Advances in Experimental Medicine and Biology 801

John D. Ash
Christian Grimm
Joe G. Hollyfield
Robert E. Anderson
Matthew M. LaVail
Catherine Bowes Rickman *Editors*

# Retinal Degenerative Diseases

## Mechanisms and Experimental Therapy

Springer

# Advances in Experimental Medicine and Biology

Volume 801



For further volumes:
http://www.springer.com/series/5584

John D. Ash • Christian Grimm
Joe G. Hollyfield • Robert E. Anderson
Matthew M. LaVail • Catherine Bowes Rickman
Editors

# Retinal Degenerative Diseases

## Mechanisms and Experimental Therapy

Springer

*Editors*
John D. Ash
Department of Ophthalmology
University of Florida
Gainesville
Florida
USA

Christian Grimm
University Hospital Zurich
Zurich
Switzerland

Joe G. Hollyfield
Cole Eye Institute at the Cleveland Clin
Division of Ophthalmology
Cleveland
Ohio
USA

Robert E. Anderson
Dean A. McGee Eye Institute
University of Oklahoma Health Science
Center
Oklahoma City
Oklahoma
USA

Matthew M. LaVail
Beckman Vision Center
University of California
San Francisco School of Medicine
San Francisco
California
USA

Catherine Bowes Rickman
Department of Ophthalmology
Duke University Medical Center
Durham
North Carolina
USA

ISSN 0065-2598 ISSN 2214-8019 (electronic)
ISBN 978-1-4614-3208-1 ISBN 978-1-4614-3209-8 (eBook)
DOI 10.1007/978-1-4614-3209-8
Springer New York Heidelberg Dordrecht London

Library of Congress Control Number: 2014930315



Printed on acid-free paper

Springer is part of Springer Science+Business Media (www.springer.com)

***Elizabeth Jean Ozan Anderson***

*April 17, 1941–April 11, 2011*
*Each of the preceding volumes of these Retinal Degeneration Symposia have been dedicated to an individual who has been an important sponsor or contributor to the field of retinal degeneration research. This volume is dedicated to the late Elizabeth Anderson, an avid and enthusiastic supporter of the young scientists who attend these meetings, and wife of Robert E. (Gene) Anderson, one of the original organizers of these meetings. At several RD Symposia, Elizabeth was the principal organizer of the spouses' program, actively planning and supervising excursions for the non-scientists in attendance. She functioned as special "hostess" for*

*young scientists, making sure that they were introduced to many of the senior investigators in retinal degeneration research. Because of our close friendship with Gene and Elizabeth, the Editors of this volume asked that we contribute some personal remembrances of Elizabeth for this dedication.*

*Although we have known Gene since 1970, we first met Elizabeth after our move to Houston in 1977 to become a part of the Cullen Eye Institute at Baylor College of Medicine. During our 17 years at Baylor, we were with Elizabeth and Gene on numerous occasions; we traveled together and became close friends.*

*Elizabeth was in college working on a bachelor's degree in nursing when she and Gene first met. This completed, Elizabeth went on to become an accredited nurse anesthetist and worked in a number of hospitals in Houston. Elizabeth was my anesthetist (JGH) when I required oral surgery in the early 1980s. The surgeon and peridontist that were treating me warned me on how painful these procedures might be and quickly convinced me to have this performed under general anesthesia in a local hospital. I checked into the hospital the night before the surgery scheduled for early the next morning. I remember being quite anxious when wheeled to the operating room, but Elizabeth had already started an IV and was by my side assuring me that she would not let me feel any pain. The next thing I remember is being awakened by a nurse back in my room who was insistent that I stay awake and drink lots of fluid to flush the remaining anesthetics from my system. Quickly the copious fluid volumes consumed required a visit to the toilet, and I called for a nurse to assist me, because I was still quite unsteady. With the nurse's help, I clumsily got out of the bed with my hospital gown in disarray and made my way to the facilities. I noticed that the nurse giggled as I moved off the bed but thought nothing of it until I discovered, as she had already observed, a big red ribbon tied securely around the most intimate part of my anatomy. Immediately I knew that Elizabeth had been up to some mischief while I was under sedation! Later when I confronted her, she assured me that she had not touched me, but that others in the OR were involved. She did finally admit to bringing the red ribbon into the OR that morning. When I questioned her about the choice of color she smiled and*

*said, "Darlin', I had a blue ribbon, but that color is reserved for my husband!"*

*Over the years, we traveled with Elizabeth and Gene to many interesting parts of the world, and on each trip, museums were always one of her favorite destinations. She loved paintings and sculpture. Many who frequent museums stroll slowly through the galleries, pausing when a painting catches one's eye, and then move on, but not Elizabeth. She would read every word of every description on every painting in every room. Gene and Joe would quickly look for a gallery with a bench or chair on which to rest while Elizabeth devoured each display. This love of art prompted her to formally enroll in a local college, and she was working toward a degree in art history at the time of her death.*

*Elizabeth had very strong opinions about a variety of issues, or perhaps we should say, about most issues. She was fearless, with no reservations whatsoever in sharing her views, and rarely softened her position to please others. One example of this occurred in 2002 during the week of the International Conference of Eye Research that convened in Geneva, Switzerland. The four of us, along with a few other couples, were dinner guests in the home of a Swiss vision scientist. As the evening progressed, and the empty wine bottles accumulated, politics became the subject and it quickly became apparent that Elizabeth and our host's husband did not share the same views. Frustrated that her pronouncements were being challenged, she pushed her chair back, stood up at the table and sang "I'm Proud to be an American", in which she was joined by several others. At the end, everyone at the table, including Elizabeth, had a great laugh, and fortunately the discussion moved on to another subject.*

*Elizabeth loved to travel, and many of her recurring annual trips were as an accompanying spouse when Gene's profession took him to a scientific meeting, usually held at some exotic destination. Early on at these conferences Elizabeth showed her concern for the young scientists in attendance. It was her personal goal to see that each young scientist she interacted with at the meeting's social function would be able to meet their most admired senior researcher.*

*It was this special characteristic that prompted Ann Milam, a retired vision scientist in Seattle and long time friend of Elizabeth's,*

*to organize an endowment in Elizabeth's name to support travel for young scientists working in the area of retinal degeneration research to attend the annual meeting of the Association for Research in Vision and Ophthalmology. Solicitations were initially made to Elizabeth and Gene's closest friends and family; then to the nearly 1,000 researchers who have attended the biennial Retinal Degeneration Symposia. Jeff Boatright also distributed a solicitation of support to the distribution list of* Molecular Vision*. Only a few days before Elizabeth's death, donations had reached $ 50,000, a level sufficient to provide support for one travel fellow each year. Elizabeth was extremely pleased to be honored and recognized with this tribute. Over 300 individuals have contributed to this endowment that now exceeds $ 120,000, a sum sufficient to fund 2–3 annual travel fellowships. Recipients of these fellowships will be designated as an* Elizabeth Anderson Travel Fellow, *allowing Elizabeth's name to appear every year in the ARVO program in perpetuity.*

*Following this travel fellowship tribute in her honor, the Foundation Fighting Blindness announced the naming of a 5-year grant, the* Elizabeth Anderson Career Development Award. *A few days later the American Health Assistance Foundation named one of their two-year, $ 120,000 awards, the* Elizabeth Anderson Macular Degeneration Grant. *Collectively, these numerous tributes to Elizabeth are a clear indication how she and Gene are respected and admired by the vision research and ophthalmology community. At the end of her struggle, death became Elizabeth's friend, because it alone brought her the peace from her illness that money could not buy, and it removed the suffering that her physicians could not cure. She left a wonderful legacy: that of a devoted wife, loving mother, devoted grandmother and an unforgettable friend to many who work in vision research and ophthalmology.*

*Mary E. Rayborn and Joe G. Hollyfield*
*Cleveland, Ohio*

Death leaves a heartache that no one can heal,
Love leaves a memory that no one can steal.
*(from an old Irish tombstone)*

# Preface

The International Symposia on Retinal Degeneration have been held in conjunction with the biennial International Congress of Eye Research (ICER) since 1984. These RD Symposia have been highly successful and have become one of the most well attended meetings in the field. The RD Symposia are successful because they allow basic and clinician scientists from around the world to convene and present their new research findings in a format that allows sufficient time for discussions and one-on-one interactions in a relaxed atmosphere, where international friendships and collaborations can be fostered.

The XVth International Symposium on Retinal Degeneration (RD2012) was held in Bad Gögging, Bavaria, Germany July 16–21, 2012. The RD2012 meeting ties the RD2010 meeting in size, which was the largest ever. The meeting brought together 230 basic and clinician scientists, retinal specialists in ophthalmology, and trainees in the field from all parts of the world. In the course of the meeting, we had 6 plenary lectures, 43 platform presentations and 117 poster presentations. A majority of these are presented in this proceedings volume. New discoveries and state of the art findings from most research areas in the field of retinal degenerations were presented.

For the first time, the RD Symposium was organized around a theme, this time focused on the role of innate and acquired immunity in the initiation and progression of retinal degenerative diseases. The recent discovery that mutations in genes related to regulation of the immune system are responsible for 50 % of the familial forms of age-related macular degeneration (AMD) demonstrates the important role the immune system plays in this disease. Based on these findings, it seemed appropriate to focus part of the RD2012 on the role of the immune system in degenerative retinal diseases. To accomplish this goal, six plenary speakers who work in the field of innate and acquired immunity were invited to participate in the RD2012 meeting. The speakers included: *V. Michael Holers*, Professor of Rheumatology, University of Colorado, School of Medicine, Denver, Colorado, USA; *Paul McMenamin*, Professor of Anatomy & Developmental Biology, School of Biomedical Sciences, Faculty of Medicine, Monash University, Melbourne, Australia; *Scott Cousins*, Professor of Ophthalmology, Duke University School of Medicine, Durham, North Carolina, USA; *Frederic Geissmann*, Professor and Chairman, Inflammation

Biology, King's College, London, United Kingdom; *Thomas Langmann*, Professor and group leader at the Institute of Human Genetics, Regensburg, Germany; and *Chi-Chao Chan*, Chief of Immunopathology Section, Laboratory of Immunology, National Eye Institute (NEI), National Institutes of Health (NIH), Bethesda, Maryland, USA. These speakers are world leaders in the fields of complement activation and signaling, the role of monocytes and microglia in retinal degeneration, and the role of cytokines in retinal degeneration. The remainder of the program included topics important to retinal degeneration including: gene therapy, neuroprotective therapy, mechanisms of cell death, mechanisms of neuroprotection, novel animal models of inherited retinal degenerations and AMD, macular degeneration, phenotype/genotype correlations, and transplantation and other cell-based approaches. The resulting program was one of the most comprehensive and up-to-date of any meeting dealing with retinal degeneration.

The meeting was organized by a nine-member committee that included the permanent members Joe G. Holyfield, Christian Grimm, Robert E. Anderson, Matthew LaVail, Catherine Bowes Rickman, and John D. Ash; and the local organizing committee members, Bernhard Webber, Ernst Tamm, and Olaf Strauss. The Symposium received international financial support from a number of organizations. We are particularly pleased to thank The Foundation Fighting Blindness, Columbia, Maryland, for its continuing support of this and all previous biennial Symposia, without which we could not have held these important meetings. In addition, for the sixth time, the NEI of the National Institutes of Health contributed in a major way to the meeting. In the past, funds from these two organizations allowed us to provide 25–35 Travel Awards to young investigators and trainees working in the field of retinal degenerations. In addition, we received generous funding from Pro Retina Germany and the Fritz Tobler Foundation Switzerland. In total, we were able to fund 57 Travel Awards, the largest number ever for these Symposia.

We thank the outstanding management and staff of the beautiful Monarch Hotel in Bad Gögging, which is located midway between Regensburg and Munich. The hotel was easily accessible, but relatively remote, which created the ideal atmosphere to encourage participation of attendees in all scientific sessions and informal meetings during meals. We would like to thank the hotel staff for all of their assistance in making this an exceptionally smooth-running conference and a truly memorable experience for all of the attendees. We would like to express our appreciation for the musical talent of Franz Badura. During our excursion to the Weltenburg monastery, Franz played several beautiful pieces in a Baroque church. Many attendees mentioned this as a highlight of the excursion. We thank Barbara Gareis and her staff in coordinating with the hotel and assisting with the poster boards and other meeting logistics. Barbara is an assistant to Ernst Tamm at the University of Regensburg. We also acknowledge the diligent and outstanding efforts of Ms. Holly Whiteside, who carried out most of the administrative aspects of the RD2012 Symposium. Holly is the Administrative Manager of Dr. Anderson's laboratory at the University of Oklahoma Health Sciences Center, and she has become the permanent Coordinator for the Retinal Degeneration Symposia. Her dedicated efforts with the Symposia since RD2000 have provided continuity not available previously, and we

are deeply indebted to her. Holly worked with Bo Dong and John D. Ash to develop the RD2012 website that for the first time included electronic submission of abstracts, registrations, and online payments.

Finally, we honor the memory of a most beloved regular attendee and supporter of the RD symposium by dedicating this book to Elizabeth Anderson. Elizabeth was a constant advocate for young scientists, as she often encouraged them to get involved in the meeting and to interact socially and informally with the senior scientists. Elizabeth was a major proponent of such interactions, and her encouragement is one of those intangible acts that influence our careers more than we could know.

John D. Ash
Christian Grimm
Joe G. Hollyfield
Robert E. Anderson
Matthew M. LaVail
Catherine Bowes Rickman

# Travel Awards

We gratefully acknowledge National Eye Institute, NIH, USA; the Foundation Fighting Blindness, USA; Pro Retina Germany; and the Fritz Tobler Foundation, Switzerland for their generous support of 57 Travel Awards to attend the RD2012 meeting. Eligibility was restricted to graduate students, postdoctoral fellows, instructors and assistant professors actively involved in retinal degeneration research. These awards were based on the quality of the abstract submitted by each applicant. Catherine Bowes Rickman chaired the Travel Awards Committee of eleven senior retinal degeneration investigators. The travel awardees are listed below. Each awardee submitted a chapter to this proceedings volume.

**Daniel Adesse**
University of Rio de Janeiro, Rio de Janeiro, Brazil
**Martin-Paul Agbaga**
University of Oklahoma HSC, Oklahoma, USA
**Cavit Agca**
University of Zürich, Zürich, Switzerland
**Alexander Aslanidis**
University of Regensburg, Regensburg, Germany
**Travis Bailey**
University of Notre Dame, Notre Dame, Indiana, USA
**Vera Bonilha**
Cole Eye Institute, Cleveland, Ohio, USA
**Barbara Maria Braunger**
University of Regensburg, Regensburg, Germany
**Leah Byrne**
University of California, Berkeley, USA
**Nora Caberoy**
University of Miami, Miami, FL, USA
**Matthew Campbell**
Trinity College Dublin, Dublin, Ireland
**Xue Cai**
University of Oklahoma HCS, Oklahoma, USA

**Timothy Day**
University of California, Berkeley, Berkeley, CA, USA
**Astra Dinculescu**
University of Florida, Gainesville, Florida USA
**Jindong Ding**
Duke University Medical Center, Durham, USA
**Xi-Qin Ding**
University of Oklahoma HSC, Oklahoma, USA
**Theodore Drivas**
University of Pennsylvania, Philadelphia, Pennsylvania, USA
**Frank Dyka**
University of Florida, Gainesville, FL, USA
**Katayoon Ebrahimi**
Johns Hopkins Hospital, University Baltimore, Baltimore, MD, USA
**Julian Esteve-Rudd**
Jules Stein Eye Institute, Los Angeles, USA
**Joseph Fogerty**
Medical College of Wisconsin, Milwaukee, USA
**Tembei Forkwa**
University of Regensburg, Regensburg, Germany
**Yingbin Fu**
University of Utah, Salt Lake City, USA
**John Fuller**
Johns Hopkins Hospital, University of Baltimore, Baltimore, MD, USA
**Sem Genini**
University of Pennsylvania, Philadelphia, Pennsylvania, USA
**Marina Gorbatyuk**
University of North Texas HSC, Fort Worth, USA
**Felix Grassmann**
University of Regensburg, Regensburg, Germany
**Gregory Grossman**
Cole Eye Institute, Cleveland, USA
**Michelle Grunin**
Hebrew University, Hadassah Ein Kerem Med Ctr, Jerusalem, Israel
**Zongchao Han**
University of Oklahoma HCS, Oklahoma, USA
**Hong Hao**
National Institutes of Health, Bethesda, USA
**Stefanie Hauck**
Helmholtz Zentrum, Munich, Germany
**Marcus Karlstetter**
University Hospital of Cologne, Cologne, Germany
**Saravanan Kolandaivelu**
West Virginia University Morgantown, West Virginia, USA
**Heike Kroeger**
University of California, San Diego San Diego, USA

**Toshihide Kurihara**
The Scripps Research Institute, La Jolla, USA
**Aparna Lakkaraju**
University of Wisconsin, Madison, Wisconsin, USA
**Jonathan Lin**
University of California, La Jolla, California, USA
**Sreemathi Logan**
University of Oklahoma HCS, Oklahoma, USA
**Vanda Lopes**
University of Coimbra, Coimbra, Portugal
**Ulrich Luhmann**
UCL Institute of Ophthalmology, London, UK
**Haoyu Mao**
University of Florida, Gainesville, USA
**Lea Marchette**
University of Oklahoma HSC, Oklahoma, USA
**Emeline Nandrot**
Institut de la Vision, Paris, France
**Anh Thi Nguyen**
Trinity College Dublin, Dublin, Ireland
**Ema Ozaki**
Trinity College Dublin, Dublin, Ireland
**David Rabin**
Albany Medical College, Albany, USA
**Alison Reynolds**
University College Dublin, Dublin, Ireland
**Linda Ruggiero**
Fordham University New York, USA
**Marijana Samardzija**
University of Zürich, Zürich, Switzerland
**Gloriane Schnabolk**
Medical University of South Carolina, Charleston, South Carolina, USA
**Chloe Stanton**
University of Edinburgh MRC IGMM, Edinburgh, Scotland
**Preeti Subramanian**
National Eye Institute, Bethesda, USA
**Peter Westenskow**
The Scripps Research Institute La Jolla, USA
**Kerstin Nagel-Wolfrum**
Johannes Gutenberg University, Mainz, Germany
**Alex Woodell**
Medical University of South Carolina, Charleston, USA
**Frank Zach**
University of Regensburg, Regensburg, Germany
**Houbin Zhang**
University of Utah, Salt Lake City, Utah, USA

# Contents

**Part XI Therapy: Protection**

# Contributors

**Toshiaki Abe** Division of Clinical Cell Therapy, Center for Advanced Medical Research and Development (ART), Graduate School of Medicine, Tohoku University, Sendai, Japan

**Martin-Paul Agbaga** Departments of Ophthalmology, University of Oklahoma Health Sciences Center, Oklahoma City, OK, USA

Dean McGee Eye Institute, Oklahoma City, OK, USA

**Cavit Agca** Lab for Retinal Cell Biology, Department of Ophthalmology, University of Zurich, Zurich, Switzerland

**Gustavo D. Aguirre** Department of Clinical Studies, School of Veterinary Medicine, University of Pennsylvania, Philadelphia, PA, USA

**Saeed Akhtar** Cornea Research Chair, College of Applied Medical Sciences, King Saud University, Riyadh, Saudi Arabia

**Eduardo C. Alfonso** Bascom Palmer Eye Institute, University of Miami, Miami, FL, USA

**Robin R Ali** Department of Genetics, UCL Institute of Ophthalmology, London, UK

NIHR Biomedical Research Centre for Ophthalmology at Moorfields Eye Hospital NHS Foundation Trust and UCL Institute of Ophthalmology, London, UK

**Turki M Al-Mubrad** Cornea Research Chair, College of Applied Medical Sciences, King Saud University, Riyadh, Saudi Arabia

**Muayyad R. Al-Ubaidi** Department of Cell Biology, University of Oklahoma Health Sciences Center, Oklahoma City, Oklahoma, USA

Oklahoma Center for Neurosciences, University of Oklahoma Health Sciences Center, Oklahoma City, Oklahoma, USA

**Noemí Álvarez-Lindo** 3D Lab (Development, Differentiation and Degeneration), Department of Cellular and Molecular Medicine, Centro de Investigaciones Biológicas, CSIC, Madrid, Spain

**Robert E. Anderson** Department of Cell Biology, University of Oklahoma Health Sciences Center, Oklahoma City, OK, USA

Department of Ophthalmology, University of Oklahoma Health Sciences Center, Oklahoma City, OK, USA

Dean McGee Eye Institute, University of Oklahoma Health Sciences Center, Oklahoma City, OK, USA

**Kunizo Arai** Department of Clinical Drug Informatics, Faculty of Pharmacy, Institute of Medical, Pharmaceutical and Health Sciences, Kanazawa University, Kanazawa, Japan

**Daniel Ardeljan** Section of Immunopathology, Laboratory of Immunology, National Eye Institute, National Institutes of Health, Bethesda, MD, USA

**Ana I. Arroba** 3D Lab (Development, Differentiation and Degeneration), Department of Cellular and Molecular Medicine, Centro de Investigaciones Biológicas, CSIC, Madrid, Spain

**John D. Ash** Department of Ophthalmology, University of Florida, Gainesville, FL, USA

**Alexander Aslanidis** Department of Ophthalmology, University of Cologne, Cologne, Germany

**Timor Baasov** Edith and Joseph Fischer Enzyme Inhibitors Laboratory, Schulich Faculty of Chemistry, Technion-Israel Institute of Technology, Haifa, Israel

**Wolfgang Baehr** Department of Ophthalmology, John A. Moran Eye Center, University of Utah Health Science Center, Salt Lake City, UT, USA

Department of Neurobiology and Anatomy, University of Utah, Salt Lake City, UT, USA

Department of Biology, University of Utah, Salt Lake City, UT, USA

**Travis J. Bailey** Department of Biological Sciences and Center for Zebrafish Research, University of Notre Dame, Notre Dame, IN, USA

**James WB Bainbridge** Department of Genetics, UCL Institute of Ophthalmology, London, UK

NIHR Biomedical Research Centre for Ophthalmology at Moorfields Eye Hospital NHS Foundation Trust and UCL Institute of Ophthalmology, London, UK

**Gabe Baltazar** Department of Anatomy and Cell Biology, University of Pennsylvania, Philadelphia, PA, USA

**Colin J. Barnstable** Department of Neural and Behavioral Sciences, Pennsylvania State University College of Medicine, Hershey, PA, USA

**Katharina Bauss** Institute of Zoology, Dept. Cell & Matrix Biology, Johannes Gutenberg University Mainz, Mainz, Germany

**S. Patricia Becerra** National Eye Institute, National Institutes of Health, Bethesda, MD, USA

**Elvir Becirovic** Center for Integrated Protein Science Munich (CIPSM), Department of Pharmacy—Center for Drug Research, Ludwig-Maximilians-Universität München, Munich, Germany

**Susanne C. Beck** Division of Ocular Neurodegeneration, Institute for Ophthalmic Research, Centre for Ophthalmology, University of Tübingen, Tübingen, Germany

**Craig D. Beight** Department of Ophthalmic Research, Cole Eye Institute, Cleveland Clinic, Cleveland, OH, USA

**William A. Beltran** Department of Clinical Studies, School of Veterinary Medicine, University of Pennsylvania, Philadelphia, PA, USA

**Jean Bennett** Kirby Center for Molecular Ophthalmology, University of Pennsylvania Perelman School of Medicine, Philadelphia, PA, USA

**Cynthia A. Berlinicke** Wilmer Eye Institute, Johns Hopkins University School of Medicine, Baltimore, MD, USA

**Maude Bernasconi** University of Lausanne, Lausanne, Switzerland

**Joseph C. Besharse** Department of Cell Biology, Neurobiology, and Anatomy, Medical College of Wisconsin, Milwaukee, WI, USA

**Faizah Bhatti** Department of Ophthalmology, University of Oklahoma Health Sciences Center, Oklahoma City, OK, USA

Department of Pediatrics, University of Oklahoma Health Sciences Center, Oklahoma City, OK, USA

**Yogesh Bhootada** Department of Molecular Genetics and Microbiology, University of Florida, Gainesville, FL, USA

**Martin Biel** Center for Integrated Protein Science Munich (CIPSM), Department of Pharmacy—Center for Drug Research, Ludwig-Maximilians-Universität München, Munich, Germany

**Susan H. Blanton** Miami Institute for Human Genomics, Univ. of Miami, Miami, FL, USA

**Jeffrey H. Boatright** Department of Ophthalmology, Emory University, Atlanta, GA, USA

Department of Ophthalmology, Emory University School of Medicine, Atlanta, GA, USA

**Sylvia Bolz** Division of Experimental Ophthalmology, Institute for Ophthalmic Research, University Eye Clinic Tübingen, Tübingen, Germany

**Vera L. Bonilha** Department of Ophthalmology, Cleveland Clinic Lerner College of Medicine, The Cole Eye Institute, i31, Cleveland, OH, USA

**Delphine Bonnet-Wersinger** Wilmer Eye Institute, Johns Hopkins University School of Medicine, Baltimore, MD, USA

**Sara J. Bowne** Human Genetics Center, School of Public Health, Univ. of Texas HSC, Houston, TX, USA

**Sanford L. Boye** Department of Ophthalmology, College of Medicine, University of Florida, Gainesville, FL, USA

**Shannon E. Boye** Department of Ophthalmology, College of Medicine, University of Florida, Gainesville, FL, USA

**Barbara M. Braunger** Institute of Human Anatomy and Embryology, University of Regensburg, Regensburg, Germany

**Richard S. Brush** Department of Ophthalmology, University of Oklahoma Health Sciences Center, Oklahoma City, OK, USA

Dean McGee Eye Institute, University of Oklahoma Health Sciences Center, Oklahoma City, OK, USA

**Marie S. Burstedt** Department of Clinical Sciences/Ophthalmology, University of Umeå, Umeå, Sweden

**Ronald A. Bush** STRRMD, National Institute on Deafness and Other Communication Disorders, National Institutes of Health, Bethesda, MD, USA

**Leah C. Byrne** Helen Wills Neuroscience Institute, The University of California Berkeley, Berkeley, CA, USA

**Nora Blanca Caberoy** School of Life Sciences, University of Nevada Las Vegas, Las Vegas, NV, USA

**Huaibin Cai** Laboratory of Neurogenetics, National Institute of Aging, NIH, Bethesda, MD, USA

**Xue Cai** Department of Ophthalmology, Dean McGee Eye Institute, University of Oklahoma Health Sciences Center, Oklahoma City, OK, USA

**Matthew Campbell** Ocular Genetics Unit, Smurfit Institute of Genetics, Trinity College Dublin, Ireland

Department of Clinical Medicine, School of Medicine, Trinity College Dublin, Ireland

National Childrens Research Centre, Our Ladys Childrens Hospital, Crumlin, Dublin, Ireland

**Marisol Cano** Wilmer Eye Institute, Johns Hopkins School of Medicine, Baltimore, MD, USA

**Daniel J. J. Carr** Department of Ophthalmology, OUHSC, Oklahoma City, OK, USA

Dean A. McGee Eye Institute, Oklahoma City, OK, USA

Department of Microbiology and Immunology, OUHSC, Oklahoma City, OK, USA

**Annie Y. Chan** Department of Ophthalmology, OUHSC, Oklahoma City, OK, USA

Dean A. McGee Eye Institute, Oklahoma City, OK, USA

**Chi-Chao Chan** Section of Immunopathology, Laboratory of Immunology, National Eye Institute, National Institutes of Health, Bethesda, MD, USA

**M. Chan** Department of Ophthalmology, University of Oklahoma Health Sciences Center, Oklahoma City, OK, USA

Dean McGee Eye Institute, University of Oklahoma Health Sciences Center, Oklahoma City, OK, USA

**Min-Lee Chang** Laboratory for Nutrition and Vision Research, Jean Mayer USDA Human Nutrition Research Center on Aging, Tufts University, Boston, MA, USA

**Hui Chen** Department of Ophthalmology, OUHSC, Oklahoma City, OK, USA

Dean A. McGee Eye Institute, Oklahoma City, OK, USA

Department of Ophthalmology, Sichuan Academy of Medical Sciences & Sichuan Provincial People's Hospital, Chengdu, Sichuan, China

**Rui Chen** Dept. of Molecular and Human Genetics, Baylor College of Medicine, Houston, TX, USA

**Vince A. Chiodo** Department of Ophthalmology, College of Medicine, University of Florida, Gainesville, FL, USA

**Chung-Jung Chiu** Laboratory for Nutrition and Vision Research, Jean Mayer USDA Human Nutrition Research Center on Aging, Tufts University, Boston, MA, USA

Department of Ophthalmology, School of Medicine, Tufts University, Boston, MA, USA

**Jonathan Chou** Department of Ophthalmology, Northwestern Feinberg School of Medicine, Chicago, IL, USA

**Shreyasi Choudhury** Department of Cell Biology and Anatomy, University of North Texas Health Science Center, Fort Worth, TX, USA

**Itay Chowers** Department of Ophthalmology, Hadassah-Hebrew University Medical Center, Jerusalem, Israel

**Micah A. Chrenek** Department of Ophthalmology, Emory University, Atlanta, GA, USA

**Joseph G. Christenbury** Department of Ophthalmology, Duke University Medical Center, Durham, NC, USA

**Vincent T. Ciavatta** Ophthalmology, School of Medicine, Emory University, Atlanta, GA, USA

**Alex W. Cohen** Department of Ophthalmology, University of Oklahoma Health Sciences Center, Oklahoma City, OK, USA

Dean McGee Eye Institute, Oklahoma City, OK, USA

**Shannon M. Conley** Department of Cell Biology, University of Oklahoma Health Sciences Center, Oklahoma City, OK, USA

**Anda Cornea** Division of Neuroscience, Oregon National Primate Research Center, Oregon Health & Science University, Beaverton, OR, USA

**Cheryl M. Craft** Mary D. Allen Laboratory for Vision Research, Doheny Eye Institute, Departments of Ophthalmology and Cell & Neurobiology, Keck School of Medicine of the University of Southern California, Los Angeles, CA, USA

**Stephen P. Daiger** Human Genetics Center, School of Public Health, Univ. of Texas HSC, Houston, TX, USA

**Nupur Dalal** Department of Ophthalmology, Emory University, Atlanta, GA, USA

**Julia E. Dallman** Department of Integrative Biology, University of Miami, Miami, FL, USA

**Joy Davis** Department of Ophthalmology and Visual Sciences, University of Michigan, Kellogg Eye Center, Ann Arbor, MI, USA

**Timothy P. Day** Helen Wills Neuroscience Institute, The University of California Berkeley, Berkeley, CA, USA

**Enrique J. de la Rosa** 3D Lab (Development, Differentiation and Degeneration), Department of Cellular and Molecular Medicine, Centro de Investigaciones Biológicas, CSIC, Madrid, Spain

**Cora Demmer** Institute of Human Anatomy and Embryology, University of Regensburg, Regensburg, Germany

**Wen-Tao Deng** Department of Ophthalmology, College of Medicine, University of Florida, Gainesville, FL, USA

**Tanja Diemer** Departments of Ophthalmology and Neurobiology, Stein Eye Institute, UCLA School of Medicine, Los Angeles, CA, USA

**J. Dietter** François Paquet-Durand, Institute for Ophthalmic Research, University of Tübingen, Tübingen, Germany

**Astra Dinculescu** Department of Ophthalmology, College of Medicine, University of Florida, Gainesville, FL, USA

**Jin-Dong Ding** Department of Ophthalmology, Duke University Medical Center, Durham, NC, USA

**Xi-Qin Ding** Departments of Cell Biology, University of Oklahoma Health Sciences Center, Oklahoma City, OK, USA

**Shuqian Dong** Department of Medicine Endocrinology, University of Oklahoma Health Sciences Center, Oklahoma City, OK, USA

Harold Hamm Diabetes Center, University of Oklahoma Health Sciences Center, Oklahoma City, OK, USA

Department of Ophthalmology, Xiangya Hospital of Central South University, Changsha, China

**Sarah L. Doyle** Ocular Genetics Unit, Smurfit Institute of Genetics, Trinity College Dublin, Ireland

Department of Clinical Medicine, School of Medicine, Trinity College Dublin, Ireland

National Childrens Research Centre, Our Ladys Childrens Hospital, Crumlin, Dublin, Ireland

**Arlene V. Drack** Department of Ophthalmology and Visual Sciences, The University of Lowa, Lowa City, USA

**Theodore G. Drivas** Cell and Molecular Biology Department, 404 Anatomy and Chemistry, University of Pennsylvania Perelman School of Medicine, Philadelphia, PA, USA

**Frank M. Dyka** Department of Ophthalmology, College of Medicine, University of Florida, Gainesville, FL, USA

**Lindsey A. Ebke** Department of Ophthalmic Research, Cole Eye Institute, Cleveland Clinic, Cleveland, OH, USA

**Katayoon B. Ebrahimi** Wilmer Eye Institute, Johns Hopkins School of Medicine, Baltimore, MD, USA

**Charles E. Egwuagu** Molecular Immunology Section, Laboratory of Immunology, National Eye Institute, National Institutes of Health, Bethesda, MD, USA

**P. A. R. Ekström** Department of Clinical Sciences, University of Lund, Lund, Sweden

**Michael H. Elliott** Department of Ophthalmology, University of Oklahoma Health Sciences Center, Oklahoma City, OK, USA

Department of Physiology, University of Oklahoma Health Sciences Center, Oklahoma City, OK, USA

Oklahoma Center for Neuroscience, University of Oklahoma Health Sciences Center, Oklahoma City, OK, USA

Dean McGee Eye Institute, Oklahoma City, OK, USA

**Pascal Escher** IRO, Institute for Research in Ophthalmology, Sion, Switzerland

University of Lausanne, Lausanne, Switzerland

**Julian Esteve-Rudd** Stein Eye Institute, UCLA David Geffen School of Medicine, Los Angeles, CA, USA

**Tatiana Favez** IRO, Institute for Research in Ophthalmology, Sion, Switzerland

**Amani A Fawzi** Department of Ophthalmology, Northwestern Feinberg School of Medicine, Chicago, IL, USA

**Jonathan D. Fay** Department of Ophthalmology, Casey Eye Institute, Oregon Health & Science University, Portland, OR, USA

**Shu Feng** Department of Ophthalmology, Casey Eye Institute, Oregon Health & Science University, Portland, OR, USA

**Natalia Fijalkowski** Wilmer Eye Institute, Johns Hopkins School of Medicine, Baltimore, MD, USA

**Silvia C. Finnemann** Department of Biological Sciences, Center for Cancer, Genetic Diseases, and Gene Regulation, Fordham University, Bronx, NY, USA

**John G. Flannery** Helen Wills Neuroscience Institute, The University of California Berkeley, Berkeley, CA, USA

**Joseph Fogerty** Department of Cell Biology, Neurobiology, and Anatomy, Medical College of Wisconsin, Milwaukee, WI, USA

**Tembei K. Forkwa** Institute of Human Anatomy and Embryology, University of Regensburg, Regensburg, Germany

**Jeanne M. Frederick** Department of Ophthalmology, John A. Moran Eye Center, University of Utah Health Science Center, Salt Lake City, UT, USA

**Martin Friedlander** Department of Cell and Molecular Biology, The Scripps Research Institute, San Diego, CA, USA

Department of Cell Biology, The Scripps Research Institute, La Jolla, CA, USA

**Joachim Fruebis** External R&D Innovations,, Pfizer Inc., Cambridge, MA, USA

**Suhua Fu** Department of Ophthalmology, The Second Affiliated Hospital of Nanchang University, Nanchang, China

Departments of Medicine Endocrinology, University of Oklahoma Health Sciences Center, Oklahoma City, OK, USA

Harold Hamm Diabetes Center, University of Oklahoma Health Sciences Center, Oklahoma City, OK, USA

**Yingbin Fu** Department of Ophthalmology & Visual Sciences, University of Utah, Salt Lake City, UT, USA

**John A. Fuller** Wilmer Eye Institute, Johns Hopkins University School of Medicine, Baltimore, MD, USA

**Robert S. Fulton** Genome Institute, Washington Univ. School of Med., St. Louis, MO, USA

**Chun Y Gao** Biological Imaging Core Facility, National Eye Institute, Bethesda, MD, USA

**Christopher Gardner** Department of Ophthalmology, Emory University, Atlanta, GA, USA

**Anupam K. Garg** Department of Ophthalmology, Casey Eye Institute, Oregon Health & Science University, Portland, OR, USA

**Marina Garcia Garrido** Division of Ocular Neurodegeneration, Institute for Ophthalmic Research, Centre for Ophthalmology, University of Tübingen, Tübingen, Germany

**Andreas Genewsky** Department of Experimental Ophthalmology, Klinikum der Universitaet Regensburg, Regensburg, Germany

**Sem Genini** Department of Clinical Studies, School of Veterinary Medicine, University of Pennsylvania, Philadelphia, PA, USA

**Shanti Kaligotla Ghosh** Department of Ophthalmology and Cell Biology, Columbia University, New York, NY, USA

**Irina Golovleva** Department of Medical Biosciences/Medical and Clinical Genetics, University Hospital of Umeå, Umeå, Sweden

**Nestor Mas Gomez** Experimental Ophthalmology, Eye Hospital, University Medical Center Regensburg, Regensburg, Germany

Department of Clinical Studies, School of Veterinary Medicine, University of Pennsylvania, Philadelphia, USA

**Marina Gorbatyuk** Department of Molecular Genetics and Microbiology, University of Florida, Gainesville, FL, USA

1670 University Blvd., Birmingham, AL, USA

**Oleg Gorbatyuk** Department of Vision Sciences, University of Alabama at Birmingham, Birmingham, AL, USA

**Felix Grassmann** Institute of Human Genetics Institute of Human Genetics, University of Regensburg, Regensburg, Germany

**Janina Gregorski** Graduate School of Basic Medical Sciences, New York Medical College, Valhalla, NY, USA

**Christian Grimm** Lab for Retinal Cell Biology, Department of Ophthalmology, University of Zurich, Zurich, Switzerland

**Marybeth Groelle** Department of Ophthalmology, Duke University Medical Center, Durham, NC, USA

**Jeffrey Gross** Section of Molecular, Cell and Developmental Biology, Institute of Cell and Molecular Biology, University of Texas at Austin, Austin, TX, USA

**Gregory H. Grossman** Department of Ophthalmic Research, Cole Eye Institute, Cleveland Clinic, Cleveland, OH, USA

**Hans E. Grossniklaus** Department of Ophthalmology, Emory University, Atlanta, GA, USA

**Michelle Grunin** Department of Ophthalmology, Hadassah-Hebrew University Medical Center, Jerusalem, Israel

**Xiaowu Gu** Department of Ophthalmology, University of Oklahoma Health Sciences Center, Oklahoma City, OK, USA

Oklahoma Center for Neuroscience, University of Oklahoma Health Sciences Center, Oklahoma City, OK, USA

Dean McGee Eye Institute, Oklahoma City, OK, USA

**Sonia Guha** Department of Anatomy and Cell Biology, University of Pennsylvania, Philadelphia, PA, USA

**Shira Hagbi-Levi** Department of Ophthalmology, Hadassah-Hebrew University Medical Center, Jerusalem, Israel

**Stephanie A. Hagstrom** Department of Ophthalmic Research, Cole Eye Institute, Cleveland Clinic, Cleveland, OH, USA

Department of Ophthalmology, Cleveland Clinic Lerner College of Medicine of Case Western Reserve University, Cleveland, OH, USA

**Zongchao Han** Department of Cell Biology, University of Oklahoma Health Sciences Center, Oklahoma City, OK, USA

**James T. Handa** Wilmer Eye Institute, Johns Hopkins School of Medicine, Baltimore, MD, USA

**Baranda S. Hansen** Wilmer Eye Institute, Johns Hopkins University School of Medicine, Baltimore, MD, USA

**Hong Hao** Neurobiology-Neurodegeneration & Repair Laboratory, National Eye Institute, NIH, Bethesda, MD, USA

**Stefanie M. Hauck** Research Unit Protein Science, Helmholtz Zentrum München, Neuherberg, Germany

**William W. Hauswirth** Department of Ophthalmology, College of Medicine, University of Florida, Gainesville, FL, USA

**John R. Heckenlively** Department of Ophthalmology and Visual Sciences, University of Michigan, Kellogg Eye Center, Ann Arbor, MI, USA

**Iris M. Heid** Department of Genetic Epidemiology, University of Regensburg, Regensburg, Germany

Institute of Genetic Epidemiology, Helmholtz Zentrum München, German Research Center for Environmental Health, Neuherberg, Germany

**Anita Hendrickson** Department of Ophthalmology, University of Washington, Seattle, WA, USA

Department of Biological Structure, University of Washington, Seattle, WA, USA

**John R. Hetling** Bioengineering, University of Illinois at Chicago, Chicago, IL, USA

**B. Hitzmann** Institute of Food Science and Biotechnology, University of Stuttgart Hohenheim, Stuttgart, Germany

**Jing Huang** Department of Ophthalmology, University of Washington, Seattle, WA, USA

**Marian M. Humphries** Ocular Genetics Unit, Smurfit Institute of Genetics, Trinity College Dublin, Ireland

Department of Clinical Medicine, School of Medicine, Trinity College Dublin, Ireland

National Childrens Research Centre, Our Ladys Childrens Hospital, Crumlin, Dublin, Ireland

**Peter Humphries** Ocular Genetics Unit, Smurfit Institute of Genetics, Trinity College Dublin, Ireland

Department of Clinical Medicine, School of Medicine, Trinity College Dublin, Ireland

National Childrens Research Centre, Our Ladys Childrens Hospital, Crumlin, Dublin, Ireland

**Sawan Hurst** Division of Neuroscience, Oregon National Primate Research Center, Oregon Health & Science University, Beaverton, OR, USA

**David R. Hyde** Department of Biological Sciences and Center for Zebrafish Research, University of Notre Dame, Notre Dame, IN, USA

**Sana Idrees** School of Medicine, The George Washington University, NW , Washington, DC, USA

**James Inglese** National Center for Advancing Translational Sciences, NIH, Rockville, MD, USA

National Human Genome Institute, NIH, Bethesda, MD, USA

**P. Michael Iuvone** Department of Ophthalmology, Emory University School of Medicine, Atlanta, GA, USA

**Herbert Jägle** Department of Ophthalmology, University Hospital Regensburg, Regensburg, Germany

Department of Ophthalmology, University Eye Clinic Regensburg, Regensburg, Germany

**Thiran Jayasundera** Department of Ophthalmology and Visual Sciences, University of Michigan, Kellogg Eye Center, Ann Arbor, MI, USA

**Wei-Chieh Jerry Chiang** Department of Pathology, University of California at San Diego, La Jolla, CA, USA

**Mei Jiang** Stein Eye Institute, UCLA David Geffen School of Medicine, Los Angeles, CA, USA

**Yi Jiang** Department of Mathematics and Statistics, Georgia State University, Atlanta, GA, USA

**Frida Jonsson** Department of Medical Biosciences/Medical and Clinical Genetics, University Hospital of Umeå, Umeå, Sweden

**Pratibha Joshi** Department of Ophthalmology, Bascom Palmer Eye Institute, University of Miami Miller School of Medicine, Miami, FL, USA

**Hirokazu Kaji** Department of Bioengineering and Robotics, Graduate School of Engineering, Tohoku University, Sendai, Japan

**Marie Kamiya** Department of Clinical Drug Informatics, Faculty of Pharmacy, Institute of Medical, Pharmaceutical and Health Sciences, Kanazawa University, Kanazawa, Japan

**Marcus Karlstetter** Department of Ophthalmology, University of Cologne, Cologne, Germany

**Satoru Kato** Department of Molecular Neurobiology, Graduate School of Medical Science, Kanazawa University, Kanazawa, Ishikawa, Japan

**Yuki Katsukura** Division of Clinical Cell Therapy, Center for Advanced Medical Research and Development (ART), Graduate School of Medicine, Tohoku University, Sendai, Japan

**Christine N. Kay** Department of Ophthalmology, University of Florida College of Medicine, Gainesville, FL, USA

**Una Kelly** Department of Ophthalmology, Duke University Medical Center, Durham, NC, USA

**Paul F. Kenna** Ocular Genetics Unit, Smurfit Institute of Genetics, Dublin 2, Ireland

**Breandán N. Kennedy** School of Biomolecular and Biomedical Science, Conway Institute, University College Dublin, Dublin 4, Ireland

**David Kent** The Vision Clinic, Kilkenny, Ireland

Pharmacology and Therapeutics, University of Florida, Gainesville, FL, USA

**Naheed Khan** Department of Ophthalmology and Visual Sciences, University of Michigan, Kellogg Eye Center, Ann Arbor, MI, USA

**Aditi Khanna** Department of Ophthalmology and Visual Sciences, The University of Lowa, Lowa City, USA

**Anna-Sophia Kiang** Ocular Genetics Unit, Smurfit Institute of Genetics, Trinity College Dublin, Ireland

Department of Clinical Medicine, School of Medicine, Trinity College Dublin, Ireland

National Childrens Research Centre, Our Ladys Childrens Hospital, Crumlin, Dublin, Ireland

**Claire Kilty** School of Biomolecular and Biomedical Science, Conway Institute, University College Dublin, Dublin 4, Ireland

**Kathryn E. Klump** Oklahoma Center for Neuroscience, University of Oklahoma Health Sciences Center, Oklahoma City, USA

Dean A. McGee Eye Institute, Oklahoma City, OK, USA

**Daniel C. Koboldt** Genome Institute, Washington Univ. School of Med., St. Louis, MO, USA

**Fred Koch** Center for Integrated Protein Science Munich (CIPSM), Department of Pharmacy—Center for Drug Research, Ludwig-Maximilians-Universität München, Munich, Germany

**Susanne Koch** Center for Integrated Protein Science Munich (CIPSM), Department of Pharmacy—Center for Drug Research, Ludwig-Maximilians-Universität München, Munich, Germany

**Adarsha Koirala** Department of Cell Biology, University of Oklahoma Health Sciences Center, Oklahoma City, OK, USA

**Saravanan Kolandaivelu** Ophthalmology and Biochemistry, Center for Neuroscience, Eye Institute, West Virginia University, Morgantown, WV, USA

**Naoka Komori** Departments of Cell Biology, University of Oklahoma Health Sciences Center, Oklahoma City, OK, USA

**Yoshiki Koriyama** Department of Molecular Neurobiology, Graduate School of Medical Science, Kanazawa University, Kanazawa, Ishikawa, Japan

**Heike Kroeger** Department of Pathology, University of California, San Diego, USA

**Kannan Kunchithapautham** Department of Ophthalmology, Medical University of South Carolina, Charleston, SC, USA

**Mansi Motiwale Kunte** Department of Cell Biology and Anatomy, University of North Texas Health Science Center, Fort Worth, TX, USA

**Toshihide Kurihara** Department of Cell and Molecular Biology, The Scripps Research Institute, San Diego, CA, USA

Department of Cell Biology, The Scripps Research Institute, La Jolla, CA, USA

**Ayaka Kuwana** Division of Health Sciences, Graduate School of Medical Science, Kanazawa University, Kanazawa, Ishikawa, Japan

**Aparna Lakkaraju** Department of Ophthalmology and Visual Sciences, School of Medicine and Public Health, University of Wisconsin-Madison, Madison, WI, USA

McPherson Eye Research Institute, University of Wisconsin-Madison, Madison, WI, USA

**Byron L. Lam** Bascom Palmer Eye Institute, University of Miami, Miami, FL, USA

**Thomas Langmann** Department of Ophthalmology, University of Cologne, Cologne, Germany

Department of Experimental Immunology of the Eye, University of Cologne, Cologne, Germany

**David Larsen** Genome Institute, Washington Univ. School of Med., St. Louis, MO, USA

**Alan M. Laties** Department of Ophthalmology, University of Pennsylvania, Philadelphia, PA, USA

**Matthew M. LaVail** Departments of Anatomy and Ophthalmology, University of California, San Francisco, USA

**Yun-Zheng Le** Department of Medicine Endocrinology, University of Oklahoma Health Sciences Center, Oklahoma City, OK, USA

Department of Cell Biology, University of Oklahoma Health Sciences Center, Oklahoma City, OK, USA

Harold Hamm Diabetes Center, University of Oklahoma Health Sciences Center, Oklahoma City, OK, USA

**Wen-Hsiang Lee** Department of Ophthalmology, Bascom Palmer Eye Institute, University of Miami Miller School of Medicine, Miami, FL, USA

**Alfred S. Lewin** Department of Vision Sciences, University of Alabama at Birmingham, Birmingham, AL, USA

**Qiuhong Li** Department of Ophthalmology, College of Medicine, University of Florida, Gainesville, FL, USA

**Yichao Li** Visual Function Core, National Eye Institute, Bethesda, MD, USA

**Yiwen Li** Bascom Palmer Eye Institute, University of Miami, Miami, FL, USA

**Yumei Li** Dept. of Molecular and Human Genetics, Baylor College of Medicine, Houston, TX, USA

**Jonathan H. Lin** Department of Pathology, University of California at San Diego, La Jolla, CA, USA

**Ji Liu** Department of Ophthalmology, University of Pennsylvania, Philadelphia, PA, USA

**Yan Liu** Department of Medicine Endocrinology, University of Oklahoma Health Sciences Center, Oklahoma City, OK, USA

Harold Hamm Diabetes Center, University of Oklahoma Health Sciences Center, Oklahoma City, OK, USA

Department of Ophthalmology, Xiangya Hospital of Central South University, Changsha, China

**Zhao Liu** Department of Ophthalmology and Cell Biology, Columbia University, New York, NY, USA

**Zhenzhen Liu** Laboratory for Nutrition and Vision Research, Jean Mayer USDA Human Nutrition Research Center on Aging at Tufts University, Boston, USA

**S. Logan** Department of Cell Biology, University of Oklahoma Health Sciences Center, Oklahoma City, OK, USA

Dean A. McGee Eye Institute, Oklahoma City, OK, USA

**Sreemathi Logan** Dean McGee Eye Institute, Oklahoma City, OK, USA

Department of Cell Biology, University of Oklahoma Health Sciences Center, Oklahoma City, OK, USA

**Vanda S. Lopes** Stein Eye Institute, UCLA David Geffen School of Medicine, Los Angeles, CA, USA

**Hubert Löwenheim** Otolaryngology Department, University of Tübingen, Tübingen, Germany

**Ulrich FO Luhmann** Department of Genetics, UCL Institute of Ophthalmology, London, UK

**Mahdi Mahmood** Department of Ophthalmology and Visual Sciences, University of Michigan, Kellogg Eye Center, Ann Arbor, MI, USA

**Goldis Malek** Duke University Eye Center, Albert Eye Research Institute, Department of Ophthalmology, Duke University, Durham, NC, USA

**Nawajes A. Mandal** Department of Ophthalmology, University of Oklahoma Health Sciences Center, Oklahoma City, OK, USA

Dean McGee Eye Institute, University of Oklahoma Health Sciences Center, Oklahoma City, OK, USA

Dean A. McGee Eye Institute, Oklahoma City, OK, USA

Department of Physiology, OUHSC, Oklahoma City, OK, USA

Department of Oklahoma Center for Neuroscience (OCNS), OUHSC, Oklahoma City, OK, USA

**Shivani N. Mann** Department of Ophthalmology, OUHSC, Oklahoma City, OK, USA

Dean A. McGee Eye Institute, Oklahoma City, OK, USA

**L. D. Marchette** Department of Cell Biology, University of Oklahoma Health Sciences Center, Oklahoma City, OK, USA

Dean McGee Eye Institute, University of Oklahoma Health Sciences Center, Oklahoma City, OK, USA

**Julien Maruotti** Department of Ophthalmology, The Johns Hopkins University School of Medicine, Baltimore, MD, USA

**Hiroyuki Matsumoto** Departments of Cell Biology, University of Oklahoma Health Sciences Center, Oklahoma City, OK, USA

**Alexander Matveev** Departments of Cell Biology, University of Oklahoma Health Sciences Center, Oklahoma City, OK, USA

**Kazuhiro Mawatari** Division of Health Sciences, Graduate School of Medical Science, Kanazawa University, Kanazawa, Ishikawa, Japan

**Michael McClintock** Department of Ophthalmology, University of Florida College of Medicine, Gainesville, FL, USA

**Daphne L. McCulloch** Department of Life Sciences, Glasgow Caledonian University, Glasgow, Scotland

**Trevor J. McGill** Department of Ophthalmology, Casey Eye Institute, Oregon Health & Science University, Portland, OR, USA

**James F. McGinnis** Oklahoma Center for Neuroscience, University of Oklahoma Health Sciences Center, Oklahoma City, USA

Department of Cell Biology, University of Oklahoma Health Sciences Center, Oklahoma City, USA

Department of Ophthalmology, University of Oklahoma Health Sciences Center, Oklahoma City, USA

Department of Ophthalmology, College of Medicine, University of Oklahoma Health Sciences Center (OUHSC) and Dean McGee Eye Institute, Oklahoma City, OK, USA

Cell Biology and Oklahoma Center for Neuroscience, OUHSC, Oklahoma City, OK, USA

Department of Ophthalmology, Dean McGee Eye Institute, University of Oklahoma Health Sciences Center, Oklahoma City, OK, USA

Neuroscience Center, University of Oklahoma Health Sciences Center, Oklahoma City, OK, USA

**Keith V. Michaels** Department of Ophthalmology, Casey Eye Institute, Oregon Health & Science University, Portland, OR, USA

**Stylianos Michalakis** Center for Integrated Protein Science Munich (CIPSM), Department of Pharmacy—Center for Drug Research, Ludwig-Maximilians-Universität München, Munich, Germany

**Seok-Hong Min** Department of Ophthalmology, College of Medicine, University of Florida, Gainesville, FL, USA

**Myriam Mirza** Instutute of Human Genetics, University of Regensburg, Regensburg, Germany

Department of Experimental Immunology of the Eye, University of Cologne, Cologne, Germany

**Claire H. Mitchell** Department of Anatomy and Cell Biology, University of Pennsylvania, Philadelphia, PA, USA

**Regine Mühlfriedel** Division of Ocular Neurodegeneration, Institute for Ophthalmic Research, Centre for Ophthalmology, University of Tübingen, Tübingen, Germany

**Claudia Müller** Experimental Ophthalmology, Eye Hospital, University Medical Center Regensburg, Regensburg, Germany

**Robert F. Mullins** Department of Ophthalmology and Visual Sciences, The University of Lowa, Lowa City, USA

**Muna I. Naash** Department of Cell Biology, University of Oklahoma Health Sciences Center, Oklahoma City, OK, USA

**Nobuhiro Nagai** Division of Clinical Cell Therapy, Center for Advanced Medical Research and Development (ART), Graduate School of Medicine, Tohoku University, Sendai, Japan

**Kerstin Nagel-Wolfrum** Institute of Zoology, Dept. Cell & Matrix Biology, Johannes Gutenberg University Mainz, Mainz, Germany

**Hiroshi Nakashima** Division of Health Sciences, Graduate School of Medical Science, Kanazawa University, Kanazawa, Ishikawa, Japan

**Emeline F. Nandrot** INSERM, Paris, France

Institut de la Vision, UPMC Univ Paris 06, Paris, France

CNRS, Paris, France

**Sonali Nashine** Department of Cell Biology and Anatomy, University of North Texas Health Science Center, Fort Worth, TX, USA

**Martha Neuringer** Department of Ophthalmology, Casey Eye Institute, Oregon Health & Science University, Portland, OR, USA

Division of Neuroscience, Oregon National Primate Research Center, Oregon Health & Science University, Beaverton, OR, USA

**Anh T. H. Nguyen** The Ocular Genetics Unit, Smurfit Institute of Genetics, Trinity College Dublin, Dublin 2, Ireland

**John M. Nickerson** Department of Ophthalmology, Emory University, Atlanta, GA, USA

**Maki Nishitani** Division of Health Sciences, Graduate School of Medical Science, Kanazawa University, Kanazawa, Ishikawa, Japan

**Matsuhiko Nishizawa** Department of Bioengineering and Robotics, Graduate School of Engineering, Tohoku University, Sendai, Japan

**Anna Norberg** Department of Medical Biosciences/Medical and Clinical Genetics, University Hospital of Umeå, Umeå, Sweden

**Kazuhiro Ogai** Division of Health Sciences, Graduate School of Medical Science, Kanazawa University, Kanazawa, Ishikawa, Japan

**Andreas Ohlmann** Institute of Human Anatomy and Embryology, University of Regensburg, Regensburg, Germany

**Hideyuki Onami** Division of Clinical Cell Therapy, Center for Advanced Medical Research and Development (ART), Graduate School of Medicine, Tohoku University, Sendai, Japan

**Ema Ozaki** Ocular Genetics Unit, Smurfit Institute of Genetics, Trinity College Dublin, Ireland

Department of Clinical Medicine, School of Medicine, Trinity College Dublin, Ireland

National Childrens Research Centre, Our Ladys Childrens Hospital, Crumlin, Dublin, Ireland

**Francois Paquet-Durand** François Paquet-Durand, Institute for Ophthalmic Research, University of Tübingen, Tübingen, Germany

Division of Experimental Ophthalmology, Institute for Ophthalmic Research, University Eye Clinic Tübingen, Tübingen, Germany

**O. Paquet-Durand** Institute of Food Science and Biotechnology, University of Stuttgart Hohenheim, Stuttgart, Germany

**Machelle T. Pardue** Ophthalmology, School of Medicine, Emory University, Atlanta, GA, USA

Rehab R&D Center of Excellence, US Department of Veterans Affairs, Decatur, GA, USA

Research Service (151Oph), Atlanta VA Medical Center, Decatur, GA, USA

**Gayle J. T. Pauer** Department of Ophthalmic Research, Cole Eye Institute, Cleveland Clinic, Cleveland, OH, USA

**Marc C. Peden** Department of Ophthalmology, University of Florida College of Medicine, Gainesville, FL, USA

**Crandall Peeler** Department of Ophthalmology and Visual Sciences, University of Michigan, Kellogg Eye Center, Ann Arbor, MI, USA

**Mark E. Pennesi** Department of Ophthalmology, Casey Eye Institute, Oregon Health & Science University, Portland, OR, USA

**Margaret A. Peričak-Vance** John P. Hussman Institute for Human Genomics, University of Miami, Miami, FL, USA

**Eric A. Pierce** Ocular Genomics Institute, Massachusetts Eye and Ear Infirmary, Boston, MA, USA

**Evgenya Y. Popova** Department of Neural and Behavioral Sciences, Pennsylvania State University College of Medicine, Hershey, PA, USA

**Daniel E. Possin** Department of Ophthalmology, University of Washington, Seattle, WA, USA

**Constantin J. Pournaras** Department of NEUCLID, Geneva University Hospitals, Geneva, Switzerland

**Nathalie Produit-Zengaffinen** Institute for Research in Ophthalmology, Sion, Switzerland

**X Qi** Department of Mathematics and Statistics, Georgia State University, Atlanta, GA, USA

**Haohua Qian** Visual Function Core, National Eye Institute, Bethesda, MD, USA

**Tingyu Qin** Laboratory for Nutrition and Vision Research, Jean Mayer USDA Human Nutrition Research Center on Aging at Tufts University, Boston, USA

**Rakesh Kotapati Raghupathy** Department of Life Sciences, Glasgow Caledonian University, Glasgow, Scotland

**Visvanathan Ramamurthy** Ophthalmology and Biochemistry, Center for Neuroscience, Eye Institute, West Virginia University, Morgantown, WV, USA

**Matthew Rapp** National Eye Institute, National Institutes of Health, Bethesda, MD, USA

**Mary E. Rayborn** Department of Ophthalmology, Cleveland Clinic Lerner College of Medicine, The Cole Eye Institute, i31, Cleveland, OH, USA

**Alaina Reagan** Department of Ophthalmology, University of Oklahoma Health Sciences Center, Oklahoma City, OK, USA

Oklahoma Center for Neuroscience, University of Oklahoma Health Sciences Center, Oklahoma City, OK, USA

Dean McGee Eye Institute, Oklahoma City, OK, USA

**Nadine Reichhart** Experimental Ophthalmology, Department of Ophthalmology, Charite University Medicine Berlin, Berlin, Germany

Experimental Ophthalmology, Eye Hospital, University Medical Center Regensburg, Regensburg, Germany

**Laurie M. Renner** Division of Neuroscience, Oregon National Primate Research Center, Oregon Health & Science University, Beaverton, OR, USA

**Alison L. Reynolds** School of Biomolecular and Biomedical Science, Conway Institute, University College Dublin, Dublin 4, Ireland

**Catherine Bowes Rickman** Departments of Ophthalmology and Cell Biology, Duke University Medical Center, Durham, NC, USA

Department of Cell Biology, Duke University Medical Center, Durham, NC, USA

Duke Eye Center, Duke University Medical Center, Durham, NC, USA

**Kay D. Rittenhouse** External R&D Innovations,, Pfizer Inc., Cambridge, MA, USA

**Scott J Robbie** Department of Genetics, UCL Institute of Ophthalmology, London, UK

NIHR Biomedical Research Centre for Ophthalmology at Moorfields Eye Hospital NHS Foundation Trust and UCL Institute of Ophthalmology, London, UK

**Bärbel Rohrer** Department of Ophthalmology, Medical University of South Carolina, Charleston, SC, USA

Research Service, Ralph H. Johnson VA Medical Center, Charleston, SC, USA

Departments of Neurosciences, Division of Research, Medical University of South Carolina, Charleston, SC, USA

Departments of Neurosciences and Ophthalmology, Medical University of South Carolina, Charleston, SC, USA

Research Service, Ralph H. Johnson VA Medical Center, Medical University of South Carolina, Charleston, SC, USA

Ralph H. Johnson VA Medical Center, Division of Research, Charleston, SC, USA

Division of Research and Ophthalmology, Medical University of South Carolina, Charleston, SC, USA

**Stuart Rollins** Department of Ophthalmology, Northwestern Feinberg School of Medicine, Chicago, IL, USA

**Linda Ruggiero** Department of Biological Sciences, Center for Cancer, Genetic Diseases, and Gene Regulation, Fordham University, Bronx, NY, USA

**Renee C. Ryals** Department of Ophthalmology, College of Medicine, University of Florida, Gainesville, FL, USA

**Ayse Sahaboglu** François Paquet-Durand, Institute for Ophthalmic Research, University of Tübingen, Tübingen, Germany

Division of Experimental Ophthalmology, Institute for Ophthalmic Research, University Eye Clinic Tübingen, Tübingen, Germany

**Marijana Samardzija** Lab for Retinal Cell Biology, Department of Ophthalmology, University of Zurich, Zurich, Switzerland

**Ola Sandgren** Department of Clinical Sciences/Ophthalmology, University of Umeå, Umeå, Sweden

**Temitope Sasore** School of Biomolecular and Biomedical Science, Conway Institute, University College Dublin, Dublin 4, Ireland

**David V. Schaffer** Helen Wills Neuroscience Institute, The University of California Berkeley, Berkeley, CA, USA

Department of Chemical and Biomolecular Engineering, The University of California, Berkeley, CA, USA

**Gloriane Schnabolk** Ralph H. Johnson VA Medical Center, Division of Research, Charleston, SC, USA

**Desi P. Schoo** Department of Ophthalmology and Visual Sciences, The University of Lowa, Lowa City, USA

**Daniel F. Schorderet** IRO, Institute for Research in Ophthalmology, Sion, Switzerland

University of Lausanne, Lausanne, Switzerland

Faculty of Life Sciences, Ecole polytechnique fédérale de Lausanne, Lausanne, Switzerland

Department of Ophthalmology, University of Lausanne, Lausanne, Switzerland

**Elisabeth Schulze** Center for Integrated Protein Science Munich (CIPSM), Department of Pharmacy—Center for Drug Research, Ludwig-Maximilians-Universität München, Munich, Germany

**Sudipta Seal** Materials Science and Engineering, Advanced Materials Processing Analysis Center and Nanoscience Technology Center, University of Central Florida, Orlando, FL, USA

**Mathias W. Seeliger** Division of Ocular Neurodegeneration, Institute for Ophthalmic Research, Centre for Ophthalmology, University of Tübingen, Tübingen, Germany

**Christina Seide** Division of Ocular Neurodegeneration, Institute for Ophthalmic Research, Centre for Ophthalmology, University of Tübingen, Tübingen, Germany

**Roswitha Seitz** Institute of Human Anatomy and Embryology, University of Regensburg, Regensburg, Germany

**Fu Shang** Laboratory for Nutrition and Vision Research, Jean Mayer USDA Human Nutrition Research Center on Aging at Tufts University, Boston, USA

**Gillian C. Shaw** Wilmer Eye Institute, Johns Hopkins University School of Medicine, Baltimore, MD, USA

**Ryan A. Shaw** Department of Cell Biology, University of Oklahoma Health Sciences Center, Oklahoma City, OK, USA

**D. M. Sherry** Department of Cell Biology, University of Oklahoma Health Sciences Center, Oklahoma City, OK, USA

Oklahoma Center for Neuroscience, University of Oklahoma Health Sciences Center, Oklahoma City, OK, USA

Department of Pharmaceutical Sciences, University of Oklahoma Health Sciences Center, Oklahoma City, OK, USA

**Lisa Shine** School of Biomolecular and Biomedical Science, Conway Institute, University College Dublin, Dublin 4, Ireland

**Xinhua Shu** Department of Life Sciences, Glasgow Caledonian University, Glasgow, Scotland

**Paul A. Sieving** National Eye Institute, National Institutes of Health, Bethesda, MD, USA

**Anil Singh** Departments of Cell Biology, University of Oklahoma Health Sciences Center, Oklahoma City, OK, USA

**C. Sippl** Institute of Human Anatomy and Embryology, University of Regensburg, Regensburg, Germany

**Travis B. Smith** Department of Ophthalmology, Casey Eye Institute, Oregon Health & Science University, Portland, OR, USA

**Elliott H. Sohn** Department of Ophthalmology and Visual Sciences, The University of Lowa, Lowa City, USA

**Nasrin Sorusch** Institute of Zoology, Dept. Cell & Matrix Biology, Johannes Gutenberg University Mainz, Mainz, Germany

**Vithiyanjali Sothilingam** Division of Ocular Neurodegeneration, Institute for Ophthalmic Research, Centre for Ophthalmology, University of Tübingen, Tübingen, Germany

**Janet R. Sparrow** Department of Ophthalmology, Columbia University, New York, USA

Department of Ophthalmology and Cell Biology, Columbia University, New York, NY, USA

Department of Pathology and Cell Biology, Columbia University, New York, NY, USA

**Marvin Sperling** External R&D Innovations,, Pfizer Inc., Cambridge, MA, USA

**Chloe M. Stanton** MRC Human Genetics Unit, MRC Institute of Genetics and Molecular Medicine, University of Edinburgh, Edinburgh, UK

**Veronika M. Stein** Department of Small Animal Medicine and Surgery, University of Veterinary Medicine Hannover, Hannover, Germany

**Heidi Stöhr** Institute of Human Genetics, University Regensburg, Regensburg, Germany

**Donald U. Stone** Department of Ophthalmology, OUHSC, Oklahoma City, OK, USA

Dean A. McGee Eye Institute, Oklahoma City, OK, USA

**Edwin M. Stone** Department of Ophthalmology and Visual Sciences, The University of Lowa, Lowa City, USA

**Olaf Strauß** Experimental Ophthalmology, Department of Ophthalmology, Charite University Medicine Berlin, Berlin, Germany

Experimental Ophthalmology, Eye Hospital, University Medical Center Regensburg, Regensburg, Germany

Department of Experimental Ophthalmology, Klinikum der Universitaet Regensburg, Regensburg, Germany

Experimental Ophthalmology, Department of Ophthalmology, Charite Universitaetsmedizin Berlin, Berlin, Germany

**Michael W. Stuck** Department of Cell Biology, University of Oklahoma Health Sciences Center, Oklahoma City, OK, USA

**Preeti Subramanian** National Eye Institute, National Institutes of Health, Bethesda, MD, USA

**Kayo Sugitani** Division of Health Sciences, Graduate School of Medical Science, Kanazawa University, Kanazawa, Ishikawa, Japan

**Lori S. Sullivan** Human Genetics Center, School of Public Health, Univ. of Texas HSC, Houston, TX, USA

**Ernst R. Tamm** Institute of Human Anatomy and Embryology, University of Regensburg, Regensburg, Germany

**Naoyuki Tanimoto** Division of Ocular Neurodegeneration, Institute for Ophthalmic Research, Centre for Ophthalmology, University of Tübingen, Tübingen, Germany

**Allen Taylor** Laboratory for Nutrition and Vision Research, Jean Mayer USDA Human Nutrition Research Center on Aging, Tufts University, Boston, MA, USA

Department of Ophthalmology, School of Medicine, Tufts University, Boston, MA, USA

**Leila Tiab** IRO, Institute for Research in Ophthalmology, Sion, Switzerland

**Yumi Tokita-Ishikawa** Division of Clinical Cell Therapy, Center for Advanced Medical Research and Development (ART), Graduate School of Medicine, Tohoku University, Sendai, Japan

**Stephen Tomlinson** Departments of Microbiology and Immunology, Medical University of South Carolina, Charleston, SC, USA

**Kimberly A. Toops** Department of Ophthalmology and Visual Sciences, School of Medicine and Public Health, University of Wisconsin-Madison, Madison, WI, USA

McPherson Eye Research Institute, University of Wisconsin-Madison, Madison, WI, USA

**Gianluca Tosini** Department of Ophthalmology, Emory University School of Medicine, Atlanta, GA, USA

Department of Pharmacology and Toxicology and Neuroscience Institute, Morehouse School of Medicine, Atlanta, GA, USA

**Budd A. Tucker** Department of Ophthalmology and Visual Sciences, The University of Lowa, Lowa City, USA

**Marius Ueffing** François Paquet-Durand, Institute for Ophthalmic Research, University of Tübingen, Tübingen, Germany

Research Unit Protein Science, Helmholtz Zentrum München, Neuherberg, Germany

Centre of Ophthalmology, Institute for Ophthalmic Research, University of Tübingen, Tübingen, Germany

**Nico van Rooijen** 3D Lab (Development, Differentiation and Degeneration), Department of Cellular and Molecular Medicine, Centro de Investigaciones Biológicas, CSIC, Madrid, Spain

**Jeffery M. Vance** John P. Hussman Institute for Human Genomics, University of Miami, Miami, FL, USA

**Camasamudram Vijayasarathy** STRRMD, National Institute on Deafness and Other Communication Disorders, National Institutes of Health, Bethesda, MD, USA

**Cornelia Volz** Department of Ophthalmology, University Eye Clinic Regensburg, Regensburg, Germany

**Christine von Toerne** Research Unit Protein Science, Helmholtz Zentrum München, Neuherberg, Germany

**Karl J. Wahlin** Department of Ophthalmology, The Johns Hopkins University School of Medicine, Baltimore, MD, USA

**Yana Walczak** Department of Ophthalmology, University of Cologne, Cologne, Germany

**J. Wang** University of Florida, Gainesville, FL, USA

**Minhua Wang** Unit on Neuron-Glia Interactions in Retinal Diseases, National Eye Institute, National Institutes of Health, Bethesda, MD, USA

**Yunchang Wang** Department of Ophthalmology, The Second Affiliated Hospital of Nanchang University, Nanchang, China

**Bernhard H. F. Weber** Institute of Human Genetics Institute of Human Genetics, University of Regensburg, Regensburg, Germany

**George M. Weinstock** Genome Institute, Washington Univ. School of Med., St. Louis, MO, USA

**Alison R. Weiss** Division of Neuroscience, Oregon National Primate Research Center, Oregon Health & Science University, Beaverton, OR, USA

**Rong Wen** Department of Ophthalmology, Bascom Palmer Eye Institute, University of Miami Miller School of Medicine, Miami, FL, USA

**Y. Wen** Amherst College, Amherst, MA, USA

**Peter D. Westenskow** Department of Cell and Molecular Biology, The Scripps Research Institute, San Diego, CA, USA

Department of Cell Biology, The Scripps Research Institute, La Jolla, CA, USA

**David S. Williams** Stein Eye Institute, UCLA David Geffen School of Medicine, Los Angeles, CA, USA

Departments of Ophthalmology and Neurobiology, Stein Eye Institute, UCLA School of Medicine, Los Angeles, CA, USA

**Roman Wolf** Department of Comparative Medicine, University of Oklahoma Health Sciences Center, Oklahoma City, OK, USA

**Uwe Wolfrum** Department of Cell and Matrix Biology, Institute of Zoology, Johannes Gutenberg University of Mainz, Mainz, Germany

**Lily L. Wong** Department of Ophthalmology, College of Medicine, University of Oklahoma Health Sciences Center (OUHSC) and Dean McGee Eye Institute, Oklahoma City, OK, USA

**Wai T. Wong** Unit on Neuron-Glia Interactions in Retinal Diseases, National Eye Institute, National Institutes of Health, Bethesda, MD, USA

**Grace Woo** National Eye Institute, National Institutes of Health, Bethesda, MD, USA

**Alex Woodell** Departments of Neurosciences, Division of Research, Medical University of South Carolina, Charleston, SC, USA

**Alan F. Wright** MRC Human Genetics Unit, MRC Institute of Genetics and Molecular Medicine, University of Edinburgh, Edinburgh, UK

**Kirsten Wunderlich** Institute of Zoology, Dept. Cell & Matrix Biology, Johannes Gutenberg University Mainz, Mainz, Germany

**Chengsong Xie** Laboratory of Neurogenetics, National Institute of Aging, NIH, Bethesda, MD, USA

**Jin Xu** Department of Ophthalmology and Visual Sciences, School of Medicine and Public Health, University of Wisconsin-Madison, Madison, WI, USA

**Xueliang Xu** Department of Ophthalmology, Xiangya Hospital of Central South University, Changsha, China

**Xiaoping Yang** Department of Ophthalmology, Cleveland Clinic Lerner College of Medicine, The Cole Eye Institute, i31, Cleveland, OH, USA

**Keqiang Ye** Department of Pharmacology and Toxicology and Neuroscience Institute, Morehouse School of Medicine, Atlanta, GA, USA

Department of Pathology and Laboratory Medicine, Emory University School of Medicine, Atlanta, GA, USA

**Allen Yen** Department of Ophthalmology, University of Oklahoma Health Sciences Center, Oklahoma City, OK, USA

Dean McGee Eye Institute, Oklahoma City, OK, USA

**Junji Yodoi** Department of Biological Responses, Institute for Virus Research, Kyoto University, Kyoto, Japan

**Frank Zach** Institute of Human Genetics, University Regensburg, Regensburg, Germany

**Donald J. Zack** Department of Ophthalmology, The Johns Hopkins University School of Medicine, Baltimore, MD, USA

Department of Neuroscience, The Johns Hopkins University School of Medicine, Baltimore, MD, USA

Department of Molecular Biology and Genetics, The Johns Hopkins University School of Medicine, Baltimore, MD, USA

Institute of Genetic Medicine, The Johns Hopkins University School of Medicine, Baltimore, MD, USA

Institut de la Vision, Paris, France

Wilmer Eye Institute, Johns Hopkins University School of Medicine, Baltimore, MD, USA

Departments of Molecular Biology and Genetics, Neuroscience, and Institute of Genetic Medicine, The Johns Hopkins University School of Medicine, Baltimore, MD, USA

**Sarwar Zahid** Department of Ophthalmology and Visual Sciences, University of Michigan, Kellogg Eye Center, Ann Arbor, MI, USA

**Bin Zhang** Genomic Medicine Institute, Lerner Research Institute, Cleveland Clinic Foundation, Cleveland, OH, USA

**Houbin Zhang** Department of Ophthalmology, John A. Moran Eye Center, University of Utah Health Science Center, Salt Lake City, UT, USA

**Samuel Shao-Min Zhang** Department of Neural and Behavioral Sciences, Pennsylvania State University College of Medicine, Hershey, PA, USA

**Tao Zhang** Department of Ophthalmology & Visual Sciences, University of Utah, Salt Lake City, UT, USA

**Wenlan Zhang** Department of Ophthalmology, Duke University Medical Center, Durham, NC, USA

**Jilin Zhou** Department of Ophthalmology, Columbia University, New York, USA

Department of Ophthalmology and Cell Biology, Columbia University, New York, NY, USA

**Meili Zhu** Department of Medicine Endocrinology, University of Oklahoma Health Sciences Center, Oklahoma City, OK, USA

Harold Hamm Diabetes Center, University of Oklahoma Health Sciences Center, Oklahoma City, OK, USA

**Lucia Ziccardi** G. B. Bietti Foundation, Istituto di Ricovero e Cura a Carattere Scientifico (IRCCS), Rome, Italy

**Stephan L. Züchner** John P. Hussman Institute for Human Genomics, University of Miami, Miami, FL, USA

# About the Editors

**John D. Ash, Ph.D.** Francis M. Bullard Eminent Scholar Chair in Ophthalmological Sciences, Department of Ophthalmology, College of Medicine at the University of Florida. Dr. Ash received his Ph.D. from the Ohio State University Biochemistry Program in 1994, and completed postdoctoral training in the Cell Biology Department at Baylor College of Medicine, in Houston, Texas, and began his faculty career at the University of Oklahoma Health Sciences Center, Oklahoma. Dr. Ash is also a Visiting Professor of the Dalian Medical University, Dalian China. Dr. Ash has written and published 51 manuscripts including research articles, book chapters and invited reviews. He is currently an Executive editor for *Experimental Eye research*, and a Scientific Review Editor for *Molecular Vision*. Dr. Ash is an active reviewer for these journals as well as *Investigative Ophthalmology & Visual Science*. In 2009, Dr. Ash received a research award from Hope for Vision, and in 2010 he received a Lew R. Wasserman Merit award from Research to Prevent Blindness, Inc. Dr. Ash has received grants from the National Institutes of Health, the Foundation Fighting Blindness, Research to Prevent Blindness, Inc., Hope for Vision, and the American Diabetes Association. Dr. Ash has served on the Program Committee of the Association for Research in Vision and Ophthalmology, and currently serving on their Advocacy Committee. Dr. Ash has served on the scientific review panel for Fight For Sight (2005–2008), and is currently serving on the Scientific Advisory Board of the Foundation Fighting Blindness (Columbia, MD) where he chairs the review committee on Novel Medical Therapies Program. He also serves on the scientific review panel for the Macular Degeneration program of the Bright Focus Organization (formally the American Health Assistance Foundation, Clarksburg, MD).

**Christian Grimm, Ph.D.** is Professor for Experimental Ophthalmology at the University of Zurich, Switzerland. He received his Ph.D. degree at the Institute for General Microbiology at the University of Berne in 1990. After an initial postdoc position in the field of snRNP maturation, Dr. Grimm conducted research at the University of Wisconsin in Madison, WI, where he studied nucleo-cytoplasmic transport of small RNAs. In 1997 Dr. Grimm moved back to Switzerland where he joined the Lab for Retinal Cell Biology in the department of Ophthalmology at the University of Zurich. Dr. Grimm has led the Lab for Retinal Cell Biology since

2006 and was appointed Professor for Experimental Ophthalmology and joined the medical faculty in 2008. Dr. Grimm has published more than 100 original research and review articles, more than 90 in the field of retinal degeneration. His research focuses on molecular mechanisms of photoreceptor cell death, neuroprotection and hypoxic signaling. Dr. Grimm has received the Alfred Vogt Award (2000), the Retinitis Pigmentosa Award of Pro Retina Germany (2003) and the Pfizer Research Award in Neuroscience (2004). He serves on the Editorial Boards of *Current Eye Research, Experimental Eye Research* and *Molecular Vision*, is Honorary Board member of *Hypoxic Signaling* and acts as a Scientific Review Associate for the *European Journal of Neuroscience*. Dr. Grimm has received research grants from the Swiss National Science Foundation, the European Union, the University of Zurich and several private funding organizations. He serves on the Scientific Advisory Board of the Foundation Fighting Blindness, ProRetina Germany, Retina Suisse and the Swiss Society of Ophthalmology, and is Vice Chairman of the Center for Integrative Human Physiology, a priority research program of the University of Zurich.

**Joe G. Hollyfield, Ph.D.** is Chairman of Ophthalmic Research and the Llura and Gordon Gund Professor of Ophthalmology Research in the Cole Eye Institute at the Cleveland Clinic, Cleveland, Ohio. He received a Ph.D. from the University of Texas at Austin and did postdoctoral work at the Hubrecht Laboratory in Utrecht, The Netherlands. He has held faculty positions at Columbia University College of Physicians and Surgeons in New York City and at Baylor College of Medicine in Houston, Texas. He was Director of the Retinitis Pigmentosa Research Center in The Cullen Eye Institute at Baylor from 1978 until his move to The Cleveland Clinic Foundation in 1995. He is currently Director of the Foundation Fighting Blindness Research Center at the Cleveland Clinic and oversees activity of the Foundation Fighting Blindness Histopathology Center and Donor Eye Program. Dr. Hollyfield has published over 200 papers in the area of cell and developmental biology of the retina and retinal pigment epithelium in health and disease. He has edited 16 books, 15 on retinal degenerations and one on the structure of the eye. Dr. Hollyfield received the Marjorie W. Margolin Prize (1981, 1994), the Sam and Bertha Brochstein Award (1985) and the Award of Merit in Retina Research (1998) from the Retina Research Foundation; the Olga Keith Weiss Distinguished Scholars' Award (1981) and two Senior Scientific Investigator Awards (1988, 1994) from Research to Prevent Blindness, Inc.; an award from the Alcon Research Institute (1987); the Distinguished Alumnus Award (1991) from Hendrix College, Conway, Arkansas; the Endre A. Balazs Prize (1994) from the International Society for Eye Research (ISER); the Proctor Medal (2009) from the Association for Research in Vision and Ophthalmology (ARVO), and the 2009 Cless "Best of the Best" Award, given by the University of Illinois Eye and Ear Infirmary. He was named an inaugural Gold Fellow by ARVO in 2009. Since 1991 he has been Editor-in-Chief of the journal, *Experimental Eye Research* published by Elsevier. Dr. Hollyfield has been active in ARVO, serving on the Program Committee (1976), as Trustee (Retinal Cell Biology, 1989–1994), as President (1993–1994) and as Immediate

Past President (1994–1995). He also served as President (1988–1991) and Secretary (1984–1987) of the International Society of Eye Research. He is Chairman of the scientific review panel for the Macular Degeneration program of the Bright Focus Foundation (Clarksburg, MD), serves on the scientific advisory boards of the Foundation Fighting Blindness (Owings Mills, MD), the Helen Keller Eye Research Foundation (Birmingham, AL), the South Africa Retinitis Pigmentosa Foundation (Johannesburg, South Africa), is Co-Chairman of the Medical and Scientific Advisory Board of Retina International (Zurich, Switzerland), and is a member of the Board of Trustees of Hendrix College.

**Robert E. Anderson, M.D., Ph.D.** is George Lynn Cross Research Professor, Dean A. McGee Professor of Ophthalmology, Professor of Cell Biology, and Adjunct Professor of Geriatric Medicine at The University of Oklahoma Health Sciences Center in Oklahoma City, Oklahoma. He is also Director of Research at the Dean A. McGee Eye Institute. He received his Ph.D. in Biochemistry (1968) from Texas A&M University and his M.D. from Baylor College of Medicine in 1975. In 1968, he was a postdoctoral fellow at Oak Ridge Associated Universities. At Baylor, he was appointed Assistant Professor in 1969, Associate Professor in 1976, and Professor in 1981. He joined the faculty of the University of Oklahoma Health Sciences Center in January of 1995. Dr. Anderson served as director of the Oklahoma Center for Neuroscience (1995–1999) and chairman of the Department of Cell Biology (1998–2007). He has received several honorary appointments including Visiting Professor, West China School of Medicine, Sichuan University, Chengdu, China; Honorary Professorship, Xi'an Jiaotong University, Xi'an, China; and Honorary Professor of Sichuan Medical Science Academy, Sichuan Provincial People's Hospital, Sichuan, China. Dr. Anderson has received the Sam and Bertha Brochstein Award for Outstanding Achievement in Retina Research from the Retina Research Foundation (1980), and the Dolly Green Award (1982) and two Senior Scientific Investigator Awards (1990 and 1997) from Research to Prevent Blindness, Inc. He received an Award for Outstanding Contributions to Vision Research from the Alcon Research Institute (1985), and the Marjorie Margolin Prize (1994). He has served on the editorial boards of *Investigative Ophthalmology and Visual Science, Journal of Neuroscience Research, Neurochemistry International, Current Eye Research*, and *Experimental Eye Research*. Dr. Anderson has published extensively in the areas of lipid metabolism in the retina and biochemistry of retinal degenerations. He has edited 15 books, 14 on retinal degenerations and one on the biochemistry of the eye. Dr. Anderson has received grants from the National Institutes of Health, The Retina Research Foundation, the Foundation Fighting Blindness, and Research to Prevent Blindness, Inc. He has been an active participant in the program committees of the Association for Research in Vision and Ophthalmology (ARVO) and was a trustee representing the Biochemistry and Molecular Biology section. He was named a Gold Fellow by ARVO in 2009 and received the Proctor Medal from ARVO in 2011. He received the Llura Liggett Gund Lifetime Achievement Award from the Foundation Fighting Blindness in June 2011. In 2012, he received the Paul A. Kayser International Award, Retina Research Foundation. He has served on the

Vision Research Program Committee and Board of Scientific Counselors of the National Eye Institute and the Board of the Basic and Clinical Science Series of The American Academy of Ophthalmology. Dr. Anderson is a past Councilor, Treasurer, and President of the International Society for Eye Research.

**Matthew M. LaVail, Ph.D.** is Professor of Anatomy and Ophthalmology at the University of California, San Francisco School of Medicine. He received his PhD degree in Anatomy (1969) from the University of Texas Medical Branch in Galveston and was subsequently a postdoctoral fellow at Harvard Medical School. Dr. LaVail was appointed Assistant Professor of Neurology-Neuropathology at Harvard Medical School in 1973. In 1976, he moved to UCSF, where he was appointed Associate Professor of Anatomy. He was appointed to his current position in 1982, and in 1988, he also became Director of the Retinitis Pigmentosa Research Center at UCSF, later named the Kearn Family Center for the Study of Retinal Degeneration. Dr. LaVail has published extensively in the research areas of photoreceptor-retinal pigment epithelial cell interactions, retinal development, circadian events in the retina, genetics of pigmentation and ocular abnormalities, inherited retinal degenerations, light-induced retinal degeneration, and neuroprotective and gene therapy for retinal degenerative diseases. He has identified several naturally occurring murine models of human retinal degenerations and has developed transgenic mouse and rat models of others. He is the author of more than 160 research publications and has edited 14 books on inherited and environmentally induced retinal degenerations. Dr. LaVail has received the Fight for Sight Citation (1976); the Sundial Award from the Retina Foundation (1976); the Friedenwald Award from the Association for Research in Vision and Ophthalmology (ARVO, 1981); two Senior Scientific Investigators Awards from Research to Prevent Blindness (1988 and 1998); a MERIT Award from the National Eye Institute (1989); an Award for Outstanding Contributions to Vision Research from the Alcon Research Institute (1990); the Award of Merit from the Retina Research Foundation (1990); the first John A. Moran Prize for Vision Research from the University of Utah (1997); the first Trustee Award from The Foundation Fighting Blindness (1998); the fourth Llura Liggett Gund Award from the Foundation Fighting Blindness (2007); and he has received the Distinguished Alumnus Award from both his university (University of North Texas) and his graduate school (University of Texas Medical Branch). He has served on the editorial boards of *Investigative Ophthalmology and Visual Science* and *Experimental Eye Research*. Dr. LaVail has been an active participant in the program committee of ARVO and has served as a Trustee (Retinal Cell Biology Section) of ARVO. In 2009, he was appointed an inaugural ARVO Fellow, Gold, of the 12,000-member organization. Dr. LaVail has been a member of the program committee and a Vice President of the International Society for Eye research. He also served on the Scientific Advisory Board of the Foundation Fighting Blindness from 1973–2011.

**Catherine Bowes Rickman, Ph.D.** is a tenured Associate Professor of Ophthalmology and of Cell Biology at Duke University located in Durham, NC. Dr. Bowes Rickman leads a team of researchers focused on developing and using mouse models to understand the pathobiology of age-related macular degeneration (AMD)

and on developing and testing therapeutic targets for AMD. Dr. Bowes Rickman received her undergraduate degree at the University of California at Santa Barbara, specializing in Biochemistry/Molecular Biology and Aquatic Biology. She did her Ph.D. at the University of California at Los Angeles and postdoctoral fellowship at the Jules Stein Eye Institute, CA, where she focused on models of retinitis pigmentosa. Dr. Bowes Rickman has a long-standing interest in the molecular and cell biology and pathology of the retina. Amongst her seminal discoveries was the identification of the gene responsible for retinal degeneration in the *rd* mouse. She has applied her expertise in mouse genetics to develop models to study age-related macular degeneration (AMD). Currently, she is using several mouse models developed in her program that faithfully recapitulate many aspects of the human AMD phenotype to provide *in vivo* means to examine the pathogenic contribution of genetic, inflammatory and environmental factors to AMD onset and progression. Recently, she successfully demonstrated therapeutic rescue from dry AMD in one of these models. She has spent the last few years expanding her research program into studying the impact of the complement system on the onset and progression of AMD. Dr. Bowes Rickman's research program has been continually funded by the NIH and is also currently supported by an Edward N. and Della L. Thome Memorial Foundation Award. She has received support from Research to Prevent Blindness (RPB) Foundation, the Foundation Fighting Blindness, the Macular Degeneration program of the American Health Assistance Foundation, Macula Vision Research Foundation, and The Ruth and Milton Steinbach Fund. Dr. Bowes Rickman has received a RPB Career Development Award and a RPB William and Mary Greve Special Scholars Award. She has published more than 40 original research and review articles. She currently serves on the Scientific Advisory Boards of the Foundation Fighting Blindness and Applied Genetics Technologies Corp Scientific Advisory Board and is a consultant for GlaxoSmithKline and Pfizer.

# Part I
# Basic Processes: Development, Physiology and Function

# Chapter 1
# Cell Type-Specific Epigenetic Signatures Accompany Late Stages of Mouse Retina Development

**Evgenya Y. Popova, Colin J. Barnstable and Samuel Shao-Min Zhang**

**Abstract** We have used ChIP-seq to map the distribution of two important histone H3 modifications, H3K4me2 and H3K27me3, over the whole genome at multiple time points during late mouse retina development. We merged these data with our previous retina developmental expression profiles and show that there are several epigenetic signatures specific for different functional groups of genes. The main conclusion from our study is that epigenetic signatures defined by H3K4me2 and H3K27me3 can distinguish cell-type specific genes from widespread transcripts and may be reflective of cell specificity during retina maturation. Rod photoreceptor-specific genes have a striking signature, a de novo accumulation of H3K4me2 and a complete absence of H3K27me3. We were able to use this signature in an unbiased search of the whole genome and identified essentially all the known rod photoreceptor genes as well as a group of novel genes that have a high probability of being rod photoreceptor specific. Comparison of our genome-wide chromatin signature maps with available data sets for Polymerase-II (Pol-II) and CRX binding sites and DNase1 Hypersensitive Sites (DHS) for retina shows great agreement. Because our approach is not dependent on high levels of gene expression, it provides a new way of identifying cell type-specific genes, particularly genes that may be involved in retinal diseases.

**Keywords** Retina development · Epigenetic · Chromatin · Histone

The retina begins as an early compartment of the forebrain and has frequently served as a model of CNS development [1, 2]. Retinal cell types are formed in a characteristic sequence from E12 to PN5 with ganglion cells, amacrine cells, and

C. J. Barnstable (✉) · E. Y. Popova · S. Shao-Min Zhang
Department of Neural and Behavioral Sciences, Pennsylvania State University College of Medicine, Hershey, PA 17033, USA
e-mail: cbarnstable@hmc.psu.edu

E. Y. Popova
e-mail: eyp1@psu.edu

S. Shao-Min Zhang
e-mail: ssz3@psu.edu

J. D. Ash et al. (eds.), *Retinal Degenerative Diseases,* Advances in Experimental Medicine and Biology 801, DOI 10.1007/978-1-4614-3209-8_1,

horizontal cells among the early formed types and rod photoreceptors and bipolar cells formed predominantly during the later postnatal period. Control of retinogenesis is a complex process involving changing levels of expression regulation of large groups of genes. Change in chromatin structure around promoters and genes is an important factor in tissue specification, but knowledge about this epigenetic contribution to retina development is just beginning to emerge. Previously, studies have focused on chromatin changes in promoter areas of individual genes, for example rhodopsin [3, 4]. New genome-wide technologies provide the opportunity to study simultaneously developmental changes in large groups of genes during retinogenesis and to better understand how tissue-specific gene expression is established and maintained in retina. Here we have combined and reviewed both our and several other recently published genome-wide data sets for retina development. We have created custom tracks in the UCSC Mouse Genome Browser by using data from our study for H3K4me2 ChIP-Seq [5], Pol-II ChIP-on-Chip data from [6], data for CRX ChIP-Seq [7], and ENCODE project tracts for retina's DHS (University of Washington). This approach provides a new way of identifying cell type-specific genes, particularly genes that may be involved in retinal diseases.

We generated a comprehensive genomic map of H3K4me2 and H3K27me3 using ChIP-seq on mouse retinas of various ages [5]. When the H3K4me2 and H3K27me3 reads were mapped to the genome it was clear that most of these two-histone modifications were in gene-rich regions of the genome (Fig. 1.1a, b). The accumulation of H3K4me2 reads in the genome were primarily localized in the area around the transcription start site (TSS), showing two sharp peaks (Fig. 1.1c) of enrichment approximately ± 1 Kb surrounding the TSS as defined for the 25,158 genes from the NCBI RefSeq database, including splice variants and alternative TSS. The peaks of H3K27me3 were less pronounced and were even less distinct at PN15 than at E17.5 (Fig. 1.1d). A small set of genes from this large collection was used for confirmation by ChIP-qPCR analysis and the results perfectly matched those of the ChIP-Seq experiments. Analysis of these data has revealed a number of important and surprising results.

*First*, genes that are never expressed in retina, such as erythrocyte-specific globin or olfactory receptor genes, showed no accumulation of either H3K4me2 or H3K27me3. This appears to be a good diagnostic criterion for whether a gene is ever expressed in retina. Interestingly, when we examined available databases of other cell types (ChIP-Seq analysis of C2C12 myogenic cell line, LICR Histone Track, UCSC Genome Informatics) that do not express these genes we found a similar lack of both H3K4me2 and H3K27me3, suggesting that this criterion may be general.

*Second,* we found different histone signatures for retinal genes with the same gene expression pattern. In our earlier developmental gene expression studies we had identified a group of 123 genes whose expression increased in parallel with maturation of rod photoreceptors, and a pool of 119 genes whose expression decreased between E16.5 and PN15. When we carried out a hierarchical cluster analysis on the upregulated genes they fell into four distinct clusters, each with its own epigenetic signature (Fig. 1.1e). Similarly the downregulated genes fell into three distinct clusters.

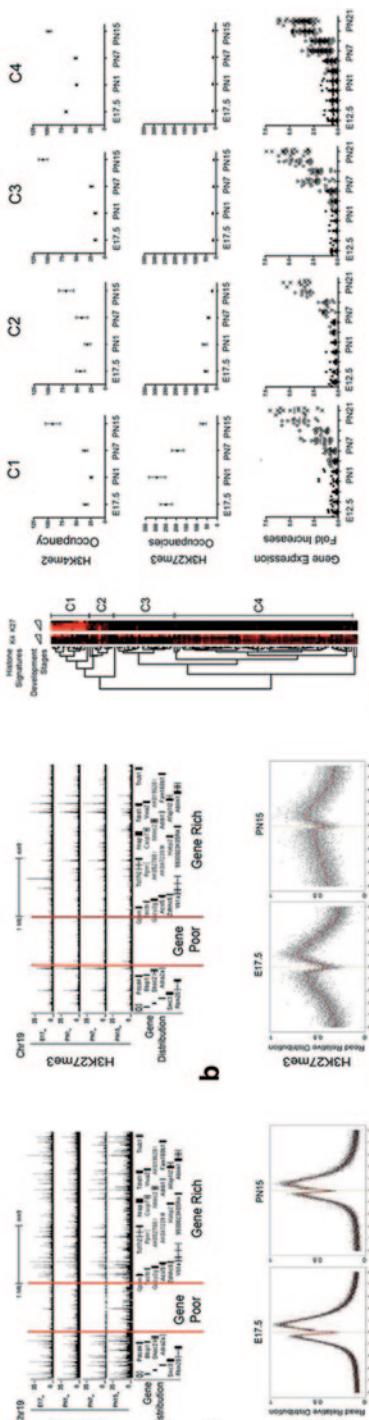


**Fig. 1.1** H3K4me2 and H3K27me3 profiles during retina organogenesis. **a**, b Histone modifications patterns at part of chromosome 19. Peaks of normalized sequenced tags from ChIP-Seq analysis of mouse retina at four developmental stages. **c**, d Histone modifications for all NCBI RefSeq genes around TSS. **e** Cluster analysis of H3K4me2 and H3K27me3 occupancy around TSS (± 2.5 Kb) for genes upregulated in mature retina. Tree-view shows 4 clusters (*C1—C4*) with distinct epigenetic patterns for H3K4me2 (*upper panel*) and H3K27me3 (*middle panel*), but with same expression patterns (*lower panel*). Adapted from [5]

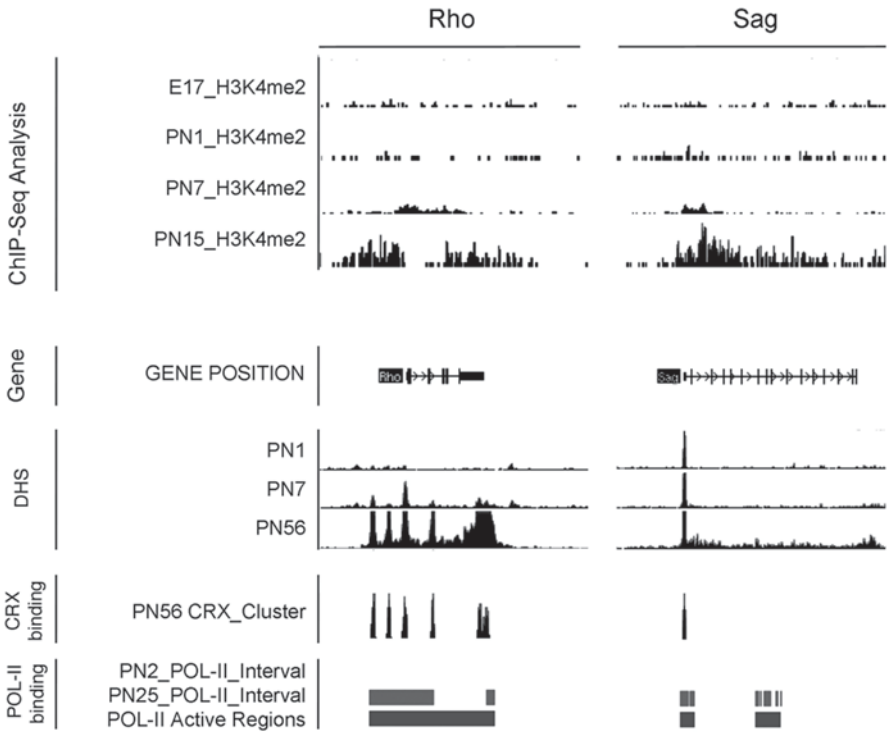


**Fig. 1.2** Combine genome-wide tracks of H3K4me2 ChIP-Seq analysis, DNase1 Hypersensitive Sites (DHS) and CRX- and Pol-II-binding sites for known rod-specific genes

*Third,* we found that a unique signature of H3K4me2 and H3K27me3 marks rod photoreceptor-specific genes. Our initial analysis identified a cluster that contained a group of known rod-specific genes. The signature of this cluster (C3 on Fig. 1.1e) was a de novo increase in H3K4me2 and no H3K27me3 at any stage. To test whether this was a signature for rod-specific genes we did an unbiased cluster analysis of all 25,158 genes in the RefSeq database. This analysis identified 107 genes with the "rod signature". This cluster contained all known rod-specific genes, including *rho, Nrl, and Nr2E3,* mouse orthologues of recently described disease genes such as *BC027072,* and genes such as *Ppef2*, *Lrit1,* and *Lrit2* that have been implicated in phototransduction but whose exact function is unknown. Many other genes in this cluster are predominantly expressed in the retina (data sets from [8]; Stanford SOURCE; MGI from Jackson Lab), but exact localization has yet to be carried out. Since the epigenetic signatures are unrelated to the level of gene expression, we have suggested that they may be a novel way of identifying cell type-specific genes particularly those expressed at low levels.

*Fourth*, the accumulation of H3K4me2 at rod-specific genes was over the whole gene, not just the TSS, as indicated for the example genes in Fig. 1.2. We have suggested that this histone modification is involved in the maintenance of rod gene expression not its initial onset. This is in agreement with other recent genome-wide

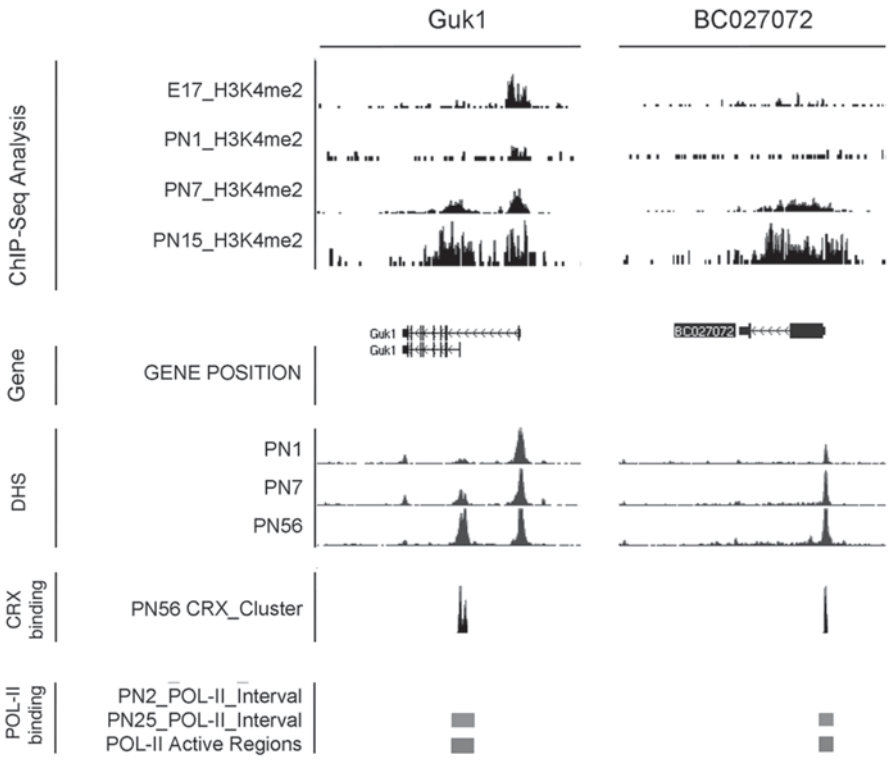


**Fig. 1.3** Combine genome-wide tracks of H3K4me2 ChIP-Seq analysis, DNase1 Hypersensitive Sites (DHS), and CRX- and Pol-II-binding sites for newly predicted rod-specific genes

studies, that genes specially expressed in blood cells displayed high levels of H3K-4me2 over the whole gene bodies [9, 10].

The conclusion from our study is that epigenetic signatures defined by H3K-4me2 and H3K27me3 can distinguish cell type-specific genes from widespread transcripts and may be reflective of cell specificity during retina maturation.

We then compared our genome-wide chromatin signature maps with available data sets for retina for ChIP-on-Chip study of Polymerase-II (Pol-II) binding sites [6], ChIP-Seq study for CRX binding sites [7], and DHS (University of Washington data, available on UCSC mouse Genome Browser as a part of ENCODE project) with a focus on the cluster of genes with a "rod signature". In this cluster of 107 genes, 95 genes (or 89 %) have CRX binding site around the TSS and gene, with average ~2 CRX binding sites per gene. ENCODE project retina's DHS tracks are available for three developmental stages: PN1, PN7, PN56. During development DHS could spread widely, for example at the promoter or TSS of developmentally upregulated genes, or could disappear at the TSS and promoter of downregulated genes. We monitored developmentally upregulated DHS for our rod-specific cluster genes and 105 of them (or 98 %) have such DHS around gene or its promoter with average three upregulated DHS per gene. Pol-II binding data is available for retina

at PN2 and PN25 developmental stages with a list of genes that have ratio of Pol-II PN25/ Pol-II PN2 more than 1.8. 67 genes (or 63 %) from our cluster of rod-specific genes are in this list with the average level of Pol-II PN25/Pol-II PN2 around 4.2. When compared, combination of tracks (CRX and Pol-II binding sites, DHS and H3K4me2 accumulation) for known rod-specific genes (Fig. 1.2) looks very similar to the tracks of newly predicted genes (Fig. 1.3).

The agreement between our whole-genome data and other data sets shows the predictive power of epigenetic signatures and the importance of studying changes in the epigenome and chromatin structure of promoters and genes during retina development. Rod photoreceptors also provide us with an almost unique model to address the question of whether epigenetic changes are controlled by the same transcription factors that regulate gene expression or by some as yet unknown mechanism.

**Acknowledgment** We thank K.P. Mitton for providing an access to genome tracks for the Pol-II binding sites. This work was supported by NIH grant EY013865 and Macular Vision Research Foundation to C.J.B.

**Funding/Support:** Pfizer Ophthalmology External Research Unit, The Foundation Fighting Blindness CDA (MEP), Research to Prevent Blindness (Unrestricted grant to Casey Eye Institute, CDA to MEP), NIH grant P51OD011092 (MN), K08 EY021186-01 (MEP).

## References

1. Barnstable CJ (1987) A molecular view of vertebrate retinal development. Mol Neurobiol 1:9–46
2. Dyer MA, Cepko CL (2001) Regulating proliferation during retinal development. Nat Rev Neurosci 2:333–342
3. Peng GH, Chen S (2007) Crx activates opsin transcription by recruiting HAT-containing co-activators and promoting histone acetylation. Hum Mol Genet 16:2433–2452
4. Peng GH, Chen S (2011) Active opsin loci adopt intrachromosomal loops that depend on the photoreceptor transcription factor network. Proc Natl Acad Sci U S A 108:17821–17826
5. Popova EY, Xu X, Dewan AT, Salzberg AC, Berg A, Hoh J, Zhang SS, Barnstable CJ (2012) Stage and gene specific signatures defined by histones H3K4me2 and H3K27me3 accompany mammalian retina maturation in vivo. PLoS One 7:e46867
6. Tummala P, Mali RS, Guzman E, Zhang X, Mitton KP (2010) Temporal ChIP-on-Chip of RNA-polymerase-II to detect novel gene activation events during photoreceptor maturation. Mol Vis 16:252–271
7. Corbo JC, Lawrence KA, Karlstetter M, Myers CA, Abdelaziz M, Dirkes W, Weigelt K, Seifert M, Benes V, Fritsche LG et al (2010) CRX ChIP-seq reveals the cis-regulatory architecture of mouse photoreceptors. Genome Res 20:1512–1525
8. Su AI, Cooke MP, Ching KA, Hakak Y, Walker JR, Wiltshire T, Orth AP, Vega RG, Sapinoso LM, Moqrich A et al. (2002) Large-scale analysis of the human and mouse transcriptomes. Proc Natl Acad Sci U S A 99:4465–4470
9. Wong P, Hattangadi SM, Cheng AW, Frampton GM, Young RA, Lodish HF (2011) Gene induction and repression during terminal erythropoiesis are mediated by distinct epigenetic changes. Blood 118:e128–138
10. Pekowska A, Benoukraf T, Ferrier P, Spicuglia S (2010) A unique H3K4me2 profile marks tissue-specific gene regulation. Genome Res 20:1493–1502

# Chapter 2
# Programmed Cell Death During Retinal Development of the Mouse Eye

**Barbara M. Braunger, Cora Demmer and Ernst R. Tamm**

**Abstract** Similar to other parts of the central nervous system, there are two types of programmed cell death during retinal development. In early development, the neuronal progenitor population is affected. In the mouse eye, this kind of programmed cell death begins at around embryonic day (E) 12.5 and peaks between E14.5 and E16.5. The second phase of programmed cell death occurs during synaptogenesis within the first 2 postnatal weeks. Important signaling mechanisms that induce programmed cell death of retinal progenitors appear to involve nerve growth factor acting on the proapoptotic receptor to p75 neurotrophin receptor ($p75^{NTR}$) and transforming growth factor-β.

**Keywords** Retina · Programmed cell death · Neuronal development · Apoptosis

## 2.1 Introduction

Programmed cell death constitutes an important element of the morphogenetic processes during development of the central nervous system in which up to 70% of neurons that have been generated do not survive until adulthood. This article will briefly review the process of programmed cell death in the mouse retina.

## 2.2 Programmed Cell Death in the Mouse Retina

Similar to other parts of the central nervous system, there are two types of programmed cell death during retinal development. In early development, the neuronal progenitor population is affected. In the mouse eye, this kind of programmed cell

E. R. Tamm (✉) · B. M. Braunger · C. Demmer
Institute of Human Anatomy and Embryology,
University of Regensburg, Universitätsstr. 31,
93053 Regensburg, Germany
e-mail: ernst.tamm@vkl.uni-regensburg.de

J. D. Ash et al. (eds.), *Retinal Degenerative Diseases,* Advances in Experimental Medicine and Biology 801, DOI 10.1007/978-1-4614-3209-8_2,

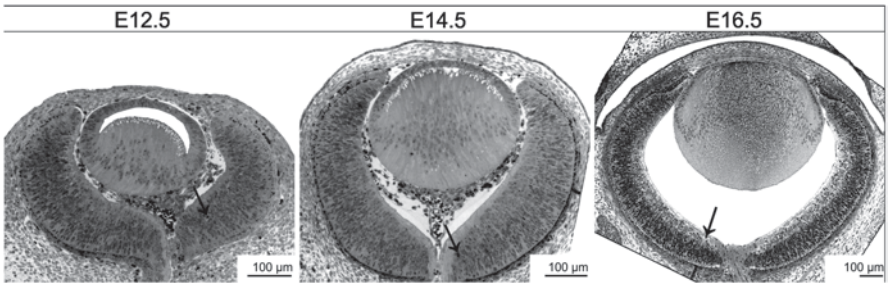


**Fig. 2.1** Retinal development: semithin sections of the mouse eye at different embryonic time-points (*E*). The *arrows* indicate pycnotic cell nuclei

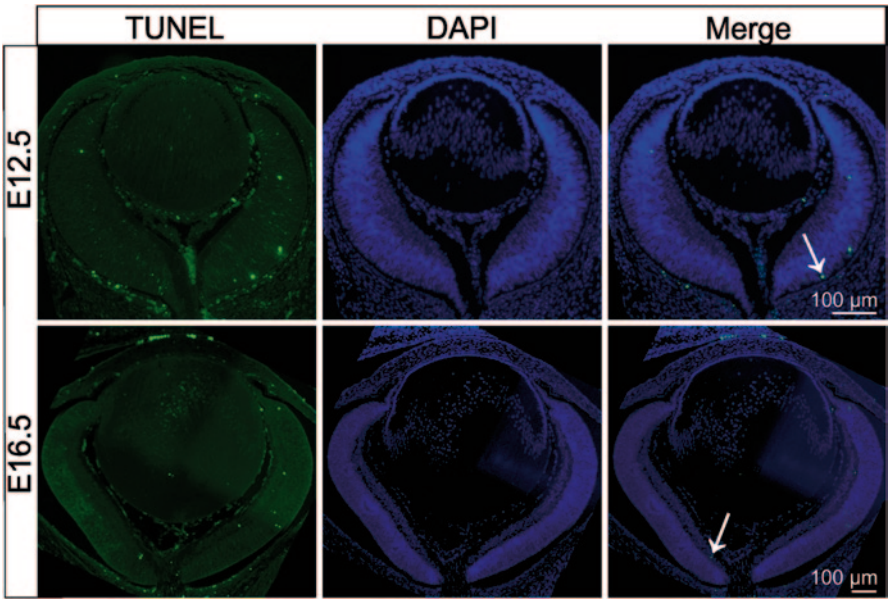


**Fig. 2.2** Apoptotic cell death during embryonic retinal development. TUNEL staining visualizes apoptotic cells (*arrows*). Paraffin sections of mouse embryonic eyes at embryonic day (*E*) 12.5 and E16.5

death begins at around embryonic day (E) 12.5 [1] and peaks between E14.5 and E16.5, a period where numerous pycnotic or TUNEL-positive progenitor cells can be identified (Figs. 2.1 and 2.2). It has been discussed that the advantage of this kind of cell death is the adaptation of the size of the progenitor cell population [2, 3]. The second phase of programmed cell death in the developing central nervous system occurs during synaptogenesis. The cells are sorted out in order to promote optimal target innervation. According to the neurotrophin hypothesis, neurons that are in the process to seek connectivity compete with other neurons for a limited supply of neurotrophic factors provided by the target cell. The winner cell will survive, while those cells that are unsuccessful in this competition will die [4–6].

In the mouse retina, programmed cell death during synaptogenesis occurs during the first 2 postnatal weeks. Young et al. [7] showed that degenerating cells were found in all layers of the retina at the day of birth, but they were distributed unevenly. Retinal ganglion cells die during the first 11 days of life with a peak between postnatal (P) days 2–4. Death of amacrine cells takes place during the first 11 days, with its peak during P4–5. Bipolar and Müller cells die between P5–18 with highest cell death between P8–9. Inner rods die between P5–10 with the peak at P7, whereas outer rods undergo programmed cell death during P5–24, and the peak at P11 [7]. Overall, photoreceptors are affected less than other retinal neurons by programmed cell death [8].

## 2.3 Neurotrophins

Neurotrophins constitute a family of secreted proteins which are involved in proliferation, growth, and maintenance of neurons. Family members are nerve growth factor (NGF), brain-derived neurotrophic factor (BDNF), neurotrophin-3 (NT3), and neurotrophin-4 (NT4). In the adult rodent retina, NGF is expressed in astrocytes, retinal ganglion cells, Müller cells, and the retinal pigment epithelium [9], while BDNF is detected in Müller cells [10], retinal ganglion cells, and cells of the inner nuclear layer [11, 12]. NT-3 is expressed in a small subset of cells in the inner nuclear layer and the ganglion cell layer, and NT-4 in the inner and outer nuclear layer of the retina[13]. Neurotrophins mediate their function through binding to the family of tropomyosin related kinase receptors (Trk) and the p75 neurotrophin receptor ($p75^{NTR}$) [14]. NGF binds to TrkA, BDNF and NT-3 to TrkB and NT-4 to TrkC. Nevertheless, there is some crossreactivity, e.g., NT-3 is able to bind to TrkA and TrkB. The classic view is that through binding to their Trk receptors, neurotrophins primarily mediate their neurotrophic functions like promoting axonal and dendritic growth, synapse formation, neuroprotection, and maintenance [15]. After receptor binding, the receptor dimerizes and autophosphorylates the cytoplasmatic kinase domain. Briefly, this results in an activation of Ras, which then triggers PI3K, p38MAPK, and c-Raf/ERK pathways [15].

The $p75^{NTR}$ receptor, which belongs to the tumor necrosis factor superfamily, was the first receptor identified for NGF. All neurotrophins can bind to $p75^{NTR}$ with similar affinity [16–18].

## 2.4 Signaling Mechanisms During Programmed Cell Death of the Mouse Retina

In the retina of birds, programmed cell death of progenitors is under control of NGF released from microglia: NGF acts on those neuronal progenitors that express $p75^{NTR}$, but not TrkA [17]. $P75^{NTR}$ is a proapoptotic receptor in the absence of TrkA, and NGF induces programmed cell death in this context [17, 19]. The relevance

of this mechanism for development of the mammalian retina is unclear. There is a significant decrease in programmed cell death of neuronal progenitors during early embryonic development of $p75^{NTR}$-deficient retinae [20, 21]. Still, this appears to be a transitory event which does not result in obvious changes in retinal morphology of $p75^{NTR}$-deficient mice past E15 [21].

In addition, TGF-β signaling appears to modulate programmed cell death of neuronal progenitors in the avian retina as the application of antibodies that neutralize signaling of all three avian TGF-β isoforms (TGF-β1, -β2, -β3) reduces programmed cell death of neuronal progenitors in treated embryos, effects that appear to be independent from the action of NGF and its binding to $p75^{NTR}$ [22]. Again, the relevance of these findings in birds for the development of the mammalian retina is unclear. Embryos of double TGF-β2/TGF-β3-deficient mice show a reduction of neuronal progenitors undergoing programmed cell death at E 14.5 [23], but die around E 15.5, a time when programmed cell death of retinal progenitors has reached its peak and well before the time when death of differentiated retinal neurons begins [7, 24].

## References

1. Farah MH (2004, April 30) Cumulative labeling of embryonic mouse neural retina with bromodeoxyuridine supplied by an osmotic minipump. J Neurosci Methods 134(2):169–78
2. Buss RR, Sun W, Oppenheim RW (2006) Adaptive roles of programmed cell death during nervous system development. Annu Rev Neurosci 29:1–35
3. Yeo W, Gautier J (2004, Oct 15) Early neural cell death: dying to become neurons. Dev Biol 274(2):233–244
4. Henderson CE (1996, Oct) Programmed cell death in the developing nervous system. Neuron. 17(4):579–585
5. Yuen EC, Howe CL, Li Y, Holtzman DM, Mobley WC (1996, Oct) Nerve growth factor and the neurotrophic factor hypothesis. Brain Dev 18(5):362–368
6. Ichim G, Tauszig-Delamasure S, Mehlen P (2012, July 1) Neurotrophins and cell death. Exp Cell Res 318(11):1221–1228
7. Young RW (1984, Nov 1) Cell death during differentiation of the retina in the mouse. J Comp Neurol 229(3):362–373
8. Cepko CL, Austin CP, Yang X, Alexiades M, Ezzeddine D (1996, Jan) Cell fate determination in the vertebrate retina. Proc Natl Acad Sci U.S.A. 93(2):589–595
9. Chakrabarti S, Sima AAF, Lee J, Brachet P, Dicou E (1990, July) Nerve growth factor (NGF), proNGF and NGF receptor-like immunoreactivity in BB rat retina. Brain Res 523(1):11–15
10. Seitz R, Hackl S, Seibuchner T, Tamm ER, Ohlmann A (2010, April 28) Norrin mediates neuroprotective effects on retinal ganglion cells via activation of the Wnt/beta-catenin signaling pathway and the induction of neuroprotective growth factors in Muller cells. J Neurosci 30(17):5998–6010
11. Bennett JL, Zeiler SR, Jones KR (1999, Nov) Patterned expression of BDNF and NT-3 in the retina and anterior segment of the developing mammalian eye. Invest Ophthalmol Vis Sci 40(12):2996–3005
12. Braunger BM, Ohlmann A, Koch M, Tanimoto N, Volz C, Yang Y et al. (2013) Constitutive overexpression of Norrin activates Wnt/β-catenin and endothelin-2 signaling to protect photoreceptors from light damage. Neurobiol Dis Februar 50:1–12

13. Bennett JL, Zeiler SR, Jones KR (1999, Nov) Patterned expression of BDNF and NT-3 in the retina and anterior segment of the developing mammalian eye. Invest Ophthalmol Vis Sci 40(12):2996–3005
14. Arévalo JC, Wu SH (2006, July) Neurotrophin signaling: many exciting surprises! Cell Mol Life Sci 63(13):1523–1537
15. Parada LF, Tsoulfas P, Tessarollo L, Blair J, Reid SW, Soppet D (1992) The Trk family of tyrosine kinases: receptors for NGF-related neurotrophins. Cold Spring Harb Symp Quant Biol 57:43–51
16. Rodríguez-Tébar A, Dechant G, Barde YA (1991, March 29) Neurotrophins: structural relatedness and receptor interactions. Philos Trans R Soc Lond, B Biol Sci 331(1261):255–258
17. Frade JM, Barde YA (1998, Feb) Nerve growth factor: two receptors, multiple functions. Bioessays 20(2):137–145
18. Bronfman FC, Fainzilber M (2004, Sep) Multi-tasking by the p75 neurotrophin receptor: sortilin things out? EMBO Rep 5(9):867–871
19. Nykjaer A, Willnow TE, Petersen CM (2005, Feb) p75NTR–live or let die. Curr Opin Neurobiol 15(1):49–57
20. Frade JM, Barde YA (1999, Feb) Genetic evidence for cell death mediated by nerve growth factor and the neurotrophin receptor p75 in the developing mouse retina and spinal cord. Development 126(4):683–690
21. Harada C, Harada T, Nakamura K, Sakai Y, Tanaka K, Parada LF (2006, Feb 1) Effect of p75NTR on the regulation of naturally occurring cell death and retinal ganglion cell number in the mouse eye. Dev Biol 290(1):57–65
22. Dünker N, Schuster N, Krieglstein K (2001, June) TGF-beta modulates programmed cell death in the retina of the developing chick embryo. Development 128(11):1933–1942
23. Dünker N, Krieglstein K (2003, July) Reduced programmed cell death in the retina and defects in lens and cornea of Tgfbeta2(-/-) Tgfbeta3(-/-) double-deficient mice. Cell Tissue Res 313(1):1–10
24. Farah MH, Easter SS Jr (2005, Aug 15) Cell birth and death in the mouse retinal ganglion cell layer. J Comp Neurol 489(1):120–134

# Chapter 3
# Spatial and Temporal Localization of Caveolin-1 Protein in the Developing Retina

**Xiaowu Gu, Alaina Reagan, Allen Yen, Faizah Bhatti, Alex W. Cohen and Michael H. Elliott**

**Abstract** Caveolin-1 (Cav-1), the signature protein of caveolae is expressed in several cell types in the adult retina and is linked to ocular pathologies including uveitis, diabetic retinopathy, and primary open angle glaucoma. Genetic ablation of Cav-1 causes retinal functional deficits due to disruptions in environmental homeostasis. To better understand Cav-1 function in the retina, we examined its expression/localization during postnatal retinal development. From P0–P5, Cav-1 was detected only in the developing superficial retinal vessels, in hyaloid and choroidal vasculature, and in the retinal pigment epithelium (RPE). At P7, staining began to be observed centrally in radial cells in the neuroretina, and this staining increased dramatically by P9/10 in identifiable Müller glia. Prominent vascular staining continued throughout development. These results support the idea that Cav-1 is an indicator of Müller glial differentiation and suggests that it plays an important role in Müller cell function.

M. H. Elliott (✉) · X. Gu · A. Reagan · A. Yen · F. Bhatti · A. W. Cohen
Department of Ophthalmology, University of Oklahoma Health Sciences Center, Oklahoma City, OK, USA
e-mail: Michael-Elliott@ouhsc.edu

X. Gu · A. Reagan · M. H. Elliott
Oklahoma Center for Neuroscience, University of Oklahoma Health Sciences Center, Oklahoma City, OK, USA

X. Gu · A. Reagan · A. Yen · A. W. Cohen · M. H. Elliott
Dean McGee Eye Institute, 608 Stanton L. Young Blvd., DMEI B423, Oklahoma City, OK 73104, USA

F. Bhatti
Department of Pediatrics, University of Oklahoma Health Sciences Center, Oklahoma City, OK, USA

M. H. Elliott
Department of Physiology, University of Oklahoma Health Sciences Center, Oklahoma City, OK, USA

J. D. Ash et al. (eds.), *Retinal Degenerative Diseases,* Advances in Experimental Medicine and Biology 801, DOI 10.1007/978-1-4614-3209-8_3,

**Keywords** Caveolin-1 · Retina · Müller glia · Vasculature · Development · Differentiation

**Abbreviations**

| | |
|---|---|
| Cav-1 | Caveolin-1 |
| RPE | Retinal pigment epithelium |
| GS | Glutamine synthetase |
| SV2 | Synaptic vesicle glycoprotein 2 |
| ONH | Optic nerve head |
| CD31 | Cluster of differentiation 31 |

## 3.1 Introduction

Caveolin-1 (Cav-1) is the primary structural protein of specialized, 50–100 nm flask-shaped caveolae membrane domains [1]. Cav-1 is intrinsically involved in multiple caveolar functions including lipid trafficking, endocytosis, mechanotransduction, and cell signaling [1, 2]. Our understanding of Cav-1 and caveolae function in the eye is limited. Changes in Cav-1 expression are associated with blood-retinal barrier breakdown in experimental diabetic retinopathy [3] and with chronic inflammation in posterior uveitis [4]. Polymorphisms in the *CAV1* gene are also linked to primary open angle glaucoma [5]. We recently reported that loss of Cav-1 compromises retinal environmental homeostasis leading to retinal functional deficits [6]. In adult retinas, Cav-1 protein is expressed in several cell types including RPE, Müller glia, photoreceptors, and vascular cells [6–8]. At the transcript level, Cav-1 is dramatically enriched in Müller glia compared to retinal neurons [9] and our immunohistochemical staining confirms this prominent expression in Müller glia in adult retinas [6]. Intriguingly, Cav-1 mRNA expression in FACS-purified Müller cells increases in a temporal pattern matching that of markers of Müller glial differentiation [10], but whether other cell types express Cav-1 during retinal development is not known.

The purpose of the present study was to determine the localization of Cav-1 protein during postnatal retinal development. The temporal and spatial expression indicated that differentiating and adult Müller glia and retinal vasculature are the major cell types expressing Cav-1. These results support the idea that Cav-1 is an indicator of Müller glial maturation and suggest that it plays an important role in the function of differentiated Müller glia.

## 3.2 Methods

*Mice* C57BL/6J (The Jackson Laboratory, Bar Harbor, ME) mice were used for these studies. All procedures were carried out according to the Association for Research in Vision and Ophthalmology Statement for the Use of Animals in

Ophthalmic and Vision Research and were approved by Institutional Animal Care and Use Committees of the University of Oklahoma Health Sciences Center and Dean McGee Eye Institute.

*Immunohistochemistry and Confocal Microscopy* Mice were euthanized at the indicated postnatal ages, eyes were fixed in Prefer fixative (Anatech, Ltd., Battlefield, MI), embedded in paraffin, and 5-μm sections were cut. Immunohistochemistry was performed as previously described [6] with the following antibodies: rabbit anti-Cav-1 (1:100, BD Biosciences, San Jose, CA); rat anti-CD31 (1:300, Dianova GmbH, Hamburg, Germany); and mouse antibodies against glutamine synthetase (GS; 1:500, clone GS-6) and rhodopsin (1:500, clone 4D2) from Millipore (Billerica, MA), and synaptic vesicle glycoprotein 2 (SV2, 1:500, clone 10H3, gift from Erik Floor, University of Kansas). Immunoreactivity was detected with Alexa Fluor-labeled secondaries (Life Technologies, Grand Island, NY) and nuclei were stained with DAPI or propidium iodide. Pseudocolors were assigned to images as follows: Cav-1 (green), other proteins (red), nuclei (blue).

## 3.3 Results

### *3.3.1 Cav-1 is Expressed by the Vasculature During Retinal Development*

Mouse retinal vasculature develops postnatally with the superficial vascular plexus forming from the optic nerve head (ONH) and progressing to the retinal periphery by P8. From P7, superficial capillaries sprout perpendicularly toward the outer retina to form deep and intermediate capillary plexuses in the outer and inner plexiform layers which are interconnected by P21. At early postnatal days, Cav-1 is predominantly colocalized with the endothelial marker, CD31, in superficial retinal vessels (*vertical red arrows* in Fig. 3.1 highlight representative vessels) and choroidal vasculature. It is also detected in vesicular structures at the apical RPE. At P7, weak, nonvascular radial staining in the neuroretina begins to be observed (*horizontal green arrow* in P7 panels). Cav-1 immunoreactivity remains prominent in retinal vessels throughout development but is less apparent as Cav-1 expression in presumptive Müller glia increases between P7 and P21.

### *3.3.2 Cav-1 Expression Increases Dramatically in Neuroretina as Müller glia Mature*

As shown in Fig. 3.1, nonvascular Cav-1 staining in the neuroretina was first detected in radial cells at P7. This staining was initially most pronounced near the ONH and decreased toward the retinal periphery (not shown), but eventually a radial expression pattern with Müller glial morphology was apparent panretinally. The morphology of Cav-1-localized cells and the temporal expression,

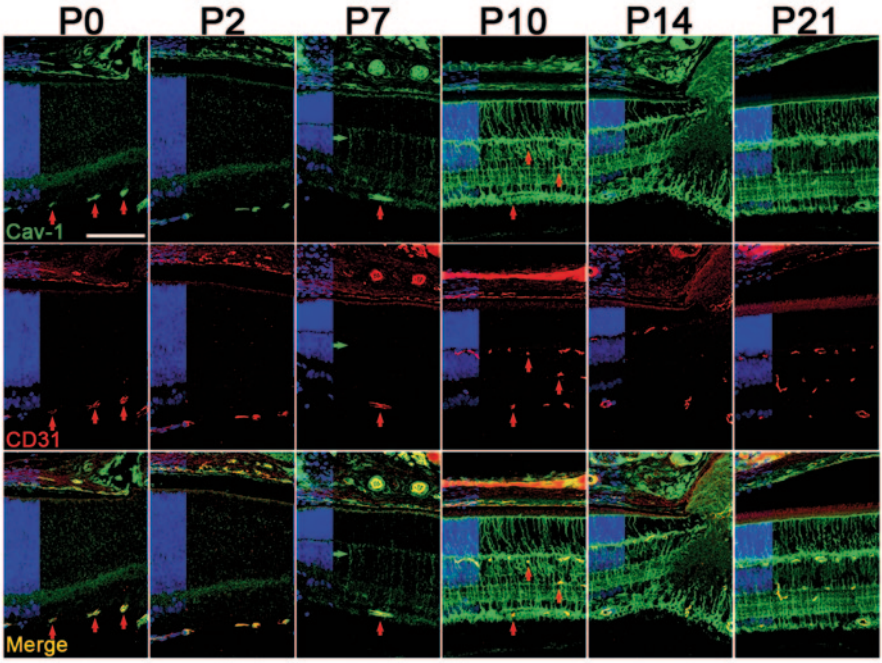


**Fig. 3.1** Caveolin-1 (*Cav-1*) is expressed in developing vessels and increases in the neuroretina from P7–P10. *Cav-1* (*green*) colocalizes with the endothelial marker, cluster of differentiation 31 (*CD31, red*) in vessels throughout postnatal retinal development. *Red vertical arrows* highlight several vessels at various developmental stages. The *green horizontal arrow* at P7 indicates a *CD31*-negative radial cell. Nuclear layers are indicated in *blue* on the *left* of each panel. (Scale bar = 100 μm)

coinciding with the timing of Müller glial differentiation [11], suggested that these nonvascular Cav-1-positive cells were Müller cells. To confirm this, we co-labeled with the Müller glial marker, GS (Fig. 3.2). Prior to P9, no specific GS immunoreactivity was detected in retinal sections. The staining observed in the inner retina at early time points was indistinguishable from sections incubated without primary antibodies (not shown) suggesting that this represents secondary antibody reaction with endogenous murine immunoglobulins. Specific GS-positive immunoreactivity could be localized to Müller cell bodies in the inner nuclear layer by P9 when Cav-1 staining was clearly detected in Müller glia. At P12, characteristic GS immunoreactivity could be observed in the same cells that express Cav-1. Perfect colocalization is not achieved as GS is a cytosolic enzyme and Cav-1 is an integral protein but it is clear from Fig. 3.2 that Cav-1 and GS are both present in the same cells. In addition to GS, we also labeled sections with rod photoreceptor and synaptic markers, rhodopsin and SV2, respectively. As shown in Fig. 3.3, these markers did not display the same localization or temporal expression as Cav-1.

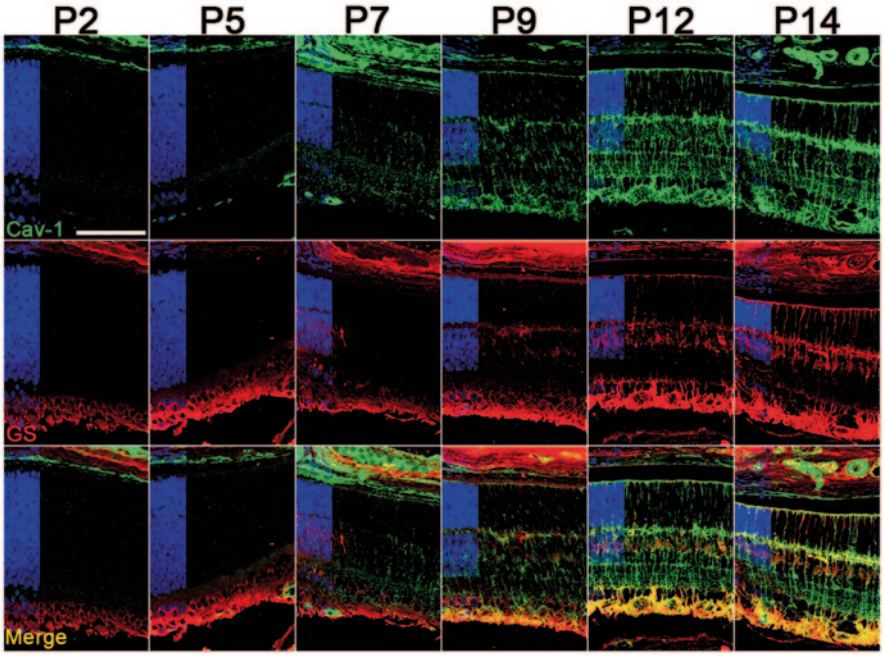


**Fig. 3.2** Caveolin-1 (*Cav-1*)-positive radial cells (*green*) detected after P7 are also positive for glutamine synthetase (*GS, red*), a marker of mature Müller glia. Nuclear layers are indicated in *blue*. (Scale bar = 100 μm)

## 3.4 Discussion

Based on the timing and localization of immunoreactivity and the morphology of immunopositive cells, we conclude that Müller glia and vascular endothelium are the principal cell types that express Cav-1 in the retina. The pronounced immunoreactivity in the developing retinal vasculature is consistent with the well-established abundant expression of Cav-1 and numerous caveolae detected in vascular endothelium in other tissues [1, 2]. The expression in the developing retinal vasculature is not surprising given that caveolae in retinal vascular endothelium have been suggested as sites of vascular endothelial growth factor (VEGF) signaling [8].

Less is understood about Cav-1 function in cells derived from neuroretinal progenitors. Our results agree with those of Roesch et al. [9], who identified Cav-1 as a Müller-cell-enriched transcript in individual adult Müller cells and with our previous immunolocalization of Cav-1 in adult retinas [6]. The temporal increase in Cav-1 in maturing Müller glia agrees precisely with the timing of expression of Cav-1 mRNA in fluorescence-activated cell sorting (FACS)-isolated Müller cells [10]. Importantly, Cav-1 expression increases dramatically between P7 and P10 at the time when Müller cells increase expression of markers of functional maturation, e.g., Kir4.1, aquaporin-4 [10], and GS (this study). Collectively, these results

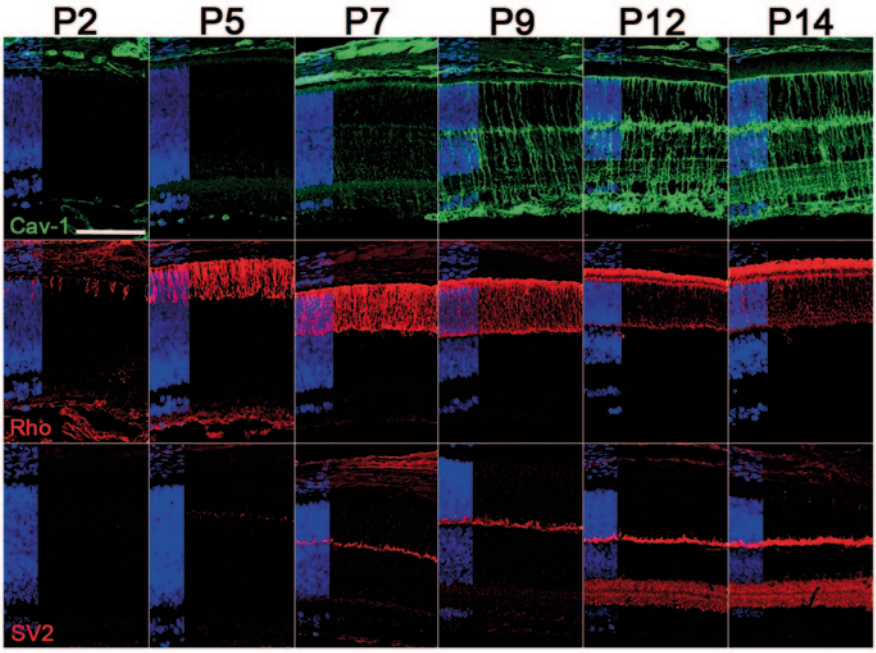


**Fig. 3.3** Caveolin-1 (*Cav-1*) immunoreactivity (*green*) does not spatially or temporally associate with rod photoreceptors or synaptic development. Middle panels are labeled for rhodopsin (*red*) and lower panels for the synaptic vesicle protein (*SV2, red*). Nuclear layers are indicated in *blue*. (Scale bar = 100 μm)

suggest that Cav-1 plays an important role in Müller cell function in the fully developed retina.

Müller glia span the entire retina, contact all retinal neurons, and form the outer and inner limiting membranes. They perform many functions including: regulation of ion homeostasis, neurotransmitter recycling, neuroprotection, retinal structure scaffolding, and possibly neuronal regeneration [12]. Given the myriad functions of Müller glia [12], we can presently only speculate on which of these might be Cav-1 associated. We have recently reported reduced electroretinogram (ERG) responses and changes in ion homeostasis in retinas from Cav-1 null mice [6]. We speculate that these deficits result from loss of Cav-1-dependent functions in Müller cells.

**Acknowledgments** This work was supported by NIH Grants EY019494, RR017703, and P30EY021725, and by Research to Prevent Blindness, Inc. (unrestricted grant and Sybil B. Harrington Special Scholar Award for Macular Degeneration).

## References

1. Parton RG, Simons K (2007) The multiple faces of caveolae. Nat Rev Mol Cell Biol 8:185–194
2. Cohen AW, Hnasko R, Schubert W, Lisanti MP (2004) Role of caveolae and caveolins in health and disease. Physiol Rev 84:1341–1379

3. Klaassen I, Hughes JM, Vogels IM, Schalkwijk CG, Van Noorden CJ, Schlingemann RO (2009) Altered expression of genes related to blood-retina barrier disruption in streptozotocin-induced diabetes. Exp Eye Res 89:4–15
4. Hauck SM, Dietter J, Kramer RL, Hofmaier F, Zipplies JK, Amann B et al (2010) Deciphering membrane-associated molecular processes in target tissue of autoimmune uveitis by label-free quantitative mass spectrometry. Mol Cell Proteomics 9:2292–2305
5. Thorleifsson G, Walters GB, Hewitt AW, Masson G, Helgason A, DeWan A et al (2010) Common variants near CAV1 and CAV2 are associated with primary open-angle glaucoma. Nat Genet 42:906–909
6. Li X, McClellan ME, Tanito M, Garteiser P, Towner R, Bissig D et al (2012) Loss of caveolin-1 impairs retinal function due to disturbance of subretinal microenvironment. J Biol Chem 287:16424–16434
7. Mora RC, Bonilha VL, Shin BC, Hu J, Cohen-Gould L, Bok D, Rodriguez-Boulan E (2006) Bipolar assembly of caveolae in retinal pigment epithelium. Am J Physiol Cell Physiol 290:C832–C843
8. Feng Y, Venema VJ, Venema RC, Tsai N, Behzadian MA, Caldwell RB (1999) VEGF-induced permeability increase is mediated by caveolae. Invest Ophthalmol Vis Sci 40:157–167
9. Roesch K, Jadhav AP, Trimarchi JM, Stadler MB, Roska B, Sun BB, Cepko CL (2008) The transcriptome of retinal Muller glial cells. J Comp Neurol 509:225–238
10. Nelson BR, Ueki Y, Reardon S, Karl MO, Georgi S, Hartman BH, Lamba DA, Reh TA (2011) Genome-wide analysis of Muller glial differentiation reveals a requirement for Notch signaling in postmitotic cells to maintain the glial fate. PLoS One 6:e22817
11. Jadhav AP, Roesch K, Cepko CL (2009) Development and neurogenic potential of Muller glial cells in the vertebrate retina. Prog Retin Eye Res 28:249–262
12. Bringmann A, Pannicke T, Grosche J, Francke M, Wiedemann P, Skatchkov SN, Osborne NN, Reichenbach A (2006) Muller cells in the healthy and diseased retina. Prog Retin Eye Res 25:397–424

# Chapter 4
# Glutathione S-Transferase Pi Isoform (GSTP1) Expression in Murine Retina Increases with Developmental Maturity

**Wen-Hsiang Lee, Pratibha Joshi and Rong Wen**

**Abstract**

Background and Aims

Glutathione S-transferase pi isoform (GSTP1) is an intracellular detoxification enzyme that catalyzes reduction of chemically reactive electrophiles and is a zeaxanthin-binding protein in the human macula. We have previously demonstrated that GSTP1 levels are decreased in human age-related macular degeneration (AMD) retina compared to normal controls (Joshi et al., Invest Ophthalmol Vis Sci, e-abstract, 2009). We also showed that GSTP1 levels parallel survival of human retinal pigment epithelial (RPE) cells exposed to ultraviolet (UV) light, and GSTP1 overexpression protects them against UV light damage (Joshi et al., Invest Ophthalmol Vis Sci, e-abstract, 2010). In the present work, we determined the developmental time course of GSTP1 expression in murine retina and in response to light challenge.

Methods

Eyes from BALB/c mice at postnatal day 20, 1 month, and 2 months of age were prepared for retinal protein extraction and cryo sectioning, and GSTP1 levels in the retina were analyzed by Western blot and immunohistochemistry (IHC). Another group of BALB/c mice with the same age ranges was exposed to 1000 lx of white fluorescent light for 24 h, and their retinas were analyzed for GSTP1 expression by Western blot and IHC in a similar manner.

W.-H. Lee (✉) · P. Joshi · R. Wen
Department of Ophthalmology, Bascom Palmer Eye Institute,
University of Miami Miller School of Medicine, Miami, FL, USA
e-mail: LWEN@med.miami.edu

P. Joshi
e-mail: pjoshi@med.miami.edu

R. Wen
e-mail: rwen@med.miami.edu

J. D. Ash et al. (eds.), *Retinal Degenerative Diseases,* Advances in Experimental Medicine and Biology 801, DOI 10.1007/978-1-4614-3209-8_4,

Results

GSTP1 levels in the murine retina increased in ascending order from postnatal day 20, 1 month, and 2 months of age. Moreover, GSTP1 expression in murine retina at postnatal day 20, 1 month, and 2 months of age increased in response to brief light exposure compared to age-matched controls under normal condition.

Conclusions

GSTP1 expression in retina increases with developmental age in mice and accompanies murine retinal maturation. Brief exposure to light induces GSTP1 expression in the murine retina across various developmental ages. GSTP1 induction may be a protective response to light-induced oxidative damage in the murine retina.

**Keywords** Glutathione S-transferase pi (GSTP1) · Retinal pigment epithelieum (RPE) · Light toxicity · Oxidative stress · Retinal development · Retinal degeneration · Age-related macular degeneration (AMD)

## 4.1 Introduction

### *4.1.1 GSTP1 and Oxidative Stress*

Glutathione S-transferases (GSTs) are a family of intracellular detoxification enzymes that catalyze the reduction of electrophiles by conjugating them to glutathione. The human GSTs are classified into at least four families: alpha, mu, pi, and theta [3]. Different isomers exist for each of the four classes of GSTs, but only one isoform of the pi-class GST (GSTP1) is known to be expressed in human tissues. GSTP1 has been identified as a zeaxanthin-binding protein and found to be localized in the retina [4]. GSTP1 has been shown to play a role in oxidative damage in cancer [5–9]. GSTP1 also has been shown to protect against endothelial dysfunction induced by exposure to tobacco smoke in mice [10]. Overall, it is speculated that GSTP1 is induced in order to scavenge toxic electrophiles, including reactive oxygen species. Thus, if GSTP1 expression is down-regulated, the cells become susceptible to oxidative damage leading to diseased states, such as age-related chronic degenerative disorders.

### *4.1.2 GSTP1 and Maturation*

Not much is known about the association between GSTP1 and developmental maturation and aging. GSTP1 and GSTA3 proteins have been shown to increase in rat cochlea during early development [11]. GSTP1 and GSTA4 expression increased with age in rat cerebral cortex [12]. Intracellular translocation of GST-pi, a marker for mature oligodendrocytes in adult mammalian brain, from the nucleus to the cytosol occurs during oligodendrocyte differentiation in adult rat cerebral cortex [13].

### *4.1.3 Light Toxicity*

High-energy photons can create free radicals which are damaging to DNA and cellular organelles such as mitochondria. It has been suggested that ultraviolet (UV) radiation may cause retinal damage and may contribute to the development of age-related macular degeneration (AMD) [14]. Phototoxic damage also has been demonstrated in cultured human retinal pigment epithelial (RPE) cells [15, 16]. Animal studies have shown that excessive exposure to visible or UV light induced retinal damages to photoreceptors and RPE [17–19].

The retina is particularly susceptible to oxidative stress because of its high consumption of oxygen, high proportion of polyunsaturated fatty acids (PUFAs), and exposure to visible light [20, 21]. GSTP1's localization in the macula as a zeaxanthin-binding protein suggests that GSTP1 plays an important role in modulating the levels of antioxidants in the macula. We have previously demonstrated that GSTP1 levels are decreased in human AMD retina compared to normal controls. We also showed that GSTP1 levels parallel survival of human RPE cells exposed to UV light, and GSTP1 over-expression protects them against UV light damage. In the present work, we determined the developmental time course of GSTP1 expression in murine retina and in response to light challenge.

## 4.2 Materials and Methods

### *4.2.1 Experiment with Animals*

All animal experiments were in accordance with the guidelines of the Declaration of Helsinki and the Association for Research in Vision and Ophthalmology, as approved by the University of Miami Institutional Animal Care and Use Committee.

### *4.2.2 Light Exposure*

BALB/c mice at postnatal day 20 (P20), 1 month (1mo), and 2 months (2mo) of age were exposed to 1,000 lx of white fluorescent light for 24 h. The age-matched control group of BALB/c mice was kept under normal condition. The eyes were enucleated and prepared for retinal protein extraction and for cryo sectioning.

### *4.2.3 Immunohistochemistry*

The enucleated mouse eyes were embedded whole in O.C.T. (Tissue Tek), frozen at −80 °C, cryo-sectioned, and stored at −20 °C. Retinal sections were fixed with 4% paraformaldehyde and processed using standard protocol for IHC by probing with polyclonal antibodies (Abcam, Inc.) against murine GST3/GST pi protein (murine

homolog of GSTP1), followed by secondary antibodies coupled to Alexa 488 (Invitrogen) showing green fluorescence. DAPI was used to stain nuclei (blue). The immunostaining was detected using a confocal Leica TSP microscope.

### *4.2.4 Western Blot Analysis*

Protein extracts from mouse retinas were subject to Western blot analysis. The proteins were separated on 4–20% SDS-PAGE (Invitrogen), transferred onto a polyvinylidene fluoride (PVDF) membrane, blocked with 5% BSA in 0.2% TBST, and subsequently probed with polyclonal antibodies against murine GST3/GST pi protein (Abcam, Inc.), followed by secondary antibodies (Santa Cruz Biotechnology, Inc). For control, the membrane was also probed with polyclonal antibodies against murine GAPDH protein (Cell Signalling, Inc.), followed by secondary antibodies (Invitrogen). The Western blots were developed by electrochemiluminescence (ECL) (Pierce Biotechnology) and exposed to films.

## 4.3 Results

### *4.3.1 GSTP1 Expression in Retina Accompanied Murine Retinal Maturation*

To determine the murine retinal GSTP1 expression at baseline in the early developmental spectrum, the retinas from BALB/c mice at P20, 1mo, and 2mo of age kept under normal light-dark cycle condition were assessed by IHC analysis. GSTP1 was detected in all layers of murine retina as early as P20, and the intensity of GSTP1 expression increased correspondingly with retinal maturation as the age increased from P20 to 1mo to 2mo of age (Fig. 4.1a, (−) Light). GSTP1 levels in retina from mice at P20, 1mo, and 2mo of age also increased in response to light exposure when compared to baseline (Fig. 4.1b, (+) Light). The increase in GSTP1 expression was observed in all retinal layers and slightly more so in the RPE layer.

### *4.3.2 GSTP1 Levels in Murine Retina Increased with Developmental Age and with Light Exposure*

Retinal GSTP1 levels from BALB/c mice at P20, 1mo, and 2mo of age kept under normal light-dark cycle condition (Fig. 4.2a, b, (−) Light) were compared to those exposed to light for 24 h (Fig. 4.2c, d, (+) Light) by Western blot analysis, and the relative GSTP1 levels were quantified by optical density using the Image J software. GSTP1 levels in murine retina increased with developmental age from P20 to

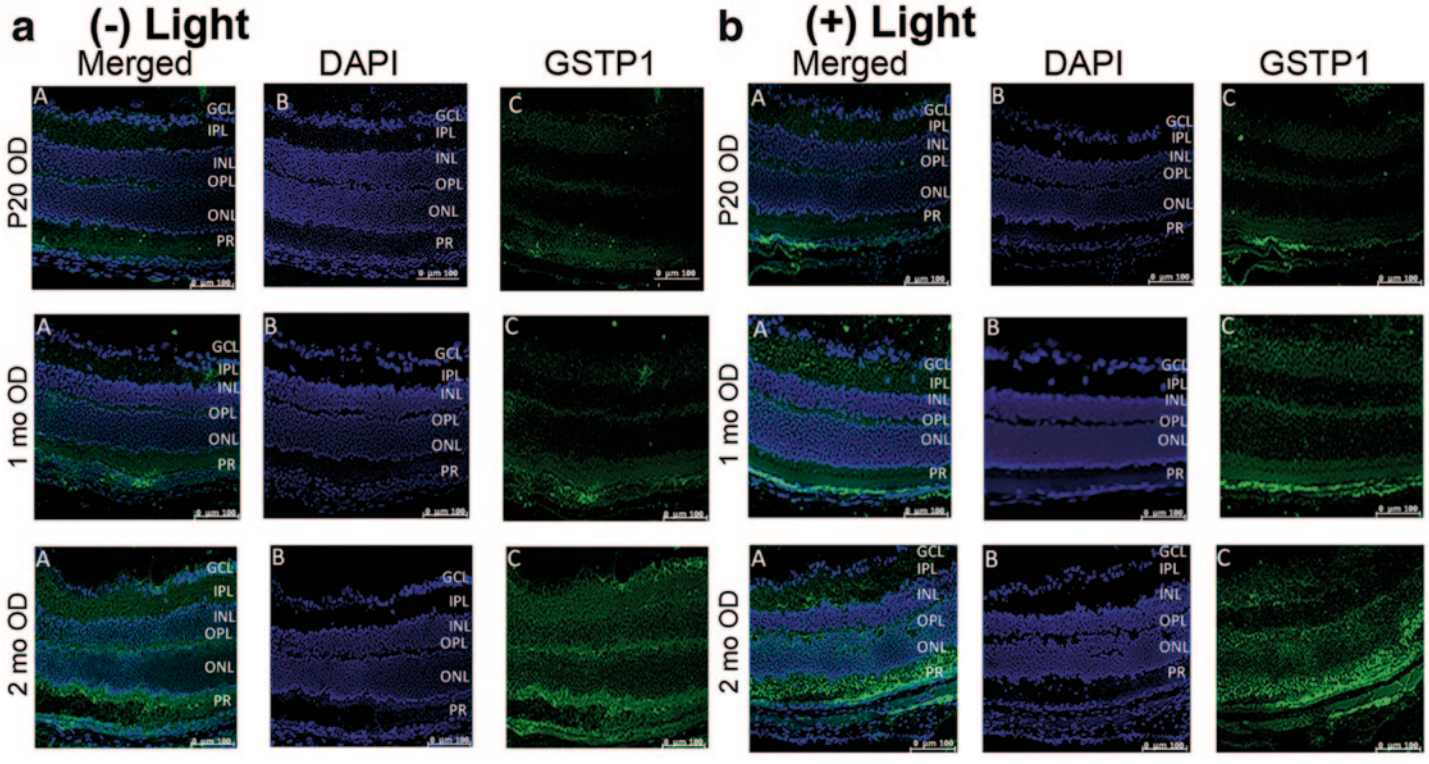


**Fig. 4.1** GSTP1 in murine retina increased with retinal maturation and with light exposure by IHC. Representative images of IHC analysis of GSTP1 in the retina from BALB/c mice at postnatal day 20 (*P20*), 1 month (*1mo*), and 2 months (*2mo*) of age kept under normal light-dark cycle condition (**a** (−) Light), compared to those exposed to light for 24 h (**b** (+) Light). Merged image (*Panel A*) and separate images showed GSTP1 staining as green fluorescence (*Panel C*) and DAPI staining the nuclei blue (*Panel B*). *OD* right eye

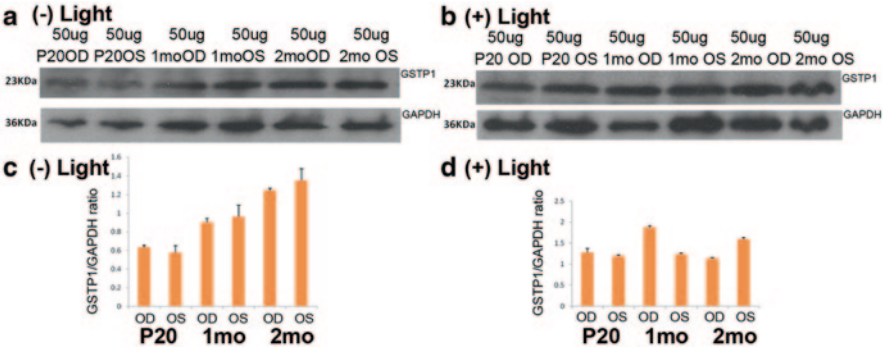


**Fig. 4.2** GSTP1 in murine retina increased with developmental age and with light exposure by Western blot analysis. Retinal GSTP1 levels from BALB/c mice at postnatal day 20 (*P20*), 1 month (*1mo*), and 2 months (*2mo*) of age kept under normal light-dark cycle condition (**a, b** (−) *Light*) were compared to those exposed to light for 24 h (**c, d** (+) *Light*). The optical density of each band was measured using the Image J software, and relative GSTP1 levels were quantified (**b, d**). *OD* right eye, *OS* left eye

1mo to 2mo. In addition, at each of these developmental stages, the retinal GSTP1 levels also were induced by exposure to light, some by nearly two folds.

## 4.4 Discussion

GSTP1 is an intracellular detoxification enzyme that catalyzes reduction of chemically reactive electrophiles and is a zeaxanthin-binding protein in the human macula. We have previously demonstrated that GSTP1 levels are decreased in human AMD retina compared to normal controls. We also showed that GSTP1 levels parallel survival of human RPE cells exposed to UV light, and GSTP1 over-expression protects them against UV light damage. In the present work, we determined the developmental time course of GSTP1 expression in murine retina and in response to light challenge.

In this study, we used BALB/c mice at ages P20, 1mo, and 2mo that represent roughly from infancy to sexual maturation in the early spectrum of development. We found that GSTP1 expression was present in murine retina as early as age P20. Our data demonstrated that GSTP1 expression in retina increased with developmental age in mice and accompanied murine retinal maturation. This suggests that GSTP1 is expressed in retina as early as P20 in murine development and increases in expression levels with retinal maturation as the mouse reaches sexual maturity. This also suggests that GSTP1 may play a role in normal development in the murine retina. We also showed that brief exposure to light induced GSTP1 expression in the murine retina across various developmental ages from P20 to 2mo. This suggests that GSTP1 induction may be a protective response to light-induced oxidative damage in the murine retina in normal development. It is tantalizing to speculate that

disturbance in GSTP1 expression at baseline or failure to induce GSTP1 in response to oxidative stress may render the retina susceptible to damages leading to retinal degenerative disorders.

**Acknowledgments** We thank Gabriel Gaidosh for his assistance with confocal imaging. This work was supported in part by funds from NIH grant K08EY20864, Hope for Vision, SanBio, Inc., R01EY018586, NIH Center Core Grant P30EY14801, Research to Prevent Blindness Unrestricted Grant, and Department of Defense (DOD- Grant #W81XWH-09-1-0675).

## References

1. Joshi PM, Franko M, Dubovy S, Bhattacharya SK, Lee W-H (2009) Decreased expression of GSTP1 in the macula leads to AMD pathogenesis. Invest Ophthalmol Vis Sci. 2009:ARVO E-Abstract 2346
2. Joshi PM, Dubovy S, Bhattacharya SK, Lee W-H (2010) Glutathione S-Transferase Pi isoform (GSTP1) expression plays a role in the health of retinal pigment epithelium (RPE). Invest Ophthalmol Vis Sci. ARVO eAbstract 51:4105
3. Mannervik B, Awasthi YC, Board PG, Hayes JD, Di Ilio C, Ketterer B, Listowsky I, Morgenstern R, Muramatsu M, Pearson WR, Pickett CB, Sato K, Widersten M, Wolf CR (2007) Nomenclature for human glutathione transferases. Biochem J 282(Pt 1):305–306
4. Bhosale P, Larson AJ, Frederick JM, Southwick K, Thulin CD, Bernstein PS (2004) Identification and characterization of a Pi isoform of glutathione S-transferase (GSTP1) as a zeaxanthin-binding protein in the macula of the human eye. J Biol Chem 279(47):49447–49454
5. Ritchie KJ, Henderson CJ, Wang XJ, Vassieva O, Carrie D, Farmer PB, Gaskell M, Park K, Wolf CR (2007) Glutathione transferase pi plays a critical role in the development of lung carcinogenesis following exposure to tobacco-related carcinogens and urethane. Cancer Res 67(19):9248–9257
6. Huang J, Tan PH, Tan BK, Bay BH (2004) GST-pi expression correlates with oxidative stress and apoptosis in breast cancer. Oncol Rep 12(4):921–925
7. Matsui A, Ikeda T, Enomoto K, Hosoda K, Nakashima H, Omae K, Watanabe M, Hibi T, Kitajima M (2000) Increased formation of oxidative DNA damage, 8-hydroxy-2′-deoxyguanosine, in human breast cancer tissue and its relationship to GSTP1 and COMT genotypes. Cancer Lett 151(1):87–95
8. Fryer AA, Ramsay HM, Lovatt TJ, Jones PW, Hawley CM, Nicol DL, Strange RC, Harden PN (2005) Polymorphisms in glutathione S-transferases and non-melanoma skin cancer risk in Australian renal transplant recipients. Carcinogenesis 26(1):185–191
9. Lee WH, Morton RA, Epstein JI, Brooks JD, Campbell PA, Bova GS, Hsieh WS, Isaacs WB, Nelson WG (1994) Cytidine methylation of regulatory sequences near the pi-class glutathione S-transferase gene accompanies human prostatic carcinogenesis. Proc Natl Acad Sci USA 91(24):11733–11737
10. Conklin DJ, Haberzettl P, Prough RA, Bhatnagar A (2009) Glutathione-S-transferase P protects against endothelial dysfunction induced by exposure to tobacco smoke. Am J Physiol Heart Circ Physiol 296:1586–1597
11. Whitlon DS, Wright LS, Nelson SA, Szakaly R, Siegel FL (1999) Maturation of cochlear glutathione-S-transferases correlates with the end of the sensitive period for ototoxicity. Hear Res 137:43–50
12. Martinez-Lara E, Siles E, Hernandez R, Canuelo AR, del Moral ML, Jimenez A, Blanco S, Lopez-Ramos JC, Esteban FJ, Pedrosa JA, Peinado MA (2003) Glutathione S-transferase isoenzymatic response to aging in rat cerebral cortex and cerebellum. Neurobiol Aging 24:501–509
13. Tamura Y, Kataoka Y, Cui Y, Takamori Y, Watanabe Y, Yamada H (2007) Intracellular translocation of glutathione S-transferase pi during oligodendrocyte differentiation in adult rat cerebral cortex in vivo. Neuroscience 148:535–540

14. Braustein RE, Sparrow JR (2005) A blue-blocking intraocular lens should be used in cataract surgery. Arch Ophthalmol 123:547–549
15. Gao X, Talalay P (2004) Induction of phase 2 genes by sulforaphane protects retinal pigment epithelial cells against photooxidative damage. Proc Natl Acad Sci USA 101(28):10446–10451
16. Youn H-Y, Chou BR, Cullen AP, Sivak JG (2009) Effects of 400 nm, 420 nm, and 435.8 nm radiations on cultured human retinal pigment epithelial cells. J Photochem Photobiol B 95: 64–70
17. Organisciak DT, Darrow RM, Barsalou L, Kutty RK, Wiggert B (2003) Susceptibility to retinal light damage in transgenic rats with rhodopsin mutations. Invest Ophthalmol Vis Sci 44(2):486–492
18. Grimm C, Wenzel A, Hafezi F, Yu S, Redmond TM, Remé CE (2000) Protection of Rpe65-deficient mice identifies rhodopsin as a mediator of light-induced retinal degeneration. Nat Genet 25(1):63–66
19. Rattner A, Toulabi L, Williams J, Yu H, Nathans J (2008) The genomic response of the retinal pigment epithelium to light damage and retinal detachment. J Neurosci 28(39):9880–9889.
20. Bazan NG (1989) The metabolism of omega-3 polyunsaturated fatty acids in the eye: the possible role of docosahexaenoic acid and docosanoids in retinal physiology and ocular pathology. Prog Clin Biol Res 312:95–112
21. Dargel R (1992) Lipid peroxidation–a common pathogenetic mechanism? Exp Toxicol Pathol 44(4):169–181

# Chapter 5
# RETINA-Specific Expression of *Kcnv2* Is Controlled by Cone-Rod Homeobox (Crx) and Neural Retina Leucine Zipper (Nrl)

**Alexander Aslanidis, Marcus Karlstetter, Yana Walczak, Herbert Jägle and Thomas Langmann**

**Abstract** Cone dystrophy with supernormal rod response (CDSRR) is an autosomal recessive disorder that leads to progressive retinal degeneration with a distinct electroretinogram (ERG) phenotype. CDSRR patients show reduced sensitivity to dim light, augmented response to suprathreshold light and reduced response to flicker. The disorder is caused by mutations in the *KCNV2* gene, which encodes the Kv11.1 subunit of a voltage-gated potassium channel. Here, we studied the retina-specific expression and *cis*-regulatory activity of the murine *Kcnv2* gene using electroporation of explanted retinas. Using qRT-PCR profiling of early postnatal retinas, we showed that *Kcnv2* expression increased towards P14, which marks the beginning of visual activity in mice. In vivo electroporation of GFP-*Kcnv2* expressing plasmids revealed that Kv11.1 localizes to the inner segment membranes of adult P21 photoreceptors. Using bioinformatic prediction and chromatin immunoprecipitation (ChIP), we identified two Crx binding sites (CBS) and one Nrl binding site (NBS) in the *Kcnv2* promoter. Reporter electroporation of the wild type promoter region induced strong DsRed expression, indicating high regulatory activity, whereas shRNA-mediated knockdown of Crx and Nrl resulted in reduced *Kcnv2* promoter activity and low endogenous *Kcnv2* mRNA expression in the retina. Site-directed mutagenesis of the CBS and NBS demonstrated that CBS2 is crucial for *Kcnv2* promoter activity. We conclude that nucleotide changes in evolutionary conserved CBS could impact retina-specific expression levels of *Kcnv2*.

**Keywords** Photoreceptor · Genetics · Gene regulation · Gene expression · Transcription factor · *cis*-regulatory element · Cone dystrophy · Electroporation · ERG

T. Langmann (✉) · A. Aslanidis · M. Karlstetter · Y. Walczak
Department of Ophthalmology, University of Cologne, Joseph-Stelzmann-Str. 9, 50931 Cologne, Germany
e-mail: thomas.langmann@uk-koeln.de

H. Jägle
Department of Ophthalmology, University Hospital Regensburg, Regensburg, Germany

J. D. Ash et al. (eds.), *Retinal Degenerative Diseases,* Advances in Experimental Medicine and Biology 801, DOI 10.1007/978-1-4614-3209-8_5,

## 5.1 Introduction

Cone dystrophy with supernormal rod response (CDSRR) is an autosomal recessive retinal disorder with progressive loss of cone-mediated visual acuity, reduced color perception, elevated sensitivity to bright light and night blindness. Lipofuscin deposits and atrophy of photoreceptors and retinal pigment epithelium surrounding the macula are characteristic for this disease [1–3]. CDSRR patients show a distinct electroretinogram (ERG) phenotype with reduced sensitivity to dim light, augmented response to suprathreshold light and reduced response to flicker [4, 5].

CDSRR is caused by mutations in the *KCNV2* gene [5–7]. *KCNV2* encodes the Kv11.1 subunit of a voltage-gated potassium channel. These channel types regulate resting potentials and influence the shape, duration and frequency of action potentials [8]. Kv11.1 forms heterotetramers with the *KCNB1, KCNC1* and *KCNF1* gene products to build a functional potassium channel [9]. *KCNV2* is predominantly expressed in neuronal and pacemaker tissue like photoreceptors and the heart [10].

Photoreceptor-specific gene expression is regulated by a hierarchical network of transcription factors, including cone-rod homeobox (Crx) and neural retina leucine zipper (Nrl) [11, 12]. Crx is expressed in the developing retina where it critically influences the transcription of photoreceptor genes [13]. CRX mutations lead to cone-rod dystrophy or Leber's congenital amaurosis and Crx knockout mice lack photoreceptor outer segments [14–16]. Nrl is activated by Crx and acts as a decision factor in rod differentiation. Mice lacking Nrl show an elevated number of cone-like photoreceptors [17]. In mature photoreceptors, Nrl interacts synergistically with Crx in order to drive expression of photoreceptor-specific genes [18]. ChIP-seq experiments revealed that Crx and Nrl coordinate the expression of several hundreds of photoreceptor genes including most known retinal disease genes [19, 20].

The aim of our work was to study the retina-specific expression of the murine *Kcnv2* gene using qRT-PCR, chromatin immunoprecipitation and electroporation of fluorescent reporters into living mouse retinas.

## 5.2 Materials and Methods

### *5.2.1 Mouse Husbandry*

CD1 and C57BL/6 mice were purchased from Charles River Laboratories (Sulzfeld, Germany) and maintained on a 12-h light/dark schedule at 22 °C with free access to water and food. The health of the animals was regularly monitored, and all procedures were approved by the University of Regensburg animal rights committee.

### 5.2.2 DNA Constructs

Mouse retinal cDNA was used to amplify the full-length 1,691 bp *Kcnv2* open reading frame. The pCAG-GFP, pRho-2.2K-DsRed, Crx/Nrl shRNA and No-basal DsRed vectors have been described previously [21]. A scrambled shRNA expressing plasmid was electroporated as a control for Crx/Nrl knockdown experiments. To create the CAG-GFP-*Kcnv2*CDS construct, a 2,386-bp GFP-*Kcnv2*CDS fusion was cloned into a CAG vector. To create the *Kcnv2* reporter construct, a 479-bp region containing the mouse *Kcnv2* promoter was amplified. This fragment was cloned upstream of DsRed in the No-basal reporter vector. Site-directed mutagenesis was performed using the QuikChange Multi Site-Directed Mutagenesis Kit (Stratagene, La Jolla, CA, USA).

### 5.2.3 RNA-Isolation, RT-PCR and qRT-PCR

Total RNA was isolated from different mouse tissues using the RNeasy Mini Kit (Qiagen, Hilden, Germany). Reverse transcription was performed using the RevertAid H Minus First Strand cDNA Synthesis kit (Fermentas, St. Leon-Rot, Germany). RT-PCR to amplify 531 bp of mouse *Kcnv2* was performed with 50-ng cDNA and intron-spanning primers using the Taq Core kit (Qiagen, Hilden, Germany) and standard PCR conditions. A 290-bp fragment of *Lrrc58* was amplified as reference. qRT-PCR was carried out with the TaqMan 7900HT PCR detection system (Invitrogen Life Technologies, San Diego, CA). For the detection of mouse *Kcnv2* transcripts, intron-spanning primers were used. *Atp5b* was amplified as a reference gene. The PCR reaction parameters were as follows: 40 s at 95 °C melting, 1 min at 60 °C annealing, and 2 min at 72 °C extension. Each run was performed for 40 cycles and each measurement was performed in triplicates. Results were analysed with the ABI RQ Manager software using the $\Delta\Delta C_T$ method for relative quantitation.

### 5.2.4 Bioinformatic Analysis

The UCSC Genome Browser was used to display the Crx and Nrl ChIP-seq and PolII ChIP-on-Chip tracks. Genomatix MatInspector (Genomatix Software GmbH, Munich, Germany) was used to identify potential transcription factor binding sites in the *Kcnv2* promoter. Weight matrices V$BCDF and V$AP1R were used to predict Crx and Nrl binding, respectively.

### 5.2.5 Chromatin Immunoprecipitation

ChIP assays were performed as described previously [22]. The immunoprecipitated DNA was analysed by PCR using specific primers for detection of *Kcnv2* CBS1, CBS2 and NBS.

### 5.2.6 *Electroporation of Mouse Retinas*

Electroporation of mouse retinas was performed as described previously [21]. Plasmids were electroporated at a final concentration of 0.5 μg/μl per construct for in vitro and 4 μg/μl for in vivo electroporation, respectively. DsRed fluorescence was quantified and normalized to GFP control fluorescence. At P21, in vivo electroporated animals were sacrificed, the eyes harvested, fixed and cryosectioned. After staining with 4,6-diamidino-2-phenylindol, cover slides were applied and fluorescence pictures were taken.

## 5.3 Results

### 5.3.1 Kcnv2 *is Highly Expressed in the Murine Retina*

To investigate the tissue-specific expression of the murine *Kcnv2* gene, total RNA of ten different mouse tissues was analysed using PCR. Semi-quantitative RT-PCR analysis showed that *Kcnv2* expression is mainly confined to the retina with weak transcript levels in the heart (Fig. 5.1a). Early postnatal temporal analysis of *Kcnv2* expression showed a continuous increase in *Kcnv2* mRNA levels towards P14, reaching a plateau at P21 (Fig. 5.1b).

### 5.3.2 Kcnv2 *Localizes to Inner Segment Membranes of Photoreceptors*

Next, we studied the subcellular localization of the Kv11.1 protein using in vivo electroporation of a GFP-*Kcnv2* fusion construct. Fluorescence microscopy analysis at P21 showed a prominent GFP signal in the inner segments and membrane regions of photoreceptors (Fig. 5.1c).

### 5.3.3 *Retinal* Kcnv2 *Expression Is Regulated by Crx and Nrl*

We next characterized the regulatory potential of the *Kcnv2* promoter. Using bioinformatic analysis and ChIP-seq data, we identified two Crx binding sites (CBS) and one Nrl binding site (NBS) in the proximal promoter region (Fig. 5.2a). All three binding sites show high-evolutionary conservation (Fig. 5.2b). Although both CBS represent Crx motifs, CBS2 exhibits a sequence (antisense 5′-TAATC-3′), which perfectly represents the most overrepresented canonical Crx binding motif, whereas CBS1 does not.

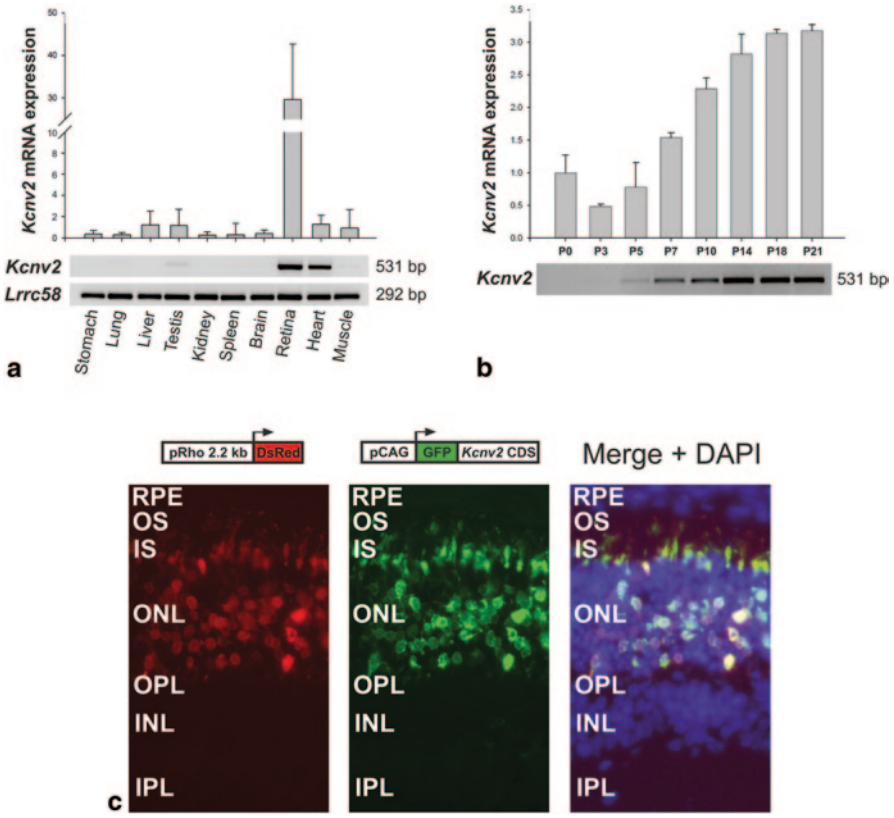


**Fig. 5.1** **a** RT-PCR and qRT-PCR analysis of mouse tissues reveals *Kcnv2* expression in the retina and in heart. **b** Early postnatal *Kcnv2* expression levels in the mouse retina. **c** Kv11.1 localization studies using in vivo electroporation and fluorescence microscopy at P21 revealed membrane-associated Kv11.1 localization in inner segments

To verify in vivo binding of Crx and Nrl to the murine *Kcnv2* promoter, we carried out chromatin immunoprecipitation experiments. Crx ChIP demonstrated Crx binding at both CBS, with CBS2 showing stronger binding than CBS1 (Fig. 5.2b). Nrl ChIP also confirmed Nrl binding to the predicted NBS.

To investigate the regulatory potential of the *Kcnv2* promoter region, a 479-bp fragment, containing CBS1, CBS2 and NBS, was cloned into the No-basal DsRed reporter vector (Fig. 5.2c), and in vitro electroporations were carried out. After eight days of culture, the intensity of DsRed signals was determined in retinal flat mounts and cross sections to quantify *cis*-regulatory activities. The wild type *Kcnv2* promoter construct induced a strong DsRed signal, depicting high regulatory activity (Fig. 5.3a).

We then determined the effect of a Crx and Nrl deficiency on the regulatory activity of the *Kcnv2* promoter. For this purpose, in vitro electroporations of the

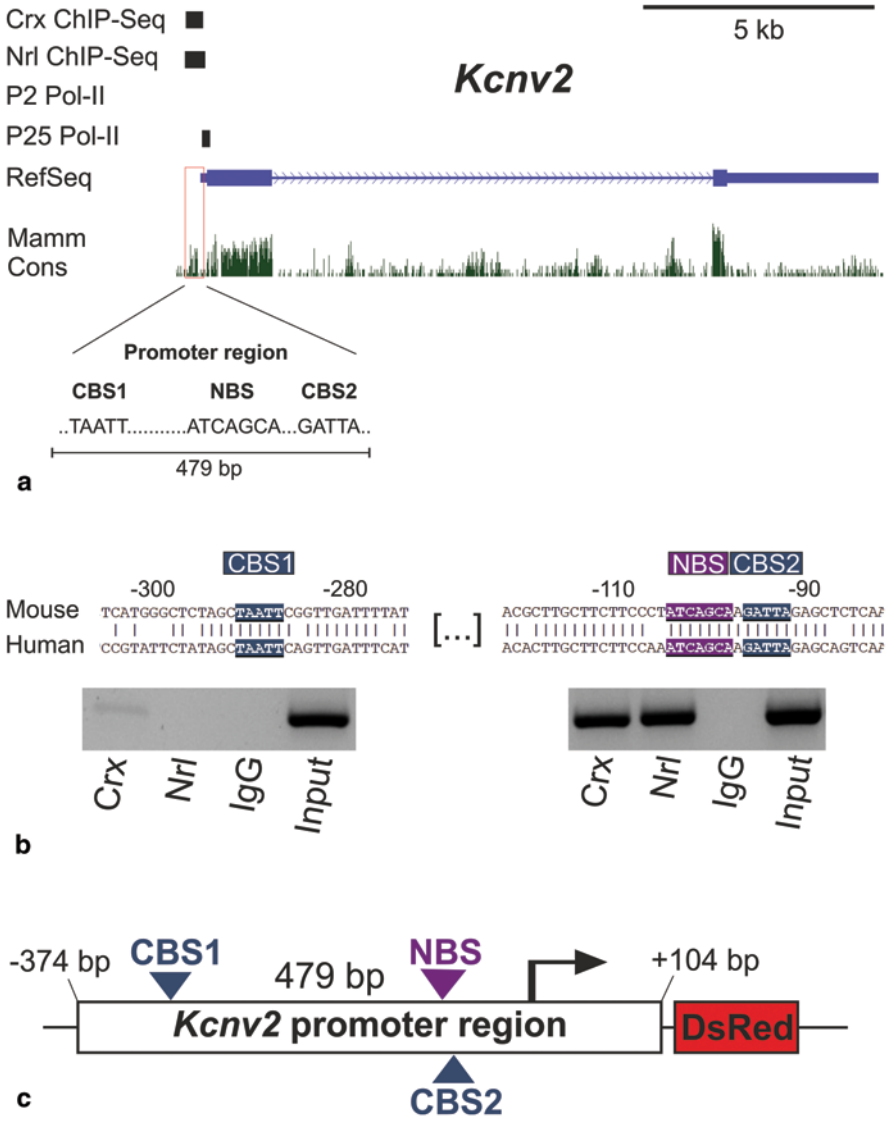


**Fig. 5.2** **a** Crx and Nrl enriched ChIP-seq regions are present in the proximal *Kcnv2* promoter. Pol-II ChIP indicates transcriptional activity in *P25* retinas, in contrast to *P2*. The nucleotide sequences of Crx binding sites (*CBS*) and Nrl binding sites (*NBS*) are depicted. **b** Evolutionary conservation and Crx/Nrl ChIP-PCR signals at *CBS1* and *CBS2/NBS*. **c** Reporter construct including a 479-bp *Kcnv2* promoter region used for in vitro electroporation

wild type reporter construct were carried out together with knockdown plasmids expressing shRNA against Crx and Nrl (Fig. 5.3a). We observed a ~20-fold reduction of *Kcnv2* promoter activity in the Crx knockdown and a ~fivefold reduction in the Nrl knockdown retina (Fig. 5.3b). Double knockdown of Crx and Nrl abolished

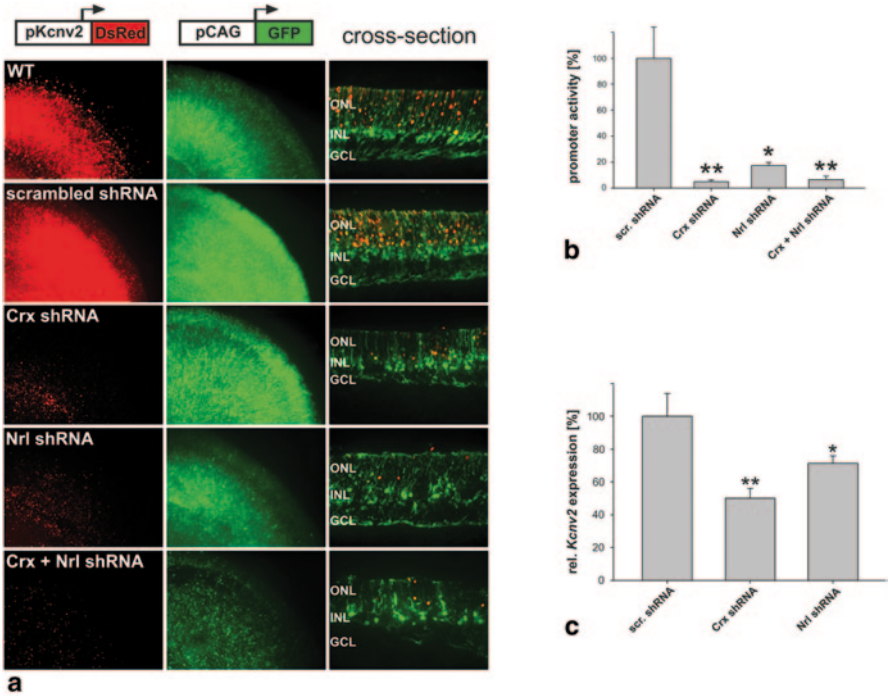


**Fig. 5.3** **a** Activity of the *Kcnv2* promoter region in explanted mouse retinas without and with Crx/Nrl knockdown. **b** Quantitative analysis of DsRed signal intensity. **c** qRT-PCR analysis of endogenous *Kcnv2* expression after Crx/Nrl shRNA electroporation

reporter activity. Endogenous *Kcnv2* expression was also decreased by ~50% in the Crx knockdown and ~30% in the Nrl knockdown retina (Fig. 5.3c).

To determine the importance of the individual transcription factor binding sites, we performed site-directed mutagenesis and quantified the regulatory activity by in vitro electroporation. Mutagenesis of CBS1 had no significant effect on DsRed expression (Fig. 5.4a). In contrast, depletion of the Crx motif in CBS2 led to an almost complete loss of regulatory activity. Depleting NBS did not affect the regulatory potential of the *Kcnv2* promoter.

Although both, CBS1 and CBS2, are Crx binding sites, their nucleotide compositions differ with CBS2 showing a higher Crx binding affinity. To investigate whether this difference could be used to modulate *Kcnv2* promoter activity, we switched the nucleotide of interest towards a "better" or "worse" Crx affinity. Modulation of CBS1 towards a more ideal Crx motif led to a significant decrease of reporter activity (Fig. 5.4b). A functional CBS2 drove strong DsRed expression, almost regardless of its Crx affinity. A higher CBS1 Crx affinity did not manage to compensate the loss of reporter activity caused by CBS2 depletion. Swapping of CBS1 and CBS2 Crx affinities led to a significant decrease of reporter activity, indicating the importance of sequence integrity in these evolutionary highly conserved regions.

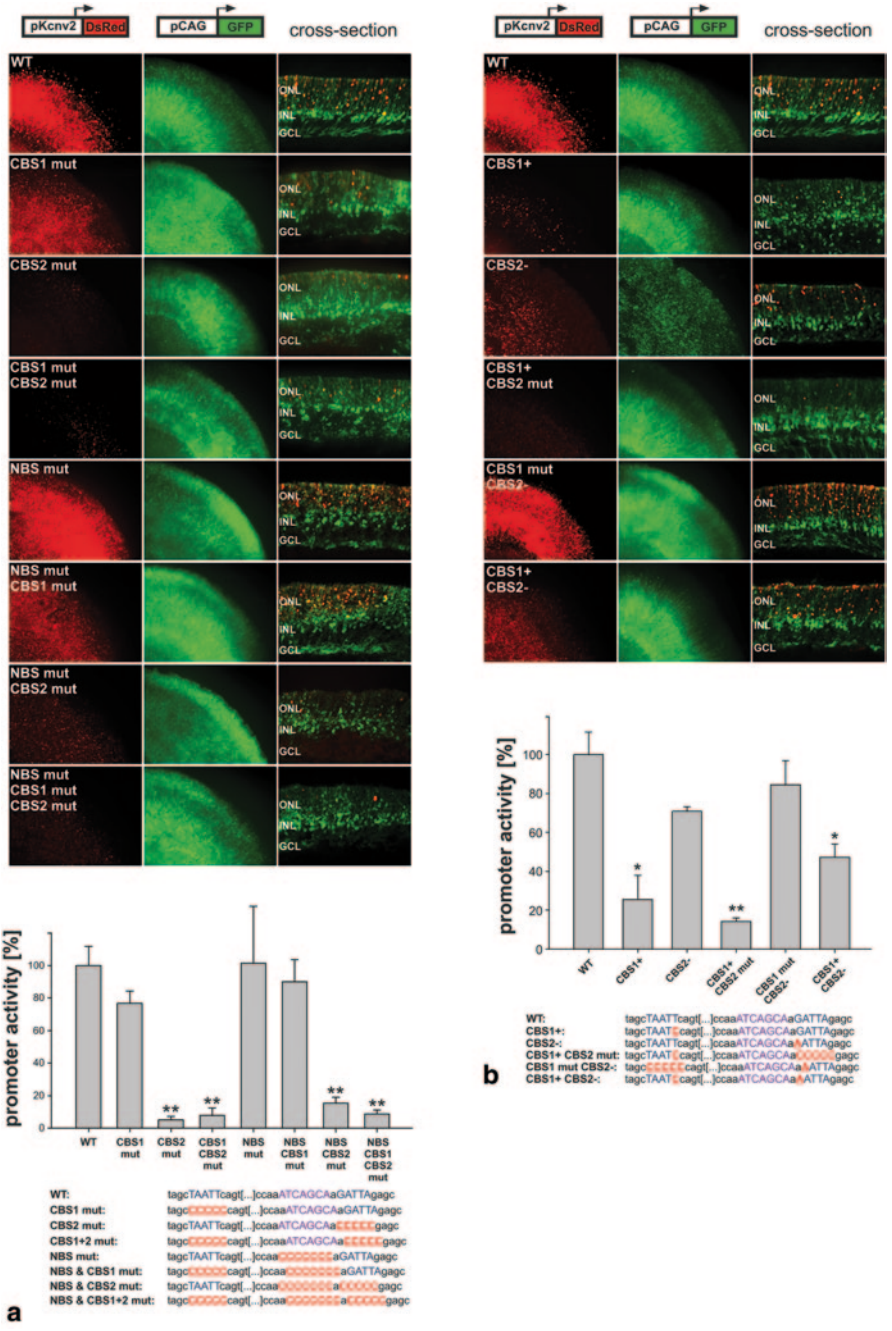


**Fig. 5.4** **a** In vitro electroporation of *Kcnv2* promoter constructs with depleted Crx/Nrl binding sites (*CBS*/*NBS*). **b** Attempts of modulating the Crx motifs towards a higher (+) or lower (−) Crx affinity. Quantitative analyses of DsRed signal intensity and sequence compositions are depicted

## 5.4 Discussion

*Kcnv2* is predominantly expressed in the retina and in heart tissue. Accordingly, *Kcnv2* mutations can also cause heart malfunction [23]. Temporal *Kcnv2* expression showed a correlation with postnatal developmental stages in the retina. The rapid increase of expression levels towards P14 hints at an important role of *Kcnv2* in processing visual signals since postnatal day 14 marks the time point of eyelid opening and thus the beginning of visual activity in mice. Other retinal genes, like rhodopsin, show a similar developmental expression pattern [24]. These findings are in accordance with recent RNA Pol-II ChIP-on-Chip data, which showed an active transcription site at the *Kcnv2* promoter in the murine P25 retina, in contrast to the P2 retina [25].

Using in vivo electroporation of a GFP-*Kcnv2* overexpressing plasmid, we investigated the localization of the *Kcnv2* gene product in the murine retina. Our observations suggest a membrane association of the Kv11.1 potassium channel subunit in photoreceptor inner segments. Accordingly, immunohistochemical experiments in murine and in situ hybridization in human retinas showed Kv11.1 localization in the inner segment membranes [26, 27].

Bioinformatic analyses revealed two CBS and one NBS in the murine *Kcnv2* promoter. All three sites show evolutionary conservation, which is a hallmark of important regulatory sites [28]. Using ChIP, we confirmed in vivo binding of Crx and Nrl at all three sites. The stronger Crx binding at CBS2 could be due to its high affinity Crx motif, its closer localization to the transcription start site or the coexistence of the NBS close by.

*Kcnv2* promoter activity was strongly reduced in shRNA-mediated Crx and Nrl knockdown retinas. In the Crx knockdown retina, a ~20-fold decrease of reporter activity was observed, indicating a direct regulation of *Kcnv2* by Crx. The observed ~fivefold decrease of *Kcnv2* promoter activity in the Nrl knockdown retina also demonstrated a regulatory influence of Nrl on *Kcnv2* expression. Since Nrl is known to synergistically interact with Crx [18], this effect could also be of indirect nature. This hypothesis is supported by ChIP-seq data showing a genome-wide overlap of CBS and NBS of 65 %, and the fact that 51 % of downregulated genes in $Nrl^{-/-}$ mice also show reduced expression in $Crx^{-/-}$ retinas [13, 20]. *Kcnv2* promoter activity in Crx and Nrl double knockdown retinas was nearly completely abolished. Additional qRT-PCR analyses of Crx and Nrl knockdown retinas showed a decrease of endogenous *Kcnv2* expression. Likewise, a recent study using $Nrl^{-/-}$ mice demonstrated low retinal *Kcnv2* expression [29].

To investigate the direct effects of the binding sites on *Kcnv2* promoter activity, in vitro mutagenesis was carried out. Mutations in the Crx core motif of CBS2 abolished promoter activity, while CBS1 mutations affected DsRed expression only mildly. Mutagenesis of NBS did not affect *Kcnv2* promoter activity, which indicates an indirect regulation of *Kcnv2* by Nrl. Recent studies show a strong correlation between induced gene expression and association duration of transcription factors with their binding site [30]. Thus, CBS2 could allow for a more stable and prolonged Crx binding compared to CBS1.

Finally, we introduced single nucleotide changes to modulate Crx binding affinities. A recent study showed that fine-tuning of a single CBS could modulate the activity of the rhodopsin promoter by up to ~225-fold [31]. In our study, modification of CBS1 alone towards a "better" Crx affinity resulted in a loss of *Kcnv2* promoter activity. An explanation for this effect could be that a higher Crx affinity at CBS1 leads to withdrawal of Crx from the regulatory more important CBS2. A "better" CBS1 Crx motif also failed to compensate the lost promoter activity induced by CBS2 depletion. In contrast, a "weaker" CBS2 Crx motif still induced significant DsRed expression. Swapping of CBS1 and CBS2 Crx affinities significantly decreased reporter activity, indicating the importance of sequence integrity in these evolutionary conserved regions. In summary, our findings highlight important genomic elements required for *Kcnv2* expression and could be helpful for the design of CDSRR gene therapy vectors.

## References

1. Gouras P, Eggers HM, MacKay CJ (1983) Cone dystrophy, nyctalopia, and supernormal rod responses. A new retinal degeneration. Archi Ophthalmol 101(5):718–724
2. Robson AG, Michaelides M, Saihan Z, Bird AC, Webster AR, Moore AT et al (2008) Functional characteristics of patients with retinal dystrophy that manifest abnormal parafoveal annuli of high density fundus autofluorescence; a review and update. Documenta Ophthalmologica Adv Ophthalmol 116(2):79–89
3. Sergouniotis PI, Holder GE, Robson AG, Michaelides M, Webster AR, Moore AT (2012) High-resolution optical coherence tomography imaging in KCNV2 retinopathy. British J Ophthalmol 96(2):213–217
4. Michaelides M, Holder GE, Webster AR, Hunt DM, Bird AC, Fitzke FW et al (2005) A detailed phenotypic study of "cone dystrophy with supernormal rod ERG". British J Ophthalmol 89(3):332–339
5. Robson AG, Webster AR, Michaelides M, Downes SM, Cowing JA, Hunt DM et al (2010) "Cone dystrophy with supernormal rod electroretinogram": a comprehensive genotype/phenotype study including fundus autofluorescence and extensive electrophysiology. Retina 30(1):51–62
6. Ben Salah S, Kamei S, Senechal A, Lopez S, Bazalgette C, Bazalgette C et al (2008) Novel KCNV2 mutations in cone dystrophy with supernormal rod electroretinogram. American J Ophthalmol 145(6):1099–1106
7. Wissinger B, Dangel S, Jagle H, Hansen L, Baumann B, Rudolph G et al (2008) Cone dystrophy with supernormal rod response is strictly associated with mutations in KCNV2. Investig Ophthalmol Visual Sci 49(2):751–757
8. Pongs O (1999) Voltage-gated potassium channels: from hyperexcitability to excitement. FEBS letters 452(1–2):31–35
9. Balijepalli RC, Delisle BP, Balijepalli SY, Foell JD, Slind JK, Kamp TJ et al (2007) Kv11.1 (ERG1) K + channels localize in cholesterol and sphingolipid enriched membranes and are modulated by membrane cholesterol. Channels 1(4):263–272
10. Czirjak G, Toth ZE, Enyedi P (2007) Characterization of the heteromeric potassium channel formed by kv2.1 and the retinal subunit kv8.2 in Xenopus oocytes. J neurophysiol 98(3):1213–1222
11. Furukawa T, Morrow EM, Cepko CL (1997) Crx, a novel otx-like homeobox gene, shows photoreceptor-specific expression and regulates photoreceptor differentiation. Cell 91(4):531–541
12. Mears AJ, Kondo M, Swain PK, Takada Y, Bush RA, Saunders TL et al (2001) Nrl is required for rod photoreceptor development. Nat Genetics 29(4):447–452

13. Hsiau TH, Diaconu C, Myers CA, Lee J, Cepko CL, Corbo JC (2007) The cis-regulatory logic of the mammalian photoreceptor transcriptional network. PloS one 2(7):e643
14. Freund CL, Gregory-Evans CY, Furukawa T, Papaioannou M, Looser J, Ploder L et al (1997) Cone-rod dystrophy due to mutations in a novel photoreceptor-specific homeobox gene (CRX) essential for maintenance of the photoreceptor. Cell 91(4):543–553
15. Freund CL, Wang QL, Chen S, Muskat BL, Wiles CD, Sheffield VC et al (1998) De novo mutations in the CRX homeobox gene associated with Leber congenital amaurosis. Nat Genetics 18(4):311–312
16. Furukawa T, Morrow EM, Li T, Davis FC, Cepko CL (1999) Retinopathy and attenuated circadian entrainment in Crx-deficient mice. Nat Genetics 23(4):466–470
17. Corbo JC, Cepko CL (2005) A hybrid photoreceptor expressing both rod and cone genes in a mouse model of enhanced S-cone syndrome. PLoS genetics 1(2):e11
18. Mitton KP, Swain PK, Chen S, Xu S, Zack DJ, Swaroop A (2000) The leucine zipper of NRL interacts with the CRX homeodomain. A possible mechanism of transcriptional synergy in rhodopsin regulation. J Biol Chem 275(38):29794–29799
19. Corbo JC, Lawrence KA, Karlstetter M, Myers CA, Abdelaziz M, Dirkes W et al (2010) CRX ChIP-seq reveals the cis-regulatory architecture of mouse photoreceptors. Genome Res 20(11):1512–1525
20. Hao H, Kim DS, Klocke B, Johnson KR, Cui K, Gotoh N et al (2012) Transcriptional Regulation of Rod Photoreceptor Homeostasis Revealed by In Vivo NRL Targetome Analysis. PLoS genetics 8(4):e1002649
21. Matsuda T, Cepko CL (2004) Electroporation and RNA interference in the rodent retina in vivo and in vitro. Proc Natl Acad Sci United States of America 101(1):16–22
22. Langmann T, Lai CC, Weigelt K, Tam BM, Warneke-Wittstock R, Moritz OL et al (2008) CRX controls retinal expression of the X-linked juvenile retinoschisis (RS1) gene. Nucleic acids Res 36(20):6523–6534
23. Smirnov SV, Robertson TP, Ward JP, Aaronson PI (1994) Chronic hypoxia is associated with reduced delayed rectifier K + current in rat pulmonary artery muscle cells. American J Physiol 266(1 Pt 2):H365–370.
24. Blackshaw S, Fraioli RE, Furukawa T, Cepko CL (2001) Comprehensive analysis of photoreceptor gene expression and the identification of candidate retinal disease genes. Cell 107(5):579–589
25. Tummala P, Mali RS, Guzman E, Zhang X, Mitton KP (2010) Temporal ChIP-on-Chip of RNA-Polymerase-II to detect novel gene activation events during photoreceptor maturation. Mol Vision 16:252–271
26. Cordeiro S, Guseva D, Wulfsen I, Bauer CK (2011) Expression pattern of Kv11 (Ether a-go-go-related gene; erg) K + channels in the mouse retina. PloS one 6(12):e29490
27. Wu H, Cowing JA, Michaelides M, Wilkie SE, Jeffery G, Jenkins SA et al (2006) Mutations in the gene KCNV2 encoding a voltage-gated potassium channel subunit cause "cone dystrophy with supernormal rod electroretinogram" in humans. American J Hum Genetics 79(3):574–579
28. Hardison RC (2000). Conserved noncoding sequences are reliable guides to regulatory elements. Trends Genetics: TIG 16(9):369–372
29. Brooks MJ, Rajasimha HK, Roger JE, Swaroop A (2011) Next-generation sequencing facilitates quantitative analysis of wild-type and Nrl(–/–) retinal transcriptomes. Mol Vision 17:3034–3054
30. Lickwar CR, Mueller F, Hanlon SE, McNally JG, Lieb JD (2012) Genome-wide protein-DNA binding dynamics suggest a molecular clutch for transcription factor function. Nature 484(7393):251–255
31. Lee J, Myers CA, Williams N, Abdelaziz M, Corbo JC (2010) Quantitative fine-tuning of photoreceptor cis-regulatory elements through affinity modulation of transcription factor binding sites. Gene therapy 17(11):1390–1399

# Chapter 6
# AIPL1 Protein and its Indispensable Role in Cone Photoreceptor Function and Survival

**Saravanan Kolandaivelu and Visvanathan Ramamurthy**

**Abstract** Mutations in *Aryl hydrocarbon receptor interacting protein like-1* (AIPL1) are linked to Leber congenital amaurosis (LCA), a severe blinding disease that occurs in early childhood. The severity of disease is due to requirement for AIPL1 in both rod and cone photoreceptor cell survival and function. *Aipl1* is expressed very early during retinal development in both rods and cones. In adult primates, robust expression of *Aipl1* is found in rods but not in cones. Mouse models revealed the importance of AIPL1 in stability and function of heteromeric phosphodiesterase 6 (PDE6), an enzyme needed for visual response. However, the need for AIPL1 in cone cell survival and function is not clearly understood. In this chapter, using results obtained from multiple lines of animal models, we discuss the role for AIPL1 in photoreceptors.

**Keywords** Retina · Photoreceptor · Rod · Cone · Phosphodiesterase 6 · AIPL1 and LCA

## 6.1 Introduction

Leber congenital amaurosis (LCA) is the most severe inherited retinal disorder affecting rod and cone mediated vision and thus very often leading to complete blindness in humans [1]. At present, 16 genes have been implicated in LCA with varying severity and progression of retinal degeneration [2]. Among the genes linked to LCA, mutations in "*Aryl hydrocarbon receptor interacting protein like 1*" (*Aipl1*) leads to severe and devastating retinal blinding disease affecting both

S. Kolandaivelu (✉) · V. Ramamurthy
Ophthalmology and Biochemistry, Center for Neuroscience, Eye Institute,
West Virginia University, One Stadium Drive, Room number E363,
Morgantown, WV 26506, USA
e-mail: kolandaivelus@wvuhealthcare.com

V. Ramamurthy
e-mail: ramamurthyv@wvuhealthcare.com

J. D. Ash et al. (eds.), *Retinal Degenerative Diseases,* Advances in Experimental Medicine and Biology 801, DOI 10.1007/978-1-4614-3209-8_6,

rods and cones [3]. As the name indicates, AIPL1 is a close homologue to AIP (Aryl hydrocarbon receptor Interacting Protein). AIPL1 contains 3 tetratricopeptide repeat (TPR) domains, a helix-loop-helix structure thought to play a role in protein-protein interaction at its C-terminal. AIPL1 also contains an inactive prolyl peptidyl isomerase domain (PPI) at their N-terminal. PPI domains are typically present in chaperones such as heat shock proteins. In primates including humans, a unique unstructured C-terminal proline rich region is present [1]. Mutations in AIPL1 linked to blinding diseases can be classified into three different categories depending on the domain where these changes occur. Class I representing mutations in the N-terminal PPI domain and class II changes occurring in TPR domains are linked to LCA. Mutations in unique C-termini are linked to dominant cone dystrophy or juvenile retinitis pigmentosa suggesting the importance of this region in function of AIPL1 in primates [3]. Based on sequence similarity and known function of AIP, AIPL1 was predicted to function as a chaperone in folding of some essential protein needed for vision.

## 6.2 Animal Models of AIPL1 Deficiency

Generation and characterization of animal models has led to remarkable progress in our understanding of this devastating disease [4–6]. Two complete knockouts eliminating *Aipl1* expression in mouse showed dramatic degeneration of both rod and cone photoreceptor cells [4, 5]. However, photoreceptor cells were formed suggesting normal development of rods and cone cells. Characterization of photoreceptors by electroretinogram (ERG) demonstrated lack of function in response to light stimuli. A mouse model with reduced levels of *Aipl1* expression also showed degenerating rod and cone photoreceptor cells [6]. The molecular mechanism behind degeneration of both rods and cones in AIPL1 deficient animal model is due to de-stabilization of phosphodiesterase 6 (PDE6) [4, 7]. PDE6 is a crucial effector enzyme that hydrolyzes cGMP and is needed for conversion of light into electrical signal. It is a heterotetrameric enzyme composed of two catalytic subunits and two inhibitory subunits. In rods, α and β subunits dimerize to form catalytic core [8–10]. In cones, PDE6 hydrolyzes cGMP using two identical catalytic subunits (α′). Absence of PDE6 leads to blindness in humans. Furthermore, in a well characterized animal model lacking PDE6β subunit (*rd1* animal), rapid degeneration of photoreceptor cells similar to animals lacking AIPL1 is observed [11]. Altogether, these evidences point to an important role for AIPL1 in PDE6 stability and function.

## 6.3 Link Between AIPL1 and Rod PDE6

Detailed biochemical analysis showed that in absence of AIPL1, rod PDE6 subunits (α, β and γ) are synthesized normally but are not stable and do not assemble properly. Misassembled PDE6 subunits are likely rapidly degraded by proteasomal

machinery in the photoreceptor inner segment leading to decline in PDE6 levels [12]. A previous yeast two-hybrid study had demonstrated a stable interaction between prenylated proteins and AIPL1 [13]. Prenylation is the modification of the C-terminal, cysteine residue in proteins containing "CAAX" box motif (C = cysteine, A = Aliphatic amino acid residue and X = any amino acid residue). If X = leucine, the cysteine residue is covalently modified by C-20 geranylgeranyl group otherwise it is modified by a less hydrophobic, C-15 farnesyl group [13, 14]. Interestingly, rod PDE6 catalytic subunits are differentially prenylated with α- subunit modified with farnesyl group while PDE6β subunit is geranylgeranylated. Immunoprecipitation with AIPL1 specific monoclonal antibodies show the primary interacting partner as α- subunit of PDE6 [12]. In addition, studies show direct interaction between AIPL1 and chaperone, heat shock protein-90 (Hsp90) [15]. Altogether, these evidences show a crucial role for AIPL1 in folding of PDE6 subunits perhaps with farnesyl group being one of the interacting surfaces with AIPL1. Unfortunately, lack of suitable functional expression system for PDE6 has impeded our progress in understanding the mechanism behind the need for AIPL1 in PDE6 stability. However, generation of novel animal models with altered prenyl groups in PDE6 catalytic subunits, albeit slow and expensive, will provide greater clarity needed to understand this process.

## 6.4 AIPL1 in Mouse Cones

Rapid degeneration of cone cells in animal lacking AIPL1 could be due to 'bystander' effect of massive rod loss. Alternatively, AIPL1 may play a direct role in cones. Electroretinogram (ERG) in AIPL1 complete knockout suggested a direct role as photopic ERG response was absent at any age tested. This is in contrast to findings in *rd1* animals, where cone ERG responses could be elicited prior to significant degeneration. To unequivocally answer the importance of AIPL1 in cones, we created an animal model where human AIPL1 isoform was expressed in rod cells [7]. These transgenic animals were then bred into complete knockout background to create animals where AIPL1 is expressed only in rod cells. ERG analysis shows a robust scotopic response demonstrating functional rod cells. In contrast, photopic or cone responses were completely absent. In absence of rod degeneration, cone cells were lost but at a much slower rate demonstrating a direct and an important role for AIPL1 in cones. Slower rate of cone degeneration in our transgenic animal models suggests that rapid rod cell death was partly responsible for fast rate of cone cell death observed in animals with complete knockout of AIPL1. Prior to cone degeneration, we observed significant reduction in levels of cone PDE6 catalytic subunits [7]. This finding suggests a role for AIPL1 in stability of cone PDE6 subunits. It also puts our finding that AIPL1 interacts with farnesylated proteins into question as cone PDE6 catalytic subunits are thought to be geranylgeranylated. However, there is no direct evidence that cone PDE6 catalytic subunits are geranylgeranylated. Online prediction programs suggest that cone PDE6 subunits are farnesylated rather

than geranylgeranylated. To resolve this issue unambiguously, future studies using animal models as proposed in earlier section are needed to test this hypothesis.

## 6.5 AIPL1 in Primate Cones

Animal models and biochemical studies show that AIPL1 is needed for stability of rod and cone PDE6 enzymes necessary for functional vision [4, 7]. This finding suggests that AIPL1 is needed for proper functioning of fully-developed adult cones. In contrary to this expectation, studies show expression of AIPL1 is absent in adult cones [7, 16]. To avoid possible tissue processing problems that may arise in human samples, we tested the expression of AIPL1 in well-preserved retinas from developing and adult macaque. Robust expression of AIPL1 was observed in early developing photoreceptors (rods and cones) in macaque and was absent in adult macaque cones [17]. AIPL1 expression was observed in inner segment, nuclei and synaptic regions. Within inner segment, closer to tips of connecting cilia, we observe a strong signal for AIPL1 suggesting a role of AIPL1 in trafficking of assembled PDE6 in photoreceptor cells. After birth, loss of AIPL1 in cones was progressive with inner segment losing staining first and synapse the last. By end of year 1, AIPL1 staining in cones was dramatically reduced or absent (*Ramamurthy and Hendrickson, unpublished results*). We cannot rule out the possibility of epitope masking confounding our detection of AIPL1 in cones despite using a robust polyclonal antibody (1:25,000 dilution) against human AIPL1. It must be noted that we did observe strong expression of AIPL1 in adult rods. The reason and the mechanism behind the down regulation of AIPL1 proteins in primate cone photoreceptor cells remains a mystery.

Interestingly, mutations in C-terminal primate specific region of AIPL1 are linked to cone dystrophy and juvenile RP in humans [3]. These linkage studies suggest the importance of AIPL1 in proper functioning of cone cells. Recent imaging studies in human patients with AIPL1-LCA suggest a role for AIPL1 in development of cones and rods [18]. In agreement with this early role in development, we find early expression of AIPL1 in both rods and cones of humans. However, in mouse, it is clear that AIPL1 is dispensable for early development of photoreceptor cells.

## 6.6 Conclusions and Future Directions

In the last 10 years, work on AIPL1 by scientific community has raised our understanding about AIPL1 and its role in retina tremendously. AIPL1 is required for stability and function of rod and cone PDE6 enzymes. Absence of AIPL1 also leads to dramatic degeneration of photoreceptor cells which can be successfully halted if treated by gene therapy prior to significant damage. Studies on AIPL1 have also led to several interesting questions that need to be addressed to make a significant

impact in our treatment of humans afflicted with AIPL1-LCA. Some of these questions are briefly summarized below.

1. What is the mechanism behind the role for AIPL1 as PDE6 chaperone? It is clear that in the absence of AIPL1, PDE6 subunits do not assemble, function and are degraded. Lack of proper assembly and degradation is likely due to AIPL1's role as a chaperone. It is likely that AIPL1 in concert with Hsp90 aids in folding of PDE6. Does AIPL1 help in folding of α or β subunit or both? Is there a role for lipid groups (farnesyl or geranyl geranyl) in this process? What regions in AIPL1 or PDE6 are involved in this interaction? How do these interactions vary between cone and rod PDE6 subunits? The answers to some of these questions may be a predictor of the severity of particular AIPL1 mutation, associated disease progression and treatment potential.
2. Does the role of AIPL1 in rods and cones differ? In rod cells, lack of AIPL1 leads to reduction in PDE6 and consequent increase in cGMP levels leading to rapid rod cell death. The exact mechanism behind death of cones in the absence of AIPL1 is not known. Animal models lacking AIPL1 in cones show reduction of PDE6 which likely leads to increases in cGMP levels. However, observed cone cell death is slow in transgenic animal model that lack AIPL1 exclusively in cones This could be due to intrinsic ability of cones to tolerate higher levels of cGMP and calcium. Alternatively, cones might possess a compensatory mechanism to maintain cGMP levels. In addition, it is not clear if AIPL1, similar to its role in rods cells, affects the assembly of cone PDE6 subunits. Absence of detectable AIPL1 in adult primate cones poses another conundrum. If AIPL1 is important for PDE6 stability and assembly, continued expression of AIPL1 or its homologue throughout adulthood is needed for phototransduction. Immunocytochemistry demonstrates the opposite in both adult human and macaque tissue. It is possible that epitope masking occludes our ability to detect AIPL1 in cones. Further experimentation is needed to fully address this question.
3. What is the role for C-terminal unique extension? In primates, AIPL1 possess a unique proline rich C-termini. The need for this extension is not clear. Mutations in this region are linked to cone dystrophy and RP suggesting the importance of this domain in functioning of AIPL1 in primates. Human *Aipl1* gene is able to efficiently compensate for the lack of mouse *Aipl1* suggesting that both isoforms fundamentally operate by similar mechanism. Presence of fovea in primates may entail some special role for the C-terminal extension or human isoform of AIPL1 in cone development.
4. In conclusion, we envision three roles for AIPL1 in photoreceptor cells.: a) Folding of PDE6 catalytic subunits, b) transport of assembled PDE6 complex and c) early development of rods and cones in primates.

**Acknowledgments** We thank National Eye Institute for the travel grant award (to SK) to attend and present the work in the RD2012 meeting. We acknowledge help from members of Dr. Ramamurthy lab and collaborators for their support in this study. This work was supported by NIH grants RO1EY017035 (VR), West Virginia Lions, Lion Club International Foundation and Unrestricted grant from Research to Prevent Blindness (RPB).

## References


1. Sohocki MM, Bowne SJ, Sullivan LS, Blackshaw S, Cepko CL, Payne AM et al (2000) Mutations in a new photoreceptor-pineal gene on 17p cause Leber congenital amaurosis. Nat Genet 24(1):79–83
2. Tan MH, Mackay DS, Cowing J, Tran HV, Smith AJ, Wright GA et al (2012) Leber congenital amaurosis associated with AIPL1: challenges in ascribing disease causation, clinical findings, and implications for gene therapy. PLoS One 7(3):e32330
3. Sohocki MM, Perrault I, Leroy BP, Payne AM, Dharmaraj S, Bhattacharya SS et al (2000) Prevalence of AIPL1 mutations in inherited retinal degenerative disease. Mol Genet Metab 70(2):142–150
4. Ramamurthy V, Niemi GA, Reh TA, Hurley JB (2004) Leber congenital amaurosis linked to AIPL1: a mouse model reveals destabilization of cGMP phosphodiesterase. Proc Natl Acad Sci U S A 101(38):13897–13902
5. Dyer MA, Donovan SL, Zhang J, Gray J, Ortiz A, Tenney R et al (2004) Retinal degeneration in Aipl1-deficient mice: a new genetic model of Leber congenital amaurosis. Brain Res Mol Brain Res 132(2):208–220
6. Liu X, Bulgakov OV, Wen XH, Woodruff ML, Pawlyk B, Yang J et al (2004) AIPL1, the protein that is defective in Leber congenital amaurosis, is essential for the biosynthesis of retinal rod cGMP phosphodiesterase. Proc Natl Acad Sci U S A 101(38):13903–13908
7. Kirschman LT, Kolandaivelu S, Frederick JM, Dang L, Goldberg AF, Baehr W et al (2010) The Leber congenital amaurosis protein, AIPL1, is needed for the viability and functioning of cone photoreceptor cells. Hum Mol Genet 19(6):1076–1087
8. Burns ME, Arshavsky VY (2005) Beyond counting photons: trials and trends in vertebrate visual transduction. Neuron 48(3):387–401
9. Lamb TD, Pugh EN Jr (2004) Dark adaptation and the retinoid cycle of vision. Prog Retin Eye Res 23(3):307–380
10. Zhang X, Cote RH (2005) cGMP signaling in vertebrate retinal photoreceptor cells. Front Biosci 10:1191–1204
11. Farber DB (1995) From mice to men: the cyclic GMP phosphodiesterase gene in vision and disease. The Proctor Lecture. Invest Ophthalmol Vis Sci 36(2):263–275
12. Kolandaivelu S, Huang J, Hurley JB, Ramamurthy V (2009) AIPL1, a protein associated with childhood blindness, interacts with alpha-subunit of rod phosphodiesterase (PDE6) and is essential for its proper assembly. J Biol Chem 284(45):30853–30861
13. Ramamurthy V, Roberts M, van den Akker F, Niemi G, Reh TA, Hurley JB (2003) AIPL1, a protein implicated in Leber's congenital amaurosis, interacts with and aids in processing of farnesylated proteins. Proc Natl Acad Sci U S A 100(22):12630–12635
14. Christiansen JR, Kolandaivelu S, Bergo MO, Ramamurthy V (2011) RAS-converting enzyme 1-mediated endoproteolysis is required for trafficking of rod phosphodiesterase 6 to photoreceptor outer segments. Proc Natl Acad Sci U S A 108(21):8862–8866
15. Hidalgo-de-Quintana J, Evans RJ, Cheetham ME, van der Spuy J (2008) The Leber congenital amaurosis protein AIPL1 functions as part of a chaperone heterocomplex. Invest Ophthalmol Vis Sci 49(7):2878–2887
16. van der Spuy J, Kim JH, Yu YS, Szel A, Luthert PJ, Clark BJ et al (2003) The expression of the Leber congenital amaurosis protein AIPL1 coincides with rod and cone photoreceptor development. Invest Ophthalmol Vis Sci 44(12):5396–5403
17. Hendrickson A, Bumsted-O'Brien K, Natoli R, Ramamurthy V, Possin D, Provis J (2008) Rod photoreceptor differentiation in fetal and infant human retina. Exp Eye Res 87(5): 415–426
18. Jacobson SG, Cideciyan AV, Aleman TS, Sumaroka A, Roman AJ, Swider M et al (2011) Human retinal disease from AIPL1 gene mutations: foveal cone loss with minimal macular photoreceptors and rod function remaining. Invest Ophthalmol Vis Sci 52(1):70–79

# Chapter 7
# Primate Short-Wavelength Cones Share Molecular Markers with Rods

**Cheryl M. Craft, Jing Huang, Daniel E. Possin and Anita Hendrickson**

**Abstract** *Macaca, Callithrix jacchus* marmoset monkey, *Pan troglodytes* chimpanzee and human retinas were examined to define if short wavelength (S) cones share molecular markers with L&M cone or rod photoreceptors. S cones showed consistent differences in their immunohistochemical staining and expression levels compared to L&M cones for "rod" Arrestin1 (S-Antigen), "cone" Arrestin4, cone alpha transducin, and Calbindin. Our data verify a similar pattern of expression in these primate retinas and provide clues to the structural divergence of rods and S cones versus L&M cones, suggesting S cone retinal function is "intermediate" between them.

**Keywords** L&M opsins · Monkey · Neural retina leucine zipper · Primate · Photoreceptor · S-antigen · S opsin · Visual arrestins

C. M. Craft (✉)
Mary D. Allen Laboratory for Vision Research, Doheny Eye Institute,
Departments of Ophthalmology and Cell & Neurobiology,
Keck School of Medicine of the University of Southern California,
1355 San Pablo St., DVRC 405, Los Angeles, CA 90033, USA
e-mail: ccraft@usc.edu

J. Huang · D. E. Possin · A. Hendrickson
Department of Ophthalmology, University of Washington,
Seattle, WA 98195, USA
e-mail: jinghu@u.washington.edu

D. E. Possin
e-mail: danpossn@u.washington.edu

A. Hendrickson
Department of Biological Structure, University of Washington, Seattle,
WA 98195, USA
e-mail: anitah@u.washington.edu

J. D. Ash et al. (eds.), *Retinal Degenerative Diseases,* Advances in Experimental Medicine and Biology 801, DOI 10.1007/978-1-4614-3209-8_7,

**Abbreviations**

| | |
|---|---|
| Arr | Arrestin |
| Calb | Calbindin |
| CTr | Cone Transducin |
| IHC | Immunohistochemistry |
| S | Short wavelength |
| M | Medium wavelength |
| L | Long wavelength |
| RTr | Rod Transducin |
| Mab | Monoclonal |
| Pab | Polyclonal |
| OS | Outer segment |
| NRL | Neural retina leucine zipper |
| NR2E3 | Nuclear receptor subfamily 2, group E, member 3 |

## 7.1 Introduction

The primate retina has one type of rod photoreceptor and three types of cone photoreceptors. In humans, rods outnumber cones 15–20:1 and form a single group that expresses photosensitive rhodopsin in their outer segments (OS), while 90 % of cone OS have photosensitive pigments containing either long- (L or red) or medium-wavelength (M or green) selective opsin or 5–10 % contain short-wavelength (S or blue) selective opsin.

The cones expressing L or M opsin are remarkably similar in their anatomy and physiology, but the cones with S opsin have unique differences, reviewed in [1]. S opsin has a 42 % molecular homology to rod, L or M opsin and is an "intermediate" visual opsin [2]. Thus, specific reagents cannot distinguish L from M cones (L&M). However, S opsin specific reagents distinguish S from both L&M cones and rods. Morphologically, the S cone differs from the L&M cones in inner segment (IS) size and shape, smaller synaptic pedicle. Their cell body lies deeper from the external limiting membrane [3–5] and extracellular sheath around their OS that stains more heavily with peanut agglutinin [6, 7].

There are unexplained species differences within the primates for S cone distribution. In all primates, L&M cones are found throughout the retina in diminishing density from the foveal center. In macaque and marmoset, S cones are found at lower density throughout the fovea [8, 9]; while in human, S cones are lacking in the foveal center in both adults and fetuses [4–10]. In all Old World primates, S cones are spaced semi-regularly throughout the retina [11]. In New World squirrel monkey but not New World marmosets, S cones occur in small clumps [9].

Using specific antibodies for visual arrestins (Arr), transducins, and calbindin, we examined monkey, ape, and human retinas to define if S cones share molecular markers with rod or L&M cones photoreceptors.

## 7.2 Materials and Methods

### *7.2.1 Tissue*

Adult Macaca monkey, Callithrix jacchus marmoset monkey, and Pan troglodytes chimpanzee eyes were obtained under authorized animal protocols from Tissue Programs at San Antonio, Emory, Washington, or Wisconsin Regional Primate Centers. Human eyes were obtained through the University of Washington, Willed Body Program. Eyes were enucleated, cornea and lens removed, and posterior globe immersion fixed in 4% paraformaldehyde in 0.1 M phosphate buffer for 2–4 h. Selected areas of the retina were removed, cryo-protected, and serial frozen sections were cut at 12–20 μm. Every tenth slide was stained with 1% azure II-methylene blue in borax buffer pH 10.5 to identify retinal morphology and locate the fovea.

### *7.2.2 Immunohistochemical (IHC) Staining*

Selected sections were double IHC labeled using a combination of mouse monoclonal (Mab) and rabbit polyclonal (Pab) antibodies. IHC labeling used standard methods [9]. Pab were generated to S cone opsin (JH455; 1/10,000, J. Nathans, Johns Hopkins), L&M cone opsin (1/5,000, J. Saari, Univ. Washington), human cone Arr4 (Luminaire Founders [hCARR-LUMIf]; 1/15,000), [12] S-antigen or "rod" Arr1 (C10C10; 1/10,000) [13], and rod alpha transducin (RTr; sc389; 1/2,000, Santa Cruz Biotechnology).

Mabs were generated to S cone opsin (OS2; 1/20,000, A. Szél, Semilweiss Univ.), Arr4 (7G6; 1/300, P. MacLeish, Morehouse Univ.), Arr1 (S-antigen, D9F2: 1/7,000, L.A. Donoso, Wills Eye Hospital), calbindin D28k (#C8666; 1/2000, Sigma-Aldrich), and alpha subunit of cone transducin (CTr; A1.1; 1/300, J. Hurley, Univ. Washington). For detection, the tissue was incubated in a mixture of 1/500 goat anti-rabbit IgG coupled to Alexa 488 and goat anti-mouse IgG coupled to Alexa 594 (Molecular Probes).

To detect differences in IHC labeling intensity within the photoreceptors, adjacent sections were incubated in primary antibodies diluted 2, 5, and 10 times normal working dilution. Sections were imaged either using a Zeiss LSM two-photon confocal microscope or a Nikon E1000 wide field digital microscope equipped with deconvolution software (Scientific Volume Imaging, The Netherlands). All images were processed in Adobe Photoshop CS3 for color balance, sharpness, and contrast.

## 7.3 Results

In all four primates, S cones showed a consistent difference in their IHC staining pattern compared to L&M cones, but some species differences were also noted.

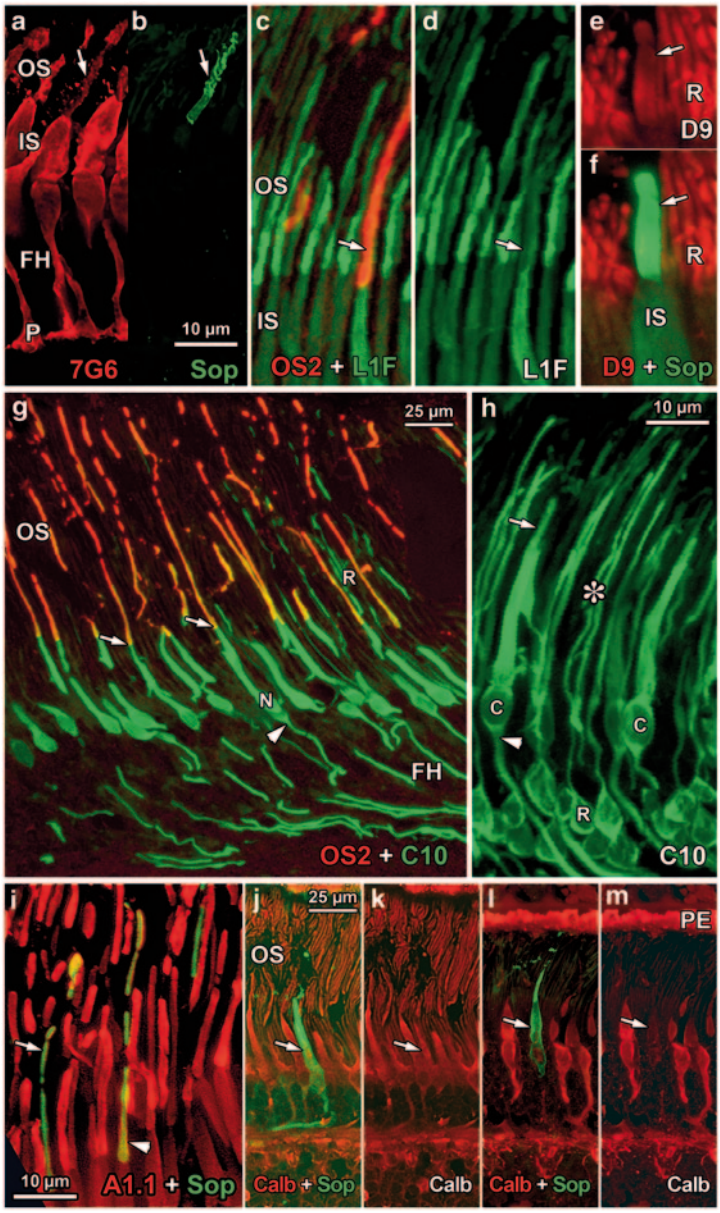


**Fig. 7.1** Sections of adult primate retina stained IHC for the designated antibodies. **a–d** Cone Arr4 labeling in human peripheral retina (**a**, **b**) shows S cone opsin (*red*) labeled by Pab *Sop* and both S and L&M cone cytoplasm labeled by Mab *7G6* to hARR4 (*green*). Staining in macaque central (**c**, **d**) retina is similar for Mab *OS2* and Pab hCARR-LUMIf (*LIF*). In both combinations, S cone outer segments (*OS*; *arrows,* **a–d**) are labeled more lightly than L&M *OS*. Scale in **b** for **a–d**. **e, f** Chimpanzee S cone OS (*arrows*) label for Arr1 at a similar intensity to surrounding rod OS. **g** Marmoset foveal edge shows S cone *OS* labeling by *OS2* (*red*) and intense labeling (*green*) by Pab C10C10 to Arr1 of S cones *OS* (*arrows*), IS, cell body (*N*) and synaptic axon or fiber of Henle (*FH*).

### 7.3.1 Cone Arr4 (Pab LUMIf; Mab 7G6)

All cones heavily labeled throughout the IS, cell body, axonal Fiber of Henle (FH), and synaptic pedicle with both antibodies to Arr4 (Fig. 7.1a, b, c, d); rods were unlabeled. The S cone OS labeling intensity was much lighter than neighboring L&M OS or S cone cell body (Fig. 7.1a–d, arrows). At 5x dilution, S cone OS labeling was almost undetectable while L&M cone OS immunostained up to 10x dilution (data not shown).

### 7.3.2 Rod Arr1 (S-Antigen; Mab D9F2; Pab C10C10)

OS labeling pattern was similar for both antibodies to Arr1. L&M cone OS were negative for both antibodies, while the S cone OS labeled for both (Fig. 7.1e, f; arrow) at similar intensity as surrounding rod OS (Fig. 7.1e, f, R). In the marmoset and macaque fovea (Fig. 7.1g) and parafovea (Fig. 7.1h), OS2+Arr1 double IHC marked the distinctive sparse S cone OS (arrows) lying between the numerous unlabeled L&M cone OS. The S cone was heavily labeled from OS to pedicle. Some FH axons could be traced from Arr1+ S cone cell bodies (Fig. 7.1g, h; arrowheads). Heavy Arr1 IHC in rod OS (Fig. 7.1g, R; Fig. 7.1h, asterisk), IS, cell body (Fig. 7.1h, R), and axon can be seen on the foveal edge (Fig. 7.1g, right side) where rods are sparse. Mab D9F2 labeled the same regions of S cones and rods, but much less intensely (not shown).

### 7.3.3 Cone Alpha Transducin (CTr; Mab A1.1)

IHC labeling for CTr was similar to Arr4 for both cone types in all primates, but S cone OS varied in intensity (Fig. 7.1i) from light to dark. Most S cone OS were unstained at 5x dilution of A1.1.

The axons angle away from the foveal center to the left. A few Arr1 + rod OS (*R*) are present on the edge of the fovea. **h** Macaque cones (*C*) and rods (*R*) both labeled for Arr1 from OS to cell body (*C, R*) to FH (*arrowhead*) by Pab C10C10 (*C10*). S cone OS (*arrow*) labeled similar to adjacent rod OS (*arrowhead*). **i**. Both L&M and S cone OS (*green*) label heavily for cone transducin (CTr) (*red*) with Mab *A1.1*. The cytoplasm from IS to pedicle heavily labeled in both (not shown). The S cone OS varies in CTr intensity, with some OS clearly double labeled (*arrowhead*) and others with lighter CTr labeling (*arrow*). **j**, **k** Macaque L&M cones labeled for calbindin with Mab *CalB* used at 2x dilution from IS to pedicle, but S cones only lightly labeled. Cone *OS* labeled lightly. **l, m** Human L&M cones label from IS throughout the rest of the cytoplasm for Mab *CalB* used at 2x dilution, but S cones show little labeling. Neither type of OS contains detectible labeling. Retinal pigment epithelium (*PE*) indicates inherent auto-fluorescence in this layer. Scale in **j** for **j–m**

### *7.3.4 Rod Transducin (RTr; sc389)*

No labeling was detected in either L&M or S cones while rods were heavily labeled (data not shown).

### *7.3.5 Calbindin-D24k (CalB; Mab C8666)*

In monkeys and chimps, all L&M and S cones labeled from IS to synaptic pedicle, with light to negligible labeling in the OS (Fig. 7.1j, k, arrow). In humans the OS were unstained and the S cone contained little CalB compared to surrounding L&M cones (Fig 7.1l, m, arrow).

## 7.4 Discussion

An earlier immuno-electron microscopy study showed that rod and S cone OS, but not L&M cone OS, in baboon retina are labeled with S-antigen, renamed "rod" Arr1 [14]. By contrast, Arr1 is expressed in all mouse rods and cones [15]. Later, a second visual arrestin, "cone" Arr4, was discovered that was highly expressed in all cones but no rods of many vertebrates [12, 16, 17]. Our data extend these earlier observations to several other primate retinas and verify a similar pattern of "intermediate" expression of both "rod" and "cone" visual Arr in S cones.

Close molecular ties exist during development between S cones and rods. The nuclear transcription factors, neural retina leucine zipper (NRL), and nuclear receptor subfamily 2, group E, member 3 (NR2E3), are essential for normal rod development. If one or both of these regulators are genetically altered, progenitors that should have a rod fate shift their genetic program to become S cones [18, 19]. Another similarity is that S cone inner retinal circuitry is more similar to that of rods than L&M cones [20, 21]. In central retina, two to five S cones converge onto a single "blue ON" bipolar cell and multiple rods converge onto a "rod" bipolar. In inner retina there is further convergence by blue bipolars onto a subset of ganglion cells. By contrast, a single L&M cone synapses onto a single "midget" ON and a single "midget" OFF bipolar. Each midget bipolar, in turn, synapses onto a single ganglion cell. Thus, this "midget" pathway is the basis of high visual acuity as well as red/green color vision, while the S cone system seems to be designed for chromatic sensitivity.

In all four primates, S cones showed a consistent difference in their IHC staining pattern and level of expression compared to L&M cones and rods. Both cone types labeled heavily for Cone Arr4 and CTr from IS to synaptic pedicle, but S cone OS were typically stained less intensely than L&M. "Rod" Arr1 did not label L&M primate cones, but S cones and rods were labeled heavily. In monkeys, the L&M cone cytoplasm, but not OS, was well labeled for CalB in both cone types, while in

chimps and humans the S cone was lightly labeled. Rods were negative for CalB in all primates. Our results show that human, monkey, and ape S and L&M cones share Cone Arr4, CTr, and CalB expression. Only S cones share "rod" Arr1 expression with rods while RTr expression is confined to rods.

Why do S cones and rods share any molecular markers? It is possible that rod developmental signals are not turned off appropriately in the S cones, although Bumsted et al. found no coexpression of NRL or NR2E3 in primate cones [22]. Alternatively, perhaps the functional and structural similarities between the rhodopsin in rods and S opsin in cones recruit this transduction shutoff molecule to maintain visual sensitivity with lower intensity light and to protect the rods and S cones from retinal degeneration.

**Acknowledgments** Dr. Craft holds the Mary D. Allen Chair in Vision Research, Doheny Eye Institute. We thank Drs. Donoso, MacLeisch, Nathans, and Saari for generously providing antibodies. This work was supported, in part, by EY015851 (CMC), Kayser Award (AH), CORE grants EY01730 (UW) and EY03040 (DEI), and Research to Prevent Blindness. We gratefully acknowledge the assistance of the Willed Body Program and the Tissue Programs at University of Washington, University of Wisconsin Regional Primate Research Center (P51RR000167), San Antonio Primate Center (P51-RR13986), and Yerkes Regional Primate Center.

## References

1. Calkins DJ (2001) Seeing with S cones. Prog Retin Eye Res 20(3):255–287
2. Nathans J (1989) The genes for color vision. Sci Am 260(2):42–49
3. Ahnelt P, Keri C, Kolb H (1990) Identification of pedicles of putative blue-sensitive cones in the human retina. J Comp Neurol 293(1):39–53
4. Curcio CA, Allen KA, Sloan KR, Lerea CL, Hurley JB, Klock IB et al (1991) Distribution and morphology of human cone photoreceptors stained with anti-blue opsin. J Comp Neurol 312(4):610–624
5. Xiao M, Hendrickson A (2000) Spatial and temporal expression of short, long/medium, or both opsins in human fetal cones. J Comp Neurol 425(4):545–559
6. Yan Q, Bumsted K, Hendrickson A (1995) Differential peanut agglutinin lectin labeling for S and L/M cone matrix sheaths in adult primate retina. Exp Eye Res 61(6):763–766
7. Rohlich P, Szel A, Johnson LV, Hageman GS (1989) Carbohydrate components recognized by the cone-specific monoclonal antibody CSA-1 and by peanut agglutinin are associated with red and green-sensitive cone photoreceptors. J Comp Neurol 289(3):395–400
8. Hendrickson A, Troilo D, Djajadi H, Possin D, Springer A (2009) Expression of synaptic and phototransduction markers during photoreceptor development in the marmoset monkey *Callithrix jacchus*. J Comp Neurol 512(2):218–331
9. Bumsted K, Hendrickson A (1999) Distribution and development of short-wavelength cones differ between Macaca monkey and human fovea. J Comp Neurol 403(4):502–516
10. Curcio CA, Sloan KR Jr, Packer O, Hendrickson AE, Kalina RE (1987) Distribution of cones in human and monkey retina: individual variability and radial asymmetry. Science 236(4801):579–582
11. Roorda A, Metha AB, Lennie P, Williams DR (2001) Packing arrangement of the three cone classes in primate retina. Vision Res 41(10–11):1291–1306
12. Zhang Y, Li A, Zhu X, Wong CH, Brown B, Craft CM (2001) Cone arrestin expression and induction in retinoblastoma cells. In: Hollyfield JG, Anderson RE, LaVail MM (eds) Retinal degeneration diseases and experimental therapy. Kluwer Academic: Plenum Publishers, New York, pp 309–318

13. Brown BM, Ramirez T, Rife L, Craft CM (2010) Visual arrestin 1 Contributes to cone photoreceptor survival and light adaptation. Invest Ophthalmol Vis Sci 51(5):2372–2380
14. Nir I, Ransom N (1992) S-antigen in rods and cones of the primate retina: different labeling patterns are revealed with antibodies directed against specific domains in the molecule. J Histochem Cytochem 40(3):343–352
15. Nikonov SS, Brown BM, Davis JA, Zuniga FI, Bragin A, Pugh EN Jr et al (2008) Mouse cones require an arrestin for normal inactivation of phototransduction. Neuron 59(3):462–474
16. Zhu X, Li A, Brown B, Weiss ER, Osawa S, Craft CM (2002) Mouse cone arrestin expression pattern: light induced translocation in cone photoreceptors. Mol Vis 8:462–471
17. Zhang H, Cuenca N, Ivanova T, Church-Kopish J, Frederick JM, MacLeish PR et al (2003) Identification and light-dependent translocation of a cone-specific antigen, cone arrestin, recognized by monoclonal antibody 7G6. Invest Ophthalmol Vis Sci 44(7):2858–2867
18. Mears AJ, Kondo M, Swain PK, Takada Y, Bush RA, Saunders TL et al (2001) Nrl is required for rod photoreceptor development. Nat Genet 29(4):447–452
19. Haider NB, Jacobson SG, Cideciyan AV, Swiderski R, Streb LM, Searby C et al (2000) Mutation of a nuclear receptor gene, NR2E3, causes enhanced S cone syndrome, a disorder of retinal cell fate. Nat Genet 24(2):127–131
20. Calkins DJ, Sterling P (1999) Evidence that circuits for spatial and color vision segregate at the first retinal synapse. Neuron 24(2):313–321
21. Dacey DM, Packer OS (2003) Colour coding in the primate retina: diverse cell types and cone-specific circuitry. Curr Opin Neurobiol 13(4):421–427
22. Bumsted O'Brien KM, Cheng H, Jiang Y, Schulte D, Swaroop A, Hendrickson AE (2004) Expression of photoreceptor-specific nuclear receptor NR2E3 in rod photoreceptors of fetal human retina. Invest Ophthalmol Vis Sci 45(8):2807–2812

# Chapter 8
# Exploration of Cone Cyclic Nucleotide-Gated Channel-Interacting Proteins Using Affinity Purification and Mass Spectrometry

**Xi-Qin Ding, Alexander Matveev, Anil Singh, Naoka Komori and Hiroyuki Matsumoto**

**Abstract** Photopic (cone) vision essential for color sensation, central vision, and visual acuity is mediated by the activation of photoreceptor cyclic nucleotide-gated (CNG) channels. Naturally occurring mutations in the cone channel subunits CNGA3 and CNGB3 are associated with achromatopsia and cone dystrophies. This work investigated the functional modulation of cone CNG channel by exploring the channel-interacting proteins. Retinal protein extracts prepared from cone-dominant *Nrl*$^{-/-}$ mice were used in CNGA3 antibody affinity purification, followed by sodium dodecyl sulfate polyacrylamide gel electrophoresis (SDS-PAGE) separation and matrix-assisted laser desorption/ionization time-of-flight (MALDI-TOF) mass spectrometry analysis. The peptide mass fingerprinting of the tryptic digests and database search identified a number of proteins including spectrin alpha-2, ATPase ($Na^+/K^+$ transporting) alpha-3, alpha and beta subunits of ATP synthase ($H^+$ transporting, mitochondrial F1 complex), and alpha-2 subunit of the guanine nucleotide-binding protein. In addition, the affinity-binding assays demonstrated an interaction between cone CNG channel and calmodulin but not cone $Na^+/Ca^{2+}$–$K^+$ exchanger in the mouse retina. Results of this study provide insight into our understanding of cone CNG channel-interacting proteins and the functional modulations.

**Keywords** CNG channel · Cone · Photoreceptor · Retina · Achromatopsia · Mass spectrometry

X.-Q. Ding (✉) · A. Matveev
Departments of Cell Biology, University of Oklahoma Health Sciences Center,
940 Stanton L. Young Blvd., BMSB 553,
Oklahoma City, OK 73104 USA
e-mail: xi-qin-ding@ouhsc.edu

A. Matveev
e-mail: xi-qin-ding@ouhsc.edu

A. Singh · N. Komori · H. Matsumoto
Departments of Cell Biology, University of Oklahoma Health Sciences Center,
940 Stanton L. Young Blvd., BMSB 553,
Oklahoma City, OK 73104 USA

J. D. Ash et al. (eds.), *Retinal Degenerative Diseases,* Advances in Experimental Medicine and Biology 801, DOI 10.1007/978-1-4614-3209-8_8,

## 8.1 Introduction

The photoreceptor cyclic nucleotide-gated (CNG) channels are operated by binding of cyclic guanosine mononucleotide (cGMP) and are fundamental to visual function. Phototransduction mediated by cone CNG channel is essential for central and color vision and for visual acuity. Naturally occurring mutations in the cone CNG channel subunits CNGA3 and CNGB3 are associated with achromatopsia and cone dystrophy. Indeed, mutations in the cone CNG channel subunits account for 75% of achromatopsia patients. Nevertheless, our understanding of the functional modulation of cone CNG channel is limited, and little is known about the CNG channel-interacting proteins. The lack of understanding of cone CNG channel is primarily due to the difficulty of investigating the cone system in a mammalian retina since cones comprise only 3–5% of the total photoreceptor population. We have shown the robust expression of cone CNG channel and the lack of rod CNG channel in the cone-dominant *Nrl*$^{-/-}$ mice [1]. In this work, we explored potential cone CNG channel-interacting proteins using *Nrl*$^{-/-}$ retinas. By using affinity purification and mass spectrometry analysis, we identified several CNGA3-interacting proteins including spectrin alpha-2, ATPase ($Na^+/K^+$ transporting) alpha-3, and guanine nucleotide-binding protein G(o) subunit alpha-2. Using affinity-binding and chemical cross-linking assays, we demonstrated the interaction of cone CNG channel with calmodulin but not with cone $Na^+/Ca^{2+}$–$K^+$ exchanger 2 (NCKX2). The findings of this study shed light on the cone CNG channel's interaction with other proteins and the channel's functional modulation.

## 8.2 Materials and Methods

### *8.2.1 Animals, Antibodies, and Other Materials*

The *Nrl*$^{-/-}$ mouse line was provided by Dr. Anand Swaroop (National Eye Institute, Bethesda, MD). Wild-type mice (C57BL/6 background) were purchased from Charles River Laboratories (Wilmington, MA). All experiments and animal maintenance were approved by the local Institutional Animal Care and Use Committee (Oklahoma City, OK) and conformed to the guidelines on the care and use of animals adopted by the Society for Neuroscience and the Association for Research in Vision and Ophthalmology (Rockville, MD).

Rabbit polyclonal antibodies against mouse CNGA3 and mouse CNGB3 [1] were used in this study. Rabbit polyclonal antibody against NCKX2 was provided by Dr. Jonathan Lytton (University of Calgary Health Sciences Centre, Calgary, Canada). Chemical cross-linkers 1,4-bismaleimidyl-2,3-dihydroxybutane, thiol specific (BMDB) and bis-sulfosuccinimidyl suberate, amino-specific ($BS^3$) were purchased from Pierce (Rockford, IL). Calmodulin affinity resin and 8-pCPT-cGMP were purchased from Sigma-Aldrich (St. Louis, MO). All other chemicals were purchased from Sigma-Aldrich (St. Louis, MO), Bio-Rad (Hercules, CA) or Invitrogen (Carlsbad, CA).

### 8.2.2 Antibody Affinity Purification, Mass Spectrometry, and Tandem Mass Spectrometry (MS/MS) Analyses

Retinal protein extracts were prepared by 3-[(3-cholamidopropyl) dimethylammonio]-1-propanesulfonate (CHAPS) solubilization as described previously [1]. The anti-CNGA3 affinity column was generated by covalent cross-linking of the purified antibody to the cyanogen bromide (CNBr)-activated Sepharose 4B resin (Sigma-Aldrich, St. Louis, MO) following the manufacturer's instructions. The CHAPS-solubilized protein extracts were incubated with antibody resin at 4 °C, overnight, followed by wash and peptide elution. In the affinity purification experiments, the control assays with normal immunoglobulin G (IgG) were included. The affinity-purified products were resolved on a 4–12 % sodium dodecyl sulfate polyacrylamide gel electrophoresis (SDS-PAGE) and visualized by Coomassie blue staining. The mass spectrometry and MS/MS analyses were performed as described by Takemori et al. [2]. Briefly, the bands were excised, eluted, and subjected to in-gel trypsin digestion. The tryptic peptides were applied to a target plate for mass spectrometry analysis using a matrix-assisted laser desorption/ionization time-of-flight mass spectrometer (MALDI-TOF MS) (Voyager Elite; PerSeptive Biosystems, Framingham, MA), and analyzed with a MASCOT peptide mass fingerprinting program (Matrix Science, London; http://www.matrixscience.com) against the nonredundant mouse protein sequence data bank of the National Center for Biotechnology Information (NCBI).

### 8.2.3 Immunoprecipitation, Chemical Cross-Linking, and Calmodulin Binding

Immunoprecipitation assays with anti-NCKX2, anti-CNGA3 and anti-CNGB3 antibodies were performed as described previously [1]. Briefly, CHAPS-solubilized membrane proteins were incubated with antibody in solubilization buffer at 4 °C overnight. Protein-A sepharose beads were then added, and incubation continued at 4 °C for another 1°h. After adsorption, the beads were washed and the bound proteins were eluted with Laemmli sample buffer, followed by SDS-PAGE separation and immunoblotting.

Chemical cross-linking experiments were performed using retinal membrane preparations and chemical cross-linkers BMDB and $BS^3$ as described previously [1]. After cross-linking reaction, the intermediate crosslink products were identified by terminating the reaction with dithiothreitol (DTT, 500 μM; for BMDB) or tris(hydroxymethyl) amino methane (Tris-HCl, 500 mM, pH 7.5; for $BS^3$). Cross-linking products were then resolved on 3–8 % Nu-PAGE, and analyzed by immunoblotting.

Calmodulin binding to cone CNG channel was examined using calmodulin affinity resin as described previously [1]. Briefly, CHAPS-solubilized retinal membrane proteins were incubated with calmodulin affinity resin in CHAPS-binding buffer in the presence and absence of ethylenediaminetetraacetic acid (EDTA, 5.0 mM) at

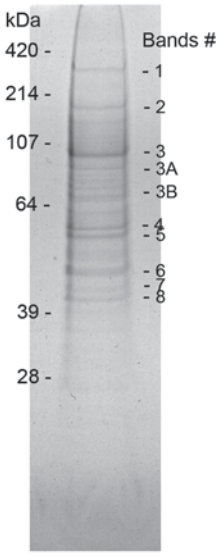


**a**

**b**

| Band # in Figure | Observed MW (kDa) | Protein | Theoretical MW/PI | NCBI Accession # | PMF MOWSE score | Sequence coverage (%) |
|---|---|---|---|---|---|---|
| 1 | 300 | Spectrin alpha 2 mCG18286 | 283715/5.2 289940/5.25 | 126540868 148676482 | 102 112 | 12 12 |
| 2 | | There are some peaks, but no positive results | | | | |
| 3 | 98 | ATPase, Na+/K+ transporting, alpha 3 | 113396/5.26 | 19855078 | 68 | 21 |
| 3A | 85 | aconitase 2, mitochondreal | 86334/8.08 | 18079339 | 108 | 27 |
| 3B | | There are some peaks, but no positive results | | | | |
| 4 | 56 | ATP synthase, H+ transporting, mitochondrial F1 complex, alpha subunit | 54703/8.24 | 148677501 | 112 | 36 |
| 5 | 52 | ATP synthase, H+ transporting, mitochondrial F1 complex, beta subunit | 56265/5.19 | 31980648 | 114 | 38 |
| 6 | | There are some peaks, but no positive results | | | | |
| 7 | 44 | Guanine nucleotide-binding protein G (o) subunit alpha 2 | 40650/5.69 | 120979 | 57 | 29 |
| 8 | | There are some peaks, but no positive results | | | | |

**Fig. 8.1** Identification of cone CNG channel-interacting proteins using immunoaffinity purification and MALDI-TOF MS analysis. **a** Coomassie blue-stained SDS–PAGE gel of proteins separated from affinity purification using *Nrl*$^{-/-}$ retinal extracts. Band numbers of excised bands subjected to mass spectrometric analysis are shown and correspond to those indicated in panel b. **b** List of identified proteins from CNGA3 immunoaffinity purification and MALDI-TOF MS analysis. *MW* molecular weight, *PI* isoelectric point, *PMF* peptide mass fingerprinting

4 °C for 2 h, followed by wash and elution with Laemmli sample buffer. The bound proteins were resolved by 10 % SDS-PAGE and analyzed by immunoblotting.

## 8.3 Results

### *8.3.1 Identification of Cone CNG Channel-Interacting Proteins Using Affinity Purification and MALDI-TOF MS Analysis*

The CNGA3 antibody affinity purifications resulted in several bands on the SDS-PAGE gel visualized by Commassie blue staining (Fig. 8.1a). The protein bands were excised, digested with trypsin, and subjected to MALDI-TOF MS analysis.

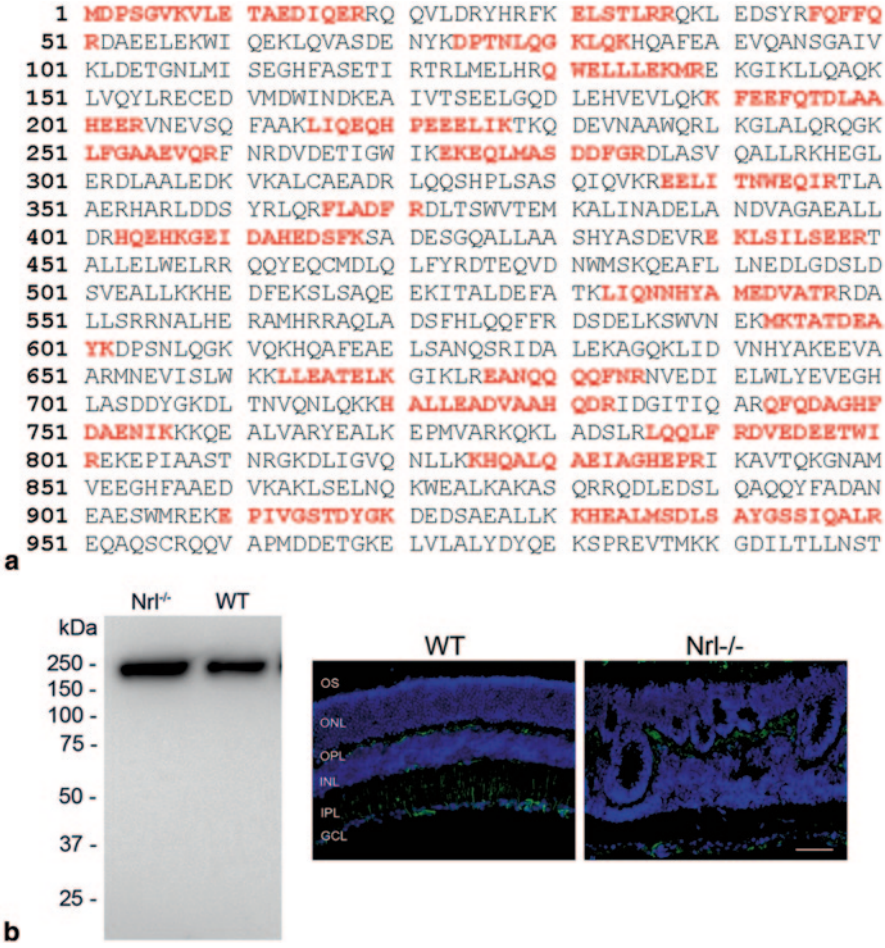


**Fig. 8.2** Spectrin alpha-2 peptide sequence with amino acids identified by MALDI-TOF. **a** In *red*, amino acid sequence of spectrin alpha-2 showing the peptide sequences matching the spectrum peaks obtained from MALDI-TOF. Due to the space limitation, only the sequence 1 through 1000 of sepctrin alpha-2 peptide (full-length peptide has 2457 amino acid residues) is shown. **b** Immunoblotting (*left panel*) and immunofluorescence labeling (*right panel*) showing expression of spectrin alpha-2 in retinas from Nrl knockout (Nrl-/-) and wild type (WT) mice

Using peptide mass fingerprinting of the tryptic digests and database search, we identified several proteins including spectrin alpha-2, ATPase ($Na^+/K^+$ transporting) alpha-3, and guanine nucleotide-binding protein G(o) subunit alpha-2 (Fig. 8.1b). Spectrin alpha-2 was identified with the highest-probability-based MOWSE scores (scores: 195 and 191 in two independent experiments) where the scores corresponded to the probability of $p < 0.05$. Figure 8.2a shows the amino acid sequences in the spectrin alpha-2 peptide with matched amino acid sequences marked in red color. About 25% of spectrin alpha-2 sequences were identified. Expression of spectrin alpha-2 in the mouse retinas was shown by immunoblotting and immunofluorescence labeling (Fig. 8.2b).

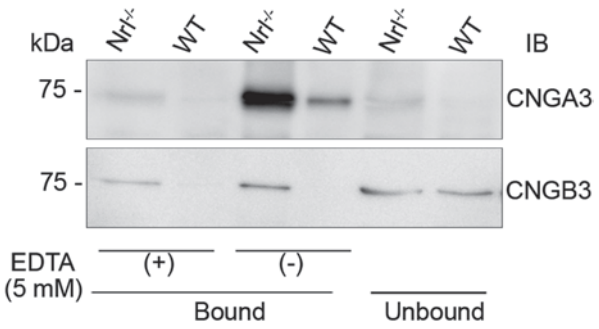


**Fig. 8.3** Binding of calmodulin to cone CNG channel in the mouse retina. Representative images of Western blot (IB) using antibodies to CNGA3 or CNGB3 against proteins bound to calmodulin affinity-binding products. (Adapted from [1])

### *8.3.2 Binding of Calmodulin to Cone CNG Channel in the Mouse Retina*

Calcium-binding protein calmodulin is an important modulator for olfactory and rod CNG channels [3, 4]. However, its role in cone CNG channel remains unclear. We examined calmodulin binding to cone CNG channel in the mouse retina using calmodulin affinity resin. In the binding assays, we observed a strong binding signal for CNGA3 and a weak binding for CNGB3 (Fig. 8.3). Addition of EDTA abolished the binding, demonstrating a specific, $Ca^{2+}$-dependent binding.

### *8.3.3 Lack of Interaction Between Cone CNG Channel and NCKX2 in the Mouse Retina*

Photoreceptor CNG channel is the only known source for $Ca^{2+}$ influx into the outer segments. Interaction of rod CNG channel with Na/Ca–K exchanger 1 (NCKX1) and the functional significance of such association in control of the intracellular $Ca^{2+}$ concentration and dynamics of $Ca^{2+}$ homeostasis have been well characterized [5, 6]. Little is known about the association between cone CNG channel and NCKX2. Hence, we examined the potential interaction between CNGA3 and NCKX2 by co-immunoprecipitation and chemical cross-linking. As shown in Fig. 8.4a, no NCKX2 signal was detected in the CNGA3 immunoprecipitation assays though interaction between CNGA3 and CNGB3 was detected. In the NCKX2 immunoprecipitation assays, abundant amount of NCKX2 was detected but no signal of CNGA3 or CNGB3 was detected (Fig. 8.4a). Thus, co-immunoprecipitation assays with antibodies against CNGA3 or against NCKX2 did not show evidence of interaction between the cone channel and this type of exchanger. The potential interaction of cone CNG channel with NCKX2 was also examined by chemical cross-linking. Though association between CNGA3 and CNGB3 was demonstrated, no NCKX2-associated cross-linking products were detected in these assays (Fig. 8.4b).

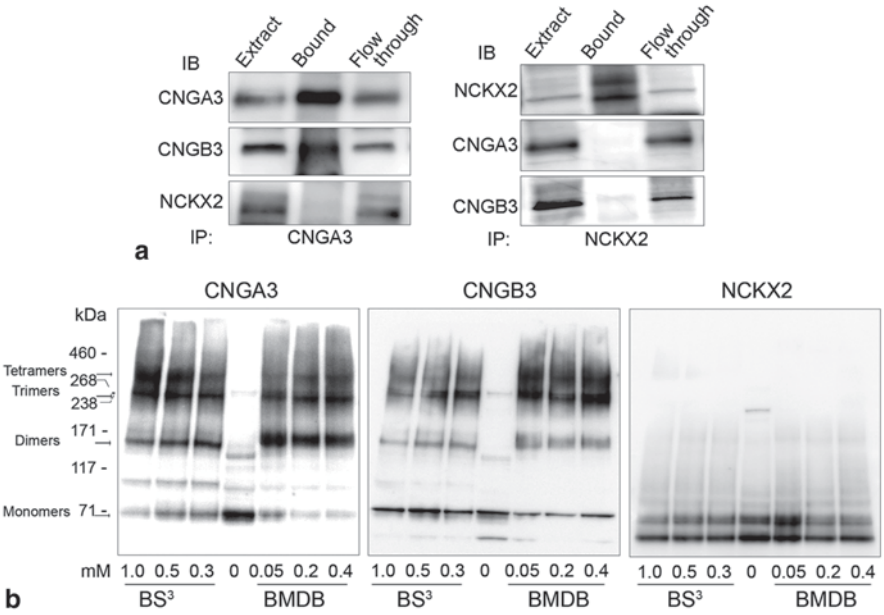


**Fig. 8.4** Lack of interaction between cone CNG channel and NCKX2 in the mouse retina. **a** Representative images of immunoblotting for detection of immunoprecipitation products. **b** Representative images of immunoblotting for detection of chemical cross-linking products. (Adapted from [1]). IB and IP indicates antibodies used in the immunoblot or immunoprecipitation respectively

## 8.4 Discussion

This work explores cone CNG channel-interacting proteins in order to understand the channel's functional modulation. By using affinity purification and mass spectrometry analysis, we identified several cone channel-interacting proteins. Spectrin alpha-2 was identified with the highest probability-based MOWSE scores. Spectrins are ~200–400 kDa proteins that form extended, flexible protein dimers and contain actin-binding domains. Spectrin dimers composed of alpha- and beta-subunits associate laterally to form heterotetramers that are linked to short actin filaments, and the spectrin-actin network is coupled to the plasma membrane primarily by association with the adaptor protein ankyrin [7]. Spectrin has been recognized as a ubiquitous scaffolding protein that acts in conjunction with a variety of adaptor proteins to organize membrane microdomains on both the plasma membrane and on intracellular organelles [8]. Indeed, spectrin-ankyrin *cytoskeletons* have been shown to interact with the transient receptor potential cation 4 (TRPC4) channel [9], bind to the N-methyl-D-aspartate (NMDA) receptor [8], and regulate sodium channel clustering. More interestingly, ankyrin-promoting CNG channel transport to rod outer segment has been demonstrated recently [10]. The finding of spectrin-ankyrin network association with a subcompartment of the endoplasmic reticulum in honeybee photoreceptors [11] also supports its role in the channel complex trafficking

in photoreceptors. This work identified spectrin alpha-2 subunit as one of the most promising channel-interacting proteins, supporting a role of spectrin-ankyrin network in the cone channel's cellular trafficking.

Calmodulin is known as an important negative modulator for olfactory and rod CNG channels [4]. However, its role in cone CNG channel is less understood although the binding motif has been demonstrated in CNGA3 and CNGB3 in various in vitro binding assays [12, 13]. This work examined binding of calmodulin to cone CNG channel complexes in the mouse retina and demonstrated its binding to both CNGA3 and CNGB3, supporting a potential role of calmodulin in the channel's functional modulation in cones.

The potential interaction between cone CNG channel and NCKX2 was also examined in this study. Cone specific expression of NCKX2 was detected in *Nrl*$^{-/-}$ retina, but no evidence of such interaction was obtained as analyzed by co-immunoprecipitation and chemical cross-linking assays. The observation of the lack of interaction between the cone channel and cone exchanger is in agreement with the report showing a normal retinal phenotype in *Nckx2*$^{-/-}$ mice [14]. Thus, NCKX2 may not be the major component required for $Ca^{2+}$ extrusion in cones, and a distinct modulatory mechanism of $Ca^{2+}$ influx and efflux may exist.

**Acknowledgments** This work was supported by grants from the National Center for Research Resources (P20RR017703), the National Eye Institute (EY12190, EY019490, and EY17888), and the Oklahoma Center for the Advancement of Science & Technology (OCAST). We thank Drs. Anand Swaroop and Jonathan Lytton for providing *Nrl*$^{-/-}$ mouse line and anti-NCKX2 antibody, respectively.

## References

1. Matveev AV, Quiambao AB, Browning Fitzgerald J, Ding XQ (2008) Native cone photoreceptor cyclic nucleotide-gated channel is a heterotetrameric complex comprising both CNGA3 and CNGB3: a study using the cone-dominant retina of *Nrl*$^{-/-}$ mice. J Neurochem 106:2042–2055
2. Takemori N, Komori N, Thompson JN Jr, Yamamoto MT, Matsumoto H (2007) Novel eye-specific calmodulin methylation characterized by protein mapping in *Drosophila melanogaster*. Proteomics 7:2651–2658
3. Kaupp UB, Seifert R (2002) Cyclic nucleotide-gated ion channels. Physiol Rev 82:769–824
4. Trudeau MC, Zagotta WN (2002) Mechanism of calcium/calmodulin inhibition of rod cyclic nucleotide-gated channels. Proc Natl Acad Sci USA 99:8424–8429
5. Kang K, Schnetkamp PP (2003) Signal sequence cleavage and plasma membrane targeting of the retinal rod NCKX1 and cone NCKX2 $Na^+/Ca^{2+}$-$K^+$ exchangers. Biochemistry 42:9438–9445
6. Paillart C, Winkfein RJ, Schnetkamp PP, Korenbrot JI (2007) Functional characterization and molecular cloning of the $K^+$-dependent $Na^+/Ca^{2+}$ exchanger in intact retinal cone photoreceptors. J Gen Physiol 129:1–16
7. Bennett V, Baines AJ (2001) Spectrin and ankyrin-based pathways: metazoan inventions for integrating cells into tissues. Physiol Rev 81:1353–1392
8. Wechsler A, Teichberg VI (1998) Brain spectrin binding to the NMDA receptor is regulated by phosphorylation, calcium and calmodulin. EMBO J 17:3931–3939

9. Odell AF, Van Helden DF, Scott JL (2008) The spectrin cytoskeleton influences the surface expression and activation of human transient receptor potential channel 4 channels. J Biol Chem 283:4395–4407
10. Kizhatil K, Sandhu NK, Peachey NS, Bennett V (2009) Ankyrin-B is required for coordinated expression of beta-2-spectrin, the Na/K-ATPase and the Na/Ca exchanger in the inner segment of rod photoreceptors. Exp Eye Res 88:57–64
11. Baumann O (1998) Association of spectrin with a subcompartment of the endoplasmic reticulum in honeybee photoreceptor cells. Cell Motil Cytoskelet 41:74–86
12. Muller F, Vantler M, Weitz D, Eismann E, Zoche M, Koch KW, Kaupp UB (2001) Ligand sensitivity of the 2 subunit from the bovine cone cGMP-gated channel is modulated by protein kinase C but not by calmodulin. J Physiol 532:399–409
13. Peng C, Rich ED, Thor CA, Varnum MD (2003) Functionally important calmodulin-binding sites in both $NH_2$- and COOH-terminal regions of the cone photoreceptor cyclic nucleotide-gated channel CNGB3 subunit. J Biol Chem 278:24617–24623
14. Li XF, Kiedrowski L, Tremblay F, Fernandez FR, Perizzolo M, Winkfein RJ, Turner RW, Bains JS, Rancourt DE, Lytton J (2006) Importance of $K^+$-dependent $Na^+/Ca^{2+}$-exchanger 2, NCKX2, in motor learning and memory. J Biol Chem 281:6273–6282

# Chapter 9
# Electrophysiological Characterization of Rod and Cone Responses in the Baboon Nonhuman Primate Model

**Michael W. Stuck, Shannon M. Conley, Ryan A. Shaw, Roman Wolf and Muna I. Naash**

**Abstract** Many monogenic retinal diseases target the human macula, and evaluating genetic treatments for these diseases in rodent models which lack a macula can be limiting. To better test the likelihood that novel treatments will be relevant to patients, assessing expression and distribution may be undertaken in a nonhuman primate (NHP) model. The purpose of this study was to establish baseline functional characteristics in the baboon (*Papio anubis*) eye to establish a control dataset for future experiments testing novel genetic therapies. Electroretinography (ERG) was conducted on 12 young (~3 years of age) dark-adapted baboons. Scotopic responses were measured in response to a series of light intensities followed by a 10-min period of light adaptation after which photopic responses were measured following the same series of light intensities. At the highest flash intensity, scotopic amplitudes were 334±10 μV and 458±15 μV for a- and b-waves, respectively. At the highest flash intensity, photopic amplitudes were 82±5 μV and 81±4 μV for a- and b-waves, respectively. Waveforms for scotopic responses were similar in

M. I. Naash (✉) · M. W. Stuck · S. M. Conley · R. A. Shaw
Department of Cell Biology, University of Oklahoma Health Sciences Center,
940 Stanton L. Young Blvd., BMSB 781,
73104 Oklahoma City, OK, USA
e-mail:muna-naash@ouhsc.edu

M. W. Stuck
e-mail: Michael-stuck@ouhsc.edu

S. M. Conley
e-mail: Shannon-conley@ouhsc.edu

R. A. Shaw
e-mail: ryan-shaw@ouhsc.edu

R. Wolf
Department of Comparative Medicine, University of Oklahoma
Health Sciences Center, 940 Stanton L. Young Blvd., BMSB 781,
73104 Oklahoma City, OK, USA
e-mail: roman-wolf@ouhsc.edu

J. D. Ash et al. (eds.), *Retinal Degenerative Diseases,* Advances in Experimental Medicine and Biology 801, DOI 10.1007/978-1-4614-3209-8_9,

shape to rodent scotopic responses. In contrast, photopic baboon waveforms were quite different in shape from those of rodents and were more similar to waveforms recorded from humans or other NHPs. These results are consistent with the differences in the photopic visual system in rodents versus primates (presence of a macula) and provide an excellent baseline for future studies testing novel therapies in the baboon model.

**Keywords** Baboon · Gene therapy · Nonhuman primate · ERG

**Abbreviations**

| | |
|---|---|
| NHP | Nonhuman primate |
| ERG | Electroretinography |

## 9.1 Introduction

Human color vision and high-resolution central vision is accomplished through the macula; a specialized retinal structure of high cone density [1]. Disruption of this region by genetic defects causes a debilitating group of retinal diseases which lead to significant vision loss and blindness. Many of the genetic defects that lead to inherited macular dystrophies have been identified; however, effective treatments for patients afflicted with these diseases are still lacking. Gene therapy is a promising approach that is currently being developed. Replacement of the defective gene to repair the cellular machinery necessary for normal vision holds the potential to cure many of these inherited genetic defects if the treatment is effective and can be delivered prior to significant loss of retinal cells [2].

The majority of gene therapy work has been done in species such as the mouse that can be easily manipulated genetically and have high fecundity [3]. Through the use of these models, effective techniques and potential treatments have been developed that involve the intravitreal or subretinal injection of viral or non-viral particles containing genetic cargo [4, 5]. Unfortunately, these models have a significantly different retinal topography from humans. Rodent models completely lack a macular region, which is limited to humans and nonhuman primates (NHPs) [3]. Certain critical issues cannot be addressed using models that have small eyes and lack a macula. First, the anatomy of the macula makes targeting macular cones difficult, so assessing the ability of genetic therapies to generate sufficient distribution of expression in the primate model (in contrast to the small eye of the rodent) is important. Second, macular cones have been shown to be extremely sensitive to disruption from subretinal injection. Injection-associated damage has been a primary concern in gene therapy clinical trials, and the good recovery most rodents exhibit after subretinal injection has made it a difficult problem to study in lower organisms. Developing genetic therapies that can target macular cones after intravitreal or non-macular subretinal injection is a critical step and relies on testing in NHPs.

With the goal of using an NHP model for assessment of the efficacy of therapeutic delivery, we established an electroretinography (ERG) protocol and evaluated baseline ERG values for the baboon eye. Baboons have some advantages over other primate species; in particular their body and eye size is closer to humans than that of other monkeys. Our results show that baboon scotopic and photopic ERG responses are similar in shape and magnitude to previously reported human ERGs.

## 9.2 Materials and Methods

### *9.2.1 Animal Handling*

All baboons were housed and cared for according to the standards detailed in the Guide for the Care and Use of Laboratory Animals (National Research Council 1996) and the Association for Assessment and Accreditation of Laboratory Animal Care International (AAALAC). They were fed Harlan primate diet 2055 as well as fresh fruit, vegetables, trail-mix, and dry cereal. Potable water was available ad libitum from automatic waterers. All baboons receive daily health checks by the responsible animal care technicians for each area. Considerable effort is placed toward promoting psychological well-being and providing environmental enhancement for the baboon colonies. Procedures used here have been approved by the University of Oklahoma Health Sciences Center (OUHSC) Institutional Animal Care and Use Committee.

ERGs were performed in an aseptic surgical suite. The baboons were first dark adapted overnight. One of the faculty veterinarians (Dr. Wolf) anesthetized the baboons using a mixture of ketamine (10 mg/kg) and xylazine (1 mg/kg) administered intramuscularly and, along with veterinary staff, remained in the operating room to monitor the health of the animal before, during, and after the procedure. After anesthetizing the animal, the pupil was dilated using 1 % cyclopentolate hydrochloride (Pharmaceutical Systems, Inc., Tulsa OK). The animal was placed in ventral recumbency on a procedure table, and body temperature was maintained using a heated water blanket. The animal's head rested on a stand sized to fit into the ERG ganzfeld (UTAS Visual Diagnostic System with BigShot™ Ganzfeld, LKC Technologies, Inc., Gaithersburg, MD, USA). The reference electrode was placed under the skin in the medial region just above the orbital ridge of the baboon. The ground electrode was placed under the skin near the base of the skull. The eye electrodes used were disposable ERG-jet contact lens electrodes (Micro Components, Grenchen, Switzerland). Eye electrodes were replaced after every two animals. Animals were subjected to a scotopic series of tests followed by a photopic series of tests with an intervening 10-min light adaptation at a rod desensitizing intensity of 30 cd/m$^2$. During this light adaptation, the veterinary staff administered a booster shot of ketamine and xylazine. The whole procedure took approximately 50–60 min per animal. After the ERGs, the electrodes were removed and a triple antibiotic ophthal-

mic ointment (Vetropolycin; Dechra Veterinary Products, Overland Park, KS) was administered to each eye. Post-operative care was managed by a veterinarian and included the administration of the analgesic buprenorphine (0.01 mg/kg I.M. b.i.d.) as necessary. To minimize distress caused by the isolation during the procedure, the animal was returned to the colony/cagemate as soon as possible after full recovery from anesthesia.

### *9.2.2 ERG Protocol*

For scotopic evaluation, a series of ten tests using a single, white light flash was administered to each baboon. The flashes were −3.62, −2.35, −1.77, −1.43, −0.99, −0.996, 0.612, 1.38, 2.14, and 2.86 log cd-s/$m^2$ in intensity. The protocol began at the lowest intensity and moved up with a 2-min wait between each flash. All scotopic tests were performed in a completely dark room. After light adaptation, a series of ten tests were administered using 25 flashes at 2.1 Hz. For each test the individual responses from all 25 flashes were averaged to obtain an individual photopic waveform. The intensities for photopic recording were the same as for scotopic, and again there was a 2-min wait between tests.

### *9.2.3 ERG Analysis*

Analysis used the EMWIN software (LKC Technologies). The a-wave amplitude was determined by measuring from the baseline to the bottom of the a-wave trough for both scotopic and photopic responses. The b-wave amplitude was determined by measuring from the bottom of the a-wave trough to the highest point of the b-wave for both scotopic and photopic responses. Values are shown as means +/− SEM.

## 9.3 Results and Discussion

### *9.3.1 Scotopic ERG Response*

ERGs were performed on 12 baboons of ~3 years of age. The scotopic waveforms were similar in shape to what has been observed in both humans and rodents [6, 7]. At low flash intensities only a second-order neuronal response (b-wave) is detectable (Fig. 9.1a). At approximately −1.43 log cd-s/$m^2$ the rod photoreceptor a-wave is visible with a mean amplitude (±SEM) of 16 ± 1 μV and becomes significantly more pronounced at −0.40 log cd-s/$m^2$ with a mean amplitude of 73 ± 3 μV. A-wave amplitudes continued to increase up to the maximum intensity tested (2.86 log cd-s/$m^2$) with a maximum value of 334 ± 10 μV (Fig. 9.1b). Scotopic a-wave amplitudes

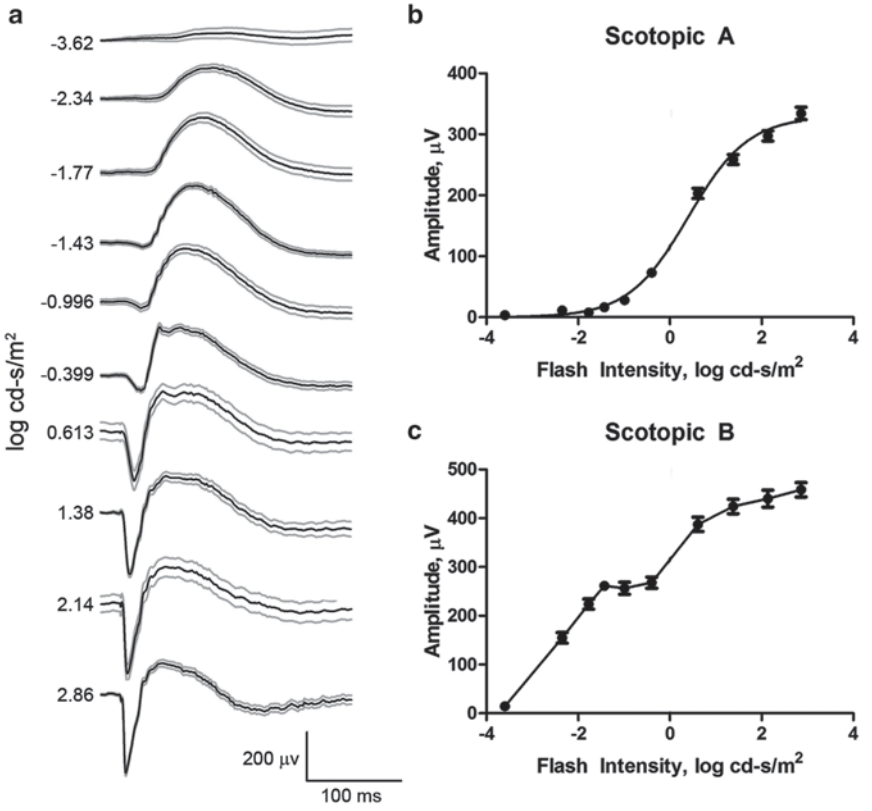


**Fig. 9.1** Scotopic ERGs. **a** Mean waveforms (*black line*) generated by averaging individual traces from all scotopic ERGs. *Grey lines* represent the standard error. Mean scotopic a-wave (**b**) and b-wave (**c**) amplitude (µV, ± SEM) plotted relative to flash intensity. $N = 12$ baboons

fit a sinusoidal curve when plotted against flash intensity, consistent with expected rod responses (Fig. 9.1b). While scotopic b-wave amplitudes also increase with flash intensity, they do not exhibit this shape (Fig. 9.1c).

### *9.3.2 Photopic ERG Response*

Photopic ERG waveforms from the baboon (Fig. 9.2a) are quite different in shape from rodent responses. They are similar in shape to human waveforms, consistent with the differences in the photopic visual system in rodents versus primates. The photopic a-wave is first detectable at −0.40 log cd-s/m$^2$ (13 ± 1 µV) and becomes more pronounced as the flash intensities increase with a maximum amplitude of 82 ± 5 µV at 2.86 log cd-s/m$^2$ (Fig. 9.2b). The photopic a-wave responses also fit a sinusoidal distribution, consistent with being photoreceptor (cone in this case) in

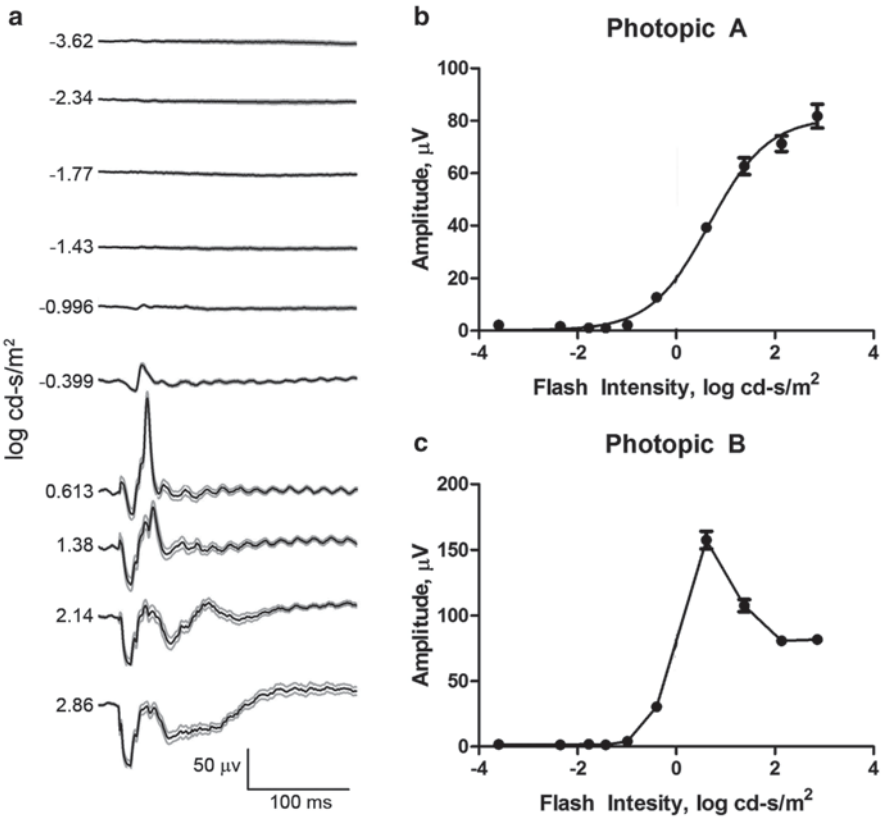


**Fig. 9.2** Photopic ERGs. **a** Mean waveforms (*black line*) generated by averaging individual traces from all photopic ERGs. *Grey lines* represent the standard error. Mean scotopic a-wave (**b**) and b-wave (**c**) amplitude (μV, ± SEM) plotted relative to flash intensity. $N = 9$ baboons

origin. Photopic second-order neuron responses peak at 0.62 log cd-s/m$^2$ with an amplitude of 157 ± 7 μV before dropping with increased flash intensity to a mean value of 82 ± 3 μV at 2.86 log cd-s/m$^2$ (Fig. 9.2c). This "photopic hill" effect is also seen in humans [8]. The b-wave amplitude is primarily a combination of positive signals from the ON and OFF second-order neuron pathways, and the photopic hill is thought to be tied to a reduction in the magnitude of the ON- and a delay in the peak of the OFF-pathway contributions as flash intensity increases [9].

## 9.4 Conclusions

The lack of a macula in rodent models commonly used in biomedical research has been a great hindrance to the development of clinically effective gene therapies for macular pathologies. The ability to assess safety of the delivery procedure, immune

response to the drug, and levels and distribution of gene expression in a model that has similar ocular architecture to humans is highly valuable. Our data clearly show that ERG is a suitable technique for functional analysis of the baboon eye; importantly, this technique is non-invasive, simple to perform with readily available equipment and trained personnel, and requires no behavioral training. Furthermore, our data show that the ERG responses of the baboon are similar in shape and magnitude to that of humans [7], underscoring the value of this species as a good model for the human eye. The work provides a functional baseline for the baboon eye, thus facilitating its use in subsequent ocular gene therapy experiments, and hopefully accelerating the translation of novel therapies from the bench to the clinic.

**Acknowledgments** The authors thank Dr. Gary White and the staff of the OUHSC Baboon Research Resource, especially Mr. David Carey, for their technical support. This work was supported by the NIH (R01EY18656, R01EY022778, P40RR12317), the Foundation Fighting Blindness, and the Oklahoma Center for the Advancement of Science and Technology. Content is solely the responsibility of the authors and does not necessarily represent the official views of the National Institutes of Health.

## References

1. Mustafi D, Engel AH, Palczewski K (2009) Structure of cone photoreceptors. Prog Retin Eye Res 28(4):289–302
2. Han Z, Conley SM, Naash MI (2011) AAV and compacted DNA nanoparticles for the treatment of retinal disorders: challenges and future prospects. Invest Ophthalmol Vis Sci 52(6):3051–3059
3. Pennesi ME, Neuringer M, Courtney RJ (2012) Animal models of age related macular degeneration. Mol Aspects Med 33(4):487–509
4. Cai X, Conley SM, Naash MI (2010) Gene therapy in the Retinal Degeneration Slow model of retinitis pigmentosa. Adv Exp Med Biol 664:611–619
5. Mowat FM, Breuwer AR, Bartoe JT, Annear MJ, Zhang Z, Smith AJ, Bainbridge JW, Petersen-Jones SM, Ali RR (2013) RPE65 gene therapy slows cone loss in Rpe65-deficient dogs. Gene Ther 20(5):545–555
6. Chakraborty D, Ding XQ, Conley SM, Fliesler SJ, Naash MI (2009) Differential requirements for retinal degeneration slow intermolecular disulfide-linked oligomerization in rods versus cones. Hum Mol Genet 18(5):797–808
7. Freund PR, Watson J, Gilmour GS, Gaillard F, Sauve Y (2011) Differential changes in retina function with normal aging in humans. Doc Ophthalmol 122(3):177–190
8. Freund PR, Watson J, Gilmour GS, Gaillard F, Sauve Y (2011) Differential changes in retina function with normal aging in humans. Doc Ophthalmol 122(3):177–190
9. Ueno S, Kondo M, Niwa Y, Terasaki H, Miyake Y (2004) Luminance dependence of neural components that underlies the primate photopic electroretinogram. Invest Ophthalmol Vis Sci 45(3):1033–1040

# Part II
# Basic Processes: RPE

# Chapter 10
# Animal Models, in "*The Quest to Decipher RPE Phagocytosis*"

**Emeline F. Nandrot**

**Abstract** Renewal and elimination of aged photoreceptor outer segment (POS) tips by cells from the retinal pigment epithelial (RPE) is a daily rhythmic process that is crucial for long-term vision. Anomalies can arise during any of the sequential steps required for completion of this phagocytic function, from POS recognition to complete digestion of POS components. During the past 15 years, many animal models helped us characterize the molecular machinery implicated in RPE phagocytosis as well as understand associated defects leading to various retinal pathologies. Depending on which part of the machinery is flawed, phenotypes can either appear early in life, such as retinitis pigmentosa or Usher syndrome, or develop with aging of the individual, like age-related macular degeneration, affecting first either the peripheral or the central retina. This chapter describes mouse and rat models related to defective phagocytosis, and how they have been a tremendous help for us to comprehend RPE phagocytosis, its rhythm, and its failures.

**Keywords** Retinal pigment epithelium · Photoreceptor outer segments · Phagocytosis · Circadian rhythm · Animal models

E. F. Nandrot (✉)
INSERM, U968, 17 rue Moreau, 75012 Paris, France
e-mail: emeline.nandrot@inserm.fr

E. F. Nandrot
Institut de la Vision, UPMC Univ Paris 06, UMR_S 968, 17 rue Moreau, 75012 Paris, France

CNRS, UMR_7210, 17 rue Moreau, 75012 Paris, France

J. D. Ash et al. (eds.), *Retinal Degenerative Diseases,* Advances in Experimental Medicine and Biology 801, DOI 10.1007/978-1-4614-3209-8_10,

## 10.1 Introduction

The existence of a renewal mechanism of the stacks of membranous disks in photoreceptor outer segments (POS) and subsequent aged POS tips elimination by retinal pigment epithelial (RPE) cells has been discovered in the 1960s [1]. Animal studies in rats revealed that rod phagocytosis peaks within 2 h after the light onset [2]. RPE cells serve between 20 and 40 POS, hence digesting POS tips constitutes an important daily job for RPE cells.

Various phenotypes are linked to phagocytic defects, ranging from early-onset retinal dystrophies such as retinitis pigmentosa (RP) to aging diseases like age-related macular degeneration (AMD). In this context, animal models have played a central role in the understanding of the phagocytic machinery, its timely regulation, and sequential activation. This chapter reviews the various phagocytic steps that are now better understood thanks to mice and rats (Table 10.1).

## 10.2 Animals Models and the Deciphering of the Phagocytic Machinery

### *10.2.1 POS Binding and Phagocytosis Synchronization*

One of the first proteins identified as playing a role in RPE phagocytosis, αvβ 5 is the only integrin receptor expressed at the RPE apical surface [3]. Its inhibition decreases POS binding and internalization, and it co-localizes with POS during phagocytosis in vitro. *β 5−/−* mice allowed us to show that α vβ 5 integrin receptors are responsible for the daily rhythm of retinal phagocytosis via the activation of MerTK receptors just after light onset [4]. Indeed, in *β 5−/−* mice the phagocytic peak is replaced by a steady-state level of phagosome numbers in RPE cells. This arrhythmia leads to the development of an aging phenotype close to AMD, including loss of vision and lipofuscin accumulation, most probably due to the gradual buildup of improperly digested materials. Surprisingly, no photoreceptor loss was detected even in older animals, suggesting that lipofuscin deposits alone are not sufficient to lead to cell loss. So far, no mutation in the *β 5 integrin* (*ITGB5*) gene has been associated with a retinal phenotype in humans.

The milk fat globule-EGF8 factor (MFG-E8) is one of the α vβ 3 integrin receptor ligands for macrophages, and α vβ 3 and α vβ 5 integrin receptors seem to function similarly in macrophages and RPE cells [5]. The availability of *Mfg-e8−/−* mice provided the link between MFG-E8 and α vβ 5 integrin receptors for the bridging of POS to RPE cells in vivo. *Mfg-e8−/−* mice replicated the loss of diurnal phagocytic rhythm observed in *β 5−/−* mice [6], but it was not accompanied by an aging phenotype.

**Table 10.1** Molecules of the RPE phagocytic machinery, related animal models and associated human phenotypes

| Protein | Function in RPE | Animal model | Retinal phenotype | Human disease |
|---|---|---|---|---|
| α vβ 5 Integrin receptor | POS binding<br>Phagocytic rhythm synchronization | *β 5*−/− mouse [4] | Phagocytic rhythm loss<br>Aging phenotype:<br>Decreased ERG<br>Lipofuscin accumulation<br>No PR loss | Unknown |
| MFG-E8 | αvβ5 integrin ligand<br>Phagocytic rhythm synchronization | *MFG-E8*−/− mouse [6] | Phagocytic rhythm loss<br>No aging phenotype | Unknown |
| MerTK receptor | Control of POS binding capacity | RCS rat [8, 9, 10] | No POS internalization | Atypical RP or RCD with macular lesions [11] |
| | Required for POS internalization | | By 3 months of age:<br>Complete PR loss<br>Flat ERG | CRD [12] |
| Gas6, Protein S | MerTK ligands (both required) | *ProS1* and *Gas6* DKO [15] | Moderate to severe retinal degeneration | Unknown |
| CD36 | Regulator of internalization dynamics | *CD36*−/− mouse [17, 18] | No phagocytic defect<br>RPE aging phenotype:<br>Oxidized LDL build-up<br>Bruch's membrane thickening | Unknown |
| Annexin 2 | Regulator of actin dynamics | *Anx2*−/− mouse [19] | Delay in phagosome transport | Present in drusens [20] |
| Myosin VIIA | Trafficking of phagosomes | Shaker1 (*myo7a*) mouse [21, 22, 23] | Organelle transport anomalies, slow phagosome degradation<br>Deafness, slightly decreased ERG | Usher Syndrome type 1B |
| Cathepsin D (CatD) | Lysosomal enzyme | *mcd/mcd* [25] and *mcd2/mcd2* mice [26] | Impaired phagosome degradation<br>RPE aging phenotype:<br>Lipofuscin granules<br>Basal deposits | Unknown |
| β A3/A1-Crystallin | Lysosomal component<br>Required for normal CatD levels | Nuc1 rat [27] | Impaired phagosome degradation<br>RPE aging phenotype:<br>Lipid accumulation<br>RPE cell displacement | Autosomal dominant zonular cataract |
| Melano-regulin | Required for lysosome maturation | *Mreg*−/− mouse [28] | Delayed phagosome degradation<br>Lipofuscin/A2E accumulation | Unknown |

*PR* photoreceptors, *DKO* double knockout

### *10.2.2 POS Internalization*

The most known and used rodent model is the RCS rat strain from the Royal College of Surgeons [7]. This rat develops a rapid loss of visual responses and death of photoreceptor cells between 3 weeks and 3 months of age. It was also shown that the defect originated in RPE cells that are not able to ingest shed POS provoking accumulation of POS debris. Thanks to a genomic deletion present in RCS rats, the MerTK tyrosine kinase was identified as the POS internalization receptor [8, 9]. More recently, analysis of primary RPE cells from RCS rats highlighted a novel role for MerTK in controlling the amounts of POS that can be bound by RPE cells [10]. In humans, mutations in the *MERTK* gene are quite rare and appear in various forms, from rod-cone dystrophies (RCD) with some macular defects [11] to cone-rod dystrophies (CRD) [12].

Gas6 and Protein S are the two cognate ligands for the MerTK family of tyrosine kinase receptors. Gas6 and Protein S were shown to be able to increase POS phagocytosis [13], and both ligands are expressed in the mouse retina [14]. Only very recently, the generation of multiple mouse models inactivated in *Gas6* and/or *Protein S* genes showed that both ligands are interchangeable and required in vivo [15]: Double knockouts develop a severe retinal degeneration while simple knockouts remain unaffected.

CD36 is a membrane receptor from the scavenger family that participates in POS phagocytosis by RPE cells seeming to intervene on the POS internalization speed post binding [16]. Primary cultures of *CD36*−/− RPE cells helped determine that CD36 receptors recognize photo-oxidized phospholipids that could serve as POS ligands [17]. Surprisingly, *CD36*−/− mouse retinas' morphology and RPE cells' phagocytosis were similar to wild type animals. However, *CD36*−/− mice accumulated oxidized LDL (low-density lipoprotein particles) and a thickening of the Bruch's membrane was observed during aging. Therefore, CD36 might contribute for the clearance of sub-retinal deposits observed during the development of AMD [18].

Lately, in vivo data were obtained related to the participation of the small signaling molecule annexin 2 in the stimulation of actin dynamics for phagosome closure and engulfment [19]. *ANXA2*−/− mice show an accumulation of phagocytosed POS in the apical processes of RPE cells. Moreover, phosphorylation of Annexin 2 tyrosine residues occurring before light onset in wild type animals is delayed in *ANXA2*−/− mice, suggesting that annexin 2 acts upstream of the synchronized activation of αvβ5 integrin/MerTK just after light onset. To date, no mutation in *ANXA2* has been found directly linked to any retinal disease. However, annexin A2 expression has been identified in drusens from AMD patients [20].

In humans, mutations in the *MYOSIN VIIA* gene (*MYO7A*) cause blindness and deafness, collectively known as Usher Type 1B syndrome (USH1B). Shaker1 mice, mutated in the *Myo7a* gene, are deaf but not blind although having slightly abnormal electroretinogram (ERG) responses [21]. The shaker1 mouse permitted the identification of the participation of myosin VIIA for melanosome [22] and phagosome transport in RPE cells [23]: Melanosomes are absent from while phagosomes accumulate in the RPE apical processes, resulting in slower phagosome degradation.

### *10.2.3 POS Degradation*

RPE cells degrade phagosome components via fusion with lysosomes containing enzymes like Cathepsin D (CatD), the major lysosomal component required for proper POS degradation [24]. *Mcd/mcd* and *mcd2/mcd2* mice expressing enzymatically inactive mutant forms of CatD confirmed the in vivo function of CatD [25, 26]. Indeed, mutant mice accumulate hyperfluorescence and cell abnormalities, as well as age-related lipofuscin granules and basal deposits in the RPE, both considered hallmarks of AMD. The defects appear earlier in *mcd2/mcd2* compared to *mcd/mcd* mice, the gene deletion being bigger.

Recently, Nuc1 mutant rats, harboring a mutation in the *βA3/A1-crystallin* gene, allowed the characterization of βA3/A1-crystallin as a novel lysosomal component required for the correct degradation of internalized POS [27]. Mutant β A3/A1-crystallin proteins fail to localize to lysosomes, decreasing CatD protein levels and impairing completion of POS digestion. Mutant animals also showed a defect in the autophagy process with age as well as associated lipid accumulation, which are suggested to be linked to impaired lysosomal function.

Yet another animal model pinpointed the role of melanoregulin in POS degradation [28]. In *Mreg*−/− mice, POS degradation is delayed due to the failed maturation of lysosomes and diminished CatD activity. This leads to the accumulation of POS derivatives such as lipofuscin and A2E from 9 months of age.

## 10.3 Perspectives

The molecules described above constitute an efficient and well-organized machinery. However, it is not excluded that other proteins participate actively in retinal phagocytosis. Moreover, all the molecular mechanisms identified so far have been obtained with nocturnal rodents and are thus mostly related to rod phagocytosis. Therefore, the question remains open regarding the constituents of the phagocytic machinery in cone photoreceptors. Cone phagocytosis seems to peak either after light offset or onset depending on the species studied. Hence, the use of new animal models living a mostly diurnal life and/or possessing a retina richer in cones [29] seems pertinent to the characterization of potential cone-specific phagocytic machinery components and the understanding of pathologies linked to phagocytic defects, especially in cone-rich areas like the macula.

## References

1. Young RW, Bok D (1969) Participation of the retinal pigment epithelium in the rod outer segment renewal process. J Cell Biol 42:392–403
2. LaVail MM (1976) Rod outer segment disk shedding in rat retina: relationship to cyclic lighting. Science 194:1071–1074

3. Finnemann SC, Bonilha VL, Marmorstein AD, Rodriguez-Boulan E (1997) Phagocytosis of rod outer segments by retinal pigment epithelial cells requires alpha(v)beta5 integrin for binding but not for internalization. Proc Natl Acad Sci USA 94:12932–12937
4. Nandrot EF, Kim Y, Brodie SE, Huang X, Sheppard D, Finnemann SC (2004) Loss of synchronized retinal phagocytosis and age-related blindness in mice lacking alphavbeta5 integrin. J Exp Med 200:1539–1545
5. Finnemann SC, Rodriguez-Boulan E (1999) Macrophage and retinal pigment epithelium phagocytosis: apoptotic cells and photoreceptors compete for alphavbeta3 and alphavbeta5 integrins, and protein kinase C regulates alphavbeta5 binding and cytoskeletal linkage. J Exp Med 190:861–874
6. Nandrot EF, Anand M, Almeida D, Atabai K, Sheppard D, Finnemann SC (2007) Essential role for MFG-E8 as ligand for alphavbeta5 integrin in diurnal retinal phagocytosis. Proc Natl Acad Sci USA 104:12005–12010
7. Strauss O, Stumpff F, Mergler S, Wienrich M, Wiederholt M (1998) The Royal College of Surgeons rat: an animal model for inherited retinal degeneration with a still unknown genetic defect. Acta Anat (Basel) 162(2–3):101–111
8. Nandrot E, Dufour EM, Provost AC, Péquignot MO, Bonnel S, Gogat K, Marchant D, Rouillac C, Sépulchre deCB, Bihoreau MT, Shaver C, Dufier JL, Marsac C, Lathrop M, Menasche M, Abitbol MM (2000) Homozygous deletion in the coding sequence of the c-mer gene in RCS rats unravels general mechanisms of physiological cell adhesion and apoptosis. Neurobiol Dis 7:586–599
9. D'Cruz PM, Yasumura D, Weir J, Matthes MT, Abderrahim H, La Vail MM, Vollrath D (2000) Mutation of the receptor tyrosine kinase gene mertk in the retinal dystrophic RCS rat. Hum Mol Genet 9(4):645–651
10. Nandrot EF, Silva KE, Scelfo C, Finnemann SC (2012) Retinal pigment epithelial cells use a MerTK-dependent mechanism to limit the phagocytic particle binding activity of α vβ 5 integrin. Biol Cell 104(6):326–341
11. Tschernutter M, Jenkins SA, Waseem NH, Saihan Z, Holder GE, Bird AC, Bhattacharya SS, Ali RR, Webster AR (2006) Clinical characterisation of a family with retinal dystrophy caused by mutation in the Mertk gene. Br J Ophthalmol 90(6):718–723
12. Ebermann I, Walger M, Scholl HP, Charbel Issa P, Lüke C (2007) Nürnberg G, Lang-Roth R, Becker C, Nürnberg P, Bolz HJ. Truncating mutation of the DFNB59 gene causes cochlear hearing impairment and central vestibular dysfunction. Hum Mutat 28(6):571–577
13. Hall MO, Obin MS, Heeb MJ, Burgess BL, Abrams TA (2005) Both protein S and Gas6 stimulate outer segment phagocytosis by cultured rat retinal pigment epithelial cells. Exp Eye Res 81(5):581–591
14. Prasad D, Rothlin CV, Burrola P, Burstyn-Cohen T, Lu Q, Garcia deFP, Lemke G (2006) TAM receptor function in the retinal pigment epithelium. Mol Cell Neurosci 33:96–108
15. Burstyn-Cohen T, Lew ED, Través PG, Burrola PG, Hash JC, Lemke G (2012) Genetic dissection of TAM receptor-ligand interaction in retinal pigment epithelial cell phagocytosis. Neuron 76(6):1123–1132
16. Finnemann SC, Silverstein RL (2001) Differential roles of CD36 and alphavbeta5 integrin in photoreceptor phagocytosis by the retinal pigment epithelium. J Exp Med 194:1289–1298
17. Sun M, Finnemann SC, Febbraio M, Shan L, Annangudi SP, Podrez EA, Hoppe G, Darrow R, Organisciak DT, Salomon RG, Silverstein RL, Hazen SL (2006) Light-induced oxidation of photoreceptor outer segment phospholipids generates ligands for CD36-mediated phagocytosis by retinal pigment epithelium: a potential mechanism for modulating outer segment phagocytosis under oxidant stress conditions. J Biol Chem 281(7):4222–4230
18. Picard E, Houssier M, Bujold K, Sapieha P, Lubell W, Dorfman A, Racine J, Hardy P, Febbraio M, Lachapelle P, Ong H, Sennlaub F, Chemtob S (2010) CD36 plays an important role in the clearance of oxLDL and associated age-dependent sub-retinal deposits. Aging (Albany NY) 2(12):981–999
19. Law AL, Ling Q, Hajjar KA, Futter CE, Greenwood J, Adamson P, Wavre-Shapton ST, Moss SE, Hayes MJ (2009) Annexin A2 regulates phagocytosis of photoreceptor outer segments in the mouse retina. Mol Biol Cell 20:3896–3904

20. Crabb JW, Miyagi M, Gu X, Shadrach K, West KA, Sakaguchi H, Kamei M, Hasan A, Yan L, Rayborn ME, Salomon RG, Hollyfield JG (2002) Drusen proteome analysis: an approach to the etiology of age-related macular degeneration. Proc Natl Acad Sci USA 99(23):14682–14687
21. Libby RT, Steel KP (2001) Electroretinographic anomalies in mice with mutations in Myo7a, the gene involved in human Usher syndrome type 1B. Invest Ophthalmol Vis Sci 42(3):770–778
22. Liu X, Ondek B, Williams DS (1998) Mutant myosin VIIa causes defective melanosome distribution in the RPE of shaker-1 mice. Nat Genet 19(2):117–118
23. Gibbs D, Kitamoto J, Williams DS (2003) Abnormal phagocytosis by retinal pigmented epithelium that lacks myosin VIIa, the Usher syndrome 1B protein. Proc Natl Acad Sci USA 100:6481–6486
24. Deguchi J, Yamamoto A, Yoshimori T, Sugasawa K, Moriyama Y, Futai M, Suzuki T, Kato K, Uyama M, Tashiro Y (1994) Acidification of phagosomes and degradation of rod outer segments in rat retinal pigment epithelium. Invest Ophthalmol Vis Sci 35(2):568–579
25. Rakoczy PE, Zhang D, Robertson T, Barnett NL, Papadimitriou J, Constable IJ, Lai CM (2002) Progressive age-related changes similar to age-related macular degeneration in a transgenic mouse model. Am J Pathol 161(4):1515–1524
26. Zhang D, Brankov M, Makhija MT, Robertson T, Helmerhorst E, Papadimitriou JM, Rakoczy PE (2005) Correlation between inactive cathepsin D expression and retinal changes in mcd2/mcd2 transgenic mice. Invest Ophthalmol Vis Sci 46(9):3031–3038
27. Zigler JS Jr, Zhang C, Grebe R, Sehrawat G, Hackler L Jr, Adhya S, Hose S, McLeod DS, Bhutto I, Barbour W, Parthasarathy G, Zack DJ, Sergeev Y, Lutty GA, Handa JT, Sinha D (2011) Mutation in the βA3/A1-crystallin gene impairs phagosome degradation in the retinal pigmented epithelium of the rat. J Cell Sci 124(Pt 4):523–531
28. Damek-Poprawa M, Diemer T, Lopes VS, Lillo C, Harper DC, Marks MS, Wu Y, Sparrow JR, Rachel RA, Williams DS, Boesze-Battaglia K (2009) Melanoregulin (MREG) modulates lysosome function in pigment epithelial cells. J Biol Chem 284(16):10877–10889
29. Bobu C, Craft CM, Masson-Pevet M, Hicks D (2006) Photoreceptor organization and rhythmic phagocytosis in the nile rat Arvicanthis ansorgei: a novel diurnal rodent model for the study of cone pathophysiology. Invest Ophthalmol Vis Sci 47(7):3109–3118

# Chapter 11
# In Vivo and in Vitro Monitoring of Phagosome Maturation in Retinal Pigment Epithelium Cells

**Julian Esteve-Rudd, Vanda S. Lopes, Mei Jiang and David S. Williams**

**Abstract** The ingestion and degradation of photoreceptor disk membranes is a critical and major role for the retinal pigment epithelium (RPE). To help elucidate the cellular events involved in this role, functional in vivo and in vitro assays need to be developed further. Here we propose a method to help monitor phagosome maturation, using antibodies against different epitopes of opsin. We show that antibodies specific for the C-terminus of opsin label only immature phagosomes located in the apical region of the RPE. In contrast, antibodies recognizing the N-terminus also label more mature phagosomes, located more basally. The combined use of antibodies against different opsin epitopes thus provides a valuable tool in the study of phagosome maturation in the RPE.

**Keywords** RPE · Phagocytosis · Opsin · Protein degradation · Phagosome

## 11.1 Introduction

Each day the tips of the photoreceptor outer segments (POSs) are ingested and degraded by the adjacent retinal pigment epithelium (RPE) cells [1]. A defect at any stage of this process can lead to photoreceptor impairment and degeneration. Photoreceptor degeneration in the RCS rat and *Mertk* knockout mouse is caused by

J. E.-Rudd (✉) · V. S. Lopes · M. Jiang · D. S. Williams
Stein Eye Institute, UCLA David Geffen School of Medicine, Doris Stein Building, 200 Stein Plaza, Los Angeles, 90095 CA, USA
e-mail: jesteve@ucla.edu

V. S. Lopes
e-mail: vslopes@ucla.edu

M. Jiang
e-mail: JIANGM@UCLA.EDU

D. S. Williams
e-mail: dswilliams@ucla.edu

J. D. Ash et al. (eds.), *Retinal Degenerative Diseases,* Advances in Experimental Medicine and Biology 801, DOI 10.1007/978-1-4614-3209-8_11,

a failure at the ingestion stage [2, 3]. After ingestion, phagosomes are transported from the apical RPE towards the basal side and undergo degradation by fusion with lysosomes [4–6]. Defects in degradation lead to the accumulation of undigested debris in the RPE, the formation of sub-RPE deposits, and photoreceptor degeneration, as shown in transgenic mice overexpressing mutant Cathepsin D, the main proteolytic enzyme involved in opsin degradation [7]. Phagosome degradation can also be impaired by defects in the transport of phagosomes and/or lysosomes, causing a delay in the fusion of the two organelles. Lack of MYO7A retards the transition of POSs from the apical to the basal RPE, resulting in a delay in phagosome digestion [8].

We have developed a method for measuring POS digestion in cultured mouse primary RPE cells [9, 10], based on previously described assays [2]. Here, we describe a more detailed method for the monitoring of POS maturation both in vivo and in cell culture, based on the detection of different epitopes by different opsin antibodies. This approach was suggested by previous immunoelectron microscopy (immunoEM) studies [11; and C.E. Futter, personnal communication]. The method allows us to differentiate early phagosomes from late-stage phagosomes and can be used to identify photoreceptor or RPE defects in mutant mice.

## 11.2 In Vivo Assessment of Phagosome Maturation in the RPE

Ultrathin retinal sections were obtained as described previously [12]. They were double-labeled with mAb1D4, which was generated in a mouse and specifically recognizes the C-terminus of opsin [13, 14], and pAb01 made in a rabbit against bovine opsin [15]. ImmunoEM of RPE showed that the mAb1D4 antibody labeled apical phagosomes, while the pAb01 antibody-labeled apical, central, and basal phagosomes (Fig. 11.1). Given the apical to basal migration of phagosomes during their maturation [5, 6], this result suggests that the C-terminus epitope of opsin Opsin is lost quickly during the phagosome maturation process.

## 11.3 Phagocytosis of POSs by Cultured Mouse RPE Cells

Primary cultures of RPE from wild-type mice were prepared, and the phagocytosis assay was performed as described [8, 9], with the following modifications. Cells, grown on transwell filters for 7–10 days, were incubated for 20 min with a suspension of 1 to $5 \times 10^6$ gradient-purified POSs. Unbound POSs were then removed by extensive washing with PBS, and cells were either fixed or incubated for an additional period ("chase" following the POS "pulse"), and then fixed (Fig. 11.2a). Immunofluorescence labeling of bound and total POSs was performed using a combination of mAb1D4 and pAb01 (Fig. 11.2). POSs that were only bound to the

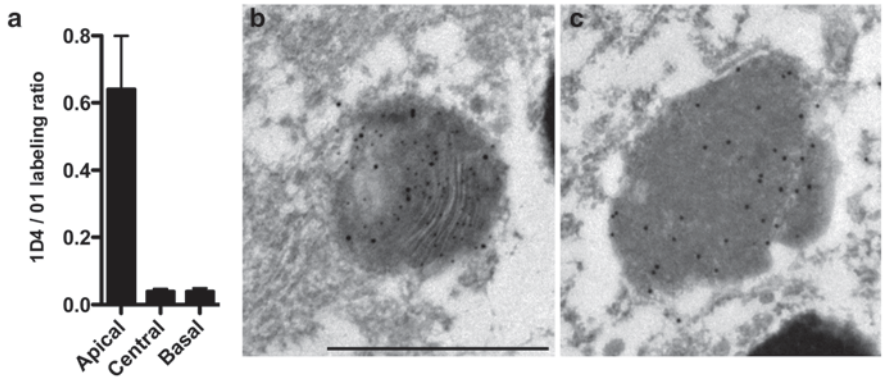


**Fig. 11.1** ImmunoEM opsin labeling of RPE phagosomes. **a** Quantification of gold particles corresponding to mAb1D4 or pAb01 labeling on phagosomes located in the apical, central, and basal regions of the RPE. The concentration of immunogold label per area of all the phagosomes in each of the three regions of the RPE was measured for each antibody on double-labeled sections. A phagosome was identified by the presence of pAb01 labeling. Significant mAb1D4 labeling was present only on phagosomes in the apical region. **b**, **c** Electromicroscopies (EMs) showing labeled phagosomes from the apical (**b**) and basal (**c**) regions; mAb1D4 is indicated by the smaller 12-nm *gold* particles and pAb01 by the larger 15-nm particles. Scale bar: 1 μm

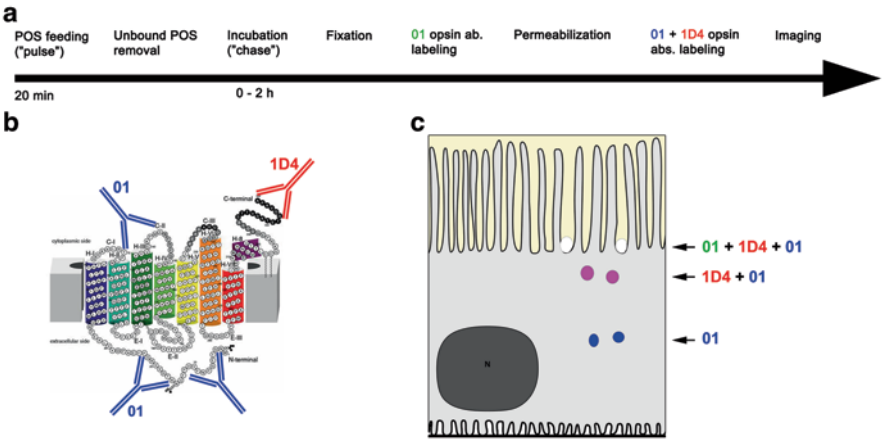


**Fig. 11.2** Method for phagocytosis assay on RPE cells in culture using a combination of opsin antibodies. **a** Time course of phagocytosis assay and immunolabeling. Color-coded 01 and 1D4 correspond to secondary antibodies that were used to detect primary antibodies in each case (*green* corresponds to Alexa-488, *red* to Alexa-568 and *blue* to Alexa-647). **b** Scheme of opsin structure (From [16]. Permission pending) with different epitopes for pAb01 and mAb1D4 indicated. **c** Scheme illustrating possible combinations of opsin immunolabeling of bound and ingested POSs, after merging the three acquisition channels. POSs that are bound to the external cell surface (i.e., not ingested) are labeled with pAb01 before permeabilization, and mAb1D4 and pAb01 after permeabilization, and appear *white*. Phagosomes labeled with mAb1D4 and pAb01 after permeabilization appear in *magenta*. Phagosomes labeled only with pAb01 after permeabilization appear in *blue*

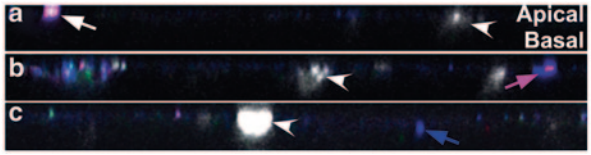


**Fig. 11.3** Phagosome localization at different digestion stages in cultured RPE cells. **a, b, c** Orthogonal projections from a stack of confocal slices of a single RPE cell from a culture fed with POSs and immunolabeled as described. **a** POS that is bound to the external cell surface and labeled by all three secondary antibodies (*white arrow*). **b** Phagosome labeled with mAb1D4 and pAb01 after permeabilization (*magenta arrow*) in the apical region of the RPE cell. **c** Phagosome labeled with pAb01 only after permeabilization (*blue arrow*), located in the central soma region of the cell. *Arrowheads* indicate RPE cell nuclei stained with DAPI (shown in *white*). Scale bar: 20 μm

cell surface were labeled first, and then, after cell permeabilization by treatment with 50% ethanol, all POSs were labeled with mAb1D4 and pAb01, followed by Alexa-568 and Alexa-647 secondary antibodies. Ingested POSs were identified by subtracting the bound-only POSs (white) from the total POSs. POSs labeled by mAb1D4 are shown in magenta, while POSs labeled by pAb01 but not mAb1D4 are in blue (Fig. 11.2c). POSs at least 1 μm in diameter were counted at × 400 magnification in all cells within five fields of view chosen randomly. Images were collected with a Fluoview FV1000 confocal microscope (Olympus) and analyzed on ImageJ.

## 11.4 Assessment of Phagosome Maturation in Cultured RPE

To determine the localization of phagosomes on the apical-basal plane of RPE cells grown on filters, stacks of confocal slices separated by 0.3 μm were projected orthogonally (Fig. 11.3). Our results are consistent with our observations in vivo. Bound POSs appear at the apical surface of RPE cells. POSs labeled with both mAb1D4 and pAb01 after permeabilization are ingested but reside within the apical region, while POSs labeled only with pAb01 after permeabilization are located more basally.

We also performed quantitative assays to evaluate the digestion rate of phagosomes, by assessing the decay rate of different opsin epitopes. We observed that the mAb1D4 labeling disappeared more quickly than the pAb01 labeling during the chase period. Figure 11.4 illustrates an experiment with a chase period of 2 h. These experiments indicate that loss of a C-terminal epitope of opsin constitutes an early step in phagosome digestion.

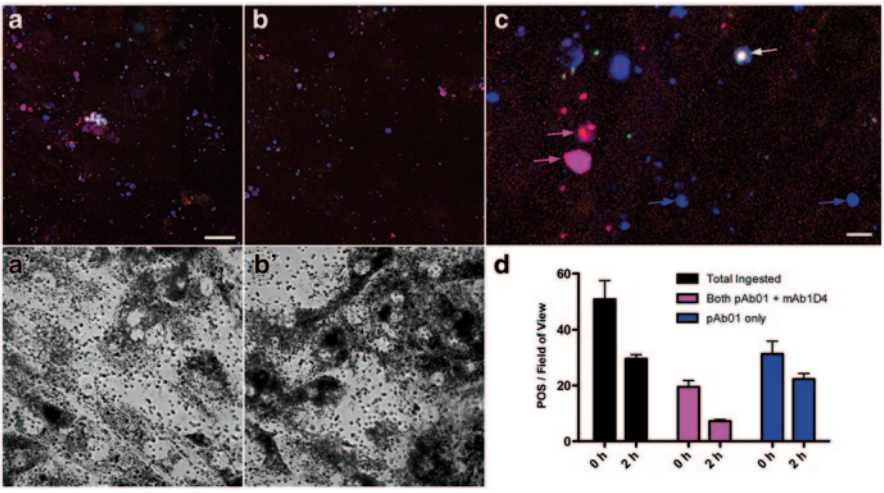


**Fig. 11.4** Time-course of POS digestion in cultured RPE cells. **a, b** Micrographs showing immunofluorescence labeling of POSs with mAb1D4 + pAb01, as described, immediately after removal of the POSs (end of pulse, 0 h) (**a**) and after 2 h subsequent incubation (chase) (**b**). **a'**, **b'** Bright field images of the same areas shown in **a** and **b**, respectively. **c** High-magnification detail of **a**, showing phagosomes at different stages of maturation. **d** Quantification of POSs in cultured RPE cells after 0 h (pulse only) and 2 h chase periods. Graph shows total ingested POSs (*black*), ingested POSs that were labeled with both pAb01 and mAb1D4 (*magenta*), and ingested POSs that were labeled with pAb01 only—no mAb1D4 labeling (*blue*). The overall reduction in the number of phagosomes during the 2-h chase was 42 %. The number of POSs labeled with both mAb1D4 and pAb01 decreased by 63 %, while the number of POSs labeled with pAb01 alone decreased by 29 %. Scale bars: **a**, **b**: 20 µm; **c**: 5 µm

## 11.5 Conclusions

Observations of phagosome location and the rate of phagosome degradation indicate that the mAb1D4, which binds to a C-terminal epitope on opsin, recognizes only early phagosomes. Thus, in comparison with an opsin antibody that binds to epitopes elsewhere, different stages of phagosome maturation can be identified. This assay could be used to help identify defects in phagosome degradation in retinal disease.

**Acknowledgments** Supported by National Institutes of Health (NIH) grant EY07042. David S. Williams is a Jules and Doris Stein RPB Professor.

## References


1. Young RW, Bok D (1969) Participation of the retinal pigment epithelium in the rod outer segment renewal process. J Cell Biol 42:392–403
2. Chaitin MH, Hall MO (1983) Defective ingestion of rod outer segments by cultured dystrophic rat pigment epithelial cells. Invest Ophthalmol Vis Sci 24:812–820
3. Duncan JL, LaVail MM, Yasumura D, Matthes MT, Yang H, Trautmann N, Chappelow AV, Feng W, Earp HS, Matsushima GK, Vollrath D (2003) An RCS-like retinal dystrophy phenotype in mer knockout mice. Invest Ophthalmol Vis Sci 44:826–838
4. Bosch E, Horwitz J, Bok D (1993) Phagocytosis of outer segments by retinal pigment epithelium: phagosome-lysosome interaction. J Histochem Cytochem 41:253–263
5. Herman KG, Steinberg RH (1982) Phagosome degradation in the tapetal retinal pigment epithelium of the opossum. Invest Ophthalmol Vis Sci 23:291–304
6. Herman KG, Steinberg RH (1982) Phagosome movement and the diurnal pattern of phagocytosis in the tapetal retinal pigment epithelium of the opossum. Invest Ophthalmol Vis Sci 23:277–290
7. Rakoczy PE, Zhang D, Robertson T, Barnett NL, Papadimitriou J, Constable IJ et al (2002) Progressive age-related changes similar to age-related macular degeneration in a transgenic mouse model. Am J Pathol 161:1515–1524
8. Gibbs D, Kitamoto J, Williams DS (2003) Abnormal phagocytosis by retinal pigmented epithelium that lacks myosin VIIa, the Usher syndrome 1B protein. Proc Natl Acad Sci U S A 100:6481–6486
9. Diemer T, Gibbs D, Williams DS (2008) Analysis of the rate of disk membrane digestion by cultured RPE cells. Adv Exp Med Biol 613:321–326
10. Gibbs D, Williams DS (2003) Isolation and culture of primary mouse retinal pigmented epithelial cells. Adv Exp Med Biol 533:347–352
11. Law AL, Ling Q, Hajjar KA, Futter CE, Greenwood J, Adamson P, et al (2009) Annexin A2 regulates phagocytosis of photoreceptor outer segments in the mouse retina. Mol Biol Cell 20:3896–3904
12. Lopes VS, Gibbs D, Libby RT, Aleman TS, Welch DL, Lillo C et al (2013) The Usher 1B protein, MYO7A, is required for normal localization and function of the visual retinoid cycle enzyme, RPE65. Hum Mol Genet 20:2560–2570
13. Hodges RS, Heaton RJ, Parker JM, Molday L, Molday RS (1988) Antigen-antibody interaction. Synthetic peptides define linear antigenic determinants recognized by monoclonal antibodies directed to the cytoplasmic carboxyl terminus of rhodopsin. J Biol Chem 263:11768–11775
14. MacKenzie D, Arendt A, Hargrave P, McDowell JH, Molday RS (1984) Localization of binding sites for carboxyl terminal specific anti-rhodopsin monoclonal antibodies using synthetic peptides. BioChemistry 23:6544–6549
15. Liu X, Udovichenko IP, Brown SD, Steel KP, Williams DS (1999) Myosin VIIa participates in opsin transport through the photoreceptor cilium. J Neurosci 19:6267–6274
16. Salom D, Lodowski DT, Stenkamp RE, Le Trong I, Golczak M, Jastrzebska B et al (2006) Crystal structure of a photoactivated deprotonated intermediate of rhodopsin. Proc Natl Acad Sci U S A 103:16123–16128

# Chapter 12
# Lack of Effect of Microfilament or Microtubule Cytoskeleton-Disrupting Agents on Restriction of Externalized Phosphatidylserine to Rod Photoreceptor Outer Segment Tips

**Linda Ruggiero and Silvia C. Finnemann**

**Abstract** In the mammalian retina, life-long renewal of rod photoreceptor outer segments involves circadian shedding of distal outer segment tips and their prompt phagocytosis by the adjacent retinal pigment epithelium (RPE) every morning after light onset. Failure of this process causes retinal dystrophy in animal models and its decline likely contributes to retinal aging and some forms of degeneration of the human retina. We previously found that surface exposure of the membrane phospholipid phosphatidylserine (PS) is restricted to outer segment tips with discrete boundaries in mouse retina and that both frequency and length of tips exposing PS peak after light onset. Here, we sought to test mechanisms photoreceptors use to restrict PS specifically to their outer segment tips. To this end, we tested whether nocodazole or cytochalasin D, perturbing microtubule or F-actin microfilament cytoskeleton, respectively, affect localization of externalized PS at outer segment tips. Fluorescence imaging of PS exposed by rods in freshly dissected, live mouse retina showed normal PS demarcation of outer segment tips regardless of drug treatment. These results suggest that the mechanism that restricts externalized PS to rod tips is independent of F-actin and microtubule cytoskeletal systems.

**Keywords** Actin · Cytoskeleton · Microtubules · Outer segment · Phosphatidylserine · Photoreceptor · Retina · Shedding

**Abbreviations**

| | |
|---|---|
| HBSS | Hank's buffered saline solution |
| PS | Phosphatidylserine |
| pSIVA | Polarity-sensitive indicator of viability and apoptosis |
| POS | Photoreceptor outer segments |
| RPE | Retinal pigment epithelium |

S. C. Finnemann (✉) · L. Ruggiero
Department of Biological Sciences, Center for Cancer, Genetic Diseases, and Gene Regulation, Fordham University, 441 East Fordham Road, Larkin Hall, Bronx, 10458 NY, USA
e-mail: finnemann@fordham.edu

L. Ruggiero
e-mail: pixietail@gmail.com

J. D. Ash et al. (eds.), *Retinal Degenerative Diseases,* Advances in Experimental Medicine and Biology 801, DOI 10.1007/978-1-4614-3209-8_12,

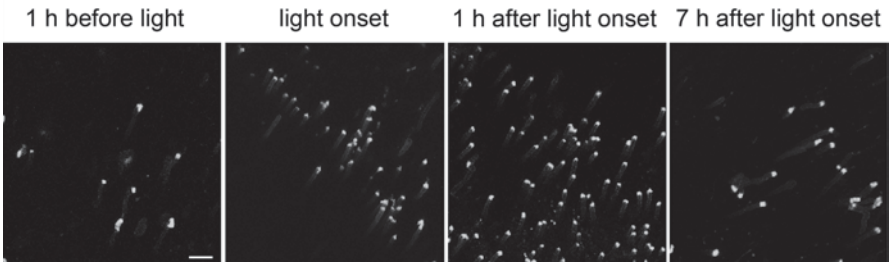


**Fig. 12.1** PS-biosensor imaging of live mouse rods reveals precise retention of externalized PS to distal POS tips at all times of day and increased frequency of POS exposing PS after light onset. Fields show representative confocal maximal projections of pSIVA labeling of rod POS of live retinal tissue freshly dissected from wild-type mice at different times with respect to light onset as indicated. Scale bar, 20 μm. (© Ruggiero et al. 2012, originally published in Proc Natl Acad Sci USA [2])

## 12.1 Introduction

In the mammalian retina, life-long renewal of light-sensitive rod photoreceptor outer segments (POS) involves circadian shedding of distal POS tips and their subsequent phagocytosis by the adjacent retinal pigment epithelium (RPE) every morning after light onset [1]. We previously examined plasma membrane asymmetry of mouse POS by quantifying surface exposure of the membrane phospholipid phosphatidylserine (PS) [2]. In these studies we first used recombinant annexin V to specifically label exposed PS in live, freshly dissected retina. Quantification of annexin V association with retinas either by fluorescence microscopy of samples fixed after labeling or by immunoblotting analysis of recombinant annexin V of samples lysed after labeling revealed that PS exposure is significantly elevated at light onset, the time of POS shedding, as compared to 7 h later [2]. Furthermore, we monitored the subcellular localization of externalized PS on POS by imaging freshly dissected mouse retina samples live in the presence of a novel annexin-based biosensor with switchable states of fluorescence, termed pSIVA ("polarity-sensitive indicator of viability and apoptosis") [3]. pSIVA imaging revealed for the first time PS externalization restricted to POS tips with discrete boundaries. Tips were slightly but significantly longer immediately after light onset than at all other times of day tested [2]. Most strikingly, changes in frequency of these tips correlated with circadian changes in POS renewal (Fig. 12.1). Altogether, our findings suggest that enhanced PS exposure precedes rod POS shedding and phagocytosis to promote these processes.

We have been intrigued by the precise retention of PS exposure to distal POS tips that suggest that rod outer segments possess mechanisms exposing PS solely at tips and preventing lateral diffusion of externalized PS toward the proximal end of POS. In this study, we set out to determine POS mechanisms that restrict PS mobility. Specifically, we tested if short-term treatment with pharmacological agents that selectively disrupt either the F-actin or the microtubule cytoskeleton alters PS restriction to POS tips in freshly dissected mouse retina.

## 12.2 Materials and Methods

### *12.2.1 Animals*

All procedures were performed in accordance with the National Institutes of Health Guide for the Care and Use of Laboratory Animals and reviewed and approved by the Fordham University Institutional Animal Care and Use Committee. Wild-type 129T2/SvEms mice originally obtained from Jackson Laboratories were reared and housed under cyclic 12 h light/12 h dark conditions and fed ad libitum. Three- to four-month-old male and female mice were used for experiments.

### *12.2.2 Tissue Preparation, Drug Treatment, pSIVA Labeling, and Fluorescence Imaging*

Mice were sacrificed by $CO_2$ asphyxiation at specific times before or after light onset. Retinas were immediately dissected and either stained with pSIVA and imaged immediately as described below or treated with cytoskeleton disrupting agents before staining and imaging. To destabilize F-actin, one retina of a mouse was placed into Hank's buffered saline solution (HBSS) containing 2.5 μM cytochalasin D, and the other retina was placed into HBSS alone for incubation at room temperature for 15 min. To destabilize microtubules, one retina of each mouse was placed into HBSS containing 10 μM nocodazole, and the other retina was placed into HBSS alone for incubation at 37 °C for 15 min. Both agents were diluted from 100-fold stock solutions in dimethyl sulfoxide (DMSO, Sigma) directly before use. Retinas were rinsed in HBSS at room temperature for 5 min before being placed onto glass slides photoreceptor side up in HBSS supplemented with pSIVA at 1:100. Retinas were covered with a cover glass and imaged immediately on a Leica TSP5 laser scanning confocal microscopy system. Image acquisition parameters were kept constant for all experiments. Maximal projections of image stacks were recompiled in Adobe Photoshop.

## 12.3 Results

### *12.3.1 Effects of Cytochalasin D on Localization of Externalized PS at POS Tips*

We sought to examine the potential role of cytoskeletal components, namely F-actin microfilaments and microtubules, in restricting external plasma membrane PS localization to rod POS tips. To this end, we first examined the effects of cytochalasin D, a pharmacological agent that is well characterized to disrupt specifically the

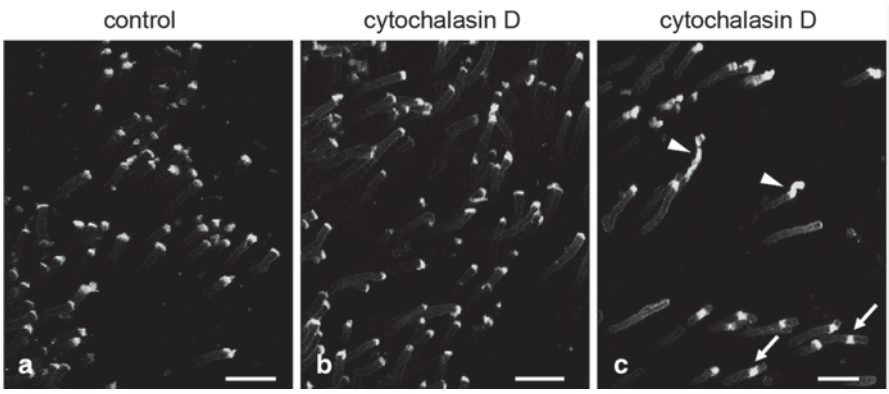


**Fig. 12.2** Cytochalasin D F-actin destabilizing agent has no effect on precise retention of externalized PS to distal POS as detected by PS-biosensor imaging of live mouse rods in samples that do not display signs of cytotoxicity. Fields show representative confocal maximal projections of pSIVA labeling of rod POS of live retinal tissue freshly prepared from wild-type mice at light onset. **a** Control retina incubated in buffer alone. **b** Retina incubated in buffer with cytochalasin D showing normal pSIVA labeling and no cytotoxicity. **c** Retina incubated in buffer with cytochalasin D showing displaced PS exposure (*arrows*) and cytotoxicity (*arrowheads*). Note that the image shown in **b** is representative of the majority of samples. Scale bar, 20 μm

F-actin cytoskeleton. F-actin is present in POS, and it has been shown earlier to play an important role in disk morphogenesis at the proximal end of outer segments [4]. Disruption of F-actin in dissected mouse retinas with attached RPE disturbs the light-driven translocation of arrestin and transducin between inner and outer segment [5]. Whether or not F-actin also plays a role at distal POS tips of rods has not yet been studied. However, in human erythroleukemia cells in culture, the F-actin cytoskeleton contributes to PS exposure such that treatment with cytochalasin D diminishes PS externalization [6]. Here, we incubated freshly dissected whole retinas with cytochalasin D for 15 min followed by labeling with pSIVA and live imaging. We found in most samples that cytochalasin D-treated POS displayed very little disruption in localization of PS when compared to control POS (Fig. 12.2, compare panels b and a). In some samples, we observed a fraction of rods in which pSIVA labeled not the tips of POS but discrete bands along POS (Fig. 12.2, panel c). In these samples, we also found a significant number of POS that appeared to be disorganized. We conclude that cytochalasin D at the concentration applied does not specifically affect PS localization to POS tips but causes some cytotoxicity, the extent of which is variable among samples.

### *12.3.2 Effects of Nocodazole on Localization of Externalized PS at POS Tips*

We next turned our attention to the potential relevance of microtubules in restricting externalized PS to POS tips. Microtubules are abundant in rod POS, and distal POS

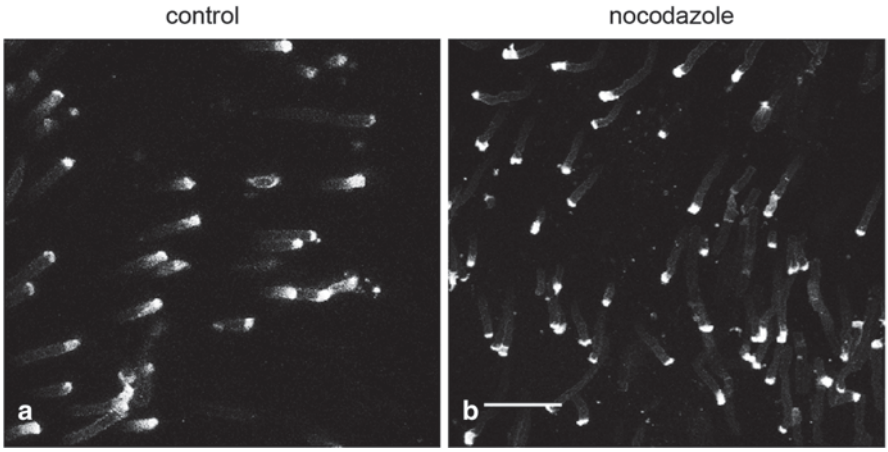


**Fig. 12.3** Nocodazole microtubule destabilizing agent has no effect on precise retention of externalized PS to distal POS as detected by PS-biosensor imaging of live mouse rods. Fields show representative confocal maximal projections of pSIVA labeling of rod POS of live retinal tissue freshly prepared from wild-type mice at light onset. **a** Control retina incubated in buffer alone. **b** Retina incubated in buffer with nocodazole. Scale bar, 20 µm

tips in toads have been reported to contain distinct microtubule-like elements [7]. We incubated freshly dissected mouse retinas in nocodazole, which interferes with microtubule polymerization, and labeled them with pSIVA. We found that retinas treated with nocodazole displayed no obvious differences in PS localization at POS tips when compared to control retinas (Fig. 12.3). This experiment suggests that retention of externalized PS to POS tips is independent of microtubules that are sensitive to nocodazole.

## 12.4 Discussion

In this study, we tested how short-term incubation of freshly isolated mouse retina with pharmacological agents disturbing F-actin or microtubules affected the distribution of externalized PS on distal rod POS tips.

To manipulate F-actin, we applied cytochalasin D, which prevents F-actin polymerization and promotes depolymerization of existing F-actin filaments. We found that cytochalasin D as applied had negligible effect on samples that did not show signs of cytotoxicity. These data suggest that cytochalasin D does not specifically perturb PS retention at POS tips.

To manipulate microtubules, we applied nocodazole, which prevents microtubule polymerization. We found that nocodazole as used had no effect on the localization of externalized PS at POS tips. These data suggest that nocodazole-sensitive microtubules are not required for restriction of externalized PS to POS tips. It is

important to note, however, that POS contain a distinct population of microtubules, some of which are not affected by nocodazole [8]. Further studies are needed to determine their potential role in positioning of externalized PS on rod POS.

**Acknowledgments** We are grateful for the Young Investigator Travel Award from the National Eye Institute that supported the participation at the RD2012 Symposium of Linda Ruggiero. We thank all members of the Finnemann lab for helpful discussions. This study was supported by NIH grant EY13295.

## References

1. Ruggiero L, Finnemann SC (In Press) Photoreceptor-RPE interactions: diurnal phagocytosis. In: Werner JS, Chalupa LM (eds) The new visual neurosciences. MIT Press
2. Ruggiero L, Connor MP, Chen J, Langen R, Finnemann SC (2012) Diurnal, localized exposure of phosphatidylserine by rod outer segment tips in wild-type but not Itgb5-/- or Mfge8-/- mouse retina. Proc Natl Acad Sci USA 109:8154–8158
3. Kim YE, Chen J, Langen R, Chan JR (2010) Monitoring apoptosis and neuronal degeneration by real-time detection of phosphatidylserine externalization using a polarity-sensitive indicator of viability and apoptosis. Nature Protoc 5:1396–1405
4. Williams DS, Linberg KA, Vaughan DK, Fariss RN, Fisher SK (1988) Disruption of microfilament organization and deregulation of disk membrane morphogenesis by cytochalasin D in rod and cone photoreceptors. J Comp Neurol 272:161–176
5. Reidel B, Goldmann T, Giessl A, Wolfrum U (2008) The translocation of signaling molecules in dark adapting mammalian rod photoreceptor cells is dependent on the cytoskeleton. Cell Motil Cytoskeleton 65:785–800
6. Kunzelmann-Marche C, Freyssinet JM, Martinez MC (2001) Regulation of phosphatidylserine transbilayer redistribution by store-operated $Ca^{2+}$ entry: role of actin cytoskeleton. J Biol Chem 276:5134–5139
7. Roof D, Adamian M, Jacobs D, Hayes A (1991) Cytoskeletal specializations at the rod photoreceptor distal tip. J Comp Neurol 305:289–303
8. Sale WS, Besharse JC, Piperno G (1988) Distribution of acetylated alpha-tubulin in retina and in vitro-assembled microtubules. Cell Motil Cytoskeleton 9:243–253

# Chapter 13
# Vacuolar ATPases and Their Role in Vision

**Lisa Shine, Claire Kilty, Jeffrey Gross and Breandan Kennedy**

**Abstract** Vacuolar ATPases (v-ATPases) hydrolyze adenosine triphospate (ATP) to pump protons across cell membranes. Mutations in v-ATPase subunits are implicated in three human disorders: distal renal tubular acidosis, osteopetrosis, and cutis laxa type II. In the eye, the role of v-ATPases is only emerging. Mutations in v-ATPase subunits are not linked to human blindness, but altered proton pump function may underlie ocular pathologies. For example, inhibition of v-ATPase by A2E may accentuate age-related macular degeneration (AMD). In animal models, v-ATPase mutations perturb the retinal pigment epithelium (RPE) and photoreceptor outer segment (OS) phagocytosis, an event linked to retinal degeneration. As the RPE plays essential roles in eye development and vision, the study of v-ATPase-induced RPE dysfunction may improve our understanding of RPE diseases.

**Keywords** Bafilomycin · Phagocytosis · Photoreceptor outer segments · RPE · Vacuolar ATPases

**Abbreviations**

| | |
|---|---|
| AMD | Age related macular degeneration |
| $Ca^{2+}$ | Calcium |

B. Kennedy (✉) · L. Shine · C. Kilty
School of Biomolecular and Biomedical Science, Conway Institute,
University College Dublin, Belfield, Dublin 4, Ireland
e-mail: brendan.kennedy@ucd.ie

Lisa Shine
e-mail: Lisa.shine@ucd.ie

C. Kilty
e-mail: Claire.kilty@ucd.ie

J. Gross
Section of Molecular, Cell and Developmental Biology, Institute of
Cell and Molecular Biology, University of Texas at Austin,
1 University Station, Austin TX 78712, USA
e-mail: jmgross@austin.utexas.edu

J. D. Ash et al. (eds.), *Retinal Degenerative Diseases,* Advances in Experimental Medicine and Biology 801, DOI 10.1007/978-1-4614-3209-8_13,

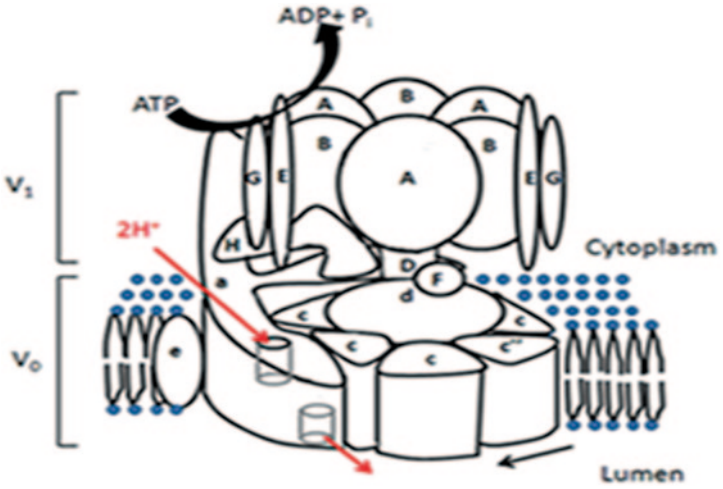


**Fig. 13.1** The v-ATPase complex. The v-ATPase complex consists of a peripheral domain ($V_1$), and an integral domain ($V_0$). These domains consist of 14 different subunits types. The $V_1$ domain catalyses the hydrolysis of adenosine triphosphate (*ATP*) and the $V_0$ domain transports H+ ions across the membrane. *ADP* adenosine diphosphate

| | |
|---|---|
| CMZ | Ciliary marginal zone |
| $H_2S$ | Hydrogen sulphide |
| OKR | Optokinetic response |
| OS | Outer segment |
| RPE | Retinal pigment epithelium |
| V-ATPase | Vacuolar ATPase |

## 13.1 Introduction to V-ATPases

Vacuolar ATPases (v-ATPases) are adenosine triphosphate (ATP)-dependent proton pumps present in eukaryotic cells. These large, multisubunit complexes hydrolyze ATP to pump $H^+$ ions across membranes regulating pH homeostasis in intracellular compartments. They function in receptor-mediated endocytosis, intracellular membrane trafficking, neurotransmitter uptake, and protein processing and degradation [1]. V-ATPases consist of two, reversibly associated domains: a peripheral domain ($V_1$), involved in ATP hydrolysis, and an integral domain ($V_0$), involved in proton transport [2] (Fig. 13.1). The $V_1$ domain is composed of eight different subunits (A–H) and the $V_0$ domain of six subunits (*a, d, e, c, c'* and *c''* [Table 13.1]). The c' subunit, found in yeast, is absent from higher eukaryotes which also possess the accessory subunits, Ac45 (encoded by *ATP6ap1*) [3], and a truncated form of the pro-renin receptor (encoded by *ATP6ap2)* [4]. Many v-ATPase isoforms exist, and, although the role of specific isoforms is unclear, they appear to target v-ATPases to specific organelles or cells.

**Table 13.1** Characteristics of v-ATPase subunits and accessory subunits

| Subunit | Isoforms | Subunit function [2] | Known expression/role in eye |
|---|---|---|---|
| $V_1$ | | | |
| A | – | ATP hydrolytic site, stator subunit | – |
| B | B1, B2 | Non-catalytic ATP site, stator subunit, binds actin and aldolase | Rodent: *B*1 in ciliary epithelium. Aqueous humor production [21] *B*1/*B*2 in horizontal cells [31] |
| C | C1, C2a, b | Regulatory, stator subunit, binds actin | Rodent: in horizontal cells [31] |
| D | – | Rotary subunit | Zebra fish: in RPE. Retinoblast proliferation and survival, retinal morphogenesis and pigmentation [12] |
| E | E1, E2 | Stator sub unit, binds RAVE and aldolase | Zebra fish: in RPE. Retinoblast proliferation and survival, retinal morphogenesis and pigmentation [12] |
| F | – | Rotary subunit | Zebra fish: in RPE. Retinoblast proliferation and survival, retinal morphogenesis and pigmentation [12] |
| G | G1, G3 | Stator subunit, binds RAVE | – |
| H | 2 splice variants | Regulatory, stator subunit, binds NEF | Zebra fish: in RPE. Retinoblast proliferation and survival, retinal morphogenesis and pigmentation [12] |
| $V_0$ | | | |
| a | a1I–a1IV a2, a3, a3I–a3III, a4I–a4II | H+ transport, targeting, stator subunit, binds aldolase | Rodent: *a*1, *a*2 in photoreceptors, *a*3 in capillary rich tissue. Foramina development. *a*4 in RPE, ciliary bodies, uveal tissue [22] *Drosophila: a*1 in photoreceptor presynaptic terminals. Membrane fusion, acidification and synaptic vesicle exocytosis [15, 18] |
| d | d1, d2 | Coupling, rotary subunit | – |
| e | – | Unknown | Zebra fish: in RPE. Retinoblast proliferation and survival, retinal morphogenesis and pigmentation [12] |
| c | – | H+ transport, rotary subunit | – |
| c’ | None | H+ transport, rotary subunit, binds Vma21, assembly factor | – |
| c” | – | H+ transport, rotary subunit | – |
| Ac45 | – | Unknown | – |
| PRR | – | Unknown | – |

Pharmacological and genetic (see below) approaches can assess v-ATPase complex function, and bafilomyin A1 (b-A1), a plecomacrolide antibiotic, is widely used to study the physiological roles of v-ATPases [5]. v-ATPase inhibitors have potential clinical applications in the treatment of cancer [6] and lytic bone disease

[7]. However, as the existing inhibitors are toxic, current research focuses on developing subunit-specific inhibitors with reduced side effects [6].

## 13.2 Function of V-ATPase Subunits and Accessory Proteins

Mutations in v-ATPase subunits are implicated in the human disorders: distal renal tubular acidosis, cutis laxa type II, and osteopetrosis [8–10]. Knockdown of the v-ATPase accessory subunit Ac45 (*Atp6ap1*) in osteoclasts demonstrates that Ac45 regulates extracellular acidification, lysosomal trafficking, and exocytosis [11]. A zebra fish *atp6ap1* mutant displays a reduced optokinetic response (OKR), a hypopigmented RPE, and accumulation of undigested outer segments (OSs) in RPE cells [12]. Knockdown of the v-ATPase accessory subunit PRR (*Atp6ap2*), in mouse cardiomyocytes, results in heart failure associated with extensive vacuolation [13].

Some vacuolar ATPase subunits promote membrane fusion [14, 15]. Mice with *a3* subunit deletions secrete insulin inefficiently [16], *d2* mouse knockouts display a failure of cell fusion in osteoclasts [17], and the *a* subunit of the $V_0$ complex interacts with SNAREs, mediators of membrane fusion [18]. $V_0$ subunits also function in the phagocytic pathway. Knockdown of the zebra fish $V_0$ *a1* subunit results in the accumulation of apoptotic corpses in phagosomes, due to defects in phagosome-lysosome fusion [19]. In addition, mutation of the *C. elegans* $V_1$ B subunit results in defects in apoptotic corpse clearance due to lysosomal acidification defects [20].

## 13.3 The Role of V-ATPases in the Eye

The v-ATPase complex is vital for the production of aqueous humor in the rabbit ocular ciliary epithelium, suggesting that v-ATPases may contribute to glaucoma [21]. Additionally, v-ATPase mutations perturb the RPE in animal models, suggesting that v-ATPase dysfunction may underlie human retinopathies. In osteopetrosis, a narrowed foramina results in optic nerve compression in humans and mice [22, 23].

In rats injected intravitreally with b-A1, a reduction in phagolysosome acidification in the RPE is observed, significantly delaying the degradation of OSs [24]. Additionally, A2-E, the major component of lipofusin, inhibits v-ATPase activity in purified human RPE lysosomes, resulting in increased intralysosomal pH, impaired phagocytosis, and an accumulation of undergraded OSs [25].

*Drosophila* mutants lacking the *a1* subunit accumulate synaptic vesicles at photoreceptor presynaptic terminals [18], and lysosomes in these mutants display reduced acidification and a reduced degradative capacity, resulting in neurodegeneration [15]. In fact, the *a1* subunit in *Drosophila* has a dual function that incorporates

both membrane fusion and acidification, to provide an integrated neuronal degradation mechanism [15]. This is in addition to its role in synaptic vesicle exocytosis.

Zebra fish v-ATPase mutants display a reduced OKR and most are dead by 6 dpf [12, 26]. They exhibit oculocutaneous albinism, the RPE contains membrane-bound vacuoles full of undigested OSs and apoptosis is observed near the ciliary marginal zone (CMZ), as well as throughout the retina and brain of these mutants. While all retinal cell types are present, photoreceptor OSs are described as "dishevelled," and in situ hybridization reveals RPE-specific ocular expression of v-ATPase genes. It is hypothesized that defects in melanosome maturation, localization, and survival cause the pigmentation defects in v-ATPase mutants [12]. It is unclear what causes increased cell death in these mutants, but v-ATPases may maintain cell proliferation and promote differentiation and survival. In the developing mouse cortex, v-ATPases maintain neural stem cells by regulating notch signalling [27], and, in many mammalian cells, inhibition of the v-ATPase complex triggers apoptosis [28]. The apoptotic cells in the eye of zebra fish v-ATPase mutants are located adjacent to the CMZ, which suggests that newly born neurons are dying. The role of v-ATPases in the survival of these cells appears to be an indirect one, possibly mediated by the RPE, as RPE cells express v-ATPase transcripts [12] and the RPE is known to regulate the growth and survival of retinal cells [29].

The center surround antagonism of the receptive field is a vital component of vertebrate vision, regulated by negative feedback signals produced by horizontal cells [30]. Utilizing b-A1, v-ATPase is implicated in this antagonism through a mechanism whereby horizontal cell depolarization leads to acidification, proton release and inhibition of L-type calcium ($Ca^{2+}$) channels on photoreceptor presynaptic termini [31]. V-ATPase activation and suppression of $Ca^{2+}$, due to the upregulation of Hydrogen sulphide ($H_2S$) in the retina, provide further evidence for this process [32]. Additionally, activation of v-ATPases by $H_2S$ is protective against light-induced retinal degeneration [32].

## 13.4 Expression of V-ATPase Subunits in the Eye

In *Drosophila,* the *a1* ortholog *V100* is known to be expressed in the presynaptic terminal of photoreceptors and plays a role in synaptic vesicle release [15, 18]. In mice, four *a* subunit isoforms are expressed in the eye. The *a3* subunit is localized to the choriocapillary meshwork of uveal tissue, but is absent from the eyes of *a3* deficient *Tcirg1*$^{-/-}$ mice which display impaired vision due to optic nerve compression. The *a4* isoform is predominantly expressed in the RPE and ciliary body. However, in *Tcirg1*$^{-/-}$ mice, *a4* is upregulated in uveal tissues, suggesting a mechanism whereby *a4* compensates for *a3*. The *a1* and *a2* isoforms localize to retinal photoreceptor layers [22]. In the goldfish retina, the *B1/B2* and *C* subunits are expressed in isolated horizontal cells, suggesting a putative role for these subunits in center surround antagonism [31]. *B1* is also expressed in the ocular ciliary epithelium, indicating that it may regulate aqueous humor production [21, 22].

## 13.5 Conclusion

While v-ATPases function in many cellular processes, their exact function in visual function is unknown. v-ATPase subunits are expressed in retinae of *Drosophila,* zebra fish, and rodents. Human patients with osteopetrosis, resulting from a mutation in the v-ATPase *a3* subunit, display visual impairment. RPE dysfunction and accumulation of undigested OSs in the RPE are a feature common to zebra fish v-ATPase mutants and rats injected with v-ATPase inhibitors. Defective OS phagocytosis is also linked to the human retinal diseases AMD, retinitis pigmentosa, and Usher syndrome type IB [24, 25, 29]. It is not known whether neuroretinal defects observed in animals lacking functional v-ATPase complexes are cell autonomous or a secondary consequence of RPE defects. It will be fascinating to determine if specifically restoring v-ATPase expression to mutant RPE recovers these phenotypes. In summary, increasing evidence suggests a crucial role for v-ATPases in the retina, which warrant further study and which may provide novel drug targets for treating retinal degeneration.

## References

1. Forgac M (1999) Structure and properties of the vacuolar (H+)-ATPases. J Biol Chem 274(19):12951–12954
2. Forgac M (2007) Vacuolar ATPases: rotary proton pumps in physiology and pathophysiology. Nat Rev Mol Cell Biol 8(11):917–929
3. Supek F, Supekova L, Mandiyan S, Pan YC, Nelson H, Nelson N (1994) A novel accessory subunit for vacuolar H(+)-ATPase from chromaffin granules. J Biol Chem 269(39):24102–24106
4. Nguyen G (2011) Renin, (pro)renin and receptor: an update. Clin Sci (Lond) 120(5):169–178
5. Huss M, Wieczorek H (2009) Inhibitors of V-ATPases: old and new players. J Exp Biol 212(Pt 3):341–346
6. Perez-Sayans M, Somoza-Martin JM, Barros-Angueira F, Rey JM, Garcia-Garcia A (2009) V-ATPase inhibitors and implication in cancer treatment. Cancer Treat Rev 35(8):707–713
7. Niikura K, Takeshita N, Takano M (2005) A vacuolar ATPase inhibitor, FR167356, prevents bone resorption in ovariectomized rats with high potency and specificity: potential for clinical application. J Bone Miner Res 20(9):1579–1588
8. Karet FE, Finberg KE, Nelson RD, Nayir A, Mocan H, Sanjad SA et al (1999) Mutations in the gene encoding B1 subunit of H+ -ATPase cause renal tubular acidosis with sensorineural deafness. Nat Genet 21(1):84–90
9. Kornak U, Reynders E, Dimopoulou A, van Reeuwijk J, Fischer B, Rajab A, et al (2008) Impaired glycosylation and cutis laxa caused by mutations in the vesicular H+ -ATPase subunit ATP6V0A2. Nat Genet 40(1):32–34
10. Frattini A, Orchard PJ, Sobacchi C, Giliani S, Abinun M, Mattsson JP et al (2000) Defects in TCIRG1 subunit of the vacuolar proton pump are responsible for a subset of human autosomal recessive osteopetrosis. Nat Genet 25(3):343–346
11. Yang DQ, Feng S, Chen W, Zhao H, Paulson C, Li YP (2012) V-ATPase subunit ATP6AP1 (Ac45) regulates osteoclast differentiation, extracellular acidification, lysosomal trafficking, and protease exocytosis in osteoclast-mediated bone resorption. J Bone Miner Res 27(8):1695–1707
12. Nuckels RJ, Ng A, Darland T, Gross JM (2009)The vacuolar-ATPase complex regulates retinoblast proliferation and survival, photoreceptor morphogenesis, and pigmentation in the zebrafish eye. Invest Ophthalmol Vis Sci 50(2):893–905

13. Kinouchi K, Ichihara A, Sano M, Sun-Wada GH, Wada Y, Kurauchi-Mito A et al (2010) The (pro)renin receptor/ATP6AP2 is essential for vacuolar H+ -ATPase assembly in murine cardiomyocytes. Circ Res 107(1):30–34
14. El Far O, Seagar M (2011) A role for V-ATPase subunits in synaptic vesicle fusion? J Neurochem 117(4):603–612
15. Williamson WR, Wang D, Haberman AS, Hiesinger PR (2010) A dual function of V0-ATPase a1 provides an endolysosomal degradation mechanism in Drosophila melanogaster photoreceptors. J Cell Biol 189(5):885–899
16. Sun-Wada GH, Toyomura T, Murata Y, Yamamoto A, Futai M, Wada Y (2006) The a3 isoform of V-ATPase regulates insulin secretion from pancreatic beta-cells. J Cell Sci 119(Pt 21):4531–4540
17. Lee SH, Rho J, Jeong D, Sul JY, Kim T, Kim N et al (2006) v-ATPase V0 subunit d2-deficient mice exhibit impaired osteoclast fusion and increased bone formation. Nat Med 12(12):1403–1409
18. Hiesinger PR, Fayyazuddin A, Mehta SQ, Rosenmund T, Schulze KL, Zhai RG et al (2005) The v-ATPase V0 subunit a1 is required for a late step in synaptic vesicle exocytosis in Drosophila. Cell 121(4):607–620
19. Peri F, Nusslein-Volhard C (2008) Live imaging of neuronal degradation by microglia reveals a role for v0-ATPase a1 in phagosomal fusion in vivo. Cell 133(5):916–927
20. Ernstrom GG, Weimer R, Pawar DR, Watanabe S, Hobson RJ, Greenstein D et al (2012) V-ATPase V1 sector is required for corpse clearance and neurotransmission in Caenorhabditis elegans. Genetics 191(2):461–475
21. Wax MB, Saito I, Tenkova T, Krupin T, Becker B, Nelson N et al (1997) Vacuolar H+ -ATPase in ocular ciliary epithelium. Proc Nat Acad Sci 94(13):6752–6757
22. Kawamura N, Tabata H, Sun-Wada GH, Wada Y (2010) Optic nerve compression and retinal degeneration in Tcirg1 mutant mice lacking the vacuolar-type H-ATPase a3 subunit. PloS One 5(8):e12086
23. Steward CG (2003) Neurological aspects of osteopetrosis. Neuropathol Appl Neurobiol 29(2):87–97
24. Deguchi J, Yamamoto A, Yoshimori T, Sugasawa K, Moriyama Y, Futai M et al (1994) Acidification of phagosomes and degradation of rod outer segments in rat retinal pigment epithelium. Invest Ophthalmol Vis Sci 35(2):568–579
25. Bergmann M, Schutt F, Holz FG, Kopitz J (2004) Inhibition of the ATP-driven proton pump in RPE lysosomes by the major lipofuscin fluorophore A2-E may contribute to the pathogenesis of age-related macular degeneration. FASEB J 18(3):562–564
26. Gross JM, Perkins BD, Amsterdam A, Egana A, Darland T, Matsui JI et al (2005) Identification of zebrafish insertional mutants with defects in visual system development and function. Genetics 170(1):245–261
27. Lange C, Prenninger S, Knuckles P, Taylor V, Levin M, Calegari F (2011) The H(+) vacuolar ATPase maintains neural stem cells in the developing mouse cortex. Stem Cells Dev 20(5):843–850
28. Tanigaki K, Sasaki S, Ohkuma S (2003) In bafilomycin A1-resistant cells, bafilomycin A1 raised lysosomal pH and both prodigiosins and concanamycin A inhibited growth through apoptosis. FEBS Lett 537(1–3):79–84
29. Strauss O (2005) The retinal pigment epithelium in visual function. Physiol Rev 85(3):845–881
30. Baylor DA, Fuortes MG, O'Bryan PM (1971) Receptive fields of cones in the retina of the turtle. J Physiol 214(2):265–294
31. Jouhou H, Yamamoto K, Homma A, Hara M, Kaneko A, Yamada M (2007) Depolarization of isolated horizontal cells of fish acidifies their immediate surrounding by activating V-ATPase. J Physiol 585(Pt 2):401–412
32. Mikami Y, Shibuya N, Kimura Y, Nagahara N, Yamada M, Kimura H (2011) Hydrogen sulfide protects the retina from light-induced degeneration by the modulation of $Ca^{2+}$ influx. J Biol Chem 286(45):39379–39386

# Chapter 14
# Rescue of Compromised Lysosomes Enhances Degradation of Photoreceptor Outer Segments and Reduces Lipofuscin-Like Autofluorescence in Retinal Pigmented Epithelial Cells

**Sonia Guha, Ji Liu, Gabe Baltazar, Alan M. Laties and Claire H. Mitchell**

**Abstract** Healthful cell maintenance requires the efficient degradative processing and removal of waste material. Retinal pigmented epithelial (RPE) cells have the onerous task of degrading both internal cellular debris generated through autophagy as well as phagocytosed photoreceptor outer segments. We propose that the inadequate processing material with the resulting accumulation of cellular waste contributes to the downstream pathologies characterized as age-related macular degeneration (AMD). The lysosomal enzymes responsible for clearance function optimally over a narrow range of acidic pH values; elevation of lysosomal pH by compounds like chloroquine or A2E can impair degradative enzyme activity and lead to a lipofuscin-like autofluorescence. Restoring acidity to the lysosomes of RPE cells can enhance activity of multiple degradative enzymes and is therefore a logical target in early AMD. We have identified several approaches to reacidify lysosomes of compromised RPE cells; stimulation of beta-adrenergic, $A_{2A}$ adenosine and D5 dopamine receptors each lowers lysosomal pH and improves degradation of outer segments. Activation of the CFTR chloride channel also reacidifies lysosomes and increases degradation. These approaches also restore the lysosomal pH of RPE cells from aged ABCA4$^{-/-}$ mice with chronically high levels of A2E,

C. H. Mitchell (✉) · S. Guha · G. Baltazar
Department of Anatomy and Cell Biology, University of Pennsylvania,
440 Levy Bldg., 240 S. 40th St., Philadelphia, PA 19104, USA
e-mail: chm@exchange.upenn.edu

S. Guha
e-mail: guha@jsei.ucla.edu

J. Liu · C. H. Mitchell
Department of Physiology, University of Pennsylvania, Philadelphia, PA 19104, USA
e-mail: ji.liu.jl2383@yale.edu

G. Baltazar
e-mail: Gabo823@gmail.com

A. M. Laties
Department of Ophthalmology, University of Pennsylvania, Philadelphia, PA 19104, USA
e-mail: laties@mail.med.upenn.edu

J. D. Ash et al. (eds.), *Retinal Degenerative Diseases,* Advances in Experimental Medicine and Biology 801, DOI 10.1007/978-1-4614-3209-8_14,

suggesting that functional signaling pathways to reacidify lysosomes are retained in aged cells like those in patients with AMD. Acidic nanoparticles transported to RPE lysosomes also lower pH and improve degradation of outer segments. In summary, the ability of diverse approaches to lower lysosomal pH and enhance outer segment degradation support the proposal that lysosomal acidification can prevent the accumulation of lipofuscin-like material in RPE cells.

**Keywords** Retinal pigment epithelium (RPE) · Age-related macular degeneration (AMD) · Lipofuscin · Autophagy · Lysosomal pH · Stargardt's disease · Enzymatic degradation · Signal transduction · Nanoparticles

## 14.1 AMD, Lysosomes and pH

The cardinal features of age-related macular degeneration (AMD) pathogenesis have been defined. A series of observations have clarified a step-wise progression consequent to inadequate internal maintenance of the RPE cell [1]. Failure to properly degrade and/or recycle protein and lipid derived from the daily ingestion of phagosomes, as well as internal material through autophagy, leads to the slow accumulation of lipoprotein aggregates [2]. Such aggregates are in part retained and in part exocytosed basolaterally. In time those that are retained impede essential cell function, while the exocytosed material forms deposits in the subretinal space and infiltrates into Bruch's membrane. Characterized by pathologists as basal laminar deposits, basal linear deposits and drusen, these aggregates engender a series of local reactions that include incitement of innate immunity [3]. By their volume, the subretinal deposits lengthen the distance between the choroidal circulation and the inner segments of photoreceptors. Further, lipoprotein infiltration of Bruch's membrane leads to a series of pathologies that include breakdown of the elastic lamina, swelling, and loss of permeability. Since the RPE, as one of its essential functions, aids in the maintenance of retinal transparency by constantly acting as an outward water pump—a necessary prerequisite for transparency, the impedance to outward water movement is responsible for the frequently observed pigment epithelial detachment noted in subjects with AMD.

While the phenotypes associated with AMD are likely due to numerous overlapping pathologies, we propose that the inadequate breakdown of material by RPE lysosomes provides a common locus that may explain many of the subsequent effects. The sharp pH sensitivity of lysosomal enzymes, combined with evidence that this pH is elevated by compounds associated with AMD-like retinopathies, make lysosomal pH an ideal target in addressing AMD at its early stages (Fig. 14.1).

## 14.2 Pathological Elevation of Lysosomal pH in RPE Cells

The lysosomal pH of RPE cells can be elevated by numerous insults. For example, the anti-malarial drug chloroquine has long been known to alkalinize lysosomes [4]. This tertiary amine accumulates in acidic organelles, freely diffusing across the

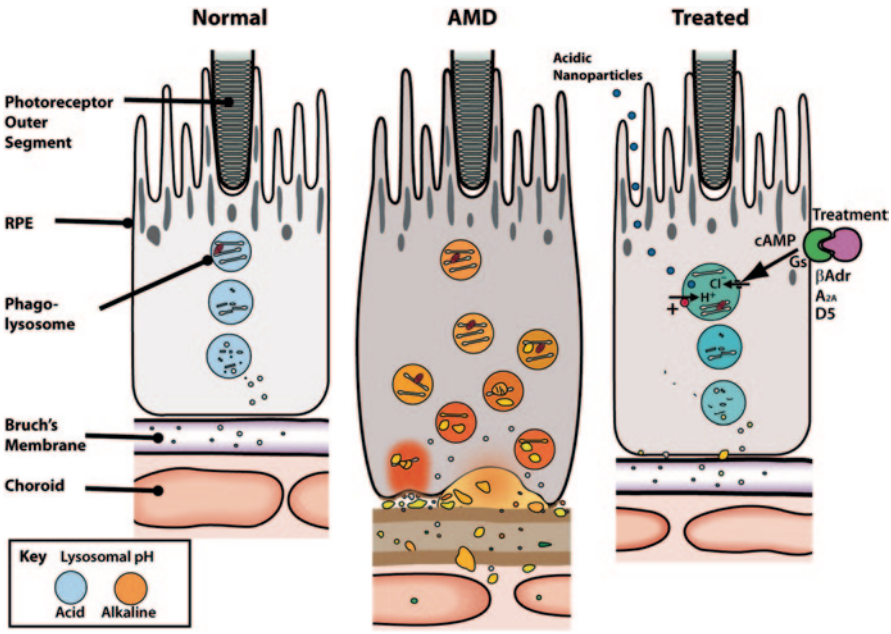


**Fig. 14.1** The restoration of an acidic lysosomal pH is proposed to enhance the degradation of phagocytosed POS and autophagic material in RPE cells. Activation of receptors linked to the $G_s$ protein such as the beta-adrenergic, $A_{2a}$ adenosine, and D5 dopamine receptor lead to a rise in cytoplasmic cAMP which can enhance the conductance through an anionic channel and acidify lysosomes, or increase activity of the vesicular proton pump. Acidic nanoparticles trafficed to lysosomes also improve the activity of degradative enzymes and enhance clearance. The degree to which treatment can forstall the pathological developments in AMD such as drusen formation may depend upon how early it is begun

membrane and then becoming trapped upon protonation. Tamoxifen also elevates lysosomal pH in RPE cells independently of its estrogenic actions; while a similar trapping mechanism is suspected a detergent-like effect may also contribute to the alkalinization [5, 6].

Of particular interest to RPE cells is the observation that lysosomal pH may also be increased by chronic exposure to N-retinylidene-N-retinylethinolamide (A2E), a byproduct of the visual cycle. A2E accumulates with age in most individuals, but rises to higher levels at an earlier age when the ABCA4 transporter is defective as in recessive Stargardt's disease [7]. A2E rapidly localizes to the lysosomes of RPE cells [8]. Although short term exposure to high levels can impair cholesterol and phospholipid metabolism, it does not change lysosomal pH [9, 10]. However, chronic exposure to A2E does raise lysosomal pH; several weeks of A2E reduces the ATPase activity of isolated lysosomes, slows degradation of photoreceptor outer segments (POS) and reduces autophagy [11, 12]. Further evidence for an alkalinizing effect of A2E comes from the RPE cells of ABCA4$^{-/-}$ mice, whose lysosomes have a substantially higher pH as compared to that of age matched controls [6]. Whether the delayed alkalinization by A2E is caused by its detergent-like effects in the membrane, by changes to cholesterol metabolism or changes in expression of

lysosomal genes remains unclear, but as quaternary amines like A2E do not display the rapid protonation in acidic environments seen by tertiary amines like chloroquine, the lack of rapid alkalinization is expected.

## 14.3 Consequences of Lysosomal Alkalinization on Degradation

Lysosomal enzymes function optimally over a narrow range of acidic pH values and the predominant lysosomal enzymes of the RPE reflect this tight pH dependence. For instance, activity of the major RPE enzyme lysosomal acid lipase decreases by 60% when the pH is raised from 4.5 to 5.2, while activity of major protease cathepsin D falls by 80% when the pH rises from 4.5 to 5.0 [13, 14]. This sharp pH dependence of enzyme activity implies that alkalinizing lysosomes of RPE cells will lower the activity of multiple enzymes and interfere with the degradation of internalized outer segments. Autofluorescence associated with POS was increased in RPE cells exposed to cholorquine while lysosomal alkalinization decreased accessability of lysosomal enzyme cathepsin D [15, 16]. POS clearance is also reduced when lysosomal pH is elevated with tamoxifen [17]. Lysosomal alkalinization also disrupts outer segment degradation by RPE cells *in vivo*. Chronic treatment of rats with chloroquine leads to the accumulation of lysosomal-associated organelles and multilamellar bodies within the RPE cells and of partially degraded material of photoreceptor origin in and around Bruch's membrane [18, 19]. Together, these studies imply lysosomal alkalinization is itself sufficient to impair POS degradation by RPE calls and promote deposition of exocytosed debris onto Bruch's membrane.

## 14.4 Restoration of An Acidic Lysosomal pH to Compromised RPE Cells

The restoration of an acidic lysosomal pH to compromised RPE cells can simultaneously increase the activity of numerous degradative enzymes. Our laboratory employed a screening approach to identify drugs capable of reacidifying lysosomes in damaged RPE cells. Epinephrine, norepinephrine, and beta-adrenergic agonist isoproterenol reacidified lysosomes [6]. The non-specific adenosine receptor agonist 5′-*N*-ethylcarboxamidoadenosine (NECA) and the $A_{2A}$ adenosine receptor agonist CGS21680 reacidified lysosomes, while $A_1$ adenosine receptor agonists were not effective [6]. Dopamine agonists A68930, A77636, and SKF81297 all reacidified lysosomes in compromised RPE cells; siRNA identified the D5 dopamine receptor as mediating the response; while, SFK81297 sustained reacidification for at least 12 days [16].

Beta adrenergic, $A_{2A}$ adenosine, and D5 dopamine receptors are all linked to the $G_s$ protein. As activation of $G_s$ elevates cytoplasmic cAMP, the second messenger

was implicated in the reacidification. This was confirmed when the direct elevation of cytoplasmic cAMP with membrane permeant cpt-cAMP reacidified lysosomes in treated cells [6]. Protein kinase A was also identified as involved in the pathway.

Lysosomal reacidification is partially dependent upon enhanced $Cl^-$ influx into the lysosomes [17]. The entry of anions into the lysosomal lumen can minimize the change in electrical potential that accompanies an accumulation of protons, allowing a higher concentration of protons, and thus a lower pH, to be established. Specific activators of the $Cl^-$ channel CFTR restored lysosomal pH. The effect of CFTR-associated drugs was larger in cells with alkalinized lysosomes, consistent with the pH dependence of channel selectivity. This suggests the transport mechanisms underlying this receptor-mediated reacidification may be distinct from those that set the baseline pH levels of the lysosome. This implies that activation of the cAMP-dependent pathway may target damaged lysosomes with little effect on the healthy organelle.

This approach was effective on RPE cells from older ABCA4$^{-/-}$ mice. Direct activation of cAMP substantially reacidified lysosomes of RPE cells from 6-month-old ABCA4$^{-/-}$ mice [6], while dopamine D5 receptor agonists lowered lysosomal pH in RPE cells from 11-month-old ABCA4$^{-/-}$ mice [16]. Together these findings imply that the cAMP pathway and receptors can function in damaged cells from older animals. As most patients with AMD have lysosomes that have been perturbed for many years, any putative treatment must be effective on cells that have been likewise disrupted.

In addition to the pharmacological approaches above, acidic nanoparticles have also been used to reacidify lysosomes from compromised RPE cells [15]. Poly DL-lactide spheres were rapidly taken up unto the RPE cells and colocalized with lysosomes within 60 min. These acidic nanospheres reduced the pH in cells exposed to chloroquine when measured after 1 hr. Remarkably, lysosomal pH remained significantly acidified 12 days after one application of nanoparticles.

## 14.5 Functional Effects of Lysosomal Reacidification

The lysosomal reacidification induced by the above treatments leads to functional improvements in RPE cells. For example, exposure of RPE cells to POS for a week increased the lipofuscin-like autofluorescence, but treatment with the D5 dopamine receptor agonist SKF81297 completely prevented this. SKF 81297 also restored access to the cathepsin D binding sites, consistent with the improved degradation [16]. Stimulation of $A_{2A}$ adenosine and beta adrenergic receptors, and activation of CFTR, also enhanced the degradation of POS [6, 17]. Poly-DL lactide nanospheres restored access to the cathepsin D binding site and reduced the lipofuscin-like autofluorescence from outer segments. The nanospheres also reduced opsin levels by over 90%, confirming their role in degradation of outer segments. The ability of acidic nanoparticles to induce analogous enhancement in outer segment degradation clearly demonstrates that functional effects are downstream of lysosomal acidification and not due to non-specific actions of cAMP.

## 14.6 Summary

In conclusion, these studies have identified several different approaches to reacidify compromised lysosomes in RPE. Reacidification enhances the degradation of spent POS and lessens lipofuscin-like autofluorescence. This strategy may potentially have a general utility in prevention of AMD at an early stage.

## References

1. Ambati J, Fowler BJ (2012) Mechanisms of age-related macular degeneration. Neuron 75:26–39
2. Brunk UT, Terman A (2002) Lipofuscin: mechanisms of age-related accumulation and influence on cell function. Free Rad Biol Med 33:611–619
3. Curcio CA, Johnson M, Rudolf M, Huang JD (2011) The oil spill in ageing Bruch membrane. The Br J Ophthalmol 95:1638–1645
4. de Duve C, de Barsy T, Poole B, Trouet A, Tulkens P, Van Hoof F (1974) Lysosomotropic agents. Biochem Pharmacol 23:2495–2531
5. Altan N, Chen Y, Schindler M, Simon SM (1999) Tamoxifen inhibits acidification in cells independent of the estrogen receptor. Proc Nat Acad Sci USA 96:4432–4437
6. Liu J, Lu W, Reigada D, Nguyen J, Laties AM, Mitchell CH (2008) Restoration of lysosomal pH in RPE cells from cultured human and ABCA4(-/-) mice: pharmacologic approaches and functional recovery. Invest Ophthalmol Vis Sci 49:772–780
7. Mata NL, Weng J, Travis GH (2000) Biosynthesis of a major lipofuscin fluorophore in mice and humans with ABCR-mediated retinal and macular degeneration. Proc Nat Acad Sci USA 97:7154–7159
8. Sparrow JR, Parish CA, Hashimoto M, Nakanishi K (1999) A2E, a lipofuscin fluorophore, in human retinal pigmented epithelial cells in culture. Invest Ophthalmol Vis Sci 40:2988–2995
9. Finnemann SC, Leung LW, Rodriguez-Boulan E (2002) The lipofuscin component A2E selectively inhibits phagolysosomal degradation of photoreceptor phospholipid by the retinal pigment epithelium. Proc Nat Acad Sci USA 99:3842–3847
10. Lakkaraju A, Finnemann SC, Rodriguez-Boulan E (2007) The lipofuscin fluorophore A2E perturbs cholesterol metabolism in retinal pigment epithelial cells. Proc Nat Acad Sci USA 104:11026–11031
11. Holz FG, Schutt F, Kopitz J, Eldred GE, Kruse FE, Volcker HE et al (1999) Inhibition of lysosomal degradative functions in RPE cells by a retinoid component of lipofuscin. Invest Ophthalmol Vis Sci 40:737–743
12. Bergmann M, Schutt F, Holz FG, Kopitz J (2004) Inhibition of the ATP-driven proton pump in RPE lysosomes by the major lipofuscin fluorophore A2-E may contribute to the pathogenesis of age-related macular degeneration. FASEB J 18:562–564
13. Hayasaka S, Hara S, Mizuno K (1975) Degradation of rod outer segment proteins by cathepsin D. J Biochem 78:1365–1367
14. Barrett A (1977) Proteinases in mammalian cells and tissues. Biomedical Press, New York
15. Baltazar GC, Guha S, Boesze-Battaglia K, Laties AM, Tyagi P, Kompella UB et al (2012) Acidic nanoparticles restore lysosomal pH and degradative function in compromised RPE cells. PloS One 7:e49635
16. Guha S, Baltazar GC, Tu LA, Liu J, Lim JC, Lu W et al (2012) Stimulation of the D5 dopamine receptor acidifies the lysosomal pH of retinal pigmented epithelial cells and decreases accumulation of autofluorescent photoreceptor debris. J Neurochem 122:823–833

17. Liu J, Lu W, Guha S, Baltazar GC, Coffey EE, Laties AM et al (2012) Cystic fibrosis transmembrane conductance regulator (CFTR) contributes to reacidification of alkalinized lysosomes in RPE cells. Am J Physiol Cell Physiol 303:C160–C169
18. Peters S, Reinthal E, Blitgen-Heinecke P, Bartz-Schmidt KU, Schraermeyer U (2006) Inhibition of lysosomal degradation in retinal pigment epithelium cells induces exocytosis of phagocytic residual material at the basolateral plasma membrane. Ophthal Res 38:83–88
19. Mahon GJ, Anderson HR, Gardiner TA, McFarlane S, Archer DB, Stitt AW (2004) Chloroquine causes lysosomal dysfunction in neural retina and RPE: implications for retinopathy. Curr Eye Res 28:277–284

# Chapter 15
# The Role of Bestrophin-1 in Intracellular $Ca^{2+}$ Signaling

**Olaf Strauß, Claudia Müller, Nadine Reichhart, Ernst R. Tamm and Nestor Mas Gomez**

**Abstract** Mutations in the BEST1 gene lead to a variety of retinal degenerations, among them Best's vitelliforme macular degeneration. To clarify the mechanism of the disease, the understanding of the function of BEST1 gene product, bestrophin-1, is mandatory. In overexpression studies bestrophin-1 appeared to function as a $Ca^{2+}$-dependent Cl channel. On the other hand, bestrophin-1 is able to participate in intracellular $Ca^{2+}$ signaling. Endogenously expressed bestrophin-1 largely localized to the cytosolic compartment close to the basolateral membrane of the retinal pigment epithelium (RPE) as it can be shown using differential centrifugation, immunohistochemistry, and transmission electron microscopy. To elucidate a cytosolic function of bestrophin-1, we explored the store-operated $Ca^{2+}$ entry in short-time cultured porcine RPE cells. Depletion of cytosolic $Ca^{2+}$stores by SERCA inhibition led to activation of Orai-1 $Ca^{2+}$ channels. This resulted in an influx of extracellular $Ca^{2+}$ into the cell which was reduced when bestrophin-1 expression was knocked down using siRNA techniques. Quantification of $Ca^{2+}$ which can be released from cytosolic $Ca^{2+}$ stores revealed that after reduction of bestrophin-1 expression less $Ca^{2+}$ is stored in ER $Ca^{2+}$ stores. Thus, bestrophin-1 functions as an intracellular Cl channel which helps to accumulate and to release $Ca^{2+}$ from stores by conducting the counterion for $Ca^{2+}$.

**Keywords** Bestrophin-1 · Stim-1 · Orai-1 · $Ca^{2+}$-signaling · Store-operated $Ca^{2+}$ entry

O. Strauß (✉) · N. Reichhart
Experimental Ophthalmology, Department of Ophthalmology,
Charite University Medicine Berlin, Berlin, Germany
e-mail: olaf.strauss@charite.de

O. Strauß · C. Müller · N. Reichhart · N. M. Gomez
Experimental Ophthalmology, Eye Hospital, University Medical Center Regensburg,
Regensburg, Germany

E. R. Tamm
Institute of Human Anatomy and Embryology, University of Regensburg, Regensburg, Germany

N. M. Gomez
Department of Clinical Studies, School of Veterinary Medicine, University of Pennsylvania,
Philadelphia, USA

J. D. Ash et al. (eds.), *Retinal Degenerative Diseases,* Advances in Experimental Medicine and Biology 801, DOI 10.1007/978-1-4614-3209-8_15,

## 15.1 Bestrophin-1, a Cl Channel and Modulator of Voltage-Dependent $Ca^{2+}$ Channels

Bestrophin-1 is the product of the BEST1 gene [1, 2]. Mutations in BEST1 lead to a variety of retinal degenerations, among them Best's vitelliforme macular dystrophy [1–8]. Bestrophin-1 is expressed in the retinal pigment epithelium (RPE) and there localized to the basolateral membrane [3, 6, 9–12]. In overexpression studies, bestrophin-1 appeared as a $Ca^{2+}$-dependent and swelling-activated Cl channel [3, 6, 13–20]. Furthermore, bestrophin-1 is able to modulate the activity of L-type $Ca^{2+}$ channels [12, 21–24].

## 15.2 Mutations in the BEST1 Gene and Best's Disease

In overexpression studies, disease-leading mutant bestrophin-1 showed a loss of anion conductance [3, 6, 13, 17, 19, 24–26] and/or a loss of trafficking from the endoplasmic reticulum (ER) to the cell membrane [26]. The loss of function possibly explains the pathomechanism of Best's disease: the inability to regulate intracellular ion homeostasis and cell volume regulation of RPE cells [3].

In contrast, the bestrophin-1 knock-out mouse and the W93C knock-in mouse model showed no retinal degeneration and no changes in the Cl conductance in RPE cells [27, 28]. Thus the phenotypes of the bestrophin-1 mouse models challenge the idea that a loss of Cl channel activity of mutant bestrophin-1 cause retinal degeneration. However, the W93C knock-in mouse showed signs of retinal degeneration with comparable symptoms to that of the human disease [28].

## 15.3 Evidence for an Intracellular Localization of Bestrophin-1

The bestrophin-1 functions in overexpression systems and in cells which endogenously expressed bestrophin-1 appears to be controversial. An explanation could be that bestrophin-1 is an intracellular protein. In differential centrifugation, a major proportion of endogenously expressed bestrophin-1 can be found in the fraction of intracellular membrane proteins which contains, for example, the intracellular ClC-3 Cl channel [11]. Co-staining of bestrophin-1 and the membrane protein cadherin in retina sections showed bestrophin-1 on the cytosolic side close to the cadherin staining [11]. Also Barro-Soria et al. found in human airway epithelial cells co-localization of endogenously expressed bestrophin-1 with ER proteins calreticulin and calnexin [29]. Transmission electron microscopy with bestrophin-1 immunogold labeling shows that bestrophin-1 can be found in diffuse electron dense material close to the basolateral membrane (Fig. 15.1). In glutaraldehyde fixation, we

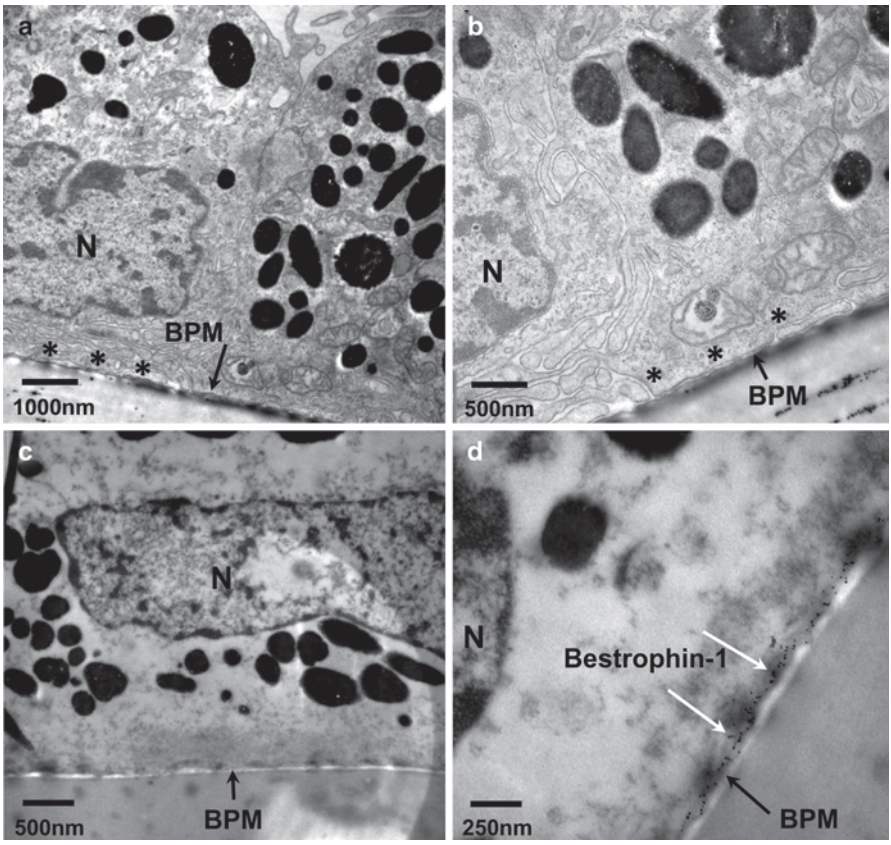


**Fig. 15.1** Intracellular bestrophin-1 detection by means of transmission electron microscopy. Polarized primary porcine RPE cells growing on filter were labeled against bestrophin-1. **a**, **b** Cells were fixed with 2.5% glutaraldehyde, postfixed with 1% $OsO_4$, 0.8% $K_4[Fe(CN)_6]$, and embedded in Epon. Ultrathin sections were stained with uranyl acetate and lead citrate enabling analysis of membranous structures in the RPE. **b** Higher magnification of **a**. **c**, **d** Cells were fixed with 4% (w/v) paraformaldehyde, incubated with antibodies, processed for silver enhancement, postfixed, and embedded in Epon. For controls (**c**), cells were incubated only with the secondary antibody (CFTM 568 Fluor Nano Gold). Immunoreactivity for bestrophin-1 (**d**) was detected using specific primary antibodies, Fluo Nano Gold secondary antibodies as probe and silver enhancement: Gold particles (*white arrows*) indicating the presence of bestrophin-1 are detected in electron dense material close to, but not within the basal plasma membrane. *BPM* basal plasma membrane, *N* nucleus, * smooth ER

can show that these electron dense structures are a network of membranes from the ER. Thus, at least a part of bestrophin-1 is localized to the ER.

## 15.4 Function of Intracellular Bestrophin-1

A detailed analysis of the cytosolic bestrophin-1 function by Barro-Soria et al. [29] showed that bestrophin-1 is required to handle $Ca^{2+}$ in ER $Ca^{2+}$ stores in lung airway cells. As a mechanism bestrophin-1 was able to directly interact with the stromal-interacting molecule-1 (Stim-1) [30] which is a membrane protein of ER $Ca^{2+}$ stores [29].

We have recently investigated a comparable mechanism in RPE cells [31]. Here, we directly addressed the interaction between $Ca^{2+}$ stores and calcium release-activated calcium channel protein 1 (Orai-1) $Ca^{2+}$ channels in cultured porcine RPE cells which show a robust endogenous bestrophin-1 expression. Orai-1 is a $Ca^{2+}$ channel which is activated by direct interaction with Stim-1 [30]. In RPE cells with reduced bestrophin-1 expression induced by siRNA treatment, Orai-1 activation was reduced by 80 % (Fig. 15.2). This was due to a smaller amount of $Ca^{2+}$ releasable from ER store. Thus bestrophin-1 is required to take up and to release $Ca^{2+}$ from ER $Ca^{2+}$ stores [31].

## 15.5 The Cytosolic Bestrophin-1 Function and Best's Disease

A considerable amount of bestrophin-1 functions as an intracellular $Ca^{2+}$-dependent Cl channel. Bestrophin-1 helps to accumulate or to release $Ca^{2+}$ from ER $Ca^{2+}$ stores by conducting the counterion for transfer of positively charged $Ca^{2+}$ ions [29, 31, 32]. Bestrophin-1 as a $Ca^{2+}$-dependent Cl channel would have increased activity at high $Ca^{2+}$ levels and facilitate re-uptake of $Ca^{2+}$ into the ER stores to re-establish basal $Ca^{2+}$ concentrations. Furthermore, the cytosolic localization of bestrophin-1 explains why RPE cells from bestrophin-1 knock-out and W93C knock-in mice show no differences in the membrane conductance for $Cl^-$ and the changes in the $Ca^{2+}$-signaling of these mouse models [27, 28]. However, it is still possible that a fraction of bestrophin-1 functions as plasma membrane Cl channel.

Bestrophin-1 is expressed in the RPE which is a close interaction partner of the photoreceptors [33]. Thus, mutation-dependent changes of bestrophin-1 likely lead to changes in $Ca^{2+}$-dependent regulation of RPE cell function and in consequence to photoreceptor degeneration. These functions are growth-factor secretion, transepithelial transport of $Cl^-$, and the diurnal phagocytosis of photoreceptor outer segments in their renewal process [34–37].

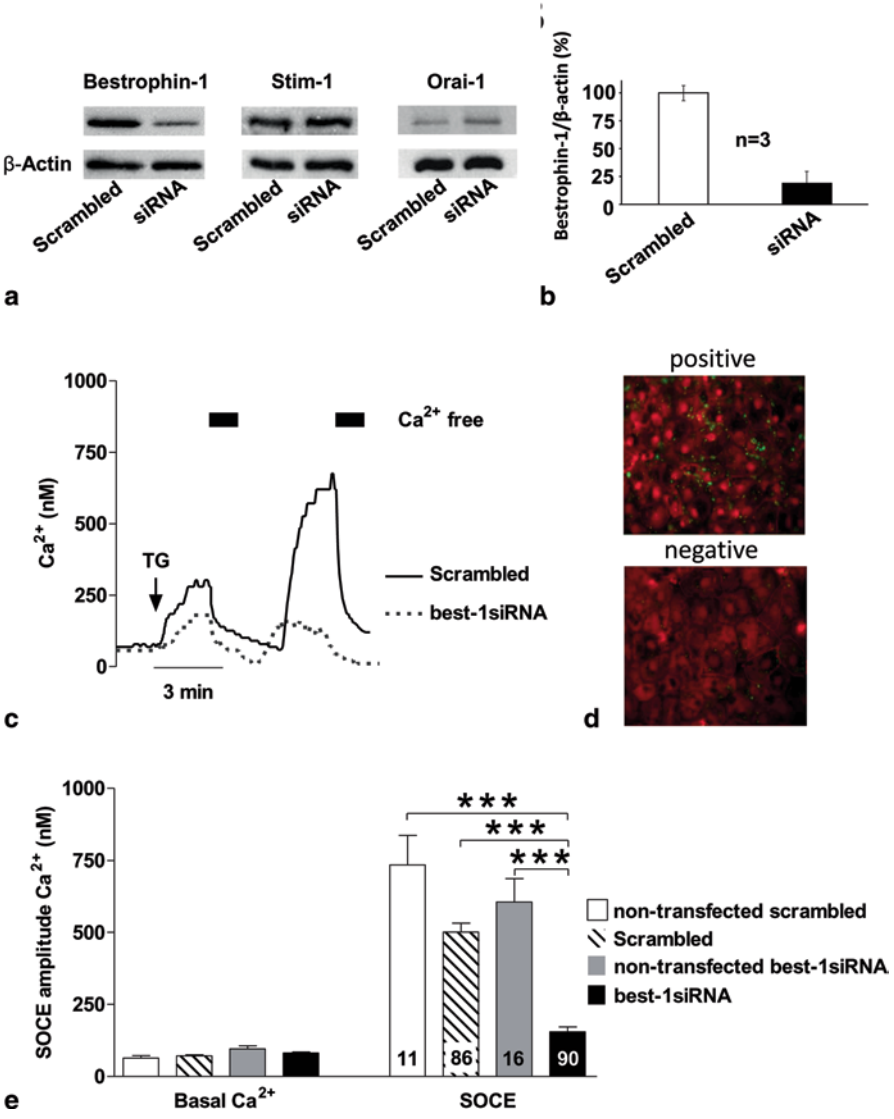


**Fig. 15.2** Knockdown of bestrophin-1 protein. **a** Western blot shows the knockdown of bestrophin-1 protein in best-1siRNA-transfected cells compared to scrambled siRNA-transfected cells. Stromal-interacting molecule-1 (*stim-1*) and calcium release-activated calcium channel protein 1 (*Orai-1*) proteins did not show any expression changes due to best-1siRNA. Equal amounts of protein were loaded to the blot. **b** Quantification of knockdown bestrophin-1 after a densitometric analysis. **c** Calcium tracing of SOCE in scrambled (*solid line*) and best-1siRNA (*dashed line*) transfected cells. Cells were treated previously with Ringer solution, after thapsigargin (1 μM) was applied for 3 min and followed by $Ca^{2+}$-free solution for 80 s, and later, extracellular $Ca^{2+}$ was re-added to the cells. **d** Detection of best-1siRNA transfected cells. Cells transfected (*upper panel*) and not transfected (*lower panel*) with Alexa 488 fluorophor-labeled best-1siRNA. **e** Statistic analysis of basal $Ca^{2+}$ and SOCE activation amplitude between scrambled siRNA and best-1siRNA transfected cells. Transfected cells and non-transfected (n.t) cells were also compared within each set of experiment (best-1siRNA and scrambled; $*P \leq 0.05$; $**P \leq 0.01$; $***P \leq 0.001$; $n_{\text{scrambled}} = 86$ and $n_{\text{scrambled(n.t)}} = 11$; $n_{\text{best-1siRNA}} = 90$, and $n_{\text{best-1siRNA(n.t)}} = 16$; all experiments were done in three different rounds of primary cells isolation; number of scrambled experiment = 8 and number of best-1siRNA experiment = 6). (Source: Mas Gomez et al. [31], with permission by Springer)

## References


1. Petrukhin K, Koisti MJ, Bakall B, Li W, Xie G, Marknell T et al (1998) Identification of the gene responsible for best macular dystrophy. Nat Genet 19(3):241–247
2. Marquardt A, Stohr H, Passmore LA, Kramer F, Rivera A, Weber BH (1998) Mutations in a novel gene, VMD2, encoding a protein of unknown properties cause juvenile-onset vitelliform macular dystrophy (Best's disease). Hum Mol Genet 7(9):1517–1525
3. Hartzell HC, Qu Z, Yu K, Xiao Q, Chien LT (2008) Molecular physiology of bestrophins: multifunctional membrane proteins linked to best disease and other retinopathies. Physiol Rev 88(2):639–672
4. Marmorstein AD, Cross HE, Peachey NS (2009) Functional roles of bestrophins in ocular epithelia. Prog Retin Eye Res 28(3):206–226
5. Boon CJ, Klevering BJ, Leroy BP, Hoyng CB, Keunen JE, den Hollander AI (2009) The spectrum of ocular phenotypes caused by mutations in the BEST1 gene. Prog Retin Eye Res 28(3):187–205
6. Xiao Q, Hartzell HC, Yu K (2010) Bestrophins and retinopathies. Pflugers Arch 460(2):559–569
7. Planells-Cases R, Jentsch TJ (2009) Chloride channelopathies. Biochim Biophys Acta 1792(3):173–189
8. White K, Marquardt A, Weber BH (2000) VMD2 mutations in vitelliform macular dystrophy (Best disease) and other maculopathies. Hum Mutat 15(4):301–308
9. Milenkovic VM, Rivera A, Horling F, Weber BH (2007) Insertion and topology of normal and mutant bestrophin-1 in the endoplasmic reticulum membrane. J Biol Chem 282(2):1313–1321
10. Marmorstein AD, Marmorstein LY, Rayborn M, Wang X, Hollyfield JG, Petrukhin K (2000) Bestrophin the product of the Best vitelliform macular dystrophy gene (VMD2), localizes to the basolateral plasma membrane of the retinal pigment epithelium. Proc Natl Acad Sci USA 97(23):12758–12763
11. Neussert R, Muller C, Milenkovic VM, Strauss O (2010) The presence of bestrophin-1 modulates the $Ca^{2+}$ recruitment from $Ca^{2+}$ stores in the ER. Pflugers Arch 460(1):163–175
12. Reichhart N, Milenkovic VM, Halsband CA, Cordeiro S, Strauss O (2010) Effect of bestrophin-1 on L-type $Ca^{(2+)}$ channel activity depends on the $Ca^{(2+)}$ channel beta-subunit. Exp Eye Res 91(5):630–639
13. Sun H, Tsunenari T, Yau KW, Nathans J (2002) The vitelliform macular dystrophy protein defines a new family of chloride channels. Proc Natl Acad Sci USA 99(6):4008–4013
14. Hartzell C, Putzier I, Arreola J (2005) Calcium-activated chloride channels. Annu Rev Physiol 67:719–758
15. Fischmeister R, Hartzell HC (2005) Volume sensitivity of the bestrophin family of chloride channels. J Physiol 562(Pt 2):477–491
16. Xiao Q, Yu K, Cui YY, Hartzell HC (2009) Dysregulation of human bestrophin-1 by ceramide-induced dephosphorylation. J Physiol 587(Pt 18):4379–4391
17. Marchant D, Yu K, Bigot K, Roche O, Germain A, Bonneau D et al (2007) New VMD2 gene mutations identified in patients affected by Best vitelliform macular dystrophy. J Med Genet 44(3):e70
18. Yu K, Cui Y, Hartzell HC (2006) The bestrophin mutation A243V, linked to adult-onset vitelliform macular dystrophy, impairs its chloride channel function. Invest Ophthalmol Vis Sci 47(11):4956–4961
19. Qu Z, Hartzell HC (2008) Bestrophin Cl− channels are highly permeable to HCO3−. Am J Physiol Cell Physiol 294(6):C1371–C1377
20. Chien LT, Hartzell HC (2008) Rescue of volume-regulated anion current by bestrophin mutants with altered charge selectivity. J Gen Physiol 132(5):537–546
21. Rosenthal R, Heimann H, Agostini H, Martin G, Hansen LL, Strauss O (2007) $Ca^{2+}$ channels in retinal pigment epithelial cells regulate vascular endothelial growth factor secretion rates in health and disease. Mol Vis 13:443–456

22. Milenkovic VM, Krejcova S, Reichhart N, Wagner A, Strauss O (2011) Interaction of bestrophin-1 and $Ca^{2+}$ channel β-subunits: identification of new binding domains on the bestrophin-1 C-terminus. PLoS One; in revision
23. Yu K, Xiao Q, Cui G, Lee A, Hartzell HC (2008) The best disease-linked Cl− channel hBest1 regulates Ca V 1 (L-type) $Ca^{2+}$ channels via src-homology-binding domains. J Neurosci 28(22):5660–5670
24. Burgess R, Millar ID, Leroy BP, Urquhart JE, Fearon IM, De Baere E et al (2008) Biallelic mutation of BEST1 causes a distinct retinopathy in humans. Am J Hum Genet 82(1):19–31
25. Davidson AE, Millar ID, Urquhart JE, Burgess-Mullan R, Shweikh Y, Parry N et al (2009) Missense mutations in a retinal pigment epithelium protein, bestrophin-1, cause retinitis pigmentosa. Am J Hum Genet 85(5):581–592
26. Milenkovic VM, Roehrl E, Weber BH, Strauss O (2011) Disease-associated missense mutations in bestrophin-1 affect cellular trafficking and anion conductance. J Cell Sci (submitted)
27. Marmorstein LY, Wu J, McLaughlin P, Yocom J, Karl MO, Neussert R et al (2006) The light peak of the electroretinogram is dependent on voltage-gated calcium channels and antagonized by bestrophin (best-1). J Gen Physiol 127(5):577–589
28. Zhang Y, Stanton JB, Wu J, Yu K, Hartzell HC, Peachey NS et al (2010) Suppression of $Ca^{2+}$ signaling in a mouse model of Best disease. Hum Mol Genet 19(6):1108–1118
29. Barro-Soria R, Aldehni F, Almaca J, Witzgall R, Schreiber R, Kunzelmann K (2010) ER-localized bestrophin 1 activates $Ca^{2+}$-dependent ion channels TMEM16A and SK4 possibly by acting as a counterion channel. Pflugers Arch 459(3):485–497
30. Putney JW Jr (2005) Capacitative calcium entry: sensing the calcium stores. J Cell Biol 169(3):381–382
31. Mas Gomez N, Tamm ER, Strauss O (2012) Involvement of bestrophin-1 in store-operated calcium entry in porcine retinal pigment epithelium. Pflugers Arch (Dec.4, Epub ahead of print)
32. Kunzelmann K, Kongsuphol P, Aldehni F, Tian Y, Ousingsawat J, Warth R et al (2009) Bestrophin and TMEM16-$Ca^{(2+)}$ activated Cl(−) channels with different functions. Cell Calcium 46(4):233–241
33. Strauss O (2005) Retinal pigment epithelium in visual function. Physiol Rev 85(3):845–881
34. Wimmers S, Karl MO, Strauss O (2007) Ion channels in the RPE. Prog Retin Eye Res 26(3):263–301
35. Maminishkis A, Jalickee S, Blaug SA, Rymer J, Yerxa BR, Peterson WM et al (2002) The P2Y(2) receptor agonist INS37217 stimulates RPE fluid transport in vitro and retinal reattachment in rat. Invest Ophthalmol Vis Sci 43(11):3555–3566
36. Mitchell CH (2001) Release of ATP by a human retinal pigment epithelial cell line: potential for autocrine stimulation through subretinal space. J Physiol 534(Pt 1):193–202
37. Peterson WM, Meggyesy C, Yu K, Miller SS (1997) Extracellular ATP activates calcium signaling, ion, and fluid transport in retinal pigment epithelium. J Neurosci 17(7):2324–233715

# Part III
# Basic Processes: Methodology

# Chapter 16
# Application of Next-Generation Sequencing to Identify Genes and Mutations Causing Autosomal Dominant Retinitis Pigmentosa (adRP)

**Stephen P. Daiger, Sara J. Bowne, Lori S. Sullivan, Susan H. Blanton, George M. Weinstock, Daniel C. Koboldt, Robert S. Fulton, David Larsen, Peter Humphries, Marian M. Humphries, Eric A. Pierce, Rui Chen and Yumei Li**

**Abstract** The goal of our research is to identify genes and mutations causing autosomal dominant retinitis pigmentosa (adRP). For this purpose we established a cohort of more than 250 independently ascertained families with adRP in the Houston Laboratory for Molecular Diagnosis of Inherited Eye Diseases. Affected members of each family were screened for disease-causing mutations in genes and gene regions that are commonly associated with adRP. By this approach, we detected mutations in 65 % of the families, leaving 85 families that are likely to harbor mutations outside of the "common" regions or in novel genes. Of these, 32 families were tested by several types of next-generation sequencing (NGS), including (a) targeted polymerase chain reaction (PCR) NGS, (b) whole exome NGS, and (c) targeted retinal-capture NGS. We detected mutations in 11 of these families (31 %) bringing the total detected in the adRP cohort to 70 %. Several large families have also been tested for linkage using Afymetrix single nucleotide polymorphism (SNP) arrays.

**Keywords** Retinitis pigmentosa · Next-generation sequencing · Linkage mapping · Mutation prevalence · Retinal gene capture · Whole-exome sequencing

S. P. Daiger (✉) · S. J. Bowne · L. S. Sullivan
Human Genetics Center, School of Public Health, Univ. of Texas HSC,
1200 Herman Pressler Dr., 77030 Houston, TX, USA
e-mail: Stephen.P.Daiger@uth.tmc.edusss

S. H. Blanton
Miami Institute for Human Genomics, Univ. of Miami, Miami, FL, USA

G. M. Weinstock · D. C. Koboldt · R. S. Fulton · D. Larsen
Genome Institute, Washington Univ. School of Med., St. Louis, MO, USA

P. Humphries · M. M. Humphries
Dept. of Genetics, Trinity College, Dublin, Ireland

E. A. Pierce
Ocular Genomics Institute, Massachusetts Eye and Ear Infirmary, Boston, MA, USA

R. Chen · Y. Li
Dept. of Molecular and Human Genetics, Baylor College of Medicine, Houston, TX, USA

J. D. Ash et al. (eds.), *Retinal Degenerative Diseases,* Advances in Experimental Medicine and Biology 801, DOI 10.1007/978-1-4614-3209-8_16,

## 16.1 Introduction

Retinitis pigmentosa (RP) is a highly heterogeneous set of inherited retinopathies with many causative genes, thousands of reported mutations, and complicated relationships between genotypes and phenotypes [1, 2]. For example, mutations in more than 23 genes are known to cause autosomal dominant RP (adRP), and mutations in 36 genes may cause autosomal recessive RP [3]. Our research focuses on adRP and dominant-acting mutations in X-linked RP genes. Over the past two decades, we have enrolled more than 600 unrelated families with a provisional diagnosis of adRP in our studies. Of these, 256 currently meet or exceed criteria for inclusion in our adRP cohort. To establish prevalences for genes and mutations causing RP, we have applied a staged set of genetic tests to affected members of the cohort. (Newly detected genes are then confirmed in the extended collection of families.) Initial screening includes Sanger sequencing of 12 adRP genes or gene regions known to cause approximately 50% of adRP cases among Americans of European origin and Europeans [4–6], followed by screening for deletions not detected by conventional sequencing [7], and sequencing of the X-linked RP genes RPGR and RP2 to detect mutations which may cause clinically significant retinal disease in carrier females [8].

Disease-causing mutations were found in 65% of the adRP cohort families based on these sequential steps. The remaining families then became candidates for different sequencing approaches based on high-throughput, next-generation sequencing (NGS). Methods included targeted polymerase chain reaction (PCR) of 46 genes, linkage mapping using Affymetrix 6.0 single nucleotide variation (SNV) arrays, whole-exome sequencing, and targeted retinal-capture NGS.

## 16.2 Methods

### *16.2.1 AdRP Cohort*

Families in the adRP cohort were ascertained by clinical collaborators including Dr. David Birch, Retina Foundation of the Southwest, Dallas and Dr. John Heckenlively, Kellogg Eye Center, Univ. of Michigan, Ann Arbor. Clinical examinations included visual acuity, visual fields and dark adaptation, and, in most cases, optical coherence tomography and electroretinography [9]. Criteria for enrollment in the adRP cohort were three affected generations with affected females, or two affected generations with male-to-male transmission (to minimize X-linked RP). DNAs were first tested by Sanger sequencing in our CLIA-certified diagnostic laboratory and then, if no mutation was found, entered into our NGS research protocols. See Fig. 16.1 for sample staging.

The study was performed in accordance with the Declaration of Helsinki, and was approved by the Committee for the Protection of Human Subjects of the University of Texas Health Science Center at Houston and by the respective human subjects' review boards at each participating institution.

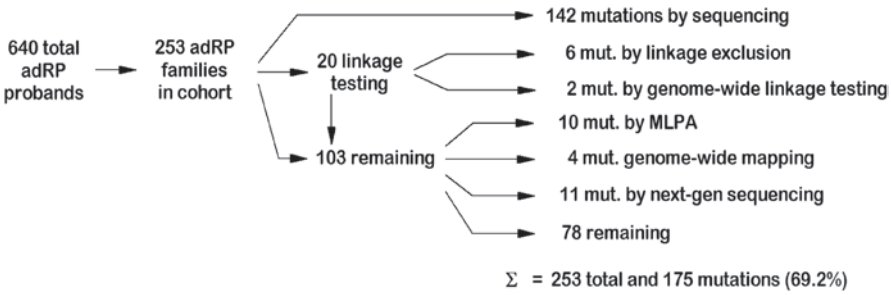


**Fig. 16.1** Flow chart of testing stages for families in the adRP cohort of the Houston Laboratory for Molecular Diagnosis of Inherited Eye Diseases (LMDIED)

### *16.2.2 Targeted PCR NGS*

Twenty-one families were tested by targeted PCR amplification of 46 known RP genes, equivalent to 1,000 PCR amplimer products, followed by NGS using 454GS FLX Titanium GAIIx and Illumina/Solexa platforms to an average sequence depth of 70X and 150X, respectively [10, 11].

### *16.2.3 Linkage Mapping*

Whole-exome linkage testing was conducted using Affymetrix 6.0 single nucleotide polymorphism (SNP)/copy number variation (CNV) arrays and the data were analyzed using the Affymetrix Genotyping Console™ and PLINK [12]. Linkage testing was done in collaboration with Dr. Susan Blanton, Univ. of Miami.

### *16.2.4 Whole-Exome NGS*

Whole-exome NGS was done at the Genome Institute, Washington Univ., St. Louis and in collaboration with Dr. Eric Pierce, Massachusetts Eye and Ear Infirmary, Boston. A variety of platforms, capture reagents and sequencing platforms were used, including Agilent and NimbleGen arrays, Illumina HiSeq and Roche 454 FLX sequencing, and custom resequencing and validation arrays [11, 13]. At least four affected family members and an unaffected parent were tested in each family.

### *16.2.5 Targeted Retinal-Capture NGS*

Targeted retinal-capture NGS was done in collaboration with Dr. Rui Chen, Baylor College of Medicine, Houston. All coding exons, including retina-specific exons, of 172 genes known to cause inherited retinal diseases were captured using Agilent probes and sequenced using the Illumina platform.

**Table 16.1** Pathogenic variants detected in the 1,000 amplimer project

| Family | Gene | Chromosome | Functional class | Coding | Protein | Frequency in controls (%) |
|---|---|---|---|---|---|---|
| VCH010 | KLHL7 | 7p15.3 | missense | c.458C>T | p.Ala153Val | 0.00 |
| VCH012 | GUCY2D | 17p13.1 | missense | c.2512C>T | p.Arg838Cys | 0.00 |
| VCH017 | RPGR | Xp11.4 | nonsense | c.2212C>A | p.Gly738* | 0.00 |
| VCH018 | RPGR | Xp11.4 | missense | c.194C>T | p.Gly65asp | 0.00 |
| VCH020 | PRPF31 | 19q13.42 | splice-site | c.946-1 | unknown | 0.00 |

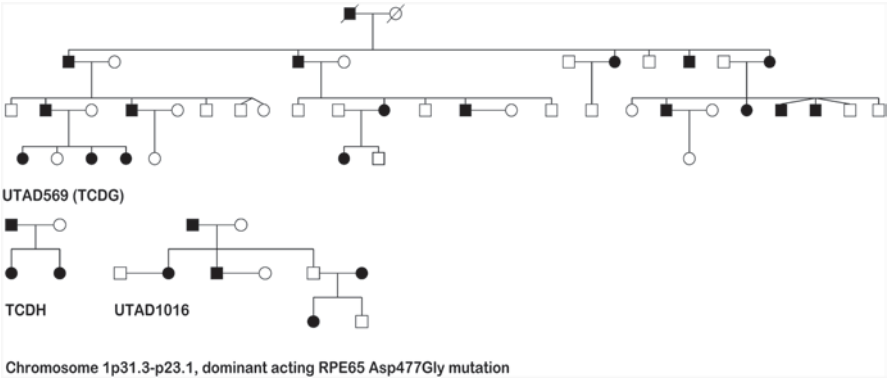


**Fig. 16.2** Pedigrees of Irish and Canadian adRP families with a dominant-acting mutation in RPE65, detected using whole-exome NGS

## 16.3 Results

Starting with 253 families in the adRP cohort, we screened for disease-causing mutations by a variety of approaches (Fig. 16.1) Based on conventional Sanger sequencing, linkage mapping, and multiplex ligation-dependent probe amplification (MLPA) to detect large deletions [7], we determined the disease-causing gene and mutation in 164 families. Of the remaining families, 32 were tested by NGS using three approaches, targeted PCR NGS, whole-exome NGS and targeted retinal-capture NGS. We also mapped the disease locus in several large adRP families by whole-exome linkage mapping. Results, in summary, were as follows.

A. We applied targeted PCR NGS to 21 families. By this approach we identified disease-causing mutations in 5 families (24%) [10] (see Table 16.1).
B. Linkage mapping and whole-exome NGS identified a dominant-acting mutation in RPE65 on chromosome 1p31 in a large Irish family. Novel mutations in known genes were identified in two additional families (Fig. 16.2). No other variants were detected; in vitro studies indicated protein instability; and two additional adRP families with this mutation were observed [13]. Mutations in RPE65 are usually associated with recessive Leber congenital amaurosis. This illustrates that mutations in retinal disease genes may be recessive acting in some cases but different mutations in the same gene may be dominant acting in other cases.

**Table 16.2** Families in the adRP cohort with mapped loci

| Family | People for linkage | Chromosome | Mb (genes) |
|---|---|---|---|
| RFS132 | 25 | 19p13.3 | 1.1 (15) |
| UTAD055 | 20 | 19q13.2–q13.42 | 15.7 (400+) |
| UTAD562 | 15 | 20q13.33-qter | 4.1 (150) |
| UTAD569 | 32 | 1p31.3–p31.1 | 8.8 (50) |
| UTAD598 | 16 | 2q24.1–q31.1 | 14.0 (81) |

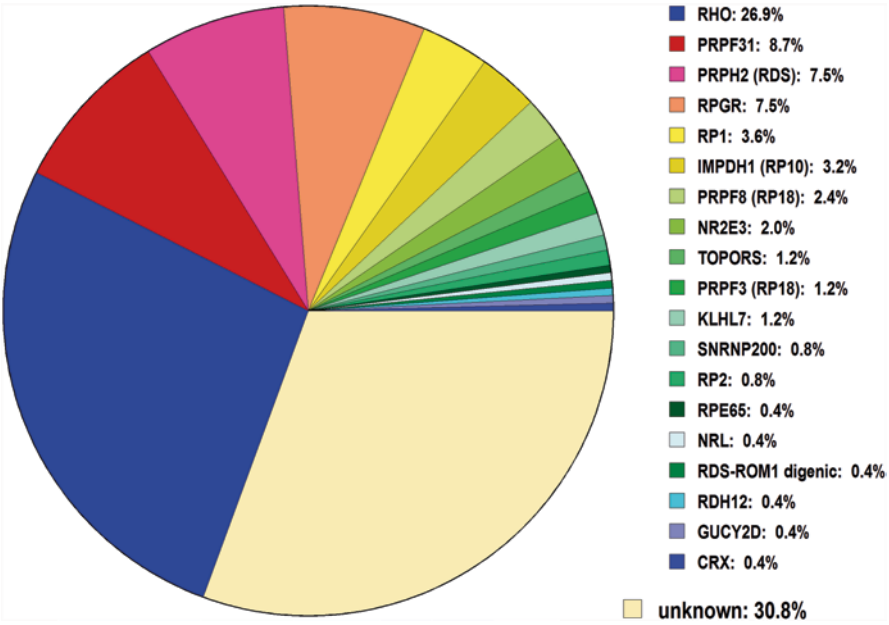


**Fig. 16.3** Mutations detected to date in the Houston LMDIED adRP cohort (including dominant X-linked RP mutations)

C. Further linkage mapping in other families identified potentially-novel adRP loci on 2q24, 19q13, and 20q13 in unrelated families (Table 16.2). These families are currently the subject of whole-exome sequencing, focusing on the minimal linkage region in each case.
D. Targeted retinal-capture NGS involves liquid capture of exons of 172 retinal disease genes (the "RetNet set") using a NimbleGen capture panel, followed by Illumina NGS. In early trials of targeted retinal-capture NGS we detected novel disease-causing mutations in 3 of 13 adRP families tested (23%). This is potentially a rapid, reliable, and highly effective method to detect disease-causing mutations in adRP patients.

Altogether, using several NGS approaches and whole-exome linkage mapping, we detected the disease-causing mutation in 11 of 32 families tested (34%) or 5% of the total adRP cohort (Fig. 16.3 and Table 16.3).

**Table 16.3** Summary of NGS findings in the adRP cohort

| ID | WU-GSC 42 genes | WU-GSC exome | Baylor | Final result |
|---|---|---|---|---|
| RFS021 | – | RP2 | – | RP2 del EX04-flanking |
| RFS038 | KLHL7 | – | – | KLHL7 Ala153Val |
| RFS048 | – | – | SNRNP200 | SNRNP200 Ala542Val benign? |
| RFS066 | GUCY2D | – | – | GUCY2D Arg838Cys |
| RFS191 | RPGR | – | – | RPGR Gly738* |
| RFS296 | RPGR | – | – | RPGR Gly65Asp |
| RFS397 | – | PROM1 | – | PROM1 Arg373Cys |
| UTAD037 | PRPF31 | – | – | PRPF31 946-1 G>C |
| UTAD198 | – | NRL | NRL | NRL Pro51Ala |
| UTAD388 | – | – | PRPF31 | PRPF31 Gly272Val |
| UTAD565 | – | SNRNP200 | SNRNP200 | SNRNP200 Arg681Lys |
| UTAD569 | – | RPE65 | – | RPE65 Asp477Gly |

## 16.4 Discussion

NGS is a highly versatile and effective approach to detection of novel disease-causing genes and mutations in families with autosomal dominant forms of retinopathy. Linkage mapping is a critical adjunct to NGS, significantly reducing the number of genes to consider and helping to distinguish pathogenic variants from the many rare, potentially deleterious variants in the human genome.

**Acknowledgments** This work was supported by NIH grant EY007142 and the Foundation Fighting Blindness. We thank Dr. David Birch, Dr John Heckenlively, Dr. Richard Lewis, Dr. Dianna Wheaton, Ms. Kari Branham, and Ms. Elizabeth Cadena for clinical assistance; and Ms. Cheryl Avery, Ms. Aimee Buhr, and Ms. Elizabeth Quimby for technical assistance.

## References

1. Berger W, Kloeckener-Gruissem B, Neidhardt J (2010) The molecular basis of human retinal and vitreoretinal diseases. Prog Retin Eye Res 29:335–75
2. Daiger SP, Bowne SJ, Sullivan LS (2007) Perspective on genes and mutations causing retinitis pigmentosa. Arch Ophthalmol 125:151–158
3. RetNet (2013) The Retinal Information Network. (Stephen P. Daiger, PhD, Administrator, The University of Texas Health Science Center at Houston). http://www.sph.uth.tmc.edu/RetNet/
4. Daiger SP, Sullivan LS, Gire AI, Birch DG, Heckenlively JR, Bowne SJ (2008) Mutations in known genes account for 58% of autosomal dominant retinitis pigmentosa (adRP). Adv Exp Med Biol 613:203–209
5. Sohocki MM, Daiger SP, Bowne SJ, Rodriquez JA, Northrup H, Heckenlively JR et al (2001) Prevalence of mutations causing retinitis pigmentosa and other inherited retinopathies. Hum Mutat 17:42–51
6. Sullivan LS, Bowne SJ, Birch DG, Hughbanks-Wheaton D, Heckenlively JR, Lewis RA et al (2006) Prevalence of disease-causing mutations in families with autosomal dominant retinitis pigmentosa (adRP): a screen of known genes in 200 families. Invest Ophthalmol Vis Sci 47:3052–3064

7. Sullivan LS, Bowne SJ, Seaman CR, Blanton SH, Lewis RA, Heckenlively JR et al (2006) Genomic rearrangements of the PRPF31 gene account for 2.5 % of autosomal dominant retinitis pigmentosa. Invest Ophthalmol Vis Sci 47:4579–4588
8. Churchill JD, Bowne SJ, Sullivan LS, Lewis RA, Wheaton DK, Birch DG et al (2013) Mutations in the X-linked retinitis pigmentosa genes RPGR and RP2 found in 8.5 % of families with a provisional diagnosis of autosomal dominant retinitis pigmentosa. Invest Ophthalmol Vis Sci 54:1411–1416
9. Wen Y, Locke KG, Klein M, Bowne SJ, Sullivan LS, Ray JW et al (2011) Phenotypic characterization of 3 families with autosomal dominant retinitis pigmentosa due to mutations in KLHL7. Arch Ophthalmol 129:1475–1482
10. Bowne SJ, Sullivan LS, Koboldt DC, Ding L, Fulton R, Abbott RM et al (2010) Identification of disease-causing mutations in autosomal dominant retinitis pigmentosa (adRP) using next-generation DNA sequencing. Invest Ophthalmol Vis Sci 52:494–503
11. Daiger SP, Sullivan LS, Bowne SJ, Birch DG, Heckenlively JR, Pierce EA et al (2010) Targeted high-throughput DNA sequencing for gene discovery in retinitis pigmentosa. Adv Exp Med Biol 664:325–331
12. Purcell S, Neale B, Todd-Brown K, Thomas L, Ferreira MA, Bender D et al (2007) PLINK: a tool set for whole-genome association and population-based linkage analyses. Am J Hum Genet 81:559–575
13. Bowne SJ, Humphries MM, Sullivan LS, Kenna PF, Tam LCS, Kiang AS et al (2011) A dominant-acting mutation in RPE65 identified by whole-exome sequencing causes retinitis pigmentosa with choroidal involvement. Euro J Hum Genet 10:1074–1081

# Chapter 17
# Digital Quantification of Goldmann Visual Fields (GVFs) as a Means for Genotype–Phenotype Comparisons and Detection of Progression in Retinal Degenerations

**Sarwar Zahid, Crandall Peeler, Naheed Khan, Joy Davis, Mahdi Mahmood, John R. Heckenlively and Thiran Jayasundera**

**Abstract**

Purpose
To develop a reliable and efficient digital method to quantify planimetric Goldmann visual field (GVF) data to monitor disease course and treatment responses in retinal degenerative diseases.

Methods
A novel method to digitally quantify GVFs using Adobe Photoshop CS3 was developed for comparison to traditional digital planimetry (Placom 45C digital planimeter; EngineerSupply, Lynchburg, Virginia, USA). GVFs from 20 eyes from 10 patients with Stargardt disease were quantified to assess the difference between the two methods (a total of 230 measurements per method). This quantification ap-

J. R. Heckenlively (✉) · S. Zahid · C. Peeler · N. Khan · J. Davis · M. Mahmood · T. Jayasundera
Department of Ophthalmology and Visual Sciences, University of Michigan,
Kellogg Eye Center, 1000 Wall Street, 48105 Ann Arbor, MI, USA
e-mail: jrheck@umich.edu

S. Zahid
e-mail: zahids@med.umich.edu

C. Peeler
e-mail: cpeeler@med.umich.edu

N. Khan
e-mail: nwkhan@med.umich.edu

J. Davis
e-mail: jsdav@umich.edu

M. Mahmood
e-mail: mahdi.n.mahmood@gmail.com

T. Jayasundera
e-mail: thiran@umich.edu

J. D. Ash et al. (eds.), *Retinal Degenerative Diseases,* Advances in Experimental Medicine and Biology 801, DOI 10.1007/978-1-4614-3209-8_17,

proach was also applied to 13 patients with X-linked retinitis pigmentosa (XLRP) with mutations in *RPGR*.

Results
Overall, measurements using Adobe Photoshop were more rapidly performed than those using conventional planimetry. Photoshop measurements also exhibited less inter- and intraobserver variability. GVF areas for the $I_{4e}$ isopter in patients with the same mutation in *RPGR* who were nearby in age had similar qualitative and quantitative areas.

Conclusions
Quantification of GVFs using Adobe Photoshop is quicker, more reliable, and less user dependent than conventional digital planimetry. It will be a useful tool for both retrospective and prospective studies of disease course as well as for monitoring treatment response in clinical trials for retinal degenerative diseases.

**Keywords** Retinal dystrophies · Goldmann visual fields · Disease course · Treatment response · Genotype–phenotype correlations

## 17.1 Introduction

Kinetic perimetry is broadly less utilized today in ophthalmic care. However, it remains critical in the evaluation of progression of inherited and autoimmune retinal degenerations. The visual fields of these patients are better assessed with kinetic perimetry [1] and their visual field defect or scotoma may lie beyond 30° of the visual field tested by the Humphrey Visual Field analyzer. Descriptive methods for evaluating Goldmann visual fields (GVFs) have been described in the past, with central and peripheral losses reflecting cone-rod and rod-cone patterns of retinal degeneration, respectively [2]. Linstone et al. [3] described the use of planimetry to quantify GVFs over two decades ago and this technique has been successfully used to monitor treatment responses in patients with autoimmune retinopathy [4, 5].

Despite the potential for quantification, planimetric measurements are often time-consuming and can vary widely between users. In order to determine efficacy of immunosuppressive agents used for treatment of autoimmune retinopathies [4], and as new therapies for retinal dystrophies enter into clinical trials, it has become increasingly important to accurately quantify visual field areas in both clinical and research settings. We describe a novel technique that is faster, more reliable, and less operator dependent using Adobe Photoshop CS3 (Photoshop). We also apply this technique to patients with X-linked retinitis pigmentosa (XLRP) who have the same mutations in *RPGR* to explore the potential for quantified GVFs in future studies of genotype–phenotype relationships.

1. Scan Goldmann visual field sheet (Haag-Streit, Bern, Switzerland) and convert the file to TIFF format.
2. Open the file in Adobe Photoshop CS3.
3. Set Scale in Photoshop by going to **ANALYSIS > SET MEASUREMENT SCALE > CUSTOM**
   - Take the on-screen ruler onto the GVF sheet and measure from the center to 10 degrees in any direction.
   - This should give a specific pixel length (94 pixels)
   - Set Logical Length to "12"
   - Set Logical Units to "mm"
   - [Logical Lengths and Units can also be set to centimeters (0.12 cm) or degrees (10 degrees)]
   - Click "SAVE PRESET" and name "GVF Quantification" (naming is arbitrary)
4. Open Adobe Photoshop CS3 and go to FILE > OPEN.
5. Open the file of interest and record the date and eye (OD or OS) examined.
6. Ensure the measurement scale is set as "GVF Quantification"
7. Click the MAGIC WAND button on the left panel.
8. Start with the largest test target isopter and click a certain area that it includes. You may modify this area by "ADDING" and "SUBTRACTING" with the wand. Click to include up to the outer boundaries.
9. If there are scotomata within the field of a certain target, use the "SUBTRACT" function on the wand to remove them from the area you are selecting. Ensure you extend to the outer border of a line. (Depending on your study, you may choose to include or subtract the **physiologic blind spot**)
10. If there are islands of functional vision, these can be selected by "ADDING" with the wand cursor.
11. Once your area of choice is selected, go to ANALYSIS > RECORD MEASUREMENTS and a small box of measurements appear. The area will be measured in square millimeters ($mm^2$). If there are multiple islands of vision, you will find multiple measurements – each individual island as well as the cumulative sum (total selected area).
12. Repeat for other isopters.

**Fig. 17.1** Goldmann visual field (*GVF*) digital quantification methodology using Adobe Photoshop CS3 is delineated in a stepwise fashion

## 17.2 Methods

This study was approved by the University of Michigan Institutional Review Board. A novel method of quantifying GVFs digitally using Photoshop was developed at the University of Michigan (Fig. 17.1). Measurements made using this technique were compared to traditional digital planimetry (Placom 45C digital planimeter; EngineerSupply, Lynchburg, Virginia, USA). 38 GVF tests from 10 patients (20 eyes) with different stages of Stargardt disease were quantified in planimetric square centimeters ($cm^2$) to evaluate the difference between the two methods (230 measurements/method). The average difference between measurements using each method was assessed.

Inter- and intraobserver variations of the two methods were also evaluated. Two observers each measured one full visual field comprising the $I_{4e}$, $III_{4e}$, and $IV_{4e}$ isopters. Each set of measurements for each isopter was performed three times using both methodologies. The three measurements of each parameter were averaged to obtain one value/parameter/observer/methodology. The average difference between the measurements of each observer using a particular measurement method was defined as the interobserver variability. Given that each measureable parameter was measured three times by each observer, intraobserver variability for each measure was assessed by calculating the standard deviation (SD) within the three measurements. The average SDs for each measurement using each methodology were compared to assess overall intraobserver variability.

GVFs from 13 patients with proven mutations in *RPGR* were evaluated in an application of this quantification technique. Descriptive phenotypes were assigned to each patient's pattern of GVF loss. Predominantly peripheral losses represented a rod-cone phenotype, and predominantly central vision loss represented a cone-rod phenotype, as described by Heckenlively [2]. The GVF areas for the $I_{4e}$ isopter were quantified as described above and expressed as percentages of the normal mean for the total $I_{4e}$ area as derived from 10 normal eyes (176.78 $cm^2$). Qualitative GVF phenotypes and quantified areas from patients with the same mutation who were near in age were compared in square centimeters.

## 17.3 Results

### *17.3.1 Verification of Quantification Technique*

Measurements using Photoshop were on average 2.33 % (SD = 0.65 %) greater than measurements by digital perimetry for visual field areas measured by the $I_{4e}$, $III_{4e}$, and $IV_{4e}$ isopters ($N = 20$ eyes; 10 patients). An example comparing measurements of these isopters from a 35-year-old female patient with Stargardt disease is shown in Fig. 17.2.

Interobserver variability taken from an average of three measurements per user per isopter was 0.216 $cm^2$ for digital planimetry versus 0.067 $cm^2$ for Photoshop. Intraobserver variability, as reflected by the average standard deviation of 18 sets of 3 measurements each from two users measuring all available isopters from one visual field, was 0.227 $cm^2$ for digital planimetry versus 0.0 $cm^2$ for measurements using Photoshop. Of note, for a GVF with full peripheral fields, on average greater than 10 min was required for digital planimetry measurements, while less than 5 min were required using Photoshop.

### *17.3.2 Application of Quantification Technique*

Qualitative and quantitative GVF phenotypes in 13 patients with XLRP representing 6 distinct proven mutations in *RPGR* were compared. Patients were compared only to other patients who had the same mutation and were nearby (less than 6 years) in age. The patients with a rod-cone GVF phenotype tended to have qualitatively and quantitatively smaller areas when compared to other patients with the same mutation. In contrast, patients with a cone-rod phenotype tended to have larger GVF areas. The difference in areas for all comparisons of patients with the same mutations was minimal.

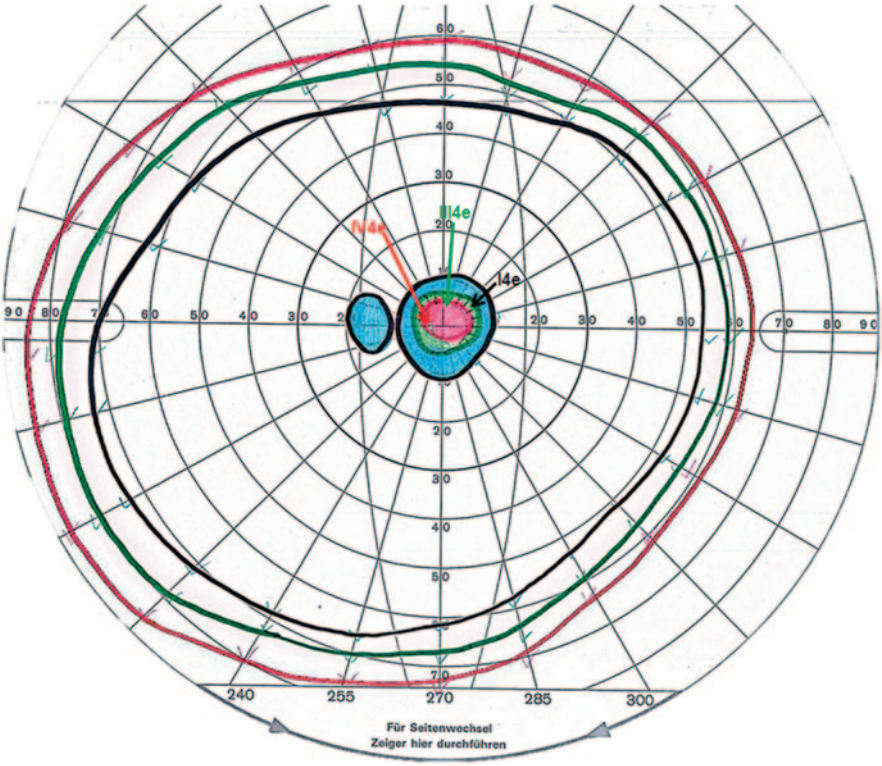


| Measurements | | | |
|---|---|---|---|
| | Digital Planimeter (in cm²) | Digitized Quantification (in cm²) | Difference (in cm²) |
| I4e Total | 154.9 | 158.1 | 3.20 |
| I4e Central Scotoma | 4.9 | 5.1 | 0.20 |
| I4e Blind Spot | 1.3 | 1.3 | 0.00 |
| III4e Total | 188.6 | 193.4 | 4.80 |
| III4e Central Scotoma | 2 | 2.3 | 0.30 |
| IV4e Total | 222.2 | 227.2 | 5.00 |
| IV4e Central Scotoma | 1.2 | 1.1 | -0.10 |

**Fig. 17.2** Comparison of traditional versus novel digital GVF quantification. Quantification of the total extent of peripheral fields, physiologic blind spot, and central scotoma were performed by a single observer in square centimeters ($cm^2$) for the $I_{4e}$, $III_{4e}$, and $IV_{4e}$ isopters using digital planimetry and Adobe Photoshop for a 35-year-old female patient with Stargardt disease. The absolute differences between the two methodologies are shown in the table

## 17.4 Discussion

We have shown that Photoshop can be a useful measurement tool for GVFs. This technique is less time consuming, more reliable, and less user dependent than previous techniques such as digital planimetry. It can enable the precise longitudinal assessment of GVFs to evaluate the progression and therapeutic responses of retinal degenerative diseases. This may be especially useful for clinical trials involving novel therapies (e.g., gene therapy), where accurately quantified scotomata may be monitored longitudinally as an outcome measure.

There are some limitations to our technique. First, it is most useful for retrospective studies that utilize standardized methodology. Even when standardized technique is utilized, there may be significant test–retest variability [6]. Second, although newer perimeters (e.g., Octopus® 900) can provide automated GVF quantification, there exists a wealth of quantifiable retrospective GVF data that can be utilized to study disease course and genotype to phenotype correlations in various diseases.

Another limitation of our technique is that it provides planimetric, rather than retinal, areas, which does not account for perimetric distortions [7, 8]. However, these distortions are minimal at smaller eccentricities [9]. Therefore, for defects such as central scotomata, an accurate technique such as the one described herein is useful in both clinical and research settings.

The application of our quantitative technique in patients with XLRP caused by mutations in *RPGR* illustrates the potential for using our technique to analyze retrospective GVF data to explore genotype to phenotype relationships. Most importantly, it shows the greatest utility when patients with the same mutation who are near in age are compared, as it reveals whether visual field loss is comparable both qualitatively and quantitatively at similar points of the disease course for each mutation. Given that most retinal dystrophies often take years to decades to progress, the data currently available is mostly retrospective (often with incomplete follow-up). Therefore, accurate quantification of visual parameters such as GVFs is important to assess the disease course in each unique mutation.

**Acknowledgments** We would like to specially thank Dr. Michael D. Abramoff, MD, PhD for his advice on Goldmann visual field quantification.

This research was supported by the Foundation Fighting Blindness and the National Eye Institute (Core Center for Vision Research—EY007003).

## References

1. Barton JJS, Benatar M (April 2003) Field of vision: a manual and atlas of perimetry. Springer, New York
2. Heckenlively JR (1988) Retinitis pigmentosa. Lippincott, Philadelphia
3. Linstone FA, Heckenlively JR, Solish AM (1982) The use of planimetry in the quantitative analysis of visual fields. Glaucoma 4:17–19

4. Ferreyra HA, Jayasundera T, Khan NW, He S, Lu Y, Heckenlively JR (2009) Management of autoimmune retinopathies with immunosuppression. Archives of ophthalmology 127(4):390–397
5. Heckenlively JR, Ferreyra HA (2008) Autoimmune retinopathy: a review and summary. Semin Immunopathol 30(2):127–134
6. Bittner AK, Iftikhar MH, Dagnelie G (2011) Test-retest, within-visit variability of Goldmann visual fields in retinitis pigmentosa. Invest Ophthalmol Vis Sci 52(11):8042–8046
7. Drasdo N, Fowler CW (1974) Non-linear projection of the retinal image in a wide-angle schematic eye. Br J Ophthalmol 58(8):709–714
8. Kirkham TH, Meyer E (1981) Visual field area on the Goldmann hemispheric perimeter surface. Correction of cartographic errors inherent in perimetry. Curr Eye Res 1(2):93–99
9. Dagnelie G (1990) Conversion of planimetric visual field data into solid angles and retinal areas. Clin Vision Sciences 5:95–100

# Chapter 18
# Simplified System to Investigate Alteration of Retinal Neurons in Diabetes

**Shuqian Dong, Yan Liu, Meili Zhu, Xueliang Xu and Yun-Zheng Le**

**Abstract** Diabetic retinopathy (DR) is traditionally considered as a microvascular complication in diabetic retinas. Emerging evidences suggest that the alteration of neuronal function and the death of retinal neurons are part of DR pathology. However, surprisingly little is known about how retinal neurons behave in DR. As diabetic animals are chronicle models that are difficult and expensive to maintain, we used a chemical hypoxia model that mimics the later stage of diabetes and investigated its potential in predicting retinal cell behaviors in diabetes in an efficient manner. In this chapter, we discuss the similarities and differences between diabetic and hypoxic models and the usefulness and limitation of the cobalt-chloride-generated hypoxia system in mice for studying retinal neurobiology in diabetes.

**Keywords** Diabetes · $CoCl_2$ · Hypoxia · Retina · Neurons

These authors contributed equally to this work.

Y.-Z. Le (✉) · S. Dong · Y. Liu · M. Zhu
Department of Medicine Endocrinology, University of Oklahoma Health Sciences Center,
941 S. L. Young Blvd., BSEB 302G, 73104 Oklahoma City, OK, USA
e-mail: Yun-Le@ouhsc.edu

S. Dong · Y. Liu · M. Zhu · Y.-Z. Le
Harold Hamm Diabetes Center, University of Oklahoma Health Sciences Center,
941 S. L. Young Blvd., BSEB 302G, 73104 Oklahoma City, OK, USA

Y.-Z. Le
Department of Cell Biology, University of Oklahoma Health Sciences Center,
941 S. L. Young Blvd., BSEB 302G, 73104 Oklahoma City, OK, USA

S. Dong · Y. Liu · X. Xu
Department of Ophthalmology, Xiangya Hospital of Central South University,
410008 Changsha, China

J. D. Ash et al. (eds.), *Retinal Degenerative Diseases,* Advances in Experimental Medicine and Biology 801, DOI 10.1007/978-1-4614-3209-8_18,

## 18.1 Introduction

Diabetic retinopathy (DR) is traditionally regarded as a microvascular complication of the retinal vessels in diabetic patients, which is characterized clinically by retinal hemorrhages, microaneurysms, cotton-wool spots, lipid exudates, macular edema, capillary occlusion, and retinal neovascularization. While it is increasingly recognized that the loss of neuronal function and viability occurs before the onset of retinal microvascular abnormalities in diabetic humans and animals [1], the mechanisms governing diabetes-induced alteration of retinal neurons are largely unexplored. A major contributing factor for the current situation is: Diabetic animals are chronicle models that are difficult and expensive to maintain. To circumvent this problem and to obtain critical clues relevant to diabetic retinal cells in a simplified and efficient manner, we explored the potential utility of cobalt chloride which is capable of reacting to oxygen and causing hypoxia, a pathological condition similar to that in the later stage of diabetes. We hereby discuss our investigation on the usefulness and limitation of the cobalt-chloride-generated hypoxia for studying retinal neurobiology in diabetic rodents.

## 18.2 Methods

All animal experiments were performed according to the Association for Research in Vision and Ophthalmology Statement for the Use of Animals in Ophthalmic and Vision Research and were approved by Institutional Animal Care and Use Committee at the University of Oklahoma Health Sciences Center. To induce hypoxia in the retina, we adopted a previous method by intravitreal delivering cobalt chloride prepared in phosphate buffered saline (PBS) [4]. Mice were anesthetized with ketamine (15 mg/kg) and xylazine (100 mg/kg). Pupils were dilated with 5% tropicamide. Local anesthesia was administered with 0.5% proparacaine. Intravitreal injections of 1 μl solution were performed at a location 1 mm posterior to the limbus. Antibiotic ointment was applied to prevent infection after the injection. Diabetes was induced in C57BL6 background mice by streptozotocin (STZ) injection, as described previously [15]. Examination of retinal function with electroretinography (ERG) and morphology in hematoxylin and eosin (H&E)-stained retinal sections were performed according to procedures described previously [16]. Analysis of gene expression with Western blot was carried out according to methods described previously [2, 15].

## 18.3 Results and Discussions

### *18.3.1 Degeneration of Retinal Neurons by Hypoxia with Cobalt Chloride*

Hypoxia induced by cobalt chloride was used to manipulate retinal neurons and was served as a retinal degeneration model in rodents [4]. To determine whether hypoxic

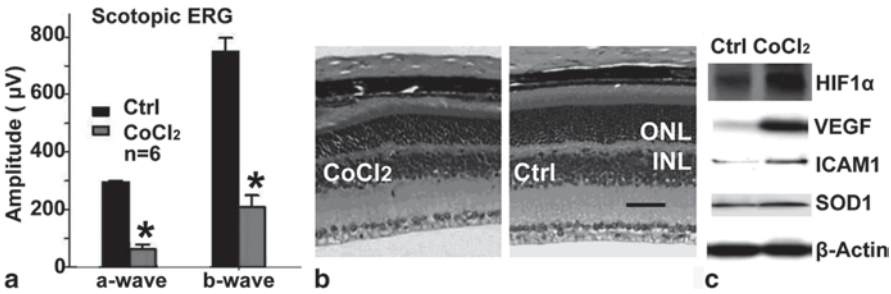


**Fig. 18.1** Cobalt chloride (5 nmole) induced functional, morphological, and biochemical alterations in the retina. **a** *Scotopic ERG* showing a significant reduction of both *a-wave* ($p<0.05$) and *b-wave* ($p<0.05$) amplitudes in C57BL6 background mice ($n>6$) 1 week after intravitreal delivery of cobalt chloride. **b** Representative images of H&E-stained retinal section showing a significant loss of photoreceptor outer nuclear layer (*ONL*) thickness, inner nuclear layer (*INL*) thickness, and ganglion cell layer neuron density in wild-type mice 1 week after intravitreal delivery of cobalt chloride (scale bar equal to 40 μm). **c** Representative Western blot images showing that the expression of biomarkers commonly upregulated in diabetic retinas was also elevated in hypoxic model 2 days after intravitreal delivery of cobalt chloride. *Ctrl* control

system, which provides a cellular environment very similar to that in the late stage of diabetes, is suitable for providing clues to study retinal neurobiology in diabetes, we examined retinal function and morphology in cobalt-chloride-treated weanling aged mice first. While a high dosage of cobalt chloride caused almost complete loss of retinal function and massive retinal neuron degeneration (data not shown), a moderate amount of cobalt chloride (5 nmole) resulted in a measurable reduction in retinal function, as judged by scotopic ERG a-wave and b-wave (Fig. 18.1a), 1 week after cobalt chloride injection. Under such a condition, there was also an apparent loss of photoreceptor outer nuclear layer (ONL) thickness, inner nuclear layer (INL) thickness, and ganglion cell layer neuron density (Fig. 18.1b). These data suggest that cobalt chloride can generate detectable but controllable levels of retinal degeneration for all retinal neurons. Therefore, this may be a useful model for retinal degeneration under hypoxia, a key pathological characteristic in late stage of DR.

### *18.3.2 Expression of Major DR Biomarkers in Cobalt-Chloride-Induced Hypoxia*

While we did observe the loss of retinal function with ERG and the degeneration of retinal neurons in H&E-stained retinal sections in cobalt-chloride-induced hypoxic model (Fig. 18.1a, b), as observed previously [4], it was more striking that major parameters supposedly upregulated in diabetes were also increased substantially. Cobalt-chloride-injected animals demonstrated a significant upregulation of hypoxia-inducible factor 1α (HIF-1α), vascular endothelial growth factor (VEGF), intercellular adhesion molecule-1 (ICAM-1), and superoxide dismutase-1 (SOD-1), major biomarkers in DR.

During the development of DR, a number of biochemical changes occur as a consequence of hyperglycemia/high retinal glucose, including the increase of reactive oxygen species (ROS) and oxidative stress [3, 8], activation of protein kinase C [6], and the formation of advanced glycation end products [5, 14]. Presence of excessive amount of ROS is considered a determining factor that activates many downstream pathways in DR [11]. SOD-1 is considered as a major biomarker for oxidative stress in DR, which was upregulated in the retina of cobalt-chloride-induced hypoxia (Fig. 18.1).

Retinal inflammation is an early pathological change in DR, which is reflected in the increase of adherent leukocytes and the upregulation of inflammatory markers, such as ICAM-1 and tumor necrosis factor-α (TNF-α [15]. To determine whether cobalt-chloride-induced hypoxia upregulated retinal inflammation, we examined the expression of ICAM-1. Our result showed that ICAM-1 expression was increased substantially in the retina, suggesting that a significant increase of inflammatory responses occurs as a consequence of cobalt-chloride-induced hypoxia.

HIF-1α is a major sensor of hypoxia and a master transcriptional regulator for many pathways, including pathological angiogenesis in intraocular neovascularization in age-related macular degeneration (AMD) and DR [9, 10]. A major downstream effector of HIF-1α is VEGF, an essential growth factor for vasculogenesis during development [7], neuronal differentiation and survival [13], physiological angiogenesis in maintaining normal blood-retina barrier (BRB) function [12], and pathological angiogenesis in neovascular AMD and retinal neovascularization and macular edema in DR [12]. At present, VEGF has been considered as a major therapeutic target of neovascular AMD and BRB breakdown in DR [12]. A significant upregulation of HIF-1α and VEGF in cobalt-chloride-induced hypoxia demonstrates the resemblance of major parameters in this system to that in DR.

### *18.3.3 Benefits and Limitations of Cobalt-Chloride-Induced Hypoxic System*

As demonstrated above, cobalt-chloride-induced hypoxic retinas expressed major biomarkers that represent key biochemical and physiological changes in DR. While a complete development of these changes in DR may take a few months, the biochemical alteration triggered by cobalt-chloride-induced hypoxia can be readily detected within a day or two, and the physiological consequences can be analyzed in a week. Therefore, the cobalt-chloride-induced hypoxia system allows one to obtain clues for a specific mechanistic question in the late stage of DR in a very short time, which is also cost-effective for the maintenance of experimental animals. However, there are fundamental differences between acute hypoxia-stimulated changes and diabetes-induced chronic pathological progression. Cobalt-chloride-induced hypoxia will not provide full information related to DR. Cautions must be taken in interpreting data. While the cobalt-chloride-induced hypoxic system allows efficient predication of biochemical, cellular, and pathological alterations that may occur in DR, all conclusions must be verified in diabetic animals eventually.

**Acknowledgments** We thank our laboratory members for preliminary data and helpful discussions. Our work was supported by NIH grants GM104934, EY020900, and EY21725, Grants from American Diabetes Association, Foundation Fighting Blindness, Beckman Initiative for Macular Research, and Oklahoma Center for the Advancement of Science and Technology, and an endowment from Choctaw Nation and Oklahoma State.

## References

1. Antonetti DA, Klein R, Gardner TW (2012) Diabetic retinopathy. N Engl J Med 366:1227–1239
2. Bai Y, Ma JX, Guo J, Wang J, Zhu M, Chen Y, Le YZ (2009) Muller cell-derived VEGF is a significant contributor to retinal neovascularization. J Pathol 219:446–454
3. Catherwood MA, Powell LA, Anderson P, McMaster D, Sharpe PC, Trimble ER (2002) Glucose-induced oxidative stress in mesangial cells. Kidney Int 61:599–608
4. Hara A, Niwa M, Aoki H, Kumada M, Kunisada T, Oyama T, Yamamoto T, Kozawa O, Mori H (2006) A new model of retinal photoreceptor cell degeneration induced by a chemical hypoxia-mimicking agent, cobalt chloride. Brain Res 1109:192–200
5. Horie K, Miyata T, Maeda K, Miyata S, Sugiyama S, Sakai H, van Ypersole de Strihou C, Monnier VM, Witztum JL, Kurokawa K (1997) Immunohistochemical colocalization of glycoxidation products and lipid peroxidation products in diabetic renal glomerular lesions. Implication for glycoxidative stress in the pathogenesis of diabetic nephropathy. J Clin Invest 100:2995–3004
6. Koya D, King GL (1998) Protein kinase C activation and the development of diabetic complications. Diabetes 47:859–866
7. Le YZ, Bai Y, Zhu M, Zheng L (2010) Temporal requirement of RPE-derived VEGF in the development of choroidal vasculature. J Neurochem 112:1584–1592
8. Li JM, Shah AM (2003) ROS generation by nonphagocytic NADPH oxidase: potential relevance in diabetic nephropathy. J Am Soc Nephrol 14:S221–S226
9. Lin M, Chen Y, Jin J, Hu Y, Zhou KK, Zhu M, Le YZ, Ge J, Johnson RS, Ma JX (2011) Ischaemia-induced retinal neovascularisation and diabetic retinopathy in mice with conditional knockout of hypoxia-inducible factor-1 in retinal Muller cells. Diabetologia 54:1554–1566
10. Lin M, Hu Y, Chen Y, Zhou KK, Jin J, Zhu M, Le YZ, Ge J, Ma JX (2012) Impacts of hypoxia-inducible factor-1 knockout in the retinal pigment epithelium on choroidal neovascularization. Invest Ophthalmol Vis Sci 53:6197–6206
11. Madsen-Bouterse SA, Kowluru RA (2008) Oxidative stress and diabetic retinopathy: pathophysiological mechanisms and treatment perspectives. Rev Endocr Metab Disord 9:315–327
12. Penn JS, Madan A, Caldwell RB, Bartoli M, Caldwell RW, Hartnett ME (2008) Vascular endothelial growth factor in eye disease. Prog Retin Eye Res 27:331–371
13. Rosenstein JM, Krum JM, Ruhrberg C (2010) VEGF in the nervous system. Organogenesis 6:107–114
14. Stitt AW, Li YM, Gardiner TA, Bucala R, Archer DB, Vlassara H (1997) Advanced glycation end products (AGEs) co-localize with AGE receptors in the retinal vasculature of diabetic and of AGE-infused rats. Am J Pathol 150:523–531
15. Wang J, Xu X, Elliott MH, Zhu M, Le YZ (2010) Muller cell-derived VEGF is essential for diabetes-induced retinal inflammation and vascular leakage. Diabetes 59:2297–2305
16. Zheng L, Anderson RE, Agbaga MP, Rucker EB 3rd, Le Y.Z. (2006) Loss of BCL-XL in rod photoreceptors: Increased susceptibility to bright light stress. Invest Ophthalmol Vis Sci 47:5583–5589

# Chapter 19
# What Is the Nature of the RGC-5 Cell Line?

**C. Sippl and E. R. Tamm**

**Abstract** The immortalized RGC-5 cell line has been widely used as a cell culture model to study the neurobiology of retinal ganglion cells (RGCs). The cells were originally introduced as derived from rat RGC showing expression of various neuronal markers, in particular the RGC-characteristic proteins Brn3 and Thy1. Recent data gave rise to concerns regarding the origin and nature of the cells. RGC-5 cells were identified to be of mouse origin and their expression of RGC characteristics was questioned by some laboratories. This article summarizes the available data on the properties of RGC-5, discusses common protocols for their differentiation and is aimed at providing researchers some guidelines on the benefits and limitations of RGC-5 for research.

**Keywords** RGC-5 · Retinal ganglion cells · Ocular neurons · Cell line · Staurosporine · Trichostatin A · Succinylated concanavalin A · Brn3 · Thy1 · Glaucoma

## 19.1 Introduction

Retinal ganglion cells (RGCs) are the neurons that transmit visual signals from the retina to the brain. Dysfunction or loss of RGCs is associated with various optic neuropathies including glaucoma, a complex, heterogeneous disease that constitutes the major cause of irreversible blindness worldwide. Despite its diverse causes, a common hallmark of primary open-angle glaucoma is the apoptotic cell death of RGCs [15]. Other ocular diseases characterized by affected RGCs include diabetic retinopathy [3], optic neuritis [13] or Leber's hereditary optic neuropathy [5].

Using purified primary RGCs as a model to study physiological processes and the largely unknown mechanisms of RGC death is laborious and results in a limited number of cells that will survive only for a few days [11]. Due to these difficulties,

E. R. Tamm (✉) · C. Sippl
Institute of Human Anatomy and Embryology, University of Regensburg, Universitätsstr. 31, 93053 Regensburg, Germany
e-mail: ernst.tamm@vkl.uni-regensburg.de

C. Sippl
e-mail: christiane.sippl@vkl.uni-regensburg.de

J. D. Ash et al. (eds.), *Retinal Degenerative Diseases,* Advances in Experimental Medicine and Biology 801, DOI 10.1007/978-1-4614-3209-8_19,

it is helpful to use proliferating cells from a transformed cell line. Currently, RGC-5 cells represent the only available immortalized cell line that has been introduced as being of RGC origin. RGC-5 cells were originally established by Krishnamoorthy et al. in 2001 [16]. The group around Neeraj Agarwal reported on studies in which they permanently transformed a mixed retinal cell culture from postnatal day 1 rats using the ψ2E1A adenovirus [6] to induce proliferation and immortalization. To ensure RGC origin of the cells, clones were tested for the expression of specific markers. Clone number 5 expressed certain molecules characteristic of primary RGCs including Thy1 and Brn3C, and was termed RGC-5 [16].

RGC-5 cells were first regarded as a highly beneficial tool and widely used in ocular research. So far, there are around 200 publications listed in PubMed in which this cell line was utilized as a model system. In 2009, doubts emerged when Van Bergen et al. [29] published a recharacterization of the cell line including the finding that RGC-5 is of murine (*Mus musculus*) and not of rat (*Rattus norvegicus*) origin, an observation that has been independently confirmed [26]. To our knowledge, the laboratory which first introduced the RGC-5 cell line has not provided a comment on this issue which is in the public domain. Clearly, since RGC-5 cells are from a different species than originally reported, there are considerable doubts if the cells are derived from retinal neurons, let alone from RGC.

In the present report, we will provide an overview on the properties of the RGC-5 cell line that have been described in the literature over the years. Furthermore, we will discuss common protocols for their differentiation to induce a neuronal phenotype. Our goal is to provide researchers with some guidelines on the benefits and limitations of RGC-5 for research.

## 19.2 Expression of Markers

RGC-5 cells grow as a monolayer and proliferate rapidly with a doubling time of approximately 20 h. Decreasing the percentage of serum in the medium may slow down their proliferation. The morphology of RGC-5 cells is flat and polygonal with short extensions (Fig. 19.1a).

Originally, Krishnamoorthy et al. [16] described the expression of Thy1, a general marker for RGCs [4], and of Brn3C, which is characteristic of a subset of smaller RGCs [34]. In addition, the expression of neuronal markers including neuritin, N-methyl-D-aspartate (NMDA) receptor, gamma-aminobutyric acid B (GABA-B) receptor and synaptophysin was reported while no expression of other retinal cell markers such as glial fibrillary acidic protein (GFAP) for Müller cells, syntaxin or human plasma cell antigen-1 (HPC1) for amacrine cells and 8A1 for horizontal and ganglion cells was observed [16]. Furthermore, the expression of the neurotrophic factors ciliary neurotrophic factor (CNTF), glial cell-derived neurotrophic factor (GDNF), nerve growth factor (NGF), brain-derived neurotrophic factor (BDNF), neurotrophin-3 (NT3) and neurotrophin-4 (NT4) and their cognate (tyrosine kinase) receptors TrkA, TrkB, TrkC and p75 neurotrophin receptor (p75NTR) was reported [1].

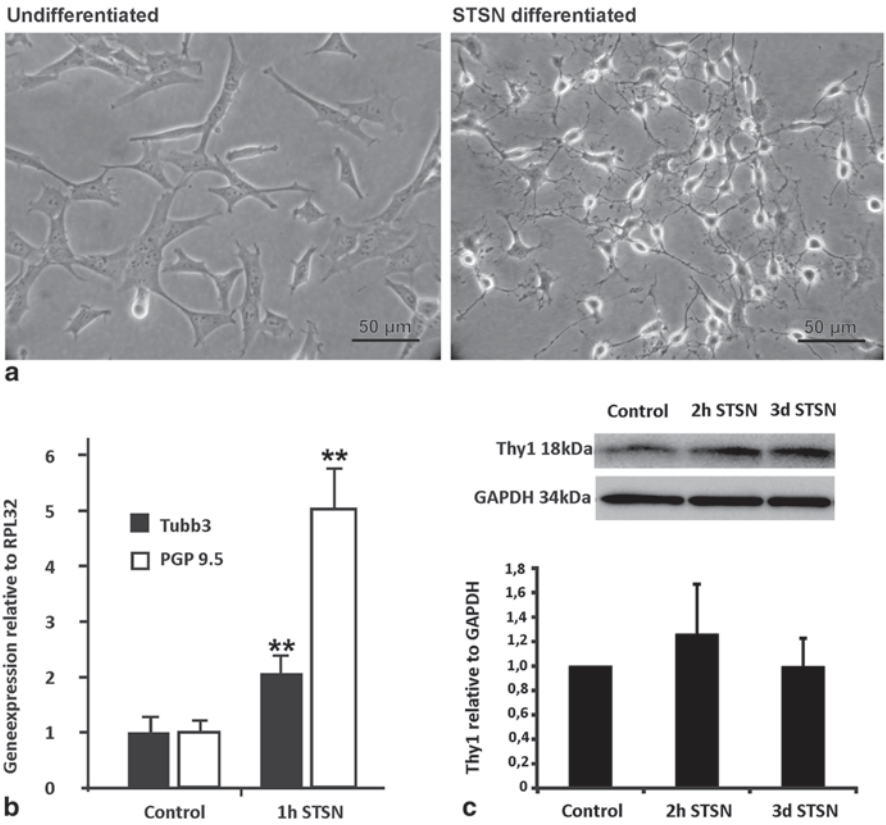


**Fig. 19.1** Characteristics of RGC-5. **a** Phase contrast microscopy of RGC-5 cells before and after treatment with 1 µM staurosporine (*STSN*). Following treatment, RGC-5 cells change their phenotype from flat and polygonal to neuron-like. **b** Real-time reverse transcription-polymerase chain reaction (RT-PCR) for messenger RNA (mRNA) of tubulin beta-3 (TUBB3) and protein gene product 9.5 (PGP 9.5) in RNA from RGC-5 cells before and after treatment with 1 µM STSN for 24 h. Ribosomal protein L32 (*RPL32*) served as a reference gene. **c** Western blot analysis and densitometry for Thy1 in protein extracts from RGC-5 cells before and after treatment with STSN. *GAPDH* glyceraldehyde 3-phosphate dehydrogenase. ** $p<0.01$, $n\geq3$. (Modified [26])

Table 19.1 gives an overview on the markers that were investigated in RGC-5 cells. Clearly, there is currently some controversy regarding the presence of certain markers in RGC-5, notably regarding Thy1. Overall, it can be stated that a larger percentage of authors reported RGC-5 cells to be positive for Thy1 [1, 7, 8, 10, 12, 16, 26, 29, 33, 35]. The differences may be due to an ongoing dedifferentiation of the cells in different laboratories. Interestingly, the expression of nestin has been described [33] suggesting an origin from neuronal precursor cells lineage. Quite surprisingly, the RGC-5 cells have been reported to express cone opsin [20, 33].

**Table 19.1** List of published markers expressed in undifferentiated RGC-5 cells

| Gene symbol | Protein name | Expression confirmed | No expression found |
|---|---|---|---|
| *RGC markers* | | | |
| Brn3 (Pou4f) | POU domain, class 4, transcription factor | [7, 12, 16, 24, 35] | [33] |
| Sncg | Gamma-synuclein | [7] | |
| Thy1 | Thy-1 membrane glycoprotein | [1, 7, 8, 10, 12, 16, 26, 35] | [29, 33] |
| *Neuronal markers* | | | |
| GABABR1 (Gabbr1) | Gamma-aminobutyric acid type B receptor subunit 1 | [16] | |
| Map1b | Microtubule-associated protein 1B | [33] | |
| Map2 | Microtubule-associated protein 2 | [8, 22, 23, 26, 33] | |
| Nefh | Neurofilament heavy polypeptide | [22, 23] | [29] |
| Nefl | Neurofilament light polypeptide | [10] | [29, 33] |
| Nefm | Neurofilament medium polypeptide | [7] | [29, 33] |
| NMDAR (Grin) | Glutamate [NMDA] receptor | [8, 16] | |
| Nrn1 | Neuritin | [16] | |
| PGP 9.5 (Uchl1) | Ubiquitin carboxyl-terminal hydrolase isozyme L1 | [26, 29, 33] | |
| Syp | Synaptophysin | [16] | [33] |
| Tau (Mapt) | Microtubule-associated protein tau | [22, 23, 29, 33] | |
| Tubb3 | Tubulin beta-3 chain | [22, 23, 26, 33] | |
| *Neurotrophins* | | | |
| Bdnf | Brain-derived neurotrophic factor | [1, 16] | |
| Cntf | Ciliary neurotrophic factor | [16, 26] | |
| Gdnf | Glial cell line-derived neurotrophic factor | [16] | |
| Ngf | Beta-nerve growth factor | [1, 16] | |
| NT3 (Ntf3) | Neurotrophin-3 | [1, 16, 26] | |
| NT4 (Ntf4) | Neurotrophin-4 | [1, 16] | |
| *Neurotrophin receptors* | | | |
| TrkA (Ntrk1) | High-affinity nerve growth factor receptor | [1, 16] | |
| TrkB (Ntrk2) | BDNF/NT-3 growth factors receptor | [1, 12, 16] | |
| TrkC (Ntrk3) | NT-3 growth factor receptor | [16] | [1] |

**Table 19.1** (continued)

| Gene symbol | Protein name | Expression confirmed | No expression found |
|---|---|---|---|
| p75 (Tnfrsf1b) | Tumor necrosis factor receptor superfamily member 1B | [1, 16] | |
| *Precursor markers* | | | |
| Chx10 (Vsx2) | Visual system homeobox 2 | | [33] |
| Dcx | Neuronal migration protein doublecortin | | [33] |
| Musashi1 (Msi1) | RNA-binding protein Musashi homolog 1 | | [33] |
| Nes | Nestin | [33] | |
| *Opsins* | | | |
| Opn1sw | Short-wave-sensitive opsin 1 | [33] | |
| Opn1mw | Medium-wave-sensitive opsin 1 | [20] | |
| Opn3 | Opsin-3 | [20] | |
| Opn4 | Melanopsin | | [20] |
| Opn5 | Opsin-5 | [20] | |
| Rgr | RPE-retinal G protein-coupled receptor | [20] | |
| Rho | Rhodopsin | | [20, 33] |
| *Amacrine cells* | | | |
| Stx1a | Syntaxin-1A | | [16] |
| Calb2 | Calretinin | | [33] |
| Astrocytes | | | |
| Gfap | Glial fibrillary acidic protein | | [16, 33] |
| *Horizontal cells* | | | |
| Calb1 | Calbindin | | [33] |
| *Müller glia* | | | |
| Vim | Vimentin | | [10] |
| *On-bipolar cells* | | | |
| Prkca (Pkcα) | Protein kinase C alpha type | | [33] |

## 19.3 Characteristics of Physiological Relevance

Glutamate-induced excitotoxicity is a common feature of RGCs and is discussed to be associated with glaucoma [21, 30]. Since RGCs are more vulnerable to excitotoxic injury than other retinal neurons [17], glutamate sensitivity would support an RGC origin of RGC-5. Indeed, glutamate sensitivity was reported for succinylated concanavalin A differentiated [1] and undifferentiated RGC-5 cells [2]. Still, later studies rather noted an increased resistance to glutamate [19, 29]. Currently, differentiation with trichostatin A [33], staurosporine [12] or conditioned medium

from human nonpigmented ciliary epithelial (HNPE) cells [28] is recommended to induce glutamate sensitivity in RGC-5 cells.

Various experiments were performed to investigate cell death induced by oxidative stress [12, 19], exposure to light [32] or hydrostatic pressure [14] to name a few. Another vital characteristic of RGC research is their dependency on trophic factors [1, 26]. These factors are able to prevent RGC-5 cells from undergoing apoptosis induced by glutamate or oxidative stress [12] and depletion of optineurin [26].

Being intrinsically photosensitive potentially due to the expression of visual and nonvisual opsins offers an additional possibility for investigation [20]. In addition, RGC-5 cells have been used to study various aspects of retinal neurons by electrophysiology [8, 31].

## 19.4 Protocols for Differentiation

In RGC-5 cells, differentiation is disrupted by ψ2E1A adenovirus infection. This leads to a mitotically active state and a transformed phenotype which is distinct from primary RGCs. To stop proliferation and induce cell differentiation, the following four methods were proposed and will be discussed in detail. Table 19.2 gives an overview of expression changes following differentiation using these methods.

### *19.4.1 Succinylated Concanavalin A*

Succinylated concanavalin A (sConA), a nontoxic derivative of the lectin concanavalin A, was originally recommended as differentiation agent. Following this, protocol cells are cultured for 24 h in the absence of serum, followed by a 7-day period in growth medium supplemented with sConA to a final concentration of 50 μg/ml [16]. This treatment was reported to induce differentiation and responsiveness to glutamate toxicity [16]. Meanwhile, alternative methods for differentiation are preferred, as subsequent reports did not find changes in the expression of any markers or induction of glutamate sensitivity by sConA treatment [29, 33].

### *19.4.2 Staurosporine*

Staurosporine (STSN) treatment leads to a rapid induction of a neuronal-like morphology. Within minutes, an increased outgrowth of branched neurites (Fig. 19.1a) associated with cell cycle arrest can be observed [26, 29, 33]. This nonselective protein kinase inhibitor induces increased expression of outward rectifying channels as well as neuronal markers including Thy1 and MAP2 [8]. STSN represents a reliable agent to induce neuronal differentiation of RGC-5. The most commonly used protocol is 316 nM STSN in normal growth medium for usually 24 h, which can be extended for up to 5 days [10, 18, 24].

**Table 19.2** Comparison of expression changes following different methods for differentiation in RGC-5 cells

| Gene symbol | sConA | STSN | TSA | HNPE-medium |
|---|---|---|---|---|
| *RGC markers* | | | | |
| Brn3 (Pou4f) | ND [33] | ND [33], −[24], + [12] | ND [33], + [24] | |
| Thy1 | ND [29, 33] | ND [33], = [26], + [8, 10, 12] | ND [33] | + [35] |
| *Neuronal markers* | | | | |
| Map1b | = [33] | + [33] | + [33] | |
| Map2 | = [33] | + [8, 18, 23, 33] | + [22, 33] | |
| Nefh | ND[29] | + [33] | + [22] | |
| Nefl | ND [29, 33] | ND [33], + [10] | ND [33] | |
| Nefm | ND [29, 33] | ND [33] | ND [33] | |
| NMDAR (Grin) | | + [8] | | |
| PGP 9.5 (Uchl1) | = [29, 33] | + [26, 33] | + [33] | |
| Tau (Mapt) | = [29, 33] | = [33], + [23] | + [22, 33] | |
| Tubb3 | = [33] | = [33], + [23, 26] | + [22, 33] | |
| TrkB (Ntrk2) | | + [12] | | |

*ND* not detectable, = no changes in expression following differentiation, − down-regulation following differentiation, + up-regulation following differentiation, *HNPE* human nonpigmented ciliary epithelial, *RGC* retinal ganglion cell, *sConA* succinylated concanavalin A, *STSN* staurosporine, *TSA* trichostatin A

### *19.4.3 Trichostatin A*

Another differentiation-inducing agent is trichostatin A (TSA), a histone deacetylase inhibitor, which induces cell cycle arrest, morphological changes and upregulation of certain markers: Map1b, Map2, beta tubulin, Tau, PGP9.5 and NFH [22, 33]. Following TSA incubation, excitotoxic responsiveness was reported [33]. For differentiation, cells are cultured for 24 h under serum-free conditions and subsequently with 500 nM TSA for 3 up to 5 days [24, 33].

### *19.4.4 Conditioned HNPE Medium*

A promising method is differentiation using conditioned medium collected from HNPE cells. According to this protocol, RGC-5 cells are incubated for 48 h with HNPE-conditioned medium. This induces a more neuron-like phenotype with elongated neurites and condensed soma comparable to STSN-treated cells. Besides, sensitivity to glutamate is induced [28], and Thy1 expression is enhanced [35].

So far, it is challenging to find the most appropriate agent for differentiation. Still, mechanisms are unclear and it is questionable which method is able to achieve the most RGC-like results. While sConA is not sufficient to induce differentiation [29, 33], there is not enough information about conditioned HNPE medium for dif-

ferentiation available [35] to compare this method with STSN and TSA treatment. Both agents, STSN and TSA, cause, in a dose- and time-dependent manner, non-proliferative cells, upregulation of certain neuronal markers and neuritogenesis underlying separate and largely unknown mechanisms [24, 33]. It has to be mentioned that STSN treatment induces cell death even in lowest concentrations that can be used for differentiation [23], and the same applies to TSA [22]. In contrast to STSN, there is a significantly higher percentage of cell death caused by TSA, which can be reduced using neurotrophic factors; this is not the case for STSN. The dependency on neurotrophic factors appears to be an attribute that is similar to RGCs in vivo [24]. Following treatment with TSA [33], STSN [13] or conditioned HNPE medium [28], cells can be rendered glutamate sensitive.

## 19.5 Conclusion

Although originally designated to be derived from *Rattus norvegicus*, we now consider confirmed that RGC-5 cells take their origin from *Mus musculus* [26, 29]. With regards to the expression of the RGC-typical proteins Thy1 and Brn3, there is some controversy, as it was not confirmed by some authors [29, 33]. On the other hand, the majority of authors demonstrated an expression [1, 7, 8, 10, 12, 16, 26, 35].

RGC-5 cells have some properties in common with neural progenitor cells, being mitotically active and positive for nestin, but not for other neural progenitor cell markers [33]. It should be taken into account though that in injured neuronal tissue, like dissociated retina culture, a general upregulation of nestin occurs [9]. Nestin expression in RGC-5 could be a sign of dedifferentiation induced by bringing the cell to culture conditions.

Remarkably, RGC-5 cells are intrinsically photosensitive [20] and positive for blue (Opn1SW) [33] and green cone opsins (Opn1MW) as well as for other visual and nonvisual opsins [20]. This finding appears to indicate an origin not from RGC but rather from cone photoreceptor lineage. Alternatively, a cross-contamination in the laboratory of origin with the cone photoreceptor cell line 661W, which possesses similar properties, was proposed [27]. Still, while the expression of cone opsin is surprising, it was previously described for a subset of RGCs. The numbers of the cells increased particularly in response to photoreceptor cell loss [25]. As RGC-5 cells are cultured isolated without other cell types, an upregulation of markers that are unspecific to mature RGCs but were described to be induced after lesion might explain this observation.

In general, it is important to keep in mind that in any transformed cell line, the process of transformation invariably leads to dedifferentiation of the cells. Accordingly, transformed cell lines will always miss characteristic properties of their cells of origin. This is also true for RGC-5. While the available data support the concept that RGC-5 cells are of neuronal origin from the retina, it is less clear if they derived from RGC and/or if they still express the defining characteristics of mature RGC. In addition, there is some evidence that the original properties became modified by

high passage numbers or progressive subculturing. With all these caveats considered, RGC-5 may still be a tool in the hand of researchers who want to follow up on some initial hypotheses that require a transformed retina cell line of neuronal origin. Still, it is highly recommended that such findings are subsequently tested in a more biologically relevant background.

## References

1. Agarwal N, Agarwal R, Kumar DM, Ondricek A, Clark AF, Wordinger RJ et al (2007) Comparison of expression profile of neurotrophins and their receptors in primary and transformed rat retinal ganglion cells. Mol Vis 13:1311–1318
2. Aoun P, Simpkins JW, Agarwal N (2003) Role of PPAR-gamma ligands in neuroprotection against glutamate-induced cytotoxicity in retinal ganglion cells. Invest Ophthalmol Vis Sci 44:2999–3004
3. Barber AJ, Lieth E, Khin SA, Antonetti DA, Buchanan AG, Gardner TW (1998) Neural apoptosis in the retina during experimental and human diabetes. Early onset and effect of insulin. J Clin Invest 102:783–791
4. Beale R, Osborne NN (1982) Localization of the Thy-1 antigen to the surfaces of rat retinal ganglion cells. Neurochem Int 4:587–595
5. Carelli V, La Morgia C, Valentino ML, Barboni P, Ross-Cisneros FN, Sadun AA (2009) Retinal ganglion cell neurodegeneration in mitochondrial inherited disorders. Biochim Biophys Acta 1787:518–528
6. Cone RD, Grodzicker T, Jaramillo M (1988) A Retrovirus Expressing the 12S Adenoviral ElA gene product can immortalize epithelial cells from a broad range of rat tissues. Mol Cell Biol 8:1036–1044
7. Fragoso MA, Yi H, Nakamura RE, Hackam AS (2011) The Wnt signaling pathway protects retinal ganglion cell 5 (RGC-5) cells from elevated pressure. Cell Mol Neurobiol 31:163–173
8. Frassetto LJ, Schlieve CR, Lieven CJ, Utter AA, Jones MV, Agarwal N et al (2006) Kinase-dependent differentiation of a retinal ganglion cell precursor. Invest Ophthalmol Vis Sci 47:427–438
9. Frisén J, Johansson CB, Török C, Risling M, Lendahl U (1995) Rapid, widespread, and longlasting induction of nestin contributes to the generation of glial scar tissue after CNS injury. J Cell Biol 131:453–464
10. Ganapathy PS, Dun Y, Ha Y, Duplantier J, Allen JB, Farooq A et al (2010) Sensitivity of staurosporine-induced differentiated RGC-5 cells to homocysteine. Curr Eye Res 35:80–90
11. Grozdanov V, Müller A, Sengottuvel V, Leibinger M, Fischer D (2010) A method for preparing primary retinal cell cultures for evaluating the neuroprotective and neuritogenic effect of factors on axotomized mature CNS neurons. Curr Protoc Neurosci; Chapter 3:Unit3.22
12. Harper MM, Adamson L, Blits B, Bunge MB, Grozdanic SD, Sakaguchi DS (2009) Brain-derived neurotrophic factor released from engineered mesenchymal stem cells attenuates glutamate- and hydrogen peroxide-mediated death of staurosporine-differentiated RGC-5 cells. Exp Eye Res 89:538–548
13. Hobom M, Storch MK, Weissert R, Maier K, Radhakrishnan A, Kramer B et al (2004) Mechanisms and time course of neuronal degeneration in experimental autoimmune encephalomyelitis. Brain Pathol 14:148–157
14. Ju WK, Liu Q, Kim KY, Crowston JG, Lindsey JD, Agarwal N et al (2007) Elevated hydrostatic pressure triggers mitochondrial fission and decreases cellular ATP in differentiated RGC-5 cells. Invest Ophthalmol Vis Sci 48:2145–2151
15. Kerrigan LA, Zack DJ, Quigley HA, Smith SD, Pease ME (1997) TUNEL-positive ganglion cells in human primary open-angle glaucoma. Arch Ophthalmol 115:1031–1035

16. Krishnamoorthy RR, Agarwal P, Prasanna G, Vopat K, Lambert W, Sheedlo HJ et al (2001) Characterization of a transformed rat retinal ganglion cell line. Mol Brain Res 86:1–12
17. Li Y, Schlamp CL, Nickells RW (1999) Experimental induction of retinal ganglion cell death in adult mice. Invest Ophthalmol Vis Sci 40:1004–1008
18. Lieven CJ, Millet LE, Hoegger MJ, Levin LA (2007) Induction of axon and dendrite formation during early RGC-5 cell differentiation. Exp Eye Res 85:678–683
19. Maher P, Hanneken A (2005) The molecular basis of oxidative stress-induced cell death in an immortalized retinal ganglion cell line. Invest Ophthalmol Vis Sci 46:749–757
20. Nieto PS, Valdez DJ, Acosta-Rodríguez VA, Guido ME (2011) Expression of novel opsins and intrinsic light responses in the mammalian retinal ganglion cell line RGC-5. Presence of OPN5 in the rat retina. PLoS One 6: e26417
21. Olney JW (1969) Glutamate-induced retinal degeneration in neonatal mice: Electron microscopy of the acutely evolving lesion. J Neuropathol Exp Neurol 28:455–474
22. Schnichels S, Schultheiss M, Hofmann J, Szurman P, Bartz-Schmidt KU, Spitzer MS (2012) Trichostatin A induces cell death at the concentration recommended to differentiate the RGC-5 cell line. Neurochem Int 60:581–591
23. Schultheiss M, Schnichels S, Miteva K, Warstat K, Szurman P, Spitzer MS et al (2012) Staurosporine-induced differentiation of the RGC-5 cell line leads to apoptosis and cell death at the lowest differentiating concentration. Graefes Arch Clin Exp Ophthalmol 250:1221–1229
24. Schwechter BR, Millet LE, Levin LA (2007) Histone deacetylase inhibitionmediated differentiation of RGC-5 cells and interaction with survival. Invest Ophthalmol Vis Sci 48:2845–2857
25. Semo M, Vugler AA, Jeffery G (2007) Paradoxical opsin expressing cells in the inner retina that are augmented following retinal degeneration. Eur J Neurosci 25:2296–2306
26. Sippl C, Bosserhoff AK, Fischer D, Tamm ER (2011) Depletion of optineurin in RGC-5 cells derived from retinal neurons causes apoptosis and reduces the secretion of neurotrophins. Exp Eye Res 93:669–680
27. Tan E, Ding XQ, Saadi A, Agarwal N, Naash MI, Al-Ubaidi MR (2004) Expression of cone-photoreceptor-specific antigens in a cell line derived from retinal tumors in transgenic mice. Invest Ophthalmol Vis Sci 45:764–768
28. Tchedre KT, Yorio T (2008) Sigma-1 receptors protect RGC-5 cells from apoptosis by regulating intracellular calcium, Bax levels, and caspase-3 activation. Invest Ophthalmol Vis Sci 49:2577–2588
29. Van Bergen NJ, Wood JP, Chidlow G, Trounce IA, Casson RJ, Ju WK et al (2009) Recharacterization of the RGC-5 retinal ganglion cell line. Invest Ophthalmol Vis Sci 50:4267–4272
30. Vorwerk CK, Lipton SA, Zurakowski D, Hyman BT, Sabel BA, Dreyer EB (1996) Chronic low-dose glutamate is toxic to retinal ganglion cells: Toxicity blocked by memantine. Invest Ophthalmol Vis Sci 37:1618–1624
31. Wang SJ, Xie LH, Heng B, Liu YQ (2012) Classification of potassium and chlorine ionic currents in retinal ganglion cell line (RGC-5) by whole-cell patch clamp. Vis Neurosci 29:275–282
32. Wood JP, Lascaratos G, Bron AJ, Osborne NN (2007) The influence of visible light exposure on cultured RGC-5 cells. Mol Vis 14:334–344
33. Wood JP, Chidlow G, Tran T, Crowston JG, Casson RJ (2010) A comparison of differentiation protocols for RGC-5 cells. Invest Ophthalmol Vis Sci 51:3774–3783
34. Xiang M, Zhou L, Macke JP, Yoshioka T, Hendry SH, Eddy RL et al (1995) The Brn-3 family of POU-domain factors: primary structure, binding specificity, and expression in subsets of retinal ganglion cells and somatosensory neurons. J Neurosci 15:4762–4785
35. Yang MH, Krishnamoorthy RR, Jong SB, Chu PY, Yang YH, Chen et al (2011). Protein profiling of human nonpigmented ciliary epithelium cell secretome: the differentiation factors characterization for retinal ganglion cell line. J Biomed Biotechnol 2011:901329

# Part IV
# Genetics in Retinal Disease

# Chapter 20
# Modeling Retinal Dystrophies Using Patient-Derived Induced Pluripotent Stem Cells

**Karl J. Wahlin, Julien Maruotti and Donald J. Zack**

**Abstract** *Retinal* degenerative disease involving photoreceptor (PR) cell loss results in permanent vision loss and often blindness. Generation of induced pluripotent stem cell (iPSC)-derived retinal cells and tissues from individuals with retinal dystrophies is a relatively new and promising method for studying retinal degeneration mechanisms in vitro. Recent advancements in strategies to differentiate human iPSCs (hiPSCs) into 3D retinal eyecups with a strong resemblance to the mature retina raise the possibility that this system could offer a reliable model for translational drug studies. However, despite the potential benefits, there are challenges that remain to be overcome before stem-cell-derived retinal eyecups can be routinely used to model human retinal diseases. This chapter will discuss both the potential of these 3D eyecup approaches and the nature of some of the challenges that remain.

**Keywords** Retinal degeneration · Patient · Dystrophy · Stem cell · hiPSC · Pluripotent · Eyecup

K. J. Wahlin (✉) · J. Maruotti · D. J. Zack
Department of Ophthalmology, The Johns Hopkins University School of Medicine, Smith Building Rm 3029, 400 N Broadway, Baltimore, MD, USA
e-mail: kwahlin1@jhmi.edu

D. J. Zack
Department of Neuroscience, The Johns Hopkins University School of Medicine, Baltimore, MD, USA
e-mail: dzack@jhmi.edu

Department of Molecular Biology and Genetics, The Johns Hopkins University School of Medicine, Baltimore, MD, USA

Institute of Genetic Medicine, The Johns Hopkins University School of Medicine, Baltimore, MD, USA

Institut de la Vision, Paris 75012, Paris, France

J. D. Ash et al. (eds.), *Retinal Degenerative Diseases,* Advances in Experimental Medicine and Biology 801, DOI 10.1007/978-1-4614-3209-8_20,

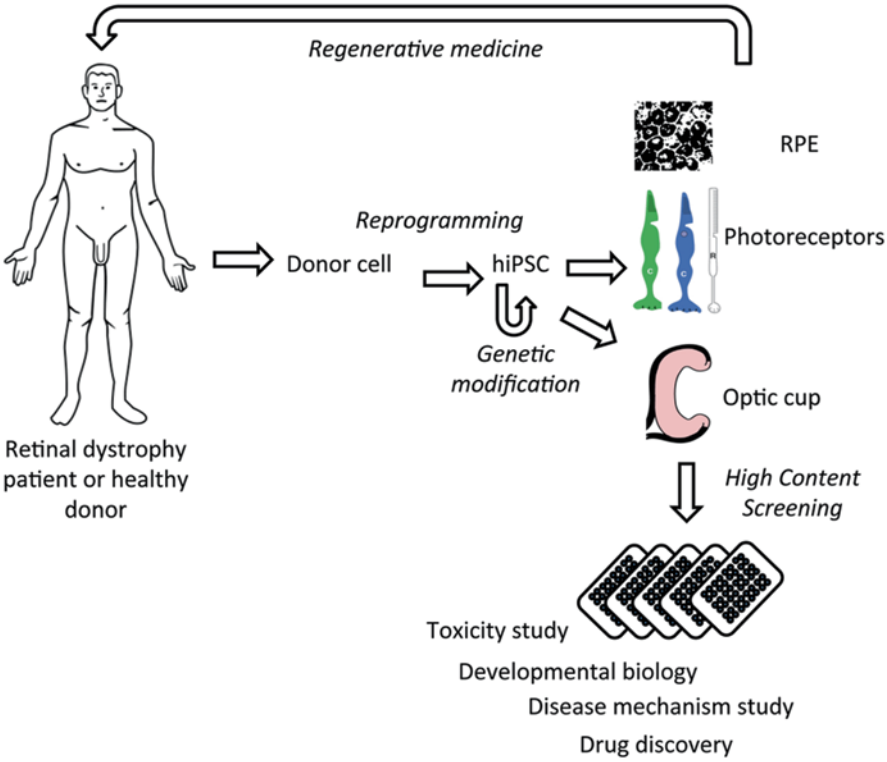


**Fig. 20.1** A strategy to utilize human-induced pluripotent stem cell (*hiPSC*)-derived PR or retinal pigment epithelial (*RPE*) cells for cell replacement therapies or to generate retinal eyecups to be used to model human eye disease and for high-content drug screening

## 20.1 Introduction

Retinal degenerative diseases include Mendelian orphan diseases such as retinitis pigmentosa (RP) and the complex genetics disease age-related macular degeneration (AMD), which is the second most common cause of irreversible blindness in the western world. Vision loss in these diseases results from the dysfunction and death of photoreceptor (PR) cells and/or adjacent retinal pigment epithelial (RPE) cells. While both environmental and genetic causes have been implicated in retinal degeneration, in many cases the particular gene(s) and/or risk factor(s) involved are unknown, making it difficult to develop targeted therapies [1]. Even when the mutation is known, FDA-approved therapies are in general not yet available. Pluripotent stem cells (PSCs) of human origin offer exciting new approaches to study human "diseases in a dish," offering a new means to explore mechanisms of retinal disease and opening the possibility of novel cell-based therapeutic approaches (Fig. 20.1). PSC-derived retinal cells could also facilitate high-content screening of human disease-based cells for neuroprotective and other therapeutic compounds.

One approach for such studies is to use dissociated cell cultures. Another approach, which has the advantage of better modeling the in vivo situation, is the use of 3D retinal cultures in the form of retinal eyecups that preserve the stereotypical laminar pattern of the mature neural retina, complete with a thin RPE layer [2].

## 20.2 Retinal Dystrophies Can Arise from Mutations in Genes Predominantly Expressed in Photoreceptors or the RPE

The Retinal Information Network, or Retnet (https://sph.uth.edu/RetNet/), which maintains a curated list of genes causing retinal disease, lists well over 200 retinal disease-associated genes and loci. Rhodopsin gene mutations are the most common causes of autosomal dominant RP (adRP), with the P23H mutation being the most common opsin mutation. Rhodopsin mutations can result in protein mis-folding and trafficking defects, and eventually result in PR death [3]. Defects in cells other than PRs can also result in PR degeneration. For example, defects in the Mer tyrosine kinase (*MERTK*) can result in a childhood onset rod-cone dystrophy by altering the normal phagocytic functions of RPE cells, which disrupts the normal cycling of visual pigments that are shed on a daily basis from PR outer segments [4]. Similarly, mutations in the *RPE-65* gene, which encodes a retinoid isomerase that is predominantly expressed in the RPE, can result in Leber congenital amaurosis (LCA), a severe early onset form of childhood retinal degeneration [5].

## 20.3 Existing Models of Retinal Degeneration Using hiPSCs

Although mouse models of human *RP* exist and are being used for mechanism and drug development purposes, mice and humans are not equivalent, and species-specific differences have been an issue in translational studies. In a mouse model of Usher 3 syndrome, a form of RP with hearing loss, the causal mutation in *clarin-1* expressed in mice, leads to auditory deficits but no detectable retinal degeneration phenotypes [6]. It is hoped that by generating models of human eye disease in a dish through the use of human-induced pluripotent stem cells (hiPSCs) some of these species-related issues can be avoided.

Several studies of human retinal disease have used hiPSCs to study *RP* and gyrate atrophy (GA) [7, 8]. GA of the retina can arise from a defect in the metabolism of ornithine-δ-aminotransferase (OAT) and begins in childhood, often resulting in total vision loss in 30–40-year olds [9, 10]. From an individual with a form of GA that is responsive to dietary supplementation with pyridoxine (vitamin B6), hiPSCs were generated by Meyers et al. who then directed them to become RPE cells, a cell type affected by this disease [8]. Restoration of OAT activity was observed upon treatment with high doses of vitamin B6. Furthermore, showing the power of hiPSC

technology, it was shown that mutant cells could be restored to normal function by genetically correcting the OAT gene mutation via bacterial artificial chromosome (BAC)-mediated homologous recombination.

In another recent report, whole exome sequencing of stem-cell-derived retinal cells from a single patient with RP was used to identify a homozygous Alu insertion in exon 9 of Male germ cell Associated kinase (MAK) [11]. In hiPSCs from healthy unaffected donors, a transcript-lacking exon9 was found in undifferentiated cells, whereas a transcript-bearing exon 9 and a previously unrecognized exon 12 were seen in differentiated retinal precursors. In the RP-based hiPSCs with the Alu insertion, this splicing switch never occurred, suggesting a defect in alternative splicing. For retinal disorders in which the basis for disease is not yet known, this strategy demonstrates the usefulness of exome sequencing to uncover differences in altered gene expression and/or alternatively spliced variants due to retinal degeneration.

Another important study involved a model for RP in which Jin et al. generated hiPSCs from RP patients with early (RP9) or late onset (RP1, PRPH2, or RHO) retinal degeneration [7]. Compared with unaffected controls, stem-cell-derived rod PRs from disease backgrounds decreased over time, and markers for oxidative and/or ER stress became elevated. These observations bode well for retinal disease modeling—a major concern has been that since many retinal dystrophies occur only after many decades of life, they would not demonstrate a detectable phenotype in relatively short-term cell culture. There is mounting evidence that some neurodegenerative disorders with later-stage onset can also be modeled in vitro [12].

## 20.4 Generating hiPSCs and PRs

Lineage-specific variation can affect hiPSC generation, maintenance, and PR differentiation. Numerous studies suggest that not all stem cell lines are created equal; stem cells created by different labs, by different reprogramming methods, and even different cell lines derived from the same patient with the same methods can show variable differentiation potential [13]. To reduce this inherent variation, it is important that microenvironmental, epigenetic, and other factors that contribute to retinal differentiation be better understood.

Studies of stem-cell-derived retinal cells have traditionally been carried out with mouse PSCs [14–19]. In the past few years, however, newer protocols for generating retinal and RPE cells of human origin have also been developed. These new methodologies include improvements in microenvironment, extracellular matrices, timing, and cell purity [2, 8, 20–23]. One of the most noteworthy improvements has focused on self-organized pseudostratified optic cup structures bearing all the retinal cell types in their proper orientation (Fig. 20.2, unpublished data) [2, 8]. Rax positive neural retina can be distinguished after 2–3 weeks while early PR markers can be distinguished by 30–45 days in vitro. With a brief treatment with the small molecule Wnt agonist, CHIR99021, these cultures can even be coaxed to develop a thin layer of pigmented RPE cells. The advanced morphology and mature gene expression in 3D systems demonstrate the importance of cell–cell interactions; such

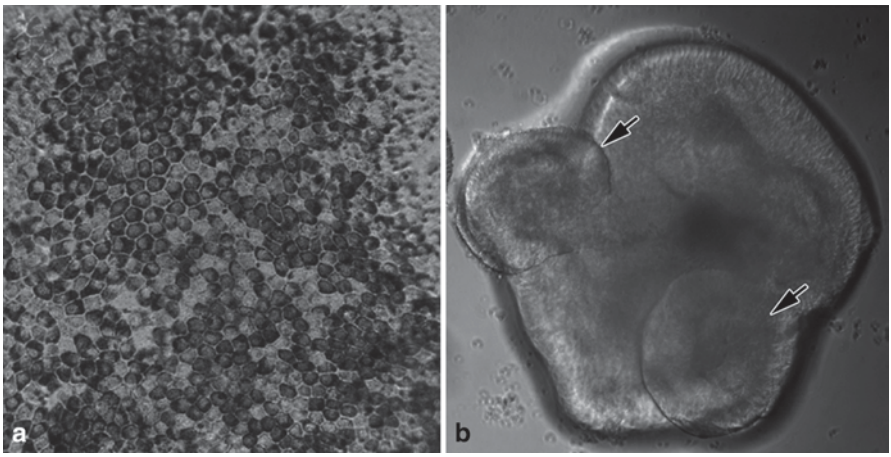


**Fig. 20.2** A representative RPE monolayer (**a**) and pseudo-stratified optic cup-like structure (b) from human iPS cells. *Arrows* indicate retinal eyecup structures in 18-day-old human stem-cell-derived retinas

retinal progenitors injected in vivo have been observed to have elevated expression of visual pigment and other PR-specific genes and bear outer segment-like structures that do not normally develop in simple monolayer cultures in vitro [2, 18, 21]. Collectively, these features should make it easier to develop in vitro assays for studying retinal degenerative disorders.

## 20.5 Limitations to Using hiPSC for Modeling Human Disease

When a disease source can be isolated to a single primary cell with a single gene mutation identified, the disease can be studied rather successfully, as exemplified in the case of the defective RPE cells in *GA*. When a disease affects PRs directly, purified PR progenitors can be grown in monolayer culture or as more complex optic cup structures. Unfortunately many retinal diseases result from a complex interplay between distinct cell and tissue types. Additionally, systemic factors can play a role, and these complex interactions can be difficult or impossible to adequately model in vitro.

There are also technical reasons why a disease phenotype might not be easily observed, especially when dealing with a subtle disease phenotype. Human iPSC-derived embryoid bodies and neurospheres can vary considerably in terms of cell type composition, number and size of optic cups, and demonstrate differences in the timing of differentiation (Wahlin et al., unpublished observations). Parameters such as oxygen tension, cell medium composition, and feeding frequency can also adversely affect cell culture variability and can act as additional sources of experimental variability. As stem cell and retinal differentiation protocols become better refined, such issues will hopefully become less problematic.

## 20.6 Exciting New Tools to Study Disease-Specific Cell Lines

Major sources of variation are the stem cells themselves, and this poses challenging problems when studying diseases with subtle phenotypes [13]. Variation in hiPSC-derived retinal cells from different individuals, which could result from genetic and epigenetic differences, might mask any retinal degeneration phenotype induced by an actual disease-causing mutation. Using new genome editing tools including zinc fingers nucleases (ZFNs), TALE effector nucleases (TALENs), or the type II bacterial CRISPR RNA-guided nucleases, one can now generate mutant cell lines with congenic controls rather than relying on genetically unmatched controls [24–26]. Due to decreased variability, these controls could greatly simplify interpretation of experimental findings. This technology could also be used to repair genetic mutations for the purpose of replacing defective retinal cells by transplantation.

## 20.7 Small Molecule Screens for Neuroprotective Compounds

Platforms for identifying neuroprotective small molecule chemicals are being investigated for many neurodegenerative models and have proven successful in some cases. For instance, a screen for proneurogenic compounds has uncovered molecules that protect against animal models of ALS and Parkinson's disease [27, 28]. For retinal survival assays, there are ongoing small molecule screens to protect primary rodent retinal ganglion and PR cell cultures (unpublished data). The recently developed eyecup methods should offer a new and powerful tool for investigating PR development and neuroprotection in a more in vivo-like environment.

Although much work remains, hiPSCs show great potential to contribute to the development of personalized medicine approaches and will likely help in the study of diseases for which no working model exists. Future studies should shed light on a plethora of retinal diseases, leading to greater understanding of disease mechanisms and hopefully also to advances in therapy.

## References

1. Sullivan LS, Bowne SJ, Birch DG et al (2006) Prevalence of disease-causing mutations in families with autosomal dominant retinitis pigmentosa: a screen of known genes in 200 families. Invest Ophthalmol Vis Sci 47(7):3052–3064 (Available at: http://eutils.ncbi.nlm.nih.gov/entrez/eutils/elink.fcgi?dbfrom=pubmed&id=16799052&retmode=ref&cmd=prlinks)
2. Nakano T, Ando S, Takata N et al (2012) Self-Formation of optic cups and storable stratified neural retina from human ESCs. STEM 10(6):771–785
3. Daiger SP, Bowne SJ, Sullivan LS (2007) Perspective on genes and mutations causing retinitis pigmentosa. Arch Ophthalmol 125(2):151–158

4. Mackay DS, Henderson RH, Sergouniotis PI et al (2010) Novel mutations in MERTK associated with childhood onset rod-cone dystrophy. Mol Vis 16:369–377
5. Marlhens F, Bareil C, Griffoin JM et al (1997) Mutations in RPE65 cause Leber's congenital amaurosis. Nat Genet 17(2):139–141
6. Geller SF, Guerin KI, Visel M, et al (2009) CLRN1 is nonessential in the mouse retina but is required for cochlear hair cell development. PLoS Genet 5(8):e1000607
7. Jin Z-B, Okamoto S, Osakada F et al (2011) Modeling retinal degeneration using patient-specific induced pluripotent stem cells. PLoS ONE 6(2):e17084
8. Meyer JS, Howden SE, Wallace KA et al (2011) Optic vesicle-like structures derived from human pluripotent stem cells facilitate a customized approach to retinal disease treatment. STEM CELLS 29(8):1206–1218
9. Valle D, Kaiser-Kupfer M (1982) Gyrate atrophy of the choroid and retina. Prog Clin Biol Res 82:123–134
10. Valle D, Simell O (2001) The hyperornithemias. In: Scriver CR, Beaudet AL, Sly WS, Valle D (eds) The metabolic & molecular bases of inherited disease, 8th ed. McGraw-Hill, New York, p 1857
11. Tucker BA, Scheetz TE, Mullins RF et al (2011) Exome sequencing and analysis of induced pluripotent stem cells identify the cilia-related gene male germ cell-associated kinase (MAK) as a cause of retinitis pigmentosa. Proc Natl Acad Sci USA 108(34):E569–E576
12. Marchetto MCN, Winner B, Gage FH (2010) Pluripotent stem cells in neurodegenerative and neurodevelopmental diseases. Hum Mol Genet 19(R1):R71–R76
13. Boulting GL, Kiskinis E, Croft GF et al (2011) A functionally characterized test set of human induced pluripotent stem cells. Nat Biotechnol 29(3):279–286
14. Ikeda H, Osakada F, Watanabe K et al (2005) Generation of Rx+/Pax6+neural retinal precursors from embryonic stem cells. Proc Natl Acad Sci USA 102(32):11331–11336
15. Lamba DA, Karl MO, Ware CB, Reh TA (2006) Efficient generation of retinal progenitor cells from human embryonic stem cells. Proc Natl Acad Sci USA 103(34):12769–12774
16. Maclaren RE, Pearson RA, MacNeil A et al (2006) Retinal repair by transplantation of photoreceptor precursors. Nature 444(7116):203–207
17. Osakada F, Ikeda H, Sasai Y, Takahashi M (2009) Stepwise differentiation of pluripotent stem cells into retinal cells. Nat Protoc 4(6):811–824
18. Tucker BA, Park I-H, Qi SD et al (2011) Transplantation of adult mouse iPS cell-derived photoreceptor precursors restores retinal structure and function in degenerative mice. PLoS ONE 6(4):e18992
19. Eiraku M, Takata N, Ishibashi H et al (2011) Self-organizing optic-cup morphogenesis in three-dimensional culture. Nature 472(7341):51–56
20. Osakada F, Jin Z-B, Hirami Y et al (2009) In vitro differentiation of retinal cells from human pluripotent stem cells by small-molecule induction. J Cell Sci 122(Pt 17):3169–3179
21. Meyer J, Shearer R, Capowski EE et al (2009) Modeling early retinal development with human embryonic and induced pluripotent stem cells. Proc Natl Acad Sci USA 106(39):16698–16703
22. Lamba DA, McUsic A, Hirata RK, Wang P-R, Russell D, Reh TA (2010) Generation, purification and transplantation of photoreceptors derived from human induced pluripotent stem cells. PLoS ONE 5(1):e8763
23. Boucherie C, Mukherjee S, Henckaerts E, Thrasher AJ, Sowden JC, Ali RR (2013) Self-organising neuroepithelium from human pluripotent stem cells facilitates derivation of photoreceptors. STEM CELLS 31(2):408–414
24. Briggs AW, Rios X, Chari R et al (2012) Iterative capped assembly: rapid and scalable synthesis of repeat-module DNA such as TAL effectors from individual monomers. Nucleic Acids Res 40(15):e117
25. Mali P, Yang L, Esvelt KM et al (2013) RNA-guided human genome engineering via Cas9. Science 339(6121):823–826
26. Soldner F, Laganière J, Cheng AW et al (2011) Generation of isogenic pluripotent stem cells differing exclusively at two early onset Parkinson point mutations. Cell 146(2):318–331

27. Tesla R, Wolf HP, Xu P et al (2012) Neuroprotective efficacy of aminopropyl carbazoles in a mouse model of amyotrophic lateral sclerosis. Proc Natl Acad Sci USA 109(42):17016–17021
28. De Jesús-Cortés H, Xu P, Drawbridge J et al (2012) Neuroprotective efficacy of aminopropyl carbazoles in a mouse model of Parkinson disease. Proc Natl Acad Sci USA 109(42):17010–17015

# Chapter 21
# Mutation K42E in Dehydrodolichol Diphosphate Synthase (DHDDS) Causes Recessive Retinitis Pigmentosa

**Byron L. Lam, Stephan L. Züchner, Julia Dallman, Rong Wen, Eduardo C. Alfonso, Jeffery M. Vance and Margaret A. Peričak-Vance**

**Abstract** A single-nucleotide mutation in the gene that encodes DHDDS has been identified by whole exome sequencing as the cause of the non-syndromic recessive retinitis pigmentosa (RP) in a family of Ashkenazi Jewish origin in which three of the four siblings have early onset retinal degeneration. The peripheral retinal degeneration in the affected siblings was evident in the initial examination in 1992 and only one had detectable electroretinogram (ERG) that suggested cone-rod dysfunction. The pigmentary retinal degeneration subsequently progressed rapidly. The identified mutation changes the highly conserved residue Lys42 to Glu, resulting in lower catalytic efficiency. Patterns of plasma transferrin isoelectric focusing gel were normal in all family members, indicating no significant abnormality in protein glycosylation. Dolichols have been shown to influence the fluidity and of the membrane and promote vesicle fusion. Considering that photoreceptor outer segments contain stacks of membrane discs, we believe that the mutation may lead to low dolichol levels in photoreceptor outer segments, resulting in unstable membrane structure that leads to photoreceptor degeneration.

**Keywords** Retinitis pigmentosa · Autosomal recessive · Dehydrodolichol diphosphate synthase (DHDDS) · Genotype · Ashkenazi Jewish · Whole exome sequencing · Transferrin isoelectric focusing · Hereditary retinal degeneration

B. L. Lam (✉) · R. Wen · E. C. Alfonso
Bascom Palmer Eye Institute, University of Miami, 900 NW 17th St, Miami, FL 33136, USA
e-mail: BLam@med.miami.edu

S. L. Züchner · J. M. Vance · M. A. Peričak-Vance
John P. Hussman Institute for Human Genomics, University of Miami, Miami, FL 33136, USA
e-mail: SZuchner@med.miami.edu

J. Dallman
Department of Integrative Biology, University of Miami, Miami, FL 33136, USA
e-mail: jdallman@bio.miami.edu

J. D. Ash et al. (eds.), *Retinal Degenerative Diseases,* Advances in Experimental Medicine and Biology 801, DOI 10.1007/978-1-4614-3209-8_21,

**Table 21.1** Systemic tests performed

| Systemic tests performed | |
|---|---|
| Neurological examination | Brain MRI with contrast |
| X-ray bone body survey | Bone density scan |
| Echocardiogram | Cholesterol and lipid profile |
| Thyroid function studies (TSH, free T4, free T3, TBG) | |
| Serum IGF binding protein 1 and 2 | |
| Serum clotting factors (II, V VII, VIII, IX, X, XI, XII) | |
| Antithrombin III | |

## 21.1 Introduction

Hereditary retinal degenerations, including retinitis pigmentosa (RP), are a group of blinding diseases of which no effective treatments are available. More than 50 genes are implicated in RP, a group of retinal degenerative disorders that share similar phenotypes that affect 1 in 3,000–4,500 of the population [1–4]. However, the genetic mutations in close to 50% of the autosomal recessive RP cases remain unknown (http://www.sph.uth.tmc.edu/retnet/sum-dis.htm). Identification of the genetic mutations improves the understanding of the disease process and promotes development of treatments.

We studied a family of Ashkenazi Jewish (AJ) origin in which three of the four siblings were diagnosed with RP in their teenage years. Using whole exome sequencing, a single-nucleotide mutation, c.124A > G in the DHDDS gene was found to be the cause of retinal degeneration in this family [5]. This mutation has subsequently been confirmed in other similar patients and is found to 10–20% of autosomal recessive RP in AJ population [6]. It is estimated that 1 in 332 in the AJ population is a heterozygous carrier of this mutation [6].

## 21.2 Materials and Methods

Clinical characterization of the patients included comprehensive ophthalmologic examination, Goldmann visual field, optical coherence tomography (OCT). A list of systemic tests were also performed (Table 21.1). Whole exome sequencing was used to identify the mutation. The pattern of plasma transferrin isoelectric focusing gel (IEF) analysis was carried out to detect abnormal protein glycosylation.

## 21.3 Results

### *21.3.1 Clinical Characterization of the Patients*

Three of the four siblings of this AJ family are homozygous of the K42E DHDDS mutation, as shown in the family pedigree (Fig. 21.1). Fundus images of the three

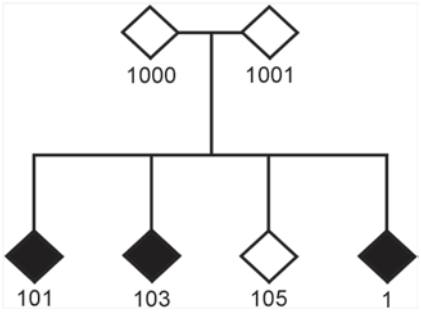


**Fig. 21.1** Family pedegree. Three out of the four siblings of this family of AJ origin are affected by autosomal recessive RP associated with the DHDDS genotype. (Modified from [5])

affected siblings show diffuse pigmentary retinal degeneration with vascular attenuation consistent with RP (Fig. 21.2). Patient 101 experienced impaired peripheral vision at age 16 years. By age 20, visual acuity was 20/25 OU with non-detectable ERG. Visual acuity at age 36 was 20/40 OD, 20/200 OS with constricted visual fields of < 10° (Fig. 21.2a). Patient 103 experienced impaired night and peripheral vision at age 15. By age 17, visual acuity was 20/30 and 20/25 with non-detectable ERG. Visual acuity at age 35 was 20/300 and 20/400 with visual fields of < 10° (Fig. 21.2b). Patient 1 was asymptomatic at age 14 with ERG indicated cone-rod dysfunction. Vision was reduced to LP OU by the time the patient was near age 30 (Fig. 21.2c).

### *21.3.2 Normal Pattern of Plasma Transferrin Isoelectric Focusing Gel*

Although biological functions of free dolichols are not well understood, the role of dolichyl phosphate as a lipid carrier for the assembly of oligosaccharides in protein glycosylation is well established. Does dolichol deficiency caused by this mutation lead to N-glycosylation deficiency? Plasma transferrin IEF was performed to address that question. Transferrin IEF is a common test for the diagnosis of congenital disorders of glycosylation (CDG), a group of inherited metabolic diseases with glycosylation deficiency that affect almost all organs and systems [7–9]. Results from the plasma transferrin IEF showed no appreciable carbohydrate-deficient transferrin in any of the patients (Fig. 21.3), suggesting no N-glycosylation deficiency in affected patients and thus deficiency in glycosylation is unlikely to be the cause of DHDDS-related RP.

## 21.4 Discussion

Using whole-exome sequencing, we identified a mutation in DHDDS as the cause of autosomal recessive RP in a family of AJ origin [5]. Subsequent work confirmed this mutation in other patients of AJ origin and found that this mutation accounts

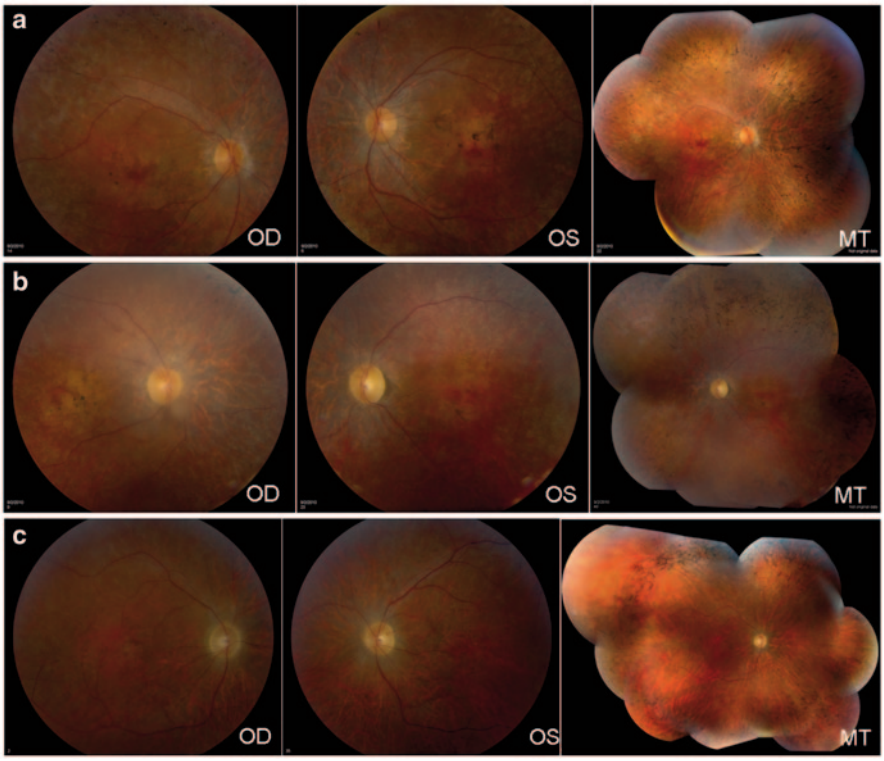


**Fig. 21.2** Retinal photographs of the affected family members with DHDDS RP (**a** Subject 101, **b** Subject 103, **c** Subject 1). The fundus photographs of the right eye (*OD*), left eye (*OS*), and montage (*MT*) retinal photograph of one eye are shown, demonstrating pigmentary retinal degeneration and vascular attenuation

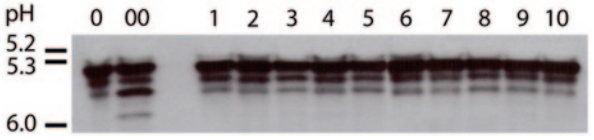


**Fig. 21.3** IEF of serum transferrin. No obvious abnormal serum transferrin pattern was found in patients with the K42E mutation in DHDDS. Lane *0,* negative control, *00,* positive control; Lane *1–6,* serum samples from patients; Lane *7–8,* from a carrier, and *9–10,* from an unaffected sibling (duplicated samples)

for 10–20 % of the autosomal recessive RP cases in AJ patients [6]. In addition, 1 in 332 in the AJ population is a carrier of this mutation [6]. The onset of the symptoms in this family where the genotype was first discovered was in their teenager years, and the degeneration progressed steadily resulting in legal blindness by age 30. The identification of this mutation presents at least two important challenges to us: (1) to

understand the mechanism by which this particular mutation leads to photoreceptor degeneration and (2) to design effective treatment strategies to save the vision of the affected patients.

Molecular modeling shows that this particular mutation changes a highly conserved Lys42 to Glu and causes distortion of the active site of the enzyme, which is likely to lead to dolichol deficiency. Dolichols were discovered more than 50 years ago [10, 11], but the biological functions of free dolichols remain poorly understood, except that the phosphorylated derivative dolichol is known to serve as the required lipid carrier for biosynthesis of oligosaccharides for protein glycosylation [12–17]. Since the patients show no systemic syndromes, it is unlikely that their protein glycosylation is impaired. This is confirmed by their normal pattern of plasma transferrin IEF. Previous studies showed that as a component of cell membrane, dolichols exert significant influence on the physical properties of the membrane. Photoreceptor outer segments are membrane rich structures. It is possible that insufficient amount of dolichols in photoreceptor outer segments could alter their normal physical properties that leads to photoreceptor degeneration.

The identification of the mutation and the autosomal recessive nature of the disease make gene therapy an effective way to treat this subtype of RP, as gene therapy has become a treatment for hereditary retinal degenerations [18–20]. In addition, neuroprotective therapies with specific neurotrophic factors may be considered to slow down the degeneration and thus to delay the loss of vision.

To further understand the link between the DHDDS mutation and to test potential treatment, transgenic mice are being created that carry the same mutation in our labs, which are expected to help us in further studies of this subtype of RP.

**Acknowledgments** We thank Drs. Yiwen Li and Zhengying Wang for technical assistance. This study was supported by grants from the National Institute of Health (P30-EY14801, R01-EY012118, R01-EY018586, and U54-NS065712), Department of Defense (W81XWH-09-1-0674), Hope for Vision, an unrestricted grant from Research to Prevent Blindness, and a grant from the Florida Office of Tourism, Trade and Economic Development (OTTED).

## References

1. Hartong DT, Berson EL, Dryja TP (2006) Retinitis pigmentosa. Lancet 368(9549):1795–1809
2. Heckenlively JR, Yoser SL, Friedman LH, Oversier JJ (1988) Clinical findings and common symptoms in retinitis pigmentosa. Am J Ophthalmol 105(5):504–511
3. Pagon RA (1988) Retinitis pigmentosa. Surv Ophthalmol 1988 33(3):137–177
4. Fahim AT, Daiger SP, Weleber RG (1993) Retinitis pigmentosa overview. In: Pagon RA, Adam MP, Bird TD, Dolan CR, Fong CT, Smith RJH, Stephens K, (eds) GeneReviews(tm) [Internet]. University of Washington, Seattle
5. Zuchner S, Dallman J, Wen R, Beecham G, Naj A, Farooq A et al (2011) Whole-exome sequencing links a variant in DHDDS to retinitis pigmentosa. Am J Hum Genet 88(2):201–206
6. Zelinger L, Banin E, Obolensky A, Mizrahi-Meissonnier L, Beryozkin A, Bandah-Rozenfeld D et al (2011) A missense mutation in DHDDS, encoding dehydrodolichyl diphosphate synthase, is associated with autosomal-recessive retinitis pigmentosa in Ashkenazi Jews. Am J Hum Genet 88(2):207–215

7. Freeze HH (2006) Genetic defects in the human glycome. Nat Rev Genet 7(7):537–551
8. Jaeken J, Matthijs G (2007) Congenital disorders of glycosylation: a rapidly expanding disease family. Annu Rev Genomics Hum Genet 8:261–278
9. Jaeken J (2010) Congenital disorders of glycosylation. Ann N Y Acad Sci 1214:190–198
10. Pennock JF, Hemming FW, Morton RA (1960) Dolichol: a naturally occurring isoprenoid alcohol. Nature 186:470–472
11. Burgos J, Hemming FW, Pennock JF, Morton RA (1963) Dolichol: a naturally-occurring C100 isoprenoid alcohol. Biochem J 88:470–482
12. Schenk B, Fernandez F, Waechter CJ (2001) The ins(ide) and out(side) of dolichyl phosphate biosynthesis and recycling in the endoplasmic reticulum. Glycobiology 11(5):61R–70R
13. Marquardt T, Denecke J (2003) Congenital disorders of glycosylation: review of their molecular bases, clinical presentations and specific therapies. Eur J Pediatr 162(6):359–379
14. Denecke J, Kranz C (2009) Hypoglycosylation due to dolichol metabolism defects. Biochim Biophys Acta 1792(9):888–895
15. Burda P, Aebi M (1999) The dolichol pathway of N-linked glycosylation. Biochim Biophys Acta 1426(2):239–257
16. Lehle L, Strahl S, Tanner W (2006) Protein glycosylation, conserved from yeast to man: a model organism helps elucidate congenital human diseases. Angew Chem Int Ed Engl 45(41):6802–6818
17. Behrens NH, Leloir LF (1970) Dolichol monophosphate glucose: an intermediate in glucose transfer in liver. Proc Natl Acad Sci U S A 66(1):153–159
18. den Hollander AI, Black A, Bennett J, Cremers FP (2010) Lighting a candle in the dark: advances in genetics and gene therapy of recessive retinal dystrophies. J Clin Invest 120(9):3042–3053
19. Cideciyan AV (2010) Leber congenital amaurosis due to RPE65 mutations and its treatment with gene therapy. Prog Retin Eye Res 29(5):398–427
20. Jacobson SG, Cideciyan AV, Ratnakaram R, Heon E, Schwartz SB, Roman AJ et al (2012) Gene therapy for leber congenital amaurosis caused by RPE65 mutations: safety and efficacy in 15 children and adults followed up to 3 years. Arch Ophthalmol 130(1):9–24

# Chapter 22
# IROme, a New High-Throughput Molecular Tool for the Diagnosis of Inherited Retinal Dystrophies—A Price Comparison with Sanger Sequencing

**Daniel F. Schorderet, Maude Bernasconi, Leila Tiab, Tatiana Favez and Pascal Escher**

**Abstract** The molecular diagnosis of retinal dystrophies (RD) is difficult because of genetic and clinical heterogeneity. Previously, the molecular screening of genes was done one by one, sometimes in a scheme based on the frequency of sequence variants and the number of exons/length of the candidate genes. Payment for these procedures was complicated and the sequential billing of several genes created endless paperwork. We therefore evaluated the costs of generating and sequencing a hybridization-based DNA library enriched for the 64 most frequently mutated genes in RD, called IROme, and compared them to the costs of amplifying and sequencing these genes by the Sanger method. The production cost generated by the high-throughput (HT) sequencing of IROme was established at CHF 2,875.75 per case. Sanger sequencing of the same exons cost CHF 69,399.02. Turnaround time of the analysis was 3 days for IROme. For Sanger sequencing, it could only be estimated, as we never sequenced all 64 genes in one single patient. Sale cost for IROme calculated on the basis of the sale cost of one exon by Sanger sequencing is CHF 8,445.88, which corresponds to the sale price of 40 exons. In conclusion, IROme is cheaper and faster than Sanger sequencing and therefore represents a sound approach for the diagnosis of RD, both scientifically and economically. As a drop in the costs of HT sequencing is anticipated, target resequencing might become the new gold standard in the molecular diagnosis of RD.

D. F. Schorderet (✉) · L. Tiab · T. Favez · P. Escher
IRO, Institute for Research in Ophthalmology, 64 Avenue du Grand-Champsec, 1950 Sion, Switzerland
e-mail: daniel.schorderet@irovision.ch

D. F. Schorderet · M. Bernasconi · P. Escher
University of Lausanne, Lausanne, Switzerland

M. Bernasconi
e-mail: maude.bernasconi@unil.ch

D. F. Schorderet
Faculty of Life Sciences, Ecole polytechnique fédérale de Lausanne, Lausanne, Switzerland

J. D. Ash et al. (eds.), *Retinal Degenerative Diseases,* Advances in Experimental Medicine and Biology 801, DOI 10.1007/978-1-4614-3209-8_22,

**Keywords** Retinitis pigmentosa · Retinal degeneration · Rod-cone dystrophy · Cone-rod dystrophy · Molecular diagnosis · High-throughput sequencing

## 22.1 Introduction

Retinitis pigmentosa (RP) and cone-rod dystrophies are a group of retinal diseases characterized by genetic heterogeneity. Not only mutations in different genes can induce the development of similar clinical phenotypes, but also different well-defined retinal diseases can be due to mutations in one particular gene. Therefore, a precise molecular diagnosis is essential in all patients for the following reasons: first, an accurate diagnosis makes long and sometimes painful examinations unnecessary; second, obtaining a precise diagnosis reduces the anxiety of the patients and their parents that a potentially treatable diagnosis was missed. It also allows some predictions to be made on the development and outcome of the disease. This will help to delineate potential treatments, i.e., vitamin A supplements in some RP patients. Conversely, such supplements are dangerous in Stargardt patients with mutations in *ABCA4* [1]. Third, a precise molecular diagnosis is a prerequisite for accurate genetic counseling. This can be illustrated by the family reported by Escher et al. [2]. In this family, two patients were affected with Enhanced-S-Cone syndrome (ESCS), an autosomal recessive disease caused by mutations in *NR2E3*. In such a situation, genetic counseling seems easy. If no patient/spouse consanguinity exists and assuming a *NR2E3* carrier frequency of 1/1,000, all children would most likely be carriers. Only 1 in 2,000 would develop ESCS. Molecular analysis in this family showed that both patients carried one of the *NR2E3* allele, a G56R mutation, responsible for a severe autosomal dominant RP when present in a heterozygous state with a wild-type allele [3, 4]. Therefore, the true risk for developing retinal disease in the offspring of this family is 0.5 rather than 0.002.

Molecular diagnosis is usually done by PCR amplification of specific exons followed by Sanger sequencing. Recently, many groups, including our own, developed solution- or chip-based approaches to specifically enrich for target genes followed by high-throughput sequencing [5–14]. We developed an in-solution array, called IROme, which enriched for a total of 942 exons contained in the 63 most prevalent genes involved in RP and macular dystrophies [14]. Here, we compared the cost between the IROme and high-throughput sequencing approach and regular Sanger sequencing.

## 22.2 Methods

The costs for Sanger and Roche 454 Junior-based high-throughput sequencing (Junior-HT) were evaluated from the diagnostic protocols used by the Laboratory of Molecular Ophthalmology at the Institute for Research in Ophthalmology (IRO),

in Sion. First, a flow chart describing both approaches was established. Common and specific steps were then identified. The duration of each step, the collaborators involved and the reagents needed were tabulated in an Excel sheet. In order to compare methods, time and price for the Sanger sequencing method were calculated for one exon. As a technician can work on more than one exon at a time with the Sanger approach, we compared the number of exons analyzed per week with the Sanger method to the number of patients per week with the Junior-HT technique. Prices of reagents, wages of the collaborators, and depreciation of the equipment were obtained from the financial section of IRO. It was assumed that each exon could be analyzed with one PCR/Sanger sequencing reaction. The production costs of both approaches were then compared. Finally, a sale price for the Junior-HT approach was calculated by analogy with the Sanger sequencing official billing amounts as set by the Swiss Federal Office of Public Health (http://www.bag.admin.ch/org/index.html?lang=en).

## 22.3 Results

The various pre-analytic, analytic, and post-analytic steps are described in Fig. 22.1 and differences between the two methods are individualized. The costs involved at each step are described in Table 22.1. IROme interrogates 942 exons in a single run. The main costs are related to three positions: target enrichment, HT sequencing and data analysis. One technician handling one machine can sequence one patient a day, 20 days a month. The same technician could sequence 1,920 exons per month. Adding monthly depreciation and maintenance as well as technician and supervisor wages, the production cost for one patient is estimated at CHF 69,399.05 and CHF 2,875.75 for Sanger and IROme Junior-HT sequencing, respectively. The latter price includes the Sanger sequencing of two exons, as many diseases are recessive.

The Swiss Federal Office of Public Health used a 2.9 ratio to calculate the sale costs of sequencing one exon by the Sanger method. Using a similar ratio would put the sale cost of IROme at CHF 9,000.05 per patient, which is equivalent to Sanger sequencing approx. 42 exons.

## 22.4 Discussion

RD are a group of heterogeneous diseases and no clear genotype-phenotype correlations have been established. Therefore, there are no accurate flow-charts to guide the molecular diagnosis of these diseases. Recently, high-throughput sequencing of targeted regions has emerged as an alternative method. Many aspects are in favor of such a trend, including better overall results, fast turnaround time, and global approach. However, we wanted to have a comparative cost analysis of this method in order to evaluate the financial burden of both approaches and decide which one

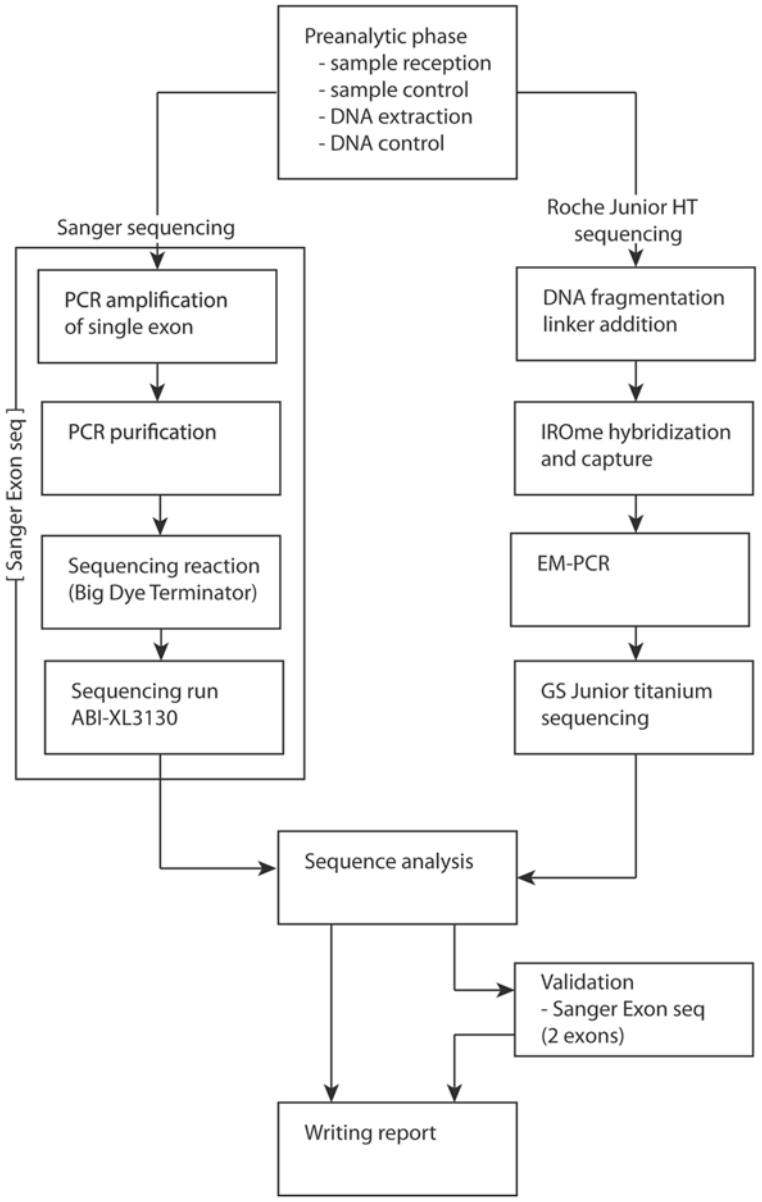


**Fig. 22.1** Flow chart of the Sanger and Roche-HT sequencing approaches

was the most economical. We evaluated the costs involved in running IROme, an in liquid enrichment kit followed by high-throughput sequencing on a Roche 454 Junior system [14]. The benefits of the HT approach were by far in favor of the use of IROme when compared to the Sanger sequencing of individual exons. We established that the costs involved in using IROme were equivalent to the costs generated

**Table 22.1** Description and cost (in Swiss Francs) involved at each step

| | Sanger sequencing | IROme |
|---|---|---|
| | (ABI 3130XL) | Roche 454 Junior-HT sequencing |
| Cost of reagents for NimbleGen enrichment/patient | | 600 |
| Cost of reagents for sequencing one exon (Sanger) per patient (1 run, Junior) | 68.50 | 1,940.65 |
| Cost of reagents for 942 exons/run | 64,527.00 | 2,540.65 |
| Number of analyzed exons, per day | 96 | 948 |
| Number of analyzed exons, per month (20 days) | 1920 | 18,960 |
| Number of patient/month | 2 | 20 |
| Number of days to analyze 942 exons/run | 10 | 0.5 |
| Time (in h) for supervisor to validate sequencing of 942 exons (15 min/exon) and write report | 20 | 3 |
| Cost of hardware | 550,000.00 | 250,000.00 |
| Depreciation, 10% per year calculated by month | 4,625.00 | 2,083.33 |
| Maintenance contract, per month | 1,666.67 | 1,041.67 |
| Technician wage, per month | 6,000.00 | 6,000.00 |
| Technician cost for one patient (942 exons) | 3,000.00 | 300.00 |
| Cost for one exon by Sanger | 73.21 | |
| Sanger validation (2 exons) of IROme results | | 146.42 |
| Cost for one patient | 69,399.02 | 2,875.75 |
| Sale cost estimate of IROme based on Sanger sequencing ratio | 215.00 | 8,445.88 |

by sequencing 40 exons with the Sanger approach. As our comparison was based on Swiss prices, this equivalence should help the reader to translate this price in his/her own currency and work conditions.

In conclusion, the potential of new technologies to control the steady worldwide IROme enrichment followed by high-throughput sequencing on a Roche 454 Junior system is not only scientifically sound but also economically.

**Conflict of Interest** The authors have no conflict of interest.

## References

1. Ma L, Kaufman Y, Zhang J, Washington I (2011) C20-D3-vitamin A slows lipofuscin accumulation and electrophysiological retinal degeneration in a mouse model of Stargardt disease. J Biol Chem 286(10):7966–7974
2. Escher P, Gouras P, Roduit R, Tiab L, Bolay S, Delarive T et al (2009) Mutations in NR2E3 can cause dominant or recessive retinal degenerations in the same family. Hum Mutat 30(3):342–351
3. Roduit R, Escher P, Schorderet DF (2009) Mutations in the DNA-binding domain of NR2E3 affect in vivo dimerization and interaction with CRX. PloS One 4(10):e7379

4. Schorderet DF, Escher P (2009) NR2E3 mutations in enhanced S-cone sensitivity syndrome (ESCS), Goldmann-Favre syndrome (GFS), clumped pigmentary retinal degeneration (CPRD), and retinitis pigmentosa (RP). Hum Mutat 30(11):1475–1485
5. Zernant J, Kulm M, Dharmaraj S, den Hollander AI, Perrault I, Preising MN et al (2005) Genotyping microarray (disease chip) for Leber congenital amaurosis: detection of modifier alleles. Investig Ophthalmol Vis Sci 46(9):3052–3059
6. Vallespin E, Cantalapiedra D, Riveiro-Alvarez R, Wilke R, Aguirre-Lamban J, Avila-Fernandez A et al (2007) Mutation screening of 299 Spanish families with retinal dystrophies by Leber congenital amaurosis genotyping microarray. Investig Ophthalmol Vis Sci 48(12):5653–5661
7. Avila-Fernandez A, Cantalapiedra D, Aller E, Vallespin E, Aguirre-Lamban J, Blanco-Kelly F et al (2010) Mutation analysis of 272 Spanish families affected by autosomal recessive retinitis pigmentosa using a genotyping microarray. Mol Vis 16:2550–2558
8. Bowne SJ, Sullivan LS, Koboldt DC, Ding L, Fulton R, Abbott RM et al (2011) Identification of disease-causing mutations in autosomal dominant retinitis pigmentosa (adRP) using next-generation DNA sequencing. Investig Ophthalmol Vis Sci 52(1):494–503
9. Gonzalez-del Pozo M, Borrego S, Barragan I, Pieras JI, Santoyo J, Matamala N et al (2011) Mutation screening of multiple genes in Spanish patients with autosomal recessive retinitis pigmentosa by targeted resequencing. PloS One 6(12):e27894
10. Simpson DA, Clark GR, Alexander S, Silvestri G, Willoughby CE (2011) Molecular diagnosis for heterogeneous genetic diseases with targeted high-throughput DNA sequencing applied to retinitis pigmentosa. J Med Genet 48(3):145–151
11. Song J, Smaoui N, Ayyagari R, Stiles D, Benhamed S, MacDonald IM et al (2011) High-throughput retina-array for screening 93 genes involved in inherited retinal dystrophy. Investig Ophthalmol Vis Sci 52(12):9053–9060
12. Kim C, Kim KJ, Bok J, Lee EJ, Kim DJ, Oh JH et al (2012) Microarray-based mutation detection and phenotypic characterization in Korean patients with retinitis pigmentosa. Mol Vis 18:2398–2410
13. Neveling K, Collin RW, Gilissen C, van Huet RA, Visser L, Kwint MP et al (2012) Next-generation genetic testing for retinitis pigmentosa. Hum Mutat 33(6):963–972
14. Schorderet DF, Iouranova A, Favez T, Tiab L, Escher P (2013) IROme, a new high-throughput molecular tool for the diagnosis of inherited retinal dystrophies. BioMed Res Int 2013 (Article ID 198089)

# Chapter 23
# Genetic Heterogeneity and Clinical Outcome in a Swedish Family with Retinal Degeneration Caused by Mutations in *CRB1* and *ABCA4* Genes

**Frida Jonsson, Marie S. Burstedt, Ola Sandgren, Anna Norberg and Irina Golovleva**

**Abstract** Genetic mechanisms underlying severe retinal dystrophy in a large Swedish family presenting two distinct phenotypes, Leber congenital amaurosis and Stargardt disease were investigated. In the family, four patients with Leber congenital amaurosis were homozygous for a novel c.2557C>T (p.Q853X) mutation in the *CRB1* gene, while of two cases with Stargardt disease, one was homozygous for c.5461-10T>C in the *ABCA4* gene and another was a compound heterozygous for c.5461-10T>C and a novel *ABCA4* mutation c.4773+3 A>G. Sequence analysis of the entire *ABCA4* gene in patients with Stargardt disease revealed complex alleles with additional sequence variants.

Our results provide evidence of genetic complexity causative of different clinical features present in the same family, which is an obvious challenge for ophthalmologists, molecular geneticists and genetic counsellors.

**Keywords** *CRB1* · *ABCA4* · Mutation · SNP-array · Stargardt disease · Leber Congenital Amaurosis

I. Golovleva (✉) · F. Jonsson · A. Norberg
Department of Medical Biosciences/Medical and Clinical Genetics,
University Hospital of Umeå, SE 901 85 Umeå, Sweden
e-mail: Irina.Golovleva@medbio.umu.se

F. Jonsson
e-mail: frida.jonsson@medbio.umu.se

A. Norberg
e-mail: anna.norberg@vll.se

M. S. Burstedt · O. Sandgren
Department of Clinical Sciences/Ophthalmology, University of Umeå,
SE 901 85 Umeå, Sweden
e-mail: marie.burstedt@ophthal.umu.se

O. Sandgren
e-mail: ola.sandgren@ophthal.umu.se

J. D. Ash et al. (eds.), *Retinal Degenerative Diseases,* Advances in Experimental Medicine and Biology 801, DOI 10.1007/978-1-4614-3209-8_23,

**Abbreviations**

| | |
|---|---|
| *ABCA4* | ATP-binding cassette, sub-family A (ABC1), member 4 |
| APEX | Arrayed primer extension |
| *CRB1* | Crumbs homolog 1 (Drosophila) |
| ERG | Electroretinography |
| LCA | Leber congenital amaurosis |
| ROH | Region of homozygosity |
| RP | Retinitis pigmentosa |
| RPE | Retinal pigment epithelium |
| STGD1 | Stargardt disease |

## 23.1 Introduction

Leber congenital amaurosis (LCA) is a severe retinal dystrophy with onset in early childhood. LCA is characterised by poor visual function, photophobia, high hyperopia, nystagmus and severe retinal dysfunction [1]. The electroretinogram (ERG) is usually undetectable or severely reduced. LCA has typically autosomal recessive inheritance mode and diagnosis is established by clinical findings. Fifteen genes associated with LCA are available for genetic testing. One of the most studied LCA genes is *CRB1* at 1q31-q32.1, encoding a protein *Crumbs homolog* that participates in determination and maintenance of photoreceptor architecture. Sequence changes in *CRB1* can cause LCA, retinitis pigmentosa (RP) [2] or RP with preserved parararteriolar retinal pigment epithelium (RPE) [3].

Stargardt disease (STGD1) is another autosomal recessive trait representing a severe form of retinal degeneration that affects the macula and begins in childhood. The gene responsible for STGD1 is *ABCA4* at 1p22, which encodes a protein involved in energy transport to and from photoreceptor cells in the retina. Clinical diagnosis of the disease is difficult during the first few years of onset when discrete yellow spots or atrophy are occasionally seen in the macula. So far, more than 600 *ABCA4* mutations have been annotated [4]. Mutations in *ABCA4* cause not only STGD1 but also cone-rod dystrophy and RP [5, 6].

Molecular genetic testing is desirable for facilitating the diagnosis of LCA, early-onset RP and STGD1. This study was conducted to investigate the genetic defects in a Swedish family that manifests two distinct retinal degenerations: STGD1 and LCA.

## 23.2 Materials and Methods

### *23.2.1 Patients and Clinical Examination*

DNA was available from six affected and ten unaffected individuals from a family originating from Jämtland County in northern Sweden (Fig. 23.1). The research

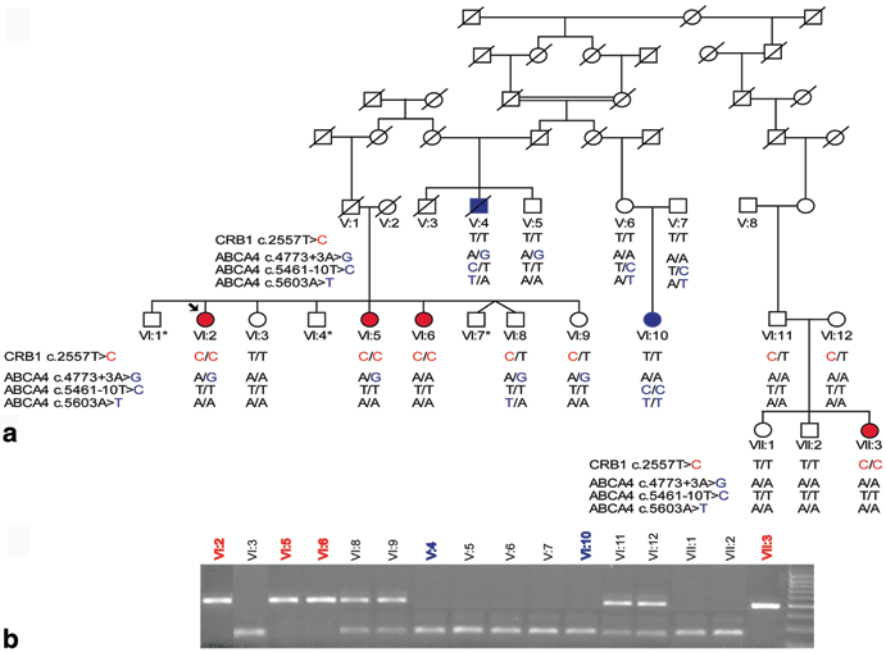


**Fig. 23.1** Pedigree of the Swedish family segregating *CRB1* and *ABCA4* mutations. **a** DNA from index patient VI:2 (marked by an *arrow*) and V:4 were used for targeted mutation screening. Affected individuals are shown in shaded *black* and healthy subjects are shown as open *circles* for women and *square*s for men. *CRB1* and *ABCA4* genotypes and corresponding LCA and STGD1 phenotypes are drawn in *red* and *blue,* respectively. * DNA was not available. **b** Segregation analysis of *CRB1* c.2557T>C mutation was carried out by PCR-RFLP analysis of the *CRB1* exon 7. 472 bp PCR fragments were digested with *Dde*I endonuclease and results were visualised on 2% agarose gel. c.2557T>C mutation abolishes *Dde*I restriction site. LCA cases are indicated in *red* and STGD1 in *blue*

followed the tenets of the Helsinki Declaration and was approved by the Ethics Committee of University of Umeå.

Clinical ophthalmological and electrophysiological examinations were performed and medical chats of affected individuals were requested from their home clinics.

## *23.2.2 Molecular Genetic Analysis*

Testing for LCA, autosomal recessive RP and STGD1 mutations was performed by arrayed primer extension (APEX) at AsperBiotech (Tartu, Estonia). High resolution genome-wide SNP-array genotyping was applied for identification of homozygosity regions containing potential disease causing genes (Illumina, CA, USA). Coding exons and adjacent intronic sequences of *CRX1, CRB1,* and *ABCA4* were analysed by sequencing. To predict the impact of sequence variants on the CRB1 and ABCA4 function, bioinformatics tools included in the Alamut software version 2.0 (Interactive Biosoftware, Rouen, France) were applied.

## 23.3 Results

### *23.3.1 Clinical Findings*

In a large Swedish family two different phenotypes were recognised; four of the cases (Fig. 23.1a, VI:2, VI:5, VI:6, VII:3) presented an early-onset RP, LCA, and two of the cases (Fig. 23.1a, V:4, VI:10) presented an early-onset maculopathy, STGD1.

The LCA cases showed severely reduced visual acuity or blindness in childhood, nystagmus, convergent strabismus and severe hyperopia. In early childhood, the macular area showed central diffuse atrophy and the peripheral retina had an overall granulated appearance. In the central retina, areolar atrophy surrounded by prominent pigmentation of the macular area was found with generally dispersed pigmentary changes of more peripheral retina. The full-field ERG responses described at the age of 3 were extinguished in early childhood.

Visual acuity in the STGD1 cases was affected at age of 8–14 years. Macular atrophy was present with some hyperpigmentation and yellowish flecks of the posterior pole. The peripheral retina was preserved in young adulthood, although peripheral retinal function and visual fields diminished in adulthood. In the full-field ERGs the rod, mixed rod-cone and cone amplitudes were within normal range but the 30 Hz flicker amplitude was decreased to 40 % of normal level with prolonged implicit time.

### *23.3.2 Molecular Genetic Findings*

#### Genetic Testing for Known Mutations

First, 641 mutations in 13 LCA genes and 594 mutations in 19 RP genes were genotyped by APEX in LCA patient VI:2 and STGD1 patient V:4. No mutations were identified in the LCA patient. In the STGD1 patient, heterozygous variant c.5461-10T>C in the *ABCA4* gene was detected.

#### Homozygosity Regions Detection

Based on recessive inheritance pattern and presence of consanguinity loops in the family (Fig. 23.1a), high resolution SNP-array genotyping was undertaken aiming to reveal regions of homozygosity (ROH). In the STGD1 patient only one ROH was identified which did not contain any known retinal genes and did not overlap with any of eight ROH detected in the LCA case. In ROH of the LCA patient, two retinal genes were present, the *Crumbs homolog* gene (*CRB1*) on chromosome 1 and the cone-rod homeobox gene (*CRX1*) on chromosome 19.

**Table 23.1** *ABCA4* sequence variants in STGD1 patient

| Position | Nucleotide change | Aminoacid change | RefSNP | Splice site effect | MAF (minor allele frequency, %) |
|---|---|---|---|---|---|
| Exon 10 | c.1268A>G | p.H423R | rs3112831 | – | C=26.0649[a] |
| Exon 28 | c.4203C>A | p.P1401P | rs1801666 | – | A=2.5604[a] |
| Exon 40 | c.5603A>T | p.N1868I | rs1801466 | – | A=4.7747[a]<br>A=13.9[b] |
| Exon 40 | c.5682G>C | p.L1894L | rs1801574 | – | G=24.927[a] |
| Intron 3 | c.302+26A>G | – | rs2297634 | None | T=47.3089[a] |
| Intron 7 | c.769-32T>C | – | rs526016 | None | G=24.4881[a] |
| Intron 9 | c.1240-14C>T | – | rs4147830 | None | G=46.5477[a] |
| Intron 13 | c.1761-54G>A | – | rs4147833 | Cryptic site? | T=0.377/824[c] |
| Intron 26 | c.3863-73_3863-64delA | – | rs4147892 | None | N/A[a] |
| Intron 33 | c. 4773+3A>G | | New variant | Weak | N/A[a]<br>G=0.009/113[b] |
| Intron 38 | c.5461-10T>C | | rs1800728 | Weak | C=0.0231[a]<br>C=0.000/116[b] |
| Intron 38 | c.5461-51delA | | rs4147899 | None | –=24.9002[a] |

[a] http://evs.gs.washington.edu/EVS/
[b] this study
[c] http://www.ncbi.nlm.nih.gov/SNP

## Sequence Analysis of CRX1 and CRB1 in LCA

Sequencing of *CRX1* in the LCA patient did not reveal any mutations. A novel homozygous mutation c.2557C>T in exon 7, resulting in a premature stop codon, p.Q853X was identified in *CRB1*. Segregation analysis in the family (Fig. 23.1b) demonstrated that four LCA patients (VI:2, VI:5, VI:6, VII:3) were homozygous, while healthy parents of individual VII:3 were heterozygous for c.2557C>T mutation. The mutation was absent in 356 controls from a matched population.

## Sequence Analysis of ABCA4 in STGD1

Heterozygous c.5461-10T>C in *ABCA4* intron 38 was detected in STGD1 patient V:4 and in healthy parents to another STGD1 patient (VI:10) who appeared to be homozygous (Fig. 23.1a). Testing of 116 clinically matched controls revealed no other carriers. To determine if V:4 was a compound heterozygote, all exons and flanking intronic sequences of the *ABCA4* were sequenced. Of the identified variants (Table 23.1), the most interesting were the novel sequence variant c.4773+3A>G and the exonic variants, p.N1868I and p.H423R. Bioinformatics analysis predicted p.N1868I to be possibly damaging for protein function, whereas p.H423R was predicted to be benign. However, p.N1868I did not segregate with the disease in the

family (Fig 23.1a) and was a common variant in northern Sweden with an estimated allele frequency of 0.139 (16/115).

The novel variant c.4773+3A>G was found in heterozygous form in the two LCA patients, three unaffected individuals and STGD1 patient V:4 (Fig. 23.1a). Allele frequency estimated in matched healthy controls was low, 0.009 (1/113). As follows from haplotype analysis, STGD1 patient V:4 is presumably compound heterozygous for the two rare splice variants c.5461-10T>C and c.4773+3A>G.

## 23.4 Discussion

In this study, we approached patients with different clinical presentation belonging to the same multi-generation family of Swedish origin. Clinical diagnosis of LCA was recognised in four of six patients. Molecular testing of LCA patients is quite laborious due to genetic heterogeneity. Testing for known mutations by array technology provides fast and reliable results; however, it does not detect novel mutations. In our study, array revealed no mutations in the LCA patient, and only one heterozygous mutation in the *ABCA4* gene in the STGD1 patient.

Several regions of homozygosity were detected by genome-wide genotyping in the LCA case, of which the most promising candidate gene was *CRB1* on chromosome 1. Subsequent sequencing of *CRB1* resulted in detection of a novel null mutation p.Q853X.

The c.5461-10T>C in *ABCA4* was first reported by Maugeri et al. [7], although its function is still not resolved. The c.5461-10T>C variant was found to be the most prevalent allele among patients with autosomal recessive cone and cone-rod dystrophy (8 of 64 patients) [8]. It is to be noticed that another STGD1 patient was homozygous for the c.5461-10T>C mutation. Notably, none of our healthy controls carried the c.5461-10T>C mutation. The heterozygous STGD1 patient was also a carrier of sequence variant c.4773+3A>G, predicted to reduce the strength of the donor splice site. This variant was not detected in 3,510 controls of European American descent [9], and in our study only one carrier of 113 tested was found.

Interestingly, our STGD1 patients carried the sequence variant *ABCA4* p.N1868I that was predicted to be possibly damaging, as well as acting as a risk-increasing factor in age-related macular degeneration [9]. In our study, this variant was detected in almost 14 % of the healthy controls, which is much higher compared to the frequency of 7.5 % in a Finnish population [9].

In conclusion, in a large Swedish family we have identified the underlying genetic mechanisms consisting of a novel null mutation in the *CRB1* gene, p.Q853X as a cause of LCA. In the same family, STGD1 appears to be caused by compound heterozygosity of the two *ABCA4* mutations c.4773+3A>G and c.5461-10T>C, or by homozygosity of the mutation c.5461-10T>C. Presence of different genetic mechanisms resulting in variable phenotype within the family is not rare and can challenge molecular geneticists, ophthalmologists and genetic counsellors.

**Acknowledgments** This study was supported by grants from Visare Norr, KMA and University Hospital of Umeå.

## References

1. Chung DC, Traboulsi EI (2009) Leber congenital amaurosis: clinical correlations with genotypes, gene therapy trials update, and future directions. J AAPOS 13(6):587–592
2. den Hollander AI, Heckenlively JR, van den Born LI, de Kok YJ, van der Velde-Visser SD, Kellner U, Jurklies B, van Schooneveld MJ, Blankenagel A, Rohrschneider K, Wissinger B, Cruysberg JR, Deutman AF, Brunner HG, Apfelstedt-Sylla E, Hoyng CB, Cremers FP (2001) Leber congenital amaurosis and retinitis pigmentosa with Coats-like exudative vasculopathy are associated with mutations in the crumbs homologue 1 (*CRB1*) gene. Am J Hum Genet 69(1):198–203
3. den Hollander AI, ten Brink JB, de Kok YJ, van Soest S, van den Born LI, van Driel MA, van de Pol DJ, Payne AM, Bhattacharya SS, Kellner U, Hoyng CB, Westerveld A, Brunner HG, Bleeker-Wagemakers EM, Deutman AF, Heckenlively JR, Cremers FP, Bergen AA (1999) Mutations in a human homologue of Drosophila crumbs cause retinitis pigmentosa (RP12). Nat Genet 23(2):217–221
4. Zernant J, Schubert C, Im KM, Burke T, Brown CM, Fishman GA, Tsang SH, Gouras P, Dean M, Allikmets R (2011) Analysis of the *ABCA4* gene by next-generation sequencing. Invest Ophthalmol Vis Sci 52(11):8479–8487
5. Cremers FP, van de Pol DJ, van Driel M, den Hollander AI, van Haren FJ, Knoers NV, Tijmes N, Bergen AA, Rohrschneider K, Blankenagel A, Pinckers AJ, Deutman AF, Hoyng CB (1998) Autosomal recessive retinitis pigmentosa and cone-rod dystrophy caused by splice site mutations in the Stargardt's disease gene *ABCR*. Hum Mol Genet 7(3):355–362
6. Maugeri A, Klevering BJ, Rohrschneider K, Blankenagel A, Brunner HG, Deutman AF, Hoyng CB, Cremers FP (2000) Mutations in the *ABCA4* (ABCR) gene are the major cause of autosomal recessive cone-rod dystrophy. Am J Hum Genet 67(4):960–966
7. Maugeri A, van Driel MA, van de Pol DJ, Klevering BJ, van Haren FJ, Tijmes N, Bergen AA, Rohrschneider K, Blankenagel A, Pinckers AJ, Dahl N, Brunner HG, Deutman AF, Hoyng CB, Cremers FP (1999) The 2588G->C mutation in the ABCR gene is a mild frequent founder mutation in the Western European population and allows the classification of ABCR mutations in patients with Stargardt disease. Am J Hum Genet 64(4):1024–1035
8. Kitiratschky VB, Grau T, Bernd A, Zrenner E, Jagle H, Renner AB, Kellner U, Rudolph G, Jacobson SG, Cideciyan AV, Schaich S, Kohl S, Wissinger B (2008) *ABCA4* gene analysis in patients with autosomal recessive cone and cone rod dystrophies. Eur J Hum Genet 16(7):812–819
9. Fritsche LG, Fleckenstein M, Fiebig BS, Schmitz-Valckenberg S, Bindewald-Wittich A, Keilhauer CN, Renner AB, Mackensen F, Mossner A, Pauleikhoff D, Adrion C, Mansmann U, Scholl HP, Holz FG, Weber BH (2012) A subgroup of age-related macular degeneration is associated with mono-allelic sequence variants in the *ABCA4* gene. Invest Ophthalmol Vis Sci 53(4):2112–2118

# Chapter 24
# FAM161A, a Novel Centrosomal-Ciliary Protein Implicated in Autosomal Recessive Retinitis Pigmentosa

**Frank Zach and Heidi Stöhr**

**Abstract** Retinitis pigmentosa (RP) is an inherited disease of the retina leading to vision impairment due to progressive photoreceptor cell death. Homozygous and compound heterozygous null mutations in the CRX-regulated *FAM161A* gene of unknown function were identified as a cause for autosomal recessive RP (RP28) in patients from India, Germany, Israel, the Palestinian territories, and the USA. The FAM161A protein has been found to be localized to the connecting cilium, the basal body, and the adjacent centriole in mammalian photoreceptors and was also present in synaptic layers and ganglion cells of the retina. In addition, FAM161A was shown to be part of microtubule-organizing centers in cultured cells and associates with the intracellular microtubule network. Moreover, FAM161A directly binds to microtubules and increases the acetylation of α-tubulin. An evolutionary highly conserved, C-terminal protein domain (UPF0564) of FAM161A was shown to mediate microtubule association, homo- and heterotypic interaction among UPF0564-containing proteins and binding to several ciliopathy-associated proteins. In summary, FAM161A is a novel centrosomal-ciliary protein that likely is implicated in the regulation of microtubule-based cellular processes in the retina.

**Keywords** Retinitis pigmentosa · FAM161A · Microtubules · Connecting cilium · Basal body

H. Stöhr (✉) · F. Zach
Institute of Human Genetics, University Regensburg, Franz-Josef-Strauss-Allee 11, 93053, Regensburg, Germany
e-mail: heidi.stoehr@klinik.uni-regensburg.de

F. Zach
e-mail: frank.zach@klinik.uni-regensburg.de

J. D. Ash et al. (eds.), *Retinal Degenerative Diseases,* Advances in Experimental Medicine and Biology 801, DOI 10.1007/978-1-4614-3209-8_24,

**Abbreviations**

| | |
|---|---|
| CEP290 | Centrosomal protein 290 |
| CRX | Cone-rod homeobox |
| MDH1 | Malate dehydrogenase 1 |
| OFD1 | Orofacialdigital 1 |
| RP | Retinitis pigmentosa |
| RP1 | Retinitis pigmentosa 1 |
| SDCCAG8 | Serologically defined colon cancer antigen 8 |
| siRNA | Small interfering RNA |
| TACC3 | Transforming acidic coiled-coil 3 |
| UPF0564 | Uncharacterized protein family 0564 |

## 24.1 Identification of Mutations in the *FAM161A* Gene as a Cause of Retinitis Pigmentosa

Retinitis pigmentosa (RP) is the most common form of inherited retinal degeneration with approximately 1.5 million affected individuals worldwide [1]. RP is genetically heterogeneous and can be inherited in an autosomal recessive, autosomal dominant, or X-linked pattern. So far, 50 different loci have been associated with nonsyndromic RP [https://sph.uth.edu/retnet/home.htm]. This includes RP28, an autosomal recessive form of RP, originally mapped to chromosome 2p11-p15 in a consanguineous Indian family in 1999 [2]. After attempts to refine the RP28 candidate region [3] and the exclusion of the putative candidate gene *MDH1* (encoding a cytosolic malate dehydrogenase) by mutational analysis [4], a homozygous c.685C>T (p.Arg229X) nonsense mutation in exon 3 of the human *FAM161A* gene has eventually been identified as the cause for *RP28* by a combined approach of chromatin immunoprecipitation and parallel sequencing of genomic DNA (Fig. 24.1) [5]. At about the same time, homozygosity mapping in several RP families from Israel and the Palestinian territories and subsequent sequencing of candidate genes in the shared homozygous regions on the short arm of chromosome 2 revealed additional null mutations c.1355_6delCA (p.Thr452SerfsX3), c.1567C>T (p.Arg523X) and c.1786C>T (pArg596X) in the *FAM161A* gene of RP patients (Fig. 24.1) [6]. Further screening of the *FAM161A* gene in a German RP patient cohort identified homozygous nonsense mutation c.1309A>T (pArg437X) in three individuals (Fig. 24.1) [5]. Taken together, these data implicate that a loss of FAM161A function leads to RP in humans. Whereas *FAM161A* mutations are considered to be a major cause (~12 %) of autosomal recessive RP in Israel and the Palestinian territories, they appear to be less frequent in other parts of the world, e.g., Germany and the USA (~1, 5–3 %) [5, 7].

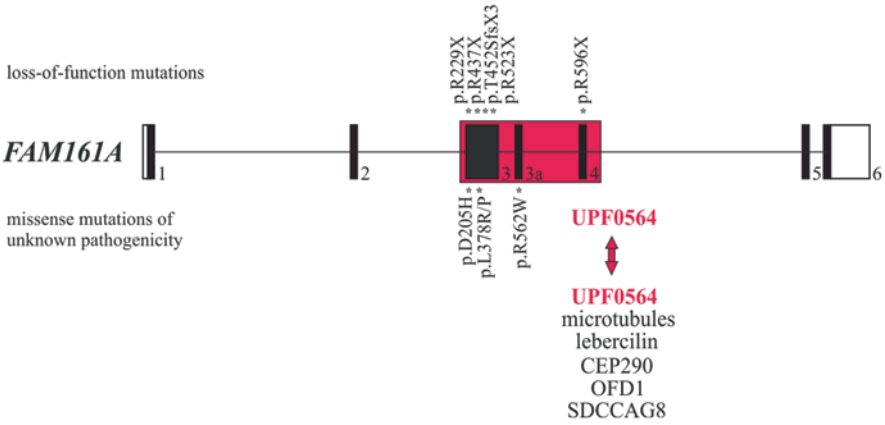


**Fig. 24.1** Structure and characteristics of the *FAM161A* gene/protein. The exon-intron structure of the human *FAM161A* gene is indicated by boxes and lines, respectively. Untranslated regions are shown as *open boxes,* coding regions as *black boxes,* known mutations are marked by *asterisks*. The conserved *UPF0564* domain encoded by exon *3–4* is boxed and mediates microtubule binding, homo- and heterotypic multimerization and interactions with other centrosomal/ciliary proteins

*FAM161A*-associated retinal disease displays typical features of autosomal recessive RP but shows a wide phenotypic variability in terms of age of onset and the severity of clinical symptoms.

Besides loss-of-functions mutations, four rare nonsynonymous *FAM161A* sequence variants have been found in RP patients that affect evolutionary conserved amino acids (Fig. 24.1) [5, 7]. The pathogenicity of these missense mutations need to be further clarified.

## 24.2 Structure and Expression of the *FAM161A* Gene

The human *FAM161A* gene consists of seven exons and spans approximately 30 Kb of genomic DNA on chromosome 2p15 (Fig. 24.1). Two protein coding transcript variants are produced by alternative splicing of central exon 3a (exon 4 in [6]) to generate isoforms of 660 amino acids (76 kDa) and 716 amino acids (83 kDa), respectively. Both variants have similar expression profiles with high transcript levels in the retina and testis. The mouse *Fam161a* gene is also highly expressed in the developing and adult retina [5]. In situ hybridization revealed *Fam161a* gene expression in the entire neuroblastic layer during embryogenesis whereas at postnatal stages *Fam161a* transcripts were only found in nuclei of mouse photoreceptors [6]. A region bound by the retina-specific transcription factor CRX within the first intron of *Fam161a* was shown to activate expression of reporter constructs in the outer nuclear layer of mouse retinal explants and could therefore be responsible for postnatal, photoreceptor-specific *Fam161a* gene expression [5].

## 24.3 *In silico* Characterization of the FAM161A Protein

The deduced FAM161A protein sequence is evolutionary conserved among vertebrates. It has one human paralogue, named FAM161B, which is encoded by the *FAM161B* gene on chromosome 14q23.2. FAM161A and FAM161B share an overall protein sequence identity of 25%. Both proteins contain a single highly conserved ~400 amino acid protein domain of unknown function (UPF0564) in their C-terminal portion that can also be found in a variety of eukaryotic species as well as in bacteria (Fig. 24.1). Secondary structure prediction of UPF0564 revealed putative alpha-helical regions separated by highly conserved amino acid residues that typically mediate oligomerization and protein–protein interaction [6, 8].

## 24.4 Subcellular Localization of *FAM161A* in the Retina

Immunohistochemical analysis of FAM161A protein localization in retinal sections from adult mouse, rat and human eyes using antibodies directed against different regions of the FAM161A protein revealed an abundance of the protein in the inner segments of rod and cone photoreceptor cells and smaller amounts in other retinal layers [5, 8, 9]. Proteomic analyses have shown that FAM161A is part of the cytoskeleton fraction of the mouse photoreceptor sensory cilium complex and a component of human centrosomes [10, 11]. Further investigation using variations in immunohistochemistry protocols and co-localization studies with marker proteins of the photoreceptor ciliary regions (e.g., RP1, centrin, acetylated α-tubulin) indicated the presence of FAM161A in the connecting cilium, basal body, and the adjacent centriole of mouse and human photoreceptors [8]. High-resolution immunoelectron microscopy showed that the FAM161A protein associates with the microtubule doublet in the connecting cilium, at the basal body, and the adjacent centriole at the ciliary base of mouse rod photoreceptor as well as at centrosomes in the outer nuclear layer [8]. In the outer plexiform layer, FAM161A appears to be present in postsynaptic terminals of second-order neurons [8].

## 24.5 Subcellular Localization and Microtubule Association of FAM161A in Cell Culture

Recombinant FAM161A was found at the base of primary cilia, the centrosomes, and spindle poles of cultured cells of different origin [8, 9]. In ciliated hTERT-RPE-1 cells, endogenous FAM161A was shown to be present at the level of the basal body [9]. These data confirmed an association of FAM161A with microtubule-organizing centers. Moreover, ectopic FAM161A decorated the intracellular microtubule network, a property that could be mapped to the C-terminal part

including the UPF0564 domain by heterologous expression of deletion mutants [8]. Direct binding of FAM161A-UPF0564 to microtubules was further demonstrated by in vitro microtubule co-sedimentation assays [8]. Overexpressed FAM161A significantly increased the acetylation level of α-tubulin and resistance to nocodazole depolymerization, indicative of a role of FAM161A in the stabilization of existing microtubules [8]. FAM161A knockdown experiments in hTERT-RPE-1 cells via siRNA treatment led to a significant reduction in the number of ciliated cells suggesting a role for FAM161A also in the assembly of the primary cilium [9].

## 24.6 Protein–Protein Interaction Mediated by FAM161A

Binding studies revealed that the conserved UPF0564 domain mediates homotypic FAM161A and heterotypic FAM161A-FAM161B protein–protein interaction [8]. The human *FAM161B* gene is expressed in the retina and several other neuronal tissues [8]. It encodes a physical interaction partner of transforming acidic coiled-coil 3 (TACC3), which plays an important role in centrosome-dependent microtubule assembly, kinetochore attachment, chromosome alignment, and the regulation of mitotic exit in different species [12]. Similar to FAM161A, FAM161B localizes at microtubules when overexpressed in cultured cells [8]. UPF0564 domain-containing proteins may therefore form a novel family of microtubule-associated proteins. A recent study revealed decreased expression of *FAM161B* in adenoma and tumor samples [13], which indicates a role of FAM161B and maybe other UPF0564 domain-containing proteins in carcinogenesis.

Yeast-two-hybrid binding assays using FAM161A and a series of other known ciliary/centrosomal proteins identified an interaction of FAM161A with ciliopathy-associated proteins lebercilin, CEP290, OFD1, and SDCCAG8 that was shown to be mediated by the C-terminal moiety of FAM161A [9]. Thus, FAM161A could be part of one or more protein complexes with each component playing a vital role in ciliary function.

## 24.7 Conclusion and Perspectives

The absence of FAM161A in the retina leads to progressive RP in humans. First insights into the functional role of FAM161A showed that FAM161A is a novel ciliary/centrosomal protein capable of UPF0564 domain-mediated microtubule binding and protein–protein interaction. This appears to be essential for cilium assembly and may be important to establish and maintain microtubule tracks. The elucidation of basic mechanisms underlying FAM161A-triggered microtubule stabilization and the dynamics of FAM161A self-association versus interaction with microtubules and other proteins will be most interesting and important to study in further detail.

In addition, the generation of animal models will help to unravel the pathomechanism leading to FAM161A-associated retinal degeneration.

## References


1. Ayuso C, Millan JM (2010) Retinitis pigmentosa and allied condiditions today: a paradigm of translational research. Genome Med 2(5):34
2. Gu S, Kumaramanickavel G, Srikumari CR, Denton MJ, Gal A (1999) Autosomal recessive retinitis pigmentosa locus RP28 maps between D2S1337 and D2S286 on chromosome 2p11-p15 in an Indian family. J Med Genet 36(9):705–707
3. Kumar A, Shetty J, Kumar B, Blanton SH (2004) Confirmation of linkage and refinement of the RP28 locus for autosomal recessive retinitis pigmentosa on chromosome 2p14-p15 in an Indian family. Mol Vis 10:399–402
4. Rio Frio T, Panek S, Iseli C, Di Gioia SA, Kumar A, Gal A et al (2009) Ultra high throughput sequencing excludes MDH1 as candidate gene for RP28-linked retinitis pigmentosa. Mol Vis 15:2627–2633
5. Langmann T, Di Gioia SA, Rau I, Stöhr H, Maksimovic NS, Corbo JC et al (2010) Nonsense mutations in FAM161A cause RP28-associated recessive retinitis pigmentosa. Am J Hum Genet 87(3):376–381
6. Bandah-Rozenfeld D, Mizrahi-Meissonnier L, Farhy C, Obolensky A, Chowers I, Pe'er J et al (2010) Homozygosity mapping reveals null mutations in FAM161A as a cause of autosomal recessive retinitis pigmentosa. Am J Hum Genet 87(3):382–391
7. Ransijn A, Venturini G, Di Gioia S, Harper S, Weigel-DiFranco C, Rivolta C, Berson EL. FAM161A mutations in patients with early-onset retinitis pigmentosa in the United States. ARVO 2012 Annual Meeting Abstracts; program number 4545.
8. Zach F, Grassmann F, Langmann T, Sorusch N, Wolfrum U, Stöhr H (2012) The retinitis pigmentosa 28 protein FAM161A is a novel ciliary protein involved in intermolecular protein interaction and microtubule association. Hum Mol Genet 21(21):4573–4586
9. Di Gioia SA, Letteboer SJ, Kostic C, Bandah-Rozenfeld D, Hetterschiji L, Sharon D et al (2012) FAM161A, associated with retinitis pigmentosa, is a component of the cilia-basal body complex and interacts with proteins involved in ciliopathies. Hum Mol Genet 21(23):5174–5184
10. Liu Q, Tan G, Levenkova N, Li T, Pugh EN Jr, Rux JJ et al (2007) The proteome of the mouse photoreceptor sensory cilium complex. Mol Cell Proteomics 6(8):1299–1317
11. Jakobsen L, Vanselow K, Skogs M, Toyoda Y, Lundberg E, Poser I et al (2011) Novel asymmetrically localizing components of human centrosomes identified by complementary proteomics methods. EMBO J 30(8):1520–1535
12. Gómez-Baldó L, Schmidt S, Maxwell CA, Bonifaci N, Gabaldón T, Vidalain PO et al (2010) TACC3-TSC2 maintains nuclear envelope structure and controls cell division. Cell Cycle 9(6):1143–1155
13. Spisák S, Kalmár A, Galamb O, Wichmann B, Sipos F, Péterfia B et al (2012) Genome-wide screening of genes regulated by DNA methylation in colon cancer development. PloS One 7(10):e46215

# Part V
# AMD: Novel Developments

# Chapter 25
# Molecular Pathology of Macrophages and Interleukin-17 in Age-Related Macular Degeneration

**Chi-Chao Chan and Daniel Ardeljan**

**Abstract** The pathology of age-related macular degeneration (AMD) is characterized by degeneration of photoreceptors and retinal pigment epithelial cells as well as by changes of choroidal capillaries in the macula. Although AMD is not a typical uveitis, there is a consistence and an imbalance of ocular para-inflammation. Ocular inflammation, particularly in the macula, plays a critical role in AMD pathogenesis. The inflammatory and immune-related elements involved in AMD include inflammatory and related cells as well as the secreted molecules and factors from these cells. Innate immune system elements such as macrophages and cytokines play an important role in AMD pathology and pathogenesis. This chapter reviews the observed deviation in macrophage plasticity and the elevated expression of interleukin-17 in AMD eyes while discussing potential contributions to AMD pathogenesis. Targeting of these specific inflammatory pathways and molecules at appropriate times should be explored and may become promising novel adjunct agents to AMD therapy.

**Keywords** Age-related macular degeneration · Macrophage · IL-17 · Inflammation · Eye

**Abbreviations**

| | |
|---|---|
| AMD | Age-related macular degeneration |
| RPE | Retinal pigment epithelium |
| IL-17 | Interleukin-17 |
| iNO | Inducible nitric oxide |
| IL-17R | Interleukin-17 Receptor |
| RT-PCR | Real time polymerase chain reaction |

C.-C. Chan (✉) · D. Ardeljan
Section of Immunopathology, Laboratory of Immunology, National Eye Institute, National Institutes of Health, 10 Center Drive, 10/10N103, 20892-1857, Bethesda, MD, USA
e-mail: chanc@nei.nih.gov

D. Ardeljan
e-mail: ardeljand@mail.nih.gov

J. D. Ash et al. (eds.), *Retinal Degenerative Diseases,* Advances in Experimental Medicine and Biology 801, DOI 10.1007/978-1-4614-3209-8_25,

## 25.1 Introduction

In 1875, Hutchison and Tay described 10 cases of "symmetrical central chorioretinal disease occurring in senile persons" characterized by whitish spots (drusen) in the macula [1]. This was the first description of what was then called "senile macular degeneration" and what has since been renamed "age-related macular degeneration" (AMD) in the 1980s. The aging eye exists in a para-inflammatory state to keep normal physiological functions of photoreceptors and retinal pigment epithelium (RPE) cells and thus maintain retinal homeostasis [2]. Loss of retinal homeostasis is permissive for development of AMD in the macula resulting from photoreceptor and RPE pathology as well as subtle or mild chronic inflammation.

The etiology of AMD involves multiple factors such as aging, genetic predisposition, environmental elements including smoke and diet, oxidative stress, and inflammation [3]. Unlike uveitis, inflammation in the AMD eye is subtle or mild, never severe or overwhelming. This chapter describes recent pathological findings of macrophage and interleukin (IL)-17 involvements in AMD.

## 25.2 Macrophage

Macrophages, a predominant cell type associated with chronic inflammation, are the most prominent inflammatory cells observed in AMD tissue, outnumbering subretinal microglia (resident myeloid cells/macrophages) as well as lymphocytes in AMD eyes [3–5]. The findings have been well documented in and/or near the lesions of drusen, neovascular, and geographic atrophy AMD [6–8]. Macrophages secrete a wide range of cytokines, chemokines, complement factors, and growth factors, including vascular endothelial growth factor in response to pathogens and damaged tissues; most of them are implicated in AMD. Using immunohistochemistry, choroidal macrophages expressing inducible nitric oxide (iNO) were only found in the Bruch's membrane of early AMD eyes with soft drusen or thick basal laminar deposits, in active disciform scars, and in eyes with subclinical choroidal neovascularization. Choroidal macrophages in the normal macula do not express iNO [9].

Each macrophage can secrete more than 100 different molecules for biologic activities including inflammation, immunity, phagocytosis, cell growth, and cell death [10]. The secretion of these products depends on the inciting stimulus, macrophage subtype, and location. Diversity and plasticity have long been recognized for cells of monocyte-macrophage lineage. In response to signals derived from microbes, damaged tissues, or activated lymphocytes, macrophages polarize into distinct functional phenotypes. Two main macrophage phenotypes are classified based on functional properties, surface markers, and cytokine profiles: the classically activated M1 macrophage and the alternatively activated M2 macrophage [11, 12]. In general, M1 macrophages are pro-inflammatory, microbicidal, and anti-tumoral; M2 macrophages are anti-inflammatory, tissue remodeling, pro-tumoral, immunoregulatory, and proliferative. Recently, some suggested that the M2 macrophages should

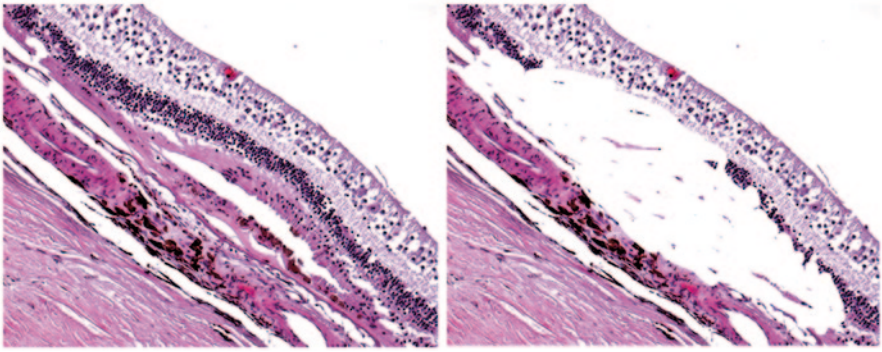

**Fig. 25.1** Macular lesion in an AMD eye before and after microdissection. The outer neuroretinal cells, hypertrophic RPE, and irregular Bruch's membrane were microdissected and subjected for quantitative real-time polymerase chain reaction (RT-PCR). (*left,* before microdissection, *right,* after microdissection; hematoxylin and eosin, x100)

be further divided into at least two groups: pro-angiogenic and anti-angiogenic [13]. However, there are still uncertainties regarding distinct expression patterns of surface markers that clearly define macrophage subtypes, particularly in the case of human macrophages. Furthermore, macrophages often retain their plasticity, so the phenotypes of a macrophage population can change over time [14]. M1 and M2 macrophages may undergo phenotype switching towards M2 prominence during the normal aging process [15, 16].

Distinct chemokine patterns are also associated with M1 and M2 macrophage activation and production. CXCL9, CXCL10, and CXCL11 represent M1 chemokines, and CCL17 and CCL22 represent M2 chemokines [17]. Using molecular pathology including microdissection (Fig. 25.1) and immunochemistry, a pathological imbalance of macrophage polarization was reported in AMD lesions; a relatively higher M1 infiltration in geographic atrophy AMD and an aberrantly higher M2 in neovascular AMD were reported [15]. The findings suggest that macrophage polarization and plasticity could contribute to AMD development and progression.

## 25.3 IL-17A

The IL-17 cytokine family includes six members named A–F. IL-17A is the main cytokine in the IL-17 family produced mostly by Th17 cells [18, 19]. However, other inflammatory cells such as neutrophils and even macrophages under specific conditions may produce IL-17A [20, 21]. IL-17A homodimers bind IL-17 receptor (R)C/IL-17RA heterodimers. The most notable role of IL-17 is its involvement in inducing and mediating pro-inflammatory responses. It controls extracellular pathogens and induces matrix destruction and neovascularization. Th17-type cytokines have been linked to neurodegenerative diseases such as multiple sclerosis and Alzheimer's disease [22, 23].

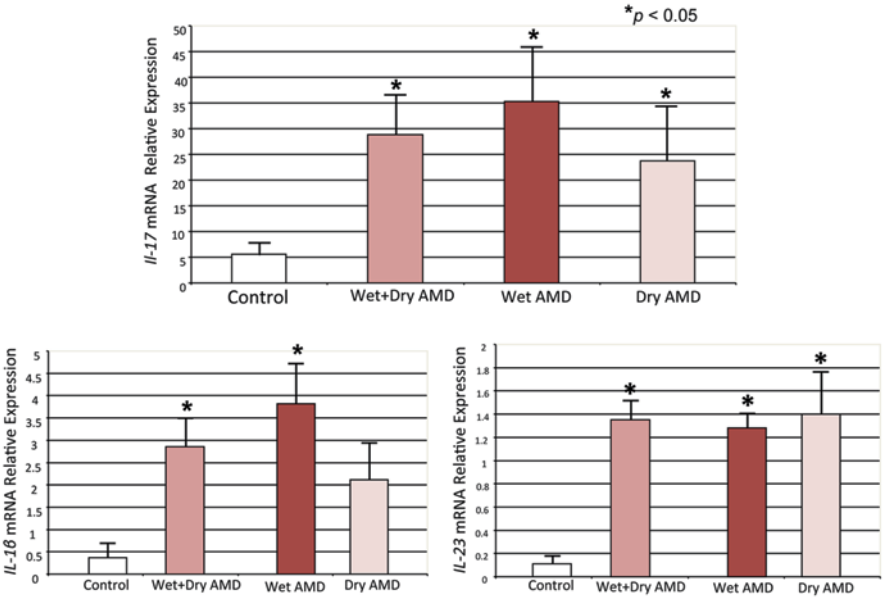


**Fig. 25.2** Transcript expression of *IL-1β, IL-23,* and *IL-17* in macular cells of four normal and nine age-related macular degeneration (*AMD,* five geographic atrophy "dry" and four neovascular "wet" AMD) eyes. Significant elevations of these three cytokines are detected in maculae with AMD lesions compared to the normal controls

In a recent report, serum levels of IL-17 were significantly higher in 23 AMD patients compared to 30 age-matched non-AMD individuals; serum levels of IL-22, a Th17 family cytokine, were also significantly higher in 25 AMD patients as compared to 29 control individuals [24]. This study also showed that the C5a anaphylatoxin can promote Th17 cytokine expression from human $CD4^+$ T cells. More recently, hypomethylation of the IL-17RC promoter was associated with AMD [25]. The epigenetic alteration leads to elevation of IL-17RC transcript and protein in peripheral blood as well as in macular cells of AMD patients. Since the IL-17RC subunit plays a key role in modulating the IL-17 response [26], the association of IL-17RC with AMD suggests that IL-17 could be an important player in AMD pathogenesis.

Our preliminary experiments have shown that IL-17A reduces cellular viability, alters cell metabolism, and induces apoptosis in ARPE-19 cells [27]. This in vitro study supports the harmful role of IL-17 on RPE cells, a critical cell in AMD. In addition, we detected significantly high expression of not only *IL-17* but also *IL-1β* and *IL-23* mRNA in AMD lesions (Fig. 25.2) [28]; these two cytokines promote Th17 cell differentiation and are secreted mainly by macrophages [18, 19]. Our data offer convincing support for an increase of IL-17 in AMD eyes and the role of IL-17 in neurodegenerative disease. Two recent independent studies have linked the inflammasome to AMD pathogenesis [29, 30]. Inflammasome is expressed in

macrophages and activates the release of IL-1β and IL-18, which can subsequently drive an IL-17 response [31].

## 25.4 Conclusion

Immunopathology and molecular pathology of AMD lesions clearly prove that there is an important role for inflammation and innate immune cells such as macrophages in AMD. IL-17A and IL-17RC in AMD eyes and patients demonstrate IL-17 involvement in AMD pathogenesis. Targeting IL-17, IL-17RC, and cells producing IL-17 to deter retinal degeneration might be a potential treatment strategy for AMD. However, we should consider genetic background and clinical manifestation of each patient, duration of the therapy, and adverse effects of individual therapeutic agents.

## References

1. Hutchison J, Tay W (1875) Symmetrical central chorioretinal disease occurring in senile persons. R London Ophthal Hosp Rep 8:231–244
2. Xu H, Chen M, Forrester JV (2009) Para-inflammation in the aging retina. Prog Retin Eye Res 28(5):348–368
3. Coleman HR, Chan CC, Ferris FL III, Chew EY (2008) Age-related macular degeneration. The Lancet 372(9652):1835–1845
4. Penfold PL, Killingsworth MC, Sarks SH (1985) Senile macular degeneration: the involvement of immunocompetent cells. Graefes Arch Clin Exp Ophthalmol 223(2):69–76
5. Dastgheib K, Bressler SB, Green WR (1993) Clinicopathologic correlation of laser lesion expansion after treatment of choroidal neovascularization. Retina 13(4):345–352
6. Grossniklaus HE, Miskala PH, Green WR, Bressler SB, Hawkins BS, Toth C et al (2005) Histopathologic and ultrastructural features of surgically excised subfoveal choroidal neovascular lesions: submacular surgery trials report no. 7. Arch Ophthalmol 123(7):914–921
7. Ding X, Patel M, Chan CC (2009) Molecular pathology of age-related macular degeneration. Prog Retin Eye Res 28(1):1–18
8. Killingsworth MC, Sarks JP, Sarks SH (1990) Macrophages related to Bruch's membrane in age-related macular degeneration. Eye (Lond) 4(Pt 4):613–621
9. Cherepanoff S, McMenamin P, Gillies MC, Kettle E, Sarks SH (2010) Bruch's membrane and choroidal macrophages in early and advanced age-related macular degeneration. Br J Ophthalmol 94(7):918–925
10. Nathan CF (1987) Secretory products of macrophages. J Clin Invest 79(2):319–326
11. Mantovani A, Biswas SK, Galdiero MR, Sica A, Locati M (2013) Macrophage plasticity and polarization in tissue repair and remodelling. J Pathol 229(2):176–185
12. Biswas SK, Chittezhath M, Shalova IN, Lim JY (2012) Macrophage polarization and plasticity in health and disease. Immunol Res 53(1–3):11–24
13. Dick AD (2012) Road to fulfilment: taming the immune response to restore vision. Ophthalmic Res 48(1):43–49
14. Mosser DM, Edwards JP (2008) Exploring the full spectrum of macrophage activation. Nat Rev Immunol 8(12):958–969
15. Cao X, Shen D, Patel MM, Tuo J, Johnson TM, Olsen TW et al (2011) Macrophage polarization in the maculae of age-related macular degeneration: a pilot study. Pathol Int 61(9):528–535

16. Mahbub S, Deburghgraeve CR, Kovacs EJ (2012) Advanced age impairs macrophage polarization. J Interferon Cytokine Res 32(1):18–26
17. Mantovani A, Sica A, Sozzani S, Allavena P, Vecchi A, Locati M (2004) The chemokine system in diverse forms of macrophage activation and polarization. Trends Immunol 25(12):677–686
18. Miossec P, Korn T, Kuchroo VK (2009) Interleukin-17 and type 17 helper T cells. N Engl J Med 361(9):888–898
19. Gaffen SL (2011) Recent advances in the IL-17 cytokine family. Curr Opin Immunol 23(5):613–619
20. Song C, Luo L, Lei Z, Li B, Liang Z, Liu G et al (2008) IL-17-producing alveolar macrophages mediate allergic lung inflammation related to asthma. J Immunol 181(9):6117–6124
21. Vazquez N, Rekka S, Gliozzi M, Feng CG, Amarnath S, Orenstein JM et al (2012) Modulation of innate host factors by Mycobacterium avium complex in human macrophages includes interleukin 17. J Infect Dis 206(8):1206–1217
22. Gold R, Luhder F (2008) Interleukin-17-extended features of a key player in multiple sclerosis. Am J Pathol 172(1):8–10
23. Hu WT, Chen-Plotkin A, Grossman M, Arnold SE, Clark CM, Shaw LM et al (2010) Novel CSF biomarkers for frontotemporal lobar degenerations. Neurology 75(23):2079–2086
24. Liu B, Wei L, Meyerle C, Tuo J, Sen HN, Li Z et al (2011) Complement Component C5a Promotes Expression of IL-22 and IL-17 from Human T cells and its Implication in Age-related Macular Degeneration. J Transl Med 9(1):111
25. Wei L, Liu B, Tuo J, Shen D, Chen P, Li Z et al (2012) Hypomethylation of the IL17RC Promoter Associates with Age-Related Macular Degeneration. Cell Rep 2(5):1151–1158
26. Ho AW, Gaffen SL (2010) IL-17RC: a partner in IL-17 signaling and beyond. Semin Immunopathol 32(1):33–42
27. Ardeljan D, Wang Y, Shen D, Tuo J, Chan CC (2012) Treatment with recombinant interleukin-17A reduces ARPE-19 cell viability. ARVO Abstr. #1227, 06 May 2012
28. Chan CC, Shen D, Cao X, Wang VM, Wang Y, Tuo J (2011) Expression of IL-17 in Eyes of Age-related Macular Degeneration. ARVO Abstr. #1228, 2011
29. Tarallo V, Hirano Y, Gelfand BD, Dridi S, Kerur N, Kim Y et al (2012) DICER1 loss and Alu RNA induce age-related macular degeneration via the NLRP3 inflammasome and MyD88. Cell 149(4):847–859
30. Doyle SL, Campbell M, Ozaki E, Salomon RG, Mori A, Kenna PF et al (2012) NLRP3 has a protective role in age-related macular degeneration through the induction of IL-18 by drusen components. Nat Med 18(5):791–798
31. Mills KH, Dungan LS, Jones SA, Harris J (2012) The role of inflammasome-derived IL-1 in driving IL-17 responses. J Leukoc Biol 93(4):489–497

# Chapter 26
# The Role of Monocytes and Macrophages in Age-Related Macular Degeneration

**Michelle Grunin, Shira Hagbi-Levi and Itay Chowers**

**Abstract** White blood cells, particularly monocytes and their descendants, macrophages, have been implicated in age-related macular degeneration (AMD) pathology. In this minireview, we describe the current knowledge of monocyte and macrophage involvement in AMD. Chemokine receptors present on these cells such as CCR1, CCR2, and CX3CR1, and their roles in monocyte/macrophage recruitment to sites of injury and inflammation in the context of AMD will be reviewed. Mice models for perturbation of chemokine receptors that recapitulate some of the features of AMD are also described. The body of evidence from human and rodent studies at this point in time suggests that monocyte and macrophages may modulate the course of AMD.

**Keywords** Monocytes/macrophages · Age-related macular degeneration · Chemokine signaling · Mouse models of retinal degeneration

## 26.1 Introduction

While the complement system receives much of the attention with respect to the role of inflammation in age-related macular degeneration (AMD), data show that mononuclear cells and specifically the monocytes and macrophages may have a significant role in the disease. Here, we briefly present the current knowledge on this topic.

I. Chowers (✉) · M. Grunin · S. Hagbi-Levi
Department of Ophthalmology, Hadassah-Hebrew University Medical Center, 91120, Jerusalem, Israel
e-mail: chowers@hadassah.org.il

M. Grunin
e-mail: michelle.grunin@mail.huji.ac.il

S. Hagbi-Levi
e-mail: shira.hagbi@mail.huji.ac.il

J. D. Ash et al. (eds.), *Retinal Degenerative Diseases,* Advances in Experimental Medicine and Biology 801, DOI 10.1007/978-1-4614-3209-8_26,

## 26.2 Macrophage and Monocyte Involvement in AMD

The presence of macrophages and other leukocytes in the vicinity of drusen and choroidal neovascularization (CNV), the hallmarks of neovascular AMD (NVAMD), have been reported [1–4]. While macrophages are detected in normal eyes, their number, spatial distribution, and phenotype are different in AMD. It was suggested that macrophages engulf fragments of the outer chollagenous zone of Bruch's membrane in AMD [1], that there is an increase in the number of macrophages and lymphocytes in the choroid as AMD progresses, and that the cells may be related to breaks in Bruch's membrane [2, 3]. Macrophage recruitment was associated with extracellular deposits in the form of soft drusen and thick, continuous basal laminar deposits. Furthermore, immunostaining for inducible nitric oxide synthase (iNOS) was detected among choroidal macrophages from AMD eyes, but not in controls—an observation which provides an insight into the potential phenotype of these macrophages [5].

Studies of rodent model for laser-induced CNV provide insight into the variable and even contradictory effects of macrophages [6–11]. The majority of F4/80 positive macrophages found in the choroid near laser-induced CNV lesions are derived from the peripheral circulation [8]. Ablation of peripheral macrophages via treatment with clodronate liposomes results in smaller and less vascular CNV [6]. Using the same model, it has been found that interleukin (IL)-10 deficient mice are impaired in their ability to generate CNV [10, 12]. Since IL-10 is involved in polarization to the M2 macrophage phenotype, this may indicate that macrophage phenotype contributes towards CNV development. Intravitreal delivery of F4/80+ splenic macrophages from young mice causes reduced CNV area, but macrophages from aged mice fail to inhibit CNV growth [12]. This may suggest that an altered anti-angiogenic effect of aged macrophages plays a role in NVAMD.

Such contradictory results may be explained by the heterogeneity of monocyte [13–17] and macrophage populations [18, 19]. Macrophages can polarize to at least two phenotypes; M1 macrophages having a pro-inflammatory and anti-angiogenic effect, and M2, which can have a pro-angiogenic and anti-inflammatory effect. Such polarization may be relevant in the context of AMD. For example, IL-10 may lead to M2 polarization, thus, its ablation may reduce the aniogenic stimuli derived by an M2 phenotype. The number of M2 macrophages compared to M1 macrophages was also reported to be increased in normal aging eyes [20]. Such an environment predominated by the M2 phenotype may exacerbate NVAMD. It is also possible that macrophage function is affected by infection, as macrophage activation associated with chronic murine cytomegalovirus infection results in more severe CNV [21].

Subclasses of monocytes also exist and may be a factor underlying the heterogeneous effect of their macrophage descendants. Two major monocyte subsets have been previously described: the classical CD14++CD16−, non-classical CD14+CD16++ monocytes, and a third subset, intermediate monocytes, with a phenotype of CD14++CD16+, recently described [15]. The classical subset was associated with the immune response, while the non-classical subset was associated with

a “patrolling” phenotype and the intermediate subset with T cell stimulation and a pro-inflammatory phenotype, expanded in specific diseases [15, 22]. Yet, it is still unclear if these specific subsets differentiate to the macrophage phenotypes which have been implicated with AMD. Also noteworthy is that as monocytes age, they are associated with chronic immune activation and expansion of the inflammatory CD16+ monocyte subset with resulting changes in function [23, 24].

## 26.3 Chemokine Receptors, Monocytes, and AMD

It is known that retinal pigment epithelium (RPE) cells can induce chemotaxis of monocytic cells [25]. Chemokine signaling leads to recruitment of all subsets of monocytes and is primarily mediated by the chemokine receptors CCR2 and CX3CR1, and their ligands CCL2 (monocyte chemotactic protein-1, MCP-1) and CX3CL1 (fractalkine), respectively [26, 27]. In in-vitro experiments, monocytes activated by MCP-1 co-cultured with RPE cells led to increased RPE apoptosis [28]. Photooxidative stress, that is also suspected to have a role in AMD, may lead to increased MCP-1 and subsequent macrophage recruitment [29]. Recruitment of macrophages via MCP-1 to the retina have also been found due to anti-retinal autoantibodies (ARA) that were created in response to dying photoreceptors, leading to further breakdown of the blood-retinal barrier [30]. Accordingly, a greater concentration of MCP-1 has been found in the aqueous humor of patients with AMD. [31, 32]. Activated CCR2 has also been shown to be a precursor to retinal inflammation and angiogenesis [33], and silencing of CCR2 using small interfering RNA (siRNA) for MCP-1 injected intravitreally in rats, which were then exposed to light damage, inhibits apoptosis, photoreceptor cell death, and infiltration of monocytes/microglia into the retina [34].

The other receptor, CX3CR1, has been known to mediate monocyte recruitment to sites of injury and is involved in the signaling pathway between dying photoreceptors and activated resident retinal microglia [35]. Recent work suggests that in mouse retinas exposed to oxidative injury, the absence of CX3CR1 may add insult to injury in the development of inflammation and retinal degeneration as well as an increase in infiltrating white blood cells to the retina, and subsequently higher amounts of markers of inflammation and apoptosis such as TNF-α, iNOS, and Casp-1 [36].

Thorough studies on the chemokine receptors have been done using knockout (KO) mouse models, among them CCR2, CX3CR1, CCL2 KO, and CCL2/CX-3CR1 double KOs and were thought to be relevant AMD models. However, it was recently discovered that the rd8 mutation in the CRB1 gene, causing retinal degeneration, is prevalent in the chemokine KO mice and may underlie their phenotype [37–39]. Contradicting data were then reported with respect to the effect of chemokine receptor deficiencies in the presence of wild type CRB1. Subtle alterations were reported in such mice, and a potential protective role has been suggested to

CX3CR1-mediated signaling, while CCR2-mediated signaling might have a deleterious effect in degenerating mouse retinas [38–40].

## 26.4 Gene Expression Studies on Monocytes and Retina

We reported a differential gene expression signature in peripheral blood mononuclear cells (PBMC) from patients with NVAMD [41], and upregulation of the chemokine receptors CCR1 and CCR2 on CD14+CD16+ monocytes from NVAMD patients, suggesting the involvement of non-classical monocyte in the disease [42]. Other signs of AMD in peripheral blood include the lower expression of CD46 and CD59 and higher expression of CD35 on monocytes, all of which are involved in the regulation of the complement system [43, 44]; they include the potential association between high TNF-α expression on cultured monocytes and prevalence of CNV among AMD patients [45], all of which implicate peripheral mononuclear cells with AMD.

## 26.5 Conclusions

Current data suggest that peripheral blood monocytes are recruited to the retina potentially through CCR2 and CX3CR1 and differentiate to macrophages, and that these cells may affect the course of all stages of AMD. The effect of these cells in the context of AMD may be variable, and at time opposing. Further investigation is required to understand the role of inflammation in the pathogenesis of AMD, what part monocytes/macrophages play in that system, and how they interact with additional factors important in AMD such as oxidative injury, complement activation, cell death, and angiogenesis. Targeting these cells and their signaling pathways may be the key to discovery of new avenues and treatments for the disease.

## References

1. Killingsworth MC, Sarks JP, Sarks SH (1990) Macrophages related to Bruch's membrane in age-related macular degeneration. Eye (Lond) 4(Pt 4):613–621
2. Penfold P, Killingsworth M, Sarks S (1984) An ultrastructural study of the role of leucocytes and fibroblasts in the breakdown of Bruch's membrane. Aust J Ophthalmol 12(1):23–31
3. Penfold PL, Killingsworth MC, Sarks SH (1985) Senile macular degeneration: the involvement of immunocompetent cells. Graefes Arch Clin Exp Ophthalmol 223(2):69–76
4. Sarks SH, Van Driel D, Maxwell L, Killingsworth M (1980) Softening of drusen and subretinal neovascularization. Trans Ophthalmol Soc U K 100(3):414–422
5. Cherepanoff S, McMenamin P, Gillies MC, Kettle E, Sarks SH (2010) Bruch's membrane and choroidal macrophages in early and advanced age-related macular degeneration. Br J Ophthalmol 94(7):918–925

6. Espinosa-Heidmann DG, Suner IJ, Hernandez EP, Monroy D, Csaky KG, Cousins SW (2003) Macrophage depletion diminishes lesion size and severity in experimental choroidal neovascularization. Invest Ophthalmol Vis Sci 44(8):3586–3592
7. Sakurai E, Anand A, Ambati BK, van Rooijen N, Ambati J (2003) Macrophage depletion inhibits experimental choroidal neovascularization. Invest Ophthalmol Vis Sci 44(8):3578–3585
8. Caicedo A, Espinosa-Heidmann DG, Pina Y, Hernandez EP, Cousins SW (2005) Blood-derived macrophages infiltrate the retina and activate Muller glial cells under experimental choroidal neovascularization. Exp Eye Res 81(1):38–47
9. Shi YY, Wang YS, Zhang ZX, Cai Y, Zhou J, Hou HY et al (2011) Monocyte/macrophages promote vasculogenesis in choroidal neovascularization in mice by stimulating SDF-1 expression in RPE cells. Graefes Arch Clin Exp Ophthalmol 249(11):1667–1679
10. Apte RS, Richter J, Herndon J, Ferguson TA (2006) Macrophages inhibit neovascularization in a murine model of age-related macular degeneration. PLoS Med 3(8):e310
11. Tsutsumi C, Sonoda KH, Egashira K, Qiao H, Hisatomi T, Nakao S et al (2003) The critical role of ocular-infiltrating macrophages in the development of choroidal neovascularization. J Leukoc Biol 74(1):25–32
12. Kelly J, Ali Khan A, Yin J, Ferguson TA, Apte RS (2007) Senescence regulates macrophage activation and angiogenic fate at sites of tissue injury in mice. J Clin Invest 117(11):3421–3426
13. Weber C, Belge KU, von Hundelshausen P, Draude G, Steppich B, Mack M et al (2000) Differential chemokine receptor expression and function in human monocyte subpopulations. J Leukoc Biol 67(5):699–704
14. Ziegler-Heitbrock L, Ancuta P, Crowe S, Dalod M, Grau V, Hart DN et al (2010) Nomenclature of monocytes and dendritic cells in blood. Blood 116(16):e74–80
15. Wong KL, Tai JJ, Wong WC, Han H, Sem X, Yeap WH et al (2011) Gene expression profiling reveals the defining features of the classical, intermediate, and nonclassical human monocyte subsets. Blood 118(5):e16–31
16. Geissmann F, Jung S, Littman DR (2003) Blood monocytes consist of two principal subsets with distinct migratory properties. Immunity 19(1):71–82
17. Frankenberger M, Sternsdorf T, Pechumer H, Pforte A, Ziegler-Heitbrock HW (1996) Differential cytokine expression in human blood monocyte subpopulations: a polymerase chain reaction analysis. Blood 87(1):373–377
18. Mantovani A, Sica A, Sozzani S, Allavena P, Vecchi A, Locati M (2004) The chemokine system in diverse forms of macrophage activation and polarization. Trends Immunol 25(12):677–686
19. Martinez FO, Gordon S, Locati M, Mantovani A (2006) Transcriptional profiling of the human monocyte-to-macrophage differentiation and polarization: new molecules and patterns of gene expression. J Immunol 177(10):7303–7311
20. Cao X, Shen D, Patel MM, Tuo J, Johnson TM, Olsen TW et al (2011) Macrophage polarization in the maculae of age-related macular degeneration: a pilot study. Pathol Int 61(9):528–535
21. Cousins SW, Espinosa-Heidmann DG, Miller DM, Pereira-Simon S, Hernandez EP, Chien H et al (2012) Macrophage activation associated with chronic murine cytomegalovirus infection results in more severe experimental choroidal neovascularization. PLoS Pathog 8(4):e1002671
22. Shi C, Pamer EG (2011) Monocyte recruitment during infection and inflammation. Nat Rev Immunol 11(11):762–774
23. Hearps AC, Martin GE, Angelovich TA, Cheng WJ, Maisa A, Landay AL et al (2012) Aging is associated with chronic innate immune activation and dysregulation of monocyte phenotype and function. Aging Cell 11(5):867–875
24. Seidler S, Zimmermann HW, Bartneck M, Trautwein C, Tacke F (2010) Age-dependent alterations of monocyte subsets and monocyte-related chemokine pathways in healthy adults. BMC Immunol 11:30

25. Rosenbaum JT, O'Rourke L, Davies G, Wenger C, David L, Robertson JE (1987) Retinal pigment epithelial cells secrete substances that are chemotactic for monocytes. Curr Eye Res 6(6):793–800
26. Ancuta P, Rao R, Moses A, Mehle A, Shaw SK, Luscinskas FW et al (2003) Fractalkine preferentially mediates arrest and migration of CD16+ monocytes. J Exp Med 197(12):1701–1707
27. Shantsila E, Wrigley B, Tapp L, Apostolakis S, Montoro-Garcia S, Drayson MT et al (2011) Immunophenotypic characterization of human monocyte subsets: possible implications for cardiovascular disease pathophysiology. J Thromb Haemost 9(5):1056–1066
28. Yang D, Elner SG, Chen X, Field MG, Petty HR, Elner VM (2011) MCP-1-activated monocytes induce apoptosis in human retinal pigment epithelium. Invest Ophthalmol Vis Sci 52(8):6026–6034
29. Suzuki M, Tsujikawa M, Itabe H, Du ZJ, Xie P, Matsumura N et al (2012) Chronic photo-oxidative stress and subsequent MCP-1 activation as causative factors for age-related macular degeneration. J Cell Sci 125(Pt 10):2407–2415
30. Kyger M, Worley A, Adamus G (2013) Autoimmune responses against photoreceptor antigens during retinal degeneration and their role in macrophage recruitment into retinas of RCS rats. J Neuroimmunol 254(1–2):91–100
31. Kramer M, Hasanreisoglu M, Feldman A, Axer-Siegel R, Sonis P, Maharshak I et al (2012) Monocyte chemoattractant protein-1 in the aqueous humour of patients with age-related macular degeneration. Clin Experiment Ophthalmol 40(6):617–625
32. Jonas JB, Tao Y, Neumaier M, Findeisen P (2012) Cytokine concentration in aqueous humour of eyes with exudative age-related macular degeneration. Acta Ophthalmol 90(5):e381–388
33. Chen M, Copland DA, Zhao J, Liu J, Forrester JV, Dick AD et al (2012) Persistent inflammation subverts thrombospondin-1-induced regulation of retinal angiogenesis and is driven by CCR2 ligation. Am J Pathol 180(1):235–245
34. Rutar M, Natoli R, Provis JM (2012) Small interfering RNA-mediated suppression of Ccl2 in Muller cells attenuates microglial recruitment and photoreceptor death following retinal degeneration. J Neuroinflammation 9:221
35. Zhang M, Xu G, Liu W, Ni Y, Zhou W (2012) Role of fractalkine/CX3CR1 interaction in light-induced photoreceptor degeneration through regulating retinal microglial activation and migration. PLoS One 7(4):e35446
36. Chen M, Luo C, Penalva R, Xu H (2013) Paraquat-induced retinal degeneration is exaggerated in CX3CR1 deficient mice and is associated with increased retinal inflammation. Invest Ophthalmol Vis Sci 54(1):682–690
37. Mattapallil MJ, Wawrousek EF, Chan CC, Zhao H, Roychoudhury J, Ferguson TA et al (2012) The Rd8 mutation of the Crb1 gene is present in vendor lines of C57BL/6N mice and embryonic stem cells, and confounds ocular induced mutant phenotypes. Invest Ophthalmol Vis Sci 53(6):2921–2927
38. Luhmann UF, Lange CA, Robbie S, Munro PM, Cowing JA, Armer HE et al (2012) Differential modulation of retinal degeneration by Ccl2 and Cx3cr1 chemokine signalling. PLoS One 7(4):e35551
39. Luhmann UF, Carvalho LS, Robbie SJ, Cowing JA, Duran Y, Munro PM et al (2013) Ccl2, Cx3cr1 and Ccl2/Cx3cr1 chemokine deficiencies are not sufficient to cause age-related retinal degeneration. Exp Eye Res 107C:80–87
40. Vessey KA, Greferath U, Jobling AI, Phipps JA, Ho T, Waugh M et al (2012) Ccl2/Cx3cr1 knockout mice have inner retinal dysfunction but are not an accelerated model of AMD. Invest Ophthalmol Vis Sci 53(12):7833–7846
41. Lederman M, Weiss A, Chowers I (2010) Association of neovascular age-related macular degeneration with specific gene expression patterns in peripheral white blood cells. Invest Ophthalmol Vis Sci 51(1):53–58
42. Grunin M, Burstyn-Cohen T, Hagbi-Levi S, Peled A, Chowers I (2012) Chemokine receptor expression in peripheral blood monocytes from patients with neovascular age-related macular degeneration. Invest Ophthalmol Vis Sci 53(9):5292–5300

43. Haas P, Aggermann T, Nagl M, Steindl-Kuscher K, Krugluger W, Binder S (2011) Implication of CD21, CD35, and CD55 in the pathogenesis of age-related macular degeneration. Am J Ophthalmol 152(3):396–399e1
44. Singh A, Faber C, Falk M, Nissen MH, Hviid TV, Sorensen TL (2011) Altered expression of CD46 and CD59 on leukocytes in neovascular age-related macular degeneration. Am J Ophthalmol 154(1):193–199e2
45. Cousins SW, Espinosa-Heidmann DG, Csaky KG (2004) Monocyte activation in patients with age-related macular degeneration: a biomarker of risk for choroidal neovascularization? Arch Ophthalmol 122(7):1013–1018

# Chapter 27
# Microglia in the Aging Retina

**Marcus Karlstetter and Thomas Langmann**

**Abstract** In the healthy retina, microglial cells represent a self-renewing population of innate immune cells, which constantly survey their microenvironment. Equipped with receptors, a microglial cell detects subtle cellular damage and rapidly responds with activation, migration, and increased phagocytic activity. While the involvement of microglial cells has been well characterized in monogenic retinal disorders, it is still unclear how they contribute to the onset of retinal aging disorders including age-related macular degeneration (AMD). There is evidence, that microglial activation is not solely a secondary manifestation of retinal tissue damage in age-related disorders. Thus, work in the aging rodent and human retina suggests that long-lived and genetically predisposed microglia transform into a dystrophic state, with loss of neuroprotective functions. In this concept, malfunction of aging microglia can trigger a chronic low-grade inflammatory environment that favors the onset and progression of retinal degeneration.

**Keywords** Microglia · AMD · Aging · Retinal degeneration · Inflammation · Complement system

## 27.1 Introduction

Retinal degeneration represents a common cause for vision impairment in the industrialized world, and apoptotic photoreceptor death represents the common hallmark [1]. In monogenic disorders, the progression of degenerative processes is determined by the underlying genetic defect and cellular dysfunction. These strong effects can be modified by factors like age and lifestyle. In contrast, the development

T. Langmann (✉) · M. Karlstetter
Department of Ophthalmology, University of Cologne, Kerpener Straße 62,
D-50924 Cologne, Germany
e-mail: thomas.langmann@uk-koeln.de

M. Karlstetter
e-mail: marcus.karlstetter@uk-koeln.de

J. D. Ash et al. (eds.), *Retinal Degenerative Diseases,* Advances in Experimental Medicine and Biology 801, DOI 10.1007/978-1-4614-3209-8_27,

of complex retinal diseases like age-related macular degeneration (AMD), is based on the interaction of genetic variants that modify the risk of disease susceptibility and environmental factors like smoking, diet, physique, and age [2, 3].

The role of innate immune cells has been extensively studied in various mouse models of inherited retinal degeneration [4]. Moderate immune activation during initiation stages is followed by a cascade of neurotoxic proinflammatory events at acute phases of the degenerative process. Morphological studies with retinas of AMD patients revealed activated microglia in the photoreceptor layer and subretinal space. The subretinal microglia incorporated rhodopsin-positive particles, indicating high phagocytic activity [5]. However, microglial cells not only are involved in acute degeneration but may also play a role in the initiation of age-related changes in the retina [6]. The retina provides a susceptible environment for age-related changes, and aging is a major risk factor for retinal disorders like AMD, glaucoma, and diabetic retinopathy [7]. In the aging retina, microglial cells are surrounded by long-lived neurons and play an essential role in tissue maintenance and repair. Any perturbance in this machinery may have serious consequences for retinal health.

## 27.2 Aging Processes in Microglia

Microglial cells populate the mammalian central nervous system (CNS) before blood brain barrier formation and have to be maintained through self-renewal [8]. Microglia lack a stem cell reservoir in the CNS and thus underlie aging processes which result from multiple cell divisions. In particular, the telomeres of microglial cells isolated from old rats are shortened compared to young animals [9]. Telomere shortening is a result of multiple cell divisions and represents a general cellular process in aging [10]. Brains of young rats contain cells with extra long telomeres specialized to replenish microglial cells during development. This “rejuvenation reservoir” is exhausted in older animals, which has profound consequences on the homeostatic functions of microglia. Ramified microglial cells are characterized by static cell bodies, with radially outreaching and highly dynamic protrusions. This specialized morphology allows the entire microglial population to cover every angle of the retina which is essential for the maintenance of tissue homeostasis [11]. Studies in mice revealed that ramifications of retinal microglia lose motility, branching complexity, and process length with age [12]. Thus, the area covered by microglial surveillance is decreased, and phagocytosis performance per time and area is diminished. Insufficient phagocytic clearance leads consequently to the accumulation of neurotoxic debris.

In contrast to the amoeboid cytoplasmic shape of young, activated microglial cells after tissue damage, histological analyses in the aging CNS identified dystrophic microglial cells characterized by swelling, beading, or deramification of their processes [13]. Dystrophic microglial cells also form cellular aggregates which deregulate the high order of the “native” cellular network.

## 27.3 The Retinal Microenvironment Controls the Innate Immune Status

During retinal aging, oxidative stress leads to the modification of retinal molecules and subsequent deposition of insoluble debris. This material contains oxidized retinal proteins which are commonly classified as advanced glycation end products (AGEs) and advanced lipoxidation end products (ALEs) [14]. AGEs and ALEs are preferentially deposited in the retinal pigment epithelium (RPE) and the subretinal space [15].

Microglial cells can detect AGEs via specific receptors (RAGE) and downstream signaling pathways lead to proinflammatory activation and impairment of neuronal function [16]. Although receptors for ALEs have not been identified yet, synthetic ALE malondialdehyde-lysine (MDA-Lys) induces a proinflammatory response and production of oxidative stress in myeloid cells. This suggests that ALEs evoke AGE-like effects during aging [17]. The humoral immune system seems to play an important role in clearance of AGEs. The complement factor H (CFH) variant His402, which shows a strong genetic association with AMD, has decreased binding affinity to malondialdehyde (MDA). CFH is an inhibitory complement component, which catalyzes the formation of iC3b, which then recruits microglial cells and stimulates phagocytosis. Decreased binding activity of CFH-His402 consequently leads to decreased phagocytic clearance of MDA, resulting in increased secretion of the proinflammatory cytokine interleukin 8 from RPE-cells [18, 19].

In addition to immune-activating mechanisms, aging also leads to a loss of immune-suppressive signals. In the healthy CNS, the neuronal "sugar" coat of the cell, the glycocalyx is decorated with sialic acid caps which serve as ligands for the immunosuppressive receptor Siglec-11 on microglial cells. During aging, oxidative stress triggers the cleavage of sialic acid caps and thereby interrupts Siglec-11 inhibitory signals [20–22]. Neuronal surfaces devoid of an intact glycocalyx also favor complement C1q binding. C1q flags damaged cells for phagocytic clearance, which is mediated by complement receptor 3 expressed on microglial cells [23].

Another important receptor in phagocytic clearance is triggering receptor expressed on myeloid cells 2 (TREM2). TREM2 mediates noninflammatory activation of microglial phagocytosis, and genetic variants in TREM2 are associated with an increased risk of developing Alzheimer's disease [20, 24–26].

## 27.4 Chronic Immune Activation in the Aging Retina

In contrast to acute retinal damage, the aging retina provides low-level immune stimuli, inducing a parainflammatory environment over a long time span. Transcriptome analysis from 20-month-old mice showed that their retinas had significantly increased expression levels of innate immune and complement genes compared to young mice [27]. Isolated microglial cells from 18-month-old mice

showed morphological signs of activation and expressed proinflammatory markers, indicating low-grade immune activation in the aging retina [28]. Microglial cells tend to translocate to the subretinal space during aging in the murine and human retina. Proinflammatory microglial cells transplanted into the subretinal space perturb the function of RPE cells and evoke secretion of angiogenic factors [6, 15]. Chronic inflammation is a result of numerous stimulation events, and cells can memorize stimulus challenge over time. Thus, microglial cells derived from LPS-injected old mice responded with an excessive and prolonged immune response compared to young mice [28]. This suggests that gradual priming with lifelong subinflammatory stimuli mounts a pronounced inflammatory activation.

Transcriptome analysis in retinas from A/J mice, a mouse model for multifactorial age-related retinal degeneration, could identify immune activation prior to any signs of degeneration. This suggests that background-specific genetic predisposition leads to immune activation and retinal degeneration. Interestingly, Interferon-β (IFN-β) signaling could be identified as major pathway involving the target genes Irf7, Stat1 and Mx2 [29]. IFN-β signaling also precedes degenerative processes in the blue-light-damaged mouse retina, and thus may represent a common immunological principle for age-related tissue changes [30].

## 27.5 Conclusions

In the healthy retina, microglial activation is tightly controlled to maintain the essential housekeeping functions, yet avoiding chronic immune activation. During aging, augmented deposition of cellular debris demands increased phagocytic capacity of microglia. However, microglial cells themselves undergo aging processes with morphological changes, diminished housekeeping potential, and latent immune activation. Acquired or inherited retinal damage may accelerate these aging processes and tip the balance to pathology. Thus, preservation of microglial functions during aging as well as prevention of oxidative stress in the retina are promising concepts to delay the onset of age-dependent retinal diseases and slow down their progression.

## References

1. Stone J, Maslim J, Valter-Kocsi K, Mervin K, Bowers F, Chu Y et al (1999) Mechanisms of photoreceptor death and survival in mammalian retina. Prog Retin Eye Res 18(6):689–735
2. Jager RD, Mieler WF, Miller JW (2008) Age-related macular degeneration. N Engl J Med 358(24):2606–2617
3. Swaroop A, Branham KEH, Chen W, Abecasis G (2007) Genetic susceptibility to age-related macular degeneration: a paradigm for dissecting complex disease traits. Hum Mol Genet 16:R174–182

4. Karlstetter M, Ebert S, Langmann T (2010) Microglia in the healthy and degenerating retina: insights from novel mouse models. Immunobiology 215(9–10):685–691
5. Gupta N, Brown KE, Milam AH (2003) Activated microglia in human retinitis pigmentosa, late-onset retinal degeneration, and age-related macular degeneration. Exp Eye Res 76(4):463–471
6. Ma W, Zhao L, Fontainhas AM, Fariss RN, Wong WT (2009) Microglia in the mouse retina alter the structure and function of retinal pigmented epithelial cells: a potential cellular interaction relevant to AMD. PLoS One 4(11):e7945
7. Chen M, Forrester J (2009) Para-inflammation in the aging retina. Prog Retin Eye Res 28(5):348–368
8. Ginhoux F, Greter M, Leboeuf M, Nandi S, See P, Gokhan S et al (2010) Fate mapping analysis reveals that adult microglia derive from primitive macrophages. Science 330(6005):841–845
9. Flanary BE, Sammons NW, Nguyen C, Walker D, Streit WJ (2007) Evidence that aging and amyloid promote microglial cell senescence. Rejuvenation Res 10(1):61–74
10. Kirkwood TBL (2005) Understanding the odd science of aging. Cell 120(4):437–447
11. Nimmerjahn A, Kirchhoff F, Helmchen F (2005) Resting microglial cells are highly dynamic surveillants of brain parenchyma in vivo. Science 308(5726):1314–1318
12. Damani MR, Zhao L, Fontainhas AM, Amaral J, Fariss RN, Wong WT (2010) Age-related alterations in the dynamic behavior of microglia. Glia 10:263–276
13. Streit WJ (2006) Microglial senescence: does the brain's immune system have an expiration date? Trends Neurosci 29(9):506–510
14. Glenn JV, Stitt AW (2009) The role of advanced glycation end products in retinal ageing and disease. Biochim Biophys Acta 1790(10):1109–1116
15. Ma W, Coon S, Zhao L, Fariss RN, Wong WT (2012) A2E accumulation influences retinal microglial activation and complement regulation. Neurobiol Aging 34(3):943–960
16. Fang F, Lue LF, Yan S, Xu H, Luddy JS, Chen D et al (2010) RAGE-dependent signaling in microglia contributes to neuroinflammation, Aβ accumulation, and impaired learning/memory in a mouse model of Alzheimer's disease. FASEB J 24(4):1043–1055
17. Shanmugam N, Figarola JL, Li Y, Swiderski PM, Rahbar S, Natarajan R (2008) Proinflammatory effects of advanced lipoxidation end products in monocytes. Diabetes 57(4):879–888
18. Klein RJ, Zeiss C, Chew EY, Tsai JY, Sackler RS, Haynes C et al (2005) Complement factor H polymorphism in age-related macular degeneration. Science 308(5720):385–389
19. Weismann D, Hartvigsen K, Lauer N, Bennett KL, Scholl HPN, Charbel Issa P et al (2011) Complement factor H binds malondialdehyde epitopes and protects from oxidative stress. Nature 478(7367):76–81
20. Linnartz B, Neumann H (2013) Microglial activatory (immunoreceptor tyrosine-based activation motif)- and inhibitory (immunoreceptor tyrosine-based inhibition motif)-signaling receptors for recognition of the neuronal glycocalyx. Glia 61(1):37–46
21. Moseley R, Waddington RJ, Embery G (1997) Degradation of glycosaminoglycans by reactive oxygen species derived from stimulated polymorphonuclear leukocytes. Biochim Biophys Acta 1362(2–3):221–231
22. Moseley R, Waddington R, Evans P, Halliwell B, Embery G (1995) The chemical modification of glycosaminoglycan structure by oxygen-derived species in vitro. Biochim Biophys Acta 1244(2–3):245–252
23. Linnartz B, Kopatz J, Tenner AJ, Neumann H (2012) Sialic acid on the neuronal glycocalyx prevents complement C1 binding and complement receptor-3-mediated removal by microglia. J Neurosci 32(3):946–952
24. Takahashi K (2005) Clearance of apoptotic neurons without inflammation by microglial triggering receptor expressed on myeloid cells-2. J Exp Med 201(4):647–657
25. Guerreiro R, Wojtas A, Bras J, Carrasquillo M, Rogaeva E, Majounie E et al (2012) TREM2 variants in Alzheimer's disease. N Engl J Med 368(2):117–127
26. Jonsson T, Stefansson H, Ph D SS, Jonsdottir I, Jonsson PV, Snaedal J et al (2012) Variant of TREM2 associated with the risk of Alzheimer's disease. N Engl J Med 368(2):107–116

27. Chen M, Muckersie E, Forrester JV, Xu H (2010) Immune activation in retinal aging: a gene expression study. Invest Ophthalmol Vis Sci 51(11):5888–5896
28. Sierra A, Gottfried-Blackmore AC, McEwen BS, Bulloch K (2007) Microglia derived from aging mice exhibit an altered inflammatory profile. Glia 55(4):412–424
29. Mustafi D, Maeda T, Kohno H, Nadeau JH, Palczewski K (2012) Inflammatory priming predisposes mice to age-related retinal degeneration. J Clin Invest 122(8):2989–3001
30. Ebert S, Walczak Y, Remé C, Langmann T (2012) Microglial activation and transcriptomic changes in the blue light-exposed mouse retina. Adv Exp Med Biol 723:619–632

# Chapter 28
# The Role of Complement Dysregulation in AMD Mouse Models

**Jin-Dong Ding, Una Kelly, Marybeth Groelle, Joseph G. Christenbury, Wenlan Zhang and Catherine Bowes Rickman**

**Abstract** Variations in several complement genes are now known to be significant risk factors for the development of age-related macular degeneration (AMD). Despite dramatic effects on disease susceptibility, the underlying mechanisms by which common polymorphisms in complement proteins alter disease risk have remained unclear. Genetically modified mice in which the activity of the complement has been altered are available and can be used to investigate the role of complement in the pathogenesis of AMD. In this mini review, we will discuss some existing complement models of AMD and our efforts to develop and characterize the ocular phenotype in a variety of mice in which complement is either chronically activated or inhibited. A spectrum of complement dysregulation was modeled on the *APOE4* AMD mouse model by crossing these mice to complement factor H

C. B. Rickman (✉) · J.-D. Ding · U. Kelly · M. Groelle · J. G. Christenbury · W. Zhang
Department of Ophthalmology, Duke University Medical Center, 2351 Erwin Rd, Durham, NC 27710, USA
e-mail: bowes007@duke.edu

J.-D. Ding
jd84@duke.edu

U. Kelly
e-mail: una.kelly@duke.edu

M. Groelle
e-mail: groel003@duke.edu

J. G. Christenbury
e-mail: jgchristenbury@gmail.co

W. Zhang
e-mail: wz15@duke.edu

C. B. Rickman
Departments of Ophthalmology and Cell Biology, Duke University Medical Center, 2351 Erwin Rd, Durham, NC 27710, USA

Duke Eye Center, Duke University Medical Center, AERI Rm 5010, Post Box 3802, Durham, NC 27710, USA

J. D. Ash et al. (eds.), *Retinal Degenerative Diseases,* Advances in Experimental Medicine and Biology 801, DOI 10.1007/978-1-4614-3209-8_28,

knockout (*cfh−/−*) mice to test the impact of excess complement activation, and by crossing them to soluble-complement-receptor-1-related protein y (sCrry) mice, in which sCrry acts as a potent inhibitor of mouse complement acting in a manner similar to CFH. In addition, we have also generated humanized *CFH* mice expressing normal and risk variants of CFH.

**Keywords** Age-related macular degeneration · Complement · Alternative pathway · Complement factor H (CFH)

## 28.1 Introduction

Age-related macular degeneration (AMD) is the leading cause of blindness in the developed world. It is a late onset, progressive retinal degenerative disease influenced by both environmental and genetic factors. Early AMD is characterized by the accumulation of lipid- and protein-containing deposits, between the retinal pigmented epithelium (RPE) and Bruch's membrane (BrM). These sub-RPE deposits may be focal (drusen) or diffuse and likely contribute to disease pathogenesis and progression. As AMD progresses to late-stage disease, it is categorized as either "dry" (geographic atrophy, with photoreceptor loss and extensive RPE atrophy) or "wet" (exudative, with subsequent choroidal neovascularization, CNV).

Over the past decade, a large body of evidence has emerged that implicates complement in the pathogenesis and progression of AMD. For example, pathobiologic investigations have led to the identification of numerous complement proteins in drusen [1–3], and genetic studies have led to the discovery of variants in several complement genes that confer significant risk for, or protection from, development of AMD late in life [4]. Genetic association studies have identified the complement factor H (*CFH*) gene, which encodes an alternative complement pathway inhibitor, as the strongest genetic factor associated with AMD risk [4]. It is now apparent that dysregulation of the complement cascade, and of the alternative pathway (AP) in particular [5], is a critical predisposing step in AMD development.

Complement is a key system for immune surveillance and homeostasis. It is a proteolytic cascade triggered by three activation routes, the classical, alternative, and lectin pathways (reviewed in [6]). The AP is constantly activated at low levels, initiated by spontaneous hydrolysis of complement factor 3 (C3). Thus inhibitory regulators are crucial to maintain the AP at minimum activity under normal physiological conditions. These include membrane-bound factors such as decay-accelerating factor (DAF), CD46, complement receptor 1 (CR1), and, in rodents, complement-receptor-1-related protein y (Crry) as well as soluble proteins like CFH and factor I [6].

The associated risk of *CFH* variants supports the hypothesis that local inflammation and activation of the complement cascade contributes to AMD pathogenesis. However, it has not been clearly established whether *CFH* variants contribute to AMD risk by a loss or gain of function although studies to date support loss of function [7]. To test the effect of complement on AMD pathobiology, we and other

researchers have taken advantage of various complement dysregulated transgenic mice. Through analysis of the ocular phenotype, complement activation, and visual function of these mouse models, we hope to answer whether chronic inhibition or unregulated activation of complement contributes to AMD pathogenesis.

## 28.2 *cfh−/−* Mice, Complement Inhibitor Loss of Function Model

CFH is the major inhibitor of the AP C3 convertase. Absence of cfh in *cfh* knockout (*cfh−/−*) mice leads to continuous uncontrolled C3 cleavage, resulting in very low C3 in plasma [8]. Coffey et al. analyzed the ocular phenotype of 2-year-old *cfh−/−* mice and found that the visual acuity and rod response were impaired, as measured by behavior and electroretinogram (ERG) [9]. Although the anatomy of the retina did not appear to be damaged compared to wild-type mice, the rod photoreceptor outer segments were disorganized. In a subsequent study of these mice the retina blood vessels were found to be restricted, resulting in a reduction of retinal blood supply [10].

These results from *cfh−/−* mice studies clearly demonstrate the importance of CFH in the maintenance of retina structure and function. However, the reported ocular phenotype in this mouse model does not replicate a key AMD feature, sub-RPE deposits. In fact, the authors reported that the sub-RPE deposit in the *cfh−/−* mice was decreased compared to wild-type mice of the same age. The serum levels of C3 and factor B were below detection due to the lack of cfh-mediated inhibition. C3 is produced but is rapidly activated in the absence of CFH inhibition resulting in the bulk of the plasma C3 being in the form of C3b. Using immunohistochemistry, C3 was previously detected in BrM and RPE and extending into the photoreceptor outer segments of old *cfh−/−* mice [9] as well as in the glomerular basement membrane [8].

## 28.3 Soluble Crry (sCrry) Mice, a Chronic Inhibition of Complement Model

Crry, a rodent homologue of human CR1, is a potent membrane inhibitor of complement C3 convertases [11]. In order to create an animal model in which there was continuous increased inhibition of complement, Quigg et al. generated a transgenic mouse that expresses recombinant sCrry, controlled by the broadly active and heavy-metal-inducible metallothionein-I promotor [12]. *sCrry* transcripts are widely expressed in various tissues with and without zinc (Zn)-induced activation of the metallothionein promotor, and complement activation was significantly inhibited in the serum during short-term Zn-induced sCrry expression [12].

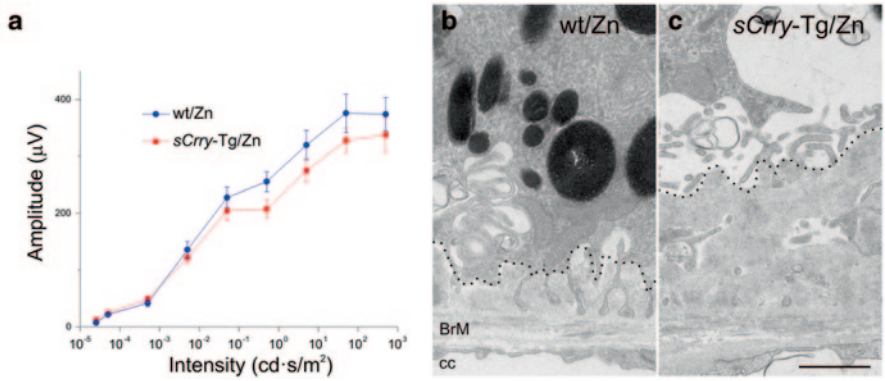


**Fig. 28.1** Visual function and RPE/Bruch's histopathology in old *sCrry* mice. **a** Scotopic ERG flash responses. Stimulus response curves of b-wave amplitudes. Baseline ERGs obtained from Zn-fed 2-year-old C57Bl/6N wild-type controls (*blue, wt/Zn*) and Zn-fed age-matched transgenic *sCrry* (*red, sCrry*-Tg/Zn) mice. b-Wave amplitudes are decreased in the *sCrry* mice compared to controls. Data are expressed as standard error of the mean (±SEM). **b** Retina from 2-year-old Zn-fed wt mouse retina shows mild basal deposit accumulation between *dashed line* and Bruch's membrane (*BrM*), whereas in **c** 2-year-old *sCrry*-Tg mouse retina, the basal deposit accumulations was significantly increased (Scale: 1 μm). *cc* choriocapillaris

Wyss-Coray et al. crossed this mouse with an Alzheimer's disease mouse model, the human amyloid precursor protein (*hAPP*) transgenic mouse [13] and found that the amyloid β (Aβ) accumulation in 1-year-old *hAP, sCrry* mouse brain was two- to threefold higher than in age-matched *hAPP* mice. Alzheimer's disease and AMD share many pathological mechanisms, including accumulation of extracellular deposits, increased oxidative stress, inflammation, and complement activation [14, 15]. Thus, we examined how inhibition of complement through expression of the *sCrry* transgene affects the retina structure and function in aged mice.

We compared cohorts of 2-year-old *sCrry* and wild-type mice, all fed Zn-fortified water post weaning. The overall morphology of the retina was unchanged but the ERG b-wave amplitude was attenuated in *sCrry* mice compared to wild-type controls, and there was significant accumulation of sub-RPE deposits in the *sCrry* mice (Fig. 28.1).

## 28.4 Humanized CFH Mice

Among the nonsynonymous coding variants of *CFH,* a tyrosine (Y) to histidine (H) change at amino acid position 402, H402, is most strongly associated with the major AMD risk haplotype [4]. Ultimately, more subtle approaches than using a *cfh* null will be needed to understand why an isoform variant of CFH increases the "risk" of developing AMD. For this reason, we generated full-length human CFH-transgenic mice using bacterial artificial chromosomes. These CFH-transgenic mice were then crossed to the *cfh*−/− mice, so that only the full-length human CFH is expressed in

the mouse [16]. We verified the presence of CFH isoforms using mass spectrometry. Biochemical analyses established that the human CFH can functionally interact with mouse complement by inhibiting C3 hydrolysis, and the ERG b-wave of the *CFH, cfh−/−*, mice was recovered compared to *cfh−/−* animals [16]. We are now in the process of analyzing the retina and RPE structure of these mice and determining the extent of the protective effect of the two CFH isoforms.

Ufret-Vincenty et al. generated chimeric mice by replacing the short consensus repeats (SCR) 6–8 of mouse cfh with human CFH SCR6–8 including the Y- or H402 amino acid using constructs driven by an apolipoprotein (ApoE) promotor [17]. Using a C3 enzyme-linked immunosorbent assay (ELISA), they showed that the chimeric proteins are functional in vivo and, somewhat surprisingly, that there is accumulation of subretinal macrophages in these 13- to 14-month-old chimeras.

## 28.5 Modification of Complement Activation in the *APOE4* AMD Model

We developed a murine model of AMD (aged human *APOE4*-targeted replacement mice on a high fat, cholesterol-enriched diet (*APOE4*~HFC)) that faithfully recapitulates many aspects of the human AMD phenotype—particularly RPE cell pathology, visual function deficits, and formation of sub-RPE deposits [18]. Moreover, complement activation is a factor in the development of the AMD-like pathology in this mouse model. Activated complement components accumulate within the sub-RPE deposits of the *APOE4*~HFC mice [18, 19]. To directly interrogate the impact of complement activation and inhibition in our AMD model, we crossed the *sCrry* mice and *cfh−/−* mice to the *APOE4* mice. The *APOE4* mouse model provides a platform in which both recovery and aggravation of the AMD-like phenotype can be manipulated and analyzed. Initial analyses of these mice is ongoing, but early results suggest the constant increase in complement activation in *APOE4,cfh−/−* mice has a more detrimental effect than the enhanced inhibition of complement seen in the *APOE4,sCrry* mice.

## 28.6 Conclusions

Complement activation products, produced as part of the inflammatory response, can have beneficial effects by facilitating phagocytosis and removal of cellular debris, or they can be detrimental by causing bystander damage to surrounding tissues. The various mouse models of complement dysregulation described have a different capacity to accumulate activated complement components in the eye, providing us a spectrum of complement deposition and complement-related phenotypes to compare and analyze. Based on the initial analyses of the ocular phenotype of these mouse models, it appears that it is not simply chronic inhibition (*sCrry*) versus unregulated activation (*cfh−/−*) of complement that contributes to AMD pathogenesis since both

models demonstrated some features of AMD-like pathology. We hypothesize that the balance of complement activation is critical in AMD pathogenesis and that characterization of these new complement models of AMD should help define that balance.

**Acknowledgments** *sCrry* and *cfh−/−* mice were kindly provided by Drs. R. J. Quigg (University of Chicago, IL) and M. Botto (Imperial College, London), respectively. The work of the authors is supported by NIH Grants EY019038, P30 EY005722, an Edward N. & Della L. Thome Memorial Foundation Award, and Research to Prevent Blindness, Inc. Medical Student Fellowship awards to JGC and WZ.

## References

1. Anderson DH, Mullins RF, Hageman GS, Johnson LV (2002) A role for local inflammation in the formation of drusen in the aging eye. Am J Ophthalmol 134(3):411–431
2. Hageman GS, Luthert PJ, Victor Chong NH, Johnson LV, Anderson DH, Mullins RF (2001) An integrated hypothesis that considers drusen as biomarkers of immune-mediated processes at the RPE-Bruch's membrane interface in aging and age-related macular degeneration. Prog Retin Eye Res 20(6):705–732
3. Johnson LV, Leitner WP, Staples MK, Anderson DH (2001) Complement activation and inflammatory processes in Drusen formation and age related macular degeneration. Exp Eye Res 73(6):887–896
4. Zipfel PF, Lauer N, Skerka C (2010) The role of complement in AMD. Adv Exp Med Biol 703:9–24
5. Anderson DH, Radeke MJ, Gallo NB, Chapin EA, Johnson PT, Curletti CR, Hancox LS, Hu J, Ebright JN, Malek G, Hauser MA, Bowes Rickman C, Bok D, Hageman GS, Johnson LV (2010) The pivotal role of the complement system in aging and age-related macular degeneration: hypothesis re-visited. Prog Retin Eye Res 29(2):95–112
6. Thurman JM, Holers VM (2006) The central role of the alternative complement pathway in human disease. J Immunol 176(3):1305–1310
7. Johnson PT, Betts KE, Radeke MJ, Hageman GS, Anderson DH, Johnson LV (2006) Individuals homozygous for the age-related macular degeneration risk-conferring variant of complement factor H have elevated levels of CRP in the choroid. Proc Natl Acad Sci U S A 103(46):17456–17461
8. Pickering MC, Cook HT, Warren J, Bygrave AE, Moss J, Walport MJ, Botto M (2002) Uncontrolled C3 activation causes membranoproliferative glomerulonephritis in mice deficient in complement factor H. Nat Genet 31(4):424–428
9. Coffey PJ, Gias C, McDermott CJ, Lundh P, Pickering MC, Sethi C, Bird A, Fitzke FW, Maass A, Chen LL, Holder GE, Luthert PJ, Salt TE, Moss SE, Greenwood J (2007) Complement factor H deficiency in aged mice causes retinal abnormalities and visual dysfunction. Proc Natl Acad Sci U S A 104(42):16651–16656
10. Lundh von Leithner P, Kam JH, Bainbridge J, Catchpole I, Gough G, Coffey P, Jeffery G (2009) Complement factor h is critical in the maintenance of retinal perfusion. Am J Pathol 175(1):412–421
11. Foley S, Li B, Dehoff M, Molina H, Holers VM (1993) Mouse Crry/p65 is a regulator of the alternative pathway of complement activation. Eur J Immunol 23(6):1381–1384
12. Quigg RJ, He C, Lim A, Berthiaume D, Alexander JJ, Kraus D, Holers VM (1998) Transgenic mice overexpressing the complement inhibitor crry as a soluble protein are protected from antibody-induced glomerular injury. J Exp Med 188(7):1321–1331
13. Wyss-Coray T, Yan F, Lin AH, Lambris JD, Alexander JJ, Quigg RJ, Masliah E (2002) Prominent neurodegeneration and increased plaque formation in complement-inhibited Alzheimer's mice. Proc Natl Acad Sci U S A 99(16):10837–10842

14. Ding JD, Lin J, Mace BE, Herrmann R, Sullivan P, Bowes Rickman C (2008) Targeting age-related macular degeneration with Alzheimer's disease based immunotherapies: anti-amyloid-beta antibody attenuates pathologies in an age-related macular degeneration mouse model. Vision Res 48(3):339–345
15. Johnson LV, Leitner WP, Rivest AJ, Staples MK, Radeke MJ, Anderson DH (2002) The Alzheimer's A beta -peptide is deposited at sites of complement activation in pathologic deposits associated with aging and age-related macular degeneration. Proc Natl Acad Sci U S A 99(18):11830–11835
16. Ding JD, Kelly U, Smith SG, Groelle M, Bowes Rickman C (2011) Development and characterization of humanized complement factor H (CFH) transgenic mice. Association for Research in Vision and Ophthalmology:Abstract 958
17. Ufret-Vincenty RL, Aredo B, Liu X, McMahon A, Chen PW, Sun H, Niederkorn JY, Kedzierski W (2010) Transgenic mice expressing variants of complement factor H develop AMD-like retinal findings. Invest Ophthal Vis Sci 51(11):5878–5887
18. Malek G, Johnson LV, Mace BE, Saloupis P, Schmechel DE, Rickman DW, Toth CA, Sullivan PM, Bowes Rickman C (2005) Apolipoprotein E allele-dependent pathogenesis: a model for age-related retinal degeneration. Proc Natl Acad Sci U S A 102(33):11900–11905
19. Ding JD, Johnson LV, Herrmann R, Farsiu S, Smith SG, Groelle M, Mace BE, Sullivan P, Jamison JA, Kelly U, Harrabi O, Bollini SS, Dilley J, Kobayashi D, Kuang B, Li W, Pons J, Lin JC, Rickman CB (2011) Anti-amyloid therapy protects against retinal pigmented epithelium damage and vision loss in a model of age-related macular degeneration. Proc Natl Acad Sci U S A 108(28):E279–E287

# Chapter 29
# Prolonged Src Kinase Activation, a Mechanism to Turn Transient, Sublytic Complement Activation into a Sustained Pathological Condition in Retinal Pigment Epithelium Cells

**Bärbel Rohrer, Kannan Kunchithapautham, Andreas Genewsky and Olaf Strauß**

**Abstract** Age-related macular degeneration (AMD) is a slowly progressing multifactorial disease involving genetic abnormalities and environmental insults. Genetic studies have demonstrated that polymorphisms in different complement proteins increase the risk for developing AMD. Previously, we have shown that in retinal pigment epithelium (RPE) monolayers, exposure to oxidative stress reduced complement inhibition on the cell surface, with the resulting increase in complement activation leading to vascular endothelial growth factor (VEGF) release and VEGF-receptor-2-mediated disruption of the monolayer barrier function. Complement activation was found to be sublytic and transient and require the assembly of the membrane attack complex (MAC). Here, we asked how this transient, sublytic complement activation could trigger long-term pathological changes in RPE cells. The initial activation of the L-type voltage-gated calcium channels was followed by calcium influx and activation of several kinases. While Erk/Ras activation was

B. Rohrer (✉) · K. Kunchithapautham
Department of Ophthalmology, Medical University of South Carolina,
167 Ashley Ave, SEI614, 29425 Charleston, SC, USA
e-mail: rohrer@musc.edu

K. Kunchithapautham
e-mail: kunchit@musc.edu

B. Rohrer
Research Service, Ralph H. Johnson VA Medical Center, 29401 Charleston, SC, USA

A. Genewsky · O. Strauß
Department of Experimental Ophthalmology,
Klinikum der Universitaet Regensburg, Regensburg, Germany
e-mail: andreas_genewsky@mpipsykl.mpg.de

O. Strauß
Experimental Ophthalmology, Department of Ophthalmology,
Charite Universitaetsmedizin Berlin, Berlin, Germany
e-mail: olaf.strauss@charite.de

J. D. Ash et al. (eds.), *Retinal Degenerative Diseases,* Advances in Experimental Medicine and Biology 801, DOI 10.1007/978-1-4614-3209-8_29,

found to be transient, Src kinase phosphorylation was sustained. We have shown previously that Src kinase controls VEGF release from RPE cells by altering the activity of the L-type channel. We propose that the prolonged Src kinase activation, and its resulting effects on membrane depolarization and calcium influx, leads to sustained VEGF secretion. In addition, the previously shown effect of the autocrine positive feedback loop in RPE cells, involving VEGF-induced VEGF production and secretion via VEGFR-2 receptors, will augment and prolong the effects of sublytic complement activation. In summary, identification of the links between oxidative stress, chronic, low-grade activation of the complement system, and elevated VEGF expression and secretion might offer opportunities to selectively inhibit pathological VEGF release only.

**Keywords** Complement activation · Vascular endothelial growth factor · Voltage-dependent calcium channel · Calcium imaging · Patch clamp analysis

## 29.1 Introduction

Age-related macular degeneration (AMD) has been described as the leading cause of vision loss in the elderly of industrialized nations [1]. The progressive vision loss results from damage to the photoreceptor cells in the central area of the retina, the macula. Damage to the photoreceptors can be caused by two mechanisms, severe damage or loss of retinal pigment epithelium (RPE, atrophic, dry AMD) or choroidal neovascularization and leakage of these new vessels (neovascular, wet AMD). Both forms of AMD are associated with pathological lesions at the RPE/choroid interface in the macular region [2]; and both are associated with the same environmental and genetic risk factors, persistent oxidative stress [3] and polymorphisms in genes including those for complement proteins [4]. The complement cascade is part of the innate and adaptive immune system [5]. Its normal role is to eliminate pathogens by recognizing and binding to nonself cell surface molecules to initiate the complement cascade ultimately leading to cell lysis. While self-cells are protected by both soluble and membrane-bound complement inhibitors, this protection may be compromised under pathological conditions.

We have previously formulated a dual-hit hypothesis in RPE cell damage, which is based on work initially collected in ARPE-19 cells [6] and confirmed in primary RPE cells [7]. Oxidative stress was found to reduce the levels of membrane-bound complement inhibitors CD55 and CD59 and eliminate the activity of complement factor H to reduce C3 deposition on the cell surface. Together, these two impairments sensitize the RPE to complement attack, resulting in sublytic membrane attack complex (MAC) activation, the final step in the complement cascade. Sublytic MAC in RPE cells results in increased vascular endothelial growth factor (VEGF) release, which by acting on apically located VEGF-R2 receptors impairs RPE barrier function. Loss of barrier function could facilitate choroidal neovascularization and might impair other essential RPE cell function(s). Here, we further examined the immediate and transient effects of complement activation.

## 29.2 Results

### *29.2.1 Sublytic MAC Leads to Transient Activation of Mitogen-Activated Protein (MAP) Kinases Known to Be Involved in Regulating Stimulated VEGF Secretion*

Our initial observation is that sublytic MAC activation results in increased VEGF release from the apical and basal side of the RPE [6]. Furthermore, we have shown that VEGF secretion can be controlled by the activity of voltage-gated L-type $Ca^{2+}$ channels, which themselves are activated by Src kinase [8]; Klettner and Roider have shown that VEGF secretion from RPE cells is controlled by two pathways: P38 MAP kinase controls constitutive secretion whereas Erk- and Ras-kinase signaling controls stimulated secretion [9]. These two mechanisms were explored in our recent publication [10], using ARPE-19 cells grown as monolayers on permeable membrane inserts. Using Western blotting with appropriate antibodies that recognize the active form of the respective kinase (Erk, Src, and P38 MAP kinase) or the kinase itself (Ras), we established that oxidative stress generated by 0.5 mM $H_2O_2$ together with 25 % complement sufficient normal human serum (NHS) leads to rapid activation of Erk/Ras and Src, but not of P38 MAP kinase. Treatment with either $H_2O_2$ or NHS alone had no effect. Ras and Erk activation was found to be transient, returning to baseline levels by 10 min, whereas Src activity was prolonged (60 min was the longest time point examined). Utilizing enzyme-linked immunosorbent assays (ELISA) to measure the amount of VEGF secreted apically from RPE cell monolayers, it was confirmed that VEGF secretion 4 h after stimulation is low in control cells and cells treated with either $H_2O_2$ or NHS alone. In the presence of $H_2O_2$ + NHS, VEGF secretion is increased > 100-fold. However, in the presence of $H_2O_2$ + NHS plus inhibitors (nifedipine for L-type channels; U0124 for Erk; FTS for Ras; PP1 for Src), VEGF secretion is significantly reduced. SB203580, the inhibitor of P38 MAP kinase, however, had no effect on modulating $H_2O_2$ + NHS-mediated VEGF secretion. As VEGF triggers disruption of monolayer barrier function via VEGF-R2, VEGF secretion levels were found to correlate with barrier properties of the RPE cell monolayers [10].

### *29.2.2 Oxidative Stress and Complement Activation Modulate L-type $Ca^{2+}$ Channel Activity and Membrane Potential*

Sublytic complement activation by $H_2O_2$ + NHS was found to involve the complement C7 protein, an essential component of the MAC. The fully assembled MAC (C5b6-9) has been shown to form nonspecific pores in unprotected cell membranes, which are permeable to calcium ions ($Ca^{2+}$) [11] and small molecules. Other, nonlytic effects of MAC have been observed, depending on the cellular context [12]. In unpublished experiments (Rohrer B., Kunchithapautham K., Genewsky A., and

Strauß O. 2011, 2012), we have analyzed intracellular $Ca^{2+}$ levels using Fura-2 imaging. Fura-2 is a ratiometric fluorescent dye that binds free, intracellular $Ca^{2+}$. Upon NHS stimulation in the presence or absence of oxidative stress, within a minute, the $Ca^{2+}$ signal rapidly and transiently increased, followed by a prolonged plateau phase. A detailed analysis of the $Ca^{2+}$ signal revealed that both phases were dependent upon heat-labile compounds in serum, since heat-inactivating (HI) NHS completely abolished the $Ca^{2+}$ signal. If the intracellular free $Ca^{2+}$ measured here were to enter the cells through a MAC pore, the $Ca^{2+}$ ions would be expected to carry positive charges, leading to membrane depolarization. Membrane potential was assessed by patch-clamp analysis of ARPE-19 cells. Current clamp recordings revealed that after a transient hyperpolarization of the cell, NHS application resulted in a sustained depolarization. Thus, the transient phase of $Ca^{2+}$ elevation is correlated with the transient hyperpolarization of the cell whereas the prolonged phase of $Ca^{2+}$ elevation is correlated with the prolonged depolarization of the membrane potential. Hence, the transient $Ca^{2+}$ elevation cannot be due to the influx of $Ca^{2+}$ through MAC pores. How about the prolonged phase of $Ca^{2+}$ elevation? In the presence of an L-type channel inhibitor, Bayk8644, the plateau phase of the $Ca^{2+}$ signal is eliminated, with only the transient phase of the signal remaining. Thus, the prolonged phase is carried by L-type channel activation. Analysis of L-type channel (Cav1.3) phosphorylation revealed that Cav1.3 phosphorylation occurs within 5 min after exposure to $H_2O_2$ + NHS whereas only minimal increase in phosphorylation occurs upon exposure to $H_2O_2$ + HI serum. Taken together, sublytic Mac does not appear to involve pore formation; rather the two phases of the $Ca^{2+}$ signal are carried by intracellular $Ca^{2+}$ release (transient signal, mechanism to be determined) and L-type channel activation (prolonged signal).

## 29.3 Discussion

Overall, the study was designed to explore how a sublytic MAC signal might be translated into a sustained pathological signal. In previous experiments [6], we have shown that exposure to $H_2O_2$ + NHS leads to complement activation, requiring participation of the alternative pathway amplification loop as well as components of the MAC. This activation was considered sublytic, since no cell death was observed, as well as transient, since MAC could be identified within less than 30 min in the supernatant of $H_2O_2$ + NHS treated as opposed to control cells. Yet effects on VEGF secretion, gene expression, and barrier function were long lasting [6]. The results outlined here provide a hypothesis for a mechanism how sublytic MAC might exert long-term effects on the regulated VEGF secretory pathway (Fig. 29.1). Complement activation triggers rapid (observable 1 min after exposure) responses, which include membrane hyperpolarization and the development of $Ca^{2+}$ transients due to intracellular free $Ca^{2+}$ increase. The increases in intracellular free $Ca^{2+}$ presumably lead to the activation of kinases. Transient Erk/Ras signaling might be mediating an immediate, but transient phase of regulated VEGF secretion. However,

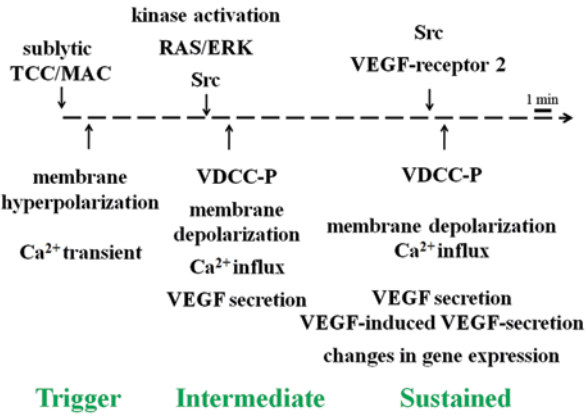


**Fig. 29.1** Summary on a proposed mechanism how sublytic MAC triggers long-term effects on regulated vascular endothelial growth factor (*VEGF*) secretory pathways by modulating Src kinase and voltage-dependent calcium channels (*VDCC*) activity

since prolonged Src activity also results in Cav1.3 phosphorylation which increases the L-type channel activity and leads to significant $Ca^{2+}$ influx concomitant with membrane depolarization, VEGF secretion could become sustained. Two additional mechanisms that have been identified, but were not described here, contribute to the development of a sustained pathological environment. Sublytic MAC activation leads to an increase in VEGF messenger RNA (mRNA) production presumably via $Ca^{2+}$ or kinase signaling, and VEGF secretion is augmented via VEGF-induced VEGF secretion mediated via the VEGF-R2 receptor [6]. Taken together, prolonged Src kinase activation and the voltage-dependent calcium channels (VDCC) are a link to turn the transient sublytic MAC signal into a sustained pathological environment.

Current therapies for AMD are limited. The main target for the treatment of early dry AMD is oxidative stress (e.g., [13]) whereas patients suffering from late-stage dry AMD (geographic atrophy) have no treatment available. The wet form of AMD can currently be treated by interrupting blood vessel growth (summarized in [14]), accomplished most successfully by depriving vessels of their essential growth factor, VEGF, using various VEGF-inhibitors [15]. However, VEGF is an important trophic factor for all ocular tissues, including the RPE [16, 17]. In addition, anti-VEGF-based therapy does fail, and failure seems to correlate with high-risk alleles in the complement inhibitor complement factor H, the mitochondrial age-related maculopathy susceptibility protein 2 (ARMS2), and vascular endothelial growth factor A (VEGFA) [18]. Hence, identifying pathways involved in pathology, specifically those involved in triggering the release of pathological levels of VEGF (e.g., mediated via Ras/Erk and Src) is crucial for the development of alternative treatments for AMD. Targeting complement activation in AMD at the level of the RPE by increasing the level of either CD59 [19] or complement factor H [6] both of which would prevent or reduce complement activation, reduce VEGF secretion,

stabilize the RPE, and generate a healthier RPE cell environment might prove to be suitable for breaking the vicious cycle between oxidative stress and inflammation thought to contribute to AMD pathology [20].

**Acknowledgments** This work was supported in part by the National Institutes of Health (R01EY019320), Veterans Affairs (I01 RX000444), Foundation Fighting Blindness, and an unrestricted grant to MUSC from Research to Prevent Blindness. The authors have no financial conflicts of interest.

## References

1. Council N (1999) Vision research-a national plan: 1999–2003, In: A report of the National Advisory Eye Council of the National Eye Institute, National Institutes of Health. Washington, DC. https://www.nei.nih.gov/resources/strategicplans/nei_vision_report.pdf
2. Nowak JZ (2006) Age-related macular degeneration (AMD): pathogenesis and therapy. Pharmacol Rep 58:353–363
3. Snodderly DM (1995) Evidence for protection against age-related macular degeneration by carotenoids and antioxidant vitamins. Am J Clin Nutr 62(6 Suppl):1448S–1461S
4. Charbel Issa P, Chong NV, Scholl HP (2011) The significance of the complement system for the pathogenesis of age-related macular degeneration-current evidence and translation into clinical application. Graefes Arch Clin Exp Ophthalmol 249:163–174
5. Muller-Eberhard HJ (1988) Molecular organization and function of the complement system. Annu Rev Biochem 57:321–347
6. Thurman JM, Renner B, Kunchithapautham K, Ferreira VP, Pangburn MK, Ablonczy Z et al (2009) Oxidative stress renders retinal pigment epithelial cells susceptible to complement-mediated injury. J Biol Chem 284:16939–16947
7. Bandyopadhyay M, Rohrer B (2012) Matrix metalloproteinase activity creates pro-angiogenic environment in primary human retinal pigment epithelial cells exposed to complement. Invest Ophthalmol Vis Sci 53:1953–1961
8. Rosenthal R, Heimann H, Agostini H, Martin G, Hansen LL, Strauss O (2007) $Ca^{2+}$ channels in retinal pigment epithelial cells regulate vascular endothelial growth factor secretion rates in health and disease. Mol Vis 13:443–456
9. Klettner A, Roider J (2009) Constitutive and oxidative-stress-induced expression of VEGF in the RPE are differently regulated by different Mitogen-activated protein kinases. Graefes Arch Clin Exp Ophthalmol 247:1487–1492
10. Kunchithapautham K, Rohrer B (2011) Sublytic membrane-attack-complex (MAC) activation alters regulated rather than constitutive vascular endothelial growth factor (VEGF) secretion in retinal pigment epithelium monolayers. J Biol Chem 286:23717–23724
11. Sala-Newby GB, Taylor KM, Badminton MN, Rembold CM, Campbell AK (1998) Imaging bioluminescent indicators shows $Ca^{2+}$ and ATP permeability thresholds in live cells attacked by complement. Immunology 93:601–609
12. Cole DS, Morgan BP (2003) Beyond lysis: how complement influences cell fate. Clin Sci (Lond) 104:455–466
13. Bartlett H, Eperjesi F (2003) Age-related macular degeneration and nutritional supplementation: a review of randomised controlled trials. Ophthalmic Physiol Opt 23:383–399
14. Augustin AJ, Scholl S, Kirchhof J (2009) Treatment of neovascular age-related macular degeneration: Current therapies. Clin Ophthalmol 3:175–182
15. Stewart MW (2012) Clinical and differential utility of VEGF inhibitors in wet age-related macular degeneration: focus on aflibercept. Clin Ophthalmol 6:1175–1186

16. Saint-Geniez M, Maharaj AS, Walshe TE, Tucker BA, Sekiyama E, Kurihara T et al (2008) Endogenous VEGF is required for visual function: evidence for a survival role on Muller cells and photoreceptors. PLoS ONE 3:e3554
17. Alon T, Hemo I, Itin A, Pe'er J, Stone J, Keshet E (1995) Vascular endothelial growth factor acts as a survival factor for newly formed retinal vessels and has implications for retinopathy of prematurity. Nat Med 1:1024–1028
18. Smailhodzic D, Muether PS, Chen J, Kwestro A, Zhang AY, Omar A et al (2012) Cumulative effect of risk alleles in CFH, ARMS2, and VEGFA on the response to ranibizumab treatment in age-related macular degeneration. Ophthalmology 119:2304–2311
19. Cashman SM, Ramo K, Kumar-Singh R (2011) A non membrane-targeted human soluble CD59 attenuates choroidal neovascularization in a model of age-related macular degeneration. PLoS ONE 6:e19078
20. Zarbin MA, Rosenfeld PJ (2010) Pathway-based therapies for age-related macular degeneration: an integrated survey of emerging treatment alternatives. Retina 30:1350–1367

# Chapter 30
# Inflammation in Age-Related Macular Degeneration

**Ema Ozaki, Matthew Campbell, Anna-Sophia Kiang, Marian Humphries, Sarah L. Doyle and Peter Humphries**

**Abstract** Age-related macular degeneration (AMD) is the leading cause of legal blindness in elderly individuals in the developed world, affecting 30–50 million people worldwide. AMD primarily affects the macular region of the retina that is responsible for the majority of central, color and daytime vision. The presence of drusen, extracellular protein aggregates that accumulate under the retinal pigment epithelium (RPE), is a major pathological hallmark in the early stages of the disease. The end stage 'dry' and 'wet' forms of the disease culminate in vision loss and are characterized by focal degeneration of the RPE and cone photoreceptors, and choroidal neovascularization (CNV), respectively. Being a multifactorial and genetically heterogeneous disease, the pathophysiology of AMD remains unclear, yet, there is ample evidence supporting immunological and inflammatory processes. Here, we review the recent literature implicating some of these immune processes in human AMD and in animal models.

**Keywords** Age-related macular degeneration · Inflammation · Drusen · Immune cells · Chemokine signaling

---

E. Ozaki (✉) · M. Campbell · A.-S. Kiang · M. Humphries · S. Doyle · P. Humphries
Ocular Genetics Unit, Smurfit Institute of Genetics, Trinity College Dublin, Ireland

Department of Clinical Medicine, School of Medicine, Trinity College Dublin, Ireland

National Childrens Research Centre, Our Ladys Childrens Hospital, Crumlin, Dublin 12, Ireland
e-mail: ozakie@tcd.ie

M. Campbell
e-mail: Matthew.Campbell@tcd.ie

A.-S. Kiang
e-mail: skiang@tcd.ie

M. Humphries
e-mail: mhumphri@tcd.ie

S. L. Doyle
e-mail: doyles8@tcd.ie

P. Humphries
e-mail: pete.humphries@tcd.ie

J. D. Ash et al. (eds.), *Retinal Degenerative Diseases,* Advances in Experimental Medicine and Biology 801, DOI 10.1007/978-1-4614-3209-8_30,

**Abbreviations**

| | |
|---|---|
| AMD | Age-related macular degeneration |
| RPE | Retinal pigment epithelium |
| CNV | Choroidal neovascularization |
| CEP | Carboxyethylpyrrole |
| BRB | Blood retinal barrier |
| MSA | Mouse serum albumin |
| IL | Interleukin |
| CCDKO | Ccl2/Cx3cr1 double knockout |
| Crb1 | Crumbs-like 1 |
| DAMPs | Danger-associated molecular patterns |
| NLRs | Nod-like receptors |
| NLRP3 | NLR family, pyrin domain containing 3 |

## 30.1 Introduction

Age-related macular degeneration (AMD) is a progressive disease of the retina and is the leading cause of vision loss in elderly individuals in the industrialized world. Early clinical signs of disease are the presence of drusen accumulating between the retinal pigment epithelium (RPE) and Bruch's membrane. Some of the first studies implicating the role of the immune system in AMD came from the extensive analysis of drusen constituents and its immunoreactivity for immunoglobulins and complement components. Lipid, protein, carbohydrate and cellular components have all been found, many of which are made locally in the eye, but extraocular proteins are also present. Several of the molecules can modulate immune responses or are involved in acute phase responses, including amyloid P component, vitronectin and apolipoprotein E, and nearly every component of the complement system has been found. Carboxyethylpyrrole (CEP)-protein adducts, which are oxidative stress-related protein modifications and advanced glycation end products have also been identified [1].

The physiology and structure of the retina and choroid change as AMD progresses. Atrophy as well as hypertrophy of the RPE cells are observed along with thickening of Bruch's membrane, making it less permeable. These changes ultimately lead to the degeneration of photoreceptor cells in the macula and culminate in vision loss. This end-stage blinding form of the disease is known as geographic atrophy. Initially, all AMD patients exhibit the dry form, but in ~10% of patients, the disease suddenly switches to the wet form, characterized by CNV. CNV occurs when endothelial cells begin to proliferate in the choroid and angiogenic blood vessels grow through a break in Bruch's membrane and enter the RPE. These vessels are leaky and often hemorrhage causing almost immediate central retinal blindness.

As a multifactorial disease, AMD pathogenesis involves a range of environmental factors such as age, smoking and diet that integrate with genetic predispositions.

Together, they modify and disrupt various homeostatic pathways and eventually lead to AMD disease progression. Inflammation and immune regulation are key pathways that constantly recur and integrate with other processes in the manifestation of this disorder.

## 30.2 Inflammation and Autoimmunity

Inflammation is a defensive biological response of the body to dangerous stimuli such as pathogens, damaged cells or irritants. The inflammatory response in the central nervous system is characterized by increased pro-inflammatory cytokine concentration, blood-brain-barrier permeability and leukocyte invasion, and activation of neuroglia. It is now widely accepted that inflammation plays a vital role in AMD pathogenesis. The retina is a purported 'immune privileged' site, protected by the blood-retinal barrier (BRB), ocular anti-inflammatory and anti-immune proteins and the anterior chamber-associated immune deviation. However, it is now evident that peripheral immune cells can invade the intact BRB and resident immune cells inhabit the retina.

Yet, due to the higher degree of immune protection compared to other organs, when immune cells invade the retina, some sense ocular antigens as 'not-self' resulting in autoantibody production. Indeed, studies have shown that the sera of patients with early and wet forms of AMD have significantly higher levels of anti-retinal autoantibodies [2]. It is not clear, however, if these autoantibodies play a primary causative role in AMD or if they are products generated during the disease process. Nevertheless, their importance in AMD pathogenesis is highlighted in studies where mice immunized with CEP-adducted to mouse serum albumin (CEP-MSA), show complement component C3 deposition in Bruch's membrane along with drusen accumulation, and ultimately AMD-like lesions, features of which are not observed in mice lacking T- and B-lymphocytes [3].

An important concept in age-related diseases is para-inflammation [4]. Tissues generally experience noxious stress conditions and the innate immune system is alerted to restore tissue homeostasis. The response elicited, known as para-inflammation, is generally between that of basal and inflammatory states and is thought to be beneficial for the host. However, if tissue malfunction is sustained over long periods, para-inflammation can become chronic and maladaptive, causing disease pathology. The retina undergoes a vast amount of pathophysiological changes with age, including the formation of oxidized lipids, proteins and DNA, a decrease in neuronal and RPE cell number, accumulation of lipofuscin, increased Bruch's membrane thickness and breakdown of the BRB. Thus, para-inflammation is induced to restore retinal homeostasis. But in AMD the balance between stress-induced damage and para-inflammation is often disrupted due to environmental and genetics factors, resulting in a chronic inflammatory state.

## 30.3 Involvement of Immune Cells and Chemokine Signaling

Although it is evident that inflammatory cells are present in regions of Bruch's membrane breakdown, RPE atrophy and CNV lesions in AMD, there remains a lot of debate to whether they play a causative or adaptive/protective role. While neutrophils have not yet been reported in human CNV specimens, they have been shown to infiltrate lesions in the laser-induced CNV mouse model and correlate with elevated transcript levels of neutrophil chemotactic proteins. Neutrophil depletion was shown to reduce CNV size with a concomitant decrease in vascular endothelial growth factor protein expression [5]. Similar observations have also been seen with macrophage depletion. More recently, a group using Ccl2 siRNA showed decreased monocyte/microglia recruitment to the injured retina after bright continuous light exposure and a reduction in photoreceptor death [6]. In contrast, others have found a protective role for macrophages in CNV development. In one study, *Ccr2*$^{-/-}$ *or Ccl2*$^{-/-}$ mice that have defects in macrophage mobilization were shown to accumulate typical AMD features including CNV [7]. In another study, *interleukin-(Il)-10*$^{-/-}$ mice that exhibit increased macrophage recruitment were shown to have a decreased susceptibility to CNV development [8], an effect blocked by inhibition of macrophage entry using neutralizing antibodies or by IL-10 supplementation.

Other immune cells that may play a role in AMD are the resident immune cells in the retina, the microglia, that have roles in neuronal homeostasis and immune surveillance. Microglia are normally absent from the outer retina but with age and in AMD, they infiltrate into subretinal space and get activated, probably to support the RPE and clear age-related debris. However, they may also induce oxidative stress and promote further degeneration. Two chemokines, CX3CL1 and CCL2, and their respective receptors, CX3CR1 and CCR2, play important functions in macrophage/microglia recruitment to tissue lesions, and in the retina, they have been shown to direct the dynamics and redistribution of resting microglia during ageing, injury and stress. Indeed, numerous studies have shown that a single nucleotide polymorphism in the *Cx3cr1* gene, M280, is associated with impaired cell migration and an enhanced AMD risk [9]. Aqueous concentrations of CCL2 have also been shown to be elevated in AMD patients, levels of which correlated with macular thickness [10].

The role of microglia in AMD pathogenesis has also been explored using *Cx3cr1*$^{-/-}$ and *Ccl2/Cx3cr1* double knockout (CCDKO) mice. *Cx3cr1*$^{-/-}$ mice have been shown to accumulate drusen-like deposits and microglia in subretinal space after laser-induced injury that exacerbates CNV [11]. Other studies have used the CCD-KO mouse model and have found that AMD-like lesions, drusen deposits, Bruch's membrane thickening and photoreceptor atrophy develop by 6 weeks of age, with CNV occurring in ~15% of animals [12].

An important consideration, which may explain some of these contradictory findings is that macrophages are not a homogenous population of cells but display different subclasses, namely the M1 and M2 macrophages. M1 macrophages have been shown to be pro-inflammatory with an IL-12$^{high}$, IL-23$^{high}$, IL-10$^{low}$ phenotype, while the M2 macrophages are relatively anti-inflammatory with an IL-12$^{low}$,

IL-23$^{low}$, IL-10$^{high}$ phenotype [13]. Therefore, it is important to investigate which subtypes of macrophages are observed at the various stages of AMD in such studies.

It has recently been reported that the autosomal recessive *rd8* mutation, a single nucleotide deletion in the *Crumbs-like 1 (Crb1)* gene, is present in vendor lines of C57BL/6N mice and embryonic stem cells, and results in a retinal degeneration phenotype that is clinically visible as light-colored spots in the fundus, representing retinal folds, pseudorosettes and focal retinal dysplasia [14]. Many of the *Cx3cr1*$^{-/-}$ and *Ccl2*$^{-/-}$*Cx3cr1*$^{-/-}$ lines contain this mutation and it is speculated to be the cause of the early retinal degeneration phenotype seen in these mice. To understand the contribution of the *rd8* mutation in retinal degeneration in the CCDKO mouse line, a recent study has compared primary and secondary pathological events during AMD pathogenesis in these mice to re-derived *Ccl2* or *Cx3cr1* single knockout lines and *Ccl2/Cx3cr1* double knockout mice, which do not carry the *rd8* mutation [15]. They show the *rd8* mutation as the primary cause of early retinal degeneration in the CCDKO mouse line, but also that the genetic background and the deficiency of *Ccl2* and/or *Cx3cr1* can differentially modulate the retinal phenotype caused by the *rd8* mutation. For example, all *Cx3cr1* deficient mice with the *rd8* mutation exhibit a more severe phenotype than those only deficient in *Ccl2* with *rd8*, which may even exhibit a slight protective effect.

## 30.4 Sterile Inflammation and the Inflammasome

The inflammation observed in AMD is likely to be sterile, i.e., not caused by microorganisms or infectious agents. Sterile inflammation is provoked by endogenous factors called danger-associated molecular patterns (DAMPs) that are not normally found in extracellular space and hidden from the immune system. However, in times of cellular stress or injury, necrotic cell death typically ensues, resulting in the release of intracellular DAMPs, e.g., high-mobility group box 1, heat shock proteins, cholesterol, monosodium urate, ATP, IL-33, IL-1α DAMPs are recognized by a range of germline-encoded pathogen recognition receptors, e.g., Toll-like receptors, C-type lectins, Nod-like receptors (NLRs) and the Rig-I-like receptors.

It has recently been shown that drusen deposits can evoke a sterile inflammatory response mediated through the NLR family, pyrin domain containing 3 (NLRP3) inflammasome [16]. Stimulation of the NLRP3 inflammasome with drusen results in activation of caspase-1 that then cleaves pro-IL-1β and pro-IL-18 into their mature pro-inflammatory forms. Activated caspase-1 and NLRP3 were also observed in macrophages surrounding the drusen-like lesions in mice immunized with CEP-MSA, a dry mouse model of AMD. As NLRP3 activation results in the secretion of highly inflammatory cytokines, inappropriate activation may be detrimental to the host. Interestingly, it was found that laser-induced CNV, is exacerbated in *Nlrp3*$^{-/-}$ and *Il-18*$^{-/-}$, but not *Il-1r1*$^{-/-}$ mice, implicating a protective role for NLRP3 activation and IL-18 secretion. These results suggest that acute inflammation to a certain extent is beneficial in wet-AMD and oppose the current dogma that is directed

at the suppression of inflammatory processes in disease prevention. In support of these observations, recent clinical trials of wet AMD patients treated with infliximab (Remicade), which targets tumor necrosis factor α, resulted in exacerbated symptoms in over 50 % of individuals [17].

## 30.5 Conclusions

There is now escalating data from histopathologic, genetic and animal studies that implicate a strong role of inflammation and immune regulation in AMD development. Not discussed here is the major significance of the complement system in AMD pathogenesis [18]. Polymorphisms in the *Complement factor H* gene remains one of the largest risk factors for AMD and polymorphisms in other complements components and regulators have also been associated with the disease. Additionally, numerous studies have reported that bacterial or viral infections, like *Cytomegalovirus* and *Chlamydia pneumoniae*, are associated with AMD incidence, and may be a risk factor for dry to wet AMD progression, a phenomenon that may be due to latent infection of macrophages with the virus. Interestingly, however, it has recently been observed that pretreatment of mice with a low-dose of lipopolysaccharide is protective in laser-induced CNV [19]. As to whether inflammation plays a beneficial or adverse role in the disease remains elusive and likely depends on the stage of the disease.

## References

1. Crabb JW, Miyagi M, Gu X, Shadrach K, West KA, Sakaguchi H et al (2002) Drusen proteome analysis: an approach to the etiology of age-related macular degeneration. Proc Natl Acad Sci U S A 99(23):14682–14687
2. Patel N, Ohbayashi M, Nugent AK, Ramchand K, Toda M, Chau KY et al (2005) Circulating anti-retinal antibodies as immune markers in age-related macular degeneration. Immunology 115:422–430
3. Hollyfield JG, Bonilha VL, Rayborn ME, Yang X, Shadrach KG, Lu L et al (2008) Oxidative damage-induced inflammation initiates age-related macular degeneration. Nat Med 14:194–198
4. Xu H, Chen M, Forrester JV (2009) Para-inflammation in the aging retina. Prog Retin Eye Res 28:348–368
5. Zhou J, Pham L, Zhang N, He S, Gamulescu MA, Spee C et al (2005) Neutrophils promote experimental choroidal neovascularization. Mol Vis 11:414–424
6. Rutar MV, Natoli RC, Provis JM (2012) Small interfering RNA-mediated suppression of Ccl2 in Muller cells attenuates microglial recruitment and photoreceptor death following retinal degeneration. J Neuroinflammation 9:221
7. Ambati J, Anand A, Fernandez S, Sakurai E, Lynn BC, Kuziel WA et al (2003) An animal model of age-related macular degeneration in senescent Ccl-2- or Ccr-2-deficient mice. Nat Med 9:1390–1397

8. Apte RS, Richter J, Herndon J, Ferguson TA (2006) Macrophages inhibit neovascularization in a murine model of age-related macular degeneration. PLoS Med 3:e310
9. Raoul W, Auvynet C, Camelo S, Guillonneau X, Feumi C, Combadière C et al (2010) CCL2/CCR2 and CX3CL1/CX3CR1 chemokine axes and their possible involvement in age-related macular degeneration. J Neuroinflammation 7:87
10. Jonas JB, Tao Y, Neumaier M, Findeisen P (2010) Monocyte chemoattractant protein 1, intercellular adhesion molecule 1, and vascular cell adhesion molecule 1 in exudative age-related macular degeneration. Arch Ophthalmol 128:1281–1286
11. Combadière C, Feumi C, Raoul W, Keller N, Rodéro M, Pézard A et al (2007) CX3CR1-dependent subretinal microglia cell accumulation is associated with cardinal features of age-related macular degeneration. J Clin Invest 117:2920–2928
12. Chan CC, Ross RJ, Shen D, Ding X, Majumdar Z, Bojanowski CM et al (2008) Ccl2/Cx-3cr1-deficient mice: an animal model for age-related macular degeneration. Ophthalmic Res 40:124–128
13. Olefsky JM, Glass CK (2010) Macrophages, inflammation, and insulin resistance. Annu Rev Physiol 72:219–246
14. Mattapallil MJ, Wawrousek EF, Chan CC, Zhao H, Roychoudhury J, Ferguson TA et al (2012) The rd8 mutation of the Crb1 gene is present in vendor lines of C57BL/6N mice and embryonic stem cells, and confounds ocular induced mutant phenotypes. Invest Ophthalmol Vis Sci 53:2921–2927
15. Luhmann UF, Lange CA, Robbie S, Munro PM, Cowing JA, Armer HE et al (2012) Differential modulation of retinal degeneration by Ccl2 and Cx3cr1 chemokine signalling. PLoS One 7:e35551
16. Doyle SL, Campbell M, Ozaki E, Salomon RG, Mori A, Kenna PF et al (2012) NLRP3 has a protective role in age-related macular degeneration through the induction of IL-18 by drusen components. Nat Med 18:791–798
17. Giganti M, Beer PM, Lemanski N, Hartman C, Schartman J, Falk N (2010) Adverse events after intravitreal infliximab (Remicade). Retina 30:71–80
18. Anderson DH, Radeke MJ, Gallo NB, Chapin EA, Johnson PT, Curletti CR et al (2010) The pivotal role of the complement system in aging and age-related macular degeneration: hypothesis re-visited. Prog Retin Eye Res 29:95–112
19. Matsumura N, Kamei M, Tsujikawa M, Suzuki M, Xie P, Nishida K (2012) Low-dose lipopolysaccharide pretreatment suppresses choroidal neovascularization via IL-10 induction. PLoS One 7:e39890

# Chapter 31
# Impairment of the Ubiquitin-Proteasome Pathway in RPE Alters the Expression of Inflammation Related Genes

**Zhenzhen Liu, Tingyu Qin, Jilin Zhou, Allen Taylor, Janet R. Sparrow and Fu Shang**

**Abstract** The ubiquitin-proteasome pathway (UPP) plays an important role in regulating gene expression. Retinal pigment epithelial cells (RPE) are a major source of ocular inflammatory cytokines. In this work we determined the relationship between impairment of the UPP and expression of inflammation-related factors. The UPP could be impaired by oxidative stress or chemical inhibition. Impairment of the UPP in RPE increased the expression of several inflammatory cytokines, such as IL-6 and IL-8. However, the expression of monocyte chemoattractant protein-1 (MCP-1) and complement factor H (CFH) and was reduced upon impairment of the UPP. These data suggest that impairment of the UPP in RPE may be one of the causes of retinal inflammation and abnormal functions of monocyte and the complement system during the pathogenesis of age-related macular degeneration.

F. Shang (✉) · Z. Liu · T. Qin · A. Taylor · F. Shang
Laboratory for Nutrition and Vision Research, Jean Mayer USDA Human Nutrition Research Center on Aging at Tufts University, Boston, USA
e-mail: fu.shang@tufts.edu

Z. Liu
e-mail: 723179127@qq.com

T. Qin
e-mail: tingyuqin@126.com

A. Taylor
e-mail: allen.taylor@tufts.edu

J. Zhou
Department of Ophthalmology, Columbia University, New York, USA
email: jz219@columbia.edu

J. R. Sparrow
Department of Ophthalmology, Columbia University, New York, USA
e-mail: jrs88@columbia.edu

J. D. Ash et al. (eds.), *Retinal Degenerative Diseases,* Advances in Experimental Medicine and Biology 801, DOI 10.1007/978-1-4614-3209-8_31,

**Keywords** Age-related macular degeneration · Inflammation · Ubiquitin · Proteasome · Retinal pigment epithelial cells · IL-6, IL-8, MCP-1 · Complement factor H

## 31.1 Introduction

Age-related macular degeneration (AMD) is a multifactorial disease and a leading cause of blindness in industrialized countries. The factors that contribute to the onset and progression of AMD include aging, genetic background, cigarette smoking, and dietary patterns [1–7]. It has been proposed that oxidative damage to the retina and retinal pigment epithelial cells (RPE) is a major trigger for the onset and progress of AMD [5, 8, 9]. However, the mechanism for the relationship between oxidative damage and AMD pathogenesis remains to be elusive. Recent studies indicate that innate immunity and inflammation are related to AMD pathogenesis [4, 10]. The evidence for the involvement of innate immunity and inflammation in AMD pathogenesis includes accumulation of immunoglobulin and complement components in drusen [11–13], the association between genetic variants of complement factor H, factor B, C2, C3, factor I, and risk for AMD [14–22], and elevated serum CRP levels in AMD patients [23–25]. Emerging evidence indicates oxidative stress and inflammation is closely related. Oxidative stress may trigger inflammatory response and inflammation also exacerbates oxidative damage [26, 27]. Mechanistic investigation into the causal relationship between oxidative damage and inflammatory response will help to elucidate how oxidative damage triggers the onset and progression of AMD. This information is important for development of novel strategies for prevention or treatment of AMD.

The ubiquitin-proteasome pathway (UPP) is the major non-lysosomal proteolytic pathway within cells [28–31]. Proteins destined for degradation are first conjugated with a polyubiquitin chain by the sequential action of three classes of enzymes: E1, E2, and E3. The ubiquitin-protein conjugates are then recognized and degraded by a large protease complex called the proteasome [29, 32]. The UPP has been involved in a myriad of cellular processes [30, 31, 33], including regulation of immune response and inflammation [34, 35]. Dysfunction of the UPP has been implicated in the pathogenesis of many degenerative diseases such as Alzheimer's disease [36], Parkinson's disease [37], diabetic retinopathy [38], and cataract [39, 40]. A fully functional UPP is required for cells to cope with various stresses, including oxidative stress [41]. However, an extensive oxidative insult also impairs the function of critical components of the UPP [42–47]. Oxidative inactivation of the proteasome not only results in accumulation of damaged proteins [39, 40, 47], but also impairs cell signaling process [48–50]. Our previous work indicates that the proteasome is more susceptible to oxidative inactivation than other components of the UPP. Sustained physiologically relevant levels of oxidative reduce proteasome activity, but not reduce ubiquitin conjugating activities [47, 48]. Oxidative inactivation of the proteasome increases production of IL-8 in cultured RPE [50], suggesting that oxidative inactivation of the proteasome may be a mechanistic link between oxidative stress and inflammation. Since RPE is a major ocular source of pro-inflammatory mediators and a primary

target of photooxidative insult, oxidative impairment of the UPP in RPE may contribute to ocular inflammation and AMD-related lesions. To further explore the relationship between proteasome inactivation and retinal inflammation, we systematically investigated the effect of impairment of the UPP and expression of several inflammation-related factors in cultured RPE. The data indicate that impairment of the UPP by photooxidation or chemical inhibition of the proteasome resulted in an increase in IL-6 and IL-8 expression, and suppressed the expression of complement factor H and MCP-1 by RPE cells, supporting the hypothesis that impairment of the UPP is a mechanistic link between oxidative stress and inflammation and the possible mechanism by which oxidative damage triggers the pathogenesis of AMD.

## 31.2 Materials and Methods

### *31.2.1 Materials*

Cell culture supplies were obtained from Invitrogen (Carlsbad, CA, USA). The DuoSet ELISA kits for human MCP-1, human IL-6 and IL-8, and MG132 were obtained from R&D Systems (Minneapolis, MN, USA). Mouse monoclonal antibody (capture antibody) to human CFH was purchased from Abcam (Cambridge MA, USA) and goat-polyclonal antibody (detecting antibody) to human CFH was purchased from EMD Chemicals (Gibbstown, NJ, USA). All other reagents were obtained from Sigma Aldrich (St. Louis, MO, USA).

### *31.2.2 Exposure to A2E and Blue Light*

ARPE-19 cells were grown to confluence and then cultured in DMEM with 10% heat-inactivated fetal calf serum and 0.1 mM nonessential amino acid solution with or without 10 μM A2E for 14 days. The medium with fresh A2E was changed twice a week. After washing twice with PBS, cell cultures were transferred to PBS with calcium, magnesium, and glucose and were exposed to 430 nm light delivered from a tungsten halogen source (430 nm ± 20; 15 min; 2.62 mW/cm$^2$). The cells were then incubated for an additional 6 h in DMEM with 1% FBS. After collection of the media, cells were washed twice with cold PBS and then the dishes were placed on ice and the cells were harvested with a cell scraper. Cells that had neither accumulated A2E nor been exposed to blue light were used as controls. Cells that had accumulated A2E alone or exposed to blue light along were also tested. The control cells were treated in the same manner as the cells that were exposed to A2E and blue light. Levels of IL6 and IL-8, MCP-1, and CFH in the medium were determined by ELISA. The latter were performed according to the manufacturer's instructions. Total RNA was also isolated from the cells for the quantitation of mRNA levels of IL-6, IL-8, MCP-1, and CFH. To determine the effects of proteasome inhibition on expression and secretion, confluent RPE were treated with 10 μM MG132

for 8 h. Levels of mRNA levels of IL-6, IL-8, MCP-1, and CFH in the cells were determined by RT-PCR and protein levels of these factors in the medium were determined by ELISA as described previously.

### *31.2.3 Proteasome Activity Assay*

ARPE-19 cells were lysed in 25 mM Tris-HCl buffer, pH 7.6. The chymotrypsin-like activity of the proteasome was determined using the fluorogenic peptide succinyl-Leu-Leu-Val-Tyr-amidomethylcoumarin (LLVY-AMC) as a substrate, trypsin-like activity of the proteasome was determined using *N*-*t*-butyloxycarbonyl-Leu-Ser-Thr-Arg-amidomethylcoumarin (LSTR-AMC) as a substrate [51]. The mixture, containing 20 μl of cell supernatant in 25 mM Tris-HCl, pH 7.6, was incubated at 25 °C with respective peptide substrates (25 μM) in a buffer containing 50 mM Tris-HCl, pH 8.0, 100 mM NaCl, 5 mM EDTA, 1 mM EGTA, 3 mM NaN3, and 0.04 % 3-[(3-Cholamidopropyl) dimethylammonio]-1-propanesulfonate (CHAPS). The final volume of the assay was 200 μl. Rates of reactions were measured in a temperature-controlled microplate fluorometric reader. Excitation/emission wavelengths were 380/440 nm. Proteasome activity was defined as the portion of peptidase activity in the cell extracts that was inhibited by 20 μM MG132, a potent proteasome inhibitor.

## 31.3 Results

### *31.3.1 Photooxidation Alters the Expression and Secretion of Inflammation-Related Factors*

To investigate the relationship between oxidative stress and inflammatory response in cultured RPE, we used the physiologically relevant A2E-mediated photooxidation protocol [26, 47, 52, 53] to investigate the effects of oxidative stress on the expression of inflammation-related genes. We chose Il-6, IL-8, MCP-1, and CFH as targets in this study. Exposure of A2E-containing RPE cells to blue light dramatically increased the mRNA levels of IL-6 and IL-8 (Fig. 31.1a, b). The increase in mRNA levels for IL-6 was ~6-fold and the increase in mRNA levels for IL-8 was ~55-fold. In contrast, exposure of A2E-containing RPE to blue light reduced the mRNA levels for MCP-1 and CFH by ~90 % and ~70 %, respectively (Fig. 31.1c, d). Interestingly, accumulation of A2E alone increased mRNA levels of IL-8, MCP-1, and CFH by 2 to 3-fold. Exposure to blue light alone increased mRNA levels for CFH by ~2 fold, but did not alter the expression of other genes. These data indicate photooxidation differentially alters the expression of inflammation-related genes. The data also suggest that A2E accumulation may regulate the expression of IL-8, MCP-1, and CFH independent of photooxidation.

To determine whether A2E-mediated photooxidation also alters the secretion of these inflammation-related factors, we determined the levels of these factors in the

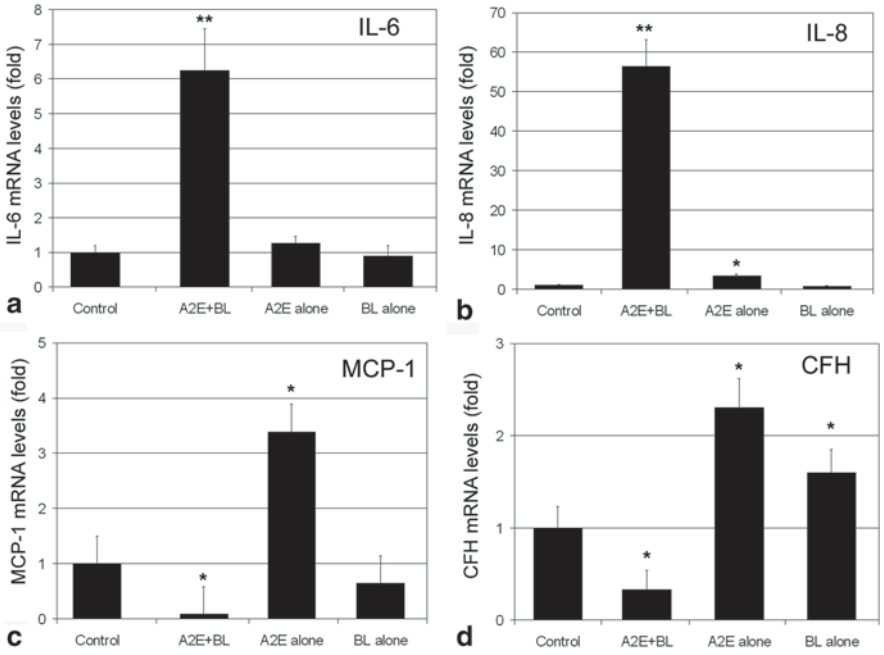


**Fig. 31.1** A2E-mediated photooxidation alters the expression of inflammation-related genes. Confluent cultured ARPE-19 cells were loaded with 10 μM *A2E* for 14 days. The cells were then transferred to PBS and exposed to blue light for 15 min. Cells that accumulated *A2E alone*, exposed to blue light alone, or neither accumulated *A2E* nor exposed to blue light were used as *control*. The cells were then cultured in fresh medium containing 1 % FBS for 6 h. Total RNA were extracted from these cells and levels of *mRNA* for *IL-6*, *IL-8*, *MCP-1*, and *CFH* were determined by RT-PCR. GADPH was used as a reference for relative quantitation. The relative levels of *mRNA* for each gene in control cells were arbitrarily designated as 1 and relative levels of *mRNA* for these genes in treated cells were expressed as fold of that in the *control* cells. The data are mean ± SD of the results from 6 samples in each group. *indicates $p < 0.05$ and ** indicates $p < 0.001$ as compared the control cells that were neither treated with *A2E* nor blue light

medium. As shown in Fig. 31.2, exposure of A2E-containing RPE to blue light resulted in a 20 % and >2-fold increase in levels of IL-6 and IL-8 and a 70–80 % decrease in levels of MCP-1 and CFH in the medium. Accumulation of A2E alone increased the levels of IL-6, IL-8, MCP-1, and CFH marginally (Fig. 31.2), whereas exposure to blue light alone had no significant effect on levels of these inflammation-related factors in the medium.

### *31.3.2 Photooxidation impairs the function of the UPP*

Our previous work showed that the proteasome is the most sensitive component of the UPP to oxidative inactivation [47, 48]. It is also known that the UPP is involved in regulating gene expressions by controlling signaling pathways and levels of transcript

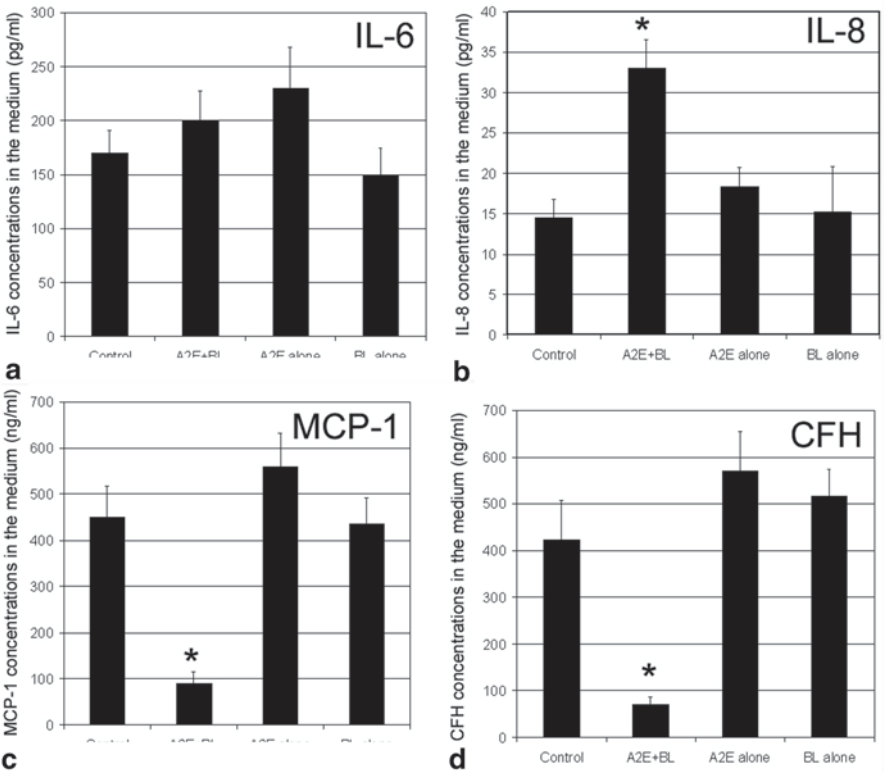


**Fig. 31.2** A2E-mediated photooxidation alters the secretion of inflammation related factors. Confluent cultured ARPE-19 cells were loaded with 10 μM *A2E* for 14 days. The cells were then transferred to PBS and exposed to blue light for 10 min. Cells that accumulated *A2E* alone, exposed to blue light alone, or neither accumulated *A2E* nor exposed to blue light were used as *control*. The cells were then cultured in fresh medium containing 1 % FBS for 6 h. The medium was collected and levels of *IL-6*, *IL-8*, *MCP-1*, and *CFH* in the medium were determined by ELISA. The data are mean ± SD of the results from 6 samples in each group. * indicates $p < 0.01$ as compared the control cells that were neither treated with *A2E* nor blue light

factors. It is plausible that the photooxidation induced changes in expression and secretion of the inflammation-related factors were related to the impairment of the UPP. To confirm previous results that physiologically relevant levels of oxidative stress inactivate the proteasome, we determine the effects of A2E-mediated photooxidation on the chymotrypsin-like and trypsin-like activities of the proteasome. As shown in Fig. 31.3, exposure of A2E-containing RPE to blue light resulted in a 70–80 % decrease in trypsin-like and chymotrypsin-like peptidase activities of the proteasome. Accumulation of A2E alone or exposure to blue light alone had no detectible difference in these peptidase activities of the proteasome. This data confirmed our previous results that the proteasome is a sensitive target of oxidative insults.

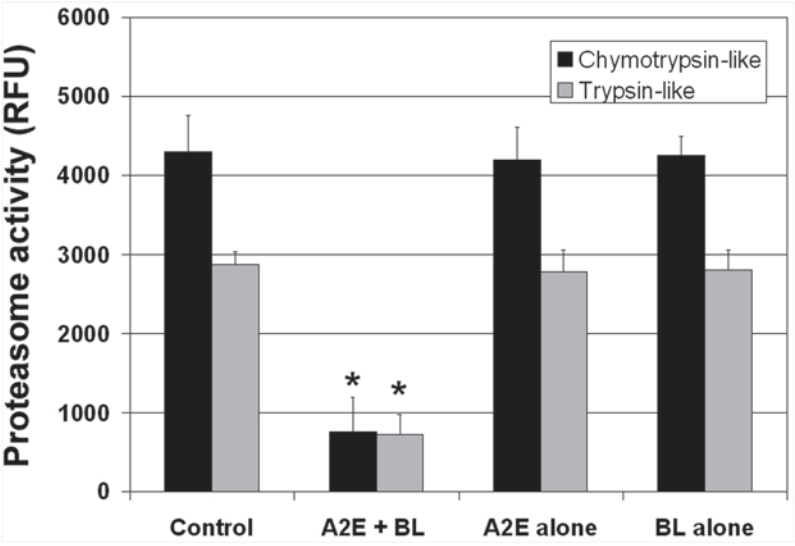


**Fig. 31.3** A2E-mediated photooxidation inactivates the proteasome in cultured RPE. Confluent cultured ARPE-19 cells were loaded with 10 μM *A2E* for 14 days. The cells were then transferred to PBS and exposed to blue light for 15 min and harvested. Cells that accumulated *A2E* alone, exposed to blue light alone, or neither accumulated *A2E* nor exposed to blue light were used as *control*. The *chymotrypsin-like* activity and *trypsin-like* activity of the proteasome in the cells were determined using a fluorogenic peptide as a substrate. The proteasome activity was expressed as increase in the relative fluorescence unit (*RFU*) during a 5 min period. The experiments were repeated twice with triplicates each time. The data are mean ± SD of the results from 6 samples in each group. * indicates $p < 0.001$ as compared the control cells

### *31.3.3 Chemical Inhibition of the Proteasome in RPE Results in Similar Changes to that Caused by Photooxidation in Expression and Secretion of Inflammation-Related Factors*

To test the hypothesis that photooxidation alters the expression and secretion of inflammation-related factors via impairment of the UPP, we inhibited proteasome activity in RPE by MG132 and determined the expression and secretion of these inflammation-related factors. We found that inhibition of proteasome resulted in a dramatic increase in mRNA levels for IL-6 and IL-8 (Fig. 31.4a, b). Levels of mRNA for IL-8 increased over 50-fold upon inhibition of the proteasome (Fig. 31.4b). Similar to photooxidation, proteasome inhibition resulted in a 70–80 % decrease in levels of mRNA for MCP-1 and CFH (Fig. 31.4c, d).

To determine whether proteasome inhibition also alter the secretion of these inflammation-related factors, we determined the levels of these factors in the medium. As shown in Fig. 31.5, inhibition of the proteasome only marginally increased the secretion of IL-6 (Fig. 31.5a), but increased the secretion of IL-8 by > 2-fold

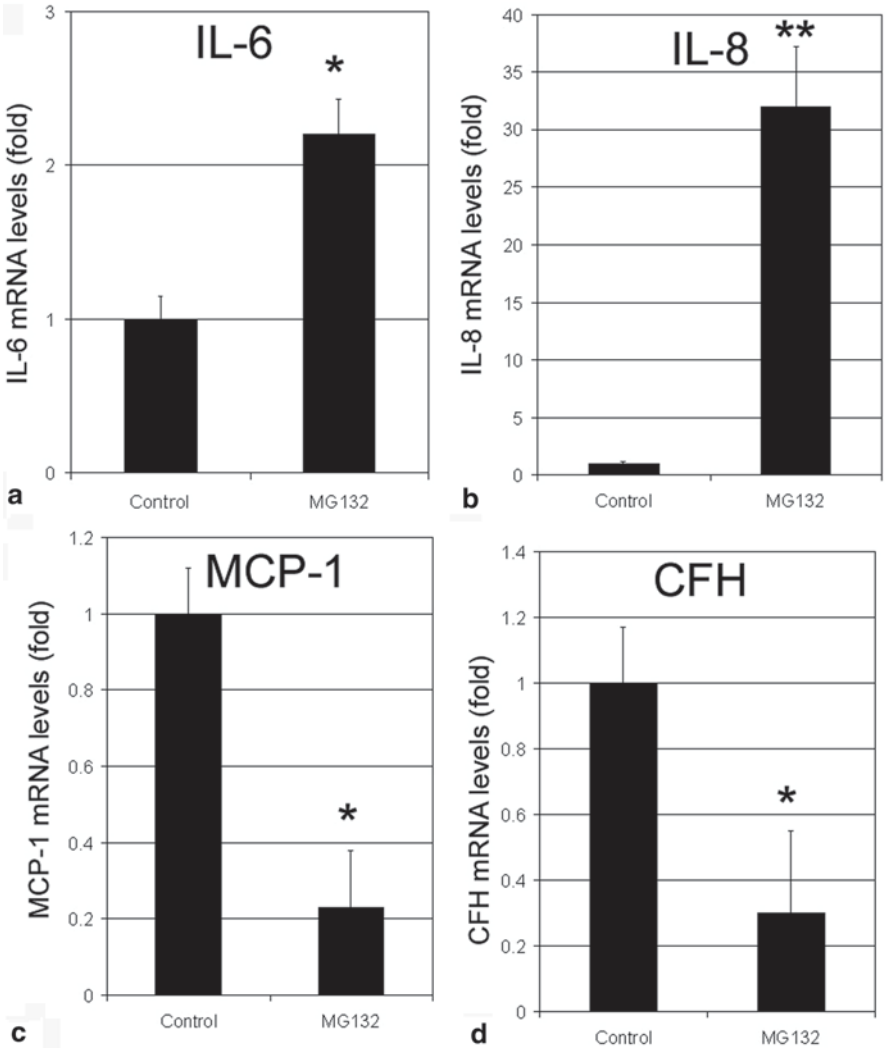


**Fig. 31.4** Inhibition of the proteasome alters the expression of inflammation-related genes. Confluent cultured ARPE-19 cells were incubated in fresh medium in the absence or presence of 10 μM *MG132* for 8 h. Levels of *mRNA* for *IL-6*, *IL-8*, *MCP-1*, and *CFH* in the cells were determined by real-time quantitative RT-PCR using levels of *mRNA* for GAPDH as a reference. The relative levels of *mRNA* for these genes in control cells were arbitrarily designated as 1 and levels of *mRNA* for these genes in *MG132*-treated cells were expressed as fold of that in the *control* cells. The data are mean ± SD of the results from 4 samples in each group. * indicates $p < 0.01$ and ** indicates $p < 0.001$ as compared to the controls

(Fig. 31.5). Consistent with the decrease in mRNA levels, protein levels of MCP-1 and CFH in the medium decreased 80–90% when the proteasome in RPE was inhibited (Fig. 31.5c, d). These data demonstrate that impairment of the UPP in RPE

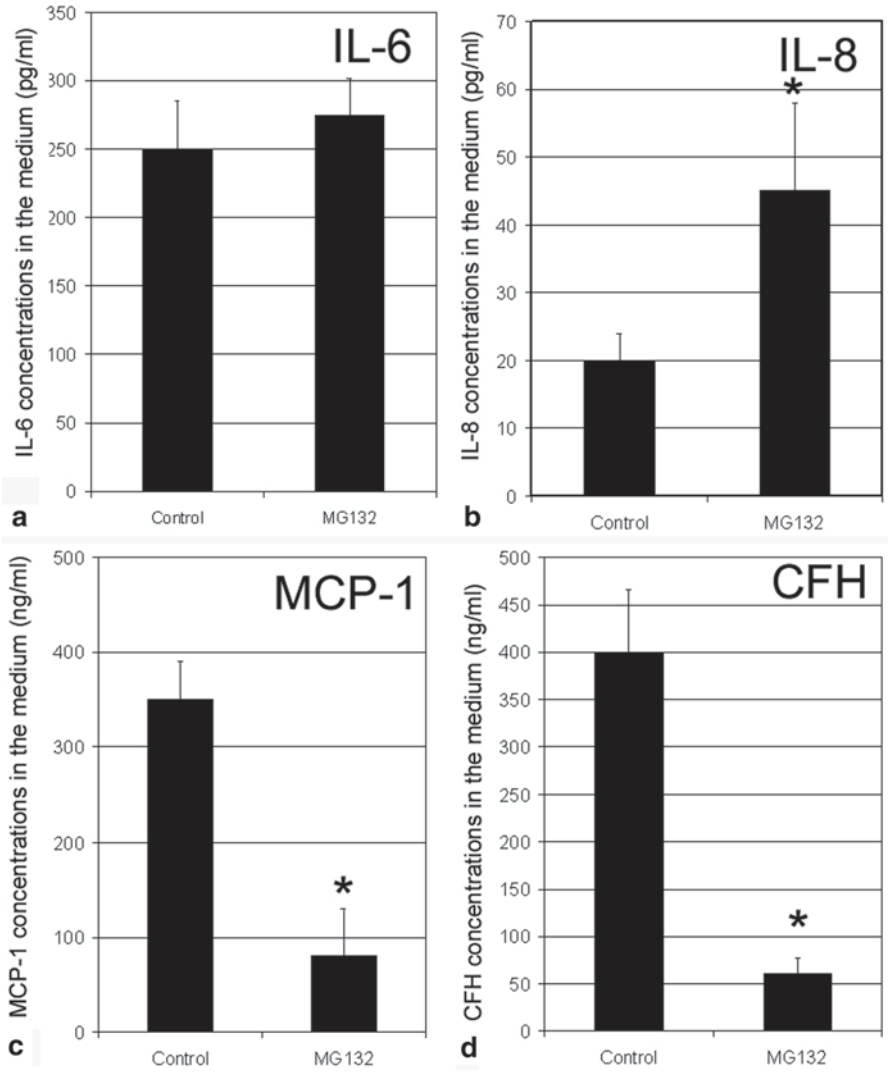


**Fig. 31.5** Inhibition of the proteasome alters secretion of inflammation-related factor by cultured RPE. Confluent cultured ARPE-19 cells were incubated in fresh medium in the absence or presence of 10 μM *MG132* for 8 h. The medium was collected and protein levels of *IL-6*, *IL-8*, *MCP-1*, and *CFH* in medium were determined by ELISA. The data are mean ± SD of the results from 4 samples in each group. * indicates $p < 0.001$ as compared to the controls

alters the expression and secretion of inflammation-related factors in a similar manner as photooxidative stress, suggesting oxidative inactivation of the proteasome is at least one of the mechanisms by which photooxidation alters the expression and secretion of inflammation-related factors by RPE.

## 31.4 Discussion

Oxidative stress and inflammation are interrelated biological events [54] and both are implicated in the pathogenesis of AMD [3, 9, 27]. There is a vicious cycle in which oxidative stress triggers inflammatory responses, and inflammation also enhances the production of reactive oxygen species, all of them cause oxidative damage [55, 56]. Due to high metabolic rate and age-related accumulation of lipofuscin, RPE is a primary target of photooxidative damage in the eye [8]. RPE is also a major source of cytokines that regulate inflammatory response in the retina [50, 57, 58]. The vicious interaction between oxidative stress and inflammatory responses in RPE may contribute to the onset and progression of AMD. Any means that break the vicious cycle between oxidative stress and inflammation in RPE could be a potential strategy for prevention or treatment of AMD.

Results from this study show that photooxidative stress inactivates the proteasome in RPE and subsequently alters the expression of inflammation-related genes, such as up-regulation of IL-6 and IL-8 and down-regulation of MCP-1 and CFH. These data are consistent with our previous work which indicates that inactivation of the proteasome is a mechanistic link between oxidative stress and altered inflammatory responses [49, 50, 59].

An increasing body of evidence indicated dysregulation of inflammatory response, including improper complement activation is involved in the pathogenesis of AMD [10]. Oxidative stress is apparently one of the triggers of dysregulation of inflammatory response and the innate immune system. The data presented in the paper suggest that impairment of the UPP, particularly the proteasome, is an important step for oxidation-induced dysregulation of the inflammatory responses. However, it remains to be determined how impairment of the UPP alters the expression and secretion of these inflammation-related factors. The UPP is involved in many aspects of cellular functions. In addition to selective degradation of damaged or obsolete proteins, the UPP is involved in regulation of signal transduction and expression via controlling the levels of regulatory proteins and transcription factors. For example, UPP-mediated degradation of inhibitors of NF-κB is required for activation of the NF-κB pathway [60–62]. We found that inhibition of the proteasome in RPE suppressed the expression and secretion of MCP-1 and the suppression is related to down regulation of NF-κB signaling pathway [59]. The down-regulation of MCP-1 may have physiological consequences since MCP-1 knockout mice development of AMD-like phenotypes [63]. We also found the inactivation of the proteasome enhances the expression and secretion of IL-8 by activation of p38 signaling pathway [49, 50]. Elevated levels of IL-8 may not only promote inflammation, but also trigger neovascularization, because IL-8 is a neutrophil attractant and a strong pro-angiogenesis factor [64–67]. This study showed that inactivation of the proteasome also contributed to the down-regulation of CFH upon photooxidative stress. Although it is unknown at present how proteasome inhibition suppresses the expression of CFH, it is likely that the proteasome is involved in regulating levels of transcription factors and signaling molecules that control the expression of CFH.

The down-regulation of CFH may play a role in complement activation [26] and complement attack to RPE [68] in response to oxidative stress.

Together, these results show that impairment of the UPP in RPE alters the expression and secretion of inflammation-related factors, suggest that inactivation of the proteasome by oxidation stress may be a mechanistic link between oxidative stress and dysregulation of inflammatory responses. Therefore, to preserve or to improve UPP activity in RPE may be a valid strategy for AMD prevention or treatment.

**Acknowledgment** This work is supported by USDA AFRI Award 2009–35200-05014, NIH grant EY 011717, USDA contract 1950-510000-060-01A.

## References

1. Landrum JT, Bone RA (2001) Lutein, zeaxanthin, and the macular pigment. Arch Biochem Biophys 385(1):28–40
2. Ambati J, Ambati BK, Yoo SH, Ianchulev S, Adamis AP (2003) Age-related macular degeneration: etiology, pathogenesis, and therapeutic strategies. Surv Ophthalmol 48(3):257–293
3. Rattner A, Nathans J (2006) Macular degeneration: recent advances and therapeutic opportunities. Nat Rev Neurosci 7(11):860–872
4. Patel M, Chan CC (2008) Immunopathological aspects of age-related macular degeneration. Semin Immunopathol 30(2):97–110
5. Khandhadia S, Lotery A (2010) Oxidation and age-related macular degeneration: insights from molecular biology. Expert Rev Mol Med 12:e34
6. Chiu CJ, Taylor A (2007) Nutritional antioxidants and age-related cataract and maculopathy. Exp Eye Res 84(2):229–245
7. Chiu CJ, Taylor A (2010) Nutritional antioxidants, dietary carbohydrates, and age-related maculopathy and cataract. In: Bendich A, Deckelbaum R (eds) Preventive nutrition, 4 ed. pp 501–543, Humana Press
8. Sparrow JR, Boulton M (2005) RPE lipofuscin and its role in retinal pathobiology. Exp Eye Res 80(5):595–606
9. Zarbin MA (2004) Current concepts in the pathogenesis of age-related macular degeneration. Arch Ophthalmol 122(4):598–614
10. Anderson DH, Radeke MJ, Gallo NB, Chapin EA, Johnson PT, Curletti CR et al (2010) The pivotal role of the complement system in aging and age-related macular degeneration: hypothesis re-visited. Prog Retin Eye Res 29(2):95–112
11. Umeda S, Suzuki MT, Okamoto H, Ono F, Mizota A, Terao K et al (2005) Molecular composition of drusen and possible involvement of anti-retinal autoimmunity in two different forms of macular degeneration in cynomolgus monkey (Macaca fascicularis). Faseb J 19(12):1683–1685
12. Crabb JW, Miyagi M, Gu X, Shadrach K, West KA, Sakaguchi H et al (2002) Drusen proteome analysis: an approach to the etiology of age-related macular degeneration. Proc Natl Acad Sci USA 99(23):14682–14687
13. Donoso LA, Kim D, Frost A, Callahan A, Hageman G (2006) The role of inflammation in the pathogenesis of age-related macular degeneration. Surv Ophthalmol 51(2):137–152
14. Souied EH, Leveziel N, Richard F, Dragon-Durey MA, Coscas G, Soubrane G et al (2005) Y402H complement factor H polymorphism associated with exudative age-related macular degeneration in the French population. Mol Vis 11:1135–1140
15. Klein RJ, Zeiss C, Chew EY, Tsai JY, Sackler RS, Haynes C et al (2005) Complement factor H polymorphism in age-related macular degeneration. Science 308(5720):385–389

16. Edwards AO, Ritter R 3rd, Abel KJ, Manning A, Panhuysen C, Farrer LA (2005) Complement factor H polymorphism and age-related macular degeneration. Science 308(5720):421–424
17. Haines JL, Hauser MA, Schmidt S, Scott WK, Olson LM, Gallins P et al (2005) Complement factor H variant increases the risk of age-related macular degeneration. Science 308(5720):419–421
18. Postel EA, Agarwal A, Caldwell J, Gallins P, Toth C, Schmidt S et al (2006) Complement factor H increases risk for atrophic age-related macular degeneration. Ophthalmology 113(9):1504–1507
19. Despriet DD, Klaver CC, Witteman JC, Bergen AA, Kardys I, de Maat MP et al (2006) Complement factor H polymorphism, complement activators, and risk of age-related macular degeneration. Jama 296(3):301–309
20. Simonelli F, Frisso G, Testa F, di Fiore R, Vitale DF, Manitto MP et al (2006) Polymorphism p.402Y>H in the complement factor H protein is a risk factor for age related macular degeneration in an Italian population. Br J Ophthalmol 90(9):1142–1145
21. Lau LI, Chen SJ, Cheng CY, Yen MY, Lee FL, Lin MW et al (2006) Association of the Y402H polymorphism in complement factor H gene and neovascular age-related macular degeneration in Chinese patients. Invest Ophthalmol Vis Sci 47(8):3242–3246
22. Gold B, Merriam JE, Zernant J, Hancox LS, Taiber AJ, Gehrs K et al (2006) Variation in factor B (BF) and complement component 2 (C2) genes is associated with age-related macular degeneration. Nat Genet 38(4):458–462
23. Schaumberg DA, Christen WG, Buring JE, Glynn RJ, Rifai N, Ridker PM (2007) High-sensitivity C-reactive protein, other markers of inflammation, and the incidence of macular degeneration in women. Arch Ophthalmol 125(3):300–305
24. Seddon JM, Gensler G, Milton RC, Klein ML, Rifai N (2004) Association between C-reactive protein and age-related macular degeneration. Jama 291(6):704–710
25. Seddon JM, George S, Rosner B, Rifai N (2005) Progression of age-related macular degeneration: prospective assessment of C-reactive protein, interleukin 6, and other cardiovascular biomarkers. Arch Ophthalmol 123(6):774–782
26. Zhou J, Jang YP, Kim SR, Sparrow JR (2006) Complement activation by photooxidation products of A2E, a lipofuscin constituent of the retinal pigment epithelium. Proc Natl Acad Sci USA 103(44):16182–16187
27. Hollyfield JG, Bonilha VL, Rayborn ME, Yang X, Shadrach KG, Lu L et al (2008) Oxidative damage-induced inflammation initiates age-related macular degeneration. Nat Med 14(2):194–198
28. Ciechanover A (2003) The ubiquitin proteolytic system and pathogenesis of human diseases: a novel platform for mechanism-based drug targeting. Biochem Soc Trans 31(2):474–481
29. Glickman MH, Ciechanover A (2002) The ubiquitin-proteasome proteolytic pathway: destruction for the sake of construction. Physiol Rev 82(2):373–428
30. Shang F, Taylor A (2011) Ubiquitin-proteasome pathway and cellular responses to oxidative stress. Free Radic Biol Med 51(1):5–16
31. Shang F, Taylor A (2012) Roles for the ubiquitin-proteasome pathway in protein quality control and signaling in the retina: Implications in the pathogenesis of age-related macular degeneration. Mol Aspects Med 33(4):446–466
32. Pickart CM (2001) Mechanisms underlying ubiquitination. Annu Rev Biochem 70:503–533
33. Welchman RL, Gordon C, Mayer RJ (2005) Ubiquitin and ubiquitin-like proteins as multifunctional signals. Nat Rev Mol Cell Biol 6(8):599–609
34. Qureshi N, Vogel SN, Van Way C 3rd, Papasian CJ, Qureshi AA, Morrison DC (2005) The proteasome: a central regulator of inflammation and macrophage function. Immunol Res 31(3):243–260
35. Kloetzel PM (2004) Generation of major histocompatibility complex class I antigens: functional interplay between proteasomes and TPPII. Nat Immunol 5(7):661–669

36. Hope AD, de Silva R, Fischer DF, Hol EM, van Leeuwen FW, Lees AJ (2003) Alzheimer's associated variant ubiquitin causes inhibition of the 26S proteasome and chaperone expression. J Neurochem 86(2):394–404
37. Dawson TM, Dawson VL (2003) Molecular pathways of neurodegeneration in Parkinson's disease. Science 302(5646):819–822
38. Fernandes R, Ramalho J, Pereira P (2006) Oxidative stress upregulates ubiquitin proteasome pathway in retinal endothelial cells. Mol Vis 12:1526–1535
39. Dudek EJ, Shang F, Valverde P, Liu Q, Hobbs M, Taylor A (2005) Selectivity of the ubiquitin pathway for oxidatively modified proteins: relevance to protein precipitation diseases. Faseb J 19(12):1707–1709
40. Shang F, Nowell TR Jr, Taylor A (2001) Removal of oxidatively damaged proteins from lens cells by the ubiquitin-proteasome pathway. Exp Eye Res 73(2):229–238
41. Shang F, Deng G, Liu Q, Guo W, Haas AL, Crosas B et al (2005) Lys6-modified ubiquitin inhibits ubiquitin-dependent protein degradation. J Biol Chem 280(21):20365–20374
42. Jahngen-Hodge J, Obin M, Gong X, Shang F, Nowell T, Gong J et al (1997) Regulation of ubiquitin conjugating enzymes by glutathione following oxidative stress. J Biol Chem 272:28218–28226
43. Obin M, Shang F, Gong X, Handelman G, Blumberg J, Taylor A (1998) Redox regulation of ubiquitin-conjugating enzymes: mechanistic insights using the thiol-specific oxidant diamide. FASEB J 12(7):561–569
44. Yao D, Gu Z, Nakamura T, Shi ZQ, Ma Y, Gaston B et al (2004) Nitrosative stress linked to sporadic Parkinson's disease: S-nitrosylation of parkin regulates its E3 ubiquitin ligase activity. Proc Natl Acad Sci USA 101(29):10810–10814
45. Ishii T, Sakurai T, Usami H, Uchida K (2005) Oxidative modification of proteasome: identification of an oxidation-sensitive subunit in 26 s proteasome. BioChemistry 44(42):13893–13901
46. Caballero M, Liton PB, Epstein DL, Gonzalez P (2003) Proteasome inhibition by chronic oxidative stress in human trabecular meshwork cells. Biochem Biophys Res Commun 308(2):346–352
47. Zhang X, Zhou J, Fernandes AF, Sparrow JR, Pereira P, Taylor A et al (2008) The proteasome: a target of oxidative damage in cultured human retina pigment epithelial cells. Invest Ophthalmol Vis Sci 49(8):3622–3630
48. Wu M, Bian Q, Liu Y, Fernandes AF, Taylor A, Pereira P et al (2009) Sustained oxidative stress inhibits NF-kappaB activation partially via inactivating the proteasome. Free Radic Biol Med 46(1):62–69
49. Fernandes AF, Bian Q, Jiang JK, Thomas CJ, Taylor A, Pereira P et al (2009) Proteasome inactivation promotes p38 mitogen-activated protein kinase-dependent phosphatidylinositol 3-kinase activation and increases interleukin-8 production in retinal pigment epithelial cells. Mol Biol Cell 20(16):3690–3699
50. Fernandes AF, Zhou J, Zhang X, Bian Q, Sparrow J, Taylor A et al (2008) Oxidative inactivation of the proteasome in retinal pigment epithelial cells. A potential link between oxidative stress and up-regulation of interleukin-8. J Biol Chem 283(30):20745–20753
51. Bulteau AL, Lundberg KC, Humphries KM, Sadek HA, Szweda PA, Friguet B et al (2001) Oxidative modification and inactivation of the proteasome during coronary occlusion/reperfusion. J Biol Chem 276(32):30057–30063
52. Sparrow JR, Parish CA, Hashimoto M, Nakanishi K (1999) A2E, a lipofuscin fluorophore, in human retinal pigmented epithelial cells in culture. Invest Ophthalmol Vis Sci 40(12):2988–2995
53. Zhou J, Cai B, Jang YP, Pachydaki S, Schmidt AM, Sparrow JR (2005) Mechanisms for the induction of HNE- MDA- and AGE-adducts, RAGE and VEGF in retinal pigment epithelial cells. Exp Eye Res 80(4):567–580
54. Nicholls SJ (2008) The complex intersection of inflammation and oxidation: implications for atheroprotection. J Am Coll Cardiol 52(17):1379–1380

55. Gill R, Tsung A, Billiar T (2010) Linking oxidative stress to inflammation: toll-like receptors. Free Radic Biol Med 48(9):1121–1132
56. Khaper N, Bryan S, Dhingra S, Singal R, Bajaj A, Pathak CM et al (2010) Targeting the vicious inflammation-oxidative stress cycle for the management of heart failure. Antioxid Redox Signal 13(7):1033–1049
57. Larrayoz IM, Huang JD, Lee JW, Pascual I (2010) Rodriguez IR. 7-ketocholesterol-induced inflammation: involvement of multiple kinase signaling pathways via NFkappaB but independently of reactive oxygen species formation. Invest Ophthalmol Vis Sci 51(10):4942–4955
58. Anderson DH, Mullins RF, Hageman GS, Johnson LV (2002) A role for local inflammation in the formation of drusen in the aging eye. Am J Ophthalmol 134(3):411–431
59. Fernandes AF, Guo W, Zhang X, Gallagher M, Ivan M, Taylor A et al (2006) Proteasome-dependent regulation of signal transduction in retinal pigment epithelial cells. Exp Eye Res 83(6):1472–1481
60. Palombella VJ, Rando OJ, Goldberg AL, Maniatis T (1994) The ubiquitin-proteasome pathway is required for processing of NF-kB procursor protein and the activation of NF-kB. Cell 78:773–785
61. Wang C, Deng L, Hong M, Akkaraju GR, Inoue J, Chen ZJ (2001) TAK1 is a ubiquitin-dependent kinase of MKK and IKK. Nature 412(6844):346–351
62. Yaron A, Gonen H, Alkalay I, Hatzubai A, Jung S, Beyth S et al (1997) Inhibition of NF-kappa-B cellular function via specific targeting of the I-kappa-B-ubiquitin ligase. Embo J 16(21):6486–6494
63. Ambati J, Anand A, Fernandez S, Sakurai E, Lynn BC, Kuziel WA et al (2003) An animal model of age-related macular degeneration in senescent Ccl-2- or Ccr-2-deficient mice. Nat Med 9(11):1390–1397
64. Simonini A, Moscucci M, Muller DW, Bates ER, Pagani FD, Burdick MD et al (2000) IL-8 is an angiogenic factor in human coronary atherectomy tissue. Circulation 101(13):1519–1526
65. Yoshida S, Ono M, Shono T, Izumi H, Ishibashi T, Suzuki H et al (1997) Involvement of interleukin-8, vascular endothelial growth factor, and basic fibroblast growth factor in tumor necrosis factor alpha-dependent angiogenesis. Mol Cell Biol 17(7):4015–4023
66. Li A, Dubey S, Varney ML, Dave BJ, Singh RK (2003) IL-8 directly enhanced endothelial cell survival, proliferation, and matrix metalloproteinases production and regulated angiogenesis. J Immunol 170(6):3369–3376
67. Heidemann J, Ogawa H, Dwinell MB, Rafiee P, Maaser C, Gockel HR et al (2003) Angiogenic effects of interleukin 8 (CXCL8) in human intestinal microvascular endothelial cells are mediated by CXCR2. J Biol Chem 278(10):8508–8515
68. Thurman JM, Renner B, Kunchithapautham K, Ferreira VP, Pangburn MK, Ablonczy Z et al (2009) Oxidative stress renders retinal pigment epithelial cells susceptible to complement-mediated injury. J Biol Chem 284(25):16939–16947

# Chapter 32
# Inflammatory Biomarkers for AMD

**Chloe M. Stanton and Alan F. Wright**

**Abstract** Age-related macular degeneration (AMD) is the leading cause of blindness worldwide, affecting an estimated 50 million individuals aged over 65 years.

Environmental and genetic risk-factors implicate chronic inflammation in the etiology of AMD, contributing to the formation of drusen, retinal pigment epithelial cell dysfunction and photoreceptor cell death. Consistent with a role for chronic inflammation in AMD pathogenesis, several inflammatory mediators, including complement components, chemokines and cytokines, are elevated at both the local and systemic levels in AMD patients. These mediators have diverse roles in the alternative complement pathway, including recruitment of inflammatory cells, activation of the inflammasome, promotion of neovascularisation and in the resolution of inflammation. The utility of inflammatory biomarkers in assessing individual risk and progression of the disease is controversial. However, understanding the role of these inflammatory mediators in AMD onset, progression and response to treatment may increase our knowledge of disease pathogenesis and provide novel therapeutic options in the future.

**Keywords** Inflammation · Age-related macular degeneration · Complement · Cytokine · Chemokine · Biomarker

**Abbreviations**

| | |
|---|---|
| AMD | Age-related macular degeneration |
| RPE | Retinal pigment epithelial |
| CNV | Choroidal neovascularisation |
| VEGF | Vascular endothelial growth factor |

C. M. Stanton (✉) · A. F. Wright
MRC Human Genetics Unit, MRC Institute of Genetics and Molecular Medicine, University of Edinburgh, Western General Hospital, Crewe Road, Edinburgh EH4 2XU, UK
e-mail: chloe.stanton@igmm.ed.ac.uk

A. F. Wright
e-mail: alan.wright@igmm.ed.ac.uk

J. D. Ash et al. (eds.), *Retinal Degenerative Diseases,* Advances in Experimental Medicine and Biology 801, DOI 10.1007/978-1-4614-3209-8_32,

| | |
|---|---|
| CRP | C-reactive protein |
| A2E | N-retinylidene-N retinylethanolamine |
| CEP | Carboxyethylpyrrole |
| NLRP3 | NACHT, LRR and PYD domains-containing protein 3 |
| CFH | Complement factor H |
| CFD | Complement factor D |
| CCL2 | Chemokine, CC motif, ligand 2 |
| CCR2 | Chemokine, CC motif, receptor type 2 |
| IL-6 | Interleukin-6 |

## 32.1 Introduction

Age-related macular degeneration (AMD) is the leading cause of blindness in people aged over 65 years in developed countries [1]. In most cases, atrophic or "dry" AMD leads to the progressive impairment of central vision as the retinal pigment epithelial (RPE) cells become dysfunctional, overlying photoreceptor cells atrophy and the macula degenerates over time. A more severe neovascular or "wet" form of the disease affects 10% of cases and results in the development of abnormal choroidal neovascularisation (CNV). These fragile vessels may lead to bleeding below or within the retina, and scarring in the macular region, dramatically decreasing central vision. There is currently no treatment for dry AMD, but anti-angiogenic therapy targeting vascular endothelial growth factor (VEGF) is available for those affected by wet AMD. However, identifying those patients at risk of progression is an on-going challenge due to the multifactorial nature of this complex disease. One possibility is that genetic susceptibility factors and systemic biomarkers could be used in combination to monitor disease progression, improve therapeutic intervention and monitor treatment responses. This chapter discusses the evidence for inflammatory biomarkers in AMD and their current value in monitoring disease prediction or progression.

## 32.2 Inflammation is a Key Mechanism in the Pathogenesis of AMD

Evidence that inflammation has a role in AMD pathogenesis comes from numerous studies implicating the innate immune system at the proteomic, histopathological and genetic levels. Known AMD-risk factors, such as smoking, also contribute to inflammation.

Many proteins involved in the immune response have been localised to the sub-RPE drusen deposits that are characteristic of AMD. These include immunoglobulins, activators of complement (C5, C5b-9, C3b, C3d, C3a and C5a), complement

regulators and acute-phase proteins such as C-reactive protein (CRP) [2–4]. Thus, drusen formation may be a consequence of a local immune response against molecules originating from dysfunctional RPE. These molecules, including N-retinylidene-N retinylethanolamine (A2E) [5], amyloid β [6] and carboxyethylpyrrole (CEP) [7] can trigger an inflammatory response—possibly by activating the NACHT, LRR and PYD domains-containing protein 3 (NLRP3) inflammasome [8]. The resulting pro-inflammatory signalling induces local expression of pro-inflammatory molecules, recruits inflammatory cells and activates the alternative complement pathway. Such a response may be induced to clear the debris. However, chronic inflammation may occur, injuring the Bruch's membrane, exacerbating RPE cell dysfunction, promoting CNV formation and leading to AMD.

Additional evidence that aberrant regulation of inflammatory processes in the eye plays an important role in AMD pathogenesis came with the identification of the first AMD susceptibility locus on chromosome 1 (1q25–31). This region contains the complement factor H (*CFH*) gene [9–11], encoding a key regulator of the alternative pathway. Risk variants in other components of the alternative pathway have also been reported, including factor B[12] and complement component *C3* [13]. Some of these variants directly affect protein function, potentially resulting in increased activation of the pathway in affected individuals [14]. Such genetic markers are useful for predicting the risk of disease, but it remains unclear how these susceptibility factors contribute to progression from early to late forms of AMD.

## 32.3 Evidence for the Association of Inflammatory Markers with AMD

From a pathological perspective, many of the stages observed in AMD may be considered to be the result of a chronic inflammatory response. Complement and other inflammatory proteins have been shown to be elevated, both locally at the AMD lesion, and systemically, in plasma, serum or urine.

### *32.3.1 Complement Proteins*

Genetic and proteomic studies have shown that dysregulation of the alternative pathway plays an important role in AMD pathogenesis. Alternative pathway components in plasma are also altered [15–18]. Recent studies consistently show chronic activation of the pathway in AMD cases compared with controls. Significantly raised concentrations of the complement components Factor D (CFD), Ba, Bb, C3d, C3a and C5a were detected in plasma from AMD cases in one or more of these studies [15–18]. The concentration of some complement proteins is under genetic control, and the ability to predict AMD using genetic risk factors was only slightly improved by including plasma CFD concentration [15]. Systemic

concentrations of complement components may reflect local complement activation. In AMD eyes, dying RPE cells accumulate CRP and C5 in the cytoplasm [2], and C3a and C5a (products of C3 and C5 cleavage) are present in drusen in AMD eyes. These fragments are anaphylatoxins that promote inflammation, chemotaxis, cytotoxic oxygen radical production and secretion of VEGF.

### *32.3.2 C-Reactive Protein*

An elevated plasma concentration of CRP, a non-specific marker of inflammation, has been suggested as a biomarker for AMD and for its progression. Significantly elevated levels of CRP in serum from severe AMD cases compared to those with no or minimal maculopathy has been detected in some studies [19–21], but not in others [22–24]. Prospective studies show conflicting results on the validity of CRP as a biomarker for AMD progression [23, 25]. The disparity in these data may reflect the importance of accounting for additional genetic and environmental risk factors, such as smoking and AMD-susceptibility genotypes [19, 20, 22].

### *32.3.3 Cytokines*

During an inflammatory response, cytokines contribute to the inflammatory cascade at the local and systemic levels. Monocytes are recruited from the choroidal blood by the combined action of CCL2 (chemokine, CC motif, ligand 2) and its receptor CCR2, and differentiate into macrophages in response to specific stimuli—including signalling by cytokines. In the AMD eye, activated microglia [26] and macrophages [27] secrete and respond to cytokines and migrate to sites of injury. Depending on their activation state, macrophages may clear sub-retinal deposits or exacerbate inflammation and contribute to CNV [28, 29]. Determining the balance of inflammatory signals in AMD is likely to provide an insight into the stage or progression of the disease.

Commonly used as a marker of systemic inflammation, interleukin-6 (IL-6) is a pro-inflammatory cytokine produced at sites of acute and chronic inflammation by cells including macrophages. IL-6 may contribute to RPE degeneration [30]. Transcriptional profiling of the RPE-choroid from eyes with geographic atrophy (a severe form of dry AMD) revealed higher *IL-6* transcript levels than in control eyes [31] and IL-6 was elevated in the aqueous humour of eyes with wet AMD [32]. Although IL6 appears to be consistently elevated at the local level in AMD, the association is less clear at the systemic level. High IL-6 concentrations in serum may predict AMD progression [25], but a significant difference in IL-6 serum concentrations between AMD cases and controls has not yet been proven [23, 33].

Elevated expression of some or all of the cytokines *CXCL1*, *CXCL2*, *CXCL9*, *CXCL10*, *CXCL11*, *CCL2*, and *CCL8* was detected in the RPE-choroid of all AMD subtypes studied [31]. These chemokines are involved in leukocyte recruitment, and

some have been implicated in AMD previously. The intraocular concentration of CCL2 was elevated in wet AMD eyes [32] and in urine from wet AMD patients [34] but there was no significant difference in serum from wet AMD cases compared to controls [35].

*CXCL9* and *CXCL10* were elevated even at the earliest stages of AMD, prior to detectable visual loss, making them attractive candidates for inflammatory biomarkers in AMD [31]. CXCL10 was localised to the choroid in AMD eyes, and significantly elevated CXCL10 concentrations measured in serum from AMD patients of all stages, relative to controls [33]. However, no such difference was observed in a study using a similar number of CNV cases (18) and controls (18) [35]. Larger sample sizes are required to validate CXCL10 as a biomarker for AMD.

## 32.4 Conclusions

The search for clinically useful inflammatory biomarkers in AMD is complicated by the influence of other diseases, infection, systemic inflammation, and by the widespread effects of ageing, which can be under distinct genetic control. This combination of factors may explain the inconsistency between studies investigating inflammatory proteins as biomarkers for AMD. Another difficulty results from trying to determine the difference between a risk factor, which participates in the causal disease pathway, and a risk marker, which is only indirectly associated with disease. The ideal inflammatory biomarker(s) should provide information about disease pathogenesis, disease progression and response to therapy. At the current time, no inflammatory biomarkers significantly improve prediction of AMD risk compared with using genetic markers alone. However, if suppression of inflammation, by therapeutic intervention or lifestyle changes is required for AMD treatment, the use of inflammatory biomarkers may still become a useful means of monitoring treatment response in AMD although whether they can usefully monitor disease progression remains to be determined.

## References

1. Friedman D, O'Colmain B, Munoz B, Tomany S, McCarty C, Jong P et al (2004) Prevalence of age-related macular degeneration in the United States. Arch Ophthalmol 122(4):564–572
2. Anderson DH, Mullins RF, Hageman GS, Johnson LV (2002) A role for local inflammation in the formation of drusen in the aging eye. Am J Ophthalmol 134(3):411–431
3. Crabb JW, Miyagi M, Gu X, Shadrach K, West KA, Sakaguchi H et al (2002) Drusen proteome analysis: an approach to the etiology of age-related macular degeneration. Proc Natl Acad Sci USA 99(23):14682–14687
4. Hageman GS, Luthert PJ, Victor Chong NH, Johnson LV, Anderson DH Mullins RF (2001) An integrated hypothesis that considers Drusen as biomarkers of immune-mediated processes at the RPE-Bruch's membrane interface in aging and age-related macular degeneration. Prog Retin Eye Res 20(6):705–732

5. Zhou J, Jang YP, Kim SR, Sparrow JR (2006) Complement activation by photooxidation products of A2E, a lipofuscin constituent of the retinal pigment epithelium. Proc Natl Acad Sci USA 103(44):16182–16187
6. Johnson LV, Leitner WP, Rivest AJ, Staples MK, Radeke MJ, Anderson DH (2002) The Alzheimer's Aβ-peptide is deposited at sites of complement activation in pathologic deposits associated with aging and age-related macular degeneration. Proc Natl Acad Sci USA 99(18):11830–11835
7. Hollyfield JG, Bonilha VL, Rayborn ME, Yang X, Shadrach KG, Lu L et al (2008) Oxidative damage-induced inflammation initiates age-related macular degeneration. Nat Med 14(2):194–198
8. Doyle SL, Campbell M, Ozaki E, Salomon RG, Mori A, Kenna PF et al (2012) NLRP3 has a protective role in age-related macular degeneration through the induction of IL-18 by drusen components. Nat Med 18(5):791–798
9. Edwards AO, Ritter R, Abel KJ, Manning A, Panhuysen C Farrer LA (2005) Complement factor H polymorphism and age-related macular degeneration. Science 308(5720):421–424
10. Hageman GS, Anderson DH, Johnson LV, Hancox LS, Taiber AJ, Hardisty LI et al (2005) A common haplotype in the complement regulatory gene factor H (HF1/CFH) predisposes individuals to age-related macular degeneration. Proc Natl Acad Sci USA 102(20):7227–7232
11. Haines JL, Hauser M, Schmidt S, Scott WK, Olson LM, Gallins P et al (2005) Complement factor H variant increases the risk of age-related macular degeneration. Science 308:419–421
12. Gold B, Merriam JE, Zernant J, Hancox LS, Taiber AJ, Gehrs K et al (2006) Variation in factor B (BF) and complement component 2 (C2) genes is associated with age-related macular degeneration. Nat Genet 38(4):458–462
13. Yates JRW, Sepp T, Matharu BK, Khan JC, Thurlby DA, Shahid H et al (2007) Complement C3 Variant and the Risk of Age-Related Macular Degeneration. N Engl J Med 357(6):553–561
14. Heurich M, Martínez-Barricarte R, Francis NJ, Roberts DL, Rodríguez deCS, Morgan BP et al (2011) Common polymorphisms in C3, factor B, and factor H collaborate to determine systemic complement activity and disease risk. Proc Natl Acad Sci USA 108(21):8761–8766
15. Hecker LA, Edwards AO, Ryu E, Tosakulwong N, Baratz KH, Brown WL et al (2010) Genetic control of the alternative pathway of complement in humans and age-related macular degeneration. Hum Mol Genet 19(1):209–215
16. Reynolds R, Hartnett ME, Atkinson JP, Giclas PC, Rosner B, Seddon JM (2009) Plasma complement components and activation fragments: associations with age-related macular degeneration genotypes and phenotypes. Invest Ophthalmol Vis Sci 50(12):5818–5827
17. Scholl HPN, Issa PC, Walier M, Janzer S, Pollok-kopp B, Fritsche LG et al (2008) Systemic Complement Activation in Age-Related Macular Degeneration. PLoS One 3(7):e2593
18. Stanton CM, Yates JRW, den Hollander AI, Seddon JM, Swaroop A, Stambolian D et al (2011) Complement Factor D in Age-Related Macular Degeneration. Invest Ophthalmol Vis Sci 52(12):8828–8834
19. Seddon J, Gensler G, Milton R, Klein M, Rifai N (2004) Association between c-reactive protein and age-related macular degeneration. JAMA 291(6):704–710
20. Seddon JM, Gensler G, Rosner B (2010) C-Reactive Protein and CFH ARMS2/HTRA1 Gene Variants Are Independently Associated with Risk of Macular Degeneration. Ophthalmology 117(8):1560–1566
21. Vine AK, Stader J, Branham K, Musch DC, Swaroop A (2005) Biomarkers of Cardiovascular Disease as Risk Factors for Age-Related Macular Degeneration. Ophthalmology 112(12):2076–2080
22. Dasch B, Fuhs A, Behrens T, Meister A, Wellmann J, Fobker M et al (2005) Inflammatory markers in age-related maculopathy: Cross-sectional analysis from the muenster aging and retina study. Arch Ophthalmol 123(11):1501–1506
23. Klein R, Klein BEK, Knudtson MD, Wong TY, Shankar A, Tsai MY (2005) Systemic markers of inflammation, endothelial dysfunction, and age-related maculopathy. Am J Ophthalmol 140(1):35–44

24. McGwin G, Hall TA, Xie A, Owsley C (2005) The relation between C reactive protein and age related macular degeneration in the cardiovascular health study. Br J Ophthalmol 89(9):1166–1170
25. Seddon J, George S, Rosner B, Rifai N (2005) Progression of age-related macular degeneration: Prospective assessment of c-reactive protein, interleukin 6, and other cardiovascular biomarkers. Arch Ophthalmol 123(6):774–782
26. Langmann T (2007) Microglia activation in retinal degeneration. J Leukoc Biol 81(6): 1345–1351
27. Forrester JV (2003) Macrophages eyed in macular degeneration. Nat Med 9(11):1350–1351
28. Espinosa-Heidmann DG, Suner IJ, Hernandez EP, Monroy D, Csaky KG Cousins SW (2003) Macrophage depletion diminishes lesion size and severity in experimental choroidal neovascularization. Invest Ophthalmol Vis Sci 44(8):3586–3592
29. Sakurai E, Anand A, Ambati BK, van Rooijen N Ambati J (2003) Macrophage depletion inhibits experimental choroidal neovascularization. Invest Ophthalmol Vis Sci 44(8):3578–3585
30. Leung KW, Barnstable CJ, Tombran-Tink J (2009) Bacterial endotoxin activates retinal pigment epithelial cells and induces their degeneration through IL-6 and IL-8 autocrine signaling. Mol Immunol 46(7):1374–1386
31. Newman A, Gallo N, Hancox L, Miller N, Radeke C, Maloney M et al (2012) Systems-level analysis of age-related macular degeneration reveals global biomarkers and phenotype-specific functional networks. Genome Med 4(2):16
32. Jonas J, Tao Y, Neumaier M, Findeisen P (2010) Monocyte chemoattractant protein 1, intercellular adhesion molecule 1, and vascular cell adhesion molecule 1 in exudative age-related macular degeneration. Arch Ophthalmol 128(10):1281–1286
33. Mo FM, Proia AD, Johnson WH, Cyr D, Lashkari K (2010) Interferon γ-Inducible Protein-10 (IP-10) and Eotaxin as Biomarkers in Age-Related Macular Degeneration. Invest Ophthalmol Vis Sci 51(8):4226–4236
34. Guymer RH, Tao LW, Goh JK, Liew D, Ischenko O, Robman LD et al (2011) Identification of urinary biomarkers for age-related macular degeneration. Invest Ophthalmol Vis Sci 52(7):4639–4644
35. Grunin M, Burstyn-Cohen T, Hagbi-Levi S, Peled A Chowers I (2012) Chemokine receptor expression in peripheral blood monocytes from patients with neovascular age-related macular degeneration. Invest Ophthalmol Vis Sci 53(9):5292–5300

# Chapter 33
# Oxidized Low-Density-Lipoprotein-Induced Injury in Retinal Pigment Epithelium Alters Expression of the Membrane Complement Regulatory Factors CD46 and CD59 through Exosomal and Apoptotic Bleb Release

**Katayoon B. Ebrahimi, Natalia Fijalkowski, Marisol Cano and James T. Handa**

**Abstract** Genetic and immunohistochemical studies have identified the alternative complement pathway as an important component of age-related macular degeneration (AMD). The objective of this chapter is to review the impact of complement regulators on complement activation in the macula as it relates to AMD. Our laboratory and other investigators have identified CD46 and CD59 as important retinal pigment epithelium (RPE) cell membrane complement regulators, which are decreased in AMD. Using oxidized low-density lipoproteins (oxLDLs), which are found in Bruch's membrane in AMD, we found that CD46 and CD59 were decreased in RPE cells in part, by their release in exosomes and apoptotic particles. The release of complement regulators could potentially impair complement regulation on RPE cells and contribute to lesion formation in the outer retina and Bruch's membrane during the development of AMD.

**Keywords** Ageing · Age-related macular degeneration · Apoptosis · Complement · Exosome · Oxidative stress

**Abbreviations**

| | |
|---|---|
| OxLDL | Oxidized low-density lipoprotein |
| RPE | Retinal pigment epithelium |
| AMD | Age-related macular degeneration |
| CFH | Complement factor H |

J. T. Handa (✉) · K. B. Ebrahimi · N. Fijalkowski · M. Cano
Wilmer Eye Institute, Johns Hopkins School of Medicine, 400 N. Broadway, Smith Building, room 3015, Baltimore, MD 21287,USA
e-mail: jthanda@jhmi.edu

K. B. Ebrahimi
e-mail: kebrahi2@jhmi.edu

N. Fijalkowski
e-mail: nfijalk1@gmail.com

M. Cano
e-mail: mcano1@jhmi.edu

J. D. Ash et al. (eds.), *Retinal Degenerative Diseases,* Advances in Experimental Medicine and Biology 801, DOI 10.1007/978-1-4614-3209-8_33,

| | |
|---|---|
| MAC | Membrane attack complex |
| RCA | Regulators of complement activation |
| MCP | Membrane cofactor protein |
| DAF | Decay-accelerating factor |
| GA | Geographic atrophy |
| SNP | Single nucleotide polymorphism |
| GPI | Glycophosphoinositol |
| IL | Interleukin |
| MCP-1 | Monocytic chemoattractant protein-1 |
| VEGF | Vascular endothelial growth factor |
| MMPs | Matrix metalloproteinases |
| OSEs | Oxidation-specific epitopes |

## 33.1 Introduction

The complement pathway has been proposed to have a role in the pathogenesis of age-related macular degeneration (AMD). Evidence of this insightful concept came with the identification of polymorphisms in complement factor H (CFH), a circulating regulator of the alternative pathway, with risk for AMD [1–4]. This finding paved the way for uncovering several other complement factors associated with AMD. Despite intensive study, however, the exact mechanism of how complement contributes to AMD remains unresolved. For example, the identification of complement components in Bruch's membrane does not establish whether complement activation is protective or pathologic. In testing whether complement activation induces the development of AMD markers, it will be necessary to evaluate not complement, but the influence by complement regulators. In a study "Decreased Membrane Complement Regulators in the Retinal Pigmented Epithelium Contributes to Age-Related Macular Degeneration," published in the *Journal of Pathology* [5] and presented at the XVth International Symposium on Retinal Degeneration, we proposed that multiple complement regulators are impaired during the development of AMD. This chapter reviews some of this work and outlines elements of complement that could be involved in the conversion from aging to AMD.

## 33.2 Complement and AMD

The complement system is a major component of the innate immune system. It consists of the classical, alternative, and lectin pathways, which activate the final common pathway through C3 convertase, cleaving C3 into C3a and C3b. C3b binds to the target and C5 convertase, which forms the membrane attack complex (MAC), composed of C5b-9, inducing cell lysis. C3, C5, and the MAC are three critical steps where complement can be activated. Activation of complement at one or all

of these three steps could potentially play a role in early AMD. While controlled activation protects, on the other hand, uncontrolled activation can contribute to inflammation and tissue injury during disease. Complement therefore, is tightly controlled by regulators of complement activation (RCA), mainly at C3 and the MAC, preventing unintended host tissue injury. C3 is controlled by membrane cofactor protein (MCP) CD46 and decay-accelerating factor (DAF) CD55 on cells, and by fluid phase factor H. The MAC is controlled by CD59, which inhibits assembly of a C5b-8 complex at C9, preventing lytic pore formation.

Complement activation appears to play an important role in AMD based on genetic and immunohistochemical studies. The identification of the factor H polymorphism associated with AMD emphasizes the relevance of alternative pathway regulation at C3. Genetic studies have also found that variations in other complement components are associated with AMD risk. Immunohistochemical studies implicate inflammation and complement-mediated attack as early events in drusen biogenesis. All of the components in the final common pathway have been identified in Bruch's membrane, and many are synthesized by the retinal pigment epithelium (RPE). For example, two fluid phase regulators, vitronectin (Vn) and clusterin (apolipoprotein J), are present in drusen. Vn is also present in the cytoplasm of RPE cells that are associated with drusen. The membrane-associated complement inhibitors complement receptor 1 and complement component C3 are also detected in drusen [6]. These studies however, do not tell us whether the complement response is protective or pathologic.

Dysregulated complement is thought to play a role in pathogenesis of AMD, but the specific mechanisms have yet to be determined. Evidence in support of this concept includes RPE apoptosis through inadequately controlled MAC formation [7]. Likewise, uncontrolled complement activation may induce an inflammatory cascade leading to the accumulation of insoluble extracellular deposits consisting of cellular debris, serum, and inflammatory molecules, otherwise known as basal deposits [8]. Definitive mechanistic evidence however, is lacking.

## 33.3 CD46 and AMD

CD46 is a transmembrane regulator that is a cofactor for complement factor I (CFI), which cleaves C3b into iC3b. By inhibiting C3, CD46 regulates complement-mediated cell death by limiting the number of C5b-9 lytic pores formed. Importantly, Elward et al. found that apoptotic cells have reduced CD46, which increased C3b opsonization following an oxidative stress insult [9]. While this would promote phagocytic removal of dying cells, in contrast to iC3b, the C3b opsonizing signal promotes unwanted inflammation. McLaughlin et al. suggested that CD46, in addition to protecting host cells from complement attack, may have interaction with beta1 integrin in the eye which may have a role in the adhesion of the RPE to its basement membrane and Bruch's membrane [10].

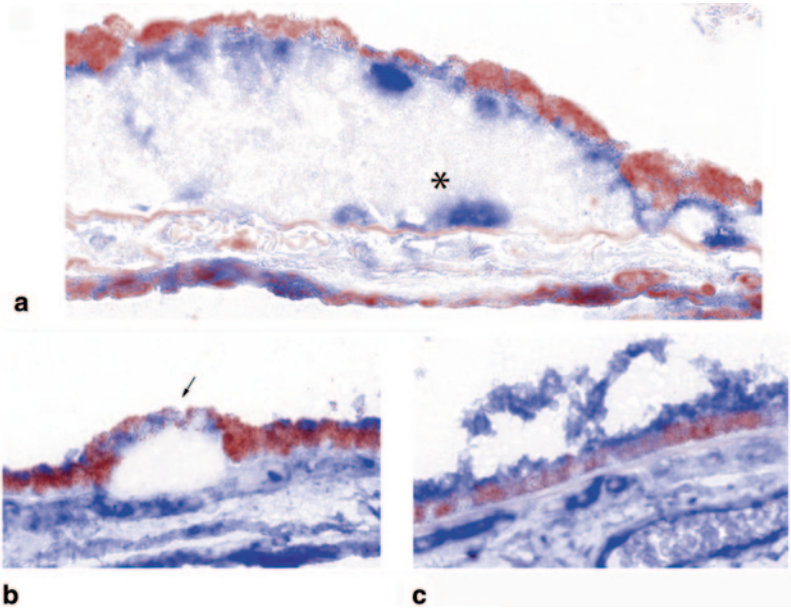


**Fig. 33.1** **a** Distribution of CD46 in the RPE of early AMD eyes. Dysmorphic macular RPE cells adjacent to a druse with reduced CD46 labeling at their lateral and basal surfaces. CD46 labeling is diffusely distributed within the druse (*asterisk*). **b** Distribution of CD59 in early AMD eyes. Macular RPE cells overlying normal Bruch's membrane have strong CD59 labeling at the apex of cells. Dysmorphic RPE cells display weaker labeling (*arrow*). **c** Material in the subretinal space also has CD59 labeling

Of cell membrane regulators expressed by the RPE, CD46 is the predominant regulator. In the human RPE, CD46 is highly expressed while CD55 has low expression. CD46 is expressed on the basolateral surface of the human RPE cells. Importantly, Vogt et al. found that CD46 is decreased in geographic atrophy (GA) before any changes to the RPE, Bruch's membrane, and photoreceptors. They showed progressive loss of staining with increasing grades of RPE degeneration. Marked reduction of CD46 labeling was present in migrating RPE cells. The authors concluded that changes in RPE CD46 expression occurred before morphological RPE change [11]. This work coincides with our discovery that CD46 was basolaterally distributed in the RPE of normal control and the unaffected RPE of AMD eyes, and was decreased in diseased areas of early AMD samples. Lateral CD46 labeling was lost in RPE cells adjacent to drusen and overlying large drusen while basal CD46 labeling was lost with the appearance of CD46 within drusen (Fig. 33.1a). The basolateral distribution of CD46 in RPE cells and localization of CD46 in the vesicles within drusen have been also reported by other groups.

CD46 expression changes were also shown on leukocytes in neovascular AMD. In a prospective, case-controlled study by Singh et al., CD46 was lower on CD14-labeled monocytes in patients with neovascular AMD compared with controls. Lower expression of CD46 was also observed on lymphocytes in patients with disciform

scars compared with patients without fibrosis [12]. Their study again supports a role for complement regulation to prevent AMD. However, a study looking specifically for single nucleotide polymorphisms (SNPs) in CD46 did not find susceptibility for AMD risk [13]. Further study on CD46 in AMD, therefore, appears warranted.

## 33.4 CD59 and AMD

Complement defense 59 (CD59) is a cell surface glycophosphoinositol (GPI)-anchored protein that prevents complement MAC assembly by binding to C5b678, and preventing C9 from binding to the forming MAC. The reduction of CD59 has been suggested to be a factor in the pathogenesis of AMD. Normally, CD59 levels are low in RPE cells, but with a stimulus, such as oxidative stress, CD59 increases. Incubation of RPE cells with CD59 antiserum followed by 5 % normal human serum induced sublytic formation of MAC. This treatment induced release of interleukin (IL)-6, IL-8, monocytic chemoattractant protein-1 (MCP-1), vascular endothelial growth factor (VEGF), vitronectin, and matrix metalloproteinases (MMPs). Therefore, sublytic MAC might have a role in generating a proinflammatory environment during both early and late AMD [14]. Recently, we showed that the macular and peripheral RPE of unaffected eyes and the peripheral RPE of early AMD eyes did not have CD59 staining. In early AMD, strong CD59 labeling was observed at the apex of the morphologically normal RPE and in the subretinal space (Fig. 33.1b, c). Decreased CD59 was observed in flattened RPE over drusen and GA while CD59 labeling remained unchanged in the choroid [5]. Normal human eyes have been shown to express CD59 throughout the nerve fiber layer and blood vessels within the ganglion cell, inner plexiform, and inner nuclear layers [15]. Our observations also demonstrated strong CD59 labeling in retinal blood vessel walls. Like CD46, CD59 was found to be lower on CD14-labeled monocytes in patients with neovascular AMD [12]. Replacing CD59 using an adenovirus vector protected cells from complement-mediated lysis and attenuated choroidal neovascularization [16]. Thus, replenishing decreased CD59 may offer a novel treatment approach for AMD.

## 33.5 Oxidized low-density lipoprotein (OxLDL) and AMD

The stimuli for complement activation by the RPE are not known. It is particularly important to determine factors that activate the alternative pathway. Drusen are hallmark clinical and histopathological lesions that are composed of a heterogeneous accumulation of lipids, proteins, and cellular debris. Many of these components are oxidatively modified, and due to their ability to induce inflammation, they are considered oxidation-specific epitopes (OSEs). Oxidative stress in general has been

shown to influence the expression of CD59 in RPE cells. Oxidative stress reduces the surface abundance of CD59, resulting in increased MAC formation. This sublytic degree of MAC formation, however, resulted in VEGF release, suggesting that oxidative stress-mediated reduction of cell surface complement regulators may sensitizes RPE cells to complement-mediated injury [17, 18]. Lipoproteins that become oxidized (oxLDL) are strong stimulators of the alternative pathway in part due to the presence of OSEs [19]. The step(s) in the final pathway at which modified lipoproteins activate complement is (are) unknown although recent evidence suggests that oxLDL can activate complement at C5 [20]. Our work demonstrated that oxLDL reduced CD46 and CD59 in RPE cells by a combination of apoptotic particles and exosomes [5]. With the immunohistochemical profile observed in AMD specimens, we suggest that the reduction of CD46 is due, in part, to apoptotic shedding of CD46 possibly toward Bruch's membrane, and is involved in both reduced protection of the RPE and in drusen biogenesis. Likewise, we propose that the reduction of CD59 is due, in part, to exosomal release possibly into the subretinal space, or with disease progression, as apoptotic blebs into Bruch's membrane during drusen formation. These results suggest that OSE formation from inadequately neutralized oxidative stress in the RPE contributes to AMD by decreasing the protective effects of complement regulators on RPE cells and contributes to AMD lesion formation in the outer retina, RPE, and Bruch's membrane. Defining the extent of this hypothesis is the subject of ongoing research in our laboratory.

**Acknowledgement** Funding: NIH EY14005 (JTH), EY019904 (JTH), Thome Foundation (JTH), AHAF (JTH), Research to Prevent Blindness Senior Scientist Award (JTH), unrestricted grant from Research to Prevent Blindness to the Wilmer Eye Institute, NIH P30EY001765 core grant, Robert Bond Welch Professorship, and a gift from the Merlau family and Aleda Wright.

## References

1. Edwards AO, Ritter R 3rd, Abel KJ, Manning A, Panhuysen C, Farrer LA (2005) Complement factor H polymorphism and age-related macular degeneration. Science 308:421–424
2. Hageman GS, Anderson DH, Johnson LV, Hancox LS, Taiber AJ, Hardisty LI, Hageman JL, Stockman HA, Borchardt JD, Gehrs KM, Smith RJ, Silvestri G, Russell SR, Klaver CC, Barbazetto I, Chang S, Yannuzzi LA, Barile GR, Merriam JC, Smith RT, Olsh AK, Bergeron J, Zernant J, Merriam JE, Gold B, Dean M, Allikmets R (2005) A common haplotype in the complement regulatory gene factor H (HF1/CFH) predisposes individuals to age-related macular degeneration. Proc Natl Acad Sci U S A 102:7227–7232
3. Haines JL, Hauser MA, Schmidt S, Scott WK, Olson LM, Gallins P, Spencer KL, Kwan SY, Noureddine M, Gilbert JR, Schnetz-Boutaud N, Agarwal A, Postel EA, Pericak-Vance MA (2005) Complement factor H variant increases the risk of age-related macular degeneration. Science 308(5720):419–421
4. Klein RJ, Zeiss C, Chew EY, Tsai JY, Sackler RS, Haynes C, Henning AK, SanGiovanni JP, Mane SM, Mayne ST, Bracken MB, Ferris FL, Ott J, Barnstable C Hoh J (2005) Complement factor H polymorphism in age-related macular degeneration. Science 308(5720):385–389
5. Ebrahimi KB, Fijalkowski N, Cano M, Handa JT (2013) Decreased Membrane Complement Regulators in the Retinal Pigmented Epithelium Contributes to Age-Related Macular Degeneration. J Pathol. 229:729–742

6. Johnson LV, Leitner WP, Staples MK, Anderson DH (2001) Complement activation and inflammatory processes in Drusen formation and age related macular degeneration. Exp Eye Res 73(6):887–896
7. Thurman JM, Holers VM (2006) The central role of the alternative complement pathway in human disease. J Immunol 176(3):1305–1310
8. Anderson DH, Mullins RF, Hageman GS, Johnson LV (2002) A role for local inflammation in the formation of drusen in the aging eye. Am J Ophthalmol 134(3):411–431
9. Elward K, Griffiths M, Mizuno M, Harris CL, Neal JW, Morgan BP, Gasque P (2005) CD46 plays a key role in tailoring innate immune recognition of apoptotic and necrotic cells. J Biol Chem 280(43):36342–36354
10. McLaughlin BJ, Fan W, Zheng JJ, Cai H, Del Priore LV, Bora NS, Kaplan HJ (2003) Novel role for a complement regulatory protein (CD46) in retinal pigment epithelial adhesion. Invest Ophthalmol Vis Sci 44(8):3669–3674
11. Vogt SD, Curcio CA, Wang L, Li CM, McGwin G Jr, Medeiros NE, Philp NJ, Kimble JA, Read RW (2011) Retinal pigment epithelial expression of complement regulator CD46 is altered early in the course of geographic atrophy. Exp Eye Res 93(4):413–423
12. Singh A, Faber C, Falk M, Nissen MH, Hviid TV, Sørensen TL (2012) Altered expression of CD46 and CD59 on leukocytes in neovascular age-related macular degeneration. Am J Ophthalmol 154(1):193–199
13. Cipriani V, Matharu BK, Khan JC, Shahid H, Stanton CM, Hayward C, Wright AF, Bunce C, Clayton DG, Moore AT, Yates JR (2012) Genetic variation in complement regulators and susceptibility to age-related macular degeneration. Immunobiology 217(2):158–161
14. Lueck K, Wasmuth S, Williams J, Hughes TR, Morgan BP, Lommatzsch A, Greenwood J, Moss SE, Pauleikhoff D (2011) Sub-lytic C5b-9 induces functional changes in retinal pigment epithelial cells consistent with age-related macular degeneration. Eye (Lond) 25(8):1074–1082
15. Vogt SD, Barnum SR, Curcio CA, Read RW (2006) Distribution of complement anaphylatoxin receptors and membrane-bound regulators in normal human retina. Exp Eye Res 83(4):834–840
16. Cashman SM, Ramo K, Kumar-Singh R (2011) A non membrane-targeted human soluble CD59 attenuates choroidal neovascularization in a model of age related macular degeneration. PLoS One 6(4):e19078
17. Thurman JM, Renner B, Kunchithapautham K, Ferreira VP, Pangburn MK, Ablonczy Z, Tomlinson S, Holers VM, Rohrer B (2009) Oxidative stress renders retinal pigment epithelial cells susceptible to complement-mediated injury. J Biol Chem 284(25):16939–16947
18. Thurman JM, Renner B, Kunchithapautham K, Holers VM, Rohrer B (2010) Aseptic injury to epithelial cells alters cell surface complement regulation in a tissue specific fashion. Adv Exp Med Biol 664:151–158
19. Malek G, Li CM, Guidry C, Medeiros NE, Curcio CA (2003) Apolipoprotein B incholesterol-containingdrusen and basal deposits of human eyes with age-related maculopathy. Am J Pathol 162:413–425
20. Bhakdi S, Dorweiler B, Kirchmann R, Torzewski J, Weise E, Tranum-Jensen J, Walev I, Wieland E (1995) On the pathogenesis of atherosclerosis: enzymatic transformation of human low density lipoprotein to an atherogenic moiety. J Exp Med 182(6):1959–1971

# Chapter 34
# Should I Stay or Should I Go? Trafficking of Sub-Lytic MAC in the Retinal Pigment Epithelium

**Aparna Lakkaraju, Kimberly A. Toops and Jin Xu**

**Abstract** Assembly of sub-lytic C5b-9 membrane attack complexes (MAC) on the plasma membrane of retinal pigment epithelial cells contributes to the pathogenesis of age-related macular degeneration. C5b-9 pores induce calcium influx, which activates signaling pathways that compromise cell function. Mechanisms that limit sub-lytic MAC activity include: cell surface complement regulatory proteins CD46, CD55, and CD59 that inhibit specific steps of MAC formation; elimination of assembled MAC by exocytosis of membrane vesicles or by endocytosis and subsequent lysosomal degradation; and rapid resealing of pores by the exocytosis of lysosomes. Aging in the post-mitotic retinal pigment epithelium is characterized by the accumulation of cellular debris called lipofuscin, which has also been associated with retinal diseases such as age-related macular degeneration. Lipofuscin has been shown to activate complement components both in vitro and in vivo, suggesting that it could contribute complement-mediated dysfunction in the retinal pigment epithelium. Here, we discuss emerging evidence that vesicular trafficking in the retinal pigment epithelium is critical for efficient removal of MAC from the cell surface and for limiting inflammation in the outer retina.

**Keywords** Retinal pigment epithelium · Age-related macular degeneration · Inflammation · Lysosome exocytosis · Complement-regulatory proteins · Exosomes · Membrane integrity · Membrane attack complex

A. Lakkaraju (✉) · K. A. Toops · J. Xu
Department of Ophthalmology and Visual Sciences, School of Medicine and Public Health, University of Wisconsin-Madison, 1300 University Ave, MSC 3385, Madison, WI 53706, USA
e-mail: lakkaraju@wisc.edu

A. Lakkaraju . K. A. Toops
McPherson Eye Research Institute, University of Wisconsin-Madison, 1300 University Ave, MSC 3385, Madison, WI 53706, USA
e-mail: toops@wisc.edu

J. Xu
e-mail: jxu3@wisc.edu

J. D. Ash et al. (eds.), *Retinal Degenerative Diseases,* Advances in Experimental Medicine and Biology 801, DOI 10.1007/978-1-4614-3209-8_34,

**Abbreviations**

| | |
|---|---|
| AMD | Age-related macular degeneration |
| ESCRT | Endosomal sorting complexes required for transport |
| GPI | Glycosylphosphatidylinositol |
| MAC | Membrane attack complex |
| RPE | Retinal pigment epithelium |
| SNARE | Soluble N-ethylmaleimide sensitive factor Attachment protein Receptor |

## 34.1 Introduction

Age-related macular degeneration (AMD) is a multifactorial disease with many genetic and environmental factors that contribute to disease susceptibility and progression [1]. Development of effective therapies for the chronic version of the disease, called geographic atrophy or dry AMD, has been hampered by a lack of clear insight into disease mechanisms [2]. However, it is now accepted that the initial damage that eventually results in vision loss occurs in cells of the retinal pigment epithelium (RPE) [3, 4]. The alternative pathway of the complement system has been implicated in AMD pathogenesis. Complement factor H polymorphisms that reduce complement-inhibitory activity are associated with $\geq 50\%$ of AMD cases [3]. Many complement components, including activated proteins and complement-regulatory molecules, have been detected in drusen, the extracellular lipid-protein aggregates that accumulate beneath the RPE and are a risk factor for AMD [5, 6].

The final step in the complement cascade is the formation of the C5b-9 membrane attack complexes (MAC, also called "terminal complement complexes") by a sequential assembly of C5b, C6, C7, C8, and C9 proteins on the cell membrane to form a lytic pore. The C9 protein is an amphipathic molecule that, when inserted in the cell membrane, polymerizes to form rigid channel. Deposition of a large number of MAC blasts holes in membranes, leading to cell lysis and death [7]. The earliest detectable event after MAC pore formation is a large influx of calcium into the cell. At high concentrations, calcium causes loss of mitochondrial membrane potential and eventually cell death. It is now appreciated that at low numbers or at "sub-lytic" doses, MAC pores do not cause cell lysis, but can nevertheless lead to compromised cell function. Since calcium is an important second messenger, a sustained influx of calcium into the cell can cause aberrant signaling and secretion of pro-inflammatory mediators [7, 8]. In the RPE in vitro, assembly of sub-lytic MAC either alone [9] or in combination with oxidative stress [10] has been shown to increase the secretion of interleukins IL-6, IL-8 and other pro-inflammatory proteins and pro-angiogenic proteins such as vascular endothelial growth factor. Further, lipofuscin and its major component, A2E, have been shown to activate complement both in vitro in the RPE and in vivo in the *abca4*$^{-/-}$ mouse model of recessive Stargardt's macular dystrophy [11, 12]. These data suggest that lipofuscin-mediated activation of complement and subsequent chronic inflammation could be one significant mechanism that contributes to AMD.

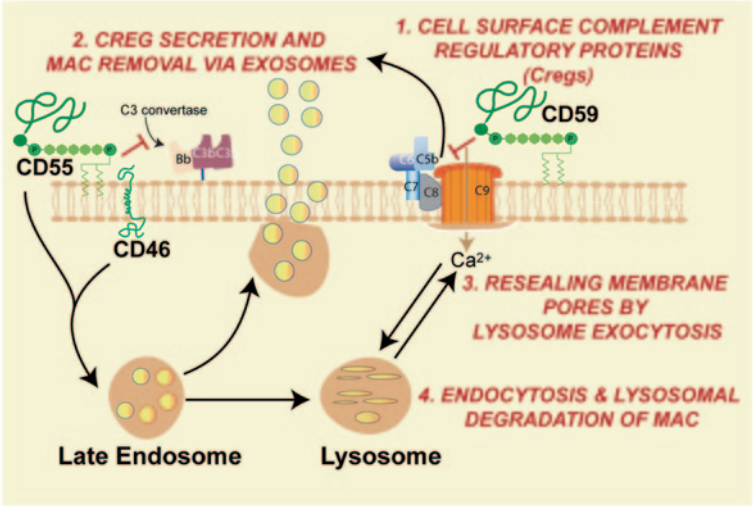


**Fig. 34.1** Mechanisms that help cells remove or recover from damage induced by sub-lytic membrane attack complexes (MAC) deposition. *1* Complement-regulatory proteins on the cell membrane such as the GPI-anchored *CD55* and *CD59* and the transmembrane *CD46* inhibit specific steps of MAC assembly. *2* MAC can also be removed by shedding from the cell surface or by secretion of exosomes; complement-regulatory proteins can also be secreted via exosomes, presumably to protect neighboring cells from MAC attack. *3* Fusion of lysosomes with the plasma membrane in response to calcium influx (lysosome exocytosis) is a crucial survival mechanism that helps maintain membrane integrity. *4* MAC can also be removed from the cell membrane by endocytosis and subsequent lysosomal degradation. These mechanisms are discussed in detail in the text in relation to the RPE

Nucleated cells have evolved numerous ways to protect themselves from sub-lytic MAC attack (Fig. 34.1) including (1) cell-surface complement regulatory proteins, (2) secretion of anti-inflammatory proteins via exosomes and removal of MAC by surface shedding of microvesicles, (3) resealing MAC pores by lysosome exocytosis, and (4) endocytosis and subsequent lysosomal degradation of MAC [7, 13]. Here, we will review how these mechanisms operate in the RPE and how endo-lysosome trafficking is central to the efficient functioning of these protective mechanisms.

## 34.2 Membrane-Bound Complement-Regulatory Proteins

CD46, CD55, and CD59 are cell-surface complement-regulatory proteins that inhibit specific steps of MAC formation [14]. CD59 in particular blocks the assembly of the C9 pore and prevents MAC deposition [15]. CD46 is a trans-membrane protein whereas CD55 and CD59 are attached to the membrane by a glycosylphosphatidylinositol (GPI) anchor. GPI-anchored proteins preferentially associate with

cholesterol-enriched domains of the cell membrane and upon internalization and undergo slow recycling back to the cell surface [16]. Studies have shown that recycling of GPI-anchored proteins depends on the cholesterol content of the cell, and recycling kinetics can be accelerated by depleting the cell of cholesterol [17]; conversely, excess cholesterol diverts GPI-anchored proteins away from the recycling pathway towards the lysosomal degradative pathway. In both early and late AMD, studies have documented decreased expression of CD59 apically and CD46 basolaterally on the RPE [18, 19]. These data suggest that a decrease in the amount of cell-surface complement-regulatory proteins would facilitate the deposition of sub-lytic MAC on the RPE membrane and predispose towards inflammation.

## 34.3 Exosomes and Microvesicles

MAC can be removed from the plasma membrane either by the secretion of exosomes or by shedding of microvesicles from the cell surface [13]. Exosomes are internal vesicles of late endosomes that are released upon fusion of the late endosomal-limiting membrane with the plasma membrane [20]. Exosomes have emerged as an important mode of intercellular communication and have been implicated in various diseases including cancer, Alzheimer's disease, and Parkinson's disease [21, 22]. Exosomes released by antigen-presenting cells have CD55 and CD59, which presumably protect them from complement-mediated lysis [23]. Alternatively, complement-regulatory proteins carried by RPE cell exosomes could protect neighboring cells from MAC attack. Cells also shed MAC-enriched microvesicles, called "ectosomes," from the surface as a rapid mechanism to limit the residence time of MAC on the plasma membrane. In many cell types, including oligodendrocytes, platelets, erythrocytes, and neutrophils, multiple membrane protrusions enriched in C9 appear on the cell surface following MAC deposition [24, 25]. These protrusions are then shed from the cell by pinching off. In addition to MAC and complement-regulatory proteins, both exosomes and ectosomes are enriched in cell-specific repertoire of proteins and lipids, indicative of active sorting processes that contribute to vesicle biogenesis [13].

## 34.4 Membrane Repair

Rapid resealing of membrane holes is a crucial survival mechanism that is important for patching MAC pores and preventing further influx of calcium. The additional membrane required to reseal the pore is provided by organelles such as lysosomes, endosomes, or small vesicles. Calcium-induced fusion of lysosomes with the plasma membrane has emerged as an important mechanism of membrane repair in non-polarized cells [26]. This phenomenon, called lysosome exocytosis, involves the fusion of lysosomes docked at the cell periphery with the plasma membrane and

was first identified during cell invasion by the protozoan parasite *Trypanosoma cruzi* [27]. Lysosome exocytosis can also function as an exit route for cellular debris: In rat hepatocytes, secretion of copper-laden lysosomes into bile is one mechanism by which cells deal with excess copper [28]; in a mouse model of the lysosomal storage disease metachromatic leukodystrophy, lysosomes containing sulfatide are exocytosed in response to increased $[Ca^{2+}]_i$ [29]. Machinery required for $Ca^{2+}$-induced lysosome exocytosis in non-polarized cells includes the calcium sensor synaptotagmin VII, the vesicular soluble N-ethylmaleimide sensitive factor attachment protein receptor (v-SNARE) VAMP7, and the target SNAREs (t-SNAREs) SNAP23 and syntaxin 4 [30]. A localized increase in intracellular calcium induces a conformational change in syntaptotagmin VII, which then allows the formation of the four helical SNARE bundles involving the v- and t-SNAREs [26]. We recently investigated the mechanism of lysosome exocytosis in polarized epithelial cells in response to calcium ionophores and pore-forming toxins. Our data implicate the actin cytoskeleton, membrane cholesterol content, and the t-SNARE syntaxin 4 in polarized lysosome exocytosis [31]. It is therefore likely that in the RPE, lysosome exocytosis participates in membrane repair following MAC deposition (Toops, Xu, Lakkaraju, et al., in preparation).

## 34.5 Endocytosis and Degradation

MAC and other pore-forming toxins can also be removed by rapid endocytosis and subsequent lysosomal degradation [32, 33]. Once internalized, MAC can be transported to late endosomes or multivesicular bodies and secreted out as exosomes. Alternatively, MAC can be trafficked to the lysosome for degradation. In erythroleukemic cells, recent work shows that endocytosis of MAC occurs by a clathrin-independent, caveolin-1-dependent route [32]. Endocytosis of MAC requires membrane cholesterol (which maintains the structure of caveolae) and the large GTPase dynamin-2, which is required for fission of endocytic vesicles. In normal rat kidney cells, the pore-forming toxin streptolysin O first induces lysosome exocytosis to facilitate membrane repair, followed by rapid removal of streptolysin O pores by internalization into endosomes. The toxin is then targeted to lysosomes by ubiquitination/ESCRT-dependent sorting and subsequently degraded [33]. It remains to be seen if the endosomal sorting complexes required for transport (ESCRT) machinery is also required for lysosomal degradation of MAC.

## 34.6 Conclusions and Perspectives

The RPE, like other nucleated cells, has numerous protective mechanisms that help limit damage caused by sub-lytic MAC deposition. The studies summarized in this review indicate that many, if not all, of these processes depend on efficient endo-

lysosome trafficking in the RPE. We have shown that the lipofuscin component A2E causes cholesterol storage in RPE late endosomes and lysosomes [34], and this excess cholesterol inhibits organelle motility (Toops, Xu, Lakkaraju, et al., in preparation). In agreement with this hypothesis, we have recently shown that excess cholesterol inhibits lysosome exocytosis in polarized epithelia [31]. Ongoing work in our laboratory is focused on how lipofuscin and cholesterol accumulation affect lipid-protein trafficking, secretion of exosomes, and lysosome exocytosis in the RPE. With age, declining lysosome function in the RPE can lead to a reciprocal increase in lipofuscin formation and, possibly, cholesterol storage, which can in turn cause intracellular traffic jams and interfere with endo-lysosome function. A decrease in the efficiency of protective mechanisms that help the cell remove and recover from sub-lytic MAC attack would compromise RPE membrane integrity, lead to aberrant signaling, and likely contribute to a chronic inflammatory environment in the outer retina.

**Acknowledgments** The work was supported by the American Health Assistance Foundation (M2009093), Carl Marshall and Mildred Almen Reeves Foundation, Karl Kirchgessner Foundation, Research to Prevent Blindness Career Development Award, and Retina Research Foundation Rebecca Meyer Brown Professorship.

## References

1. Swaroop A, Chew EY, Rickman CB, Abecasis GR (2009) Unraveling a multifactorial late-onset disease: from genetic susceptibility to disease mechanisms for age-related macular degeneration. Annu Rev Genomics Hum Genet 10:19–43
2. Bird AC (2010) Therapeutic targets in age-related macular disease. J Clin Invest 120(9):3033–3041
3. Bok D (2005) Evidence for an inflammatory process in age-related macular degeneration gains new support. Proc Natl Acad Sci U S A 102(20):7053–7054
4. Ambati J, Fowler BJ (2012) Mechanisms of age-related macular degeneration. Neuron 75(1):26–39
5. Anderson DH, Mullins RF, Hageman GS, Johnson LV (2002) A role for local inflammation in the formation of drusen in the aging eye. Am J Ophthalmol 134(3):411–431
6. Hageman GS, Anderson DH, Johnson LV, Hancox LS, Taiber AJ, Hardisty LI, Hageman JL, Stockman HA, Borchardt JD, Gehrs KM, Smith RJ, Silvestri G, Russell SR, Klaver CC, Barbazetto I, Chang S, Yannuzzi LA, Barile GR, Merriam JC, Smith RT, Olsh AK, Bergeron J, Zernant J, Merriam JE, Gold B, Dean M, Allikmets R (2005) A common haplotype in the complement regulatory gene factor H (HF1/CFH) predisposes individuals to age-related macular degeneration. Proc Natl Acad Sci U S A 102(20):7227–7232
7. Cole DS, Morgan BP (2003) Beyond lysis: how complement influences cell fate. Clin Sci 104(5):455–466
8. Bohana-Kashtan O, Ziporen L, Donin N, Kraus S, Fishelson Z (2004) Cell signals transduced by complement. Mol Immunol 41(6-7):583–597
9. Lueck K, Wasmuth S, Williams J, Hughes TR, Morgan BP, Lommatzsch A, Greenwood J, Moss SE, Pauleikhoff D (2011) Sub-lytic C5b-9 induces functional changes in retinal pigment epithelial cells consistent with age-related macular degeneration. Eye 25(8):1074–1082
10. Kunchithapautham K, Rohrer B (2011) Sublytic membrane-attack-complex (MAC) activation alters regulated rather than constitutive vascular endothelial growth factor (VEGF) secretion in retinal pigment epithelium monolayers. J Biol Chem 286(27):23717–23724

11. Radu RA, Hu J, Yuan Q, Welch DL, Makshanoff J, Lloyd M, McMullen S, Travis GH, Bok D (2011) Complement system dysregulation and inflammation in the retinal pigment epithelium of a mouse model for Stargardt macular degeneration. J Biol Chem 286(21):18593–18601
12. Sparrow JR, Ueda K, Zhou J (2012) Complement dysregulation in AMD: RPE-Bruch's membrane-choroid. Mol Aspects Med 33(4):436–445
13. Pilzer D, Gasser O, Moskovich O, Schifferli JA, Fishelson Z (2005) Emission of membrane vesicles: roles in complement resistance, immunity and cancer. Springer Semin Immunopathol 27(3):375–387
14. Longhi MP, Harris CL, Morgan BP, Gallimore A (2006)Holding T cells in check-a new role for complement regulators? Trends Immunol 27(2):102–108
15. Meri S, Morgan BP, Davies A, Daniels RH, Olavesen MG, Waldmann H, Lachmann PJ (1990) Human protectin (CD59), an 18,000-20,000 MW complement lysis restricting factor, inhibits C5b-8 catalysed insertion of C9 into lipid bilayers. Immunology 71(1):1–9
16. Mayor S, Riezman H (2004) Sorting GPI-anchored proteins. Nat Rev Mol Cell Biol 5(2):110–120
17. Mayor S, Sabharanjak S, Maxfield FR (1998) Cholesterol-dependent retention of GPI-anchored proteins in endosomes. EMBO J 17(16):4626–4638
18. Ebrahimi KB, Fijalkowski N, Cano M, Handa JT (2012) Decreased membrane complement regulators in the retinal pigmented epithelium contributes to age-related macular degeneration. J Pathol 229(5):729–742
19. Vogt SD, Curcio CA, Wang L, Li CM, McGwin G Jr, Medeiros NE, Philp NJ, Kimble JA, Read RW (2011) Retinal pigment epithelial expression of complement regulator CD46 is altered early in the course of geographic atrophy. Exp Eye Res 93(4):413–423
20. Lakkaraju A, Rodriguez-Boulan E (2008) Itinerant exosomes: Emerging roles in cell and tissue polarity. Trends Cell Biol 18:199–209
21. Thery C, Ostrowski M, Segura E (2009) Membrane vesicles as conveyors of immune responses. Nature reviews. Immunology 9(8):581–593
22. Bellingham SA, Guo BB, Coleman BM, Hill AF (2012) Exosomes: vehicles for the transfer of toxic proteins associated with neurodegenerative diseases? Frontiers Physiol 3:124
23. Clayton A, Harris CL, Court J, Mason MD, Morgan BP (2003) Antigen-presenting cell exosomes are protected from complement-mediated lysis by expression of CD55 and CD59. Eur J Immunol 33(2):522–531
24. Scolding NJ, Morgan BP, Houston WA, Linington C, Campbell AK, Compston DA (1989) Vesicular removal by oligodendrocytes of membrane attack complexes formed by activated complement. Nature 339(6226):620–622
25. Moskovich O, Fishelson Z (2007) Live cell imaging of outward and inward vesiculation induced by the complement c5b-9 complex. J Biol Chem 282(41):29977–29986
26. Idone V, Tam C, Andrews NW (2008) Two-way traffic on the road to plasma membrane repair. Trends Cell Biol 18(11):552–559
27. Andrews NW (2002) Lysosomes and the plasma membrane: trypanosomes reveal a secret relationship. J Cell Biol 158(3):389–394
28. Gross JB Jr, Myers BM, Kost LJ, Kuntz SM, LaRusso NF (1989) Biliary copper excretion by hepatocyte lysosomes in the rat. Major excretory pathway in experimental copper overload. J Clin Invest 83(1):30–39
29. Klein D, Bussow H, Fewou SN, Gieselmann V (2005) Exocytosis of storage material in a lysosomal disorder. Biochem Biophys Res Commun 327(3):663–667
30. Rao SK, Huynh C, Proux-Gillardeaux V, Galli T, Andrews NW (2004) Identification of SNAREs involved in synaptotagmin VII-regulated lysosomal exocytosis. J Biol Chem 279(19):20471–20479
31. Xu J, Diaz F, Carvajal-Gonzalez JM, Mazzoni F, Schreiner R, Rodriguez-Boulan E, Lakkaraju A (2013) Mechanism of polarized lysosome exocytosis in epithelial cells. J Cell Sci 2013:In-Press
32. Moskovich O, Herzog LO, Ehrlich M, Fishelson Z (2012) Caveolin-1 and dynamin-2 are essential for removal of the complement C5b-9 complex via endocytosis. J Biol Chem 287(24):19904–19915

33. Corrotte M, Fernandes MC, Tam C, Andrews NW (2012) Toxin pores endocytosed during plasma membrane repair traffic into the lumen of MVBs for degradation. Traffic 13(3):483–494
34. Lakkaraju A, Finnemann SC, Rodriguez-Boulan E (2007) The lipofuscin fluorophore A2E perturbs cholesterol metabolism in retinal pigment epithelial cells. Proc Natl Acad Sci U S A 104(26):11026–11031

# Chapter 35
# Hypoxia-Inducible Factor (HIF)/Vascular Endothelial Growth Factor (VEGF) Signaling in the Retina

**Toshihide Kurihara, Peter D. Westenskow and Martin Friedlander**

**Abstract** Over a span of two decades, it has become increasingly clear that vascular endothelial growth factor (VEGF) plays an important role in the pathogenesis of retinal diseases including age-related macular degeneration (AMD) and diabetic retinopathy (DR). Based on these observations, anti-VEGF therapies are being developed and approved for clinical use in the treatment of neovascular eye diseases. Hypoxia-inducible factors (HIFs) are transcriptional factors that are stabilized and activated under hypoxic conditions and induce expression of gene products, including VEGF, that are required for cell survival under hypoxia. Here we discuss recent findings from our lab and others that define roles of the HIF-VEGF axis in the retina.

**Keywords** Hypoxia-inducible factors · von Hippel-Lindau tumor suppressor · Vascular endothelial growth factor · Retinal pigment epithelium · Age-related macular degeneration

**Abbreviations**

| | |
|---|---|
| VEGF | Vascular endothelial growth factor |
| AMD | Age-related macular degeneration |
| DR | Diabetic retinopathy |
| HIFs | Hypoxia-inducible factors |
| ARNTs | Aryl hydrocarbon receptor nuclear translocators |
| PHDs | HIF prolyl hydroxylases |
| NOSs | Nitric oxide synthases |

M. Friedlander (✉) · T. Kurihara · P. D. Westenskow
Department of Cell and Molecular Biology, The Scripps Research Institute, 10550 N. Torrey Pines Rd. La Jolla, San Diego, CA 92014, USA
e-mail: friedlan@scripps.edu

T. Kurihara
e-mail: kurihara@scripps.edu

P. D. Westenskow
e-mail: petewest@scripps.edu

J. D. Ash et al. (eds.), *Retinal Degenerative Diseases,* Advances in Experimental Medicine and Biology 801, DOI 10.1007/978-1-4614-3209-8_35,

| | |
|---|---|
| GLUTs | Glucose transporters |
| VHL | Von Hippel-Lindau disease gene |
| RPE | Retinal pigment epithelium |
| PHPV | Persistent hypertrophic primary vitreous |
| OIR | Oxygen-induced retinopathy |
| ROP | Retinopathy of prematurity |
| CNV | Choroidal neovascularization |

## 35.1 Introduction

Many retinal diseases are characterized by abnormal pathological neovascularization and increased vascular permeability. A significant advance in our understanding of mechanisms that underlie these changes was the identification of increased expression of vascular endothelial growth factor (VEGF) in these diseases [1]. As a result of these findings, VEGF antagonists have been developed [2, 3]. To date, three types of anti-VEGF drugs are approved for clinical use [4] and may be used to treat neovascular age-related macular degeneration (AMD), macular edema in diabetic retinopathy (DR), and retinal vein occlusion. At the molecular level, VEGF regulates proliferation and migration of vascular endothelial cells and enhances vascular permeability through activation of its tyrosine kinase receptors. Therefore, VEGF knockout mice, even heterozygotes, are embryonic lethal due to impairment of blood-island formation [5, 6]. Although the introduction of anti-VEGF drugs into the clinics has dramatically changed our ability to treat neovascular retinal diseases, a number of off-target effects have been reported in multiple organs [7–11]. Here we discuss the physiological and pathological roles of VEGF and its main transcriptional regulators, hypoxia-inducible factors (HIFs), in the retina, and their potential use for the treatment of retinal diseases.

## 35.2 Hypoxia-Inducible Factors (HIFs)

Identification and molecular cloning of Hypoxia-inducible factor-1 (HIF-1) were first shown by Semenza and his colleagues through the analysis of transcription of the *erythropoietin* (*EPO*) gene under hypoxic conditions in the early 1990s [12, 13]. HIFs are part of a basic-helix-loop-helix-PAS family of transcriptional factors that mediate heterodimer formation between α-subunits (HIF-αs that are regulated by cellular oxygen tension) and constitutively expressed β-subunits (HIF-βs also known as aryl hydrocarbon receptor nuclear translocators, ARNTs). In normoxia, specific proline residues in HIF-αs are hydroxylated by HIF prolyl hydroxylases (PHDs); these hydroxylated HIF-αs are then multi-ubiquitinated and degraded in the proteasome. Conversely, under low oxygen tension PHD activity is inhibited,

inducing stabilization of HIF-αs. Stabilized HIF-αs are translocated to the nucleus and form heterodimers with HIF-βs where they regulate the expression of a number of genes, important for cell survival under hypoxic conditions. These genes affect a number of functions including angiogenesis (VEGF), erythropoiesis (EPO), inflammation (nitric oxide synthases, NOSs), and energy homeostasis (glucose transporters, GLUTs). Importantly, the protein encoded by von Hippel-Lindau disease gene (VHL) is required for the specific degradation of HIF-α proteins in ubiquitin-proteasome system [14]. This discovery, of a molecular connection between HIF and VHL, helped reveal the mechanism of the progression of VHL disease symptoms such as retinal and brain hemangioblastoma.

## 35.3 Physiological Roles of HIFs and VEGF in the Retina

In early developmental stages, the vascular system in the retina undergoes dramatic changes. The hyaloidal vascular system in the vitreous cavity is responsible for the blood supply by the third trimester in humans and the early postnatal stages in rodents [15, 16]. At this stage, retinal vessels start to proliferate from the optic nerve head to the retinal periphery over a template of retinal astrocytes [17, 18]. The regression of the hyaloidal vasculature occurs concomitant with development of the retinal vasculature, completing the transition from embryonic to adult circulation in the retina. Retinal neurons and glia are under conditions of physiological hypoxia during the period when the hyaloidal vasculature is present [19, 20]. Development of the retinal vasculature increases cellular oxygen tension and decreases stability of the HIFαs [20]. Disruption of this physiological reduction of HIF-α by conditionally deleting VHL in retinal neurons or astrocytes induces persistence of the hyaloidal vasculature. This developmental impairment can be rescued by genetic deletion or pharmacological inhibition of VEGF [16, 20]. Interestingly, conditional deletion of either HIF-αs or VEGF in astrocytes is not associated with defects in retinal vascular formation [21, 22]. However, conditional deletion of HIF-1α during development of retinal neurons causes delayed retinal vascular formation through impairment of astrocytic template formation [23, 24]. Thus, fine-tuning of HIF-VEGF signaling as regulated by tissue oxygen tension is important for normal development of the retinal neurons and vessels.

Retinal pigment epithelium (RPE) cells, located between photoreceptors and the choriocapillaris (capillaries forming the inner vascular layer of the choroid), play an important role in maintaining retinal homeostasis. It has been shown that RPE-derived VEGF [25, 26], but not HIF-1α [25, 27], is critical for choriocapillaris formation during developmental stages. Importantly, RPE-derived VEGF has a critical function in the adult retina after establishment of the tissue. Adult-induced RPE-specific VEGF knockout mice induce choriocapillaris and cone photoreceptor atrophy within a few days [11]. The trophic effects of VEGF has also been shown using a soluble VEGF null mouse ($VEGF^{188/188}$ mice) [28] as well as with pharmacological inhibition [29–31]. In contrast, RPE-specific deletion of HIF-1α and/or

HIF-2α shows no vascular and neurological phenotypic changes. These findings indicate that basal levels of endogenous VEGF are critical for retinal function, but HIFs are not required physiologically. In fact, VEGF is also regulated and maintained in several HIF-independent pathways [32, 33].

## 35.4 Pathological Roles of HIFs in the Retina

Constitutive stabilization of HIFs by VHL deletion in retinal neurons or astrocytes results in persistent hyaloidal vasculature resembling a human developmental defect, persistent hypertrophic primary vitreous (PHPV) [16, 20]. Interestingly, targeted deletion of VHL in myeloid cells induces *accelerated* hyaloidal vascular regression [16]. Embryonic VHL deletion in RPE induces anastomoses between the retinal and choroidal vasculature [34]. These findings further demonstrate that regulated HIF expression during development is critical.

The oxygen-induced retinopathy (OIR) model is used to investigate mechanisms of ischemic retinopathy [35] and is induced by 5 days of hyperoxia (75%) between postnatal days 7 and 12, followed by return to normoxia. Increased protein levels of HIF-αs are found in OIR [36, 37], and systemic knockdown or astrocyte-specific gene deletion of HIF-2α rescue the phenotype of neovascular tuft formation, similar to that observed when VEGF is deleted [21, 38]. Clinically, acute, intensive insulin therapy is known to induce progression of DR. This mechanism may be explained by the finding of insulin-induced HIF-1α/VEGF activation through PI 3 kinase and p38 MAPK [39]. Choroidal neovascularization (CNV) is the main feature of neovascular (wet type) AMD. In an animal model, CNV can be induced by laser photocoagulation to Bruch's membrane (laser-induced CNV) [40]. RPE-specific deletion of HIF-1α and/or HIF-2α shows significant suppression of laser-induced CNV formation compared to wild-type animals [11, 27]. Although this suppressive effect is observed in RPE-specific VEGF deletion as well, RPE-derived VEGF deletion causes functional defects, unlike that observed when HIF is deleted [11]. These data indicate a therapeutic potential for HIF in the treatment of neovascular retinal diseases such as DR and AMD.

## 35.5 Conclusion

In this minireview, we have summarized the physiological and pathological roles of HIF-VEGF signaling during development and in normal and diseased adult retinas. Abnormal VEGF expression is critical for the pathogenesis of the diseases, but physiological levels are crucial in the maintenance of normal retinal function. In contrast, HIF expression is not required physiologically except in developmental stages. Pathological HIF activation that induces increases of VEGF levels is observed in several retinal disease models. Therapeutically targeting HIFs may have

advantages over antagonizing VEGF, and the therapeutic potential of specific, effective, and safe HIF inhibitors should be explored.

**Acknowledgments** We wish to warmly thank all members of the Friedlander lab and our collaborators. Work discussed in this chapter was supported by fellowships to TK (Manpei Suzuki Diabetes Foundation and The Japan Society for the Promotion of Science Postdoctoral Fellowships for Research Abroad) and to PDW (a Ruth Kirschstein Fellow NEI EY021416). MF gratefully acknowledges the generous support of the research in our lab from the National Eye Institute of the National Institutes of Health (EY11254 and EY017540), the California Institute for Regenerative Medicine (CIRM TR1–01219), the Lowy Medical Research Foundation (the MacTel Project), and the Rasmussen Foundation.

## References

1. Aiello LP, Avery RL, Arrigg PG, Keyt BA, Jampel HD, Shah ST et al (1994) Vascular endothelial growth factor in ocular fluid of patients with diabetic retinopathy and other retinal disorders. N Engl J Med 331(22):1480–1487
2. Gragoudas ES, Adamis AP, Cunningham ET Jr, Feinsod M, Guyer DR (2004) Pegaptanib for neovascular age-related macular degeneration. N Engl J Med 351(27):2805–2816
3. Rosenfeld PJ, Brown DM, Heier JS, Boyer DS, Kaiser PK, Chung CY et al (2006) Ranibizumab for neovascular age-related macular degeneration. N Engl J Med 355(14):1419–1431
4. Stewart MW, Grippon S, Kirkpatrick P (2012) Aflibercept. Nat Rev Drug Discov 11(4):269–270
5. Ferrara N, Carver-Moore K, Chen H, Dowd M, Lu L, O'Shea KS et al (1996) Heterozygous embryonic lethality induced by targeted inactivation of the VEGF gene. Nature 380(6573):439–442
6. Carmeliet P, Ferreira V, Breier G, Pollefeyt S, Kieckens L, Gertsenstein M et al (1996) Abnormal blood vessel development and lethality in embryos lacking a single VEGF allele. Nature 380(6573):435–439
7. Eremina V, Jefferson JA, Kowalewska J, Hochster H, Haas M, Weisstuch J et al (2008) VEGF inhibition and renal thrombotic microangiopathy. N Engl J Med 358(11):1129–1136
8. Maharaj AS, Walshe TE, Saint-Geniez M, Venkatesha S, Maldonado AE, Himes NC et al (2008) VEGF and TGF-beta are required for the maintenance of the choroid plexus and ependyma. J Exp Med 205(2):491–501
9. Sandler A, Gray R, Perry MC, Brahmer J, Schiller JH, Dowlati A et al (2006) Paclitaxel-carboplatin alone or with bevacizumab for non-small-cell lung cancer. N Engl J Med 355(24):2542–2550
10. Martin DF, Maguire MG, Fine SL, Ying GS, Jaffe GJ, Grunwald JE et al (2012) Ranibizumab and bevacizumab for treatment of neovascular age-related macular degeneration: two-year results. Ophthalmology 119(7):1388–1398
11. Kurihara T, Westenskow PD, Bravo S, Aguilar E, Friedlander M (2012) Targeted deletion of Vegfa in adult mice induces vision loss. J Clin Invest 122(11):4213–4217
12. Semenza GL, Wang GL (1992) A nuclear factor induced by hypoxia via de novo protein synthesis binds to the human erythropoietin gene enhancer at a site required for transcriptional activation. Mol Cell Biol 12(12):5447–5454
13. Wang GL, Jiang BH, Rue EA, Semenza GL (1995) Hypoxia-inducible factor 1 is a basic-helix-loop-helix-PAS heterodimer regulated by cellular O2 tension. Proc Natl Acad Sci U S A 92(12):5510–5514
14. Maxwell PH, Wiesener MS, Chang GW, Clifford SC, Vaux EC, Cockman ME et al (1999) The tumour suppressor protein VHL targets hypoxia-inducible factors for oxygen-dependent proteolysis. Nature 399(6733):271–275

15. Ito M, Yoshioka M (1999) Regression of the hyaloid vessels and pupillary membrane of the mouse. Anat Embryol (Berl) 200(4):403–411
16. Kurihara T, Westenskow PD, Krohne TU, Aguilar E, Johnson RS, Friedlander M (2011) Astrocyte pVHL and HIF-alpha isoforms are required for embryonic-to-adult vascular transition in the eye. J Cell Biol 195(4):689–701
17. Dorrell MI, Aguilar E, Friedlander M (2002) Retinal vascular development is mediated by endothelial filopodia, a preexisting astrocytic template and specific R-cadherin adhesion. Invest Ophthalmol Vis Sci 43(11):3500–3510
18. Gerhardt H, Golding M, Fruttiger M, Ruhrberg C, Lundkvist A, Abramsson A et al (2003) VEGF guides angiogenic sprouting utilizing endothelial tip cell filopodia. J Cell Biol 161(6):1163–1177
19. Yu DY, Cringle SJ (2001) Oxygen distribution and consumption within the retina in vascularised and avascular retinas and in animal models of retinal disease. Prog Retin Eye Res 20(2):175–208
20. Kurihara T, Kubota Y, Ozawa Y, Takubo K, Noda K, Simon MC et al (2010) von Hippel-Lindau protein regulates transition from the fetal to the adult circulatory system in retina. Development 137(9):1563–1571
21. Weidemann A, Krohne TU, Aguilar E, Kurihara T, Takeda N, Dorrell MI et al (2010) Astrocyte hypoxic response is essential for pathological but not developmental angiogenesis of the retina. Glia 58(10):1177–1185
22. Scott A, Powner MB, Gandhi P, Clarkin C, Gutmann DH, Johnson RS et al (2010) Astrocyte-derived vascular endothelial growth factor stabilizes vessels in the developing retinal vasculature. PLoS One 5(7):e11863
23. Nakamura-Ishizu A, Kurihara T, Okuno Y, Ozawa Y, Kishi K, Goda N et al (2012) The formation of an angiogenic astrocyte template is regulated by the neuroretina in a HIF-1-dependent manner. Dev Biol 363(1):106–114
24. Caprara C, Thiersch M, Lange C, Joly S, Samardzija M, Grimm C (2011) HIF1A is essential for the development of the intermediate plexus of the retinal vasculature. Invest Ophthalmol Vis Sci 52(5):2109–2117
25. Marneros AG, Fan J, Yokoyama Y, Gerber HP, Ferrara N, Crouch RK et al (2005) Vascular endothelial growth factor expression in the retinal pigment epithelium is essential for choriocapillaris development and visual function. Am J Pathol 167(5):1451–1459
26. Le YZ, Bai Y, Zhu M, Zheng L (2010) Temporal requirement of RPE-derived VEGF in the development of choroidal vasculature. J Neurochem 112(6):1584–1592
27. Lin M, Hu Y, Chen Y, Zhou KK, Jin J, Zhu M et al (2012) Impacts of hypoxia-inducible factor-1 knockout in the retinal pigment epithelium on choroidal neovascularization. Invest Ophthalmol Vis Sci 53(10):6197–6206
28. Saint-Geniez M, Kurihara T, Sekiyama E, Maldonado AE, D'Amore PA (2009) An essential role for RPE-derived soluble VEGF in the maintenance of the choriocapillaris. Proc Natl Acad Sci U S A 106(44):18751–18756
29. Robinson GS, Ju M, Shih SC, Xu X, McMahon G, Caldwell RB et al (2001) Nonvascular role for VEGF: VEGFR-1, 2 activity is critical for neural retinal development. Faseb J 15(7):1215–1217
30. Nishijima K, Ng YS, Zhong L, Bradley J, Schubert W, Jo N et al (2007) Vascular endothelial growth factor-A is a survival factor for retinal neurons and a critical neuroprotectant during the adaptive response to ischemic injury. Am J Pathol 171(1):53–67
31. Saint-Geniez M, Maharaj AS, Walshe TE, Tucker BA, Sekiyama E, Kurihara T et al (2008) Endogenous VEGF is required for visual function: evidence for a survival role on muller cells and photoreceptors. PLoS One 3(11):e3554
32. Arany Z, Foo SY, Ma Y, Ruas JL, Bommi-Reddy A, Girnun G et al (2008) HIF-independent regulation of VEGF and angiogenesis by the transcriptional coactivator PGC-1alpha. Nature 451(7181):1008–1012

33. Schmidt D, Textor B, Pein OT, Licht AH, Andrecht S, Sator-Schmitt M et al (2007) Critical role for NF-kappaB-induced JunB in VEGF regulation and tumor angiogenesis. Embo J 26(3):710–719
34. Lange CA, Luhmann UF, Mowat FM, Georgiadis A, West EL, Abrahams S et al (2012) Von Hippel-Lindau protein in the RPE is essential for normal ocular growth and vascular development. Development 139(13):2340–2350
35. Smith LE, Wesolowski E, McLellan A, Kostyk SK, D'Amato R, Sullivan R et al (1994) Oxygen-induced retinopathy in the mouse. Invest Ophthalmol Vis Sci 35(1):101–111
36. Ozaki H, Yu AY, Della N, Ozaki K, Luna JD, Yamada H et al (1999) Hypoxia inducible factor-1alpha is increased in ischemic retina: temporal and spatial correlation with VEGF expression. Invest Ophthalmol Vis Sci 40(1):182–189
37. Mowat FM, Luhmann UF, Smith AJ, Lange C, Duran Y, Harten S et al (2010) HIF-1alpha and HIF-2alpha are differentially activated in distinct cell populations in retinal ischaemia. PLoS One 5(6):e11103
38. Morita M, Ohneda O, Yamashita T, Takahashi S, Suzuki N, Nakajima O et al (2003) HLF/HIF-2alpha is a key factor in retinopathy of prematurity in association with erythropoietin. Embo J 22(5):1134–1146
39. Poulaki V, Qin W, Joussen AM, Hurlbut P, Wiegand SJ, Rudge J et al (2002) Acute intensive insulin therapy exacerbates diabetic blood-retinal barrier breakdown via hypoxia-inducible factor-1alpha and VEGF. J Clin Invest 109(6):805–815
40. Ryan SJ (1979) The development of an experimental model of subretinal neovascularization in disciform macular degeneration. Trans Am Ophthalmol Soc 77:707–745

# Chapter 36
# Is Age-Related Macular Degeneration a Microvascular Disease?

**Robert F. Mullins, Aditi Khanna, Desi P. Schoo, Budd A. Tucker, Elliott H. Sohn, Arlene V. Drack and Edwin M. Stone**

**Abstract** Age-related macular degeneration (AMD) is a common, degenerative disease of the central retina affecting millions of elderly in the USA alone and many more worldwide. A better understanding of the pathophysiology of AMD will be essential for developing new treatments. In this review, we discuss the potential impact of complement complex deposition at the choriocapillaris of aging eyes and the relationship between choriocapillaris loss and drusen formation. We further propose a model that integrates genetic and anatomical findings in AMD and suggest the implications of these findings for future therapies.

**Keywords** Age-related macular degeneration · Choriocapillaris · Choroid · Complement · RPE

R. F. Mullins (✉) · A. Khanna · D. P. Schoo · B. A. Tucker · E. H. Sohn · A. V. Drack · E. M. Stone
Department of Ophthalmology and Visual Sciences, The University of Lowa, Lowa City, IA 52242, USA
e-mail: Robert-Mullins@uiowa.edu

A. Khanna
e-mail: aditi-khanna@uiowa.edu

D. P. Schoo
e-mail: desi-schoo@uiowa.edu

B. A. Tucker
e-mail: budd-tucker@uiowa.edu

E. H. Sohn
e-mail: Elliott-sohn@uiowa.edu

A. V. Drack
e-mail: Arlene-drack@uiowa.edu

E. M. Stone
e-mail: Edwin-stone@uiowa.edu

J. D. Ash et al. (eds.), *Retinal Degenerative Diseases,* Advances in Experimental Medicine and Biology 801, DOI 10.1007/978-1-4614-3209-8_36,

## 36.1 Age-Related Macular Degeneration

Age-related macular degeneration (AMD) is a complex disease characterized by degenerative changes that are most severe in the macular region of the retina. It is characterized at its earliest stages by the formation of drusen beneath the retinal pigment epithelium (RPE) and may progress to severe atrophic degeneration, choroidal neovascularization, hemorrhage, and scarring. Due to its detrimental effect on central vision, AMD is a major societal problem in the developed world, with a substantial impact on quality of life in the elderly [1, 2].

Over the past several years, genetic insights into the risk factors that contribute to AMD have emerged. These include genes that encode members of the complement system (most notably complement factor H (*CFH*), a principal inhibitor of complement activation, but also including *CFHR* genes, as well as *CFB*, *C2*, *C3*, and in some reports *CFI* and *SERPING1*) (reviewed in [3]). Despite recent advances in genetics, the precise mechanism of AMD is not clear, and only very recently has the impact of high- and low-risk genotypes on ocular tissues been studied.

## 36.2 The Complement System

The complement system is an evolutionarily ancient defense mechanism against pathogens. It consists of a large array of proteins that are present in the circulation and can be localized to ocular tissues [4]. The complement system can be activated by multiple pathways [5]; however, regardless of the initial pathway, complement activation results in the formation of a membrane-spanning pore (the membrane attack complex, MAC), which can lyse target pathogens. Significantly, when unchecked, the same machinery that is designed to lyse microbes can similarly damage eukaryotic cells [6].

In view of the genetic finding of polymorphisms in complement genes in AMD, understanding where components of the complement system are localized (and where they assert their physiological effects) in the aging macula is an important step. While other byproducts of complement activation may have important biological activities (e.g., proinflammatory anaphylatoxins [7–9]), the MAC is intuitively the endpoint in complement activation that could have the most profound effect on ocular cells.

Solitary nodular drusen outside the macula show robust labeling with antibodies directed against the neoepitope of the MAC. Basal deposits in the macula, however, show variable immunoreactivity with anti-MAC antibodies. In contrast, we and others have shown that domains surrounding the endothelial cells (EC) of the choriocapillaris appear to be the main sites of MAC deposition in the macula [8, 10–12] (Fig. 36.1a). While this observation does not preclude RPE injury by the MAC as an important event in AMD pathogenesis, it does suggest that the cells under the greatest complement-mediated stress are choriocapillaris EC.

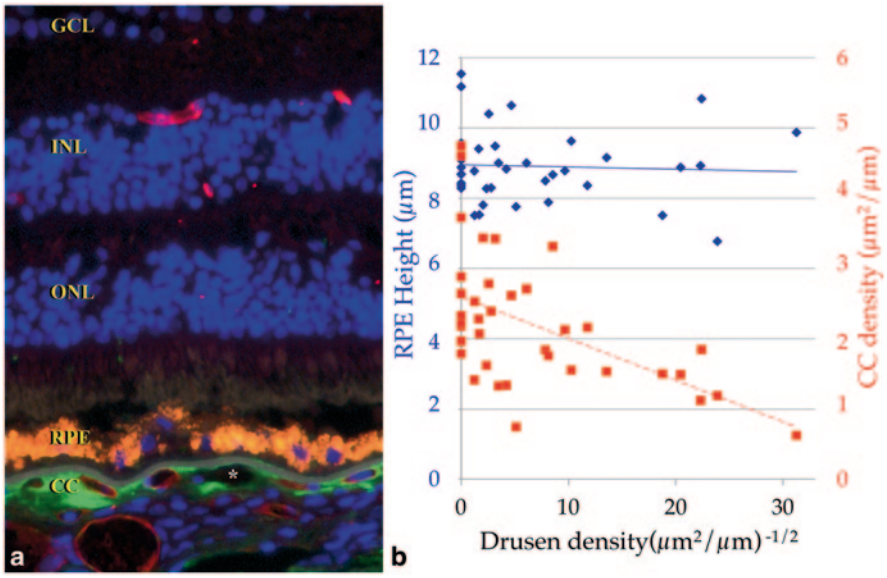


**Fig. 36.1** **a** The choriocapillaris is the main site of MAC deposition in the macula (*green fluorescence*); *red fluorescence* is UEA-I lectin. RPE lipofuscin appears *orange*. The *asterisk* indicates a choriocapillaris ghost vessel. **b** Relationship between choriocapillaris endothelial cell density (*open squares, maroon dashed trend line*), RPE height (*closed diamonds*, *blue solid trend line*), and drusen density. Note that eyes with the lowest vascular density had the largest and most numerous drusen. (Modified from [20]; copyright held by ARVO)

## 36.3 High-Risk Genotypes Associated with Increased Complement Activation

The recent identification of genetic risk factors associated with AMD has created new opportunities to study disease pathophysiology. Notably, these findings may allow the discovery of molecular changes in the tissues of interest even before the onset of detectable disease. Studies on plasma and serum from AMD patients and controls have shown increased complement activation in individuals with high-risk genotypes [13]. Enzyme-linked immunosorbent assay (ELISA) analyses of the MAC in human genotyped RPE-choroid samples show ~70% increase in eyes homozygous for the high-risk CFH allele [14], with higher levels of MAC more closely associated with genotype than AMD status. These findings in aggregate may suggest that increased MAC deposition precedes an overt AMD phenotype, as discussed below.

## 36.4 Choriocapillaris EC Loss Occurs with Increasing Density of Drusen

In addition to being the principal site of MAC localization, anatomical and functional changes occur at the level of the choriocapillaris in AMD. Prolonged filling of the choroid in early AMD was noted by Pauleikhoff and coworkers using both indocyanine green and fluorescein [15]. In laser Doppler flow studies, choroidal blood volume and choroidal blood flow are decreased in association with increasing drusen abundance [16]. Proteomic analyses of age-matched control tissues compared to AMD tissues found loss of choriocapillaris proteins CA4 and HLA-A, with persistence of RPE proteins CRALBP and RPE65 [17]. In histological studies, McLeod and colleagues found loss of choriocapillaris and preservation of RPE outside of the neovascular lesion in eyes with wet AMD, whereas in atrophic AMD, preservation of choroid with loss of the RPE was observed [18]. We employed human donor eyes labeled with the EC-binding lectin from *Ulex europaeus* (UEA-I) to detect live EC and discriminate them from unoccupied, "ghost" vessels in the choriocapillaris, and related these features to the abundance of drusen. We also assessed the height of the RPE as a measure of RPE viability. Measurement of AMD and control eyes in a masked fashion revealed that as drusen density increases, there is loss of choriocapillaris area and increase in the number of ghost vessels [19]. Superimposing the height of the RPE onto these measurements shows no correlation between RPE height and advancing drusen abundance (Fig. 36.1b). However, it should be noted that the presence of an intact RPE monolayer of normal height does not mean that the RPE is completely normal. Morphological and biochemical changes in the RPE may be occurring in eyes with drusen that our measurements do not detect.

The relationship between vascular loss and accumulation of drusen suggests that vascular changes occur early in disease, especially since drusen tend not to form over vascular lumens. We recognize the alternative (and nonexclusive) possibility that the RPE, while still present, may fail to deliver necessary trophic factors to choriocapillaris when drusen develop, such that choriocapillaris loss occurs after drusen biogenesis. It is well known that injury to the RPE can lead to loss of the choriocapillaris as a secondary phenomenon. Nevertheless, our experiments do indicate that there is a correlation between death of choriocapillaris EC and increasing drusen number and size. Further studies of selective choriocapillaris ablation in animals (see below) will refine the relationship between the RPE, Bruch's membrane deposits, and death of the choriocapillaris.

## 36.5 Choriocapillaris Loss and Implications for Therapy

The photoreceptor cells, RPE, and choriocapillaris function as an interdependent unit (recently reviewed in [20]). In light of the many roles of the RPE in maintaining retinal health, replacement of the RPE may be beneficial in AMD, and a number of trials have begun with this goal. RPE cells derived from allogeneic, embryonic, or

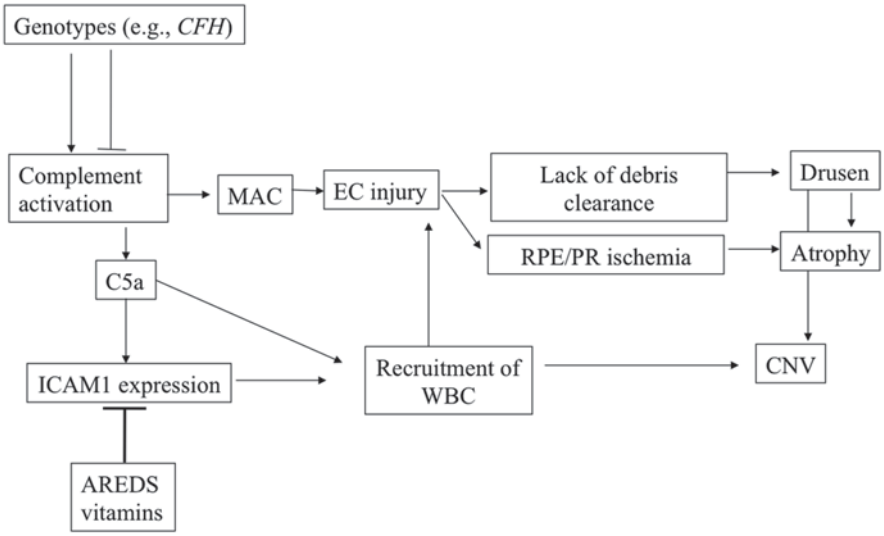


**Fig. 36.2** Model for AMD pathogenesis (see text for details)

fetal sources, or more desirably from autogenic induced pluripotent stem cells, can now be placed into the subretinal space. However in the absence of patient-specific evidence of an intact choriocapillaris (becoming possible by improvements in optical coherence tomography (OCT) [21, 22]), we suggest caution with this approach. Replacement of photoreceptor cells and/or RPE cells on top of a depleted choriocapillaris may be fruitless.

## 36.6 A Model of Early AMD Based on Vascular Loss

A model that attempts to synthesize the role of genetics, complement, vascular loss, drusen, and AMD pathogenesis is depicted in Fig. 36.2. In this model, systemic and local complement activation occurs at the level of the choriocapillaris, and this activation is more pronounced in eyes with high-risk CFH genotypes, as we have observed [14]. Increased complement activation in the choriocapillaris yields C5a anaphylatoxin, which activates vascular endothelial growth factor (VEGF) expression in the RPE and intercellular adhesion molecule 1 (ICAM1) expression in the choriocapillaris, promoting angiogenesis and leukocyte recruitment, respectively [7, 8]. The generation of MAC over the course of decades leads to loss of choriocapillaris EC (which may have a more limited repertoire of defensive proteins than the RPE). Focal loss of the choriocapillaris results in failure to remove debris from the RPE/Bruch's membrane and development of drusen, as well as retinal and RPE hypoxia.

It is interesting in this context that a solution of AREDS vitamins has been shown to attenuate at least one step in this pathway (the upregulated ICAM1 expression by choriocapillary EC [23]).

## 36.7 Future Directions

One of the critical questions is the cause–effect relationship between drusen formation and EC loss in the choriocapillaris. A clear determination of the natural history of Bruch's membrane deposit formation and EC loss needs to be established. Genetically tractable models of vascular dropout will offer insight into this relationship. A better understanding of the mechanisms by which healthy EC are lost in early AMD and the molecular basis of why drusen form in areas depleted of capillary lumens are crucial. Moreover, as noted above, the loss of choroidal EC in AMD suggests that ideal treatments of early AMD may require replacement of lost choroidal EC, through, for example, induced pluripotent stem cells. Advances in the generation, phenotyping, and replacement of these EC will be important in providing cell-based therapies for this blinding disease.

**Acknowledgments** Supported in part by NIH grant EY-017451, EY-016822, the Sramek Foundation, and the Hansjoerg E.J.W. Kolder Professorship for Best Disease Research. We regret any omissions in the bibliography, made necessary by page restrictions.

## References

1. Cahill MT, Banks AD, Stinnett SS, Toth CA (2005) Vision-related quality of life in patients with bilateral severe age-related macular degeneration. Ophthalmology 112(1):152–158
2. Coleman AL, Yu F, Ensrud KE, Stone KL, Cauley JA, Pedula KL, Hochberg MC, Mangione CM (2010) Impact of age-related macular degeneration on vision-specific quality of life: Follow-up from the 10-year and 15-year visits of the Study of Osteoporotic Fractures. Am J Ophthalmol 150(5):683–691
3. Gorin MB. (2012) Genetic insights into age-related macular degeneration: controversies addressing risk, causality, and therapeutics. Mol Aspects Med 33(4):467–486
4. Bhutto IA, Baba T, Merges C, Juriasinghani V, McLeod DS, Lutty GA (2011) C-reactive protein and complement factor H in aged human eyes and eyes with age-related macular degeneration. Br J Ophthalmol 95(9):1323–1330
5. Holers VM (2008) The spectrum of complement alternative pathway-mediated diseases. Immunol Rev 223:300–316
6. Neher MD, Weckbach S, Flierl MA, Huber-Lang MS, Stahel PF (2011) Molecular mechanisms of inflammation and tissue injury after major trauma–is complement the "bad guy"? J Biomed Sci 18:90
7. Nozaki M, Raisler BJ, Sakurai E, Sarma JV, Barnum SR, Lambris JD, Chen Y, Zhang K, Ambati BK, Baffi JZ, Ambati J (2006) Drusen complement components C3a and C5a promote choroidal neovascularization. Proc Natl Acad Sci U S A 103(7):2328–2333
8. Skeie JM, Fingert JH, Russell SR, Stone EM, Mullins RF (2010) Complement component C5a activates ICAM-1 expression on human choroidal endothelial cells. Invest Ophthalmol Vis Sci 51(10):5336–5342
9. Liu B, Wei L, Meyerle C, Tuo J, Sen HN, Li Z, Chakrabarty S, Agron E, Chan CC, Klein ML, Chew E, Ferris F, Nussenblatt RB (2011) Complement component C5a promotes expression of IL-22 and IL-17 from human T cells and its implication in age-related macular degeneration. J Transl Med 9:1–12
10. Gerl VB, Bohl J, Pitz S, Stoffelns B, Pfeiffer N, Bhakdi S (2002) Extensive deposits of complement C3d and C5b-9 in the choriocapillaris of eyes of patients with diabetic retinopathy. Invest Ophthalmol Vis Sci 43(4):1104–1108

11. Hageman GS, Anderson DH, Johnson LV, Hancox LS, Taiber AJ, Hardisty LI, Hageman JL, Stockman HA, Borchardt JD, Gehrs KM, Smith RJ, Silvestri G, Russell SR, Klaver CC, Barbazetto I, Chang S, Yannuzzi LA, Barile GR, Merriam JC, Smith RT, Olsh AK, Bergeron J, Zernant J, Merriam JE, Gold B, Dean M, Allikmets R (2005) A common haplotype in the complement regulatory gene factor H (HF1/CFH) predisposes individuals to age-related macular degeneration. Proc Natl Acad Sci U S A 102(20):7227–7232
12. Seth A, Cui J, To E, Kwee M, Matsubara J (2008) Complement-associated deposits in the human retina. Invest Ophthalmol Vis Sci 49(2):743–750
13. Hecker LA, Edwards AO (2010) Genetic control of complement activation in humans and age related macular degeneration. Adv Exp Med Biol 703:49–62
14. Mullins RF, Dewald AD, Streb LM, Wang K, Kuehn MH, Stone EM (2011) Elevated membrane attack complex in human choroid with high risk complement factor H genotypes. Exp Eye Res 93(4):565–567
15. Pauleikhoff D, Spital G, Radermacher M, Brumm GA, Lommatzsch A, Bird AC (1999) A fluorescein and indocyanine green angiographic study of choriocapillaris in age-related macular disease. Arch Ophthalmol 117(10):1353–1358
16. Berenberg TL, Metelitsina TI, Madow B, Dai Y, Ying GS, Dupont JC, Grunwald L, Brucker AJ, Grunwald JE (2012) The association between drusen extent and foveolar choroidal blood flow in age-related macular degeneration. Retina 32(1):25–31
17. Yuan X, Gu X, Crabb JS, Yue X, Shadrach K, Hollyfield JG, Crabb JW (2010) Quantitative proteomics: comparison of the macular Bruch membrane/choroid complex from age-related macular degeneration and normal eyes. Mol Cell Proteomics 9(6):1031–1046
18. McLeod DS, Grebe R, Bhutto I, Merges C, Baba T, Lutty GA (2009) Relationship between RPE and choriocapillaris in age-related macular degeneration. Invest Ophthalmol Vis Sci 50(10):4982–4991
19. Mullins RF, Johnson MN, Faidley EA, Skeie JM, Huang J (2011) Choriocapillaris vascular dropout related to density of drusen in human eyes with early age-related macular degeneration. Invest Ophthalmol Vis Sci 52(3):1606–1612
20. Bhutto I, Lutty G (2012) Understanding age-related macular degeneration (AMD): relationships between the photoreceptor/retinal pigment epithelium/Bruch's membrane/choriocapillaris complex. Mol Aspects Med 33(4):295–317
21. Zhang L, Lee K, Niemeijer M, Mullins RF, Sonka M, Abramoff MD (2012) Automated segmentation of the choroid from clinical SD-OCT. Invest Ophthalmol Vis Sci 53(12):7510–7519
22. Smailhodzic D, Klaver CC, Klevering BJ, Boon CJ, Groenewoud JM, Kirchhof B, Daha MR, den Hollander AI, Hoyng CB (2012) Risk alleles in CFH and ARMS2 are independently associated with systemic complement activation in age-related macular degeneration. Ophthalmology 119(2):339–346
23. Zeng S, Hernandez J, Mullins RF (2012) Effects of antioxidant components of AREDS vitamins and zinc ions on endothelial cell activation: implications for macular degeneration. Invest Ophthalmol Vis Sci 53(2):1041–1047

# Chapter 37
# Genetic Risk Models in Age-Related Macular Degeneration

**Felix Grassmann, Iris M. Heid and Bernhard H. F. Weber**

**Abstract** Late-stage age-related macular degeneration (AMD) is a common sight-threatening disease of the central retina affecting approximately 1 in 30 Caucasians. Besides age and smoking, common genetic variants from at least 19 gene loci have reproducibly been associated with AMD likely explaining a large proportion of disease. Based on the current knowledge, several models were calculated to predict disease risk each with its own strength and weakness. Here, we review and compare published genetic risk models for AMD with or without additionally accounting for non-genetic factors.

**Keywords** Age-related macular degeneration · Susceptibility · Logistic regression · Cox regression · Genetic risk score

## 37.1 Introduction

Age-related macular degeneration (AMD) is a common, sight-threatening disease and the leading cause of vision loss in the elderly in Western societies [1]. Advanced forms of AMD (late-stage AMD) are known as geographic atrophy (GA) of the retinal pigment epithelium (RPE) or neovascular (NV) complications. The prevalence

B. H. F. Weber (✉) · F. Grassmann
Institute of Human Genetics Institute of Human Genetics, University of Regensburg, Franz-Josef-Strauss-Allee 11, 93053, Regensburg, Germany
e-mail: bweb@klinik.uni-regensburg.de

F. Grassmann
e-mail: felix.grassmann@ukr.de

I. M. Heid
Department of Genetic Epidemiology, University of Regensburg, Franz-Josef-Strauss-Allee 11, 93053, Regensburg, Germany
e-mail: iris.heid@ukr.de

Institute of Genetic Epidemiology, Helmholtz Zentrum München, German Research Center for Environmental Health, 85764, Neuherberg, Germany

J. D. Ash et al. (eds.), *Retinal Degenerative Diseases,* Advances in Experimental Medicine and Biology 801, DOI 10.1007/978-1-4614-3209-8_37,

for late-stage AMD increases from less than 1 % at 55 years of age to more than 15 % in individuals aged 85 years and above [2].

Early stages of AMD are characterized by pigment abnormalities or the presence of large drusenoid deposits under the RPE while these early fundus changes regularly do not affect vision. Nevertheless, these early signs, also referred to as clinical risk factors, have been associated with an increased risk to develop late-stage AMD [3]. Similarly, the occurrence of late-stage AMD in one eye confers an increased risk to develop late-stage AMD in the second eye [4]. Several lifestyle factors have been suspected to be involved in AMD development, including smoking, nutritional antioxidants, and omega-3 fatty acid intake [5]. So far, only smoking has been consistently replicated.

Besides non-genetic factors, AMD risk is influenced by genetic predisposition with estimates of heritability varying from 45 to 71 % [6]. The genetics of AMD is unique among complex diseases: Several genetic loci with very strong effect sizes have been reported with odds ratios (OR) more than 2.0 per risk allele [7]. While a first strong risk variant was identified in the complement factor H (CFH) gene [8], our knowledge on the genetic basis of AMD since then has increased dramatically. Several variants in other complement genes as well as genes related to immunity, lipid metabolism, or extracellular matrix homeostasis have been identified as AMD variants over the past years. An unpublished recent meta-analysis including around 17,000 cases and 60,000 controls implicated 19 AMD loci, explaining up to 30 % of the disease or up to 65 % of the heritability.

Besides uncovering a genetic variant that modulates the risk to develop AMD compared to subjects without this variant (relative risk), it is of special interest whether a genetic variant (or a combination of those) can predict late-stage AMD or can separate those that will develop AMD from those that will not (i.e., predict the absolute risk). A reasonable prediction could facilitate early detection and possibly prevention of disease. This review explores published genetic risk models for AMD to provide an overview of study designs, the risk factors included in the various studies, and the respective discriminatory power [7, 9–22]. While we included genetic risk models without or with incorporating non-genetic factors, purely non-genetic models are scarce in the literature and were not covered in this review.

## 37.2 Statistical Methodology to Generate and Validate a Genetic Risk Model

An excellent overview on how to calculate a risk score from logistic regression models is provided in reference [7]. In brief, a genetic risk score is computed as the number of risk alleles per individual in a case-control study weighted by the single variant effect sizes (i.e., the beta estimates of the respective genetic variant from logistic regression). The predictive accuracy of such a model is usually represented as area under the curve (AUC) of the receiver-operating characteristic (ROC)

based on the sensitivity and specificity of different genetic risk score thresholds to distinguish subjects with AMD from those without the disease. For longitudinal data, the genetic risk score is calculated using weights from the Cox regression model [23]. Gold et al. [9] used a decision tree, which facilitated prediction of AMD disease, but not for computing the AUC.

An AUC of 0.75 or higher is considered to be sufficient to discriminate between individuals with high and those with low risk for disease. However, such values may not be sufficient to classify *all* patients with reasonable accuracy. Depending on the threshold set for "high risk," a fraction of the cases may not be classified appropriately, i.e., may be "missed" by the classification scheme. Alternatively, many healthy persons may be assigned high risk although they will not develop AMD [14].

Furthermore, it is important to differentiate studies using previously assessed weights (i.e., independent of the study at hand) from those using weights derived from the same data set (thus possibly inflated). For the latter, cross-validation could be helpful to eliminate such a bias. Similarly, studies which identified a new variant as AMD associated but at the same time used this variant to derive the weights or to estimate risk will tend to produce inflated weights or inflated risk estimates (the so-called "winner's curse"). Ideally, studies estimating AMD risk should be independent from variant identification and from weight estimation.

Finally, cohort studies including longitudinal information of AMD development and assessing covariates such as body mass index (BMI) or smoking at baseline (i.e., prior to AMD development) need to be considered as superior to case-control studies particularly for models including non-genetic variants. The disease prevalence—and thus absolute risk—as well as AUC values can be assessed directly. This is different in case-control studies where the disease prevalence has to be modeled and derived from external data. Cohort studies have a further advantage as they assess covariates objectively without even knowing the disease status of the individual, while case-control studies need to ascertain comparability (e.g., smoking behavior) by a careful selection of controls.

## 37.3 Methodology Applied in This Review

Here, we conducted a review of published data by selecting 15 distinguished articles from the literature. While this review summarizes and evaluates the current state-of-the-art of AMD risk models, it should be noted that this is not a systematic review using defined search criteria in public databases such as PubMed (http://www.ncbi.nlm.nih.gov/pubmed?db=pubmed). Specifically, we evaluated the characteristics of the studies with regard to (1) genetic risk factors, (2) phenotypes, (3) covariates, (4) statistical methods, (5) study design, (6) type of validation, and (7) independence of study (i.e., study not involved in identifying the genetic risk factor or in deriving the weights; Table 37.1).

**Table 37.1** Risk models for age-related macular degeneration

| Publication | Year | Genetic factors[f] | Non-genetic factors[h] | Clinical factors | Study design (sample size) | Method[c] | Risk score[d] | Discovery[g] | Validation[e] | Reported AUC |
|---|---|---|---|---|---|---|---|---|---|---|
| Maller et al.[a] [10] | 2006 | CFH (2), CFB, ARMS2 | No | No | Case control (2172) | LR | No | Yes | – | – |
| Gold et al. [9] | 2006 | CFH (2), CFB(3) | No | No | Case control (~1500) | DT | No | Yes | Independent samples | – |
| Hughes et al. [11] | 2007 | CFH (4), ARMS2 | S | No | Case control (667) | LR | Yes | Yes | – | – |
| Jakobsdottir et al. [12] | 2008 | CFH, ARMS2, C2 | No | No | Case control (675) | LR | Unclear | Yes | – | – |
| Jakobsdottir et al. [14] | 2009 | CFH, ARMS2, C2 | No | No | Case control (675) | LR | Yes | Yes | – | 0.79 |
| Seddon et al.[a] [13] | 2009 | CFH (2), ARMS2, C2, CFB, C3 | a, g, e, s, t, b | No | Longitudinal (1446) | LR | Yes | No | – | 0.83 |
| Farwick et al. [15] | 2009 | CFH, ARMS2 (2), C2, CFB | S | No | Longitudinal (913) | LR | Unclear | No | – | 0.81 |
| Gibson et al. [16] | 2010 | CFH (3), ARMS2, C3, SERPING | a, g, s | No | Case control (940) | LR | Yes | Yes | – | 0.83 |
| Chen et al.[a] [17] | 2011 | CFH (3), C2, CFB, ARMS2 (2), C3 | s, a, g, b | No | Case control (1844) | LR | Yes | No | – | 0.82 |
| Hageman et al. [19] | 2011 | CFH (4), CFHR4/5 (3), FI3B (2), C2, CFB, ARMS2, C3 | S | No | Case control (3182) | LR | Yes | Yes | Independent samples | 0.80 |
| Klein et al.[a] [18] | 2011 | CFH, ARMS2 | a, e, s,[b] | AREDS score; late-stage AMD | Longitudinal (2962) | CR | No | No | Independent samples | 0.87 |

**Table 37.1** (continued)

| Publication | Year | Genetic factors[f] | Non-genetic factors[h] | Clinical factors | Study design (sample size) | Method[c] | Risk score[d] | Discovery[g] | Validation[e] | Reported AUC |
|---|---|---|---|---|---|---|---|---|---|---|
| Seddon et al.[a] [20] | 2011 | CFH (2), ARMS2, C3, C2, CFB | e, s, b, v | Drusen size, late stage AMD | Longitudinal (2937) | CR | No | No | Cross validation | 0.92 |
| Spencer et al. [21] | 2011 | CFH, ARMS2, CFB, C3 | a, s | No | Case control (~900) | LR | Yes | No | Independent samples | 0.84 |
| McCarthy et al.[a] [22] | 2012 | CFH, ARMS2 | a, g, e, s, b, v | AREDS score, late-stage AMD | Longitudinal (2011) | LR | Yes | No | Independent samples | 0.89 |
| Grassmann et al. [7] | 2012 | CFH (3), ARMS2, CFB, C3, C2, APOE (2), CFI, LIPC (2), TIMP3 | No | No | Case control (1782) | LR | Yes | No | Cross validation | 0.82 |

[a] ARED study samples
[b] Family history of late-stage AMD was added to the model
[c] *LR* logistic regression, *CR* cox regression, *DT* decision tree
[d] Risk score calculated
[e] Methods used to avoid inflation of risk: "independent study" means independent samples were used to test the models and to obtain AUC values
[f] The number in parentheses states the number of risk variants in that locus used in the best-performing model. No number indicates only one SNP at given locus
[g] Study used to discover novel variants which were also used in model
[h] Non-genetic factors are coded: *s* smoking, *e* education, *a* age, *b* body mass index, *v* vitamins, *g* gender, *t* AREDS treatment assignment

## 37.4 Genetic Risk Models Estimate the Risk to Develop Disease Before the Onset of Symptoms

A first effort to predict risk of AMD disease estimated the combined impact of two or more genetic variants [9, 10, 12]. Maller and colleagues [10] reported absolute AMD risk values by stating that a small proportion of individuals (around 1% of the general population carrying *all* of the respective risk-increasing alleles) should have a greater than 50% absolute risk to develop AMD. However, the risk is likely inflated in all of these studies as variants were included in the model calculations which were identified as risk variants for AMD in the same studies. No AUC was reported in any of these studies.

In 2009, Jakobsdottir and colleagues [12] were the first to report an AUC value (AUC = 0.79) for an AMD risk model. Later, Hageman and colleagues calculated a genetic model including five loci [19]. A major strength of the latter study was the computation of the AUC in an independent validation study. Subsequently, Grassmann et al. [7] reported a genetic risk model for 13 variants from 8 genetic loci. At the time, these latter variants were representative for the majority of published and replicated disease-associated variants in AMD. Grassmann et al. [7] were the first to describe absolute risk in five distinct risk groups, which were based on equidistant genetic risk score intervals. Absolute risk for late-stage AMD ranged from <2% in the lowest-risk group to up to 92% in the highest-risk group, assuming a prevalence of 15% for AMD. Relative risk (assessed as OR) of the highest- versus a medium-risk group was 64.0. Furthermore, this study demonstrated that the relative AMD risk changed dramatically with age. For example, the OR for those in the two highest-risk groups compared to the medium group was 5.18 if restricted to older individuals (≥75 years) and 12.66 if focusing on younger ones (<75 years).

Current efforts are directed towards (1) increasing case-control sample sizes to identify AMD-associated variants, (2) expanding the numbers of variants by imputing genotypes from 1000G sequencing efforts (http://www.1000genomes.org/), and (3) complementing the rare to common variants with the very rare variants by exome sequencing or custom-made variant arrays. Ultimately, these efforts will identify further genetic variants, in particular very rare variants with large effects (e.g., *CFH* R1210C [24]). This is likely to reveal the full genetic content of AMD susceptibility.

## 37.5 Lifestyle/Non-genetic Factors Enhance Discriminatory Power

Several studies added non-genetic covariates such as smoking, BMI, dietary vitamins, or education to the genetic risk model. In 2009, two studies were among the first cohort studies to predict AMD risk [13, 15], a design that is optimal to account for non-genetic factors. Seddon et al. [13] described a risk score model including six

genetic variants at four gene loci and included BMI, smoking, age, and diet. However, this study did not validate their analysis, which may inflate the risk estimate. Similarly, Farwick and colleagues [15] calculated a model including two genetic variants, age, gender, and smoking as covariates.

Several case-control studies added lifestyle factors to the genetic risk model and reported AUC values between 0.75 and 0.84 [11, 16, 21]. Since these numbers are very well in line with previously published risk models without lifestyle factors, the non-genetic factors do not appear to enhance discriminatory power drastically. It should be noted, however, that most published studies including genotypic *and* phenotypic variables are underpowered to evaluate robust estimations of lifestyle or environmental contributions. Therefore, the quantification of risk due to diet or light exposure is generally limited. Also, the interaction of genetic factors with lifestyle factors such as smoking is of great interest, particularly since a genetic variant could predispose to AMD only if the person smokes. Knowledge of such interactions might specifically encourage a person with high genetic risk to change lifestyle behavior. Thus, more extensive data on population-based studies including both genotypic and phenotypic details are of great interest, in particular with respect to preventive measures.

## 37.6 Inclusion of Clinical Risk Factors Results in High Accuracy of Risk Classification

Clinical symptoms for early AMD are obvious potential risk factors for late AMD [23]. In which way the genetic factors for late AMD increase the susceptibility for early AMD itself or "only" trigger the progression from early to late AMD is not yet known. If a genetic risk model includes early AMD symptoms to predict late AMD, only the risk of progression from early AMD to late AMD is tackled as the risk for early AMD is "removed" by adding these clinical symptoms into the model.

The presence of late AMD in one eye is described as a risk factor for developing AMD in the second eye [4]. Including this "clinical factor" to a genetic risk score model does not provide an effective estimate of the genetic risk by itself or allows for preventive measures before the development of the disease. However, this points towards a substantial impact of the combined effects of genetic susceptibility and lifestyle behavior, which is not accounted for in the models by the other covariates.

Three recent studies added clinical risk factors like the presence or size of drusen, pigmentary changes in the RPE, or the presence of late-stage AMD in the fellow eye into the genetic risk models [18, 20, 22]. The clinical risk factors were either measured (e.g., drusen area) or a severity score was computed [25]. These studies reported very high AUCs for AMD, ranging from 0.87 to 0.92 and were also validated in independent samples. The best-fitting models included genetic factors, non-genetic, as well as clinical factors (e.g., early AMD, late AMD in one eye) although the addition of genetic markers failed to increase the AUC substantially.

The fact that late AMD in one eye increases the risk for late AMD in the fellow eye is an important finding in the sense that it highlights the existence of factors (genetic or non-genetic) that are yet unaccounted for in the existing models. It should be noted, however, that none of these studies reported AUCs for a model to predict late AMD from a disease-free individual or an individual affected purely with the early form of AMD. Therefore, these models cannot be compared to the pure genetic or genetic/non-genetic models described above. Although preventing disease in the fellow eye will improve quality of life of unilaterally affected individuals, preventing the disease before disease onset in either eye is favorable. There should be a note of caution as the three studies [18, 20, 22] are based on an identical study sample, namely the *age-related eye disease study* (AREDS). Therefore, a validation in a completely independent data set is missing. A detailed analysis including a step-by-step approach which compares the change of parameter estimates as well as the improvement of AUC would be required in large studies with sufficient power for each factor in order to understand the etiology of the disease.

## 37.7 Conclusions

In recent years, great efforts have been made to predict and evaluate the risk to develop AMD. Genetic models have the implicit advantage to be usable for prediction of disease risk before onset of disease symptoms. At present, these models can predict disease risk for about 50 % of AMD but for only about 10 % of cases with a reasonably high degree of confidence [7]. Although current models derive AUC values as high as 90 %, these estimates are likely not accurate. Current studies largely lack full independence from studies which identified the variants. Also, they miss the full spectrum of genetic factors that has yet to be complemented and, finally, cannot sufficiently include interactions with non-genetic factors due to insufficient study design or underpowered sample size.

The addition of lifestyle/environmental factors does not dramatically improve the prediction accuracies of the existing models. Most studies with both genotypic and lifestyle factor assessment are still underpowered to derive robust estimates for smaller-risk factors. Even more, they are underpowered to tackle potential interaction of genetic factors with, e.g., smoking or light exposure. However, this would be of great importance to delineate preventive measures for high-risk groups.

Several groups included in the modeling early- or late-stage AMD in one eye to predict progression to late AMD. Such a prediction model provides high AUC values and appears superior to pure genetic prediction. However, the objectives of such a prediction model are rather specific and take into account clinical variables that accept a certain degree of unilateral disease development. Early prevention programs may not be suited for those individuals, and the development of individual treatment options may be required.

Further studies into the full genetic content of AMD are needed to attempt to further improve on the prediction accuracy of an AMD prediction model. Such a

tool will be important to device approaches for innovative preventive measures. While lifestyle intervention programs targeted to genetic high-risk groups could be a promising option, high-risk individuals with early signs of the disease will require potent treatment options. This challenge needs to be met.

## References


1. Congdon N, O'Colmain B, Klaver CCW, Klein R, Muñoz B et al (2004) Causes and prevalence of visual impairment among adults in the United States. Arch Ophthalmol 122:477–485
2. Friedman DS, O'Colmain BJ, Muñoz B, Tomany SC, McCarty C et al (2004) Prevalence of age-related macular degeneration in the United States. Arch Ophthalmol 122:564–572
3. Klein R, Klein BEK, Knudtson MD, Meuer SM, Swift M et al (2007) Fifteen-year cumulative incidence of age-related macular degeneration: the Beaver Dam Eye Study. Ophthalmology 114:253–262
4. Solomon SD, Jefferys JL, Hawkins BS, Bressler NM, Bressler SB (2009) Risk factors for second eye progression to advanced age-related macular degeneration: SST report No. 21 Submacular Surgery Trials Research Group. Retina 29:1080–1090
5. Age-Related Eye Disease Study Research Group (2001) A randomized, placebo-controlled, clinical trial of high-dose supplementation with vitamins C and E, beta carotene, and zinc for age-related macular degeneration and vision loss: AREDS report no. 8. Arch Ophthalmol 119:1417–1436
6. Seddon JM, Cote J, Page WF, Aggen SH, Neale MC (2005) The US twin study of age-related macular degeneration: relative roles of genetic and environmental influences. Arch Ophthalmol 123:321–327
7. Grassmann F, Fritsche LG, Keilhauer CN, Heid IM, Weber BHF (2012) Modelling the genetic risk in age-related macular degeneration. PloS One 7:e37979
8. Klein RJ, Zeiss C, Chew EY, Tsai J, Sackler RS et al (2005) Complement factor H polymorphism in age-related macular degeneration. Science 308:385–389
9. Gold B, Merriam JE, Zernant J, Hancox LS, Taiber AJ et al (2006) Variation in factor B (BF) and complement component 2 (C2) genes is associated with age-related macular degeneration. Nat Genet 38:458–462
10. Maller J, George S, Purcell S, Fagerness J, Altshuler D et al (2006) Common variation in three genes, including a non-coding variant in CFH, strongly influences risk of age-related macular degeneration. Nat Genet 38:1055–1059
11. Hughes AE, Orr N, Patterson C, Esfandiary H, Hogg R et al (2007) Neovascular age-related macular degeneration risk based on CFH, LOC387715/HTRA1, and smoking. PLoS Med 4:e355
12. Jakobsdottir J, Conley YP, Weeks DE, Ferrell RE, Gorin MB (2008) C2 and CFB genes in age-related maculopathy and joint action with CFH and LOC387715 genes. PloS One 3:e2199
13. Seddon JM, Reynolds R, Maller J, Fagerness J a, Daly MJ et al (2009) Prediction model for prevalence and incidence of advanced age-related macular degeneration based on genetic, demographic, and environmental variables. Invest Ophthalmol Vis Sci 50:2044–2053
14. Jakobsdottir J, Gorin MB, Conley YP, Ferrell RE, Weeks DE (2009) Interpretation of genetic association studies: markers with replicated highly significant odds ratios may be poor classifiers. PLoS Genet 5:e1000337
15. Farwick A, Dasch B, Weber BHF, Pauleikhoff D, Stoll M et al (2009) Variations in five genes and the severity of age-related macular degeneration: results from the Muenster aging and retina study. Eye 23:2238–2244

16. Gibson J, Cree A, Collins A, Lotery A, Ennis S (2010) Determination of a gene and environment risk model for age-related macular degeneration. Br J Ophthalmol 94:1382–1387
17. Chen Y, Zeng J, Zhao C, Wang K, Trood E et al (2011) Assessing susceptibility to age-related macular degeneration with genetic markers and environmental factors. Arch Ophthalmol 129:344–351
18. Klein ML, Francis PJ, Ferris FL, Hamon SC, Clemons TE (2011) Risk assessment model for development of advanced age-related macular degeneration. Arch Ophthalmol 129(12):1543–1550
19. Hageman GS, Gehrs K, Lejnine S, Bansal AT, Deangelis MM et al (2011) Clinical validation of a genetic model to estimate the risk of developing choroidal neovascular age-related macular degeneration. Hum Genomics 5:420–440
20. Seddon JM, Reynolds R, Yu Y, Daly MJ, Rosner B (2011) Risk models for progression to advanced age-related macular degeneration using demographic, environmental, genetic, and ocular factors. Ophthalmology 118:2203–2211
21. Spencer KL, Olson LM, Schnetz-Boutaud N, Gallins P, Agarwal A, et al (2011) Using genetic variation and environmental risk factor data to identify individuals at high risk for age-related macular degeneration. PloS One 6:e17784
22. McCarthy LC, Newcombe PJ, Whittaker JC, Wurzelmann JI, Fries M a et al (2012) Predictive models of choroidal neovascularization and geographic atrophy incidence applied to clinical trial design. Am J Ophthalmol 154:568–578.e12
23. Harrell FE, Califf RM, Pryor DB, Lee KL, Rosati RA (1982) Evaluating the yield of medical tests. JAMA 247:2543–2546
24. Raychaudhuri S, Iartchouk O, Chin K, Tan PL, Tai AK et al (2011) A rare penetrant mutation in CFH confers high risk of age-related macular degeneration. Nat Genet 43:1232–1236
25. Ferris FL, Davis MD, Clemons TE, Lee L-Y, Chew EY et al (2005) A simplified severity scale for age-related macular degeneration: AREDS Report No. 18. Arch Ophthalmol 123:1570–1574

# Chapter 38
# A Mechanistic Review of Cigarette Smoke and Age-Related Macular Degeneration

**Alex Woodell and Bärbel Rohrer**

**Abstract** Age-related macular degeneration (AMD), a complex disease stemming from both genetic abnormalities and environmental insults, is the most common form of visual impairment in elderly individuals of the Western world. Many potential etiologies are linked to AMD, but smoking is the leading environmental insult associated with this maculopathy. Smoke-induced damage is mediated in part through direct oxidation, depletion of antioxidants, complement activation, and vascular transmutations. Clinically, these mechanisms manifest themselves as keystones of atrophic AMD: retinal pigment epithelium degeneration, formation of extracellular deposits such as drusen, and thickening of Bruch's membrane. Furthermore, smoking induces angiogenesis and choroidal neovascularization, advancing the course of the disease to late-stage AMD. Further exploration of the biological processes affected by cigarette smoke exposure will provide greater insight into the pathogenesis of AMD.

**Keywords** Cigarette smoke · Age-related macular degeneration · Oxidative stress · Antioxidant · Complement · Angiogenesis

B. Rohrer (✉)
Departments of Neurosciences, Division of Research, Medical University of South Carolina, 167 Ashley Ave, SEI 614, Charleston, SC 29425, USA
e-mail: rohrer@musc.edu

Departments of Neurosciences and Ophthalmology, Medical University of South Carolina, 167 Ashley Ave, SEI 614, Charleston, SC 29425, USA

Research Service, Ralph H. Johnson VA Medical Center, Medical University of South Carolina, 167 Ashley Ave, SEI 614, Charleston, SC 29401, USA

A. Woodell
Departments of Neurosciences, Division of Research, Medical University of South Carolina, 167 Ashley Ave, SEI 614, Charleston, SC 29425, USA
e-mail: woodell@musc.edu

J. D. Ash et al. (eds.), *Retinal Degenerative Diseases,* Advances in Experimental Medicine and Biology 801, DOI 10.1007/978-1-4614-3209-8_38,

## 38.1 Introduction

Age-related macular degeneration (AMD) is among the leading causes of central vision loss in the elderly of Western populations. Due to the rapid increase of the aging population in the USA, the number of individuals affected by AMD will increase from 1.75 million, currently, to 3 million by 2020 [1]. This late-onset maculopathy is diagnosed in one of two forms: atrophic, "dry" or neovascular, "wet." The hallmark sign of atrophic AMD is the presence of lipoprotein-rich deposits known as drusen, which form in the subretinal space between Bruch's membrane (BrM) and the retinal pigment epithelium (RPE) in the macula. Over time, drusen flatten and fade to become geographic atrophy [2] which can be visualized in dry AMD patients using fundoscopic imaging techniques. The neovascular form is typically associated with abnormal vascular proliferation and destruction of the RPE and photoreceptors due to the leakage of blood and proteins into either the subretinal or sub-RPE space [3]. Vision loss is more severe in neovascular AMD compared to early and intermediate stages of dry AMD. However, the most common of the two is the atrophic form, making up 90% of all cases [4].

AMD is a complex disease, influenced by a number of genetic and environmental factors. However, cigarette smoke is the only proven, modifiable risk factor associated with AMD. Previous studies found a two- to fourfold increased risk for developing AMD in smokers compared to nonsmokers [5]. Furthermore, smoking promotes the progression of AMD from the atrophic to the neovascular form [6]. In addition to these epidemiological studies, some genetic studies have identified gene–environment interactions between genetic risk factors and smoking in AMD. For example, Chakravarthy and colleagues confirmed a gene–environment interaction between age-related maculopathy susceptibility 2 (ARMS2) and cigarette smoke [7]; interactions between complement factor H and smoking have been found in some populations [8], but not others [9]; and variations in two, single-nucleotide polymorphisms of apolipoprotein E were positively or negatively associated with smoking in a genotype-specific manner [10]. Despite the links between smoking and AMD, little is known of the underlying cellular mechanisms by which cigarette smoke contributes to the pathology of AMD. The present review examines the major postulated mechanisms in the literature that contribute to AMD pathogenesis. Categories include oxidative stress, antioxidant depletion, complement activation, and vascular changes.

## 38.2 Oxidative Stress

Oxidative stress, in reference to the cellular damage caused by an inability of biological systems to detoxify reactive oxygen species (ROS), has been implicated in a number of disease processes. ROS include superoxide, hydrogen peroxide, hydroxyl radicals, and other byproducts of oxygen metabolism. These ROS can

damage all components of the cell, including proteins, lipids, and DNA, as well as disrupt cellular signaling pathways.

Previous studies have shown that oxidative stress, involving the RPE in particular, is a major contributing factor in the etiology of AMD (reviewed in [11]). The RPE layer is exposed to potentially high levels of photo-oxidative stress from photoreceptor turnover and high levels of oxygen from the systemic circulation, which is, however, minimized due to the presence of endogenous antioxidants. If the detoxification system is compromised, oxidants and stimulators of cellular oxidative metabolism can then induce damage, potentially leading to apoptosis [12]. Without support from RPE cells, overlying photoreceptors will eventually undergo apoptosis, leading to permanent vision loss. This oxidative stress hypothesis is supported by the Age-Related Eye Disease Study (AREDS), which shows that nutritional supplementation with antioxidants and zinc reduces the risk of early AMD patients progressing to advanced stages of AMD by ~25 % [13].

With each inhalation, cigarette smoke introduces a large number of free radicals [14] and likely contributes to oxidative damage loads. Oxidants found in cigarette smoke can pass through the alveolar walls and enter the systemic circulation, exerting widespread effects as evidenced by an increase in plasma markers of lipid peroxidation after smoking [15]. Oxidative damage can manifest itself in a variety of ways, including degradation of intracellular organelles, disruption of cell signaling pathways, and alterations in mitochondrial DNA. Fujihara and coworkers have shown that mice exposed to chronic cigarette smoke display signs of oxidative damage concomitant with ultrastructural changes including RPE damage and apoptosis, and thickening of BrM [16]. In addition to generating short-lived ROS, cigarette smoke contains a number of stable compounds which are also capable of generating oxidative damage. Most notable of these are acrolein, an unsaturated aldehyde capable of inducing protein modifications and enhancing the formation of advanced glycation end products and advanced lipid end products [17]; cadmium, a metal associated with zinc production that accumulates in the RPE and choroid, where it generates ROS [18]; and hydroquinone, a pro-oxidant compound, which itself can be oxidized and conjugated with glutathione to form potent mitochondrial toxins or cause DNA damage by covalently binding with DNA and inducing DNA oxidation via redoxcycling [19]. All three compounds have been shown to be associated with RPE cell damage using either in vitro or in vivo models [18, 20, 21].

## 38.3 Antioxidant Depletion

Aerobic organisms have integrated antioxidant systems to protect against oxidant-mediated cell damage. However, under pathological conditions these safeguards can easily become overwhelmed. Diet-derived vitamins B, C, and E provide protection by reacting with free radicals and preventing their propagation in tissues. However, plasma levels of vitamin C and carotenes are significantly lower in cigarette smokers when compared to nonsmokers [22], presumably as a consequence of enhanced

turnover due to smoke-induced oxidative stress. Panda and colleagues supported this line of evidence by inhibiting smoke-induced oxidative damage in vivo with vitamin C supplementation [23]. Smoke exposure also reduces the amount of endogenous circulating antioxidants; more specifically, glutathione and cysteine were both downregulated in smokers compared to nonsmokers [24]. Lastly, enzymes that degrade ROS and produce endogenous antioxidants such as superoxide dismutase (SOD) are also imperative in cellular defense against oxidative damage. SOD levels have been shown to be decreased in tissues of smokers [25], and eliminating SOD2 in mice results in "retinal damage similar to that associated with the early stages of age-related macular degeneration" [26].

## 38.4 Complement Activation

It has long been recognized that inflammation plays a role in AMD, despite the fact that it does not present itself with the classical signs of inflammation such as heat and swelling. However, inflammatory processes, possibly being triggered by local cell damage or the accumulation of debris at the level of BrM, as well as the invasion of inflammatory cells, have been documented in eyes of AMD patients. These local inflammatory alterations might then be propagated by the immune system, the choroidal vascular network, and other local cells. The complement cascade is an integral part of the innate and adaptive immune system. Its main function is to help clear pathogens or nonself cells from the organism by either marking them for clearance by phagocytosis or by direct lysis. Several complement components have been found in drusen, BrM, and choroidal neovascular (CNV) membranes, and severity of AMD is correlated with the amount of complement membrane attack complex present at the level of the RPE/BrM (reviewed in [27]). Given the destructive potential of this system, a large number of complement inhibitors are expressed by the host or self-cells. However, the majority of these membrane-bound inhibitors are misregulated in AMD [28, 29].

The inflammatory hypothesis gained further support when several genetic risk factors associated with AMD were identified as polymorphisms in complement genes such as complement inhibitor, complement factor H (CFH), complement factor B (CFB), and complement component 3 (C3) (reviewed in [30]), and when some of these gene alterations were found to be associated with the progression of atrophic to neovascular AMD. Hence, complement therapeutics are currently being explored for the treatment of AMD (e.g., [31]).

Cigarette smoke has been shown to directly activate the complement cascade via modification of C3 and subsequently activate the alternative pathway of complement [32]. Circulating CFH, the inhibitor of the alternative pathway, is also reduced in smokers. While it has yet to be proven that smoking increases the risk for AMD by increasing complement activation, it is plausible that the combination of complement-related genetic risk factors and smoke-induced activation of the complement cascade may act synergistically to promote inflammation in AMD.

## 38.5 Vascular Changes

The vascular model of AMD proposed by Friedman and coworkers suggests that changes in the choroidal vasculature, similar to those observed in atherosclerosis, are responsible for the development of AMD [33]. Chronic smoke exposure has been shown to change clot dynamics and alter fibrin structure, both of which contribute to thrombosis [34]. Thromboregulatory functions might be further disrupted by a smoke-induced decrease in NTPDase, a plasma-membrane-bound enzyme that breaks down precursor nucleotides into the antithrombotic and anti-inflammatory mediator, adenosine [35]. Smoke also induces vasoconstriction by activating α-adrenergic receptors. Collectively, these findings result in a decrease in choroidal blood flow. Friedman and colleagues proposed that this decrease in choroidal blood flow may impair the clearance of debris from the RPE and lead to the formation of deposits in BrM [36]. A decrease in blood flow might also be responsible for heat-related damage in the RPE/choroid, since light absorption by melanosomes results in an increase in temperature above 37 °C [37]. Finally, cigarette smoke might also be responsible for inducing changes in angiogenesis. Smoke exposure can change the branching pattern in proliferating vessels of chick chorioallantoic membrane [38], concomitant with an increase in the number of fibroblasts and altered composition of the extracellular matrix present in these membranes affecting their structural integrity.

## 38.6 Conclusions

AMD is a complex disease that is associated with multiple genetic and environmental etiologies. However, cigarette smoke is the most significant contributing factor known. Toxins in cigarette smoke could cause oxidative damage (directly via free radicals or indirectly by depleting antioxidants), decrease choroidal circulation (disruption of thromboregulatory function and α-adrenergic receptor activation), and activate the complement cascade (directly via activation of complement components or indirectly by downregulating complement inhibitors). Together, these effects may promote RPE damage and drusen formation, which could lead to the development of atrophic AMD. Smoke-induced alterations in the breakdown of the blood retina barrier together with blood vessel growth aid in the progression to late-stage AMD. Numerous studies implicate cigarette smoke as a risk factor for AMD, but the underlying mechanisms of action are still poorly understood. A better understanding of how cigarette smoke alters the biological milieu will enable novel treatment options for the treatment of AMD.

**Acknowledgments** The authors thank Christine Curcio for critical discussions. This review was supported in part by the National Institutes of Health (NIH) (R01EY019320), Department of Veterans Affairs (I01 RX000444), Foundation Fighting Blindness, and an unrestricted grant to MUSC from Research to Prevent Blindness (RPB), Inc., New York, NY. The authors have no financial conflicts of interest.

## References


1. Friedman DS et al (2004) Prevalence of age-related macular degeneration in the United States. Arch Ophthalmol 122(4):564–572
2. Klein ML et al (2008) Retinal precursors and the development of geographic atrophy in age-related macular degeneration. Ophthalmology 115(6):1026–1031
3. Freund KB, Zweifel SA, Engelbert M (2010) Do we need a new classification for choroidal neovascularization in age-related macular degeneration? Retina 30(9):1333–1349
4. Brown MM et al (2005) Age-related macular degeneration: economic burden and value-based medicine analysis. Can J Ophthalmol 40(3):277–287
5. Lois N et al (2008) Environmental tobacco smoke exposure and eye disease. Br J Ophthalmol 92(10):1304–1310
6. Chakravarthy U et al (2007) Cigarette smoking and age-related macular degeneration in the EUREYE Study. Ophthalmology 114(6):1157–1163
7. Chakravarthy U et al (2012) ARMS2 Increases the risk of early and late age-related macular degeneration in the european eye study. Ophthalmology 120(2):342–348
8. Delcourt C et al (2011) Associations of complement factor H and smoking with early age-related macular degeneration: the ALIENOR study. Invest Ophthalmol Vis Sci 52(8): 5955–5962
9. Sofat R et al (2012) Complement factor H genetic variant and age-related macular degeneration: effect size, modifiers and relationship to disease subtype. Int J Epidemiol 41(1):250–262
10. Adams MK et al (2012) Apolipoprotein E gene associations in age-related macular degeneration: the Melbourne Collaborative Cohort Study. Am J Epidemiol 175(6):511–518
11. Cai J et al (2000) Oxidative damage and protection of the RPE. Prog Retin Eye Res 19(2):205–221
12. Buttke TM, Sandstrom PA (1994) Oxidative stress as a mediator of apoptosis. Immunol Today 15(1):7–10
13. Age-Related Eye Disease Study Research Group (2000) The Age-Related Eye Disease Study: a clinical trial of zinc and antioxidants—Age-Related Eye Disease Study Report No. 2. J Nutr 130(5S Suppl):1516S–1519S
14. Church DF, Pryor WA (1985) Free-radical chemistry of cigarette smoke and its toxicological implications. Environ Health Perspect 64:111–126
15. Frei B et al (1991) Gas phase oxidants of cigarette smoke induce lipid peroxidation and changes in lipoprotein properties in human blood plasma. Protective effects of ascorbic acid. Biochem J 277(Pt 1):133–138
16. Fujihara M et al (2008) Chronic cigarette smoke causes oxidative damage and apoptosis to retinal pigmented epithelial cells in mice. PLoS One 3(9):e3119
17. Kirkham PA et al (2003) Cigarette smoke triggers macrophage adhesion and activation: role of lipid peroxidation products and scavenger receptor. Free Radic Biol Med 35(7):697–710
18. Wills NK et al (2008) Cadmium accumulation in the human retina: effects of age, gender, and cellular toxicity. Exp Eye Res 86(1):41–51
19. Rao GS (1996) Glutathionyl hydroquinone: a potent pro-oxidant and a possible toxic metabolite of benzene. Toxicology 106(1–3):49–54
20. Jia L et al (2007) Acrolein, a toxicant in cigarette smoke, causes oxidative damage and mitochondrial dysfunction in RPE cells: protection by (R)-alpha-lipoic acid. Invest Ophthalmol Vis Sci 48(1):339–348
21. Pons M, Marin-Castano ME (2011) Cigarette smoke-related hydroquinone dysregulates MCP-1, VEGF and PEDF expression in retinal pigment epithelium in vitro and in vivo. PLoS One 6(2):e16722
22. Chow CK et al (1986) Lower levels of vitamin C and carotenes in plasma of cigarette smokers. J Am Coll Nutr 5(3):305–312
23. Panda K et al (2000) Vitamin C prevents cigarette smoke-induced oxidative damage in vivo. Free Radic Biol Med 29(2):115–124

24. Moriarty SE et al (2003) Oxidation of glutathione and cysteine in human plasma associated with smoking. Free Radic Biol Med 35(12):1582–1588
25. Agnihotri R et al (2009) Association of cigarette smoking with superoxide dismutase enzyme levels in subjects with chronic periodontitis. J Periodontol 80(4):657–662
26. Justilien V et al (2007) SOD2 knockdown mouse model of early AMD. Invest Ophthalmol Vis Sci 48(10):4407–4420
27. Donoso LA et al (2006) The role of inflammation in the pathogenesis of age-related macular degeneration. Surv Ophthalmol 51(2):137–152
28. Fett AL et al (2012) Immunohistochemical localization of complement regulatory proteins in the human retina. Histol Histopathol 27(3):357–364
29. Ebrahimi KB et al (2012) Decreased membrane complement regulators in the retinal pigmented epithelium contributes to age-related macular degeneration. J Pathol 229(5):729–742
30. Gorin MB (2012) Genetic insights into age-related macular degeneration: controversies addressing risk, causality, and therapeutics. Mol Aspects Med 33(4):467–486
31. Rohrer B et al (2009) A targeted inhibitor of the alternative complement pathway reduces angiogenesis in a mouse model of age-related macular degeneration. Invest Ophthalmol Vis Sci 50(7):3056–3064
32. Kew RR, Ghebrehiwet B, Janoff A (1985) Cigarette smoke can activate the alternative pathway of complement in vitro by modifying the third component of complement. J Clin Invest 75(3):1000–1007
33. Friedman E (2000) The role of the atherosclerotic process in the pathogenesis of age-related macular degeneration. Am J Ophthalmol 130(5):658–663
34. Barua RS et al (2010) Effects of cigarette smoke exposure on clot dynamics and fibrin structure: an ex vivo investigation. Arterioscler Thromb Vasc Biol 30(1):75–79
35. Togna AR et al (2008) Cigarette smoke inhibits adenine nucleotide hydrolysis by human platelets. Platelets 19(7):537–42
36. Friedman E (2004) Update of the vascular model of AMD. Br J Ophthalmol. 88(2):161–163
37. Parver LM (1991) Temperature modulating action of choroidal blood flow. Eye 5 (Pt 2): 181–185
38. Melkonian G et al (2000) Normal patterns of angiogenesis and extracellular matrix deposition in chick chorioallantoic membranes are disrupted by mainstream and sidestream cigarette smoke. Toxicol Appl Pharmacol 163(1):26–37

# Chapter 39
# Measuring Cone Density in a Japanese Macaque (*Macaca fuscata*) Model of Age-Related Macular Degeneration with Commercially Available Adaptive Optics

**Mark E. Pennesi, Anupam K. Garg, Shu Feng, Keith V. Michaels, Travis B. Smith, Jonathan D. Fay, Alison R. Weiss, Laurie M. Renner, Sawan Hurst, Trevor J. McGill, Anda Cornea, Kay D. Rittenhouse, Marvin Sperling, Joachim Fruebis and Martha Neuringer**

**Abstract** The aim of this study was to assess the feasibility of using a commercially available high-resolution adaptive optics (AO) camera to image the cone mosaic in Japanese macaques (*Macaca fuscata*) with dominantly inherited drusen. The macaques examined develop drusen closely resembling those seen in humans with age-related macular degeneration (AMD). For each animal, we acquired and processed images from the AO camera, montaged the results into a composite image, applied custom cone-counting software to detect individual cone photoreceptors, and created a cone density map of the macular region. We conclude that flood-illuminated AO provides a promising method of visualizing the cone mosaic in nonhuman primates. Future studies will quantify the longitudinal change in the cone mosaic and its relationship to the severity of drusen in these animals.

**Keywords** Cone density imaging · adaptive optics · flood-illuminated adaptive optics · AMD

M. E. Pennesi (✉) · A. K. Garg · S. Feng · K. V. Michaels · T. B. Smith · J. D. Fay · T. J. McGill · M. Neuringer
Department of Ophthalmology, Casey Eye Institute, Oregon Health & Science University, 3375 SW Terwilliger Blvd, Portland, OR 97239, USA
e-mail: pennesim@ohsu.edu

A. R. Weiss · L. M. Renner · A. Cornea · M. Neuringer · S. Hurst
Division of Neuroscience, Oregon National Primate Research Center, Oregon Health & Science University, Beaverton, OR, USA

K. D. Rittenhouse · M. Sperling · J. Fruebis
External R&D Innovations, Pfizer Inc., Cambridge, MA, USA

J. D. Ash et al. (eds.), *Retinal Degenerative Diseases,* Advances in Experimental Medicine and Biology 801, DOI 10.1007/978-1-4614-3209-8_39,

## 39.1 Introduction

Age-related macular degeneration (AMD) is the leading cause of irreversible blindness in people over the age of 50 in the developed world. Its prevalence is projected to increase more than 50 % by the year 2020 [1]. The early stages of AMD are characterized by an increased frequency of drusen deposits under the retinal pigment epithelium [2]. While recent work has garnered a more detailed understanding of AMD, disease treatment and/or prevention research is currently hampered by the lack of animal models that accurately mimic the manifestation and progression of this disease in humans. We have identified a line of Japanese macaques with drusen that begin to appear early in life and increase in number and size with age. This phenotype displays an autosomal dominant inheritance pattern.

Another hindrance to understanding AMD is the low image resolution of commonly used retinal imaging systems such as the traditional scanning laser ophthalmoscope. Adaptive optics (AO) imaging, which corrects for the wavefront aberrations of the eye, provides a significant increase in retinal imaging resolution and enables the noninvasive, visualization of individual cone photoreceptor cells in vivo. Previous work with AO imaging has demonstrated the ability to image the cone mosaic in human subjects [3]. We used a new commercially available flood-illuminated AO camera to determine the feasibility of imaging and quantifying the cone mosaic in Japanese macaques with dominantly inherited drusen.

## 39.2 Materials and Methods

All procedures were approved by the Institutional Animal Care and Use Committee at Oregon Health & Science University and conformed to NIH guidelines and the ARVO Statement for the Use of Animals in Ophthalmic and Vision Research.

### *39.2.1 Subjects*

The subjects were 20 Japanese macaques aged 4–19 years old with a wide range of drusen severity. All were selected from the Japanese macaque colony resident since 1965 at the Oregon Regional Primate Research Center.

### *39.2.2 Anesthesia*

Animals were sedated with Ketamine (5–15 mg/kg) or Telazol (3–5 mg/kg) followed by endotracheal intubation and the administration of 1–3 % isoflurane vaporized in 100 % oxygen adjusted as needed, to inhibit eye movement. Pupils were

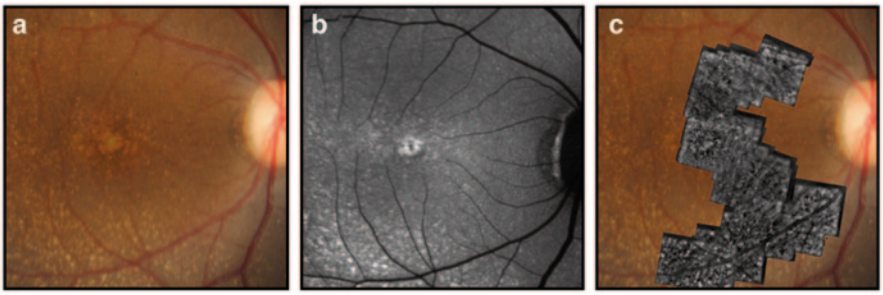


**Fig. 39.1** **a** A fundus photograph of a Japanese macaque with severe drusen. **b** An autofluorecence image of the same animal. **c** A corresponding AO montage overlaid on the fundus photograph

dilated with 2–3 applications of 1% tropicamide and 2.5% phenylephrine. Heart rate and peripheral oxygen saturation were monitored and maintained at normal levels throughout the imaging sessions.

### *39.2.3 Fundus Photography*

Retinal color and autofluorescence fundus photographs were taken of each macaque prior to AO imaging (Fig. 39.1a, b). After anesthesia and pupil dilation, images of the macula and near periphery (nasal, temporal, superior, and inferior quadrants) were acquired with a digital retinal camera system (F450, Carl Zeiss AG, Oberkochen, Germany).

### *39.2.4 Adaptive Optics Image Acquisition*

Anesthetized Japanese macaques were imaged using the rtx1 AO Retinal Camera (Imagine Eyes SA, Orsay, France). The animals were placed prone on an adjustable table. The head was positioned vertically with one eye in front of the imaging beam aperture. A Barraquer wire speculum was placed in the eye to be imaged and followed by the insertion of a plano-contact lens. Balanced salt solution or artificial tears were applied as needed.

### *39.2.5 Axial Length Measurement*

At the conclusion of image acquisition, ten of the sedated monkeys were repositioned in front of an IOLMaster 500 (Carl Zeiss AG, Oberkochen, Germany). Axial length measurements were obtained after removing the contact lens and treating the eye with artificial tears.

### 39.2.6 Image Processing and Montaging

The raw images acquired from the AO camera were automatically processed using software provided by Imagine Eyes. This software registers the 40 frames that were acquired for each image. The processed images for each subject were then montaged automatically into a wide-field composite image using i2k Retina (version 1.3.8; DualAlign LLC, Clifton Park, NY, USA) (Figs. 39.1c, 39.2a). The final montage spanned a variable field of the central macula based upon the number of images acquired. Particularly blurry or poor resolution images were omitted from the mosaic.

### 39.2.7 Cone Identification and Cone Density Measurements

For identification of cones, a modified, automatic version of the semi-automated cone photoreceptor identification software described by Li and Roorda was applied to the entire montage [4]. Li and Roorda's method applied a finite-impulse-response (FIR) low-pass filter to the retinal image and then identified local maxima of the filtered image [4]. As described by Garrioch et al., setting the cutoff frequency of the FIR filter manually can result in drastic differences in performance [5]. However, the further automated method described by Garrioch et al. is currently too computationally intensive to reasonably be applied to a full retinal montage [5]. For this reason, we empirically determined a single cutoff frequency for the FIR filter that yielded good cone identification accuracy in all retinal montages (Fig. 39.2a). Cone density was measured in both angular and metric units. Angular units were converted to metric units by using the measured axial length of each subject [6].

### 39.2.8 Density Maps

Two-dimensional depictions of cone photoreceptor density were created using a custom MATLAB (release 2011b, MathWorks, Natick, MA, USA) algorithm to visualize spatial distribution of cones across the retinal montage. Each retinal montage was spatially quantized at one bin per degree of eccentricity, or 25 bins per square degree. The final density map was created by counting the number of identified cones in each bin, normalizing by the bin area, and color-coding the bins based on the relative cone density (Fig. 39.2b, c).

### 39.2.9 Regional Cone Density Analysis

We employed two methods to quantify the cone density of the different regions of the retina. The first method measured of average cone density within the superior,

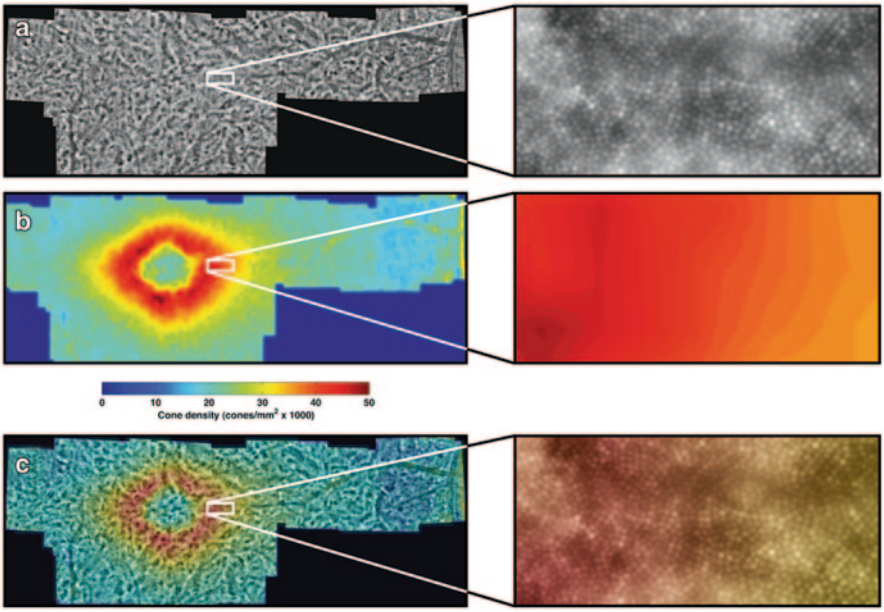


**Fig. 39.2** Example results from one animal. The areas highlighted by *white* squares are shown in detail to the right. **a** A montaged image showing the visibility of cones in the retina. **b** A cone density map created using the automated counting algorithm. **c** The density map overlaid on the original montage

inferior, nasal, and temporal quadrants of the retina (Fig. 39.3a). Cone density in each quadrant was quantified from the foveal center to 5 degrees eccentricity in steps of 0.2 degrees. The foveal center for each animal was manually estimated from the cone density maps, and the quadrants were identified using the location of the optical nerve. The second method averaged the cone density in the annulus region from 1.6 to 3.1 degrees eccentricity. This region contained the peak cone density along with a small surrounding neighborhood among all animals, and was used as an aggregate outcome measure for regression analysis.

## 39.3 Results

The axial length among 10 subjects was 19.75 ± 0.38 mm. Cone density, measured in 20 animals, exhibited an elliptical pattern (Fig. 39.3a) and generally decreased with retinal eccentricity, although there was an artificial decline within approximately 1.5 degrees where the tightly packed foveal cones were too small to be resolved by the AO camera (Fig. 39.3b). The results for the average cone density in each quadrant from 1.6 to 3.1 degrees eccentricity (corresponding to 0.35–0.73 mm for a 19.75 mm axial length) within each quadrant are listed in Table 39.1. The

**Table 39.1** Mean cone densities in an annulus spanning the region covering 1.6–3.1 degrees eccentricity from the fovea. Values are provided in cones/mm$^2$ for the four regions of the retina and the total annulus

| Region | Mean cone density (cones/mm$^2$) | Standard deviation (cones/mm$^2$) |
|---|---|---|
| Temporal | 31,397 | 4,830 |
| Inferior | 31,193 | 5,310 |
| Nasal | 31,497 | 5,335 |
| Superior | 27,192 | 5,212 |
| Total ($n$=20) | 30,303 | 4,688 |

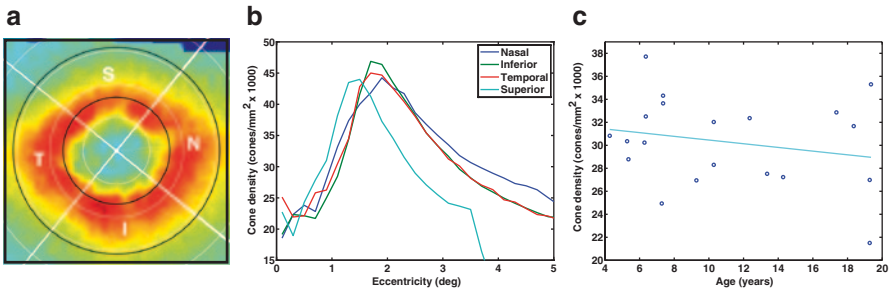


**Fig. 39.3** **a** A cone density map marked to demonstrate the regions analyzed in this study. Quadrants are labeled by letter ($N$=nasal, $S$=superior, $T$=temporal, $I$=inferior). The *white* circles represent eccentricity increments of 1 degree, and the black circles outline the annulus between 1.5 to 3.1 degrees. **b** The cone density versus retinal eccentricity in each quadrant for one animal. For the superior quadrant, the region of valid data ended at 3.5 degrees. **c** The cone density trend shows a slight, although not significant ($p$=0.1669), decrease with age. Each point represents the average cone density in the 1.5–3.1 degree annulus for one of the 20 subjects

nasal quadrant had the highest cone density followed by the temporal, inferior, and superior quadrants. Linear regression analysis revealed no significant relationship between age and cone density (Fig. 39.3c; $R^{2=}0.1034$; linear coefficient t-test $p$-value=0.1669).

The overall coefficient of variation among all 20 animals was 0.1116 within the defined annulus, indicating the cone density variation was quite small. The average cone density map, created by aligning the individual maps among the 10 subjects for which axial lengths were measured, exhibits an elliptical pattern with a tendency toward higher density in the nasal quadrant (Fig. 39.4a). The map of coefficient of variation among these 10 subjects confirms the low variation in cone densities measured in this group (Fig. 39.4b).

## 39.4 Discussion

We demonstrate that a commercially available flood-illuminated AO retinal imaging device is capable of imaging the cone mosaic in a line of Japanese macaques with drusen. Furthermore, our automated cone counting algorithm, which was originally

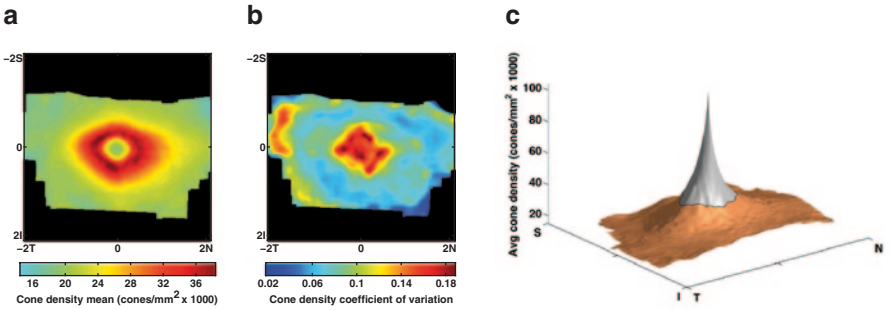


**Fig. 39.4** **a** The mean cone density map among the 10 Japanese macaques for which axial lengths were measured. **b** The map of the coefficient of variation among the same 10 animals. **c** A 3D representation of the mean density map with extrapolated data in the foveola (*gray region*) using one possible model. The extrapolation model was α/r, where r was the radius from the foveal center and α was estimated from the region of valid data (*orange*)

developed to detect cones in AO images of human subjects, was able to detect cones accurately in images from this species and permits the efficient regional analysis of cone density and the visualization of the cone mosaic (Fig. 39.3). However, many challenges remain in obtaining quality images from sedated monkeys using flood-illuminated AO. Limited anesthetic time, motion from the breathing of the animal, and loss of corneal clarity can result in reduced image quality and smaller retinal coverage.

To our knowledge, no in vivo studies of the Japanese macaque cone mosaic have been performed, but detailed studies of the rhesus macaque (*Macaca mulatta*) do exist [7, 8]. We found the axial lengths of the Japanese macaques to be significantly greater than those of rhesus macaques [9], consistent with their larger body size. As previously observed in rhesus macaques, our axial length measurements suggest a slight trend of male Japanese macaques having larger eyes than females, consistent with differences in body size (19.91 ± 0.28 mm vs. 19.59 ± 0.42 mm) [8, 9]. Our measurements of cone density (Table 39.1) fall below the cone density values measured stereologically in fixed sections of the rhesus monkey retina as reported by Wikler et al. [7]. It is well-established that cone density decreases with increasing eccentricity in macaques [10] as in humans.

Previous work by Ordy et al. showed a significant decrease in histologically measured cone density between middle-aged (12–15 years) and older (18–24 years) macaques [11]. Our study did not find any significant change in density with increasing age, although this may be due to the oldest subjects in our study being younger than most of the subjects in Ordy's older group. Ordy et al. [11] did not see a significant change in visual acuity or cone density between the young adult (4–6 years) and middle-aged macaques, in accordance with our observations (Fig. 39.3c).

Going forward, our work will focus on measuring longitudinal changes in the cone mosaic in regions with and without drusen and correlating cone density changes with drusen load and fat content in the diet. We will also explore mathematical models of cone density in Japanese macaques to extrapolate the density maps in the foveola where the AO camera cannot resolve cones. This may lead to 3D

representations of the cone density throughout the entire fovea (Fig. 39.4c). Models will be chosen based on empirical evidence gathered from histological and stereological examinations of Japanese macaque retinal tissue.

**Funding** Pfizer Ophthalmology External Research Unit, The Foundation Fighting Blindness CDA (MEP), Research to Prevent Blindness (Unrestricted grant to Casey Eye Institute, CDA to MEP), NIH grant P51OD011092 (MN), K08 EY021186-01 (MEP).

## References

1. Jager RD, Mieler WF, Miller JW (2008) Age-related macular degeneration. New Eng J Med 358(24):2606–2617
2. de Jong PT (2006) Age-related macular degeneration. New Eng J Med 355(14):1474–1485
3. Liang J, Williams DR, Miller DT (1997) Supernormal vision and high-resolution retinal imaging through adaptive optics. J Opt Soc Am A Opt Image Sci Vis 14(11):2884–2892
4. Li KY, Roorda A (2007) Automated identification of cone photoreceptors in adaptive optics retinal images. J Opt Soc Am A Opt Image Sci Vis 24(5):1358–1363
5. Garrioch R, Langlo C, Dubis AM, Cooper RF, Dubra A, Carroll J (2012) Repeatability of in vivo parafoveal cone density and spacing measurements. Optom Vis Sci 89(5):632–643
6. Bennett AG, Rudnicka AR, Edgar DF (1994) Improvements on Littmann's method of determining the size of retinal features by fundus photography. Graefes Arch Clin Exp Ophthalmol 232(6):361–367
7. Wikler KC, Williams RW, Rakic P (1990) Photoreceptor mosaic: number and distribution of rods and cones in the rhesus monkey retina. J Comp Neurol 297(4):499–508
8. Fernandes A, Bradley DV, Tigges M, Tigges J, Herndon JG (2003) Ocular measurements throughout the adult life span of rhesus monkeys. Invest Ophthalmol Vis Sci 44(6):2373–2380
9. Qiao-Grider Y, Hung LF, Kee CS, Ramamirtham R, Smith EL 3rd (2007) Normal ocular development in young rhesus monkeys (*Macaca mulatta*). Vision Res 47(11):1424–1444
10. Curcio CA, Sloan KR, Kalina RE, Hendrickson AE (1990) Human photoreceptor topography. J Comp Neurol 292(4):497–523
11. Ordy JM, Brizee KR, Hansche J (1980) Visual acuity and foveal cone density in the retina of the aged rhesus monkey. Neurobiol Aging 1(2):133–140

# Chapter 40
# Nuclear Receptors as Potential Therapeutic Targets for Age-Related Macular Degeneration

**Goldis Malek**

**Abstract** Age-related macular degeneration (AMD) is the most important cause of blindness and visual impairment among the elderly. Nuclear receptors represent one of the largest families of transcription factors, with 48 present in the human genome. They are critical regulators and modulators of developmental and physiological processes and are both targets of drugs and chemicals of environmental significance. Many of the cellular processes regulated by nuclear receptors are disrupted in AMD. With this in mind, we recently created a nuclear receptor atlas of retinal pigment epithelial (RPE) cells, cells affected in AMD, highlighting the expression of all the nuclear receptors. The results of which provided scaffold to study individual receptors in aging and disease. This study led to several candidate receptors that have become the focus of detailed studies regarding their mechanistic role in the eye. One example of a nuclear receptor potentially relevant to AMD pathobiology is presented.

**Keywords** Age-related macular degeneration · Retinal pigment epithelium · Nuclear receptors · Aryl hydrocarbon receptor

**Abbreviations**

| | |
|---|---|
| AMD | Age-related macular degeneration |
| RPE | Retinal pigment epithelium |
| AhR | Aryl hydrocarbon receptor |

G. Malek (✉)
Duke University Eye Center, Albert Eye Research Institute, Department of Ophthalmology, Duke University, 2351 Erwin Road, Room 4006,
Durham, NC 27710, USA
e-mail: gmalek@duke.edu

J. D. Ash et al. (eds.), *Retinal Degenerative Diseases,* Advances in Experimental Medicine and Biology 801, DOI 10.1007/978-1-4614-3209-8_40,

## 40.1 Introduction

Age-related macular degeneration (AMD) is the leading cause of central vision loss in the elderly population in industrialized nations [1]. Approximately 85% of patients diagnosed with AMD have the dry clinical subtype characterized by accumulation of lipid-protein-rich deposits below the retinal pigment epithelium (RPE) [2] for which currently there are no treatment options available [3, 4]. All subtypes of the disease involve physiological and pathological changes to the RPE, cells that play a vital role in retinal physiology, forming the outer blood-retina barrier while supporting photoreceptor cell function. However, the fundamental abnormalities occurring in RPE cells leading to their progressive dysfunction and deposit formation are not known. AMD is clearly multifactorial with genetic, systemic health and environmental factors regulating development of the disease. Epidemiological and animal model studies have given rise to several proposed pathogenic pathways which may be involved in the initiation and progression of disease, pathways including lipid dysregulation, mitochondrial dysfunction, choroidal non-perfusion or hyper-perfusion, growth factor-stimulated angiogenesis, chronic oxidative injury and inflammation, RPE lysosomal failure, and apoptosis to name a few.

Nuclear receptors are a superfamily of ligand-dependent transcription factors which play an important role as sensors and effectors that translate endocrine and metabolic cues including fat-soluble hormones, vitamins, dietary lipids, and toxins into gene expression programs that regulate various functions including lipid metabolism, development, cellular differentiation, proliferation, and apoptosis [5, 6]. As such, nuclear receptor dysregulation has been shown to promote disease states such as cancer, obesity, and inflammation, diseases that share pathogenic mechanisms with AMD. Nuclear receptors are also well-validated therapeutic targets as illustrated by the extensive clinical use of nuclear receptor agonists and antagonists medically. To date, no one has investigated the role of nuclear receptors in RPE cells. This led us to develop a RPE-cell-specific nuclear receptor atlas with the goal of creating a comprehensive baseline of nuclear receptor expression in order to further elucidate the biochemical and physiological pathways under normal conditions as well as identify potential pathways that may contribute to pathogenic changes seen in retinal diseases [7].

## 40.2 Nuclear Receptor Atlas of Human RPE Cells

We profiled the expression of 48 members of the human nuclear receptor superfamily of proteins using the relative standard curve method of real-time quantitative RT-PCR in three human RPE cell model system commonly used in laboratories. These model systems included the spontaneously arising RPE cell line, ARPE19 cells, primary cells derived from human donors and cultured below nine passages and freshly isolated human RPE cells. Receptors were divided based on expres-

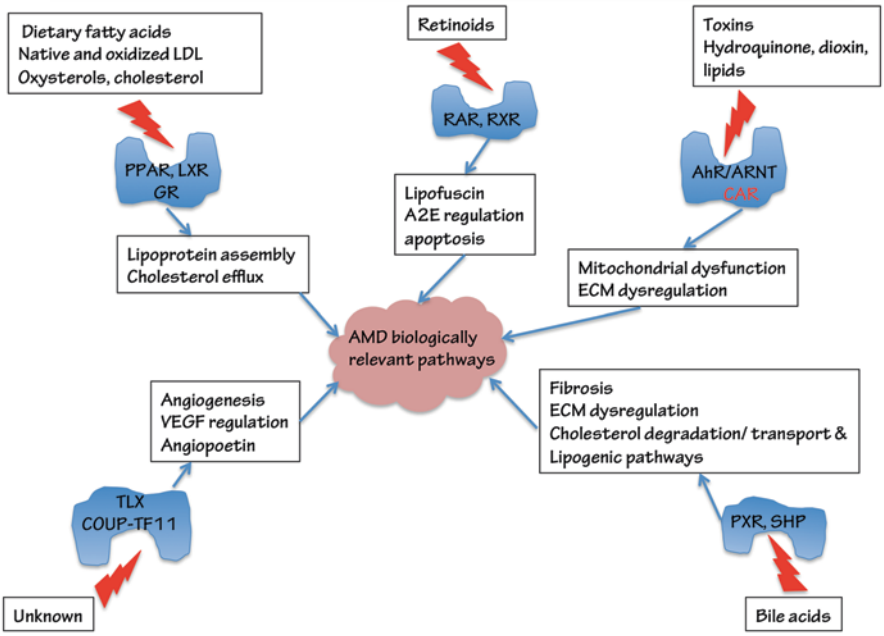


**Fig. 40.1** Potential physiologically relevant nuclear receptors in the pathogenesis of age-related macular degeneration (*AMD*). Shown are ligands for the receptors (if known) and the mechanisms and proposed pathogenic pathways through which they may impact *AMD*

sion level into the following categories: absent or undetectable, low, medium, or high expression. Analysis of the data revealed that primary RPE cells and ARPE19 cells exhibited similar expression patterns while the largest number of receptors expressed at high levels were seen in RPE cells isolated from human donor eyes [7].

To compile a list of nuclear receptors that may be important in AMD pathogenesis, we divided the receptors into functional groups with relevance to AMD based on a literature search using gene ontology terms. Select physiologically relevant receptors in the pathogenesis of AMD are shown in Fig. 40.1.

## 40.3 The Role of the Aryl Hydrocarbon Receptor (AhR) in the Pathogenesis of AMD

One receptor highly expressed in all three RPE model systems was the AhR. AhR is a ligand-dependent transcription factor activated by endogenous and environmental oxidants and plays a critical role in managing the cellular response to toxicants[8]. Recent studies propose that AhRs also demonstrate endobiotic functions regulating lipid accumulation in hepatic steatosis (fatty liver disease) and cardiovascular disease[9, 10]. To investigate the potential role of AhR in AMD, we first demonstrated

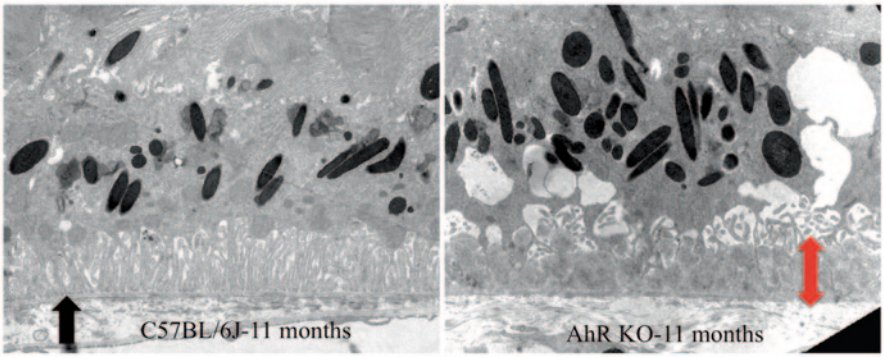


**Fig. 40.2** Morphology of wild-type and AhR knockout mice. Electron microscopic images of the RPE / Bruch's membrane / choroidal junction of 11-month-old C57BL/6J mice and AhR knockout mice. *Black arrow* points to Bruch's membrane. *Red arrow* shows the thickness of sub-RPE deposit in the AhR knockout mouse

the presence of the signaling pathway showing that known AhR ligands can increase the activity of the receptor in human RPE cells (presented at ARVO 2011). Furthermore, we also demonstrated that expression of AhR-specific target genes including the cytochrome P450 1A1 and 1B1 increase significantly following treatment of RPE cells with known AhR ligands. Next, in a preliminary study we evaluated AhR activity as a function of age in RPE cell lines derived from young (less than 55 years) and old (greater than 55 years). We found an age-related decline in activity. As result, we explored the visual function and pathology of the retina/RPE/choroid of mice carrying the AhR null allele. We found that with age there was significant impairment of vision in these mice including a decrease in a- and b-wave amplitudes following dark adaptation using electroretinography. Additionally, we found that the 11-month-aged AhR knockout mouse demonstrated several of the cardinal pathological features of human AMD including the presence of sub-RPE deposits (Fig. 40.2), thickening of Bruch's membrane, RPE hyper- and hypo-pigmentation, and ultimately RPE atrophy at 16 months of age. Current studies are exploring the mechanistic role of AhR and its regulatory role in deposit formation and apoptosis.

## 40.4 Discussion

Successful future treatments for AMD will be dependent on our understanding of the molecular and biological mechanisms that contribute to RPE dysfunction. The nuclear receptor atlas has provided us with a framework to further understand mechanistic pathways important in RPE cell function and potentially critical to retinal diseases including AMD. Identification of valid therapeutic targets will require very focused investigations of the biology of these receptors in the eye.

**Acknowledgments** Sincere thanks to the North Carolina Eye Bank, the Alabama Eye Bank, the eye donors and their families for their generosity. The author also thanks the following collaborators for their significant contributions to the studies briefly summarized herein: Donald McDonnell, Glenn Jaffe, Michael Boulton, Russell Thomas and Mary Dwyer. This work was supported in part by the US National Eye Institute grants EY02868, P30 EY005722, the Research to Prevent Blindness, Inc. (RPB) Core grants to the Duke Eye Center, the American Health Assistance Research Foundation-Macular Degeneration, the RPB special Scholars Award, and the Alcon Young Investigator Award.

## References

1. Ambati J, Ambati BK, Yoo SH, Ianchulev S, Adamis AP (2003) Age-related macular degeneration: etiology, pathogenesis, and therapeutic strategies. Surv Ophthalmol 48(3):257–293
2. Klein R, Chou CF, Klein BE, Zhang X, Meuer SM, Saaddine JB (2011) Prevalence of age-related macular degeneration in the US population. Arch Ophthalmol 129(1):75–80
3. Ciulla TA, Rosenfeld PJ (2009) Antivascular endothelial growth factor therapy for neovascular age-related macular degeneration. Curr Opin Ophthalmol 20(3):158–165
4. Klein R, Klein BE, Knudtson MD, Meuer SM, Swift M, Gangnon RE (2007) Fifteen-year cumulative incidence of age-related macular degeneration: the Beaver Dam Eye Study. Ophthalmology 114(2):253–262
5. Chawla A, Repa JJ, Evans RM, Mangelsdorf DJ (2001) Nuclear receptors and lipid physiology: opening the X-files. Science 294(5548):1866–1770
6. Bookout AL, Jeong Y, Downes M, Yu RT, Evans RM, Mangelsdorf DJ (2006) Anatomical profiling of nuclear receptor expression reveals a hierarchical transcriptional network. Cell 126(4):789–799
7. Dwyer MA, Kazmin D, Hu P, McDonnell DP, Malek G (2011) Research resource: nuclear receptor atlas of human retinal pigment epithelial cells: potential relevance to age-related macular degeneration. J Molecular Endocrinology 25(2):360–372
8. Swanson HI, Bradfield CA (1993) The AH-receptor: genetics, structure and function. Pharmacogenetics 3(5):213–230
9. Lee JH, Wada T, Febbraio M, He J, Matsubara T, Lee MJ, Gonzalez FJ, Xie W (2010) A novel role for the dioxin receptor in fatty acid metabolism and hepatic steatosis. Gastroenterology 139(2):653–663
10. Vogel CF, Sciullo E, Matsumura F (2004) Activation of inflammatory mediators and potential role of ah-receptor ligands in foam cell formation. Cardiovasc Toxicol 4(4):363–373

# Chapter 41
# Utilizing Stem Cell-Derived RPE Cells as A Therapeutic Intervention for Age-Related Macular Degeneration

**Peter D. Westenskow, Toshihide Kurihara and Martin Friedlander**

**Abstract** Purpose
Degeneration or dysfunction of the retinal pigment epithelium (RPE) can induce secondary photoreceptor atrophy and catastrophic vision loss in patients with age-related macular degeneration (AMD). AMD is the leading cause of vision loss in the elderly in industrialized countries and no cure exists for the "dry" or atrophic form to date. However, recent pre-clinical data from several groups suggests that embryonic stem cell-derived RPE cell transplantation may prevent photoreceptor degeneration in animal models of RPE degeneration. Another approach may be to derive RPE cells from autologous induced pluripotent stem cells (iPSCs) reprogrammed from dermal tissue. However, the safety of this approach has been questioned on several levels. In this chapter we will summarize work reported by several groups, including our own, that clearly demonstrate that transplanted RPE cells can provide anatomical and functional photoreceptor rescue in animal models of retinal degeneration. We will also discuss some of the prevailing concerns and challenges associated with this technique.

**Keywords** RPE · Stem cell biology · Cell-based therapy · Translational medicine · AMD

**Abbreviations**

| | |
|---|---|
| RPE | Retinal pigment epithelium |
| AMD | Age-related macular degeneration |
| iPSC | Induced pluripotent stem cell |
| iPSC-RPE | Induced pluripotent stem cell-derived RPE |

M. Friedlander (✉) · P. D. Westenskow · T. Kurihara
Department of Cell Biology, The Scripps Research Institute, MB 216, 10550 N. Torrey Pines Rd, La Jolla, CA 92014, USA
e-mail: friedlan@scripps.edu

P. D. Westenskow
e-mail: petewest@scripps.edu

T. Kurihara
e-mail: kurihara@scripps.edu

J. D. Ash et al. (eds.), *Retinal Degenerative Diseases,* Advances in Experimental Medicine and Biology 801, DOI 10.1007/978-1-4614-3209-8_41,

| | |
|---|---|
| hESC | Human embryonic stem cell |
| hESC-RPE | Human embryonic stem cell-derived RPE |
| HLA | Human leukocyte antigen |
| OSKM | Oct4, Sox2, Klf4, and c-Myc |
| OSNL | Oct4, Sox2, Nanog, and Lin28 |
| ACT | Advanced Cell Technology, Inc |

## 41.1 Introduction

The retina consists of diverse cell types stratified into organized functional tiers. Rod and cone photoreceptors and retinal pigment epithelium (RPE) cells work in conjunction to perform the energy-demanding and complicated biochemical process of converting light energy into electrical signals that ultimately are processed into "vision." The neurosensory retina rests on a monolayer of RPE cells that associates with the photoreceptors on one side while partitioning the retina from the choriocapillaris on the other. The RPE performs multiple critical diverse functions essential for maintaining photoreceptor homeostasis (for review, see [1]). In fact, death or dysfunction of RPE cells can induce devastating secondary effects on photoreceptors characteristic of age-related macular degeneration (AMD). AMD is the leading cause of vision loss in the elderly in industrialized countries [2, 3], and demographic analyses predict that it will become more widespread [4].

AMD is a multifactorial polygenic disease characterized by a broad spectrum of signs and symptoms (for review see [5]). However, RPE dysfunction and photoreceptor degeneration are shared characteristics that may be amenable to cell replacement strategies for a majority of AMD patients if delivery could be optimized and graft rejection prevented [6–9]. Compared with photoreceptor transplantation, RPE transplantation strategies are more simple since RPE cells do not need to integrate into neuronal networks that begin to degenerate and/or remodel during retinal degeneration (for review see [10]). Pluripotent stem cells may provide an excellent source of RPE, and banks of histocompatibility antigen-typed RPE derived from human embryonic stem cells (hESC-RPE) cells can be generated and used to intervene therapeutically after a patient is diagnosed with the disease.

Several NIH approved pluripotent embryonic stem cells (ESCs) are currently available, however their widespread use is still controversial due to ethical concerns. These concerns may be obviated due to a remarkable observation that the transgenic manipulation of only four transcription factors, OSKM: Oct4, Sox2, Klf4, or c-Myc [11], or OSNL: Oct4, Sox2, Nanog, and Lin28 [12], in somatic cells can "reprogram" them into induced pluripotent stem cells (iPSCs) from which autologous RPE grafts can be generated. These iPSC-RPE could be derived from individual patients and used for therapeutic transplantation since the progression of AMD is relatively slow. However, there are some prevailing safety and immunogenic concerns regarding the use of iPSCs that must first be resolved [13–20].

## 41.2 Stem Cell Derived RPE Cells Have Been Well Characterized

Pigmented RPE can be readily derived from hESCs [21–25] and hiPSCs [24, 26–30]. These cells spontaneously differentiate with appropriate morphologies and functionality, but may be more efficiently generated if exogenous factors are added to the differentiation media [21, 24, 29, 30]. hES– and hiPS–RPE cells have been well characterized. They express RPE-specific terminal differentiation markers [21–30] in polarized planes [25, 26, 29]. Using high resolution mass spectrometry-based metabolomic analyses as a measure of functional genomics, we have shown that iPS-RPE strongly resemble primary human RPE cells [29].

hES–RPE and hiPS–RPE also function as well as their human primary RPE counterparts in vitro. As observed in primary RPE [31], tightly coupled stem cell-derived RPE form fluid-filled domes, demonstrating that the ion pumps are vectorially functional [32]. Stem cell-derived RPE can also phagocytose photoreceptor outer segments in vitro [21, 25–27, 29, 33]. We have developed a flow cytometry-based method to measure the dynamics of RPE phagocytosis. Using this strategy we have shown that iPS-RPE synthesize phagocytosis receptors that phagocytose outer segments as effectively as primary human RPE do [34].

An important measure of RPE function is to determine if the cells operate in a diseased context in vivo. Studies in animal models have provided very encouraging evidence that stem cell-derived RPE transplantation can effectively promote photoreceptor cell anatomical and functional rescue in dystrophic retinas [21, 23, 25, 27, 29]. Additionally, the extremely preliminary results of a Phase 1/2 clinical trial using hES–RPE managed by Advanced Cell Technology Inc. (ACT) have shown that after four months the transplanted cells do not induce any obvious adverse side effects and may have integrated into the subretinal space of the treated patients [35].

## 41.3 Current and Future Prospects for RPE Cell Transplantation

In the majority of studies published to date (and in the ACT managed clinical trial) a bolus of RPE cells were injected into the subretinal space. With a few exceptions (including in our study in which we see a monolayer of RPE cells integrated in the subretinal space up to 17 months post injection [29]), transplanted RPE cells generally survive only for a few months after implantation and not integrate into monolayers [21, 27, 36]. For these reasons the use of alternative approaches are being advocated, including the use of intact RPE sheets or RPE cells grown on porous engineered Bruch's membrane mimics [37, 38]. The surgical techniques required to deliver sheets of cells are inherently more complicated. Furthermore, it must be demonstrated that the scaffolds can stably support RPE cells over extended periods of time and allow adequate RPE and choriocapillaris crosstalk.

The use of iPS–RPE, and personalized medicine in general, could be very expensive. One alternative approach may be to bank reduced complexity human leukocyte antigen (HLA)-homozygous iPSC (or perhaps even hESC cell-lines). It has been estimated that approximately 75 and 140 unique donors would be needed to cover ~80% and ~90% of the Japanese population, and roughly 64,000–160,000 individuals would need to be typed to find the donors [39]. However, it is also important to consider that long-term immunosuppressive therapies are expensive, associated with complications, and not well tolerated by elderly patients [40, 41]. Therefore, the expenses for both techniques, and potential consequences of life-long immunosuppression, should be directly compared before any approach is deemed to be cost prohibitive.

While still extremely premature, an alternative therapeutic approach may involve the replacement of whole degenerated regions of human retinas with large patches of intact ocular tissues grown from stem cells in 3D cultures. The idea of transplanting stratified layers of functional neural networks may be more realistic based on two ground-breaking recent reports demonstrating that aggregates of mouse and, more recently, human ES cells grown in 3-D cultures self-assembled into structures strongly resembling optic cups (rudimentary sensory retinas) with neural and RPE domains [42, 43]. If this approach could be optimized, theoretically entire autologous maculas may be generated as therapeutic interventions for AMD.

## 41.4 Conclusions

RPE that function in vitro and in vivo to maintain photoreceptor homeostasis can be readily generated from stem cells. While few conclusions can be drawn until long-term studies in human patients have been completed, and RPE derivation and delivery techniques are optimized, the evidence collected in animal models that RPE grafts can prevent continued retinal degeneration and maintain visual function is very encouraging. Therefore, stem cell-based RPE transplantation therapies for untreatable retinal degenerative diseases such as AMD may ultimately prove to be not only realistic, but also therapeutically effective.

**Acknowledgments** We wish to warmly thank all members of the Friedlander lab and our collaborators. Work discussed in this chapter was supported by generous funding to PDW, a Ruth Kirschstein Fellow (NEI EY021416), to TK (Manpei Suzuki Diabetes Foundation and The Japan Society for the Promotion of Science Postdoctoral Fellowships for Research Abroad), and to MF from the NEI (EY11254; EY017540), the California Institute for Regenerative Medicine (CIRM TR1–01219), the Lowy Medical Research Foundation (the MacTel Project), and the Rasmussen Foundation.

## References


1. Strauss O (2005) The retinal pigment epithelium in visual function. Physiol Rev 85(3):845–881
2. Congdon N, O'Colmain B, Klaver CC, Klein R, Munoz B, Friedman DS et al (2004) Causes and prevalence of visual impairment among adults in the United States. Arch Ophthalmol 122(4):477–485
3. Resnikoff S, Pascolini D, Etya'ale D, Kocur I, Pararajasegaram R, Pokharel GP et al (2004) Global data on visual impairment in the year 2002. Bull World Health Organ 82(11):844–851
4. Friedman DS, O'Colmain BJ, Munoz B, Tomany SC, McCarty C, de Jong PT et al (2004) Prevalence of age-related macular degeneration in the United States. Arch Ophthalmol 122(4):564–572
5. Bird AC (2010) Therapeutic targets in age-related macular disease. J Clin Invest 120(9):3033–3041
6. Algvere PV, Gouras P, Dafgard Kopp E (1999) Long-term outcome of RPE allografts in non-immunosuppressed patients with AMD. Eur J Ophthalmol 9(3):217–230
7. Cahill MT, Freedman SF, Toth CA (2003) Macular translocation with 360 degrees peripheral retinectomy for geographic atrophy. Arch Ophthalmol 121(1):132–133
8. Joussen AM, Joeres S, Fawzy N, Heussen FM, Llacer H, van Meurs JC et al (2007) Autologous translocation of the choroid and retinal pigment epithelium in patients with geographic atrophy. Ophthalmology 114(3):551–560
9. Zhang X, Bok D (1998) Transplantation of retinal pigment epithelial cells and immune response in the subretinal space. Invest Ophthalmol Vis Sci 39(6):1021–1027
10. Marc R (2005) Retinal remodeling. J Vis 5(12):5
11. Takahashi K, Tanabe K, Ohnuki M, Narita M, Ichisaka T, Tomoda K et al (2007) Induction of pluripotent stem cells from adult human fibroblasts by defined factors. Cell 131(5):861–872
12. Yu J, Vodyanik MA, Smuga-Otto K, Antosiewicz-Bourget J, Frane JL, Tian S et al (2007) Induced pluripotent stem cell lines derived from human somatic cells. Science 318(5858):1917–1920
13. Aoi T, Yae K, Nakagawa M, Ichisaka T, Okita K, Takahashi K et al (2008) Generation of pluripotent stem cells from adult mouse liver and stomach cells. Science 321(5889):699–702
14. Bock C, Kiskinis E, Verstappen G, Gu H, Boulting G, Smith ZD et al (2011) Reference maps of human ES and iPS cell variation enable high-throughput characterization of pluripotent cell lines. Cell 144(3):439–452
15. Hussein SM, Batada NN, Vuoristo S, Ching RW, Autio R, Narva E et al (2011) Copy number variation and selection during reprogramming to pluripotency. Nature 471(7336):58–62
16. Laurent LC, Ulitsky I, Slavin I, Tran H, Schork A, Morey R et al (2011) Dynamic changes in the copy number of pluripotency and cell proliferation genes in human ESCs and iPSCs during reprogramming and time in culture. Cell Stem Cell 8(1):106–118
17. Markoulaki S, Hanna J, Beard C, Carey BW, Cheng AW, Lengner CJ et al (2009) Transgenic mice with defined combinations of drug-inducible reprogramming factors. Nat Biotechnol 27(2):169–171
18. Mayshar Y, Ben-David U, Lavon N, Biancotti JC, Yakir B, Clark AT et al (2010) Identification and classification of chromosomal aberrations in human induced pluripotent stem cells. Cell Stem Cell 7(4):521–531
19. Quinlan AR, Boland MJ, Leibowitz ML, Shumilina S, Pehrson SM, Baldwin KK et al (2011) Genome sequencing of mouse induced pluripotent stem cells reveals retroelement stability and infrequent DNA rearrangement during reprogramming. Cell Stem Cell 9(4):366–373
20. Zhao T, Zhang Z-N, Rong Z, Xu Y (2011) Immunogenicity of induced pluripotent stem cells. Nature 474(7350):212–215
21. Idelson M, Alper R, Obolensky A, Ben-Shushan E, Hemo I, Yachimovich-Cohen N et al (2009) Directed differentiation of human embryonic stem cells into functional retinal pigment epithelium cells. Cell Stem Cell 5(4):396–408

22. Klimanskaya I, Hipp J, Rezai KA, West M, Atala A, Lanza R (2004) Derivation and comparative assessment of retinal pigment epithelium from human embryonic stem cells using transcriptomics. Cloning Stem Cells 6(3):217–245
23. Lund RD, Wang S, Klimanskaya I, Holmes T, Ramos-Kelsey R, Lu B et al (2006) Human embryonic stem cell-derived cells rescue visual function in dystrophic RCS rats. Cloning Stem Cells 8(3):189–199
24. Meyer JS, Shearer RL, Capowski EE, Wright LS, Wallace KA, McMillan EL et al (2009) Modeling early retinal development with human embryonic and induced pluripotent stem cells. Proc Natl Acad Sci 106(39):16698–16703
25. Vugler A, Carr AJ, Lawrence J, Chen LL, Burrell K, Wright A et al (2008) Elucidating the phenomenon of HESC-derived RPE: anatomy of cell genesis, expansion and retinal transplantation. Exp Neurol 214(2):347–361
26. Buchholz DE, Hikita ST, Rowland TJ, Friedrich AM, Hinman CR, Johnson LV et al (2009) Derivation of functional retinal pigmented epithelium from induced pluripotent stem cells. Stem Cells 27(10):2427–2434
27. Carr AJ, Vugler AA, Hikita ST, Lawrence JM, Gias C, Chen LL et al (2009) Protective effects of human iPS-derived retinal pigment epithelium cell transplantation in the retinal dystrophic rat. PLoS One 4(12):e8152
28. Hirami Y, Osakada F, Takahashi K, Okita K, Yamanaka S, Ikeda H et al (2009) Generation of retinal cells from mouse and human induced pluripotent stem cells. Neurosci Lett 458(3):126–131
29. Krohne T, Westenskow P, Kurihara T, Friedlander D, Lehmann M, Dorsey A et al (2012) Generation of retinal pigment epithelial cells from small molecules and OCT4-reprogrammed human induced pluripotent stem cells. Stem Cells Trans Med 1(2):96–109
30. Osakada F, Jin ZB, Hirami Y, Ikeda H, Danjyo T, Watanabe K et al (2009) In vitro differentiation of retinal cells from human pluripotent stem cells by small-molecule induction. J Cell Sci 122(Pt 17):3169–3179
31. Mircheff AK, Miller SS, Farber DB, Bradley ME, O'Day WT, Bok D (1990) Isolation and provisional identification of plasma membrane populations from cultured human retinal pigment epithelium. Invest Ophthalmol Vis Sci 31(5):863–878
32. Kokkinaki M, Sahibzada N Golestaneh N (2011) Human induced pluripotent stem-derived retinal pigment epithelium (RPE) cells exhibit ion transport, membrane potential, polarized vascular endothelial growth factor secretion, and gene expression pattern similar to native RPE. Stem Cells 29(5):825–835
33. Carr AJ, Vugler A, Lawrence J, Chen LL, Ahmado A, Chen FK et al (2009) Molecular characterization and functional analysis of phagocytosis by human embryonic stem cell-derived RPE cells using a novel human retinal assay. Mol Vis 15:283–295
34. Westenskow PD, Moreno SK, Krohne TU, Kurihara T, Zhu S, Zhang ZN et al (2012) Using flow cytometry to compare the dynamics of photoreceptor outer segment phagocytosis in iPS-derived RPE cells. Invest Ophthalmol Vis Sci 53(10):6282–6290
35. Schwartz SD, Hubschman J-P, Heilwell G, Franco-Cardenas V, Pan CK, Ostrick RM et al (2012) Embryonic stem cell trials for macular degeneration: a preliminary report. Lancet 379(9817):713–720
36. Lu B, Malcuit C, Wang S, Girman S, Francis P, Lemieux L et al (2009) Long-term safety and function of RPE from human embryonic stem cells in preclinical models of macular degeneration. Stem Cells 27(9):2126–2135
37. Sheridan C, Williams R, Grierson I (2004) Basement membranes and artificial substrates in cell transplantation. Graefes Arch Clin Exp Ophthalmol 242(1):68–75
38. Williams RL, Krishna Y, Dixon S, Haridas A, Grierson I, Sheridan C (2005) Polyurethanes as potential substrates for sub-retinal retinal pigment epithelial cell transplantation. J Mater Sci Mater Med 16(12):1087–1092
39. Okita K, Ichisaka T, Yamanaka S. 2007 Generation of germline-competent induced pluripotent stem cells. Nature 448(7151):313–317

40. Karamehic J, Ridic O, Jukic T, Ridic G, Slipicevic O, Coric J et al (2011) Financial aspects of the immunosuppressive therapy. Med Arh 65(6):357–362
41. Tezel TH, Del Priore LV, Berger AS, Kaplan HJ (2007) Adult retinal pigment epithelial transplantation in exudative age-related macular degeneration. Am J Ophthalmol 143(4):584–595
42. Eiraku M, Takata N, Ishibashi H, Kawada M, Sakakura E, Okuda S et al (2011) Self-organizing optic-cup morphogenesis in three-dimensional culture. Nature 472(7341):51–56
43. Nakano T, Ando S, Takata N, Kawada M, Muguruma K, Sekiguchi K et al (2012) Self-formation of optic cups and storable stratified neural retina from human ESCs. Cell Stem Cell 10(6):771–785

# Part VI
# Müller Cells, Microglia, and Macrophages

# Chapter 42
# Microglia-Müller Cell Interactions in the Retina

**Minhua Wang and Wai T. Wong**

**Abstract** Microglia and Müller cells are cell types that feature prominently in responses to disease and injury in the retina. However, their mutual interactions have not been investigated in detail. Here, we review evidence that indicate that these two cell populations exchange functionally significant signals under uninjured conditions and during retinal inflammation. Under normal conditions, Müller cells constitute a potential source of extracellular ATP that mediates the activity-dependent regulation of microglial dynamic process motility. Following microglial activation in inflammation, microglia can signal to Müller cells, influencing their morphological, molecular, and functional responses. Microglia-Müller cell interactions appear to be a mode of bi-directional communications that help shape the overall injury response in the retina.

**Keywords** Müller cells · Microglia · Inflammation · Retina · Gliosis

## 42.1 Introduction

Glia populations in the central nervous system (CNS) consist primarily of microglia, the main resident immune cells, and macroglia, which include astrocytes and oligodendrocytes. These non-neuronal cell populations are intimately integrated into healthy neuronal function, play important homeostatic roles in maintaining the CNS *milieu*, and participate prominently in tissue responses to diseases, inflammation, and injury [1–4].

W. T. Wong (✉) · M. Wang
Unit on Neuron-Glia Interactions in Retinal Diseases, National Eye Institute, National Institutes of Health, 6 Center Drive, 6/215, Bethesda, MD 20892, USA
e-mail: wongw@nei.nih.gov

M. Wang
e-mail: minhua.wang@nih.gov

J. D. Ash et al. (eds.), *Retinal Degenerative Diseases,* Advances in Experimental Medicine and Biology 801, DOI 10.1007/978-1-4614-3209-8_42,

In the retina, microglia and macroglia are similarly represented. Retinal microglia are found distributed throughout the inner retina in a laminated fashion [5], and are involved in retinal responses to injury and disease [6]. Retinal macroglia, consisting of astrocytes and Müller cells, play key roles in supporting neuronal functions [7–10], and demonstrate gliotic changes in response to pathological insults [11]. However, how these two retinal cell populations interact and collaborate with each other is incompletely understood. As microglial and Müller cells responses to disease and injury have been ascribed both adaptive and maladaptive aspects, it is of interest to determine if and how microglia- Müller cell interactions help shape the features of the overall retinal injury response [6, 7, 12].

## 42.2 Microglia-Müller Cell Interactions in the Healthy Retina

Live-cell imaging studies have revealed that "resting" microglial processes are highly dynamic and can occupy the surrounding extracellular milieu through these constant movements [13–17]. This "resting" phenotype has been linked to key constitutive microglial functions such as cleaning up apoptotic cells and cellular debris [18, 19], pruning excess or dysfunctional synapses [20, 21], providing trophic factors [22–24], and regulating synaptic functions and plasticity [25–27]. Recent studies have shown that microglia dynamically remodel synapses by engulfing pre-synaptic synapses in an activity-dependent manner [27]. Resting microglia can preferentially contact active neurons and down-regulate their activity, maintaining stability in overall activity levels [28]. These findings reveal that microglial process behavior and morphology are likely regulated by activity-dependent signaling involving neurons and macroglia.

As neurotransmission is the prominent mode of communication occurring between neurons and glia, it is a candidate factor for regulating microglial behavior. In live imaging experiments of ex vivo retinal explants, we found that excitatory glutamatergic neurotransmission occurring via AMPA and kainate channels exerted a positive effect on microglial morphology and process motility [15]. Blockade of glutamatergic neurotransmission using the antagonists, NBQX, and GYKI, resulted in decreased microglial dendritic arbor size and decreased process motility, while application of glutamatergic agonists AMPA and kainate exerted opposite effects. Conversely, inhibitory GABAergic neurotransmission occurring via $GABA_A$ channels was found to negatively regulate microglial morphology and process motility; bicuculline blockade of $GABA_A$ receptors increased process motility while application of GABA decreased it.

Interestingly, these effects do not appear to be mediated by direct reception of glutamatergic or GABAergic signaling on microglial cells. We were unable to co-localize ionotropic glutamate receptors GluR2/3 on microglia using immunohistochemical studies. Electrophysiological studies demonstrate that microglia do not directly respond to the application of glutamatergic or GABAergic agonists, but respond only to application of ATP, which is likely mediated through P2 receptors

expressed on microglia [15, 28]. Current evidence indicates that while microglial process motility is sensitive to overall levels of neuronal activity, which is determined by a balance between excitatory and inhibitory forms of neurotransmission, it is the activity-dependent release of extracellular ATP that constitutes the direct signal to microglia regulating their dynamic behavior [28].

The precise cellular source of ATP in the retina relevant to microglial regulation has not been definitively established, but Müller cells, a prominent source of extracellular ATP, are likely involved. Extracellular glutamate can induce Müller cells to release ATP [29] via several pathways including vesicle exocytosis [30], connexin hemichannels [31], and pannexin channels [32, 33]. In the retina, we found that probenecid, an inhibitor of pannexin channels, decreased microglial morphology and process motility, and was not rescued by the application of extracellular AMPA [15]. Taken together, these data reveal that ongoing excitatory and inhibitory neurotransmissions determine overall activity levels in the retina, which likely modulate ATP release from Müller cells via pannexin channels, thus influencing "resting" microglial behavior. This scenario posits that in the uninjured healthy retina, Müller cell-microglia communication is a constitutive ongoing phenomenon—Müller cell signals inform retinal microglia on ongoing levels of neuronal activity, which are then integrated to drive a behavioral response in microglia that is commensurate with their functions of activity-regulation, synapse modification, and trophic factor production.

## 42.3 Microglia-Müller Cell Interactions in Retinal Inflammation Help Shape the Overall Injury Response

Upon the onset of inflammation, injury, or disease, microglia react rapidly by transitioning to an activated status within minutes [13, 14, 16], initiating the first steps of the inflammatory response that precede macroglial responses [34–36]. Like astrocytes in brain, Müller cells demonstrate activation and reactive gliosis under pathological conditions. Typical features of Müller cell gliosis involve cellular hypertrophy, up-regulation of intermediate filament expression (such as GFAP and vimentin), increased rates of proliferation, and down-regulation of glutamine synthetase (GS) expression [8]. We wanted to investigate whether signals from activated microglia in the acute aftermath of injury influence Müller cells in the overall injury response.

We explored the cellular signaling between microglia and Müller cells by using a simple in vitro co-culture system in which Müller cells were cultured alone, or co-cultured with microglia with or without lipopolysaccharide (LPS) pre-treatment. We found that Müller cells which were either cultured alone or co-cultured with unactivated microglia demonstrated a symmetrical, flat cell shape with prominent lamellipodia. However, those co-cultured with activated microglia transitioned to elongated, spindle/multipolar shapes, which was confirmed by quantitative image analysis [37]. These cells also interestingly decreased their mRNA expression of

gliosis markers, such as glutamate aspartate transporter (GLAST) and vimentin. Their proliferation was also significantly decreased, without any increase in cellular apoptosis. In addition, Müller cells co-cultured with activated microglia expressed higher mRNA and protein levels of trophic factors, such as GDNF and LIF. Indeed, the conditioned media from Müller cells which had been previously co-cultured with activated microglia demonstrated greater neuroprotective effects in an in vitro assay of oxidatively-stressed 661W photoreceptors. These results indicate that Müller cells are highly responsive to the activation state of microglia, and that activated microglia can acutely induce Müller cell responses that are associated with adaptive and neuroprotective effects and do not involve expression of typical markers of gliosis.

In further experiments, we found that Müller cells co-cultured with activated microglia significantly increased their mRNA and protein expression of pro-inflammatory factors such as IL1β, IL6, and iNOS [37]. Nitrite production was increased, consistent with increased iNOS expression. When Müller cell conditioned media following activated microglia co-culture was collected and added to fresh, non-activated microglia, they were capable of inducing microglia activation as evidenced by increased microglial proliferation and pro-inflammatory cytokine production. These results suggest in response to situations of inflammation or injury, Müller cells and microglia can conduct mutual and reciprocal signaling that amplifies local inflammation in a positive feedback cycle.

We further examined whether physical interactions between microglia and Müller cells were altered in microglia-Müller cell signaling. We found that Müller cells co-cultured with activated microglia increased mRNA expression of adhesion molecules (VCAM-1 and ICAM-1). Müller cells exposed to activated microglia were also capable of retaining the largest number of microglia to their surfaces in a cell adhesion assay. Additionally, activated microglia induced Müller cells to express higher mRNA and protein levels of chemotactic cytokines (CCL2, CCL3), and the conditioned media from Müller cells exposed to activated microglia induced higher levels of microglial chemotaxis relative to controls. These results suggest that under the influence of activated microglia, Müller cells undergo changes related to their expression of cell-adhesion and chemotactic molecules, which serve to present a more conducive surface for microglial adhesion and migration. These features were recapitulated in vivo when retinal microglia activated by intravitreal injection of LPS demonstrated changes in physical contacts with Müller cells. Microglia in the unactivated, “resting” state have horizontally oriented processes that interdigitate with the orthogonally-oriented, radial Müller cell processes. Acutely following LPS injection, microglia transitioned to a more vertically-orientation where their processes fasciculated closely in an adherent manner with Müller cell processes which may serve as a scaffold for the radial migration of microglia.

Taken together, these data demonstrated the ability of microglia to induce changes in Müller cells as a function of their activation. Bi-directional microglia-Müller cell signaling appears to help shape an acute injury response that is characterized by (1) an amplification of activation, (2) adaptive neuroprotection, and (3) increased physical interaction between the two cell types that may help mobilize migratory microglia within the retina.

## 42.4 Perspectives

Given that reciprocal microglia-Müller cell interactions can shape acute retinal responses to injury and disease, future studies will examine their role in long-term responses and in chronic inflammation. The transition between acute, adaptive responses to chronic, maladaptive gliosis may be a result altered interactions changes in this particular locus. Discovery of relevant molecular signals will be instructive in understanding these multifaceted interactions. Microglia-Müller cell signaling may constitute a target for therapeutic interventions that can direct overall retinal injury responses towards beneficial, and away from detrimental, ends.

## References

1. Wake H, Moorhouse AJ, Nabekura J (2011) Functions of microglia in the central nervous system-beyond the immune response. Neuron Glia Biol 7(1):47–53
2. Ransohoff RM, Cardona AE (2011) The myeloid cells of the central nervous system parenchyma. Nature 468(7321):253–262
3. Buffo A, Rolando C, Ceruti S (2010) Astrocytes in the damaged brain: molecular and cellular insights into their reactive response and healing potential. Biochem Pharmacol 79(2):77–89
4. Hanisch UK, Kettenmann H (2007) Microglia: active sensor and versatile effector cells in the normal and pathologic brain. Nat Neurosci 10(11):1387–1394
5. Santos AM, Calvente R, Tassi M, Carrasco MC, Martin-Oliva D, Marin-Teva JL et al (2008) Embryonic and postnatal development of microglial cells in the mouse retina. J Comp Neurol 506(2):224–239
6. Karlstetter M, Ebert S, Langmann T (2010) Microglia in the healthy and degenerating retina: insights from novel mouse models. Immunobiology 215(9–10):685–691
7. Bringmann A, Iandiev I, Pannicke T, Wurm A, Hollborn M, Wiedemann P et al (2009) Cellular signaling and factors involved in Muller cell gliosis: neuroprotective and detrimental effects. Prog Retin Eye Res 28(6):423–451
8. Bringmann A, Pannicke T, Grosche J, Francke M, Wiedemann P, Skatchkov SN et al (2006) Muller cells in the healthy and diseased retina. Prog Retin Eye Res 25(4):397–424
9. Newman EA, Zahs KR (1998) Modulation of neuronal activity by glial cells in the retina. J Neurosci 18(11):4022–4028
10. Poitry-Yamate CL, Poitry S, Tsacopoulos M (1995) Lactate released by Muller glial cells is metabolized by photoreceptors from mammalian retina. J Neurosci 15(7 Pt 2):5179–5191
11. Bringmann A, Wiedemann P (2012) Muller glial cells in retinal disease. Ophthalmologica 227(1):1–19
12. Xu H, Chen M, Forrester JV (2009) Para-inflammation in the aging retina. Prog Retin Eye Res 28(5):348–368
13. Davalos D, Grutzendler J, Yang G, Kim JV, Zuo Y, Jung S et al (2005) ATP mediates rapid microglial response to local brain injury in vivo. Nat Neurosci 8(6):752–758
14. Nimmerjahn A, Kirchhoff F, Helmchen F (2005) Resting microglial cells are highly dynamic surveillants of brain parenchyma in vivo. Science 308(5726):1314–1318
15. Fontainhas AM, Wang M, Liang KJ, Chen S, Mettu P, Damani M et al (2011) Microglial morphology and dynamic behavior is regulated by ionotropic glutamatergic and GABAergic neurotransmission. PLoS One 6(1):e15973
16. Lee JE, Liang KJ, Fariss RN, Wong WT (2008) Ex vivo dynamic imaging of retinal microglia using time-lapse confocal microscopy. Invest Ophthalmol Vis Sci 49(9):4169–4176

17. Liang KJ, Lee JE, Wang YD, Ma W, Fontainhas AM, Fariss RN et al (2009) Regulation of dynamic behavior of retinal microglia by CX3CR1 signaling. Invest Ophthalmol Vis Sci 50(9):4444–4451
18. Ransohoff RM, Perry VH (2009) Microglial physiology: unique stimuli, specialized responses. Annu Rev Immunol 27:119–145
19. Kreutzberg GW (1996) Microglia: a sensor for pathological events in the CNS. Trends Neurosci 19(8):312–318
20. Trapp BD, Wujek JR, Criste GA, Jalabi W, Yin X, Kidd GJ et al (2007) Evidence for synaptic stripping by cortical microglia. Glia 55(4):360–368
21. Wake H, Moorhouse AJ, Jinno S, Kohsaka S, Nabekura J (2009) Resting microglia directly monitor the functional state of synapses in vivo and determine the fate of ischemic terminals. J Neurosci 29(13):3974–3980
22. Walton NM, Sutter BM, Laywell ED, Levkoff LH, Kearns SM, Marshall GP 2nd et al (2006) Microglia instruct subventricular zone neurogenesis. Glia 54(8):815–825
23. Elkabes S, DiCicco-Bloom EM, Black IB (1996) Brain microglia/macrophages express neurotrophins that selectively regulate microglial proliferation and function. J Neurosci 16(8):2508–2521
24. Harada T, Harada C, Kohsaka S, Wada E, Yoshida K, Ohno S et al (2002) Microglia-Muller glia cell interactions control neurotrophic factor production during light-induced retinal degeneration. J Neurosci 22(21):9228–9236
25. Bessis A, Bechade C, Bernard D, Roumier A (2007) Microglial control of neuronal death and synaptic properties. Glia 55(3):233–238
26. Roumier A, Pascual O, Bechade C, Wakselman S, Poncer JC, Real E et al (2008) Prenatal activation of microglia induces delayed impairment of glutamatergic synaptic function. PLoS One 3(7):e2595
27. Schafer DP, Lehrman EK, Kautzman AG, Koyama R, Mardinly AR, Yamasaki R et al (2012) Microglia sculpt postnatal neural circuits in an activity and complement-dependent manner. Neuron 74(4):691–705
28. Li Y, Du XF, Liu CS, Wen ZL, Du JL (2012) Reciprocal regulation between resting microglial dynamics and neuronal activity in vivo. Dev Cell 23(6):1189–1202
29. Uckermann O, Wolf A, Kutzera F, Kalisch F, Beck-Sickinger AG, Wiedemann P et al (2006) Glutamate release by neurons evokes a purinergic inhibitory mechanism of osmotic glial cell swelling in the rat retina: activation by neuropeptide Y. J Neurosci Res 83(4):538–550
30. Pankratov Y, Lalo U, Verkhratsky A, North RA (2006) Vesicular release of ATP at central synapses. Pflugers Arch 452(5):589–597
31. Stout CE, Costantin JL, Naus CC, Charles AC (2002) Intercellular calcium signaling in astrocytes via ATP release through connexin hemichannels. J Biol Chem 277(12):10482–10488
32. Dahl G, Locovei S (2006) Pannexin: to gap or not to gap, is that a question? IUBMB Life 58(7):409–419
33. Iglesias R, Dahl G, Qiu F, Spray DC, Scemes E (2009) Pannexin 1: the molecular substrate of astrocyte "hemichannels". J Neurosci 29(21):7092–7097
34. Balasingam V, Dickson K, Brade A, Yong VW (1996) Astrocyte reactivity in neonatal mice: apparent dependence on the presence of reactive microglia/macrophages. Glia 18(1):11–26
35. Graeber MB, Kreutzberg GW (1988) Delayed astrocyte reaction following facial nerve axotomy. J Neurocytol 17(2):209–220
36. Sawada M, Suzumura A, Marunouchi T (1995) Cytokine network in the central nervous system and its roles in growth and differentiation of glial and neuronal cells. Int J Dev Neurosci 13(3–4):253–264
37. Wang M, Ma W, Zhao L, Fariss RN, Wong WT (2011) Adaptive Muller cell responses to microglial activation mediate neuroprotection and coordinate inflammation in the retina. J Neuroinflammation 8:173

# Chapter 43
# Isolation and Ex Vivo Characterization of the Immunophenotype and Function of Microglia/ Macrophage Populations in Normal Dog Retina

**Sem Genini, William A. Beltran, Veronika M. Stein and Gustavo D. Aguirre**

**Abstract** Microglia are the primary resident immune cells of the retina and are involved in the pathogenesis of various retinal diseases. In this study, we optimized experimental conditions to isolate microglia from canine retinas and characterized ex vivo their immunophenotype and function using flow cytometry (FACS). The most suitable protocol included a mechanical dissociation of the retina and an enzymatic digestion using DNAse and collagenase. Extraction was carried out by density gradient centrifugation, and retinal microglia accumulated on distinct interfaces of 1.072 and 1.088 g/mL of a Percoll gradient. Immunophenotypical characterization was performed with monoclonal antibodies CD11b, CD11c, CD18, CD45, CD44, B7-1 (CD80), B7-2 (CD86), CD1c, ICAM-1 (CD54), CD14, MHCI, MHCII, CD68, CD3, CD4, CD8α, and CD21. The most prevalent microglia population in the normal canine retina is $CD11b^{high}CD45^{low}$. Functionally, retinal microglia exhibited phagocytosis and reactive oxygen species (ROS) generation activities. To conclude, ex vivo examinations of retinal microglia are feasible and possibly reflect the in vivo conditions, avoiding artifacts observed in tissue culture. The established method will be relevant to examine microglia from diseased canine retinas in order to elucidate their roles in degenerative processes.

S. Genini (✉) · W. A. Beltran · G. D. Aguirre
Department of Clinical Studies, School of Veterinary Medicine,
University of Pennsylvania, 3900 Delancey Street, Philadelphia, PA 19104, USA
e-mail: geninis@vet.upenn.edu

W. A. Beltran
e-mail: wbeltran@vet.upenn.edu

V. M. Stein
Department of Small Animal Medicine and Surgery, University of Veterinary Medicine
Hannover, 30559, Hannover, Germany
e-mail: veronika.stein@tiho-hannover.de

G. D. Aguirre
e-mail: gda@vet.upenn.edu

J. D. Ash et al. (eds.), *Retinal Degenerative Diseases,* Advances in Experimental Medicine and Biology 801, DOI 10.1007/978-1-4614-3209-8_43,

**Keywords** Dog model · Retinal microglia · Density percoll gradient extraction · Ex vivo examination · Flow cytometry (FACS) analysis · Immunophenotype characterization · Phagocytosis assay · Reactive oxygen species (ROS) generation test

**Abbreviations**

| | |
|---|---|
| FACS | Flow cytometry |
| ROS | Reactive oxygen species |
| CNS | Central nervous system |
| FSC-H | Parameter size, forward scatter |
| SSC-H | Parameter complexity, side scatter |
| PMA | Phorbol-12-myristate-13-acetate |
| DHR | Dihydrorhodamine |

## 43.1 Introduction

Microglia are important resident immune cells of the retina and central nervous system (CNS). They are particularly sensitive to changes in the surrounding environment, becoming readily activated in host response to infection or injury [1]. Microglia occur in different isoforms and respond to pathological events by progressing from a resting ramified state to an active state with retraction of processes [2]. In retina, these active sentinels have essential roles in controlling development, aging, and function by secreting growth factors and inflammatory cytokines to promote either neuroprotection or neuronal damage. They also have been implicated in the pathogenesis of various retinal diseases [3–5].

Microglia isolation and purification ex vivo is complex; difficulties include contamination with macrophages, a relatively small number of microglia present in tissues, and absence of specific markers differentiating microglia from other blood derived mononuclear cells [6, 7]. However, ex vivo analysis has the great advantage to more closely reflect in vivo conditions compared to results obtained using cell culture systems. Previous studies established microglia isolation protocols in mouse [6] and rat [8] CNS, canine spinal cord [9], and canine brain that was either normal [7] or infected with canine distemper virus [10]. Retinal microglia have been isolated and characterized in humans [11] and rats [12] using Percoll density gradient centrifugation and FACS analysis, but these experimental tools have not yet been applied to dog retinas.

With the goal of characterizing microglia immunophenotypes and function in different retinal diseases, we have developed a protocol for ex vivo isolation of microglia from canine retinas.

## 43.2 Materials and Methods

### *43.2.1 Dogs*

Normal retinas from mixed-breed dogs were examined to define optimal experimental conditions for microglia isolation and characterization. The ages were 7 (dog #1, female), 20 (dog #2, female), 25 (dog #3, female), and 35 weeks (dog #4 and #5, males). The research was conducted in full compliance with the ARVO Statement for the Use of Animals in Ophthalmic and Vision Research.

### *43.2.2 Ex Vivo Isolation of Canine Retinal Microglia*

Following an optimized protocol developed for brain [7], dogs were given 12,000 units of heparin intravenously and euthanized by pentobarbital overdose. Immediately after death, perfusion was performed with 1 L of normal saline solution via left ventricle of the heart. Sufficient perfusion was indicated by water-like fluid leaving the right atrium and the absence of blood in the retinal veins, as assessed by indirect ophthalmic examination. Following perfusion, eyes were removed and both neuroretinas separated and pooled. After mincing through a stainless-steel sieve, mechanically dissociated cells were centrifuged and then enzymatically digested for 30 min at 37 °C with type II collagenase (5.7 mg/g retina; Roche Diagnostics) and DNAse I (500 units/g retina; Sigma-Aldrich). A Percoll gradient was established in a 15 mL Falcon tube with 2 mL of Percoll (GE-Amersham Biosciences) diluted in Hanks' buffer at 1.124 g/mL, subsequently overlayed with 2 mL Percoll of 1.088 g/mL, 2 mL of 1.072 g/mL, and finally 2 mL of 1.030 g/mL containing the cell solution. After centrifugation microglia were collected from the interfaces of the 1.072 (majority of cells) and 1.088 g/mL (less cells) layers. Microglia were adjusted to a concentration of $2 \times 10^5$ cells in 50 mL, immunostained, and analyzed immediately by FACS.

The above-described protocol was applied for dog #1, while for dogs #2 and #3 neither perfusion nor DNAse and collagenase digestion were performed. The cells of dogs #4 and #5 were isolated using two successive Percoll gradients as previously done for microglia isolation from rats [8] and dogs [7, 9]; an initial gradient consisting of two densities and a major gradient with five densities, including an additional density of 1.060 g/mL. Microglia from dog #5 were collected separately from Percoll densities 1.060 and 1.072 g/mL and, as the number of cells was lower, no functional analyses were performed.

### *43.2.3 Monoclonal Antibodies (mAb) and Immunophenotyping*

Microglia characterization was performed with mAbs binding the epitopes B7–1 (CD80), B7-2 (CD86), CD11b, CD11c, CD18, CD1c, ICAM-1, CD3, CD4, CD8α,

CD21, and MHC class II (dilution 1:5; Leukocyte Antigen Biology Laboratory, University of California, Davis), CD14 (1:10; Dako), CD44 (1:10; Serotec), CD45 (1:10; Serotec), MHC class I (1:20; Veterinary Medical Research & Development), and CD68 (1:10; Santa Cruz Biotechnology). Secondary antibodies (dilution 1:100) were goat anti-mouse (Jackson Immuno Research Laboratories), rabbit anti-rat (Serotec) for CD44, and streptavidin-conjugated fluorescein-isothiocyanate (Serotec) for CD45. Cell preparations with secondary Abs only served as negative controls. Cells were measured immediately after incubation and washing using a FACSCalibur™ (BD Biosciences) flow cytometer and analyzed with the CellQuest™ software. Microglia were identified based on the parameters size (FSC), complexity (SSC), and relative expression of $CD11b^{high}$ and $CD45^{low}$, as previously shown [6, 11, 12].

### *43.2.4 Phagocytosis Assay*

Directly FITC-labeled *Staphylococcus aureus* (Life Technologies) were suspended in PBS, adjusted to a concentration of $10^8$ bacteria/mL, and incubated with either PBS (non-opsonized bacteria) or pooled dog serum (opsonized bacteria). Non-opsonized and opsonized bacteria suspensions were added to the microglia (1:100) and incubated for 60 min at 37 °C and 5 % $CO_2$ [7]. PBS served as negative control. Phagocytosis was measured immediately using a FACSCalibur™ flow cytometer.

### *43.2.5 Generation Test*

Production of reactive oxygen species (ROS) by microglia was measured as previously described [7, 10]. Briefly, $2 \times 10^6$ microglia/mL were stimulated with either PBS or phorbol-12-myristate-13-acetate (PMA; Sigma-Aldrich), followed by 15 µg/mL dihydrorhodamine (DHR) 123 (Marker Gene Technologies Inc.). A tube containing only microglia was used as negative reference. ROS generation was measured immediately using a FACSCalibur™ flow cytometer.

## 43.3 Results

We developed a protocol for ex vivo analysis of canine retinal microglia based on previous reports for brain and spinal cord [7, 9]. Five young dogs were examined and retinal cells collected under slightly different conditions to achieve the highest purified microglia populations. Retinal microglia showed a characteristic immunophenotype of $CD11b^{high}CD45^{low}$ (Fig. 43.1a). In normal dogs, retinal microglia represented a population of relatively small cells with low complexity (Fig. 43.1b, gate R1). All 17 surface markers could be detected in the microglia of the 5 dogs;

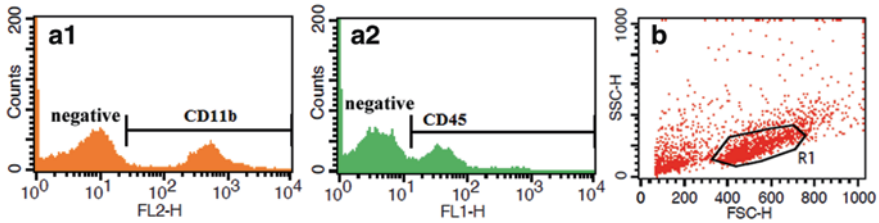


**Fig. 43.1** Retinal microglia have a characteristic immunophenotype of CD11b$^{high}$CD45$^{low}$. The histograms show expression intensities (mean fluorescent channel numbers) of *CD11b* (**a1**) and *CD45* (**a2**) measured in two fluorescence channels (*FL-H*) compared to negative controls. **b** The isolated retinal microglia form a population of relatively small cells (forward scatter, *FSC-H*) with low complexity (side scatter, *SSC-H*). Only cells within the gate R1 were further analyzed

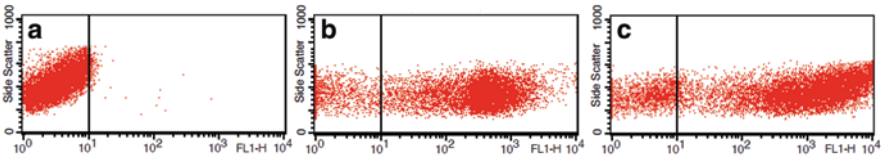


**Fig. 43.2** Retinal microglial phagocytosis after incubation with **a** PBS (negative control), **b** non-opsonized, and **c** opsonized FITC-labeled *S. aureus*. The x-axis shows fluorescence intensity and the y-axis cell complexity

the percentage of positive cells is presented in Table 43.1. Dogs #1–3 showed low contamination of the retinal microglia cell yield with lymphocytes (cells positive to CD3, CD4, or CD21 < 2.4 %), while dogs #4 and #5 (density 1.060) showed low expression of the microglia markers and high expression of the lymphocyte markers.

Phagocytosis assay and ROS generation test were performed in dogs #1–4. As duplicates showed high consistency, the median was used for analysis. Canine retinal microglia performed phagocytosis after adding both, opsonized ($\bar{x}$ = 64 %) and non-opsonized ($\bar{x}$ = 60 %) *S. aureus* (Fig. 43.2). In all dogs, the percentage of phagocytosing microglia increased with opsonized compared to non-opsonized bacteria.

ROS generation test demonstrated that canine retinal microglia were able to produce ROS. However, no increase in intensity and percentage of ROS generating microglia was noted after addition of PMA compared to PBS.

## 43.4 Discussion and Conclusions

In the present study, we developed an ex vivo extraction protocol to examine the microglia cell population from dog retinas. A total of 13 different markers known to be expressed on microglia (CD11b, CD11c, CD18, CD45, CD44, B7-1, B7-2, CD1c, ICAM-1, CD14, MHCI, MHCII, CD68) were analyzed by FACS. Additionally,

**Table 43.1** Retinal microglia expression (in percentage) of 14 microglia and 3 (CD3, CD4, CD21) lymphocyte surface molecules. Values of 5 normal dogs are shown; in dog #5 cells were collected from Percoll densities 1.060[a] and 1.072[b] g/mL and evaluated separately

| | Dog | | | | | | |
|---|---|---|---|---|---|---|---|
| Antibody | #1 | #2 | #3 | #4 | #5[a] | #5[b] | Mean |
| CD11b | 7.3 | 24.5 | 11.5 | 3.1 | 6.6 | 18.5 | 11.9 |
| CD11c | 6.8 | 23.3 | 12.7 | 2.4 | 6.7 | 39 | 15.2 |
| CD18 | 10.8 | 26.5 | 24.9 | 3.2 | 3 | 26.9 | 15.9 |
| CD45 | 6.9 | 3 | 8.1 | 1.5 | 4.5 | 26.7 | 8.5 |
| CD44 | 55.8 | 69.6 | 93.4 | 47.8 | 70.8 | 52.4 | 65 |
| B7–1 | 11.6 | 30.8 | 10 | 5.9 | 3.7 | 13 | 12.5 |
| B7-2 | 13.0 | 6.9 | 8.9 | 4.6 | 3.8 | 23.3 | 10.1 |
| CD1c | 31.5 | 37.3 | 9.7 | 3.7 | 3.9 | 33.5 | 19.9 |
| ICAM-1 | 34.2 | 39.3 | 33.2 | 6.5 | 2.7 | 36.4 | 25.4 |
| CD14 | 24.5 | 19.1 | 11.6 | 1.8 | 3 | 27.4 | 14.6 |
| MHCI | 67.1 | 12.6 | 24.2 | 33 | 23.8 | 35.1 | 32.6 |
| MHCII | 9.1 | 32.1 | 23.2 | 3.8 | 2 | 26.1 | 16.1 |
| CD68 | 3.3 | 0.3 | 1.9 | 2.3 | 1.9 | 17.8 | 4.6 |
| CD8α | 7.4 | 21.2 | 31.5 | 1.8 | 4.9 | 25 | 15.3 |
| CD3 | 0.6 | 1.4 | 0.9 | 2.6 | 5.6 | 1.3 | 2.1 |
| CD4 | 1.1 | 1.1 | 1.4 | 2.2 | 19.1 | 1.7 | 4.4 |
| CD21 | 1.3 | 0.8 | 2.5 | 1.7 | 5.6 | 2.2 | 2.4 |

CD3, CD4, CD21, and CD8α were tested to verify contamination with lymphocytes although CD8α has been shown to also be expressed by mouse microglia [13, 14]. Our data showed CD8α-positive microglia and suggested that this marker is present in canine retinal microglia.

The use of two successive Percoll gradients (dogs #4 and #5) considerably decreased the number of isolated microglia and did not result in an increased purity of the cell yield. Isolation of microglia from canine brain and spinal cord required an initial gradient in particular to remove myelin [7, 9]. As the mammalian retina is devoid of oligodendrocytes and the axons of retinal ganglion cells are not myelinated where they course through the retina, an initial gradient was not necessary. Cells from the Percoll densities 1.088 and 1.072 g/mL were highly positive to microglia markers, while cells from other interfaces (i.e. 1.060 of dog #5) were predominantly lymphocytes.

Based on these results, the optimal experimental conditions for microglia extraction and testing ex vivo seem to include perfusion, mechanical dissociation and enzymatic (DNAse and collagenase) digestion, separation with one Percoll gradient, and collection from the Percoll interfaces 1.072 and 1.088 g/mL.

Functionally, canine retinal microglia from all tested dogs exhibited phagocytosis activities, and had the capability to generate ROS. They could be triggered to ingest *S. aureus* bacteria, but not to produce more ROS with the trigger PMA. ROS generation has also been described in macrophages [15] and brain microglia [7, 10].

This method to analyze microglia ex vivo will be useful in future studies to evaluate and compare the immunophenotype and the function of different microg-

lia populations associated with photoreceptor degeneration in canine models, e.g. rcd1, XLPRA1, XLPRA2, which carry mutations in genes known to cause human inherited blindness. Indeed, this ex vivo method will be valuable in examining the effects of therapeutic strategies on microglia populations, as it might better reflect in vivo conditions compared to tissue cultures, where artifacts are often observed.

**Acknowledgments** This study was supported by NIH Grants EY06855 and EY017549, the Foundation Fighting Blindness (FFB), the Van Sloun Fund for Canine Genetic Research, and Hope for Vision. Many thanks to the National Eye Institute, NIH, for funding a travel award to SG. VMS was supported by the German Research Foundation (STE 1069/2-1).

## References

1. Garden GA, Moller T (2006) Microglia biology in health and disease. J Neuroimmune Pharmacol 1:127–137
2. Kettenmann H (2006) Triggering the brain's pathology sensor. Nat Neurosci 9:1463–1464
3. Langmann T (2007) Microglia activation in retinal degeneration. J Leukoc Biol 81:1345–1351
4. Sasahara M, Otani A, Oishi A, Kojima H, Yodoi Y, Kameda T et al (2008) Activation of bone marrow-derived microglia promotes photoreceptor survival in inherited retinal degeneration. Am J Pathol 172:1693–1703
5. Karlstetter M, Ebert S, Langmann T (2010) Microglia in the healthy and degenerating retina: insights from novel mouse models. Immunobiology 215:685–691
6. de Haas AH, Boddeke HW, Brouwer N, Biber K (2007) Optimized isolation enables ex vivo analysis of microglia from various central nervous system regions. Glia 55:1374–1384
7. Stein VM, Czub M, Hansen R, Leibold W, Moore PF, Zurbriggen A et al (2004) Characterization of canine microglial cells isolated ex vivo. Vet Immunol Immunopathol 99:73–85
8. Ford AL, Goodsall AL, Hickey WF, Sedgwick JD (1995) Normal adult ramified microglia separated from other central nervous system macrophages by flow cytometric sorting. Phenotypic differences defined and direct ex vivo antigen presentation to myelin basic protein-reactive CD4+T cells compared. J Immunol 154:4309–4321
9. Ensinger EM, Boekhoff TM, Carlson R, Beineke A, Rohn K, Tipold A et al (2010) Regional topographical differences of canine microglial immunophenotype and function in the healthy spinal cord. J Neuroimmunol 227:144–152
10. Stein VM, Czub M, Schreiner N, Moore PF, Vandevelde M, Zurbriggen A et al (2004) Microglial cell activation in demyelinating canine distemper lesions. J Neuroimmunol 153:122–131
11. Broderick C, Duncan L, Taylor N, Dick AD (2000) IFN-gamma and LPS-mediated IL-10-dependent suppression of retinal microglial activation. Invest Ophthalmol Vis Sci 41:2613–2622
12. Dick AD, Ford AL, Forrester JV, Sedgwick JD (1995) Flow cytometric identification of a minority population of MHC class II positive cells in the normal rat retina distinct from CD45lowCD11b/c+CD4low parenchymal microglia. Br J Ophthalmol 79:834–840
13. Gregerson DS, Yang J (2003) CD45-positive cells of the retina and their responsiveness to in vivo and in vitro treatment with IFN-gamma or anti-CD40. Invest Ophthalmol Vis Sci 44:3083–3093
14. Dimayuga FO, Reed JL, Carnero GA, Wang C, Dimayuga ER, Dimayuga VM et al (2005) Estrogen and brain inflammation: effects on microglial expression of MHC, costimulatory molecules and cytokines. J Neuroimmunol 161:123–136
15. Tipold A, Zurbriggen A, Moore P, Schijns V, Jungi TW (1998) Generation and functional characterisation of canine bone marrow-derived macrophages. Res Vet Sci 64:125–132

# Chapter 44
# Müller Cells and Microglia of the Mouse Eye React Throughout the Entire Retina in Response to the Procedure of an Intravitreal Injection

**Roswitha Seitz and Ernst R. Tamm**

**Abstract** The animal model of N-methyl-D-aspartate (NMDA)-induced excitotoxic damage of retinal ganglion cells (RGC) is widely used to study the molecular mechanisms of RGC death and/or its prevention by neuroprotective agents. NMDA is typically applied by intravitreal injection, while contralateral control eyes are treated by the injection of PBS as vehicle. Herein we report that the procedure of an intravitreal injection alone is sufficient to cause substantial reactive changes in Müller cells and microglia throughout the entire retina. Six week old CD1 mice received a single intravitreal injection of PBS or NMDA. Immunohistochemistry showed the presence of reactive microglia and Müller cells in both NMDA- and PBS-treated eyes during the first 24 h after injection. After 7 days, the reactive changes were only present in NMDA-injected eyes, but no longer in PBS-treated eyes. Investigators using intravitreal injections in the mouse eye should be aware that vehicle-injected control eyes will undergo phenotypic changes in microglia and Müller glia, and are likely to behave differently in their biology when compared with uninjected eyes, at least within the first 24 h after experiment.

**Keywords** NMDA · Intravitreal injection · Müller cell gliosis · Microglia activation

## 44.1 Introduction

The animal model of N-methyl-D-aspartate (NMDA)-induced excitotoxic damage of retinal ganglion cells (RGC) is widely used to study the molecular mechanisms of RGC death and/or its prevention by neuroprotective agents [1, 2]. NMDA is typically applied by an intravitreal injection of experimental eyes while contralateral

E. R. Tamm (✉) · R. Seitz
Institute of Human Anatomy and Embryology, University of Regensburg, Universitätsstr. 31, 93053 Regensburg, Germany
e-mail: ernst.tamm@vkl.uni-regensburg.de

J. D. Ash et al. (eds.), *Retinal Degenerative Diseases,* Advances in Experimental Medicine and Biology 801, DOI 10.1007/978-1-4614-3209-8_44,

control eyes are treated by the injection of PBS as vehicle at the same volume. Herein we report that the procedure of an intravitreal injection alone is sufficient to cause substantial reactive changes in Müller cells and microglia throughout the entire retina of vehicle-injected eyes.

## 44.2 Materials and Methods

All procedures in this study conformed to the National Institutes of Health Guidelines on the Care and Use of Animals in Research and the ARVO Statement for the Use of Animals in Ophthalmic and Vision Research. All experiments were at least repeated independently three times.

NMDA-mediated retinal damage was induced as reported previously [1, 2]. Briefly, adult CD1 mice were anesthetized with isoflurane and the ocular surface was disinfected by an iodine tincture. To induce retinal damage, 3 µl of NMDA (10 mM dissolved in PBS; Sigma) were injected via the ora serrata into the vitreous body of one eye while the fellow eye was treated with PBS alone. Other experimental groups included injection of 3 µl PBS in one eye whereas the fellow eye was left untouched. Mice were sacrificed 3 h to 1 week after injection and perfused with 4% paraformaldehyde (PFA) via the heart. Eyes were removed, opened at the cornea and immersed in PFA (whole mounts: 20 min, sections: 4 h). For cryosections, eyes were embedded in Tissue Tec (Sakura) and stored at −20 °C until sectioning. For retinal whole mounts eyes were transferred to PBS and retinae were dissected carefully, spread and transferred to a 96-well plate.

For immunohistochemistry, whole mounts or sections were incubated with 50 mM $NH_4Cl$ for 30 min to reduce autofluorescence. After samples were permeabilized with 0.5% Triton-X-100 for 5 min (sections) or 30 min (whole mounts) they were incubated in 1% bovine serum albumin (BSA) and 2% donkey serum for 60 min. Then sections and whole mounts were incubated overnight at 4 °C with primary antibodies (rabbit anti-Iba-1 antibodies; Wako or rabbit anti-GFAP; Dako). After three washes with PBS, samples were treated for 60 min with Cy3-labeled donkey anti-rabbit antibodies (Jackson ImmunoResearch) or Alexa 488 Fluor-labeled goat-anti-rabbit antibodies (Invitrogen). Then samples were incubated with 1:100 DAPI (Vector Laboratories). After three additional washes, sections and whole mounts were mounted in fluorescent mounting medium and analyzed on an Axiovision fluorescent microscope with apotome (Carl Zeiss).

For Western blot analyses isolated retinae were homogenized in RIPA buffer. After insoluble constituents were removed by centrifugation, up to 20 µg of protein were subjected to a 12% SDS-PAGE and transferred on a PVDF membrane. After blocking with 3% BSA in TBS-T, membranes were incubated overnight with rabbit anti-GFAP antibodies. After washing, membranes were hybridized with HRP-conjugated chicken anti-rabbit antibodies (Invitrogen). For visualization, membranes were incubated in Immobilon HRP substrate (Millipore) and visualized on a LAS 3000 Imager work station (Fujifilm). As loading control, HRP-conjugated anti-GAPDH antibodies were used (Rockland).

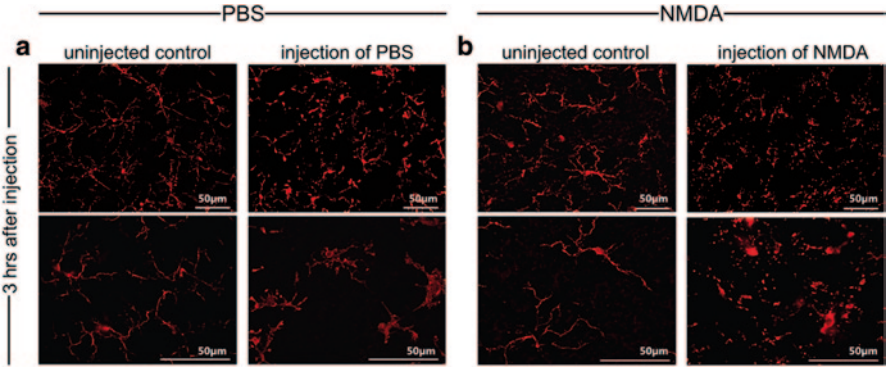


**Fig. 44.1** Staining of microglia with Iba-1 in retinal whole mounts of PBS-injected (**a**) and NMDA-injected (**b**) eyes and respective contralateral, uninjected eyes. *Lower* panels are higher magnifications. In uninjected eyes, ramified microglia cells showing their typical long branching processes and a small cellular body are readily observed. In contrast, 3 h after an intravitreal injection of PBS or NMDA the processes of the microglial cells are considerably thicker and shorter expressing the characteristic phenotype of reactive microglia. Pictures were taken in the GCL/IPL

## 44.3 Results

When retinal whole mounts from uninjected eyes of animals with an intravitreal injection of PBS (Fig. 44.1a) or NMDA (Fig. 44.1b) in their contralateral eye were stained for the microglia marker Iba-1, ramified microglia cells showing their typical long branching processes and a small cellular body were readily observed in the ganglion cell layer and both plexiform layers of the retina (Fig. 44.1a, b). An identical shape of microglia cells was observed in retinal whole mounts of untreated animals (not shown). In contrast 3 h after an intravitreal injection of PBS or NMDA, a complete different phenotype of the retinal microglia in the inner retina was observed throughout the retinal whole mount of injected eyes. The processes of the microglial cells were considerably thicker and shorter expressing the characteristic phenotype of reactive microglia (Fig. 44.1a, b). A quite similar morphology of the microglia was observed in eyes 24 h after PBS or NMDA injection (Fig. 44.2) with notable exception of the retina in immediate vicinity to the optic disc. Here, microglial cells had almost completely rounded up, while cellular processes were largely absent (Fig. 44.2). Neither 3 h nor 24 h following an intravitreal injection, differences in the shape of microglia were observed between PBS- or NMDA-injected eyes (Fig. 44.1, 44.2). Intravitreal injections of PBS or NMDA did not only cause a change in the phenotype of microglial cells, but appeared also to increase their number in the inner retina. This was likely due to their migration from the outer retina to the inner retina, as we readily observed microglial cells in the outer plexiform layer of non-injected control eyes, while they were only rarely present at this location in retinae 3 h (Fig. 44.3) and 24 h (data not shown) after PBS or NMDA injection.

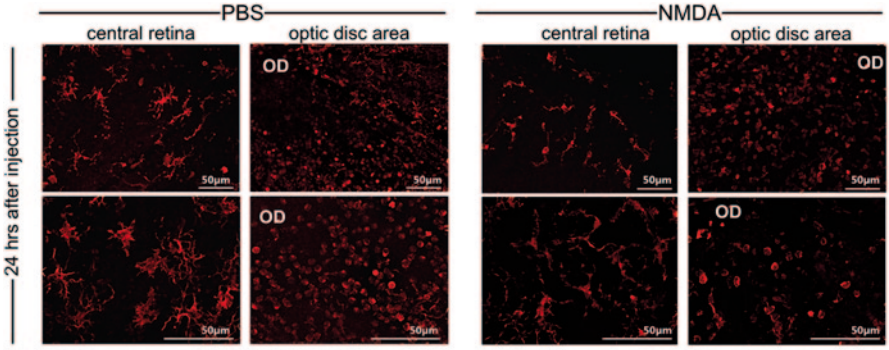


**Fig. 44.2** Staining of microglia with Iba-1 in retinal whole mounts 24 h after injection of PBS or NMDA. Lower panel shows higher magnification. In the central retina of both whole mounts, microglia shows a similar reactive phenotype as seen 3 h after injection. In contrast in close proximity to the optic disc (*OD*), microglial cells have almost completely rounded up, while cellular processes were largely absent. *OD* marks position of the optic disc. Pictures were taken in the GCL/IPL

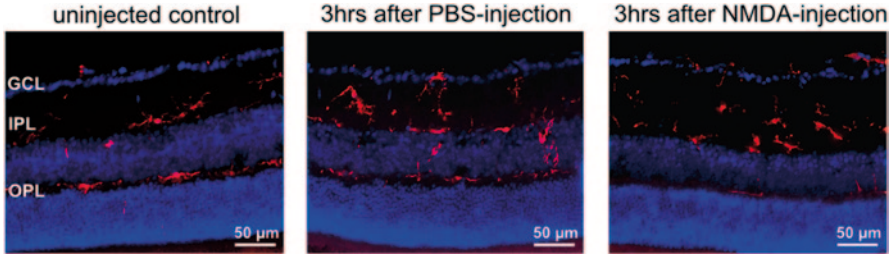


**Fig. 44.3** Immunostaining for Iba-1 in sections through the central retina of an uninjected control eye and of eyes 3 h after intravitreal injection of PBS or NMDA. In the untreated retina, most microglia cells are localized in the outer (*OPL*) and inner plexiform layers (*IPL*) and in the ganglion cell layer (*GCL*). 24 h after PBS or NMDA injection, the number of microglia cells in the *OPL* is markedly decreased. Nuclear DNA is stained with DAPI

We next investigated, if the changes in microglia occurred in parallel to changes in macroglia. To this end, we labeled retinal whole mounts for GFAP. In uninjected control eyes, we observed a dense network of astrocytes on the retinal surface (Fig. 44.4). In eyes 3 h after an intravitreal injection of PBS or NMDA, an additional immunoreactivity showing GFAP-labeled dots was regularly observed in the holes between the GFAP-positive astrocytes (Fig. 44.4). A three-dimensional view showed that GFAP labeling reached now at least 50 µm from the ganglion cell layer towards the outer retina strongly indicating its presence in reactive Müller glia. The induction of GFAP labeling in Müller glia was confirmed by staining sections through the retina. In uninjected control retinae, immunostaining for GFAP was only seen in distinct patches along the retinal surface and corresponding to the astrocyte strands that had been visualized on retinal whole mounts (Fig. 44.5). 3 h

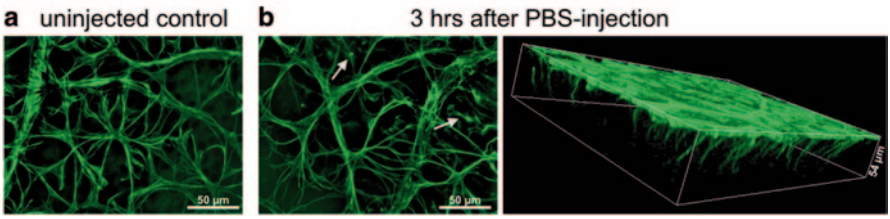


**Fig. 44.4** Immunohistochemistry for GFAP on retinal whole mounts from an uninjected eye, or from an eye 3 h after an intravitreal injection of PBS. In the uninjected control eye, a dense network of astrocytes on the retinal surface is seen. In the injected eye, an additional immunoreactivity showing GFAP-labeled dots is observed in the holes between GFAP-positive astrocytes (*arrows*). A three-dimensional view shows that GFAP labeling reaches now at least 50 µm from the ganglion cell layer towards the outer retina strongly indicating its presence in reactive Müller glia

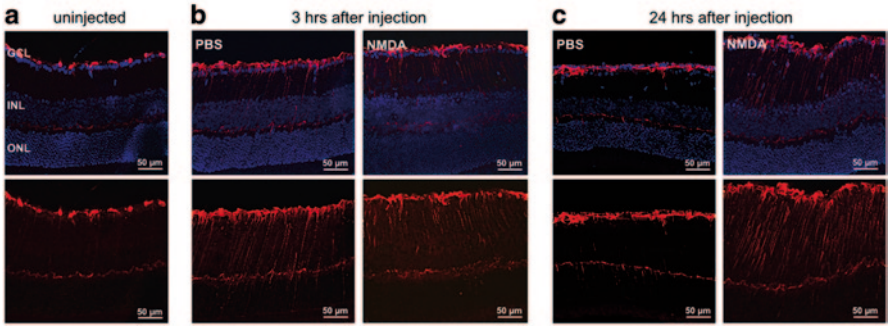


**Fig. 44.5** Immunohistochemistry for GFAP in retinal sections of an uninjected eye and of eyes *3 h* or *24 h* after an intravitreal injection of *PBS* or *NMDA*. In the *uninjected* control retinae, immunostaining for GFAP is only seen in distinct patches along the retinal surface. *3 h* after an intravitreal injection of *PBS* or *NMDA*, an additional radial GFAP-staining typical for Müller cell gliosis is visible. Müller cell immunoreactivity for GFAP is still present 24 h after NMDA injection and, albeit somewhat weaker, after *PBS* injection. Nuclear DNA is stained with DAPI

after an intravitreal injection of PBS or NMDA, an additional radial GFAP-staining typical for Müller cell gliosis became visible. Müller cell immunoreactivity for GFAP was still present 24 h after NMDA injection, and, albeit somewhat weaker, after PBS injection.

When retinal whole mounts were stained for Iba-1 one week after an intravitreal injection of PBS into the eye, only microglia with an immunologically quiescent ramified morphology was observed throughout the entire retina (Fig. 44.6a). In contrast, microglia in NMDA-injected eyes still expressed a reactive phenotype (Fig. 44.6a). In addition, radial staining of Müller glia was only detectable in NMDA-injected eyes, but not in those injected with PBS (Fig. 44.6b). Moreover, Western blot analyses of retinal proteins showed that the amounts of GFAP in retinal proteins, which were elevated 24 h after injection of PBS, had returned after 1 week to levels comparable to that seen in untouched eyes.

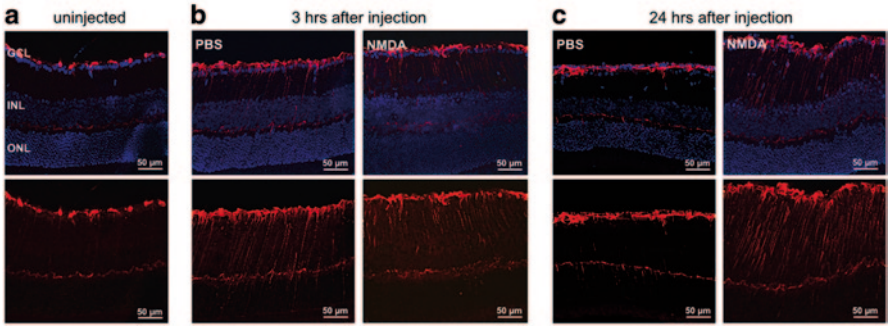


**Fig. 44.6** Immunohistochemistry for Iba-1 (**a**) or GFAP (**b**) in retinal whole mounts (**a**) and sections (**b**) 7 days after intravitreal injection of PBS or NMDA. Ramified microglia is present 7 days after *PBS*-injection, while microglia in NMDA-injected eyes expresses a reactive phenotype (**a**). OD marks position of the optic disc. Pictures were taken in the GCL/IPL. Radial staining of Müller glia is only detectable in NMDA-injected eyes, but not in those injected with PBS (**b**). Nuclear DNA is stained with DAPI. **c** Western Blot analysis for GFAP in retinal proteins of untreated eyes, or eyes 24 h or 7 days after intravitreal injection of PBS

## 44.4 Discussion

Our results show that a single injection of 3 µl PBS into the vitreous body of the mouse eye causes changes in the phenotype of microglia and Müller glia that last at least 24 h. The changes include a switch from ramified to reactive microglia, and gliosis of Müller cells as evidenced by an increase in the amounts of GFAP.

Ramified microglia is typically present in healthy tissue. In contrast, the reactive phenotype is observed following injury or pathology indicating a specific reaction that contributes to the signaling processes of the immune system, which can prevent or augment neuronal degeneration [3]. Quite comparably, gliosis refers to a reactive switch in Müller cell phenotype which is accompanied by the induction of signaling processes that may exert both protective and toxic effects on retinal neurons [4].

Mechanical piercing of ocular tissue with the injection needle in region of the ora serrata may cause or contribute to the glial changes observed in our study. Still, Müller cell gliosis following local injury such as after laser burn has been shown to occur in the immediate vicinity of the site of damage und to spread only slowly [5, 6], while we observed changes throughout the entire retina. A more likely causative factor appears to be stress or strain in the retina caused by the sudden increase in vitreous volume after injection. Astrocytes increase GFAP expression following mechanical tension [7–9] and Müller cells are likely to behave similarly. In addition, shape changes of murine microglia induced via stretch-activated ion channels have been shown [10]. Moreover, polymodal transient receptor potential vanilloid 4 (TRPV4) cation channels known to mediate mechanotransduction have been shown to be present and active on Müller glia and retinal ganglion cell perikarya, dendrites and axons in the mouse retina [11]. Our observation that changes in microglia were most pronounced around the optic disc is consistent with the assumption that stress

or strain induced by the sudden increase in vitreous volume and intraocular pressure are causative factors. In contrast to the optic disc of other species including the human, the mouse optic disc is only supported by astrocytes while a fibrillary extracellular matrix is missing [12].

Investigators using intravitreal injections in the mouse eye should be aware of the fact that vehicle-injected control eyes will undergo phenotypic changes in microglia and Müller glia, and are likely to behave differently in their biology from uninjected eyes, at least within the first 24 h after the experiment.

## References

1. Seitz R et al (2010) Norrin mediates neuroprotective effects on retinal ganglion cells via activation of the Wnt/beta-catenin signaling pathway and the induction of neuroprotective growth factors in Muller cells. J Neurosci 30(17):5998–6010
2. Seitz R, Tamm ER (2013) N-methyl-D-aspartate (NMDA)-mediated excitotoxic damage: a mouse model of acute retinal ganglion cell damage. Methods Mol Biol 935:99–109
3. Boche D, Perry VH, Nicoll JA (2012) Activation patterns of microglia and their identification in the human brain. Neuropathol Appl Neurobiol 39(1):3–18
4. Bringmann A, Wiedemann P (2012) Muller glial cells in retinal disease. Ophthalmologica 227(1):1–19
5. Humphrey MF et al (1993) A quantitative study of the lateral spread of Muller cell responses to retinal lesions in the rabbit. J Comp Neurol 334(4):545–558
6. Tackenberg MA et al (2009) Muller cell activation, proliferation and migration following laser injury. Mol Vis 15:1886–1896
7. Floyd CL et al (2004) Antagonism of group I metabotropic glutamate receptors and PLC attenuates increases in inositol trisphosphate and reduces reactive gliosis in strain-injured astrocytes. J Neurotrauma 21(2):205–216
8. Karumbaiah L et al (2012) The upregulation of specific interleukin (IL) receptor antagonists and paradoxical enhancement of neuronal apoptosis due to electrode induced strain and brain micromotion. Biomaterials 33(26):5983–5996
9. Miller WJ et al (2009) Mechanically induced reactive gliosis causes ATP-mediated alterations in astrocyte stiffness. J Neurotrauma 26(5):789–797
10. Eder C, Klee R, Heinemann U (1998) Involvement of stretch-activated Cl- channels in ramification of murine microglia. J Neurosci 18(18):7127–7137
11. Ryskamp DA et al (2011) The polymodal ion channel transient receptor potential vanilloid 4 modulates calcium flux, spiking rate, and apoptosis of mouse retinal ganglion cells. J Neurosci 31(19):7089–7101
12. Sun D et al (2009) The morphology and spatial arrangement of astrocytes in the optic nerve head of the mouse. J Comp Neurol 516(1):1–19

# Chapter 45
# Subretinal Infiltration of Monocyte Derived Cells and Complement Misregulation in Mice with AMD-Like Pathology

**Joseph Fogerty and Joseph C. Besharse**

**Abstract** We have characterized a naturally-occurring mutation in mice that causes slow, progressive photoreceptor degeneration, white fundus flecks, and late-onset RPE atrophy. These animals predictably lose visual function as photoreceptors degenerate. Genetic studies identified a deletion in the 5' coding sequence of *Mfrp*, designated $Mfrp^{174delG}$, which essentially results in a complete knockout at the protein level. We have shown in $Mfrp^{174delG}$ mice that these white fundus flecks are due to the presence of F4/80+ inflammatory cells in the subretinal space. Here we expand on our initial description of the cells with additional markers and by determining their origin. We have also begun an analysis of complement factors in the RPE and found decreased levels of C3d, suggesting that the alternative complement pathway may be misregulated. Finally, we compare and contrast the characteristics of fundus images in $Mfrp^{174delG}$ mice with those of other mutations that cause similar irregularities, including $Crb1^{rd8}$ and *RDH5,* and discuss the structural differences that may underlie them.

**Keywords** AMD · Macular degeneration · Fundus albipunctatus · Geographic atrophy · Complement · Macrophage · Microglia

## 45.1 Introduction

We have previously described a novel mutation in mouse *Mfrp* that results in AMD-like symptoms [1]. These animals have a dramatic, late-onset RPE degeneration phenotype that looks similar to human geographic atrophy. Although mice do

J. C. Besharse (✉) · J. Fogerty
Department of Cell Biology, Neurobiology, and Anatomy,
Medical College of Wisconsin, Milwaukee, WI, 53226 USA
e-mail: jbeshars@mcw.edu

J. Fogerty
e-mail: jfogerty@mcw.edu

J. D. Ash et al. (eds.), *Retinal Degenerative Diseases,* Advances in Experimental Medicine and Biology 801, DOI 10.1007/978-1-4614-3209-8_45,

not have a macula, it is possible that the patchwork atrophy that we reported in *Mfrp*$^{174delG}$ mutants simulates similar loss of RPE in humans and that these animals could provide an attractive model.

An additional feature of *Mfrp*$^{174delG}$ mice is a regular array of white retinal flecks that is seen in fundus images during the period of photoreceptor loss [1]. Our earlier work established that these white flecks were likely macrophages infiltrating the subretinal space. We expand on that analysis here by showing that the white flecks represent individual cells that express several markers indicative of a macrophage/monocyte lineage and further show in bone marrow chimeras that these macrophages are derived from circulating monocytes. We also report on an initial analysis of key complement regulators and discuss possible contributions this pathway may make to disease progression. Finally, we compare and contrast the "white fleck" phenotype seen in *Mfrp*$^{174delG}$ mice with fundus abnormalities seen in *Crb1*$^{rd8}$ mice, and discuss the possible structural basis for these observations.

## 45.2 Materials and Methods

### *45.2.1 Imaging and Image Analysis*

Animals were killed with $CO_2$ and eyes were dissected under a Leica MZFLIII microscope. The cornea and lens were removed with fine scissors and the retina was gently peeled away. The remaining eyecup was then fixed in PBS containing 4% paraformaldehyde. Images of the apical RPE surface were collected with a digital camera that was mounted on the dissecting microscope. The tissue was then stained with Hoescht, flat mounted under a coverslip, and nuclei from subretinal cells adherent to the apical RPE were imaged with a Nikon TE300 microscope and a Coolsnap HQ camera. The coordinates of each spot (in the dissecting scope image) or nucleus (in the fluorescence image) were determined, and the average nearest neighbor distance was calculated from each image. Fundus images were taken as described previously [1].

### *45.2.2 Immunohistochemistry*

Antibodies used were as follows: GFP (Torrey Pines, 1:250), Cd11b-FITC (Life Technologies, 1:250), CD68 (Millipore, 1:100), Iba1 (Wako, 1:1000), GS-IB4-488 (Life Technologies, 1:50). Fixed eyecups (see above) were permeabilized in PBS + 0.1% Triton X-100 for 2 min, blocked 1 h in PBS + 1% BSA, and incubated in the appropriate antibody overnight at 4°C. Tissue was then washed three times in PBS, incubated 30 min in the appropriate Alexa-488-conjugated secondary antibody, and counterstained with Hoescht (see above). The autofluorescence signal was collected using a long-pass rhodamine filter set. For analysis of C3d, eyecups were fixed in

2% paraformaldehyde, soaked in 50% sucrose, and embedded in OCT. 10um sections were permeabilized, blocked as above and probed with C3d antibody (R&D Systems, 1:100).

### *45.2.3 Bone Marrow Transplant*

ROSA26-YFP reporter mice [2] were bred to EIIa-Cre [3] mice to create a line of YFP+ mice ubiquitously expressing YFP. Bone marrow from these animals was then transplanted into lethally irradiated weanling *Mfrp*$^{174delG}$mice. The resulting bone marrow chimeras were then examined 8 weeks later (3 months of age) when the subretinal cells in significant numbers are first apparent in fundus images. Cells were immunostained and viewed in whole mounts using a GFP antibody (see above). Morphometry was performed as described [1].

### *45.2.4 Immunoblotting*

RPE-choroid was scraped off of eyecups (see above), sonicated directly in Laemmli buffer and western blotted using CFH and CFB antibodies (Quidel, each at 1:5000). Blots were visualized and quantitatively analyzed relative to endogenous actin with a Li-Cor Odyssey infrared detection system.

## 45.3 Results

### *45.3.1 White Spots Seen in Fundus Images of Mfrp$^{174delG}$ Mice Represent Cells in the Subretinal Space*

It has been noted previously that *Mfrp*$^{174delG}$ mice exhibit white flecks visible by fundus imaging that correspond to cells in the subretinal space [1, 4–5]. A *Mfrp*$^{174delG}$ mouse in which retinal flecks were observed by fundus photography was used to test that conclusion with more deliberate measurements. The retina was removed from the eyecup and the white spots on the RPE were directly imaged (Fig. 45.1a), and the mean distance from each spot to its nearest neighbor was determined to be 44.5 mm (±14.5 mm). The same specimen was then flattened, stained with Hoescht and imaged by fluorescence microscopy (Fig. 45.1b). The difference in focal plane between the subretinal cells and the underlying RPE, combined with the dense pigmentation of the RPE, allowed us to easily distinguish the nuclei of the two cell populations. The nearest-neighbor distance for the Hoescht-stained subretinal cells was 47.4 mm (±12.5 mm). These data are consistent with the conclusion that the white spots correspond one to one with subretinal cells.

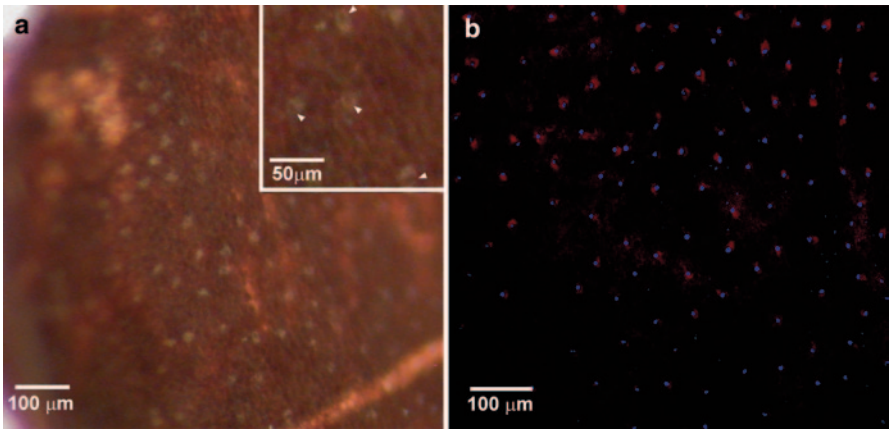


**Fig. 45.1** Correlation of fundus spots with cells in the subretinal space. **a** White spots were imaged under a dissecting microscope. Many of these spots had "holes" in their center, suggestive of a nucleus (*arrows*, *insert*). **b** The same piece of tissue was stained with Hoescht and flat mounted (*blue*= nuclei, *red* = autofluorescence)

### *45.3.2 Subretinal Cells Express Markers Characteristic of Macrophages and are Derived Directly from Circulating Monocytes*

To further phenotype the subretinal cells, we immunostained them for markers of monocyte-derived cells including Iba1, CD11b, CD68 (ED-1), and the lectin GS-IB4 [6–7] in separate preparations. Iba1, CD11b, and CD68 antibodies labeled all of the subretinal cells in their respective preparations, while GS-IB4 labeled only a subset of them (Fig. 45.2). We identified the origin of the subretinal macrophages by making bone marrow chimeras with YFP+ donor cells. Out of 8 $Mfrp^{174delG}$ bone marrow chimeras examined in detail, the subretinal macrophages were overwhelmingly YFP+ (Fig. 45.3a–b) and therefore derived from donor's bone marrow. Only a single subretinal cell among hundreds examined was not unequivocally YFP+. Furthermore, the chimeric animals, which had $Mfrp^{+/+}$ subretinal macrophages, did not exhibit any change in degree of retinal degeneration when compared to age-matched, unaltered $Mfrp^{174delG}$ mice (Fig. 45.3c), suggesting that the $Mfrp^{174delG}$ monocyte-derived cells are not primarily responsible for photoreceptor loss.

### *45.3.3 Evidence of Depressed Activity of the Alternative Complement Pathway*

Since it is widely hypothesized that the complement system is involved in AMD pathogenesis, we evaluated two candidate components of the alternative complement pathway. Western blotting of mouse RPE+choroid in weanling animals

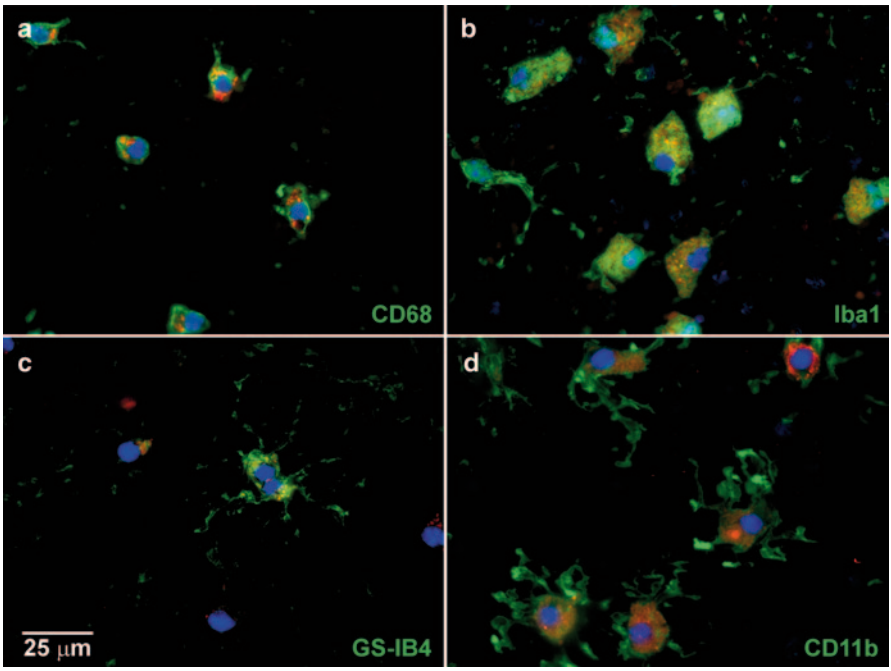


**Fig. 45.2** Immunostaining with markers of monocyte-derived cells. Subretinal cells in whole mounts all stained positive for markers of monocyte derived cells including *CD11b*, *Iba1*, and *CD68*. A fraction of the cells were also *GS-IB4* +

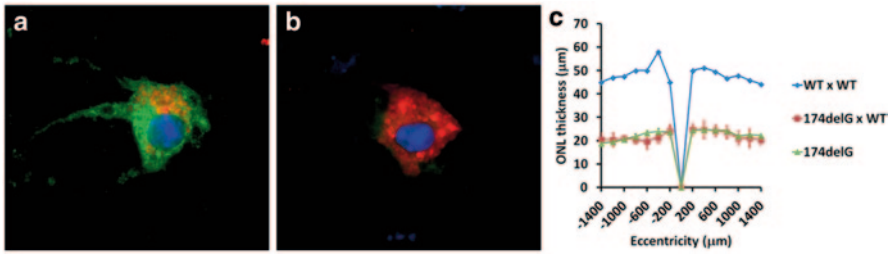


**Fig. 45.3** Subretinal cells are derived directly from circulating monocytes and replacing them with wildtype cells does not alter disease progression. YFP+ bone marrow was transplanted into irradiated *Mfrp*$^{174delG}$ mice at a young age, and then animals were examined several weeks later for evidence of donor cells in the subretinal space. **a** In animals that received a YFP + transplant, virtually all the subretinal cells contained YFP immunoreactivity. **b** In unaltered *Mfrp*$^{174delG}$ animals, no immunoreactivity was detected, indicating that the labeling is specific. *Red* signal is the intrinsic autofluorescence of these cells. They are counterstained with Hoescht to label nuclei (*blue*). **c** *Mfrp*$^{174delG}$ animals receiving *Mfrp*$^{+/+}$ YFP + bone marrow (*red line*) did not have any significant changes in retinal thickness compared to unaltered *Mfrp*$^{174delG}$ animals (*green line*)

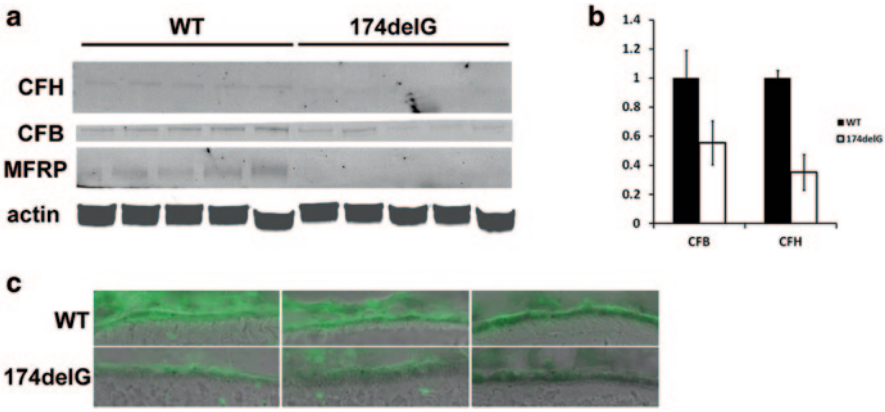


**Fig. 45.4** Downregulation of complement factors in *Mfrp*$^{174delG}$ RPE+choroid. **a** Western analysis of complement factors from RPE+choroid tissue showed a significant decrease in the abundance of CFH and CFB. Western bands are faint because individual RPE/choroids were used and the amount of material was very limiting, but the bands are accurately quantitated in (**b**). **c** C3d immunostaining in sections from three different mice of each genotype are shown. The C3d antibody labeled the RPE in both cases, although in wildtype animals staining was more intense and concentrated on the basal side of the RPE

showed that factors B and H were decreased in *Mfrp*$^{174delG}$ animals. We also evaluated C3d abundance in frozen sections from 5-month-old animals and found it to be similarly decreased (Fig. 45.4).

### 45.3.4 *Comparison of Fundus Images of Mfrp*$^{174delG}$ *and Crb1*$^{rd8}$ *Mice*

A comparison of *Mfrp*$^{174delG}$ and *Crb1*$^{rd8}$ mice illustrates the limitations of fundus imaging for delineating individual cells without additional correlative analysis. The *rd8* phenotype [8] includes white fundus spots which are stereotypically large and irregular, but can sometimes be smaller and more discrete (Fig. 45.5a–b). Some of these could easily be mistaken for the white flecks we have observed in *Mfrp*$^{174delG}$ animals. However, the lesions in *rd8* mice are due to retinal folds that protrude into and distort the outer nuclear layer [8]. The lighter appearance of the fundus in these affected areas may be due to increased reflectance from accumulations of inner and outer segment material within the retinal folds. Alternatively, it may be due to changes in light scattering properties of the outer retina due to disruption of the ONL [9]. White flecks corresponding to subretinal macrophages in *Mfrp*$^{174delG}$ mice; however, are consistently uniform and small in size, and while they can be sparse at early timepoints, they eventually cover the entire fundus with a remarkably uniform distribution (Fig. 45.5c). Interestingly, mutations in *RDH5* and *RLBP1* produce fundus images in humans with discrete white spots, similar to what we

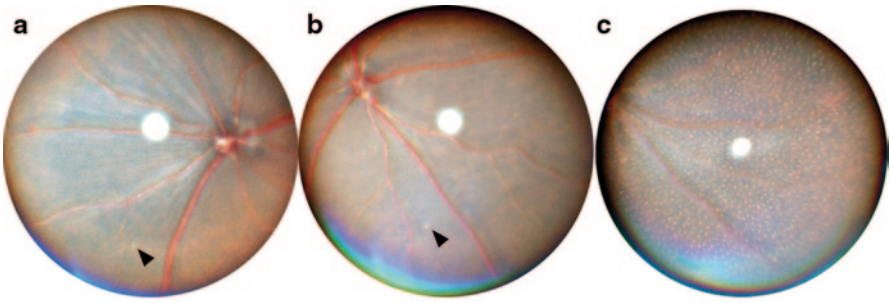


**Fig. 45.5** Comparison of rd8 lesions with fundus spots in *Mfrp*$^{174delG}$ mice. **a-b** Fundus images from 5-month old *rd8* mice. *Arrows* indicate small, discrete spots that are occasionally observed in these animals. **c** *Mfrp*$^{174delG}$ mice at this age have uniformly small spots with even distribution

see in *Mfrp*$^{174delG}$ mice [10–11]. To our knowledge, these observations have never been correlated with histological sections, although OCT scans yield results that are consistent with cells in the subretinal space [12–14]. In addition, *Rep1* mutant mice have autofluorescent retinal spots that can be seen with 488 nm SLO as well as subretinal cells [15].

## 45.4 Discussion

We have expanded on our previous analysis of the *Mfrp*$^{174delG}$ mouse and have found additional evidence of immune system involvement. More precise correlation of the white fundus flecks and the subretinal cells cements the presumption that they are the same objects. It also provides evidence that refraction caused by a single cell is not beyond the resolution of a standard fundus camera. Furthermore, we now show that these cells express additional markers characteristic of macrophages. The non-uniformity of GS-IB4 reactivity suggests that there is some degree of phenotypic heterogeneity among these cells, possibly reflecting variable degrees of cell activation [16]. We note that there is currently no clear consensus on markers that distinguish between various types of monocyte-derived cells, and that different laboratories have established different phenotyping criteria. Indeed, it has even been suggested that such a marker may not exist [17–18].

The origin of these subretinal cells is a particular point of interest. *Cx3cr1* mutant animals exhibit over-accumulation of subretinal Iba1+ cells, which appear to be derived from resident microglia that migrate down from the inner retina [19]. This is also a normal occurrence in Balb/c mice under standard lighting conditions [20]. We entertained the alternate hypothesis that the subretinal cells in *Mfrp*$^{174delG}$ mice were derived directly from circulating monocytes. Bone marrow chimeras made with YFP+donor cells clearly showed that these cells were indeed derived from the donor marrow. We considered the possibility that the donor cells might first engraft in the retina where they would mix with host microglia and then migrate to the

subretinal space. If that were the case, however, we would have expected a more mixed population of YFP+donor cells and YFP-host retinal microglial cells. The fact that they were essentially all donor-derived suggests that they arrive at this site via a more direct route.

The complement pathway has been of interest in AMD ever since the discovery that polymorphisms in key complement regulation genes are significant risk factors for developing the disease [21–22]. Factor B is a key positive regulator of the pathway, while factor H is a negative regulator; we found decreased levels of both in *Mfrp*$^{174delG}$ RPE+choroid. When the alternative pathway is activated, large amounts of C3b are produced, but the half-life of C3b is relatively short and it is rapidly cleaved to generate C3d (among other fragments), which then accumulates at the site [23]. The observation of decreases in both CFH and CFB is somewhat contradictory, but the decrease in C3d as well suggests a net depression in complement activation. The extent to which these changes may be associated with pathology in *Mfrp*$^{174delG}$ remains to be investigated. However, there is recent evidence that the disruption of baseline complement signaling results in photoreceptor degeneration [24].

## References

1. Fogerty J, Besharse JC (2011) 174delG mutation in mouse MFRP causes photoreceptor degeneration and RPE atrophy. Invest Ophthalmol Vis Sci 52(10):7256–7266
2. Srinivas S, Watanabe T, Lin CS, William CM, Tanabe Y, Jessell TM, Costantini F (2001) Cre reporter strains produced by targeted insertion of EYFP and ECFP into the ROSA26 locus. BMC Dev Biol 1:4
3. Lakso M, Pichel JG, Gorman JR, Sauer B, Okamoto Y, Lee E, Alt FW, Westphal H (1996) Efficient in vivo manipulation of mouse genomic sequences at the zygote stage. Proc Natl Acad Sci USA 93(12):5860–5865
4. Hawes NL, Chang B, Hageman GS, Nusinowitz S, Nishina PM, Schneider BS, Smith RS, Roderick TH, Davisson MT, Heckenlively JR (2000) Retinal degeneration 6 (rd6): a new mouse model for human retinitis punctata albescens. Invest Ophthalmol Vis Sci 41(10):3149–3157
5. Kameya S, Hawes NL, Chang B, Heckenlively JR, Naggert JK, Nishina PM (2002) Mfrp, a gene encoding a frizzled related protein, is mutated in the mouse retinal degeneration 6. Hum Mol Genet 11(16):1879–1886
6. Joly S, Francke M, Ulbricht E, Beck S, Seeliger M, Hirrlinger P, Hirrlinger J, Lang KS, Zinkernagel M, Odermatt B, Samardzija M, Reichenbach A, Grimm C, Reme CE (2009) Cooperative phagocytes: resident microglia and bone marrow immigrants remove dead photoreceptors in retinal lesions. Am J Pathol 174(6):2310–2323
7. Rutar MV, Natoli RC, Provis JM (2012) Small interfering RNA-mediated suppression of Ccl2 in Muller cells attenuates microglial recruitment and photoreceptor death following retinal degeneration. J Neuroinflammation 9(1):221
8. Mehalow AK, Kameya S, Smith RS, Hawes NL, Denegre JM, Young JA, Bechtold L, Haider NB, Tepass U, Heckenlively JR, Chang B, Naggert JK, Nishina PM (2003) CRB1 is essential for external limiting membrane integrity and photoreceptor morphogenesis in the mammalian retina. Hum Mol Genet 12(17):2179–2189
9. Solovei I, Kreysing M, Lanctot C, Kosem S, Peichl L, Cremer T, Guck J, Joffe B (2009) Nuclear architecture of rod photoreceptor cells adapts to vision in mammalian evolution. Cell 137(2):356–368

10. Yamamoto H, Simon A, Eriksson U, Harris E, Berson EL, Dryja TP (1999) Mutations in the gene encoding 11-cis retinol dehydrogenase cause delayed dark adaptation and fundus albipunctatus. Nat Genet 22(2):188–191
11. Demirci FY, Rigatti BW, Mah TS, Gorin MB (2004) A novel compound heterozygous mutation in the cellular retinaldehyde-binding protein gene (RLBP1) in a patient with retinitis punctata albescens. Am J Ophthalmol 138(1):171–173
12. Wang NK, Chuang LH, Lai CC, Chou CL, Chu HY, Yeung L, Chen YP, Chen KJ, Wu WC, Chen TL, Chao AN, Hwang YS (2012) Multimodal fundus imaging in fundus albipunctatus with RDH5 mutation: a newly identified compound heterozygous mutation and review of the literature. Doc Ophthalmol 125(1):51–62
13. Querques G, Carrillo P, Querques L, Bux AV, Del Curatolo MV, Delle Noci N (2009) High-definition optical coherence tomographic visualization of photoreceptor layer and retinal flecks in fundus albipunctatus associated with cone dystrophy. Arch Ophthalmol 127(5):703–706
14. Schatz P, Preising M, Lorenz B, Sander B, Larsen M, Eckstein C, Rosenberg T (2010) Lack of autofluorescence in fundus albipunctatus associated with mutations in RDH5. Retina 30(10):1704–1713
15. Tolmachova T, Anders R, Abrink M, Bugeon L, Dallman MJ, Futter CE, Ramalho JS, Tonagel F, Tanimoto N, Seeliger MW, Huxley C, Seabra MC (2006) Independent degeneration of photoreceptors and retinal pigment epithelium in conditional knockout mouse models of choroideremia. J Clin Invest 116(2):386–394
16. Tabor DR, Theus SA, Barnett JB, Tryka AF, Jacobs RF (1992) The concurrent expression of Griffonia simplicifolia-IB4 binding and tumor necrosis factor-alpha differs between alveolar and peritoneal macrophages. Proc Soc Exp Biol Med 199(3):351–359
17. Schmid CD, Melchior B, Masek K, Puntambekar SS, Danielson PE, Lo DD, Sutcliffe JG, Carson MJ (2009) Differential gene expression in LPS/IFNgamma activated microglia and macrophages: in vitro versus in vivo. J Neurochem 109(Suppl 1):117–125
18. Graeber MB, Streit WJ (2010) Microglia: biology and pathology. Acta Neuropathol 119(1):89–105
19. Kezic J, McMenamin PG (2008) Differential turnover rates of monocyte-derived cells in varied ocular tissue microenvironments. J Leukoc Biol 84(3):721–729
20. Ng TF, Streilein JW (2001) Light-induced migration of retinal microglia into the subretinal space. Invest Ophthalmol Vis Sci 42(13):3301–3310
21. Genetics DSP (2005) Was the human genome project worth the effort? Science 308(5720): 362–364
22. Gold B, Merriam JE, Zernant J, Hancox LS, Taiber AJ, Gehrs K, Cramer K, Neel J, Bergeron J, Barile GR, Smith RT, Hageman GS, Dean M, Allikmets R (2006) Variation in factor B (BF) and complement component 2 (C2) genes is associated with age-related macular degeneration. Nat Genet 38(4):458–462
23. Scholl HP, Charbel Issa P, Walier M, Janzer S, Pollok-Kopp B, Borncke F, Fritsche LG, Chong NV, Fimmers R, Wienker T, Holz FG, Weber BH, Oppermann M (2008) Systemic complement activation in age-related macular degeneration. PLoS One 3(7):e2593
24. Yu M, Zou W, Peachey NS, McIntyre TM, Liu J (2012) A novel role of complement in retinal degeneration. Invest Ophthalmol Vis Sci 53(12):7684–7692

# Chapter 46
# Ambiguous Role of Glucocorticoids on Survival of Retinal Neurons

**Tembei K. Forkwa, Ernst R. Tamm and Andreas Ohlmann**

**Abstract** Glucocorticoids (GCs) have a wide range of functions on several mammalian cell types, most of which are aimed at boosting survival, which is the raison d'être of the acute stress response. The role GCs play in the survival and viability of neurons is incongruous, as studies have revealed neuroprotective as well as neurodegenerative effects. These effects seem to depend on multiple factors amongst which are; the cell type involved, the mode of injury or underlying cause of cell death, likewise the concentration and or duration of GC exposure.

In this mini review, we discuss mechanisms of GC action and their effect on neurodegeneration in general, and specifically review the effect of GCs on retinal neurons, in animal models of retinal degeneration or acute neuronal damage. Finally, we summarize potential protective and harmful GC-mediated mechanisms, which might be involved in the determination of neuronal fate in the retina following injury or during degeneration.

**Keywords** Glucocorticoids · Glucocorticoid receptor · Neurons · Retina · Apoptosis · Neuroprotection · Retinal degeneration

T. K. Forkwa (✉)
e-mail: tembei.forkwa-kieran@ur.de

T. K. Forkwa · E. R. Tamm · A. Ohlmann
Institute of Human Anatomy and Embryology, University of Regensburg,
Universitätsstr. 31, 93053 Regensburg, Germany
e-mail: andreas.ohlmann@ur.de

E. R. Tamm
e-mail: Ernst.tamm@ur.de

J. D. Ash et al. (eds.), *Retinal Degenerative Diseases,* Advances in Experimental Medicine and Biology 801, DOI 10.1007/978-1-4614-3209-8_46,

## 46.1 Introduction

Glucocorticoids (GCs) are a class of steroid hormones that exhibit a wide range of systemic effects. Beside others, immunological and metabolic functions are the most prominent properties of glucocorticoids. In metabolism, GCs stimulate gluconeogenesis from substrates such as lactate and pyruvate, and increase lipolysis in the presence of growth hormones, amongst other functions [1]. In the immune system, GCs suppress cell mediated immunity by inhibiting genes that code for some cytokines especially interleukin 2 (IL-2), and also suppress humoral immunity by reducing expression of IL-2 receptors on B cells. In addition, GCs exhibit anti-inflammatory effects by inhibition of prostaglandins and leukotrienes, which are the two key mediators of inflammation, making GCs a widely used anti-inflammatory drug [2].

### *46.1.1 Regulation of GC Release*

Normally, GC release is underlain by a physiological, circadian rhythm with an increase in GC level in morning and low concentrations at night, and is mediated by an activation of the hypothalamic-pituitary-adrenal (HPA) axis. In addition, an enhanced GC release is also part of stress response which involves a coordinated action of the sympathetic nervous system and the HPA axis.

Once the HPA axis is activated, corticortropin releasing hormone (CRH) from neurons of the paraventricular nucleus binds to its receptors on corticotroph cells in the anterior pituitary. There, CRH induces the cleavage of the precursor proopiomelanocortin into beta-lipotrophic hormone and adrenocorticotropic hormone (ACTH) which are then released into blood. In the adrenal cortex, ACTH binds to its receptors on cells of the zona fasciculata where its main action is to stimulate the synthesis and release of GCs (cortisol in humans, corticosterone in rodents) into general circulation [3].

### *46.1.2 Mechanism of GC Action*

GCs exhibit a wide range of systemic effects which are mediated either through the ubiquitously expressed glucocorticoid receptor (GR) or with a lower affinity via binding to the mineralcorticoid receptor (MR). GR in its inactive form resides in the cytoplasm as part of a multiprotein complex. Upon binding of GCs to the GR, the GR gets activated, dissociates from its binding partners and translocates into the nucleus where it can cause activation or inhibition of transcription of several genes in two mechanisms, the genomic and nongenomic. Following activation in the genomic mechanism which generally occurs at higher GC level, the hormone-receptor complex translocates into the nucleus where it binds to glucocorticoid response elements (GRE). The nongenomic mechanism is used by GCs to achieve inhibition of genes which do not contain any GRE or any other GR-binding sites. This is possible through the transrepressive action of the GR on other transcription factors via

protein-protein interactions to block DNA binding. Like other steroid hormones, GCs may also exert non-genomic actions via membrane receptors and second messengers such as the phosphoinositide 3-kinase (PI3K) pathway [4–6].

### *46.1.3 GC Effects on Apoptotic Processes*

The role of GCs on apoptosis in general and neurodegeneration in particular is double-edged. GC pre-treatment has been shown to reduce apoptotic cell death in certain cell types such as fibroblast, glioma cells, oligodendrocytes, erythroblasts and neutrophils. Conversely, GCs also exhibit proapoptotic effects in other cell types such as those of the hematopoietic system like monocytes, macrophages and T-lymphocytes [7]. In neurons, apart from the particular type of neuron involved, the inconsistent role of GCs seems to be particularly influenced by the mechanism of damage. During oxidative stress, GCs have been shown to be deleterious and GR antagonists were protective, while a protective role has been shown in neurons during ischemia and retinal light damage as well [8–10]. This contradictory function of GCs on neurons is even more paradoxical since GCs have the ability to activate diametrically opposing processes in the same cell type or organ. For instance, in neurons of the dentate gyrus the absence of adrenal steroids following adrenalectomy (ADX) resulted in both neurogenesis [11] and neuronal apoptosis [12].

### *46.1.4 The Role of GCs on Apoptotic Processes in Retinal Neurons*

All retinal cell types including Müller cells express GRs [13], and hereby underlie the potential influence of GCs. Studies that have analyzed the effect of synthetic and endogenous GC increase on survival of damaged retinal ganglion cells (RGC) and photoreceptors have revealed incongruous results (Table 46.1). Following optic nerve crush in rats, a protective effect for cortisol on RGC has been shown [14], whereas the synthetic GC analogue methylprednisolone either had no or even a worsening effect on RGC loss [15, 16]. Further on, no or an exacerbating effect on RGC survival was described for methylprednisolone following an ischemia or an autoimmune optic neuritis, respectively [17, 18].

In line with observations on damaged RGC, the functions of GCs have been found to be contradictory for degenerating photoreceptors as well. Following light damage, dexamethasone, a synthetic GC analogue, has been shown to protect photoreceptors in BALB/c mice but not in dogs [9, 19]. Following an endogenous increase of GCs by food deprivation prior to illumination in mice, a protective role for GCs was observed as well [9]. Since following light-induced damage of photoreceptors GC level are substantially increased, these data provide strong evidence that GCs have to mediate their neuroprotective properties prior and/or during induction of injury. In line with this data, an increase in photoreceptors damage was seen in illuminated mice that were additionally treated with a GR receptor antagonist [20].

**Table 46.1** Summarized GC effects on damaged photoreceptors and RGC

| Cell type | Type of damage | Species/Treatment | Effect | Publication |
|---|---|---|---|---|
| Photoreceptors | Light exposure | Mice/Food deprivation | Protective | Wenzel et al. 2001 |
| Photoreceptors | Light exposure | Mice/Dexamethasone | Protective | |
| Photoreceptors | Light exposure | Dogs/Dexamethasone | No effect | Gu et al. 2009 |
| Photoreceptors | Hemorrhage | Rabbit/Triamcinolone | Protective | Bhisitkul et al. 2008 |
| Photoreceptors | Retinal degeneration | Rats/Fluocinolone Acetonide | Protective | Glybina et al. 2009 |
| Photoreceptors | Laser coagulation | Rhesus monkeys/ Methylprednisolone | Protective | Brown et al. 2007 |
| Photoreceptors | Laser coagulation | Cynomolgus monkeys/ Methylprednisolone | Protective | Takahashi et al. 1997 |
| Photoreceptors | Light damage | Mice/Mifepristone (GR antagonist) | Exacerbative | Cubilla et al. 2013 |
| Photoreceptors | Light damage | Rats/Systemic increase during illumination | Exacerbative | López et al. 2008 |
| RGC | Ischemia | Rats/ Methylprednisolone | No effect | Dimitriu et al. 2008 |
| RGC | Optic nerve crush | Rats/Cortisol | Protective | Heiduschka and Thanos 2006 |
| RGC | Optic nerve crush | Rats/ Methylprednisolone | No effect | Ohlsson et al. 2004 |
| RGC | Optic nerve crush | Rats/ Methylprednisolone | Exacerbative | Steinsapir et al. 2000 |
| RGC | Inflammation | Rats/ Methylprednisolone | Exacerbative | Diem et al. 2003 |

However, adrenalectomized rats showed a thicker retinal outer nuclear layer following illumination when compared to illuminated sham operated controls [21], suggesting a harmful role of GCs during illumination in rats. In addition, a protective role for GCs on photoreceptors was detected following hemorrhage, retinal degeneration and laser coagulation (Table 46.1).

Overall, these data suggest that during degeneration of retinal neurons the influence of GCs on apoptotic processes seems to vary with several factors amongst which are (1) the type of cells involved, (2) the concentration of GCs, (3) the duration of exposure (4) onset of GC treatment and (5) the underlying mechanism of neuronal death.

## 46.2 Major Pro- and Anti-Apoptotic Signaling Mechanisms of GCs

### *46.2.1 Transcriptional Regulation of Pro- and Anti-Apoptotic Genes*

Activated GR can induce transcription of either pro- and anti-apoptotic genes by direct binding to GRE or inhibition of other transcription factors. In this context,

interactions of GCs with members of the apoptotic Bcl-2 family are well characterized. This group of proteins can regulate mitochondrial outer membrane permeability and hereby induce (pro-apoptotic members) or inhibit (anti-apoptotic members) the release of cytochrome C into the cytosol, leading to apoptosis [22]. In several cell types, GC-GR complex induces the expression of pro-apoptotic Bcl-2 family members Bax, BAD, Bak and Bok and represses the expression of the anti-apoptotic proteins Bcl-2, Bcl-xL, and Bcl-w, hence promoting apoptosis [22]. However, in some circumstances, GCs can also induce anti-apoptotic gens such as Bcl-2, and hereby prevent apoptosis [23]. Besides their functions on expression of Bcl-2 family members, GCs can inhibit apoptotic processes as well by induction of the anti-apoptotic cyclin dependent kinase inhibitor (p21), GC-inducible protein kinase-1 (SGK-1) and Mitogen-activated protein kinase phosphatase-1 (MKP-1) [8, 24].

In addition, GC-GR complexes can interact with and subsequently inhibit the transcription factor activator protein (AP)-1 that is involved in mediating apoptosis of photoreceptors following light damage [9]. Likewise, GC-GR complexes can trans-repress the functioning of the transcription factor NF-κB, that can mediate pro- as well as anti-apoptotic effects, and is required for p53-mediated cell death [6].

### *46.2.2 Activation of the P13K/Akt Kinase Pathway*

GC-GR complexes can activate the phosphoinositide 3-kinase (PI3K) signaling pathway that has been shown to provide protective and anti-apoptotic effects on neurons [8]. Activated PI3K in turn leads to phosphorylation of the serine/threonine kinase Akt, a key mediator of signal transduction processes downstream of PI3K. Activated Akt is known to phosphorylate and inactivate several components of the apoptotic machinery such as pro-apoptotic BAD or caspase 9. Further on, phosphorylated Akt can activate the transcription factor NF-κB via IKK that causes phosphorylation of its p65 subunit. Once activated NF-κB can induce expression of anti-apoptotic members of the inhibitor of apoptosis (IAP) family such as c-IAP1, c-IAP2, XIAP and surviving [25].

### *46.2.3 GC-Mediated Caspase Inhibition*

Caspases are key mediators of apoptosis. In retina following light damage, the quantity of activated caspases was found to be higher in the presence of a GR antagonist, an effect that was reversed by injecting the GC analogue dexamethasone [26], suggesting that GCs can reduce apoptosis by caspase inhibition. A potential mechanism of caspase inhibition by GCs could again be provided by activation of the PI3K/Akt signaling pathway. Phosphorylated Akt has the ability to diminish caspase activity directly and via an activation of p21 [25].

## 46.3 Conclusions

Even though various reports indicate contrary functions of GCs on apoptotic processes of damaged retinal neurons, there is evidence that GCs can mediate neuroprotective effects on these cells. In line with this, GCs can influence various pathways that are involved in adjusting apoptotic processes. However, GC-mediated neuroprotective effects most likely depend on experimental conditions such as induction of damage, and the concentration, onset and duration of GC treatment. Therefore, prospective emphasis should focus on experimental setups to figure out conditions which lead to GC-mediated neuroprotection.

## References

1. Leung K, Munck A (1975) Peripheral actions of glucocorticoids. Annu Rev Physiol 37:245–272
2. Baschant U, Tuckermann J (2010) The role of the glucocorticoid receptor in inflammation and immunity. J Steroid Biochem Mol Biol 120(2–3):69–75
3. Webster JI, Sternberg EM (2004) Role of the hypothalamic-pituitary-adrenal axis, glucocorticoids and glucocorticoid receptors in toxic sequelae of exposure to bacterial and viral products. J Endocrinol 181(2):207–221
4. Buttgereit F, Scheffold A (2002) Rapid glucocorticoid effects on immune cells. Steroids 67(6):529–534
5. Buttgereit F, Burmester GR, Lipworth BJ (2009) Inflammation, glucocorticoids and risk of cardiovascular disease. Nat Clin Pract Rheumatol 5(1):18–19
6. Limbourg FP, Liao JK (2003) Nontranscriptional actions of the glucocorticoid receptor. J Mol Med (Berl) 81(3):168–174
7. Amsterdam A, Sasson R (2002) The anti-inflammatory action of glucocorticoids is mediated by cell type specific regulation of apoptosis. Mol Cell Endocrinol 189(1–2):1–9
8. Harms C et al (2007) Phosphatidylinositol 3-Akt-kinase-dependent phosphorylation of p21(Waf1/Cip1) as a novel mechanism of neuroprotection by glucocorticoids. J Neurosci 27(17):4562–4571
9. Wenzel A et al (2001) Prevention of photoreceptor apoptosis by activation of the glucocorticoid receptor. Invest Ophthalmol Vis Sci 42(7):1653–1659
10. Behl C et al (1997) Glucocorticoids enhance oxidative stress-induced cell death in hippocampal neurons in vitro. Endocrinology 138(1):101–106
11. Cameron HA, Gould E (1994) Adult neurogenesis is regulated by adrenal steroids in the dentate gyrus. Neuroscience 61(2):203–209
12. Jaarsma D, Postema F, Korf J (1992) Time course and distribution of neuronal degeneration in the dentate gyrus of rat after adrenalectomy: a silver impregnation study. Hippocampus 2(2):143–150
13. Gorovits R et al (1994) Developmental changes in the expression and compartmentalization of the glucocorticoid receptor in embryonic retina. Proc Natl Acad Sci USA 91(11):4786–4790
14. Heiduschka P, Thanos S (2006) Cortisol promotes survival and regeneration of axotomised retinal ganglion cells and enhances effects of aurintricarboxylic acid. Graefes Arch Clin Exp Ophthalmol 244(11):1512–1521
15. Ohlsson M et al (2004) Methylprednisolone treatment does not influence axonal regeneration or degeneration following optic nerve injury in the adult rat. J Neuroophthalmol 24(1):11–18

16. Steinsapir KD et al (2000) Methylprednisolone exacerbates axonal loss following optic nerve trauma in rats. Restor Neurol Neurosci 17(4):157–163
17. Diem R et al (2003) Methylprednisolone increases neuronal apoptosis during autoimmune CNS inflammation by inhibition of an endogenous neuroprotective pathway. J Neurosci 23(18):6993–7000
18. Dimitriu C et al (2008) Methylprednisolone fails to preserve retinal ganglion cells and visual function after ocular ischemia in rats. Invest Ophthalmol Vis Sci 49(11):5003–5007
19. Gu D et al (2009) Steroids do not prevent photoreceptor degeneration in the light-exposed T4R rhodopsin mutant dog retina irrespective of AP-1 inhibition. Invest Ophthalmol Vis Sci 50(7):3482–3494
20. Cubilla MA et al. (2013), Mifepristone, a blocker of glucocorticoid receptors, promotes photoreceptor death. Invest Ophthalmol Vis Sci, 54(1):313–322 2012
21. Lopez EM et al (2008) Endogenous glucocorticoids participate in retinal degeneration during continuous illumination. Int J Neurosci 118(12):1725–1747
22. Schlossmacher G, Stevens A, White A (2011) Glucocorticoid receptor-mediated apoptosis: mechanisms of resistance in cancer cells. J Endocrinol 211(1):17–25
23. Schorr K, Furth PA (2000) Induction of bcl-xL expression in mammary epithelial cells is glucocorticoid-dependent but not signal transducer and activator of transcription 5-dependent. Cancer Res 60(21):5950–5953
24. Wu W et al (2004) Microarray analysis reveals glucocorticoid-regulated survival genes that are associated with inhibition of apoptosis in breast epithelial cells. Cancer Res 64(5):1757–1764
25. Manning BD, Cantley LC (2007) AKT/PKB signaling: navigating downstream. Cell 129(7):1261–1274
26. Cubilla MA et al (2012) Glucocorticoid-dependent mechanisms in photoreceptor survival. Adv Exp Med Biol 723:101–106

# Chapter 47
# Microglia-Müller Glia Crosstalk in the *rd10* Mouse Model of Retinitis Pigmentosa

**Ana I. Arroba, Noemí Álvarez-Lindo, Nico van Rooijen and Enrique J. de la Rosa**

**Abstract** Retinitis pigmentosa refers to a large, genetically heterogeneous group of retinal dystrophies. This condition is characterized by the gradual onset of blindness due to progressive deterioration of the retina, a process that includes photoreceptor and retinal-pigmented-epithelium cell decay and death, microglial recruitment, reactive gliosis, and vascular disorganization and regression. We found that early in the degenerative process, the *rd10* mouse retina exhibits high levels of photoreceptor cell death and reactive Müller gliosis. In explant cultures, both degenerative processes were abrogated by IGF-I treatment. Moreover, the beneficial effect of IGF-I was diminished by microglial depletion using clodronate-containing liposomes. Interestingly, in the absence of IGF-I, microglial depletion partially prevented cell death without affecting Müller gliosis. These findings strongly suggest a role for microglia-Müller glia crosstalk in neuroprotection. However, a subpopulation of microglial cells appears to promote neurodegeneration in the dystrophic retina. Our findings indicate that beneficial neuroprotective effects may be achieved through strategies that modulate microglial cell responses.

**Keywords** Retinal dystrophy · Retinal degeneration · Neuroprotection · Clodronate · IGF-I

E. J. de la Rosa (✉) · A. I. Arroba · N. Álvarez-Lindo
3D Lab (Development, Differentiation and Degeneration), Department of Cellular and Molecular Medicine, Centro de Investigaciones Biológicas, CSIC, C/ Ramiro de Maeztu 9, E-28040 Madrid, Spain
e-mail: ejdelarosa@cib.csic.es

A. I. Arroba
email: anaarroba@gmail.com

N. Álvarez-Lindo
e-mail: alvarezlnl@cib.csic.es

N. van Rooijen
Department of Molecular Cell Biology, Faculty of Medicine, Vrije Universiteit, VUMC, Amsterdam, The Netherlands
e-mail: nvanrooijen@clodronateliposomes.org

J. D. Ash et al. (eds.), *Retinal Degenerative Diseases,* Advances in Experimental Medicine and Biology 801, DOI 10.1007/978-1-4614-3209-8_47,

## 47.1 Introduction

Retinitis pigmentosa (RP) comprises a large group of inherited retinal dystrophies. Despite its genetically heterogeneous origin, RP-associated vision loss is paralleled by photoreceptor cell death in most models [1], and treatments that promote cell survival moderately attenuate the degenerative process in animal models of RP [2]. Members of the insulin family are well characterized attenuators of cell death in the developing and adult nervous system [3, 4]. We previously reported that proinsulin treatment delays photoreceptor cell death and prolongs visual function in the *rd10* mouse [5]. IGF-I also reduces photoreceptor cell death in the *rd10* mouse retina, an effect mediated by microglia [6]. In the central nervous system, including the neuroretina, microglia are derived from the macrophage/monocyte lineage. Tissue damage triggers morphological and migratory adaptations in microglial cells, as well as autocrine/paracrine secretion of growth factors and proinflammatory cytokines [7]. Microglia also induce the secretion of neurotrophic factors by Müller glial cells during retinal degeneration [8]. In the present study, we explored the crosstalk between microglia and Müller glial cells in the *rd10* mouse retina.

## 47.2 Materials and Methods

### *47.2.1 Animals*

All experiments were carried out in accordance with European Union guidelines and the ARVO Statement for the Use of Animals in Ophthalmic and Vision Research. All procedures were approved by the CIB bioethics committee. Control (wild-type, WT) C57BL/6J mice and *rd10* mice homozygous for the *Pde6b*$^{rd10}$ mutation on a C57BL/6J background were reared in local facilities.

### *47.2.2 Ex vivo Retinal Explants*

Ex vivo retinal explants and cryosections were performed as previously described [6]. Briefly, postnatal day 23 (P23) *rd10* mice were euthanized and their eyes enucleated. Neuroretinas were dissected out and mounted on nitrocellulose inserts (Millicell; Millipore, Billerica, MA, USA) with the photoreceptor side facing up. Explants were cultured for 24 h in 1.2 mL R16 medium (basal), and where indicated, were treated with 20 nM IGF-I (Sigma, St. Louis, MO, USA) or with liposomes. The liposomes were a kind gift from the Clodronate Liposomes Foundation (www.clodronateliposomes.org). Clodronate was a kind gift from Roche Diagnostics GmbH, (Mannhein, Germany). Clodronate- and PBS-encapsulating liposomes were prepared as previously described [9] and applied, where indicated, to the retinal explant cultures for the entire 24 h period. Retinas were processed for

cryosectioning. Cryosections were also prepared from freshly dissected WT and *rd10* retinas (in vivo) at P24.

### *47.2.3 TUNEL*

Cell death was visualized by terminal deoxynucleotidyl transferase-mediated dUTP nick end labeling (TUNEL; Promega, Madison, WI, USA) in retinal cryosections, as previously described [6, 10]. After labeling, the sections were mounted in Fluoromount-G (Southern Biotechnology, Birmingham, AL, USA) and examined on a laser confocal microscope (TCS SP2; Leica Microsystems, Wetzlar, Germany).

### *47.2.4 Immunofluorescence*

Retinal cryosections were immunolabeled as previously described [6]. Microglia were visualized using rat anti-Cd11b or goat anti-Iba1 antibodies (Abcam, Cambridge, UK). Reactive Müller gliosis was visualized with rabbit anti-GFAP antibody (DAKO, Glostrup, Denmark). Alexa-488 or Alexa-647-conjugated secondary antibodies were used (Molecular Probes, Eugene, OR, USA). After labeling, the sections were processed as described above.

### *47.2.5 Microscopy and Quantification*

Images were acquired by confocal microscopy using a 40X objective. Stained microglial cells or TUNEL-positive nuclei were counted in an entire retinal section. The Leica Las AF Lite program was used to quantify GFAP staining in confocal images acquired under identical conditions. Intensity was normalized with respect to the area analyzed. At least three retinas and four non-adjacent sections per retina were scored for each experimental point. All results are expressed relative to those found in in vivo P24 *rd10* retinas. All data were analyzed using the STATGRAPHICS PLUS 5.1 statistical program (Statpoint Technologies Inc., Warrenton, VA, USA).

## 47.3 Results

### *47.3.1 IGF-I Treatment Attenuated Photoreceptor Cell Death and Müller Gliosis in the rd10 Mouse Retina*

We previously described the pro-survival effect of IGF-I in *rd10* mouse retinas, both in vivo and in explant cultures, and demonstrated the neuroprotective role of

microglia in this model [6]. In the present study, we sought to expand upon these findings to investigate the potential role of Müller glial cells in both the degenerative process and the neuroprotective effects of IGF-I in RP. In contrast to the WT retinas, *rd10* retinas displayed massive cell death in the outer nuclear layer and a characteristic pattern of Müller gliosis at P24, a time point at which neurodegeneration peaks, although the mice still retain visual function (Fig. 47.1a–d and see Table 47.1 for quantification) [10]. IGF-I treatment in *rd10* explant cultures prevented both photoreceptor cell death and reactive gliosis (Fig. 47.1e–h and Table 47.1).

### *47.3.2 Microglial Depletion Diminished the Neuroprotective Effect of IGF-I*

We previously observed that microglia cell numbers are increased in explant cultures in response to IGF-I treatment [6] (see also Table 47.1), suggesting a link between the microglial response and the neuroprotective effects of IGF-I. The elimination of retinal microglia by treatment with clodronate-filled liposomes attenuated the pro-survival effects of IGF-I on photoreceptor cells [6] (see also Fig. 47.1g, k). Furthermore, the effect of IGF-I on reactive Müller gliosis disappeared upon microglial depletion (Fig. 47.1h, l; and Table 47.1), indicating that these two beneficial effects of IGF-I are mediated by microglia.

Interestingly, in the absence of IGF-I, microglial depletion reduced levels of photoreceptor cell death, indicating that microglia, or a subpopulation thereof, also promote cell death during the degenerative process [6] (Fig. 47.1e, i; and Table 47.1). Microglial depletion in the absence of IGF-I had no effect on Müller gliosis (Fig. 47.1f, j; and Table 47.1), suggesting that distinct interactions between microglial and Müller glial cells occur during the induction and the resolution of the reactive glial response.

## 47.4 Discussion

In the present study, we used *rd10* retinal explants to investigate the crosstalk between microglial and Müller glial cells in both neurodegeneration and IGF-I-mediated neuroprotection in retinal dystrophies. We previously characterized the biochemical basis of IGF-I-mediated neuroprotection in *rd1* retinas and in a model of photoreceptor cell death induced by $Ca^2$+ overload [11], and demonstrated the prosurvival effect of IGF-I in the *rd10* retina both in vivo and in cultured explants [6]. The present findings further support these observations, demonstrating that microglia mediate the neuroprotective and prosurvival effects of IGF-I. However, we also found that photoreceptor cell death was induced by microglia, most likely belonging to a distinct subpopulation. While the neuroprotective effects of microglia have been described in other parts of the central nervous system [12], this cell population

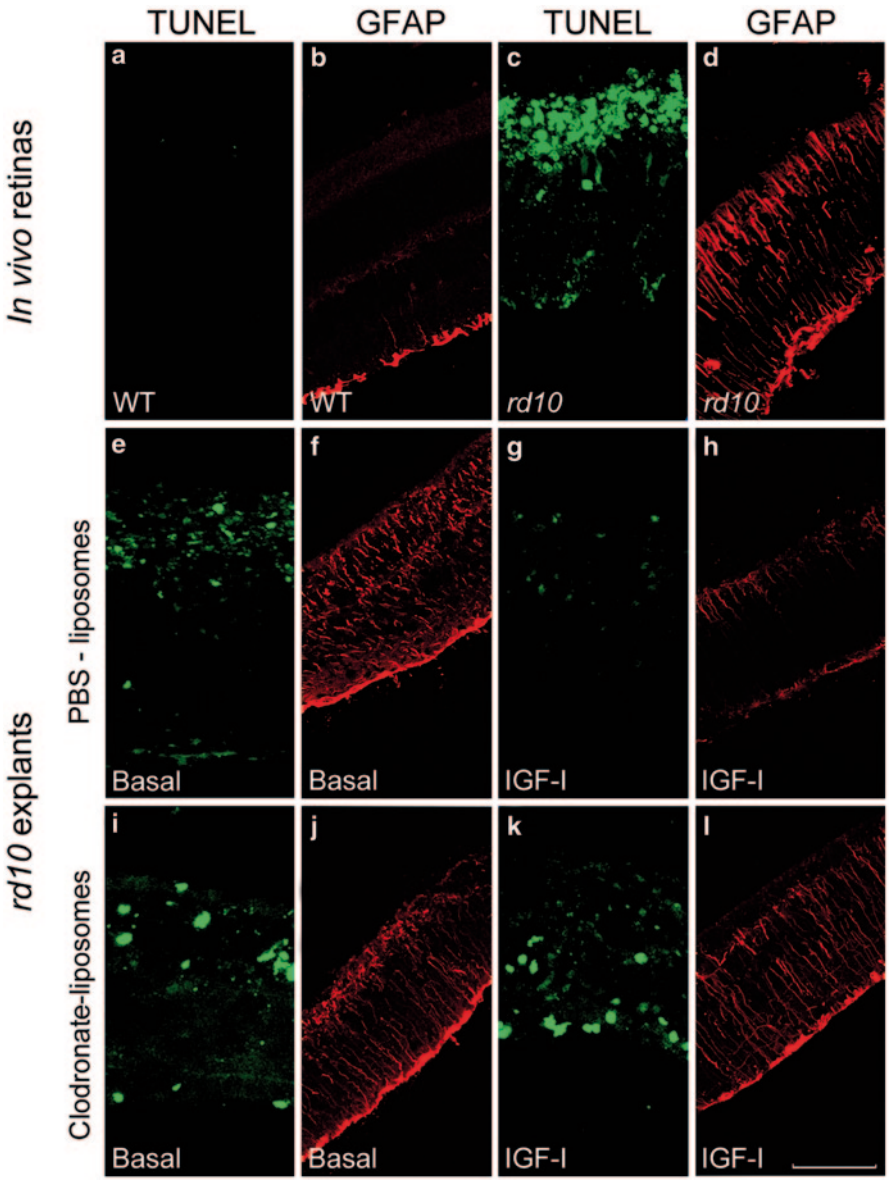


**Fig. 47.1** Photoreceptor cell death and Müller gliosis in the *rd10* mouse retina following treatment with IGF-I and/or clodronate-filled liposomes. P24 retinas from wild type (**a**, **b**) and *rd10* (**c**, **d**) mice were processed for cryosectioning. P23 retinal explants from *rd10* mice were cultured for 24 h in basal medium (**e**, **f**, **i**, **j**) in the absence or presence of IGF-I (20 nM; **g**, **h**, **k**, **l**), and subsequently processed for cryosectioning. Cell death was visualized by TUNEL (*green*; **a**, **c**, **e**, **g**, **i**, **k**). Müller gliosis was visualized by GFAP immunostaining (**b**, **d**, **f**, **h**, **j**, **l**). Scale bar = 75 µm for TUNEL and 150 µm for GFAP

**Table 47.1** Quantitative data

| Condition | | | TUNEL | GFAP | Microglia |
|---|---|---|---|---|---|
| in vivo | WT | | 2±2[a] | 43±8[a] | 107±5 |
| in vivo | *rd10* | | 100±10 | 100±23 | 100±21 |
| *rd10* explant | Basal or PBS-liposomes | −IGF-I | 60±11 | 62±19 | 248±31 |
| *rd10* explant | Basal or PBS-liposomes | +IGF-I | 10±1[b] | 27±16[c] | 395±18 |
| *rd10* explant | Clodronate-liposomes | −IGF-I | 38±4 | 60±10 | ND |
| *rd10* explant | Clodronate-liposomes | +IGF-I | 38±2[d] | 68±5[e] | ND |

*ND* not detected. Values represent the mean ± standard deviation, and are expressed relative to the in vivo situation in the P24 *rd10* retina. At least three retinas and four non-adjacent sections per retina were scored for each experimental point

[a] $p \leq 0.001$ vs *rd10* in vivo

[b] $p \leq 0.001$

[c] $p \leq 0.05$ vs the corresponding −IGF-I explant

[d] $p \leq 0.001$

[e] $p \leq 0.01$ vs the corresponding PBS-liposome-treated explant

most commonly mediates neurotoxic effects in the retina [13]. Our results reconcile these contrasting observations and support a dual role for microglia in the retina.

IGF-I exerts multiple biochemical and cellular effects and is a potent activator of survival pathways [3, 4]. It is thus surprising that microglial cell depletion significantly attenuated the effects of IGF-I. We present evidence of a possible amplifying cellular network involving microglial and Müller glial cells. In the presence of intact microglia, IGF treatment decreased photoreceptor cell death from 60 to 10% of that observed in *rd10* mice in vivo (see Table 47.1). Following microglial depletion, the proportion of dying photoreceptors increased from 10 to 38% (Table 47.1). These observations suggest a direct effect of IGF-I on photoreceptor survival, an effect that is potentiated throughout an as-yet-unidentified microglial population. Furthermore, this microglial population promoted the resolution of Müller gliosis, decreasing its putative neurotoxic effects during the course of the dystrophy. Conversely, the microglial subpopulation whose depletion attenuated photoreceptor cell death appeared not to directly affect the status of reactive Müller gliosis. Our findings are in agreement with the previously proposed crosstalk between microglia and Müller glia cells, and the secretion of neurotrophic factors by the latter [8, 14]. Taken together, our results reveal a complex signaling network that mediates the beneficial effects of IGF-I, and potentially those of other neuroprotective factors, in the dystrophic retina. Moreover, these findings may aid the identification of therapeutic targets for the treatment of RP and other retinal dystrophies.

**Acknowledgments** EJdelaR was supported by the Spanish Ministerio de Ciencia e Innovación (Grant SAF2010-21879) and the Fundación Médica Mutua Madrileña. AIA was supported by a postdoctoral contract from the Spanish Fondo de Investigaciones Sanitarias. The authors thank Prof. Julio Navascués and Dr. Amanda Sierra for scientific advice, Prof. Flora de Pablo for continuous encouragement and ideas, Dr. Owen Howard for editorial support, and Maite Seisdedos, Ana Robles and the staff of the CIB animal house for technical support.

## References

1. Sancho-Pelluz J, Arango-Gonzalez B, Kustermann S, Romero FJ, van Veen T, Zrenner E et al (2008) Photoreceptor cell death mechanisms in inherited retinal degeneration. Mol Neurobiol 38:253–269
2. Bramall AN, Wright AF, Jacobson SG, McInnes RR (2010) The genomic, biochemical, and cellular responses of the retina in inherited photoreceptor degenerations and prospects for the treatment of these disorders. Annu Rev Neurosci 33:441–472
3. de Pablo F, de la Rosa EJ (1995) The developing CNS: a scenario for the action of proinsulin, insulin and insulin-like growth factors. Trends Neurosci 18:143–150
4. Torres-Aleman I (2010) Toward a comprehensive neurobiology of IGF-I. Dev Neurobiol 70:384–396
5. Corrochano S, Barhoum R, Boya P, Arroba AI, Rodríguez-Muela N, Gómez-Vicente V et al (2008) Attenuation of vision loss and delay in apoptosis of photoreceptors induced by proinsulin in a mouse model of retinitis pigmentosa. Invest Ophthalmol Vis Sci 49:4188–4194
6. Arroba AI, Alvarez-Lindo N, van Rooijen N, de la Rosa EJ (2011) Microglia-mediated IGF-I neuroprotection in the rd10 mouse model of Retinitis Pigmentosa. Invest Ophthalmol Vis Sci 52:9124–9130
7. Karlstetter M, Ebert S, Langmann T (2010) Microglia in the healthy and degenerating retina: insights from novel mouse models. Immunobiology 215:685–691
8. Harada T, Harada C, Kohsaka S, Wada E, Yoshida K, Ohno S et al (2002) Microglia-Muller glia cell interactions control neurotrophic factor production during light-induced retinal degeneration. J Neurosci 22:9228–9236
9. Van Rooijen N, Sanders A (1994) Liposome mediated depletion of macrophages: mechanism of action, preparation of liposomes and applications. J Immunol Methods 174:83–93
10. Barhoum R, Martínez-Navarrete G, Corrochano S, Germain F, Fernandez-Sanchez L, de la Rosa EJ et al (2008) Functional and structural modifications during retinal degeneration in the rd10 mouse. Neuroscience 155:698–713
11. Arroba AI, Wallace D, Mackey A, de la Rosa EJ, Cotter TG (2009) IGF-I maintains calpastatin expression and attenuates apoptosis in several models of photoreceptor cell death. Eur J Neurosci 30:975–986
12. Lai AY, Todd KG (2008) Differential regulation of trophic and proinflammatory microglial effectors is dependent on severity of neuronal injury. Glia 56:259–270
13. Zeng HY, Zhu XA, Zhang C, Yang LP, Wu LM, Tso MO (2005) Identification of sequential events and factors associated with microglial activation, migration, and cytotoxicity in retinal degeneration in rd mice. Invest Ophthalmol Vis Sci 46:2992–2999
14. Del Río P, Irmler M, Arango-González B, Favor J, Bobe C, Bartsch U et al (2011) GDNF-induced osteopontin from Müller glial cells promotes photoreceptor survival in the Pde6b$^{rd1}$ mouse model of retinal degeneration. Glia 59:821–832

# Chapter 48
# The Neuroprotective Potential of Retinal Müller Glial Cells

**Stefanie M. Hauck, Christine von Toerne and Marius Ueffing**

**Abstract** Retinal Müller glial cells (RMG) are recognized as essential players providing neurotrophic, metabolic and structural support for retinal neurons as well as mediating inflammatory responses in the retina. While some key neuroprotective molecules in the context of retinal degeneration, such as FGF2, LIF, PEDF have been demonstrated to be of RMG origin, there is yet no comprehensive understanding on the multifaceted role of RMG in orchestrating diverse intercellular functions. In order to systematically as well as functionally analyse RMG reactivity to retinal degeneration and thus explore the RMG-derived signalling molecules in depth, we combined genomics and proteomics approaches based on profiling primary RMGs from mouse and pig. However, since modulations in cell to cell communication by secretion of molecules may not necessarily present with changes in the mRNA profile, we developed shotgun proteomics approaches enabling direct protein profiling of the RMG lysates and secretomes using label-free and SILAC quantitations. We have identified a pool of novel proteins relevant for pro-survival effects transmitted from RMG to retinal neurons and functionally valdidated selected molecules. Additionally, our approach allows to identify RMG reactions to intrinsic and extrinsic stimuli and thus enables to molecularly dissect RMG reactivity relevant for retinal health and disease.

**Keywords** Neuroprotection · Mass spectrometry · Quantitative proteomics · Secretome

S. M. Hauck (✉) · C. von Toerne · M. Ueffing
Research Unit Protein Science, Helmholtz Zentrum München, Ingolstädter Lanstr. 1, 85764, Neuherberg, Germany
e-mail: hauck@helmholtz-muenchen.de

C. von Toerne
e-mail: vontoerne@helmholtz-muenchen.de

M. Ueffing
Centre of Ophthalmology, Institute for Ophthalmic Research, University of Tübingen, Roentgenweg11, 72076 Tübingen, Germany
e-mail: marius.ueffing@uni-tuebingen.de

J. D. Ash et al. (eds.), *Retinal Degenerative Diseases,* Advances in Experimental Medicine and Biology 801, DOI 10.1007/978-1-4614-3209-8_48,

## 48.1 Introduction

Retinal Müller glial cells (RMG) have been recognised to play pivotal roles during retinal health and disease. Since RMG present the main glial cell population in the retina, their reactivation in response to all forms of injury or disease has crucial influence on pathogenesis. Such gliotic reactions are described to have both, detrimental as well as protective effects ("The Janus face of Müller cell gliosis") [1] and a comprehensive dissection of the relevant molecular processes offer the basis for rational therapy developments. Since RMG are capable to provide retinal neurons with neurotrophic support, there is a strong interest to define the molecules exerting such effects and potentially use these factors as therapeutics in selected retinal pathologies. Many neurotrophic molecules secreted by RMG have already been identified, such as bFGF, CNTF, BDNF, IGF1, LIF, PEDF and others [1, 2]. In the context of retinal gliosis, VEGF, which is released from RMG under gliosis stimulating conditions, is especially interesting, because it acts both, neuroprotective in low concentrations [3, 4], but high concentrations of VEGF cause all sorts of vascular pathologies [5] and is the main target for successful treatment against wet AMD [6].

## 48.2 In Vitro Model for Reactive RMG

In order to molecularly dissect the cell-to-cell communication processes between RMG and neurons, it is essential to isolate the respective cell types. We have established isolation of primary RMG from porcine, mouse and equine retinas [7–9] and found that those isolated cells respond to in vitro conditions with rapid changes of their protein expression patterns [7] and transformation into a proliferative phenotype. While the intermediate filament vimentin remains stably expressed in these cells [7], GFAP expression, which is likely induced during isolation of cells from the intact retina, is rapidly lost in vitro [10]. This is in line with reports from the chick retina, where only the sub-population of GFAP negative RMG become proliferative under NMDA-induced retinal damage [11] and may indicate that the primary RMG in vitro represent a subpopulation of RMG. Those RMG secrete a large variety of proteins (Fig. 48.1a), and only few of these protein in the conditioned media (CM) produced by these RMG have yet been identified. However, RMG-derived proteins have been demonstrated to rescue retinal neurons in several in vitro culture paradigms, such as retinal ganglion cells [12] and cone photoreceptors [13]. When this cocktail of proteins is supplied to primary isolated photoreceptors in vitro, specifically CM from primary RMG cultured for short periods (14 days) is able to significantly enhance survival of photoreceptors [14], while CM from RMG cultured longer (21 days) has lost this survival promoting activity (Fig. 48.1b). This setting provides a differential situation which enables to screen for the specific molecules involved in the pro-survival effects of gliotic RMG and can be used in transcriptomic and proteomic studies.

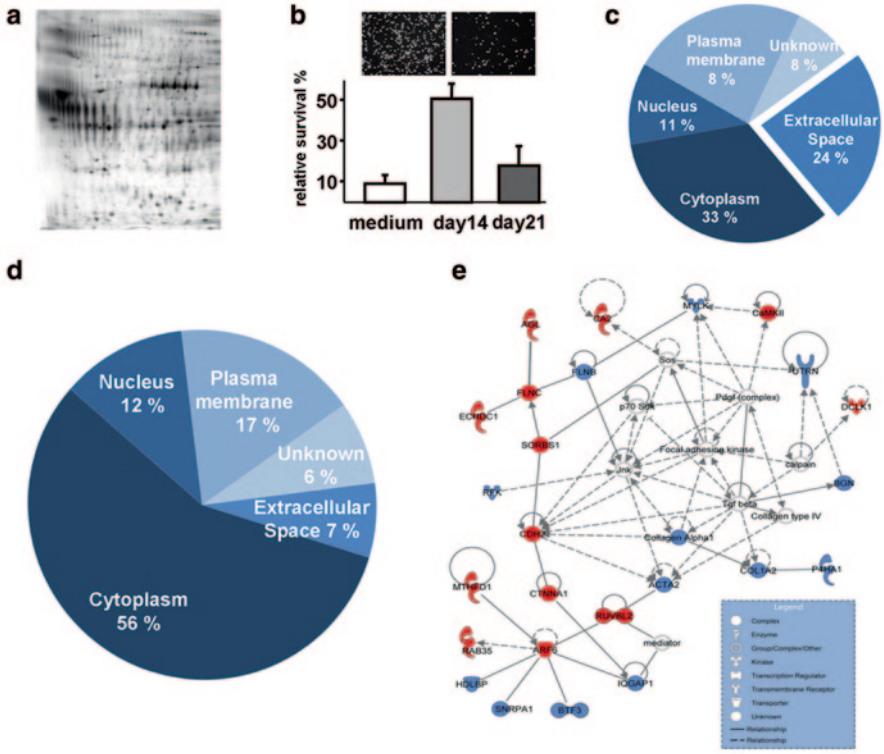


**Fig. 48.1** **a** The RMG secretome. Secreted proteins from primary porcine RMG after 14 days of in vitro cultures are labelled by $^{35}S$ incorporation and resolved by 2-dimensional SDS-PAGE. **b** Pro-survival effect of RMG secretome. Isolated primary porcine photoreceptors are treated with conditioned media (CM) containing secreted proteins from RMG cultured for either 14 days (*light grey bar*) or 21 days (*dark grey bar*) for 6 days in vitro. The amount of surviving cells is monitored by staining of life cells with esterase-driven calcein accumulation (example stainings are shown above the graph) and compared to incubation in medium alone (*white bar*). CM from day 14 RMG significantly increases the percentage of surviving cells as compared to CM from day 21 RMG. **c** Genomic profiling of primary RMG. Whole genome transcriptome arrays (Affymetrix Porcine Genome arrays containing 24000 probe sets) were probed with mRNA from RMG cultured for 14 or 21 days. The overall expression patterns are very similar and only 66 transcripts vary significantly (FDR < 5 %) between groups covering different cellular localisations. (Analysis performed with Ingenuity Pathway Analysis software). **d** Proteomic phenotyping of primary RMG. Total cell lysates of primary porcine RMG cultured for 14 and 21 days were processed for mass spectrometry and differences were retrieved by label-free analyses based on peptide peak intensities [10]. Within those lysates 272 proteins were expressed at significantly different levels (FDR < 5 %) covering different cellular localisations. **e** Top significant pathway modified during prolongued culturing. Pathway enrichment analyses (Ingenuity IPA$^{TM}$) performed with these proteins resulted in "cell-to-cell communication pathway" reported top significant. The pathway is built based on 25 of the input proteins either downregulated (*rot*) or upregulated (*blue*) during in vitro culturing

## 48.3 Genomic Profiling of Primary RMG

Transciptome studies of acutely isolated primary mouse RMG have provided a comprehensive catalogue of expression variation in these cells [15]. The specific difference between pro-survival effects of primary porcine RMG in response to in vitro culturing times prompted us to profile the respective transcriptomes with whole genome arrays [16]. Only 66 transcripts vary significantly (FDR <5%) between RMG day 14 and day 21 and subcellular localisation prediction allocates 15 of them to the secretory pathway (Fig. 48.1c). Among these potential candidates for the pro-survival effect are none of the previously reported neurotrophic molecules secreted by RMG. However, when those candidate molecules were tested on the photoreceptor survival assay, none of them proofed to be pro-survival effective (unpublished data).

## 48.4 Proteomic Phenotyping of RMG

In comparison to transcriptomic profiling, studying the proteome promises a more accurate fingerprint of the molecular phenotype defining a specific cellular condition. However, while transcriptome profiling is not limited with respect to simultaneous detection of a large variety of transcripts, proteomic profiling is often restricted to detection of highly expressed proteins and limited sensitivity is a severe obstacle. In early times of proteome analyses, two-dimensional separations of cell lysates followed by identification of isolated protein spots with MALDI mass spectrometry was the most efficient workflow. By this experimental approach, we could demonstrate that isolated primary porcine RMG profoundly change their protein profile within few days after isolation from the retina [7]. However, the proteome coverage was rather restricted and more recently we have applied state-of-the art LC-MSMS-based profiling methods to more comprehensively investigate the RMG proteome [10]. When comparing the two states of RMG which are functionally different with respect to survival supporting activity for photoreceptors, we found a total of 272 proteins significantly changed during the transition of day 14 to day 21 RMG in total cell lysates (Fig. 48.1d). This number is much higher than the result from the transcriptome arrays, although the proteome coverage can still not be expected to be complete. Interestingly, when the differentially expressed proteins are subject to pathway enrichment analysis, the top scoring pathway is “cell-to-cell communication” which suggests that the majority of changes comprise signal transduction pathways involving secreted proteins relevant for communication (Fig. 48.1e). This subset of differentially expressed proteins provides excellent candidates for the neurotrophic effect and will be functionally studied in future experiments.

## 48.5 Identification of Secreted Factors from RMG

In order to specifically screen for secreted proteins that could excert the reported pro-survival function to retinal neurons [12–14], two complementary strategies were followed. Since GDNF has been reported to functionally rescue photoreceptors in the rd1 mouse model for Retinitis Pigmentosa [17] and this effect is transmitted indirectly via activation of RMG [18, 19] we performed transcriptome profiling of mouse retina in response to GDNF and identified osteopontin (OPN) as a novel GDNF effector [8]. OPN is secreted from RMGs and supports photoreceptor survival in explant cultures of rd1 retinas and may thus be a candidate for direct pro-survival effect on photoreceptors. Complementary to the GDNF-induced screening of transcriptomes, we used mass spectrometry-based proteomic screening for directly investigating the protein inventory of RMG secretomes (Fig. 48.1a). A biochemical sub-fractionation strategy combined with high-throughput photoreceptor survival assays enabled to define a set of potential novel pro-survival proteins from RMG [14], namely connective tissue growth factor (CTGF) and insulin-like growth factor binding protein 5 (IGFBP5), which both prolongued photoreceptor survival in vitro when supplemented to CM. These two proteins are secreted from RMG and secretion of IGFBP5 was reported to decrease along in vitro culturing time [20] suggesting that this protein in contrast to other protein family members (IGFBP 1–6) is rather expressed in RMG in vivo and could thus be one of the factors functionally differentiating the efficacy of CM from RMG day 14 and day 21.

The recent advances in mass spectrometry combined with effective quantitation strategies [21] have enabled to analyse RMG cell lysates and secretomes in unprecedented detail [10, 22] and allow us to resolve the functional differences of the RMG in vitro model comprehensively. Stable isotope labelling with amino acids in cell sulture (SILAC) provides a robust mean to quantify protein expression changes identified by high resolution LC-MSMS and 39 candidate proteins correlating with the pro-survival effect were identified comprising the previously reported proteins and providing additional candiates yet to be validated [22].

## 48.6 Conclusion

Understanding RMG reactions in the context of cell-to-cell communication promises insight into neuroprotective as well as detrimental roles of these cells during retinal (patho-)physiology. We could establish quantitative proteomic methods that allow unbiased and sensitive detections of factors and molecular reactions of RMG. We currently develop strategies for effective quantitative assessment of subproteomes in response to varying stimuli, such as GDNF, IFNg and LPS. To gain insight into changes on the cell-surface and receptor level, we are further developing specific enrichment tools for plasma membrane proteins based on capturing techniques in combination with affinity purification and mass spectrometry [23].

**Acknowledgments** This work was supported by the European Community's 7th Framework Programme through Marie Curie Initial Training Network Edu-GLIA (PITN-GA-2009-237956) and the German Federal Ministry of Education and Research (HOPE – FKZ 01GM0852).

## References

1. Bringmann A, Iandiev I, Pannicke T, Wurm A, Hollborn M, Wiedemann P, Osborne NN, Reichenbach A (2009) Cellular signaling and factors involved in Muller cell gliosis: neuroprotective and detrimental effects. Progr Retin Eye Res 28(6):423–451
2. Bringmann A, Pannicke T, Grosche J, Francke M, Wiedemann P, Skatchkov SN, Osborne NN, Reichenbach A (2006) Muller cells in the healthy and diseased retina. Progr Retin Eye Res 25(4):397–424
3. Yamada H, Yamada E, Hackett SF, Ozaki H, Okamoto N, Campochiaro PA (1999) Hyperoxia causes decreased expression of vascular endothelial growth factor and endothelial cell apoptosis in adult retina. J Cell Physiol 179(2):149–156
4. Kurihara T, Westenskow PD, Bravo S, Aguilar E, Friedlander M (2012) Targeted deletion of Vegfa in adult mice induces vision loss. J Clin Invest 122(11):4213–4217
5. Tolentino MJ, McLeod DS, Taomoto M, Otsuji T, Adamis AP, Lutty GA (2002) Pathologic features of vascular endothelial growth factor-induced retinopathy in the nonhuman primate. Am J Ophthalmol 133(3):373–385
6. Kovach JL, Schwartz SG, Flynn HW Jr, Scott IU (2012) Anti-VEGF treatment strategies for wet AMD. J Ophthalmol 2012:786870
7. Hauck SM, Suppmann S, Ueffing M (2003) Proteomic profiling of primary retinal Muller glia cells reveals a shift in expression patterns upon adaptation to in vitro conditions. Glia 44(3):251–263
8. Del Rio P, Irmler M, Arango-Gonzalez B, Favor J, Bobe C, Bartsch U, Vecino E, Beckers J, Hauck SM, Ueffing M (2011) GDNF-induced osteopontin from Muller glial cells promotes photoreceptor survival in the Pde6brd1 mouse model of retinal degeneration. Glia 59(5):821–832
9. Eberhardt C, Amann B, Feuchtinger A, Hauck SM, Deeg CA (2011) Differential expression of inwardly rectifying K+ channels and aquaporins 4 and 5 in autoimmune uveitis indicates misbalance in Muller glial cell-dependent ion and water homeostasis. Glia 59(5):697–707
10. Merl J, Ueffing M, Hauck SM, von Toerne C (2012) Direct comparison of MS-based label-free and SILAC quantitative proteome profiling strategies in primary retinal Muller cells. Proteomics 12(12):10
11. Fischer AJ, Schmidt M, Omar G, Reh TA (2004) BMP4 and CNTF are neuroprotective and suppress damage-induced proliferation of Muller glia in the retina. Mol Cell Neurosci 27(4):531–542
12. Garcia M, Forster V, Hicks D, Vecino E (2002) Effects of muller glia on cell survival and neuritogenesis in adult porcine retina in vitro. Invest Ophthalmol Vis Sci 43(12):3735–3743
13. Balse E, Tessier LH, Fuchs C, Forster V, Sahel JA, Picaud S (2005) Purification of mammalian cone photoreceptors by lectin panning and the enhancement of their survival in glia-conditioned medium. Invest Ophthalmol Vis Sci 46(1):367–374
14. Hauck SM, Gloeckner CJ, Harley ME, Schoeffmann S, Boldt K, Ekstrom PA, Ueffing M (2008) Identification of paracrine neuroprotective candidate proteins by a functional assay-driven proteomics approach. Mol Cell Proteomics 7(7):1349–1361
15. Roesch K, Jadhav AP, Trimarchi JM, Stadler MB, Roska B, Sun BB, Cepko CL (2008) The transcriptome of retinal Muller glial cells. J Comp Neurol 509(2):225–238
16. Hauck SM, Schoeffmann S, del Río P, Sarioglu H, Beckers J, Ueffing M (2009) Secreted proteins from primary retinal Mueller glial cells: a combined genomics and proteomics approach. ARVO 2009

17. Frasson M, Sahel JA, Fabre M, Simonutti M, Dreyfus H, Picaud S (1999) Retinitis pigmentosa: rod photoreceptor rescue by a calcium-channel blocker in the rd mouse. Nat Med 5(10):1183–1187
18. Harada C, Harada T, Quah HM, Maekawa F, Yoshida K, Ohno S, Wada K, Parada LF, Tanaka K (2003) Potential role of glial cell line-derived neurotrophic factor receptors in Muller glial cells during light-induced retinal degeneration. Neuroscience 122(1):229–235
19. Hauck SM, Ekstrom PA, Ahuja-Jensen P, Suppmann S, Paquet-Durand F, van Veen T, Ueffing M (2006) Differential modification of phosducin protein in degenerating rd1 retina is associated with constitutively active $Ca^{2+}$/calmodulin kinase II in rod outer segments. Mol Cell Proteomics 5(2):324–336
20. King JL, Guidry C (2004) Muller cell production of insulin-like growth factor-binding proteins in vitro: modulation with phenotype and growth factor stimulation. Invest Ophthalmol Vis Sci 45(12):4535–4542
21. Gstaiger M, Aebersold R (2009) Applying mass spectrometry-based proteomics to genetics, genomics and network biology. Nat Rev Genet 10(9):617–627
22. von Toerne C, Hauck SM, Ueffing M (in preparation) Identification and relative quantification of neurotrophic factors in RMG supernatants using the SILAC approach
23. Bausch-Fluck D, Hofmann A, Wollscheid B (2012) Cell surface capturing technologies for the surfaceome discovery of hepatocytes. Methods Mol Biol 909:1–16

# Chapter 49
# Leukemia Inhibitory Factor Signaling in Degenerating Retinas

**Cavit Agca and Christian Grimm**

**Abstract** Degeneration of cells in the retina is a hallmark of various inherited and acquired blinding diseases in humans. One of the most challenging problems to establish successful treatments for these diseases is to understand the molecular mechanisms that result in retinal degeneration and to identify endogenous rescue pathways which support cell survival. In many mouse models for retinal degeneration, expression of LIF in glial cells in response to a disease condition is crucial for the activation of an elaborate protective system. This mini review will summarize the findings that are related to LIF signaling and discuss the neuroprotective effects of LIF in different animal models.

**Keywords** LIF · Retina · Neuroprotection · STAT3 · Photoreceptor apoptosis

## 49.1 Introduction

Leukemia inhibitory factor/cholinergic differentiation factor (LIF) is a glycoprotein belonging to the interleukin 6 (IL-6) family of cytokines. LIF is a pleiotropic cytokine involved in several processes during embryogenesis, development and adulthood. However, the most well-known function of LIF is the long-term maintenance of stem cell pluripotency [1].

Previously, *Lif* has been thought to be eutherian specifically due to its role in embryonic implantation. Surprisingly, however, *Lif* orthologs have also been identified in several teleost species, in a marsupial (kangaroo) and in *G. gallus* [2–5]. Human

C. Grimm (✉) · C. Agca
Lab for Retinal Cell Biology, Department of Ophthalmology, University of Zurich, Zurich, Switzerland
e-mail: cgrimm@opht.uzh.ch

C. Agca
e-mail: cavitagca@gmail.com

J. D. Ash et al. (eds.), *Retinal Degenerative Diseases,* Advances in Experimental Medicine and Biology 801, DOI 10.1007/978-1-4614-3209-8_49,

and mouse have been shown to express three LIF isoforms, LIF-D, LIF-M, and LIF-T, derived from alternative splicing. LIF-D and LIF-M have alternative first exons and identical second and third exons [6–8]. LIF-M can be either active intracellularly or secreted and localized in the extracellular matrix [6, 7]. LIF-D is the diffusible form of LIF and signals through the LIF receptor—gp130 complex, which initiates the Janus kinase/signal transducer and activator of transcription (JAK/STAT) signaling pathway [6, 7]. The truncated form of LIF, LIF-T, does not have the signal sequence, is not secreted and may induce apoptosis in cells [9].

## 49.2 Neuroprotective Role of LIF

In the early 90's, LIF's neuroprotective potential has been recognized in cultured neuronal cells [10, 11] and in various injury and disease models [12, 13]. Similarly to the central and peripheral nervous system, evidence support the existence of endogenous pathways to increase survival of neuronal cells during degenerative diseases of the retina [14–19]. Among several neurotrophic factors that are involved in retinal neuroprotection, LIF has been shown to be one of the most important endogenous proteins for both photoreceptor and retinal ganglion cell (RGC) protection [18, 20].

### *49.2.1 Neuroprotective Role of LIF During Photoreceptor Injury*

Expression of a mutant rod opsin or exposure to bright light causes photoreceptors to degenerate, induces *Lif* expression in the retina, and activates STAT3 in photoreceptors [21]. Lack of LIF accelerates degeneration [18, 22] and phosphorylation of STAT3 by exogenously applied recombinant LIF provides protection [23] that has been attributed to extensive signaling between Muller cells and photoreceptors [24]. Injured photoreceptors signal to Muller glia through photoreceptor-derived endothelin-2 (EDN2) and endothelin receptor B (EDNRB) on Muller cells [24]. Absence of LIF interrupts this signaling cascade and inhibits induction of various genes including, *Edn2*, *Stat3*, *Gfap* (glial fibrillary acidic protein), and *Fgf2* (fibroblast growth factor 2) [18], suggesting that LIF is a key protein controlling the protective response. Most likely, protection by LIF requires expression of the common receptor for IL-6 family of cytokines (gp130) in photoreceptors [25]. *Lif* upregulation and STAT3 activation have also been demonstrated in different inherited mouse models of photoreceptor degeneration including rd10 and cpfl1 [26, 27]. This indicates that induction of the protective LIF signaling cascade is a general response to photoreceptor injury supporting its importance for cell survival in the retina. However, robust overexpression of D-LIF in lens using the αA-crystallin promoter resulted in developmental defects in the retina [28, 29]. Thus, dosage and timing of LIF expression seem critical for retinal physiology and neuroprotection.

### *49.2.2 Neuroprotective Role of LIF During RGC Degeneration*

Neuroprotective effects of LIF on RGCs were first identified in a model of RGC apoptosis after removal of the superior colliculus [30]. Subsequent in vitro studies showed that LIF has also neurotrophic effects, as it enhances the neurite outgrowth of RGCs in a dose dependent manner [20]. Lack of LIF and CNTF (ciliary neurotrophic factor) in double-knockout-mice inhibited activation of STAT3 and severely impaired regeneration and survival of RGCs after optic nerve crush injury [20], further underscoring the protective effect of LIF on RGCs. Since *Lif* expression and STAT3 phosphorylation are also induced in a toxicity model of RGC degeneration [31], activation of LIF-mediated protective signaling may, in analogy to photoreceptor degeneration, constitute a general response to RGC injury.

## 49.3 Induction of LIF During Retinal Disease

Although we have now extensive knowledge on neurotrophic factors that are expressed in response to retinal disease, we still do not understand the exact mechanisms of how induction of these neuroprotective factors is regulated in the degenerative retina. One mutually accepted hypothesis depends on redox signaling [32, 33]. Redox signaling through reactive oxygen species (ROS), such as $H_2O_2$, superoxides, and hydroxyl radicals, and through the oxidation of proteins, has important roles in signal transduction and is involved in many biological pathways [34]. Strong evidence suggests that ROS production is accelerated in the damaged retina [35, 36] and that $H_2O_2$ is generated by stressed photoreceptors through an NADPH oxidase dependent pathway [33, 35, 37]. Endogenously produced ROS inhibit protein-phosphatase2A and induce extracellular signal regulated kinase 1/2, which argues that $H_2O_2$ might be one of the signaling molecules inducing survival pathways [38, 39]. Although a direct connection between redox signaling and neurotrophic factors has not yet been elucidated in vivo, a recent report showed that exogenously applied $H_2O_2$ upregulated the neuroprotective cytokine *IL-6* in a retinal pigment epithelium culture system [40].

## 49.4 Source of LIF During Retinal Degeneration

Previously, we have shown that LIF is expressed in Muller cells during light induced and inherited photoreceptor degeneration [18]. Interestingly, LIF is not induced in the whole Muller cell population, but only in a small subset of cells [18]. The discovery of a LIF-expressing subset of Muller cells argues for the existence of different classes of Muller cells with potentially diverse functions. However, it might also be possible that the pattern of *Lif* expression is a result of injury-derived subdifferentiation of Muller cells. Regardless of the model, the basis of the Muller

cell heterogeneity is not known and requires a detailed characterization of the *Lif* expressing subset, especially with respect to its neuroprotective potential. Intriguingly, LIF seems to be expressed in the whole astrocyte population during RGC degeneration [20]. This strongly argues that the source of LIF may vary in the different models of retinal degeneration and may depend on the injured cell type.

## 49.5 Perspectives

Although it is well documented that LIF is neuroprotective in the retina and that its activity strongly correlates with the activation of STAT3 transcription factor, regulation of *Lif* gene expression in response to retinal injury is still an unresolved issue. *Lif* has a distinct gene architecture and can be expressed in three isoforms. In addition, the *Lif* transcript has conserved cis-acting elements in the 3′UTR and a possible 5′UTR heterogeneity. In addition to the neuroprotective capacity of the LIF protein, these features increase the regulatory complexity of *Lif* gene expression and of potential posttranscriptional processes, which makes this cytokine very interesting to study. We are just at the beginning of understanding the mechanisms related to the activity of LIF and other neurotrophic factors in the retina. It is also intriguing to note the connection between LIF as a factor for stem cell pluripotency and evidence that mammalian Muller cells may have some stem cell properties. Might the *Lif*-expressing Muller cells define a subpopulation with increased stem cell potential in the adult retina? To uncover all aspects of LIF-mediated neuroprotection and other effects, further studies will need to focus on the transcriptional and posttranscriptional regulation of gene expression as well as on LIF target molecules and interaction partners.

## References

1. Pease S, Braghetta P, Gearing D, Grail D, Williams RL (1990) Isolation of embryonic stem (ES) cells in media supplemented with recombinant leukemia inhibitory factor (*LIF*). Dev Biol 141(2):344–352
2. Cui S, Hope RM, Rathjen J, Voyle RB, Rathjen PD (2001) Structure, sequence and function of a marsupial *LIF* gene: conservation of IL-6 family cytokines. Cytogenet Cell Genet 92(3-4):271–278
3. Abe T, Mikekado T, Haga S, Kisara Y, Watanabe K, Kurokawa T, Suzuki T (2007) Identification, cDNA cloning, and mRNA localization of a zebrafish ortholog of leukemia inhibitory factor. Comp Biochem Physiol B Biochem Mol Biol 147(1):38–44
4. Hanington PC, Patten SA, Reaume LM, Waskiewicz AJ, Belosevic M, Ali DW (2008) Analysis of leukemia inhibitory factor and leukemia inhibitory factor receptor in embryonic and adult zebrafish (Danio rerio). Dev Biol 314(2):250–260
5. Horiuchi H, Tategaki A, Yamashita Y, Hisamatsu H, Ogawa M, Noguchi T, Aosasa M, Kawashima T, Akita S, Nishimichi N, Mitsui N, Furusawa S, Matsuda H (2004) Chicken leukemia inhibitory factor maintains chicken embryonic stem cells in the undifferentiated state. J Biol Chem 279(23):24514–24520

6. Rathjen PD, Toth S, Willis A, Heath JK, Smith AG (1990) Differentiation inhibiting activity is produced in matrix-associated and diffusible forms that are generated by alternate promoter usage. Cell 62(6):1105–1114
7. Conquet F, Peyrieras N, Tiret L, Brulet P (1992) Inhibited gastrulation in mouse embryos overexpressing the leukemia inhibitory factor. Proc Natl Acad Sci U S A 89(17):8195–8199
8. Haines BP, Voyle RB, Pelton TA, Forrest R, Rathjen PD (1999) Complex conserved organization of the mammalian leukemia inhibitory factor gene: regulated expression of intracellular and extracellular cytokines. J Immunol 162(8):4637–4646
9. Haines BP, Voyle RB, Rathjen PD (2000) Intracellular and extracellular leukemia inhibitory factor proteins have different cellular activities that are mediated by distinct protein motifs. Mol Biol Cell 11(4):1369–1383
10. Martinou JC, Martinou I, Kato AC (1992) Cholinergic differentiation factor (CDF/*LIF*) promotes survival of isolated rat embryonic motoneurons in vitro. Neuron 8(4):737–744
11. Murphy M, Reid K, Hilton DJ, Bartlett PF (1991) Generation of sensory neurons is stimulated by leukemia inhibitory factor. Proc Natl Acad Sci U S A 88(8):3498–3501
12. Trouillas M, Saucourt C, Guillotin B, Gauthereau X, Taupin JL, Moreau JF, Boeuf H (2009) The LIF cytokine: towards adulthood. Eur Cytokine Netw 20(2):51–62
13. Mathieu ME, Saucourt C, Mournetas V, Gauthereau X, Theze N, Praloran V, Thiebaud P, Boeuf H (2012) *LIF*-dependent signaling: new pieces in the Lego. Stem Cell Rev 8(1):1–15
14. Azadi S, Johnson LE, Paquet-Durand F, Perez MT, Zhang Y, Ekstrom PA, van Veen T (2007) CNTF+BDNF treatment and neuroprotective pathways in the rd1 mouse retina. Brain Res 1129(1):116–129
15. Campochiaro PA, Nguyen QD, Shah SM, Klein ML, Holz E, Frank RN, Saperstein DA, Gupta A, Stout JT, Macko J, DiBartolomeo R, Wei LL (2006) Adenoviral vector-delivered pigment epithelium-derived factor for neovascular age-related macular degeneration: results of a phase I clinical trial. Hum Gene Ther 17(2):167–176
16. Frigg R, Wenzel A, Grimm C (2005) Reme CE. [Survival factors in the treatment of hereditary retinal degeneration]. Ophthalmologe 102(8):757–763
17. Grimm C, Wenzel A, Groszer M, Mayser H, Seeliger M, Samardzija M, Bauer C, Gassmann M, Reme CE (2002) HIF-1-induced erythropoietin in the hypoxic retina protects against light-induced retinal degeneration. Nat Med 8(7):718–724
18. Joly S, Lange C, Thiersch M, Samardzija M, Grimm C (2008) Leukemia inhibitory factor extends the lifespan of injured photoreceptors in vivo. J Neurosci 28(51):13765–13774
19. Sahel JA (2005) Saving cone cells in hereditary rod diseases: a possible role for rod-derived cone viability factor (RdCVF) therapy. Retina 25(8 Suppl):S38–S39
20. Leibinger M, Muller A, Andreadaki A, Hauk TG, Kirsch M, Fischer D (2009) Neuroprotective and axon growth-promoting effects following inflammatory stimulation on mature retinal ganglion cells in mice depend on ciliary neurotrophic factor and leukemia inhibitory factor. J Neurosci 29(45):14334–14341
21. Samardzija M, Wenzel A, Aufenberg S, Thiersch M, Reme C, Grimm C (2006) Differential role of Jak-STAT signaling in retinal degenerations. FASEB J 20(13):2411–2413
22. Burgi S, Samardzija M, Grimm C (2009) Endogenous leukemia inhibitory factor protects photoreceptor cells against light-induced degeneration. Mol Vis 15:1631–1637
23. Ueki Y, Wang J, Chollangi S, Ash JD (2008) STAT3 activation in photoreceptors by leukemia inhibitory factor is associated with protection from light damage. J Neurochem 105(3):784–796
24. Rattner A, Nathans J (2005) The genomic response to retinal disease and injury: evidence for endothelin signaling from photoreceptors to glia. J Neurosci 25(18):4540–4549
25. Ueki Y, Le YZ, Chollangi S, Muller W, Ash JD (2009) Preconditioning-induced protection of photoreceptors requires activation of the signal-transducing receptor gp130 in photoreceptors. Proc Natl Acad Sci U S A 106(50):21389–21394
26. Schaeferhoff K, Michalakis S, Tanimoto N, Fischer MD, Becirovic E, Beck SC, Huber G, Rieger N, Riess O, Wissinger B, Biel M, Seeliger MW, Bonin M (2010) Induction of STAT3-

related genes in fast degenerating cone photoreceptors of cpfl1 mice. Cell Mol Life Sci 67(18):3173–3186
27. Samardzija M, Wariwoda H, Imsand C, Huber P, Heynen SR, Gubler A, Grimm C (2012) Activation of survival pathways in the degenerating retina of rd10 mice. Exp Eye Res 99:17–26
28. Graham DR, Overbeek PA, Ash JD (2005) Leukemia inhibitory factor blocks expression of Crx and Nrl transcription factors to inhibit photoreceptor differentiation. Invest Ophthalmol Vis Sci 46(7):2601–2610
29. Ash J, McLeod DS, Lutty GA (2005) Transgenic expression of leukemia inhibitory factor (LIF) blocks normal vascular development but not pathological neovascularization in the eye. Mol Vis 11:298–308
30. Cui Q, Harvey AR (1995) At least two mechanisms are involved in the death of retinal ganglion cells following target ablation in neonatal rats. J Neurosci 15(12):8143–8155
31. Deparis S, Caprara C, Grimm C (2012) Intrinsically photosensitive retinal ganglion cells are resistant to N-methyl-D-aspartic acid excitotoxicity. Mol Vis 18:2814–2827
32. Groeger G, Quiney C, Cotter TG (2009) Hydrogen peroxide as a cell-survival signaling molecule. Antioxid Redox Signal 11(11):2655–2671
33. Mackey AM, Sanvicens N, Groeger G, Doonan F, Wallace D, Cotter TG (2008) Redox survival signalling in retina-derived 661W cells. Cell Death Differ 15(8):1291–1303
34. Rhee SG (2006) Cell signaling $H_2O_2$, a necessary evil for cell signaling. Science 312(5782):1882–1883
35. Bhatt L, Groeger G, McDermott K, Cotter TG (2010) Rod and cone photoreceptor cells produce ROS in response to stress in a live retinal explant system. Mol Vis 16:283–293
36. Sharma AK, Rohrer B (2007) Sustained elevation of intracellular cGMP causes oxidative stress triggering calpain-mediated apoptosis in photoreceptor degeneration. Curr Eye Res 32(3):259–269
37. Groeger G, Mackey AM, Pettigrew CA, Bhatt L, Cotter TG (2009) Stress-induced activation of Nox contributes to cell survival signalling via production of hydrogen peroxide. J Neurochem 109(5):1544–1554
38. Finnegan S, Mackey AM, Cotter TG (2010) A stress survival response in retinal cells mediated through inhibition of the serine/threonine phosphatase PP2A. Eur J Neurosci 32(3):322–334
39. Groeger G, Doonan F, Cotter TG, Donovan M (2012) Reactive oxygen species regulate prosurvival ERK1/2 signaling and bFGF expression in gliosis within the retina. Invest Ophthalmol Vis Sci 53(10):6645–6654
40. Wu WC, Hu DN, Gao HX, Chen M, Wang D, Rosen R, McCormick SA (2010) Subtoxic levels hydrogen peroxide-induced production of interleukin-6 by retinal pigment epithelial cells. Mol Vis 16:1864–1873

# Chapter 50
# In Vivo Function of the ER-Golgi Transport Protein LMAN1 in Photoreceptor Homeostasis

**Hong Hao, Janina Gregorski, Haohua Qian, Yichao Li, Chun Y Gao, Sana Idrees and Bin Zhang**

**Abstract** LMAN1 is a type I transmembrane protein that selectively transports its cargo proteins from ER to ER-Golgi intermediate compartment (ERGIC) and Golgi. *Lman1* is a direct target of the transcription factor NRL in mouse retina. Therefore, we examined the in vivo function of LMAN1 in retina. Although *Lman1*$^{-/-}$ mouse eyes did not show abnormality in histology and electroretinogram analysis at 3 months, *Lman1*$^{-/-}$ retina at 6 months showed a decrease in cis-Golgi markers

H. Hao (✉)
Neurobiology-Neurodegeneration & Repair Laboratory, National Eye Institute,
NIH, MSC0610, 6 Center Drive,
Bethesda, MD 20892, USA
e-mail: haoh@mail.nih.gov

J. Gregorski
Graduate School of Basic Medical Sciences, New York Medical College,
Valhalla, NY 10595, USA
e-mail: janina_gregorski@nymc.edu

H. Qian · Y. Li
Visual Function Core, National Eye Institute, 49 Convent Dr.,
Bethesda, MD 20892, USA
e-mail: haohua.qian@nih.gov

Y. Li
e-mail: Yichao.li@nih.gov

C. Y. Gao
Biological Imaging Core Facility, National Eye Institute, 49 Convent Drive,
Bethesda, MD 20892, USA

S. Idrees
School of Medicine, The George Washington University, 2300 Eye Street,
NW, Washington, DC 20037, USA
e-mail: sidrees@gwmail.gwu.edu

B. Zhang
Genomic Medicine Institute, Lerner Research Institute, Cleveland Clinic Foundation,
Cleveland, OH, USA
e-mail: zhangb@ccf.org

J. D. Ash et al. (eds.), *Retinal Degenerative Diseases,* Advances in Experimental Medicine and Biology 801, DOI 10.1007/978-1-4614-3209-8_50,

GM130 and GRASP65. We also observed abnormal level and location of Rhodopsin in these mice. Taken together, LMAN1 may play a role in photoreceptor gene transport and homeostasis.

**Keywords** LMAN1 · NRL · Photoreceptor · Transport · Homeostasis

## 50.1 Introduction

LMAN1 (also known as ERGIC-53) is a type I transmembrane protein that is located at ER, ER-Golgi intermediate compartment (ERGIC) and cis-Golgi [1]. LMAN1 facilitates transport of several cargo proteins including factors critical to the coagulation cascade from ER to Golgi [1, 2]. Mutations in *LMAN1* cause combined deficiency of factor V and factor VIII, a genetic bleeding disorder [1]. We previously identified *Lman1* as a direct target of the transcription factor neural retina leucine zipper (NRL) in mouse retina [3]. The rod photoreceptor specific transcription factor NRL regulates the expression of genes that are important for the rod photoreceptor development and homeostasis, and mutations in over 20 of NRL target genes have been associated with retinal diseases [4]. We hypothesize that LMAN1 facilitates transport of photoreceptor genes and is important for the functional maintenance of mature rod photoreceptors. In this study, we tested this hypothesis using the *Lman1*$^{-/-}$ mice.

## 50.2 Materials and Methods

### *50.2.1 Animal Care and Use*

*Lman1*$^{-/-}$ mice were generated previously using a gene-trap strategy [5]. The Institutional Animal Care and Use Committees at the Cleveland Clinic Foundation and the National Eye Institute approved the animal care and use procedures. PCR analysis for genotyping was performed as previously described [5].

### *50.2.2 Immunohistochemistry*

Retinas were dissected, fixed in 4% paraformaldehyde, and cryoprotecetd in 30% sucrose. Retinal sections were probed with the primary antibodies overnight. The slides were stained with secondary antibody AlexaFluor 568 (Invitrogen) and counterstained with DAPI (1 μg/mL). Sections were visualized using an Olympus FluoView FV1000 confocal laser scanner and BX61WI microscope (Center Valley).

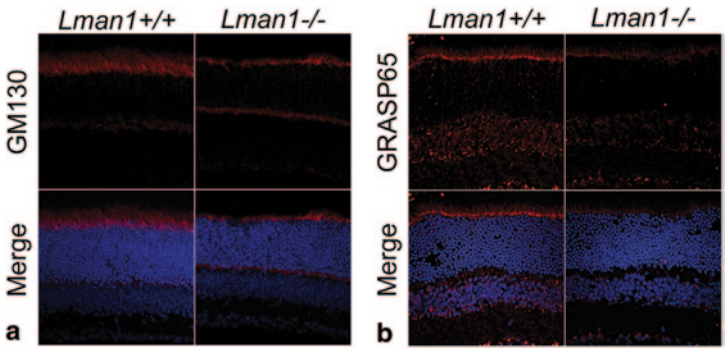


**Fig. 50.1** The effect of LMAN1 deficiency on GM130 and GRASP65. Representative images of immunohistochemistry staining of GM130 (**a**), and GRASP65 (**b**) in retinal sections of *Lman*$^{+/+}$and *Lman*$^{-/-}$ mice at 6 months. Antibody staining is shown in *red* and DAPI staining is shown in *blue*

## 50.3 Results

Hematoxylin and eosin stain did not reveal gross abnormalities in histology of *Lman1*$^{-/-}$ eyes at 3 months of age (data not shown). To examine whether photoreceptor function was compromised, we measured the electroretinogram (ERG) of these mice. No abnormalities in either scotopic or photopic ERGs were observed at 3 months, in line with the normal histology observed at this age (data not shown). These data prompted us to examine *Lman1*$^{-/-}$ eyes at a later stage.

To test the involvement of LMAN1 in ER to Golgi trafficking in photoreceptors, we examined the effect of LMAN1 deficiency on cis-Golgi markers GM130 and GRASP65, using immunohistochemistry on retina sections. We observed a small

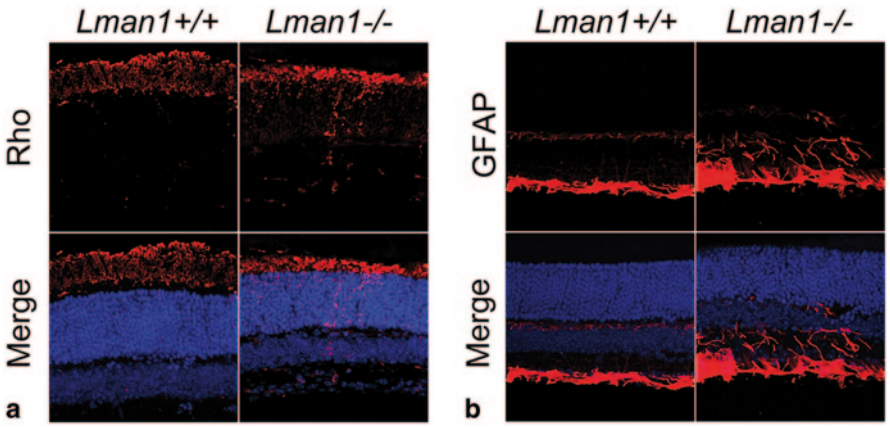


**Fig. 50.2** The effect of LMAN1 deficiency on Rhodopsin (*Rho*) and GFAP. Representative images of immunohistochemistry staining of Rho (**a**) and GFAP (**b**) in retinal sections of *Lman*$^{+/+}$and *Lman*$^{-/-}$ mice at 6 months. Antibody staining is shown in *red* and DAPI staining is shown in *blue*

decrease in GM130 and GRASP65 signal in *Lman1*$^{-/-}$ retina section compared to wild type litter-mates at 6 months (Fig. 50.1). To test the potential role of LMAN1 in photoreceptor gene transport, we examined the effect of LMAN1 deficiency on Rhodopsin (Rho). We observed a small decrease in Rho signal in outer segment and an increased staining of Rho in outer nuclear layer at 6 months, suggesting abnormal transport of Rho (Fig. 50.2a). Increased GFAP staining in *Lman1*$^{-/-}$ retina indicates that these retinas are under stress (Fig. 50.2b).

## 50.4 Discussion

Rod and cone photoreceptors are light sensing neurons responsible for vision under dim light and bright light, respectively. Photoreceptor outer segment (OS), the specialized apical cellular extension housing the phototransduction components, undergoes a complete renewal over the course of 10 days [6]. As a result, photoreceptors are under high demands for protein synthesis and transport. Abnormal expression or trafficking of the rod photoreceptor photo-pigment, Rho, has been associated with photoreceptor degeneration [7]. The mechanism of Rho transport is not clear.

The rod photoreceptor specific transcription factor NRL is the master regulator of rod photoreceptor development and homeostasis [4]. We previously identified global NRL target genes and validated the functional importance of many of the targets by in vivo shRNA knockdown experiments [3]. Although LMAN1 is expressed in numerous tissues, the levels of expression vary greatly, with strong expression observed in mouse retina [5]. In addition, *Lman1* expression in rod photoreceptors is specifically regulated by NRL [3]. These observations suggest that LMAN1 may be of functional importance to rod homoeostasis.

LMAN1 is known to cycle between the ER and ERGIC to transport selective cargo proteins from ER [1]. GM130 continuously cycles between the ERGIC and the *cis*-Golgi compartments and is tethered to the *cis*-Golgi by GRASP65 [8]. Vesicles formed from ERGIC undergo tethering and fusion at the *cis*-Golgi region to form larger membrane units and get incorporated into the Golgi stacks. Both GM130 and GRASP65 are required for this process, and hence are important for the maintenance of Golgi [9, 10]. We observed a small decrease in GM130 and GRASP65 in *Lman1*$^{-/-}$ eye. It is possible that LMAN1 deficiency affected the vesicle trafficking from ER to ERGIC, and the downstream trafficking from ERGIC to Golgi.

We observed a small decrease of Rho in outer segment and an increase of Rho in outer nuclear layer *Lman1*$^{-/-}$ eye. This suggests that LMAN1 could play a role in Rho transport. As abnormal trafficking of Rho has been associated with photoreceptor degeneration [7], we observed an increase in GFAP in *Lman1*$^{-/-}$ eye, suggesting that the *Lman1*$^{-/-}$ retina is under stress. Additional cargos and molecular mechanism of LMAN1 function in photoreceptors need to be investigated.

In summary, the ER-Golgi transport protein LMAN1 may play a role in photoreceptor gene transport. The global NRL target genes may serve as an excellent resource to facilitate the identification of retinal disease genes.

**Acknowledgments** We thank Dr. Anand Swaroop for advice and support. We also thank N-NRL members for technical assistance. This study was supported by Intramural Programs of the National Eye Institute.

## References

1. Zhang YC, Zhou Y, Yang CZ, Xiong DS (2009) A review of ERGIC-53: its structure, functions, regulation and relations with diseases. Histol histopathol 24:1193–204
2. Zhang B, Kaufman RJ, Ginsburg D (2005) LMAN1 and MCFD2 form a cargo receptor complex and interact with coagulation factor VIII in the early secretory pathway. J Biol Chem 280:25881–25886
3. Hao H, Kim DS, Klocke B, Johnson KR, Cui K, Gotoh N et al (2012) Transcriptional regulation of rod photoreceptor homeostasis revealed by in vivo NRL targetome analysis. PLoS genetics 8:e1002649
4. Swaroop A, Kim D, Forrest D (2010) Transcriptional regulation of photoreceptor development and homeostasis in the mammalian retina. Nature reviews. Neuroscience 11:563–576
5. Zhang B, Zheng C, Zhu M, Tao J, Vasievich MP, Baines A et al (2011) Mice deficient in LMAN1 exhibit FV and FVIII deficiencies and liver accumulation of alpha1-antitrypsin. Blood 118:3384–3391
6. Young RW (1967) The renewal of photoreceptor cell outer segments. J Cell Biol 33:61–72
7. Malanson KM, Lem J (2009) Rhodopsin-mediated retinitis pigmentosa. Prog Mol Biol Transl Sci 88:1–31
8. Barr FA, Nakamura N, Warren G (1998) Mapping the interaction between GRASP65 and GM130, components of a protein complex involved in the stacking of Golgi cisternae. EMBO J 17:3258–3268
9. Linstedt AD, Hauri HP (1993) Giantin, a novel conserved Golgi membrane protein containing a cytoplasmic domain of at least 350 kDa. Mol Biol Cell 4:679–693
10. Marra P, Salvatore L, Mironov A, Jr. Di Campli A, Di Tullio G, Trucco A et al (2007) The biogenesis of the Golgi ribbon: the roles of membrane input from the ER and of GM130. Mol Biol Cell 18, 1595–1608

# Chapter 51
# Investigating the Role of Retinal Müller Cells with Approaches in Genetics and Cell Biology

**Suhua Fu, Meili Zhu, John D. Ash, Yunchang Wang and Yun-Zheng Le**

**Abstract** Müller cells are major macroglia and play many essential roles as a supporting cell in the retina. As Müller cells only constitute a small portion of retinal cells, investigating the role of Müller glia in retinal biology and diseases is particularly challenging. To overcome this problem, we first generated a Cre/*lox*-based conditional gene targeting system that permits the genetic manipulation and functional dissection of gene of interests in Müller cells. To investigate diabetes-induced alteration of Müller cells, we recently adopted methods to analyze Müller cells survival/death in vitro and in vivo. We also used normal and genetically altered primary cell cultures to reveal the mechanistic insights for Müller cells in biological and disease processes. In this article, we will discuss the applications and limitations of these methodologies, which may be useful for research in retinal Müller cell biology and pathophysiology.

**Keywords** Müller glia · Cre/*lox* · Primary cultures · Apoptosis · Cell death

Y.-Z. Le (✉)
Department of Cell Biology, University of Oklahoma Health Sciences Center, 941 S. L. Young Blvd., BSEB 302G, 73104, Oklahoma City, OK, USA
e-mail: Yun-Le@ouhsc.edu

S. Fu · Y. Wang
Department of Ophthalmology, The Second Affiliated Hospital of Nanchang University, 330006, Nanchang, China

S. Fu · M. Zhu · Y.-Z. Le
Departments of Medicine Endocrinology, University of Oklahoma Health Sciences Center, 73104, Oklahoma City, OK, USA

Harold Hamm Diabetes Center, University of Oklahoma Health Sciences Center, 73104, Oklahoma City, OK, USA

J. D. Ash
Department of Ophthalmology, University of Florida, 32610, Gainesville, FL, USA

J. D. Ash et al. (eds.), *Retinal Degenerative Diseases,* Advances in Experimental Medicine and Biology 801, DOI 10.1007/978-1-4614-3209-8_51,

## 51.1 Introduction

Retinal Müller cells are major macroglia and play a pivotal role in supporting retinal maintenance, metabolism, and protection by providing neuro-trophic factors, removing metabolic wastes, regulating extracellular space volumes and ion and water homeostasis, participating visual cycles, releasing neurotransmitters, regulating endothelial barrier function, and modulating immune and inflammatory responses. They also play a major role in reactive gliosis, a process that involves in morphological, biochemical, and physiological changes, under adverse and pathological conditions. Our recent work indicates that, in addition to serve as a major retinal supporting cell, Müller cell is a major supplier of pathological angiogenic factor, vascular endothelial growth factor (VEGF) for retinal neovascularization and vascular leakage under hypoxic or diabetic conditions [1, 6]. Therefore, Müller cell is a cellular target for vascular complications in diabetic retinopathy (DR). Interestingly Müller cells may also require VEGF for their own survival under pathological conditions [3]. To establish a system amicable for studying Müller cell biology, we developed a Cre/*lox*-based conditional gene targeting system [4], which has been used successfully for a number of studies [1, 2, 4, 6]. To explore the role of Müller cells as a supporter for retinal neurons and to investigate the mechanism for maintaining the integrity of retinal Müller cells in DR, we developed in vivo and in vitro assays specifically for the quantification of Müller cells. In this article, we will discuss salient points of these methodologies in studying retinal Müller cell biology and pathophysiology.

## 51.2 Methods

All animal experiments were performed according to the ARVO Statement for the Use of Animals in Ophthalmic and Vision Research and were approved by Institutional Animal Care and Use Committee at the University of Oklahoma Health Sciences Center. Diabetes was induced in wild-type mice by streptozotocin (STZ) injection, as described previously [6]. Primary retinal Müller cells were prepared and cultured similarly as described previously with modifications [1]. Primary Müller cells were maintained in Dubelcco's Modified Eagles Medium (DMEM) containing 10% fetal bovine serum (FBS), 2 mM glutamine, and 0.1% penicillin/streptomycin. To access glucose-induced alteration, primary Müller cells were cultured separately in high glucose (HG) medium (25 mM) and low glucose (LG) medium (5 mM, supplement with 19.5 mM manitol) with daily change of media. Cultures were incubated in serum-free media overnight for analysis. The terminal deoxynucleotidyl transferase-mediated dUTP nick-end labeling (TUNEL) assay was performed to detect apoptosis in primary Müller cell cultures using an in situ apoptosis detection kit from Roche (Indianapolis, IN). The density of Müller cells in retinal sections were examined in immunohistochemically stained retinal section with an antibody (Santa Cruz, CA) against Müller cell marker glutamate synthetase (GS).

## 51.3 Results and Discussions

### *51.3.1 Conditional Gene Targeting in Müller Cells*

In our effort to generate tetracycline-inducible Cre/*lox*-based gene targeting system directed by a 3.0-kb human vitelliform macular dystrophy-2 (*Vmd2*) promoter, we identified mouse lines demonstrated Cre activated reporter expression in retinal Müller cells. This was a consistent observation identified in approximately half of the transgenic founders, suggesting that the Müller cell expression pattern is an intrinsic characteristic of the *Vmd2* gene promoter. Further characterization of a "promising" line revealed that Cre-mediated recombination was detectable at embryonic day 15, probably in progenitors of Müller cells, which resulted in the permanent deletion of *loxP*-flanked DNA in Müller cells [5]. As there was no Cre protein detectable after the birth, it was not surprising that there was no apparent Cre-toxicity in this mouse line and we did not observe any alteration in retinal function and integrity after 10 months [5].

At present, a major technical challenge for the use of Cre/*lox*-based condition gene targeting is: how we can evaluate the efficiency of Cre-mediated recombination? For proteins secreted and exerted their functions externally, such as VEGF, Western blot analysis of lysates from primary cell cultures provides a rate of protein reduction, as exemplified previously [1]. This method can also be used in a scenario that a cellular compartment protein cannot be detected by immunohistochemistry (IHC). As a cautionary note, evaluating the efficiency of Cre-mediated recombination in Müller cells by Western blot analysis can only be meaningful if one can surely exclude the possibility of a protein of interests produced by other retinal cells. In most cases, proteins with cellular localization internally, double IHC labeling with a Müller cell marker and the protein of interests will allow you to determine the percentage of Müller cells undergone Cre-mediated excessive deletion, both in vitro in primary cell cultures or in vivo in animals. Using this strategy, we were able to determine the ratio of Cre-expressing Müller cells in *Vmd2-cre* mice by counting the presence or absence of reporter gene expression in their proper cellular compartment, nuclei [5].

### *51.3.2 In Vitro Model for Mechanistic Studies in Retinal Müller Cells*

While conditional gene targeting is capable of yielding information regarding the functional aspects of a gene, it is nearly impossible to investigate biochemical mechanisms in Müller cells in vivo, as the majority of retinal cells are not Müller glia. However, there is one distinct advantage of using primary Müller cells derived from global or conditional gene knockout (KO) mice. The use of primary KO Müller cells will avoid non-specific and off-target effects resulted from using

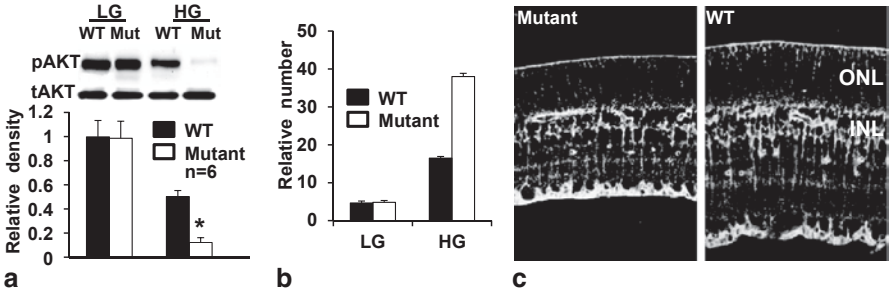


**Fig. 51.1** Analysis of mutant (mut) with defect in producing AKT survival signal. **a** Expression of total AKT (*tAKT*) and activated/phosphorylated form of AKT (*pAKT*) in primary Müller cells grown in high glucose (*HG*) and low glucose (*HG*) conditions showing an approximate 50% reduction of *pAKT* survival signal wild-type cells but a near complete loss of *pAKT* signals in the mutant in *HG* media, compared with that in LG media. *: $p < 0.05$ in student test. **b** Relative numbers of TUNEL-positive cells in primary Müller cells grown in *HG* and *LG* conditions showing *HG* media significantly exacerbated the number of TUNEL-positive cells. **c** Diabetes induced the loss of retinal Müller cells 5-months after STZ-injection. Scale bar: 40 μm

biochemical inhibitors and siRNA. The methods used in our previous experiments [1] can be readily adopted for any studies. In order to investigate the diabetes-related Müller cell pathobiology, we tested the suitability of primary cultures derived from a mutant mouse that had defect in producing activated form of survival signal, phosphorylated AKT (pAKT), in Müller cells in high glucose (HG) conditions. We then examined the survivability of Müller cells in HG media and low glucose (LG) media. While there was no apparent alteration in pAKT production, a significant down-regulation of pAKT in mutant Müller cells in HG media (Fig. 51.1a). This observation was coincided with accelerated Müller cell apoptosis in HG media (Fig. 51.1b). This result also suggests that at least two competing mechanisms are going on to regulate Müller cell survival/death in diabetes. While diabetes/HG induce the up-regulation of VEGF which is supposedly to protect Müller cells [3], it also reduced their survivability, due to a down-regulation of AKT survival signals, [7]. This example illustrated usefulness of primary cell cultures in elucidating biochemical mechanisms governing Müller cell survival in diabetes.

### *51.3.3 Evaluating Retinal Müller Cells Survival/Death*

As the percentage of Müller cells in the retina is low, it is not easy to quantify the survival/death of retinal Müller cells. While in situ apoptosis assay is capable of identifying apoptotic retinal cells, it is difficult for this assay to pin-point a particular Müller cell undergone apoptosis. Performing in situ apoptosis assay (Fig. 51.1b) and other quantitative methods, such as flow cytometry and trypan blue assay, in primary cell cultures will provide a clue on Müller cell survivability. To evaluate the survivability of Müller cells in vivo, we can take advantage of the morpho-

logical characteristic of Müller cells, which demonstrates a distinct filament shape from ganglion cell layer to out limiting membrane (Fig. 51.1c). By staining retinal sections with markers that can clearly distinguish Müller cells from other cells, we were able to count a significant loss of Müller cells in a mutant mouse that had defect in producing activated form of AKT survival signal in diabetes, as the frequency of Müller cell filament was drastically reduced in mutant retinal section stained with glutamate synthetase (Fig. 51.1c). Interestingly, the loss of pAKT survival signal-induced Müller cell death also caused a significant reduction of retinal thickness in diabetes (Fig. 51.1c), suggesting that Müller cells are a major source of trophic factors for retinal neurons in diabetes.

**Acknowledgements** We thank members of our laboratories for preliminary data and helpful discussions. Our work was supported by NIH grants GM104934, EY020900, and EY21725, Grants from American Diabetes Association, Foundation Fighting Blindness, Beckman Initiative for Macular Research, and Oklahoma Center for the Advancement of Science and Technology, and Choctaw Nation and Oklahoma State for an endowment.

## References

1. Bai Y, Ma JX, Guo J, Wang J, Zhu M, Chen Y, Le YZ (2009) Muller cell-derived VEGF is a significant contributor to retinal neovascularization. J Pathol 219:446–454
2. Lin M, Chen Y, Jin J, Hu Y, Zhou KK, Zhu M, Le YZ, Ge J, Johnson RS, Ma JX (2011) Ischaemia-induced retinal neovascularisation and diabetic retinopathy in mice with conditional knockout of hypoxia-inducible factor-1 in retinal muller cells. Diabetologia 54:1554–1566
3. Saint-Geniez M, Maharaj AS, Walshe TE, Tucker BA, Sekiyama E, Kurihara T, Darland DC, Young MJ, D'Amore PA (2008) Endogenous VEGF is required for visual function: evidence for a survival role on muller cells and photoreceptors. PLoS One 3:e3554
4. Ueki Y, Ash JD, Zhu M, Zheng L, Le YZ (2009) Expression of Cre recombinase in retinal Muller cells. Vision Res 49:615–621
5. Ueki Y, Chollangi S, Le YZ, Ash JD (2010) gp130 activation in Muller cells is not essential for photoreceptor protection from light damage. Adv Exp Med Biol 664:655–661
6. Wang J, Xu X, Elliott MH, Zhu M, Le YZ (2010) Muller cell-derived VEGF is essential for diabetes-induced retinal inflammation and vascular leakage. Diabetes 59:2297–2305
7. Xi X, Gao L, Hatala DA, Smith DG, Codispoti MC, Gong B, Kern TS, Zhang JZ (2005) Chronically elevated glucose-induced apoptosis is mediated by inactivation of Akt in cultured Muller cells. Biochem Biophys Res Commun 326:548–553

# Part VII
# Degenerative Processes: Immune-Related Mechanisms, Genes and Factors

# Chapter 52
# An Overview of the Involvement of Interleukin-18 in Degenerative Retinopathies

**Matthew Campbell, Sarah L. Doyle, Ema Ozaki, Paul F. Kenna, Anna-Sophia Kiang, Marian M. Humphries and Peter Humphries**

**Abstract** Age-related macular degeneration (AMD) is the leading cause of central vision loss worldwide and while polymorphisms in genes associated with the immune system have been identified as risk factors for disease development, the underlying pathways and mechanisms involved in disease progression have remained unclear. In AMD, localised inflammatory responses related to particulate matter accumulation and subsequent "sterile" inflammation has recently gained considerable interest amongst basic researchers and clinicians alike. Typically, inflammatory responses in the human body are caused as a result of bacterial or viral infection, however in chronic conditions such as AMD, extracellular

M. Campbell (✉) · E. Ozaki · P. F. Kenna · A.-S. Kiang · M. M. Humphries · P. Humphries
Ocular Genetics Unit, Smurfit Institute of Genetics, Lincoln Place Gate,
Dublin 2, Ireland
e-mail: Matthew.Campbell@tcd.ie

E. Ozaki
e-mail: ozakie@tcd.ie

P. F. Kenna
e-mail: pfkenna@tcd.ie

A.-S. Kiang
e-mail: skiang@tcd.ie

M. M. Humphries
e-mail: mhumphri@tcd.ie

P. Humphries
e-mail: pete.humphries@tcd.ie

S. L. Doyle
Department of Clinical Medicine, School of Medicine,
Trinity College Dublin, Dublin 2, Ireland

National Children's Research Centre, Our Lady's Children's Hospital,
Crumlin, Dublin 12, Ireland
e-mail: doyles8@tcd.ie

J. D. Ash et al. (eds.), *Retinal Degenerative Diseases,* Advances in Experimental Medicine and Biology 801, DOI 10.1007/978-1-4614-3209-8_52,

particulate matter such as drusen can be “sensed” by the NACHT, LRR and PYD domains-containing protein 3 (NLRP3) inflammasome, culminating in the release of the two pro-inflammatory cytokines IL-1β and IL-18 in the delicate local tissue of the retina. Identification at the molecular level of mediators of the inflammatory response in AMD may yield novel therapeutic approaches to this common and often severe form of blindness. Here, we will describe the role of IL-18 in AMD and other forms of retinal disorders. We will outline some of the key functions of IL-18 as it pertains to maintaining tissue homeostasis in a healthy and degenerating/diseased retina.

**Keywords** Interleukin-18 · Age-related macular degeneration (AMD) · NLRP3 · Inflammasome · Choroidal neovascularization (CNV)

## 52.1 Introduction

Age-related macular degeneration (AMD) is the leading cause of central vision loss worldwide. While it has been shown that activation of the immune system and oxidative stress are key mediators of disease progression, the exact pathways involved have remained elusive to date. Common to both “dry” and “wet” AMD is the presence on Bruch’s membrane of extracellular deposits below the retinal pigment epithelium (RPE) in the macula of the eye, recognized in an eye examination as drusen [1]. The presence of drusen in the macula and the density/area covered by these deposits represent early stages in the AMD disease process. Individuals with increased levels of drusen are considered at risk for progressing to the end-stage blinding forms of AMD. Geographic atrophy (GA), the end stage of the atrophic “dry” form of AMD, culminates in vision loss following focal degeneration of the RPE below the fovea [2, 3]. When the RPE degenerates, the foveal cone photoreceptors subsequently die, causing central retinal blindness. The end stage of the “wet” form of AMD is termed choroidal neovascularization (CNV) and is caused when new choroidal blood vessels breaking through Bruch’s membrane/RPE hemorrhage and cause a blood clot to form between the RPE and foveal photoreceptors resulting in almost immediate blindness [4–7]. This occurs in approximately 10 % of cases of AMD. Current antibody-based therapies for AMD target advanced forms of the disease by inhibiting the bioactivity of vascular endothelial growth factor (VEGF). While this is the only form of effective therapy for wet AMD currently in use clinically, it has brought immense relief to patients suffering from the condition and has represented a tremendous advance in disease treatment. This form of therapy is not however without risks and requires direct and regular intraocular injection of monoclonal antibodies (Lucentis®, Avastin® or more recently the fusion protein Eyelea®) which carries with it a risk of retinal detachment, hemorrhage and infection [8]. In addition, the use of these medicines is limited to end-stage disease where CNV already presents. There are currently no treatments available for dry AMD and lifestyle changes are the only clinical

intervention that can be suggested to patients. Like other chronic conditions associated with neural tissues, AMD development appears to have a very strong "immune" component, however the molecular aetiology of these processes is very poorly understood. The disease is multi-factorial, with both environmental and genetic factors apparently playing key roles. Sequence variants associated with disease susceptibility have now been characterized in a growing number of immune regulated genes, with activation of complement on ocular surfaces thought to play a major role in the early disease process, resulting in drusen deposition [9–11].

## 52.2 The Inflammasome and AMD

Recently, localised inflammatory responses related to particulate matter accumulation and subsequent "sterile" inflammation has gained considerable interest. Typically, inflammation and inflammatory responses in the human body are caused as a result of bacterial or viral infection; however, in chronic conditions such as AMD, particulate matter can be "sensed" by the NACHT, LRR and PYD domains-containing protein 3 (NLRP3) inflammasome, culminating in the release of the two pro-inflammatory cytokines IL-1β and IL-18 in the delicate neural tissue of the retina [12–15]. We have discovered that the NLRP3 inflammasome is central to AMD development. Specifically, we discovered a protective role for the NLRP3 inflammasome in wet AMD development that appeared to be mediated by drusen accumulation in Bruch's membrane behind the retina. Specifically, we discovered that components of the NLRP3 inflammasome such as cleaved caspase-1 are present in macrophages surrounding the drusen-like lesions in the retinas of a murine model mimicking characteristics of dry AMD. In addition, we discovered that a commonly used animal model of wet AMD (laser induced (CNV), is dependent on NLRP3 activation and "sterile" inflammation, but unexpectedly in the absence of NLRP3 or IL-18, CNV development was exacerbated [16]. These findings indicated that a key component of the inflammasome, IL-18, is a central regulator of pathological neovascularisation and suggests that therapeutic strategies aimed at producing or delivering IL-18 to the eye, may prove beneficial in preventing the progression of CNV in the context of wet AMD. Indeed, IL-18 has previously been reported to be a critical mediator of other forms of ocular neovascularization and its therapeutic potential is extremely promising.

Importantly however, it has been reported that enhanced NLRP3 inflammasome activation in the retinal pigment epithelium (RPE) as a result of *alu*RNA accumulation and DICER deficits in that distinct cell layer can lead to the development of a geographic atrophy (GA)-like phenotype in a mouse model, with subsequent degeneration of the RPE and in this regard, controlling activation of the inflammaosme and indeed levels of IL-18 in the eye and systemically appears to be a critical mediator of disease progression in AMD [17]. It is of note that human recombinant IL-18

(SB-485232) has already entered a range of clinical trials for the treatment of solid tumours, metastatic melanoma, peritoneal carcinoma, non-Hodgkin's lymphoma and a range of other cancers. It has previously been administered systemically and therefore there is a very large cohort of data pertaining to systemic tolerance of recombinant human IL-18 in patients; however it has never been deployed for use in AMD, but interestingly, retinal pathology has never been reported as an adverse effect in patients [18–20].

## 52.3 IL-18 and AMD

IL-18 is a member of the IL-1 super-family and is synthesized as a 23 kDa biologically inactive precursor protein, which can be cleaved by caspase-1 after inflammasome activation. Through its signalling via the IL18R accessory protein and the IL18Rα proteins it creates an important link between the innate and adaptive immune response, as it is predominantly produced by monocytes and macrophages, inducing the production of IFN-γ and the activation of the adaptive immune response [21]. Indeed, IL-18 when first described in 1989 was termed "IFN-γ-inducing factor". The primary source of IL-18 is macrophages and dendritic cells; however, the immature form of the cytokine pro-IL-18 is constitutively expressed in epithelial cells in various regions of the body. However, very little is known about the interface of the innate and adaptive immune responses in AMD progression. Interestingly, IL-18 can induce up-regulation of cell adhesion molecules, nitric oxide and chemokine production, while also being able to induce expression of Fas ligand.

Levels of IL-18 can be regulated by the IL-18 binding protein (IL-18BP). IL-18BP is a secreted protein that binds IL-18 with high affinity and prevents its interaction with the IL-18 receptor (IL-18R). IL-18BP is a constitutively expressed and secreted protein that resembles the extracellular domains of Ig-like receptors but does not have a transmembrane form. Because IL-18 is one of the early signals leading to IFN-γ production by T-helper (Th) type-1 cells, blocking IL-18 activity by IL-18BP may be involved in down-modulation of the early phases of immune responses. Alternatively, blocking IL-18BP function can augment IL-18 levels [22].

It is now widely accepted that a certain degree of inflammation termed "para-inflammation", may actually be beneficial to the host [23, 24]. In AMD, inflammatory processes have long been associated with dry and wet AMD pathology however complete inhibition of inflammation in the retina in AMD may not be a sound therapy given the apparent importance of IL-18 signalling for both dry and wet AMD. During clinical trials of Infliximab (Remicade®) in individuals with wet AMD [25, 26] it has been observed that patients can display greatly exacerbated symptoms, likely due to inhibition of inflammation that is, in itself, protective. In addition, the NLRP3 inflammasome has also been implicated in conferring protection, through IL-18 production, against experimental colitis and colorectal cancer in mice [27, 28].

## 52.4 Future Perspectives

In the retina, IL-18 has previously been shown to regulate pathological neovascularisation and it appears to have a role in preventing the progression of retinopathy in an animal model of retinopathy of prematurity (ROP) through an apparent ability to regulate levels of pro-angiogenic VEGF. These studies showed that IL-18 plays a very important role in retinal vascular development, with *Il-18*−/− mice showing angiectasis and vascular leakage. VEGF and bFGF levels were also observed to be up-regulated in the *Il-18*−/− mouse retinas [29, 30]. Anti-angiogenic roles for IL-18 have also been observed in post-ischemic injury [31] and in the inhibition of tumour angiogenesis [32]. In addition, while IL1-beta can stimulate the onset of a uveitis-like pathology, IL-18 does not cause this effect and its role as a mature cytokine in the retina is still unknown.

It is clear that controlling inflammasome activation in the retina and systemically plays a fundamental role in how AMD develops and strategies aimed at regulating the levels of IL-18 either systemically or locally in the retina will help us to understand the molecular basis of AMD pathology while also directing clinical deployment of new therapies aimed at augmenting or inhibiting the NLRP3 inflammasome.

## References

1. Swaroop A, Chew EY, Rickman CB, Abecasis GR (2009) Unravelling a multifactorial late-onset disease: from genetic susceptibility to disease mechanisms for age-related macular degeneration. Annu Rev Genomics Hum Genet 10:19–43
2. Resnikoff S et al (2004) Global data on visual impairment in the year 2002. Bull World Health Organ 82:844–851
3. Bressler SB, Maguire MG, Bressler NM, Fine SL (1990) Relationship of drusen and abnormalities of the retinal pigment epithelium to the prognosis of neovascular macular degeneration. The macular photocoagulation study group. Arch Ophthalmol 108:1442–1447
4. Sarks SH, van Driel D, Maxwell L, Killingsworth M (1980) Softening of drusen and subretinal neovascularization. Trans Ophthalmol Soc UK 100:414–422
5. Vinding T (1990) Occurrence of drusen, pigmentary changes, and exudative changes in the macula with reference to age-related macular degeneration. An epidemiological study of 1000 aged individuals. Acta Ophthalmol 68:410–414
6. Holz FG, Bellman C, Staudt S, Schutt F, Volcker HE (2001) Fundus autofluorescence and development of geographic atrophy in age-related macular degeneration. Invest Ophthalmol Vis Sci 42:1051–1056
7. Seddon JM, George S, Rosner B (2006) Cigarette smoking, fish consumption, omega-3 fatty acid intake, and associations with age-related macular degeneration: the US twin study of age-related macular degeneration. Arch Ophthalmol 124(7):995–1001
8. Crabb JW et al (2002) Drusen proteome analysis: an approach to the etiology of age-related macular degeneration. Proc Natl Acad Sci U S A 99(23):14682–14687
9. Gao H, Hollyfield JG (1992) Aging of the human retina. Differential loss of neurons and retinal pigment epithelial cells. Invest Ophthalmol Vis Sci 33(1):1–17

10. Curcio CA, Millican CL, Allen KA, Kalina RE (1993) Aging of the human photoreceptor mosaic: evidence for selective vulnerability of rods in central retina. Invest Ophthalmol Vis Sci 34(12):3278–3296
11. Mariathasan S et al (2006) Cryopyrin activates the inflammasome in response to toxins and ATP. Nature 440(7081):228–232
12. Martinon F, Pétrilli V, Mayor A, Tardivel A, Tschopp J(2006) Gout-associated uric acid crystals activate the NALP3 inflammasome. Nature 440(7081):237–241
13. Halle A et al (2008) The NALP3 inflammasome is involved in the innate immune response to amyloid-beta. Nat Immunol 9(8):857–865
14. Zhou R, Yazdi AS, Menu P Tschopp J (2011) A role for mitochondria in NLRP3 inflammasome activation. Nature 469(7329):221–225
15. West XZ et al (2010) Oxidative stress induces angiogenesis by activating TLR2 with novel endogenous ligands. Nature 467(7318):972–976
16. Doyle SL, Campbell M, Ozaki E, Salomon RG, Mori A, Kenna PK, Farrar GJ, Kiang AS, Humphries MM, Lavelle EC, O'Neill LAJ, Hollyfield JG, Humphries P (2012, May) NLRP3 has a protective role during the development of age-related macular degeneration through the induction of IL-18 by drusen components. Nat Med 18(5):791–798
17. Tarallo V et al (2012, May 11) DICER1 loss and Alu RNA induce age-related macular degeneration via the NLRP3 inflammasome and MyD88. Cell 149(4):847–859
18. Tarhini AA, Millward M, Mainwaring P, Kefford R, Logan T, Pavlick A, Kathman SJ, Laubscher KH, Dar MM, Kirkwood JM (2009, Feb 15) A phase 2, randomized study of SB-485232, rhIL-18, in patients with previously untreated metastatic melanoma. Cancer 115(4):859–868
19. Robertson MJ, Kirkwood JM, Logan TF, Koch KM, Kathman S, Kirby LC, Bell WN, Thurmond LM, Weisenbach J, Dar MM (2008, Jun 1) A dose-escalation study of recombinant human interleukin-18 using two different schedules of administration in patients with cancer. Clin Cancer Res 14(11):3462–3469
20. Robertson MJ, Mier JW, Logan T, Atkins M, Koon H, Koch KM, Kathman S, Pandite LN, Oei C, Kirby LC, Jewell RC, Bell WN, Thurmond LM, Weisenbach J, Roberts S, Dar MM (2006, Jul 15) Clinical and biological effects of recombinant human interleukin-18 administered by intravenous infusion to patients with advanced cancer. Clin Cancer Res 12(14 Pt 1):4265–4273
21. Smith DE (2011, Mar) The biological paths of IL-1 family members IL-18 and IL-33. J Leukoc Biol 89(3):383–392
22. Boraschi D, Dinarello CA (2006, Dec) IL-18 in autoimmunity: review. Eur Cytokine Netw 17(4):224-252
23. Xu H, Chen M, Forrester JV (2009) Para-inflammation in the aging retina. Prog Retin Eye Res 28(5):348–368
24. Medzhitov R (2008) Origin and physiological roles of inflammation. Nature 454(7203):428–435
25. Arias L et al (2010, Nov-Dec) Intravitreal infliximab in patients with macular degeneration who are nonresponders to antivascular endothelial growth factor therapy. Retina 30(10):1601–1608
26. Giganti M et al (2010, Jan) Adverse events after intravitreal infliximab (Remicade). Retina 30(1):71–80
27. Dupaul-Chicoine J et al (2010) Control of intestinal homeostasis, colitis, and colitis-associated colorectal cancer by the inflammatory caspases. Immunity 32(3):367–378
28. Allen IC et al (2010) The NLRP3 inflammasome functions as a negative regulator of tumorigenesis during colitis-associated cancer. J Exp Med 207(5):1045-1056
29. Qiao H et al (2004) Abnormal retinal vascular development in IL-18 knockout mice. Lab Invest 84(8):973–980

30. Qiao H et al (2007) Interleukin-18 regulates pathological intraocular neovascularization. J Leukoc Biol 81(4):1012–1021
31. Mallat Z et al (2002) Interleukin-18/interleukin-18 binding protein signaling modulates ischemia-induced neovascularization in mice hindlimb. Circ Res 91(5):441–448
32. Coughlin CM et al (1998) Interleukin-12 and interleukin-18 synergistically induce murine tumor regression which involves inhibition of angiogenesis. J Clin Invest 101(6):1441–1452

# Chapter 53
# Chronic Intraocular Inflammation and Development of Retinal Degenerative Disease

**Charles E. Egwuagu**

**Abstract** Elevated levels of inflammatory cytokines in the vitreous of patients with chronic intraocular inflammatory (uveitis) have long been suspected to contribute to the pathogenesis of retinal degenerative diseases. However, direct connection between chronic inflammation and development of retinal degenerative diseases has been difficult to establish because we lack an appropriate animal model of co-existing chronic intraocular inflammation and neurodegeneration. This report discusses new developments in immunological and diabetic research that suggest that persistent secretion of pro-inflammatory cytokines during uveitis might induce insulin resistance and retinal degenerative changes that contribute to the pathogenesis of Diabetic Retinopathy (DR), a retinal dystrophy of significant public health importance.

**Keywords** Uveitis · Retinal degeneration · Insulin resistance · Interferon-γ · Cytokines · Suppressor of cytokine signaling · Experimental autoimmune uveitis · EAU

## 53.1 Introduction

Retinopathy results from acute or persistent damage to the retina and is a major cause of blindness or severe vision loss, especially if the pathologic changes extend to the macular. Chronic inflammation and inflammatory cytokines or growth factors that promote neovascularization and angiogenesis are suspected to play important role in retinopathies that lead to retinal degeneration and blindness [1]. Although retinal dystrophy such as retinitis pigmentosa can be inherited, most retinopathies are caused by other underlying pathologic conditions such as, diabetes mellitus,

C. E. Egwuagu (✉)
Molecular Immunology Section, Laboratory of Immunology, National Eye Institute, National Institutes of Health, Building 10, Room 10N116, 10 Center Drive, Bethesda, MD 20892-1857, USA
e-mail: egwuaguc@nei.nih.gov

J. D. Ash et al. (eds.), *Retinal Degenerative Diseases,* Advances in Experimental Medicine and Biology 801, DOI 10.1007/978-1-4614-3209-8_53,

sickle cell disease, prematurity of the newborn, retinal vein or artery occlusion or arterial hypertension. Diabetic retinopathy (DR) is of particular public health importance because it is a major cause of vision loss in the developing world and the leading cause of blindness among adults under the age of 65 in the USA [2]. It is projected to affect more than 300 million people worldwide over the next decade. Although the pathogenesis of DR is not known, elevated levels of inflammatory cytokines and chemotactic molecules that recruit leukocytes have been detected in the vitreous of patients with DR in several studies [2], suggesting inflammation mediated etiology.

However, DR is generally considered a glucose-mediated microvascular disease that derives in part from inability of the retina to adapt to metabolic stress and insulin-resistance as a risk factor for developing DR [1, 2]. In animal studies, insulin resistance precedes appearance of early features of DR and neuronal cell death. However, early features of DR such as vascular permeability, edema and increase in inflammatory proteins in the vitreous are also hallmarks of ocular inflammation [1]. Despite the apparent involvement of chronic inflammation and insulin resistance in DR, establishing a direct connection between inflammation, diabetes and the development of retinal degenerative diseases has been difficult because we lack an appropriate animal model of co-existing chronic intraocular inflammation and neurodegeneration.

Recent studies in a mouse model of chronic uveitis have revealed that prolonged inflammation can cause insulin resistance and retinal degeneration [3]. Proof-of-principle studies have also shown that targeted expression of a pro-inflammatory cytokine in the eye induces retinal degenerative changes [4]. Here, I discuss additional data that might provide mechanistic explanation for the link between inflammation, insulin resistance and retinal degeneration.

## 53.2 Mouse Model of Chronic Intraocular Inflammation (Uveitis)

Uveitis is a group of potentially sight-threatening inflammatory diseases that includes, Behçet's disease, VKH, ocular sarcoidosis and about 10% of severe visual handicap in the USA are attributed to this group of disorders. It is characterized by progressive photoreceptor cell loss, neovascularization and retinal degeneration. However, investigation of mechanisms underlying the progression of uveitis to retinal degenerative changes in the retina is impeded because of the lack of a suitable animal model. Experimental autoimmune uveitis (EAU) shares essential features with human uveitis and current understanding of the pathophysiology of uveitis derives largely from study of EAU [5]. However, EAU in the mouse is generally considered a self-limiting disease and does not present with clinically manifestations of human chronic uveitis, including neovascularization and retinal degeneration. This limitation is attributable in part to the apparent absence of inflammatory cells in the vitreous of EAU mice 35 days after inception of EAU and this has led to the prevailing view that EAU is mainly an acute disease with complete recovery after 28–35

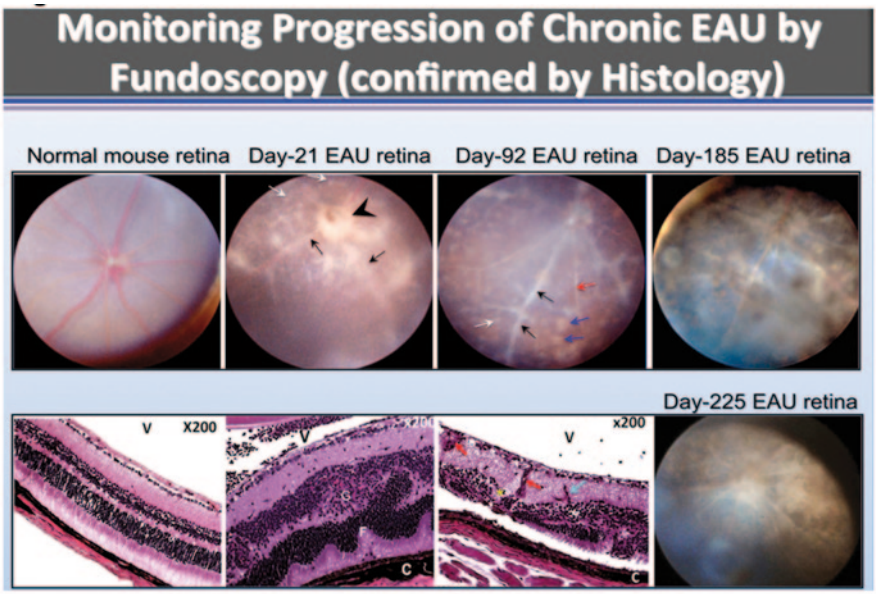


**Fig. 53.1** Chronic intraocular inflammation induces retinal degeneration and neovascularization. Fundus images were taken from normal or EAU mice over a 225 days period (top panels). Fundus images reveal blurred optic disc margins and enlarged juxtapapillary area (*black arrowhead*), retinal vasculitis with moderate cuffing (*black arrows*) and yellow-whitish retinal and choroidal infiltrates (*white arrows*). Histological analysis (Lower panels) reveals retinal structural damage, including evidence of atrophic retina (thinning) and sclerotic vessel (*red arrow*) with multiple whitish infiltrates (*white arrow*) and brownish chorioretinal scars (*blue arrows*), photoreceptor cell loss (*red asterisk*), retinal vasculitis (*black arrows*), retinal sclerotic vessel (*white arrow*), choroiditis (*black arrowhead*), and retinal degeneration (bottom panels). *OpN* optic nerve, *V* vitreous, *R* retina, *GCL* ganglion cell layer, *INL* inner nuclear layer, *ONL* outer nuclear layer, *RPE* retinal pigment epithelial layer, *CH* choroid

days. Development and adaptation of non-invasive techniques used in Opthalmology to mouse studies have made it possible to study mouse uveitis over extended period and these include fundoscopy, Optical Coherence Tomography (OCT) and electroretinography (ERG). These techniques have recently been used to monitor EAU over a 7 months period and results from these studies have revealed that the rapid decline of the severe acute retinal inflammation gives rise to a chronic phase of retinal inflammation that persists and did not completely resolve during the 225 days of the study [3]. Features of the chronic phase include severe retinal vasculitis with cuffing, sclerotic vessels, multifocal choroiditis and scaring and/or atrophy of the retina (Fig. 53.1). These pathological changes were observed by fundoscopic examination and histology beginning around day-50 after inception of EAU and persisted. OCT provided unprecedented clarity showing evolution of the acute disease to its long-term sequelae characterized by retina edema and neuroretinal degeneration (Fig. 53.2). Serial ERG tracings revealed that prolonged inflammation of the neuroretina adversely affected visual acuity in mouse. These studies established

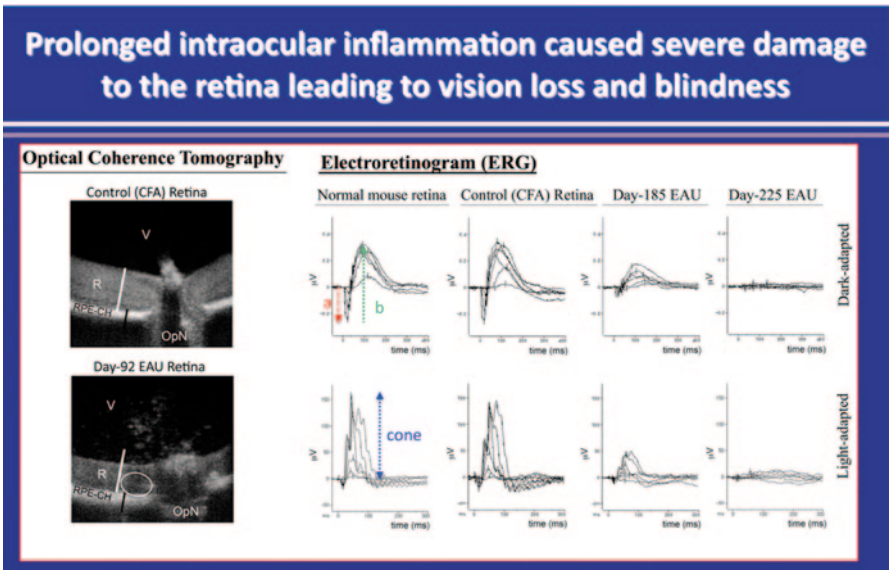


**Fig. 53.2** Mice were immunized with CFA alone or IRBP/CFA emulsion and electroretinogram (ERG) recordings were obtained and analyzed 185 or 225 days post-immunization. ERGs of control unimmunized mice or control mice immunized with CFA alone, show the characteristic normal a-, b- and cone waves. In contrast to control mice, light-induced response was barely elicited from retina of day-225 IRBP-induced EAU mice

for the first time that, as is the case in human, mice development progressive retina degeneration, severe vision loss and blindness as a result of chronic intraocular inflammation.

## 53.3 Up-Regulation of SOCS Proteins During EAU Induces Insulin Resistance and Inhibits Insulin Signaling in the Retina

Although direct connection between inflammation and insulin-resistance in etiology of DR has not been established, studies on obesity or metabolic syndrome provide a framework for understanding how these disparate processes can converge in the etiology of DR [6]. Suppressors of cytokine signaling (SOCS) are an eight-member family of intracellular proteins that regulates the intensity and duration of cytokine/growth-factor signals [7, 8]. They are rapidly induced in many cell types in response to cytokines (IFN-γ and IL-6) or growth factors (CNTF, LIF, insulin) and their inhibitory effects derive from direct interaction with cytokine/growth-factor receptors or signaling proteins, leading to proteosomal degradation of the recep-

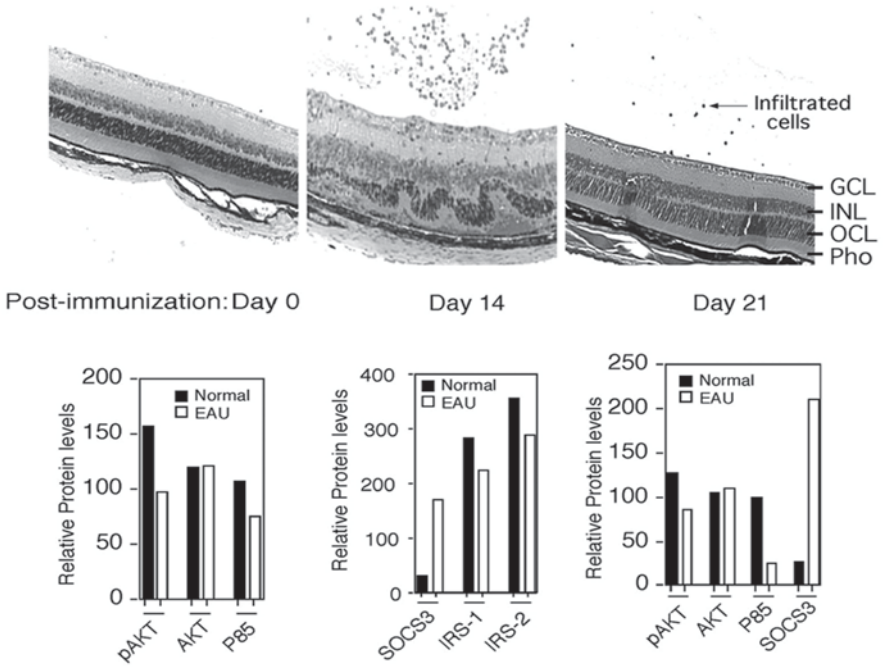


**Fig. 53.3** Induction of SOCS1 and SOCS3 during EAU correlates with inhibition of insulin signaling in the retina. **a** Six-week-old mouse was immunized with IRBP in CFA and eyes were enucleated and analyzed by histology at various times. Four microns thick sections were cut through the retina and stained with H&E. **b** Corresponding Western Blot analysis was performed. Relative Intensities of the western blot bands were analyzed in a densitometer to quantify the relative expression levels of SOCS3, IRS-1 and IRS-2

tor complex and termination of the signal [7, 8]. Because of the relatively short half-life of SOCS proteins, their negative regulatory effects are generally transient. However, constitutive SOCS expression occurs in some tissues due to unabated stimulation by chronic inflammation or cellular stress, leading to silencing of critical cellular pathways. Chronic inflammation and cellular stress induces persistent elevation of SOCS1 and SOCS3 and these SOCS members have been implicated in etiology of diabetes, obesity and metabolic-syndrome [9]. We have shown that inflammatory cytokines produced by inflammatory lymphocytes that mediate EAU induce expression of SOCS1 and SOCS3 (Fig. 53.3) [10]. The increase in SOCS3 protein is accompanied by decrease in pAKT, p85 and IRS proteins, suggesting that elevation of SOCS proteins can inhibit PI3K/AKT-mediated insulin signaling in the retina during EAU (Fig. 53.4) [10]. We have also shown that light damage, hypoxia and metabolic stress caused by type1 diabetes increases SOCS3 expression in the retina [10]. In addition, over-expression of SOCS1 and SOCS3 in human or rodent retinal cells or targeted expression of SOCS1 expression in the retina of transgenic

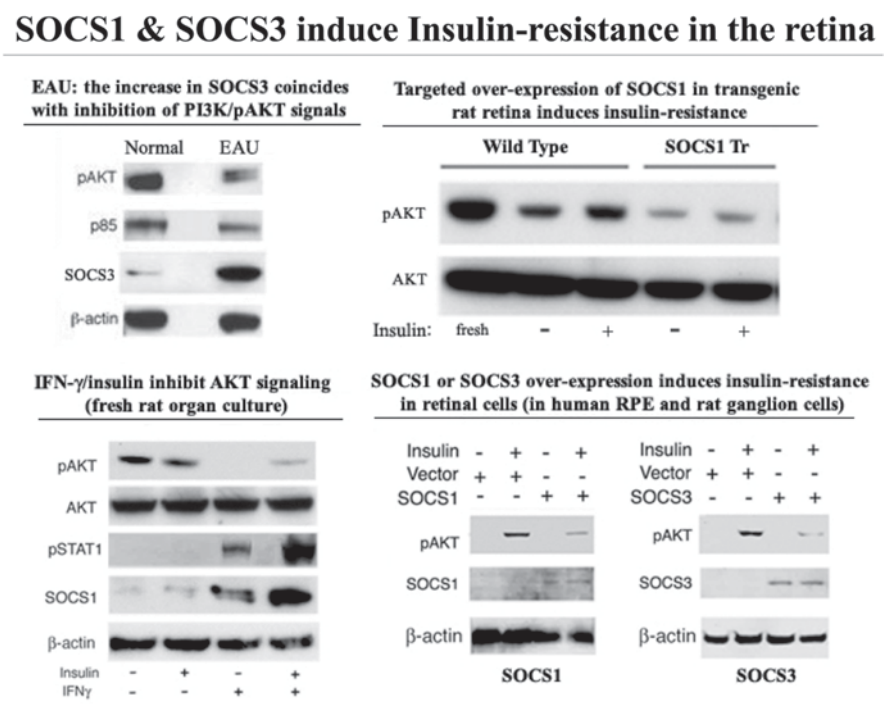


**Fig. 53.4** SOCS1 & SOCS3 induce Insulin-resistance in the retina

rats inhibited PI3K/AKT pathway [10]. These observations suggest that SOCS3-mediated inhibition during EAU can induce insulin-resistance, an important risk factor of DR and may thus provide a mechanistic link between inflammation, insulin resistance and DR.

## 53.4 Targeted Expression of Interferon-γ (IFN-γ) in the Eye Induced Retinal Degeneration

During uveitis Th1 and Th17 lymphocytes are recruited into the retina and mediate ocular pathology through the production of inflammatory cytokines including IFN-γ, TNF-α, IL-6 and IL-17 [11, 12]. These cytokines are also detected at elevated levels in the vitreous of patients with uveitis. Several of these factors induce production of SOCS1 and SOCS3. In a proof-of-principle experiment we sought to directly test the notion that chronic inflammation leading to persistent production of pro-inflammatory cytokines that up-regulate SOCS1 or SOCS3 can cause uveitis and retinal degeneration [13]. IFN-γ expression was targeted to the lens of TR rats and the lens served as a depot to release IFN-γ to retina. The IFN-γ expression induced degeneration of the lens and as the transgenic lens continued to degenerate it began to

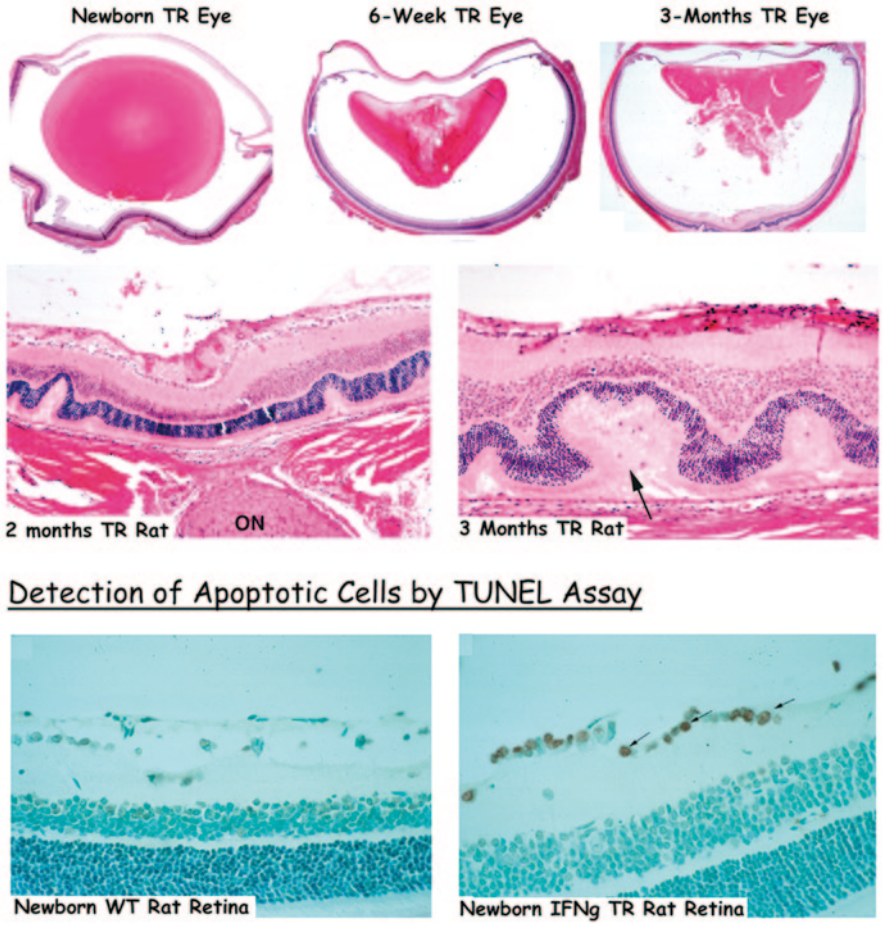


**Fig. 53.5** Phenotypes of wild-type (*WT*) and aAcry/IFN-γ transgenic (*TR*) Lewis rat eyes. Note the time-dependent disintegration of the lens capsule and inception of retinal degenerative changes. *Arrow* in middle panel shows areas of retinal in-folding, a hallmark of severe uveitis. *Arrows* in lower panel show TUNEL-stained apoptotic ganglion cells

release copious amounts of the cytokine into the vitreous (Fig. 53.5). By 3 months of age this led to significant degeneration of the retina characterized by significant apoptotic death of ganglion cells and photoreceptors [13].

## 53.5 Conclusions

Retinal dystrophies including DR cause severe vision impairment or blindness and understanding of cellular pathways that promote the survival or repair of damaged neurons is essential to efforts aimed at developing effective treatment for

retinopathies. Although molecular cues that influence the decision to allow death or survival of partially damaged neurons and photoreceptors are largely unknown, neurotrophic factors are thought to be involved in reparative processes in retina. Retinal neurotrophic factors such as CNTF, OSM or LIF activate and utilize JAK/STAT pathways and are therefore under negative-feedback regulation by SOCS proteins. Data presented here indicate that retinal cells respond to chronic inflammation, light-damage, oxidative-stress or metabolic stress due diabetes by up-regulating expression of SOCS1 and SOCS3 [10]. Although the induction of SOCS proteins undoubtedly confer protection from cytotoxic effects of pro-inflammatory cytokines or deleterious effects of excessive cellular stress, persistently high SOCS levels in retina is potentially pathogenic because it would inhibit survival signals that emanate from neurotrophic factors. In this report I have also presented evidence showing that persistent secretion of pro-inflammatory cytokines during uveitis elevated SOCS1 and SOCS3 levels in the retina, resulting in insulin resistance retinal degeneration. The recent establishment of a chronic EAU model showing that, as is the case with humans, that chronic intraocular inflammation induces retina degeneration, severe vision loss and blindness, now provides a useful system to fully investigate the mechanistic link between chronic inflammation, insulin resistance and pathogenesis of RD.

## References

1. Antonetti DA, Barber AJ, Bronson SK, Freeman WM, Gardner TW, Jefferson LS et al (2006) Diabetic retinopathy: seeing beyond glucose-induced microvascular disease. Diabetes 55(9):2401–2411
2. Meleth AD, Agron E, Chan CC, Reed GF, Arora K, Byrnes G et al (2005) Serum inflammatory markers in diabetic retinopathy. Invest Ophthalmol Vis Sci 46(11):4295–4301
3. Oh HM, Yu CR, Lee Y, Chan CC, Maminishkis A, Egwuagu CE (2011) Autoreactive memory CD4+ T lymphocytes that mediate chronic uveitis reside in the bone marrow through STAT3-dependent mechanisms. J Immunol 187(6):3338–3346
4. Egwuagu CE, Mahdi RM, Chan CC, Sztein J, Li W, Smith JA et al (1999) Expression of interferon-gamma in the lens exacerbates anterior uveitis and induces retinal degenerative changes in transgenic Lewis rats. Clin Immunol 91(2):196–205
5. Nussenblatt RB (1991) Proctor lecture. Experimental autoimmune uveitis: mechanisms of disease and clinical therapeutic indications. Invest Ophthalmol Vis Sci 32(13):3131–3141
6. Taniguchi CM, Emanuelli B, Kahn CR (2006) Critical nodes in signalling pathways: insights into insulin action. Nat Rev Mol Cell Biol 7(2):85–96
7. Naka T, Fujimoto M, Kishimoto T (1999) Negative regulation of cytokine signaling: STAT-induced STAT inhibitor. Trends Biochem Sci 24(10):394–398
8. Hilton DJ (1999) Negative regulators of cytokine signal transduction. Cell Mol Life Sci 55(12):1568–1577
9. Emanuelli B, Glondu M, Filloux C, Peraldi P, Van Obberghen E (2004) The potential role of SOCS-3 in the interleukin-1beta-induced desensitization of insulin signaling in pancreatic beta-cells. Diabetes 53(Suppl 3):S97–S103
10. Liu X, Mameza MG, Lee YS, Eseonu CI, Yu CR, Kang Derwent JJ et al (2008) Suppressors of cytokine-signaling proteins induce insulin resistance in the retina and promote survival of retinal cells. Diabetes 57(6):1651–1658

11. Liu X, Lee YS, Yu CR, Egwuagu CE (2008) Loss of STAT3 in CD4+ T cells prevents development of experimental autoimmune diseases. J Immunol 180(9):6070–6076
12. Amadi-Obi A, Yu CR, Liu X, Mahdi RM, Clarke GL, Nussenblatt RB et al (2007) T(H)17 cells contribute to uveitis and scleritis and are expanded by IL-2 and inhibited by IL-27/STAT1. Nat Med 13(6):711–718
13. Egwuagu CE, Mahdi RM, Chan CC, Sztein J, Li W, Smith JA et al (1999) Expression of interferon-gamma in the lens exacerbates anterior uveitis and induces retinal degenerative changes in transgenic Lewis rats. Clin Immunol 91(2):196–205

# Chapter 54
# The Relevance of Chemokine Signalling in Modulating Inherited and Age-Related Retinal Degenerations

**Ulrich FO Luhmann, Scott J Robbie, James WB Bainbridge and Robin R Ali**

**Abstract** Systemic monocytes, tissue resident macrophages, dendritic cells and microglia have specific roles in immune surveillance and maintenance of tissue homeostasis and are key regulator and effector cells of the local immune response to acute and chronic tissue injury.

Two major signalling pathways that differentially define trafficking behaviour and activation of systemic and local myeloid cell populations in response to exogenous and endogenous inflammatory stimuli are the Ccl2-Ccr2 and the Cx3cl1-Cx3cr1 chemokine pathways.

Alterations in these pathways have been implicated in controlling myeloid cell activation during normal ageing and in age-related retinal degenerations, including age-related macular degeneration (AMD).

We review the evidence for how altered chemokine signalling in acute and chronic inflammatory conditions regulate local and systemic myeloid cell responses in the retina and how this may contribute to or attenuate pathology in inherited and age-related retinal diseases. We discuss the role of environmental factors (e.g. light exposure) and the influence of genetic factors on the manifestation of pathology in experimental models and in human patients and how we envisage harnessing this knowledge for the development of targeted, more broadly applicable anti-inflammatory treatment strategies for a wide range of retinal degenerations.

U. F. Luhmann (✉) · S. J. Robbie · J. W. Bainbridge · R. R. Ali
Department of Genetics, UCL Institute of Ophthalmology,
11-43 Bath Street, London, EC1V 9EL, UK
e-mail: u.luhmann@ucl.ac.uk

S. J. Robbie · J. W. Bainbridge · R. R. Ali
NIHR Biomedical Research Centre for Ophthalmology at Moorfields Eye Hospital NHS Foundation Trust and UCL Institute of Ophthalmology, London, UK
e-mail: s.robbie@ucl.ac.uk

J. W. Bainbridge
e-mail: j.bainbridge@ucl.ac.uk

R. R. Ali
e-mail: r.ali@ucl.ac.uk

J. D. Ash et al. (eds.), *Retinal Degenerative Diseases,* Advances in Experimental Medicine and Biology 801, DOI 10.1007/978-1-4614-3209-8_54,

**Keywords** Innate immunity · Microglia · Monocytes · Chemokine knockout mice · *Ccl2* · *Ccr2* · *Cx3cl1* · *Cx3cr1* · Age-related macular degeneration · Retinal degeneration · Genetic background · Light

## 54.1 Introduction

The innate immune system senses infections, tissue injury or noxious stress in the tissue by danger associated molecular pattern and mounts a physiological inflammatory response to remove the danger, initiate tissue repair and restore homeostasis. While infections and tissue injury result in acute inflammation (characterised by immune cell infiltration, vasodilatation and plasma protein accumulation), tissue malfunction and cellular stress lead to a low-grade inflammation (para-inflammation). This para-inflammatory response depends on the degree of tissue damage and can range from local cytokine production and activation of local immune cells in response to near-basal tissue stress to a higher level of involvement of systemic cells during more pronounced tissue damage. If the initial danger is not removed by these responses inflammation may become persistent and lead to pathological consequences for the surrounding tissue. The major cellular components of the innate immune system mediating these functions are monocytes, macrophages, dendritic cells and microglia [1].

## 54.2 The Role of Microglia in the Local Innate Immune Response

Microglia are the resident immune cells of the central nervous system (CNS). In the retina they are either localized adjacent to vessels (perivascular microglia) or distributed in a parenchymal network at the level of the inner and outer plexiform layers. Microglia express high levels of Cx3cr1 [2] and normally show a continuous surveillance behaviour with highly dynamic movements of their processes but stable soma position. In response to any disturbance of tissue homeostasis, including normal aging, inherited or multi-factorial age-related retinal degenerations, microglia sense associated foreign or endogenous danger signals and become activated by pattern recognition receptors and by chemokines and cytokines from the damaged tissue. Activated microglia release inflammatory mediators, alter their morphology from a ramified to amoeboid appearance and can migrate to the site of tissue injury to eliminate danger signals and restore retinal homeostasis, e.g. by phagocytosis or through the controlled production of cytokines and growth factors. The released signalling molecules may lead to an additional recruitment of bone marrow-derived systemic macrophages and also define various heterogeneous effector functions that can be pro-inflammatory (classical activation), tissue-protective (alternative activation) or immune suppressive [3].

## 54.3 Differential Recruitment of Functional Monocyte Subsets by Chemokine Signalling

Systemic monocyte subsets can be distinguished by the expression pattern of chemokine surface receptors and adhesion molecules, that include CD14, CD16 and CD64 (in human) and CD115, CD11b, Gr1/Ly6C (in mouse) as well as the C-C chemokine receptor 2 (CCR2) and fractalkine receptor CX3CR1 (in both) [4]. Pro-inflammatory CCR2-expressing monocytes infiltrate sites of inflammation and give rise to inflammatory macrophages and dendritic cells in response to local stimuli such as the CC-chemokine ligand 2 (Ccl2) [5]. In contrast "resting" monocytes, which express high levels of *Cx3cr1*, but not *Ccr2*, patrol non-inflamed tissue, may be involved in resolution of inflammation and are regulated by CX3CL1 (fraktalkine) [6].

## 54.4 Ccl2 and Cx3cl1 Expression Changes During Inflammatory Conditions in the Eye

While CX3CL1 is constitutively expressed in retinal neurons and the RPE, CCL2 expression is very low in the healthy RPE or retina [2]. During inflammation, local expression of both chemokines is induced. Muller glia, microglia, retinal pigment epithelial cells (RPE) and choroidal and retinal endothelial cells are prominent sources of CCL2 and CX3CL1 [7]. CX3CL1 is expressed as a transmembrane protein from which a soluble, chemotactic variant can be released by proteolytic cleavage [8].

## 54.5 CCL2-CCR2 and CX3CR1-CX3CR1 Signalling Differentially Modulate Retinal Pathology Associated With Acute Retinal Inflammation

In acute inflammation CCL2-CCR2 signalling plays an important role in the recruitment of systemic $CCR2^{+}$ monocytes that appear to mediate retinal pathology. This is supported by the observation that ablation of *Ccr2* in the endotoxin-induced autoimmune uveitis model (EAU) leads to reduced photoreceptor loss [9] and attenuated intra-retinal vascular remodelling [10]. Ablation of *Ccl2*-*Ccr2* signalling results in reduced choroidal neovascularisation (CNV) in the laser-induced CNV model and attenuates photoreceptor loss in acute light damage and retinal detachment, indicating that systemically derived $CCR2^{+}$ macrophages mediate pathological vascular remodelling and photoreceptor loss [11–13]. However, local Ccl2 up-regulation alone is not sufficient to induce pathology as transgenic overexpression

of CCL2 in astrocytes in the brain only leads to neurological impairment after additional systemic pertussis injection [14].

Conversely, Cx3cl1-Cx3cr1 signalling in acute retinal inflammation controls the activation of local *Cx3cr1*$^{hi}$ microglia. Interestingly, the ablation of Cx3cl1-Cx3cr1 signalling seems not to affect photoreceptor loss in EAU [15] but does result in increased CNV after laser treatment [16], suggesting that local microglia activation in EAU appears to have a minor role while it suppresses CNV. In acute light damage, *soluble* CX3CL1 is released from photoreceptors and leads to microglia migration and activation with associated photoreceptor loss. In contrast, increased cell-cell-signalling via the *transmembrane* form suppresses microglia migration. This suggests that CX3CL1 signalling can have pro-inflammatory or suppressive effects on microglia activation [17].

## 54.6 Normal Age-Related Changes in Chemokine Signalling in Human Ageing and Retinal Ocular Disease

A role for chemokines signalling during ageing and in age-related retinal disease has been suggested by alterations in systemic and local expression levels of *Ccl2*, *Cx3cl1* and their cognate receptors. With ageing, CX3CR1 expression in human non-classical monocytes decreases and plasma levels of CCL2 increases [18]. Furthermore, neovascular AMD patients show increased expression of CCR2 on systemic pro-inflammatory monocytes [19] and elevated aqueous humour levels of CCL2 [20] indicating a role of this chemokine pathway in age-related ocular pathology.

## 54.7 Discrepancies in the Reports Between Chemokines Knockout Mouse Models

Although there is agreement that during ageing and age-related retinal disease chemokine signalling controls myeloid cell migration and activation, there are conflicting reports as to what degree dysfunctional chemokine signalling results in retinal degeneration. For *Ccl2*$^{-/-}$ and *Ccr2*$^{-/-}$ mice, one study has reported that RPE and choroidal changes occur from 9 months and are followed by retinal degeneration at around 16 months [21]. A second report describes the development of RPE lesions with a variable penetrance of 40 % in *Ccl2*$^{-/-}$ and 25 % in *CCR2*$^{-/-}$ mice at 18–27 months [22]. In contrast, we only observed normal age-related changes in two different *Ccl2*$^{-/-}$ lines [11, 23].

Conflicting data have also been reported for *Cx3cr1* deficient mice. While some *Cx3cr1*$^{-/-}$ and *Cx3cr1*$^{GFP/GFP}$ lines on C57Bl/6 background show a pronounced

age-related retinal degeneration [16], another *Cx3cr1*$^{-/-}$ C57Bl/6 line did not [23]. Furthermore, *Cx3cr1*$^{GFP/GFP}$ albino Balb/c lines show higher variability and earlier onset of age-related retinal degeneration between different laboratories [16, 24]

## 54.8 Additional Genetic and/or Environmental Actors May Explain Discrepancies Between Different Studies

Some senescent C57Bl/6.*Ccl2*$^{-/-}$ and C57Bl/6.*Cx3cr1*$^{-/-}$ lines show no age-related retinal degeneration, indicating that additional factors are required for the manifestation of age-related retinal degeneration in chemokine deficient mice. These may include different ages, genetic background, housing conditions (light, pathogen load) or the presence of unknown mutant alleles, such as the recently identified homozygous *Crb1 rd8* mutation that was shown to be a major confounding factor for the early onset retinal degeneration in *CCKO* (*Ccl2*$^{-/-}$/*Cx3cr1*$^{-/-}$) mice [25]. This *rd8* mutation as an additional trigger for an innate immune response revealed a differential modulatory role of the two chemokine pathways for the manifestation of retinal degeneration. While Ccl2 deficiency did not alter retinal pathology significantly, Cx3cr1 deficiency led to a more pronounced manifestation of the *rd8* phenotype associated with local microglia activation [25]. Light is another factor that modulates retinal pathology. Increased exposure accelerates the development of retinal degeneration in *Cx3cr1* deficient mice, while dark-rearing is protective [16]. The genetic background is a prominent influence on subretinal microglia accumulation and retinal degeneration as observed in several chemokine lines [16, 24] and in a model of light-induced retinal damage in which albino *C57Bl/6 J-Tyr*$^{c2j}$ mice show much lower subretinal microglia and retinal degeneration than two other albino strains (Balb/c and A/J) [26].

## 54.9 The Dysfunctional Innate Immune Response Due to Defective Chemokine Signalling Only Manifests in the Presence of Additional Inflammatory Triggers

These findings suggest that the two chemokine pathways have distinct functions during retinal inflammation and that retinal pathology is modulated either by the recruitment of systemic monocytes (*CCl2-CCR2*) or by regulating local activation of microglia (*Cx3cl1-Cx3cr1*). Dysfunctional chemokine signalling alone without inflammatory triggers does not result in retinal pathology, but it rather seems to prime tissue for the activation and recruitment of myeloid cells. Their pathological or protective effects depend on the integration of multiple factors at the cellular level that include the type and strength of the trigger (mutation, light, pathogen, injury) and

susceptibility factors (chemokine deficiencies, inherited retinal degenerations, and other genetic modifiers) that influence the activation state and function of resident microglia and recruited macrophages in the retina.

## 54.10 Targeting Chemokine Pathways as an Immune Modulatory Therapy for Retinal Degenerations

A major challenge for future research involves understanding the relative contributions of protective or detrimental cell- and signal- specific responses of local microglia and recruited macrophages in retinal disease. Studying chemokine and cytokine signalling in the context of all the above mentioned factors may help identify biomarkers for disease progression and novel therapeutic target pathways that may be utilized to modulate innate immune responses in a wide range of inherited and multi-factorial age-related retinal diseases.

## References

1. Xu H, Chen M, Forrester JV (2009) Para-inflammation in the ageing retina. Prog Retin Eye Res 28:348–368
2. Jung S, Aliberti J, Graemmel P, Sunshine MJ, Kreutzberg GW et al (2000) Analysis of fractalkine receptor CX3CR1 function by targeted deletion and green fluorescent protein reporter gene insertion. Mol Cell Biol 20:4106–4114
3. Colton C (2009) Heterogeneity of microglial activation in the innate immune response in the brain. J Neuroimmune Pharmacol 4:399–418
4. Tacke F, Randolph GJ (2006) Migratory fate and differentiation of blood monocyte subsets. Immunobiology 211:609–618
5. Lu B, Rutledge BJ, Gu L, Fiorillo J, Lukacs NW et al (1998) Abnormalities in monocyte recruitment and cytokine expression in monocyte chemoattractant protein 1-deficient mice. J Exp Med 187:601–608
6. Geissmann F, Jung S, Littman DR (2003) Blood monocytes consist of two principal subsets with distinct migratory properties. Immunity 19:71–82
7. Silverman MD, Zamora DO, Pan Y, Texeira PV, Baek SH et al (2003) Constitutive and inflammatory mediator-regulated fractalkine expression in human ocular tissues and cultured cells. Invest Ophthalmol Vis Sci 44:1608–1615
8. Bazan JF, Bacon KB, Hardiman G, Wang W, Soo K et al (1997) A new class of membrane-bound chemokine with a CX3C motif. Nature 385:640–644
9. Xu H, Manivannan A, Dawson R, Crane IJ, Mack M et al (2005) Differentiation to the CCR2+ inflammatory phenotype in vivo is a constitutive, time-limited property of blood monocytes and is independent of local inflammatory mediators. J Immunol 175:6915–6923
10. Chen M, Copland DA, Zhao J, Liu J, Forrester JV et al (2012) Persistent inflammation subverts thrombospondin-1-induced regulation of retinal angiogenesis and is driven by CCR2 Ligation. Am J Pathol 180:235–245
11. Luhmann UFO, Robbie S, Munro PM, Barker SE, Duran Y et al (2009) The drusen-like phenotype in aging Ccl2 knockout mice is caused by an accelerated accumulation of swollen autofluorescent subretinal macrophages. Invest Ophthalmol Vis Sci 50:5934–5943

12. Nakazawa T, Hisatomi T, Nakazawa C, Noda K, Maruyama K et al (2007) From the cover: monocyte chemoattractant protein 1 mediates retinal detachment-induced photoreceptor apoptosis. PNAS 104:2425–2430
13. Rutar M, Natoli R, Provis J (2012) Small interfering RNA-mediated suppression of Ccl2 in Muller cells attenuates microglial recruitment and photoreceptor death following retinal degeneration. J Neuroinflammation 9:221
14. Huang D, Tani M, Wang J, Han Y, He TT et al (2002) Pertussis toxin-induced reversible encephalopathy dependent on monocyte chemoattractant protein-1 overexpression in mice. J Neurosci 22:10633–10642
15. Kezic J, McMenamin PG (2010) The monocyte chemokine receptor CX3CR1 does not play a significant role in the pathogenesis of experimental autoimmune uveoretinitis. Invest Ophthalmol Vis Sci 51:5121–5127
16. Combadiere C, Feumi C, Raoul W, Keller N, Rodero M et al (2007) CX3CR1-dependent subretinal microglia cell accumulation is associated with cardinal features of age-related macular degeneration. J Clin Invest 117:2920–2928
17. Zhang M, Xu G, Liu W, Ni Y, Zhou W (2012) Role of fractalkine/CX3CR1 interaction in light-induced photoreceptor degeneration through regulating retinal microglial activation and migration. PLoS ONE 7:e35446
18. Seidler S, Zimmermann H, Bartneck M, Trautwein C, Tacke F (2010) Age-dependent alterations of monocyte subsets and monocyte-related chemokine pathways in healthy adults. BMC Immunol 11:30
19. Grunin M, Burstyn-Cohen T, Hagbi-Levi S, Peled A, Chowers I (2012) Chemokine receptor expression in peripheral blood monocytes from patients with neovascular age-related macular degeneration. Invest Ophthalmol Vis Sci 53:5292–5300
20. Jonas JB, Tao Y, Neumaier M, Findeisen P (2012) Cytokine concentration in aqueous humour of eyes with exudative age-related macular degeneration. Acta Ophthalmol 90(5):e381–388
21. Ambati J, Anand A, Fernandez S, Sakurai E, Lynn BC et al (2003) An animal model of age-related macular degeneration in senescent Ccl-2- or Ccr-2-deficient mice. Nat Med 9:1390–1397
22. Chen M, Forrester JV, Xu H (2011) Dysregulation in retinal para-inflammation and age-related retinal degeneration in CCL2 or CCR2 deficient mice. PLoS ONE 6:e22818
23. Luhmann UFO, Carvalho LS, Robbie SJ, Cowing JA, Duran Y et al (2013) Ccl2, Cx3cr1 and Ccl2/Cx3cr1 chemokine deficiencies are not sufficient to cause age-related retinal degeneration. Exp Eye Res 107:80–87
24. Chinnery HR, McLenachan S, Humphries T, Kezic JM, Chen X et al (2012) Accumulation of murine subretinal macrophages: effects of age, pigmentation and CX3CR1. Neurobiol Aging 33(8):1769–1776
25. Luhmann UFO, Lange CA, Robbie S, Munro PMG, Cowing JA et al (2012) Differential modulation of retinal degeneration by *Ccl2* and *Cx3cr1* chemokine signalling. PLoS ONE 7:e35551
26. Ng TF, Streilein JW (2001) Light-induced migration of retinal microglia into the subretinal space. Invest Ophthalmol Vis Sci 42:3301–3310

# Chapter 55
# The Complement Regulatory Protein CD59: Insights into Attenuation of Choroidal Neovascularization

**Gloriane Schnabolk, Stephen Tomlinson and Bärbel Rohrer**

**Abstract** Complement activation is associated with age-related macular degeneration (AMD), with the retinal pigment epithelium (RPE) being one of the main target tissues. In AMD, disease severity is correlated with the formation of the membrane attack complex (MAC), the terminal step in the complement cascade, as well as diminished RPE expression of CD59, a membrane-bound regulatory protein of MAC formation. This has prompted the search for therapeutic strategies based on MAC inhibition, and soluble forms of CD59 (sCD59) have been investigated in mouse laser-induced choroidal neovascularization, a model for "wet" AMD. Unlike membrane-bound CD59, sCD59 provides relatively poor cell protection from complement, and different strategies to increase sCD59 activity at the cell membrane level have been investigated. These include increasing the circulatory half-life of sCD59 by the addition of an Fc moiety; increasing the half-life of sCD59 in target tissues by modifying CD59 with a (non-specific) membrane-targeting domain; and by locally overexpressing sCD59 via adenoviral vectors. Finally, a different strategy currently under investigation employs complement receptor (CR)2-mediated

B. Rohrer (✉). G. Schnabolk
Ralph H. Johnson VA Medical Center, Division of Research,
Charleston, SC 29401, USA
e-mail: faith@musc.edu

S. Tomlinson
Departments of Microbiology and Immunology, Medical University of South Carolina,
Charleston, SC 29425, USA
e-mail: faith@musc.edu

B. Rohrer
Departments of Ophthalmology and Neurosciences, Medical University of South Carolina,
Charleston, SC 29425, USA
e-mail: rohrer@musc.edu

J. D. Ash et al. (eds.), *Retinal Degenerative Diseases,* Advances in Experimental Medicine and Biology 801, DOI 10.1007/978-1-4614-3209-8_55,

targeting of CD59 exclusively to membranes under complement attack. CR2 recognizes long-lasting membrane-bound breakdown activation fragments of complement C3. CR2-CD59 may have greater therapeutic potential than other complement inhibitory approaches, since it can be administered either systemically or locally, it will bind specifically to membranes containing activated complement activation fragments, and dosing can be regulated. Hence, this strategy might offer opportunities for site-specific inhibition of complement in diseases with restricted sites of inflammation such as AMD.

**Keywords** AMD · CD59 · Complement · Choroidal neovascularization (CNV) · Membrane attack complex (MAC)

## 55.1 Introduction

Age-related macular degeneration (AMD) is the leading cause of blindness in developed countries, generally affecting individuals over the age of 50. Divided into two forms, AMD is classified as “dry” and “wet”. Dry AMD results in atrophy of the retinal pigment epithelium (RPE), and eventually leads to photoreceptor loss [1, 2]. Patients with this form of AMD exhibit drusen, deposits found on the basal surface of the RPE [3]. Wet AMD is so called due to subretinal fluid leakage, and is further characterized by choroidal neovascularization of the RPE and Bruch’s membrane. While this disease was first described over 80 years ago, current methods to treat AMD are limited. Early dry AMD is treated with antioxidants (NIH Publication No. 03-2294), whereas no treatment is currently available for advanced dry AMD (geographic atrophy, GA). Therapeutics to treat wet AMD rely on invasive techniques, administering compounds that block vascular endothelial growth factor (VEGF), required for neovascularization. However, it is unclear as to the efficacy and safety for long-term treatment. In a search for more effective strategies to treat AMD, researchers have been exploring various pathways involved in the development and progression of AMD. One such pathway, the complement system, has been linked to AMD. Drusen deposits have been found to contain various complement proteins [2]. In addition, single nucleotide polymorphisms, such as those identified with complement factor H (fH), have also been associated with an increased AMD risk [4].

The complement system is made up of three activation pathways, the classical (CP), the lectin (LP), and the alternative pathway (AP). Providing innate defense against pathogens, these pathways are initiated in a pathway and pattern-recognition molecule (PRM)-specific manner [5]. Following activation, the three pathways converge with the cleavage and activation of C3, and the subsequent initiation of the common terminal pathway. Complement activation results in the generation of powerful soluble anaphylactic peptides C3a and C5a, as well as the membrane attack complex (MAC), which can mediate cell lysis and inflammation, as well as cell activation when the MAC is deposited at sublytic concentrations [6]. Due to

the ability of the complement cascade to be spontaneously activated, and the inability of the PRM to distinguish between self- and nonself-cells, various soluble and membrane-bound regulators and inhibitors that act on different steps along the complement cascade are present to keep the complement system in check. In this chapter, we will focus on CD59, an inhibitor of MAC formation, and discuss implications for its possible use as a treatment for AMD.

## 55.2 CD59

CD59, also known as protectin, is an 18–21 kDA glycoprotein which anchors to cell membranes by way of a glycophosphatidylinositol (GPI) anchor [6]. CD59 inhibits MAC formation by binding to C8 and C9 in the assembling MAC, where it has a high affinity for the α-chain of C8 and the "b"-domain of C9 [7]. Reflecting its importance as the terminal inhibitor in the complement pathway, CD59 is widely expressed, although absolute levels vary with tissue type. Human CD59 is encoded by a single gene, whereas in the mouse it is encoded by two homologous genes, *CD59a* and *CD59b* [8]. The expression profile of mouse CD59a more closely mirrors that seen in humans, and CD59a is the protein most studied in mouse models. In terms of evaluating the function and activity of sCD59 in mouse models, it is appropriate to use mouse CD59, not only because of protein immunogenicity, but because CD59 activity is species selective.

The MAC appears to play a pathological role in various diseases, including AMD. In AMD, a high concentration of MAC in the area of Bruch's membrane and the RPE has been documented, with the density of MAC deposition, in particular in the macula, correlating with the severity of AMD. Furthermore, there is a correlation between the amount of MAC deposition and the loss of RPE cells [2]. Localization and levels of CD59 have been examined in donor eyes with and without AMD. All eyes had strong choroidal labeling, whereas RPE cell labeling differed with disease. Control donor eyes exhibited minimal CD59 labeling in the RPE, and early AMD eyes labeled strongly for CD59, in particular on the apical side; whereas staining was reduced in areas overlying drusen (e.g., early AMD) or atrophic regions (e.g., GA) [9]. Taken together, the evidence suggests that the regulation of MAC by CD59 may represent a therapeutic treatment for AMD.

## 55.3 Testing CD59-Based Therapeutics in Mouse CNV

Since MAC formation correlates with AMD severity and loss of RPE cells [2], and since endogenous membrane-bound CD59 levels are inversely correlated with disease (high in early AMD; low to absent in late AMD) [9], CD59 has been investigated as a possible method to regulate MAC formation and AMD. One such approach that has been investigated is the administration of a soluble form of CD59 (sCD59).

Endogenous soluble CD59 has been identified in various human bodily fluids [10, 11]. In many of these fluids, sCD59 retains a GPI anchor, which can insert into a cell membrane, whereas sCD59 found in human urine is without a GPI anchor [10]. Results from hemolytic assays have suggested that both forms of sCD59 show MAC inhibitory activity, but that the inhibitory activity of sCD59 containing a GPI linker is reduced due to its association with unidentified serum proteins [12]. Thus, recombinant sCD59 has typically been produced without the GPI anchor. However, while these studies have illustrated that sCD59 is capable of inhibiting cell lysis, this inhibition is relatively poor when compared to membrane-bound CD59. The importance of membrane targeting was demonstrated in a study performed by He et al., comparing the efficacy of a membrane-targeted CD59 with that of sCD59 [13].

Testing the effects of sCD59 in vivo is hampered by its small size and rapid elimination from the circulation. To increase the circulatory half-life of sCD59, the Bora group utilized a recombinant soluble CD59a-IgG2a fusion-protein. Systemic injections of CD59a-IgG2a reduced CNV, reduced MAC activation in the laser lesion site, and reduced pro-angiogenic growth factor expression [14]. Alternatively, CD59 can be delivered locally to the eye, which various publications have taken advantage of. Intravitreal injection of CD59a-IgG2a [14], as well as injection of CD59a modified with a membrane inserting moiety (APT542) [15], both reduced CNV lesion size. Finally, overexpression of sCD59 in target tissues via adenoviral vectors [16] and utilizing subretinal or intravitreal delivery, significantly reduced CNV size and MAC formation. Together, these results suggest that sCD59 might be suitable as a potential therapy for AMD. However, both approaches have their inherent limitations: CD59a-IgG2a and sCD59-APT542 do not target to sites of complement activation; IgG2a by itself mediates complement activation via the classical pathway [17]; and gene therapy poses significant problems since it relies on an invasive delivery route and inhibitor levels are difficult to control.

As a means to directly target sites of complement activation, CR2 fusion proteins containing different complement inhibitor proteins have been developed. Recently, CR2-fH and CR2-Crry constructs have been created by joining the C3d-binding fragment of mouse CR2 to complement inhibitory regions of mouse fH or Crry [18–20]. The CR2 moiety of the fusion protein binds to iC3b, C3dg, and C3d, which are long-lived complement activation products deposited at sites of complement activation. Hence, CR2 linked to various complement inhibitors allows for site-specific targeting with prolonged tissue retention times. In studies performed by Rohrer et al., intravenous injection of either mouse or human CR2-fH significantly reduced CNV lesion size, and bioavailability of CR2-fH within the lesion was shown to be at least 24 h [19, 21]. Experiments are currently under way to construct and characterize mouse CR2-CD59, and based on the forgoing review of the role of CD59 and the MAC in AMD, we anticipate it will provide effective therapy. If effective, a significant potential advantage of a CD59-based inhibitor over fH, or other C3 inhibitors, is that the generation of early complement activation products that have host defense and homeostatic functions (e.g., clearance of dead and dying cells) will not be affected. These aspects of CR2-CD59 activity will need to be investigated, and it will also be interesting to investigate the use of CR2-CD59 in models of dry AMD.

## 55.4 Conclusions

CD59 expression is altered in the RPE of AMD patients. Early in AMD, healthy RPE expresses high levels of CD59, whereas RPE overlying pathological structures (drusen or atrophic areas) lacks CD59. This suggests that early, but non-pathological alterations in RPE cells trigger an increase in CD59 as a protective response. On the flip-side, this suggests that elevating CD59 at the level of the RPE might prevent pathology in both dry and wet AMD. This hypothesis has been tested by inhibition of MAC using different forms of CD59 in mouse CNV. A consensus seems to have emerged regarding an optimal therapeutic form of CD59. First, CD59 without a GPI anchor should be used. Second, if used locally within the eye, efficacy can be increased by either membrane targeting or by increasing availability by viral vector delivery. And third, if used systemically, half-life needs to be increased either within the circulation, or within the tissue by utilizing a site-specific targeted version of the inhibitor. We suggest that CR2-CD59 will provide the most versatile inhibitor since it would allow for either systemic or local administration, with potentially long-lasting local effects due to its long retention at sites of complement activation.

**Acknowledgments** This review was supported in part by the National Institutes of Health (NIH) (R01EY019320), Department of Veterans Affairs (I01 RX000444), Foundation Fighting Blindness, and an unrestricted grant to MUSC from Research to Prevent Blindness (RPB), Inc., New York, NY. The authors have no financial conflicts of interest.

## References

1. Gehrs KM, Anderson DH, Johnson LV, Hageman GS (2006) Age-related macular degeneration- emerging pathogenetic and therapeutic concepts. Ann of Med 38:450–471
2. Hageman GS, Luthert PJ, Victor Chong NH, Johnson LV, Anderson DH, Mullins RF (2001) An integrated hypothesis that considers drusen as biomarkers of immune-mediated processes at the RPE-Bruch's membrane interface in aging and age-related macular degeneration. Prog Retinal Eye Res 20:705–732
3. Johnson LV, Leitner WP, Staples MK, Anderson DH (2001) Complement activation and inflammatory processes in drusen formation and age related macular degeneration. Exp Eye Res 73:887–896
4. Hageman GS, Anderson DH, Johnson LV, Hancox LS, Taiber AJ, Hardisty LI et al (2005) A common haplotype in the complement regulatory gene factor H (HF1/CFH) predisposes individuals to age-related macular degeneration. Proc Natl Acad Sci U S A 102:7227–7232
5. Muller-Eberhard HJ (1988) Molecular organization and function of the complement system. Ann Rev Biochem 57:321–347
6. Davies A, Simmons DL, Hale G, Harrison RA, Tighe H, Lachmann PJ et al (1989) CD59, an LY-6-like protein expressed in human lymphoid cells, regulates the action of the complement membrane attack complex on homologous cells. J Exp Med 170:637–654
7. Ninomiya H, Sims PJ (1992) The human complement regulatory protein CD59 binds to the alpha-chain of C8 and to the "b"domain of C9. J Biol Chem 267:13675–13680
8. Qin X, Miwa T, Aktas H, Gao M, Lee C, Qian YM et al (2001) Genomic structure, functional comparison, and tissue distribution of mouse Cd59a and Cd59b. Mamm Genome 12:582–589

9. Ebrahimi KB, Fijalkowski N, Cano M, Handa JT (2012) Decreased membrane complement regulators in the retinal pigmented epithelium contributes to age-related macular degeneration. J Pathol (in press)
10. Hakulinen J, Meri S (1995) Shedding and enrichment of the glycolipid-anchored complement lysis inhibitor protectin (CD59) into milk fat globules. Immunology 85:495–501
11. Meri S, Waldmann H, Lachmann PJ (1991) Distribution of protectin (CD59), a complement membrane attack inhibitor, in normal human tissues. Lab Invest 65:532–537
12. Sugita Y, Ito K, Shiozuka K, Suzuki H, Gushima H, Tomita M et al (1994) Recombinant soluble CD59 inhibits reactive haemolysis with complement. Immunology 82:34–41
13. He C, Imai M, Song H, Quigg RJ, Tomlinson S (2005) Complement inhibitors targeted to the proximal tubule prevent injury in experimental nephrotic syndrome and demonstrate a key role for C5b-9. J Immunol 174:5750–5757
14. Bora NS, Kaliappan S, Jha P, Xu Q, Sivasankar B, Harris CL et al (2007) CD59, a complement regulatory protein, controls choroidal neovascularization in a mouse model of wet-type age-related macular degeneration. J Immunol 178:1783–1790
15. Bora NS, Jha P, Lyzogubov VV, Kaliappan S, Liu J, Tytarenko RG et al (2010) Recombinant membrane-targeted form of CD59 inhibits the growth of choroidal neovascular complex in mice. J Biol Chem 285:33826–33833
16. Cashman SM, Ramo K, Kumar-Singh R (2011) A non membrane-targeted human soluble CD59 attenuates choroidal neovascularization in a model of age related macular degeneration. PloS One 6:e19078
17. Leatherbarrow RJ, Dwek RA (1984) Binding of complement subcomponent C1q to mouse IgG1, IgG2a and IgG2b: a novel C1q binding assay. Mol Immunol 21:321–327
18. Atkinson C, Song H, Lu B, Qiao F, Burns TA, Holers VM et al (2005) Targeted complement inhibition by C3d recognition ameliorates tissue injury without apparent increase in susceptibility to infection. J Clin Invest 115:2444–2453
19. Rohrer B, Long Q, Coughlin B, Wilson RB, Huang Y, Qiao F et al (2009) A targeted inhibitor of the alternative complement pathway reduces angiogenesis in a mouse model of age- related macular degeneration. Invest Ophthalmol Vis Sci 50:3056–3064
20. Song H, He C, Knaak C, Guthridge JM, Holers VM, Tomlinson S (2003) Complement receptor 2-mediated targeting of complement inhibitors to sites of complement activation. J Clin Invest 111:1875–1885
21. Rohrer B, Coughlin B, Bandyopadhyay M, Holers VM (2012) Systemic human CR2-targeted complement alternative pathway inhibitor ameliorates mouse laser-induced choroidal neovascularization. J Ocular Pharmacol Ther 28:402–409

# Chapter 56
# Regeneration-Associated Genes on Optic Nerve Regeneration in Fish Retina

**Kazuhiro Ogai, Maki Nishitani, Ayaka Kuwana, Kazuhiro Mawatari, Yoshiki Koriyama, Kayo Sugitani, Hiroshi Nakashima and Satoru Kato**

**Abstract** It has been well documented that fish central nervous system, including retina and optic nerve, can regenerate and recover its function after nerve injury. Within a few decades, a number of regeneration-associated genes (RAGs) have been identified in fish retina following optic nerve injury (ONI). RAGs can be classified into two groups: cell survival- and axonal outgrowth-related genes. In fish retina after ONI, cell survival-related genes were upregulated in 1–6 days after ONI, which corresponds to the preparation stage for cell survival and axonal sprouting. Subsequently, axonal outgrowth-related genes were upregulated in 1–6 weeks after ONI, which corresponds to the axonal regrowth stage. Recently, we've found a novel type of RAGs, dedifferentiation-related genes, that are upregulated in overlapping time between cell survival and axonal regrowth (3–10 days after ONI). In this chapter we summarize these three types of RAGs that promote optic nerve regeneration in the fish retina after ONI.

**Keywords** Optic nerve regeneration · Fish · Retina · Regeneration-associated genes · Cell survival · Axonal elongation

S. Kato (✉) · Y. Koriyama
Department of Molecular Neurobiology, Graduate School of Medical Science, Kanazawa University, 13-1 Takaramachi, Kanazawa, Ishikawa, 920-8640, Japan
e-mail: satoru@med.kanazawa-u.ac.jp

K. Ogai · M. Nishitani · A. Kuwana · K. Mawatari · K. Sugitani · H. Nakashima
Division of Health Sciences, Graduate School of Medical Science, Kanazawa University, 5-11-80 Kodatsuno, Kanazawa, Ishikawa, 920-0942, Japan
e-mail: kazu0208@stu.kanazawa-u.ac.jp

Y. Koriyama
e-mail: koriyama@med.kanazawa-u.ac.jp

K. Sugitani
e-mail: sugitani@staff.kanazawa-u.ac.jp

H. Nakashima
e-mail: hinaka@staff.kanazawa-u.ac.jp

J. D. Ash et al. (eds.), *Retinal Degenerative Diseases,* Advances in Experimental Medicine and Biology 801, DOI 10.1007/978-1-4614-3209-8_56,

**Abbreviation**

| | |
|---|---|
| Dpi | Day(s) post-injury |
| FXIII-A | Cellular factor XIII A subunit |
| GAP43 | Growth associated protein 43 |
| IGF-1 | Insulin-like growth factor 1 |
| NO | Nitric oxide |
| NOS | Nitric oxide synthase |
| ONI | Optic nerve injury |
| PI3K | Phosphatidylinositol-3 kinase |
| RAG | Regeneration-associated gene |
| RGC | Retinal ganglion cell |
| $TG_R$ | Retinal transglutaminase |

## 56.1 Introduction

Visual loss caused by glaucoma or optic nerve injury (ONI) is thought to be one of the problematic diseases, as once retinal ganglion cells (RGCs) have degenerated, they cannot survive and, if survived, they cannot regenerate their axons [1]. In contrast to such a tragic situation, fish are able to regain the visual function even after ONI. We have conducted behavioral and morphological studies of fish during optic nerve regeneration, and revealed the temporal change of regenerative stages [2]. First, the injured RGCs should be survived following injury, and be ready to promote axon regrowth (Fig. 56.1, stage *I*). Next, they should continue to extend their axons to the visual center of the brain (Fig. 56.1, stage *II*). Finally, the synaptic reorganization should be taken place in the brain (Fig. 56.1, stage *III*) followed by functional recovery (Fig. 56.1, stage *IV*). However, there had been little insight into molecular mechanisms that govern these regenerative functions. For more than a decade, therefore, we have studied a number of "regeneration-associated genes" (RAGs) that are related to each regeneration stage. Thus far, we have found a number of genes that are responsible for cell survival (Fig. 56.1, (*1*)) and for axonal regeneration (Fig. 56.1, (*3*)) [2]. Recently we found a novel candidate of RAGs: dedifferentiation-associated genes (Fig. 56.1, (*2*)) between cell survival and axonal regrowth stage. Here we summarize these RAGs with regeneration stages following ONI in adult fish.

## 56.2 Cell Survival-Related Genes

In mammals after ONI, more than half of RGCs are lost through the induction of pro-apoptotic pathway and the inhibition of anti-apoptotic pathway. For example in rat model, injured RGCs upregulate Bax protein, which is an effective molecule of apoptotic pathway (cytochrome-*c*, caspase-9 and caspase-3), leading to apoptotic

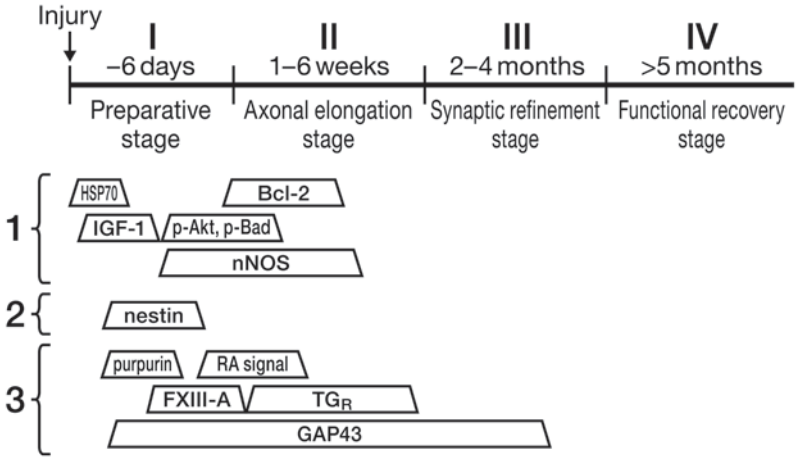


**Fig. 56.1** Classification of various regeneration-associated genes (RAGs) during optic nerve regeneration in fish. Factors in (*1*) are cell survival-related genes, which are contributing to the cell survival of RGCs following ONI. Factors in (*3*) are axonal regeneration-related genes, which are responsible for axonal regeneration. Note that the factors in (*1*) are upregulated in the early stage of optic nerve regeneration (stage *I–II*) whereas factors in (*3*) are mainly expressed in axonal regenerative stages (stage *II–III*). We propose a novel type of RAGs: dedifferentiation-related genes (*2*) that appear in the transitional period of stage *I* and *II*

cell death at 6 days post-injury (dpi). In addition, insulin-like growth factor 1 (IGF-1), which activates anti-apoptotic p-Akt, p-Bad and Bcl-2 through phosphatidylinositol-3 kinase (PI3K) system, is downregulated in injured RGCs within 1 week after ONI [3]. Because of such rapid adverse changes on cell survival, mammalian RGCs are difficult to survive following ONI. On the other hand, in fish retina, anti-apoptotic p-Akt, p-Bad and Bcl-2 are upregulated through IGF-1/PI3K system in 3–20 dpi [4]. Indeed, the number of surviving RGCs in fish retina after ONI is not much changed even at 30 dpi. Moreover, heat shock protein 70 and heat shock factor 1, both are contributing to protecting cells from a variety of stress conditions and from apoptotic cell death, are upregulated very rapidly after nerve injury (30 min to 24 h post-injury) to protect RGCs from the onset of apoptotic cell death in fish retina [5].

There are another factors for cell survival: nitric oxide (NO) and NO synthase (NOS). NO is a gaseous molecule which is produced by three types of NOS: neuronal, endothelial, and inducible NOS (nNOS, eNOS and iNOS, respectively). NO appears to be both toxic and protective to neurons in central nervous system. In mammalian retina, iNOS is expressed in Müller cells after ONI [6]. Then iNOS produces a massive amount of NO, which is thought to be the cause of apoptotic cell death of RGCs [7]. In fish retina after nerve injury; however, only nNOS is upregulated in RGCs after ONI. The nNOS produces a mild amount of NO, leading to a survival of injured RGCs of fish. Therefore, the amount of NO is a crucial factor for the decision between cell death and survival after ONI.

In summary, fish RGCs can survive after ONI owing to a number of survival factors (Fig. 56.1, (*1*)) that are not detected, or excess, in mammalian RGCs.

## 56.3 Axonal Regeneration-Related Genes

Only promoting molecules for cell survival is not sufficient for optic nerve regeneration; promoting molecules for axonal regeneration is also crucial. In mammals, although a small number of injured RGCs could avoid apoptosis, none of them can regenerate their axons [8]. In contrast, injured fish RGCs successfully regenerate their axons, and regenerating axons can reach to the optic tectum within 20–30 dpi [2, 9]. A number of molecules have been described to be involved in such capacity of axonal regeneration in fish (Fig. 56.1, (*3*)).

A retinol-binding protein, purpurin, is upregulated in 1–7 dpi and peaked at 3 dpi in the photoreceptors [10], and retinol is transported with purpurin from photoreceptors to RGCs. Subsequently, in RGCs at 5–10 dpi, retinol is converted to retinoic acid which activates the transcription of neurite outgrowth-related genes [11]. Combining with the fact that the knockdown of purpurin inhibits normal RGCs' differentiation in the early development of zebrafish retina [12], purpurin and retinoic acid signaling are important factors for both development and regeneration of RGCs.

Growth associated protein 43 (GAP43) is known as a marker of growing and regrowing axons [13] and is activated by phosphorylation at the growth cone [14]. In zebrafish retina following ONI, GAP43 expression and phosphorylation of GAP43 are both upregulated for a long term (~60 dpi); interestingly, the expression pattern of phospho-GAP43 is biphasic [9]. The first peak (>10 folds) around 10 dpi corresponds to the axon regrowth period, and the following long plateau (~4 folds) between 20–60 dpi corresponds to the synaptic refinement period when the synapses in optic tectum are restored in order.

Two types of transglutaminase, cellular factor XIII A subunit (FXIII-A) and retinal transglutaminase ($TG_R$) are upregulated in goldfish retina 3–10 dpi and 10–40 dpi, respectively [15, 16]. Although the substrate catalyzed by FXIII-A or $TG_R$ are still unknown, it is proved that both FXIII-A and $TG_R$ promote axonal sprouting and elongation on retinal explant culture system, and the effects are regressed by treatment of anti-FXIII-A or anti-$TG_R$ antibody. Interestingly, the effect of FXIII-A is different depending on its expression site. In goldfish retina after ONI, FXIII-A is upregulated in RGCs between 3 and 10 dpi. Whereas, in optic nerve, FXIII-A upregulation is maintained for more than 20 days after ONI, and is produced by non-neuronal cells (e.g., glial cells). Sugitani et al. provide a rationale for such a distinct effect as follows; FXIII-A in RGCs is thought to be related to sprouting of new axons following injury, and FXIII-A in optic nerve, secreted from glial cells, is supporting the elongation of regrowing axons following injury.

Taken together, many factors contributing to axonal regrowth are upregulated intrinsically in fish retina after ONI. An exogenous induction of these factors to the mammalian retina following injury would be a reliable approach to the treatment against optic nerve disorders in mammals [4, 15].

## 56.4 Dedifferentiation-Related Genes

In fish retina, once photoreceptors undergo cell death by constant and intense light, Müller cells proliferate, dedifferentiate and serve as a source of new photoreceptor cells [17]. However, under ONI there is no supplement of new RGCs from either Müller cells, because the number of RGCs does not change, and there is no sign of cell death [4] or cell proliferation (K. Ogai, unpublished data) after ONI. It is natural, therefore, to think that there is a transition of RGCs' states so that they can regrow new axons.

Till date, we have observed an upregulation of nestin in RGCs after ONI in zebrafish. Nestin is an intermediate filament protein, and its expression is specific for neural stem cells [18]. In unlesioned retina, *nestin* mRNA is rarely expressed. At 5 dpi, the expression of *nestin* is increased about 4-fold as compared to the unlesioned retina (Fig. 56.1, (*2*)), and its upregulation is limited in RGCs. That is, injured RGCs express the "neural stem cell-specific protein", implying that the state of RGCs might be changed from mature ($nestin^{-}$) to immature ($nestin^{+}$) state which enables them to regrow new axons.

However, we have not found the factors that transit RGCs from mature to immature state. Our next goal is to determine such factors that are intrinsically upregulated in fish RGCs and able to change RGCs' state.

## 56.5 Conclusion

As shown here, many factors are upregulated in fish RGCs after ONI, and all of which have regenerative properties (Fig. 56.1). Such regenerative properties provide us a useful and reliable therapeutic tool for regeneration of mammalian RGCs after ONI [3, 15].

## References

1. Ramón y Cajal S (1928) Degeneration and regeneration in the nervous system. Haffner Publishing Co, New York
2. Matsukawa T, Arai K, Koriyama Y, Liu Z, Kato S (2004) Axonal regeneration of fish optic nerve after injury. Biol Pharm Bull 27:445–451
3. Homma K, Koriyama Y, Mawatari K, Higuchi Y, Kosaka J, Kato S (2007) Early downregulation of IGF-I decides the fate of rat retinal ganglion cells after optic nerve injury. Neurochem Int 50:741–748

4. Koriyama Y, Homma K, Sugitani K, Higuchi Y, Matsukawa T, Murayama D, Kato S (2007) Upregulation of IGF-I in the goldfish retinal ganglion cells during the early stage of optic nerve regeneration. Neurochem Int 50:749–756
5. Nagashima M, Fujikawa C, Mawatari K, Mori Y, Kato S (2012) HSP70, the earliest-induced gene in the zebrafish retina during optic nerve regeneration: its role in cell survival. Neurochem Int 58:888–895
6. Koeberle PD, Ball AK (1999) Nitric oxide synthase inhibition delays axonal degeneration and promotes the survival of axotomized retinal ganglion cells. Exp Neurol 158:366–381
7. Goureau O, Régnier-Ricard F, Courtois Y (1999) Requirement for nitric oxide in retinal neuronal cell death induced by activated Müller glial cells. J Neurochem 72:2506–2515
8. Leon S, Yin Y, Nguyen J, Irwin N, Benowitz LI (2000) Lens injury stimulates axon regeneration in the mature rat optic nerve. J Neurosci 20:4615–4626
9. Kaneda M, Nagashima M, Nunome T, Muramatsu T, Yamada Y, Kubo M, Muramoto K, Matsukawa T, Koriyama Y, Sugitani K, Vachkov IH, Mawatari K, Kato S (2008) Changes of phospho-growth-associated protein 43 (phospho-GAP43) in the zebrafish retina after optic nerve injury: a long-term observation. Neurosci Res 61:281–288
10. Tanaka M, Murayama D, Nagashima M, Higashi T, Mawatari K, Matsukawa T, Kato S (2007) Purpurin expression in the zebrafish retina during early development and after optic nerve lesion in adults. Brain Res 1153:34–42
11. Nagashima M, Sakurai H, Mawatari K, Koriyama Y, Matsukawa T, Kato S (2008) Involvement of retinoic acid signaling in goldfish optic nerve regeneration. Neurochem Int 54: 229–236
12. Nagashima M, Mawatari K, Tanaka M, Higashi T, Saito H, Muramoto K, Matsukawa T, Koriyama Y, Sugitani K, Kato S (2009) Purpurin is a key molecule for cell differentiation during the early development of zebrafish retina. Brain Res 1302:54–63
13. Skene JH (1989) Axonal growth-associated proteins. Annu Rev Neurosci 12:127–156
14. Coggins PJ, Zwiers H (1989) Evidence for a single protein kinase C-mediated phosphorylation site in rat brain protein B-50. J Neurochem 53:1895–1901
15. Sugitani K, Matsukawa T, Koriyama Y, Shintani T, Nakamura T, Noda M, Kato S (2006) Upregulation of retinal transglutaminase during the axonal elongation stage of goldfish optic nerve regeneration. Neuroscience 142:1081–1092
16. Sugitani K, Ogai K, Hitomi K, Nakamura-Yonehara K, Shintani T, Noda M, Koriyama Y, Tanii H, Matsukawa T, Kato S (2012) A distinct effect of transient and sustained upregulation of cellular factor XIII in the goldfish retina and optic nerve on optic nerve regeneration. Neurochem Int 61:423–432
17. Thummel R, Kassen SC, Enright JM, Nelson CM, Montgomery JE, Hyde DR (2008) Characterization of Müller glia and neuronal progenitors during adult zebrafish retinal regeneration. Exp Eye Res 87:433–444
18. Lendahl U, Zimmerman LB, McKay RD (1990) CNS stem cells express a new class of intermediate filament protein. Cell 60:585–595

# Chapter 57
# Dominant Stargardt Macular Dystrophy (STGD3) and ELOVL4

**Sreemathi Logan and Robert E. Anderson**

**Abstract** Autosomal dominant Stargardt3 Macular Dystrophy (STGD3) results from mutations in the *ELOVL4* gene. ELOVL4 protein localizes to the endoplasmic reticulum (ER), where it mediates the rate-limiting condensation reaction during very long-chain (VLC, ≥ C28) fatty acid biosynthesis. The defective gene product is truncated at the C-terminus, leading to mislocalization and aggregation in other organelles. In this review, we summarize our current understanding of the disease-causing mutation and its potential role in STGD3 pathogenesis.

**Keywords** Retinal degeneration · Fatty acids · Macular dystrophy · Autosomal dominant · Stargardt · Endoplasmic reticulum

## 57.1 Introduction

The etiology of autosomal-dominant Stargardt Macular Dystrophy (STGD3) in humans was described by three independent research groups as resulting from mutations in the *ELOVL4* gene [1–4]. Patients with STGD3 suffer from early onset loss of central vision with progressive degeneration of the macula and subsequently the peripheral retina.

R. E. Anderson (✉) · S. Logan
Department of Cell Biology, University of Oklahoma Health Sciences Center,
608 Stanton L. Young Boulevard, Oklahoma City, OK 73104, USA
e-mail: robert-anderson@ouhsc.edu

Dean A. McGee Eye Institute, Oklahoma City, OK, USA

R. E. Anderson
Department of Ophthalmology, University of Oklahoma Health Sciences Center,
608 Stanton L. Young Boulevard, Oklahoma City, OK 73104, USA

S. Logan
e-mail: slogan1@ouhsc.edu

J. D. Ash et al. (eds.), *Retinal Degenerative Diseases,* Advances in Experimental Medicine and Biology 801, DOI 10.1007/978-1-4614-3209-8_57,

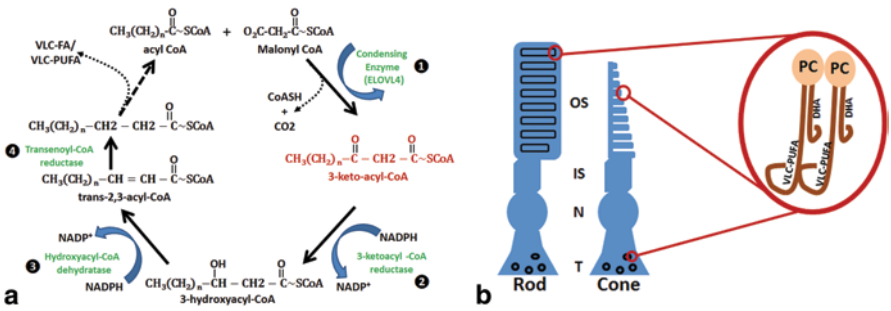


**Fig. 57.1** VLC fatty acid elongation in the retina. **a** ELOVL4 catalyzes the initial rate-limiting condensation reaction between a fatty acyl-CoA and malonyl-CoA (the 2-carbon donor) generating a 3-keto intermediate. *1* The 3-keto intermediate is reduced by KAR, *2* dehydrated by HACD1, *3* and reduced by TER to yield the final product, *4* a fatty acid elongated by two carbons, or further elongated by this cyclical process. **b** VLC-PUFA are enriched in the phosphatidylcholine (*PC*) fraction in photoreceptor membranes. *OS* outer segment, *IS* inner segment, *N* nucleus, *T* synaptic terminal

ELOVL4 has been shown to elongate very long chain (VLC) saturated (FA) and polyunsaturated fatty acids (PUFA) ≥C28 [5, 6]. ELOVL4 is an integral membrane protein with predicted five transmembrane segments, a C-terminal di-lysine endoplasmic reticulum (ER) retention signal (KXKXX), and a histidine motif (HXXHH) shown to sequester dioxy iron in fatty acid desaturases and other iron-binding enzymes during catalysis [3, 7]. VLC fatty acid synthesis occurs in the ER via a four-step cyclical process of condensation, reduction, dehydration, and reduction (Fig. 57.1a), yielding a fatty acid elongated by two carbons [8].

VLC-PUFA in the retina are enriched in the phosphatidylcholine (PC) fraction of retinal lipids [9] and are present in ~13% of the PC in rod photoreceptor outer segments, with DHA (22:6n−3) as the predominant partner (Fig. 57.1b) in the dipolyunsaturated molecular species [9–11]. In the retina, VLC-PUFA have been shown to be tightly associated with rhodopsin, and were suggested to possibly aid in phototransduction via maintenance of the curvature and fluidity of the membranes [12]. VLC fatty acids are also components of brain lipids [13], levels of which accumulate in patients with peroxisomal disorders, such as Zellweger syndrome [14]. In mammalian testes, VLC-PUFA are enriched in the sphingomyelin and ceramide fractions of the total lipids, levels of which increase during spermatogenesis [15]. VLC-PUFA levels remain high in fertile adult rats and decline with age [16], suggesting an important role of these fatty acids in fertility.

## 57.2 STGD3 Mutations

In 2001, two independent groups revealed a 5-bp deletion (797–801del*AACTT*) in exon 6 of the *Elongation of Very Long chain fatty acids-4* (*ELOVL4*) gene, which resulted in STGD3 pathology [2, 3]. Another study in the same year reported two

1-bp deletions (*790ΔT and 794ΔT*) in *ELOVL4* [1]. A third mutation, *810C>G* (Tyr270X), in *ELOVL4* was identified in 2004 with similar pathophysiology [4].

Mouse models of STGD3 have failed to recapitulate the human condition. Homozygous KI and KO of *Elovl4* confer neonatal lethality in mice due to compromised skin barrier permeability [17–19]. As a result, the retinal function in these animals remains unknown. *Elovl4* knock-in (KI; 5-bp del) and knock-out (KO) mice show reduced levels of VLC-FA in acyl-ceramide in the skin of heterozygous mice [17, 18, 20, 21]. In addition, retinal levels of VLC-PUFA in the PC are decreased in heterozygous *Elovl4* KI mice [22]. *ELOVL4* transgenic mice (TG1, TG2, and TG3) exhibit progressive retinal degeneration and lipofuscin accumulation in the RPE [23]. The transgenic data are, however, marred by the overexpression of the human mutant transgene (2-fold in TG2 and 5-fold in TG3 mice) compared to the wild-type transgene (WT1) expressing controls. Thus, it is difficult to parse out the contribution of the mutant transgene to the observed phenotype from the effects of over-expression alone. Nevertheless, TG1 mice that show overexpression of the transgene comparable to WT1 show a modest decline in retinal structure and function with age. Transgenic pigs also exhibit diminished electroretinogram with overexpressing of the disease-causing mutation [24].

## 57.3 STGD3 Truncating Mutation Affects Enzyme Activity

Mutations in *ELOVL4* occur downstream of the conserved histidine motif, preserving the active site residues, but resulting in a truncated product that is mislocalized to the Golgi, and forms aggresomes in cultured cells [23, 25–27]. Thus, death of photoreceptors in STGD3 may arise from three possible scenarios: (1) reduction in VLC-PUFA may affect structure and function of photoreceptors, (2) cellular stress generated from the mislocalization of the truncated protein, and (3) generation of toxic products (i.e., 3-ketone intermediates) from the enzymatic activity of the truncated protein due to the preserved active site. Production and accumulation of these toxic ketone intermediates by the truncated ELOVL4 could be an additive insult to the overall reduction in the VLC-PUFA products (Fig. 57.2). In our most recent publication, we clearly showed that despite the preservation of the active site, the mislocalized STGD3 truncated protein lacks innate enzyme activity [6]. We also showed that redirecting the truncated protein to the ER did not restore its function. Thus, the structural modifications due to the mutation render the STGD3 protein inactive. Furthermore, we showed that although there were gross morphological changes associated with the expression of the truncated protein in cultured cells, it did not upregulate the ER-stress pathway.

Over-expressed tagged STGD3 mutant constructs have revealed a dominant-negative effect on the localization of wild-type ELOVL4 in cultured cells [4, 23, 26–28]. In agreement with these studies, we recently showed that the synthesis of VLC-PUFA by wild-type (WT) ELOVL4 was inhibited by the truncated mutant

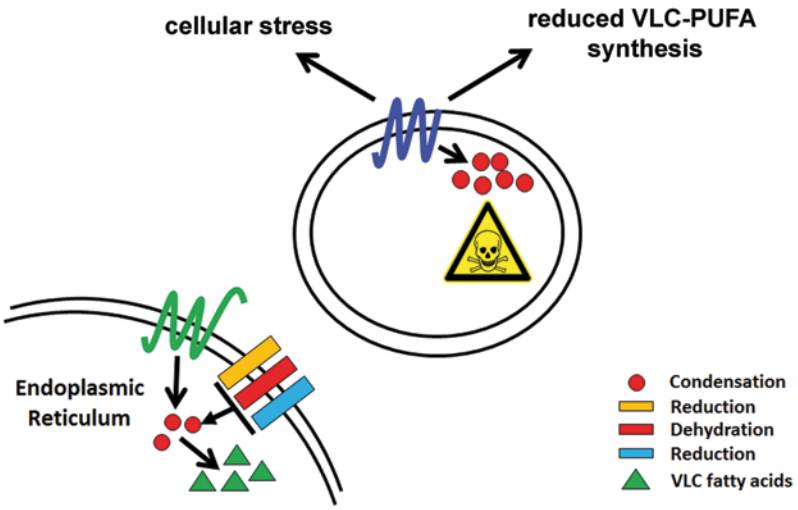


**Fig. 57.2** Mislocalized 3-keto intermediates could be toxic. The mislocalization of catalytically active STGD3 mutant ELOVL4 from the site of fatty acid biosynthesis (endoplasmic reticulum) may generate ketone intermediates in other cellular compartments. In the absence of further processing to the fatty acid product, the ketone intermediates could be toxic

protein [6]. This inhibition was further exacerbated when the mutant was redirected to the ER. We further illustrated using the cell-free microsome assay that the truncated protein, while lacking innate activity, inhibited the condensation activity of WT-ELOVL4, thereby exerting a dominant-negative effect (Fig. 57.3).

## 57.4 Future Directions

Currently, there is no existing treatment for STGD3. There are conflicting reports on DHA supplementation as a means of therapy in animal models of STGD3 [29, 30]. However, a 15-year-old patient with STGD3 who underwent supplementation with DHA for a period of 2 months showed improved visual function, both subjectively via questionnaire and objectively via multifocal electroretinography (mfERG) [31]. Interestingly, the predominant effect was in the b-wave amplitudes of both rod and cone responses, which improved 30% after supplementation, suggesting a role of VLC-PUFA in synaptic transmission. Thus, it is conceivable that direct supplementation with VLC-PUFA, such as 34:5n3, may serve as a viable treatment option for STGD3. In conjunction with dietary supplementation, STGD3 patients may benefit further from ribozyme or RNAi- mediated knock-down of the defective gene product to possibly rescue dominant-negative effects and alterations in photoreceptor structure and function.

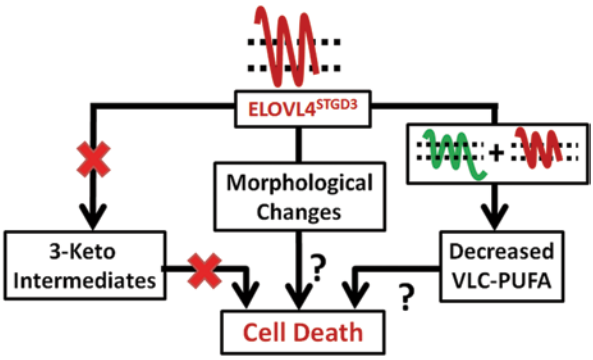


**Fig. 57.3** STGD3 mutant and its effect on ELOVL4 enzymatic activity. The mislocalized STGD3 mutant protein (ELOVL4$^{STGD3}$) is unable to produce the condensation product (3-keto intermediate) and thus the VLC-PUFA. Gross morphological changes induced by the STGD3 mutant may contribute to cell death through unknown mediators ("?"). Furthermore, the STGD3 mutant alters wild-type ELOVL4 localization and has a dominant-negative effect on ELOVL4-mediated synthesis of VLC-PUFA. In photoreceptors, reduction in VLC-PUFA beyond critical levels may culminate in photoreceptor degeneration

**Acknowledgment** This work was supported by NIH Grants EY00871, EY04149, EY21725, EY21725 and RR17703; Foundation Fighting Blindness, Inc., and Research to Prevent Blindness, Inc.

## References

1. Bernstein PS, Tammur J, Singh N, Hutchinson A, Dixon M, Pappas CM, Zabriskie NA, Zhang K, Petrukhin K, Leppert M, Allikmets R (2001) Diverse macular dystrophy phenotype caused by a novel complex mutation in the ELOVL4 gene. Invest Ophthalmol Vis Sci 42(13):3331–3336
2. Edwards AO, Donoso LA, Ritter R 3rd (2001) A novel gene for autosomal dominant Stargardt-like macular dystrophy with homology to the SUR4 protein family. Invest Ophthalmol Vis Sci 42(11):2652–2663
3. Zhang K, Kniazeva M, Han M, Li W, Yu Z, Yang Z, Li Y, Metzker ML, Allikmets R, Zack DJ, Kakuk LE, Lagali PS, Wong PW, MacDonald IM, Sieving PA, Figueroa DJ, Austin CP, Gould RJ, Ayyagari R, Petrukhin K (2001) A 5-bp deletion in ELOVL4 is associated with two related forms of autosomal dominant macular dystrophy. Nat Genet 27(1):89–93
4. Maugeri A, Meire F, Hoyng CB, Vink C, Van Regemorter N, Karan G, Yang Z, Cremers FP, Zhang K (2004) A novel mutation in the ELOVL4 gene causes autosomal dominant Stargardt-like macular dystrophy. Invest Ophthalmol Vis Sci 45(12):4263–4267
5. Agbaga MP, Brush RS, Mandal MN, Henry K, Elliott MH, Anderson RE (2008) Role of Stargardt-3 macular dystrophy protein (ELOVL4) in the biosynthesis of very long chain fatty acids. Proc Natl Acad Sci U S A 105(35):12843–12848
6. Logan S, Agbaga MP, Chan MD, Kabir N, Mandal NA, Brush RS, Anderson RE (2013) Deciphering mutant ELOVL4 activity in autosomal-dominant Stargardt macular dystrophy. Proc Natl Acad Sci U S A 110(14):5446–5451

7. Shanklin J, Whittle E, Fox BG (1994) Eight histidine residues are catalytically essential in a membrane-associated iron enzyme, stearoyl-CoA desaturase, and are conserved in alkane hydroxylase and xylene monooxygenase. BioChemistry 33(43):12787–12794
8. Nugteren DH (1965) The enzymic chain elongation of fatty acids by rat-liver microsomes. Biochim Biophys Acta 106(2):280–290
9. Aveldano MI (1987) A novel group of very long chain polyenoic fatty acids in dipolyunsaturated phosphatidylcholines from vertebrate retina. J Biol Chem 262(3):1172–1179
10. Aveldano MI, Sprecher H (1987) Very long chain (C24 to C36) polyenoic fatty acids of the n-3 and n-6 series in dipolyunsaturated phosphatidylcholines from bovine retina. J Biol Chem 262(3):1180–1186
11. Poulos A (1995) Very long chain fatty acids in higher animals—a review. Lipids 30(1):1–14
12. Aveldano MI (1988) Phospholipid species containing long and very long polyenoic fatty acids remain with rhodopsin after hexane extraction of photoreceptor membranes. BioChemistry 27(4):1229–1239
13. Poulos A, Sharp P, Singh H, Johnson D, Fellenberg A, Pollard A (1986) Detection of a homologous series of C26-C38 polyenoic fatty acids in the brain of patients without peroxisomes (Zellweger's syndrome). Biochem J 235(2):607–610
14. Poulos A (1989) Lipid metabolism in Zellweger's syndrome. Prog Lipid Res 28(1):35–51
15. Poulos A, Sharp P, Johnson D, White I, Fellenberg A (1986) The occurrence of polyenoic fatty acids with greater than 22 carbon atoms in mammalian spermatozoa. Biochem J 240(3):891–895
16. Furland NE, Zanetti SR, Oresti GM, Maldonado EN, Aveldano MI (2007) Ceramides and sphingomyelins with high proportions of very long-chain polyunsaturated fatty acids in mammalian germ cells. J Biol Chem 282(25):18141–18150
17. Vasireddy V, Uchida Y, Salem N Jr, Kim SY, Mandal MN, Reddy GB, Bodepudi R, Alderson NL, Brown JC, Hama H, Dlugosz A, Elias PM, Holleran WM, Ayyagari R (2007) Loss of functional ELOVL4 depletes very long-chain fatty acids (> or = C28) and the unique omega-O-acylceramides in skin leading to neonatal death. Hum Mol Genet 16(5):471–482
18. Cameron DJ, Tong Z, Yang Z, Kaminoh J, Kamiyah S, Chen H, Zeng J, Chen Y, Luo L, Zhang K (2007) Essential role of Elovl4 in very long chain fatty acid synthesis, skin permeability barrier function, and neonatal survival. Int J Biol Sci 3(2):111–119
19. Li W, Chen Y, Cameron DJ, Wang C, Karan G, Yang Z, Zhao Y, Pearson E, Chen H, Deng C, Howes K, Zhang K (2007) Elovl4 haploinsufficiency does not induce early onset retinal degeneration in mice. Vision Res 47(5):714–722
20. Li W, Sandhoff R, Kono M, Zerfas P, Hoffmann V, Ding BC, Proia RL, Deng CX (2007) Depletion of ceramides with very long chain fatty acids causes defective skin permeability barrier function, and neonatal lethality in ELOVL4 deficient mice. Int J Biol Sci 3(2):120–128
21. McMahon A, Butovich IA, Mata NL, Klein M, Ritter R 3rd, Richardson J, Birch DG, Edwards AO, Kedzierski W (2007) Retinal pathology and skin barrier defect in mice carrying a Stargardt disease-3 mutation in elongase of very long chain fatty acids-4. Mol Vis 13:258–272
22. McMahon A, Jackson SN, Woods AS, Kedzierski W (2007) A Stargardt disease-3 mutation in the mouse Elovl4 gene causes retinal deficiency of C32-C36 acyl phosphatidylcholines. FEBS Lett 581(28):5459–5463
23. Karan G, Lillo C, Yang Z, Cameron DJ, Locke KG, Zhao Y, Thirumalaichary S, Li C, Birch DG, Vollmer-Snarr HR, Williams DS, Zhang K. (2005) Lipofuscin accumulation, abnormal electrophysiology, and photoreceptor degeneration in mutant ELOVL4 transgenic mice: a model for macular degeneration. Proc Natl Acad Sci U S A 102(11):4164–4169
24. Sommer JR, Estrada JL, Collins EB, Bedell M, Alexander CA, Yang Z, Hughes G, Mir B, Gilger BC, Grob S, Wei X, Piedrahita JA, Shaw PX, Petters RM, Zhang K (2011) Production of ELOVL4 transgenic pigs: a large animal model for Stargardt-like macular degeneration. Br J Ophthalmol 95(12):1749–1754

25. Ambasudhan R, Wang X, Jablonski MM, Thompson DA, Lagali PS, Wong PW, Sieving PA, Ayyagari R (2004) Atrophic macular degeneration mutations in ELOVL4 result in the intracellular misrouting of the protein. Genomics 83(4):615–625
26. Grayson C, Molday RS (2005) Dominant negative mechanism underlies autosomal dominant Stargardt-like macular dystrophy linked to mutations in ELOVL4. J Biol Chem 280(37):32521–32530
27. Vasireddy V, Vijayasarathy C, Huang J, Wang XF, Jablonski MM, Petty HR, Sieving PA, Ayyagari R (2005) Stargardt-like macular dystrophy protein ELOVL4 exerts a dominant negative effect by recruiting wild-type protein into aggresomes. Mol Vis 11:665–676
28. Karan G, Yang Z, Zhang K (2004) Expression of wild type and mutant ELOVL4 in cell culture: subcellular localization and cell viability. Mol Vis 10:248–253
29. Li F, Marchette LD, Brush RS, Elliott MH, Le YZ, Henry KA, Anderson AG, Zhao C, Sun X, Zhang K, Anderson RE (2009) DHA does not protect ELOVL4 transgenic mice from retinal degeneration. Mol Vis 15:1185–1193
30. Dornstauder B, Suh M, Kuny S, Gaillard F, Macdonald IM, Clandinin MT, Sauve Y (2012) Dietary docosahexaenoic acid supplementation prevents age-related functional losses and A2E accumulation in the retina. Invest Ophthalmol Vis Sci 53(4):2256–2265
31. MacDonald IM, Hebert M, Yau RJ, Flynn S, Jumpsen J, Suh M, Clandinin MT (2004) Effect of docosahexaenoic acid supplementation on retinal function in a patient with autosomal dominant Stargardt-like retinal dystrophy. Br J Ophthalmol 88(2):305–306

# Chapter 58
# Modulation of the Rate of Retinal Degeneration in T17M RHO Mice by Reprogramming the Unfolded Protein Response.

**Shreyasi Choudhury, Sonali Nashine, Yogesh Bhootada, Mansi Motiwale Kunte, Oleg Gorbatyuk, Alfred S. Lewin and Marina Gorbatyuk**

**Abstract** The goal of this study is to validate whether reprogramming of the UPR via modulation of pro-apoptotic caspase-7 and CHOP proteins could be an effective approach to slow down the rate of retinal degeneration in ADRP mice. In order to pursue our goal we created the T17M *RHO* CASP7 and T17M *RHO* CHOP mice to study the impact of the CASP7 or CHOP ablations in T17M *RHO* retina by ERG, SD-OCT, histology and western blot analysis. The scotopic ERG demonstrated that the ablation of the CASP7 in T17M *RHO* retina leads to significant preservation of the function of photoreceptors compared to control. Surprisingly, the ablation of pro-apoptotic CHOP protein in T17M *RHO* mice led to a more severe form of retinal degeneration. Results of the SD-OCT and histology were in agreement with the ERG data. The further analysis demonstrated that the preservation of the structure and function or the acceleration of the onset of the T17M *RHO* photoreceptor degeneration occurred via reprogramming of the UPR. In addition, the CASP7 ablation leads to the inhibition of cJUN mediated apoptosis, while the ablation of

M. Gorbatyuk (✉)
1670 University Blvd., Birmingham, AL 35294, USA
e-mail: mgortk@uab.edu

S. Choudhury · S. Nashine · M. M. Kunte
Department of Cell Biology and Anatomy, University of North Texas Health Science Center, Fort Worth, TX, USA
e-mail: shreyasi.choudhury@live.unthsc.edu

S. Nashine
e-mail: sonali.nashine@live.unthsc.edu

M. M. Kunte
e-mail: mansikunte@yahoo.com

Y. Bhootada · M. Gorbatyuk
Department of Molecular Genetics and Microbiology, University of Florida, Gainesville, FL, USA
e-mail: yb0022@uab.edu

O. Gorbatyuk · A. S. Lewin
Department of Vision Sciences, University of Alabama at Birmingham, Birmingham, AL, USA
e-mail: olegor@ufl.edu

J. D. Ash et al. (eds.), *Retinal Degenerative Diseases,* Advances in Experimental Medicine and Biology 801, DOI 10.1007/978-1-4614-3209-8_58,

CHOP induces an increase in the HDAC. Thus, manipulation with the UPR requires careful examination in order to achieve a therapeutic effect.

**Keywords** ADRP · UPR · Caspase-7 · CHOP · Apoptosis

## 58.1 Introduction

The T17M mutation within *Rhodopsin* (*RHO*) gene affects the assembly of the opsin protein with 11-cis-retinal [1] and presumably impairs protein stability, folding and trafficking [1, 2] leading to a severe form of retinal degeneration known as autosomal dominant retinitis pigmentosa (ADRP). Recently, we have shown that the ER stress associated caspase-7 and the pro-apoptotic CHOP protein are elevated in ADRP retina [3–5]. However, no direct evidence of the important role of the caspase-7 and CHOP proteins in the mechanism of ADRP progression has been found so far. Therefore, our goal is to verify whether the genetic manipulation with pro-apoptotic UPR-associated caspase-7 and CHOP proteins is beneficial for ADRP photoreceptors.

## 58.2 Materials and Methods

### *58.2.1 Animal Models*

C57BL/6 (wild type, WT), Caspase 7−/− (CSP7) and CHOP−/− (CHOP) were purchased from the Jackson Laboratory. The T17M CSP7 and T17M CHOP mice were obtained from the breeding of knockout mice with T17M RHO (T17M) mice. All mice were raised under a 12-h light/12-h dark cycle.

### *58.2.2 Electroretinography*

The scotopic ERG with dark-adapted (12 h) and anesthetized mice at postnatal day (P) 30, 60, and 90 was performed using LKC Technologies as previously described [3].

### *58.2.3 Spectra-Domain Optical Coherent Tomography (SD-OCT)*

The SD-OCT was performed in P30 mice using the SDOIS as previously described [3]. The thickness of the outer nuclear layer (ONL) was determined by averaging

10 measurements within 100, 200, 300, and 400 μm of the optic nerve head in the superior and inferior hemispheres of the retina.

### *58.2.4 H and E staining*

The histological analysis and H and E staining in WT, T17M, T17M CSP7, and T17M CHOP mice was conducted as previously described [6].

### *58.2.5 Western Blot*

Protein extracts from P30 retinas were obtained and analyzed as previously described [4]. Antibodies detected the pATF6, peIf2α, ATF4, spliced XBP1 (sXBP1), and β-actin proteins were purchased from Imgenex (1:1000), Abcam (1:1000), and Sigma-Aldrich (1:1000).

## 58.3 Results

### *58.3.1 Both the CSP-7 and CHOP Ablations Modulate the Loss of Vision in T17M Retina*

The a and b-waves of the ERG were measured in mice at P30, P60, and P90 (Fig. 58.1). The a-wave amplitudes in T17M CSP7 retina were significantly increased by 138, 233, and 422% at P30, P60, and P90, respectively, whereas the T17M CHOP mice showed a significant decrease in the a-wave amplitudes by 57% at P30 and no difference at P60 and P90 compared to T17M mice. The b-wave amplitudes in T17M CSP7 mice were also significantly elevated by 154, 187, and 179% at P30, P60, and P90, respectively. The T17M CHOP mice had 26% lower the b-wave amplitude at P30 than T17M mice and no difference at P60 and P90.

### *58.3.2 Both the CSP7 and CHOP Ablations Alter the Retinal Structure in T17M Mice.*

The thickness of the ONL of the inferior and superior in P30 T17M CSP7 retina was significantly increased by 166%, whereas the T17M CHOP mice demonstrated 25% reduction (Fig. 58.2). The histological analysis confirmed the OCT results and revealed that the number of the nuclei is higher by 30% in T17M CSP7 retina and is lower by 55% in T17M CHOP retina compared to T17M mice.

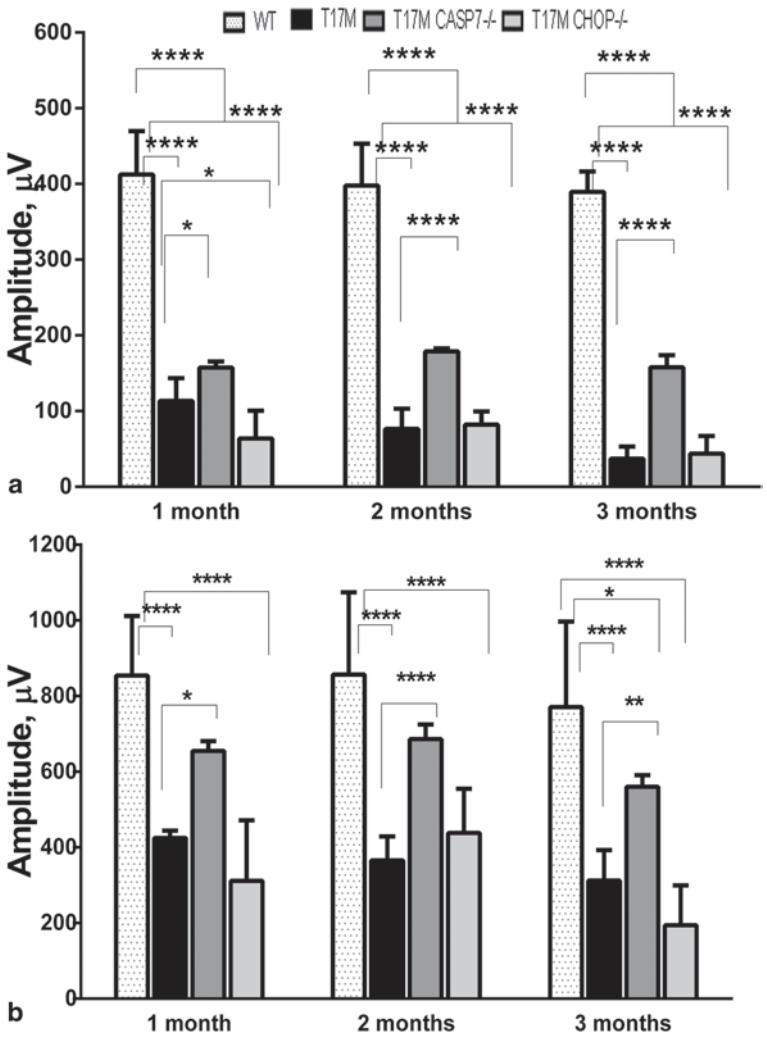


**Fig. 58.1** The lack of CSP7 and CHOP proteins modulates the vision loss in T17M photoreceptors. **a** The a-wave of ERG amplitudes are modified in T17M CSP7 and T17M CHOP mice compared to control. **b** The B-wave of ERG amplitudes are modified in T17M CSP7 and T17M CHOP mice compared to control. (*-$p<0.05$, **-$p<0.01$, ***-$p<0.001$, ****-$p<0.0001$)

### *58.3.3 Both the CSP7 and CHOP Ablations Reprogram the UPR in T17M Retina*

Both ablations reprogram the UPR in transgenic retina (Fig. 58.3). The PERK pathway was modified in T17M CSP7 and T17M CHOP mice. For example, in T17M CSP7 retina the ATF4 protein was decreased by 55 % compared to T17M retina. In

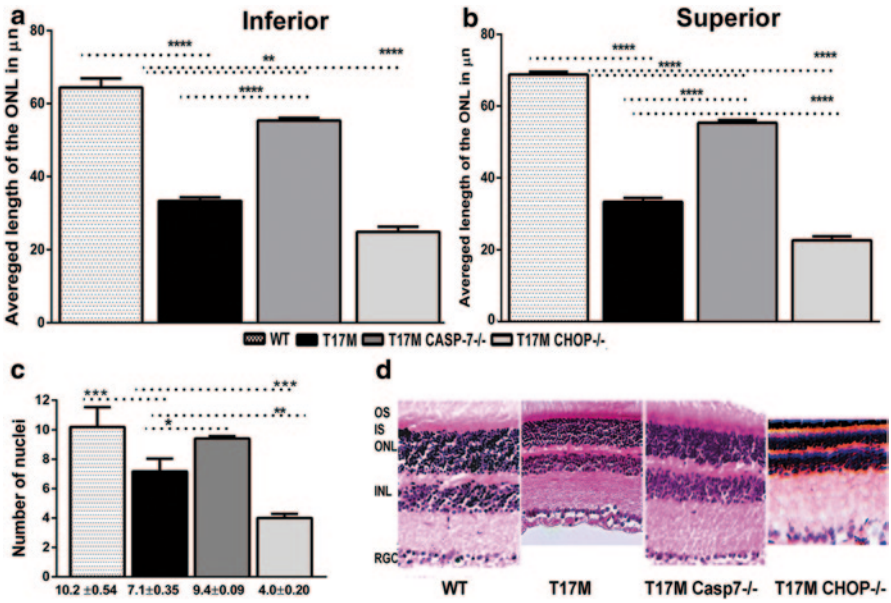


**Fig. 58.2** The lack of CSP7 and CHOP proteins modifies the retinal structure and morphology in T17M mice. **a** and **b** The average thickness of the ONL in the superior and inferior retinas correspondingly. **c** The number of the nuclei measured by H and E histological analysis in the retina. **d** Images of the H and E staining in the retina. (*-$p<0.05$, **-$p<0.01$, ***-$p<0.001$, ****-$p<0.0001$)

T17M CHOP mice the peIF2α protein was dramatically (over 10-fold) increased compared to T17M mice. The ATF6 signaling was modified in T17M CSP7 mice as well. The pATF6(50) was decreased by 57% compared to T17M mice and was no different compared to wt retina. The IRE1 signaling was not altered in T17M CSP7 retina. However, in T17M CHOP retina the sXbp1 protein was 30% lower compared to T17M mice.

### *58.3.4 Both the CSP7 and CHOP Ablations Modify the Cellular Signaling in T17M Retina*

In T17M retina we found that the level of mTOR protein was significantly (over 2-fold) higher compared to wt (Fig. 58.4). The CSP7 ablation led to down-regulation of the mTOR by 33% in these mice that was not statistically different compared to wt. In T17M CSP7 retina this alteration was accompanied by 160% increase in pAKT compared to T17M suggesting that in T17M CSP7 the mTOR/AKT pathway is modified in similar to wt manner.

In T17M retina we also found that the levels of PARP1, TNFα, TRAf2, and pcJUN proteins were significantly higher compared to wt by 180, 235, 217, and

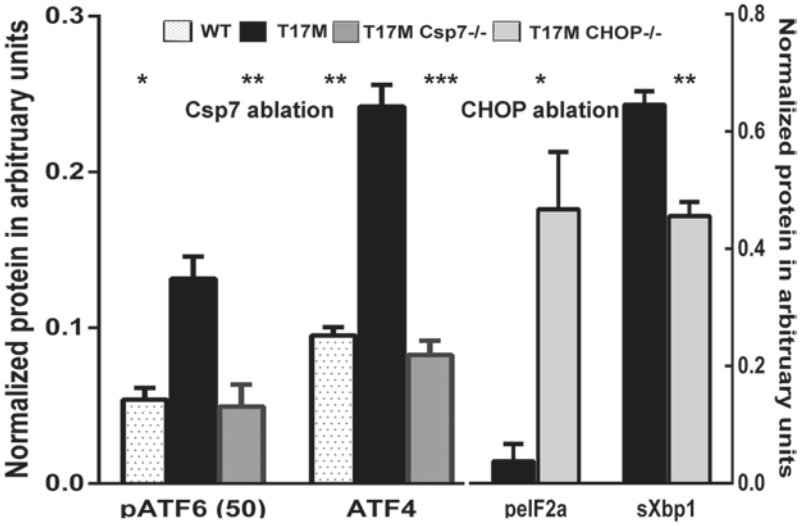


**Fig. 58.3** The UPR is modified in T17M retina deficient either in CSP7 or CHOP protein. **a** The ATF4 and pATF6 protein are reduced in T17M retina deficient in CSP7. **b** Increase in peIF2 and decreased in sXBP1 protein are found in T17M retina deficient in the CHOP. (*-$p<0.05$, **-$p<0.01$, ***-$p<0.001$)

300%, correspondingly. The CSP7 ablation; however, significantly reduced the level of these proteins by 51, 72, 31, and 54%, respectively

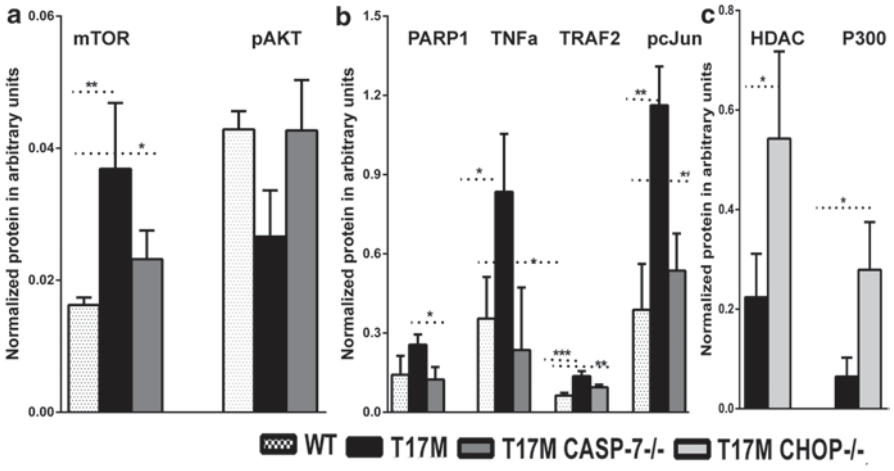


**Fig. 58.4** Modulation of the cellular signaling in T17M CSP7 and T17M CHOP mice. **a** Modulation of the mTOR/pAKT signaling in T17M CSP7 retina. **b** Modulation of the PAR1-TNFa-TRAF2-pcJUN pathways in T17M CSP7 retina. **c** The HDAC and P300 protein expressions are modified in T17M CHOP retina. (*-$p<0.05$, **-$p<0.01$, ***-$p<0.001$, ****-$p<0.0001$)

Ablation of the CHOP protein also altered the cellular signaling in T17M retina. For example, we found that the HDAC1 protein was over 2-fold elevated in T17M CHOP retina compared to T17M. On the contrary, the P300 transcription factor, the co-activator of the RHO gene transcription [7] was found to be decreased by 77% in T17M CHOP mice. Along with RHO mRNA the CRX and NRL gene expressions were diminished in T17M CHOP retina as well (data not shown).

## 58.4 Discussion

In this study, we tested the hypothesis of whether the ablation of pro-apoptotic UPR markers, CSP7 and CHOP proteins are beneficial for ADRP retina. Despite the fact that the increase of the a- and b-waves of ERG amplitudes in T17M CSP7 did not reach the level of wt, the vision loss in these animals was significantly prevented. The results of the SD-OCT and histology confirm the ERG data and indicate the significant improvement of the T17M CSP7 retinal morphology. Controversially, the CHOP ablation expedites the ADRP progression. The ERG, SD-OCT, and histological results indicate the acceleration of the vision loss and the loss of photoreceptor cells.

We found that the reprogramming of the PERK pathway is a common consequence in ADRP retina deficient either in CSP7 or CHOP proteins. For example, in T17M CSP7 mice the decrease in ATF4 could negatively regulate the CHOP protein production and dampen the apoptosis. In T17M CHOP mice the increase in peIF2α at P30 suggests that these animals experience a long-term activation of the PERK UPR arm compared to previously detected in these mice at P15 [3]. Therefore, a prolonged activation of the PERK pathway may induce the inhibition of a global protein translation in ADRP retina and expedite the rate of photoreceptor degeneration. In favor of this hypothesis, we found that the sXBP1 protein (the IRE1 pathway) is significantly diminished in T17M CHOP mice, suggesting that the function of the pro-survival arm is compromised in this retina [3]. The second UPR arm, the ATF6 pathway is also modulated in T17M CSP7. Diminishing of the pro-apoptotic outcomes from the ATF6 activation could be potentially responsible for slowing down the ADRP progression.

Both ablations modify cellular signaling in T17M retina. We found first that the PARP1-TNFα-TRAF2-pcJUN pathway is elevated in T17M retina and the ablation of the CSP7 attenuates the apoptosis in these mice via the modulation of the PARP1 protein and decrease in pcJUN. Evidently, the reduction in pro-apoptotic pcJUN protein is responsible for slowing down the rate of the ADRP progression in T17M CSP7 mice suggesting that the anti-apoptotic therapeutic strategy could be applied to treat the ADRP photoreceptors. This data also reveal that the inflammatory component may be involved in the mechanism of the ADRP pathology.

In T17M CHOP mice, the elevation of HDAC1, a binding partner of the CHOP transcriptional factor [8], evidently suggests that increased histone deacetylation could repress a general transcription and accelerate retinal degeneration in these

mice. The HDAC's function is an opposite of the histone acetyl-transferase P300. Therefore, it is not surprise, that the level of P300 is diminished in T17M RHO, evidently leading to decrease in the CRX, NRL and RHO mRNA. This down-regulation serves as an essential proof for the decline in P300 expression, and additionally for global translation attenuation in ADRP photoreceptors by increased peIF2α.

Therefore, in this study we demonstrated that the rate of the ADRP progression could be modulated by reprogramming of the UPR and, in order to achieve a therapeutic effect based on manipulation with pro-apoptotic UPR proteins in ADRP retina, a careful examination should be taken.

**Acknowledgments** This study was supported by NIH R01EY020905, FFB and "Hope for Vision" grants.

## References

1. Mendes HF, van der Spuy J, Chapple JP, Cheetham ME (2005) Mechanisms of cell death in rhodopsin retinitis pigmentosa: implications for therapy. Trends Mol Med 11:177–185
2. Krebs MP, Holden DC, Joshi P, Clark CL, Lee AH, Kaushal S (2010) Molecular mechanisms of rhodopsin retinitis pigmentosa and the efficacy of pharmacological rescue. J Mol Biol 395:1063–1078
3. Kunte MM, Choudhury S, Manheim JF, Shinde VM, Miura M, Chiodo VA et al (2012) ER stress is involved in T17M rhodopsin-induced retinal degeneration. Invest Ophthalmol Vis Sci 53:3792–3800
4. Shinde VM, Sizova OS, Lin JH, Lavail MM, Gorbatyuk MS (2012) ER Stress in Retinal Degeneration in S334ter Rho Rats. PLoS One 7:e33266
5. Gorbatyuk MS, Knox T, LaVail MM, Gorbatyuk OS, Noorwez SM, Hauswirth WW et al (2010) Restoration of visual function in P23H rhodopsin transgenic rats by gene delivery of BiP/Grp78. Proc Natl Acad Sci U S A 107:5961–5966
6. White DA, Hauswirth WW, Kaushal S, Lewin AS (2007) Increased sensitivity to light-induced damage in a mouse model of autosomal dominant retinal disease. Invest Ophth Vis Sci 48:1942–1951
7. Peng GH, Chen S (2007) Crx activates opsin transcription by recruiting HAT-containing coactivators and promoting histone acetylation. Hum Mol Genet 16:2433–2452
8. Ohoka N, Hattori T, Kitagawa M, Onozaki K, Hayashi H (2007) Critical and functional regulation of CHOP (C/EBP homologous protein) through the N-terminal portion. J Biol Chem 282:35687–35694

# Chapter 59
# Expression of Poly(ADP-Ribose) Glycohydrolase in Wild-Type and PARG-110 Knock-Out Retina

**Ayse Sahaboglu, Sylvia Bolz, Hubert Löwenheim and Francois Paquet-Durand**

**Abstract** Poly(ADP-ribose) (PAR) turnover is required for many cellular processes, and highly relevant for cell death and survival. This post-translational protein modification is regulated by the synthesizing enzyme poly(ADP)ribose-polymerase (PARP) and the degrading enzyme poly(ADP-ribose) glycohydrolase (PARG). Previously, PARP activity was found to be involved in photoreceptor degeneration in the *rd1* mouse and in *rd1*-like conditions PARP-1 was the main PARP family member contributing to photoreceptor cell death. Despite the manifest role of PARP and PAR accumulation in photoreceptor cell death, the influence of PAR degradation on photoreceptor viability was still unknown. Here, we investigated the role of PARG in photoreceptor degeneration using the PARG-110 knock out mouse and report for the first time on PARG expression in wild-type and knock-out retina.

**Keywords** Retina · PARG · PARP · Poly (ADP) ribosylation · Neuroprotection

## 59.1 Introduction

Poly(ADP-ribosyl)ation is a post-translational modification involved in many cellular pathways such as transcription, replication, histone modification, telomere maintenance, cell differentiation, DNA repair, and cell death [1, 2]. Poly(ADP-

A. Sahaboglu (✉) · S. Bolz · F. Paquet-Durand
Division of Experimental Ophthalmology, Institute for Ophthalmic Research, University Eye Clinic Tübingen, Röntgenweg 11, 72076 Tübingen, Germany
e-mail: aysesahaboglu@hotmail.com

S. Bolz
e-mail: sylvia.bolz@uni-tuebingen.de

H. Löwenheim
Otolaryngology Department, University of Tübingen, 72076 Tübingen, Germany

F. Paquet-Durand
e-mail: francois.paquet-durand@klinikum.uni-tuebingen.de

J. D. Ash et al. (eds.), *Retinal Degenerative Diseases,* Advances in Experimental Medicine and Biology 801, DOI 10.1007/978-1-4614-3209-8_59,

ribose) (PAR) is synthesized by poly(ADP)ribose-polymerase (PARP) . So far, 17 PARP family members have been identified and among them PARP-1, is the best known. PARP-1 attaches ADP-ribose residues to generate PAR chains on target proteins using $NAD^+$ as a substrate. PARP-1 also auto-modifies itself by PARylation, to reduce and thereby regulate PARP-1 activity [1].

Acceptor proteins become negatively charged by PARylation. This electrical charge-shift of proteins facilitates association of DNA and proteins [3].

PARylation turnover is regulated by PARP and poly (ADP) ribose glycohydrolase (PARG), which is responsible for degradation of PAR polymers [4]. ADP-ribose residues or protein-free PAR polymers are released from acceptor proteins by exoglycosidase activity and PAR polymers are released by endoglycosidic activity [5]. Even at low levels, endoglycosidic activity is effective in preventing hypermodification of nuclear proteins with very long chains of PAR. This endoglycosidic activity of PARG also serves to maintain PARP-1 activity by removing PAR polymers from the PARP-1 automodification domain [5]. In addition, PARG activity is much higher than PARP activity, so that in DNA damage PAR in vivo half life is approximately 1 min [6]. There is a single *Parg* gene in mammals with at least five different isoforms with differing subcellular localizations and different molecular weights [7]. PARG-110/111 localizes to the nucleus, PARG-102 and PARG-99 isoforms are cytoplasmic and PARG-59/60, PARG-55 isoforms are targeted to the mitochondria [8]. Presently it is not clear whether these different *Parg* isoforms exist in all mammalian species [1].

In 2007, it was shown that PARP activity was involved in rod photoreceptor degeneration in the *rd1* mouse. We confirmed this observation by mimicking the *rd1* situation in wild-type (*wt*) and PARP-1 KO retina. PARP-1 KO retina was more resistant to *rd1*-like degeneration than *wt* [9], indicating that, within the PARP family, PARP-1 was the main contributor to *rd1*-like photoreceptor cell death. Interestingly, preliminary data from several genetically different animal models for RP showed an involvement of PARP over activation in photoreceptor degeneration [Arango-Gonzalez et al., *in preparation*]. In connection with the importance of PARP activity and PARylation in photoreceptor degeneration, we investigated the expression of PARG 110 and PARG-56 in *wt* and PARG-110 KO retina.

## 59.2 Materials and Methods

### *59.2.1 Experimental Animals*

PARG-110 KO and wild-type (*wt*) animals were housed under standard white cyclic lighting and had free access to food and water. All procedures were performed in accordance with the ARVO statement for the use of animals in ophthalmic and visual research and were approved by the Tübingen University committee on animal protection (Einrichtung für Tierschutz, Tierärztlicher Dienst und Labortierkunde di-

rected by Dr. Franz Iglauer). Because of the critical molecular changes apparent at postnatal day (P) 11 [10], comparisons between *wt* and PARG-110 KO retinae were carried out at postnatal (P) day 11 and 30.

### *59.2.2 PARG-110 KO Mice*

PARG-110 KO mice were generated by deletion of exons 2 and 3 of *PARG* gene which results in depletion of the PARG-110 protein [11]. PARG-110 KO mice are phenotypically normal, although they exhibit hypersensitivity to radiation, DNA alkylating agents, and chemotherapeutics [11, 12]. PARG-110 KO mice were kindly provided by Zhao-Qi Wang, Leibniz Institute for Age Research, Fritz Lipmann Institute, Jena.

### *59.2.3 Immunostaining*

Immunostaining was performed on *wt* and PARG-110 KO mice at P11 and P30. Retinae were fixed with 4 % PFA for 1 h. Frozen sections from fixed tissue were air dried for 30–60 min at 37° C. Tissue was rinsed in PBS and preincubated in blocking solution containing 10 % goat normal serum, 1 % bovine serum albumin (BSA), and 0.1 % Triton X in PBS (PBST) for 1 h at room temperature. Incubation of primary antibodies directed against PARG (detects PARG-110 and PARG-56° kDa proteins; Abcam, Cambridge, UK; dilution 1:100), mouse-anti-Calbindin (Swant, Switzerland; dilution 1:500), and mouse-anti PKCα (BioTrend, Billerica, USA; dilution 1:50) were diluted in blocking solution overnight at 4° C. Subsequently, the tissue was rinsed in PBS and incubated with Alexafluor 488 conjugated secondary antibody (Invitrogen; dilution 1:250–1:750). Sections were washed in PBS and mounted in Vectashield with DAPI (Vector, Burlingame, CA, USA).

### *59.2.4 TUNEL Assay*

Cell death was assessed using the terminal deoxynucleotidyl transferase dUTP nick end labeling (TUNEL) assay and an in situ cell death detection kit conjugated with fluorescein isothiocyanate (Roche Diagnostics, Mannheim, Germany).

### *59.2.5 Microscopy, Cell counting and Statistic*

Microscopy was performed by Zeiss Imager Z1 Apotome Microscope. Images were taken with a Zeiss Axiocam digital camera by using Zeiss Axiovision 4.7 software. Corel Draw X3 software was used for image enhancements (Contrast, Colors).

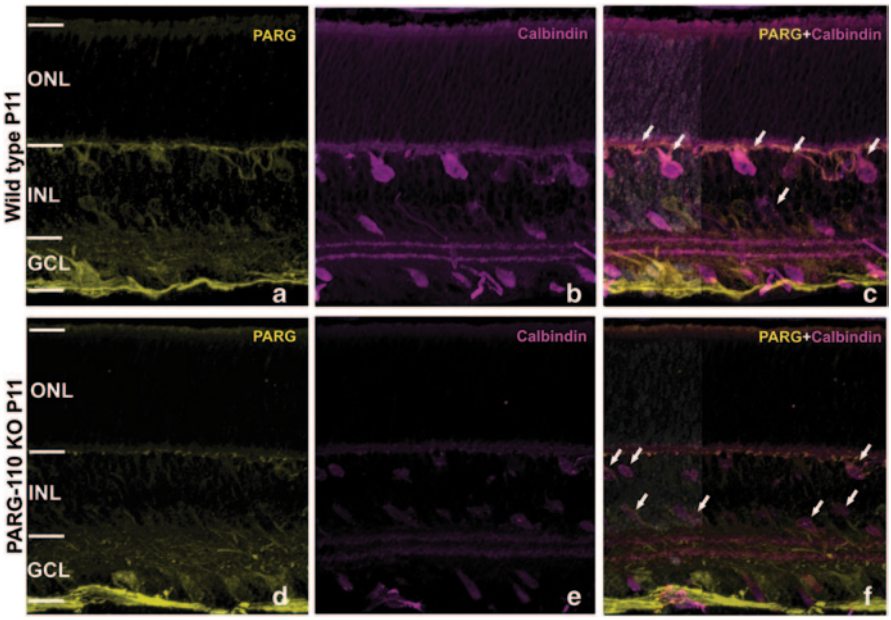


**Fig. 59.1** Immunohistochemical analysis of *PARG* and *calbindin* expression: *wt* retinae at P11 and P30 (data not shown) showed immunoreactivity for *PARG* in the *ONL*, *INL*, *IPL*, *GCL*, and optic nerve fiber layer (**a**). *PARG* labeling intensity was weaker for *PARG-110 KO* retina and showed less reactivity when compared with *wt* (**d**). Calbindin immunoreactivity was identified in cell bodies, dentrites, and axons of horizontal cells in *wt* and *PARG-110 KO* at P11 (**b**, **e**) and P30 (data not shown). There was colocalization between *calbindin* and *PARG* in the *wt* and *PARG-110 KO* retina (**c**, **f**). *ONL* outer nuclear layer, *OPL* outer plexiform layer, *INL* inner nuclear layer, *IPL* inner plexiform layer, *GCL* ganglion cell layer

## 59.3 Results

### *59.3.1 PARG Expression in the Retina*

PARG expression was analyzed by immunofluorescent detection on ex vivo sections from *wt* at P11 and P30. PARG expressions with an antibody against PARG110 and PARG 56 were shown in the outer plexiform layer (OPL), inner nuclear layer (INL), inner plexiform layer (IPL), ganglion cell layer and the retinal nerve fiber layer (Figs. 59.1a and 59.2a). PARG antibody was used also for ex vivo sections from PARG-110 KO retina and there was some positive immunostaining, probably relating to other PARG isoforms (Figs. 59.1d and 59.2d).

### *59.3.2 Colocalization of PARG Expression with Calbindin*

Calbindin-D28K is a calcium-binding protein expressed in horizontal, amacrine, and ganglion cells [13]. All PARG staining in the outer plexiform layer was colocal-

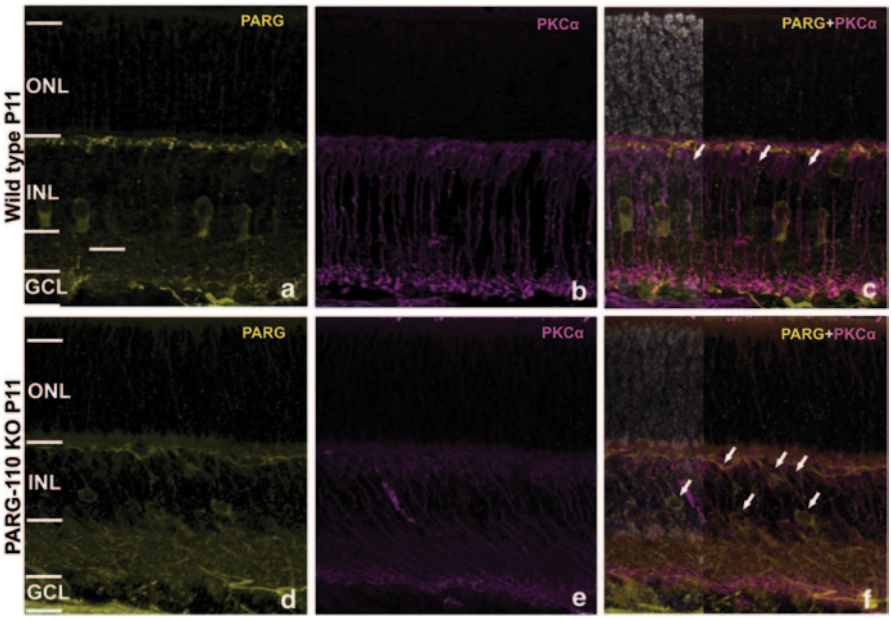


**Fig. 59.2** Immunohistochemical analysis of *PARG* and *PKCα* expression: *PKCα* immunoreactivity showed rod bipolar cells extending from the *INL* to the *IPL* of *wt* (**b**) and *PARG-110 KO* (**e**) retinae at P11 and P30 (data not shown). *PKCα* was colocalized with *PARG* in *wt* (**a**) and *PARG-110* (**d**) retinae (**c**, **f**). *ONL* outer nuclear layer, *OPL* outer plexiform layer, *INL* inner nuclear layer, *IPL* inner plexiform layer, *GCL* ganglion cell layer

ized with calbindin (Fig. 59.1c) indicating PARG expression in horizontal cells in *wt* retina. In the inner retina, PARG staining was also colocalized with calbindin in amacrine cells and ganglion cells (Fig. 59.1c). Calbindin staining appeared weaker in PARG-110 retina when compared with *wt*, and there was also colocalization between PARG and calbindin (Fig. 59.1f).

### *59.3.3 Colocalization of PARG Expression with PKCα*

Bipolar cells were detected by a PKCα antibody and there were colocalizations between PKCα and PARG in *wt* retina (Fig. 59.2c). There was colocalization also for PKCα and PARG in PARG-110 KO retina (Fig. 59.2f).

## 59.4 Discussion

### *59.4.1 PARG in the Retina*

PARylation is regulated by PARP and PARG. Previous studies showed the importance of PARP activity for retinal degeneration in the *rd1* mouse [14] or in retinae in

which an *rd1*-like degeneration was chemically induced by inhibition of PDE6 [9]. Moreover, S334ter and P23H rats for retinal degeneration showed PARP activation during photoreceptor degeneration [15]. Also several other animal models showed a strong activation of PARP during retinal degeneration [Arango-Gonzalez et al., *in preparation*]. Therefore, PARP may constitute a common denominator of photoreceptor degeneration. Nevertheless, further investigations are needed to understand clearly the role of PARylation and PARP activity during photoreceptor degeneration. The turnover of PARylation is regulated by PARG which is the major enzyme involved in degradation of poly (ADP-ribose) [1].

### *59.4.2 PARG Inhibition as a Therapeutic Target*

A number of animal studies have highlighted PARP inhibition as a promising new form of treatment for neurodegenerative diseases such as stroke and neurotrauma [16]. In addition, PARP-1 inhibitors are in use in anticancer clinical trials [17, 18]. Although many publications address the anticancer and neuroprotective potential of PARP inhibitors, there is only limited data about PARG inhibition [6]. Loss of PARG activity by isoform specific knockout and knockdown of the *Parg* gene showed protective effects against cell death or neurodegeneration [19, 20].

The fact that all PARG isoforms are encoded by a single *Parg* gene and that the cellular abundance of PARG proteins with approximately 2,000 molecules per cell is very low [12] suggests PARG as an attractive therapeutic target. Unfortunately, highly specific, satisfactory small-molecule inhibitors of PARG are currently not available [6, 12]. Future neuroprotection studies using specific PARG inhibitors or genetic *Parg* knock-down approaches may be developed into a novel treatment option for inherited eye diseases.

Although some studies showed importance of PARP activity in the photoreceptor degeneration, there is no study available about PARG, an antagonist of PARP, in the retina. Here, we demonstrate the expression of PARG isoforms (PARG-110, PARG-56) in the outer plexiform layer, inner nuclear layer, inner plexiform layer, ganglion cell layer, and nerve fiber layer retina in wild-type mice. PARG-110 KO retina showed relatively weak staining for PARG antibody. Further investigations with a PARG antibody against specifically PARG-110 protein are needed to evaluate the relative expression differences between different retinal cell types.

**Acknowledgment** We thank K. Gültig for excellent technical assistance. This work has been supported by grants from the Kerstan Foundation, the EU (NEUROTRAIN: MEST-CT-2005-020235), and Deutsche Forschungsgemeinschaft (DFG; PA1751/4-1).

## References

1. Hassa PO, Hottiger MO (2008) The diverse biological roles of mammalian PARPS, a small but powerful family of poly-ADP-ribose polymerases. Front Biosci 13:3046–3082

2. Heeres JT, Hergenrother PJ (2007) Poly(ADP-ribose) makes a date with death. Curr Opin Chem Biol 11(6):644–653
3. Osada T, Masutani M (2012) PolyADP-Ribosylation in postfertilization and genome reprogramming: implications for carcinogenesis. In: de Souza Gomes A (ed) Polymerization. Intech, Croatia. doi:10.5772/46097
4. Miwa M, Sugimura T (1971) Splitting of the ribose-ribose linkage of poly(adenosine diphosphate-robose) by a calf thymus extract. J Biol Chem 246(20):6362–6364
5. D'Amours D, Desnoyers S, D'Silva I, Poirier GG (1999) Poly(ADP-ribosyl)ation reactions in the regulation of nuclear functions. Biochem J 342:249–268
6. Putt KS, Hergenrother PJ (2004) A nonradiometric, high-throughput assay for poly(ADP-ribose) glycohydrolase (PARG): application to inhibitor identification and evaluation. Anal Biochem 333(2):256–264
7. Burns DM, Ying W, Kauppinen TM, Zhu K, Swanson RA (2009) Selective down-regulation of nuclear poly(ADP-ribose) glycohydrolase. PLoS One 4(3):e4896
8. Mortusewicz O, Fouquerel E, Amé JC, Leonhardt H, Schreiber V (2011) PARG is recruited to DNA damage sites through poly(ADP-ribose)- and PCNA-dependent mechanisms. Nucleic Acids Res 39(12):5045–5056
9. Sahaboglu A, Tanimoto N, Kaur J, Sancho-Pelluz J, Huber G, Fahl E, Arango-Gonzalez B, Zrenner E, Ekström P, Löwenheim H, Seeliger M, Paquet-Durand F (2010) PARP1 gene knock-out increases resistance to retinal degeneration without affecting retinal function. PLoS One 5(11):e15495
10. Sancho-Pelluz J, Arango-Gonzalez B, Kustermann S, Romero FJ, van Veen T, Zrenner E, Ekström P, Paquet-Durand F (2008) Photoreceptor cell death mechanisms in inherited retinal degeneration. Mol Neurobiol 38(3):253–269
11. Cortes U, Tong WM, Coyle DL, Meyer-Ficca ML, Meyer RG, Petrilli V, Herceg Z, Jacobson EL, Jacobson MK, Wang ZQ (2004) Depletion of the 110-kilodalton isoform of poly(ADP-ribose) glycohydrolase increases sensitivity to genotoxic and endotoxic stress in mice. Mol Cell Biol 24(16):7163–7178
12. Finch KE, Knezevic CE, Nottbohm AC, Partlow KC, Hergenrother PJ (2012) Selective small molecule inhibition of poly(ADP-ribose) glycohydrolase (PARG). ACS Chem Biol 7(3):563–570
13. Haverkamp S, Wässle H (2000) Immunocytochemical analysis of the mouse retina. J Comp Neurol 424(1):1–23
14. Paquet-Durand F, Silva J, Talukdar T, Johnson LE, Azadi S, van Veen T, Ueffing M, Hauck SM, Ekström PA (2007) Excessive activation of poly(ADP-Ribose) polymerase contributes to inherited photoreceptor degeneration in the retinal degeneration 1 mouse. J Neurosci 27(38):10311–10319
15. Kaur J, Mencl S, Sahaboglu A, Farinelli P, van Veen T, Zrenner E, Ekström P, Paquet-Durand F, Arango-Gonzalez B (2011) Calpain and PARP activation during photoreceptor cell death in P23H and S334ter rhodopsin mutant rats. PLoS One 6(7):e22181
16. Virág L, Szabó C (2002) The therapeutic potential of poly(ADP-ribose) polymerase inhibitors. Pharmacol Rev 54(3):375–429
17. Graziani G, Szabó C (2005) Clinical perspectives of PARP inhibitors. Pharmacol Res 52(1):109–118
18. Kling J (2009) PARP inhibitors blaze a trail in difficult-to-treat cancers. Nat Biotechnol 27(9):784–786
19. Blenn C, Althaus FR, Malanga M (2006) Poly(ADP-ribose) glycohydrolase silencing protects against H2O2-induced cell death. Biochem J 396(3):419–429
20. Lu XC, Massuda E, Lin Q, Li W, Li JH, Zhang J (2003) Post-treatment with a novel PARG inhibitor reduces infarct in cerebral ischemia in the rat. Brain Res 978(1–2):99–103

# Chapter 60
# Current Therapeutic Strategies for P23H RHO-Linked RP

**Anh T. H. Nguyen, Matthew Campbell, Anna-Sophia Kiang, Marian M. Humphries and Peter Humphries**

**Abstract** The first autosomal dominant mutation identified to cause retinitis pigmentosa in the North American population was the substitution of proline to histidine at position 23 of the *rhodopsin* gene (P23H RHO). Many biochemical studies have demonstrated that P23H mutation induces rhodopsin (RHO) misfolding leading to endoplasmic reticulum stress. Herein, we review current thinking of this topic.

**Keywords** ER stress · RP · P23H · Rhodopsin · Retinal degeneration

## 60.1 Introduction

### *60.1.1 Rhodopsin and Autosomal Dominant Retinitis Pigmentosa (adRP)*

Rhodopsin (RHO) is the most abundant protein in photoreceptors accounting for nearly 30% of the entire proteome and over 90% of outer segment proteins [1]. RHO is critical in phototransduction and is expressed only in rod photoreceptors. Being a transmembrane protein, RHO synthesis occurs at the endoplasmic reticulum (ER) where nascent RHO polypeptides are co-translationally transported to the ER and subjected to post-translational modifications including disulfide bond

A. T. H. Nguyen (✉) · M. Campbell · A.-S. Kiang · M. M. Humphries · P. Humphries
The Ocular Genetics Unit, Smurfit Institute of Genetics, Trinity College Dublin, College Green, Dublin 2, Ireland
e-mail: nguyenat@tcd.ie

M. Campbell
e-mail: campbem2@tcd.ie

A.-S. Kiang
e-mail: skiang@tcd.ie

M. M. Humphries
e-mail: mhumphri@tcd.ie

P. Humphries
e-mail: pete.humphries@tcd.ie

J. D. Ash et al. (eds.), *Retinal Degenerative Diseases,* Advances in Experimental Medicine and Biology 801, DOI 10.1007/978-1-4614-3209-8_60,

formation and glycosylation at asparagines residues 2 and 15, the latter being important in signal transduction [2–4]. Once properly folded, RHO exits the ER and undergoes additional sugar modifications within the Golgi from where it is finally transported to the rod photoreceptor outer segment [5].

Mutations in the *RHO* gene are the most common cause of dominant retinitis pigmentosa (RP) accounting for ~30–40% while the first RHO mutation discovered, Pro23His (P23H), alone accounts for about 12% of all adRP cases and one third of such cases containing RHO mutations [6, 7]. Some RHO mutations cause recessive RP and congenital stationary night blindness; however, the vast majority of them are associated with dominant disease. The proline residue at position 23 is highly conserved among vertebrates and inverterbrate opsins and in other G-protein coupled receptors such as beta-2-adrenergic receptor [8]. This class II mutant is misfolded at the N-terminal plug, the binding site for 11-cis-retinal chromophore. Many biochemical studies have demonstrated that P23H mutation induces RHO misfolding. Mutant RHO forms oligomeric aggregates, and instead of being properly glycolysated as wild type RHO, P23H RHO is complexed with endoplasmic reticulum chaperones such as BiP or Grp94 [9–11]. Unlike wild type RHO which is translocated to the surface membrane, P23H RHO is localized to the ER/Golgi [12]. Several studies also suggested a dominant negative effect related to P23H mutation. Co-expression of wild type (WT) and P23H RHO resulted in the formation of inclusions containing the WT RHO and disruption of trafficking of wild-type RHO synthesized in the same cell [13, 14]. Furthermore, P23H mutant enhanced proteasome mediated degradation of the WT protein thus strongly implying a dominant negative mechanism of P23H mutation [15]. The chaperone folding machinery is expected to be highly efficient in photoreceptor cells since RHO is continuously synthesised in large amounts of up to $10^7$ molecules per day per photoreceptor. Therefore, accumulation of misfolded P23H RHO in the ER can induce ER stress leading to induction of the unfolded protein response (UPR) and ultimately photoreceptor degeneration [16]. Indeed, more than 140 RP-linked RHO mutations have been identified and those that result in protein misfolding and ER retention are the most prevalent [17]. Li et al. [9] also suggested that most point mutations in the intradiscal domain linked to adRP lead to either complete or partial misfolding of RHO.

### *60.1.2 Unfolded Protein Response*

Once the homeostasis of the ER environment is unbalanced by accumulation of misfolded proteins which are toxic to cells impairing normal cellular function, a signal transduction cascade termed Unfolded Protein Response (UPR) or ER stress response is activated in order to alleviate ER stress. Protein misfolding has been associated with variety of disorders such as conformational diseases; however, UPR has also been shown to be activated during normal cellular events such as B-cell differentiation, muscle differentiation, or viral infections [18–20]. Typically, the UPR transduction cascade is composed of translation attenuation to prevent further production of unfolded proteins, transcriptional induction of various ER resident

proteins such as chaperones to further assist folding, induction of ER-associated degradation (ERAD) to target misfolded proteins for degradation, and enlargement of the ER to handle the accumulation of unfolded proteins [21].

There are three main trans-membrane proteins within the ER that respond to prolonged ER stress: inositol-requiring kinase 1 (IRE1), activating transcription factor 6 (ATF6) and double stranded RNA activated protein kinase-like endoplasmic reticulum kinase (PERK). These proteins have a transmembrane domain that spans the ER, a cytosolic domain and an ER luminal domain and initially activate transcription of certain genes such as ER resident chaperones to increase ER protein folding capacity, reduce synthesis of new proteins and enhance degradation of misfolded proteins through ER associated degradation (ERAD) by ubiquitination within the cytoplasm. However, cyto-protective and pro-apoptotic outputs coexist in the UPR cascade. Under prolonged ER stress where ER homeostasis cannot be re-established, UPR signalling eventually induces cell death by apoptosis.

## 60.2 Current Therapeutic Strategies for P23H RHO Linked RP

### *60.2.1 Upstream of ER Stress*

Pharmacological chaperones such as 11-cis-retinal and its isomer 9-cis-retinal have been found to promote the correct folding, the ability to bind to retinal and the proper trafficking to the plasma membrane of P23H RHO in mammalian cells [10, 22]. Moreover, 11-cis-7-ring-retinal, a modified form of retinal that cannot undergo isomerisation upon light exposure has a higher binding affinity for P23H RHO than for WT RHO and increase P23H RHO folding in mammalian cells [23]. Although there is no effective cure for RP or any beneficial effects on functional vision such as visual acuity or visual field, vitamin A supplementation has been shown to delay the rate of retinal degeneration thus slowing diseases progression in RP patients [24, 25]. However, potential disadvantages of retinal derivatives are their chemical instability, photolability and the potential toxic effects of their metabolites (such as retinoic acid) in other tissues. Recently, retinobenzaldehydes, a class of more stable RHO ligands with less toxicity compared to retinals have been developed [26]. In a recent high-throughput screen in HEK293 cells, novel pharmacological chaperones such as β-Ionone and NSC45012 have also been found to improve P23H RHO folding to a certain extent by occupying the same hydrophobic region of the retinal binding site [7]. Excitingly, the use of natural cytoprotective compounds such as curcumin and safranal have been tested recently in rat models of P23H [27, 28]. These compounds were shown to disrupt protein aggregation, facilitate protein trafficking to the plasma membrane in vitro and provide beneficial effects on retinal degeneration in terms of retinal morphology and physiology in vivo. In addition, 17-AAG, derived from geldanamycin and currently under clinical trials for cancer, also prevented P23H aggregation and inclusion formation; and reduced cell death and caspase activation [29].

A second strategy to restore ER homeostasis is to target the mutant RHO at the genetic level. Mutation independent therapies including ribozymes or RNAi are useful in suppressing both mutant and wild type RHO, whereas gene replacement can be used in parallel to introduce WT RHO cDNA [30]. For example, subretinal injection of AAV2/5 expressing shRNAs targeting both WT and mutant RHO in combination with WT RHO cDNA shows suppression of retinal degeneration in mice expressing P23H RHO [31]. On the other hand, recent report showed that AAV2/5 delivery of WT RHO alone is sufficient to suppress the disease progression in mice expressing P23H RHO [32].

### *60.2.2 At the Level of ER Stress Sensors*

BiP is an important sensor in unfolded protein induced ER stress, BiP transcript levels have been shown to be reduced while CHOP mRNA levels were increased in P23H-3 rats, a model of adRP [33]. Indeed, administration of AAV2/5 expressing BiP has been demonstrated to delay retinal degeneration and lead to rescue of visual function and preservation of retinal structure in these animals [34]. Although, addition of BiP does not seem to promote proper trafficking of P23H to the plasma membrane in vitro, it does alleviate ER stress by reducing the production of phosphorylated eIF2α and cleaved ATF6 which are important in the UPR transduction cascade in both in vivo and in vitro. In addition, BiP also interacted with caspase-12 and pro-apoptotic Bik, and suppressed ER stress-induced CHOP expression in vivo.

### *60.2.3 Downstream of ER Stress Response*

Furthermore, IRE1 activation can also promote apoptosis via ASK1-JNK signalling and caspase-12 activation. Therefore, suppression of this pathway by a JNK inhibitor, such as SP600125, could inhibit cell death in retinitis pigmentosa since it has been shown to reduce ganglion cell loss in a rat model of acute ocular hypertension [35].

In addition to proteasomal degradation, autophagy also plays an essential role in clearing up protein aggregation. This cellular process can be induced by stimuli toxic to the cell such as aggregation of misfolded protein, accumulation of damaged organelles or amino acid derivation. Indeed, rapamycin targeting the mTOR signalling pathway, has been found to induce autophagy in cells expressing P23H RHO and specifically reduce mutant RHO while leaving the wild type protein intact [36].

## 60.3 Conclusion

Protein aggregation is a common theme in many other retinal degenerative diseases such as RP10 retinitis pigmentosa which is caused by mutations in IMPDH1 [37] and ElovL4 mutations in Stargardt-like macular degeneration [38]. Thus, increas-

ing our understanding of the biochemical pathways involved in P23H RHO adRP will also shed light on disease mechanisms in these other protein conformational diseases of the retina in addition to pinpointing molecular and cellular targets for development of therapeutic approaches.

## References


1. Hargrave PA (2001) Rhodopsin structure, function, and topography the Friedenwald lecture. Invest Ophthalmol Vis Sci 42(1):3–9
2. Fukuda MN, Papermaster DS, Hargrave PA (1979) Rhodopsin carbohydrate. Structure of small oligosaccharides attached at two sites near the NH2 terminus. J Biol Chem 254(17):8201–8207
3. Kaushal S, Ridge KD, Khorana HG (1994) Structure and function in rhodopsin: the role of asparagine-linked glycosylation. Proc Natl Acad Sci U S A 91(9):4024–4028
4. Krebs MP, Noorwez SM, Malhotra R, Kaushal S (2004) Quality control of integral membrane proteins. Trends Biochem Sci 29(12):648–655
5. Liang CJ, Yamashita K, Muellenberg CG, Shichi H, Kobata A (1979) Structure of the carbohydrate moieties of bovine rhodopsin. J Biol Chem 254(14):6414–6418
6. Dryja TP, McEvoy JA, McGee TL, Berson EL (2000) Novel rhodopsin mutations Gly114Val and Gln184Pro in dominant retinitis pigmentosa. Invest Ophthalmol Vis Sci 41(10):3124–3127
7. Noorwez SM, Ostrov DA, McDowell JH, Krebs MP, Kaushal S (2008) A high-throughput screening method for small-molecule pharmacologic chaperones of misfolded rhodopsin. Invest Ophthalmol Vis Sci 49(7):3224–3230
8. Applebury ML, Hargrave PA (1986) Molecular biology of the visual pigments. Vision Res 26(12):1881–1895
9. Liu X, Garriga P, Khorana HG (1996) Structure and function in rhodopsin: correct folding and misfolding in two point mutants in the intradiscal domain of rhodopsin identified in retinitis pigmentosa. Proc Natl Acad Sci U S A 93(10):4554–4559
10. Noorwez SM, Malhotra R, McDowell JH, Smith KA, Krebs MP, Kaushal S (2004) Retinoids assist the cellular folding of the autosomal dominant retinitis pigmentosa opsin mutant P23H. J Biol Chem 279(16):16278–16284
11. Anukanth A, Khorana HG (1994) Structure and function in rhodopsin. Requirements of a specific structure for the intradiscal domain. J Biol Chem 269(31):19738–19744
12. Tam BM, Moritz OL (2006) Characterization of rhodopsin P23H-induced retinal degeneration in a Xenopus laevis model of retinitis pigmentosa. Invest Ophthalmol Vis Sci 47(8):3234–3241
13. Saliba RS, Munro PM, Luthert PJ, Cheetham ME (2002) The cellular fate of mutant rhodopsin: quality control, degradation and aggresome formation. J Cell Sci 115(Pt 14):2907–2918
14. Illing ME, Rajan RS, Bence NF, Kopito RR (2002) A rhodopsin mutant linked to autosomal dominant retinitis pigmentosa is prone to aggregate and interacts with the ubiquitin proteasome system. J Biol Chem 277(37):34150–34160
15. Rajan RS, Kopito RR (2005) Suppression of wild-type rhodopsin maturation by mutants linked to autosomal dominant retinitis pigmentosa. J Biol Chem 280(2):1284–1291
16. Chapple JP, Grayson C, Hardcastle AJ, Saliba RS, van der Spuy J, Cheetham ME (2001) Unfolding retinal dystrophies: a role for molecular chaperones? Trends Mol Med 7(9):414–421
17. Mendes HF, van der Spuy J, Chapple JP, Cheetham ME (2005) Mechanisms of cell death in rhodopsin retinitis pigmentosa: implications for therapy. Trends Mol Med 11(4):177–185
18. Reimold AM, Iwakoshi NN, Manis J, Vallabhajosyula P, Szomolanyi-Tsuda E, Gravallese EM et al (2001) Plasma cell differentiation requires the transcription factor XBP-1. Nature 412(6844):300–307

19. Nakanishi K, Sudo T, Morishima N (2005) Endoplasmic reticulum stress signaling transmitted by ATF6 mediates apoptosis during muscle development. J Cell Biol 169(4):555–560
20. Benali-Furet NL, Chami M, Houel L, De Giorgi F, Vernejoul F, Lagorce D et al (2005) Hepatitis C virus core triggers apoptosis in liver cells by inducing ER stress and ER calcium depletion. Oncogene 24(31):4921–4933
21. Haeri M, Knox BE (2012) Endoplasmic reticulum stress and unfolded protein response pathways: potential for treating age-related retinal degeneration. J Ophthal Vision Res 7(1):45–59
22. Krebs MP, Holden DC, Joshi P, Clark CL 3rd, Lee AH, Kaushal S (2010) Molecular mechanisms of rhodopsin retinitis pigmentosa and the efficacy of pharmacological rescue. J Mol Biol 395(5):1063–1078
23. Noorwez SM, Kuksa V, Imanishi Y, Zhu L, Filipek S, Palczewski K et al (2003) Pharmacological chaperone-mediated in vivo folding and stabilization of the P23H-opsin mutant associated with autosomal dominant retinitis pigmentosa. J Biol Chem 278(16):14442–14450
24. Shintani K, Shechtman DL, Gurwood AS (2009) Review and update: current treatment trends for patients with retinitis pigmentosa. Optometry 80(7):384–401
25. Berson EL, Rosner B, Sandberg MA, Hayes KC, Nicholson BW, Weigel-DiFrano C et al (1993) Vitamin A supplementation for retinitis pigmentosa. Arch Ophthalmol 111(11):1456–1459
26. Ohgane K, Dodo K, Hashimoto Y (2010) Retinobenzaldehydes as proper-trafficking inducers of folding-defective P23H rhodopsin mutant responsible for retinitis pigmentosa. Bioorg Med Chem 18(19):7022–7028
27. Fernandez-Sanchez L, Lax P, Esquiva G, Martin-Nieto J, Pinilla I, Cuenca N (2012) Safranal, a saffron constituent, attenuates retinal degeneration in P23H rats. PLoS One 7(8):e43074
28. Vasireddy V, Chavali VR, Joseph VT, Kadam R, Lin JH, Jamison JA et al (2011) Rescue of photoreceptor degeneration by curcumin in transgenic rats with P23H rhodopsin mutation. PLoS One 6(6):e21193
29. Mendes HF, Cheetham ME (2008) Pharmacological manipulation of gain-of-function and dominant-negative mechanisms in rhodopsin retinitis pigmentosa. Hum Mol Genet 17(19):3043–3054
30. Farrar GJ, Kenna PF, Humphries P (2002) On the genetics of retinitis pigmentosa and on mutation-independent approaches to therapeutic intervention. EMBO J 21(5):857–864
31. O'Reilly M, Palfi A, Chadderton N, Millington-Ward S, Ader M, Cronin T et al (2007) RNA interference-mediated suppression and replacement of human rhodopsin in vivo. Am J Hum Genet 81(1):127–135
32. Mao H, James T Jr, Schwein A, Shabashvili AE, Hauswirth WW, Gorbatyuk MS et al (2011) AAV delivery of wild-type rhodopsin preserves retinal function in a mouse model of autosomal dominant retinitis pigmentosa. Hum Gene Ther 22(5):567–575
33. Lin JH, Li H, Yasumura D, Cohen HR, Zhang C, Panning B et al (2007) IRE1 signaling affects cell fate during the unfolded protein response. Science 318(5852):944–949
34. Gorbatyuk MS, Knox T, LaVail MM, Gorbatyuk OS, Noorwez SM, Hauswirth WW et al (2010) Restoration of visual function in P23H rhodopsin transgenic rats by gene delivery of BiP/Grp78. Proc Nat Acad Sci U S A 107(13):5961–5966
35. Sun H, Wang Y, Pang IH, Shen J, Tang X, Li Y et al (2011) Protective effect of a JNK inhibitor against retinal ganglion cell loss induced by acute moderate ocular hypertension. Mol Vis 17:864–875
36. Kaushal S (2006) Effect of rapamycin on the fate of P23H opsin associated with retinitis pigmentosa (an American Ophthalmological Society thesis). Trans Am Ophthalmol Soc 104:517–529
37. Aherne A, Kennan A, Kenna PF, McNally N, Lloyd DG, Alberts IL et al (2004) On the molecular pathology of neurodegeneration in IMPDH1-based retinitis pigmentosa. Hum Mol Genet 13(6):641–650
38. Vasireddy V, Vijayasarathy C, Huang J, Wang XF, Jablonski MM, Petty HR et al (2005) Stargardt-like macular dystrophy protein ELOVL4 exerts a dominant negative effect by recruiting wild-type protein into aggresomes. Mol Vis 11:665–676

# Chapter 61
# Pathogenesis of X-linked RP3: Insights from Animal Models

**Rakesh Kotapati Raghupathy, Daphne L. McCulloch, Saeed Akhtar, Turki M Al-Mubrad and Xinhua Shu**

**Abstract** Retinitis Pigmentosa (RP) is a genetically heterogeneous disorder characterized by rod and cone photoreceptor cell dysfunction. X-linked RP (XLRP) is one of the most severe forms of human retinal degeneration, as determined by age-of-set and progression, and accounts for six to 20 % of all RP cases. At least six XLRP loci have been identified, but RP3 is the major subtype of XLRP, accounting for 70 to 80 % of affected families. The *RPGR* gene is responsible for the RP3 form of XLRP and is mutated in 10–20 % of all RP patients. The pathogenesis of retinitis pigmentosa GTPase regulator (RPGR) mutant-causing RP is not clear, different animal models have been used to understand the pathogenesis of these diseases. In this brief review, we will summarize the functional characterization of RPGR and highlight recent studies in animal models, which will not only shed light on the disease mechanisms in XLRP but will also provide therapeutic strategies for RP treatment.

**Keywords** Retinitis pigmentosa · X-linked retinitis pigmentosa · Pathogenesis · Animal models · Dog · Mouse · Zebrafish

X. Shu (✉) · R. K. Raghupathy · D. L. McCulloch
Department of Life Sciences, Glasgow Caledonian University, Cowcaddens Road, Glasgow, C4 0BA, Scotland
e-mail: Rakesh.Kotapati@gcu.ac.uk

D. L. McCulloch
e-mail: D.L.Mcculloch@gcu.ac.uk

Saeed Akhtar · T. M Al-Mubrad
Cornea Research Chair, College of Applied Medical Sciences, King Saud University, Riyadh, Saudi Arabia
e-mail: akhtars@ksu.edu.sa

T. M Al-Mubrad
turkim@ksu.edu.sa

X. Shu
e-mail: Xinhua.Shu@gcu.ac.uk

J. D. Ash et al. (eds.), *Retinal Degenerative Diseases,* Advances in Experimental Medicine and Biology 801, DOI 10.1007/978-1-4614-3209-8_61,


**Fig. 61.1** Schematic structures of RPGR$^{ex1\text{-}19}$ (AAC50481) and RPGR$^{ORF15}$ (DAA05713.1) proteins. The N- and C-terminal, *RCC1-like*, *glutamic acid rich* ORF15 C-terminal (*C2*) domains, and the isoprenylation signal motif are shown

## 61.1 Introduction

Retinitis pigmentosa (RP) refers to a heterogeneous group of retinal disorders characterized by the primary death of the rod photoreceptors, affecting 1 in 4,000 individuals [1]. RP can be inherited in the autosomal, X-linked, or mitochondrial manner. X-linked RP (XLRP) represents the most severe form of RP, accounting for 10–25% of the RP familial cases. Previous reports suggested that the average age at onset in XLRP was 7.2 ± 1.7 years [2, 3]. The earliest clinical symptom of XLRP is night blindness. Patients have a reduction in visual acuity by 20 years of age, which progresses to severe visual loss (< 6/60) by age 40 [4]. Genetic mapping data have shown at least six loci of genetic defects in XLRP, including RP2, RP3, RP23, RP24, and RP34. RP3 is the major RP locus identified to date, accounting for 70–90% of XLRP case [5–7].

## 61.2 The *RP3 Gene: Retinitis Pigmentosa GTPase Regulator*

The human RP3 locus was identified as the *retinitis pigmentosa GTPase regulator* (*RPGR*) gene, which is localized in chromosomal region Xp21.1. RPGR has a complex expression patterns with multiple alternatively spliced transcripts, all of which encode an N-terminal RCC1-like domain structurally similar to the RCC1 protein, a guanine nucleotide exchange factor for the small G protein, Ran [8, 9]. There are two major RPGR isoforms, RPGR$^{ex1\text{-}19}$ and RPGR$^{ORF15}$ (Fig. 61.1). RPGRex$^{1\text{-}19}$ contains exon 1-19, coding a protein with predicted size of 90 kDa. RPGR$^{ORF15}$ contains 15 exons, encoding a 145 kDa protein. Both RPGR$^{ex1\text{-}19}$ and RPGR$^{ORF15}$ share the N-terminal RCC1-like domain but with different C-terminals. RPGR$^{ex1\text{-}19}$ has a C-terminal isoprenylation anchorage signal, whereas RPGR$^{ORF15}$ has a repetitive glycine and glutamic acid-rich domain with a basic C-terminal domain [10]. RPGR$^{ex1\text{-}19}$ is widely expressed in different tissues of tested species. RPGR$^{ORF15}$ is predominantly expressed in the retina and highly conserved in the evolution (Fig. 61.2). RPGR$^{ORF15}$ is the only transcript involving in retinal dystrophies [9].

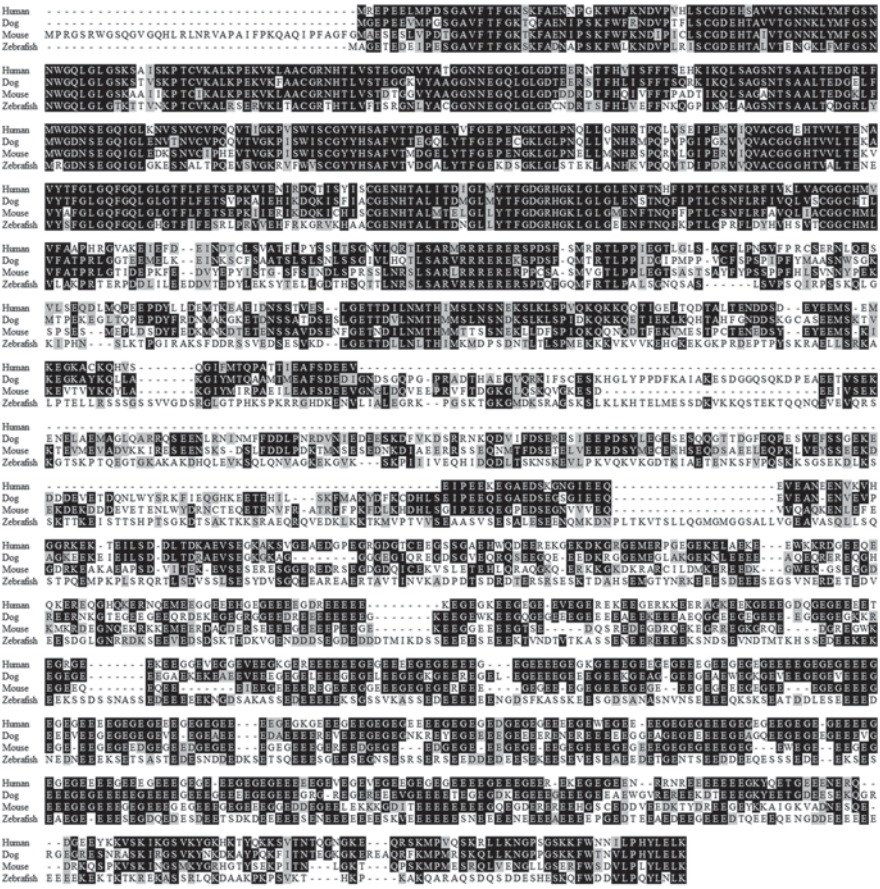


**Fig. 61.2** Conservation of RPGR$^{ORF15}$ in *human* (DAA05713.1), *dog* (NP_001003126.1 and AAM22073.1), *mouse* (NP_001030025.1), and *zebrafish* (ADA84472.1), which have been used as models for investigating the RPGR function

About 300 mutations have been reported, the majority of which are implicated in XLRP, but some cause cone-rod dystrophy, cone dystrophy, atrophic macular degeneration, or a systemic disorders [7, 10].

RPGR is predominantly localized in photoreceptor connecting cilia and basal bodies, but localization has also reported in outer segments in some species [11–13]. RPGR has also been shown to localize in the centrosome/basal body in mammalian and Xenopus cells [12, 13]. RPGR has been shown to interact with a number of different photoreceptor and ciliary proteins. The RCC1-like domain was shown to interact with the delta subunit of the rod cyclic GMP phosphodiesterase (PDE6D), which can bind several prenylated proteins, including Rab13, Ras, Rap, and Rho6 [14]. The RCC1-like domain also interacts with the RPGR-interacting protein 1 (RPGRIP1), which is localized to the photoreceptor connecting cilium [15–17].

The function of RPGRIP1 is not clear but mutations in RPGRIP1 caused Leber's congenital amaurosis. The C-terminal of $RPGR^{ORF15}$ interacts with nucleophosmin (NPM) and with multiple whirlin isoforms [13, 18]. NPM is a multiple function protein involved in many cellular processes. It is present in the mouse photoreceptor outer segment proteome, but the functional consequence of $RPGR^{ORF15}$ interaction with NPM is not clear. Mutations in the whirlin gene cause nonsyndromic deafness and Usher syndrome (type 2D, USH2D), a condition characterized by congenital deafness and RP. The interaction between whirlin and $RPGR^{ORF15}$ suggests that RPGR may have a role in USH2D. Previous studies showed that $RPGR^{ORF15}$ co-immunoprecipitated with basal body/axonemal proteins (NPHP5, NPHP6, IFT88, 14-3-3ε, and γ-tublin) and with the microtubule-based transport proteins (Kinesin II related proteins KIF3A and KAP3, two regulators of cytoplasmic dynein p150Glued and p50-dynamitin). Disruption of dynein-dynactin motor complex by overexpressing p50-dynamitin abrogates RPGR localization to basal bodies [19]. So $RPGR^{ORF15}$ appears to have a role in regulating microtubule-based transport both to and from the basal bodies and within photoreceptor axonemes.

## 61.3 Dog Models for the *RPGR* Gene

Canine X-linked progressive retinal atrophy (XLPRA) is a naturally-occurring animal model of X-linked retinal disease. The phenotypes of XLPRA in the Siberian husky dog are similar to XLRP in human. Histological study found that rod outer segments of affected male dogs were fragmented and disorganized at the early stage, the outer nuclear layer became thin with a reduction to 50% of the original thickness at the middle stage, and almost all photoreceptor cells were degenerated and the retinal architecture was disorganized at the late stage [20]. Two-point linkage analysis found XLPRA was tightly linked to the RPGR gene with an lod score of 11.7 and zero recombination, establishing XLPRA as the homological locus to human RP3. According to the published human $RPGR^{ex1-19}$ at that time, the canine $RPGR^{ex1-19}$ cDNA was cloned showing that the RCC1-like domain is highly homologous to that of human RPGR (Fig. 61.2). Four canine RPGR splice variants were sequenced, but no mutation was found [21]. After human $RPGR^{ORF15}$ was identified by Dr. Wright's group in 2000 [9], the canine RPGR exon ORF15 was cloned and two disease-associated mutations were identified. Canine XLPRA1 (the original XLPRA in Siberian husky and samoyed) carries a 5-base pair deletion (delGAGAA) in exon ORF15, resulting in a frameshift and an immediate premature stop codon; while canine XLPRA2, derived from mongrel dogs which maps to the same disease locus, carries a 2-base deletion (delGA) in exon ORF15, resulting in a frameshift and premature stop codon 71 amino acids downstream with 34 additional basic residues [22]. The XLPRA1 mutant demonstrates normal retinal development and function till age of 6 months old or later. Rod degeneration was detected by histological assay at 11 months of age, progressing to cone degeneration at late stage. In contrast, the XLPRA2 phenotype is very severe with abnormal photoreceptor

development and a faster degeneration. XLPRA2 mutant showed outer segment disruption and misalignment at the age of 4.9 weeks, severe outer segment disintegration at the age of 7.9 weeks, and significant rod loss with the thickness of the outer nuclear layer reduced to about 60% of its original thickness at age of 16 weeks. The density of both rod and cone cells was clearly decreased at the age of 26 weeks, and only two to three rows of nuclei in outer nuclear layer remained at the age of 40.6 weeks [22, 23]. The severe retinal degeneration of early onset in XLPRA2 was presumably caused by a toxic gain of function of $RPGR^{ORF15}$ mutant protein, which was shown to aggregate in the endoplasmic reticulum of the transfected cells [22].

## 61.4 Mouse Models for the *RPGR* Gene

Mouse RPGR also has two major isoforms: RPGEex1-19 and RPGRORF15, which are highly homologous to human and dog RPGR (Fig. 61.2) [21]. The RPGR knock-out (KO) mouse has normal retinal histology and function at the completion of retinal development (at ≈30 postnatal days), but mislocalization of cone opsins was found as early as postnatal day 20 and degenerative changes were underway at the age of 2 months. Rhodopsin was not mislocalized in the rod photoreceptors at the early stage though the content of rhodopsin in outer segments was reduced in RPGR KO mice. Photoreceptor cell loss in RPGR-deficient mice became apparent at 6 months of age. Electroretinography (ERG) measurements also showed 25% reduction of rod a-wave amplitude and 31% reduction of cone b-wave amplitude in RPGR mutant mice at the age of 6.5 months. Ultrastructural studies revealed that the mutant mice have well-packed discs in outer segments and well-maintained structure of the connecting cilium axoneme, however the newly formed discs at the base of outer segments were highly disorganised [24]. These results suggest that while the photoreceptors initially develop normally in the absence of RPGR, they degenerate subsequently due to a slower turnover of the outer segment membrane.

A newly-characterised naturally-occurring mouse model, rd9, carries a 32-bp duplication in RPGR exon ORF15, causing a reading frameshift with additional 108 basic residues. The $RPGR^{ex1\text{-}19}$ isoform was expressed in the rd9 mouse retina but the $RPGR^{ORF15}$ isoform was not detected. The rd9 mice developed a slower degeneration than that of RPGR KO mice [25]. Rd9 mice showed normal retinal structure and outer nuclear layer thickness at the age of 2 months. Mislocalization of M-opsin was seen in the rd9 superior retina as young as 2 months of age and the intensity of rhodopsin staining was shown to decrease at 12 months of age. Photoreceptor cell loss also became evident by 12 months of age, with about 50% photoreceptors degenerated by 24 months of age. ERG measurements showed a- and b-wave amplitudes in Rd9/Y male and Rd9/Rd9 female reduced gradually and continuously to 24 months of age [25]. These results suggested the loss of $RPGRP^{ORF15}$ isoform only caused a slow retinal degeneration with features resembling XLRP with mutations in RPGR exon ORF15 [26].

There are five transgenic mouse models with over-expression RPGR. Hong et al expressed an abbreviated $RPGR^{ORF15}$ variant with 654 bp deletion in the repetitive region of exon ORF15 in RPGR KO mouse and found that the short $RPGR^{ORF15}$ variant could substantially rescue the retinal degeneration phenotype due to loss of endogenous RPGR [27]. A transgenic mouse model harbouring a murine $RPGR^{ORF15}$ truncation mutant was also made by Hong et al. This mutant showed a rapid photoreceptor degeneration, compared with the relatively slow degeneration observed in the knockout mouse alone, suggesting a gain-of-function role in retina [28]. Brunner et al made a transgenic mouse model by increasing gene copies of RPGR and found that the male transgenic mice were infertile due to defects in flagellar formation [29]. The severity of the flagellar defect was correlated to the increased RPGR copy number, since very high RPGR copy numbers leaded to completely abolished assembly of the flagellum. Those transgenic mice expressed high levels of 80, 90, and 125 kDa RPGR isoforms, especially the expression of testis specific RPGR isoform (165 kDa) was significantly increased in RPGR over-expressing males. The high molecular isoforms (125 and 165 kDa) might not contain exon ORF15, since an antibody against RPGRORF15 did not detect both isofroms [29]. Wright et al made a transgenic mouse models with overexpression of $RPGR^{ex1\text{-}19}$ or $RPGR^{ORF15}$ and found only high levels of $RPGR^{ex1\text{-}19}$ in the retinal caused more severe retinal degeneration than that of *RPGR* KO mouse [30]. A transgenic model harbouring an in-frame deletion of RPGR exon 4 showed that genetic background plays a role in determining the retinal phenotype. The transgenic mice exhibited a mild rod-dominant phenotype on the B6 background, whereas a cone dominant phenotype was exhibited on the BALB/cJ background [31].

## 61.5 Zebrafish Models for the *RPGR* Gene

The structure and function of zebrafish neural retina closely resembles that of the human retina, and many genes and functional pathways are also conserved with those of humans. The zebrafish is increasingly used as a model to study retinal neurogenesis and diseases. Zebrafish has two *RPGR* genes (*ZFRPGR1* and *ZFRPGR2*) due to a genome duplication that occurred in teleosts. ZFRPGR1 is homology to $RPGR^{ORF15}$ transcript but does not appear to have $RPGR^{ex1\text{-}19}$, ZFRPGR2 has two major transcripts: $ZFRPGR2^{ex1\text{-}17}$ and $ZFRPGR2^{ORF15}$, similar to human $RPGR^{ex1\text{-}19}$ and $RPGR^{ORF15}$, respectively [32]. *ZFRPGR1* and *ZFRPGR2* have different expression patterns, but expression patterns of *ZFRPGR2* are very similar to that of other vertebrate species. With depletion of *ZFRPGR1* and *ZFRPGR2* by morpholino injection, only *ZFRPGR2* depletion cause developmental defects, affecting gastrulation, tail and head development. *ZFRPGR2* morphants also exhibited abnormal development in the eyes, including lamination defects, failure to develop photoreceptor outer segments and a small eye phenotype, associated with an ongoing increasing cell death throughout the retina. Those abnormalities could be rescued by expression of wild-type but not RP-causing mutant forms of human RPGR [32]. Ghosh et al also

knock-downed zebrafish RPGR (*ZFRPGR2*) by translation-blocking morpholinos and found that *ZFRPGR2* morphants had significantly shortened Kupffer's vesicle cilia, associated with ciliary defects, but did not show any defect in retinal development. The authors evaluated RP-causing alleles of the human *RPGR* gene based on the phenotypes of *RPGR* knock-down morphants and found some RP-associated alleles could rescue the phenotypes, whereas other alleles did not yield any rescue [33]. Gerner et al have also identified a zebrafish ortholog (same as ZFRPGR1$^{ORF15}$) and found that morpholino knock-down of ZFRPGR1$^{ORF15}$ caused developmental defects including abnormal and shortened body-axis, small eyes, and hydrocephalus [34]. However, Shu et al. found that *ZFRPGR1$^{ORF15}$* depletion did not produce any defect throughout early development [32].

## 61.6 Conclusion

Mutations in the *RPGR* are the most common single cause of RP but the disease mechanisms are not fully understood. Studies in canine and murine models suggested RPGR was not critical for photoreceptor development but had an important role in regulating protein transport to and from the basal bodies and within photoreceptor axonemes. Those results also suggested that RPGR$^{ORF15}$ was a functional and RP-associated isoform in retina and that a subset of frameshift mutations in *RPGR* exon ORF15 had a gain-of-function effect. Studies in zebrafish suggested RPGR had a role in zebrafish photoreceptor development. The zebrafish model provides a platform for evaluating RP-associated alleles before proposing *RP3* gene therapy trials.

**Acknowledgements** We would like to acknowledge the financial support of the Royal Society London, the TENOVUS Scotland, the WH Ross Foundation, the National Eye Research Centre, the Rosetrees Trust, the Visual Research Trust, the UK Fight for Sight and the Carnegie Trust for the University of Scotland.

## References

1. Rattner A, Sun H, Nathan J (1999) Molecular genetics of human retinal disease. Annu Rev Genet 33:89–131
2. Maumenee IH, Pierce ER, Bias WB, Schleutermann DA (1975) Linkage studies of typical retinitis pigmentosa and common markers. Am J Hum Genet 27:505–508
3. Wright AF, Shu X (2007) X-linked retinal dystrophies and microtubular functions within the retina. In: Tombran-Tink J, Barnstable CJ (eds) Retinal degenerations: biology, diagnostics, and therapeutics. The Human Press, pp 257–268
4. Bird AC (1975) X-linked retinitis pigmentosa. Br J Ophthalmol 59:177–199
5. Breuer DK, Yashar BM, Filippova E, Hiriyanna S, Lyons RH, Mears AJ et al (2002) A comprehensive mutation analysis of RP2 and RPGR in a North American cohort of families with X-linked retinitis pigmentosa. Am J Hum Genet 70:1545–1554
6. Shu X, McDowall E, Brown AF, Wright AF (2008) The human retinitis pigmentosa GTPase regulator gene variant database. Hum Mutat 29:605–608

7. Shu X, Black GC, Rice JM, Hart-Holden N, Jones A, O'Grady A et al (2007) RPGR mutation analysis and disease: an update. Hum Mutat 28:322–328
8. Meindl A, Dry K, Herrmann K, Manson F, Ciccodicola A, Edgar A et al (1996) A gene (RPGR) with homology to the RCC1 guanine nucleotide exchange factor is mutated in X-linked retinitis pigmentosa (RP3). Nat Genet 13:35–42
9. Vervoort R, Lennon A, Bird AC, Tulloch B, Axton R, Miano MG et al (2000) Mutational hot spot within a new RPGR exon in X-linked retinitis pigmentosa. Nat Genet 25:462–466
10. Wright AF, Shu X (2007) Focus on Molecules: RPGR. Exp Eye Res 85:1–2
11. Hong DH, Pawlyk B, Sokolov M, Strissel KJ, Yang J, Tulloch B et al (2003) RPGR isoforms in photoreceptor connecting cilia and the transitional zone of motile cilia. Invest Ophthalmol Vis Sci 44:2413–2421
12. Shu X, Zeng Z, Eckmiller MS, Gautier P, Vlachantoni D, Manson FD et al (2006) Developmental and tissue expression of Xenopus laevis RPGR. Invest Ophthalmol Vis Sci 47:348–356
13. Shu X, Fry AM, Tulloch B, Manson FD, Crabb JW, Khanna H et al (2005) RPGR ORF15 isoform co-localizes with RPGRIP1 at centrioles and basal bodies and interacts with nucleophosmin. Hum Mol Genet 14:1183–1197
14. Linari M, Ueffing M, Manson F, Wright AF, Meitinger T, Becker J (1999) The retinitis pigmentosa GTPase regulator, RPGR, interacts with the deta subunit of rod cyclic GMP phosphodiesterase. Proc Natl Acad Sci U S A 96:1315–1320
15. Boylan JP, Wright AF (2000) Identification of a novel protein interacting with RPGR. Hum Mol Genet 9:2085–2093
16. Roepman R, Bernoud-Hubac N, Schick DE, Maugeri A, Berger W, Ropers HH et al (2000) The retinitis pigmentosa GTPase regulator (RPGR) interacts with novel transport-like proteins in the outer segments of rod photoreceptors. Hum Mol Genet 9:2095–2105
17. Hong DH, Yue G, Adamian M, Li T (2001) Retinitis pigmentosa GTPase regulator (RPGRr)-interacting protein is stably associated with the photoreceptor ciliary axoneme and anchors RPGR to the connecting cilium. J Biol Chem 276:12091–12099
18. Wright RN, Hong DH, Perkins B (2012) RpgrORF15 connects to the usher protein network through direct interactions with multiple whirlin isoforms. Invest Ophthalmol Vis Sci 53:1519–1529
19. Khanna H, Hurd TW, Lillo C, Shu X, Parapuram SK, He S et al (2005) RPGR-ORF15, which is mutated in retinitis pigmentosa, associates with SMC1, SMC3, and microtubule transport proteins. J Biol Chem 280:33580–33587
20. Zeiss CJ, Acland GM, Aguirre GD (1999) Retinal pathology of canine X-linked progressive retinal atrophy, the locus homologue of RP3. Invest Ophthalmol Vis Sci 40:3292–3304
21. Zeiss CJ, Ray K, Acland GM, Aguirre GD (2000) Mapping of X-linked progressive retinal atrophy (XLPRA), the canine homolog of retinitis pigmentosa 3 (RP3). Hum Mol Genet 9:531–537
22. Zhang Q, Acland GM, Wu WX, Johnson JL, Pearce-Kelling S, Tulloch B et al (2002) Different RPGR exon ORF15 mutations in Canids provide insights into photoreceptor cell degeneration. Hum Mol Genet 11:993–1003
23. Beltran WA, Hammond P, Acland GM, Aguirre GD (2006) A frameshift mutation in RPGR exon ORF15 causes photoreceptor degeneration and inner retina remodelling in a model of X-linked retinitis pigmentosa. Invest Ophthalmol Vis Sci 47:1669–1681
24. Hong DH, Pawlyk BS, Shang J, Sandberg MA, Berson EL, Li T (2000) A retinitis pigmentosa GTPase regulator (RPGR)-deficient mouse model for X-linked retinitis pigmentosa (RP3). Proc Natl Acad Sci U S A 97:3649–3654
25. Thompson DA, Khan NW, Othman MI, Chang B, Jia L, Grahek G et al (2012) Rd9 is a naturally occurring mouse model of a common form of retinitis pigmentosa caused by mutations in RPGR-ORF15. PLoS One 7:e35865
26. Fahim AT, Bowne SJ, Sullivan LS, Webb KD, Williams JT, Wheaton DK et al (2011) Allelic heterogeneity and genetic modifier loci contribute to clinical variation in males with X-linked retinitis pigmentosa due to RPGR mutations. PLoS One 6:e23021

27. Hong DH, Pawlyk BS, Adamian M, Sandberg MA, Li T (2005) A single, abbreviated RPGR-ORF15 variant reconstitutes RPGR function in vivo. Invest Ophthalmol Vis Sci 46:435–441
28. Hong DH, Pawlyk BS, Adamian M, Li T (2004) Dominant gain-of-function mutant produced by truncation of RPGR. Invest Ophthalmol Vis Sci 45:36–41
29. Brunner S, Colman D, Travis AJ, Luhmann UF, Shi W, Feil S et al (2008) Overexpression of RPGR leads to male infertility in mice due to defects in flagellar assembly. Biol Reprod 79:608–617
30. Wright RN, Hong DH, Perkins B (2011) Misexpression of the constitutive RPGR(ex1–19) variant leads to severe photoreceptor degeneration. Invest Ophthalmol Vis Sci 52:5189–5201
31. Brunner S, Skosyrski S, Kirschner-Schwabe R, Knobeloch KP, Neidhardt J, Feil S et al (2010) Cone versus rod disease in a mutant Rpgr mouse caused by different genetic backgrounds. Invest Ophthalmol Vis Sci 51:1106–1115
32. Shu X, Zeng Z, Gautier P, Lennon A, Gakovic M, Patton EE et al (2010) Zebrafish Rpgr is required for normal retinal development and plays a role in dynein-based retrograde transport processes. Hum Mol Genet 19:657–670
33. Ghosh AK, Murga-Zamalloa CA, Chan L, Hitchcock PF, Swaroop A, Khanna H (2010) Human retinopathy associated ciliary protein retinitis pigmentosa GTPase regulator mediates cilia-dependent vertebrate development. Hum Mol Genet 19:90–98
34. Gerner M, Haribaskar R, Pütz M, Czerwitzki J, Walz G, SchÓ“fer T (2010) The retinitis pigmentosa GTPase regulator interacting protein 1 (RPGRIP1) links RPGR to the nephronophthisis protein network. Kidney Int 77:891–896

# Chapter 62
# Unc119 Gene Deletion Partially Rescues the GRK1 Transport Defect of *Pde6d*$^{-/-}$ Cones

**Houbin Zhang, Jeanne M. Frederick and Wolfgang Baehr**

**Abstract** PrBP/δ, encoded by the *Pde6d* gene, is an isoprenyl-binding protein that regulates trafficking of isoprenylated proteins, such as PDE6 and GRK1, from photoreceptor inner segments to outer segments. Trafficking of PDE6 and GRK1 to photoreceptor outer segments is impeded in *Pde6d* knockout mice. In *Pde6d*$^{-/-}$cones, PDE6 and GRK1 are nearly undetectable and the b-wave amplitudes of photopic ERGs in *Pde6d*$^{-/-}$ mice are reduced by over 50%. We reported recently that UNC119, a homolog of PrBP/δ highly expressed in photoreceptors, functions as an acyl-binding protein and regulates transport of G-proteins in sensory neurons. Since both PrBP/δ and UNC119 regulate peripheral protein trafficking in photoreceptors, we generated *Pde6d; Unc119* double knockout mice in order to study how PrBP/δ and UNC119 may interact. Surprisingly, knockout of Unc119 partially reversed the transport defect of GRK1 in cone photoreceptors caused by deletion of *Pde6d*, and the b-wave amplitudes of photopic ERGs in the double knockout mice were significantly higher than those in the *Pde6d*$^{-/-}$ mice. These results suggest that cone transport of isoprenylated and acylated proteins is interdependent.

**Keywords** PrBP/δ · Pde6d · UNC119 · Photoreceptors · GRK1 · PDE6 · ERG

H. Zhang (✉) · J. M. Frederick · W. Baehr
Department of Ophthalmology, John A. Moran Eye Center, University of Utah Health Science Center, 65 Mario Capecchi Drive, Salt Lake City, UT 84132, USA
e-mail: houbin.zhang@hsc.utah.edu

J. M. Frederick
e-mail: jeanne.frederick@hsc.utah.edu

W. Baehr
Department of Neurobiology and Anatomy, University of Utah, Salt Lake City, UT 84132, USA
e-mail: wbaehr@hsc.utah.edu

W. Baehr
Department of Biology, University of Utah, Salt Lake City, UT 84112, USA

J. D. Ash et al. (eds.), *Retinal Degenerative Diseases,* Advances in Experimental Medicine and Biology 801, DOI 10.1007/978-1-4614-3209-8_62,

**Abbreviations**

| | |
|---|---|
| RhoGDI | Rho GTPase guanine nucleotide dissociation inhibitor |
| ERG | Electroretinogram |
| COS | Cone outer segment |

## 62.1 Introduction

PrBP/δ, encoded by the *Pde6d* gene, is a small polypeptide consisting of 150 amino acids in mammals with an apparent molecular weight of ~17 kD [1]. As PrBP/δ co-purified with photoreceptor PDE6, it was thought initially to be a fourth subunit of rod PDE6 [2]. Many more PrBP/δ-interacting proteins, identified by yeast-two hybrid screening (e.g., GRK1, Ras, and other small GTPases in the Ras family [3–5]), suggested a more general function of PrBP/δ. Close examination of PrBP/δ-interacting proteins revealed that most share a common feature, a C-terminal isoprenyl group. The FRET assay shows that PrBP/δ has distinct affinities for farnesyl and geranylgeranyl moieties, binding farnesyl ($k_d$ = 0.7 μM) more tightly than geranylgeranyl ($k_d$ = 19 μM) [5]. Transport of isoprenylated proteins (GRK1, rod PDE6, and cone PDE6) to photoreceptor outer segments was impeded in *Pde6d* knockout photoreceptors, resulting in a slow degeneration of cones followed by degeneration of rods, a phenotype similar to human patients with cone-rod dystrophy [6].

UNC119, first discovered in *C.elegans*, shares 30–40 % sequence similarity with PrBP/δ [7]. UNC119 is highly expressed in the synaptic termini of photoreceptors, and to a less extent in the inner segments [8]. Knockout of the *Unc119* gene in mouse led to slow retinal degeneration starting at 6 months postnatally, a phenotype similar to human *RP* (*Retinitis Pigmentosa*) [8], although the mechanism of degeneration is unclear. We recently proposed that UNC119 is an acyl-binding protein. UNC119 binds the acylated N-terminal peptide of transducin α with a $k_d$ of 0.5 μM [9]. UNC119 can extract transducin from retina membranes in the presence of GTP, and is required for efficient return of transducin to photoreceptor outer segments after light-induced translocation of transducin from outer segments to inner segments during light adaptation, suggesting that UNC119 regulates trafficking of transducin in photoreceptors [9].

In this study, we generated PrBP/δ and UNC119 double knockout mice and observed that GRK1 is up-regulated in the mutant cone photoreceptors. With more GRK1 present in the cone photoreceptor cells, photopic ERGs reflecting cone function exhibit higher responses in the double knockout mice compared with those in the *Pde6d* single knockout mice.

## 62.2 Materials and Methods

### *62.2.1 Mouse Breeding Genotyping*

Procedures for the animal experiments were approved by the University of Utah IACUC and conformed to recommendations of the Association of Research for Vision and Ophthalmology. Animals were maintained in cyclic light (12 h light/12 h dark) conditions. *Unc119*$^{-/-}$ mice were provided by Dr. George Inana at the University of Miami. *Pde6d; Unc119* double knockout mice were generated by mating *Pde6d*$^{-/-}$ mice to *Unc119*$^{-/-}$ mice. Genotyping of *Pde6d*$^{-/-}$ and *Unc119*$^{-/-}$ mice was described previously [6, 8].

### *62.2.2 Immunohistochemistry*

Immunostaining of mouse retina sections was performed as described [10]. Retina cryosections were cut and immunolabeled using mouse monoclonal GRK1 antibody (G8, 1:1000, from Dr. Kris Palczewski, Case Western Reserve University) or rabbit polyclonal cone PDE6 antibody (1:500, from Dr. Tiansen Li, NEI/NIH).

### *62.2.3 Photopic Electroretinogram (ERG)*

ERGs were recorded with a UTAS E-3000 (LKC Technologies, Inc.) as described [6, 11]. For photopic ERGs to record cone function, the mice were light-adapted under background light of 10 db (1.48 logcds $m^{-2}$) for 15 min. Single-flash responses were usually recorded at stimulus intensities of −4 db (−0.6 logcds $m^{-2}$) to 15 db (1.86 log cds $m^{-2}$).

## 62.3 Results

### *62.3.1 Knockout of the Unc119 Gene in Pde6d*$^{-/-}$ *Mice Increases Expression of GRK1 in Photoreceptor Outer Segments*

PrBP/δ and UNC119 each regulate transport of lipid-conjugated peripheral proteins to photoreceptor outer segments. Both, in turn, are regulated by the small GTPase ARL3, which controls cargo release from PrBP/δ and UNC119 [12, 13]. It remains unclear whether PrBP/δ and UNC119 coordinately regulate the transport of isoprenylated proteins and acylated protein to photoreceptor outer segments.

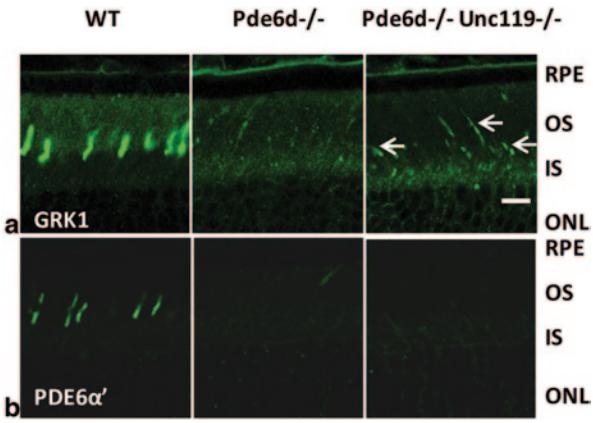


**Fig. 62.1** Immunolocalization of *GRK1* and *PDE6α'* in *WT*, *Pde6d*$^{-/-}$, and *Pde6d*$^{-/-}$ *Unc119*$^{-/-}$ retinas. The eyes were co-embedded, and central retina sections were probed simultaneously using anti-*GRK1* (**a**) and *PDE6α'* (**b**). *RPE* retinal pigment epithelium, *OS* outer segments, *IS* inner segments, *ONL* outer nuclear layer. *Arrows* point cone outer segments. Scale bar, 10 μm

We were interested to define the functional relationship of these two proteins by generating *Pde6d* and *Unc119* double knockout mice. In the *Pde6d*$^{-/-}$*Unc119*$^{-/-}$ mice, cone PDE6 is nearly undetectable, which is similar in the *Pde6d* single knockout (Fig. 62.1b). Expression of GRK1 in the *Pde6d*$^{-/-}$ and *Pde6d*$^{-/-}$*Unc119*$^{-/-}$ mice is almost absent throughout the rods (Fig. 62.1a). However, expression of GRK1 is surprisingly increased in the cone outer segments, as compared to the *Pde6d*$^{-/-}$ cones with little GRK1 in COS (Fig. 62.1a).

### 62.3.2 *Knockout of the Unc119 Gene in Pde6d*$^{-/-}$ *Background Increases Cone Photoresponses*

GRK1 is a key enzyme to shut down the phototransduction cascade. GRK1 phosphorylates rhodopsin and cone opsins, thereby desensitizing rhodopsin and cone opsins following activation. In GRK1 gene knockout mice, both rod and cone photoreceptors showed slower recovery from photoactivation [14]. In *Pde6d* knockout mice, expression of GRK1 is significantly down-regulated and photoreceptors exhibit a phenotype of slower dark-adaption [6]. Lowered GRK1 in *Pde6d*$^{-/-}$ mice essentially delays desensitization of activated cone opsins and increase basal level of photoresponses under constant light, resulting in lower amplitude of photopic ERGs. In the *Pde6d*$^{-/-}$*Unc119*$^{-/-}$ mice, the expression of GRK1 increases relative to that observed in *Pde6d* knockout mice. As expected, the amplitude of photopic ERGs in the *Pde6d*$^{-/-}$*Unc119*$^{-/-}$ is higher than that in the *Pde6d*$^{-/-}$ mice; however, it is still lower than that in wild-type mice (Fig. 62.2), which may be due to partial up-regulation of GRK1 and lower cone PDE6 expression in the double knockout.

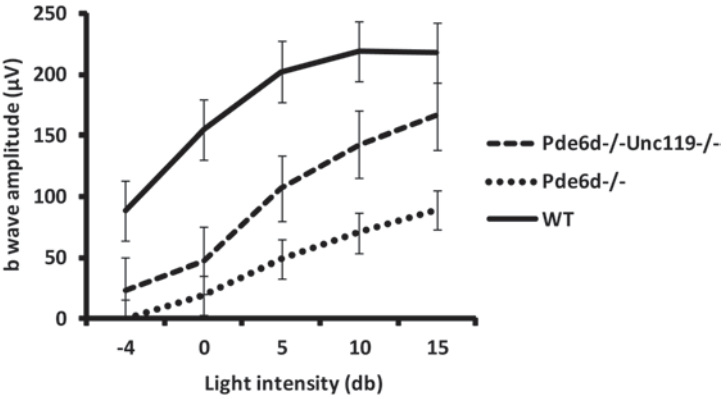


**Fig. 62.2** Photopic ERGs of *WT*, *Pde6d*$^{-/-}$, and *Pde6d*$^{-/-}$*Unc119*$^{-/-}$ mice. Photopic *b-wave amplitudes* are plotted as a function of *light intensities*. Error *bars* represent mean ± SD ($n = 3$)

## 62.4 Discussion

We show that deletion of the Unc119 gene in the *Pde6d*-/- background produced up-regulated expression of GRK1 in cone photoreceptors and consequently, cone b-wave photoresponses increased relative to that observed in *Pde6d* single knockout mice (Fig. 62.2). GRK1 is a peripheral membrane protein, and undergoes post-translational isoprenylation at its C-terminus. PrBP/δ solubilizes GRK1 from membranes by binding the isoprenyl tail of GRK1, and forming a soluble complex to facilitate transport of GRK1. PrBP/δ also interacts with a small GTPase ARL3 [15], and GTP-bound ARL3 likely promotes release of GRK1 from PrBP/δ at the target membrane, analogous to release of farnesylated Rheb from PrBP/δ [12]. In contrast, UNC119 is an acyl-binding protein. Deletion of the *UNC119* gene does not interfere with transport of GRK1 and other isoprenylated proteins [9]. However, UNC119 also interacts with ARL3, and GTP-bound ARL3 facilitates the release of acylated protein cargo from UNC119 [13]. Our result that the *UNC119*; *Pde6d* double knockout improves transport of GRK1 in cones is counter-intuitive, because ARL3 is not involved in regulating PrBP/δ cargo release when PrBP/δ is absent. However, in *Pde6d* knockout cones, residual GRK1 is present in cone outer segments, suggesting that GRK1 transport may be facilitated via alternative mechanisms. One possible mechanism is that other isoprenyl-binding proteins may play a minor role in transport of GRK1 to outer segments, and one 'candidate isoprenyl binding protein' is RhoGDI that binds geranylgeranylated CDC42. Although RhoGDI is a possible candidate that may enhance transport of GRK1 to cone outer segments, we cannot exclude other isoprenyl-binding proteins as possible candidates, such as RabGDI; nor could we exclude possible common factors that play a role in transport pathways of both isoprenylated proteins and acylated proteins.

PrBP/δ and RhoGDI each contain a hydrophobic pocket sandwiched by two β-sheets and each can bind isoprenyl groups. It is possible that RhoGDI can

accommodate isoprenyl tail of GRK1. Expression of Rho GTPase proteins in photoreceptors have been documented [16], suggesting that RhoGDI, an essential functional partner for Rho GTPase, is also expressed in photoreceptors. When PrBP/δ/GRK1 complex reaches its destination membrane, release of GRK1 requires interaction with GTP-bound ARL3. Similarly, RhoGDI/GRK1 complex may require ARL3 to discharge GRK1 from RhoGDI upon their arrival to the targeted membrane. ARL3 not only traffics isoprenylated proteins but also traffics acylated proteins, a process which is modulated by UNC119. Other factors besides ARL3 may share transport of isoprenylated and acylated proteins. Therefore, knockout of *Unc119* gene will free at least some ARL3 and other unknown factors from the pathway of trafficking acylated proteins and enhance transport of GRK1 by the alternative transport pathway.

Future investigations will determine if rescue of GRK1 transport in the *Pde6d; Unc119* double knockout mice would slow down the degeneration of cone photoreceptors. We will also investigate the expression profile of photoreceptor RhoGDI and test the binding affinity of RhoGDI to GRK1 and PDE6. This will address the role of RhoGDI in the observed rescue of GRK1 transport in *Unc119; Pde6d* double knockout mice.

## References

1. Zhang H, Constantine R, Frederick JM, Baehr W (2012) The prenyl-binding protein PrBP/δ: a chaperone participating in intracellular trafficking. Vision Res 75:19–25
2. Gillespie PG, Prusti RK, Apel ED, Beavo JA (1989) A soluble form of bovine rod photoreceptor phosphodiesterase has a novel 15-kDa subunit. J Biol Chem 264(21):12187–12193
3. Hillig RC, Hanzal-Bayer M, Linari M, Becker J, Wittinghofer A, Renault L (2000) Structural and biochemical properties show ARL3-GDP as a distinct GTP binding protein. Structure 8(12):1239–1245
4. Hanzal-Bayer M, Renault L, Roversi P, Wittinghofer A, Hillig RC (2002) The complex of Arl2-GTP and PDE delta: from structure to function. EMBO J 21(9):2095–2106
5. Zhang H, Liu XH, Zhang K, Chen CK, Frederick JM, Prestwich GD, Baehr W (2004) Photoreceptor cGMP phosphodiesterase delta subunit (PDEdelta) functions as a prenyl-binding protein. J Biol Chem 279(1):407–413
6. Zhang H, Li S, Doan T, Rieke F, Detwiler PB, Frederick JM, Baehr W (2007) Deletion of PrBP/delta impedes transport of GRK1 and PDE6 catalytic subunits to photoreceptor outer segments. Proc Natl Acad Sci USA 104(21):8857–8862
7. Maduro M, Pilgrim D (1995) Identification and cloning of *Unc-119*, a gene expressed in the Caenorhabditis elegans nervous system. Genetics 141(3):977–988
8. Ishiba Y, Higashide T, Mori N, Kobayashi A, Kubota S, McLaren MJ, Satoh H, Wong F, Inana G (2007) Targeted inactivation of synaptic HRG4 (UNC119) causes dysfunction in the distal photoreceptor and slow retinal degeneration, revealing a new function. Exp Eye Res 84(3):473–485
9. Zhang H, Constantine R, Vorobiev S, Chen Y, Seetharaman J, Huang YJ, Xiao R, Montelione GT, Gerstner CD, Davis MW, Inana G, Whitby FG, Jorgensen EM, Hill CP, Tong L, Baehr W (2011) UNC119 is required for G protein trafficking in sensory neurons. Nat Neurosci 14(7):874–880

10. Zhang H, Fan J, Li S, Karan S, Rohrer B, Palczewski K, Frederick JM, Crouch RK, Baehr W (2008) Trafficking of membrane-associated proteins to cone photoreceptor outer segments requires the chromophore 11-cis-retinal. J Neurosci 28(15):4008–4014
11. Jiang L, Zhang H, Dizhoor AM, Boye SE, Hauswirth WW, Frederick JM, Baehr W (2011) Long-term RNA interference gene therapy in a dominant retinitis pigmentosa mouse model. Proc Natl Acad Sci USA 108(45):18476–18481
12. Ismail SA, Chen YX, Rusinova A, Chandra A, Bierbaum M, Gremer L, Triola G, Waldmann H, Bastiaens PI, Wittinghofer A (2011) Arl2-GTP and Arl3-GTP regulate a GDI-like transport system for farnesylated cargo. Nat Chem Biol 7(12):942–949
13. Wright KJ, Baye LM, Olivier-Mason A, Mukhopadhyay S, Sang L, Kwong M, Wang W, Pretorius PR, Sheffield VC, Sengupta P, Slusarski DC, Jackson PK (2011) An ARL3-UNC119-RP2 GTPase cycle targets myristoylated NPHP3 to the primary cilium. Genes Dev 25(22):2347–2360
14. Chen CK, Burns ME, Spencer M, Niemi GA, Chen J, Hurley JB, Baylor DA, Simon MI (1999) Abnormal photoresponses and light-induced apoptosis in rods lacking rhodopsin kinase. Proc Natl Acad Sci USA 96(7):3718–3722
15. Linari M, Hanzal-Bayer M, Becker J (1999) The delta subunit of rod specific cyclic GMP phosphodiesterase, PDE delta, interacts with the Arf-like protein Arl3 in a GTP specific manner. FEBS Lett 458(1):55–59
16. Fontainhas AM, Townes-Anderson E (2008) RhoA and its role in synaptic structural plasticity of isolated salamander photoreceptors. Invest Ophthalmol Vis Sci 49(9):4177–4187

# Chapter 63
# Retinal Function in Aging Homozygous *Cln3*$^{\Delta ex7/8}$ Knock-In Mice

**Cornelia Volz, Myriam Mirza, Thomas Langmann and Herbert Jägle**

**Abstract** Neuronal ceroid lipofuscinoses (NCL) are characterized by lysosomal accumulation of autofluorescent material and lead to degeneration of the central nervous system. Patients affected by the juvenile form of NCL (JNCL), the most common form of the disease, develop visual failure prior to mental and motor deficits. It is currently unclear if the corresponding mouse model, *Cln3*$^{\Delta ex7/8}$ knock-in, develops the same retinal phenotype and electroretinogram (ERG) measurements as affected patients. The aim of our study was to investigate the visual disease progression in the *Cln3*$^{\Delta ex7/8}$ mice using scotopic and photopic ERGs as well as optokinetic tracking (OKT) at different ages. The results were then compared with age-matched controls.

The amplitudes of the a-wave and b-wave (scotopic ERG) decrease significantly in *Cln3*$^{\Delta ex7/8}$ mice starting at the age of 12 months. A reduction in the b/a-amplitude ratio indicates a degeneration preferentially of the inner retina. An amplitude reduction observed in the *Cln3*$^{+/+}$ control mice may be attributed to an additional *Crb1*$^{rd8}$ mutation. Using optokinetic tracking (OKT) the *Cln3*$^{\Delta ex7/8}$ mice show a progressive decline in visual acuity after 12 months of age.

C. Volz (✉)
Department of Ophthalmology, University Eye Clinic Regensburg,
Franz-Josef-Strauß Allee 11, 93053 Regensburg, Germany
e-mail: volz@eye-regensburg.de

M. Mirza
Instutute of Human Genetics, University of Regensburg, Regensburg, Germany

Department of Experimental Immunology of the Eye, University of Cologne, Cologne, Germany
e-mail: Myriam.Mirza@klinik.uni-regensburg.de

T. Langmann
Department of Experimental Immunology of the Eye, University of Cologne, Cologne, Germany
e-mail: thomas.langmann@uk-koeln.de

H. Jägle
Department of Ophthalmology, University Eye Clinic Regensburg,
Franz-Josef-Strauß Allee 11, 93053 Regensburg, Germany
e-mail: Herbert.jaegle@ukr.de

J. D. Ash et al. (eds.), *Retinal Degenerative Diseases,* Advances in Experimental Medicine and Biology 801, DOI 10.1007/978-1-4614-3209-8_63,

**Keywords** Neuronal ceroid lipofuscinosis · *Cln3* · Retinal function · Electroretinography · Optokinetic tracking

## 63.1 Introduction

Neuronal ceroid lipofuscinosis (NCL) represent a group of inherited fatal, early onset neurodegenerative diseases characterized by progressive vision loss, motor and mental deficits, and spontaneous seizures. NCL is normally caused by mutations in the CLN genes, with the most common mutation being a 1.02 kb genomic deletion of exons 7–8 in the *Cln3* gene giving rise to the juvenile form of NCL (JNCL). JNCL accounts for 85 % of NCL cases and is the most common form of childhood neurodegenerative disease. The *Cln3* function itself is not yet fully understood. It is a primarily endosomal-lysosomal protein in mammalian cells, which plays a major role in post-Golgi, endocytic, autophagic and lysosomal trafficking [1].

There are three available mouse models ($Cln3^{-/-}$ knockout, $Cln3^{\Delta ex7/8}$ knock-in and *Cln3* knockout) for JNCL [2], however the retinal phenotype in these mouse models is considered to be milder than in humans [3]. The $Cln3^{\Delta ex7/8}$ knock-in mouse model has the same common deletion as found in patients making it more clinically relevant. Thus, the aim of our study was to characterize the retinal function in homozygous $Cln3^{\Delta ex7/8}$ mice.

## 63.2 Materials and Methods

### *63.2.1 Experiments with Animals*

Wild type ($Cln3^{+/+}$) and homozygous $Cln3^{\Delta ex7/8}$ knock-in mice were all on a C57BL/6 background. $Cln3^{\Delta ex7/8}$ mice and control mice were provided by Dr. Klaus Rüther (Charité Berlin). All mice tested positive for the $Crb1^{rd8}$ mutation. Animals were maintained in an air-conditioned environment on a 12-h light–dark schedule at 22 °C, and had free access to food and water. The health of the animals was regularly monitored, and all procedures were approved by the University of Regensburg animal rights committee and complied with the German Law on Animal Protection and the Institute for Laboratory Animal Research Guide for the Care and Use of Laboratory Animals, 2011.

### *63.2.2 Behavioral Measurement of Vision*

Optokinetic tracking (OKT) was assessed as a predictor of visual acuity using a virtual optomotor system (OptoMotry, Cerebral Mechanics Inc., Lethbridge, Alberta,

Canada) as described previously [4]. Briefly, freely moving animals were exposed to moving sine-wave gratings of various spatial frequencies and reflexively tracked the gratings by head movements. An automated staircase paradigm adjusted the spatial frequency of the rotating pattern on subsequent trials until a threshold was achieved. The OKT threshold was defined as the highest spatial frequency obtained at 100 % contrast.

### *63.2.3 Electroretinography*

Mice were dark adapted for at least 12 h before the experiments and subsequently anesthetized by subcutaneous injection of ketamine and xylazine. Pupils were dilated with tropicamide eye drops (Mydriaticum Stulln; Pharma Stulln, Germany). Silver needle electrodes served as reference (fore-head) and ground (tail) and gold wire ring electrodes as active electrodes. Corneregel (Bausch & Lomb, Berlin, Germany) was applied to keep the eye hydrated and maintain good electrical contact. ERGs were recorded using a Ganzfeld bowl (Ganzfeld QC450 SCX, Roland Consult, Brandenburg, Germany) and an amplifier and recording unit (RETI-Port, Roland Consult, Brandenburg, Germany). ERGs were recorded from both eyes simultaneously, band-pass filtered (1–300 Hz) and averaged. Single flash scotopic (dark adapted) responses to a series of 10 LED-flash intensities ranging from −3.5 to 1.0 log cd.s/m$^2$ with an inter stimulus interval of 2 s up to 20 s for the highest intensity were recorded. After 10 min of adaptation to a white background illumination (25 cd/m$^2$) single flash photopic (light adapted) responses to three Xenon-flash intensities (1, 2, and 3 log cd.s/m$^2$) were also recorded. Response waveforms were analyzed by means of peak amplitude and implicit time measurement. All analysis and plotting was carried out with R 2.15.1 and ggplot 0.9.2.

## 63.3 Results

### *63.3.1 Optokinetic Tracking*

We studied the visual performance of *Cln3*$^{\Delta ex7/8}$ mice using OKT. OKT is a good predictor of visual acuity when measuring reflexive head tracking to moving gratings using stairway changes in spatial frequency. Until 12 months of age, *Cln3*$^{\Delta ex7/8}$ mice showed normal OKT thresholds that did not differ from *Cln3*$^{+/+}$ mice (Fig. 63.1). However, past 12 months of age, *Cln3*$^{\Delta ex7/8}$ mice appear to have a significant and rapid decline in OKT thresholds. The relatively large standard deviations of OKT thresholds most likely reflect variable disease progresses in the *Cln3*$^{\Delta ex7/8}$ mice. The OKT thresholds of *Cln3*$^{+/+}$ mice stay the same until 18 months of age.

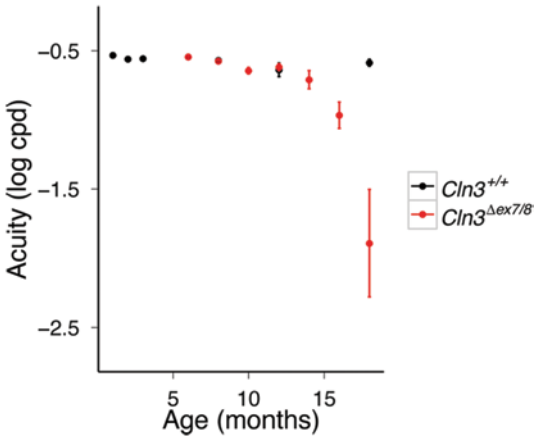


**Fig. 63.1** Temporal changes in optokinetic tracking thresholds in homozygous *Cln3*$^{\Delta ex7/8}$ and *Cln3*$^{+/+}$ mice. After 12 months of age, the visual function decreases rapidly in *Cln3*$^{\Delta ex7/8}$mice while staying the same in *Cln3*$^{+/+}$ mice

### *63.3.2 Scotopic ERG*

ERG measurements were performed as an independent measure of retinal function at 6, 12, and 18 months of age. First, we performed dark-adapted (scotopic) ERG measurements. Rod photoreceptor function, as measured by the amplitude and implicit time of the leading trough of the response waveform (a-wave), as well as the inner retinal function, represented by the amplitude and implicit time of the positive peak (b-wave), were determined for *Cln3*$^{+/+}$ and *Cln3*$^{\Delta ex7/8}$ mice (Fig. 63.2). At 6 months of age there was no amplitude difference between the *Cln3*$^{\Delta ex7/8}$ and *Cln3*$^{+/+}$group. The a-wave as well as the b-wave amplitudes decreased more in *Cln3*$^{\Delta ex7/8}$ mice compared to *Cln3*$^{+/+}$ mice starting at 12 months of age (Fig. 63.2b). The amplitude loss of both components in *Cln3*$^{\Delta ex7/8}$ mice became obvious at 18 months, with the b-wave being more affected than the a-wave (Fig. 63.2b). This is also illustrated by the b-/a-wave amplitude ratio which was lower for *Cln3*$^{\Delta ex7/8}$ mice starting at 12 month of age, indicating a preferential degeneration of the inner retina (Fig. 63.2d). Interestingly, the amplitudes also clearly decreased in aging *Cln3*$^{+/+}$ mice. A decrease of one third can be seen in 18 month old *Cln3*$^{+/+}$ mice as compared to the 6-month-old mice which may result from the presence of the Crb1$^{rd8}$ mutation. There was no difference in the implicit time between the two groups at 6 or at 12 months. At 18 months, the implicit time of the a-wave was prolonged in *Cln3*$^{\Delta ex7/8}$ mice for most flash intensities. This difference was clearer for the implicit time of the b-wave (Fig. 63.2c).

### *63.3.3 Photopic ERG*

Photopic ERG measurements were performed on light-adapted mice (Fig. 63.3). At 6 months of age, the amplitudes (measured from the leading trough to the following peak) of the *Cln3*$^{\Delta ex7/8}$ mice were already reduced as compared to *Cln3*$^{+/+}$ mice. The

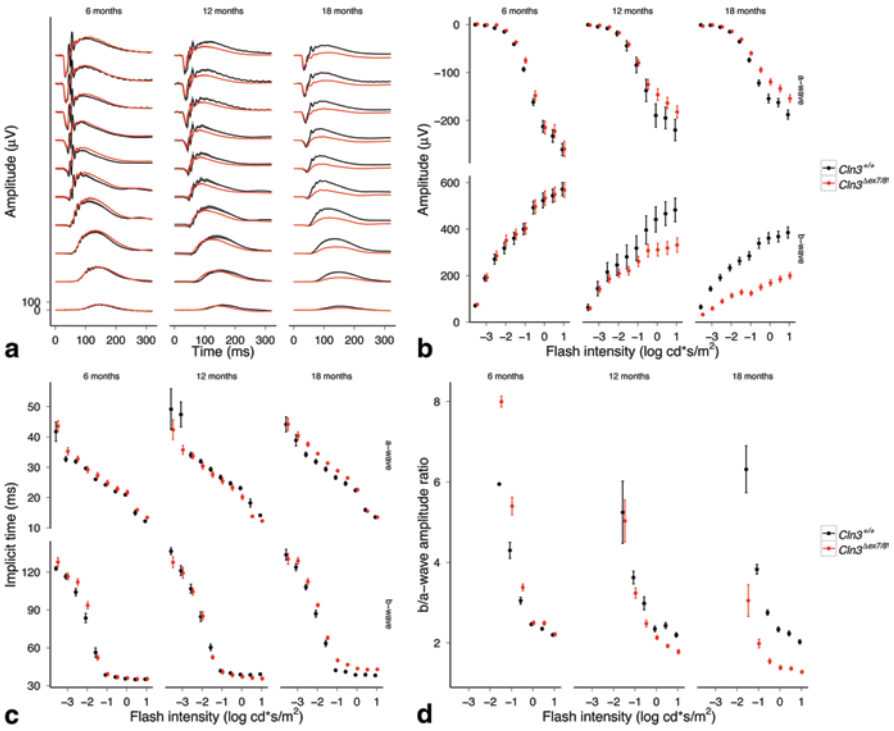


**Fig. 63.2** Dark-adapted (scotopic) ERG responses of 6, 12 and 18 months old *Cln3*$^{\Delta ex7/8}$(*red* traces) and age-matched *Cln3*$^{+/+}$ mice (*black* traces). Amplitudes of the a- and b-wave are the same in both groups at 6 months of age. At 12 months of age, the amplitudes are reduced in *Cln3*$^{\Delta ex7/8}$ mice compared to the controls. The difference is more obvious at 18 months of age and the b-wave is more affected than the a-wave (**a** and **b**). The implicit time is slightly prolonged in *Cln3*$^{\Delta ex7/8}$ at 18 months of age (**c**). The reduction of the b-/a-wave amplitude ratio indicates a preferential degeneration of the inner retina (**d**)

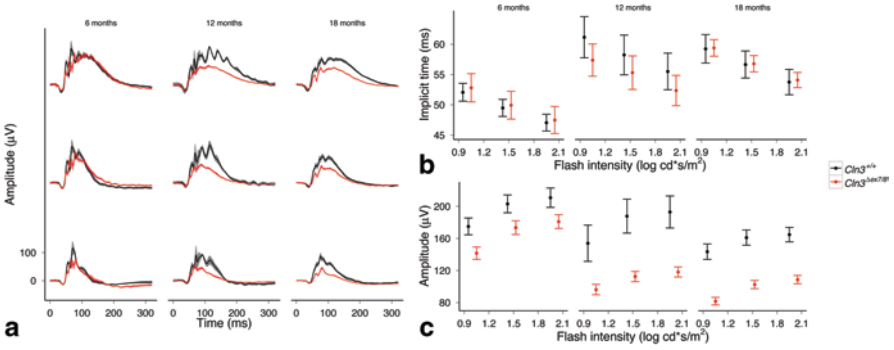


**Fig. 63.3** Light-adapted (photopic) ERG responses of 6, 12 and 18 months old *Cln3*$^{\Delta ex7/8}$ (*red* traces) and age-matched *Cln3*$^{+/+}$ mice (*black* traces). The amplitude reduction in *Cln3*$^{\Delta ex7/8}$ mice is already present at 6 months of age. The difference increases with age when comparing to the control group (**a** and **c**). There was no significant difference in the implicit time between the two groups (**b**)

difference was more obvious at 12 and 18 months. The amplitudes of *Cln3*$^{+/+}$ mice also decreased with age (Fig. 63.3c).

## 63.4 Discussion

In this study, we investigated the retinal function of the JNCL using the *Cln3*$^{\Delta ex7/8}$ mouse model. Our results suggest a delayed progressive retinal degeneration in these mice. OKT and ERG measurements demonstrate a decline in visual perception and a loss of retinal function starting at 12 months of age.

Visual acuity can be assessed by OKT [5]. To our knowledge, there has been no report so far on OKT results in aging *Cln3*$^{\Delta ex7/8}$ mice. We found significant OKT threshold changes after 12 months of age with a drastic reduction in visual acuity at 18 months of age. It is important to consider that at this time point, the visual acuity shows large inter-individual variability. The disease course is also very variable in humans and vision loss is the most common presenting symptom of JNCL, occurring between 5.5 and 8.5 years [6]. However, the results of the OKT measurements may be confounded by the effects of increasing degeneration of the central nervous system at the highest age.

The decline in the retinal function was also noticeable in the scotopic ERG at 12 months of age: the b-wave amplitude was reduced in *Cln3*$^{\Delta ex7/8}$ mice compared to *Cln3*$^{+/+}$ mice. The amplitude drop was milder, but also present in the a-wave starting at 12 months. Staropoli et al. investigated *Cln3*$^{\Delta ex7/8}$ mice up to an age of 16 months and found virtually no difference between a-wave amplitudes at any of the ages [7]. A marked drop in the a-wave amplitude possibly occurs between the 16 and 18 months of age, which may explain our findings. Additionally, the a-wave amplitude reduction may also have been occluded by additional variability introduced by mild degeneration due to the *Crb1*$^{rd8}$ mutation.

The photopic ERG seems to be affected earlier and be a more sensitive marker picking up early functional changes in the *Cln3*$^{\Delta ex7/8}$ retina. The amplitudes here were reduced in *Cln3*$^{\Delta ex7/8}$ mice by the age of 6 months, compared to *Cln3*$^{+/+}$ mice. This data are in accordance with the retinal findings in *Cln3*$^{\Delta ex7/8}$ KI mice reported by Staropoli et al. [7] and in *Cln3*-knock-out mice reported by Katz et al. [8].

Interestingly, ERG responses also considerably decline in *Cln3*$^{+/+}$ mice with age. Mattapallil et al. reported the existence of the Crb1$^{rd8}$ mutation in the C57BL/6N genetic background, which could confound retinal function studies in transgenic mouse models established on this background [9]. All mice included in our study tested positive for the Crb1$^{rd8}$ mutation, this being a possible explanation for the amplitude loss in *Cln3*$^{+/+}$ mice with increasing age. Further investigation needs to be done on how the ERG in C57BL/6N mice without the Crb1$^{rd8}$ mutation evolves over time.

Electroretinography and OKT can be used to characterize disease progression in a mouse model for JNCL. Our results indicate a preferential decline of the inner retinal function in *Cln3*$^{\Delta ex7/8}$ mice, similar to human disease, while the time of onset

does not coincide with that observed in JNCL patients. The decline seen in the optokinetic response is milder than in the electroretinography results. In the context of a therapeutic trial, electroretinography could provide important information about disease course under treatment and identify successful approaches.

**Acknowledgment** We would like to thank Dr. Klaus Rüther for providing *Cln3*$^{\Delta ex7/8}$ mice. We thank Dr. Frank Stehr for his support. This work was funded by the NCL-Foundation and the Auerbach foundation.

## References

1. Cotman SL, Vrbanac V, Lebel LA, Lee RL, Johnson KA, Donahue LR et al (2002) Cln3(Deltaex7/8) knock-in mice with the common JNCL mutation exhibit progressive neurologic disease that begins before birth. Hum Mol Genet 11(22):2709–2721
2. Cooper JD, Russell C, Mitchison HM (2006) Progress towards understanding disease mechanisms in small vertebrate models of neuronal ceroid lipofuscinosis. Biochim Biophys Acta 1762(10):873–889
3. Seigel GM, Lotery A, Kummer A, Bernard DJ, Greene ND, Turmaine M et al (2002) Retinal pathology and function in a Cln3 knockout mouse model of juvenile neuronal ceroid lipofuscinosis (batten disease). Mol Cell Neurosci 19(4):515–527
4. Douglas RM, Alam NM, Silver BD, McGill TJ, Tschetter WW, Prusky GT (2005) Independent visual threshold measurements in the two eyes of freely moving rats and mice using a virtual-reality optokinetic system. Vis Neurosci 22(5):677–684
5. Prusky GT, Alam NM, Beekman S, Douglas RM (2004) Rapid quantification of adult and developing mouse spatial vision using a virtual optomotor system. Invest Ophthalmol Vis Sci 45(12):4611–4616
6. Bozorg S, Ramirez-Montealegre D, Chung M, Pearce DA (2009) Juvenile neuronal ceroid lipofuscinosis (JNCL) and the eye. Surv Ophthalmol 54(4):463–471
7. Staropoli JF, Haliw L, Biswas S, Garrett L, Holter SM, Becker L et al (2012) Large-scale phenotyping of an accurate genetic mouse model of JNCL identifies novel early pathology outside the central nervous system. PLoS One 7(6):e38310
8. Katz ML, Johnson GS, Tullis GE, Lei B (2008) Phenotypic characterization of a mouse model of juvenile neuronal ceroid lipofuscinosis. Neurobiol Dis 29(2):242–253
9. Mattapallil MJ, Wawrousek EF, Chan CC, Zhao H, Roychoudhury J, Ferguson TA et al (2012) The Rd8 mutation of the Crb1 gene is present in vendor lines of C57BL/6N mice and embryonic stem cells, and confounds ocular induced mutant phenotypes. Invest Ophthalmol Vis Sci 53(6):2921–2927

# Chapter 64
# Synergistic Interaction of Tubby and Tubby-Like Protein 1 (Tulp1)

**Nora Blanca Caberoy**

**Abstract** Mutations in either tubby or tubby-like protein 1 (Tulp1) cause retinal degeneration with undefined mechanisms. We recently identified both proteins with unconventional secretion as novel MerTK-specific phagocytosis ligands for retinal pigment epithelium (RPE) cells. Using our newly-developed open reading frame (ORF) phage display as a technology for protein-protein interactions, we identified Tulp1 as a Tubby-binding protein. The interaction of tubby and Tulp1 was verified by yeast two-hybrid and protein pull-down assays. Tubby and Tulp1 form heterodimer or heterooligomer and their interaction was functionally revealed by their synergistic stimulation of RPE phagocytosis. Tubby and Tulp1 mediated phagocytosis through MerTK-dependent signaling with non-muscle myosin II redistribution leading to colocalization of phagocytosed vesicles with rearranged NMMIIA.

**Keywords** Synergistic interaction · Tubby · Tubby-like protein 1 · Tulp1 · Retinal pigment epithelium · Phagocytosis · MerTK · Retinal degeneration · Phagocytosis ligands · ORF phage display

## 64.1 Introduction

Tubby and tubby-like protein 1 (Tulp1) belong to tubby protein family with four members (tubby, Tulp1, 2 and 3; Tulps), which share the highly conserved C-terminal region of the 'tubby domain' with ~260 amino acids [1]. A spontaneous mutation in tubby gene causes adult onset obesity, progressive retinal and cochlear degeneration in Tubby mice with undefined mechanisms, whereas mutations in Tulp1 associate only with retinal degeneration [2-3]. Several cellular functions have been characterized for Tulp1, including interactions with F-actin and GTPase dynamin-1 [4], photoreceptor synaptic development and photoreceptor protein transport pathways [5]. Both tubby and Tulp1 were reported as signaling molecules for G

N. B. Caberoy (✉)
School of Life Sciences, University of Nevada Las Vegas, Las Vegas, NV 89154, USA
e-mail: nora.caberoy@unlv.edu

J. D. Ash et al. (eds.), *Retinal Degenerative Diseases,* Advances in Experimental Medicine and Biology 801, DOI 10.1007/978-1-4614-3209-8_64,

protein-coupled receptors (GPCRs) and putative nuclear factors that regulate gene transcription [6]. Despite their nuclear translocation and putative C-terminal binding to double-stranded DNA, no target gene transcriptionally regulated by tubby or Tulp1 have been identified. We recently reported unconventional secretion of tubby and Tulp1 [7] and characterized both proteins as MerTK-specific ligands that facilitate retinal pigment epithelium (RPE) phagocytosis [8]. Here we describe that tubby interacts with Tulp1. Their interaction synergistically facilitates RPE phagocytosis. Given the broad roles of tubby and Tulp1 in the nuclei, cytoplasm and extracellular environment, tubby and Tulp1 interaction may synergistically modulate an array of cellular functions with broad implication.

## 64.2 Materials and Methods

### *64.2.1 Screening of Tubby-Binding Proteins*

Recombinant adenovirus expressing FLAG-tubby-F or GFP-FLAG was generated as previously described [9] and used to infect HEK293 cells to express the recombinant protein. Protein was purified using anti-FLAG mAb affinity columns (Sigma), eluted with FLAG peptide (100 mg/ml), and dialyzed against PBS. Purified tubby-F and GFP were immobilized onto the ELISA plates (5 mg/ml, 100 ml/well) and used for phage binding using open reading frame (ORF) phage display [10]. After three rounds of phage selection, individual clones were randomly picked from plates of enriched phages and analyzed for their binding to purified Tubby. Positive clones were identified by DNA sequencing.

### *64.2.2 Y2H Assay*

Tubby-N-terminal cDNA was cloned into pGBT9 plasmid (Clontech) at EcoRI and BamHI sites. The cDNA inserts of identified phages were amplified by PCR and cloned into pGAD424 plasmid (Clontech) at BamHI and SalI sites. Y2H assay was performed according to the manufacturer's protocol. Briefly, *S. cerevisiae* CG-1945 strain was co-transformed with cDNA insert/pGAD424 and tubby-N/pGBT9 or pGBT9 control. The transformed yeast was selected on agar plates with double (-Leu/-Trp) or triple (-Leu/-Trp/-His) dropout of the essential amino acids. Dropout- resistant yeast clones were re-grown on YPD plates, lifted onto a filter paper and analyzed for b-galactosidase expression using X-gal as a substrate.

### *64.2.3 Protein Pull-Down Assay*

Full-length coding sequence of mouse Tulp1 or Tubby was amplified by PCR and cloned into pcDNA3 with an N-terminal FLAG tag. HEK293 cells were transfected with the plasmid expressing FLAG-tagged Tulp1 with Lipofectamine reagent (Invitrogen). The cells were harvested at 48 h post-transfection and washed. Cell lysate was prepared in PBS containing 0.5% Triton X-100, spun and incubated with purified GST-tubby-F or GST control, followed by glutathione resin. The resin was washed and analyzed by Western blot using anti-FLAG mAb.

### *64.2.4 RPE Phagocytosis Assay*

Membrane vesicles were prepared from Neuro-2a cells transfected with Tubby, Tulp1, and/or control plasmid(s) that also co-expressed plasma membrane-targeted green fluorescent protein (mGFP) [11]. Plasma membrane vesicles were incubated with human ARPE19 RPE cells for 3 h at 37 °C for phagocytosis. Phagocytosed fluorescent signals were analyzed by confocal microscopy [11].

### *64.2.5 Immunocytochemistry*

ARPE19 RPE cells were incubated with membrane targeted GFP (mGFP)-labeled membrane vesicles in the presence or absence of Mer-Fc for 3 h, washed, fixed with 4% buffered formalin, permeabilized with 0.5% Triton X-100 in PBS, and incubated with rabbit anti-myosin II-A or anti-Lamp-1 Ab (Sigma). Bound Abs were detected by Texas Red-labeled secondary Abs and analysed by confocal microscopy for colocalization of mGFP and Texas Red signals.

## 64.3 Results

### *64.3.1 Tubby and Tulp1 Facilitate Phagocytosis in Synergy*

ORF phage display screening with purified tubby N-terminal domain (Tubby-N) as bait identified Tulp1 as a tubby-binding protein. The interaction of tubby and Tulp1 was independently verified by yeast two-hybrid assay and protein pull-down assay (Fig. 64.1). Tubby or Tulp1 alone stimulated RPE phagocytosis of POS. The combination of tubby and Tulp1 synergistically stimulated RPE ingestion of membrane vesicles (Fig. 64.1).

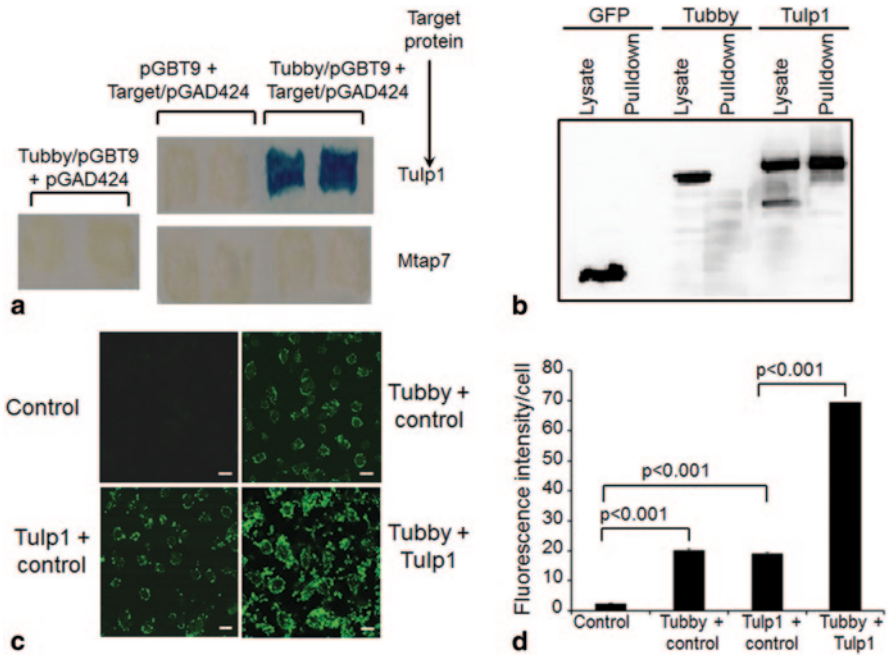


**Fig. 64.1** Tubby and Tulp1 interact and synergistically stimulate RPE phagocytosis. **a** Yeast two-hybrid assay. Tubby N-terminal domain in pGBT9 plasmid and Tulp1 in pGAD424 plasmid were co-expressed in *S. cerevisiae* CG-1945 stain, selected with -Leu/-Trp/-His triple dropout plates. Individual plasmids as controls were selected on -Leu/-Trp double dropout plates. Mtap7 was included as a negative control. Dropout-resistant yeast colonies were re-grown on a plate, lifted onto filter and analyzed for β-galactosidase expression with X-gal. *Blue* color indicated that the target protein interacts with tubby. **b** Protein pull-down assay. Glutathione S-transferase (GST)-tubby fusion protein was expressed, purified, incubated with cell lysates of FLAG-tagged tubby, Tulp1, or GFP (*green fluorescent* protein), pull-downed with glutathione resin, washed and analyzed by Western blot using anti-FLAG monoclonal antibodies. **c** A mixture of mGFP-labeled plasma membrane vesicles expressing tubby, Tulp1 or control was analyzed for RPE phagocytosis with human ARPE19 RPE cells for 3 h at 37 °C. Phagocytosed fluorescent signals were analyzed by confocal microscopy. Bar = 10 μm. **d** Relative fluorescence intensity per cell in **c** was quantified with > 100 cells counted per group (± SEM, $n > 100$, t-test). (Caberoy et al. 2010 [10] with permission from J Mol Recognit for **a**; Caberoy et al. 2010 [11] with permission from Exp Cell Res for **b–d**)

### *64.3.2 Tubby and Tulp1 Mediate Phagocytosis Through MerTK*

To identify the phagocytic receptor for tubby and Tulp1, we screened their interaction with several known receptors. Tubby and Tulp1 bound to Mer tyrosine kinase (MerTK) [8]. We then analyzed the role of MerTK in tubby- and Tulp1-mediated RPE phagocytosis. MerTK receptor dimerization is known to facilitate receptor activation and phosphorylation. Tubby or Tulp1 alone induced MerTK activation [8]

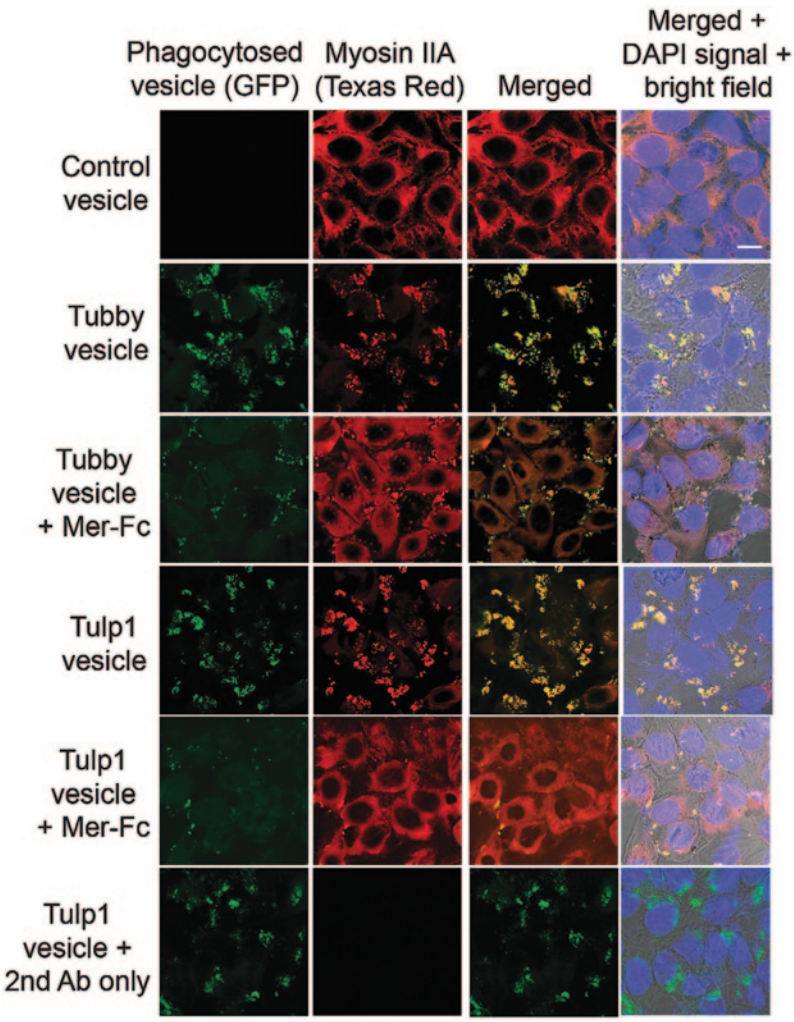


**Fig. 64.2** Tubby- and Tulp1-mediated RPE phagocytosis was MerTK-dependent. mGFP-labeled plasma membrane vesicles were prepared from Neuro-2a cells expressing tubby or Tulp1, and incubated with ARPE19 cells in the presence or absence of excess Mer-Fc (MerTK extracellular domain covalently fused to human IgG1 Fc domain, R&D Systems) for phagocytosis assay as in Fig. 64.1. After washing, ARPE19 cells were fixed, permeabilized, detected with anti-non-muscle myosin II (NMMII) A heavy chain antibodies, detected with Texas red-labeled secondary antibodies and analyzed by confocal microscopy. Fluorescence signals for mGFP and NMMII-A were co-localized. Bar = 10 μm. (Caberoy et al. 2010 [8] with permission from EMBO J)

(Fig. 64.2). Excessive soluble Mer-Fc (MerTK extracellular domain fused to human IgG1 Fc domain) blocked tubby- or Tulp1-mediated phagocytosis. Both ligands induced MerTK activation with receptor phosphorylation and signaling cascade, including non-muscle myosin II redistribution and co-localization with phagocytosed vesicles.

## 64.4 Discussion

Mutations in either tubby or Tulp1 associate with autosomal recessive retinal degeneration with unknown mechanisms. Tubby and Tulp1 facilitate phagocytosis in RPE cells and both proteins bind to and activate MerTK. RPE phagocytosis has been previously demonstrated to be critical in preventing retinal degeneration in Royal College of Surgeons (RCS) rats with a mutation in the well-characterized phagocytic receptor MerTK [12]. If tubby and Tulp1 facilitates RPE phagocytosis through MerTK, it is tempting to speculate that they are essential ligands to prevent retinal degeneration. An intriguing question is why these two functionally redundant proteins fail to compensate each other in their autosomal recessive mutations. One of the possible explanations is that tubby and Tulp1 synergistically stimulate RPE phagocytosis. The failure of mutant tubby or Tulp1 to stimulate phagocytosis in synergy may be responsible for the lack of their functional compensation, leading to autosomal recessive retinal degeneration with mutation in either gene. However, the caveat is that these data and our previous studies [8, 11] are sufficient only to support tubby and Tulp1 as RPE ligands, but not enough to support a claim that they are essential ligands to prevent retinal degeneration. Moreover, possible accumulation of unphagocytosed vesicles in POS which is characteristic of MerTK mutation in RCS rats [13] is not observed in Tubby mice and Tulp1$^{-/-}$ mice during retinal degeneration [5, 14, 15]. Similarly, ablation of other known MerTK ligand Gas6 results in minimal defect in phagocytosis and retinal homeostasis [16], possibly due to functional compensation by other MerTK ligand like protein S [17]. Hence, the lack of accumulation of unphagocytosed POS debris in Tubby mice or Tulp1$^{-/-}$ mice could be due to functional compensation by other MerTK ligands. A body of evidence, including previously described intracellular functions of tubby and Tulp1, 16 new tubby-binding proteins identified by our ORF phage display [10] and 4 distinct clinical manifestations of retinal degeneration associated with 23 different hTulp1 mutations [3], suggest that tubby and Tulp1 are proteins with diverse functions. Stimulation of RPE phagocytosis is only one of their important functions. Their critical role as eat-me signals in retinal homeostasis is yet to be delineated. It is possible that the interaction of tubby and Tulp1 may also play important roles in their cytoplasmic and nuclear functions.

**Acknowledgments** This study was supported by NIH 1K99EY020865/4R00EY020865 grant to NBC.

## References


1. Carroll K, Gomez C, Shapiro L (2004) Tubby proteins: the plot thickens. Nat Rev Mol Cell Biol 5:55–63
2. Ikeda A, Nishina PM, Naggert JK (2002) The tubby-like proteins, a family with roles in neuronal development and function. J Cell Sci 115:9–14
3. Abbasi AH, Garzozi HJ, Ben-Yosef T (2008) A novel splice-site mutation of TULP1 underlies severe early-onset retinitis pigmentosa in a consanguineous Israeli Muslim Arab family. Mol Vis 14:675–682
4. Xi Q, Pauer GJ, Ball SL, Rayborn M, Hollyfield JG, Peachey NS, Crabb JW, Hagstrom SA (2007) Interaction between the photoreceptor-specific tubby-like protein 1 and the neuronal-specific GTPase dynamin-1. Invest Ophthalmol Vis Sci 48:2837–2844
5. Hagstrom SA, Duyao M, North MA, Li T (1999) Retinal degeneration in tulp1−/− mice: vesicular accumulation in the interphotoreceptor matrix. Invest Ophthalmol Vis Sci 40:2795–2802
6. Santagata S, Boggon TJ, Baird CL, Gomez CA, Zhao J, Shan WS, Myszka DG, Shapiro L (2001) G-protein signaling through tubby proteins. Science 292:2041–2050
7. Caberoy NB, Li W (2009) Unconventional secretion of tubby and tubby-like protein 1. FEBS Lett 583:3057–3062
8. Caberoy NB, Zhou Y, Li W (2010) Tubby and tubby-like protein 1 are new ligands for MerTK. EMBO J 29:3898–3910
9. Chen J, Huber BT, Grand RJ, Li W (2001) Recombinant adenovirus coexpressing covalent peptide/MHC class II complex and B7-1: in vitro and in vivo activation of myelin basic protein-specific T cells. J Immunol 167:1297–1305
10. Caberoy NB, Zhou Y, Jiang X, Alvarado G, Li W (2010) Efficient identification of tubby-binding proteins by an improved system of T7 phage display. J Mol Recognit 23:74–83
11. Caberoy NB, Maiguel D, Kim Y, Li W (2010) Identification of tubby and tubby-like protein 1 as eat-me signal by phage display. Exp Cell Res 316:245–257
12. D'Cruz PM, Yasumura D, Weir J, Matthes MT, Abderrahim H, LaVail MM, Vollrath D (2000) Mutation of the receptor tyrosine kinase gene Mertk in the retinal dystrophic RCS rat. Hum Mol Genet 9:645–651
13. Bok D, Hall MO (1971) The role of the pigment epithelium in the etiology of inherited retinal dystrophy in the rat. J Cell Biol 49:664–682
14. Ikeda S, Shiva N, Ikeda A, Smith RS, Nusinowitz S, Yan G, Lin TR, Chu S, Heckenlively JR, North MA, Naggert JK, Nishina PM, Duyao MP (2000) Retinal degeneration but not obesity is observed in null mutants of the tubby-like protein 1 gene. Hum Mol Genet 9:155–163
15. Ohlemiller KK, Hughes RM, Lett JM, Ogilvie JM, Speck JD, Wright JS, Faddis BT (1997) Progression of cochlear and retinal degeneration in the tubby (rd5) mouse. Audiol Neurootol 2:175–185
16. Hall MO, Obin MS, Heeb MJ, Burgess BL, Abrams TA (2005) Both protein S and Gas6 stimulate outer segment phagocytosis by cultured rat retinal pigment epithelial cells. Exp Eye Res 81:581–591
17. Ravichandran KS, Lorenz U (2007) Engulfment of apoptotic cells: signals for a good meal. Nat Rev Immunol 7:964–974

# Chapter 65
# Interaction of Tubby-Like Protein-1 (Tulp1) and Microtubule-Associated Protein (MAP) 1A and MAP1B in the Mouse Retina

**Gregory H. Grossman, Craig D. Beight, Lindsey A. Ebke, Gayle J. T. Pauer and Stephanie A. Hagstrom**

**Abstract** Tubby-like protein-1 (Tulp1) is a photoreceptor-specific protein involved in the transport of specific proteins from the inner segment (IS) to the outer segment (OS) in photoreceptor cells. Mutations in the human *TULP1* gene cause an early onset form of retinitis pigmentosa. Our previous work has shown an association between *Tulp1* and the microtubule-associated protein, MAP1B. An allele of *Mtap1a,* which encodes the MAP1A protein, significantly delays photoreceptor degeneration in Tulp1 mutant mice. MAP1 proteins are important in stabilizing microtubules in neuronal cells, but their role in photoreceptors remains obscure. To investigate the relationship between Tulp1 and MAP1 proteins, we performed western blots, immunoprecipitations (IP), immunohistochemistry and proximity ligand assays (PLA) in wild-type and *tulp1−/−* mouse retinas. Our IP experiments provide evidence that Tulp1 and MAP1B interact while PLA experiments localize their interaction to the outer nuclear layer and IS of photoreceptors. Although MAP1A and MAP1B protein levels are not affected in the *tulp1−/−* retina, they are no longer localized to the OS of photoreceptors. This may be the cause for disorganized OSs in *tulp1−/−* mice, and indicate that their transport to the OS is Tulp1-dependent.

S. A. Hagstrom (✉) G. H. Grossman · C. D. Beight · L. A. Ebke · G. J. T. Pauer
Department of Ophthalmic Research, Cole Eye Institute,
Cleveland Clinic, Cleveland, OH, USA
e-mail: hagstrs@ccf.org

G. H. Grossman
e-mail: grossmg@ccf.org

C. D. Beight
e-mail: beightc@ccf.org

L. A. Ebke
e-mail: ebkel@ccf.org

G. J. T. Pauer
e-mail: pauerg@ccf.org

S. A. Hagstrom
Department of Ophthalmology, Cleveland Clinic Lerner College of Medicine
of Case Western Reserve University, Cleveland, OH 44195, USA

J. D. Ash et al. (eds.), *Retinal Degenerative Diseases,* Advances in Experimental Medicine and Biology 801, DOI 10.1007/978-1-4614-3209-8_65,

**Keywords** Photoreceptor · Retinal degeneration · MAP1 · Tulp1 · Mouse mutant · Microtubule · Cilium · Transport · Trafficking

**Abbreviations**

| | |
|---|---|
| $BS^3$ | Bis[sulfosuccinimidyl] suberate |
| CC | Connecting cilium |
| GCL | Ganglion cell layer |
| IFT | Intraflagellar transport |
| IHC | Immunohistochemistry |
| INL | Inner nuclear layer |
| IP | Immunoprecipitations |
| IPL | Inner plexiform layer |
| IS | Inner segment |
| MAP | Microtubule-associated protein |
| MW | Molecular weight |
| ONL | Outer nuclear layer |
| OPL | Outer plexiform layer |
| OS | Outer segment |
| P | Postnatal day |
| PFA | Paraformaldehyde |
| PLA | Proximity ligand assays |
| RP1 | Retinitis pigmentosa 1 protein |
| SDS | Sodium dodecyl sulfate |
| Tulp1 | Tubby-like protein-1 |
| WB | Western blot |

## 65.1 Introduction

Mutations in microtubule-associated proteins (MAPs) have been shown to underlie several neurodegenerative diseases [1, 2], including a common form of retinitis pigmentosa [3]. MAP1A and MAP1B are expressed primarily in neurons where they function in stabilizing microtubules [4]. MAP1A and MAP1B are distantly related and developmentally distinct, with MAP1A being present in adult neurons and MAP1B being largely restricted to developing neurons [5].

Tulp1 is a photoreceptor-specific protein that is localized to the connecting cilium (CC), inner segment (IS), cell body and synaptic terminal [6]. Tulp1 exhibits a genetic interaction with *Mtap1a*, whereby an allele of *Mtap1a* significantly attenuates photoreceptor degeneration in Tulp1 mutant mice [7]. Evidence pointing to a common pathway of these two proteins is their interaction with cytoskeletal elements. MAP1A and Tulp1 have been shown to bind both tubulin and actin, linking the microtubule networks to the microfilament cytoskeleton [8]. MAP1B has also been identified as a Tulp1 interacting partner [9]. Furthermore, both Tulp1 and

**Table 65.1** Primary antibodies used in the present study

| Antigen | Technique | Source | Host |
|---|---|---|---|
| MAP1A | IHC 1:200, WB 1:500 | Santa Cruz; N-18 sc-8969 | Goat polyclonal |
| MAP1B | IHC 1:200 and PLA 1:200 | Santa Cruz; N-19 sc-8970 | Goat polyclonal |
| MAP1B | WB 1:500 and IP 2–5 ug/mg lysate | Novus Biologicals; NB100-68256 | Rabbit polyclonal |
| Tulp1 | WB 1:1000 and PLA 1:200 | Stephanie Hagstrom; mTulp1 | Rabbit polyclonal |
| Peripherin/RDS | IHC 1:500 | Andrew Goldberg; pAbMPCT | Rabbit polyclonal |

MAPs have been implicated in protein transport [6, 10–12]. Thus, Tulp1 and MAP1 proteins may be involved in a functional complex in the mammalian photoreceptor. To investigate this association, we performed colocalization and interaction experiments.

## 65.2 Materials and Methods

### *65.2.1 Animals*

*Tulp1−/−* mice were generated and genotyped as previously described [6]. All experiments using mice were approved by the Institutional Animal Care and Use Committee of the Cleveland Clinic and were conducted in compliance with the ARVO Statement for the Use of Animals in Ophthalmic and Visual Research.

### *65.2.2 Western Blot Analysis*

Western blot (WB) analysis was performed as previously described [13]. Primary antibodies and conditions are listed in Table 65.1.

### *65.2.3 Immunoprecipitations*

Immunoprecipitation (IP) was performed per the manufacturer's instructions (Dynabeads Protein A, Invitrogen). Postnatal (P) 16 wild-type (wt) mouse retinas were homogenized in lysis buffer supplemented with protease inhibitors (Fisher Scientific). The suspension was centrifuged at 9,000 rpm for 15 min, and the supernatant removed. Retinal lysate protein concentration (3.8 μg/μl) was determined by BCA protein assay (Thermo Scientific). 10 μg of MAP1B antibody or non-specific rab-

bit IgG (Southern Biotech) serving as a negative control was used. Prior to this, the antibody was crosslinked to the magnetic beads using $BS^3$ (Thermo Scientific) for 30 min at rt. Binding of the lysate (500 µl per IP) to the bead-bound antibody occurred overnight at 4 °C. After three washes with buffer, proteins were eluted with 20 µl of SDS sample buffer. IP products were fractionated on SDS-PAGE gels followed by WB to detect proteins of interest.

### *65.2.4 Immunohistochemistry*

Immunohistochemistry (IHC) was conducted as previously reported [11]. Six sections from five different mice were examined for each antibody. Table 65.1 lists the antibodies and conditions used in IHC experiments.

### *65.2.5 Proximity Ligand Assays*

Proximity ligand assays (PLA) were performed on fresh-frozen 10 µm retinal sections.

PLAs were accomplished using a Duolink In Situ Kit (Olink Bioscience) according to the manufacturer's directions. Briefly, 10 µg of mTulp1 antibody and 4 µg of MAP1B antibody were conjugated to Plus and Minus PLA oligonucleotides arms respectively using Duolink Probemaker kits. After blocking, 40 µl of conjugated antibody solution was applied to each section, and the slides were placed in a humidity chamber at 4 °C overnight. Ligation-ligase solution was then added to each section for 30 min at 37 °C followed by the amplification solution containing nucleotides, polymerase, and fluorescently labeled oligonucleotides. After several washes, the slides were coverslipped with Vectashield with DAPI. The slides were then imaged as described for IHC.

## 65.3 Results

### *65.3.1 MAP1A and MAP1B are Expressed in the Mouse Retina*

MAP1 protein expression was analyzed in mouse wt and *tulp1*−/− retinas by WB at P13 and P16. P13 was chosen as a developmental age in which the OSs have formed and are beginning to lengthen [14]. P16 was chosen as a fully developed age but prior to photoreceptor degeneration in the *tulp1*−/− retina [6, 14]. In (Fig. 65.1a) MAP1A immunoreactivity is detected in the developing (P13) and young adult (P16) retina and brain at its known molecular weight (MW) of ~350 kDa. As ex-

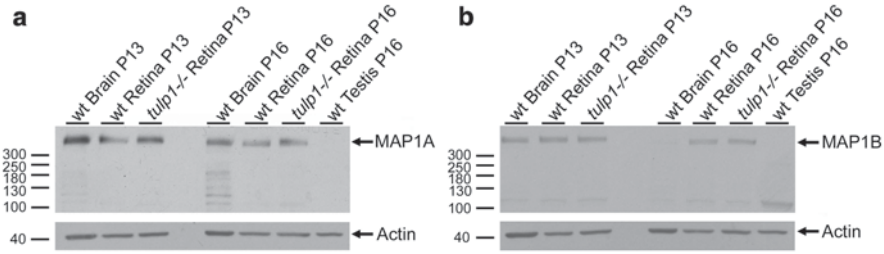


**Fig. 65.1** WB analysis of *MAP1A* and *MAP1B* expression. **a** *MAP1A* is detected in P13 and P16 brain and retina of wt and *tulp1−/−* mice, but not in testis. **b** *MAP1B* is detected in the wt and *tulp1−/−* brain and retina at P13, and wt and *tulp1−/−* retina at P16. It is absent from wt brain at P16. Neither *MAP1A* nor *MAP1B* appear to exhibit an alteration in protein levels in the *tulp1−/−* retina. *Actin* is shown in *lower* blots as a control for loading equivalency

pected, MAP1A is not detected in the testis [15]. Expression of MAP1A does not appear to be affected in the *tulp1−/−* retina. Figure 65.1b shows that MAP1B is expressed in the developing (P13) and young adult (P16) retina, as well as the P13 brain at its known molecular weight of ~350 kDa. However, it is not detected in the young adult (P16) brain, in agreement with previous studies [16]. MAP1B expression does not appear to be affected in the *tulp1−/−* retina. Probing with antibodies against actin supports equal protein loading across lanes.

### *65.3.2 MAP1A and MAP1B are Mislocalized in the tulp1−/− Retina*

MAP1 protein localization was analyzed in mouse wt and *tulp1−/−* retinas by IHC at P16.In the wt retina, MAP1A staining is present in the inner plexiform layer (IPL), the ganglion cell layer (GCL) and in the OS of photoreceptors (Fig. 65.2a). Peripherin/RDS was chosen as an OS marker because its transport to the OS is not Tulp1-dependent [11]. In the *tulp1−/−* retina, MAP1A exhibits a severe mislocalization (Fig. 65.2b). In the photoreceptor, it is no longer restricted to the OS but is mislocalized throughout all compartments. MAP1B is also present in the IPL and GCL; however, in contrast to MAP1A, it is localized throughout the photoreceptor layer (Fig. 65.2c). In the *tulp1−/−* retina, MAP1B is no longer present in the OS (Fig. 65.2d). These results indicate that both MAP1 proteins are absent from photoreceptor OSs in the *tulp1−/−* retina.

### *65.3.3 MAP1B and Tulp1 are Binding Partners*

IPs using MAP1B antibodies were conducted and Fig. 65.3a shows a representative result. WB analysis of the IP experimental samples probed with Tulp1 antibodies

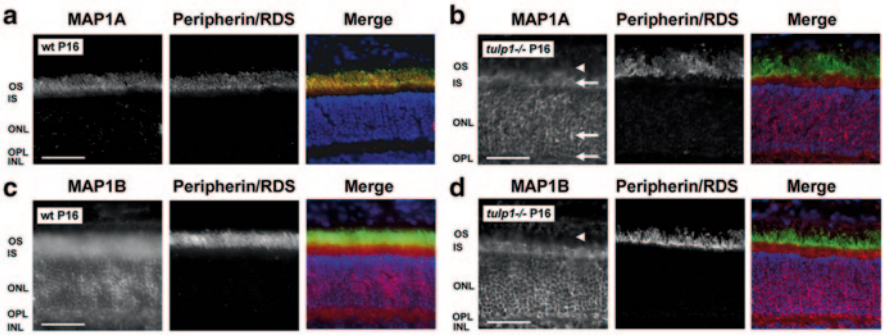


**Fig. 65.2** Immunofluorescent images of MAP1A and MAP1B staining in P16 mouse retinas. **a** In the wt retina, MAP1A colocalizes with the OS-specific protein Peripherin/RDS (merge column: nuclei in *blue*, MAPs in *red* and Peripherin/RDS in *green*). **b** In the *tulp1-/-* retina, MAP1A is no longer present in the OS (*arrowhead*, 1st column), and is mislocalized throughout the photoreceptor compartment (*arrows*). **c** In the wt retina, MAP1B is present throughout all photoreceptor compartments. **d** In the *tulp1−/−* retina, MAP1B staining is no longer localized to the OS (*arrowhead*, 1st column). Scale bars = 50 μm

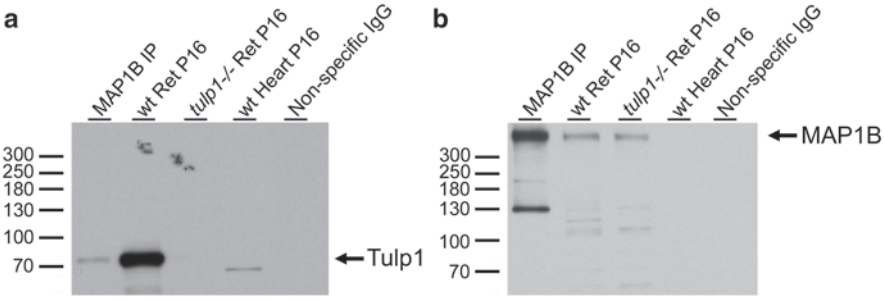


**Fig. 65.3** IP of retinal lysate with MAP1B antibodies. **a** WB of the MAP1B IP experimental samples probed with Tulp1 antibodies. In the IP product lane, a band corresponding to Tulp1 is detected. A corresponding band is seen in the wt retinal lysate but not in the *tulp1−/−* retinal lysate, heart lysate or non-specific IgG IP lanes. **b** WB of the *MAP1B IP* experimental samples probed with MAP1B antibodies. In the IP product, wt retinal lysate and *tulp1−/−* retinal lysate lanes, a band corresponding to MAP1B is detected. No bands are seen in the heart or non-specific IgG IP sample lanes

shows a band corresponding to the correct MW of Tulp1 (~78 kDa) is detected in the MAP1B IP product lane. A corresponding band is also detected in the wt retinal lysate lane but not in the *tulp1−/−* retinal lysate, heart lysate, or non-specific IgG IP lanes. To verify the efficacy of the MAP1B IP, the blot was probed with MAP1B antibodies (Fig. 65.3b). A band corresponding to MAP1B is detected in the wt and *tulp1-/-* retinal lysate lanes, and the IP product lane. No bands were detected in the heart lysate or non-specific IgG IP lanes.

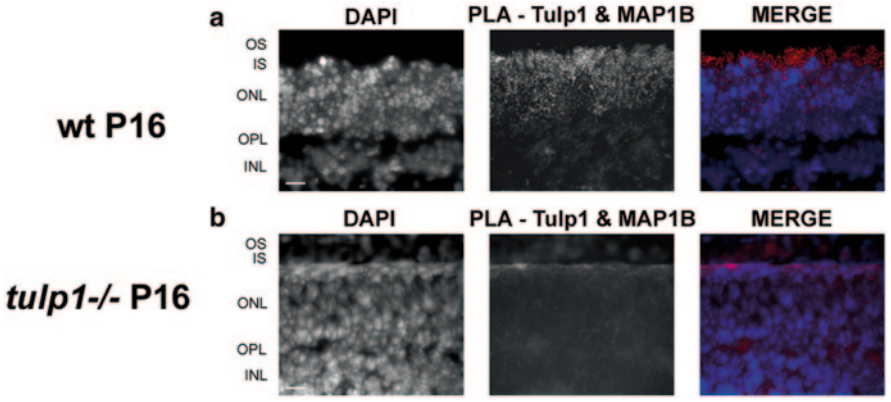


**Fig. 65.4** *PLA* analysis in mouse retinal sections. (**a**) In the wt retina analyzed with MAP1B and Tulp1 antibodies, positive signals (*white dots*) are found throughout the ONL and near the apical region of the IS, indicating the detection of Tulp1-MAP1B complexes. In the wt retina analyzed with only Tulp1 antibodies, the wt retina analyzed with only MAP1B antibodies, or the *tulp1−/−* retina analyzed with both antibodies (**b**), positive signals are not detected. Scale bars = 20 μm

### *65.3.4 MAP1B and Tulp1 Endogenously Interact*

PLA allows for the detection of in situ protein interactions. A fluorescent signal is generated only when the two primary antibodies, and thus their target proteins, are in close proximity. Figure 65.4 shows the result of a representative PLA experiment examining the endogenous interaction of MAP1B and Tulp1. In the wt retina, positive signals are seen throughout the outer nuclear layer (ONL) and the apical IS when using both Tulp1 and MAP1B antibodies (Fig. 65.4a). Signals are not detected when analyzing only Tulp1 antibodies, only MAP1B antibodies, or in the *tulp1−/−* retina when using both Tulp1 and MAP1B antibodies (Fig. 65.4b).

## 65.4 Discussion

We confirm that the expression of MAP1B is retained in the adult retina, possibly playing a role in photoreceptor OS and axonal plasticity [17]. Tulp1 colocalizes with MAP1B in the IS, and was identified as a MAP1B interacting protein by IP. This interaction was verified in situ by PLA. In the *tulp1−/−* retina, MAP1A and MAP1B are no longer localized to the OS. This may indicate that MAP1 protein transport is Tulp1-dependent, as determined for several other OS-resident proteins [11]. Since MAP1A and MAP1B stabilize microtubules, their absence in the OS of *tulp1−/−* mice may destabilize microtubule networks in the axoneme of the photoreceptor, and thus be the underlying cause for the disorganized OSs and ultimately

photoreceptor cell death in these mice. Further experiments are needed to support this hypothesis and test whether Tulp1 is a retinal-specific MAP.

**Acknowledgments** This study was supported by NIH Grant EY15638 (SAH), a Research to Prevent Blindness Center Grant and a Knights Templar Pediatric Ophthalmology Career-Starter Research Grant (GHG).

## References

1. Higuchi M, Lee VM, Trojanowski JQ (2002) Tau and axonopathy in neurodegenerative disorders. Neuromolecular Med 2(2):131–150
2. Puls I, Jonnakuty C, LaMonte BH, Holzbaur EL, Tokito M, Mann E et al (2003) Mutant dynactin in motor neuron disease. Nat Genet 33(4):455–456
3. Liu Q, Zuo J, Pierce EA (2004) The retinitis pigmentosa 1 protein is a photoreceptor microtubule-associated protein. J Neurosci 24(29):6427–6436
4. Halpain S, Dehmelt L (2006) The MAP1 family of microtubule-associated proteins. Genome Biol 7(6):224
5. Schoenfeld TA, McKerracher L, Obar R, Vallee RB (1989) MAP 1A and MAP 1B are structurally related microtubule associated proteins with distinct developmental patterns in the CNS. J Neurosci 9(5):1712–1730
6. Hagstrom SA, Duyao M, North MA, Li T (1999) Retinal degeneration in tulp1-/- mice: vesicular accumulation in the interphotoreceptor matrix. Invest Ophthalmol Vis Sci 40(12): 2795–2802
7. Maddox DM, Ikeda S, Ikeda A, Zhang W, Krebs MP, Nishina PM et al (2012) An allele of microtubule-associated protein 1A (Mtap1a) reduces photoreceptor degeneration in Tulp1 and Tub mutant mice. Invest Ophthalmol Vis Sci 53(3):1663–1669
8. Noiges R, Eichinger R, Kutschera W, Fischer I, Nemeth Z, Wiche G et al (2002) Microtubule-associated protein 1A (MAP1A) and MAP1B: light chains determine distinct functional properties. J Neurosci 22(6):2106–2114
9. Xi Q, Pauer GJ, West KA, Crabb JW, Hagstrom SA (2003) Retinal degeneration caused by mutations in TULP1. Adv Exp Med Biol 533:303–308
10. Dixit R, Ross JL, Goldman YE, Holzbaur EL (2008) Differential regulation of dynein and kinesin motor proteins by tau. Science 319(5866):1086–1089
11. Grossman GH, Watson RF, Pauer GJ, Bollinger K, Hagstrom SA (2011) Immunocytochemical evidence of Tulp1-dependent outer segment protein transport pathways in photoreceptor cells. Exp Eye Res 93(5):658–668
12. Hagstrom SA, Adamian M, Scimeca M, Pawlyk BS, Yue G, Li T (2001) A role for the Tubby-like protein 1 in rhodopsin transport. Invest Ophthalmol Vis Sci 42(9):1955–1962
13. Xi Q, Pauer GJ, Ball SL, Rayborn M, Hollyfield JG, Peachey NS et al (2007) Interaction between the photoreceptor-specific tubby-like protein 1 and the neuronal-specific GTPase dynamin-1. Invest Ophthalmol Vis Sci 48(6):2837–2844
14. Zhang X, Serb JM, Greenlee MH (2011) Mouse retinal development: a dark horse model for systems biology research. Bioinform Biol Insights 5:99–113
15. Neely MD, Boekelheide K (1988) Sertoli cell processes have axoplasmic features: an ordered microtubule distribution and an abundant high molecular weight microtubule-associated protein (cytoplasmic dynein). J Cell Biol 107(5):1767–1776
16. Tucker RP, Matus AI (1988) Microtubule-associated proteins characteristic of embryonic brain are found in the adult mammalian retina. Dev Biol 130(2):423–434
17. Pattnaik B, Jellali A, Sahel J, Dreyfus H, Picaud S (2000) GABAC receptors are localized with microtubule-associated protein 1B in mammalian cone photoreceptors. J Neurosci 20(18):6789–6796

# Chapter 66
# CEP290 and the Primary Cilium

**Theodore G. Drivas and Jean Bennett**

**Abstract** The protein CEP290 has recently emerged as a major player in the biology of the cilium and as a causative protein in a number of human syndromic diseases, most of which are associated with the devastating blinding disease Leber congenital amaurosis. (Coppieters et al., Hum Mutat 31, 2010, 1097–1108) CEP290 is known to be an important component of the primary cilium, localizing to the Y-links of the ciliary transition zone and having a role in the regulation of transport in and out of the ciliary compartment (Craige et al., J Cell Biol 190, 2010, 927–940). While many mutations in *CEP290* have been identified in human patients, how these mutations result in the spectrum of human disease attributed to the protein remain unknown. As we begin to learn more about the normal role of CEP290, it is likely that we will begin to shed light on how these mutations result in the various CEP290 disease phenotypes. Here we discuss many of these diverse aspects of CEP290 biology and pathology in an attempt to link what we know about the molecular mechanisms of CEP290 function with what we know about CEP290-asociated disease.

**Keywords** CEP290 · Primary cilium · Ciliopathy · Intraflagellar transport · Leber congenital amaurosis

J. Bennett (✉)
Kirby Center for Molecular Ophthalmology, University of Pennsylvania Perelman School of Medicine, 305 Stellar Chance, 422 Curie Boulevard, Philadelphia, PA 19104, USA
e-mail: jebennet@mail.med.upenn.edu

T. G. Drivas
Cell and Molecular Biology Department, 404 Anatomy and Chemistry, University of Pennsylvania Perelman School of Medicine, 3620 Hamilton Walk, Philadelphia, PA 19104, USA
e-mail: tdrivas@mail.med.upenn.edu

J. D. Ash et al. (eds.), *Retinal Degenerative Diseases,* Advances in Experimental Medicine and Biology 801, DOI 10.1007/978-1-4614-3209-8_66,

## 66.1 Introduction

Upon exit from the cell cycle and entry into $G_0$, the mammalian cell sequesters its centrosome in a structure known as the primary cilium [3, 4]. Until recently, the functional role of the primary cilium, a single, antenna-like projection of the apical membrane that is found in nearly every human cell type, had not been well studied or appreciated. It is clear now that this organelle has important sensory roles affecting multiple cellular processes, with a large proportion of G-protein coupled receptors, ion channels, and downstream effector molecules sequestered and confined to its membrane and lumen [3]. Additionally, it has recently been shown that defects in primary cilium formation and function are responsible for a variety of human diseases and developmental disorders, collectively termed ciliopathies [5].

The cilium is formed as a membrane-bound microtubule extension, known as the ciliary axoneme, protruding from the distal end of the mother centriole at the apical surface of the cell. It is a biochemically distinct organelle, and, in fact, it is thought that all proteins within the ciliary compartment must be specifically and actively transported there through a highly regulated process known as intraflagellar transport (IFT) [4]. This process has recently been shown to require carrier proteins, localization signals, molecular switches, and microtubule based motors, and shares certain similarities with the machinery of the nuclear pore complex and nuclear transport. The tight regulation of IFT not only ensures the efficient import of cilium-destined cargos into the cilium, but also serves to prevent the passive diffusion of non-ciliary proteins into the ciliary compartment [4].

The barrier between the cilium and the cytosol is maintained at the transition zone of the cilium, the region of the organelle just proximal to the axoneme, in plane with the cortex of the cell. Here, the dense proteinaceous Y-links and ciliary necklace have been shown to closely couple the ciliary membrane to the microtubule axoneme, likely presenting a barrier to the passive diffusion of molecules in and out of the ciliary compartment, and potentially forming the scaffold for a pore-like structure for the selective transport of cilium-destined cargos [2, 5].

Elegant work in the *Chlamydomonas* model system has shown that the ciliary protein CEP290 is a critical component of these Y-link junctions [2]. Additionally, numerous studies have demonstrated that CEP290's function is critical for IFT—in *CEP290* knockdown experiments, many proteins that would normally localize to the cilium fail to do so, and cilium formation is disrupted or absent [5, 6]. While the precise role that CEP290 plays in IFT and cilium formation remains unknown, we are beginning to discover more and more, both about CEP290's function and about how dysfunction of the protein can lead to disease. In this review, we discuss what is known about CEP290 on a molecular level, the diversity of CEP290 mutations discovered in patients, and how deficiencies in CEP290 can manifest as a whole spectrum of syndromic disease.

## 66.2 CEP290 Structure and Function

To begin to understand how mutations in *CEP290* can cause disease, it is best to try to understand exactly what the protein does. At first glance, this seems a daunting task, as the protein itself is very large, composed of nearly 2500 amino acids and with a molecular weight of 290 kiloDaltons. The protein can, however, be divided into a number of regions defined by various putative protein motifs. Dividing CEP290 this way, it becomes clear that, while nearly the entire protein is predicted to fold into coiled-coils, a number of interesting putative domains are scattered throughout the protein's length [7]. These domains include three tropomyosin homology domains, a structural maintenance of chromosomes homology domain, a large hook domain, an even larger myosin-tail homology domain, numerous kinase-inducible domains, and a potential bipartite nuclear localization signal [7].

The presence of these domains seems to implicate CEP290 in multiple diverse activities throughout different compartments of the cell. Accordingly, CEP290 appears to localize to at least two different cellular locations. Primarily, CEP290 is thought of as a centriolar/ciliary protein, and localizes to the distal ends of centrioles and to the cloud of pericentriolar material that surrounds the centrosome [6, 8]. When the cell initiates its program of ciliogenesis, the centrosome migrates to the apical surface of the cell and, through the degradation of the CEP290 inhibitory protein CP110 at only the distal end of the mother centriole, CEP290 is activated, resulting in the growth of the ciliary axoneme and the formation of the primary cilium [8].

While much of the work surrounding CEP290 focuses on its role at the cilium, a number of groups have presented data showing that CEP290 is also at least partially localized to the nucleus and seems to activate the transcription factor ATF4 [9]. Exactly what CEP290 is doing in the nucleus and how its nuclear functions may affect human disease remain unknown.

While there are clearly many gaps to fill in, and likely many functional domains left to be identified within CEP290, we can say with certainty that CEP290 is essential to the regular function and formation of the primary cilium. A number of groups have looked at the effects of decreased CEP290 levels in both artificial and naturally occurring models. The shRNA-mediated knockdown of CEP290 resulted in a dramatic decrease in the percent of cells that were able to form primary cilia [8]. These same cells also exhibited marked mislocalization of normal ciliary proteins. The same protein mislocalization was seen in the retinas of rd16 mice, an animal model characterized by an in-frame deletion of 298 amino acids of Cep290 [6]. In these mice, a number of photoreceptor-specific proteins that are normally transported, by IFT, through the cilium and into the photoreceptor outer segment instead accumulated in the inner segment of the cell. All these data indicate that CEP290 plays an indispensible role in cilium formation and maintenance and trafficking.

## 66.3 CEP290 Interacting Partners

CEP290 has been shown to interact with a large number of proteins and has been identified as a member of many protein complexes. Many of these interactions are with other primary cilium proteins—it has been shown that CEP290 interacts with Nephrocystin 5 (NPHP5) and can directly bind to the proteins Coiled-coil and C2 domain-containing 2a (CC2DA) [1] and RPGR-interacting protein 1-like (RPGRIP1 L), [10] all of which are critical for cilium function. RPGRIP in turn is capable of binding the protein Retinitis pigmentosa GTPase regulator (RPGR), [10] which recruits the small GTPase Rab8, [11] and all three of these proteins have been identified in CEP290 co-immunoprecipitation (IP) experiments. In fact, CEP290 knockdown results in the mislocalization of these proteins, implying that CEP290 is the sole protein responsible for their recruitment to the cilium. CEP290 can also bind to PCM1, a protein component of the pericentriolar material which surrounds the centrioles [12]. In the absence of CEP290, PCM1 fails to localize correctly, implying that CEP290 has important functionality at the centriole beyond being a mediator of primary cilium formation.

Another interesting interacting partner of CEP290 is the protein CP110. CP110 binds to the N-terminal region of CEP290 and inhibits CEP290's activity [8]. Overexpression of *CP110* results in fewer cells capable of forming primary cilia, while knockdown of *CP110* results in longer cilia and an increase in the percent of ciliated cells [8].

One of CEP290's most interesting interacting partners, however, may be itself. It has been shown that the C-terminus of CEP290 is cable of binding itself through homotypic interactions [13]. Similarly, the very N-terminus of the protein can do the same [13]. Most interestingly, however, it has also been shown that the N- and C- termini are also capable of binding each other [13]. This presents a range of possibilities for CEP290 tertiary and quaternary structure, with the potential for CEP290 to dimerize (in either parallel or antiparelel conformations), form long filaments, (through head-to-head, tail-to-tail, or head-to-tail interactions), and potentially for the molecule to fold back over on itself, with its N-terminus bound to its C-terminus.

## 66.4 CEP290 and Disease

Dysfunction or disruption of IFT can lead to a variety of different syndromic human diseases, all of which are characterized by the dysfunction or absence of primary cilia. These ciliopathies are diverse in both phenotype and etiology, but specific genes have been implicated as having causative roles in multiple cilium-associated syndromes. *CEP290* is one of these genes. Mutations in *CEP290* have been described in up to 25 % of patients with the devastating blinding disease Leber's Congenital Amaurosis, in which dysfunction of the connecting cilium of the rod photoreceptors leads to cellular dysfunction and eventual death [14]. LCA is, however,

the least dramatic of the *CEP290* phenotypes. Mutations in *CEP290* are also accountable for cases of nephronophthisis, the most common genetic cause of childhood kidney failure, and Senior Løken syndrome, characterized by both renal and retinal dysfunction [1]. *CEP290* mutations are also accountable for many cases of Joubert syndrome. In mild cases of Joubert syndrome, pathology is confined to the cerebellum and brain stem, while more severe cases are characterized by polydactyly, mental retardation, and renal, retinal, and hepatic pathology [1]. Bardet-Biedl syndrome, also resulting from CEP290 deficiencies, is characterized by a number of seemingly unrelated phenotypes including retinal degeneration, hypogonadism, obesity, polydactyly, renal dysfunction, and mental retardation [1]. Finally, CEP290 deficiencies, in their most severe form, can manifest themselves as the lethal disease known as Meckel-Gruber syndrome. This disorder, characterized by numerous pathological findings, is uniformly lethal, with death occurring in utero or shortly after birth [1].

## 66.5 *CEP290* Mutations

As is apparent from the above discussion of CEP290 disease, numerous mutations in *CEP290* have been identified in human patients. What is perhaps most striking about the mutations that have been identified is that they are, with only very few exceptions, truncating mutations, with only a handful of missense mutations identified [1]. This is surprising for a protein like CEP290, which is so highly conserved across species [7] and which one would think not amenable to point mutations and alterations in the coding sequence. We still cannot reconcile these two observations, but further research into the protein's function and functional domains may help us to better understand this phenomenon.

The most common *CEP290* mutation is a point mutation in intron 26 [1]. This particular mutation is interesting in that it creates a novel splice site, resulting in the inclusion of a cryptic exon, encoding a stop codon, between exons 26 and 27 [1]. Till date, this mutation has only been identified in LCA patients and is being extensively researched as a potential target for exon-skipping therapeutics.

Looking at all of the other identified mutations, an obvious question arises—can we correlate the location of patient mutations to patient phenotype? Surprisingly, the answer to that question is no. Till date, no group has been able to explain why particular mutations result in particular phenotypes. It stands to reason that if, as proposed, the nonsense and frame-shift mutations lead to truncated protein products with partial functionality, then the location of the truncation should correlate with the severity of the phenotype. Analyzing the known *CEP290* mutations this way has failed to yield any meaningful correlations.

There are numerous theories as to why this may be the case. One idea is that modifying alleles may be modulating the effects of *CEP290* mutations, and that our analyses are confounded by our lack of knowledge of what these modifying alleles are and how they might be interacting with CEP290. Another theory is that

the different *CEP290* phenotypes may be a result of a spectrum of CEP290 protein levels—it has recently been shown that mRNAs harboring early stop codons are subject to degradation through a process known as nonsense-mediated decay [1]. If this were the case, certain early stop and frame shift mutations may be more subject to nonsense-mediated decay than others, leading to diverse levels of CEP290 protein (either truncated or full length) that may correlate with disease phenotype. Experiments designed to test this hypothesis could yield interesting results.

## 66.6 Conclusions

As we continue to identify more patients with CEP290-based disease, we will undoubtedly continue to learn more about the correlation between *CEP290* mutations, protein function, and disease phenotype. We are already beginning to appreciate just how central and important CEP290 is to the processes of ciliogenesis and IFT. As evidenced by the spectrum of disease caused by mutations in the gene, CEP290 is critical for nearly every organ system of the body, with devastating consequences when it is deficient. Whether these deficiencies are caused by reduced protein levels, truncating mutations, modifying alleles, or some combination of these, it is clear that we have a lot more to learn about the gene, what it does, and how it can be manipulated to ameliorate disease.

## References

1. Coppieters F, Lefever S, Leroy BP, De Baere E (2010) CEP290, a gene with many faces: mutation overview and presentation of CEP290base. Hum Mutat 31:1097–1108
2. Craige B et al (2010) CEP290 tethers flagellar transition zone microtubules to the membrane and regulates flagellar protein content. J Cell Biol 190:927–940
3. Gerdes JM, Davis EE, Katsanis N (2009) The vertebrate primary cilium in development, homeostasis, and disease. Cell 137:32–45
4. Qin H (2012) Regulation of intraflagellar transport and ciliogenesis by small G proteins. Int Rev Cell Mol Biol 293:149–168
5. Waters AM, Beales PL (2011) Ciliopathies: an expanding disease spectrum. Pediatr Nephrol 26:1039–1056
6. Chang B et al (2006) In-frame deletion in a novel centrosomal/ciliary protein CEP290/NPHP6 perturbs its interaction with RPGR and results in early-onset retinal degeneration in the rd16 mouse. Hum Mol Genet 15:1847–1857
7. Moradi P, Davies WL, Mackay DS, Cheetham ME, Moore AT (2011) Focus on molecules: centrosomal protein 290 (CEP290). Exp Eye Res 92:316–317
8. Tsang WY et al (2008) CP110 suppresses primary cilia formation through its interaction with CEP290, a protein deficient in human ciliary disease. Dev Cell 15:187–197
9. Sayer JA et al (2006) The centrosomal protein nephrocystin-6 is mutated in Joubert syndrome and activates transcription factor ATF4. Nat Genet 38:674–681
10. Zhao Y et al (2003) The retinitis pigmentosa GTPase regulator (RPGR)- interacting protein: subserving RPGR function and participating in disk morphogenesis. Proc Natl Acad Sci USA 100:3965–3970

11. Murga-Zamalloa CA, Atkins SJ, Peranen J, Swaroop A, Khanna H (2010) Interaction of retinitis pigmentosa GTPase regulator (RPGR) with RAB8A GTPase: implications for cilia dysfunction and photoreceptor degeneration. Hum Mol Genet 19:3591–3598
12. Kim J, Krishnaswami SR, Gleeson JG (2008) CEP290 interacts with the centriolar satellite component PCM-1 and is required for Rab8 localization to the primary cilium. Hum Mol Genet 17:3796–3805
13. Schäfer T et al (2008) Genetic and physical interaction between the NPHP5 and NPHP6 gene products. Hum Mol Genet 17:3655–3662
14. Den Hollander AI et al (2006) Mutations in the CEP290 (NPHP6) gene are a frequent cause of Leber congenital amaurosis. Am J Hum Genet 79:556–561

# Chapter 67
# Usher Syndrome Protein Network Functions in the Retina and their Relation to Other Retinal Ciliopathies

**Nasrin Sorusch, Kirsten Wunderlich, Katharina Bauss, Kerstin Nagel-Wolfrum and Uwe Wolfrum**

**Abstract** The human Usher syndrome (USH) is the most frequent cause of combined hereditary deaf-blindness. USH is genetically and clinically heterogeneous: 15 chromosomal loci assigned to 3 clinical types, USH1-3. All USH1 and 2 proteins are organized into protein networks by the scaffold proteins harmonin (USH1C), whirlin (USH2D) and SANS (USH1G). This has contributed essentially to our current understanding of the USH protein function in the eye and the ear and explains why defects in proteins of different families cause very similar phenotypes. Ongoing in depth analyses of USH protein networks in the eye indicated cytoskeletal functions as well as roles in molecular transport processes and ciliary cargo delivery in photoreceptor cells. The analysis of USH protein networks revealed molecular links of USH to other ciliopathies, including non-syndromic inner ear defects and isolated retinal dystrophies but also to kidney diseases and syndromes like the Bardet-Biedl syndrome. These findings provide emerging evidence that USH is a ciliopathy molecularly related to other ciliopathies, which opens an avenue for common therapy strategies to treat these diseases.

**Keywords** Usher syndrome · Deaf-blindness · Retinitis pigmentosa · LCA · BBS · Ciliopathy · Protein networks · Interactome · Ciliary transport

U. Wolfrum (✉) · N. Sorusch · K. Wunderlich · K. Bauss · K. N.-Wolfrum
Institute of Zoology, Dept. Cell & Matrix Biology,
Johannes Gutenberg University Mainz, Mainz, Germany
e-mail: wolfrum@uni-mainz.de

N. Sorusch
e-mail: sorusch@uni-mainz.de

K. Wunderlich
e-mail: wunderlk@uni-mainz.de

K. Bauss
e-mail: kbauss@students.uni-mainz.de

K. N.-Wolfrum
e-mail: nagelwol@uni-mainz.de

J. D. Ash et al. (eds.), *Retinal Degenerative Diseases,* Advances in Experimental Medicine and Biology 801, DOI 10.1007/978-1-4614-3209-8_67,

**List of Abbreviations**

| | |
|---|---|
| Ax | Axoneme |
| BB | Basal body |
| BBS | Bardet-Biedl syndrome |
| CC | Connecting cilium |
| Cdh 23 | Cadherin 23 |
| Cep290 | Centrosomal protein of 290 kDa |
| CP | Calycal processes |
| Gpr98 | G protein-coupled receptor 98 |
| IFT | Intraflagellar transport |
| IS | Inner segment |
| LCA | Leber congenital amaurosis |
| MKS | Meckel-Gruber syndrome |
| NPHP | Nephronophthisis |
| Nlp | Ninein-like protein |
| $Nlp^{isoB}$ | Ninein-like protein isoform B |
| OLM | Outer limiting membrane |
| OS | Outer segment |
| P | Perikaryon |
| PMC | Periciliary membrane complex |
| Pcdh15 | Protocadherin 15 |
| RP | Retinitis pigmentosa |
| RPE | Retinal pigment epithelium |
| RPGR | RP GTPase regulator |
| RPGRIP1 | RPGR interacting protein 1 |
| S | Synapse |
| SANS | Scaffold protein containg ankyrin repeats and SAM domain |
| SLS | Senior-Loken syndrome |
| Tz | Transition zone |
| USH | Human Usher syndrome |
| VLGR1 | Very large G-protein coupled receptor protein 1 |

## 67.1 Introduction to the Human Usher Syndrome

The human Usher syndrome (USH), with a prevalence of ~1/6.000, is categorized as rare disease but is also the most frequent cause of combined hereditary deaf-blindness [1, 2]. It is characterized by hearing impairment, vestibular dysfunction and retinal degeneration, *Retinitis pigmentosa* (RP). The three clinical subtypes (USH1-3) differ in severity, age of onset, and progression of symptoms. USH is genetically heterogeneous; 10 identified USH genes encode proteins from various families [2, 3]: myosin VIIa (USH1B) is a molecular motor protein; harmonin (USH1C), SANS (scaffold protein containing ankyrin repeats and SAM

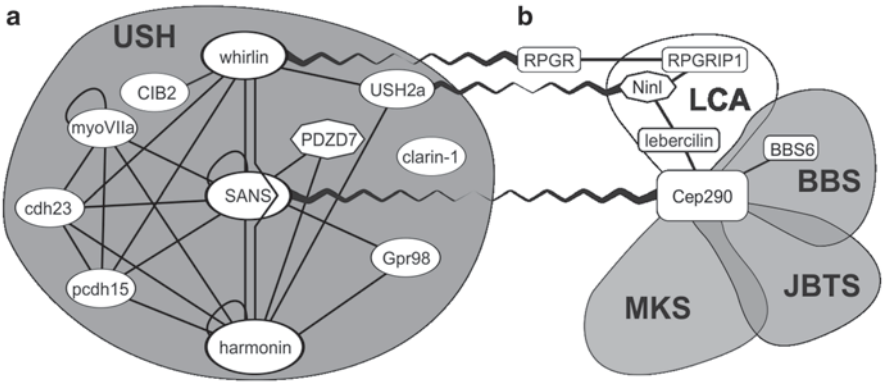


**Fig. 67.1** The USH protein interactome (*solid lines*) (**a**) and links to molecules of other ciliopathies (*zig-zag lines*) (**b**)

domain/USH1G), and whirlin (USH2D) are scaffold proteins; cadherin 23 (cdh23/USH1D) and protocadherin 15 (pcdh15/USH1F) are adhesion proteins; the recently identified CIB2 (USH1J) is a calcium- and integrin-binding protein; the G protein-coupled receptor 98 (Gpr98 = VLGR1b, very large G protein coupled receptor/USH2C) is the largest known adhesion GPCR and like USH2a ("usherin") a transmembrane protein; clarin-1 (USH3A) is a transmembrane protein of the tetraspanin family. Most USH genes are alternatively spliced and expressed as several isoforms which most probably serve in different cellular functions. Moreover, *PDZD7* alleles contribute to digenic USH or act as modifiers of the retinal phenotype [4].

## 67.2 USH Protein Networks

The diversity of the affected proteins is surprising, given that the clinical phenotypes of the three USH types are very similar. The successive identification of supramolecular protein networks related to USH has provided an explanation to this phenomenon and thereby insights into the complex pathophysiology of USH. In the USH protein interactome all USH1 and USH2 proteins are integrated mainly by direct interactions to the USH scaffold proteins harmonin, SANS, and whirlin as well as the tail of myosin VIIa (Fig. 67.1a) [2, 3, 5, 6]. In addition, the USH3 protein clarin-1 may also associate with the USH1/USH2 protein network [7]. Furthermore, the genetic modifier PDZD7 is part of the USH interactome [4, 8]. Beyond that, direct links of USH protein networks to the actin and the microtubule cytoskeleton are described [5, 9]. Systematic proteomic screens for USH protein network partners revealed direct and indirect interactions of USH proteins with several dozen non-USH proteins including disease related proteins [9, 10]. Interestingly, the set of recently identified interaction partners of USH proteins include proteins related to retinal and syndromic ciliopathies (Fig. 67.1b).

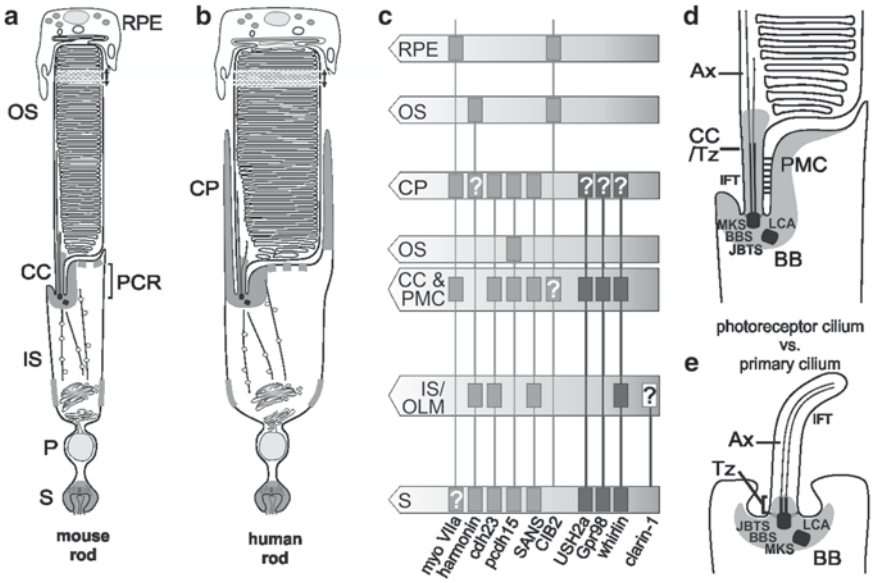


**Fig. 67.2** Ciliopathy related protein localization in photoreceptors and primary cilia. Rodent (**a**) and human rods (**b**) are composed of the photosensitive outer segment (*OS*), resembling a modified primary cilium, and the synthetic active inner segment (*IS*) connected by the connecting cilium (*CC*). *CP*, calycal processes; *PMC*, periciliary membrane complex; *P*, perikaryon; *S*, synapse; *OLM*, outer limiting membrane; *RPE*, retinal pigment epithelium; *Grey* areas: USH protein networks. **c** USH protein localization, controversial data. **d**, **e** Localization of ciliopathy protein networks in the photoreceptor cilium (**d**) and in the primary cilium (**e**). *Grey* areas: co-localization of USH and ciliopathy proteins. *Ax*, axoneme; *BB*, basal body; *Tz*, transition zone

## 67.3 USH Interactome is Molecularly Linked to Other Ciliopathies

Ciliopathies are a group of disorders that affect the formation, function and maintenance of cilia (Fig. 67.2a–67.2d). There has been growing evidence that USH, affecting ciliated sensory cells in the inner ear and the retina, displays characteristics of a ciliopathy. Recently discovered molecular links to other ciliopathies support this hypothesis: the USH2 protein whirlin connects USH networks to the RP GTPase regulator (RPGR) [11]. In photoreceptor cells, the splice variant $RPGR^{ORF15}$ is suggested to interact with multiple proteins that are related to cilia function, including the intraflagellar transport (IFT) protein IFT88, the IFT motor KIF3A, and the RPGR interacting protein (RPGRIP1), which is part of the nephrocystin protein network [12, 13]. Mutations in the *RPGRIP1* gene can lead to Leber congenital amaurosis (LCA), probably the most severe form of retinal dystrophy. An additional molecular link between USH and LCA exists through the direct binding of USH2a to the centriolar ninein-like protein (Nlp) isoform B which mediates the molecular bond to the LCA5 protein lebercilin [14]. Lebercilin is a ciliary protein associated with components of the IFT protein complex B in photoreceptor cells [15, 16].

Finally, we have recently shown that the USH1G protein SANS binds to the centrosomal protein of 290 kDa (Cep290) (Sorusch et al., in prep.). Cep290 is essential for biogenesis and maintenance of cilia. Mutations in *CEP290* are causative for multiple non-syndromic and syndromic ciliopathies of diverse severity: LCA, nephronophthisis (NPHP), Senior-Loken syndrome (SLS), Joubert syndrome (JBTS), Bardet-Biedl syndrome (BBS), and the lethal Meckel-Gruber syndrome (MKS) [17]. Moreover, Cep290 participates in protein complexes with numerous of other ciliopathy molecules, e.g. RPGR, RPGRIP1, lebercilin, Nlp, and BBS6 [17]. The SANS interaction with the comprehensive ciliopathy molecule Cep290 provides additional molecular links of the USH interactome to other ciliopathy networks.

## 67.4 USH Protein Networks in the Inner Ear and Eye

Mutations in USH genes lead to dysfunction of mechanosensory hair cells in the inner ear and photo-sensitive photoreceptor cells as well as the cells of the retinal pigment epithelium (RPE). Intense mouse model analyses revealed that USH proteins and their networks are essential for interstereovilli links in the signal perceiving hair bundles [18]. Defects in USH proteins lead to altered stereovilli organization during hair cell differentiation. In addition, USH proteins are present in ribbon synapses of auditory hair cells [2]. In inner hair cell synapses harmonin scaffolds ion channel complexes regulating the synaptic electrical and $Ca^{2+}$ signaling [19].

In ocular RPE cells, myosin VIIa is the only USH protein, essential for melanosome transport into the apical microvillar compartment and for phagocytosis of outer segment tips (Fig. 67.2) [20]. In photoreceptor cells, most USH proteins seem to be expressed at ribbon synapses indicating the formation of protein networks [1, 2]. Nevertheless, there is no consistent knowledge on their function in photoreceptor synapses, so far.

However, prominent USH protein networks associate with adhesion complexes in calycal processes and in the periciliary membrane complex (PMC) of photoreceptor cells [2]. Calycal processes are characteristic for vertebrate photoreceptor cells and resemble microvilli-like apical extensions of the inner segment that shield the basolateral region of the outer segment like the calyx of a flower (Fig. 67.2b). Recent systematic analysis has indicated USH1 proteins localization in calycal processes [21]. In contrast, our data revealed the absence of harmonin in the presence of other USH1 and all three USH2 proteins [2]. Anyhow, USH proteins may serve in adhesion complexes to stabilize the calyx in the fragile area of the *de novo* genesis of outer segment disks. The presence of USH proteins in calycal processes, which are absent in the slender photoreceptor cells of rodents (Fig. 67.2a, b), may explain the incoherency in phenotypes of human patients and USH mouse models [2].

In the PMC, USH proteins provide the molecular basis for the membrane adhesion between the inner segment and the connecting cilium [6, 10]. Fibrous links of the photoreceptor PMC are homologue to hair cell ankle-links, composed of the extracellular domains of Gpr98 and USH2a. These transmembrane proteins are anchored via their intracellular tail by whirlin in the periciliary cytoplasm. There is

growing evidence that SANS links this complex to the microtubule-based transport routes for outer segment cargoes though the cytoplasm of the inner segment [9, 12]. However, USH proteins are also localized in the photoreceptor connecting cilium, the transition zone between the inner and the outer segment. Myosin VIIa is thought to participate in opsin transport across this zone [2, 22].

## 67.5 USH Networks in Ciliary Transport of Photoreceptor Cells

The periciliary compartment plays an extraordinary role in the ciliary cargo transport in general [12]: the transport of cargo through the cytoplasm is specifically targeted to the periciliary region before the cargo import occurs, through the transition zone into the ciliary axoneme. Molecules related to ciliopathies are essential for these processes [17, 23]. In the periciliary region of photoreceptor cells, the periciliary USH protein network molecularly characterizes the PMC. The inner segment membrane region of the PMC is thought to serve as the target for the cytoplasmic vesicle transport towards the photoreceptor cilium [6, 10, 24]. Current research provides accretive evidence that USH proteins work in concert with BBSome components and other ciliopathy proteins in the cargo transfer from the inner segment transport to the ciliary transport module, in which IFT particles and myosin VIIa take over powering the cargo transport to its ciliary destination [2, 24].

## 67.6 Conclusions

The protein interactome related to USH is linked with proteins and networks of other ciliopathies. The participation of ciliopathy related proteins in common cellular mechanisms explain the overlap of pathogenic defects in ciliogenesis, cilia maintenance and ciliary transport. Shared molecular features of USH and other ciliopathies may open an avenue for common therapeutic strategies for the treatment of patients affected by these diseases.

**Supports** DFG; EU FP7 “SYSCILIA” and “TREATRUSH”; FAUN-Stiftung; Foundation Fighting Blindness (FFB); Forschung contra Blindheit; ProRetina Deutschland.

## References

1. Saihan Z et al (2009) Update on Usher syndrome. Curr Opin Neurol 22:19–27
2. Wolfrum U (2011) Protein networks related to the Usher syndrome gain insights in the molecular basis of the disease. In: Ahuja S (ed) Usher syndrome: pathogenesis, diagnosis and therapy. Nova Sci Pub Inc, USA, p. 51–73

3. Riazuddin S et al (2012) Alterations of the CIB2 calcium- and integrin-binding protein cause Usher syndrome type 1J and nonsyndromic deafness DFNB48. Nat Genet 44:1265–1271
4. Ebermann I et al (2010) PDZD7 is a modifier of retinal disease and a contributor to digenic Usher syndrome. J Clin Invest 120:1812–1823
5. Reiners J et al (2006) Molecular basis of human Usher syndrome: deciphering the meshes of the Usher protein network provides insights into the pathomechanisms of the Usher disease. Exp Eye Res 83:97–119
6. Yang J (2012) Usher syndrome: genes, proteins, models, molecular mechanisms, and therapies. In: Naz DS (ed) Hearing loss. Intech, Rijeka
7. Zallocchi M et al (2012) Role for a novel Usher protein complex in hair cell synaptic maturation. PLoS One 7:e30573
8. Schneider E et al (2009) Homozygous disruption of PDZD7 by reciprocal translocation in a consanguineous family: a new member of the Usher syndrome protein interactome causing congenital hearing impairment. Hum Mol Genet 18:655–666
9. Overlack N et al (2011) Direct interaction of the Usher syndrome 1G protein SANS and myomegalin in the retina. Biochim Biophys Acta 1813:1883–1892
10. Maerker T et al (2008) A novel Usher protein network at the periciliary reloading point between molecular transport machineries in vertebrate photoreceptor cells. Hum Mol Genet 17:71–86
11. Wright RN et al (2012) RpgrORF15 connects to the usher protein network through direct interactions with multiple whirlin isoforms. Invest Ophthalmol Vis Sci 53:1519–1529
12. Roepman R, Wolfrum U (2007) Protein networks and complexes in photoreceptor cilia. In: Faupel M, Bertrand E (eds) Subcellular proteomics-from cell deconstruction to system reconstruction. Springer, Dordrecht, pp. 209–235
13. Sang L et al (2011) Mapping the NPHP-JBTS-MKS protein network reveals ciliopathy disease genes and pathways. Cell 145:513–528
14. van Wijk E et al (2009) Usher syndrome and Leber congenital amaurosis are molecularly linked via a novel isoform of the centrosomal ninein-like protein. Hum Mol Genet 18:51–64
15. den Hollander AI et al (2007) Mutations in LCA5, encoding the ciliary protein lebercilin, cause Leber congenital amaurosis. Nat Genet 39:889–895
16. Boldt K et al (2011) Disruption of intraflagellar protein transport in photoreceptor cilia causes Leber congenital amaurosis in humans and mice. J Clin Invest 121:2169–2180
17. Coppieters F et al (2010) CEP290, a gene with many faces: mutation overview and presentation of CEP290base. Hum Mutat 31:1097–1108
18. Gillespie P, Muller U (2009) Mechanotransduction by hair cells: models, molecules, and mechanisms. Cell 139:33–44
19. Gregory FD et al (2011) Harmonin inhibits presynaptic Cav1.3 Ca(2)(+) channels in mouse inner hair cells. Nat Neurosci 14:1109–1111
20. Gibbs D et al (2010) Function of MYO7A in the human RPE and the validity of shaker1 mice as a model for Usher syndrome 1B. Invest Ophthalmol Vis Sci 51:1130–1135
21. Sahly I et al (2012) Localization of Usher 1 proteins to the photoreceptor calyceal processes, which are absent from mice. J Cell Biol 199:381–399
22. Wolfrum U, Schmitt A (2000) Rhodopsin transport in the membrane of the connecting cilium of mammalian photoreceptor cells. Cell Motil Cytoskeleton 46:95–107
23. Zaghloul NA, Katsanis N (2009) Mechanistic insights into Bardet-Biedl syndrome, a model ciliopathy. J Clin Invest 119:428–437
24. Sedmak T, Wolfrum U (2010) Intraflagellar transport molecules in ciliary and nonciliary cells of the retina. J Cell Biol 189:171–186

# Chapter 68
# The Phenotype of the *Good Effort* Mutant Zebrafish is Retinal Degeneration by Cell Death and is Linked to the *Chromosome Assembly Factor 1b* Gene

**Travis J. Bailey and David R. Hyde**

**Abstract** In a screen to identify zebrafish eye mutants, we isolated the *good effort* (*gef*) mutant. The retina of *gef* embryos is characterized by the successful initiation of the optic primordium and normal retinal development over the first 2 days post fertilization (dpf). The mutant retina, however, fails to continue to grow. Embryos from *gef* heterozygous incrosses were analyzed for cell death by acridine orange and by TUNEL labeling at 2 dpf. Significantly more TUNEL-positive and acridine orange-labeled dying cells were found in *gef* mutant embryos at 2 dpf relative to wild-type embryos. Because this time was earlier than any observable gross morphological differences, this cell death was likely the cause of the gross morphological defects. Meiotic mapping localized the mutation interval to a one-megabase interval on zebrafish chromosome 9.

**Keywords** Zebrafish · Mutant allele · *Good effort* · Chromosome assembly factor 1b · Cell death · Retinal degeneration

## 68.1 Introduction

A genetic screen to uncover mutations in genes critical for eye development was previously performed in our lab [1]. A number of recessive alleles were isolated and categorized as mutants in either Development (Class I), Cell death (Class II), Pigmentation (Class III), or Lens Defects (Class IV). Class I and II mutants were

T. J. Bailey (✉) · D. R. Hyde
Department of Biological Sciences and Center for Zebrafish Research, University of Notre Dame, 027B Galvin Building, Notre Dame, IN 46556, USA
e-mail: tbailey@nd.edu

D. R. Hyde
e-mail: dhyde@nd.edu

J. D. Ash et al. (eds.), *Retinal Degenerative Diseases,* Advances in Experimental Medicine and Biology 801, DOI 10.1007/978-1-4614-3209-8_68,

characterized by smaller eyes relative to sibling fry, but only Class II mutants exhibited pyknotic nuclei. The abnormal eye size in the mutants was revealed at different stages of embryonic development. The first Class I mutant, *barely started,* has a noticeably smaller eye at 2 dpf by gross morphological inspection. By contrast, the *good effort* (*gef*) mutant embryos seem to develop normally for 2 days, but have noticeably smaller eyes than normal by 3 dpf [1]. The mutant lens is normal sized, however it protrudes from the eye. Upon close inspection, the retina seemed subtly smaller at 3 dpf relative to 2 dpf. This suggests that the *gef* mutant retinas were degenerating, rather than failing to form properly.

## 68.2 Materials and Methods

### *68.2.1 Animals and Husbandry*

The genetic screen used to isolate the *good effort* mutant zebrafish was described previously [1]. All animal procedures were performed according to the guidelines of the ARVO statement for the "Use of Animals in Ophthalmic and Vision Research" and were approved by the Institutional Animal Care and Use Committees at the University of Notre Dame. Adult zebrafish (*Danio rerio*) were raised using standard husbandry techniques [2]. The *Tg*(*fli1-eGFP*)$^{y1}$ transgenic zebrafish was described [3].

### *68.2.2 Mapping and Cloning of the gef Mutation*

Meiotic mapping was done as previously described using 828 meioses [4]. Genomic DNA samples from homozygous *gef*$^{nt2}$ mutant embryos were genotyped using SSLP markers from Research Genetics (Huntsville, AL) and data analyzed for the indication of linkage.

### *68.2.3 Cell Death Assay in Embryos*

Cell death was monitored using whole mount acridine orange labeling as described [5], with embryos incubated in 0.2 mM phenylthiourea (PTU) to block pigmentation [2]. Alternatively, embryos were fixed in 4% paraformaldehyde in 1 X PBS and whole mount TUNEL labeling was done according to the manufacturer's protocol (Clontech), with the embryos being permeabilized in pre-chilled −20 °C methanol for 20 min and then rehydrated in 0.1% sodium citrate and 0.1% Triton X-100 buffer.

**Table 68.1** Chronology of degenerative or missing tissue in the *gef* mutant

| Age (dpf) | Eye | Brain | Heart | Jaw | Pectoral fin | Head vasculature | Spinal cord | Swim bladder |
|---|---|---|---|---|---|---|---|---|
| 1 | No | No | No | No | NA | No | No | NA |
| 2 | No/Degen | Degen | No | Degen | Degen | Alt | Degen | NA |
| 3 | Degen | Degen | Abnor | Miss | Miss | Alt | Degen | NA |
| 4 | Degen | Degen | Abnor | Miss | Miss | Alt | Degen | Missing |
| 5 | Miss | Degen | Abnor | Miss | Miss | Alt | Degen | Missing |

*No* normal morphology, *Abnor* abnormal shape and looping by gross inspection, *Alt* altered morphology as determined by *Tg*(*fli1:eGFP*)$^{y1}$ transgenic reporter, *Miss* missing tissue or organ, but no obvious cell death association, *Degen* tissue degeneration as assayed by acridine orange or TUNEL labeling, *NA* not applicable as tissue has not developed at this age

## 68.3 Results

### 68.3.1 *The* gef *Mutant Small Eye Phenotype is Due to Cell Death*

We tested if the small eye phenotype in the *gef* mutant was due to cell death by identifying cells unable to exclude the fluorescent vital dye acridine orange in whole mount embryos. We found elevated levels of cell death in the retina and spinal cord of *gef* mutant embryos at 2 dpf, a time prior to gross morphological differences (Table 68.1). These data were confirmed by increased numbers of TUNEL-positive retinal cells in *gef* embryos relative to wild-type embryos.

### 68.3.2 *Meiotic Mapping of the Good Effort Mutation*

SSLP genomic DNA mapping of the *gef*$^{ht2}$ mutation placed it in a 1 MB interval on zebrafish chromosome 9 (Fig. 68.1a). This interval contained 11 predicted genes (*dacd*, *gpr18*, *gpr183*, *clybl*, *zic5a*, *zic2*, *tmtc4*, *hpld1*, *nalcn*, *itgbl1*, and *fgf14*). Sequencing of cDNA isolated from *gef* mutant embryos failed to show any coding region defects and analysis of mRNA transcript levels by qRT-PCR failed to show significant differences in expression for any gene except *itgbl1*, which showed a reduction in expression to one third of wild-type levels. A flanking gene, *chaf1b*, which was 5' to the interval, was also considered in the case that one of the embryos was misphenotyped. This cDNA clone of the gene, showed a missing exon (Fig. 68.1c) and genomic sequencing demonstrated a 3 bp deletion in the splice donor site for exon 3, (Fig. 68.1b), which results in a premature truncation in the protein (Fig. 68.1d).

### 68.3.3 *Extra Ocular Phenotypes in the gef Mutant Zebrafish*

After high amounts of cell death in 2 and 3 dpf *gef* mutant embryos, little cell death was seen in the developing retina until the ultimate necrosis of the dying embryo

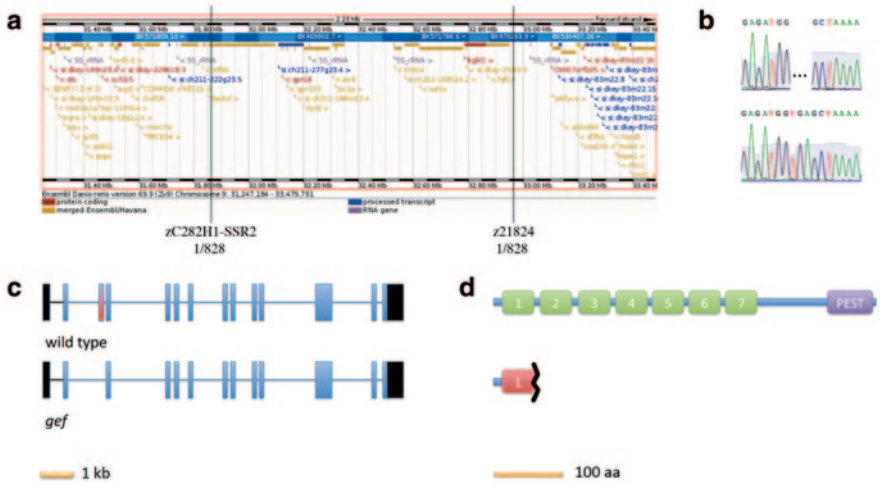


**Fig. 68.1** The *good effort* mutation maps to zebrafish chromosome 9. **a** Schematic of the interval of chromosome 9 indicated by SNP analysis of 828 embryos. **b** Electropherogram generated by sequencing the deletion near the splice donor site of exon3. **c** Schematic representing how sequence of the cDNA (*boxes*) of wild type *chaf1b* (*top*) and *gef* mutant *chaf1b* (*bottom*) aligns to the genomic sequence (*line*). **d** Schematic representation of wild-type Chaf1b$^{wt}$ protein (*green*, 68 kDa) showing the *seven* WD40 repeats and PEST motifs compared with to Chaf1b$^{gef}$ (*red*, 5 kDa) illustrating the predicted premature stop, which results in a severely truncated polypeptide

(Table 68.1 summarizes the phenotypes observed in *gef* mutant embryos at different days of development). Because of cell death at 2 dpf in the pectoral fin bud and branchial arches, the pectoral fin and jaw structures failed to form, respectively. The vascular network was present, but malformed, as determined by GFP expression of *gef* mutants crossed to the *Tg*(*fli1*:*eGFP*)$^{y1}$ transgenic line. The heart appears normal until pericardial edema stretched the looping cardiac tissue, but there was no evidence of cell death. A swim bladder was never observed in *gef* mutant embryos, although edema was seen between the spinal cord and the yolk sac and lateral to the yolk at 5 dpf. TUNEL and acridine orange labeling at 2 dpf in the retina, brain, and spinal cord did not appear to affect the areas of post-mitotic cells. The tail and heads of *gef* mutant embryos appeared normal.

## 68.4 Discussion

### *68.4.1 Genetic Screens for Zebrafish Mutants in Retinal Development and Degeneration*

The *good effort* zebrafish mutant is characterized by a period of normal development, followed by rapid cell death in highly proliferative developing tissues,

including the retina, brain, and pectoral fins. Strikingly, the retinal cell death phenotype appears to be confined to those cells of the retinoblastic layer that are making the transition from proliferating progenitors to post-mitotic differentiating cells. This phenotype also leaves other developing tissue, such as the lens, unperturbed. A number of genetic screens have been carried out in zebrafish embryos that affect the eye [1, 6–8], including some that exhibit general neural degeneration [9]. In contrast, the *good effort* mutant likely belongs to the Group V—non-specific retinal degeneration class characterized by Malicki et al., [8], the Group 1 class of the Rodriguez and Driever [10], and the Growth Retardation and Central Retinal Defects group described by Gross et al. [7].

Although zebrafish mutants that perturb vascular integrity, exhibit CNS degeneration [11], mutants such as *cloche*, which fail to develop any head vasculature, as determined by endothelial cell markers and lack of circulating blood, form morphologically normal retina and brain structures for over a day later than the onset of the *gef* mutant phenotype. This suggests that the vasculature defects seen in the *gef* mutant embryos are downstream of the cranial crest defects rather than upstream of the neural defects.

### *68.4.2 The Timing of the* gef *Mutant Phenotype Suggests a Defect in the Switch From Cell Cycling to Post-Mitotic Differentiation*

Although highly proliferative tissues appear to be most affected by the *gef* mutation, cycling retinal circumferential marginal zone progenitor cells seem unaffected at 2 dpf. This suggests a requirement for Chaf1b in the switch from cycling retinal progenitor cells (analogous to transit amplifying cells) to post-mitotic differentiating cells. The surviving *gef* retinal neurons observed in whole mount immunohistochemistry of photoreceptors [1] are likely due to their differentiation prior to a requirement of Chaf1b protein. Interestingly, morpholinos designed to inhibit translation or transcription of the Chaf1b protein phenocopy equally well the mutant phenotypes, without being more severe. Fischer et al. [12] suggested that, despite being expressed in the eight-cell embryo, the delayed phenotype might not be due to maternally-deposited mRNA in the affected cells, but rather to persistent protein. However, the C terminus of Chaf1b has a PEST domain, common to proteins specifically degraded during cell cycle regulation [13], suggesting no need for Chaf1b translation in embryos less than 2 dpf.

### *68.4.3 Comparison of* gef *Mutant Phenotype with Other Models*

Deleting the *chaf1b* homolog in proliferating human cells in vitro is lethal [18]. A growing number zebrafish mutants that disrupt cell cycle machinery have been described, which show similar stage cell death in highly proliferative tissues [12, 14, 15].

The *yellow head* (*yhd*) and *neural degeneration 1* (*ned*-1) zebrafish mutants display similar central retina cell death at without affecting the CMZ or lens [16, 17]. However the *ned*-1 mutant possesses elevated numbers of pyknotic retina nuclei as early as 1.5 dpf, which is earlier than *gef* mutants. The *yhd* and *ned*-1 mutant genes have not been mapped. The *young* mutant zebrafish, which has a nonsense mutation in the coding region of the SWI/SNF-related, matrix-associated, actin-dependent regulator of chromatin (*smarca4*), shares the central retinal degeneration phenotype with *gef*, without affecting the circumferential marginal zone (CMZ) or the lens dramatically [4]. Other mutants in the chromatin remodeling complexes such as *baf53a*$^{hi1052Tg}$ and *smarca5*$^{hi550Tg}$, cyclin genes like *ccna2*$^{hi2696Tg}$, and DNA replication genes *fen1*$^{hi4026Tg}$ also display a central retinal degeneration, also with little affect on the lens or peripheral retina [4, 7]. The fact that these mutant fish all display similar effects on the central, but not peripheral retina suggests a common genetic pathway. It is unclear if the retinal degeneration is due to a failure of these genes to facilitate the cell cycle (their ascribed function) or another unknown function. The fact that the marginal cells, which are still cycling, are unaffected in the mutants suggests the latter case. This possibility could be tested by evaluating expression of genes in retinal developmental pathways in *gef* mutant and *chaf1b* morphant embryos.

**Acknowledgment** We thank Ronald R. Gregg (University of Louisville) for SNP mapping. This study was supported by the NIH (R01-EY018417) and the Center for Zebrafish Research at the University of Notre Dame.

## References

1. Vihtelic TS, Hyde DR (2002) Zebrafish mutagenesis yields eye morphological mutants with retinal and lens defects. Vision Res 42(4):535–540
2. Westerfield M (1993) The Zebrafish Book, 3rd edn. Univeristy of Oregon Press, Eugene
3. Lawson ND, Weinstein BM (2002) In vivo imaging of embryonic vascular development using transgenic zebrafish. Dev Biol 248(2):307–318
4. Gregg RG et al (2003) Positional cloning of the young mutation identifies an essential role for the Brahma chromatin remodeling complex in mediating retinal cell differentiation. Proc Natl Acad Sci U S A 100(11):6535–6540
5. Begemann G et al (2001) The zebrafish neckless mutation reveals a requirement for raldh2 in mesodermal signals that pattern the hindbrain. Development 128(16):3081–3094
6. Fadool JM et al (1997) Mutations affecting eye morphology in the developing zebrafish (Danio rerio). Dev Genet 20(3):288–295
7. Gross JM et al (2005) Identification of zebrafish insertional mutants with defects in visual system development and function. Genetics 170(1):245–261
8. Malicki J et al (1996) Mutations affecting development of the zebrafish retina. Development 123:263–273
9. Furutani-Seiki M et al (1996) Neural degeneration mutants in the zebrafish, Danio rerio. Development 123:229–239
10. Rodriguez M, Driever W (1997) Mutations resulting in transient and localized degeneration in the developing zebrafish brain. Biochem Cell Biol 75(5):579–600
11. Stainier DY et al (1996) Mutations affecting the formation and function of the cardiovascular system in the zebrafish embryo. Development 123:285–292

12. Fischer S et al (2007) Mutation of zebrafish caf-1b results in S phase arrest, defective differentiation, and p53-mediated apoptosis during organogenesis. Cell Cycle 6(23):2962–2969
13. Kaufman PD et al (1995) The p150 and p60 subunits of chromatin assembly factor I: a molecular link between newly synthesized histones and DNA replication. Cell 81(7):1105–1114
14. Plaster N et al (2006) p53 deficiency rescues apoptosis and differentiation of multiple cell types in zebrafish flathead mutants deficient for zygotic DNA polymerase delta1. Cell Death Differ 13(2):223–235
15. Yamaguchi M et al (2008) Mutation of DNA primase causes extensive apoptosis of retinal neurons through the activation of DNA damage checkpoint and tumor suppressor p53. Development 135(7):1247–1257
16. Daly FJ, Sandell JH (2000) Inherited retinal degeneration and apoptosis in mutant zebrafish. Anat Rec 258(2):145–155
17. Grunwald DJ et al (1988) A neural degeneration mutation that spares primary neurons in the zebrafish. Dev Biol 126(1):115–128
18. Nabatiyan A, Krude T (2004) Silencing of chromatin assembly factor 1 in human cells leads to cell death and loss of chromatin assembly during DNA synthesis. Mol Cell Biol 24(7):2853–2862

# Chapter 69
# Knock-Down DHDDS Expression Induces Photoreceptor Degeneration in Zebrafish

**Rong Wen, Julia E. Dallman, Yiwen Li, Stephan L. Züchner, Jeffery M. Vance, Margaret A. Peričak-Vance and Byron L. Lam**

**Abstract** A mutation in the dehydrodolichol diphosphate synthase (DHDDS) was recently identified as the cause of a subtype of recessive retinitis pigmentosa (RP). Molecular modeling indicates that this mutation could result in low enzymatic efficiency of DHDDS. To investigate the possible link between insufficient DHDDS activity and photoreceptor degeneration, the expression of DHDDS was knocked down by morpholino oligonucleotides (MO) injected into zebrafish one cell embryos. The general appearance and behavior of 4-day-old MO-injected fish were normal, but they failed to respond to light-off, suggesting loss of visual function. Morphological analysis showed that photoreceptor outer segments in retinas of MO-injected fish are very short and in many cases completely missing. Peanut agglutinin (PNA) staining confirmed the absence of cone outer segments. These results demonstrate that suppression of DHDDS expression in zebrafish leads to the

R. Wen (✉) · Y. Li · B. L. Lam
Bascom Palmer Eye Institute, University of Miami, 506 McKnight Building, 1638 NW 10th Ave, Miami, FL 33136, USA
e-mail: rwen@med.miami.edu

Y. Li
e-mail: YLi2@med.miami.edu

B. L. Lam
e-mail: BLam@med.miami.edu

J. E. Dallman
Department of Integrative Biology, University of Miami, Miami, FL 33136, USA
e-mail: jdallman@bio.miami.edu

S. L. Züchner · J. M. Vance · M. A. Peričak-Vance
John P. Hussman Institute for Human Genomics, University of Miami, Miami, FL 33136, USA
e-mail: SZuchner@med.miami.edu

J. M. Vance
e-mail: JVance@med.miami.edu

M. A. Peričak-Vance
e-mail: MPericak@med.miami.edu

J. D. Ash et al. (eds.), *Retinal Degenerative Diseases,* Advances in Experimental Medicine and Biology 801, DOI 10.1007/978-1-4614-3209-8_69,

loss of photoreceptor outer segments and visual function. These results support the hypothesis that insufficient DHDDS function leads to retinal degeneration.

**Keywords** DHDDS · Retinal degeneration · Photoreceptor outer segments · Zebrafish · Morpholino · PNA

## 69.1 Introduction

Retinitis pigmentosa (RP) is a group of genetically heterogeneous retinal degenerative disorders with the prevalence of 1 in 3,000–4,500 people [1–4]. Known mutations in more than 50 genes are implicated in RP (http://www.sph.uth.tmc.edu/retnet/sum-dis.htm). However, mutations have only been identified in about 50% of autosomal recessive RP cases. For the other 50% patients the disease-causing mutations remain unknown [1].

Using whole-exome sequencing, we recently identified a single-nucleotide mutation, c.124A>G in the dehydrodolichol diphosphate synthase-encoding *DHDDS* gene as the cause of retinal degeneration in a family of Ashkenazi Jewish (AJ) origin in which three of the four siblings were diagnosed with RP in their teenage years [5]. This discovery was subsequently confirmed to causes 10–20% of autosomal recessive RP cases in patients of (AJ) origin [6]. DHDDS, a cis-prenyltransferase, is a key enzyme in dehydrodolichol diphosphate biosynthesis [7]. The identified mutation changes a highly conserved wild-type Lys42 to Glu. Lys42 is located in the vicinity of active site residue Arg38, where it facilitates the optimal orientation of Arg38 for ion pairing with the substrate farnesyl-pyrophosphate (FPP) via charge-charge repulsive forces between the two residues [5]. The mutant Glu residue reverses the repulsive forces of Lys42, causing misorientation of Arg38, weakening substrate binding, and thus lowering catalytic efficiency.

To test the hypothesis that retinal degeneration in patients with the K42E DHDDS mutation is the result of low DHDDS activity, the expression of DHDDS in zebrafish was knocked down by morpholino oligonucleotides (MO) against exone1/intron1 of the zebrafish *DHDDS*. Injection of the MO into one-cell embryos resulted in loss of photoreceptor outer segments and visual impairment. These results provide evidence supporting the hypothesis that insufficient DHDDS function leads to retinal degeneration

## 69.2 Materials and Methods

Morpholino was designed to block the splice-junction of zebrafish *DHDDS* exone1/intron1 (GeneTools, Philomoth, OR). One-cell embryos were injected with MO allowed to develop for 4 days when the visual system is functional. RNA was extracted for RT-PCR analysis to confirm retention of intron1. Visual function was

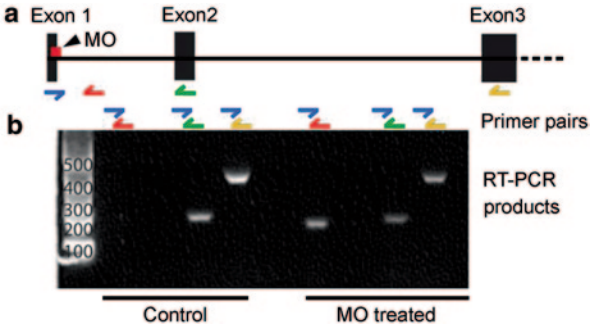


**Fig. 69.1** Suppression of *DHDDS* expression by morpholino oligonucleotides (MO). To study the effects of low DHDDS expression on photoreceptors, MO were used to suppress DHDDS in zebrafish. A splicing junction blocking morpholino (a, *red square*) was designed against the junction between exon1 and exon2 (**a**). Four days after MO injection, total RNA was harvested. RT-PCR showed that MO induced retention of intron1 (*red-blue* primer pair in MO-treated fish), which introduced a stop codon after exon1, leading to severe truncation of the encoded protein. (**b**) (Modified from [5] with permission)

assessed by the light-off response test in which the typical zebrafish response to light-off with bursts of swimming was captured at 60 frames per second by a high-speed camera, FASTCAM 1024 PCI (Photron San Diego CA). Morphological analysis of the retina and photoreceptors were performed with semi-thin sections (1 μm) of eyes along the vertical meridian by light microscopy. Additional morphological analysis of cone outer segments was carried out by PNA staining (peanut agglutinin conjugated with Alexa Fluor 488, Invitrogen, Carlsbad, CA) of cryosections (10 μm) and confocal microscopy.

## 69.3 Results

### *69.3.1 Confirmation of Intron1 Retention*

To confirm that MO injection resulted in suppression of DHDDS expression, RNA was extracted from 4-day-old fish injected with MO and RT-PCR was performed with primers designed to detect retention of intron1 (red arrow, Fig. 69.1a). Retention of intron1 was clearly shown in MO treated fish and not in controls (Fig. 69.1b). Intron1 retention introduces a stop codon after exon1, resulting in severe truncation of the encoded DHDDS protein.

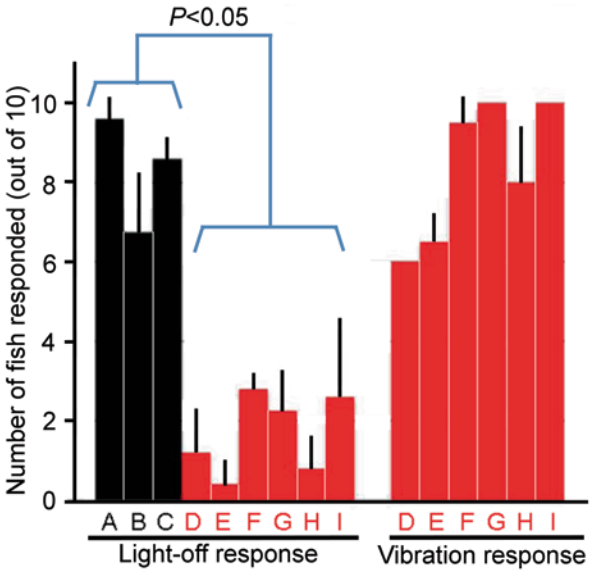


**Fig. 69.2** Light-off response. Zebrafish typically respond to light-off with bursts of swimming. The light-off responses were evoked in MO-treated fish to assess their visual function. Each bar represents the response of a group of 10 control (*black bars*) or MO-injected fish (*red bars*) to 5 trials of light-off transitions (mean ± SD). Light-off responses were significantly reduced in MO-treatment fish. The response of control fish to light-off is 8.3 ± 1.4 ($n = 30$), whereas the response of MO-injected fish is 1.7 ± 1.0 ($n = 60$). Response of MO-injected fish to vibration is 8.3 ± 1.8, similar to light-off responses in control fish. Thus, MO-treated fish were fully capable to swim. (Modified from [5] with permission)

### *69.3.2 Loss of Visual Function in MO-Injected Fish*

The light-off response test takes advantage of a natural behavior of zebrafish. They typically respond to sudden reductions in light intensity with bursts of swimming, which can be reliably observed in 4-day-old wild-type fish. Ten fish were placed in 35 mm Petri dish and their behavior was recorded. Almost all untreated fish responded to light-off whereas most MO-injected fish failed to respond to light transition (Fig. 69.2). To rule out the possibility that the failure to respond to light transition was because MO-treated fish were unable to swim, vibration response test was performed by lightly tapping the side of the Petri dishes. Most MO-treated fish responded to vibration normally (Fig. 69.2).

### *69.3.3 Loss of Photoreceptor Outer Segments*

After the visual function test, fish were prepared for morphological analysis with either semi-thin or cryo-sections of the retina. The general organization and structure of the retina in MO-treated fish retinas (Fig. 69.3b) appeared similar to the

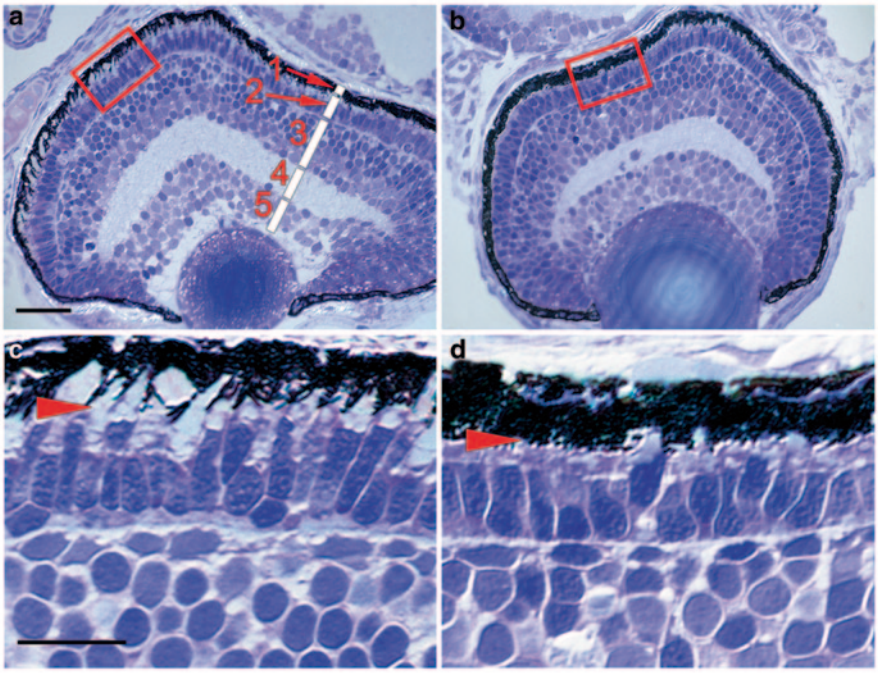


**Fig. 69.3** Suppression of DHDDS expression in zebrafish and photoreceptor morphology. Fish were killed and embedded in epoxy resin for semi-thin sections after the light-off response test. The gross morphology seems not significantly changed in MO-treated eye (**b**) as compared with the WT one (**a**). However, photoreceptors in MO-treated fish had very short outer segments and in many cells, the outer segments were completely missing (*arrowhead*, **d**, high power image of the area indicated by a *red rectangle* in **b**), as compared to photoreceptors in the control fish (*arrowhead*, **c**, high power image of the area indicated by a *red rectangle* in **a**). The layers of the retina are indicated by the *white bars* in (**a**), including the retinal pigment epithelium *1*, the outer nuclear layer *2*, the inner nuclear layer *3*, the inner plexiform layer *4*, and the retinal ganglion cell layer 5. Scale bar: 25 μm for **a** and **b**, and 10 μm for **c** and **d**. (Modified from [5] with permission)

controls (Fig. 69.3a). Close examination of photoreceptors, however, revealed that in MO-treated fish, photoreceptor outer segments were very short or in most cases completely missing (Fig. 69.3d), whereas normal outer segments were seen in the control retinas (Fig. 69.3d). The lack of photoreceptor outer segments were further confirmed by PNA staining, which specifically label cone outer segments of a variety of species [8, 9]. Unlike in the control fish retinas where cone outer segments were heavily stained by PNA (Fig. 69.4a), almost no PNA staining was detected in retinas from MO-treated fish (Fig. 69.4b).

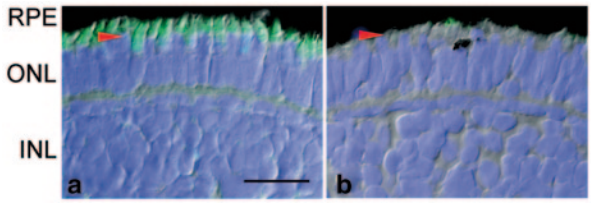


**Fig. 69.4** Staining of cone outer segments with PNA. PNA staining was used to identify cone outer segments. In the control retina (**a**), cone outer segments were nicely stained, whereas the staining is almost missing in the retina from an MO-treated fish (**b**) retinal pigment epithelium (*RPE*), outer nuclear layer (*ONL*), inner nuclear layer (*INL*), Scale bar: 20 μm. (Modified from [5] with permission)

## 69.4 Discussion

We have demonstrated that when DHDDS expression is suppressed in zebrafish, photoreceptors failed to develop outer segments properly and that leads to visual function impairment. Our results therefore support the hypothesis that the K42E mutation of DHDDS identified in human patients results in lower DHDDS enzymatic activity and dolichol deficiency, which in turn leads to photoreceptor degeneration.

Dolichol is a membrane component found in all tissues and organs [10, 11]. Discovered over 50 years ago [12, 13], the biological functions of free dolichols are still largely unknown. One well established function of dolichols is that that the phosphorylated derivative dolichols, dolichyl phosphate, is the required lipid carrier upon which oligosaccharides involved in *N*-linked protein glycosylation are assembled [14–19]. Could the dolichol deficiency caused by the K42E DHDDS mutation lead to deficiency in protein glycosylation? We believe it is unlikely. Patients with the DHDDS mutation have no systemic syndromes, different from those with congenital disorders of glycosylation (CDG), a group of inherited metabolic diseases with glycosylation deficiency that affect almost all organs and systems [20–22]. The fact that MO-treated fish developed normally in the present work also suggest protein glycosylation is perhaps not significantly affected by the suppression of DHDDS expression. These observations suggest that glycosylation deficiency is perhaps not the cause of retinal degeneration in this case.

DHDDS is ubiquitously expressed as a house keeping protein, yet the mutation only affects photoreceptors. Why photoreceptors are more susceptible to dolichol deficiency? To answer this question request more research in the future. Existing data indicate that dolichols, as a membrane component, help to shape the physical properties of the membrane, including increasing membrane fluidity and promoting vesicle fusion [23–25]. Considering that photoreceptor outer segments are membrane rich organelles which are renewed constantly, dolichol deficiency could impair the structure and renewal of photoreceptor outer segments, leading to retinal degeneration.

**Acknowledgment** We thank Dr. Deqiang Huang for technical assistance. This study was supported by grants from the National Institute of Health (P30-EY14801, R01-EY012118, R01-EY018586, and U54-NS065712), Department of Defense (W81XWH-09-1-0674), Hope for Vision, an unrestricted grant from Research to Prevent Blindness, and a grant from the Florida Office of Tourism, Trade and Economic Development (OTTED).

## References

1. Hartong DT, Berson EL, Dryja TP (2006) Retinitis pigmentosa. The Lancet 368(9549):1795–1809
2. Heckenlively JR, Yoser SL, Friedman LH, Oversier JJ (1988) Clinical findings and common symptoms in retinitis pigmentosa. Am J Ophthalmol 105(5):504–511
3. Pagon RA (1988) Retinitis pigmentosa. Surv Ophthalmol 33(3):137–177
4. Fahim AT, Daiger SP, Weleber RG (1993) Retinitis pigmentosa overview. In: Pagon RA, Adam MP, Bird TD, Dolan CR, Fong CT, Smith RJH, Stephens K, (eds) GeneReviews(tm) [Internet]. University of Washington, Seattle
5. Zuchner S, Dallman J, Wen R, Beecham G, Naj A, Farooq A et al (2011) Whole-exome sequencing links a variant in DHDDS to retinitis pigmentosa. Am J Hum Genet 88(2):201–206
6. Zelinger L, Banin E, Obolensky A, Mizrahi-Meissonnier L, Beryozkin A, Bandah-Rozenfeld D et al (2011) A missense mutation in DHDDS, encoding dehydrodolichyl diphosphate synthase, is associated with autosomal-recessive retinitis pigmentosa in Ashkenazi Jews. Am J Hum Genet 88(2):207–215
7. Endo S, Zhang YW, Takahashi S, Koyama T (2003) Identification of human dehydrodolichyl diphosphate synthase gene. Biochim Biophys Acta 1625(3):291–295
8. Blanks JC, Johnson LV (1983) Selective lectin binding of the developing mouse retina. J Comp Neurol 221(1):31–41
9. Hageman GS, Johnson LV (1986) Biochemical characterization of the major peanut-agglutinin-binding glycoproteins in vertebrate retinae. J Comp Neurol 249(4):499–510, 482–483
10. Chojnacki T, Dallner G (1988) The biological role of dolichol. Biochem J 251(1):1–9
11. Rip JW, Rupar CA, Ravi K, Carroll KK (1985) Distribution, metabolism and function of dolichol and polyprenols. Prog Lipid Res 24(4): 269–309
12. Pennock JF, Hemming FW, Morton RA (1960) Dolichol: a naturally occurring isoprenoid alcohol. Nature 186:470–472
13. Burgos J, Hemming FW, Pennock JF, Morton RA (1963) Dolichol: a naturally-occurring C100 isoprenoid alcohol. Biochem J 88:470–482
14. Schenk B, Fernandez F, Waechter CJ (2001) The in(side) and out(side) of dolichyl phosphate biosynthesis and recycling in the endoplasmic reticulum. Glycobiology 11(5):61R–70R
15. Marquardt T, Denecke J (2003) Congenital disorders of glycosylation: review of their molecular bases, clinical presentations and specific therapies. Eur J Pediatr 162(6):359–379
16. Denecke J, Kranz C (2009) Hypoglycosylation due to dolichol metabolism defects. Biochim Biophys Acta 1792(9):888–895
17. Burda P, Aebi M (1999) The dolichol pathway of N-linked glycosylation. Biochim Biophys Acta 1426(2):239–257
18. Lehle L, Strahl S, Tanner W (2006) Protein glycosylation, conserved from yeast to man: a model organism helps elucidate congenital human diseases. Angew Chem Int Ed Engl 45(41):6802–6818
19. Behrens NH, Leloir LF (1970) Dolichol monophosphate glucose: an intermediate in glucose transfer in liver. Proc Natl Acad Sci U S A 66(1):153–159
20. Freeze HH (2006) Genetic defects in the human glycome. Nature reviews Genetics 7(7):537–551

21. Jaeken J, Matthijs G (2007) Congenital disorders of glycosylation: a rapidly expanding disease family. Annu Rev Genomics Hum Genet 8:261–278
22. Jaeken J (2010) Congenital disorders of glycosylation. Ann N Y Acad Sci 1214:190–198
23. Valtersson C, van Duyn G, Verkleij AJ, Chojnacki T, de Kruijff B, Dallner G (1985) The influence of dolichol, dolichol esters, and dolichyl phosphate on phospholipid polymorphism and fluidity in model membranes. J Biol Chem 260(5):2742–2751
24. van Duijn G, Valtersson C, Chojnacki T, Verkleij AJ, Dallner G, de Kruijff B (1986) Dolichyl phosphate induces non-bilayer structures, vesicle fusion and transbilayer movement of lipids: a model membrane study. Biochim Biophys Acta 861(2):211–223
25. Wang X, Mansourian AR, Quinn PJ (2008) The effect of dolichol on the structure and phase behaviour of phospholipid model membranes. Mol Membrane Biol 25(6–7):547–556

# Chapter 70
# Spectral Domain Optical Coherence Tomography Findings in CNGB3-Associated Achromatopsia and Therapeutic Implications

**Michael McClintock, Marc C. Peden and Christine N. Kay**

**Abstract** We describe the spectral domain OCT findings in two siblings with CNGB3-associated achromatopsia. A 33-year-old female and her 31-year-old sibling were evaluated for mild nystagmus and decreased visual acuity which had been present since childhood. They were each evaluated with full field Ganzfeld electroretinography which demonstrated flat photopic responses and preserved rod function. Genetic testing performed at Carver lab at the University of Iowa confirmed a diagnosis of achromatopsia with identical mutations in the CNGB3 gene. Spectral domain optical coherence tomography was performed which revealed foveal changes in both siblings, with slight phenotypic variations in these genotypically identical siblings. OCT findings in achromatopsia emphasize the importance of early identification and treatment in this disorder.

**Keywords** Achromatopsia · Spectral domain OCT · Fovea · Cones · Gene therapy · CNGB3 · Inner segment · Outer segment · Photoreceptor · Macula

---

Supported in part by Foundation Fighting Blindness and by an unrestricted grant to the Department of Ophthalmology from Research to Prevent Blindness.

None of the authors have any relevant financial disclosures.

---

C. N. Kay (✉) · M. McClintock · M. C. Peden
Department of Ophthalmology, University of Florida College of Medicine,
Gainesville, FL 32610-0284, USA
e-mail: ckay@ufl.edu

M. McClintock
e-mail: mlmccl01@ufl.edu

M. C. Peden
e-mail: mpeden@ufl.edu

J. D. Ash et al. (eds.), *Retinal Degenerative Diseases,* Advances in Experimental Medicine and Biology 801, DOI 10.1007/978-1-4614-3209-8_70,

## 70.1 Achromatopsia

Complete achromatopsia is an autosomal recessive inherited retinal disorder characterized by severely reduced visual acuity and complete loss of color discrimination. Patients with achromatopsia lack functional cones, which are the photoreceptors responsible for color vision and central visual acuity. In 45 % of patients with achromatopsia, the disease is caused by mutations in the human cone photoreceptor cyclic nucleotide gated channel beta subunit (CNGB3) gene. Clinical findings include poor visual acuity, photophobia, pendular nystagmus, paradoxical pupil response, normal peripheral visual fields with central scotoma, and poor color discrimination. There is complete absence of cone function on electroretinography (ERG) with preservation of scotopic ERG responses. A clinical distinction is sometimes made between complete achromatopsia and incomplete achromatopsia. Incomplete, or atypical, achromatopsia is associated with some preservation of cone function on ERG with higher levels of visual acuity and color vision. The overall prevalence of achromatopsia has been estimated to be 1:30,000 to 1:50,000 [1]. There is currently no treatment available for patients with achromatopsia.

## 70.2 Genetics of Achromatopsia

There are several known genetic mutations associated with achromatopsia, most of which are involved in the phototransduction cascade within cone photoreceptors. These include mutations in the CNGA3, CNGB3, GNAT2, and PDE6C genes. The CNGA3 and CNGB3 gene products are among the most important as combined they may account for up to 75 % of achromatopsia cases with 50 % or more of all cases being attributed to CNGB3 and another 25 % attributed to CNGA3 [2]. The products of these genes are subunits of the cyclic nucleotide gated (CNG) plasma membrane cation channel. Each CNG channel is composed of two A3 and two B3 dimeric subunits which combine to form a tetrameric integral plasma membrane protein [1, 3–6]. In the phototransduction cascade incident light causes decreased concentrations of cGMP which results in closure of the channel thus decreasing intracellular flow of sodium and calcium cations. This influx hyperpolarizes the photoreceptor cell. The PDE6C gene encodes the catalytic alpha subunit of cone cyclic nucleotide phosphodiesterase which catalyzes the hydrolysis of cGMP to GMP. GNAT2 codes for the alpha subunit of cone transducin. GNAT2 and PDE6C mutations combined account for approximately 2 % of cases of achromatopsia.

## 70.3 Gene Therapy for Achromatopsia

Preliminary studies in animal models have shown benefit from gene therapy in achromatopsia caused by mutations in CNGA3, CNGB3, and GNAT2 [7]. There have been promising results with gene replacement using a subretinally injected

AAV5 vector in a murine model of CNGA3-associated achromatopsia with restoration of cone function [8]. Gene therapy using a recombinant subretinally injected adeno-associated virus expressing a normal human CNGB3 gene has been shown to be of potential benefit in restoring cone photoreceptor function in a CNGB3 knockout mouse model as well as in a naturally occurring canine model of this disease [9, 10]. The canine studies showed functional cone rescue after subretinal gene therapy to be age-dependent, with older dogs not showing restoration of function after treatment [10]. Knockout GNAT2 mice have also been treated with a subretinal AAV5 vector carrying wild-type mouse GNAT2, with restoration of visual acuity by optomotor behavioral testing and electrophysiologic response.

## 70.4 Optical Coherence Tomography Findings in Achromatopsia

Time domain and spectral domain optical coherence tomography (OCT) findings characterizing the structural changes in achromatopsia have been described. Regarding time domain OCT, a study by Barthelmes et al. [11] demonstrated alterations in foveolar structure but no change in overall retinal thickness compared to controls whereas a study by Varsanyi et al. [12] demonstrated significant reductions in central retinal thickness as well as macular volume.

A more recent study by Thomas et al. [13] using higher resolution spectral domain OCT demonstrated disruption of the photoreceptor inner segment and outer segment (IS/OS) junction in the foveal and parafoveal areas in all patients with congenital achromatopsia. In this same study, one of the more conspicuous findings was that of a "punched-out" appearing hyporeflective zone (HRZ) in the outer foveola. The presence of this zone correlated well with an age-dependent reduction in outer nuclear layer thickness. It was postulated that the HRZ arises secondary to a progressive extrusion of outer nuclear layer nuclei into the photoreceptor layer or alternatively to progressive autolysis of cone outer segments. Also observed, but less frequently, was the presence of altered cone outer segment tip (COST) reflectance.

Another study by Thiadens et al. [14] demonstrated that loss of inner and outer segments did appear to be age dependent in a study of 40 achromatopsia patients, with cone cell loss evident in 42% of patients under 30 years of age, and 95% of patients over 30. The age-dependent nature of many of these findings supports the notion of achromatopsia as a progressive disorder.

## 70.5 A Brief Case Report of OCT Findings in Siblings with CNGB3-Associated Achromatopsia

Here we present a case report of two female siblings of similar age with a proven high pathogenicity heterozygous mutation in CNGB3 and their associated SD-OCT findings. Molecular testing was performed at Carver laboratory at the University

of Iowa with bidirectional DNA sequencing using ABI 3730 sequencers (Applied Biosystems, Carlsbad, California). The sisters were found to each have one mutation in CNGB3 gene (Thr383 del 1aC het). There was phenotypic variation between siblings as exhibited by variations in SD-OCT findings.

The first and elder sister, Subject 1, was a 33-year-old Hispanic female who presented to our clinic with a history of decreased vision since childhood, who had been seen by multiple other ophthalmologists with no diagnosis. On clinical examination, her visual acuity was noted to be 20/100 in both eyes with mild hyperopic correction. The patient noted mild photophobia reduced but not eliminated with sunglasses. Motility examination revealed mild nystagmus and exophoria. Dilated funduscopic exam revealed retinal pigment epithelium mottling in the macula. Color vision testing with Ishihara plates revealed sensitivity only to the control plate in both eyes. Goldmann kinetic perimetry demonstrated a central scotoma in both eyes with otherwise full fields. Full field Ganzfeld electroretinography (ERG) was performed under photopic and scotopic conditions. Recordings were obtained from the corneal apexes using a DTL micro fiber electrode. All testing was in accordance with international standards and was performed on the LKC UTAS visual electrodiagnostic testing system. ERG results showed a flat photopic response and preserved rod function. There was strong clinical suspicion for achromatopsia and subsequent independent genetic analysis conducted through the John and Marcia Carver nonprofit genetic testing laboratory at the University of Iowa revealed a heterozygous sequence variation 1 base pair deletion of C at codon 383 in the CNGB3 gene. The second disease-causing mutation has not yet been identified.

Her sister, subject 2, was 31 years old, and presented with a nearly identical clinical history and examination. Her visual acuity was 20/200 in both eyes, also with mild hyperopic correction. Her SD-OCT findings showed some residual hyperreflective material with partial degradation of the IS/OS junction. Figures 70.1 and 70.2 show heidelberg spectralis spectral domain OCT findings for both subjects.

## 70.6 Discussion

Several characteristic morphological changes evident in SD-OCT imaging in patients with congenital achromatopsia have been previously described. The cases presented here demonstrate that a defect in the IS/OS junction, disruption of COST reflectivity, and the presence of a hyporeflective zone are indeed indicative findings in routine SD-OCT imaging of the fovea. Both patients demonstrate central degradation of the IS/OS junction and a central outer hyporeflective zone as well as attenuation of the cone outer segment tips in both eyes. Of note, the hyporeflective in the left eye in the younger sister (subject 2) was less well-defined and there was notable presence of hyperreflective material within the hyporeflective zone which may represent residual photoreceptor outer segment material or debris (Fig. 70.2). The macular OCT of subject 1 demonstrates a hyporeflective zone that is larger and more well-defined, lack of residual hyperreflective material within this zone, and more notable attenuation in the IS/OS junction (Fig. 70.1).

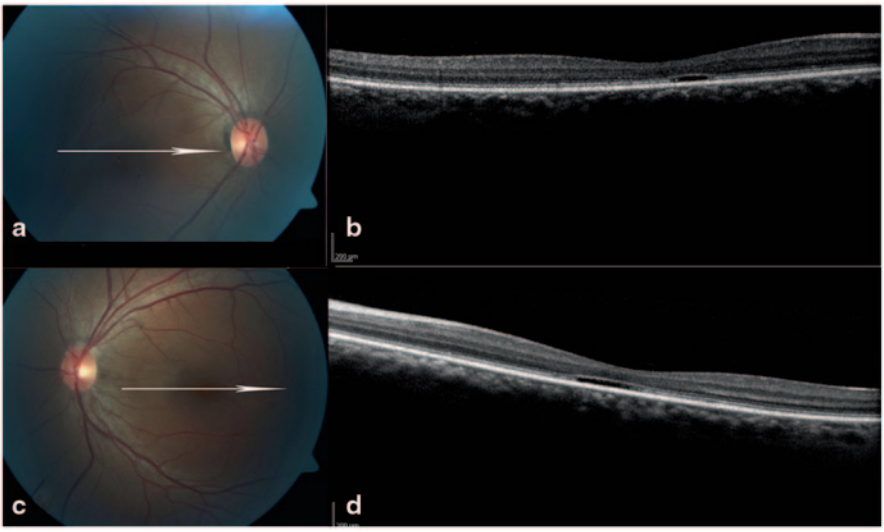


**Fig. 70.1** This figure depicts fundus photographs and OCT images from the 33-year-old sibling. **a**, **c** Color fundus photograph of the right, left eyes. **b**, **d** Corresponding SD-OCT images show a complete loss of the IS/OS junction at the fovea with an associated notable hyporeflective zone

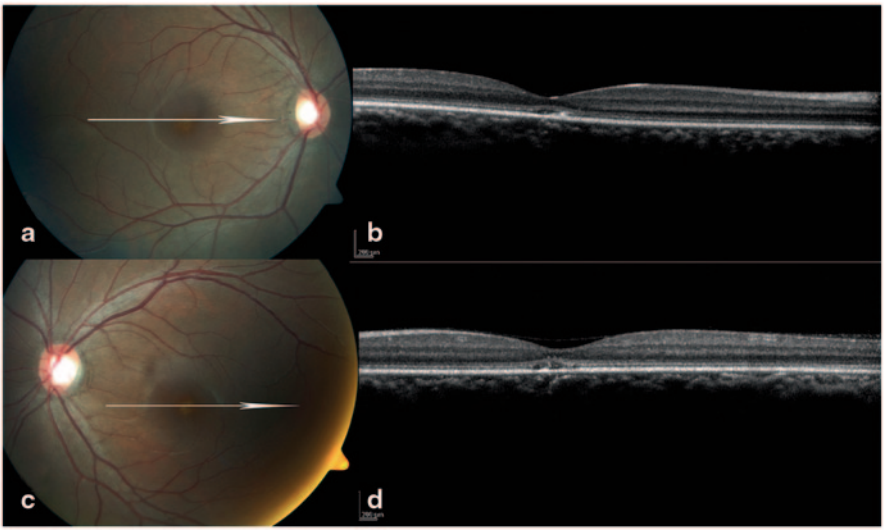


**Fig. 70.2** This figure depicts fundus photographs and OCT images from the 31–year-old sibling. **a**, **c** Color fundus photograph of the right, left eyes. **b**, **d** Corresponding SD-OCT images show only partial degradation of the inner segment/outer segment IS/OS junction with some residual hyperreflective material within the hyporeflective zone

Importantly, it should be noted that phenotypic variation exists between siblings described in our case report, with preservation of outer segment residual material in the younger sibling and loss of all evidence of normal photoreceptor outer segment anatomy in sibling who was 2 years older. This suggests an age-related component to progressive loss of the cone outer segment tips as illustrated with these two siblings, and this is consistent with prior publications [5]. This age-dependent progression of disease course as evidenced by OCT change emphasizes the importance of early treatment in a disorder that has previously been considered to be stationary.

The finding of variable deterioration in foveal architecture evident between two genotypically identical siblings who differ in age by only 2 years, with more notable outer retinal atrophy evident in the older sibling, emphasizes the importance of early and accurate identification of patients with achromatopsia. Restoring function with gene therapy requires presence of a living cell body for vector transduction (unlike regenerative methodologies such as stem cell therapy), and retention of outer retinal normal architecture at the fovea as detected by SD-OCT would imply an increased plausibility for visual acuity recovery after gene therapy. SD-OCT findings in patients with CNGB3-achromatopsia suggest a time sensitive critical window for gene therapy. Patients with retained foveal architecture are the most likely to experience an improvement in visual acuity from gene therapy, and early identification and characterization of these patients is of utmost importance to screen for potential clinical trial candidates for future gene therapy trials.

## References

1. Kohl S et al (2002) Mutations in the cone photoreceptor G-protein alpha-subunit gene GNAT2 in patients with achromatopsia. Am J Hum Genet 71(2):422–425
2. Kohl S et al (2005) CNGB3 mutations account for 50% of all cases with autosomal recessive achromatopsia. Eur J Hum Genet 13(3):302–308
3. Kohl S et al (2000) Mutations in the CNGB3 gene encoding the beta-subunit of the cone photoreceptor cGMP-gated channel are responsible for achromatopsia (ACHM3) linked to chromosome 8q21. Hum Mol Genet 9(14):2107–2116
4. Michaelides M et al (2006) Progressive cone and cone-rod dystrophies: phenotypes and underlying molecular genetic basis. Surv Ophthalmol 51(3):232–258
5. Thiadens AA et al (2009) Homozygosity mapping reveals PDE6C mutations in patients with early-onset cone photoreceptor disorders. Am J Hum Genet 85(2):240–247
6. Wissinger B et al (2001) CNGA3 mutations in hereditary cone photoreceptor disorders. Am J Hum Genet 69(4):722–737
7. Pang JJ et al (2010) Achromatopsia as a potential candidate for gene therapy. Adv Exp Med Biol 664:639–646
8. Pang JJ et al (2012) AAV-Mediated Cone Rescue in a Naturally Occurring Mouse Model of CNGA3-Achromatopsia. PLoS One 7(4):e35250
9. Carvalho LS et al (2011) Long-term and age-dependent restoration of visual function in a mouse model of CNGB3-associated achromatopsia following gene therapy. Hum Mol Genet 20(16):3161–3175

10. Komaromy AM et al (2010) Gene therapy rescues cone function in congenital achromatopsia. Hum Mol Genet 19(13):2581–2593
11. Barthelmes D et al (2006) Quantitative analysis of OCT characteristics in patients with achromatopsia and blue-cone monochromatism. Invest Ophthalmol Vis Sci 47(3):1161–1166
12. Varsanyi B et al (2007) Optical coherence tomography of the macula in congenital achromatopsia. Invest Ophthalmol Vis Sci 48(5):2249–2253
13. Thomas MG et al (2011) High-resolution in vivo imaging in achromatopsia. Ophthalmology 118(5):882–887
14. Thiadens AA et al (2010) Progressive loss of cones in achromatopsia: an imaging study using spectral-domain optical coherence tomography. Invest Ophthalmol Vis Sci 51(11):5952–5957

# Chapter 71
# Photoreceptor Pathology in the X-Linked Retinoschisis (XLRS) Mouse Results in Delayed Rod Maturation and Impaired Light Driven Transducin Translocation

**Lucia Ziccardi, Camasamudram Vijayasarathy, Ronald A. Bush and Paul A. Sieving**

**Abstract** Light-activated movement of transducin-α ($G_{\alpha t1}$) from rod photoreceptor outer segments (ROS) into inner segments (IS) enables rods to rapidly adapt to changes in light intensity. The threshold light intensity at which $G_{\alpha t1}$ translocates from ROS into IS is primarily determined by the rates of activation and inactivation of $G\alpha t_1$. Loss- of- expression of the retina specific cell surface protein, retinoschsin (*Rs1*-KO), led to a dramatic 3–10 fold increase, depending on age, in the luminance threshold for transducin translocation from ROS into IS compared with wild-type control. In contrast, arrestin translocated from IS into ROS at the same light intensity both in WT and Rs1-KO mice. Biochemical changes, including reduced transducin protein levels and enhanced transducin GTPase activity, explain the shift in light intensity threshold for $G_{\alpha t1}$ translocation in *Rs1*-KO mice. These changes in *Rs1*-KO mice were also associated with age related alterations in photoreceptor

Supported by the Intramural Research Program of the National Institutes of Health, National Institute on Deafness and Other Communication Disorders, and the National Eye Institute.

P. A. Sieving (✉)
National Eye Institute, National Institutes of Health, 31 Center Drive,
Room 6A03, Bethesda, MD 20892, USA
e-mail: paulsieving@nei.nih.gov

L. Ziccardi
G. B. Bietti Foundation, Istituto di Ricovero e Cura a Carattere Scientifico
(IRCCS), 00198, Rome, Italy
e-mail: luxzic@hotmail.com

C. Vijayasarathy · R. A. Bush
STRRMD, National Institute on Deafness and Other Communication Disorders,
National Institutes of Health, Bldg 50 Room 4339,
Bethesda, MD 20892, USA
e-mail: camasamv@nidcd.nih.gov

R. A. Bush
e-mail: bushr@nidcd.nih.gov

J. D. Ash et al. (eds.), *Retinal Degenerative Diseases,* Advances in Experimental Medicine and Biology 801, DOI 10.1007/978-1-4614-3209-8_71,

morphology and transcription factor expression that suggest delayed photoreceptor maturation.

**Keywords** Transducin · Arrestin · Translocation · Photoreceptors · Retinoschisis

## 71.1 Introduction

Vertebrate vision is initiated in the retinal rod and cone photoreceptor outer segments, where light is captured and converted to a neuronal signal that ultimately leads to a reduction in cGMP levels [1]. The sequence of events commonly referred to as the phototransduction cascade include: activation of rhodopsin through photoisomerization of chromophore 11-*cis* retinal to all-*trans* retinal (R*) and activation of transducin by GTP/GDP exchange on $G_{\alpha t1}$ subunit which in turn leads to activation of cGMP phosphodiesterase 6 (PDE6) that hydrolyses cGMP. The decrease in cGMP concentration leads to closure of cGMP-gated cation channels (CNG) in the plasma membrane and membrane hyperpolarization. In the photoresponse deactivation phase**,** R* is shut off by $Ca^{2+}$/recoverin mediated phosphorylation of R* by rhodopsin kinase and the subsequent binding of arrestin to phosphorylated rhodopsin. $G_{\alpha t1}$* turns itself off by hydrolyzing GTP to GDP (intrinsic GTPase activity) which is accelerated by retinal RGS9 (regulator of G-protein signaling) protein. A drop in calcium levels caused by light exposure stimulates guanylate cyclase and restores cGMP concentration to the resting dark level.

## 71.2 Light Dependent Translocation of Phototransdction Proteins

The kinetics of phototransduction, i.e. the amplitude and speed of the photoresponse, are critical factors for the function of the visual system allowing it to respond to wide range of light levels from starlight to bright sunlight. There are several different mechanisms involved in light adaptation, but the activities and expression levels of phototransduction proteins and the calcium concentration are the key modulators [1]. Research over the past decade has demonstrated that light driven translocation of signaling molecules, namely, transducin and arrestin, between outer and inner segments contributes to photoreceptor cell adaptation to light [2]. When the light intensity reaches a critical threshold at which the rate of activation of $G_{\alpha t1}$ exceeds the rate of inactivation by GTP hydrolysis, $G_{\alpha t1}$ moves from the ROS into the IS and the cell body. Cone α-transducin, which is compartmentalized in the cone outer segment, does not translocate as cones function in much brighter light than rods and cone $G\alpha_{t2}$ can turn off about a factor of two more rapidly than $G\alpha_{t1}$. Arrestin, which quenches photoactivated rhodopsin, moves in reciprocal manner from the IS to the ROS when the intensity of background illumination approaches the upper

limit of rod responsiveness. Diffusion is believed to be the basic principle driving this protein movement. Gat1 translocation is expected to contribute to photoreceptor light adaptation, as it allows rods to escape saturation and extends their range of light responsiveness. Alternatively, the process may reduce metabolic stress in the retina by reducing excess GTP consumption by rods and thereby the activation of Gat1 molecules in cone dominated bright light vision.

## 71.3 X-Linked Retinoschisis (XLRS)

Retinoschisin (RS1), a discoidin domain family member, is a retina specific cell surface protein expressed predominantly in photoreceptor IS and bipolar cells and functions in retinal cell adhesion and lamination processes [3]. Loss of function mutations in the X-linked RS1 gene causes XLRS a form of macular degeneration seen in young males [3, 4]. The disease phenotype is mimicked in the mouse model (*Rs1*-KO), which has delamination of inner retinal layers with decreased ERG b-wave amplitudes and diminished bipolar cell signaling. Because of the robust expression of RS1 in photoreceptors and its role in maintaining the photoreceptor inner segment stability and architecture [5, 6], it is surprising that only a third of XLRS patients display photoreceptor pathology with reduced a-wave amplitude [4]. By comparison, Rs1-KO mice display reduced ERG a-wave amplitude and have shortened rod outer segment (ROS) length as early as 1 month. The mice also have slow photoreceptor loss that progresses over more than a year [7]. To address the role of RS1 in photoreceptor function, we determined the threshold light intensities for transducin and arrestin translocation in *Rs1*-KO mice at postnatal days 21 (P21) and 60 (P60) when retinal degeneration is minimal [8]

## 71.4 Translocation in *RS1*-KO Mice

*Rs1*-KO mice required higher light intensity for $G\alpha_{t1}$ translocation than age-matched WT mice at both P21 and P60 (Fig. 71.1) [8]. Complete translocation of $G\alpha_{t1}$ from ROS to the IS, ONL and OPL in adult P60 *Rs1*-KO retinas required 2.5-fold higher light intensity compared with P60 WT retinas (1 h exposure at 30 sc. cd/m$^2$ vs. 12 sc.cd/m$^2$). However, at P21, complete movement of $G\alpha_{t1}$ into the OPL was seen in *Rs1*-KO retinas only at 10-fold higher light intensity (300 sc.cd/m$^2$) compared with P21 WT retinas (30 sc.cd/m$^2$) (Fig. 71.1). Exposure for 3 h to 60 sc. cd/m$^2$ failed to cause $G\alpha_{t1}$ translocation in P21 *Rs1*-KO retinas, thus ruling out the possibility of slow movement of $G\alpha_{t1}$ as the reason for the elevated translocation threshold. In contrast to $G\alpha_{t1,}$ arrestin translocated from IS to the ROS at the same light intensity (between 1 and 2 sc.cd/m$^2$) both in WT and *Rs1*-KO retinas at P21 (Fig. 71.2). Loss of RS1 protein did not impair the axial diffusion of $G\alpha_{t1}$ and

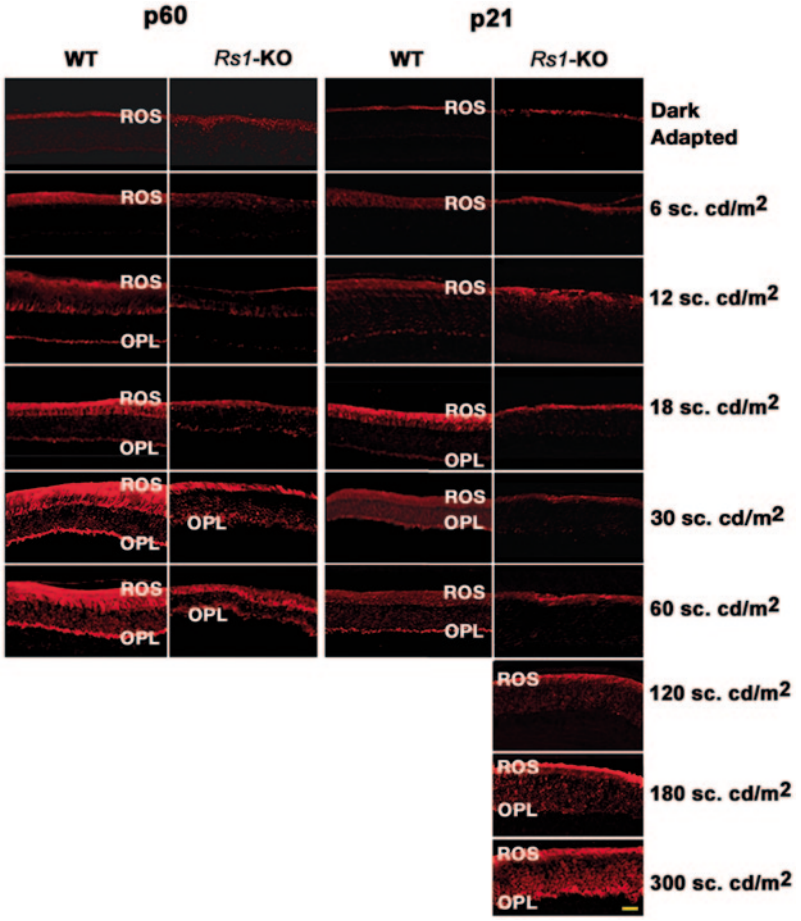


**Fig. 71.1** Light-intensity-dependent transducin translocation in WT and *Rs1*-KO mice at P21 and P60. Animals were either dark adapted or exposed to 1 h of light of different intensities (indicated on the *right*). Comparison of $G\alpha_{t1}$ distribution in WT and *Rs1*-KO mice retinas shows that, in P21 and P60 WT retinas, $G\alpha_{t1}$ translocates from *ROS* and distributes into OPL at much lower light intensities compared with *Rs1*-KO retinas. Immunofluorescence of $G\alpha_{t1}$ in P21 *Rs1*-KO retinas shows persistent staining only in the ROS. Only exposure to very bright light (180–300 sc.cd/$m^2$) caused $G\alpha_{t1}$ distribution into the OPL. Scale bar, 20 μm

arrestin between the photoreceptor compartments because re-translocation of $G\alpha_{t1}$ in the dark **(**from IS to the ROS**)** and arrestin (from ROS to IS) occurred similarly in WT and *Rs1*-KO retinas at P21.

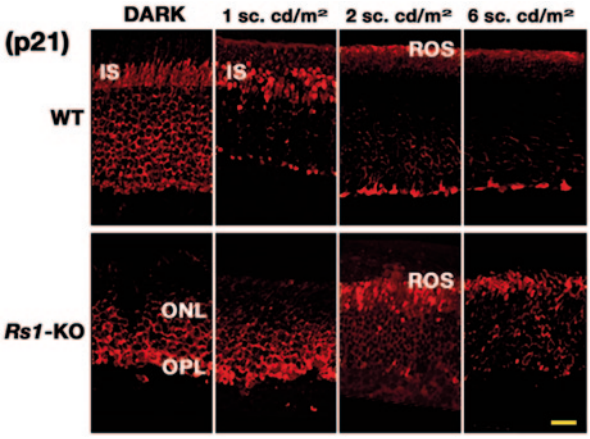


**Fig. 71.2** Arrestin movement in response to light in P21 WT and *Rs1*-KO mice: Animals were either dark adapted or exposed to 1 h of light of different intensities as indicated. Light of 2 sc.cd/m$^2$ was able to mobilize arrestin from the IS to the ROS both in WT and *Rs1*-KO mice. Scale bar, 15 µm

## 71.5 Photoreceptor Maturation and Translocation Threshold Light Intensity

Another interesting finding was the progressive decrease in luminance threshold for transducin translocation in WT mice as they mature from P18 to P21 to P60 indicating that changes in the sensitivity of transducin translocation are part of normal rod maturation [8]. *Rs1*-KO mice also showed a decrease in luminance threshold for transducin translocation from p21 to p60. However, *Rs1*-KO mice had a much higher threshold relative to WT at P21 (10X) than at P60 (2.5X, Fig. 71.1), suggesting a delay in maturation of the translocation threshold in *Rs1*-KO mice. The age related biochemical and morphological changes seen in *Rs1*-KO mice also suggest a delay in rod cell maturation processes. ROS length normally reaches adult levels in WT mice at P21 [9], but in *Rs1*-KO mice ROS length was significantly shorter at P21 but it reached adult levels by P60. *Rs1*-KO mice had reduced levels of the photoreceptor development specific transcription factors NRL and CRX at P21, but the levels were similar to WT at P60. Taken together, this indicates a delay in photoreceptor maturation in the *Rs1*-KO mouse.

## 71.6 Phototransduction in *Rs1*-KO mice

Kinetics of rhodopsin and transducin deactivation are key factors that set the speed and sensitivity of the photoresponse. Transducin levels were decreased 15–30% relative to rhodopsin in *Rs1*-KO mice at P21 but not at P60 (Fig. 71.3a) [8]. Whereas, RGS9, the GTPase-accelerating protein (GAP) for $G\alpha_{t1}$, was elevated 1.7- to 2.5-fold above WT at P21, PDE$\alpha$ and PDE$\gamma$ were slightly elevated relative to rhodopsin in *Rs1*-KO photoreceptors (Fig. 71.3b–d). Consistent with this observation, the rate of $G\alpha_{t1}$ inactivation by GTP hydrolysis was nearly two fold higher in ROS

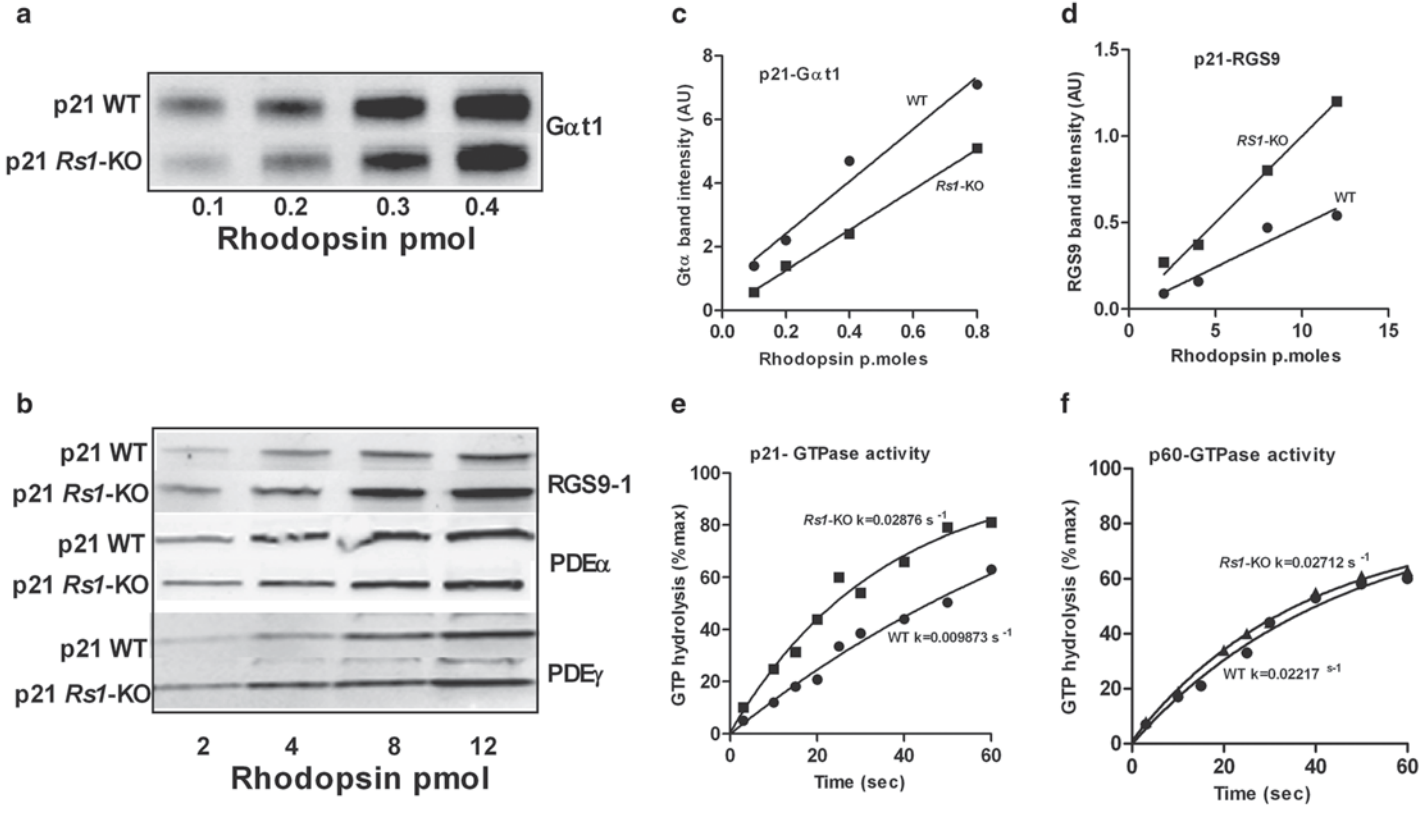
a
p21 WT
p21 Rs1-KO
Gαt1
0.1 0.2 0.3 0.4
Rhodopsin pmol
b
p21 WT
p21 Rs1-KO
RGS9-1
p21 WT
p21 Rs1-KO
PDEα
p21 WT
p21 Rs1-KO
PDEγ
2 4 8 12
Rhodopsin pmol
c
p21-Gαt1
WT
Rs1-KO
Gtα band intensity (AU)
Rhodopsin p.moles
d
p21-RGS9
RS1-KO
WT
RGS9 band intensity (AU)
Rhodopsin p.moles
e
p21- GTPase activity
Rs1-KO k=0.02876 s -1
WT k=0.009873 s -1
GTP hydrolysis (% max)
Time (sec)
f
p60-GTPase activity
Rs1-KO k=0.02712 s -1
WT k=0.02217 s-1
GTP hydrolysis (% max)
Time (sec)

of *Rs1*-KO mice (Fig. 71.3e) than in WT retinas at P21 but indistinguishable from WT at P60 (Fig. 71.3f). The increased inactivation rate in *Rs1*-KO mice at P21 results in a shorter lifetime of activated transducin, which could shift the light intensity threshold for transducin translocation to higher intensity by reducing the amount of activated transducin present during exposure.

Transducin and arrestin translocation defects were demonstrated in mouse models mimicking phototransduction gene linked diseases. One such example is bradyopsia **(**slow vision), a condition that results from mutations in genes encoding RGS9 or the RGS9 anchor protein (R9AP) [10]. Patients with bradyopsia have trouble adjusting to changing light conditions because of delay in the recovery from light responses (reduced rate of transducin GTPase activity). In the mouse model of bradyopsia, Gat1 translocated at lower (~2.3-fold) light intensity than in WT mice [11]. On the other hand, light activation threshold for Gat1 translocation was shifted to a higher light intensity in *Shaker1* mice, an animal model for Usher syndrome (USH1B) with mutations in *MYO7A* [12]. MYO7A is expressed in melanosomes of retinal pigment cells and in photoreceptor cilium, the region that links inner segments to outer segments (OS) and the sole route for delivering the proteins from IS to OS. Although this study did not show evidence of a mechanism for the shift in translocation threshold, it might be linked to decreased rhodopsin in rods, (Shaker 1 mice have been shown to have diminished ERG a-wave amplitudes) or to changes in melanosomes altering the effective light intensity in photoreceptors. Neither RS1 nor MYO7A is a member of the phototransduction cascade or is linked directly to phototransduction. Nevertheless, loss of their function affected light responses in photoreceptors. These results suggest that any defect intrinsic to photoreceptor function could in principle modulate photoresponses and thereby light adaptation.

**Fig. 71.3** Quantitative immunoblot analyses (Odyssey imaging system; LI-COR) of key phototransduction protein subunits, transducin ($G\alpha_{t1}$), RGS9, PDE6α, and PDE6γ, in dark-adapted outer segment extracts from P21 WT and *Rs1*-KO mice. $G\alpha_{t1}$ levels relative to rhodopsin were 15–30% lower in *Rs1*-KO mice than in WT (**a, c**). RGS9, the GAP for $G\alpha_{t1}$ was 1.7- to 2.5- fold higher in *Rs1*-KO than in WT (**d**). Both PDE6α and PDE6γ protein levels were marginally elevated in *Rs1*-KO retinas (**b**). The time course of phosphate formation during hydrolysis of [γ-32P] GTP by $G\alpha_{t1}$* in ROS: In single-turnover GTPase activity measurements in isolated ROS, GTP hydrolysis by $G\alpha_{t1}$ was nearly twofold higher in *Rs1*-KO than in WT at P21 (**e**). resulting in a shorter lifetime of activated $G\alpha_{t1}$ in *Rs1*-KO ROS. The rates were not different at P60 (**f**). The data were fitted to a single-phase exponential decay curve using GraphPad Prism (GraphPad Software)

## References


1. Burns ME, Arshavsky VY (2005) Beyond counting photons: trials and trends in vertebrate visual transduction. Neuron 48(3):387–401
2. Arshavsky VYBM (2012) Photoreceptor signaling: supporting vision across a wide range of light intensities. J Biol Chem 287(3):1620–1626
3. Molday RS, Kellner U, Weber BH (2012) X-linked juvenile retinoschisis: Clinical diagnosis, genetic analysis, and molecular mechanisms. Prog Retin Eye Res 31(3):195–212
4. Sikkink SK, Biswas S, Parry NR, Stanga PE, Trump D (2007) X-linked retinoschisis: an update. J Med Genet 44(4):225–232
5. Vijayasarathy C, Takada Y, Zeng Y, Bush RA, Sieving PA (2007) Retinoschisin is a peripheral membrane protein with affinity for anionic phospholipids and affected by divalent cations. Invest Ophthalmol Vis Sci 48(3):991–1000
6. Takada Y, Vijayasarathy C, Zeng Y, Kjellstrom S, Bush RA, Sieving PA (2008) Synaptic pathology in retinoschisis knockout (Rs1-/y) mouse retina and modification by rAAV-Rs1 gene delivery. Invest Ophthalmol Vis Sci 49(8):3677–3686
7. Kjellstrom S, Bush RA, Zeng Y, Takada Y, Sieving PA (2007) Retinoschisin gene therapy and natural history in the Rs1h-KO mouse: long-term rescue from retinal degeneration. Invest Ophthalmol Vis Sci 48(8):3837–3845
8. Ziccardi LVC, Bush RA, Sieving PA (2012) Loss of retinoschisin (RS1) cell surface protein in maturing mouse rod photoreceptors elevates the luminance threshold for light-driven translocation of transducin but not arrestin. J Neurosci 32(38):13010–13021
9. Fulton AB, Manning KA, Baker BN, Schukar SE, Bailey CJ (1982) Dark-adapted sensitivity, rhodopsin content, and background adaptation in pcd/pcd mice. Invest Ophthalmol Vis Sci 22(3):386–393
10. Nishiguchi KMSM, Kooijman AC, Martemyanov KA, Pott JW, Hagstrom SA, Arshavsky VY, Berson EL, Dryja TP (2004) Defects in RGS9 or its anchor protein R9AP in patients with slow photoreceptor deactivation. Nature 427(6969):75–78
11. Lobanova ES, Finkelstein S, Song H, Tsang SH, Chen CK, Sokolov M, Skiba NP, Arshavsky VY (2007) Transducin translocation in rods is triggered by saturation of the GTPase-activating complex. J Neurosci 27(5):1151–1160
12. Peng YW, Zallocchi M, Wang WM, Delimont D, Cosgrove D (2011) Moderate light induced degeneration of rod photoreceptors with delayed transducin translocation in shaker1 mice. Invest Ophthalmol Vis Sci 52(9):6421–6427

# Chapter 72
# Mouse Models for Cone Degeneration

**Marijana Samardzija and Christian Grimm**

**Abstract** Loss of cone vision has devastating effects on everyday life. Even though much effort has been made to understand cone physiology and pathophysiology, no successful therapies are available for patients suffering from cone disorders. As complex retinal interactions cannot be studied in vitro, utilization of different animal models is inevitable. Due to recent advances in transgenesis, mice became the most popular animal model to study human diseases, also in ophthalmology. While there are similarities in retinal anatomy and pathophysiology between mice and humans, there are also differences, most importantly the lack of a cone-rich macula in mice. Instead, cones in mice are rare and distributed over the whole retina, which makes the analysis of cone pathophysiology very difficult in these animals. This hindrance is one of the reasons why our understanding of rod pathophysiological processes is much more advanced. Recently, however, the sparseness of cones was overcome by the generation of the *Nrl*$^{-/-}$ mouse that expresses only cone photoreceptors in the retina. This paper will give a brief overview of some of the known mouse models to study cone degeneration and discuss the current knowledge gained from the analysis of these models.

**Keywords** Retina · Photoreceptors · Cones · Nrl · Dystrophy · Blindness · Degeneration · Mouse model

M. Samardzija (✉) · C. Grimm
Lab for Retinal Cell Biology, Department of Ophthalmology,
University of Zurich, Wagistr 14 Schlieren,
8952, Zurich, Switzerland
e-mail: marijana.samardzija@usz.uzh.ch

C. Grimm
e-mail: cgrimm@opht.uzh.ch

J. D. Ash et al. (eds.), *Retinal Degenerative Diseases,* Advances in Experimental Medicine and Biology 801, DOI 10.1007/978-1-4614-3209-8_72,

## 72.1 Introduction

The need for animal models to study retinal degeneration is undisputed. Its small size, short gestation time, simple maintenance, easy accessibility for genome manipulation, and both the anatomical and genetic similarity to the human retina, made mouse the most frequently used model to study retinal physiology and pathophysiology. In addition to the targeted generation of transgenic mice, large scale screens for spontaneous mutations within established mouse colonies as well as phenotyping the mice coming from systematic chemical mutagenesis screens [1] led to the discovery of the majority of mouse models for retinal degeneration. Here we will discuss specific models for cone degenerations. We should emphasize that the guiding idea was to describe models that are characterized by initial cone cell death, which may or may not be followed by rod cell death.

## 72.2 Cones in Health and in Disease

While rods are primarily responsible for dim-light vision, cones function under bright light and are responsible for high-acuity, color vision. Both types of photoreceptors utilize 11-*cis*-retinal as the light-sensitive chromophore. After photon absorption the chromophore is recycled in elaborate processes that may differ between rods and cones [2, 3]. Rods contain only one type of opsin molecule while cones have three possible types of photopigments; blue, green, and red that respond to short, medium, and long wavelengths of light, respectively. In the human retina, rods outnumber cones by far by a ratio 20:1 [4]. However, the macula with the most central foveal region is highly enriched in cones.

Diseases affecting cones share common symptoms like decreased visual acuity and color vision defects that may lead to complete loss of central vision. Diseases can be either stationary or progressive [5]. Stationary diseases such as complete or incomplete achromatopsia, typically affect color vision. Patients may have in addition poor visual acuity, juvenile nystagmus, and photophobia. Progressive diseases involve cone- or cone-rod dystrophies, and macular degenerations such as age-related-macular degeneration (AMD) or Stargardt disease (reviewed in [5]). The four major genes that have been identified in humans to cause cone or cone-rod dystrophies are *ABCA4*, *CRX*, *GUCY2D*, and *RPGR*. However, since a particular gene mutation may lead to different clinical outcomes, the analysis of the underlying pathological mechanisms is challenging [6].

## 72.3 Mouse Models for Cone Degeneration

Many natural and genetically engineered mouse models for retinal degeneration have been described (reviewed in [7]). However, most of these models exhibit primarily rod cell death and only few models exist to specifically study cone

degeneration. Naturally occurring *Cpfl* (cone photoreceptor function loss) mouse models were discovered after screens for ocular defects in normal mouse colonies. Most of the genes and their underlying mutations in *Cpfl* mutants were identified later. Mouse models for dry AMD have been reviewed recently [8] and they will not be the subject of this review.

### 72.3.1 *Pde6c$^{Cpfl1}$*

*Pde6c$^{Cpfl1}$* mice serve as a model for human achromatopsia. *Pde6c$^{Cpfl1}$* mice have an insertion in the *Pde6c* gene (phosphodiesterase 6C, cGMP-specific, cone, alpha prime) causing a frame shift and premature stop codon leading to a non-functional protein [9]. This results in non-detectable light-adapted ERG [9] and rapid cone degeneration peaking at 24 days of age [10]. Cones in *Pde6c$^{Cpfl1}$* mice degenerate due to toxic effects of increased cGMP accumulation. Caspase-independent cell death and calpain involvement have been demonstrated [10].

### 72.3.2 *Gnat2$^{Cpfl3}$*

*Gnat2* (guanine nucleotide binding protein [G protein]) encodes the α-subunit of cone transducin. *Gnat2$^{Cpfl3}$* mice have a missense mutation in the gene resulting in the amino acid change Asp200Asn [11]. *Gnat2$^{Cpfl3}$* mice have very early abnormal photopic responses that are reduced by 75 % as compared to controls and by 9 months of age, light-adapted responses are no longer detectable. However, no clear signs of cone cell loss are found in 14-week-old mice (last time-point analyzed). The dark-adapted ERG is normal at the beginning but some function is lost between 4 weeks and 9 months [11]. These mice were also used for the first successful gene therapy targeting cones. Function has been restored and visual acuity was improved by subretinal injections of AAV5 carrying a wild-type mouse cone alpha-transducin cDNA [12].

### 72.3.3 *Cnga3$^{-/-}$ and Cnga3$^{Cpfl5}$*

Cnga3 (alpha-3 cyclic nucleotide-gated channel) is an essential protein of CNG channels in the plasma membrane of cone outer segments and thus has key functions in phototransduction and calcium homeostasis in cones. Two mouse models exist: *Cnga3$^{-/-}$* mice with a targeted deletion of exon 7 [13], and *Cnga3$^{Cpfl5}$* mice with a spontaneous missense mutation in exon 5 leading to an Ala492Thr amino acid exchange [14]. Both mice have no cone-mediated light response and show progressive cone cell degeneration. Rod function is largely preserved initially but is reduced at 1 year of age, concomitantly with a slowly progressing rod degeneration

[15]. Such retinal phenotype characterized by secondary impairment of rod function was described in patients suffering from achromatopsia that are caused by mutations in the *CNGB3* gene [16].

### 72.3.4 *Cngb3*$^{-/-}$

Mutations in CNGB3 (beta-3 cyclic nucleotide-gated channel) account for 50 % of all known cases of achromatopsia in patients [17]. *Cngb3*$^{-/-}$ mice show an early-onset, slowly progressing decrease in light-adapted ERG responses and cone cell density. Scotopic ERG is normal in the young retina [18]. Loss of CNGB3 reduces biosynthesis of CNGA3 and impairs cone CNG channel function [18]. This reduces intracellular calcium concentrations and may cause the accumulation of cGMP, which may trigger oxidative stress leading to apoptotic cell death. In addition, evidence also suggest that endoplasmic reticulum stress may contribute to cone degeneration [19].

### 72.3.5 *Abca4*$^{-/-}$

ABCA4 (ATP-binding cassette transporter 4) is a photoreceptor specific transmembrane protein involved in the clearance of all-*trans*-retinal from outer segments. Mutations in *ABCA4* gene lead to diverse pathologies from Stargardts disease to retinitis pigmentosa. *Abca4*$^{-/-}$ mice accumulate toxic lipofuscin granules in the RPE, suffer from increased oxidative stress and complement activation, show thickening of the Bruch's membrane, have delayed dark adaptation and reduced clearance of all-*trans*-retinal [20, 21]. However, no retinal degeneration is detected in pigmented *Abca4*$^{-/-}$ mice up to 44 weeks of age [21].

### 72.3.6 *Elovl4 Mutant Mice*

The *ELOVL4* (elongation of very long chain fatty acids-like 4) gene encodes an elongase required for the synthesis of very long chain polyunsaturated fatty acids [22]. It is a membrane protein with an ER retention signal at the C-terminus [23]. Mutations in *ELOVL4* lead to autosomal dominant Stargardt macular dystrophy (STGD3). All mutations identified in STGD3 patients cause the expression of a truncated *ELOVL4* protein lacking the ER retention signal [22].

Several models based on ELOVL4 have been generated: transgenic mice expressing a human *ELOVL4* cDNA with a 5-bp deletion that leads to the truncated form of the protein [24], knock-in mice that harbor a similar 5-bp deletion in the endogenous mouse gene [25], knock-in mice that produce an ELOVL4 protein with an aberrant 8-amino acid C-terminal [26], two knock-out mice [27, 28], and mice

with a photoreceptor-specific *Elovl4* knock-out [29]. While homozygous knock-out mice die perinatally due to severe skin permeability defects, heterozygous mice show no apparent phenotype [25].

Heterozygous mice expressing a truncated ELOVL4 together with the wild-type protein form, mimic several features of the human disease such as lipofuscin accumulation, RPE atrophy, accumulation of subretinal debris, and retinal degeneration [24, 25]. Surprisingly, rod- or cone-specific knock-out of *Elovl4* does not result in retinal degeneration and only mildly influences function [29]. All of this argues that dysfunction and not lack of the protein is the cause of retinal disease.

### *72.3.7 Nrl$^{-/-}$*

Neural retina leucin zipper (NRL) is a transcription factor necessary to generate rod cells from progenitors. In the absence of NRL all photoreceptor precursors are driven into a cone cell fate resulting in an excessive generation of S-cones during development [30]. The all-cone retina of the *Nrl*$^{-/-}$ mouse is therefore very attractive for the analysis of cone cell death, which may be induced chemically or genetically. Indeed, cone degeneration was studied in double mutant *Nrl*$^{-/-}$*;Grk1*$^{-/-}$ which show age-related and light independent cone cell loss [31].

## 72.4 Conclusions

Several models now exist to study mechanisms of cone degeneration. However, certain limitations have to be considered when using these mice in ophthalmology. Mice have dichromatic vision, lack a macula, have a short life span and live mostly in a pathogen-free environment. All of this is important when ageing diseases and the involvement of the immune system in retinal pathologies have to be considered.

Nevertheless, the current mouse models are very helpful to acquire knowledge about cone physiology and pathophysiology. The use of the all-cone *Nrl*$^{-/-}$ mouse to express mutations, which were found to cause cone degeneration in humans, may be a promising approach to facilitate cone-related research and to gain the knowledge necessary for the development of future therapies to treat patients.

## References

1. Won J, Shi LY, Hicks W, Wang J, Hurd R, Naggert JK, Chang B, Nishina PM (2011) Mouse model resources for vision research. J Ophthalmol 2011:391384
2. Wang JS, Estevez ME, Cornwall MC, Kefalov VJ (2009) Intra-retinal visual cycle required for rapid and complete cone dark adaptation. Nat Neurosci 12:295–302
3. Wang JS, Kefalov VJ (2009) An alternative pathway mediates the mouse and human cone visual cycle. Curr Biol 19:1665–1669

4. Curcio CA, Allen KA, Sloan KR, Lerea CL, Hurley JB, Klock IB, Milam AH (1991) Distribution and morphology of human cone photoreceptors stained with anti-blue opsin. J Comp Neurol 312:610–624
5. Berger W, Kloeckener-Gruissem B, Neidhardt J (2010) The molecular basis of human retinal and vitreoretinal diseases. Prog Retin Eye Res 29:335–375
6. Hamel CP (2007) Cone rod dystrophies. Orphanet J Rare Dis 2:7
7. Samardzija M, Neuhauss SCF, Joly S, Kurz-Levin M, Grimm C (2010) Animal models for retinal degeneration. Neuromethods 46:51–79
8. Ramkumar HL, Zhang J, Chan CC (2010) Retinal ultrastructure of murine models of dry age-related macular degeneration (AMD). Prog Retin Eye Res 29:169–190
9. Chang B, Grau T, Dangel S, Hurd R, Jurklies B, Sener EC, Andreasson S, Dollfus H, Baumann B, Bolz S, Artemyev N, Kohl S, Heckenlively J, Wissinger B (2009) A homologous genetic basis of the murine cpfl1 mutant and human achromatopsia linked to mutations in the PDE6C gene. Proc Natl Acad Sci U S A 106:19581–19586
10. Trifunovic D, Dengler K, Michalakis S, Zrenner E, Wissinger B, Paquet-Durand F (2010) cGMP-dependent cone photoreceptor degeneration in the cpfl1 mouse retina. J Comp Neurol 518:3604–3617
11. Chang B, Dacey MS, Hawes NL, Hitchcock PF, Milam AH, Atmaca-Sonmez P, Nusinowitz S, Heckenlively JR (2006) Cone photoreceptor function loss-3, a novel mouse model of achromatopsia due to a mutation in Gnat2. Invest Ophthalmol Vis Sci 47:5017–5021
12. Alexander JJ, Umino Y, Everhart D, Chang B, Min SH, Li Q, Timmers AM, Hawes NL, Pang JJ, Barlow RB, Hauswirth WW (2007) Restoration of cone vision in a mouse model of achromatopsia. Nat Med 13:685–687
13. Biel M, Seeliger M, Pfeifer A, Kohler K, Gerstner A, Ludwig A, Jaissle G, Fauser S, Zrenner E, Hofmann F (1999) Selective loss of cone function in mice lacking the cyclic nucleotide-gated channel CNG3. Proc Natl Acad Sci U S A 96:7553–7557
14. Hawes N, Wang X, Hurd RE, Wang J, Davisson MT, Nusinowitz S, Heckenlively JR, Chang B (2006) A point mutation in the Cnga3 gene causes cone photoreceptor function loss (cpfl5) in mice. Invest Ophthalmol Vis Sci 47: E-Abstr 4579
15. Xu J, Morris LM, Michalakis S, Biel M, Fliesler SJ, Sherry DM, Ding XQ (2012) CNGA3 deficiency affects cone synaptic terminal structure and function and leads to secondary rod dysfunction and degeneration. Invest Ophthalmol Vis Sci 53:1117–1129
16. Khan NW, Wissinger B, Kohl S, Sieving PA (2007) CNGB3 achromatopsia with progressive loss of residual cone function and impaired rod-mediated function. Invest Ophthalmol Vis Sci 48:3864–3871
17. Kohl S, Varsanyi B, Antunes GA, Baumann B, Hoyng CB, Jagle H, Rosenberg T, Kellner U, Lorenz B, Salati R, Jurklies B, Farkas A, Andreasson S, Weleber RG, Jacobson SG, Rudolph G, Castellan C, Dollfus H, Legius E, Anastasi M, Bitoun P, Lev D, Sieving PA, Munier FL, Zrenner E, Sharpe LT, Cremers FP, Wissinger B (2005) CNGB3 mutations account for 50% of all cases with autosomal recessive achromatopsia. Eur J Hum Genet 13:302–308
18. Ding XQ, Harry CS, Umino Y, Matveev AV, Fliesler SJ, Barlow RB (2009) Impaired cone function and cone degeneration resulting from CNGB3 deficiency: down-regulation of CNGA3 biosynthesis as a potential mechanism. Hum Mol Genet 18:4770–4780
19. Thapa A, Morris L, Xu J, Ma H, Michalakis S, Biel M, Ding XQ (2012) Endoplasmic reticulum stress-associated cone photoreceptor degeneration in cyclic nucleotide-gated channel deficiency. J Biol Chem 287:18018–18029
20. Radu RA, Hu J, Yuan Q, Welch DL, Makshanoff J, Lloyd M, McMullen S, Travis GH, Bok D (2011) Complement system dysregulation and inflammation in the retinal pigment epithelium of a mouse model for Stargardt macular degeneration. J Biol Chem 286:18593–18601
21. Weng J, Mata NL, Azarian SM, Tzekov RT, Birch DG, Travis GH (1999) Insights into the function of Rim protein in photoreceptors and etiology of Stargardt's disease from the phenotype in abcr knockout mice. Cell 98:13–23

22. Agbaga MP, Brush RS, Mandal MN, Henry K, Elliott MH, Anderson RE (2008) Role of Stargardt-3 macular dystrophy protein (ELOVL4) in the biosynthesis of very long chain fatty acids. Proc Natl Acad Sci U S A 105:12843–12848
23. Ambasudhan R, Wang X, Jablonski MM, Thompson DA, Lagali PS, Wong PW, Sieving PA, Ayyagari R (2004) Atrophic macular degeneration mutations in ELOVL4 result in the intracellular misrouting of the protein. Genomics 83:615–625
24. Karan G, Lillo C, Yang Z, Cameron DJ, Locke KG, Zhao Y, Thirumalaichary S, Li C, Birch DG, Vollmer-Snarr HR, Williams DS, Zhang K (2005) Lipofuscin accumulation, abnormal electrophysiology, and photoreceptor degeneration in mutant ELOVL4 transgenic mice: a model for macular degeneration. Proc Natl Acad Sci U S A 102:4164–4169
25. Vasireddy V, Jablonski MM, Mandal MN, Raz-Prag D, Wang XF, Nizol L, Iannaccone A, Musch DC, Bush RA, Salem NJ, Sieving PA, Ayyagari R (2006) Elovl4 5-bp-deletion knock-in mice develop progressive photoreceptor degeneration. Invest Ophthalmol Vis Sci 47:4558–4568
26. McMahon A, Butovich IA, Mata NL, Klein M, Ritter R, Richardson J, Birch DG, Edwards AO, Kedzierski W (2007) Retinal pathology and skin barrier defect in mice carrying a Stargardt disease-3 mutation in elongase of very long chain fatty acids-4. Mol Vis 13:258–272
27. Raz-Prag D, Ayyagari R, Fariss RN, Mandal MN, Vasireddy V, Majchrzak S, Webber AL, Bush RA, Salem NJ, Petrukhin K, Sieving PA (2006) Haploinsufficiency is not the key mechanism of pathogenesis in a heterozygous Elovl4 knockout mouse model of STGD3 disease. Invest Ophthalmol Vis Sci 47:3603–3611
28. Li W, Chen Y, Cameron DJ, Wang C, Karan G, Yang Z, Zhao Y, Pearson E, Chen H, Deng C, Howes K, Zhang K (2007) Elovl4 haploinsufficiency does not induce early onset retinal degeneration in mice. Vision Res 47:714–722
29. Harkewicz R, Du H, Tong Z, Alkuraya H, Bedell M, Sun W, Wang X, Hsu YH, Esteve-Rudd J, Hughes G, Su Z, Zhang M, Lopes VS, Molday RS, Williams DS, Dennis EA, Zhang K (2012) Essential role of ELOVL4 protein in very long chain fatty acid synthesis and retinal function. J Biol Chem 287:11469–11480
30. Mears AJ, Kondo M, Swain PK, Takada Y, Bush RA, Saunders TL, Sieving PA, Swaroop A (2001) Nrl is required for rod photoreceptor development. Nat Genet 29:447–452
31. Yetemian RM, Brown BM, Craft CM (2010) Neovascularization, enhanced inflammatory response, and age-related cone dystrophy in the Nrl−/−Grk1−/− mouse retina. Invest Ophthalmol Vis Sci 51:6196–6206

# Chapter 73
# How Long Does a Photoreceptor Cell Take to Die? Implications for the Causative Cell Death Mechanisms

**F. Paquet-Durand, A. Sahaboglu, J. Dietter, O. Paquet-Durand, B. Hitzmann, M. Ueffing and P. A. R. Ekström**

**Abstract** The duration of cell death may allow deducing the underlying degenerative mechanism. To find out how long a photoreceptor takes to die, we used the *rd1* mouse model for retinal neurodegeneration, which is characterized by phosphodiesterase-6 (PDE6) dysfunction and photoreceptor death triggered by high cGMP levels. Based on cellular data on the progression of cGMP accumulation, cell death, and survival, we created a mathematical model to simulate the temporal development of the degeneration and the clearance of dead cells. Both cellular data and modelling suggested that at the level of the individual cell, the degenerative process was rather slow, taking around 80 h to complete. Organotypic retinal explant cultures derived from wild-type animals and exposed to the selective PDE6 inhibitor zaprinast, confirmed the surprisingly long duration of an individual photoreceptor cell's death. We briefly discuss the possibility to link different cell death stages and

F. Paquet-Durand (✉) · A. Sahaboglu · J. Dietter · M. Ueffing
François Paquet-Durand, Institute for Ophthalmic Research, University of Tübingen,
Röntgenweg 11,
72076, Tübingen, Germany
e-mail: francois.paquet-durand@klinikum.uni-tuebingen.de

A. Sahaboglu
e-mail: aysesahaboglu@hotmail.com

J. Dietter
e-mail: johannes.dietter@uni-tuebingen.de

M. Ueffing
e-mail: marius.ueffing@uni-tuebingen.de

O. Paquet-Durand · B. Hitzmann
Institute of Food Science and Biotechnology, University of Stuttgart Hohenheim, Stuttgart, Germany
e-mail: o.paquet-durand@uni-hohenheim.de

B. Hitzmann
e-mail: bernd.hitzmann@uni-hohenheim.de

P. A. R. Ekström
Department of Clinical Sciences, University of Lund, Lund, Sweden
e-mail: per.ekstrom@med.lu.se

J. D. Ash et al. (eds.), *Retinal Degenerative Diseases,* Advances in Experimental Medicine and Biology 801, DOI 10.1007/978-1-4614-3209-8_73,

their temporal progression to specific enzymatic activities known to be causally connected to cell death. This in turn opens up new perspectives for the treatment of inherited retinal degeneration, both in terms of therapeutic targets and temporal windows-of-opportunity.

**Keywords** TUNEL · Apoptosis · Necrosis · cGMP · PKG · CNG channel · HDAC · PARP

## 73.1 Introduction

Inherited photoreceptor degeneration is a currently untreatable condition that often leads to complete blindness. The mechanisms of cell death that govern retinal degeneration are poorly understood to date and have in the past been suggested to involve apoptosis [1], necrosis [2], or non-apoptotic cell death [3]. Since different cell death pathways run on different time-scales, knowledge on the temporal duration of an individual photoreceptor cell's death could potentially be used for identification of the underlying cell death mechanisms. For instance, necrosis is a rapid, chaotic, and unordered destruction of the cell, taking between a few minutes to 1–2 h to complete [4], whereas apoptosis is a comparatively slow, program driven, and orderly cellular disintegration that may take 6–18 h to complete [5]. In addition, the analysis of the time-course of cell death in a living neuronal tissue will define the window-of-opportunity for treatment and may thus determine therapeutic strategies.

Previous attempts to define the precise time-frame for cell death were limited by the lack of markers for the beginning of cellular deterioration. Therefore, most knowledge on cell death duration relates to the late phases of cell death, identified by pyknosis or DNA fragmentation (DAPI or TUNEL staining, respectively). This "clearance time" was suggested to last 1–5 h in different models for neurodegeneration [6]. However, pathological alterations of nuclear structure are late events during the death process; the clearance time therefore relates only to the duration of the final stage of cell death.

To study the total duration of photoreceptor death, we used the *rd1* mouse, a homologous animal model for Retinitis Pigmentosa with an early, rapid loss of photoreceptors. The *rd1* mutation leads to loss-of-activity in rod photoreceptor cGMP phosphodiesterase-6 (PDE6) [7] and an accumulation of cGMP, triggering cell death [8, 9]. Interestingly, and very similar to many other neurodegeneration models, the *rd1* mouse shows a constant rate of cell death, resembling the exponential decay of radioactive elements [10]. Starting from there, we used different cell death markers to create a mathematical model to estimate the temporal characteristics of photoreceptor neurodegeneration in vivo. This article summarizes the main findings presented in Poster 104 at the RD2012 meeting and published in early 2013 in Cell Death & Disease [11]. Additional conclusions are discussed.

## 73.2 Materials and Methods

C3H *rd1*/*rd1* (*rd1*) and control C3H wild-type (*wt*) mice were used according to regulations specified by the local ethics committee at Tübingen University. Day of birth was considered as postnatal day (PN) 0. Organotypic retinal explant cultures were generated using P5 *rd1* and *wt* animals as described before [8, 12]. Immunostaining and TUNEL assay were performed as reported previously [8, 12]. For modelling cell death progression, irreversible first order kinetics were assumed [10]. The model consisted of six stages, termed "healthy" (H), "transition state-1" ($Tr_1$), "cGMP-positive" (cGMP⊕), "transition state-2" ($Tr_2$), "TUNEL-positive" (TU⊕), and "dead" (D). For a complete description of materials and methods please refer to [11].

## 73.3 Results

### *73.3.1 cGMP and Photoreceptor Cell Death*

cGMP accumulation found in *rd1* photoreceptors is the first sign of imminent cellular degeneration [9], while the corresponding endpoint is easily detected using the TUNEL method. Interestingly, even though high cGMP triggers TUNEL positive *rd1* cell death [8], cGMP did not co-label with TUNEL in photoreceptor cells [11]. Thus, PDE6 dysfunction caused a temporary rise in cGMP, followed by intermediate, cGMP-negative processes, before the cells turned TUNEL positive, to be finally cleared away. Our methodology; therefore, provided an opportunity to study three different and temporally unique events during an individual photoreceptor cell's death.

Only very rarely were cGMP positive cells observed in wild-type retinal cross-sections, usually at early postnatal (PN) days. In contrast, the number of cGMP positive photoreceptors was significantly elevated in the outer nuclear layer (ONL) of the *rd1* retina already from PN8. The early postnatal mouse retina shows some developmental photoreceptor cell death [13], seen also here by the TUNEL assay in *wt* specimens. While *rd1* photoreceptor cell death was numerically higher at PN9 when compared to *wt*, statistically significant differences were found only from PN11 onwards. The delay between the significant rise of cGMP at PN8, and TUNEL at PN11, indicated that photoreceptor death execution could take as long as two to three days.

Both the percentages of cGMP positive and dying ONL cells peaked at PN13 in the *rd1* retina (Fig. 73.1a). After PN13 the numbers for cGMP and TUNEL positive cells declined, but cells with high cGMP remained more numerous than TUNEL positive cells suggesting that cGMP positivity lasted longer than TUNEL positivity. The amount of surviving photoreceptor rows showed a minor decrease in *wt* retina (due to developmental processes), while in *rd1* retina photoreceptors were rapidly

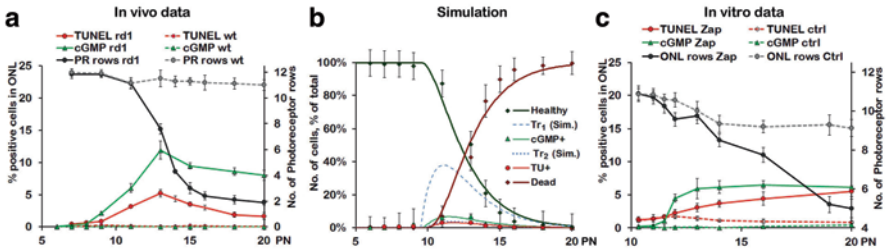


**Fig. 73.1** Comparison of *in vivo*, simulation, and *in vitro* data. **a** Progression of *cGMP* (*green*), *TUNEL* (*red*), and photoreceptor viability (*black*) in *rd1* retina during the first 20 postnatal (*PN*) days. **b** The simulation used normalized data sets and included equations for dead photoreceptors (*dark red*) and transition stages $Tr_1$, $Tr_2$ (*dotted lines*). **c** Zaprinast treatment of *wt* retina produced cell death kinetics similar to the *rd1 in vivo* situation and the model simulation. Together, these data sets suggest a total cell death duration of around 80 h (cf. Fig. 73.2). (Figure modified after [11])

lost from PN11 onwards (Fig. 73.1a). This data served as an index of the clearance of cells.

### *73.3.2 Simulating Photoreceptor Cell Death Kinetics*

Based on the in vivo data on cGMP accumulation, TUNEL positivity, and survival of photoreceptors, we constructed a mathematical model for the temporal progression of neurodegeneration in the *rd1* retina (Fig. 73.1b). We reasoned that in addition to three phases defined by cGMP, TUNEL, and clearance of cells, at least two additional transition states must exist: (1) A first one which, while cGMP-negative, eventually causes excessively high cGMP. (2) A second one in between cGMP and TUNEL positivity, since these two markers were apparently not co-localized. Together with an initial "healthy" stage a total of six different stages were considered, going from healthy (H) to transition-1 ($Tr_1$) to high cGMP (cGMP⊕) to transition-2 ($Tr_2$) to TUNEL-positive (TU⊕) to dead (D). The dynamics of these were described by differential equations yielding the average life-time for each stage. The simulated times for the different death stages were: 35.3±3.4 h for $Tr_1$, 35.7±4.0 h for cGMP⊕, 5.6±0.9 h for $Tr_2$, and 7.2±1.3 h for TU⊕. Altogether, the average time for an individual cell to die was predicted as: 83.8±9.4 h [11].

### *73.3.3 Simulating the rd1 Degeneration with Zaprinast*

To test and validate the model predictions, we used organotypic retinal explant cultures derived from *wt* animals, exposed to the selective PDE6 inhibitor zaprinast [14]. Zaprinast raises intracellular cGMP levels and induces *wt* photoreceptor degeneration similar to what is seen in *rd1* retina [8, 12]. Zaprinast treatment

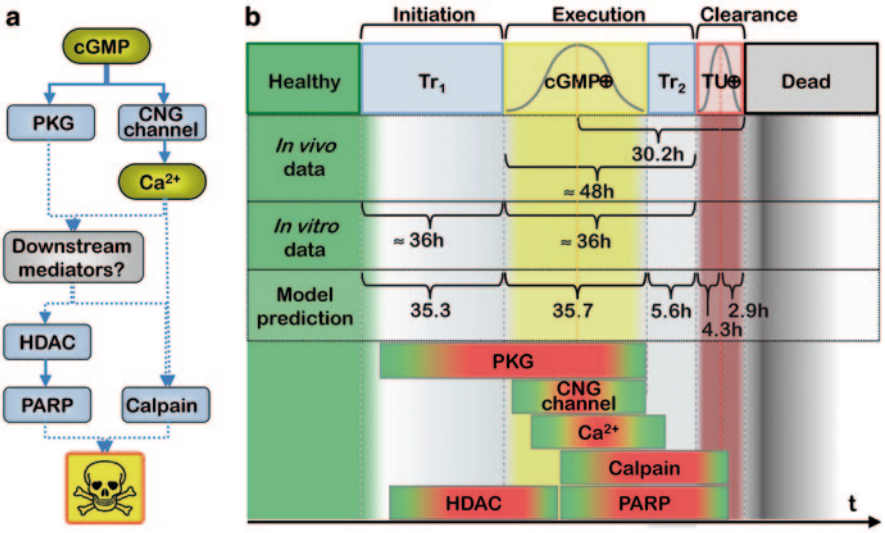


**Fig. 73.2** Proposed cell death mechanism and temporal progression. **a** Based on previous results [8, 12, 15, 16], a pathway for cGMP-dependent photoreceptor death is proposed. **b** The *in vivo, in vitro*, and modelling results suggest a total duration of cell death of approximately 80 h. The different stages of cell death and their respective durations may be linked to corresponding enzymatic activities. *TU⊕* = TUNEL. (Figure modified after [3, 11])

was started at PN10 and the effects on cGMP levels and TUNEL positivity were investigated at time-points ranging from 8 h to 10 days (d). A significant rise in cGMP positive cells was detected after 36 h of zaprinast treatment and at all later time-points assessed (Fig. 73.1c). Retinal explantation is a traumatic event and the cultures therefore displayed elevated rates of TUNEL positive cells even under control conditions. Still, zaprinast caused a significant rise in cell death, albeit only after 72 h of treatment.

In culture, the number of photoreceptor rows in the ONL in vitro is decreasing more strongly than it would in vivo, in healthy *wt* retina (Fig. 73.1c). This cell loss was further and significantly exacerbated by zaprinast from 6d of treatment onward. The delay of almost 36 h between the zaprinast induced rise of cGMP and the rise of cell death another 36 h later corresponded well to both the in vivo findings and the mathematical modelling (Fig. 73.2).

## 73.4 Discussion

Despite a rapid progression of overall tissue degeneration, inherited neuronal cell death in the retina is a surprisingly slow process at the individual cell level. Since a total duration of cell death of approximately 80 h is incompatible with the execution of necrotic or apoptotic cell death, the outcome points toward an execution of

non-necrotic, non-apoptotic, and relatively slow cell death mechanisms. This has clear relevance for the development of potential therapies, since the identification of the window-of-opportunity and the underlying degenerative mechanism will define possible treatment approaches.

Previously, photoreceptor cell death was found to be causally connected to the enzymatic activities of PKG [8], HDAC [15], PARP [12], and calpain [16] and a preliminary sketch of the corresponding cell death pathways was suggested [3] (Fig. 73.2). The mathematical model now presented may be extended to also include these processes—possibly in combination with the use of transgenic biosensors for cGMP and $Ca^{2+}$ [17]—to allow for their precise temporal delineation. This in turn could highlight novel targets for neuroprotection, namely enzymatic processes with a particularly wide window-of-opportunity.

**Acknowledgment** We thank T. Euler, B. Arango-Gonzalez, and D. Trifunović for helpful comments and discussions. This work was supported by grants from DFG [Pa1751/4-1, 1-1], EU [DRUGSFORD: HEALTH-F2-2012-304963], and the Kerstan Foundation.

## References

1. Chang GQ, Hao Y, Wong F (1993) Apoptosis: final common pathway of photoreceptor death in rd, rds, and rhodopsin mutant mice. Neuron 11:595–605
2. Trichonas G, Murakami Y, Thanos A, Morizane Y, Kayama M, Debouck CM et al (2010) Receptor interacting protein kinases mediate retinal detachment-induced photoreceptor necrosis and compensate for inhibition of apoptosis. Proc Natl Acad Sci U S A 107:21695–21700
3. Trifunovic D, Sahaboglu A, Kaur J, Mencl S, Zrenner E, Ueffing M et al (2012) Neuroprotective Strategies for the Treatment of Inherited Photoreceptor Degeneration. Curr Mol Med 12:598–612
4. Zong WX, Thompson CB (2006) Necrotic death as a cell fate. Genes Dev 20:1–15
5. Oppenheim RW, Flavell RA, Vinsant S, Prevette D, Kuan CY, Rakic P (2001) Programmed cell death of developing mammalian neurons after genetic deletion of caspases. J Neurosci 21:4752–4760
6. Gohlke JM, Griffith WC, Faustman EM (2004) The role of cell death during neocortical neurogenesis and synaptogenesis: implications from a computational model for the rat and mouse. Brain Res Dev Brain Res 151:43–54
7. Bowes C, Li T, Danciger M, Baxter LC, Applebury ML, Farber DB (1990) Retinal degeneration in the rd mouse is caused by a defect in the beta subunit of rod cGMP-phosphodiesterase. Nature 347:677–680
8. Paquet-Durand F, Hauck SM, van Veen T, Ueffing M, Ekstrom P (2009) PKG activity causes photoreceptor cell death in two retinitis pigmentosa models. J Neurochem 108:796–810
9. Lolley RN, Farber DB, Rayborn ME, Hollyfield JG (1977) Cyclic GMP accumulation causes degeneration of photoreceptor cells: simulation of an inherited disease. Science 196:664–666
10. Clarke G, Collins RA, Leavitt BR, Andrews DF, Hayden MR, Lumsden CJ et al (2000) A one-hit model of cell death in inherited neuronal degenerations. Nature 406:195–199
11. Sahaboglu A, Paquet-Durand O, Dietter J, Dengler K, Bernhard-Kurz S, Ekström P et al (2013) Retinitis pigmentosa: rapid neurodegeneration is governed by slow cell death mechanisms. Cell Death Dis 4:e488
12. Sahaboglu A, Tanimoto N, Kaur J, Sancho-Pelluz J, Huber G, Fahl E et al (2010) PARP1gene knock-out increases resistance to retinal degeneration without affecting retinal function. PLoS ONE 5:e15495-

13. Trifunovic D, Dengler K, Michalakis S, Zrenner E, Wissinger B, Paquet-Durand F (2010) cGMP-dependent cone photoreceptor degeneration in the cpfl1 mouse retina. J Comp Neurol 518:3604–3617
14. Zhang X, Feng Q, Cote RH (2005) Efficacy and selectivity of phosphodiesterase-targeted drugs in inhibiting photoreceptor phosphodiesterase (PDE6) in retinal photoreceptors. Invest Ophthalmol Vis Sci 46:3060–3066
15. Sancho-Pelluz J, Alavi M, Sahaboglu A, Kustermann S, Farinelli P, Azadi S et al (2010) Excessive HDAC activation is critical for neurodegeneration in the rd1 mouse. Cell Death Dis 1:1–9
16. Paquet-Durand F, Beck S, Michalakis S, Goldmann T, Huber G, Muhlfriedel R et al (2011) A key role for cyclic nucleotide gated (CNG) channels in cGMP-related retinitis pigmentosa. Hum Mol Genet 20:941–947
17. Wei T, Schubert T, Paquet-Durand F, Tanimoto N, Chang L, Koeppen K et al (2012) Generation and functional characterization of a transgenic mouse expressing a $Ca^{2+}$ biosensor in cone photoreceptors. J Neurosci 32:6994–6981

# Part VIII
# Degenerative Processes: RPE and Fatty Acids

# Chapter 74
# Endoplasmic Reticulum Stress in Vertebrate Mutant Rhodopsin Models of Retinal Degeneration

**Heike Kroeger, Matthew M. LaVail and Jonathan H. Lin**

**Abstract** *Rhodopsin* mutations cause many types of heritable retinitis pigmentosa (RP). Biochemical and in vitro studies have demonstrated that many RP-linked mutant *rhodopsins* produce misfolded rhodopsin proteins, which are prone to aggregation and retention within the endoplasmic reticulum, where they cause endoplasmic reticulum stress and activate the Unfolded Protein Response signaling pathways. Many vertebrate models of retinal degeneration have been created through expression of RP-linked *rhodopsins* in photoreceptors including, but not limited to, *VPP/GHL* mice, *P23H Rhodopsin* frogs, *P23H rhodopsin* rats, *S334ter rhodopsin* rats, *C185R rhodopsin* mice, *T17M rhodopsin* mice, and *P23H rhodopsin* mice. These models have provided many opportunities to test therapeutic strategies to prevent retinal degeneration and also enabled in vivo investigation of cellular and molecular mechanisms responsible for photoreceptor cell death. Here, we examine and compare the contribution of endoplasmic reticulum stress to retinal degeneration in several vertebrate models of RP generated through expression of mutant *rhodopsins*.

**Keywords** Rhodopsin · Retinitis pigmentosa · P23H rhodopsin · Endoplasmic reticulum · Unfolded Protein Response · Photoreceptors

J. H. Lin (✉) · H. Kroeger
Department of Pathology, University of California, San Diego, USA
e-mail: jlin@ucsd.edu

H. Kroeger
e-mail: hkroeger@ucsd.edu

M. M. LaVail
Departments of Anatomy and Ophthalmology, University of California, San Francisco, USA
e-mail: matthew.lavail@ucsf.edu

J. D. Ash et al. (eds.), *Retinal Degenerative Diseases,* Advances in Experimental Medicine and Biology 801, DOI 10.1007/978-1-4614-3209-8_74,

**Abbreviations**

| | |
|---|---|
| RP | Retinitis pigmentosa |
| ER | Endoplasmic reticulum |
| UPR | Unfolded Protein Response |
| *VPP* | **V**20G, **P**23H, and **P**27L mutations |
| *GHL* | V20**G**, P23**H**, and P27**L** mutations |

## 74.1 Introduction

*Rhodopsin* encodes a G protein-coupled multipass transmembrane protein that is expressed solely in rod photoreceptors and is essential for phototransduction [1]. Many heritable types of RP are caused by mutations in *rhodopsin* (www.sph.uth.tmc.edu/retnet). Biochemical studies in heterologous cell culture expression systems have found that many RP-linked *rhodopsin* mutations generate mutant rhodopsin proteins that are misfolded, abnormally aggregated, and are retained within the endoplasmic reticulum (ER) by ER protein quality control mechanisms such as the Unfolded Protein Response (UPR) [2–7]. Many animal models of retinal degeneration have also been developed through expression of mutant rhodopsins in photoreceptors. Here, we compare roles for ER stress in several vertebrate models of retinal degeneration expressing mutant rhodopsins.

## 74.2 VPP and GHL Transgenic Mice

"*VPP*" and "*GHL*" transgenic mice both express genetically modified mouse *opsin* bearing V20G, P23H, and P27L mutations under mouse opsin promoter control and have been widely studied as models of human RP [8, 9]. In these mice, in the absence of any wild-type rhodopsin (in rhodopsin knockout background), the triple mutant rhodopsin aggregates as abnormal dimers and is found mostly within the rod inner segment co-localizing with ER markers [9]. By contrast, in the presence of wild-type rhodopsin, fewer abnormal rhodopsin dimers are formed, and mutant rhodopsin can be detected in the rod outer segment [10]. These findings indicate that the photoreceptor recognizes the triple mutant rhodopsin as a misfolded protein and retains it in the ER, where it likely causes ER stress and activates UPR signaling. These findings also suggest that wild-type rhodopsin somehow reduces the levels of abnormal rhodopsin dimers and enables mutant rhodopsin protein to exit from ER to the outer segment, when both wild-type and mutant rhodopsin are co-expressed in photoreceptors. This alleviation may be incompletely sustained since these animals still ultimately develop photoreceptor cell loss.

## 74.3 P23H Rhodopsin Transgenic *Xenopus Laevis*

Transgenic *Xenopus laevis* expressing *X. laevis* rhodopsin bearing a P23H mutation under the control of the *X. laevis* opsin promoter develop progressive retinal degeneration in a transgene dose-dependent manner [11]. Mutant *X. laevis* P23H rhodopsin predominantly localizes within the rod inner segment in transgenic *X. laevis*, co-localizing with the ER-resident calnexin protein [11]. Mutant *X. laevis* P23H rhodopsin protein also forms abnormal dimers and other higher order protein aggregates in solubilized retina lysates from these animals [11]. These findings in transgenic *X. laevis* indicate that *X. laevis* mutant P23H rhodopsin is misfolded and retained in the ER. Interestingly, endogenous wild-type *X. laevis* rhodopsin is still expressed in these animals, but amelioration of the abnormal aggregation and ER retention has not been reported for P23H rhodopsin protein despite co-expression of the wild-type protein.

## 74.4 P23H Rhodopsin Transgenic Rat

Transgenic rats expressing mouse *opsin* bearing P23H mutation under mouse opsin promoter control develop retinal degeneration in a transgene dose-dependent manner and are widely used to study retinal degeneration mechanisms and therapeutics [12–14]. Molecular studies have found increased levels of ER stress-induced and UPR signaling pathway-activated mRNAs and proteins, such as the ER-resident chaperone *Grp78/BiP* and the transcription factor *Chop*, at ages that roughly correspond with the onset and early progression of retinal degeneration [6, 15]. These findings mirror cell culture studies that found activation of UPR signaling pathways and ER stress-induced genes in response to P23H rhodopsin expression [6, 16]. UPR signaling promotes selective degradation of misfolded P23H rhodopsin in vitro and could also operate in these animals to remove P23H rhodopsin protein from photoreceptors [7, 17]. P23H rhodopsin protein aggregation and subcellular localization has been difficult to determine precisely in these transgenic rats, in part because of nearly identical homology between the transgenic mouse P23H rhodopsin protein and endogenous rat rhodopsin protein.

## 74.5 S334ter Rhodopsin Transgenic Rat

Transgenic rats expressing mouse *opsin* bearing a premature termination codon at residue S334 also develop retinal degeneration in transgene dose-dependent manners [14, 18]. S334ter rhodopsin lacks carboxy-terminal residues required for accurate rhodopsin protein intracellular localization and accurate phototransduction signaling by rhodopsin [19–22]. In vitro studies have reported that many carboxy-

tail mutant rhodopsin proteins fold with sufficient fidelity that they do not form abnormal aggregates and can journey out of the ER to the outer segment [3, 23]. Surprisingly, recent reports found increased levels of ER stress-induced proteins, BiP/Grp78 and Chop, in retinas of transgenic S334ter rats compared to wild-type animals [24, 25]. It is unclear why and how S334ter rhodopsin causes ER stress, but ER stress could arise through the disruption of photoreceptor calcium homeostasis due to abnormal rhodopsin phototransduction. Recent biochemical studies have also found that some S334ter rhodopsin is retained within the ER to a greater degree compared to wild-type rhodopsin (albeit less than the ER retention seen with P23H rhodopsin) [17]. Increased ER latency of S334ter rhodopsin could also contribute to elevated ER stress levels seen in transgenic S334ter rhodopsin rats.

## 74.6 *R3* (C185R Rhodopsin) Mouse

The *R3* mouse line was identified in an N-ethyl-N-nitrosourea mutagenesis mouse screen [26]. These animals develop an autosomal dominant retinal degeneration that mapped to a C185R mutation in the native mouse *opsin* gene [26]. Coincidentally, orthologous human C185R mutations have also been identified in RP patients [27]. Structural modeling of the C185R mutant rhodopsin predicted that the long side chain of the abnormal arginine residue would interfere with rhodopsin folding and thereby lead to generation of misfolded rhodopsin protein [26]. C185R rhodopsin protein entirely localized to the inner segment in R3/R3 homozygous mice [26]. Ultrastructural studies further found that R3/R3 homozygous animals produced virtually no outer segment, while R3/+ heterozygous animals showed short outer segments with extensive disc disorganization [26]. These findings suggest that photoreceptors recognize C185R rhodopsin as a misfolded protein to be retained in the ER and targeted for degradation.

## 74.7 T17M Transgenic Mouse

Transgenic mice expressing the human *rhodopsin* gene and flanking sequences bearing the T17M mutation develop a progressive retinal degeneration and have been used to study therapeutic effects of vitamin A [28]. In vitro studies previously demonstrated that T17M rhodopsin was misfolded and retained within the ER similar to P23H rhodopsin [2, 3, 7]. Up-regulation of several ER stress-induced and UPR activated target genes were observed in the retinas of transgenic T17M mice [29]. Furthermore, increased GFP fluorescence was seen in photoreceptors when T17M mice were crossed with ER stress-sensitive GFP reporter mice [29, 30]. Multiple additional intracellular signaling pathways and cellular processes, including the Akt signaling pathway, autophagy, and mitochondrial intrinsic apop-

tosis regulators, were also dysregulated in T17M animals in addition to activation of UPR signaling pathways [29]. These findings suggest that many intracellular mechanisms are disrupted during the course of T17M rhodopsin-induced retinal degeneration.

## 74.8 P23H Rhodopsin Knock-In Mouse

P23H rhodopsin knock-in mice have recently been generated through targeted replacement of the *P23H* codon in endogenous mouse *opsin* gene [31]. By contrast to prior vertebrate P23H rhodopsin models, the P23H rhodopsin knock-in mice express no exogenous transgenic copies of rhodopsin. P23H rhodopsin knock-in heterozygous mice develop a progressive retinal degeneration that is significantly more rapid and severe in mice homozygous for the P23H rhodopsin knock-in allele. In P23H rhodopsin knock-in mice, P23H rhodopsin was incompletely glycosylated, retained within the ER, and found at very low levels compared to wild-type rhodopsin, presumably because ER-retained P23H rhodopsin was quickly targeted for degradation [31]. In heterozygous animals, 1D4-immunoreactivity to visualize rhodopsin protein localization showed rhodopsin labeling in rod outer segments with minimal rhodopsin labeling elsewhere in the photoreceptor [31]. Moreover, the outer segments were significantly shorter and contained abnormal, perpendicularly polarized discs [31]. Interestingly, the retinal degeneration seen in the P23H knock-in mice was worsened by genetic depletion of 11-cis-retinal, a molecular chaperone of P23H opsin in vitro [31].

## 74.9 P23H Rhodopsin-GFP Knock-In Mouse

P23H rhodopsin-GFP knock-in mice have also recently been generated through targeted replacement of an endogenous mouse *opsin* allele with homologous human *opsin* genomic region carrying a mutated *P23H* codon and *GFP* fused to the carboxy terminus of rhodopsin [32]. Heterozygous mice develop a mild retinal degeneration that is severely worsened in homozygous animals. In these animals, the P23H rhodopsin-GFP knock-in allele was transcribed as efficiently as endogenous *opsin* [32]. However, P23H rhodopsin-GFP protein levels were significantly lower than that of the wild-type rhodopsin protein, presumably through decreased stability and enhanced degradation of the P23H rhodopsin-GFP protein [32]. The fusion of GFP to P23H rhodopsin in these animals provided an opportunity to specifically track the subcellular localization of P23H rhodopsin-GFP independent of wild-type rhodopsin in photoreceptors. P23H rhodopsin-GFP was found to be predominantly mislocalized to the rod inner segment and outer nuclear layer, where the ER and nuclear membranes reside, with smaller amounts of GFP signal found in the outer segment and inner plexiform layer [32].

## 74.10 Discussion

Misfolded membrane proteins commonly aggregate, are retained within the ER, elicit ER stress, and activate the UPR [33, 34]. UPR signaling then enhances degradation of irreparably damaged proteins. Many mutant rhodopsins linked to RP display all of these features in heterologous cell culture expression studies. In vertebrate models of retinal degeneration generated through mutant rhodopsin expression in photoreceptors, abnormal rhodopsin protein aggregation, ER retention, and UPR activation/ER stress are also seen to varying degrees suggesting that ER stress is also involved in retinal degeneration in vivo. Vertebrate models have also revealed additional intriguing properties and effects of mutant rhodopsins in retina including: (1) photoreceptors can rapidly identify and clear mutant rhodopsins from the ER via unclear mechanisms, (2) co-expression of wild-type rhodopsin can enable mutant rhodopsin to escape ER and/or promote its degradation via unclear mechanisms in photoreceptors, and (3) disorganization of discs and outer segments are frequently in photoreceptors expressing mutant rhodopsins. Investigating functions and properties of ER unique to photoreceptors may provide further insight into the role of ER stress in retinal degeneration.

**Acknowledgment** Supported by NIH grant EY001919, EY002162, EY006842, EY020846, and the Foundation Fighting Blindness.

## References

1. Sung CH, Chuang JZ (2010) The cell biology of vision. J Cell Biol 190(6):953–963
2. Sung CH, Schneider BG, Agarwal N, Papermaster DS, Nathans J (1991) Functional heterogeneity of mutant rhodopsins responsible for autosomal dominant retinitis pigmentosa. Proc Natl Acad Sci USA 88(19):8840–8844
3. Kaushal S, Khorana HG (1994) Structure and function in rhodopsin. 7. Point mutations associated with autosomal dominant retinitis pigmentosa. BioChemistry 33(20):6121–6128
4. Illing ME, Rajan RS, Bence NF, Kopito RR (2002) A rhodopsin mutant linked to autosomal dominant retinitis pigmentosa is prone to aggregate and interacts with the ubiquitin proteasome system. J Biol Chem 277(37):34150–34160
5. Saliba RS, Munro PM, Luthert PJ, Cheetham ME (2002) The cellular fate of mutant rhodopsin: quality control, degradation and aggresome formation. J Cell Sci 115(Pt 14):2907–2918
6. Lin JH, Li H, Yasumura D, Cohen HR, Zhang C, Panning B, Shokat KM, LaVail MM, Walter P (2007) IRE1 signaling affects cell fate during the unfolded protein response. Science 318(5852):944–949
7. Chiang WC, Messah C, Lin JH (2012) IRE1 directs proteasomal and lysosomal degradation of misfolded rhodopsin. Mol Biol Cell 23(5):758–770
8. Naash MI, Hollyfield JG, al-Ubaidi MR, Baehr W (1993) Simulation of human autosomal dominant retinitis pigmentosa in transgenic mice expressing a mutated murine opsin gene. Proc Natl Acad Sci USA 90(12):5499–5503
9. Frederick JM, Krasnoperova NV, Hoffmann K, Church-Kopish J, Ruther K, Howes K, Lem J, Baehr W (2001) Mutant rhodopsin transgene expression on a null background. Invest Ophthalmol Vis Sci 42(3):826–833

10. Wu TH, Ting TD, Okajima TI, Pepperberg DR, Ho YK, Ripps H, Naash MI (1998) Opsin localization and rhodopsin photochemistry in a transgenic mouse model of retinitis pigmentosa. Neuroscience 87(3):709–717
11. Tam BM, Moritz OL (2006) Characterization of rhodopsin P23H-induced retinal degeneration in a Xenopus laevis model of retinitis pigmentosa. Invest Ophthalmol Vis Sci 47(8):3234–3241
12. Lee D, Geller S, Walsh N, Valter K, Yasumura D, Matthes M, LaVail M, Stone J (2003) Photoreceptor degeneration in Pro23His and S334ter transgenic rats. Adv Exp Med Biol 533:297–302
13. Machida S, Kondo M, Jamison JA, Khan NW, Kononen LT, Sugawara T, Bush RA, Sieving PA (2000) P23H rhodopsin transgenic rat: correlation of retinal function with histopathology. Invest Ophthalmol Vis Sci 41(10):3200–3209
14. Steinberg RH, Flannery JG, Naash MI, Oh P, Matthes MT, Yasumura D, Lau-Villacorta C, Chen J, LaVail MM (1996) Transgenic rat models of inherited retinal degeneration caused by mutant opsin genes [ARVO Abstract]. Invest Ophthalmol Vis Sci 37:S 698 (Abstract nr 3190)
15. Gorbatyuk MS, Knox T, LaVail MM, Gorbatyuk OS, Noorwez SM, Hauswirth WW, Lin JH, Muzyczka N, Lewin AS (2010) Restoration of visual function in P23H rhodopsin transgenic rats by gene delivery of BiP/Grp78. Proc Natl Acad Sci USA 107(13):5961–5966
16. Vasireddy V, Chavali VR, Joseph VT, Kadam R, Lin JH, Jamison JA, Kompella UB, Reddy GB, Ayyagari R (2011) Rescue of photoreceptor degeneration by curcumin in transgenic rats with P23H rhodopsin mutation. PLoS One 6(6):e21193
17. Chiang WC, Hiramatsu N, Messah C, Kroeger H, Lin JH (2012) Selective activation of ATF6 and PERK endoplasmic reticulum stress signaling pathways prevent mutant rhodopsin accumulation. Invest Ophthalmol Vis Sci 53(11):7159–7166
18. Pennesi ME, Nishikawa S, Matthes MT, Yasumura D, LaVail MM (2008) The relationship of photoreceptor degeneration to retinal vascular development and loss in mutant rhodopsin transgenic and RCS rats. Exp Eye Res 87(6):561–570
19. Concepcion F, Mendez A, Chen J (2002) The carboxyl-terminal domain is essential for rhodopsin transport in rod photoreceptors. Vision Res 42(4):417–426
20. Green ES, Menz MD, LaVail MM, Flannery JG (2000) Characterization of rhodopsin missorting and constitutive activation in a transgenic rat model of retinitis pigmentosa. Invest Ophthalmol Vis Sci 41(6):1546–1553
21. Lee ES, Flannery JG (2007) Transport of truncated rhodopsin and its effects on rod function and degeneration. Invest Ophthalmol Vis Sci 48(6):2868–2876
22. Chen J, Makino CL, Peachey NS, Baylor D, Simon MI (1995) Mechanisms of rhodopsin inactivation in vivo as revealed by COOH-terminal truncation mutant. Science 267:374–377
23. Sung C-H, Davenport CM, Nathans J (1993) Rhodopsin mutations responsible for autosomal dominant retinitis pigmentosa. J Biol Chem 268:26645–26649
24. Kroeger H, Messah C, Ahern K, Gee J, Joseph V, Matthes MT, Yasumura D, Gorbatyuk MS, Chiang WC, Lavail MM, Lin JH (2012) Induction of Endoplasmic Reticulum Stress Genes, BiP and Chop, in Genetic and Environmental Models of Retinal Degeneration. Invest Ophthalmol Vis Sci 53(12):7590–7599
25. Shinde VM, Sizova OS, Lin JH, Lavail MM, Gorbatyuk MS (2012) ER Stress in Retinal Degeneration in S334ter Rho Rats. PLoS One 7(3):e33266
26. Liu H, Wang M, Xia CH, Du X, Flannery JG, Ridge KD, Beutler B, Gong X (2010) Severe retinal degeneration caused by a novel rhodopsin mutation. Invest Ophthalmol Vis Sci 51(2):1059–1065
27. Sohocki MM, Daiger SP, Bowne SJ, Rodriquez JA, Northrup H, Heckenlively JR, Birch DG, Mintz-Hittner H, Ruiz RS, Lewis RA, Saperstein DA, Sullivan LS (2001) Prevalence of mutations causing retinitis pigmentosa and other inherited retinopathies. Hum Mutat 17(1):42–51
28. Li T, Sandberg MA, Pawlyk BS, Rosner B, Hayes KC, Dryja TP, Berson EL (1998) Effect of vitamin A supplementation on rhodopsin mutants threonine-17 -> methionine and

proline-347 -> serine in transgenic mice and in cell cultures. Proc Natl Acad Sci USA 95(20):11933–11938
29. Kunte MM, Choudhury S, Manheim JF, Shinde VM, Miura M, Chiodo VA, Hauswirth WW, Gorbatyuk OS, Gorbatyuk MS (2012) ER stress is involved in T17M rhodopsin-induced retinal degeneration. Invest Ophthalmol Vis Sci 53(7):3792–3800
30. Iwawaki T, Akai R, Kohno K, Miura M (2004) A transgenic mouse model for monitoring endoplasmic reticulum stress. Nat Med 10(1):98–102
31. Sakami S, Maeda T, Bereta G, Okano K, Golczak M, Sumaroka A, Roman AJ, Cideciyan AV, Jacobson SG, Palczewski K (2011) Probing mechanisms of photoreceptor degeneration in a new mouse model of the common form of autosomal dominant retinitis pigmentosa due to P23H opsin mutations. J Biol Chem 286(12):10551–10567
32. Price BA, Sandoval IM, Chan F, Simons DL, Wu SM, Wensel TG, Wilson JH (2011) Mislocalization and degradation of human P23H-rhodopsin-GFP in a knockin mouse model of retinitis pigmentosa. Invest Ophthalmol Vis Sci 52(13):9728–9736
33. Alberts B (2008) Molecular biology of the cell, 5th ed. Garland Science, New York
34. Walter P, Ron D (2011) The unfolded protein response: from stress pathway to homeostatic regulation. Science 334(6059):1081–1086

# Chapter 75
# Bisretinoid Degradation and the Ubiquitin-Proteasome System

**Janet R. Sparrow, Jilin Zhou, Shanti Kaligotla Ghosh and Zhao Liu**

**Abstract** Bisretinoid fluorophores of retinal pigment epithelial (RPE) lipofuscin have been shown to undergo degradation in two ways, the first involving photofragmentation following photooxidation of their polyene structure and the second being enzyme-mediated and limited, thus far, to in vitro models employing horseradish peroxidase (HRP). Here we show that both of these processes impact the ubiquitin–proteasome system (UPS) of the RPE cell. By measuring the consumption of A2E and all-*trans*-retinal dimer by HPLC, we confirmed that both HRP-mediated and photodegradation of the compounds occurred and that in both cases the chymotrypsin-like and trypsin-like activities of the proteasome system were decreased. With HRP-mediated degradation of A2E, there was a small negative impact on cell viability that was not mitigated by elevating gluthathione in the cell.

**Keywords** Bisretinoid · Lipofuscin · Proteasome · Retinal pigment epithelium · Enzyme degradation

J. R. Sparrow (✉) · J. Zhou · S. K. Ghosh · Z. Liu
Department of Ophthalmology and Cell Biology, Columbia University, 630 W. 168 Street, New York, NY 10032, USA
e-mail: jrs88@columbia.edu

J. Zhou
e-mail: jz219@columbia.edu

S. K. Ghosh
e-mail: shanti111us@gmail.com

J. R. Sparrow
Department of Pathology and Cell Biology, Columbia University, New York, NY, USA

J. D. Ash et al. (eds.), *Retinal Degenerative Diseases,* Advances in Experimental Medicine and Biology 801, DOI 10.1007/978-1-4614-3209-8_75,

## 75.1 Introduction

Proteasomes are protease assemblies responsible for the degradation and recycling of proteins which have been previously tagged with ubiquitin. Proteins damaged by postsynthetic alterations are important substrates for degradation by the ubiquitin–proteasome system (UPS) [1], and one such modification is the advanced glycation end product (AGEs). We have uncovered a unique source of AGEs that form in retinal pigment epithelial (RPE) cells. Specifically, we demonstrated that methylglyoxal (MG) and glyoxal (GO), two small dicarbonyls known to form AGEs, are released upon photodegradation of A2E and all-*trans*-retinal dimer, two bisretinoids that accumulate with age as lipofuscin in RPE. This cleavage of bisretinoid occurs upon exposure to wavelengths of light that reach the retina. Significantly, we have also observed that the processes of photooxidation and photodegradation of intracellular bisretinoid in RPE cells alters the function of the ubiquitin–proteasome system (UPS) [2].

In work designed to test the possibility that exogenous enzymes can be delivered so as to degrade the bisretinoid constituents of RPE lipofuscin and protect against their accumulation, we previously demonstrated that the oxo-iron heme-based enzyme horseradish peroxide (HRP) can cleave the bisretinoid A2E [3]. We also identified aldehyde-bearing fragments that were products of this activity. Here we have examined for whether the products of enzyme-mediated cleavage of A2E cause cellular stress by impacting proteasome activity and whether reduced glutathione is protective. We also compared the proteasome activity to that in cells undergoing A2E photodegradation.

## 75.2 Materials and Methods

### *75.2.1 Cell-Associated A2E*

Confluent ARPE-19 cells (ATCC, Manassas, VA) (35 mm dishes) that lack endogenous lipofuscin accumulated A2E in lysosomes as described [3, 4].

### *75.2.2 Photodegradation of Cell-Associated A2E*

For 430 nm irradiation, cultures were transferred to PBS with calcium, magnesium, and glucose and were exposed as previously reported [5] and then incubated for an additional 6 h before harvesting.

### 75.2.3 Enzymatic Degradation of Cell Associated A2E

HRP was delivered to the cells using the Bioporter reagent (Sigma-Aldrich Corp., St. Louis, MO) as previously described [3].

### 75.2.4 Proteasome Activity Assays

Trypsin-like proteasome activity was measured in a live-cell assay using a luminogenic substrate (Z-LRR-aminoluciferin; Proteasome-Glo, Promega Corporation, Madison, WI). Briefly, to cells released into a suspension (10,000 cells/100 μL) 100 μL of Proteasome-Glo cell-based reagent was added. After mixing and incubating (6 min, room temperature) luminescence was measured using the SoftMax Pro 5 microplate reader (Molecular Devices, Inc. Sunnyvale, CA). Samples were assayed in duplicate.

Chymotrypsin-like proteasome activity was measured using a fluorescence assay that employs an AMC-tagged peptide substrate (Succ-LLVY-AMC; BioVision Incorporated, Mountain View, CA) and cells homogenized in 0.5% NP-40 (Sigma-Aldrich Corp., St. Louis, MO). Fluorescence (excitation/emission, 350/440 nm) was measured in the microplate reader (37 °C from 30–60 min). Nonspecific (non-proteasome) fluorescence measured in the presence of a proteasome inhibitor was subtracted, values were adjusted to protein concentration and proteasome activity was determined from a standard curve of AMC fluorescence. Samples were assayed in duplicate.

### 75.2.5 HPLC Quantitation of A2E

Chromatographic separation and A2E quantification was performed by reverse-phase HPLC as previously described [6]. An Atlantis® dC18 (3 μm, 4.6×150 mm, Waters Corp, Milford MA) column was employed with an acetonitrile and water gradient and 0.1% trifluoroacetic acid (85–100%, 0.8 mL/min 15 min; 100% acetonitrile, 0.8–1.2 mL/min 15–20 min; monitoring at 430 nm; 30 μL injection volume).

### 75.2.6 Sulforaphane Treatment

Cells were treated with sulforaphane (1-isothiocyanato-4-(methyl sulfinyl)butane; 5 μM, 48 h; LKT Laboratories, St. Paul, MN) in DMEM and Ham's F-12 medium (1:1) with 10% FBS that had been heat- (90 min at 55 °C) and charcoal-treated (1% w/v) to reduce the presence of endogenous NQO1 inducers.

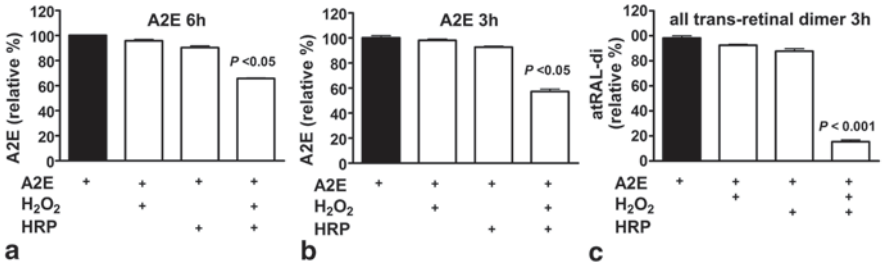


**Fig. 75.1** HPLC quantitation of the bisretinoids *A2E* (**a**, **b**) and all-*trans*-retinal dimer (*atRAL-di*) (**c**) after incubation in the presence (+) and absence (−) of horseradish peroxidase and hydrogen peroxide (*HRP/$H_2O_2$*) for time periods (hours) indicated. Mean ± SEM, 3 experiments. One-way ANOVA and Newman Keul Multiple Comparison test

### *75.2.7 GSH Measurement*

Supernatants from cell lysates containing 1 % 5-sulfosalicylic acid were submitted to GSH colorimetric assay (405 nm absorbance) in the presence of GSH reductase, NADPH, and DTNB (BioVision Research Products). GSH concentration was determined using a calibration curve and protein was measured by Bio-Rad assay (Bio-Rad, Hercules, CA).

### *75.2.8 Cell Viability Assay*

Cytotoxicity was assayed by MTT (4, 5-dimethylthiazol-2-yl)-2, 5-diphenyltetrazolium bromide) assay (Roche Diagnostics, Basel, Switzerland).

## 75.3 Results

### *75.3.1 HRP Degrades Bisretinoids in a Cell-Free Assay*

We have previously shown in non-cellular assays that HRP can degrade A2E [3]. Here we compared the degradation of A2E to another bisretinoid having a polyene structure, all-*trans*-retinal dimer. After a 3 h incubation period, A2E levels were decreased by 35 % in the presence of HRP and $H_2O_2$(Fig. 75.1). The effect of HRP on all-*trans*-retinal dimer was even more robust, with levels of the latter compound being reduced by 85 % within 3 h.

### 75.3.2 Reduced Proteasome Activity with HRP-Mediated Degradation of Intracellular A2E

We also previously showed that HRP, when delivered to cultured RPE via the Bioporter® system, becomes located in lysosomes [3].

In the current experiments, we quantified A2E by integrating HPLC peak areas 3 days after introducing HRP to the cells. A2E levels were reduced by ~40% as compared to starting levels. BioPorter in the absence of HRP conferred no changes in A2E levels (Fig. 75.1c), indicating that HRP is exclusively responsible for the oxidation and degradation of A2E.

We next assayed for proteasome activity using luminogenic and fluorogenic substrates that generate a signal upon proteasome cleavage. We found that HRP-mediated degradation of intracellular A2E reduced chymotrypsin-like and trypsin-like proteasome activity by 36% and 18% respectively (Fig.75.2). This level of interference in proteasome activity by HRP-mediated degradation of intracellular A2E was similar to that observed in RPE cells following 430 nm-irradiation of A2E-containing ARPE-19 cells.

### 75.3.3 GSH Effects on HRP-Mediated Degradation of Intracellular A2E

We also sought to determine whether reduced glutathione (GSH), a cellular source of reducing equivalents, could protect the RPE cell in the presence of HRP-mediated A2E cleavage. To this end we treated the cells with sulphoraphane, a phytochemical that increases cellular GSH levels [7, 8]. With sulphoraphane, cellular GSH levels were increased by 58% (as compared to untreated RPE) (Fig. 75.3). HRP-mediated degradation of A2E caused a 25% decline in GSH levels measured 3 days after HRP was delivered. Seven (7) and 14 days after HRP delivery, cell viability was diminished by 14% and 19%, respectively (as compared to A2E-containing cells in the absence of HRP; $p<0.05$)) and protection by sulphoraphane pretreatment was not detectable ($p>0.05$) (Fig. 75.3).

## 75.4 Discussion

Autofluorescent bisretinoid pigments such as A2E and all-*trans*-retinal dimer accumulate with age as the lipofuscin of retinal pigment epithelial (RPE) cells in the eye. These pigments originate in photoreceptor outer segments from reactions of visual cycle vitamin A aldehyde and are deposited in the RPE secondarily. The bisretinoids of RPE lipofuscin likely accumulate because they are refractory to lysosomal proteolysis. RPE lipofuscin is implicated in a number of macular diseases [9]. Pre-clinical therapeutic strategies aimed at preventing vision loss in *ABCA4*-

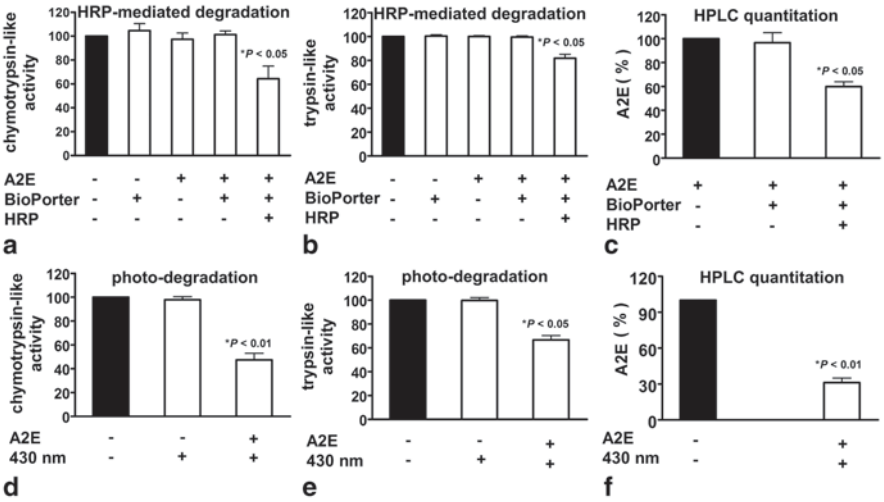


**Fig. 75.2** Enzyme-mediated degradation and photo-degradation of *A2E* impacts proteasome activity in RPE cells. HRP was delivered to *A2E*-containing RPE by BioPorter vehicle. **a**–**c** *HRP-mediated degradation* of *A2E* followed by measurement of chymotrypsin- (**a**) and trypsin-like (**b**) proteasome activity. (**c**). *HPLC quantitation* of *A2E* confirms *A2E* degradation by *HRP*. Controls include absence of *A2E*; BioPorter in absence of *HRP*. **d**–**e** Photodegradation (*430 nm* light) of *A2E* followed by measurement of chymotrypsin- (**d**) and trypsin-like (**e**) proteasome activity. **f** *HPLC* quantitation of *A2E* and *A2E* isomers confirms *A2E* photodegradation. Controls include absence of *A2E* and *A2E* in absence of 430 nm exposure. Values normalized to untreated cells; mean ± SEM, 3 experiments; one-way ANOVA and Newman Keul Multiple Comparison test

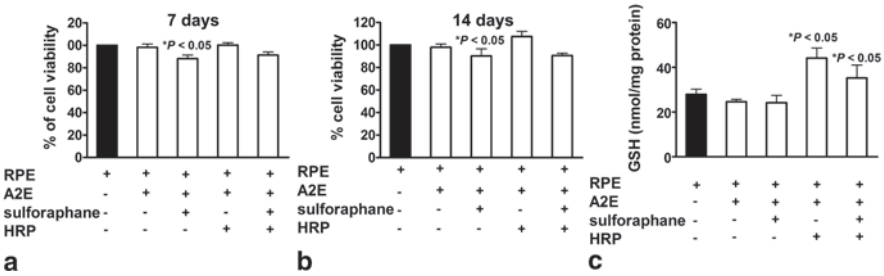


**Fig. 75.3** Cell viability and *GSH* levels in *RPE* cells pre-treated with *sulforaphane* 24 h before *HRP* was delivered to the cells to degrade *A2E*. **a**, **b** Cell viability was determined after 24 h by MTT assay, a decrease in the absorbance (570 nm) of reduced MTT being indicative of diminished cell viability. Values were normalized to untreated cells. **c** *GSH* quantitation. Total *GSH* expressed as nanomoles per milligram of cytosolic protein. Means ± SEM, 4 experiments; one-way ANOVA and Newman Keul Multiple Comparison test

associated disease have focused on viral vector mediated delivery of the wild-type gene or systemic administration of compounds that limit the retinoid cycle [10–14]. These approaches, however, cannot reverse the accumulation of lipofuscin bisreti-

noids, once it has already occurred. Thus we have been exploring an additional line of attack that would involve delivery of exogenous enzyme having the capability to cleave the bisretinoids of RPE lipofuscin. As proof of principle, we have experimented with a well-known enzyme, HRP. As shown here and previously, HRP can bring about the degradation of A2E [3]; HRP can even more effectively cleave the bisretinoid all-*trans*-retinal dimer. Interestingly, all-*trans*-retinal dimer is also more susceptible to photooxidation [15].

As shown here, one effect of this form of enzyme degradation could be perturbation of the UPS. The mechanism by which the UPS is impacted is not clear. Perhaps by engaging the proteasome, the products of HRP-mediated A2E degradation overwhelm other UPS substrates, thereby competitively inhibiting proteasome function. Alternatively, the degradation fragments could react with, and thus attenuate proteasome enzyme activity. In the future we will test additional enzyme candidates for their ability to safely degrade the bisretinoids of RPE lipofuscin.

**Acknowledgments** This study was supported by the Edward N. and Della L. Thome Memorial Foundation, National Institutes of Health grant P30EY019007, and a grant from Research to Prevent Blindness to the Department of Ophthalmology, Columbia University.

## References

1. Dudek EJ, Shang F, Valverde P, Liu Q, Hobbs M, Taylor A (2005) Selectivity of the ubiquitin pathway for oxidatively modified proteins: relevance to protein precipitation diseases. FASEB J 19(12):1707–1709
2. Fernandes AF, Zhou J, Zhang X, Bian Q, Sparrow JR, Taylor A, Pereira P, Shang F (2008) Oxidative inactivation of the proteasome in retinal pigment epithelial cells. A potential link between oxidative stress and up-regulation of interleukin-8. J Biol Chem 283:20745–20753
3. Wu Y, Zhou J, Fishkin N, Rittmann BE, Sparrow JR (2011) Enzymatic degradation of A2E, a retinal pigment epithelial lipofuscin bisretinoid. J Am Chem Soc 133:849–857
4. Sparrow JR, Parish CA, Hashimoto M, Nakanishi K (1999) A2E, a lipofuscin fluorophore, in human retinal pigmented epithelial cells in culture. Invest Ophthalmol Vis Sci 40(12):2988–2995
5. Sparrow JR, Zhou J, Ben-Shabat S, Vollmer H, Itagaki Y, Nakanishi K (2002) Involvement of oxidative mechanisms in blue light induced damage to A2E-laden RPE. Invest Ophthalmol Vis Sci 43(4):1222–1227
6. Kim SR, Jang YP, Jockusch S, Fishkin NE, Turro NJ, Sparrow JR (2007) The all-trans-retinal dimer series of lipofuscin pigments in retinal pigment epithelial cells in a recessive Stargardt disease model. Proc Natl Acad Sci U S A 104:19273–19278
7. Fahey JW, Zhang Y, Talalay P (1997) Broccoli sprouts: an exceptionally rich source of inducers of enzymes that protect against chemical carcinogens. Proc Natl Acad Sci U S A 94:10367–10372
8. Zhou J, Gao X, Cai B, Sparrow JR (2006) Indirect antioxidant protection against photooxidative processes initiated in retinal pigment epithelial cells by a lipofuscin pigment. Rejuven Res 9(2):256–263
9. Sparrow JR, Gregory-Roberts E, Yamamoto K, Blonska A, Ghosh SK, Ueda K, Zhou J (2012) The bisretinoids of retinal pigment epithelium. Prog Retin Eye Res 31:121–135

10. Allocca M, Doria M, Petrillo M, Colella P, Garcia-Hoyos M, Gibbs D, Kim SR, Maguire AM, Rex TS, Di Vicino U, Cutillo L, Sparrow JR, Williams DS, Bennett J, Auricchio A (2008) Serotype-dependent packaging of large genes in adeno-associated viral vectors results in effective gene delivery in mice. J Clin Invest 118:1955–1964
11. Kong J, Kim SR, Binley K, Pata, Doi K, Mannik J, Zernant-Rajang J, Kan O, Iqball S, Naylor S, Sparrow JR, Gouras P, Allikmets R (2008) Correction of the disease phenotype in the mouse model of Stargardt disease by lentiviral gene therapy. Gene Ther 15(19):1311–1320
12. Radu RA, Han Y, Bui TV, Nusinowitz S, Bok D, Lichter J, Widder K, Travis GH, Mata NL (2005) Reductions in serum vitamin A arrest accumulation of toxic retinal fluorophores: a potential therapy for treatment of lipofuscin-based retinal diseases. Invest Ophthalmol Vis Sci 46:4393–4401
13. Maiti P, Kong J, Kim SR, Sparrow JR, Allikmets R, Rando RR (2006) Small molecule RPE65 antagonists limit the visual cycle and prevent lipofuscin formation. Biochem 45:852–860
14. Maeda A, Maeda T, Golczak M, Palczewski K (2008) Retinopathy in mice induced by disrupted all-trans-retinal clearance. J Biol Chem 283:26684–26693
15. Yoon KD, Yamamoto K, Zhou J, Sparrow JR (2011) Photo-products of retinal pigment epithelial bisretinoids react with cellular thiols. Mol Vis 17:1839–1849

# Chapter 76
# Analysis of Mouse RPE Sheet Morphology Gives Discriminatory Categories

**Yi Jiang, X Qi, Micah A. Chrenek, Christopher Gardner, Nupur Dalal, Jeffrey H. Boatright, Hans E. Grossniklaus and John M. Nickerson**

**Abstract** We are interested in developing quantitative tools to study retinal pigmented epithelium (RPE) morphology. We want to detect changes in the RPE by strain, disease, genotype, and age. Ultimately these tools should be useful in predicting retinal disease progression. The morphometric data will also help us to understand RPE sheet formation and barrier functions. A clear disruption of the regular cell size and shape appeared in mouse mutants. Aspect ratio and cell area together gave rise to principal components that predicted age and genotype accurately and well before visually obvious damage could be seen.

**Keywords** Retinal pigmented epithelium · RPE · Morphometrics · Pattern analysis

J. M. Nickerson (✉) · M. A. Chrenek · C. Gardner · N. Dalal · J. H. Boatright · H. E. Grossniklaus
Department of Ophthalmology, Emory University, Atlanta, GA 30322, USA
e-mail: litjn@emory.edu

M. A. Chrenek
e-mail: micah.chrenek@emory.edu

C. Gardner
e-mail: christopher.gardner@emory.edu

N. Dalal
e-mail: ndalal@lsuhsc.edu

J. H. Boatright
e-mail: jboatri@emory.edu

H. E. Grossniklaus
e-mail: ophtheg@emory.edu

Y. Jiang · X Qi
Department of Mathematics and Statistics, Georgia State University, Atlanta, GA, USA
e-mail: yjiang12@gsu.edu

X Qi
e-mail: xqi3@gsu.edu

J. D. Ash et al. (eds.), *Retinal Degenerative Diseases,* Advances in Experimental Medicine and Biology 801, DOI 10.1007/978-1-4614-3209-8_76,

## 76.1 Introduction

We hypothesize that in age related macular degeneration (AMD), stage-specific mechanical stresses act on the RPE, altering morphology. In this article we describe imaging and computational analyses for staging and categorizing these morphological responses in the RPE.

The morphology of the RPE cell is affected in disease states in many retinal and macular diseases. Breakdown of the RPE leads to a loss of the blood-retina-barrier [1]. In a diseased state, RPE changes can include epithelial-mesenchymal transition and abnormal proliferation. Changes can range from minor shape changes to cell death. Here, we seek to define patterns in the local interactions of RPE cells, when viewed en face, which are characteristic of the very earliest changes in shape that precede AMD. We have begun with simple mouse model systems to study the normal and diseased RPE sheet in flatmounts. We previously established that the rd10 mouse RPE sheet experiences many abnormalities [1]. Here we quantitatively detect early changes that appear useful as predictors of subsequent damage and death of RPE in this and other strains. We created a large dataset and discovered principal components based on two metrics; aspect ratio and cell size, that provided discrimination among strains and ages of mice. With this information we can begin to build a useful model of RPE degeneration as a predictive tool for retinal disease and AMD progression.

## 76.2 Materials and Methods

All animals were cared for in an AAALAC certified facility under an approved IACUC protocol [2, 3]. Over 100 mice were used, including C57BL/6J (WT) and mutant lines (rd10, IRBP knockout (KO), and rpe65 KO) that were congenic with C57BL/6J. Dissection, fixation, flatmounting, staining, and imaging were conducted as previously described [2].

To analyze photomerged images, Cell Profiler version 1.0 (release 9717) was used [4]. About 1.0 million cells were analyzed; CellProfiler automatically collected morphometric data (in 23 metrics) on every cell. We used functional principal component analysis (FPCA) to analyze the data.

## 76.3 Results

In Fig. 76.1, Panel A is an example of a flatmount that was photomerged from 64 images, and then 21 selected rectangles were analyzed in CellProfiler. Data were collected from four radial zones from three strains of mice (WT C57BL/6J, IRBP KO, and rpe65 KO). The density distributions of cell area in Panels B-D indicate differences according to strain and zone. The shapes of the distributions varied widely.

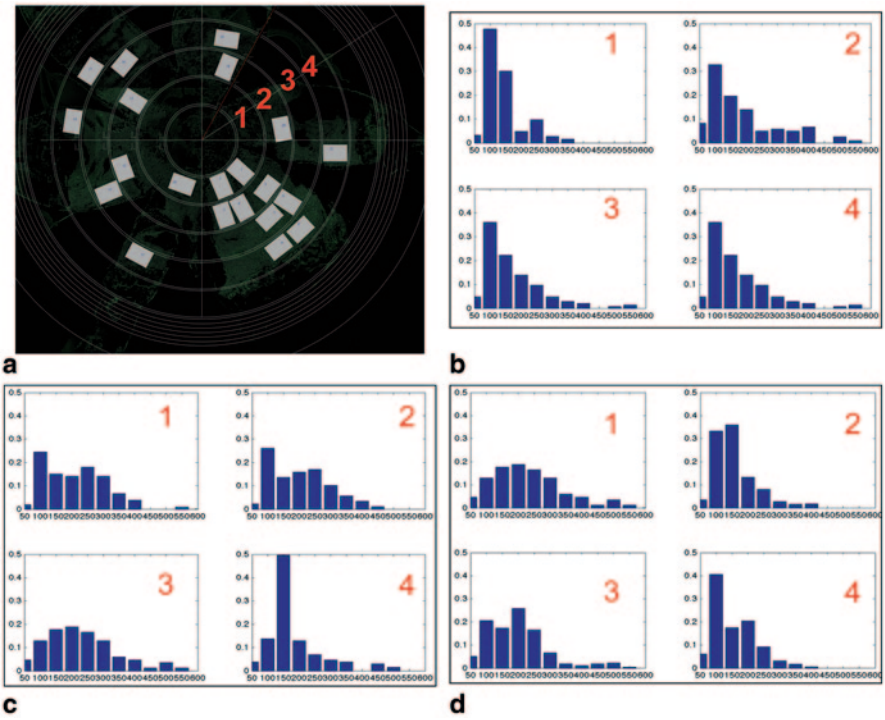


**Fig. 76.1** Inhomogeneous spatial distribution of morphology in experimental mouse RPE flatmount data. **a** RPE flat-mount defining measuring zones *1–4* (*red* numbers). **b–d** Cell area distributions for four zones: **b** Wild-type mouse at P60; **c** IRBP mutant at P60; **d** RPE65 mutant at P60. While the WT distributions were tighter and more similar from one zone to the next, most of the other distributions were more spread out and revealed no obviously similar patterns of cell sizes

In Fig. 76.2, at very young ages from P30 to P60, we observed no difference in cell size, density, or number of sides. Previously, we observed early changes in eccentricity and form factor [2], and here we detected differences in solidity and extent of the RPE cell, indicating quantitative irregularities in the shape of RPE cells from the rd10 mouse that were not detected by visual inspection.

In Fig. 76.3, we tested the hypothesis that the aspect ratio (a measure of cell shape) combined with cell area of the RPE cells would be a useful predictor of future deterioration of the RPE sheet. The figure shows function principal component analysis (FPCA) results with the first four principal components (PC). With this approach it was possible to clearly resolve young versus old in WT, rpe65, and rd10. For example, PC1 and PC2 resolved rd10 and WT at both young and old ages well. Thus, principal components allowed an accurate genotyping of each strain regardless of age. Prediction accuracy of the age and genotype of an unknown mouse RPE flatmount was > 98 %.

In Fig. 76.4, extremely large RPE cells from P100 rd10 are illustrated. These cells appeared to be multinucleate [5], though a possible confound is "show-through" of

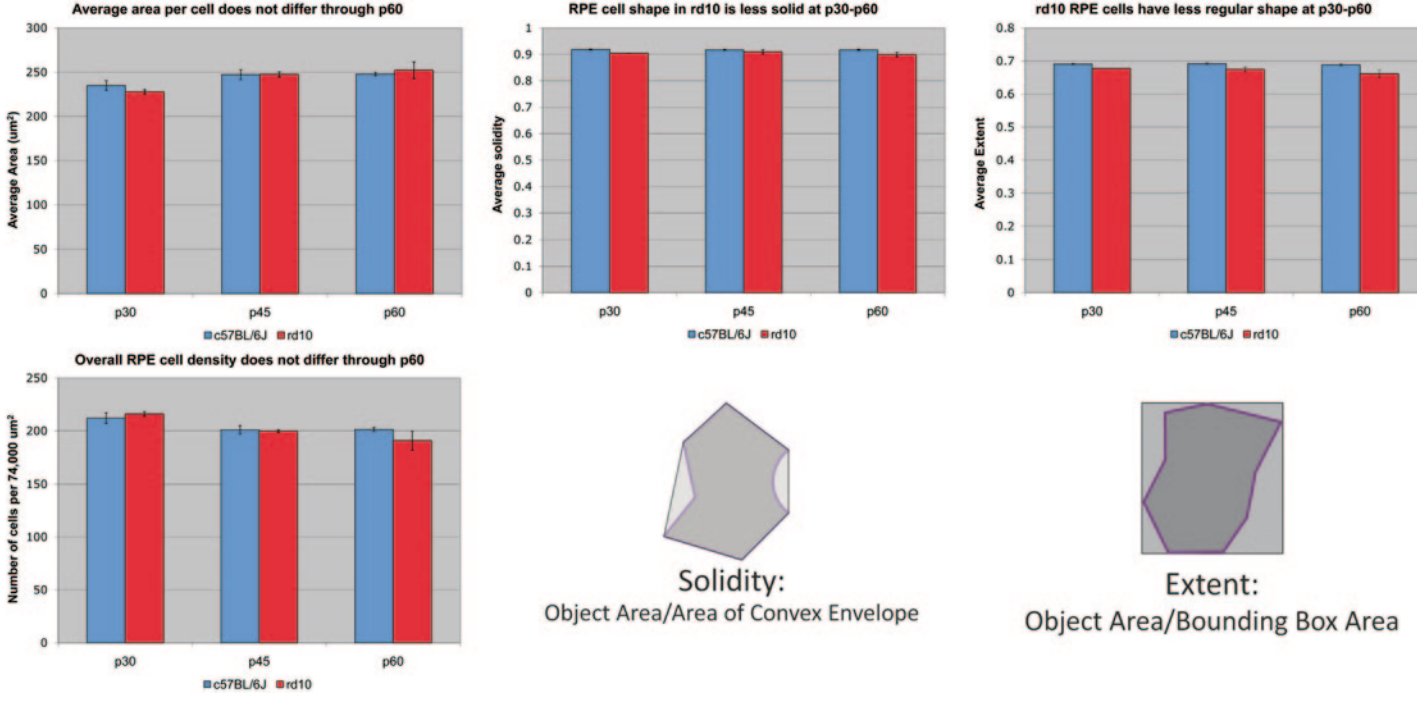


**Fig. 76.2** Comparison of *rd10* and wt *RPE* at young ages. Four metrics obtained in CellProfiler were studied for potential differences. These included cell area, cell density, solidity, and extent. The definitions of solidity and extent are diagrammed. No differences in the averaged cell area or cell density were detected comparing *rd10* to WT at *P30*, *P45*, or *P60*. The solidity and extent of *rd10 RPE* cells were reduced compared to WT at all three ages

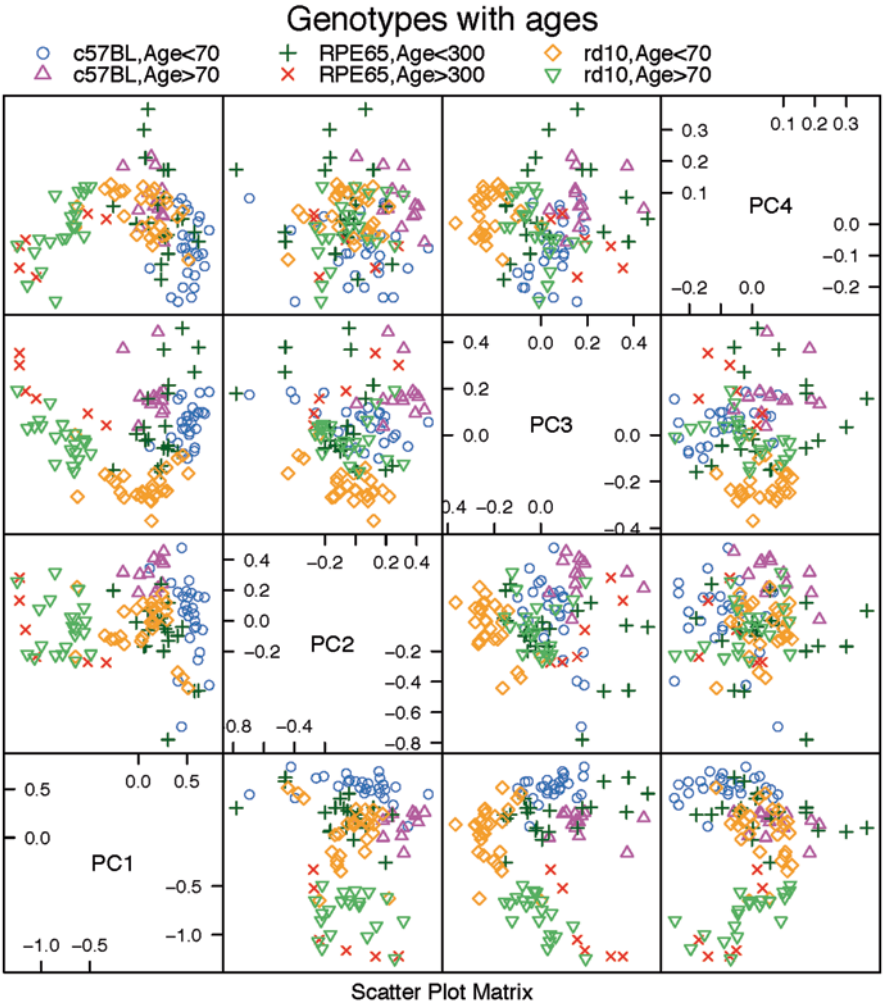


**Fig. 76.3** Scatterplot of the first four principal components from FPCA analysis using aspect ratio and cell area. Different *colors* and *marks* indicate six distinct classes: young *C57BL/6J*, old *C57BL/6J*, young *rpe65* KO, old *rpe65* KO, young *rd10*, and old *rd10*

underlying capillary endothelial cells. In normal pigmented mice, pigment granules block "show-through"; however, if stretched thin, the number of pigment granules can be so small that underlying capillary nuclei become readily visible. There was no obvious pattern or location in the appearance of the extremely large cells. For example, in Panels A and B the large cells were near highly eccentric cells, but not near many other large cells. Regardless of mutant or WT strain, at least 25 % of cells were binucleate [6].

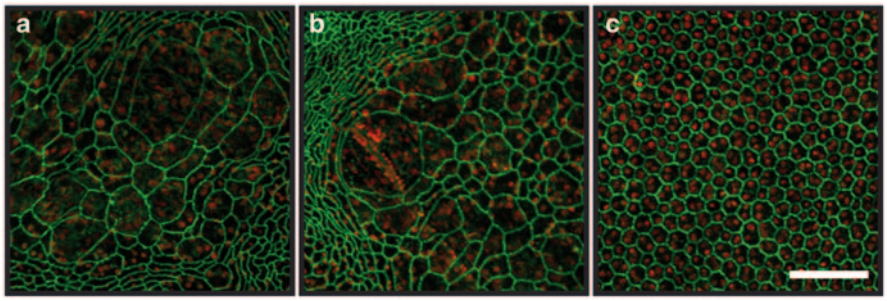


**Fig. 76.4** Highly enlarged cells in the RPE sheet of the P100 rd10 mouse. *Green* represents ZO-1 staining, and *red* represents propidium iodide staining of nuclei. Panels *A* and *B* illustrate representative large cell patches from rd10. Panel *C* represents aged matched WT. The large cells appeared multinucleate in A and B. The scale bar in Panel *C* represents 100 microns and applies to all panels

## 76.4 Discussion

RPE sheet morphometrics clearly indicate retinal disease stage and age. That is, we can predict genotype at early stages before any damage occurs in simple Mendelian inherited retinal degenerations in mouse. We speculate that this can be applied to human RPE and predict who is at risk for AMD. Further, the approach could be used to monitor treatment effectiveness and dosing schedules.

The general utility of the CellProfiler pipeline [4] was in the analysis of spatial and temporal information and in capturing quantified information on numerous metrics of millions of individual RPE cells (Fig. 76.1). The density distributions of cell areas in different regions indicates that within the eye, that spatial variation of the morphology can be almost as significant as that between different strains.

At early ages some metrics were not useful in early discrimination of rd10 from WT. However, shape-related metrics (aspect ratio, solidity, eccentricity, and extent) revealed clear differences between mutant strains and WT at early stages before a human observer could detect morphologic changes (Fig. 76.2), suggesting a promising class of metrics to pursue.

By utilizing FPCA (based on joint aspect ratio and cell size) we achieved: (1) discrimination by age in each genotype, (2) discrimination among genotypes at each age, (3) discrimination among all six age-genotype groups (Fig. 76.3). This establishes that we can make predictions of each genotype and its outcome at an early age with high accuracy and confidence.

In young wild type mice the RPE morphology resembles a regular hexagonal array of cells of uniform size throughout the retina except near the ciliary body, where the shapes of RPE resemble a soft network of teardrop- or fish scale-shaped cells at the periphery (called the transitional epithelium, an 8–10 cell-wide zone). It is common to see a few discrete dots of ZO-1 staining in the cytoplasm of these transitional cells. The regular RPE lack these dots.

Mutant eyes develop a subpopulation of large cells. To compensate for cell loss, adjacent RPE cells expand surface area to prevent gaps from emerging between adjacent cells. Over time there is an equilibration of cell sizes, leading to most cells becoming larger. However, in rd10 mice, we find some extremely large cells (Fig. 76.4), and it remains to be explained why there is no equilibration of cell size among those and nearby cells. We speculate that there are unknown permanent structures attached to some cells that hinder movement or area expansion, and this prevents cell size equilibration.

In conclusion, cell size and aspect ratio ought to be investigated to discriminate (with FPCA) between normal and early stage AMD. Morgan et al. [7] have reported noninvasive AO-FAF imaging of RPE. Flood illumination and AO, Syed et al. [8] may be useful as well. Analysis of data from such instruments with the approach we report here ought to be considered.

**Acknowledgments** Supported by NIH grants R01EY0016470, and P30EY007092, and an unrestricted grant to the Emory Eye Center from Research to Prevent Blindness.

## References

1. Rizzolo LJ (2007) Development and role of tight junctions in the retinal pigment epithelium. Int Rev Cytol 258:195–234
2. Chrenek MA, Dalal N, Gardner C, Grossniklaus H, Jiang Y, Boatright JH, Nickerson JM (2012) Analysis of the RPE sheet in the rd10 retinal degeneration model. Adv Exp Med Biol 723:641–647
3. Nickerson JM, Goodman P, Chrenek MA, Bernal CJ, Berglin L, Redmond TM, Boatright JH (2012) Subretinal delivery and electroporation in pigmented and nonpigmented adult mouse eyes. Methods Mol Biol 884:53–69 (Clifton, NJ)
4. Lamprecht MR, Sabatini DM, Carpenter AE (2007) CellProfiler: free, versatile software for automated biological image analysis. Biotechniques 42(1):71–75
5. Ding J-D, Johnson LV, Herrmann R, Farsiu S, Smith SG, Groelle M, Mace BE, Sullivan P, Jamison JA, Kelly U, Harrabi O, Bollini SS, Dilley J, Kobayashi D, Kuang B, Li W, Pons J, Lin JC, Bowes Rickman C (2011) Anti-amyloid therapy protects against retinal pigmented epithelium damage and vision loss in a model of age-related macular degeneration. Proc Natl Acad Sci USA 108(28):E279–E287
6. Bodenstein L, Sidman RL (1987) Growth and development of the mouse retinal pigment epithelium. I. Cell and tissue morphometrics and topography of mitotic activity. Dev Biol 121(1):192–204
7. Morgan JI, Dubra A, Wolfe R, Merigan WH, Williams DR (2009) In vivo autofluorescence imaging of the human and macaque retinal pigment epithelial cell mosaic. Invest Ophthalmol Vis Sci 50(3):1350–1359
8. Syed R, Sundquist SM, Ratnam K, Soudry SZ, Zhang Y, Crawford JB, Macdonald IM, Godara P, Rha J, Carroll J, Roorda A, Stepien KE, Duncan JL (2013) High resolution images of retinal structure in patients with choroideremia. Invest Ophthalmol Vis Sci 54(2):950–961

# Chapter 77
# High Glucose Activates ChREBP-Mediated HIF-1α and VEGF Expression in Human RPE Cells Under Normoxia

**Min-Lee Chang, Chung-Jung Chiu, Fu Shang and Allen Taylor**

**Abstract**

**Objective** Because retina-damaging angiogenesis is controlled by vascular endothelial growth factor (VEGF) and people with higher glucose intakes are more susceptible to retinal complications that may be due to increased VEGF, it is crucial to elucidate relations between glucose exposure and *VEGF* expression. We aimed to determine if a carbohydrate response element binding protein (ChREBP) plays a role in the transcriptional up-regulation of hypoxia-inducible factor-1α (*HIF-1α*) and the downstream *VEGF* expression in retinal pigment epithelial (RPE) cells exposed to high glucose under normoxic conditions.
**Methods** ARPE19 cells were exposed to 5.6, 11, 17, 25 and 30 mM glucose for 48 h in serum-free culture media under normoxic (21 % $O_2$) conditions. Protein and mRNA expression of indicated genes were determined by immunoblot analyses and real-time RT-PCR, respectively. An enzyme-linked immunosorbent assay (ELISA) was used to detect the concentrations of VEGF in the media. Immunofluorescence (IF) and chromatin immunoprecipitation (ChIP) for ChREBP were used to demonstrate nuclear translocation and *HIF-1α* gene promoter association, respectively.
**Results** Immunoblot analyses showed that HIF-1α levels were positively related to levels of glucose exposure between 5.6–25 mM in the RPE cells, indicating

C.-J. Chiu (✉) · M.-L. Chang · F. Shang · A. Taylor
Laboratory for Nutrition and Vision Research, Jean Mayer USDA Human Nutrition Research Center on Aging, Tufts University, Boston, MA, 02111, USA
e-mail: cj.chiu@tufts.edu

M.-L. Chang
e-mail: Min-Lee.Chang@tufts.edu

C.-J. Chiu · A. Taylor
Department of Ophthalmology, School of Medicine, Tufts University, Boston, MA, 02111, USA
e-mail: Allen.Taylor@tufts.edu

F. Shang
e-mail: Fu.Shang@tufts.edu

J. D. Ash et al. (eds.), *Retinal Degenerative Diseases,* Advances in Experimental Medicine and Biology 801, DOI 10.1007/978-1-4614-3209-8_77,

the induction and stabilization of HIF-1α by elevated glucose under normoxic conditions. Human lens epithelial cells and HeLa cells did not respond to high glucose, implying that this phenomenon is cell type-specific. Real-time RT-PCR for *HIF-1α* and *VEGF* and ELISA for VEGF indicated that high glucose is associated with elevated production of HIF-1α-induced VEGF, an established inducer of neovascularization, in the RPE cells. IF analyses showed that, although ChREBP was expressed under both low (5.6 mM) and high (25 mM) glucose conditions, it appeared more in the nuclear region than in the cytosol of the RPE cells after the high glucose treatment. ChIP analyses suggested a *HIF-1α* gene promoter association with ChREBP under the high glucose condition. These results imply that RPE cells use cytosolic ChREBP as a glucose sensor to up-regulate *HIF-1α* expression.
**Conclusion** These results suggest a high glucose-induced, ChREBP-mediated, and normoxic *HIF-1α* activation that may be partially responsible for neovascularization in both diabetic and age-related retinopathy.

**Keywords** Glucose · Hyperglycemia · Carbohydrate response element binding protein (ChREBP) · Hypoxia-inducible factor-1α (HIF-1α) · Vascular endothelial growth factor (VEGF) · Retinal pigment epithelial (RPE) · Neovascularization · Normoxia · Age-related macular degeneration (AMD) · Diabetic retinopathy (DR)

**Abbreviations**

| | |
|---|---|
| AMD | Age-related macular degeneration |
| AREDS | Age-related eye Diseases study |
| BMES | Blue mountains eye study |
| ChIP | Chromatin immunoprecipitation |
| ChRE | Carbohydrate response element |
| ChREBP | Carbohydrate response element binding protein |
| DR | Diabetic retinopathy |
| GI | Gycemic index |
| HIF-1α | Hypoxia-inducible factor-1α |
| HLE | Human lens epithelial |
| NHS | Nurses' Health Study |
| NVP | Nutrition and Vision Project |
| OEM | Osmolarity equivalent medium |
| PP2A | Protein phosphatase 2A |
| RPE | Retinal pigment epithelial |
| VEGF | Vascular endothelial growth factor |

## 77.1 Introduction

Age-related macular degeneration (AMD) is a progressive disease, the advanced forms of which account for over 50% (500,000 cases per year) of legal blindness in the USA [1]. Because the proportion of aged in our population is increasing, it is

estimated that the number of individuals affected with advanced AMD in the USA will increase more than 50 % from 1.75 million in 2,000 to 2.95 million in 2020 [2]. There is no cure for this devastating disease, so there is a high premium on preventing it or delaying its progress to debilitating stages. It is believed that dietary may be the most cost-effective strategy to address this health issue [3, 4].

In recent studies, we observed a link between glycemic index (GI) and increased risk for AMD in two American cohorts, the Nutrition and Vision Project (NVP) sub-study of the Nurses' Health Study (NHS) and the Age Related Eye Diseases Study (AREDS) of the NEI, NIH [5–9]. Both studies indicate that consuming diets that cause higher blood glucose loads (i.e. diets with higher GI) is associated with higher risk for AMD in otherwise healthy, non-diabetic individuals. The findings were corroborated in the Blue Mountains Eye Study (BMES) cohort, Australia [10]. However, the mechanism of this association remains poorly understood. Elucidating the biochemical mechanisms is critical for designing nutritional intervention strategies, furthering our understanding of the underlying pathogenesis, and would inform about the designs of new therapeutics for AMD [11].

We recently postulated that hyperglycemia (e.g. the high postprandial hyperglycemia induced by high-GI diets) may affect the risk for AMD, diabetic retinopathy (DR), and other diseases, through the activation of hypoxia-inducible factor (HIF)-inducible genes, such as vascular endothelial growth factor (*VEGF*), even under normoxia [12]. Uncontrolled VEGF is a major cause of blinding AMD, and contributes to proliferative DR.

Carbohydrate response element binding protein (ChREBP) is a key regulator of glucose metabolism, which is activated in response to high glucose and up-regulates more than 15 genes involved in the metabolic conversion of glucose to fat, such as the pyruvate kinase and lipogenesis enzyme genes, by binding to a carbohydrate response element (ChRE) of these genes [13]. Through controlling transcription of lipogenic enzyme genes in response to nutritional and hormonal inputs, ChREBP may play an important role in disease states, such as diabetes, obesity, hypertension, etc. Recently, the ChREBP has also been shown to be able to up-regulate the transcription of *HIF-1α* and, therefore, downstream HIF-inducible gene expression in human renal mesangial cells exposed to normoxia and high glucose, and it is suggested that this phenomenon is tissue (cell type)-specific [14]. However, this phenomenon has never been investigated in the human retina. In this study, we tested this hypothesis by determining if a ChREBP plays a role in the transcriptional up-regulation of hypoxia-inducible factor-1α (*HIF-1α*) and downstream *VEGF* expression in retinal pigment epithelial (RPE) cells exposed to normoxia and high glucose.

## 77.2 Materials and Methods

### *77.2.1 Cell Culture*

ARPE-19 cells, human lens epithelial (HLE) cells and HeLa cells (ATCC, Manassas, VA) were maintained in DMEM (Invitrogen, Carlsbad, CA) supplemented with

10% fetal bovine serum, 50 U/ml penicillin, and 50 μg/ml streptomycin. Before each assay, the cells were starved for 16 h in the media containing 0.2% fetal bovine serum albumin. After washing with PBS twice, the cells were incubated with serum-free culture media containing different glucose concentrations for 48 h.

### *77.2.2 Western Blot Analysis*

Whole-cells were lysed directly with SDS-gel loading buffer. Total proteins were resolved by 10% SDS-PAGE and transferred into nitrocellulose membrane (BioRad, USA). Primary antibodies were incubated in Tris-buffered saline with 2.5% milk. Secondary antibodies conjugated with horseradish peroxidase (Jackson immuno research, USA) and theSuperSignal West Pico detection system (ThermoFisher Scientific) were used for visualization. For semiquantitative analyses, the band densities were measured using Image-J software. The following primary antibodies were used: mouse anti-HIF-1α (Novus Biologicals, USA), rabbit anti-CHREBP (Novus Biologicals, USA), and mouse beta-actin (Sigma, USA).

### *77.2.3 Quantitative Real-Time PCR*

Total RNA was purified according to the manufacturer's instructions using an RNeasy mini kit (Qiagen, Valencia, CA). SuperScript III Reverse Transcriptase (Invitrogen, Carlsbad, CA), random hexadeoxynucleotide primers and oligo dT primers were used to synthesize cDNA. The real time PCR analyses were conducted on a MX3000P quantitative PCR system (Agilent technology, Willmington, DE, USA). SYBR Green PCR master mix (Qiagen, USA) was used to quantify human HIF-1α and VEGF mRNA. cDNA amplification was performed using the following set of primers: VEGF forward 5′-CAGAATCATCACGAAGTG-3′; VEGF reverse 5′-TCTGCATGGTGATGTTGGAC-3′. Quantitative RT-PCR was performed and HIF-1α mRNA or VEGF mRNA levels were normalized to beta-actin levels.

### *77.2.4 VEGF ELISA*

The concentration of VEGF in the cell culture media was measured by a VEGF ELISA kit (R&D Systems, USA), using monoclonal antibodies directed against human VEGF. Absorbance was measured at 450 nm, with wavelength correction at 570 nm.

### *77.2.5 ChIP Analysis*

Chromatin immunoprecipitation (ChIP) analysis was performed according to the instructions of EpiTect ChIP OneDay kit (QIAGEN, USA). Briefly, fragments of the

chromatin were incubated with rabbit anti-ChREBP antibodies (Novus Biologicals, USA) or rabbit polyclonal immunoglobulin G (Jackson Immune Research) and then precipitated by protein G-Sepharose. After wash and purification, PCR was performed using primers flanking the ChRE within the *HIF-1α* gene promoter: forward, 5'-CTCTTTCCTCCGCCGCTAAAC-3' and reverse, 5'-GGTTCCTCGAGATCCAATGGC-3'.

### *77.2.6 Immunofluorescence Staining*

Cells were grown on four-well chamber slides (BD Biosciences). Cells were washed with PBS, fixed for 10 min with 4 % paraformaldehyde in PBS and treated with 0.1 % Triton X-100. The slides were blocked with PBS containing 0.1 % TX-100 and 0.5 % BSA for 30 min. Staining with primary rabbit anti-CHREBP (Novus Biologicals, USA) for 2 h, and the slides were then washed with PBS and incubated with FITC conjugated secondary anti-rabbit antibody (Jackson Immuno Research) for 1 h. Slides were again washed with PBS and counterstained with DAPI for 5 min, rinsed, and briefly dried before mounting.

### *77.2.7 Statistical Analysis*

Data are reported as the mean ± 95 % confidence interval of at least three independent experiments. For comparison between two groups, the two-sided *t* test was used. In all cases, $p < 0.05$ was considered significant.

## 77.3 Results

### *77.3.1 High Glucose Induces Expression of* HIF-1α *in Human RPE Cells Under Normoxia*

ARPE-19 cells were incubated in medium containing 5.6, 11, 17, 25, and 30 mM glucose under normoxic (21 % $O_2$) condition for 48 h (Fig. 77.1). *HIF-1α* expression was then determined by immunoblot analyses and β-actin was used as a protein loading control. We observed that RPE cells maintained in the medium with normal level of glucose (5.6 mM D-glucose) under normoxic (21 % $O_2$) conditions showed weak basal *HIF-1α* expression, and HIF-1α levels were positively related to glucose concentrations between 5.6–25 mM in the RPE cells whereas at 5.6 mM glucose little HIF-1α was identified, HIF-1α was visible at 11 mM and became evident at above 17 mM. 25 mM D-glucose seemed to be a threshold for this relationship since the HIF-1α level under 30 mM D-glucose did not differ from that under 25 mM

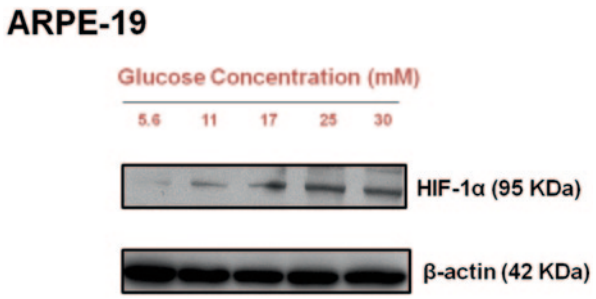


**Fig. 77.1** Dose-response of the induction and stabilization of *HIF-1α* by glucose under normoxia in RPE cells. *ARPE-19* cells were incubated in medium containing the indicated concentrations of glucose under normoxic (21 % $O_2$) conditions for 48 h. *HIF-1α* expression was determined by Western blotting. *β-actin* was used as a protein loading control

D-glucose. These results indicate that HIF-1α is induced and stabilized by glucose under normoxic conditions in RPE cells. To rule out the effect of osmolarity on this glucose-induced *HIF-1α* expression, the RPE cells were incubated in 5.6 mM D-glucose (NG), 25 mM D-glucose (HG), or osmolarity equivalent medium (OEM: 5.6 mM D-glucose and 19.4 mM L-glucose) for 48 h. HIF-1α and β-actin were then determined by Western blotting. The results showed that increasing osmolarity to levels that would be created by 25 mM glucose failed to enhance the *HIF-1α* expression (Fig. 77.2). This data suggest that glucose is responsible for the upregulation of *HIF-1α*.

We also compared this glucose-induced HIF-1α stabilization among HeLa, ARPE-19, and HLE cells. The Western blots showed stabilized HIF-1 α in the RPE cells, but not in HeLa and HLE under normoxic conditions, implying that this phenomenon is cell type-specific (Fig. 77.3).

To begin to explore the mechanism underlying high glucose-mediated upregulation of *HIF-1α*, HLE and ARPE-19 were incubated for 48 h in NG or HG medium and HIF-1α mRNA expression was determined by real-time PCR and normalized by β-actin. Interestingly, HIF-1α mRNA induction was increased by HG in the ARPE-19 cells but not in HLE cells (Fig. 77.4). Taken together, we observe a cell-type specific glucose-dependent transcriptional regulation of *HIF-1α* under normoxia.

### *77.3.2 High Glucose Induces VEGF Under Normoxia in RPE Cells*

To determine if VEGF, an established inducer of neovascularization, also respond to glucose-dependent transcriptional regulation, HLE and ARPE-19 cells were incubated in NG or HG medium for 48 h. VEGF mRNA expression was determined

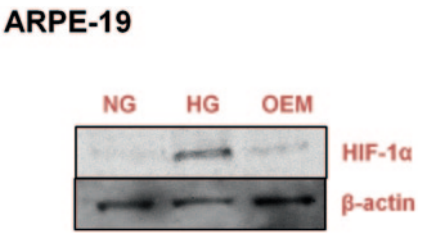


**Fig. 77.2** Ruling out osmolarity. *ARPE-19* cells were incubated in 5.6 mM glucose (*NG*), 25 mM glucose (*HG*), or osmolarity equivalent medium (*OEM*; 5.6 mM D-glucose and 19.4 mM L-glucose) for 48 h. *Hif-1α* and *β-actin* was determined by Western blot

by real-time PCR and normalized by β-actin. Similar to the results from HIF-1α, VEGF mRNA induction was increased by HG in the ARPE-19 cells but not in HLE cells (Fig. 77.5). To further determine if this glucose-dependent regulation of VEGF corresponded to the VEGF secretion, we measured VEGF secretion by ELISA. There was an over 60% increase of secreted VEGF by the RPE cells in the HG medium than in the NG. No significant difference was noted for the HLE cells (Fig. 77.6). Thus, like HIF-1α, VEGF levels are regulated in RPE cells in response to altering glucose, and the effect is cell-specific.

### *77.3.3 ChREBP has a Role in HIF-1α mRNA Induction by High Glucose*

To determine if the variations in levels of HIF-1α are a downstream effect of glucose-induced ChREBP, HLE cells and RPE cells were treated with NG or HG medium for 48 h and ChREBP protein expression was monitored by immunofluorescence. Rabbit polyclonal IgG was applied as a negative control, and input lysate was used as a positive control. We observed that, while ChREBP was expressed in the RPE cells under both NG and HG conditions, it tended to aggregate around the nucleoli under the HG condition (Fig. 77.7). We did not observe a distributional difference of ChREBP between NG and HG conditions in the HLE cells. Protein levels of ChREBP in the nucleus of the RPE cells appeared to be higher than in HLE cells, which might correlate with the cell-type specificity for *HIF-1α* induction by high glucose.

To demonstrate a role of ChREBP on the transcriptional regulation of *HIF-1α* gene in RPE cells, we carried out ChIP assays. PCR products amplifying indicated region of *HIF-1α* gene promoter by 40 cycles was then separated by 2.5% agarose gel electrophoresis. PCR product was confirmed by DNA sequencing. Anti-ChREBP antibodies efficiently precipitated the DNA fragments containing ChRE-like sequence in *HIF-1α* promoter from the ARPE-19 cells treated with HG (Fig. 77.8), indicating the binding of ChREBP to the *HIF-1α* promoter in the RPE

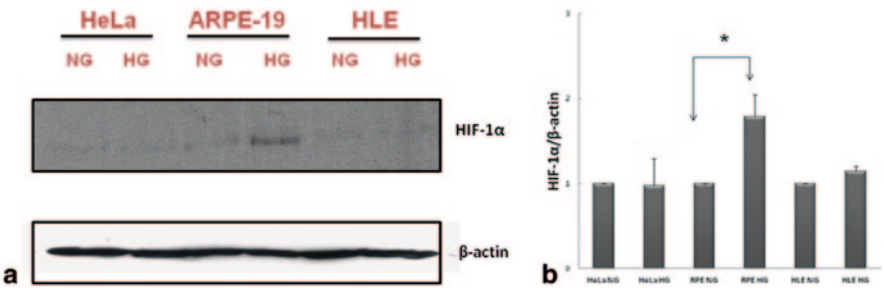


**Fig. 77.3** Induction and stabilization of *HIF-1α* by glucose under normoxia is cell-type specific. **a** *HeLa*, *ARPE-19*, and human lens epithelial (*HLE*) cells were treated with 5.6 mM glucose (*NG*) or 25 mM glucose (*HG*) for 48 h. *HIF-1α* and *β-actin* were detected by Western blotting. **b** Summary of three independent experiments. Desitometry was determined by Image J. *HIF-1α* values were normalized to *β-actin*. Data are means ($n=3$). *$p<0.05$ for 25 mM glucose versus control 5.6 mM glucose

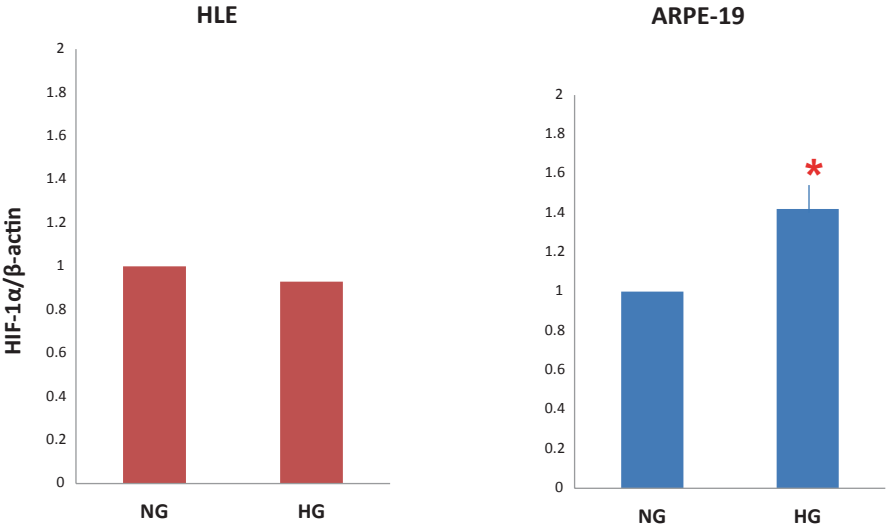


**Fig. 77.4** High glucose increases *HIF-1α* mRNA level in RPE cells under normoxia. Human lens epithelial (*HLE*) and *ARPE-19* were incubated for 48 h in 5.6 mM glucose (*NG*) or 25 mM glucose (*HG*) medium and *HIF-1α* mRNA expression was determined by real-time PCR and normalized by *β-actin*. *$p$ value $<0.05$

cells exposed to HG under nomaxia. In conclusion, *HIF-1α* uses ChREBP as a glucose sensor for regulation of its expression to participate in gene regulation in the RPE cells in response to high glucose.

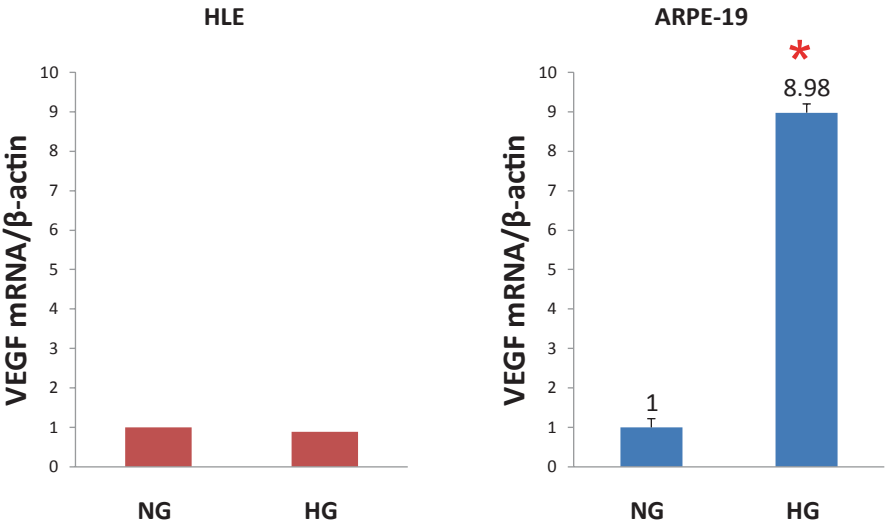


**Fig. 77.5** High glucose increases *VEGF mRNA* level in the RPE cells under normoxia. Human lens epithelial (*HLE*) and *ARPE-19* were incubated for 48 h in 5.6 mM glucose (*NG*) or 25 mM glucose (*HG*) medium and *VEGF mRNA* expression was determined by real-time PCR and normalized by *β-actin*. **p* value < 0.05

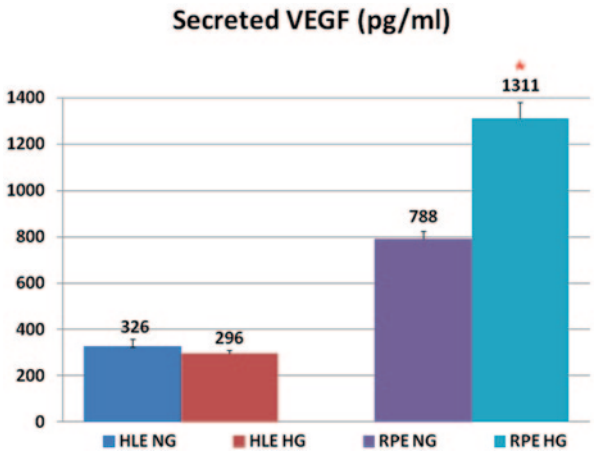


**Fig. 77.6** High glucose induces *VEGF* secretion by *RPE* cells under normoxia. *VEGF* secretions by ARPE-19 cells were measured by ELISA after incubation in the medium containing the indicated concentrations of glucose under normoxic (21 % $O_2$) condition for 48 h. Human lens epithelial (*HLE*). *Error bar* indicates 95 % CI, and **p*-value < 0.05 comparing 25 mM glucose (*HG*) to 5.6 mM (*NG*) glucose

## 77.4 Discussion

From a clinical point of view, VEGF is one of the most important HIF-inducible genes, because it induces postnatal neovascularization and angiogenesis seen after ischemic events in both DR and AMD patients [15]. It has been shown that hypoxia-induced HIF-1α mediates VEGF expression by increased binding of the

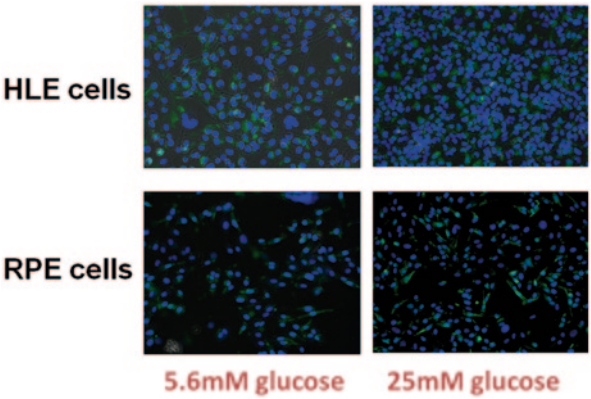


**Fig. 77.7** ChREBP is a glucose sensor in *RPE cells*. *HLE* cells and *RPE* cells treated with 5.6 mM glucose (NG) or 25 mM glucose (HG) medium for 48 h and detected for ChREBP protein expression by immunofluorescence staining. *Blue*: DAPI. *Green*: ChREBP

active HIF-1α to the HRE of the VEGF promoter and by increasing the stability of the VEGF mRNA transcript through mitogen-activated protein kinase and Akt pathways, respectively [16]. This mechanism at least partially contributes to the pathogenesis of DR and AMD, especially for the proliferative and neovascular types of the diseases. Anti-VEGF, such as Lucentis®, Avastin®, and Macugen®, has been used in clinics to treat exudative AMD [17, 18] and is currently being evaluated for the treatment of proliferative DR and neovascular glaucoma [19]. Recently, it has been shown that intravitreal ranibizumab (anti-VEGF therapy, trade name Lucentis®) with prompt or deferred laser is more effective through at least 1 year compared with prompt laser alone for the treatment of diabetic macular edema involving the central macula [20]. However, these applications of anti-VEGF therapeutics are limited to the late stages of the diseases and can only arrest the progression but not restore the compromised physiological functions. In addition to VEGF, recent studies have also explored the possibility of directly targeting HIF for a new therapeutic option for both DR and AMD [21–24]. Nevertheless, caution is advised because suppressing of HIF may be a double-edged sword because, by serving as one of the major regulators in glucose metabolism, HIF is necessary for maintaining physiological homeostasis.

Other challenges than hypoxia could also stabilize HIF and activate HIF-inducible proteins to contribute to retinal pathogenesis. It has been shown that RPE cells cultured with high concentrations of glucose enhance synthesis and accumulation of HIF under nomoxia, and the expression of VEGF is increased [25, 26]. Because cell respiration depends on the balance between glucose homeostasis and oxygen homeostasis, hyperglycemia increases the risk of oxygen depletion, which is similar to a hypoxic environment. Therefore, oxygen depletion can be viewed as frequently coincident events with hyperglycemia, even under physiological conditions [12]. This is especially true for the retina because the retina is the most metabolically active tissue in the human body, with dual blood supplies and rapid consumption of glucose and oxygen [27]. It has been proposed that even under normal tissue partial oxygen pressure diabetes-related hyperglycemia mimics the effects of true hypoxia

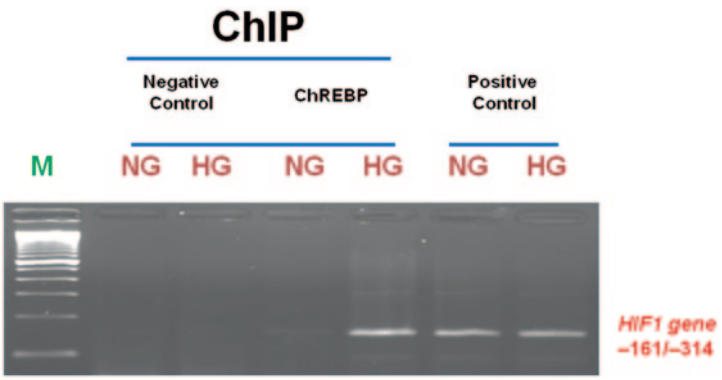


**Fig. 77.8** High glucose induces nuclear translocation of cytosolic ChREBP to up-regulate *HIF-1α* expression. RPE cells were treated in either 5.6 mM glucose (*NG*) or 25 mM glucose (*HG*) medium for 48 h, and chromatin immunoprecipitation (*ChIP*) assays using anti-ChREBP antibody were then performed. Rabbit polyclonal IgG was applied as a negative control, and input lysate was used as a positive control. PCR products amplifying indicated region of *HIF-1α* gene promoter by 40 cycles was then separated by 2.5 % agarose gel electrophoresis. PCR product was confirmed by DNA sequencing

on vascular and neural function and plays an important role in the pathogenesis of diabetic complications, including DR [28, 29]. Despite of these observations, it is unclear how the molecular mechanism works for these hyperglycemic retinal pathogeneses. In this study, we show that high glucose levels induced a ChREBP-mediated normoxic HIF-1α stabilization and VEGF expression.

Although ChREBP is a well-characterized transcription factor and playing a pivotal role in the glycolytic and lipogenic gene regulation in liver and adipose tissues [30], the role of ChREBP in the retina remains unclear. Our study is the first to demonstrate the expression of ChREBP and its role in mediating hyperglycemia-induced HIF expression in the RPE cells under normoxia. Notably, unlike hypoxia, the nomoxic hyperglycemia-induced, ChREBP-mediated HIF is regulated by increasing mRNA levels, and the phenomenon is cell-type specific, i.e., we only observed the phenomenon in the RPE cells but not in either HLE cells or HeLa cells. It has been proposed that high glucose facilitates nuclear translocation of dephosphorylated ChREBP by protein phosphatase 2A (PP2A), which is upregulated by an intermediate, xylulose-5-P, in the pentose phosphate pathway [31]. Since the pentose phosphate pathway is an alternative to glycolysis and only activated in specific cell types, this may offer an explanation for the cell-type specific glucose-induced ChREBP-mediated HIF activation under normoxia. Further deciphering this biochemical mechanism will advance our understanding of the underlying pathogenesis and enhance therapeutic options for metabolic retinal diseases, such as DR and AMD, preferably in the early stages of the diseases.

In conclusion, our observations suggest that ChREBP plays a role in the transcriptional upregulation of HIF-1α under hyperglycemic, nomoxic conditions. This observation provides support for our hypothesis that HIF can also be considered as

a hyperglycemia-inducible factor. Since the hyperglycemic HIF pathway and its interactions with other hyperglycemic pathogenesis pathways, such as hyperglycemic AGE, PKC, polyol, and hexosamine pathways, can affect oxidative stress responses, inflammation, proteolytic mechanisms, etc., all of which are involved in the pathogeneses of DR and AMD [12]. Elucidating this wide range of hyperglycemic cellular effects may open new treatment indications.

**Acknowledgment** The funding sources had no role in the design and conduct of the study; the collection, analysis, and interpretation of the data; or the preparation, review, or approval of the manuscript.

We declare that we have no conflict of interest. Any opinions, findings, conclusions, or recommendations expressed in this publication are those of the authors and do not necessarily reflect the views or policies of the USA Department of Agriculture, nor does mention of trade names, commercial products, or organizations imply endorsement by the USA Government.

**Funding** NEI R01 EY021826, EY021212, EY013250, Ross Aging Initiative, and USDA agreements 1950-5100-060-01A.

## References

1. Congdon N, O'Colmain B, Klaver CC, Klein R, Munoz B, Friedman DS, Kempen J, Taylor HR, Mitchell P, Group EDPR (2004) Causes and prevalence of visual impairment among adults in the United States. Arch Ophthalmol 122:477–485
2. Friedman DS, O'Colmain BJ, Munoz B, Tomany SC, McCarty C, de Jong PT, Nemesure B, Mitchell P, Kempen J, Group EDPR (2004) Prevalence of age-related macular degeneration in the United States. Arch Ophthalmol 122:564–572
3. Chiu CJ, Taylor A (2007) Nutritional antioxidants and age-related cataract and maculopathy. Exp Eye Res 84:229–245
4. Weikel KA, Chiu CJ, Taylor A (2012) Nutritional modulation of age-related macular degeneration. Mol Aspects Med 33:318–375
5. Chiu CJ, Hubbard LD, Armstrong J, Rogers G, Jacques PF, Chylack JLT, Hankinson SE, Willett WC, Taylor A (2006) Dietary glycemic index and carbohydrate in relation to early age-related macular degeneration. Am J Clin Nutr 83:880–886
6. Chiu CJ, Klein R, Milton RC, Gensler G, Taylor A (2009) Does eating particular diets alter risk of age-related macular degeneration in users of the age-related eye disease study supplements? Br J Ophthalmol 93:1241–1246
7. Chiu CJ, Milton RC, Gensler G, Taylor A (2007) Association between dietary glycemic index and age-related macular degeneration in the age-related eye disease study. Am J Clin Nutr 86:180–188
8. Chiu CJ, Milton RC, Klein R, Gensler G, Taylor A (2007) Dietary carbohydrate and progression of age-related macular degeneration, a prospective study from the age-related eye disease study. Am J Clin Nutr 86:1210–1218
9. Chiu CJ, Milton RC, Klein R, Gensler G, Taylor A (2009) Dietary compound score and risk of age-related macular degeneration in the age-related eye disease study. Ophthalmology 116:939–946
10. Kaushik S, Wang JJ, Flood V, Tan JS, Barclay AW, Wong TY, Brand-Miller J, Mitchell P (2008) Dietary glycemic index and the risk of age-related macular degeneration. Am J Clin Nutr 88:1104–1110
11. Chiu CJ, Liu S, Willett WC, Wolever TMS, Brand-Miller JC, Barclay AW, Taylor A (2011) Informing food choices and health outcomes by use of the dietary glycemic index. Nutr Rev 69:231–242

12. Chiu CJ, Taylor A (2011) Dietary hyperglycemia, glycemic index and metabolic retinal diseases. Prog Retin Eye Res 30:18–53
13. Uyeda K, Yamashita H, Kawaguchi T (2002) Carbohydrate responsive element-binding protein (ChREBP): a key regulator of glucose metabolism and fat storage. Biochem Pharmacol 63:2075–2080
14. Isoe T, Makino Y, Mizumoto K, Sakagami H, Fujita Y, Honjo J, Takiyama Y, Itoh H, Haneda M (2010) High glucose activates HIF-1-mediated signal transduction in glomerular mesangial cells through a carbohydrate response element binding protein. Kidney Int 78:48–59
15. Lee SH, Wolf PL, Escudero R, Deutsch R, Jamieson SW, Thistlethwaite PA (2000) Early expression of angiogenesis factors in acute myocardial ischemia and infarction. N Engl J Med 342:626–633
16. Suzuma K, Naruse K, Suzuma I, Takahara N, Ueki K, Aiello LP, King GL (2000) Vascular endothelial growth factor induces expression of connective tissue growth factor via KDR, Flt1, and phosphatidylinositol 3-kinase-akt-dependent pathways in retinal vascular cells. J Biol Chem 275:40725–40731
17. Bressler SB (2009) Introduction: understanding the role of angiogenesis and antiangiogenic agents in age-related macular degeneration. Ophthalmology 116(10 Suppl):S 1–7
18. Bressler NM (2009) Antiangiogenic approaches to age-related macular degeneration today. Ophthalmology 116(10 Suppl):S 15–23
19. Rodriguez-Fontal M, Alfaro V, Kerrison JB Jablon EP (2009) Ranibizumab for diabetic retinopathy. Curr Diabetes Rev 5:47–51
20. The Diabetic Retinopathy Clinical Research Network, Elman MJ, Aiello LP, Beck RW, Bressler NM, Bressler SB, Edwards AR, Ferris FL III, Friedman SM, Glassman AR, Miller KM, Scott IU, Stockdale CR, Sun JK (2010) Randomized trial evaluating ranibizumab plus prompt or deferred laser or triamcinolone plus prompt laser for diabetic macular edema. Ophthalmology 117:1064–1077
21. Wang X, Wang G, Wang Y (2009) Intravitreous vascular endothelial growth factor and hypoxia-inducible factor 1a in patients with proliferative diabetic retinopathy. Am J Ophthalmol 148:883–889
22. Zhang P, Wang Y, Hui Y, Hu D, Wang H, Zhou J, Du H (2007) Inhibition of VEGF expression by targeting HIF-1 alpha with small interference RNA in human RPE cells. Ophthalmologica 221:411–417
23. Arjamaa O, Nikinmaa M (2006) Oxygen-dependent diseases in the retina: role of hypoxia-inducible factors. Exp Eye Res 83:473–483
24. Arjamaa O, Nikinmaa M, Salminen A, Kaarniranta K (2009) Regulatory role of HIF-1alpha in the pathogenesis of age-related macular degeneration (AMD). Ageing Res Rev 8:349–358
25. Xiao Q, Zeng S, Ling S, Lv M (2006) Up-regulation of HIF-1alpha and VEGF expression by elevated glucose concentration and hypoxia in cultured human retinal pigment epithelial cells. J Huazhong Univ Sci Technolog Med Sci 26:463–465
26. Yao Y, Guan M, Zhao XQ, Huang YF (2003) Downregulation of the pigment epithelium derived factor by hypoxia and elevated glucose concentration in cultured human retinal pigment epithelial cells (Article in Chinese). Zhonghua Yi Xue Za Zhi 83:1989–1992
27. Cohen LH, Noell WK (1965) Relationships between visual function and metabolism. Academic Press, New York
28. Williamson JR, Chang K, Frangos M, Hasan KS, Ido Y, Kawamura T, Nyengaard JR, van den Enden M, Kilo C, Tilton RG (1993) Hyperglycemic pseudohypoxia and diabetic complications. Diabetes 42:801–813
29. Nyengaard JR, Ido Y, Kilo C, Williamson JR (2004) Interactions between hyperglycemia and hypoxia: implications for diabetic retinopathy. Diabetes 53:2931–2938
30. Uyeda K, Repa JJ (2006) Carbohydrate response element binding protein, ChREBP, a transcription factor coupling hepatic glucose utilization and lipid synthesis. Cell Metab 4:107–110
31. Haase VH (2010) The sweet side of HIF. Kidney Int 78:10–13

# Chapter 78
# Sphingolipids in Ocular Inflammation

**Annie Y. Chan, Shivani N. Mann, Hui Chen, Donald U. Stone, Daniel J. J. Carr and Nawajes A. Mandal**

**Abstract** Sphingolipids are essential to cell membrane structure and the development and maintenance of neural tissues. The role of bioactive sphingolipids has been established in numerous cellular events, including cell survival, growth, and apoptosis. Ocular inflammatory and autoimmune diseases involve activation and migration of endothelial cells, neovascularization, and infiltration of immune cells into various tissues. Clinically, the impact and role of sphingolipid-mediated signaling is increasingly being appreciated in the pathogenesis and treatment of diseases ranging from multiple sclerosis to neovascularization in age-related macular degeneration and diabetic retinopathy. In this review, we discuss our current knowledge and understanding of sphingolipid metabolism and signaling associated with the pathogenesis of ocular diseases.

N. A. Mandal (✉) · A. Y. Chan · S. N. Mann · H. Chen · D. U. Stone · D. J. J. Carr
Department of Ophthalmology, OUHSC, Oklahoma City, OK, USA
e-mail: mmandal@ouhsc.edu

A. Y. Chan · S. N. Mann · H. Chen · D. U. Stone · D. J. J. Carr · N. A. Mandal
Dean A. McGee Eye Institute, Oklahoma City, OK, USA
e-mail: annie-chan@ouhsc.edu

S. N. Mann
e-mail: shivani-mann@ouhsc.edu

H. Chen
Department of Ophthalmology, Sichuan Academy of Medical Sciences & Sichuan Provincial People's Hospital, Chengdu, Sichuan, China
e-mail: chenhuicq@yahoo.com.cn

D. U. Stone
e-mail: Donald-stone@dmei.org

D. J. J. Carr
Department of Microbiology and Immunology, OUHSC, Oklahoma City, OK, USA
e-mail: DAN-CARR@OUHSC.EDU

N. A. Mandal
Department of Physiology, OUHSC, Oklahoma City, OK, USA

Department of Oklahoma Center for Neuroscience (OCNS), OUHSC, Oklahoma City, OK, USA

J. D. Ash et al. (eds.), *Retinal Degenerative Diseases,* Advances in Experimental Medicine and Biology 801, DOI 10.1007/978-1-4614-3209-8_78,

**Keywords** Sphingolipid · Ceramide · Sphingosine-1-phosphate · Ocular inflammation · Uveitis · Apoptosis

## 78.1 Introduction

Significant progress has been made in elucidating the role of sphingolipid signaling in cellular physiology and diseases. A delicate balance is important for cellular homeostasis and signaling, which has been defined as the "sphingolipid rheostat" [1]. Any imbalance in the level of bioactive sphingolipids, such as ceramide (Cer), sphingosine (Sph), and their phosphorylated products, ceramide-1-phosphate (C1P) and sphingosine-1-phosphate (S1P) can alter the signaling for cell survival, inflammatory pathways, and apoptosis [2–5]. The association of sphingolipids in human inflammatory diseases such as asthma, ulcerative colitis and Crohn's disease has previously been reviewed [6–8]. Here, we review the role of sphingolipids in inflammatory signaling associated with ocular diseases and the implications of sphingolipids as a therapeutic target.

## 78.2 Uveitis, Multiple Sclerosis and Fingolimod

Evidences are mounting up suggesting roles of sphingolipids in autoimmune eye diseases such as optic neuritis and uveitis. Further, the application of FTY720 (fingolimod) as a drug that can modify the course of experimental uveitis and other inflammatory diseases has provided insights into sphingolipid signaling in such diseases. Multiple sclerosis (MS) is a disease characterized by immune-mediated demyelination and neurodegeneration. FTY720, a synthetic analog of sphingosine (Sph), is an FDA-approved drug used to treat relapsing MS. Once delivered in vivo, native sphingosine kinase 2 (normally phosphorylating Sph to S1P), phosphorylates FTY720, which then mimics S1P and inactivates S1P receptor-mediated signals. Thus a wide range of cell activity is affected, including inhibition of lymphocyte egress from lymph nodes into circulation [9]. As T lymphocytes are linked to the demyelination process, FTY720 can effectively reduce T lymphocyte levels and attenuate disease severity in MS patients. Treatment with FTY720 in animal models also implies a neuroprotective role for the drug by reducing axonal loss and demyelination [10].

Ocular complications in MS include retinitis, optic neuritis, and uveitis. Although it lacks myelination, the retina is a target of inflammation in MS leading to disruption of the blood-retinal barrier [11, 12]. Moreover, the extent of retinal periphlebitis correlates with MS disease severity [13], and retinal ganglion cells begin to degenerate prior to widespread neurodegenerative damage [14]. Up to 1 % of MS patients treated with FTY720 develop macular edema, an uncommon but generally reversible side effect [15, 16]. Macular edema is not typically seen in MS in the absence of uveitis or pars planitis. However, high resolution SD-OCT has led to the

finding of a 4.7% incidence of microcystic macular edema (MME) in patients with MS, none of whom were on FTY720 therapy [17]. This supports the notion of a local blood-retinal barrier breakdown due to subtle inflammatory activity in the retina [17]. Optic neuritis is also a common ocular complication of MS; however, less is known about the role of FTY720 in optic neuritis. Treatment of a rat model for optic neuritis with FTY720 reinforces the findings of reduced inflammation, demyelination, and axonal damage [18]. Yet, FTY720 does not prevent retinal ganglion cell apoptosis despite observations that it inhibits synthesis of ceramide, a pro-apoptotic molecule [19, 20].

Uveitis is the most common presentation of ocular inflammatory disease. Experimental autoimmune uveoretinitis (EAU) is a well-characterized animal model. FTY720 has been found to suppress both the incidence and intensity of inflammation in a dose-dependent manner in EAU [21]. When administered prior to the onset of EAU, FTY720 prevents inflammatory cells from infiltrating the retina [22, 23]. The same has been reported in clinical cases of uveitis [24]. While the nuances of how sphingolipids affect inflammatory cellular activity remain under investigation, the modulation of Cer and S1P biosynthesis by FTY720 strengthens the role of sphingolipids in the pathogenesis of inflammatory neural and ocular diseases [25–27].

## 78.3 The Sphingolipid Inflammatory Link to Retinopathies

Advanced age-related macular degeneration (AMD) and proliferative diabetic retinopathy characteristically develop choroidal and retinal neovascularization (CNV and RNV respectively), and currently account for the greatest number of cases of untreatable blindness. Multiple animal models exist to support inflammatory mediators (including complement, cytokines, and chemokines) as part of the pathogenesis of CNV and RNV [28]. For example, intravitreal injection of alpha-galactosylceramide (αGal-Cer), a ligand for natural killer T cells, can promote CNV, thus supporting an inflammatory link to the induction of CNV [29]. In ischemia-induced retinopathy models, while control mice develop vitreous neovascularization, S1P receptor 2 (S1P2) knockout mice do not. Furthermore, these mice demonstrate reductions in endothelial gaps and inflammatory cells in the retina, indicating a role for S1P2-mediated signaling in pathologic ocular angiogenesis [30]. Sonepcizumab, a humanized monoclonal antibody that selectively binds to S1P, is currently under evaluation in phase III clinical trials for treatment of advanced AMD. Intraocular injection of sonepcizumab in CNV mouse models results in a significant reduction in the area of CNV and degree of leakage from the residual CNV [31]. Similar results have also been achieved in laser-induced CNV models of mice [32].

Although proliferative diabetic retinopathy (characterized by RNV) does not manifest in rodent models, decreased Cer levels and a concomitant increase in glucosylceramide content have been observed in the retinas of streptozotocin-induced diabetic rats [33]. Finally, in human retinal endothelial cells (HRECs), activation

of sphingomyelinase (SMase), the enzyme that produces Cer from sphingomyelin, has been shown to mediate cytokine-induced inflammation [34]. Treatment with the SMase inhibitor, docosahexaenoic acid, significantly reduces cytokine signaling in HREC cells [34–36]. Thus, although inflammatory pathways have long been established in models for CNV and RNV, signaling via sphingolipids is an evolving theory for how these pathways interact and ultimately lead to disease.

## 78.4 Anterior Segment Diseases

As sphingolipid signaling becomes more significant in posterior segment inflammation, the mechanisms of Cer modulation of inflammation in the anterior segment of the eye are less clear. Liposomal delivery of short-chain Cer is reportedly effective in inhibiting inflammation induced by either lipopolysaccharides or *S. aureus* in mouse corneas [37]. Cer can also suppress corneal haze caused by exposure to ultraviolet B (UVB) radiation during photorefractive keratectomy (PRK) [38]. FTY720 is effective in increasing survival rates of corneal transplantation in mouse models, providing potential utility in corneal allografts [39]. Furthermore, oral administration of FTY720 in rats after corneal transplantation reduces the infiltration of lymphocytes and significantly prolongs allograft survival [40]. Finally, in primary Sjogren's syndrome (an autoimmune disease involving inflammation and destruction of lacrimal and salivary gland cells), increase of S1P receptor 1 expression in the infiltrating inflammatory cells has been noted, indication S1P signaling is involved in the autoimmune response [41].

## 78.5 Conclusions

Lysosomal storage diseases due to genetic dysfunction in sphingolipid metabolism have long been associated with various forms of ocular pathogenesis and blindness. Most recently, cellular activities associated with ocular inflammatory and autoimmune diseases have been linked with sphingolipid signaling. Investigation into sphingolipid signaling has also determined these molecules to be important mediators in the pathogenesis of blinding diseases. Nevertheless, there are still many details of how these bioactive molecules interact with each other and with other signaling pathways are yet to be elucidated. Deciphering the regulatory role of sphingolipids in these diseases ultimately presents an opportunity to pursue them as future therapeutic targets.

**Acknowledgment** Our study is supported by NIH grants EY022071; EY021725; RR17703 and Research to Prevent Blindness Inc. USA.

## References


1. Spiegel S, Milstien S (2003) Sphingosine-1-phosphate: an enigmatic signalling lipid. Nat Rev Mol Cell Biol 4(5):397–407
2. Gangoiti P, Camacho L, Arana L, Ouro A, Granado MH, Brizuela L, Casas J, Fabrias G, Abad JL, Delgado A, Gomez-Munoz A (2010) Control of metabolism and signaling of simple bioactive sphingolipids: implications in disease. Prog Lipid Res 49(4):316–334
3. Hannun YA, Obeid LM (2008) Principles of bioactive lipid signalling: lessons from sphingolipids. Nat Rev Mol Cell Biol 9(2):139–150
4. Merrill AH Jr, Schmelz EM, Dillehay DL, Spiegel S, Shayman JA, Schroeder JJ, Riley RT, Voss KA, Wang E (1997) Sphingolipids-the enigmatic lipid class: biochemistry, physiology, and pathophysiology. Toxicol Appl Pharmacol 142(1):208–225
5. Obeid LM, Linardic CM, Karolak LA, Hannun YA (1993) Programmed cell death induced by ceramide. Science 259(5102):1769–1771
6. Teichgraber V, Ulrich M, Endlich N, Riethmuller J, Wilker B, De Oliveira-Munding CC, van Heeckeren AM, Barr ML, von Kurthy G, Schmid KW, Weller M, Tummler B, Lang F, Grassme H, Doring G, Gulbins E (2008) Ceramide accumulation mediates inflammation, cell death and infection susceptibility in cystic fibrosis. Nat Med 14(4):382–391
7. El Alwani M, Wu BX, Obeid LM, Hannun YA (2006) Bioactive sphingolipids in the modulation of the inflammatory response. Pharmacol Ther 112(1):171–183
8. Nixon GF (2009) Sphingolipids in inflammation: pathological implications and potential therapeutic targets. Br J Pharmacol 158(4):982–993
9. Chun J, Hartung HP (2010) Mechanism of action of oral fingolimod (FTY720) in multiple sclerosis. Clin Neuropharmacol 33(2):91–101
10. Balatoni B, Storch MK, Swoboda EM, Schonborn V, Koziel A, Lambrou GN, Hiestand PC, Weissert R, Foster CA (2007) FTY720 sustains and restores neuronal function in the DA rat model of MOG-induced experimental autoimmune encephalomyelitis. Brain Res Bull 74(5):307–316
11. Green AJ, McQuaid S, Hauser SL, Allen IV, Lyness R (2010) Ocular pathology in multiple sclerosis: retinal atrophy and inflammation irrespective of disease duration. Brain 133(Pt 6):1591–1601
12. Trip SA, Schlottmann PG, Jones SJ, Altmann DR, Garway-Heath DF, Thompson AJ, Plant GT, Miller DH (2005) Retinal nerve fiber layer axonal loss and visual dysfunction in optic neuritis. Ann Neurol 58(3):383–391
13. Sepulcre J, Murie-Fernandez M, Salinas-Alaman A, Garcia-Layana A, Bejarano B, Villoslada P (2007) Diagnostic accuracy of retinal abnormalities in predicting disease activity in MS. Neurology 68(18):1488–1494
14. Fairless R, Williams SK, Hoffmann DB, Stojic A, Hochmeister S, Schmitz F, Storch MK, Diem R (2012) Preclinical retinal neurodegeneration in a model of multiple sclerosis. J Neurosci 32(16):5585–5597
15. Cohen JA, Barkhof F, Comi G, Hartung HP, Khatri BO, Montalban X, Pelletier J, Capra R, Gallo P, Izquierdo G, Tiel-Wilck K, de Vera A, Jin J, Stites T, Wu S, Aradhye S, Kappos L (2010) Oral fingolimod or intramuscular interferon for relapsing multiple sclerosis. N Engl J Med 362(5):402–415
16. Kappos L, Radue EW, O'Connor P, Polman C, Hohlfeld R, Calabresi P, Selmaj K, Agoropoulou C, Leyk M, Zhang-Auberson L, Burtin P (2010) A placebo-controlled trial of oral fingolimod in relapsing multiple sclerosis. N Engl J Med 362(5):387–401
17. Gelfand JM, Nolan R, Schwartz DM, Graves J, Green AJ (2012) Microcystic macular oedema in multiple sclerosis is associated with disease severity. Brain 135(Pt 6):1786–1793
18. Rau CR, Hein K, Sattler MB, Kretzschmar B, Hillgruber C, McRae BL, Diem R, Bahr M (2011) Anti-inflammatory effects of FTY720 do not prevent neuronal cell loss in a rat model of optic neuritis. Am J Pathol 178(4):1770–1781

19. Berdyshev EV, Gorshkova I, Skobeleva A, Bittman R, Lu X, Dudek SM, Mirzapoiazova T, Garcia JG, Natarajan V (2009) FTY720 inhibits ceramide synthases and up-regulates dihydrosphingosine 1-phosphate formation in human lung endothelial cells. J Biol Chem 284(9):5467–5477
20. Lahiri S, Park H, Laviad EL, Lu X, Bittman R, Futerman AH (2009) Ceramide synthesis is modulated by the sphingosine analog FTY720 via a mixture of uncompetitive and noncompetitive inhibition in an Acyl-CoA chain length-dependent manner. J Biol Chem 284(24):16090–16098
21. Kurose S, Ikeda E, Tokiwa M, Hikita N, Mochizuki M (2000) Effects of FTY720, a novel immunosuppressant, on experimental autoimmune uveoretinitis in rats. Exp Eye Res 70(1):7–15
22. Commodaro AG, Peron JP, Lopes CT, Arslanian C, Belfort R Jr, Rizzo LV, Bueno V (2010) Evaluation of experimental autoimmune uveitis in mice treated with FTY720. Invest Ophthalmol Vis Sci 51(5):2568–2574
23. Raveney BJ, Copland DA, Nicholson LB, Dick AD (2008) Fingolimod (FTY720) as an acute rescue therapy for intraocular inflammatory disease. Arch Ophthalmol 126(10):1390–1395
24. Sakaguchi M, Sugita S, Sagawa K, Itoh K, Mochizuki M (1998) Cytokine production by T cells infiltrating in the eye of uveitis patients. Jpn J Ophthalmol 42(4):262–268
25. Brinkmann V, Davis MD, Heise CE, Albert R, Cottens S, Hof R, Bruns C, Prieschl E, Baumruker T, Hiestand P, Foster CA, Zollinger M, Lynch KR (2002) The immune modulator FTY720 targets sphingosine 1-phosphate receptors. J Biol Chem 277(24):21453–21457
26. Foster CA, Mechtcheriakova D, Storch MK, Balatoni B, Howard LM, Bornancin F, Wlachos A, Sobanov J, Kinnunen A, Baumruker T (2009) FTY720 rescue therapy in the dark agouti rat model of experimental autoimmune encephalomyelitis: expression of central nervous system genes and reversal of blood-brain-barrier damage. Brain Pathol 19(2):254–266
27. Webb M, Tham CS, Lin FF, Lariosa-Willingham K, Yu N, Hale J, Mandala S, Chun J, Rao TS (2004) Sphingosine 1-phosphate receptor agonists attenuate relapsing-remitting experimental autoimmune encephalitis in SJL mice. J Neuroimmunol 153(1-2):108–121
28. Grossniklaus HE, Kang SJ, Berglin L (2010) Animal models of choroidal and retinal neovascularization. Prog Retin Eye Res 29(6):500–519
29. Hijioka K, Sonoda KH, Tsutsumi-Miyahara C, Fujimoto T, Oshima Y, Taniguchi M, Ishibashi T (2008) Investigation of the role of CD1d-restricted invariant NKT cells in experimental choroidal neovascularization. Biochem Biophys Res Commun 374(1):38–43
30. Skoura A, Sanchez T, Claffey K, Mandala SM, Proia RL, Hla T (2007) Essential role of sphingosine 1-phosphate receptor 2 in pathological angiogenesis of the mouse retina. J Clin Invest 117(9):2506–2516
31. Xie B, Shen J, Dong A, Rashid A, Stoller G, Campochiaro PA (2009) Blockade of sphingosine-1-phosphate reduces macrophage influx and retinal and choroidal neovascularization. J Cell Physiol 218(1):192–198
32. Caballero S, Swaney J, Moreno K, Afzal A, Kielczewski J, Stoller G, Cavalli A, Garland W, Hansen G, Sabbadini R, Grant MB (2009) Anti-sphingosine-1-phosphate monoclonal antibodies inhibit angiogenesis and sub-retinal fibrosis in a murine model of laser-induced choroidal neovascularization. Exp Eye Res 88(3):367–377
33. Fox TE, Han X, Kelly S, Merrill AH 2nd, Martin RE, Anderson RE, Gardner TW, Kester M (2006) Diabetes alters sphingolipid metabolism in the retina: a potential mechanism of cell death in diabetic retinopathy. Diabetes 55(12):3573–3580
34. Chen W, Esselman WJ, Jump DB, Busik JV (2005) Anti-inflammatory effect of docosahexaenoic acid on cytokine-induced adhesion molecule expression in human retinal vascular endothelial cells. Invest Ophthalmol Vis Sci 46(11):4342–4347
35. Opreanu M, Lydic TA, Reid GE, McSorley KM, Esselman WJ, Busik JV (2010) Inhibition of cytokine signaling in human retinal endothelial cells through downregulation of sphingomyelinases by docosahexaenoic acid. Invest Ophthalmol Vis Sci 51(6):3253–3263
36. Opreanu M, Tikhonenko M, Bozack S, Lydic TA, Reid GE, McSorley KM, Sochacki A, Perez GI, Esselman WJ, Kern T, Kolesnick R, Grant MB, Busik JV (2011) The unconventional role of acid sphingomyelinase in regulation of retinal microangiopathy in diabetic human and animal models. Diabetes 60(9):2370–2378

37. Sun Y, Fox T, Adhikary G, Kester M, Pearlman E (2008) Inhibition of corneal inflammation by liposomal delivery of short-chain, C-6 ceramide. J Leukoc Biol 83(6):1512–1521
38. Kim TI, Lee SY, Pak JH, Tchah H, Kook MS (2006) Mitomycin C, ceramide, and 5-fluorouracil inhibit corneal haze and apoptosis after PRK. Cornea 25(1):55–60
39. Zhang EP, Muller A, Ignatius R, Hoffmann F (2003) Significant prolongation of orthotopic corneal-graft survival in FTY720-treated mice. Transplantation 76(10):1511–1513
40. Mayer K, Birnbaum F, Reinhard T, Reis A, Braunstein S, Claas F, Sundmacher R (2004) FTY720 prolongs clear corneal allograft survival with a differential effect on different lymphocyte populations. Br J Ophthalmol 88(7):915–919
41. Sekiguchi M, Iwasaki T, Kitano M, Kuno H, Hashimoto N, Kawahito Y, Azuma M, Hla T, Sano H (2008) Role of sphingosine 1-phosphate in the pathogenesis of Sjogren's syndrome. J Immunol 180(3):1921–1928

# Chapter 79
# Biosynthesis of Very Long-Chain Polyunsaturated Fatty Acids in Hepatocytes Expressing ELOVL4

**Martin-Paul Agbaga, Sreemathi Logan, Richard S. Brush and Robert E. Anderson**

**Abstract** Elongation of Very Long chain fatty acids-4 (ELOVL4) is a fatty acid condensing enzyme that mediates biosynthesis of very long chain polyunsaturated fatty acids (VLC-PUFA; ≥C28) in a limited number of tissues. Depletion of VLC-PUFA in retinal photoreceptors leads to retinal dysfunction and likely contributes to autosomal dominant Stargardt-like macular dystrophy (STGD3) pathology. In addition, depletion of VLC-PUFA in rodent testicular tissues leads to sterility. These results suggest that VLC-PUFA synthesized in situ play a unique role that cannot be compensated for by other fatty acid species. Though liver is the major fatty acid biosynthetic organs, it does not express the ELOVL4 protein; hence, no VLC-PUFA are detected in the blood and plasma. Thus, delivery of these VLC-PUFA to target tissues to compensate for their reduction caused by disease presents a challenge. We hypothesized that expression of ELOVL4 in the liver will result in the biosynthesis of VLC-PUFA that could be transported via the bloodstream to target tissues such as retina, brain and testis. Hence, we evaluated the ability of rat hepatoma (4HIIE) and

M.-P. Agbaga (✉) · R. S. Brush · R. E. Anderson
Departments of Ophthalmology, University of Oklahoma Health Sciences Center, Oklahoma City, OK 73104, USA
e-mail: martin-paul-agbaga@ouhsc.edu

M.-P. Agbaga · S. Logan · R. S. Brush · R. E. Anderson
Dean McGee Eye Institute, Oklahoma City, OK 73104, USA

R. S. Brush
e-mail: Richard-Brush@ouhsc.edu

S. Logan · R. E. Anderson
Department of Cell Biology, University of Oklahoma Health Sciences Center, Oklahoma City, OK 73104, USA
e-mail: slogan1@ouhsc.edu

R. E. Anderson
e-mail: Robert-Anderson@ouhsc.edu

J. D. Ash et al. (eds.), *Retinal Degenerative Diseases,* Advances in Experimental Medicine and Biology 801, DOI 10.1007/978-1-4614-3209-8_79,

human hepatocyte (HepG2) cells to synthesize VLC-PUFA by expressing ELOVL4 in these cells. We showed that, in the presence of ELOVL4, both 4HIIE and HepG2 cells are capable of VLC-PUFA biosynthesis. We propose that transgenic expression of ELOVL4 in the liver will result in the biosynthesis of VLC-PUFA that can be transported to target.

**Keywords** Hepatocytes · Degeneration · Very long chain polyunsaturated fatty acids (VLC-PUFA) · Elongation of Very Long Chain Fatty Acids-4 (ELOVL4) · Autosomal dominant Stargardt-like macular dystrophy

## 79.1 Introduction

Elongation of Very Long-chain fatty acids-4 (ELOVL4) is a fatty acid condensing enzyme expressed in retina photoreceptors, brain, sperm and testis, which all contain very long-chain polyunsaturated fatty acids (VLC-PUFA; C28-C40) [1–4]. In addition, ELOVL4 expression in the skin results in the biosynthesis of saturated very long chain fatty acids (VLC-FA) that are incorporated into sphingolipids and ceramides to maintain skin barrier permeability. Hence, ablation of the ELOVL4 protein in transgenic mice results in neonatal lethality due to dehydration [5–9]. Although liver is the major fatty acid biosynthetic organs in the body, it does not express the ELOVL4 protein; hence, no VLC-PUFA are detected in the liver, blood, and plasma. This suggests that VLC-PUFA are synthesized in situ within ELOVL4-expressing tissues and incorporated into lipid species that play a unique role that cannot be compensated for by lipids containing other long-chain polyunsaturated fatty acids (LC-PUFA; C18-C26) such as arachidonic acid (AA; 20:4n6) and docosahexaenoic acid (DHA; 22:6n3).

Recent studies on fatty acid elongases, including ELOVL4, point to the essential role of VLC-PUFA for normal and long-term function of retina photoreceptors, skin, sperm and testes [7, 10, 11]. Depletion of retinal VLC-PUFA in photoreceptors due to mutations in the *ELOVL4* gene likely contributes to autosomal dominant Stargardt-like macular dystrophy (STGD3) as the truncated mutant ELOVL4 protein lacks the signal for targeting to the endoplasmic reticulum (ER), the site of fatty acid biosynthesis. Similarly, depletion of VLC-PUFA within testicular tissues of rodents leads to male sterility [10, 12]. In this study, we hypothesized that expression of ELOVL4 in hepatocyte cells will result in the biosynthesis of VLC-PUFA that can be transported via the bloodstream to target tissues such as retina, brain and testis. Hence, we evaluated the ability of Hep2G and 4HIIE cells to synthesize VLC-PUFA by expressing ELOVL4 in these cells. We showed that in the presence of ELOVL4, both HepG2 and 4HIIE cells are capable of VLC-PUFA biosynthesis.

## 79.2 Materials and Methods

### *79.2.1 Tissue Culture and VLC-PUFA Biosynthesis Assay*

We maintained rat hepatoma cell line 4HIIE and human liver cell line Hep2G in Dulbecco's modified Eagles Media (DMEM) with 10% fetal bovine serum. For VLC-PUFA biosynthesis assay, $2 \times 10^6$ HepG2 or 4HIIE cells were seeded in a 10 $cm^2$ culture plate and incubated at 37 °C and 5% $CO_2$ until they were about 70–80% confluent. The cells were then transduced overnight using *Ad5-mouse Elovl4* or *Ad5-GFP* control adenoviral particles. The following day, the viral particle-containing media was aspirated and cells were treated with fresh media containing 30 μg/ml of the sodium salt of eicosapentaenoic acid (EPA, 20:5n3) that had been conjugated with bovine serum albumin (BSA) fraction V (Sigma, St Louis, MO) in a ratio of 2:1 FA:BSA. After 48 h of fatty acid treatment, the fatty acid-containing media was removed and the cells were washed once in 0.1 M phosphate buffer (PBS) containing 50 μM of fraction V fatty acids free BSA (Sigma) to remove any remaining free fatty acids. This was followed by an additional wash with PBS only. The cell pellets were stored at −80 °C until lipid extraction.

### *79.2.2 Total Lipid Extraction and Conversion to Fatty Acid Methyl Esters (FAMES)*

Total lipids were extracted from 4HIIE and HepG2 cells by the method of Bligh and Dyer [13] and converted to fatty acid methyl esters (FAMES) by heating in 2.0 mL of 16% HCl in methanol at 100 °C overnight. After cooling, 1.2 mL water were added and the FAMES were extracted three times with 2.0 mL hexane. The hexane layer was dried down under $N_2$ and the FAMES were isolated on a TLC plate (Silica Gel 60) using 80:20 hexane:ether (v/v) as mobile phase. After staining the plates with 2,7-dichlorofluorescein, the FAMES band was scraped into a tube, 2.0 mL of water were added, and the mixture was extracted three times with 2.0 mL hexane. The resulting extract was dried down under nitrogen. The extracts were re-suspended in 20 μl of nonane and analyzed by gas chromatography-mass spectrometry (GC-MS) as previously described [3].

### *79.2.3 Analyses of Fatty Acid Methyl Esters by Gas Chromatography-Mass Spectrometry (GC-MS)*

VLC-PUFA were represented as GC-MS tracings normalized to the response of IME (isocholesteryl methyl ether), shown to be consistent regardless of experimental differences, and were analyzed by GC-MS as described in Yu et al. [14]. Fatty

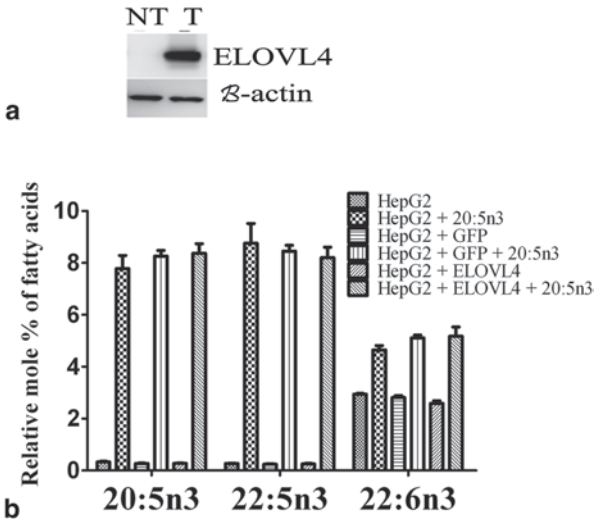


**Fig. 79.1** Expression of *ELOVL4* and fatty acid elongation in hepatocytes. **a** Western blot showing expression of *ELOVL4* in rat hepatoma cells (4HIIE cells). ELOVL4-transduced cells (*T*) have high expression of mouse *ELOVL4* compared to non-transduced (*NT*) cells. **b** Human hepatocytes (*HepG2*) elongated 20:5n3 to 22:5n3 and 22:6n3 independent of *ELOVL4* expression

acid molar percent values were determined by GC-FID (gas chromatography-flame ionization detection) as described in Yu et al. [14].

## 79.3 Results and Discussion

The liver does not express ELOVL4, hence, VLC-PUFA are not found in the liver or plasma. We show herein that hepatocyte cell lines have the biosynthetic machinery for VLC-PUFA biosynthesis when transduced with adenovirus type 5 containing mouse *ELOVL4* mini-gene. After 24 h, there was significant expression of ELOVL4, as shown in the Western blot in Fig. 79.1a. When supplemented with 20:5n3 precursor, both ELOVL4 and GFP over-expressing HepG2 cells efficiently converted it to 22:5n3 and 22:6n3, independent of ELOVL4 expression (Fig. 79.1b). As shown in Fig. 79.2, significant biosynthesis of C30-C38 n3 VLC-PUFA occurred in *Elovl4*-transduced 4HIIE cells (red), but not in control (non-transduced) cells (blue). We had similar results when we expressed ELOVL4 in human Hep2G cells (not shown).

In photoreceptor cells, mutations in ELOVL4 cause early onset retinal degeneration in STGD3 patients. Recent studies on the role of VLC-PUFA suggest that depletion/loss of these fatty acids may play a role in the pathogenesis of macular degeneration in STGD3 patients [4, 11]. This points to the possibility that VLC-PUFA play an essential role in maintaining photoreceptor structure and function that cannot be compensated for by the shorter-chain polyunsaturated fatty acids such as DHA or AA, since these fatty acids are not depleted under ELOVL4 ablation or mutation. In addition, VLC-PUFA seems to be essential for male fertility in rodents [10, 12]. As such, we seek to understand the role of these unique fatty acids

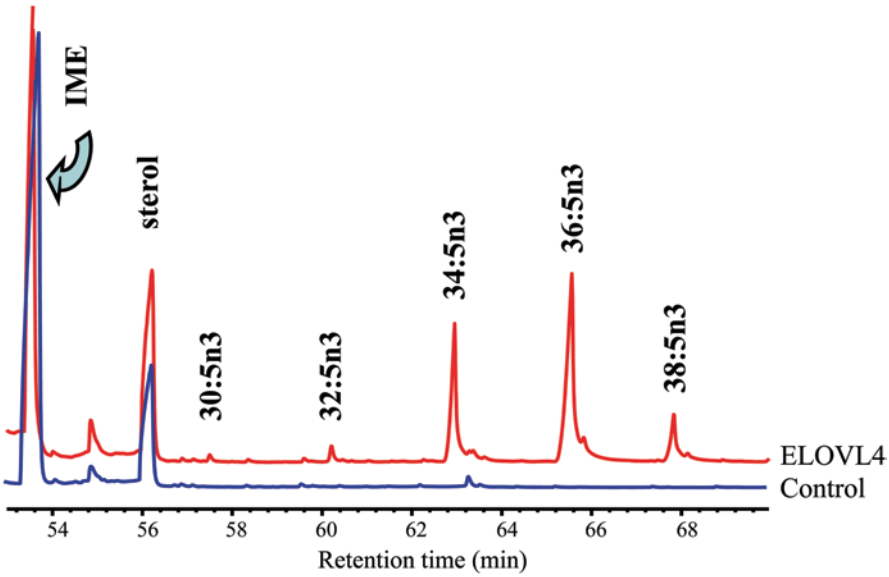


**Fig. 79.2** GC-MS of VLC-PUFA in rat hepatocytes (4HIIE). GC-MS tracings show the presence of VLC-PUFA ranging from 30 to 38 carbons in length in *ELOVL4*-expressing hepatocytes (*red* tracing). *Control* (untransduced or GFP-expressing; *blue* tracing) hepatocytes had no detectable level of the VLC-PUFA. All samples were supplemented in culture with VLC-PUFA precursor 20:5n3. Isocholesteryl methyl ether (*IME*) was used to normalize response

in maintaining retina structure and function as well as their role in maintaining male fertility.

To study the role of VLC-PUFA, we can either feed mice VLC-PUFA in diet or genetically engineer them to synthesize VLC-PUFA in the liver in vivo. While feeding VLC-PUFA represents the best approach, we currently do not have sources from which we can get these fatty acids in large amounts for feeding studies. In addition, the question remains as to whether VLC-PUFA, when supplemented in the diet, will be absorbed by intestinal cells and esterified into triacylglycerols that can be packaged into chylomicrons and be transported to the liver for further distribution to target tissues. Alternative approach is to deliver VLC-PUFA to the retina and testis by expressing *ELOVL4* in liver. We have shown that that indeed expression of ELOVL4 in liver leads to the synthesis of VLC-PUFA. We propose that transgenic expression of ELOVL4 in the liver would allow for the synthesis and delivery of VLC-PUFA to target organs where tissue function is compromised in disease states resulting from a reduction of these fatty acids. This would help us better understand and delineate the role of VLC-PUFA in tissues where they are normally found.

**Support** NIH/NEI Grants EY04149, EY00871, and EY021725; National Center for Research Resources Grant RR17703; Research to Prevent Blindness, Inc.; the Foundation Fighting Blindness to REA; Hope for Vision and Knight Templar Eye Foundation Inc. grants to MPA.

## References


1. Mandal MN, Ambasudhan R, Wong PW, Gage PJ, Sieving PA, Ayyagari R (2004) Characterization of mouse orthologue of ELOVL4: genomic organization and spatial and temporal expression. Genomics 83(4):626–635
2. Zhang K, Kniazeva M, Han M, Li W, Yu Z, Yang Z, Li Y, Metzker ML, Allikmets R, Zack DJ, Kakuk LE, Lagali PS, Wong PW, MacDonald IM, Sieving PA, Figueroa DJ, Austin CP, Gould RJ, Ayyagari R, Petrukhin K (2001) A 5-bp deletion in ELOVL4 is associated with two related forms of autosomal dominant macular dystrophy. Nat Genet 27(1):89–93
3. Agbaga MP, Brush RS, Mandal MN, Henry K, Elliott MH, Anderson RE (2008) Role of Stargardt-3 macular dystrophy protein (ELOVL4) in the biosynthesis of very long chain fatty acids. Proc Natl Acad Sci USA 105(35):12843–12848
4. McMahon A, Jackson SN, Woods AS, Kedzierski W (2007) A Stargardt disease-3 mutation in the mouse Elovl4 gene causes retinal deficiency of C32-C36 acyl phosphatidylcholines. FEBS Lett 581(28):5459–5463
5. Cameron DJ, Tong Z, Yang Z, Kaminoh J, Kamiyah S, Chen H, Zeng J, Chen Y, Luo L, Zhang K (2007) Essential role of Elovl4 in very long chain fatty acid synthesis, skin permeability barrier function, and neonatal survival. Int J Biol Sci 3(2):111–119
6. Li W, Sandhoff R, Kono M, Zerfas P, Hoffmann V, Ding BC, Proia RL, Deng CX (2007) Depletion of ceramides with very long chain fatty acids causes defective skin permeability barrier function, and neonatal lethality in ELOVL4 deficient mice. Int J Biol Sci 3(2):120–128
7. McMahon A, Butovich IA, Kedzierski W (2011) Epidermal expression of an Elovl4 transgene rescues neonatal lethality of homozygous Stargardt disease-3 mice. J Lipid Res 52(6):1128–1138
8. McMahon A, Butovich IA, Mata NL, Klein M, Ritter R 3rd, Richardson J, Birch DG, Edwards AO, Kedzierski W (2007) Retinal pathology and skin barrier defect in mice carrying a Stargardt disease-3 mutation in elongase of very long chain fatty acids-4. Mol Vis 13:258–272
9. Vasireddy V, Uchida Y, Salem N Jr, Kim SY, Mandal MN, Reddy GB, Bodepudi R, Alderson NL, Brown JC, Hama H, Dlugosz A, Elias PM, Holleran WM, Ayyagari R (2007) Loss of functional ELOVL4 depletes very long-chain fatty acids (> or = C28) and the unique omega-O-acylceramides in skin leading to neonatal death. Hum Mol Genet 16(5):471–482
10. Zadravec D, Tvrdik P, Guillou H, Haslam R, Kobayashi T, Napier JA, Capecchi MR, Jacobsson A (2011) ELOVL2 controls the level of n-6 28:5 and 30:5 fatty acids in testis, a prerequisite for male fertility and sperm maturation in mice. J Lipid Res 52(2):245–255
11. Harkewicz R, Du H, Tong Z, Alkuraya H, Bedell M, Sun W, Wang X, Hsu YH, Esteve-Rudd J, Hughes G, Su Z, Zhang M, Lopes VS, Molday RS, Williams DS, Dennis EA, Zhang K (2012) Essential role of ELOVL4 protein in very long chain fatty acid synthesis and retinal function. J Biol Chem 287(14):11469–11480
12. Zanetti SR, Maldonado EN, Aveldano MI (2007) Doxorubicin affects testicular lipids with long-chain (C18-C22) and very long-chain (C24-C32) polyunsaturated fatty acids. Cancer Res 67(14):6973–6980
13. Bligh EG, Dyer WJ (1959) A rapid method of total lipid extraction and purification. Can J Biochem Physiol 37(8):911–917
14. Yu M, Benham AF, Logan S, Brush RS, Mandal MN, Anderson RE, Agbaga MP (2011) ELOVL4 protein preferentially elongates 20:5n3 to very long chain polyunsaturated fatty acids over 20:4n6 and 22:6n3. J Lipid Res 53(3):494–504

# Chapter 80
# Very Long Chain Polyunsaturated Fatty Acids and Rod Cell Structure and Function

**L. D. Marchette, D. M Sherry, R. S Brush, M. Chan, Y. Wen, J. Wang, John D. Ash, Robert E. Anderson and N. A. Mandal**

**Abstract** The gene encoding Elongation of Very Long Chain Fatty Acids-4 (ELOVL4) is mutated in patients with autosomal dominant Stargardt's Macular Dystrophy Type 3 (STDG3). ELOVL4 catalyzes the initial condensation step in the elongation of polyunsaturated fatty acids (PUFA) containing more than 26 carbons (26C) to very long chain PUFA (VLC-PUFA; C28 and greater). To investigate the role of VLC-PUFA in rod photoreceptors, we generated mice with rod-specific deletion of *Elovl4* (RcKO). The mosaic deletion of rod-expressed ELOVL4 protein resulted in a 36% lower amount of VLC-PUFA in the retinal phosphatidylcholine (PC) fraction compared to retinas from wild-type mice. However, this reduction was not sufficient to cause rod dysfunction at 7 months or photoreceptor degeneration at 9 or 15 months.

**Keywords** ELOVL4 · VLC-PUFA · Photoreceptor · ERG · Rod

N. A. Mandal (✉) · R. S. Brush · M. Chan · R. E. Anderson
Department of Ophthalmology, University of Oklahoma Health Sciences Center, Oklahoma City, OK 73104, USA
e-mail: mmandal@ouhsc.edu

L. D. Marchette · D. M. Sherry · R. E. Anderson
Department of Cell Biology, University of Oklahoma Health Sciences Center, Oklahoma City, OK 73104, USA
e-mail: leamarchette@ouhsc.edu

D. M. Sherry
Oklahoma Center for Neuroscience, University of Oklahoma Health Sciences Center, Oklahoma City, OK 73104, USA
e-mail: david-sherry@ouhsc.edu

Department of Pharmaceutical Sciences, University of Oklahoma Health Sciences Center, Oklahoma City, OK 73104, USA

N. A. Mandal · L. D. Marchette · R. S. Brush · M. Chan · R. E. Anderson
Dean McGee Eye Institute, University of Oklahoma Health Sciences Center, 608 Stanton L. Young Blvd., Oklahoma City, OK 73104, USA

J. D. Ash et al. (eds.), *Retinal Degenerative Diseases,* Advances in Experimental Medicine and Biology 801, DOI 10.1007/978-1-4614-3209-8_80,

## 80.1 Introduction

The fatty acid condensing enzyme Elongation of Very Long Chain Fatty Acids-4 (ELOVL4) is mutated in patients with the autosomal dominant Stargardt's Macular Dystrophy Type 3 (STDG3) [1]. ELOVL4 is expressed in skin, brain, testis, and retina and is responsible for the initial rate-limiting step to elongate fatty acid species with more than 26 acyl carbons (C26) [2]. ELOVL4 expression in skin produces very long chain (VLC)-saturated fatty acids, whereas ELOVL4 in brain, testis, and retina produces VLC-PUFA (VLC-PUFA; C28-C38). To investigate the role of VLC-PUFA in rod photoreceptors, we conditionally deleted *Elovl4* in mouse rod photoreceptor cells.

## 80.2 Materials and Methods

### *80.2.1 Animal Use*

Mice with LoxP sites flanking exon 5 of the *Elovl4* (*ELO*$^{flox/flox}$) gene were mated with transgenic mice expressing Cre recombinase (Cre) driven by the rhodopsin promoter [3] (*ELO*$^{flox/flox}$ mice were a gift from Dr. Kang Zhang, USC, San Diego, CA). Progeny were backcrossed to *ELO*$^{flox/flox}$ to ultimately generate a rod-specific conditional knock out (*Cre*$^{+}$*/ELO*$^{flox/flox}$; RcKO) and littermate control wild-type (*Cre*$^{-}$*/ELO*$^{flox/flox}$; WT) mice. Mice were housed in a 12 h light ON (20 lx)/OFF cycle. All procedures were performed according to the Association for Research in Vision and Ophthalmology Statement for the Use of Animals in Ophthalmic and Vision Research and protocols were approved by the Institutional Animal Care and Use Committees of the University of Oklahoma Health Sciences Center and the Dean McGee Eye Institute.

Y. Wen
Amherst College, Amherst, MA, USA
e-mail: YWen15@Amherst.edu

J. Wang · J. D. Ash
University of Florida, Gainesville, FL, USA
e-mail: garywang@ufl.edu

R. S. Brush
e-mail: Richard-Brush@ouhsc.edu

M. Chan
e-mail: michael-chan@ouhsc.edu

### *80.2.2 Immunolabeling of Retinal Wholemounts*

Retinal wholemounts were immunolabeled as described previously [4] using the following primary antibodies: anti-ELOVL4 (1:200) [2], anti-Cre recombinase (Cre; 1:500; Abcam), and anti-cone arrestin (1:500; Gift of Dr. Cheryl Craft, USC, Los Angeles, CA). Labeling was visualized using appropriate fluorescent secondary antibodies (1:200; Invitrogen-Molecular Probes), and imaged using an Olympus BX61-WI microscope (Olympus America) with an ORCA-ER camera (Hamamatsu America) controlled by Slidebook software (Intelligent Imaging Innovations). Brightness and contrast were adjusted to highlight specific labeling using Photoshop (Adobe Systems). Images were analyzed by ImageJ software.

### *80.2.3 Tandem Mass Spectrometry Analysis of Retina Lipids*

The methods have been described previously [5]. Briefly, one mouse retina per sample was homogenized in 40 % aqueous methanol and diluted 1:20 with 2-propanol/methanol/chloroform (4:2:1 v/v/v) containing 20 mM ammonium formate and 1.00 µM phosphatidylcholine (PC, 14:0/14:0) as an internal standard. Samples were introduced into a triple quadrupole mass spectrometer (TSQ Ultra, Thermo Scientific) using a chip-based nano-ESI source (Advion NanoMate) operating in infusion mode. PC lipids were measured using precursor ion scanning of *m/z* 184. Quantification of lipid molecular species was performed using the Lipid Mass Spectrum Analysis (LIMSA) software version 1.0 peak model fit algorithm. Three to four samples per genotype were analyzed for comparison.

### *80.2.4 Electroretinography*

Electroretinography (ERG) was performed under scotopic conditions as previously described [6]. Briefly, anesthetized 7-month-old mice were subjected to 10 msec flashes of light of increasing intensities (0.004 to 400 cd.s/m$^{-2}$). The maximum amplitudes of rod-only a-waves ($Rmp^3$) were determined by analyzing the ERG responses as previously described [7]. Data were processed with MatLab software (MathWorks, Inc). The maximum rod b-wave ($V_{max}$) amplitude was determined as the least squares fit of log intensity vs. amplitude response analysis according to the previously described Naka-Rushton equation [8]. Photopic ERG was determined as response amplitudes (b-wave) to a single flash (2,000 cd.s/m$^2$) and to continuous pulses of different frequencies of light (5–30 Hz).

### *80.2.5 Statistical Analysis*

Two-way ANOVA followed by Bonferroni's multiple comparison test was used to analyze ERG responses. All other data were analyzed by Students 2-tailed t-test. Analyses were performed using GraphPad (GraphPad Prism, Inc), with statistical significance set at $p < 0.05$.

## 80.3 Results

### *80.3.1 Cre Recombinase Eliminated ELOVL4 Expression from Rods in RcKO Retina*

Immunolabeling of retinal wholemounts confirmed cell-specific expression of Cre in the RcKO retina (Fig. 80.1a) and demonstrated specific deletion of ELOVL4 from rods expressing Cre (Fig. 80.1b). Cre labeling showed a mosaic distribution in the rods of the RcKO mice that corresponded to the mosaic pattern of ELOVL4 deletion (Fig. 80.1b). As a rough estimate of the extent of Cre-mediated *elovl4* deletion in the RcKO retina, the proportion of the ONL occupied by labeling for ELOVL4 indicated that ELOVL4 was eliminated from approximately 40–60 % of the ONL, consistent with the 36 % reduction of VLC-PUFA observed by tandem mass spectroscopy (see fig. 80.1).

### *80.3.2 Retinal Phosphatidylcholine VLC-PUFA Analysis*

Tandem mass spectrometry analysis showed a smaller amount of PC VLC-PUFA (54:11 to 56:12) in 9-month-old RcKO retinas compared to the WT control retinas (Table 3.1). The only VLC-PUFA-containing species in the RcKO retina that was significantly reduced compared to WT retina was 56:11 (22:6/34:5) (Table 3.1). However, the total amount of PC VLC-PUFA in the RcKO retina was 36 % lower than WT littermates ($p < 0.001$). PC VLC-PUFA precursors (44:12 to 46:12) were more abundant in the RcKO mouse retina compared to WT retina, but 44:11 (22:6/22:5) was the only species that differed significantly (Table 3.1).

### *80.3.3 ERG Analysis*

Scotopic ERG was performed on WT and RcKO mice to determine whether the reduction in VLC-PUFA levels affected the rod photoresponse. There were no differences in a- and b-wave amplitudes between WT and RcKO mice at any of the light intensities used (Fig 80.2a). Similarly, there were no significant differences between

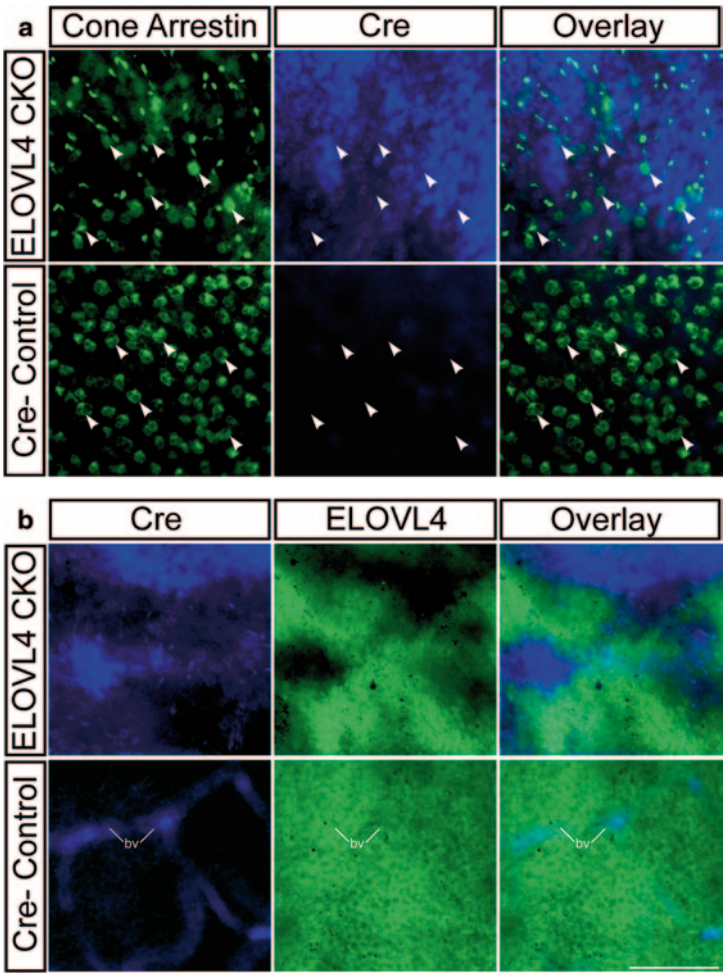


**Fig. 80.1** Rod-specific deletion of *ELOVL4*. **a** Immunolabeling for *Cone Arrestin* (*green*) and *Cre* (*Cre*; *blue*) identified the persistence of cones (*arrowheads*) and confirmed rod-specific *Cre* expression in the RcKO retina (*ELOVL4 CKO*) that was absent from the Cre negative control retina (*Cre-Control*). **b** Cre (*blue*) expression in the RcKO retina showed mosaic distribution that corresponded to the deletion of *ELOVL4* (*green*). In contrast, Cre labeling was absent in the *Cre-Control* retina, while *ELOVL4* was present in all photoreceptors. Labeling of blood vessels (*bv*) in the Cre channel was non-specific. Scale bar = 50 µm

the WT and RcKO $Rmp_3$ (421 and 359 µV; $p > 0.05$) values, although the Vmax in RcKO (828 µV) mice was significantly lower than in WT (919 µV; $p = 0.049$; Fig 80.2b). Cone ERG responses to a single flash (2,000 cd.s/$m^2$) in light-adapted WT and RcKO mice (161 and 127 µV, respectively; Fig. 80.2c), and photopic flicker ERG responses did not differ significantly between the WT and RcKO mice (Fig. 80.2c).

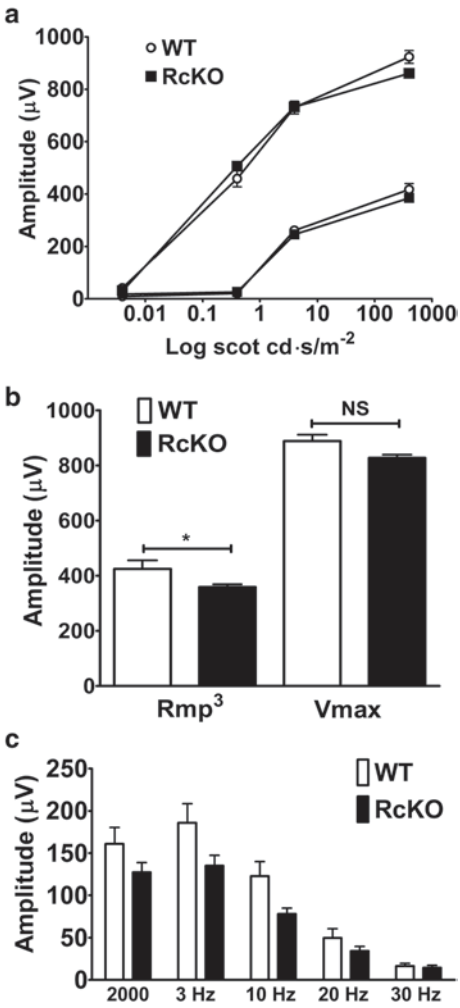


**Fig. 80.2** Electroretinography responses. **a** Scotopic ERG a- (*lower* lines) and b- (*upper* lines) waves were comparable between wild-type (*WT*) and rod-specific *Elovl4* knockout (*RcKO*) mice. **b** Maximum a- ($Rmp^3$) and b- (*Vmax*) wave responses were lower in the *RcKO* compared to *WT* but not to a level of statistical significance. **c** *WT* and *RcKO* had comparable cone responses (b-waves) to photopic single flash (2,000 cd.s/$m^2$) and flicker (5–30 Hz) ERGs. $p > 0.05$ for all photopic ERG responses. $n = 4–5$ different *WT* and *RcKO* mice respectively for all ERG. Data is mean response amplitudes (μV) ± SEM

## 80.4 Discussion

We used mice with rod-specific deletion of *Elovl4* to investigate the role of VLC-PUFA in rod photoreceptors. Heterogeneous ELOVL4 deletion was consistent with the known mosaic expression of Cre in the rods of the transgenic mouse line used to create the RcKO strain used here [3]. ELOVL4 deletion in the RcKO mice resulted in a 36 % reduction in retinal PC VLC-PUFA (Table 80.1), whereas VLC-PUFA precursors (44:11 to 46:12) were more abundant in the RcKO mouse retina compared to WT (Table 80.1). The "back up" of lipid species agrees with results of Harkewicsz et al. who showed higher amounts of precursors 44:12, 44:11, and 46:11 in their rod-specific *Elovl4* cKO compared to WT mouse retina [9].

**Table 80.1** Retinal phosphatidylcholine analysis

| Name | WT | RcKO |
|---|---|---|
| 44:11* (22:6/22:5) | 0.09±0.02 | 0.14±0.02 |
| 44:12 (22:6/22:6) | 3.92±1.79 | 6.15±0.88 |
| 46:11 (22:6/24:5) | 0.06±0.07 | 0.10±0.09 |
| 46:12 (22:6/24:6) | 0.30±0.09 | 0.31±0.04 |
| 54:11 (22:6/32:5) | 0.17±0.06 | 0.13±0.04 |
| 54:12 (22:6/32:6) | 0.75±0.35 | 0.58±0.22 |
| 56:11** (22:6/34:5) | 0.17±0.02 | 0.00±0.00 |
| 56:12 (22:6/34:6) | 0.41±0.10 | 0.26±0.08 |

*RcKO* rod conditional *Elovl4* knockout, *WT* wild type
*$p<0.05$;
**$p<0.001$

We found no differences in area occupied by ONL in 9- and 15-month-old WT and RcKO mice (data not shown). These analyses indicate that the reduction of VLC-PUFA in the RcKO mice did not cause rod cell death. These results differ from those of Harkewicsz et al., who reported that 10- and 15-month-old RcKO mice had 8 and 7 rows of photoreceptor nuclei, respectively, compared to 9 rows of nuclei in their 15-month-old WT mice [9]. In that study, the numbers of rows of photoreceptor nuclei in the ONL were counted at two points, 500 μm superior and inferior to the ONH on frozen sections of 16 μm thickness. In the current study, we measured the area occupied by the entire ONL across the vertical meridian of the entire retina in paraffin sections of 5 μm thickness. The reason for these differences is not obvious as both studies used the same rod cre-expressing mice. However, the measurement approach utilized in the current study samples a much larger area of the ONL with higher anatomical resolution and minimizes effects of orientation in relatively thick frozen sections that can make assignment of individual photoreceptor nuclei to a specific row difficult.

Rod ERG responses were comparable for WT and RcKO mice at all light intensities tested (Fig. 80.2a). The rod-only response (Rmp3) was lower in the RcKO than WT mice, but was not statistically significant ($p=0.0503$; Fig. 80.2b). However, the Vmax was significantly lower in the RcKO mice compared to WT ($p=0.049$; Fig. 80.2b). Harkewicsz et al. reported that the scotopic ERG response from RcKO mice was lower than the WT response to a light intensity of 0.0084 cd.s/m$^2$ [9], an intensity between two used in our study (0.004 and 0.4 cd.s/m$^2$), neither of which elicited statistically different responses from our WT and RcKO mice. This difference potentially might reflect the age of mice used. The mice we used were 7 months of age, but no age was given for the mice used by Harkewicsz et al., [9]. Perhaps with increasing age, our RcKO mice might also show a decline in ERG responses. The mosaic deletion of *Elovl4* by Cre also might affect the ERG results as heterogeneous photoreceptor dysfunction can bias ERG responses [10]. Cone function assessed by photopic ERG responses did not differ between RcKO and WT mice (Fig. 80.2c). These results agree with those reported by Harkewicsz et al., who showed that mice with rod-specific *Elovl4* deletion had a photopic 10 Hz flicker

ERG response comparable to WT mice [9]. These results suggest that the level of VLC-PUFA reduction in the RcKO retina did not alter rod or cone function by 7 months.

A 36% reduction in VLC-PUFA was not sufficient to cause photoreceptor cell death or rod or cone dysfunction. Our analyses of VLC-PUFA levels in retinas of *Elovl4* KO and *Elovl4* knock-in (KI) heterozygous mice showed ~50% reduction compared to WT (Mandal et al., unpublished results). The KO mice have no structural phenotype at 16 to 22 months-of-age [11] and the KI mice had minimal ERG changes and normal retinal morphology at 8 and 9 months-of-age [12, 13]. Importantly, these KO and KI mice differ from those used in the current study because the reduction in VLC-PUFA levels occurs in each rod cell, since each expresses only one WT copy of *Elovl4*. In the RcKO mice, rod cells express either two or zero copies of Elovl4, which would result in each cell having either "normal" or very low levels of VLC-PUFA. Recent studies in which we deleted *Elovl4* from over 90% of rods showed a structural and functional phenotype at 4 months-of-age (Marchette, unpublished results). Thus, in the present study, we would expect to find some phenotype in the rods of the animals in which *Elovl4* was deleted, unless there was transfer of VLC-PUFA between cells. One potential mechanism for this transfer would be recycling of VLC-PUFA from the shed tips of rod outer segments through the retinal pigment epithelium (RPE) to cells lacking *Elovl4*. This recycling phenomenon is well-known for DHA [1, 6] and retinoids involved in the visual cycle [14].

In summary, partial reduction of VLC-PUFA in rod photoreceptors is not sufficient to cause a structural or functional retinal phenotype. Even though VLC-PUFA synthesis was completely eliminated in some individual rod cells, these cells did not appear to be deleteriously affected, most likely because of sharing of these fatty acids through their efficient recycling from the RPE.

**Acknowledgments** This work was supported by NIH Grants EY00871, EY04149, EY12190, EY21725, EY22071 and RR17703; Foundation Fighting Blindness, Inc., and Research to Prevent Blindness, Inc.

## References

1. Zhang K et al (2001) A 5-bp deletion in ELOVL4 is associated with two related forms of autosomal dominant macular dystrophy. Nat Genet 27:89–93
2. Agbaga M-P, Brush RS, Mandal MNA, Henry K, Elliott MH, Anderson RE (2008) Role of Stargardt-3 macular dystrophy protein (ELOVL4) in the biosynthesis of very long chain fatty acids. Proc Nat Acad Sci 105(35):12843–12848
3. Le YZ, Zheng L, Zheng W, Ash JD, Agbaga MP, Zhu M et al (2006) Mouse opsin promoter-directed Cre recombinase expression in transgenic mice. Mol Vis 12:389–398
4. Mojumder DK, Frishman LJ, Otteson DC, Sherry DM (2007) Voltage-gated sodium channel alpha-subunits Na(v)1.1, Na(v)1.2, and Na(v)1.6 in the distal mammalian retina. Mol Vis 13:2163–2182
5. Busik JV, Reid GE, Lydic TA (2009) Global analysis of retina lipids by complementary precursor ion and neutral loss mode tandem mass spectrometry. Methods Mol Biol 579:33–70

6. Li F, Marchette LD, Brush RS, Elliott MH, Le YZ, Henry KA et al (2009) DHA does not protect ELOVL4 transgenic mice from retinal degeneration. Mol Vis 15:1185–1193
7. Hood DC, Birch DG (1994) Rod phototransduction in retinitis pigmentosa: estimation and interpretation of parameters derived from the rod a-wave. IOVS 35(7):2948–2961
8. Naka KI, Rushton WA (1966) S-potentials from luminosity units in the retina of fish (Cyprinidae). J Physiol 185(3):587–599
9. Harkewicz R, Du H, Tong Z, Alkuraya H, Bedell M, Sun W et al (2012) Essential role of ELOVL4 protein in very long chain fatty acid synthesis and retinal function. J Biol Chem 287(14):11469–11480
10. Hood DC, Shady S, Birch DG (1994) Understanding changes in the b-wave of the ERG caused by heterogeneous receptor damage. IOVS 35(5):2477–2488
11. Raz-Prag D, Ayyagari R, Fariss RN, Mandal MNA, Vasireddy V, Majchrzak S et al (2006) Haploinsufficiency is not the key mechanism of pathogenesis in a heterozygous Elovl4 knockout mouse model of STGD3 disease. IOVS 47(8):3603–3611
12. Li W, Chen Y, Cameron DJ, Wang C, Karan G, Yang Z et al (2007) Elovl4 haploinsufficiency does not induce early onset retinal degeneration in mice. Vis Res 47(5):714–722
13. McMahon A, Butovich IA, Mata NL, Klein M, Ritter R 3rd, Richardson J et al (2007) Retinal pathology and skin barrier defect in mice carrying a Stargardt disease-3 mutation in elongase of very long chain fatty acids-4. Mol Vis 13:258–272
14. Chen H, Ray J, Scarpino V, Acland GM, Aguirre GD, Anderson RE (1999) Synthesis and release of Docosahexaenoic acid by the RPE cells of prcd-affected dogs. Invest Ophthalmol Vis Sci 40(10):2418–2422

# Part IX
# Degenerative Processes: Oxidative Stress, Autophagy and Others

# Chapter 81
# Oxidative Stress Regulation by DJ-1 in the Retinal Pigment Epithelium

**Vera L. Bonilha, Mary E. Rayborn, Xiaoping Yang, Chengsong Xie and Huaibin Cai**

**Abstract** DJ-1 is a protein expressed in many tissues including the brain where it has been extensively studied due to its association with Parkinson's Disease (PD). DJ-1 was reported to function as an antioxidant, redox-sensitive molecular chaperone, and transcription regulator, which protected cells from oxidative stress by modifying signaling pathways that regulate cell survival. Here we discuss our progress toward characterization of the DJ-1 function in the protection of RPE to oxidative stress.

**Keywords** Retinal pigment epithelium · Oxidative stress · Reactive oxygen species · DJ-1 · Histology

**Abbreviations**

| | |
|---|---|
| PD | Parkinson's Disease |
| RPE | Retinal pigment epithelium |
| ROS | Reactive oxygen species |
| Carboxy-DCFDA | 5-(and-6)-carboxy-2',7'-difluorodihydrofluorescein diacetate |
| 8-oxoG | 7, 8- dihydro-8-oxoguanine |

V. L. Bonilha (✉) · M. E. Rayborn · X. Yang
Department of Ophthalmology, Cleveland Clinic Lerner College of Medicine,
The Cole Eye Institute, i31, 9500 Euclid Avenue,
Cleveland, OH 44195, USA
e-mail: bonilhav@ccf.org

M. E. Rayborn
e-mail: rayborm@ccf.org

X. Yang
e-mail: YANGX@ccf.org

C. Xie · H. Cai
Laboratory of Neurogenetics, National Institute of Aging, NIH, Bethesda, MD 20892, USA
e-mail: xiech@mail.nih.gov

H. Cai
e-mail: caih@mail.nih.gov

J. D. Ash et al. (eds.), *Retinal Degenerative Diseases,* Advances in Experimental Medicine and Biology 801, DOI 10.1007/978-1-4614-3209-8_81,

## 81.1 Introduction

*DJ-1* gene encodes a highly conserved protein with 189 amino acids and a molecular weight of ~20 kDa, which belongs to the ThiJ/PfpI protein superfamily [1]. The function of ThiJ is not fully known, but it may be related to the biosynthesis of thiamins while PfpI is an intracellular protease, responsive to growth conditions and present in most bacteria and archea [2, 3, 4]. Therefore, both DJ-1 sequence and structure suggested that this protein would be involved in cellular viability.

Initially, DJ-1 was reported as a novel oncogene showing a transforming activity when expressed together with H-ras [5]. Later, it was reported that the gene for human DJ-1 (*PARK7*) is mutated in rare forms of recessively inherited PD [6].

Recently, we have identified DJ-1 peptides in both young and aged retinal pigment epithelium (RPE) lysates starting with a proteomic approach. We also reported immunolocalization of DJ-1 protein in both young and aged rat RPE cells [7]. Here we extend our initial observations of DJ-1 expression and further discuss DJ-1 function in the RPE cells.

## 81.2 DJ-1 Function and Oxidative Stress Protection

At the subcellular level, under basal conditions, DJ-1 is found mostly in the cytoplasm and to a lesser extent in the mitochondria [6, 8, 9] and nucleus [9]. Under conditions of oxidative stress, more DJ-1 redistributes to mitochondria and later to the nucleus, and this cellular redistribution correlates with the ability of DJ-1 to confer neuroprotection [8, 10, 11]. As previously described in several cell types, under baseline conditions, DJ-1 displays a diffuse cytoplasmic and nuclear staining of all the RPE cell lines analyzed (Fig. 81.1a). Oxidative stress induced by incubation of RPE cultures with $H_2O_2$ leads to a visible increase in immunocytochemical staining for DJ-1 (Fig. 81.1b). In addition, these RPE cultures displayed an induced intracellular redistribution of DJ-1 to a perinuclear localization (mitochondria, data not shown). Confirmation of the increased DJ-1 protein levels in RPE cells under oxidative stress was also demonstrated by Western blot analysis (data not shown).

Several reports suggest that DJ-1 robustly protects cells from oxidative stress [8, 12–18]. First, reports showed that flies and mice deficient in the gene encoding DJ-1 are indeed more susceptible to oxidative toxins [13, 15, 19–21]. Second, it was reported that DJ-1 can eliminate $H_2O_2$ in vitro by becoming oxidized itself and thus functioning as a scavenger of reactive oxygen species (ROS) [17, 22]. It was also established that cysteines at residues 46, 53, and 106 become oxidized upon oxidative stress, resulting in scavenging of ROS, enhancing DJ-1 association with mitochondria and allowing DJ-1 to protect cells from oxidative stress [8, 14, 23].

To explore the functional consequences of DJ-1 mutation, adenoviruses carrying both DJ-1 full length and DJ-1 with the three cysteine at residues 46, 53, and 106 mutated to serine were generated and used as agents to induce overexpression of

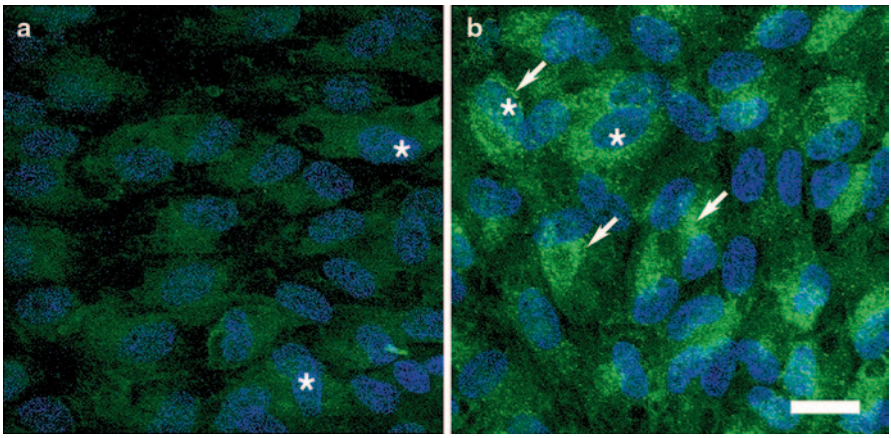


**Fig. 81.1** Immunocytochemical analysis of intracellular distribution of DJ-1 on RPE monolayers exposed to oxidative stress. Immunocytochemical staining of ARPE-19 cells for DJ-1 demonstrates that at basal conditions **a** DJ-1 is diffused in the cytoplasm and nuclei (*) of the cells. With 1 h of exposure to 800 μM $H_2O_2$, **b** a pronounced aggregated perinuclear staining (*arrows*) for DJ-1 is apparent. Bar = 20 μm

exogenous DJ-1. Control and RPE cultures overexpressing both types of exogenous DJ-1 were exposed to oxidative stress through incubation with $H_2O_2$ followed by incubation with the fluorescent indicator used to assess ROS generation 5-(and-6)-carboxy-2',7'-difluorodihydrofluorescein diacetate (carboxy-DCFDA) and confocal microscopy (Fig. 81.2). Interestingly, no significant amount of ROS was detected in ARPE-19 over-expressing exogenous full-length DJ-1 and exposed to oxidative stress (Fig. 81.2c) and in ARPE cultures at basal conditions (Fig. 81.2a). In contrast, a significant generation of ROS was observed when ARPE-19 cultures were exposed to oxidative stress (Fig. 81.2b) and when RPE cultures overexpressing the mutated DJ-1 were exposed to oxidative stress (Fig. 81.2d). This data suggested that high levels of full-length DJ-1 expression resulted in significant decrease in ROS generation in RPE cells exposed to oxidative stress.

We have also analyzed histologically the eyes of young adult DJ-1 KO mice and noted that the RPE in these mice is characterized by patchy thinning (Fig. 81.3b, arrows) when compared to the control RPE (Fig. 81.3a). Our data suggested that normal RPE structure requires DJ-1 expression. To further relate RPE DJ-1 expression with oxidative stress regulation, we analyzed the expression of 7,8-dihydro-8-oxoguanine (8-oxoG), the most abundant oxidized base generated in vivo by various types of ROS, in control and DJ-1 KO RPE with antibodies specific to this DNA oxidation (Fig. 81.3c, d). Immunocytochemical staining of 8-oxoG, was significantly elevated in the DJ-1 KO RPE (Fig. 81.3d) and photoreceptor inner segments (Fig. 81.3d, arrowheads) when compared to control RPE (Fig. 81.3c). These data indicated that lack of DJ-1 expression leads to increased oxidative stress in RPE in vivo.

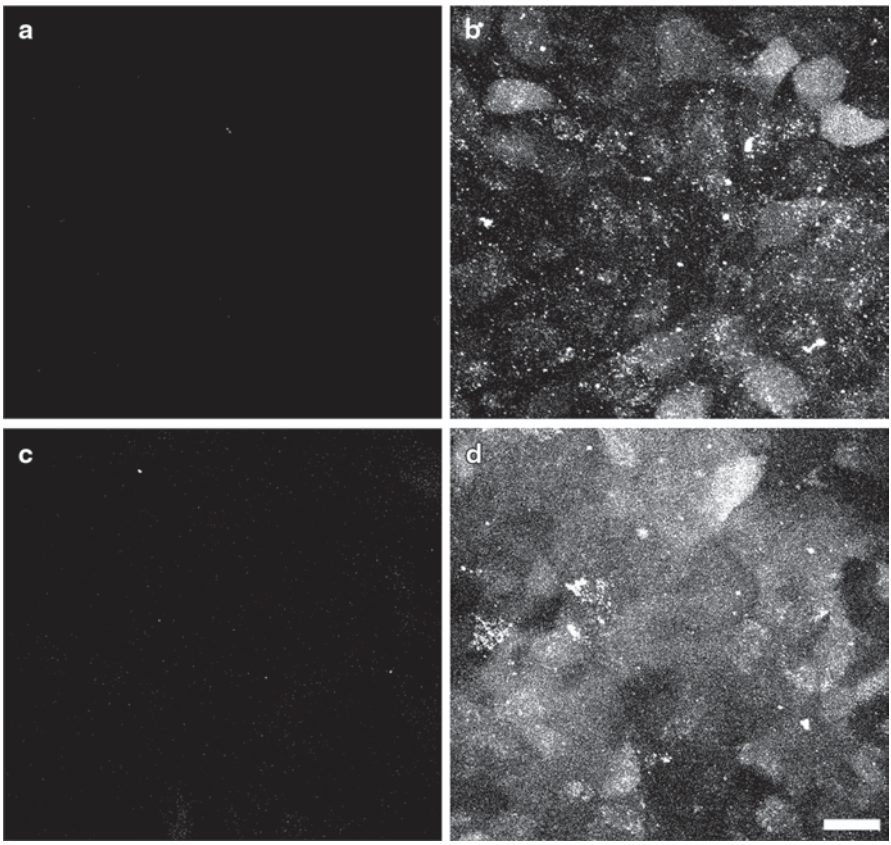


**Fig. 81.2** Staining of ROS generation on ARPE-19 monolayers expressing endogenous and exogenous DJ-1 and exposed to oxidative stress by exposure to 800 μM $H_2O_2$ for 1 h. Incubation of RPE monolayers with carboxy-DCFDA indicates that no ROS is generated by the RPE cells at basal conditions (**a**). While upon oxidative stress incubation, appreciable ROS generation throughout the entire cell body of cells is observed (**b**). RPE cultures transduced with an adenovirus carrying the full-length hDJ-1 DNA did not display ROS generation when exposed to oxidative stress (**c**). However, RPE cultures transduced with an adenovirus carrying DJ-1 with the three cysteine at residues 46, 53, and 106 mutated to serine (**d**). Displayed appreciable ROS generation when cells were exposed to oxidative stress. Bar = 20 μm

## 81.3 Conclusions

Age-related macular degeneration (AMD) is the most common cause of irreversible blindness in the elderly population in industrialized countries. Studies carried out in man, AMD animal models, and RPE cell lines point toward an important role of oxidative stress in the development of AMD. Due to the evidence presented here, connecting DJ-1 to protection against oxidative stress, it is conceivable that DJ-1 function may also be related to oxidative stress implicated in AMD pathology. The

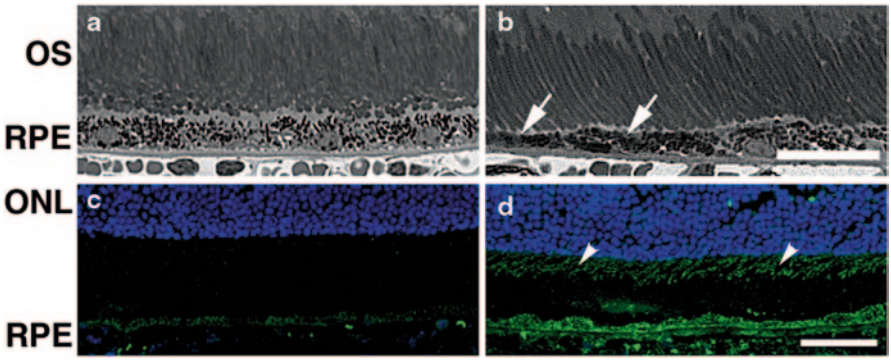


**Fig. 81.3** Degeneration in the neural retina of young adult DJ-1 KO mouse. Plastic sections of both control (**a**) and DJ-1 KO (**b**) retinas stained with toluidine blue highlighted the *RPE* and photoreceptor cells. The *RPE* of the DJ-1 KO displayed thinning (**b**, *arrows*). Cryosections of retinas were also labeled with 8-oxoG (**c**, **d**) to detect DNA oxidation. Analysis showed that 8-oxoG immunoreactivity is significantly increased in the photoreceptor inner segments (*arrowheads*) and the *RPE* cells of DJ-1 KO (**d**) when compared to the control (**c**) retinas. *ONL* outer nuclear layer, *OS* photoreceptor outer segments, *RPE* retinal pigment epithelium, Bar **a**, **b** = 25 μm and **c**, **d** = 40 μm

years to come will bring further definition of key proteins and pathways involved in the regulation of oxidative stress by DJ-1 in RPE cells as well as a better understanding of its function in AMD.

**Acknowledgment** Supported by Research Center grants from the Foundation Fighting Blindness and Research to Prevent Blindness and funds from the Cleveland Clinic Foundation and partially by the intramural research program of National Institute on Aging (HC).

## References

1. Tao X, Tong L (2003) Crystal structure of human DJ-1, a protein associated with early onset Parkinson's disease. J Biol Chem 278:31372–31379
2. Halio SB, Blumentals II, Short SA, Merrill BM, Kelly RM (1996) Sequence, expression in *Escherichia coli*, and analysis of the gene encoding a novel intracellular protease (PfpI) from the hyperthermophilic archaeon *Pyrococcus furiosus*. J Bacteriol 178:2605–2612
3. Taylor SV, Kelleher NL, Kinsland C, Chiu HJ, Costello CA et al (1998) Thiamin biosynthesis in *Escherichia coli*. Identification of ThiS thiocarboxylate as the immediate sulfur donor in the thiazole formation. J Biol Chem 273:16555–16560
4. Mizote T, Tsuda M, Smith DD, Nakayama H, Nakazawa T (1998) Cloning and characterization of the thiD/J gene of *Escherichia coli* encoding a thiamin-synthesizing bifunctional enzyme, hydroxymethylpyrimidine kinase/phosphomethylpyrimidine kinase. Microbiology 145(Pt 2):495–501
5. Nagakubo D, Taira T, Kitaura H, Ikeda M, Tamai K et al (1997) DJ-1, a novel oncogene which transforms mouse NIH3T3 cells in cooperation with ras. Biochem Biophys Res Commun 231:509–513

6. Bonifati V, Rizzu P, van Baren MJ, Schaap O, Breedveld GJ et al (2003) Mutations in the DJ-1 gene associated with autosomal recessive early-onset parkinsonism. Science 299:256–259
7. Gu X, Neric NJ, Crabb JS, Crabb JW, Bhattacharya SK et al (2012) Age-related changes in the retinal pigment epithelium (RPE). PLoS One 7:e38673
8. Canet-Aviles RM, Wilson MA, Miller DW, Ahmad R, McLendon C et al (2004) The Parkinson's disease protein DJ-1 is neuroprotective due to cysteine-sulfinic acid-driven mitochondrial localization. Proc Natl Acad Sci U S A 101:9103–9108
9. Zhang L, Shimoji M, Thomas B, Moore DJ, Yu SW et al (2005) Mitochondrial localization of the Parkinson's disease related protein DJ-1: implications for pathogenesis. Hum Mol Genet 14:2063–2073
10. Ashley AK, Hanneman WH, Katoh T, Moreno JA, Pollack A et al (2009) Analysis of targeted mutation in DJ-1 on cellular function in primary astrocytes. Toxicol Lett 184:186–191
11. Junn E, Jang WH, Zhao X, Jeong BS, Mouradian MM (2009) Mitochondrial localization of DJ-1 leads to enhanced neuroprotection. J Neurosci Res 87:123–129
12. Li HM, Taira T, Maita C, Ariga H, Iguchi-Ariga SM (2006) Protection against nonylphenol-induced cell death by DJ-1 in cultured Japanese medaka (Oryzias latipes) cells. Toxicology 228:229–238
13. Meulener MC, Xu K, Thomson L, Ischiropoulos H, Bonini NM (2006) Mutational analysis of DJ-1 in Drosophila implicates functional inactivation by oxidative damage and aging. Proc Natl Acad Sci U S A 103:12517–12522
14. Mitsumoto A, Nakagawa Y (2001) DJ-1 is an indicator for endogenous reactive oxygen species elicited by endotoxin. Free Radic Res 35:885–893
15. Park J, Kim SY, Cha GH, Lee SB, Kim S et al (2005) Drosophila DJ-1 mutants show oxidative stress-sensitive locomotive dysfunction. Gene 361:133–139
16. Sekito A, Koide-Yoshida S, Niki T, Taira T, Iguchi-Ariga SM et al (2006) DJ-1 interacts with HIPK1 and affects H2O2-induced cell death. Free Radic Res 40:155–165
17. Taira T, Saito Y, Niki T, Iguchi-Ariga SM, Takahashi K et al (2004) DJ-1 has a role in antioxidative stress to prevent cell death. EMBO Rep 5:213–218
18. Kahle PJ, Waak J, Gasser T (2009) DJ-1 and prevention of oxidative stress in Parkinson's disease and other age-related disorders. Free Radic Biol Med 47:1354–1361
19. Kim RH, Smith PD, Aleyasin H, Hayley S, Mount MP et al (2005) Hypersensitivity of DJ-1-deficient mice to 1-methyl-4-phenyl-1,2,3,6-tetrahydropyrindine (MPTP) and oxidative stress. Proc Natl Acad Sci U S A 102:5215–5220
20. Menzies FM, Yenisetti SC, Min KT (2005) Roles of Drosophila DJ-1 in survival of dopaminergic neurons and oxidative stress. Curr Biol 15:1578–1582
21. Yang Y, Gehrke S, Haque ME, Imai Y, Kosek J et al (2005) Inactivation of Drosophila DJ-1 leads to impairments of oxidative stress response and phosphatidylinositol 3-kinase/Akt signaling. Proc Natl Acad Sci U S A 102:13670–13675
22. Blackinton J, Lakshminarasimhan M, Thomas KJ, Ahmad R, Greggio E et al (2009) Formation of a stabilized cysteine sulfinic acid is critical for the mitochondrial function of the parkinsonism protein DJ-1. J Biol Chem 284:6476–6485
23. Wilson MA (2011) The role of cysteine oxidation in DJ-1 function and dysfunction. Antioxid Redox Signal 15:111–122

# Chapter 82
# The Role of Reactive Oxygen Species in Ocular Malignancy

**Kathryn E. Klump and James F. McGinnis**

**Abstract** Increased production of reactive oxygen species (ROS) is an attribute of malignant cells and is linked to the development of many of the characteristics considered "hallmarks of cancer (Hanahan and Weinberg, Cell 144(5), 2011, 646–674)." Among these are sustained proliferative signaling, induction of new vascular growth, promotion of invasion, and metastatic potential. Maintaining the balance between the beneficial biological functions of ROS and the dysregulation seen in human disease such as cancer, presents a daunting conundrum in the future of oncology research. ROS involvement is pervasive throughout the process of tumorigenesis and subsequent cancer growth, yet the response to both pro- and antioxidant based therapy is varied. We will review the ROS species in the pathogenesis of primary ocular malignancy with consideration of potential targets for therapeutic intervention.

**Keywords** Reactive oxygen species · Ocular malignancy · Retinoblastoma

K. E. Klump (✉) · J. F. McGinnis
Oklahoma Center for Neuroscience, University of Oklahoma Health Sciences Center, Oklahoma City, USA

K. E. Klump
Dean A. McGee Eye Institute, 608 Stanton L. Young Boulevard, Pavilion B, L047, Oklahoma City, OK 73104, USA
e-mail: Kathryn-Klump@ouhsc.edu

J. F. McGinnis
Department of Cell Biology, University of Oklahoma Health Sciences Center, Oklahoma City, USA

Department of Ophthalmology, University of Oklahoma Health Sciences Center, Oklahoma City, USA
e-mail: James-McGinnis@ouhsc.edu

J. D. Ash et al. (eds.), *Retinal Degenerative Diseases,* Advances in Experimental Medicine and Biology 801, DOI 10.1007/978-1-4614-3209-8_82,

## 82.1 Introduction to Reactive Oxygen Species

The generation of reactive oxygen species as a byproduct of normal intracellular processes, most notably mitochondrial respiration, is a well-characterized phenomenon with beneficial physiologic functions in normal tissues [2]. These small, highly oxidative molecules are characterized by the presence of an unpaired electron in the outer shell of electrons of an oxygen moiety and include peroxides, hydroxyl radical, and superoxide species [3]. Endogenous enzymatic mechanisms exist for coping with the potential cytotoxic interaction of ROS with lipids, nucleic acids and proteins include superoxide dismutase, catalase, thioredoxin and glutathione, and their respective reductase enzymes [4, 5]. Disruption of these homeostatic scavenging systems leads to the production of ROS in excess of these endogenous cellular defenses, and results in a redox imbalanced cellular state termed oxidative stress [6]. Oxidative stress and the chronic exposure to ROS is implicated in the pathogenesis and progression of numerous human diseases. Current data support a role for ROS of particular importance in neurodegenerative and blinding pathologies [7–9], an area that is of interest to our laboratory. Recently, there has been an increasing interest in the association of elevated ROS production with the pathogenesis of malignant tumors as a potential therapeutic target [6, 10].

## 82.2 The Problem of Primary Ocular Malignancy

Primary malignancy of the eye is a relatively rare condition with uveal melanoma and pediatric retinoblastoma together comprising approximately 15,000 annual diagnoses worldwide [11]. Retinoblastoma is a cancer of the retina that initiates during fetal development as a result of either hereditary or sporadic mutation in the Rb1 tumor suppressor gene [12]. Retinoblastoma causes significant disruption to the normal retinal structure, profound vision loss, and death in the absence of timely intervention [13]. The most common primary ocular malignancy of childhood, and most frequent primary eye cancer overall, retinoblastoma is associated with significant morbidity and a heightened risk for enucleation in advanced cases notwithstanding an approximately 95–97% cure rate in the USA and Europe [13, 14]. Uveal melanomas are the most common primary ocular cancer in the adult population. Despite prevalence in the developed world due to a predilection for occurrence in light-skinned individuals of European descent, more than half of uveal melanoma patients die from the disease [14, 15]. Uveal melanoma and retinoblastoma demonstrate metastatic and invasive potential; uveal melanoma frequently metastasizes to the liver, and retinoblastoma commonly to the central nervous system. Metastatic ocular cancers are resistant to conventional chemotherapy. Left untreated, both cancers are invariably fatal, emphasizing the need for novel targeted drug development.

## 82.3 Complex Role of ROS in Cancer

The relationship between oxidative stress and the progression of malignancy is multifaceted. Indeed, ROS are involved in the regulation of critical signal transduction pathways, and under physiologic conditions moderate quantities of ROS are necessary for cell growth [16]. Conversely, increased levels of reactive oxygen species are known to increase mutagenic events, drive genomic instability, and contribute to the amplification of tumor aggression [17]. It is clear that ROS play a significant role in carcinogenesis through oxidative damage to DNA. Elevated ROS is associated with an increase in invasive properties in human ocular malignancy and in animal models of retinoblastoma. Current data indicate that retinoblastomas are under oxidative stress accompanied by the production of reactive oxygen species [18]. Discrete areas of hypoxia within tumor tissue are associated with spontaneous production of ROS and induction of signaling through the hypoxia inducible factor-1 (HIF-1) pathway. HIF-1 regulates the expression of vascular endothelial growth factor and initiates the formation of a robust vascular supply critical for sustained tumor growth [19, 20]. In addition to the pro-angiogenic function of ROS in the hypoxic environment, ROS levels also regulate cell proliferation, tumor growth, and apoptosis through the activation of Mitogen Activated Protein Kinase (MAPK), cytokine signaling pathways, and multiple growth factor receptors [6]. Systemic antioxidant therapy has met with some challenges and conflicting data regarding efficacy in human trials. There appears to be a differential response to antioxidant therapy in different cancer types, the absence of p53 appears to confer exquisite sensitivity to the anti-proliferative effects of decreasing ROS concentrations [21].

## 82.4 Targeting ROS in Ocular Malignancy

Manipulation of the sensitive redox environment in cancer is not a new concept; however, the most effective approach remains a quandary. Some chemotherapy drugs induce oxidative stress, taking advantage of an increase in ROS to push an already stressed system over the breaking point. Chemotherapy resistance to pro-oxidant drugs occurs in a variety of cancers, including retinoblastoma, and may be linked to a robust response in the endogenous defense against ROS which is frequently upregulated in some tumors [18, 22, 23]. Dysregulation of the endogenous protective mechanisms controlling the redox environment including SOD1 and catalase, have been reported in cases of ocular malignancy. Pretreatment with antioxidant nanoparticles has been demonstrated to sensitize tumor cells to radiation therapy [24]. Targeting the need for continuous signaling through ROS-mediated pathways for sustained tumor growth is a novel approach to be considered.

The anatomy of the eye along with the pathologic characteristics of ocular malignancy, including an upregulation in VEGF, presents unique advantages for the study of ROS-targeted interventions. The ability for local delivery, using intra-arterial

or intraocular injection, of selected agents bypass problems associated with systemic antioxidant dosing [25], while the opportunity to monitor tumor response through direct observation of the fundus and non-invasive imaging modalities raises a myriad of intriguing possibilities. Therapies directed at molecular events found downstream of ROS production, such as treatment with VEGF inhibitors have met with success in in vitro and animal models [26]. These data suggest that targeting a common node in ROS mediated signaling might be of therapeutic benefit. Broad spectrum antioxidant cerium oxide nanoparticles, which are retained within the retina for extended periods of time, might provide such therapeutic benefits. Antioxidant cerium oxide nanoparticles, nanoceria, have been shown to decrease tumor invasion through an ROS-scavenging mechanism [27]. It appears that, by destroying ROS, nanoceria affect multiple downstream signal transduction pathways including ones which control the concentration of VEGF within the retina [28]. In P53TKO mice which develop inherited retinoblastomas [29], nanoceria not only decrease VEGF in the retina and inhibit tumor size but they also inhibit seeding of the anterior chamber suggesting that inhibition of tumor angiogenesis is not the only mechanism by which they exert their effects [30]. In mouse models of inherited retinal degeneration, nanoceria have been shown to inhibit AKT and ERK pathways in the Vldlr knock out mouse and to inhibit pathologic neovascularization [30, 31]. It is apparent that the up- or down-regulation of ROS concentration can have multiple effects that promote either cell death or survival of malignant cells. Agents which regulate ROS are double-edged swords, the successful wielding of which will require additional knowledge and skill.

## References

1. Hanahan D, Weinberg RA (2011) Hallmarks of cancer: the next generation. Cell 144(5):646–674
2. Droge W (2002) Free Radicals in the physiological control of cell function. Physiol Rev 82(1):47–95
3. Halliwell B, Gutteridge JMC (1999) Free radicals in biology and medicine, 3rd ed. Oxford University Press
4. McCord JM, Fridovich I (1969) The utility of superoxide dismutase in studying free radical reactions. I. Radicals generated by the interaction of sulfite, dimethyl sulfoxide, and oxygen. J Biol Chem 244(22):6056–6063
5. Lu W, Ogasawara MA, Huang P (2007) Models of reactive oxygen species in cancer. Drug Discov Today Dis Models 4(2):67–73
6. Kovacic P, Jacintho JD (2001) Mechanisms of carcinogenesis: focus on oxidative stress and electron transfer. Curr Med Chem 8(7):773–796
7. Valko M, Leibfritz D, Moncol J, Cronin MTD, Mazur M, Telser J (2007) Free radicals and antioxidants in normal physiological functions and human disease. Int J of Biochem Cell Bio 39:44–84
8. Beatty S, Koh H, Phil M, Henson D, Boulton M (2000) The role of oxidative stress in the pathogenesis of age-realted macular degeneration. Surv Ophthalmol 45(2):115–134
9. van Reyk DM, Gillies MC, Davies MJ (2003) The retina: oxidative stress and diabetes. Redox Rep 8(4):187–192

10. Trachootham D, Alexandre J, Huang P (2009) Targeting cancer cells by ROS-mediated mechanisms: a radical therapeutic approach? Nature Rev 8:579–591
11. Kivela T (2009) The epidemiological challenge of the most frequent eye cancer: retinoblastoma, an issue of birth and death. Brit J Ophthalmol 93:1129–1131
12. Friend SH, Bernards R, Rogelj S, Weinberg RA, Rapaport JM, Albert DM, Dryja TP (1986) A human DNA segment with properties of the gene that predisposes to retinoblastoma and osteosarcoma. Nature 323(6089):643–646
13. Parulekar MV (2010) Retinoblastoma—current treatment and future direction. Early Hum Dev 86(10):619–625
14. Eagle Jr. RC (2012) The pathology of ocular cancer. Eye 2012:1–9
15. Hu D, Yu GP, McCormick SA, Schneider S, Finger PT (2005) Population based incidence of uveal melanoma in various races and ethnic groups. Am J Ophthalmol 140:612–617
16. Sauer H, Wartenberg M, Hescheler J (2001) Reactive oxygen species as intracellular messengers during cell growth and differentiation. Cell Physiol Biochem 11(4):173–186
17. Valko M, Rhodes CJ, Moncol J, Izakovic M, Mazur M (2006) Free radicals, metals and antioxidants in oxidative stress-induced cancer. Chem-Biol Interact 160:1–40
18. Vandhana S, Lakshmi TSR, Indra D, Deepa PR, Krishnakumar S (2012) Microarray analysis and biochemical correlations of oxidative stress responsive genes in retinoblastoma. Curr Eye Res 37(9):830–841
19. Missotten GS, Schlingemann RO, Jager MJ (2010) Angiogenesis and vascular endothelial growth factors in intraocular tumors. Dev Ophthalmol 46:123–132
20. Stitt AW, Simpson DAC, Boocock C, Gardiner TA, Murphy GM, Archer DB (1998) Expression of vascular endothelial growth factor (VEGF) and its receptors is regulated in eyes with intra-ocular tumors. J Pathol 186:306–312
21. Khromova NV, Kopnin PB, Stephanova EV, Agapova LS Kopnin BP (2009) P53 hot-spot mutants increase tumor vascularization via ROS-mediated activation of the HIF1/VEGF-A pathway. Can Lett 276:143–151
22. Chan HS, Canton MD, Gallie BL (1989) Chemosensitivity and multidrug resistance to antineoplastic drugs in retinoblastoma cell lines. Anticancer Res 9:469–474
23. Chan HS, Thorner PS, Haddad G, Gallie BL (1991) Multidrug-resistant phenotype in retinoblastoma correlates with P-glycoprotein expression. Opthalmol 98(9):1425–1431
24. Tarnuzzer RW, Colon J, Patil S, Seal S (2005) Vacancy engineered ceria nanostructures for protection from radiation-induced cellular damage. Nano Lett 5(12):2573–2577
25. Abramson DH (2010) Super selective ophthalmic artery delivery of chemotherapy for intraocular retinoblastoma: 'chemosurgery'. Br J Ophtalmol 94:396–399
26. Lee SY, Kim DK, Cho JH, Koh JY, Yoon YH (2008) Inhibitory effect of bevacizumad on the angiogenesis and growth of retinoblastoma. Arch Ophthalmol 126(7):953–958
27. Alili L, Sack M, Karakoti AS, Teuber S, Puschmann K, Hirst SM et al (2011) Combined cytotoxic and anti-invasive properties of redox-active nanoparticles in tumor-stroma interactions. Biomaterials 32:2918–2929
28. Cai X, Sezate SA, Seal S, McGinnis JF (2012) Sustained protection against photoreceptor degeneration in tubby mice by intravitreal injection of nanoceria. Biomaterials 33(34):877–881
29. Zhang J, Schweers B, Dyer MA (2004) The first knockout mouse model of retinoblastoma. Cell Cycle 3(7):952–959
30. Klump KE, Kiosseva S, Seal S, Dyer MA, McGinnis JF (2012) Therapeutic inhibition of retinoblastoma by nanoceria. ARVO Abstr:6549
31. Zhou X, Wong LL, Karakoti AS, Seal S, McGinnis JF (2011) Nanoceria inhibit the development and promote the regression of pathologic retinal neovascularization in the Vldlr knockout mouse. PLoS One 6(2):1–10
32. Kiosseva S, Seal S, McGinnis JF (2012) Inherited neovascular retinal lesions are regressed by nanoceria-induced changes in expression of multiple cytokine and growth factor genes. ARVO Abstr:421

# Chapter 83
# The Effects of IRE1, ATF6, and PERK Signaling on adRP-Linked Rhodopsins

**Wei-Chieh Jerry Chiang and Jonathan H. Lin**

**Abstract** Many mutations in *rhodopsin* gene linked to retinitis pigmentosa (RP) cause rhodopsin misfolding. Rod photoreceptor cells expressing misfolded rhodopsin eventually die. Identifying mechanisms to prevent rhodopsin misfolding or to remove irreparably misfolded rhodopsin could provide new therapeutic strategies. IRE1, ATF6, and PERK signaling pathways, collectively called the unfolded protein response (UPR), regulate the functions of endoplasmic reticulum, responsible for accurate folding of membrane proteins such as rhodopsin. We used chemical and genetic approaches to selectively activate IRE1, ATF6, or PERK signaling pathways one at a time and analyzed their effects on mutant rhodopsin linked to RP. We found that both artificial IRE1 and ATF6 signaling promoted the degradation of mutant rhodopsin with lesser effects on wild-type rhodopsin. Furthermore, IRE1 and ATF6 signaling preferentially reduced levels of aggregated rhodopsins. By contrast, PERK signaling reduced levels of wild-type and mutant rhodopsin. These studies indicate that activation of either IRE1, ATF6, or PERK prevents mutant rhodopsin from accumulating in the cells. In addition, activation of IRE1 or ATF6 can selectively remove aggregated or mutant rhodopsin from the cells and may be useful in treating RP associated with rhodopsin protein misfolding.

**Keywords** Unfolded protein response · Rhodopsin · P23H · Misfolded protein · IRE1 · PERK · ATF6 · Retinitis pigmentosa · Retinal degeneration

**Abbreviations**

| | |
|---|---|
| ATF6 | Activating transcription factor 6 |
| eIF2α | Eukaryotic translation initiating factor 2 subunit α |

J. H. Lin (✉) · W.-C. J. Chiang
Department of Pathology, University of California at San Diego,
9500 Gilman Dr., La Jolla, CA 92093-0612, USA
e-mail: jlin@ucsd.edu

W.-C. Jerry Chiang
e-mail: wcchiang@ucsd.edu

J. D. Ash et al. (eds.), *Retinal Degenerative Diseases,* Advances in Experimental Medicine and Biology 801, DOI 10.1007/978-1-4614-3209-8_83,

| | |
|---|---|
| ER | Endoplasmic reticulum |
| ERAD | ER-associated degradation |
| IRE1 | Inositol requiring enzyme-1 |
| PERK | Protein kinase RNA-like endoplasmic reticulum kinase |
| RP | Retinitis pigmentosa |
| UPR | Unfolded protein response |
| 1NM-PP1 | 4-amino-1-tert-butyl-3-(1'-naphthylmethyl)pyrazolo[3,4-d] pyrimidine |

## 83.1 Instruction

The most common form of inherited blindness is retinitis pigmentosa (RP) [1]. Over 100 distinct mutations in *rhodopsin* have been identified that cause RP (www.sph.uth.tmc.edu/retnet/). *Rhodopsin* gene encodes a G protein-coupled receptor that is folded in the endoplasmic reticulum (ER) prior to export to the rod photoreceptor outer segment [2]. Many class II mutations in *rhodopsin* gene that cause RP generate misfolded rhodopsin proteins that are retained within the ER [3–6]. Rod photoreceptors expressing misfolded mutant rhodopsin eventually die, leading to retinal degeneration. Studies have demonstrated that reducing misfolded rhodopsin protein levels by introducing chaperones or ribozymes specifically against mutant rhodopsin mRNA can delay retinal degeneration [7–9]. Therefore, identifying strategies to reduce misfolded rhodopsin protein in cells holds promise in preventing the death of rod photoreceptor cells.

Mammalian cells respond to ER stress by activating three distinct branches of signal transduction pathways, collectively called the unfolded protein response (UPR), to restore ER proteostasis. UPR is controlled by three ER-resident membrane proteins, inositol requiring enzyme-1 (IRE1), activating transcription factor 6 (ATF6), and protein kinase RNA-like endoplasmic reticulum kinase (PERK), which all contain ER luminal domains that monitor the quality of ER proteins and cytosolic domains that activate mechanistically-distinct signal transduction cascades [10]. In response to ER stress, IRE1, PERK, and ATF6 signaling pathways are activated and restore ER proteostasis by upregulating genes involved in ER protein folding and ER-associated protein degradation (ERAD) [11–13], and attenuating protein translation [14]. IRE1, PERK, and ATF6 signaling therefore enhance ER protein folding capabilities and also reduce protein levels by dampening translation and promoting protein degradation.

UPR regulation of ER protein-folding fidelity offers potential means to repair or remove misfolded proteins, such as class II rhodopsin mutant. In this review, we summarize how activation of each pathway, using artificial chemical or genetic means, affects the fate of mutant rhodopsin in cells.

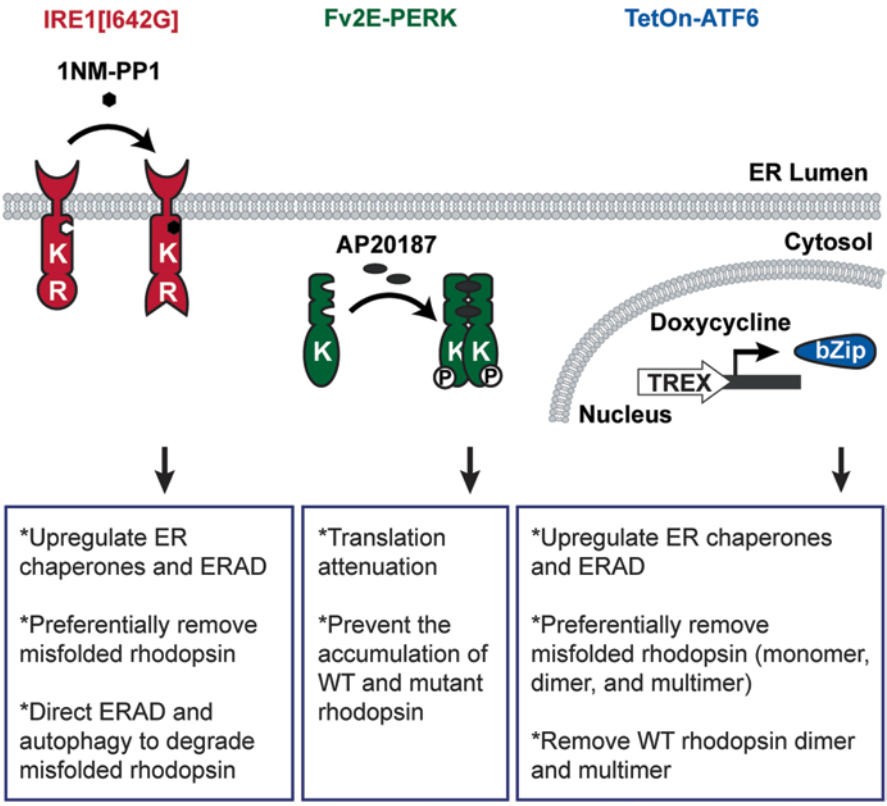


**Fig. 83.1** Chemical-genetic strategies to selectively activate IRE1, PERK, and ATF6 pathways

## 83.2 Selective Activation of IRE1 Promotes the Degradation of Misfolded Mutant Rhodopsin in the Cells

The cytosolic domain of IRE1 includes kinase and endoribonuclease (RNase) domains that control the splicing of *Xbp-1* mRNA [15–17]. To selectively activate IRE1, we used a genetically altered version of human IRE1, IRE1 [I642G], in which an isoleucine at residue 642 is substituted by a glycine. In this system, the RNase function of IRE1 [I642G] can be enabled by an ATP analog, 4-amino-1-*tert*-butyl-3-(1'-naphthylmethyl)pyrazolo[3,4-*d*]pyrimidine (1NM-PP1) [18, 19], to induce the splicing of *Xbp-1* mRNA (Fig. 83.1). Previously, we demonstrated that in cells stably expressing IRE1[I642G], the addition of 1NM-PP1 rapidly increased *Xbp-1* mRNA splicing without activating ATF6 and PERK pathways [19–21].

Using this system, we found that selectively activating IRE1 pathway tremendously reduced the protein levels of all class II rhodopsin mutants tested, including

P23H, T17M, Y178C, C185R, D190G, and K296E rhodopsin, whereas WT rhodopsin was minimally affected by the activation of IRE1. Furthermore, we found that the effects of IRE1 were almost exclusively targeted to the insoluble (aggregated) fractions of P23H rhodopsin, indicating that IRE1 removed mutant proteins at the monomeric state as well as when they were aggregated. Levels of mutant rhodopsin mRNAs were not changed in our system. Instead, activation of IRE1 promoted the degradation of mutant rhodopsin protein through two separate protein degradation pathways: the ubiquitin-proteasome system via ERAD and the autophagy-lysosome system [22].

## 83.3 Selective Activation of ATF6 Promotes the Degradation of Misfolded Mutant Rhodopsin in the Cells

In response to ER stress, ATF6 undergoes proteolysis to release its cytosolic bZIP-containing transcription factor domain (ATF6f) that migrates to the nucleus to upregulate genes involved in ER protein folding and ERAD [12, 13]. To selectively activate ATF6, we developed a system to induce the transcription of human ATF6f upon doxycycline addition (Fig. 83.1) without activating IRE1 and PERK pathways. Using this system, we showed that selectively activating ATF6 pathway significantly reduced the protein levels of class II mutant rhodopsin, such as P23H, T17M, Y178C, C185R, D190G, and K296E rhodopsin [23]. Furthermore, ATF6 reduced the protein levels of all species of P23H rhodopsin protein (monomer, dimer, and multimers). Interestingly, the protein level of WT rhodopsin was mildly reduced by ATF6, but this effect was limited to abnormal dimer and multimeric WT rhodopsin species [23]. Monomeric WT rhodopsin levels were unaffected. Our findings indicate that ATF6 signaling reduces misfolded rhodopsins as well as aggregated rhodopsin.

## 83.4 Selective Activation of IRE1 or ATF6 Promotes the Degradation of S334ter Mutant Rhodopsin

A non-class II mutant rhodopsin, S334ter rhodopsin lacking the last 15 amino acid residues in the C-terminus, also causes severe retinal degeneration.[24–28]. Surprisingly, selective activation of IRE1 or ATF6 signaling also decreased the protein level of S334ter rhodopsin in the cells [23]. Unlike the class II mutant rhodopsin that form multimers, S334ter is predominantly found as a monomer in cells, similar to the WT rhodopsin, suggesting that S334ter might not be misfolded. However, we found that S334ter is more sensitive to Endo H deglycosylation than WT rhodopsin [23]. Sensitivity to Endo H indicates that the protein contains high mannose N-

linked glycans, a typical characteristic of proteins that have not matured beyond the ER [29]. Increase of S334ter rhodopin's sensitivity to Endo H indicated that there might be more S334ter rhodopsin retained in the ER and therefore more susceptible to ER quality control upregulated by selective activation of IRE1 or ATF6 signaling.

## 83.5 Selective Activation of PERK Reduces the Accumulation of WT and P23H Rhodopsin Proteins in the Cells

PERK bears a cytosolic kinase domain that phosphorylates eukaryotic translation initiating factor 2 subunit α (eIF2α), thereby impairing ribosomal assembly on mRNAs and attenuating protein translation [14]. To selectively activate PERK, we used a genetically altered PERK protein, Fv2E-PERK, which consists of the eIF2α kinase domain of PERK fused to two modified FK506 binding domains (Fv2E) [30]. In this system, addition of a chemical dimerizer, AP20187, rapidly triggered the activation of Fv2E-PERK's eIF2α kinase domain, leading to the activation of PERK signaling (Fig. 83.1) without activating other endogenous UPR pathways [20, 30].

When we selectively activated PERK through this system, we found great reduction in protein levels of WT or P23H rhodopsin [23]. A similar reduction was also observed in cells transfected with other proteins such as VCAM-1 or GFP upon the activation of Fv2E-PERK [23]. These findings showed that PERK signaling reduced the protein levels of mutant and WT rhodopsin and other transfected proteins, consistent with the role of PERK in global attenuation of protein translation in the cells [31].

## 83.6 Conclusion

Here we dissected the effects of three separate UPR signaling pathways on rhodopsins linked to RP. We found that both IRE1 and ATF6 selectively reduced levels of misfolded rhodopsins with minimal effects on wild-type rhodopsin. Furthermore, both IRE1 and ATF6 preferentially target aggregated rhodopsins compared to the normal monomeric form. Given the ability of IRE1 and ATF6 to induce genes involved in ER protein folding and ER associated degradation, the effects of IRE1 and ATF6 signaling may be to disrupt the mutant rhodopsin aggregate and direct them for degradation. By contrast, PERK signaling non-specifically reduced levels of all rhodopsins. These findings suggest that artificial IRE1 or ATF6 signaling might be beneficial in enhancing photoreceptor cell survival in certain types of RP arising from expression of misfolded rhodopsins.

## References


1. Berson EL (1993) Retinitis pigmentosa. The Friedenwald lecture. Invest Ophthalmol Vis Sci 34(5):1659–1676
2. Sung CH, Chuang JZ (2010) The cell biology of vision. J Cell Biol 190(6):953–963
3. Kaushal S, Khorana HG (1994) Structure and function in rhodopsin. 7. Point mutations associated with autosomal dominant retinitis pigmentosa. Biochemistry 33(20):6121–6128
4. Sung CH, Schneider BG, Agarwal N, Papermaster DS, Nathans J (1991) Functional heterogeneity of mutant rhodopsins responsible for autosomal dominant retinitis pigmentosa. Proc Natl Acad Sci USA 88(19):8840–8844
5. Illing ME, Rajan RS, Bence NF, Kopito RR (2002) A rhodopsin mutant linked to autosomal dominant retinitis pigmentosa is prone to aggregate and interacts with the ubiquitin proteasome system. J Biol Chem 277(37):34150–34160
6. Saliba RS, Munro PM, Luthert PJ, Cheetham ME (2002) The cellular fate of mutant rhodopsin: quality control, degradation and aggresome formation. J Cell Sci 115(Pt 14):2907–2918
7. Lewin AS, Drenser KA, Hauswirth WW, Nishikawa S, Yasumura D, Flannery JG et al (1998) Ribozyme rescue of photoreceptor cells in a transgenic rat model of autosomal dominant retinitis pigmentosa. Nat Med 4(8):967–971
8. Kosmaoglou M, Kanuga N, Aguila M, Garriga P, Cheetham ME (2009) A dual role for EDEM1 in the processing of rod opsin. J Cell Sci 122(Pt 24):4465–4472
9. Mendes HF, Cheetham ME (2008) Pharmacological manipulation of gain-of-function and dominant-negative mechanisms in rhodopsin retinitis pigmentosa. Hum Mol Genet 17(19):3043–3054
10. Ron D, Walter P (2007) Signal integration in the endoplasmic reticulum unfolded protein response. Nat Rev Mol Cell Biol 8(7):519–529
11. Lee AH, Iwakoshi NN, Glimcher LH (2003) XBP-1 regulates a subset of endoplasmic reticulum resident chaperone genes in the unfolded protein response. Mol Cell Biol 23(21):7448–7459
12. Haze K, Yoshida H, Yanagi H, Yura T, Mori K (1999) Mammalian transcription factor ATF6 is synthesized as a transmembrane protein and activated by proteolysis in response to endoplasmic reticulum stress. Mol Biol Cell 10(11):3787–3799
13. Ye J, Rawson RB, Komuro R, Chen X, Dave UP, Prywes R et al (2000) ER stress induces cleavage of membrane-bound ATF6 by the same proteases that process SREBPs. Mol Cell 6(6):1355–1364
14. Harding HP, Zhang Y, Ron D (1999) Protein translation and folding are coupled by an endoplasmic-reticulum-resident kinase. Nature 397(6716):271–274
15. Cox JS, Shamu CE, Walter P (1993) Transcriptional induction of genes encoding endoplasmic reticulum resident proteins requires a transmembrane protein kinase. Cell 73(6):1197–1206
16. Calfon M, Zeng H, Urano F, Till JH, Hubbard SR, Harding HP et al (2002) IRE1 couples endoplasmic reticulum load to secretory capacity by processing the XBP-1 mRNA. Nature 415(6867):92–96
17. Yoshida H, Matsui T, Yamamoto A, Okada T, Mori K (2001) XBP1 mRNA is induced by ATF6 and spliced by IRE1 in response to ER stress to produce a highly active transcription factor. Cell 107(7):881–891
18. Bishop AC, Ubersax JA, Petsch DT, Matheos DP, Gray NS, Blethrow J et al (2000) A chemical switch for inhibitor-sensitive alleles of any protein kinase. Nature 407(6802):395–401
19. Lin JH, Li H, Yasumura D, Cohen HR, Zhang C, Panning B et al (2007) IRE1 signaling affects cell fate during the unfolded protein response. Science 318(5852):944–949
20. Lin JH, Li H, Zhang Y, Ron D, Walter P (2009) Divergent effects of PERK and IRE1 signaling on cell viability. PLoS ONE 4(1):e4170
21. Hiramatsu N, Joseph VT, Lin JH (2011) Monitoring and manipulating mammalian unfolded protein response. Meth Enzymol 491:183–198

22. Chiang WC, Messah C, Lin JH (2012) IRE1 directs proteasomal and lysosomal degradation of misfolded rhodopsin. Mol Biol Cell 23(5):758–770
23. Chiang WC, Hiramatsu N, Messah C, Kroeger H, Lin JH (2012) Selective activation of ATF6 and PERK endoplasmic reticulum stress signaling pathways prevent mutant rhodopsin accumulation. Invest Ophthalmol Vis Sci 53(11):7159–7166
24. Shinde VM, Sizova OS, Lin JH, Lavail MM, Gorbatyuk MS (2012) ER stress in retinal degeneration in S334ter rho rats. PLoS One 7(3):e33266
25. Dykens JA, Carroll AK, Wiley S, Covey DF, Cai ZY, Zhao L et al (2004) Photoreceptor preservation in the S334ter model of retinitis pigmentosa by a novel estradiol analog. Biochem Pharmacol 68(10):1971–1984
26. Lee D, Geller S, Walsh N, Valter K, Yasumura D, Matthes M et al (2003) Photoreceptor degeneration in Pro23His and S334ter transgenic rats. Adv Exp Med Biol 533:297–302
27. Anderson RE, Maude MB, McClellan M, Matthes MT, Yasumura D, LaVail MM (2002) Low docosahexaenoic acid levels in rod outer segments of rats with P23H and S334ter rhodopsin mutations. Mol Vis 8:351–358
28. Kroeger H, Messah C, Ahern K, Gee J, Joseph V, Matthes MT et al (2012) Induction of endoplasmic reticulum stress genes, BiP and Chop, in genetic and environmental models of retinal degeneration. Invest Ophthalmol Vis Sci 53(12):7590–7599
29. Sherblom AP, Smagula RM (1993) High-mannose chains of mammalian glycoproteins. Methods Mol Biol 14:143–149
30. Lu PD, Jousse C, Marciniak SJ, Zhang Y, Novoa I, Scheuner D et al (2004) Cytoprotection by pre-emptive conditional phosphorylation of translation initiation factor 2. EMBO J 23(1):169–179
31. Harding HP, Zhang Y, Bertolotti A, Zeng H, Ron D (2000) Perk is essential for translational regulation and cell survival during the unfolded protein response. Mol Cell 5(5):897–904

# Chapter 84
# Role of Endothelial Cell and Pericyte Dysfunction in Diabetic Retinopathy: Review of Techniques in Rodent Models

**Jonathan Chou, Stuart Rollins and Amani A Fawzi**

**Abstract** Diabetic Retinopathy is one of the hallmark microvascular diseases secondary to diabetes. Endothelial cells and pericytes are key players in the pathogenesis. Interaction between the two cell types is important in the regulation of vascular function and the maintenance of the retinal homeostatic environment. There are currently several approaches to analyze changes in morphology and function of the two cell types. Morphologic approaches include trypsin digest, while functional approaches include studying blood flow. This review explores the advantages and limitations of various methods and summarizes recent experimental studies of EC and pericyte dysfunction in rodent models of DR. An improved understanding of the role played by EC and pericyte dysfunction can lead to enhanced insights into retinal vascular regulation in DR and open new avenues for future treatments that reverse their dysfunction.

**Keywords** Endothelial cell · Pericyte · Dysfunction · Rodent · Histopathology · Trypsin digest · Blood flow · Oximetry

**List of Abbreviations**

| | |
|---|---|
| DR | Diabetic retinopathy |
| EC | Endothelial cells |
| STZ | Streptozotocin |
| H&E | Hematoxylin & eosin |
| FA | Fluorescein angiography |
| RT | Radioactive tracers |
| MT | Microsphere tracers |
| HC | Hydrogen clearance |

A. A. Fawzi (✉) · J. Chou · S. Rollins
Department of Ophthalmology, Northwestern Feinberg School of Medicine,
645 N Michigan Ave., Chicago, IL 60611, USA
e-mail: amani.fawzi@northwestern.edu

J. Chou
e:mail: jchou87@northwestern.edu

J. D. Ash et al. (eds.), *Retinal Degenerative Diseases,* Advances in Experimental Medicine and Biology 801, DOI 10.1007/978-1-4614-3209-8_84,

IVM Intravital microscopy
OCT Optical coherence tomography
SLO Scanning laser ophthalmoscope
fMRI Functional magnetic resonance spectroscopy
ΔPO2 Oxygenation response to hyperoxic provocation
PAOM Photoacoustic ophthalmoscopy

## 84.1 Introduction

Diabetic Retinopathy (DR) is one of the hallmark complications of diabetes and one of the most common causes of blindness worldwide. Endothelial cells (EC) and pericytes are key players in the pathogenesis of DR, and their role in diabetes has been extensively studied. EC line the vasculature, serve as a physical barrier between blood and the surrounding tissue, and have a critical role in maintaining the retinal homeostasis. Pericytes are found in the vascular basement membrane. Their wide-ranging functions include mediating repair to the vasculature, promoting the blood-retinal barrier, and functioning as hypoxia sensors [1]. Interactions between EC and pericytes regulate vascular stabilization and function. In diabetic microangiopathy, dysfunction in either cell type leads to abnormal function of the other, which prompted the development of many techniques to study abnormalities in vascular morphology and function. This review will address the advantages and limitations of the most common methods, and summarize important conclusions from studies in rodent models of DR.

## 84.2 Experimental Approaches in Rodent Models of Diabetic Retinopathy

A variety of animal species have been used to study the pathogenesis of DR, which have respective advantages and limitations and are described in detail, elsewhere [2]. The rodent is the most widely available animal model, given its cost efficacy and recent availability of imaging methods to study blood flow in vivo in rodents. Currently, there are several morphological and functional approaches to study EC and pericytes in rodents (Table 84.1). It is important to note that although many important abnormalities in the pathogenesis of DR have been identified (e.g. capillary degeneration, altered blood flow), not all retinal lesions that develop in diabetic patients have been reproduced in diabetic rodents (e.g. neovascularization).

**Table 84.1** Summary of morphological/functional approaches

| Morphological approaches | Benefits | Limitations |
|---|---|---|
| Flat mount | Maintains vessel integrity | Non-specific staining, poor resolution of vasculature |
| Trypsin digest | Isolates vasculature; histopathology readily seen | Technically challenging; difficult to differentiate EC/pericytes |
| Cellular markers | Identifies EC/pericytes | Not 100% specific; dynamic marker expression |
| *Functional approaches* | | |
| Imaging<br>FA<br>Hydrogen clearance<br>Intravital microscopy<br>OCT<br>SLO | Measures blood flow<br>1. Easy visualization of retinal vessels<br>2. Can measure regional/temporal fluctuations 4. Non-invasive | 1–3. Invasive; injections may alter hemodynamics<br>4. Poor resolution with cataracts |
| Oximetry | Measures oxygen tension | Invasive |
| Microelectrode<br>fMRI<br>PAOM, Phosphorescence quenching | 1. Gold standard<br>2–3. Non-invasive<br>2. Does not require media clarity | 1, 3. Requires media clarity |

## 84.3 Morphological Approaches

Whole retinal flat-mount is a commonly used method, which maintains the blood vessel integrity while vessels are highlighted by staining. However, staining is non-specific and highlights non-vascular tissue, making it difficult to differentiate vessels and to identify pathologies such as capillary degeneration. Injection of dyes has also been used to highlight vessels, but this rarely highlights the entire retinal vasculature unless given at high pressure, which risks damaging the vessels [3].

Trypsin digest has become the gold standard to analyze retinal vasculature since its description by Kuwabara and Cogan in 1960 [3]. The method removes the non-vascular tissue leaving only the vascular network intact. The retina is an ideal tissue for trypsin digest as it contains little trypsin-resistant collagen, while the EC and pericytes are protected from trypsin by a mucoproteinaceous wall. As a result, this approach provides the opportunity to study the retinal vasculature in great detail (Fig. 84.1a). Microvascular lesions such as microaneurysms, acellular capillaries, and capillary degeneration have been visualized using the technique (Fig. 84.1b). In streptozotocin-induced (STZ) rats, it has been shown that the first anatomical changes occur after 6 weeks of induction. Initially, there is the development of tortuous swollen vessels, followed by loss of EC and pericytes and subsequent microaneurysms by 28–90 weeks [4].

EC to pericyte (E/P) ratio can be used to assess pericyte dropout, one of the earliest cellular deficiencies noted in DR [1]. The accuracy of quantifying E/P ratio

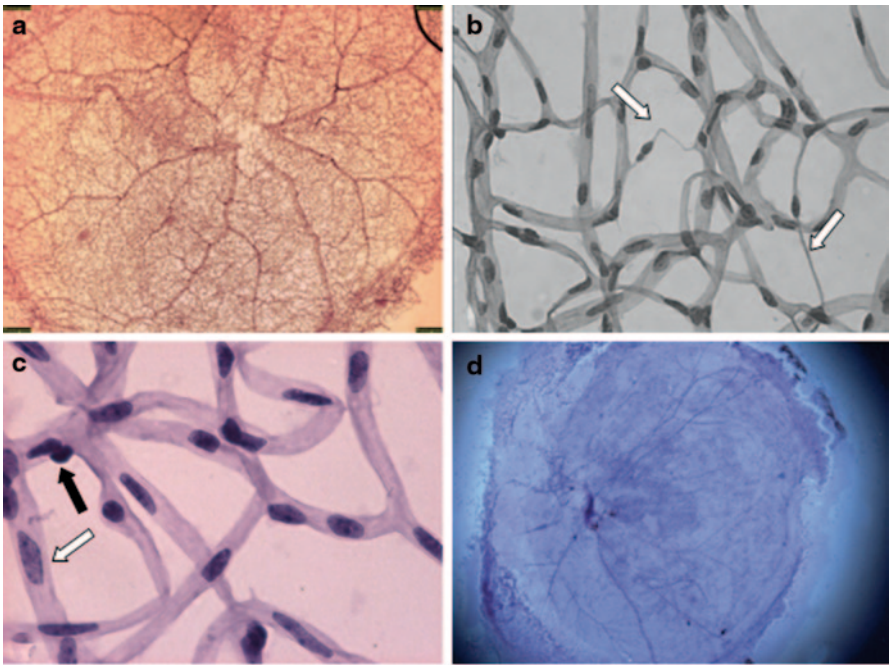


**Fig. 84.1** Trypsin digest. Flat mount mouse retina stained with H&E. **a** db/m mouse, normal retina (20×). **b** db/db mouse, capillary degeneration (*white arrow*) (500×). **c** db/m mouse, EC (*white arrow*) and pericyte (*black arrow*) highlighted (600×). **d** C57Bl6 mouse, insufficient removal of non-vascular tissue leading to impaired visualization of the blood vessels

rests on clear distinction between the two cell types. Pericyte nuclei are spherical, stain densely and have a protuberant position on the capillary wall, while EC nuclei are oval and lie within the vessel wall (Fig. 84.1c). Unfortunately, many cells can be intermediate that do not fit nicely into either group [5]. Another limitation of trypsin digest is that it is technically difficult and can lead to inconsistent results (Fig. 84.1d). Some of the potential technical challenges and approaches to overcome them are described by our group in detail elsewhere [6].

Immunohistochemistry has been used extensively to characterize pericytes and EC. A vast array of antibodies is available to identify and analyze pericyte and EC dysfunction (e.g. alpha-smooth muscle actin and intercellular adhesion molecule-1, respectively) [7, 8]. Unfortunately, none are 100% specific and can unequivocally identify all pericytes or EC [9]. Furthermore, the expression of these markers is dynamic in nature and can be up- or down-regulated in various environments. For example, alpha-smooth muscle actin is not expressed under normal circumstances in mouse retina, but is expressed in pericytes during retinopathy [1]. As a result, studies that use single markers must be viewed with caution.

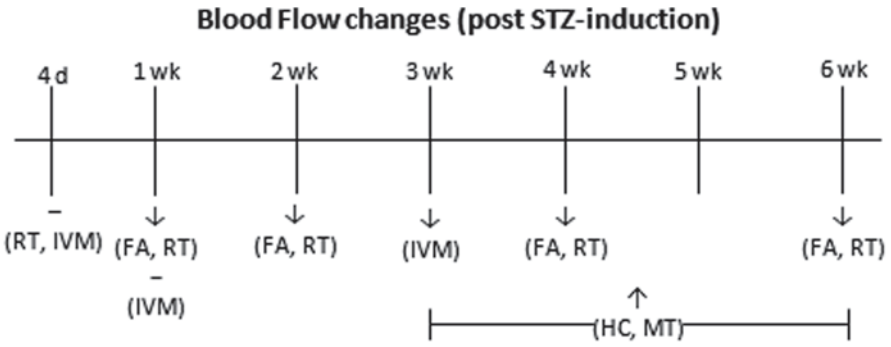


**Fig. 84.2** Blood flow changes in STZ- rats based on different techniques: Radioactive tracer (*RT*), Intravital microscopy (*IVM*), Fluorescein Angiography (*FA*), Hydrogen Clearance (*HC*), and Microsphere Tracer (*MT*). Notice conflicting data at 1 week and 3–6 weeks

## 84.4 Functional Approaches

Regulation of retinal vascular tone is one of the most important and well-studied functions of EC and pericytes. Retinal vascular auto-regulation ensures adequate delivery of oxygen, metabolic substrates, and removal of toxic substances and hence, optimal retinal function. Improved understanding of retinal blood flow can help identify new strategies to prevent DR. STZ rats have been the most widely used animal model to study retina blood flow. Unfortunately, in contrast to the morphological methods that have yielded similar conclusions, the techniques used to evaluate retinal blood flow have shown wide variability.

Fluorescein angiography (FA) and radioactive tracers (RT) are techniques to visualize the retinal circulation via injections. After injection, they can be quantified as they provide optical or radioactive contrast in the vasculature, which can be analyzed to quantify blood flow. These methods have demonstrated that blood flow decreases at 1–6 weeks after STZ-induction [10, 11]. The use of microsphere tracers is based on similar principles. Hydrogen clearance is a method that determines blood flow based on the principle that the washout rate of a non-metabolized, diffusible gas from a tissue is proportional to the blood flow [12]. This provides the opportunity to measure regional and temporal fluctuations. Contrary to FA and RT, the latter two methods have shown increases in blood flow at 3–6 weeks after STZ-induction [4, 12]. Intravital microscopy is a technique that measures flow via fluorescein injection and labeled red blood cells [13]. Using this method, it has been shown that at 1 week, there are minimal changes in blood flow, contrary to FA studies, but did support the finding that blood flow decreases by 3 weeks [14, 15].

The different principles underlying these methods may contribute to their conflicting conclusions regarding the timeline and patterns of blood flow alterations (Fig. 84.2). Furthermore, these methods are invasive and flow can be affected by the injection rate. Also, blood flow distribution throughout the retina becomes more variable with DR progression, likely due to impaired auto-regulation [4]. The com-

bination of a lack of standardized tool to measure blood flow, coupled to the overall heterogeneity of blood flow in DR has contributed to our continued limited understanding of the course of blood flow changes in DR.

Non-invasive imaging modalities are being developed to allow improved measurement of total blood flow in animal models. One example is Optical Coherence Tomography (OCT), a revolutionary technology developed in the 1990s that allows high-resolution imaging of the retina [16]. One obstacle limiting use of optical imaging in diabetic animals is the development of cataracts, which in STZ-rats begins by 5 weeks with progression to mature cataracts by 8 weeks [17]. There are various treatments that can delay cataract formation up to 3 months (e.g. glycine) after STZ-induction [17]. However, these treatments do have the potential to alter the blood flow. Interestingly, mice with congenital hyperglycemia (e.g. db/db) do not develop cataracts [18].

Measurements of retinal vascular oxygen is another important method of examining EC and pericyte function, as it allows direct quantification of oxygen delivery to the retina. Although a detailed analysis is beyond the scope of this chapter, a brief review is presented. Oxygen-sensitive microelectrodes are considered the gold standard. At 5–6 weeks after STZ-induction, rats have smaller arteriovenous oxygen tension differences suggesting vascular leakage [4]. However, interpretations need to be approached with caution as measurements are often made at only one time point and sample only a small retinal area. The procedure is also highly-invasive and hindered by cataract formation. Unlike the former, functional magnetic resonance spectroscopy (fMRI) is non-invasive, unaffected by cataracts, and is able to survey the entire retina. fMRI can measure retinal oxygenation response to hyperoxic provocation (ΔPO2), which has been shown to be a predictor of therapeutic efficacy. In STZ rats, ΔPO2 is significantly lower than control and these changes occur well before retinal histopathologic changes. STZ rats treated with aminoguanidine had restoration of normal ΔPO2 and did not develop subsequent retinal pathology [19]. Two novel techniques for measuring oxygenation are photoacoustic ophthalmoscopy (PAOM) and phosphorescence imaging [20, 21]. More research needs to be done to see whether they will become useful tools in rodent models of DR.

## 84.5 Treatment of Endothelial Cell and Pericyte Dysfunction

The importance of EC and pericytes in DR has led to research into therapies to prevent their dysfunction, before the onset of clinically overt vascular abnormalities, which become resistant to therapy over time [10]. An improved understanding of the role played by pericyte and EC dysfunction can open new avenues for treatments that reverse their dysfunction and lead to enhanced insights into retinal vascular regulation in DR.

**Support** This work was partly supported by the Illinois Society for Prevention of Blindness (JC, AAF), NIH (EY019951, AAF), Research to Prevent Blindness, NY (JC, and Northwestern Department of Ophthalmology).

## References


1. Armulik A, Abramsson A, Betsholtz C (2005) Endothelial/pericyte interactions. Circ Res 97(6):512–523
2. Robinson R, Barathi VA, Chaurasia SS, Wong TY, Kern TS (2012) Update on animal models of diabetic retinopathy: from molecular approaches to mice and higher mammals. Dis Model Mech 5(4):444–456
3. Kuwabara T, Cogan DG (1960) Studies of retinal vascular patterns. I. Normal architecture. Arch Ophthalmol 64:904–911
4. Alder VA, Su EN, Yu DY, Cringle SJ, Yu PK (1997) Diabetic retinopathy: early functional changes. Clin Exp Pharmacol Physiol 24(9–10):785–788
5. Cuthbertson RA, Mandel TE (1986) Anatomy of the mouse retina. Endothelial cell-pericyte ratio and capillary distribution. Invest Ophthalmol Vis Sci 27(11):1659–1664
6. Chou J, Rollins S, Fawzi A (in press) Trypsin digest protocol to analyze the retinal vasculature of a mouse model. JoVE 2013
7. Krueger M, Bechmann I (2010) CNS pericytes: concepts, misconceptions, and a way out. Glia 58(1):1–10
8. Portillo JA, Okenka G, Kern TS, Subauste CS (2009) Identification of primary retinal cells and ex vivo detection of proinflammatory molecules using flow cytometry. Mol Vis 15:1383–1389
9. Armulik A, Genove G, Betsholtz C (2011) Pericytes: developmental, physiological, and pathological perspectives, problems, and promises. Dev Cell 21(2):193–215
10. Higashi S, Clermont AC, Dhir V, Bursell SE (1998) Reversibility of retinal flow abnormalities is disease-duration dependent in diabetic rats. Diabetes 47(4):653–659
11. Pouliot M, Hetu S, Lahjouji K, Couture R, Vaucher E (2011) Modulation of retinal blood flow by kinin B(1) receptor in Streptozotocin-diabetic rats. Exp Eye Res 92(6):482–489
12. Cringle SJ, Yu DY, Alder VA, Su EN (1993) Retinal blood flow by hydrogen clearance polarography in the streptozotocin-induced diabetic rat. Invest Ophthalmol Vis Sci 34(5):1716–1721
13. Wang Z, Yadav AS, Leskova W, Harris NR (2010) Attenuation of streptozotocin-induced microvascular changes in the mouse retina with the endothelin receptor A antagonist atrasentan. Exp Eye Res 91(5):670–675
14. Bursell SE, Clermont AC, Shiba T, King GL (1992) Evaluating retinal circulation using video fluorescein angiography in control and diabetic rats. Curr Eye Res 11(4):287–295
15. Lee S, Morgan GA, Harris NR (2008) Ozagrel reverses streptozotocin-induced constriction of arterioles in rat retina. Microvasc Res 76(3):217–223
16. Huang D, Swanson EA, Lin CP, Schuman JS, Stinson WG, Chang W et al (1991) Optical coherence tomography. Science 254(5035):1178–1181
17. Bahmani F, Bathaie SZ, Aldavood SJ, Ghahghaei A (2012) Glycine therapy inhibits the progression of cataract in streptozotocin-induced diabetic rats. Mol Vis 18:439–448
18. Varma SD, Kinoshita JH (1974) The absence of cataracts in mice with congenital hyperglycemia. Exp Eye Res 19(6):577–582
19. Berkowitz BA, Ito Y, Kern TS, McDonald C, Hawkins R (2001) Correction of early subnormal superior hemiretinal DeltaPO(2) predicts therapeutic efficacy in experimental diabetic retinopathy. Invest Ophthalmol Vis Sci 42(12):2964–2969
20. Jiao S, Jiang M, Hu J, Fawzi A, Zhou Q, Shung KK et al (2010) Photoacoustic ophthalmoscopy for in vivo retinal imaging. Opt express 18(4):3967–3972
21. Shahidi M, Shakoor A, Blair NP, Mori M, Shonat RD (2006) A method for chorioretinal oxygen tension measurement. Curr Eye Res 31(4):357–366

# Chapter 85
# Autophagy Induction Does Not Protect Retina Against Apoptosis in Ischemia/Reperfusion Model

**Nathalie Produit-Zengaffinen, Constantin J. Pournaras and Daniel F. Schorderet**

**Abstract** The role played by autophagy after ischemia/reperfusion (I/R) in the retina remains unknown. Our study investigated whether ischemic injury in the retina, which causes an energy crisis, would induce autophagy. Retinal ischemia was induced by elevation of the intraocular pressure and modulation of autophagic markers was analyzed at the protein levels in an early and late phase of recovery. Following retinal ischemia an increase in LC3BII was first observed in the early phase of recovery but did not stay until the late phase of recovery. Post-ischemic induction of autophagy by intravitreal rapamycin administration did not provide protection against the lesion induced by the ischemic stress. On the contrary, an increase in the number of apoptotic cells was observed following I/R in the rapamycin treated retinas.

**Keywords** Retinal ischemia · Autophagy · Apoptosis · LC3 · Rapamycin

**Abbreviations**

| | |
|---|---|
| I/R | Ischemia reperfusion |
| LC3 | Microtubule associated protein light chain |
| CMA | Chaperone-mediated autophagy |

Grant support: ProVisu Foundation.

N. Produit-Zengaffinen (✉) · D. F. Schorderet
Institute for Research in Ophthalmology, 64 Avenue du Grand-Champsec, 1950, Sion, Switzerland
e-mail: nathalie.produit@irovision.ch

C. J. Pournaras
Department of NEUCLID, Geneva University Hospitals, Geneva, Switzerland
e-mail: constantin.pournaras@unige.ch

D. F. Schorderet
Department of Ophthalmology, University of Lausanne, Lausanne, Switzerland
e-mail: daniel.schorderet@irovision.ch

Faculty of Life Sciences, Ecole polytechnique fédérale de Lausanne, Lausanne, Switzerland

J. D. Ash et al. (eds.), *Retinal Degenerative Diseases,* Advances in Experimental Medicine and Biology 801, DOI 10.1007/978-1-4614-3209-8_85,

## 85.1 Introduction

Autophagy is a catabolic pathway by which mammalian cells degrade and recycle molecules and organelles. It plays a central role in maintaining intracellular homeostasis [1]. Autophagy occurs either constitutively or is induced consecutively to changes in the cellular environment. It is also a survival mechanism that can be activated in response to starvation and other stress [2]. Multiple signals are likely to trigger autophagy during ischemia/reperfusion (I/R).

Our study focused on the regulation of autophagic markers at two time points during recovery: an early (3 h after I/R) and late phase (24 h after I/R). Although ischemic retinas were obviously undergoing an apoptotic process, autophagy was not elicited over time in this experimental condition and could not be associated with a protective mechanism 24 h after I/R. To discriminate between the potential protective or harmful function of autophagy in I/R of the retina, we measured the incidence of increased autophagy on cell death in vivo. Our results reported that autophagy was initiated in an early and transient phase of recovery and further induction in a late phase after an ischemic stress compromised cell viability of the retina.

## 85.2 Methods

### *85.2.1 Animal Handling and Surgery*

Retinal ischemia was generated as described previously in male Sprague-Dawley rats [3–6]. All experimental procedures implicating rats were carried out in accordance with the ARVO Statement for the Use of Animals in Ophthalmic and Vision Research and were approved by the local Veterinary Office on Use and Care of Animals in Research of the State of Valais, Sion, Switzerland.

### *85.2.2 Western Blot Analysis*

After enucleation, retinas were quickly dissected in 1x phosphate-buffered saline (PBS) supplemented with 1x protease inhibitor cocktail, transferred in Hepes-Tween solution (Hepes 20 mM, Tween-20 0.5 %) containing phosphatases and proteases inhibitor cocktails. As loading control, β-actin was evaluated for each western blot. Quantification analysis of the proteins was performed with the Multigauge (Fujifilm) software.

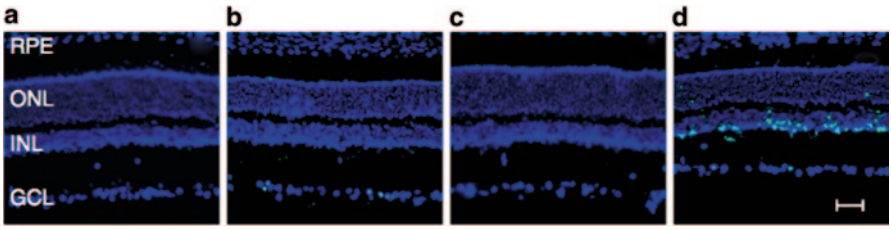


**Fig. 85.1** Retinal ischemia induced apoptosis 3 and 24 h after recovery. *Top*: several apoptotic cells were observed in the *GCL* of ischemic retinas 3 h after recovery. *Bottom*: 24 h after the ischemic insult, a high number of apoptotic cells could be visualized in the *GCL* and *INL* of ischemic retina. Scale bar: 100 µm

### *85.2.3 Immunohistology*

Eyes were fixed in 4% paraformaldehyde (PFA)/phosphate-buffered saline (PBS overnight at 4° C, followed by cryoprotection in 30% sucrose/PBS at 4° C. Twelve µm-embedded frozen sections were stained for TUNEL and with 4′,6-diamidino-2-phenylindole, dihydrochloride (DAPI) to identify retinal cell layers. Sections were then cover-slipped and observed under a microscope.

### *85.2.4 Statistics*

Results are presented as mean ± standard error of the mean (SEM) of the indicated number of independent experiments. Statistical analysis was performed using Student's *t*-test.

## 85.3 Results

### *85.3.1 Retinal Ischemia Enhanced Apoptosis in the Late Phase of Recovery*

Extent of the retinal damage induced by I/R was first assessed by analyzing cell death occurring by apoptosis (Fig. 85.1). Three hours after I/R, TUNEL positive cells were strictly located in the ganglion cell layer (GCL). After 24 h, a robust increase in the number of apoptotic cells was observed in the inner nuclear layer (INL) and, to a lower extent, in the outer nuclear layer (ONL) and persistent apoptotic cells were found in the GCL. No apoptotic cells were seen in the control retina at any time.

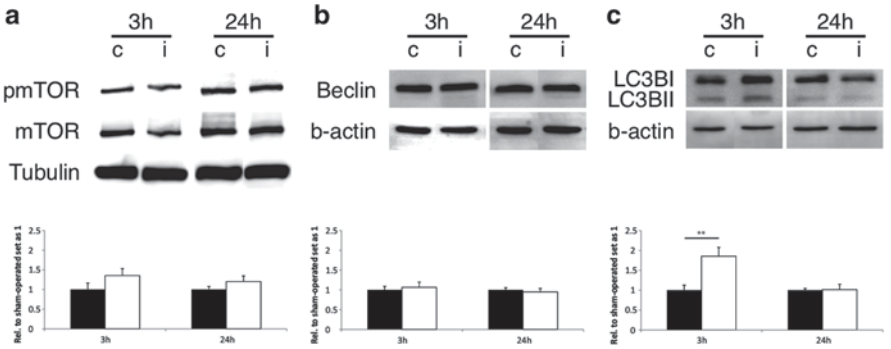


**Fig. 85.2** Effect of retinal ischemia on protein expression of autophagic markers. Ischemia did not alter **a** phospho-mTOR/mTOR nor **b** Beclin protein amount either at 3 or at 24 h after I/R. **c** Ischemia did not alter LC3B protein level 3 h after I/R but a reduction in LC3BI protein was observed 24 h after the ischemic insult. *Black columns* control retinas ($n=8$); *white columns* ischemic retinas ($n=8$). *Error bars* represent SEM ($*p<0.05$) control vs. ischemic retinas, by Student's *t*-test, *c* control retina, *i* ischemic retina

### *85.3.2 Retinal Ischemia Did Not Modify Autophagy at Protein Level in the Late Phase of Recovery*

We then evaluated autophagy involvement after I/R in the retina. Analysis of phospho-mTOR/mTOR ratio by western blot showed no significant modulation between ischemic and sham-operated retinas, either 3 or 24 h after I/R (Fig. 85.2a). Beclin 1, which is known to participate in the autophagic process, was not affected by the ischemic stress (Fig. 85.2b). LC3B-II was first highly increased 3 h after ischemia ($1\pm0.12$ vs. $1.85\pm0.22$; $p<0.05$), but was returned to normal values 24 h after the insult (Fig. 85.2c). No difference in LAMP-2 amount was observed either 3 or 24 h after I/R (data not shown), suggesting that chaperone-mediated autophagy (CMA) was not involved following an ischemic stress in the retina.

### *85.3.3 Rapamycin Administration After I/R Enhanced Retinal Apoptosis 24 h After Recovery*

We then evaluated whether autophagy induction would protect retinas against I/R induced apoptosis. Autophagy was stimulated by intravitreal injection of rapamycin, at the end of the ischemic stress, and apoptosis was evaluated 24 h post I/R. The number of apoptotic cells was then quantified by TUNEL staining (Fig. 85.3). We observed a significant increase in apoptosis in the GCL from ischemic retinas treated with rapamycin as compared to ischemic retinas ($6.12\%\pm1.26$ vs. $20.13\%\pm2.61$; $p<0.005$) and ischemic plus DMSO injected retinas ($10.14\pm3.40$ vs. $20.13\pm2.61\%$; $p<0.05$). No difference in the number of apoptotic cells was

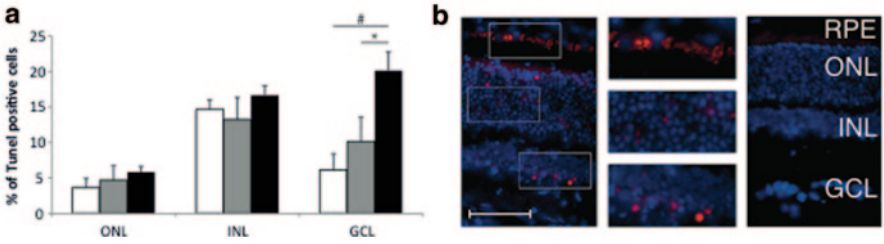


**Fig. 85.3** **a** Effect of rapamycin on the number of apoptotic cells in the *ONL*, *INL* and *GCL*. Rapamycin administration immediately after the ischemic insult enhanced the number of apoptotic cells in the *GCL* but had no effect on the number of dead cells in the *INL* or the *ONL*. *White columns*: ischemic retinas ($n=10$), *grey columns*: ischemic retinas + DMSO ($n=6$), *black columns*: ischemic retinas + rapamycin 5 mM ($n=6$). *Error bars* represent SEM (*$p<0.05$) ischemic retinas vs. ischemic retina + DMSO and (#: $p<0.005$) ischemic retinas vs. ischemic retina + rapamycin, by Student's *t*-test. **b** Effect of rapamycin on LC3B expression pattern in ischemic retinas. *Left*: Intravitreal rapamycin injection induced LC3B aggregation in *RPE*, *ONL* and *INL*. No aggregation of LC3B could be visualized in any retinal layer of the negative control (*right*). Scale bar: 100 µm

observed either in the INL or in the ONL of ischemic retinas after rapamycin administration as compared to control retinas.

## 85.4 Discussion

I/R involves a large array of pathological processes and induces highly variable outcomes that are modulated by many factors [7]. Autophagy is active at basal levels in most cells or can be stimulated by nutrient depletion [8]. It has been implicated in various diseases, including cancer and neurodegenerative diseases [9]. In all these situations, autophagy has both favorable and damaging effects. Our study investigated whether ischemic injury in the retina would induce autophagy. We then evaluated whether exogenous autophagy induction after I/R would protect or further damage the retina.

We first evaluated the extent of the damage induced by an I/R insult on the retina. Cell death after I/R in the retina has been demonstrated by TUNEL assay and a progressive increase in apoptotic cell number has already been described from 3 to 24 h after reperfusion [3–6]. In an early recovery phase (3 h), we observed some apoptotic cells restricted to the GCL of ischemic retina. In a late phase of recovery (24 h), the majority of apoptotic cells were found in the INL and to a lower extent in the GCL and in the ONL of the ischemic retinas.

Protein analysis did not highlight stable autophagy induction after I/R in the retina. Neither PmTOR/mTOR ratio nor Beclin 1 was regulated after an ischemic insult in an early or late phase of recovery. Western blot analysis of LC3 showed a first increase in LC3BII 3 h after I/R but with subsequent normalization over time. We also investigated whether CMA was induced following I/R of the retina. This

was not the case as LAMP-2A protein level was not increased in our I/R model. However, CMA activation can also occur without *de novo* synthesis of LAMP-2A and further investigation of the dynamics of LAMP-2A would be necessary to formally exclude this mode of autophagy [10, 11].

An increase in autophagy following I/R was also reported in other tissues such as brain and heart [12, 13]. As demonstrated by two studies on neurons from the central nervous system (CNS), duration of the insult induced substantial differences in gene expression and functional recovery [14, 15]. However, this did not highlight whether ischemia-reperfusion-induced autophagy could contribute to ischemic injury or cell survival in our model.

Since retinal cell death was highly augmented 24 h after I/R, we investigated whether autophagy induction protected against or, conversely, contributed to the increase in apoptosis observed at this time. Our results provided evidence that autophagy induction did not protect the retina from cell death. Specifically, autophagy induction rather increased apoptosis in the GCL, but did not affect cell death in the other layers of the retina. It seems, therefore, that autophagy could act differently in different organs as it was previously shown to be protective in ischemic injuries in kidney [16] and heart [17, 18].

Recently, Russo et al. and Piras et al. reported increased autophagy in a similar, although not identical rat model and proposed that therapeutic manipulation of autophagy could be beneficial. Although modulating autophagy may seem to have therapeutic implications, our data suggest caution as in our model, stimulation of autophagy led to retinal toxicity [19, 20].

In summary, we showed that autophagy was early activated in the retina following I/R induced by elevated IOP in the Sprague-Dawley rat. We further demonstrated that autophagy induction after I/R with rapamycin administration did not protect retinal cells against apoptosis. On the contrary, it induced an increase in the number of apoptotic cells of the GCL.

**Acknowledgement** The authors wish to thank Nicole Gilodi for expert technical help and Sue Houghton for reading the manuscript. This work was supported by a grant from the ProVisu Foundation.

## References

1. Klionsky DJ, Emr SD (2000) Autophagy as a regulated pathway of cellular degradation. Science 290(5497):1717–1721
2. Levine B, Klionsky DJ (2004) Development by self-digestion: molecular mechanisms and biological functions of autophagy. Dev Cell 6(4):463–477
3. Buchi ER (1992) Cell death in the rat retina after a pressure-induced ischaemia-reperfusion insult: an electron microscopic study. I. Ganglion cell layer and inner nuclear layer. Exp Eye Res 55(4):605–613
4. Kaneda K, Kashii S, Kurosawa T, Kaneko S, Akaike A, Honda Y et al (1999) Apoptotic DNA fragmentation and upregulation of Bax induced by transient ischemia of the rat retina. Brain Res 815(1):11–20

5. Zhang Y, Cho CH, Atchaneeyasakul LO, McFarland T, Appukuttan B, Stout JT (2005) Activation of the mitochondrial apoptotic pathway in a rat model of central retinal artery occlusion. Invest Ophthalmol Vis Sci 46(6):2133–2139
6. Produit-Zengaffinen N, Pournaras CJ, Schorderet DF (2009) Retinal ischemia-induced apoptosis is associated with alteration in Bax and Bcl-x(L) expression rather than modifications in Bak and Bcl-2. Mol Vis 15:2101–2110
7. Dirnagl U, Iadecola C, Moskowitz MA (1999) Pathobiology of ischaemic stroke: an integrated view. Trends Neurosci 22(9):391–397
8. Kuma A, Hatano M, Matsui M, Yamamoto A, Nakaya H, Yoshimori T et al (2004) The role of autophagy during the early neonatal starvation period. Nature 432(7020):1032–1036
9. Shintani T, Klionsky DJ (2004) Autophagy in health and disease: a double-edged sword. Science 306(5698):990–995
10. Cuervo AM, Dice JF (2000) Regulation of lamp2a levels in the lysosomal membrane. Traffic 1(7):570–583
11. Bandyopadhyay U, Kaushik S, Varticovski L, Cuervo AM (2008) The chaperone-mediated autophagy receptor organizes in dynamic protein complexes at the lysosomal membrane. Mol Cell Biol 28(18):5747–5763
12. Hamacher-Brady A, Brady NR, Gottlieb RA (2006) Enhancing macroautophagy protects against ischemia/reperfusion injury in cardiac myocytes. J Biol Chem 281(40):29776–29787
13. Qin AP, Zhang HL, Qin ZH (2008) Mechanisms of lysosomal proteases participating in cerebral ischemia-induced neuronal death. Neurosci Bull 24(2):117–123
14. Ikeda J, Nakajima T, Osborne OC, Mies G, Nowak TS Jr (1994) Coexpression of c-fos and hsp70 mRNAs in gerbil brain after ischemia: induction threshold, distribution and time course evaluated by in situ hybridization. Brain Res Mol Brain Res 26(1–2):249–258
15. Banasiak KJ, Haddad GG (1998) Hypoxia-induced apoptosis: effect of hypoxic severity and role of p53 in neuronal cell death. Brain Res 797(2):295–304
16. Esposito C, Grosjean F, Torreggiani M, Esposito V, Mangione F, Villa L et al (2011) Sirolimus prevents short-term renal changes induced by ischemia-reperfusion injury in rats. Am J Nephrol 33(3):239–249
17. Yang SS, Liu YB, Yu JB, Fan Y, Tang SY, Duan WT et al (2010) Rapamycin protects heart from ischemia/reperfusion injury independent of autophagy by activating PI3 kinase-Akt pathway and mitochondria K(ATP) channel. Pharmazie 65(10):760–765
18. Liu YB, Yu B, Li SF, Fan Y, Han W, Yu JB et al (2011) Mechanisms mediating the cardioprotective effects of rapamycin in ischaemia-reperfusion injury. Clin Exp Pharmacol Physiol 38(1):77–83
19. Piras A, Gianetto D, Conte D, Bosone A, Vercelli A (2011) Activation of autophagy in a rat model of retinal ischemia following high intraocular pressure. PLoS One 6(7):e22514
20. Russo R, Berliocchi L, Adornetto A, Varano GP, Cavaliere F, Nucci C et al (2011) Calpain-mediated cleavage of Beclin-1 and autophagy deregulation following retinal ischemic injury in vivo. Cell Death Dis 2:e144

# Part X
# Therapy: Gene Therapy

# Chapter 86
# Advances in AAV Vector Development for Gene Therapy in the Retina

**Timothy P. Day, Leah C. Byrne, David V. Schaffer and John G. Flannery**

**Abstract** Adeno-associated virus (AAV) is a small, non-pathogenic dependovirus that has shown great potential for safe and long-term expression of a genetic payload in the retina. AAV has been used to treat a growing number of animal models of inherited retinal degeneration, though drawbacks—including a limited carrying capacity, slow onset of expression, and a limited ability to transduce some retinal cell types from the vitreous—restrict the utility of AAV for treating some forms of inherited eye disease. Next generation AAV vectors are being created to address these needs, through rational design efforts such as the creation of self-complementary AAV vectors for faster onset of expression and specific mutations of surface-exposed residues to increase transduction of viral particles. Furthermore, directed evolution has been used to create, through an iterative process of selection, novel variants of AAV with newly acquired, advantageous characteristics. These novel AAV variants have been shown to improve the therapeutic potential of AAV vectors, and further improvements may be achieved through rational design, directed evolution, or a combination of these approaches, leading to broader applicability of AAV and improved treatments for inherited retinal degeneration.

**Keywords** Adeno-associated virus · Gene therapy · Mutagenesis · Directed evolution · Retinal degeneration

---

Authors Timothy P. Day and Leah C. Byrne contributed equally.

---

J. G. Flannery (✉) · T. P. Day · L. C. Byrne · D. V. Schaffer
Helen Wills Neuroscience Institute, The University of California Berkeley,
112 Barker Hall, Berkeley, CA 94720, USA
e-mail: flannery@berkeley.edu

T. P. Day
e-mail: timday@berkeley.edu

L. C. Byrne
e-mail: lbyrne@berkeley.edu

D. V. Schaffer
Department of Chemical and Biomolecular Engineering,
The University of California, Berkeley, CA 94720-1462 USA

J. D. Ash et al. (eds.), *Retinal Degenerative Diseases,* Advances in Experimental Medicine and Biology 801, DOI 10.1007/978-1-4614-3209-8_86,

**Abbreviations**

| | |
|---|---|
| AAV | Adeno-associated virus |
| ITR | Inverted terminal repeats |
| RPE | Retinal pigment epithelium |
| LCA2 | Leber's congenital amaurosis type 2 |
| scAAV | Self-complementary adeno-associated virus |

## 86.1 Introduction

Adeno-associated virus (AAV) is a dependovirus that has not been associated with human disease, and in the absence of co-infection with a helper virus such as adenovirus or herpes simplex virus, AAV is unable to replicate. AAV virions, which are non-enveloped and measure 25 nm in diameter, have a genome of 4.9 kB [7]. The AAV genome, which is single-stranded DNA, consists of three open reading frames (ORFs) flanked by two inverted terminal repeats (ITRs), which are 145 bp palendromic sequences that form elaborate hairpin structures and are essential for viral packaging. The first ORF is *rep,* which encodes 4 proteins involved in viral replication (Rep40, Rep52, Rep68, and Rep72). The second ORF contains *cap*, which encodes the three structural proteins that make up the icosahedral AAV capsid (VP1, VP2, and VP3). A third ORF, which exists as a nested alternative reading frame in the *cap* gene, encodes the assembly-activating protein, which localizes AAV capsid proteins to the nucleolus and participates in the process of capsid assembly (Sonntag, Schmidt, & Kleinschmidt, 2010). AAV has proven to be a safe and efficient vehicle for delivering therapeutic DNA to numerous tissue targets, in particular retinal neurons, and numerous studies have shown the potential of AAV-mediated delivery of genetic material for the treatment of inherited forms of retinal degeneration [4, 6].

## 86.2 Naturally Occurring AAV Viruses

AAV was initially discovered in 1965 as a contaminant of an adenovirus preparation, but it was not until the 1980s that AAV was first examined as a potential vector for gene therapy [8, 28]. Gene delivery vehicles or vectors based on AAV offer many advantages over other viruses as a vector for the retina. AAV vectors have the ability to infect quiescent cells and give rise to long-term expression of transgenes, and various serotypes exhibit tropisms for different subsets of retinal cells. The delivery efficacy or tropism for different retinal cells implicated in retinal degenerations—including photoreceptors, the retinal pigment epithelium (RPE), Müller glia, and ganglion cells—depends on a combination of the capsid and the route of administration, which can be either subretinal to expose virus to photoreceptors and

RPE or intravitreal to expose virus primarily to retinal ganglion and Müller cells. Over 100 different AAV capsid sequences have been isolated from both humans and primates, and canonically there are nine AAV serotypes. The first AAV serotypes, except for AAV5 which was directly obtained from a human clinical sample, were isolated as contaminants of adenovirus samples [9]. A search for new AAV serotypes with novel traits soon ensued, leading to an expansion of known variants [29]. AAV 2, 5, and 7–9 are capable of infecting photoreceptors, the most prominent cell type for retinal degenerations. Virtually every serotype is capable of infecting the RPE, and this permissiveness could be due to either the presence of AAV receptors on the cell surface or to the inherent phagocytic property of the RPE [28]. AAV2, the best characterized AAV serotype, was used in seminal clinical trials for Leber's congenital amaurosis type 2 (LCA2), an autosomal recessive retinal dystrophy caused by a mutation in *RPE65*, by three independent groups in 2008 [2, 10, 18]. In the LCA2 trials, subretinal administration of the vector was well tolerated and led to marked improvement in vision, especially in younger patients [26]. There are two additional clinical trials underway using a subretinally adminstered AAV2. The first supplies a modified soluble Flt1 receptor for the treatment of age-related macular degeneration, and the second trial seeks to treat choroideremia using an anti-VEGF molecule [16, 17].

## 86.3 Next Generation AAV Vectors

Although the safety, efficiency, and long-term expression achieved by naturally occurring AAVs make these vectors excellent tools for gene delivery, they suffer from several drawbacks that limit their utility for gene therapy in the retina. The onset of gene expression is limited by both the rate of internalization and breakdown of virions, and the time required for synthesis of the complementary strand from the single-stranded DNA genome. Transgene expression can thereby be delayed by weeks after injection of the vector. This delay in onset of expression has been reduced by self-complementary vectors (scAAV) [20], whose genomes contain both a sense copy of the transgene and a reverse complement, separated by a linker. These two copies are able to anneal and serve as a double stranded template that can be transcribed without the need for generation of any complementary strand by the host cell. scAAV2 [14], scAAV5 [24] and scAAV8 [21] have been shown to have faster onset of expression in retinal cells, with a similar pattern of expression as the single-stranded vectors. A number of rodent studies have used scAAVs to deliver a therapeutic transgene, leading to rescue in models of early onset retinal degeneration [15, 22]. However, the carrying capacity of scAAVs are further limited, roughly by one half, as two copies of the transgene must be included [30].

Another limitation to onset and extent of gene expression is AAV vector degradation, which can occur through phosphorylation of surface-exposed tyrosine residues that targets particles for ubiquitination and proteosome-mediated degradation. It has been demonstrated that mutation of these tyrosine residues to phenylalanine

(another aromatic residue that differs from tyrosine only by the lack of a para-hydroxyl group that serves as the substrate for tyrosine phosphorylation) enables vectors to partially circumvent this pathway and thereby allows highly efficient AAV transduction [31].

Several AAV serotypes have been shown to be amenable to tyrosine-to-phenylalanine mutations, leading to increased transduction after subretinal, intravitreal, and intravenous administration compared to their naturally occurring counterparts [25]. Furthermore, mutation of serine residues to valine on AAV2 has also recently been shown to increase transduction efficiency in vitro and in vivo, further supporting the benefits of a rational approach to engineering of the AAV capsid [1].

## 86.4 Directed Evolution

Both natural and rationally designed variants of AAV have been successful as gene delivery tools in the retina; however, currently existing AAVs still lack important characteristics that would greatly facility successful translation into the clinic, such as the ability to evade the immune system, the capacity to efficiently cross the physical barrier of the inner limiting membrane, and specific cell tropism. This is a result of the fact that viruses did not evolve as vectors for human gene therapy, and the mechanistic basis for these problems is often so mechanistically complex that rational design is not possible. This has led to the development of directed evolution, a high throughput molecular engineering approach, for the generation of novel AAV variants with enhanced properties for gene therapy (Fig. 86.1) [3]. For directed evolution of AAV, large ($\sim 10^7$) viral genetic capsid libraries based on wildtype AAVs are generated using one of several methods, including error prone PCR, random peptide insertion, and capsid DNA shuffling [12, 13, 23]. It is important to note that each novel capsid particle in the resulting virion library encapsidates the genome encoding that capsid, which can therefore be harnessed as "barcodes" for later identification. The viral libraries are packaged and exposed to a selective pressure such as binding to a surface receptor of a particular cell type, high affinity antibodies against AAV, or crossing a particular biological barrier. The capsid gene sequences of variants that are able to overcome the chosen selective pressure are then recovered, packaged, and subjected to additional rounds of selection. After a number of iterative rounds, a diversification step involving the introduction of new mutations to the selected capsid pool, followed by additional rounds of selection, may be conducted to further evolve the capsid toward a selected trait. The final surviving variants are individually screened and the most successful variant is determined. This method has led to novel AAV variants with enhanced properties, including viruses capable of better infecting embryonic stem cells, crossing the inner limiting membrane to infect Müller glia from the vitreous, and increased resistance to high affinity antibodies [11, 19]. Furthermore, we have recently demonstrated that AAV variants can be evolved for the ability to infect photoreceptors and RPE from the vitreous, a property with potentially strong clinical implications [5].

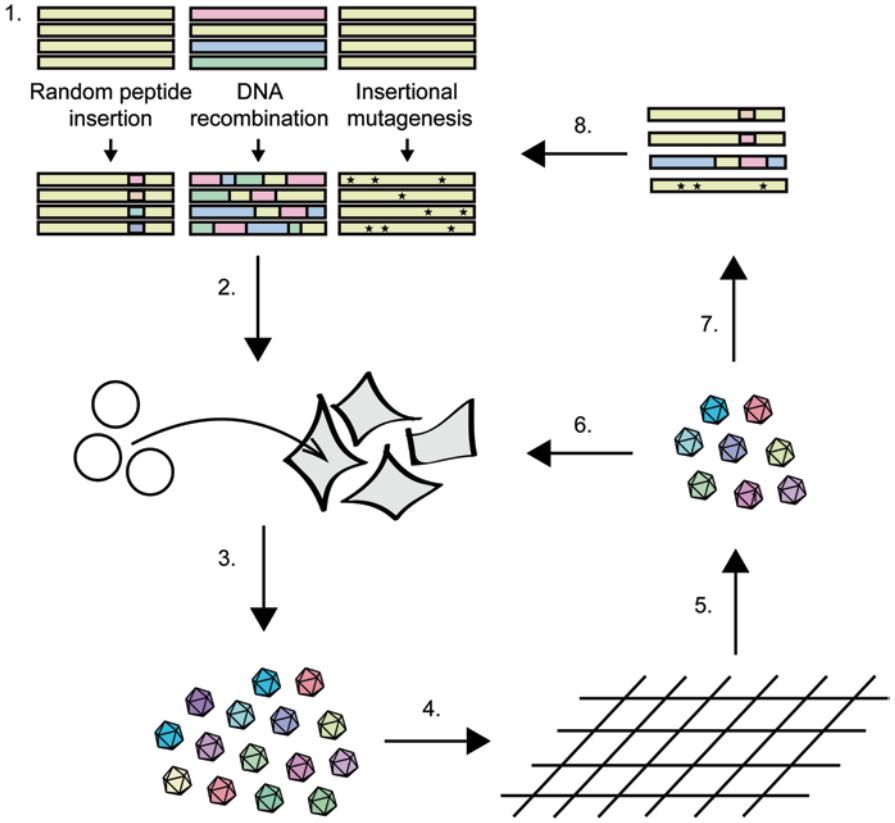


**Fig. 86.1** Steps in the directed evolution of AAV. *1* Viral libraries are created through mutation of the *cap* gene. *2* Viruses are packaged, here shown as triple transfection of HEK293 cells, so that each virion contains the *cap* gene encoding that virion's capsid proteins. *3* AAV is harvested and purified. *4* A selective pressure is applied. *5* Successful viruses are isolated. *6 Cap* genes from harvested viruses are amplified through PCR and virus is repackaged. Repeated selection steps are performed to enrich for the most successful clones. *7* Sequencing is used to analyze the sequence of *cap* genes from successful viruses. *8 Cap* genes are mutated again to introduce additional diversity. [3]

## 86.5 Conclusions

To date, significant progress has been made in the development of next generation AAV vectors. The use of tools such as directed evolution will enable the creation of AAV vectors that are able to overcome remaining formidable challenges for clinical translation. It is important to note that the benefits and efficacy of next-generation vectors must be tested in large animal models, as the size and anatomy of human eyes and the rate of cell death in human disease are significantly different from the rodent models most often used for AAV gene therapy studies. However, AAV has been shown to be flexible and amenable to structural changes that correspond to

improvements in function, indicating that the vector may be tailored to the specific demands of a variety of eyes from different species and forms of retinal degeneration. Both rational design and library selection strategies have been shown to be useful strategies for achieving improved function of AAV, and a combination of these approaches may be used to synergistically improve the function of AAV in the retina.

## References


1. Aslanidi GV, Rivers AE, Ortiz L, Govindasamy L, Ling C, Jayandharan GR et al (2012) High-efficiency transduction of human monocyte-derived dendritic cells by capsid-modified recombinant AAV2 vectors. Vaccine 30(26):3908–3917. doi:10.1016/j.vaccine.2012.03.079
2. Bainbridge JWB, Smith AJ, Barker SS, Robbie S, Henderson R, Balaggan K et al (2008) Effect of gene therapy on visual function in Leber's congenital amaurosis. N Engl J Med 358(21):2231–2239. doi:10.1056/NEJMoa0802268
3. Bartel MA, Weinstein JR, Schaffer DV (2012) Directed evolution of novel adeno-associated viruses for therapeutic gene delivery. Gene Ther 19(6):694–700. doi:10.1038/gt.2012.20
4. Cepko CL (2012) Emerging gene therapies for retinal degenerations. J Neurosci 32(19):6415–6420. doi:10.1523/JNEUROSCI.0295-12.2012
5. Dalkara D, Byrne LC, Klimczak RR, Visel M, Yu L, Merigan WH, Flannery JG, Schaffer DV (2013) In vivo directed evolution of a novel adeno-associated virus for therapeutic outer retinal gene delivery from the vitreous. Sci Transl Med 5(189): 189ra76 (Manuscript submitted to Science translational medicine)
6. den Hollander AI, Black A, Bennett J, Cremers FP(2010). Lighting a candle in the dark: advances in genetics and gene therapy of recessive retinal dystrophies. J Clin Invest 120(9):3042–3053. doi:10.1172/JCI42258
7. Fields BN, Knipe DM, Howley PM (2007) Fields virology, 5th edn. Lippincott Williams & Wilkins, Philadelphia
8. Goncalves MA (2005) Adeno-associated virus: from defective virus to effective vector. Virol J 2:43
9. Grimm D, Kay MA (2003) From virus evolution to vector revolution: use of naturally occurring serotypes of adeno-associated virus (AAV) as novel vectors for human gene therapy. Curr Gene Ther 3(4):281–304. http://eutils.ncbi.nlm.nih.gov/entrez/eutils/elink.fcgi?dbfrom=pubmed&id=12871018&retmode=ref&cmd=prlinks
10. Hauswirth WW, Aleman TS, Kaushal S, Cideciyan AV, Schwartz SB, Wang L et al (2008) Treatment of Leber congenital amaurosis due to RPE65 mutations by ocular subretinal injection of adeno-associated virus gene vector: short-term results of a phase I trial. Hum Gene Ther 19(10):979–990. doi:10.1089/hum.2008.107
11. Klimczak RR, Koerber JT, Dalkara D, Flannery JG, Schaffer DV (2009) A novel adeno-associated viral variant for efficient and selective intravitreal transduction of rat Müller cells. PLoS ONE 4(10):e7467. doi:10.1371/journal.pone.0007467
12. Koerber JT, Schaffer DV (2008) Transposon-based mutagenesis generates diverse adeno-associated viral libraries with novel gene delivery properties. Methods Mol Biol. Totowa, NJ: Humana Press, pp 161–170. doi:10.1007/978-1-60327-248-3_10
13. Koerber JT, Jang J-H, Schaffer DV (2008) DNA shuffling of adeno-associated virus yields functionally diverse viral progeny. Mol Ther 16(10):1703–1709. doi:10.1038/mt.2008.167
14. Koilkonda RD, Chou T-H, Porciatti V, Hauswirth WW, Guy J (2010) Induction of rapid and highly efficient expression of the human ND4 complex I subunit in the mouse visual system by self-complementary adeno-associated virus. Arch Ophthalmol 128(7):876–883. doi:10.1001/archophthalmol.2010.135

15. Ku CA, Chiodo VA, Boye SL, Goldberg AFX, Li TT, Hauswirth WW, Ramamurthy V (2011) Gene therapy using self-complementary Y733F capsid mutant AAV2/8 restores vision in a model of early onset Leber congenital amaurosis. Hum Mol Genet 20(23):4569–4581. doi:10.1093/hmg/ddr391
16. Lukason M, DuFresne E, Rubin H, Pechan P, Li Q, Kim I et al (2011) Inhibition of choroidal neovascularization in a nonhuman primate model by intravitreal administration of an AAV2 vector expressing a novel anti-VEGF molecule. Mol Ther 19(2):260–265. doi:10.1038/mt.2010.230
17. MacLachlan TK, Lukason M, Collins M, Munger R, Isenberger E, Rogers C et al (2011) Preclinical Safety Evaluation of AAV2-sFLT01—A gene therapy for age-related macular degeneration. Mol Ther 19(2):326–334. doi:10.1038/mt.2010.258
18. Maguire AM, Simonelli F, Pierce EA, Pugh EN Jr, Mingozzi F, Bennicelli J et al (2008) Safety and efficacy of gene transfer for Leber's congenital amaurosis. N Engl J Med 358(21):2240–2248. doi:10.1056/NEJMoa0802315
19. Maheshri N, Koerber JT, Kaspar BK, Schaffer DV (2006) Directed evolution of adeno-associated virus yields enhanced gene delivery vectors. Nat Biotechnol 24(2):198–204. doi:10.1038/nbt1182
20. McCarty DM, Monahan PE, Samulski RJ (2001) Self-complementary recombinant adeno-associated virus (scAAV) vectors promote efficient transduction independently of DNA synthesis. Gene Ther 8(16):1248–1254. doi:10.1038/sj.gt.3301514
21. Natkunarajah M, Trittibach P, McIntosh J, DURAN Y, Barker SE, Smith AJ et al (2007) Assessment of ocular transduction using single-stranded and self-complementary recombinant adeno-associated virus serotype 2/8. Gene Ther 15(6):463–467. doi:10.1038/sj.gt.3303074
22. Pang J, Boye SE, Lei B, Boye SL, Everhart D, Ryals R et al (2010). Self-complementary AAV-mediated gene therapy restores cone function and prevents cone degeneration in two models of Rpe65 deficiency. Gene Ther 17(7):815–826. doi:10.1038/gt.2010.29
23. Perabo L, Endell J, King S, Lux K, Goldnau D, Hallek M, Büning H (2006) Combinatorial engineering of a gene therapy vector: directed evolution of adeno-associated virus. J Gene Med 8(2):155–162. doi:10.1002/jgm.849
24. Petersen-Jones SM, Bartoe JT, Fischer AJ, Scott M, Boye SL, CHIODO V, Hauswirth WW (2009) AAV retinal transduction in a large animal model species: comparison of a self-complementary AAV2/5 with a single-stranded AAV2/5 vector. Mol Vision 15:1835–1842
25. Petrs-Silva H, Dinculescu A, Li Q, Min S-H, Chiodo V, Pang JJ et al (2008) High-efficiency transduction of the mouse retina by tyrosine-mutant AAV serotype vectors. Mol Ther 17(3):463–471. doi:10.1038/mt.2008.269
26. Simonelli FF, Maguire AM, Testa F, Pierce EA, Mingozzi F, Bennicelli JL et al (2010) Gene therapy for Leber's congenital amaurosis is safe and effective through 1.5 years after vector administration. Mol Ther 18(3):643–650. doi:10.1038/mt.2009.277
27. Sonntag F, Schmidt K, Kleinschmidt JA. (2010) A viral assembly factor promotes AAV2 capsid formation in the nucleolus. Proc Natl Acad of Sci U S A 107(22):10220–10225. doi:10.1073/pnas.1001673107
28. Vandenberghe LH, Auricchio A (2011) Novel adeno-associated viral vectors for retinal gene therapy. Gene Ther 19(2):162–168. doi:10.1038/gt.2011.151
29. Vandenberghe LH, Wilson JM, Gao G (2009) Tailoring the AAV vector capsid for gene therapy. Gene Ther 16(3):311–319. doi:10.1038/gt.2008.170
30. Wu J, Zhao W, Zhong L, Han Z, Li B, Ma W et al (2007) Self-complementary recombinant adeno-associated viral vectors: packaging capacity and the role of rep proteins in vector purity. Hum Gene Ther 18(2):171–182. doi:10.1089/hum.2006.088
31. Zhong LL, Li BB, Mah CSC, Govindasamy LL, Agbandje-McKenna MM, Cooper MM et al (2008) Next generation of adeno-associated virus 2 vectors: point mutations in tyrosines lead to high-efficiency transduction at lower doses. Proc Natl Acad Sci U S A 105(22):7827–7832. doi:10.1073/pnas.0802866105

# Chapter 87
# Cone Specific Promoter for Use in Gene Therapy of Retinal Degenerative Diseases

**Frank M. Dyka, Sanford L. Boye, Renee C. Ryals, Vince A. Chiodo, Shannon E. Boye and William W. Hauswirth**

**Abstract** Achromatopsia (ACHM) is caused by a progressive loss of cone photoreceptors leading to color blindness and poor visual acuity. Animal studies and human clinical trials have shown that gene replacement therapy with adeno-associate virus (AAV) is a viable treatment option for this disease. Although there have been successful attempts to optimize capsid proteins for increased specificity, it is simpler to restrict expression via the use of cell type-specific promoters. To target cone photoreceptors, a chimeric promoter consisting of an enhancer element of interphotoreceptor retinoid-binding protein promoter and a minimal sequence of the human transducin alpha-subunit promoter (IRBPe/GNAT2) was created. Additionally, a synthetic transducin alpha-subunit promoter (synGNAT2/GNAT2) containing conserved sequence blocks located downstream of the transcriptional start was created. The strength and specificity of these promoters were evaluated in murine retina by immunohistochemistry. The results showed that the chimeric, (IRBPe/GNAT2) promoter is more efficient and specific than the synthetic, synGNAT2/GNAT2 promoter. Additionally, IRBPe/GNAT2-mediated expression was found in all cone subtypes and it was improved over existing promoters currently used for gene therapy of achromatopsia.

F. M. Dyka (✉) · S. L. Boye · R. C. Ryals · V. A. Chiodo · S. E. Boye · W. W. Hauswirth
Department of Ophthalmology, College of Medicine, University of Florida,
1600 SW Archer Rd., Gainesville, FL 32610, USA
e-mail: fmdyka@ufl.edu

S. L. Boye
e-mail: sboye@ufl.edu

R. C. Ryals
e-mail: renee14@ufl.edu

V. A. Chiodo
e-mail: vchiodo@ufl.edu

S. E. Boye
e-mail: shaire@ufl.edu

W. W. Hauswirth
e-mail: hauswrth@ufl.edu

J. D. Ash et al. (eds.), *Retinal Degenerative Diseases,* Advances in Experimental Medicine and Biology 801, DOI 10.1007/978-1-4614-3209-8_87,

**Keywords** Cone photoreceptors · Chimeric promoter · Adeno-associated virus · Targeted expression · Gene replacement therapy · Achromatopsia

## 87.1 Introduction

Achromatopsia (ACHM) is an autosomal recessive disease affecting about 1:30,000 humans. It is characterized by poor visual acuity, loss of central vision, photophobia, color blindness, and reduced photopic electroretinographic amplitudes due to loss of cone photoreceptors. In humans there are three distinct subclasses of cone photoreceptors, each named for the specific wavelength of light to which they respond. L-cones respond to long wavelength light, whereas M-cones and S-cones respond to medium and short wavelength light, respectively. Spectral sensitivity is mediated by the specific form of cone opsin that each cone subclass expresses. Gene therapy-based treatments for a number of diseases affecting cone photoreceptors are currently under development [1–6].

Although ACHM is a relatively rare disorder, it presents itself as a good target for gene therapy as the causative genes are known. Additionally, proof-of-concept gene replacement studies in animal models have shown clear success [1, 3–5, 7, 8]. ACHM affects all classes of photoreceptors, including S cones. Recent evidence from case studies of patients with ACHM suggests that ACHM is progressive, with cones degenerating over time [9]. Therefore, early intervention with a therapy that targets all subclasses of cone photoreceptors would be ideal.

In recent years, adeno-associated virus (AAV) has emerged as the most efficient viral vector for gene therapy due to its ability to transduce dividing and non-dividing cells with minimal immune response[10]. Although there have been successful attempts to optimize AAV capsid proteins for increased cell specificity, a simpler way to restrict expression is through the use of cell type-specific promoters. To deliver genes safely and efficiently to cone photoreceptors of ACHM-affected individuals, therapeutic vectors should ideally utilize promoters which; (1) are capable of expressing transgene both efficiently and selectively in cones with little or no off-target expression in other retinal cell types, such as rod or retinal pigment epithelial (RPE) cells, (2) are small enough in size to accommodate the transgene within the ~4.8 kb (kilobases) packaging limit of AAV (3) are able to drive gene expression in all subclasses of cone photoreceptors.

To date, cone targeting promoters used in proof-of-concept gene therapy studies for ACHM have been deficient in one or more of these criteria. In studies by Alexander et al. [7] and Komaromy et al. [8]. A 2100 bp (base pair) version of the human red/green opsin promoter (PR2.1) was used to drive therapeutic transgene expression. In mouse, expression was limited primarily to cones with sparse expression in rods [7]. In canine, expression was highly selective for M and L cones whereas expression in S cones was not detected [8]. Furthermore the PR2.1 promoter is relatively large in size. In the case of *CNGB3* gene replacement, the AAV capsid is barely able to accommodate the PR2.1 promoter and *CNGB3* cDNA (~2.4 kb).

Such vectors may experience reduced packaging efficiency because of the oversized nature of the genome.

In addition to the PR2.1 promoter, respective, homologous regulatory regions of human and mouse S cone opsin have been tested as promoters in animal models of ACHM. In rodent, a 569 bp human S opsin promoter (HB569) led to reporter gene expression in all cone subclasses but the expression was weaker in comparison to the PR2.1 promoter [11]. In dog, the HB569 promoter performed poorly in terms of both specificity and efficiency, with relatively few L/M cones expressing the transgene and with leaky expression in rods and RPE [12].

A 500 bp version of the mouse S opsin (mBP) promoter has been tested in the context of gene replacement for *CNGA3* and performed well [3]. However it is likely that it, like the closely related human S opsin promoter, will perform poorly in higher order mammals, such as dog and human.

Finally, like the S opsin promoters described above, regulatory regions of cone arrestin identified by Craft et al. has been utilized as a promoter in AAV transduction experiments and later in gene replacement studies in ACHM animal models [1, 13]. In experiments performed in mice aimed at characterizing gene expression, respective 500 bp mouse and human cone arrestin promoters (mCAR and hCAR) drove strong expression in retina (see Results section). However specificity was poor, with rods and RPE clearly being transduced. In experiments utilizing mCAR that were performed in dog, the same general expression pattern was seen, with strong expression observed in all classes of cones and off-target expression in rods and RPE (Komáromy and Boye, unpublished).

In this work, we present data on novel cone-targeted promoters showing improved efficiency and specificity compared to existing promoters.

## 87.2 Materials and Methods

### *87.2.1 Promoter Construction*

A chimeric promoter (IRBPe/GNAT2) was constructed by fusing an enhancer element (IRBPe) from position −1619 to −1411 of the interphotoreceptor retinoid-binding protein (IRBP) to a core promoter of human transducin alpha-subunit (*GNAT2*) ranging from position −151 to +126. Additionally a synthetic promoter (synGNAT2/GNAT2) was created by aligning the *GNAT2* regulatory regions of multiple taxa (human, canine, mouse, and rat) using ClustalW and selecting conserved areas to add to the core promoter region. Both promoters were cloned in a vector plasmid to drive the expression of green fluorescent protein (GFP). Additionally a 0.5 kb version of the human and mouse cone arrestin promoter was created [1, 13]. The arrangement of the promoter constructs used in this study are depicted in Fig. 87.1.

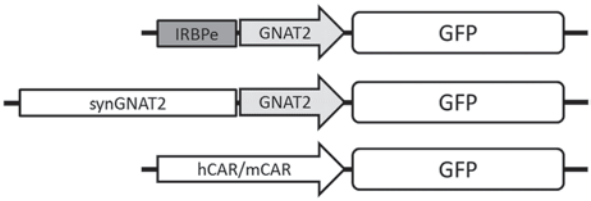


**Fig. 87.1** Schematic representation of the *IRBPe*/*GNAT2* chimeric promoter containing the *IRBPe* enhancer element and the minimal *GNAT2* promoter (*top*), the synthetic (*synGNAT2*) addition of conserved areas to the core *GNAT2* promoter (*middle*) and the cone arrestin promoter regions of human (*hCAR*) and mouse (*mCAR*) species (*bottom*)

### *87.2.2 Virus Packaging and Injection*

AAV vectors were packaged, purified, and titered according to previously published methods [14, 15]. C57BL/6 mice were injected subretinally with 1 µl of at least $5 \times 10^{12}$ virus genomes/ml of AAV5 vectors. Mice were injected at 4 to 5 weeks of age and promoter expression and tropism were analyzed by confocal microscopy 4 weeks post-injection.

All experiments were approved by the University of Florida's IACUC and conducted in accordance with the ARVO Statement for the Use of Animals in Ophthalmic and Vision Research and NIH regulations.

### *87.2.3 Histology*

Injected mice and uninjected controls were sacrificed 4 weeks post-injection and the eyes were surgically removed and fixed in 4% paraformaldehyde. Eyes were then treated with sucrose buffer of increasing concentrations of sucrose (from 5 to 20%) in phosphate buffered saline (PBS). After removing cornea and lens, the remaining eye cups were embedded in OCT (Sakura Finetek, Torrance, CA) and frozen tissue was then sectioned for analysis with a spinning disk confocal microscope (Olympus).

## 87.3 Results

To determine the efficiency and specificity of the promoters, C57BL/6 wild-type mice were injected with AAV5 containing the respective promoters driving GFP expression. Figure 87.2a, b show strong expression of GFP in the outermost nuclear region of the outer nuclear layer of the mouse retina which is known to contain the cell bodies of cone photoreceptor cells. The synthetic human transducin

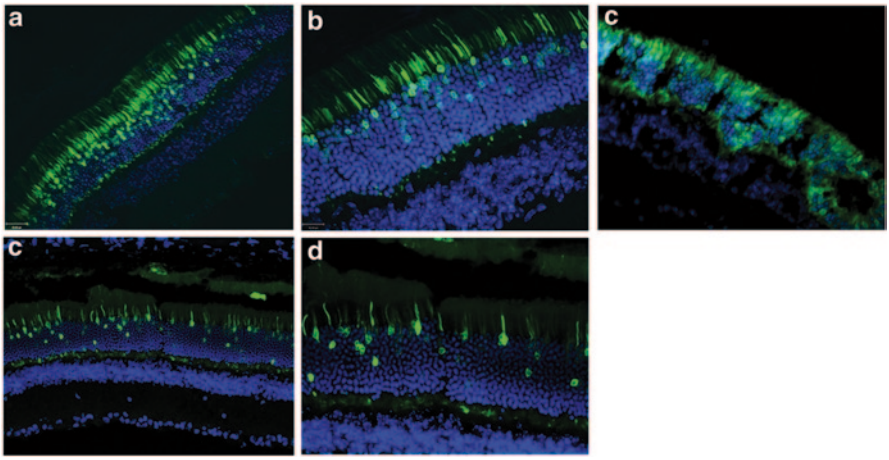


**Fig. 87.2** **a**–**d** show sections of C57BL/6 mouse retina treated subretinally with AAV5-IRBPe/GNAT2-GFPat 20 X (**a**) and 40 X (**b**) magnification and treated with AAV5-synGNAT2/GNAT2-GFP at 20 X (**c**) and 40 X (**d**) magnification. (**e**) Sections of Nrl-/- mouse treated subretinally with AAV5-IRBPe/GNAT2-GFP

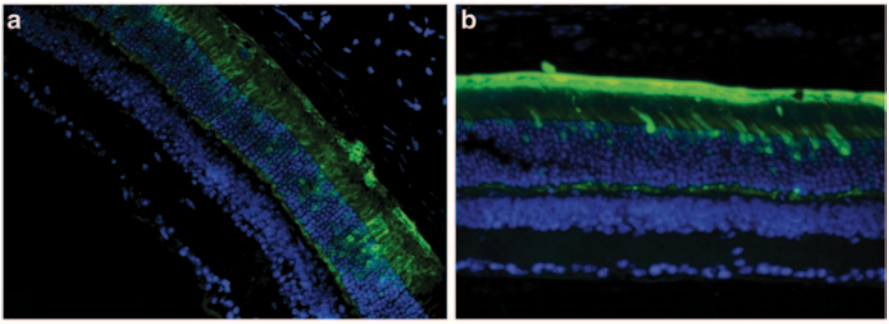


**Fig. 87.3** Sections of mouse retina were treated with AAV5-mCAR-GFP (**a**) and hCAR-GFP (**b**) at 20 X magnification

alpha-subunit (synGNAT2/GNAT2) promoter, however, shows transduction in a relatively fewer number of cells suggesting that parts of the synGNAT2 sequence act as a negative regulator in some cells (Fig. 87.2c, d). Expression in RPE or the inner retinal cell layers was not observed with either promoter. To evaluate whether IRBPe/GNAT2 would promote expression in S-cones, Nrl-/- mice were injected with AAV-IRBPe/GNAT-GFP vector. The retinas of Nrl-/- mice are composed exclusively of S cone-like photoreceptors [16, 17]. The strong, photoreceptor exclusive expression observed in Nrl -/- mice clearly support that IRBPe/GNAT2 is capable of transducing mouse S-cones (Fig. 87.2e). In contrast to the GNAT2 promoters, the mouse and human cone arrestin promoters (Fig. 87.3) resulted in strong off-target expression in the retinal pigment epithelium.

## 87.4 Discussion

In this study, an enhancer element of the interphotoreceptor retinoid-binding protein was combined with a minimal human transducin alpha-subunit promoter (IRBPe/GNAT2) and used to achieve selective expression in cone photoreceptors. Ying et al. [18] created a transgenic mouse line in which the same elements in a different configuration were used to drive chloramphenicol acetyltransferase to ablate cone photoreceptors [19]. The resulting transgenic mouse lacked cone photoreceptors. However, in ventral retina, rod photoreceptors were also absent [20]. The region-specific absence of rod photoreceptors was reported as a consequence of developmental defect due to lack of cones. However, given that only ~2.5 % of photoreceptors are cones, loss of rods was more likely due to mis-expression of the diphtheria toxin in rods. In contrast, when the IRBP enhancer element is fused upstream of the minimal GNAT2 promoter to create a chimeric promoter, expression in rods is reduced. Like IRBPe/GNAT2, a synthetic transducin alpha-subunit promoter fused to the minimal promoter (synGNAT2/GNAT2) also transduced cones, but not as efficiently. Both promoters exhibit some off-target expression in a small number of rods but not in retinal pigment epithelium or inner retinal layers. The relatively small size the IRBPe/GNAT2 chimeric promoter (less than 500 bp) and its ability to promote strong, specific expression in all cone subclasses improve on existing promoters like PR2.1. Other promoters like the cone arrestin promoters are an improvement in size and strength, however they mediate strong off-target transgene expression.

Even though both versions of the GNAT2 promoter show activity in a small number of rod photoreceptors, higher selectivity of cone expression may be likely in higher mammals. In summary, both promoters are useful tools for gene replacement therapy targeting cone photoreceptor cells in human patients.

**Acknowledgment** The authors thank Seok-Hong Min, James Peterson, and Jingfen Sun for their excellent technical assistance. They also acknowledge grants from the Foundation Fighting Blindness, Research to Prevent Blindness, Inc. for partial support of this work.

## References

1. Carvalho LS, Xu J, Pearson RA, Smith AJ, Bainbridge JW, Morris LM et al (2011) Long-term and age-dependent restoration of visual function in a mouse model of CNGB3-associated achromatopsia following gene therapy. Hum Mol Genet 20(16):3161–3175
2. Cideciyan AV, Hauswirth WW, Aleman TS, Kaushal S, Schwartz SB, Boye SL et al (2009) Human RPE65 gene therapy for Leber congenital amaurosis: persistence of early visual improvements and safety at 1 year. Hum Gene Ther 20(9):999–1004
3. Michalakis S, Muhlfriedel R, Tanimoto N, Krishnamoorthy V, Koch S, Fischer MD et al (2010) Restoration of cone vision in the CNGA3-/- mouse model of congenital complete lack of cone photoreceptor function. Mol Ther 18(12):2057–2063

4. Michalakis S, Muhlfriedel R, Tanimoto N, Krishnamoorthy V, Koch S, Fischer MD et al (2012) Gene therapy restores missing cone-mediated vision in the CNGA3-/- mouse model of achromatopsia. Adv Exp Med Biol 723:183–189
5. Pang JJ, Deng WT, Dai X, Lei B, Everhart D, Umino Y et al (2012) AAV-mediated cone rescue in a naturally occurring mouse model of CNGA3-achromatopsia. PLoS.One 7(4):e35250
6. Mancuso K, Hauswirth WW, Li Q, Connor TB, Kuchenbecker JA, Mauck MC et al (2009) Gene therapy for red-green colour blindness in adult primates. Nature 461(7265):784–787
7. Alexander JJ, Umino Y, Everhart D, Chang B, Min SH, Li Q et al (2007) Restoration of cone vision in a mouse model of achromatopsia. Nat Med 13(6):685–687
8. Komaromy AM, Alexander JJ, Rowlan JS, Garcia MM, Chiodo VA, Kaya A et al (2010) Gene therapy rescues cone function in congenital achromatopsia. Hum Mol Genet 19(13):2581–2593
9. Thiadens AA, Somervuo V, van den Born LI, Roosing S, van Schooneveld MJ, Kuijpers RW et al (2010) Progressive loss of cones in achromatopsia: an imaging study using spectral-domain optical coherence tomography. Invest Ophthalmol Vis Sci 51(11):5952–5957
10. Daya S, Berns KI (2008) Gene therapy using adeno-associated virus vectors. Clin Microbiol Rev 21(4):583–593
11. Glushakova LG, Timmers AM, Pang J, Teusner JT, Hauswirth WW (2006) Human blue-opsin promoter preferentially targets reporter gene expression to rat s-cone photoreceptors. Invest Ophthalmol Vis Sci 47(8):3505–3513
12. Komaromy AM, Alexander JJ, Cooper AE, Chiodo VA, Glushakova LG, Acland GM et al (2008) Targeting gene expression to cones with human cone opsin promoters in recombinant AAV. Gene Ther 15(14):1049–1055
13. Li A, Zhu X Craft CM (2002) Retinoic acid upregulates cone arrestin expression in retinoblastoma cells through a Cis element in the distal promoter region. Invest Ophthalmol Vis Sci 43(5):1375–1383
14. Jacobson SG, Acland GM, Aguirre GD, Aleman TS, Schwartz SB, Cideciyan AV et al (2006) Safety of recombinant adeno-associated virus type 2-RPE65 vector delivered by ocular subretinal injection. Mol Ther 13(6):1074–1084
15. Zolotukhin S, Potter M, Zolotukhin I, Sakai Y, Loiler S, Fraites TJ Jr et al (2002) Production and purification of serotype 1, 2, and 5 recombinant adeno-associated viral vectors. Methods 28(2):158–167
16. Daniele LL, Lillo C, Lyubarsky AL, Nikonov SS, Philp N, Mears AJ et al (2005) Cone-like morphological, molecular, and electrophysiological features of the photoreceptors of the Nrl knockout mouse. Invest Ophthalmol Vis Sci 46(6):2156–2167
17. Nikonov SS, Daniele LL, Zhu X, Craft CM, Swaroop A, Pugh EN Jr(2005) Photoreceptors of Nrl -/- mice coexpress functional S- and M-cone opsins having distinct inactivation mechanisms. J Gen Physiol 125(3):287–304
18. Ying S, Fong SL, Fong WB, Kao CW, Converse RL, Kao WW (1998) A CAT reporter construct containing 277 bp GNAT2 promoter and 214 bp IRBP enhancer is specifically expressed by cone photoreceptor cells in transgenic mice. Curr Eye Res 17(8):777–782
19. Ying S, Jansen HT, Lehman MN, Fong SL, Kao WW (2000) Retinal degeneration in cone photoreceptor cell-ablated transgenic mice. Mol Vis 6:101–108
20. Fong SL, Criswell MH, Belecky-Adams T, Fong WB, McClintick JN, Kao WW et al (2005) Characterization of a transgenic mouse line lacking photoreceptor development within the ventral retina. Exp Eye Res 81(4):376–388

# Chapter 88
# Episomal Maintenance of S/MAR-Containing Non-Viral Vectors for RPE-Based Diseases

**Adarsha Koirala, Shannon M Conley and Muna I. Naash**

**Abstract** The efficacy of non-viral genetic therapies has historically been limited by transient gene expression and vector loss. Scaffold matrix attachment regions (S/MARs) have been shown to augment transcription, promote episomal maintenance, and provide insulator-like function to DNA in in vitro and in vivo systems. Here we explore the ability of S/MAR elements to mediate these effects in retinal pigment epithelial (RPE) cells with the eventual goal of improving the persistence of expression of our non-viral gene delivery tools. We engineered an RPE-specific reporter vector with or without an S/MAR immediately downstream of the eGFP expression cassette. We show that the S/MAR vector is maintained as an episome for up to 1 year. Experiments in which rhodamine-labeled DNA was delivered to the subretinal space of mice show better persistence of the S/MAR-containing vector in the RPE than the non-S/MAR vector. These results suggest that inclusion of the S/MAR region promotes episomal maintenance of plasmid DNA in the RPE after subretinal delivery and that inclusion of this DNA element may be beneficial for non-viral ocular gene transfer.

**Keywords** S/MAR · RPE65 · Non-viral gene therapy · Retinal pigment epithelium · DNA nanoparticles

**Abbreviations**

| | |
|---|---|
| S/MAR | Scaffold/matrix attachment region |
| RPE | Retinal pigment epithelium |
| AAV | Adeno-associated virus |
| NPs | Nanoparticles |
| PECS | Pigment epithlium, choroid and sclera |
| PI | Post-injection |

M. I. Naash (✉) · A. Koirala · S. M. Conley
Department of Cell Biology, University of Oklahoma Health Sciences Center,
940 Stanton L. Young Blvd., BMSB 781, Oklahoma City, OK 73104, USA
e-mail: muna-naash@ouhsc.edu

A. Koirala
e-mail: adarsha_koirala@meei.harvard.edu

S. M. Conley
e-mail: Shannon-conley@ouhsc.edu

J. D. Ash et al. (eds.), *Retinal Degenerative Diseases,* Advances in Experimental Medicine and Biology 801, DOI 10.1007/978-1-4614-3209-8_88,

## 88.1 Introduction

Development of genetic therapies has been a research focus for the treatment of hereditary diseases that cause retinal/RPE degeneration and blindness. Currently, adeno-associated viral (AAV) vectors are in phase I/IIa clinical trials for the treatment of Leber's Congenital Amaurosis [1–3]. Though AAV has historically been the vector of choice for ocular gene therapy, limitations of AAV include the payload size (<5 kb), immunogenicity after re-injection and high antibody titer in patients with previous AAV exposure. We have, therefore, focused on developing alternatives. DNA nanoparticles (NPs) compacted with polyethylene glycol and polylysine (payload≥20 kb [4]) and uncompacted plasmid DNA have significantly higher genetic capacity than AAV, and we have shown them to be safe when delivered to the eye [5, 6]. More importantly, we have recently shown these NPs and plasmids successfully transfect the retinal pigment epithelium (RPE) and mediate phenotypic improvement in the *rpe65*$^{-/-}$ knockout model [7, 8]. In our previous studies [7, 8] we showed that housing our expression cassette in a plasmid containing an S/MAR region facilitated expression of eGFP for the life of the mice. Here we assess the molecular features that underlie this long-term gene expression. Specifically, we assess the integration status of the DNA and its subcellular distribution at various times after subretinal delivery of NP or plasmid vectors.

## 88.2 Materials and Methods

### *88.2.1 Animal Handling and Subretinal Injection*

Adult balb/c mice were subretinally injected as described previously [7, 8]. All experimental procedures were approved by the University of Oklahoma Health Sciences Center Institutional Animal Care and Use Committee.

### *88.2.2 Rhodamine Labeling and Fluorescence Intensity Quantification*

Endotoxin free plasmids were rhodamine-labeled prior to compaction using the *Label* IT® TM-Rhodamine labeling kit (Mirus Bio, LLC) as described [8]. NPs were compacted as described previously with the acetate counterion into rod-shaped particles of ~8 nm in diameter [7]. Labeled DNA or NPs were injected subretinally into five mice for each cohort. At post-injection (PI)-2 days, retina and RPE/choroid/sclera (PECS) were collected separately and homogenized in buffer (20 mM Tris HCl, 150 mM NaCl, 1 mM EDTA, 1% TX-100). Homogenates were incubated at 37 °C for 2 h and centrifuged at 15,000 rpm for 10 min at room temperature. Un-

injected homogenates were used for background correction. Standards contained uninjected homogenates spiked with 10–640 ng of labeled DNA (in a 2x dilution series). Fluorescence intensity was measured in a Fluostar Optima plate reader (BMG Labtech) at excitation and emission wavelength of 540 and 590 nm, respectively.

### *88.2.3 Episomal DNA Extraction and Copy Number Calculation*

Episomal DNA extraction from treated eyes was performed using Hirt's protocol as described in [9]. One microgram of resulting DNA was linearized and subjected to qPCR for assessment of copy number. A standard curve was generated using known DNA concentrations as described in [10]. Primers were against the promoter region. Regular PCR was performed using primers flanking the promoter and the S/MAR sequence to determine the integrity of the expression cassette. To assess the intactness of the plasmid, DH5α cells were transformed by standard methods using 1 µg of the Hirt's extract, and colonies were counted.

## 88.3 Results and Discussion

### *88.3.1 Uptake and Localization of Naked DNA and nps Following Subretinal Delivery*

We first asked whether uptake was dependent on inclusion of an S/MAR or nanocompaction. We rhodamine-labeled two different vectors carrying the human VMD2 promoter: one without an S/MAR (VMD2-eGFP) and one with (VMD2-eGFP-S/MAR), then subretinally delivered them as NPs or naked DNA to Balb/C mice at postnatal day 30. At PI-2 days, retinal and RPE lysates were isolated and rhodamine intensity was analyzed fluorometrically (Fig. 88.1a). Although NP compaction yielded improved uptake in the retina, there were no significant differences in DNA uptake in the RPE between groups, consistent with the phagocytic nature of the RPE, and suggesting that the beneficial effects of the S/MAR are not due to enhanced cellular uptake. Interestingly, when the total amount of isolated DNA was quantified (compared to a standard curve), we found that only ~1.8 and ~2.9% of the total DNA delivered was recovered from the RPE and retina respectively (from NP-treated samples). These data suggest that the majority of the DNA that is delivered to each eye is either not taken up and remains/is degraded in the subretinal space or is taken up by the cell and degraded prior to PI-2.

To visualize subcellular localization of the labeled DNA, RPE (Fig. 88.1b–c) whole mounts were labeled with the nuclear envelope marker Lamin-B1 (*green*), and confocal images ($N=3$ eyes/group) were captured. The bottom panels of Fig. 88.1b–c are 3D reconstructions of boxed areas in top panels. At PI-2 days,

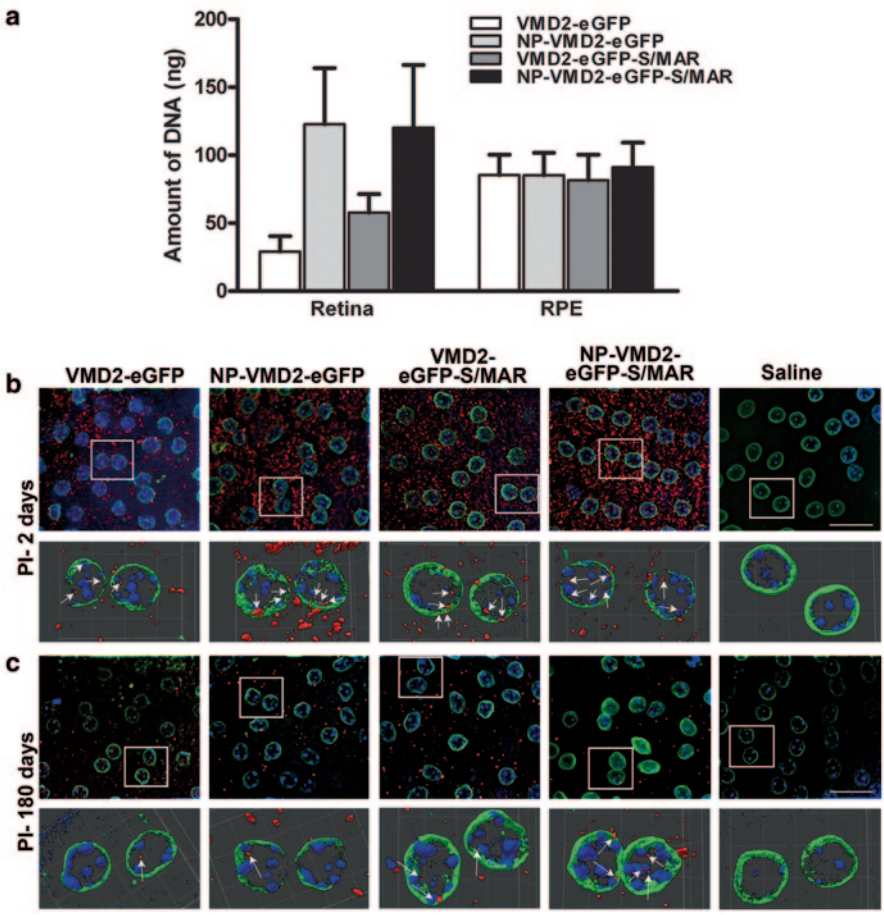


**Fig. 88.1** Inclusion of S/MAR does not affect RPE uptake of naked DNA or NPs. **a** Measurement of rhodamine fluorescence in retinal/RPE homogenates injected with labeled DNA or NPs. $N = 5$ eyes/group, shown is mean ± SEM. **b–c** Top-IHC of RPE whole mounts collected at PI-2 **b** or PI-180 **c** days after injection with rhodamine-labeled plasmids, NPs, or saline. Bottom-3D reconstructions of the boxed regions in top panels. *Blue*-DAPI, *Green*-Lamin B1, *Red*-native rhodamine fluorescence. Scale bar 10 μm

DNA (red, Fig. 88.1b) is detected in the cytoplasm and nuclei of all treated groups, although we first detect DNA in the cytoplasm at PI-6 h and in the nucleus at PI-12–24 h (not shown). At PI-180 days labeled DNA is still detected in the RPE cells of all treatment groups (Fig. 88.1c). Examination of individual RPE cells at PI-180 showed an average of 3–5 spots of rhodamine fluorescence in the samples treated with the S/MAR vector compared to ~1 or none in the non-S/MAR vector samples suggesting the S/MAR vector may have better long-term DNA retention in the nucleus than the non-S/MAR vector.

**Table 88.1** Mean number of colonies from transformation of DH5α cells with Hirt's extract. Colonies were counted after 16 h. N/A denotes that no samples were analyzed for that timepoint. Values are means, $N=3$ eyes/group

| Treatment | PI-0 | PI-2 | PI-30 | PI-60 | PI-360 |
|---|---|---|---|---|---|
| VMDe-eGFP | N/A | 815 | 305 | 57 | N/A |
| NP-VMD2-eGFP | N/A | 709 | 376 | 117 | N/A |
| VMD2-eGFP-S/MAR | 1580 | 1107 | 402 | N/A | 0 |
| NP-VMD2-eGFP-S/MAR | 1822 | 1095 | 398 | N/A | 1 |
| Saline | 0 | 0 | 0 | 0 | 0 |

### *88.3.2 Episomal Status and Long Term Integrity of the Expression Cassette*

We next assessed the episomal status and intactness of the plasmids. Episomal DNA was prepared from treated eyes using Hirts' extraction at PI-2, -30, -60 (for non-S/MAR samples) and -360 days (for S/MAR samples), and then used to transform DH5α cells. At PI-2, -30 and 60 days, we detected a substantial number of colonies from each group (Table 88.1), indicating the presence of intact vectors in the samples. However, at PI-360 days, we only observed a single colony on the plate for NP-VMD2-eGFP-S/MAR and none for naked VMD2-eGFP-S/MAR. To confirm these results, restriction digest was performed on several colonies, and bands of the size expected for intact plasmid were detected. Shown in Fig. 88.2a are representative colonies from VMD2-eGFP and NP-VMD2-eGFP samples, but VMD2-eGFP-S/MAR and NP-VMD2-eGFP-S/MAR gave the same results.

Because few colonies were detected at PI-360 days, we next performed qPCR to quantify the number of remaining plasmid copies in the RPE (per eye) at that timepoint using Hirts' extracts from treated eyes. The total number of detected plasmid copies is presented in Fig. 88.2b, but it is worth noting that this value does not account for loss during sample extraction. To determine if intact expression cassette was still present at PI-360, we conducted regular PCR using promoters flanking the expression cassette. Figure 88.2c shows PCR products of the expected size demonstrating that intact expression cassette is detected in naked and NP-VMD2-eGFP-S/MAR treated samples from both Hrti's extracts (**H**) and genomic extracts (**G**). These data indicate that at PI-360, the eGFP expression cassette is episomal, but amplification of expression cassette from genomic DNA preps indicates the possibility that some of the vectors may have integrated into the genome.

## 88.4 Conclusions

Development and characterization of non-viral alternatives for ocular gene delivery is critical for the future of gene-based medicine. We have previously shown that compacted DNA NPs and naked DNA carrying S/MARs can efficiently transduce

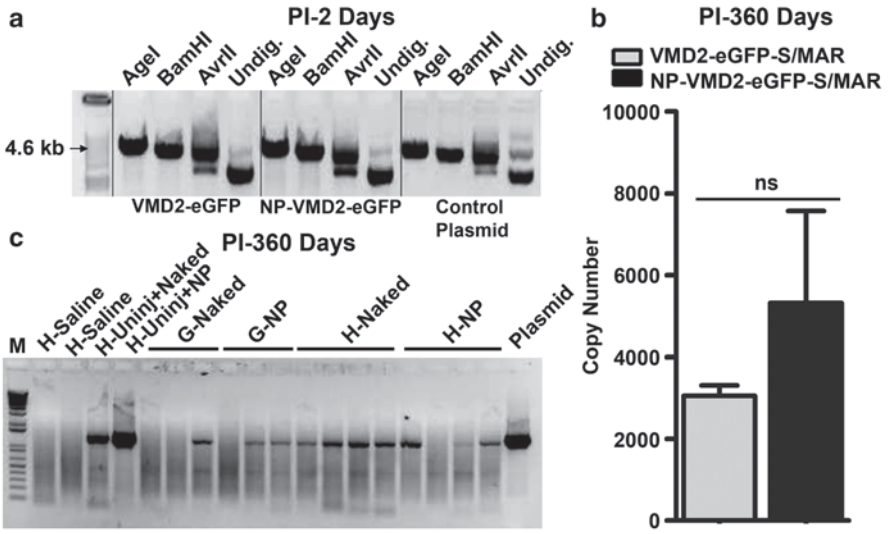


**Fig. 88.2** Episomal status and long-term integrity of the expression cassette. **a** Digestion of miniprep from colonies transformed with Hirts' extract. Control plasmid was purified original VMD2-eGFP plasmid. **b** qPCR results from amplification of PI-360 Hirts' extract of VMD2-eGFP-S/MAR and NP-VMD2-eGFP-S/MAR ($N=3$) at PI-360, shown is mean ± SEM. **c** Amplicons from regular PCR using primers which flank the expression cassette

the RPE and mediate long-term gene expression and rescue in the *rpe65*$^{-/-}$ model without detectable toxicity [6, 7]. Here, we demonstrated that the vector DNA continues to be detected in the nucleus up to PI-180 days (last timepoint tested) and that intact plasmid and expression cassette can be isolated up to PI-360 days. Vector integrity is important for long-lasting therapeutic benefit. Here, we were able to demonstrate the integrity of the expression cassette at 1 year post injection. Combined with our work demonstrating therapeutic rescue of other retinal disease models [5], these results suggest that DNA NPs (for RPE and photoreceptors) and plasmid DNA (for RPE) may be effective strategies for long-term gene targeting.

**Acknowledgment** This work was supported by the NIH, Foundation Fighting Blindness, and Oklahoma Center for the Advancement of Science and Technology.

## References

1. Jacobson SG, Cideciyan AV, Ratnakaram R, Heon E, Schwartz SB, Roman AJ, Peden MC, Aleman TS, Boye SL, Sumaroka A, Conlon TJ, Calcedo R, Pang JJ, Erger KE, Olivares MB, Mullins CL, Swider M, Kaushal S, Feuer WJ, Iannaccone A, Fishman GA, Stone EM, Byrne BJ, Hauswirth WW (2012) Gene therapy for leber congenital amaurosis caused by RPE65 mutations: safety and efficacy in 15 children and adults followed up to 3 years. Arch Ophthalmol 130(1):9–24

2. Simonelli F, Maguire AM, Testa F, Pierce EA, Mingozzi F, Bennicelli JL, Rossi S, Marshall K, Banfi S, Surace EM, Sun J, Redmond TM, Zhu X, Shindler KS, Ying GS, Ziviello C, Acerra C, Wright JF, McDonnell JW, High KA, Bennett J, Auricchio A (2010) Gene therapy for Leber's congenital amaurosis is safe and effective through 1.5 years after vector administration. Mol Ther 18(3):643–650
3. Maguire AM, High KA, Auricchio A, Wright JF, Pierce EA, Testa F, Mingozzi F, Bennicelli JL, Ying GS, Rossi S, Fulton A, Marshall KA, Banfi S, Chung DC, Morgan JI, Hauck B, Zelenaia O, Zhu X, Raffini L, Coppieters F, De Baere E, Shindler KS, Volpe NJ, Surace EM, Acerra C, Lyubarsky A, Redmond TM, Stone E, Sun J, McDonnell JW, Leroy BP, Simonelli F, Bennett J (2009) Age-dependent effects of RPE65 gene therapy for Leber's congenital amaurosis: a phase 1 dose-escalation trial. The Lancet 374(9701):1597–1605
4. Fink TL, Klepcyk PJ, Oette SM, Gedeon CR, Hyatt SL, Kowalczyk TH, Moen RC, Cooper MJ (2006) Plasmid size up to 20 kbp does not limit effective in vivo lung gene transfer using compacted DNA nanoparticles. Gene Ther 13(13):1048–1051
5. Cai X, Conley SM, Nash Z, Fliesler SJ, Cooper MJ, Naash MI (2010) Gene delivery to mitotic and postmitotic photoreceptors via compacted DNA nanoparticles results in improved phenotype in a mouse model of retinitis pigmentosa. FASEB J 24(4):1178–1191
6. Han Z, Koirala A, Makkia R, Cooper MJ, Naash MI (2012) Direct gene transfer with compacted DNA nanoparticles in retinal pigment epithelial cells: expression, repeat delivery and lack of toxicity. Nanomedicine (Lond) 7(4):521–539
7. Koirala A, Makkia RS, Conley SM, Cooper MJ, Naash MI (2013) S/MAR-containing DNA nanoparticles promote persistent RPE gene expression and improvement in RPE65-associated LCA. Hum Mol Genet 22(8):1632–1642
8. Koirala A, Makkia RS, Cooper MJ, Naash MI (2011) Nanoparticle-mediated gene transfer specific to retinal pigment epithelial cells. Biomaterials 32(35):9483–9493
9. Duan D, Sharma P, Yang J, Yue Y, Dudus L, Zhang Y, Fisher KJ, Engelhardt JF (1998) Circular intermediates of recombinant adeno-associated virus have defined structural characteristics responsible for long-term episomal persistence in muscle tissue. J Virol 72(11):8568–8577
10. Skulj M, Okrslar V, Jalen S, Jevsevar S, Slanc P, Strukelj B, Menart V (2008) Improved determination of plasmid copy number using quantitative real-time PCR for monitoring fermentation processes. Microb Cell Fact 7:6

# Chapter 89
# Gene Therapy in the Rd6 Mouse Model of Retinal Degeneration

**Astra Dinculescu, Seok-Hong Min, Wen-Tao Deng, Qiuhong Li and William W. Hauswirth**

**Abstract** The *rd6* mouse is a natural model of an RPE-based (retinal pigment epithelium) autosomal recessive retinitis pigmentosa (RP) caused by mutations in the *Mfrp* (membrane-type frizzled related protein) gene. Previously, we showed that subretinal delivery of the wild-type mouse Mfrp mediated by a tyrosine-capsid mutant scAAV8 (Y733F) vector prevented photoreceptor cell death, and rescued retinal function as assessed by electroretinography. In this study, we describe the effect of gene therapy on the retinal structure and function in *rd6* mice using a quadruple (Y272, 444, 500, 730F) tyrosine-capsid mutant scAAV2 viral vector delivered subretinally at postnatal day 14 (P14). We show that therapy is effective at slowing the photoreceptor degeneration, and in preventing the characteristic accumulation of abnormal phagocytic cells in the subretinal space. MFRP expression as driven by the ubiquitous chicken β-actin (smCBA) promoter in treated rd6 mice was found predominantly in the RPE apical membrane and the entire length of its microvilli, as well as in the photoreceptor inner segments, suggesting a potential interaction with actin filaments. In spite of preserving retinal morphology, the effects of gene therapy on retinal function were minimal, suggesting that the scAAV8 (Y733F) vector may be more efficient for the treatment of RP caused by Mfrp mutations.

**Keywords** Retinal pigment epithelium · MFRP · Adeno-associated virus · Gene therapy · Retinal degeneration

A. Dinculescu (✉) · S.-H. Min · W.-T. Deng · Q. Li · W. W. Hauswirth
Department of Ophthalmology, College of Medicine, University of Florida,
1600 SW Archer Road, Gainesville, FL32610, USA
e-mail: astra@ufl.edu

S.-H. Min
e-mail: korea@ufl.edu

W.-T. Deng
e-mail: wdeng@ufl.edu

Q. Li
e-mail: qli@ufl.edu

W. W. Hauswirth
e-mail: hauswrth@ufl.edu

J. D. Ash et al. (eds.), *Retinal Degenerative Diseases,* Advances in Experimental Medicine and Biology 801, DOI 10.1007/978-1-4614-3209-8_89,

## 89.1 Introduction

The *Mfrp* gene encodes a type II transmembrane protein of unknown function, which is highly expressed in the retinal pigment epithelium (RPE) and cilliary epithelial layers in the eye [1, 2]. Mutations in the human *Mfrp* gene, located on chromosome 11q23, can lead to autosomal recessively-inherited retinitis pigmentosa, microphthalmos, and optic disc drusen [3]. The rd6 mouse is a natural model of autosomal recessive retinal degeneration, caused by a 4 bp deletion in a splice donor site in the *Mfrp* gene [4, 5]. This results in deletion of 58 amino acids from the MFRP protein, perhaps rendering it prone to aggregation, and subsequent proteosomal degradation, since it is no longer detectable by either western blotting or immunohistochemistry in rd6 mouse eyes [6, 7]. An interesting feature of rd6 retinal pathology is the accumulation of phagocytic-like cells in the subretinal space of mice as young as P21 [4]. Although *rd6* photoreceptor degeneration is slowly progressive, it has an early onset, with outer segments already appearing shorter than normal as early as postnatal day 14, and RPE microvilli being disorganized in focal areas as early as P7 [7]. Both scotopic and photopic ERG amplitudes gradually decline with age, with cones initially appearing less affected [4, 7].

We have recently shown that despite an early onset of pathological features, subretinal delivery at postnatal day 14 of a self-complementary tyrosine-capsid mutant scAAV8 (Y733F) vector containing the mouse *Mfrp* cDNA can prevent photoreceptor degeneration and restore retinal function in *rd6* mice, indicating that this model may potentially be useful for proof-of-concept gene therapy in preparation for a clinical trial in patients [8]. In this study, we describe the effects of gene therapy on the retinal structure and function in *rd6* mice using a quadruple (Y272, 444, 500, 730F) tyrosine-capsid mutant scAAV2 viral vector and compared to the scAAV8 (Y733F) vector tested previously.

## 89.2 Materials and Methods

### *89.2.1 Production of Recombinant AAV Vectors*

The wild-type murine *Mfrp* cDNA under control of the ubiquitous, constitutive smCBA promoter was packaged either in serotype 8 capsid containing a Y733F point mutation, or the serotype 2 capsid with four Y-F mutations (Y272,444,500,730F). The full length mouse *Mfrp* cDNA was kindly provided by Dr. Xinhua Shu (Glasgow Caledonian University, Glasgow, Scotland). The viral vectors were produced by the two-plasmid co-transfection method in HEK 293 cells and purified according to previously reported methods [9].

### 89.2.2 Subretinal Vector Delivery

The *rd6* mice (originally provided by B. Chang, Jackson Laboratory, Bar Harbor, ME) were bred and maintained in the University of Florida Health Science Center Animal Care Services Facility (Gainesville, FL) under 12-hr-on/12-hr-off cyclic lighting. All experiments were approved by the University of Florida's Institutional Animal Care and Use Committee and conducted in accordance with ARVO Statement for the Use of Animals in Ophthalmic and Vision Research and NIH regulations. Subretinal injections were performed on P14 *rd6* mice under anesthesia as previously described [10]. Each eye received 1 μl of AAV vector at a titer of $1 \times 10^{12}$ vector genome copies/ml, leaving the left eye as an untreated contralateral control.

### 89.2.3 Immunostaining and Retinal Histology

Retinal sections were incubated with mouse MFRP Affinity Purified Polyclonal Antibody (AF3445, R&D Systems, Inc., Minneapolis, MN) at a 1:1000 dilution, followed by an Alexa-594 fluorophore secondary antibody (Molecular Probes/Invirogen, Eugene OR) diluted 1:500 in 1xPBS, and examined by fluorescence microscopy using a Leica TCS SP2 Laser Scanning confocal microscope (Leica, Heidelberg, Germany). For morphological analysis, the treated *rd6* and control eyes were processed for paraffin embedding, sectioned at 4 μm thickness, and stained with hematoxylin and eosin by a commercial histology laboratory (Histology Tech Services, Gainesville, FL). Adult C57BL/6 mice were used as wild-type controls.

### 89.2.4 Evaluation of Retinal Function in AAV Vector-Treated rd6 Mice

Electroretinograms were recorded at 6 weeks post-injection under scotopic and photopic conditions at various light intensities, as previously described [8]. Statistical analysis was performed using GraphPad Prism software (GraphPad, La Jolla, CA).

## 89.3 Results

In order to study the effect of subretinally delivered vector on photoreceptor cell preservation, we performed morphological analysis of *rd6* and wild-type C57BL/6 control mice using hematoxylin and eosin staining of paraffin-embedded retinal sections. Light microscopy examination of *rd6* retinas at 6 weeks post-injection clearly shows that the scAAV2 quadruple (Y272,444,500,730F)-smCBA-MFRP treated eyes have an increased number of photoreceptor nuclei (9–10 layers) in comparison to the contralateral uninjected controls which decreased to 5–7 layers

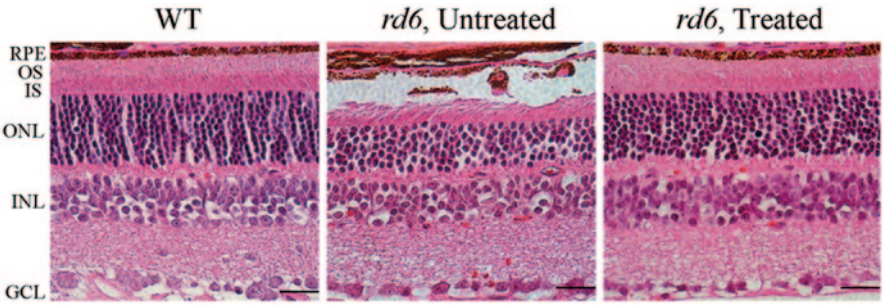


**Fig. 89.1** Histological examination of hematoxylin and eosin stained retinal sections. Representative light microscopy images of a 2-month-old retina of wild-type (*left panel*), *untreated rd6* (*middle panel*) and AAV2quadruple-treated rd6 contralateral eye (*right panel*). Note the well preserved *ONL* and *OS* of the treated rd6 eye. GCL, ganglion cell layer; *INL*, inner nuclear layer; *ONL*, outer nuclear layer; *IS*, inner segment; *OS*, outer segment; *RPE*, retinal pigment epithelium. Scale bar, 20 μm

(Fig. 89.1). Treated *rd6* retinas also contain well-organized inner and outer segments, similar to wild-type C57BL/6J eyes, and in contrast to the uninjected *rd6* eyes in which the outer segments are both shortened and disorganized. Phagocytic subretinal cells, characteristic of untreated *rd6* mouse eyes, were absent upon vector treatment.

MFRP protein expression in wild-type eyes is localized to the apical membrane and microvilli of RPE, as reported previously [7, 8]. The scAAV2 quadruple treated *rd6* eyes displayed robust MFRP labeling on the RPE apical membrane within its microvilli, as well as in photoreceptor inner segments (Fig. 89.2). An overview of the treated *rd6* retinas at low magnification shows that although subretinal vector led to widespread expression of MFRP, there were discontinuous, isolated areas in which the intensity of transgene expression was low or absent.

The effects of AAV-mediated gene therapy on retinal function were evaluated by ERG analysis at 6 weeks post-injection, and compared to those found in our previous study, which employed a scAAV8 (Y733F) vector of the same titer [8]. In order to minimize the inter-animal variation in ERG amplitudes, rescue effects were expressed as the average ratios of the treated (right) eye maximum b-wave amplitude to the corresponding control (left) eye amplitude (Fig. 89.3). The ERG amplitude ratios were significantly higher for treatment with scAAV8 (Y733F) vector than the scAAV2 quadruple (Y272,444,500,730F) ($^{*}p<0.05$), for light intensities that elicited either a dark-adapted rod response only (0.025 cds/m$^2$) or a mixed rod-cone response (2.5 cds/m$^2$). In treated mice at 2 months of age, the average pure rod-driven b-wave amplitude ratio was 1.78 ± 0.2 for the AAV8 (Y733F), and 1.09 ± 0.11 for the scAAV2 quadruple vector. The treated eye/untreated eye ratio at mixed rod-cone light intensities for the a-wave was 2.53 ± 0.21 for the AAV8 (Y733F) vector and 1.75 ± 0.15 for the scAAV2 quadruple, further demonstrating that the rod function

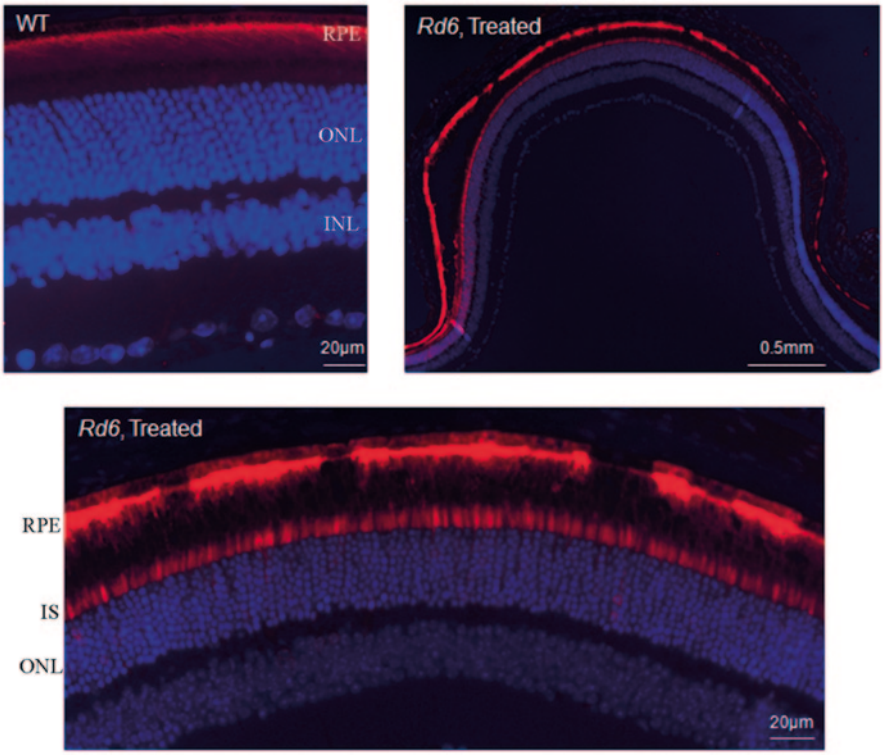


**Fig. 89.2** Expression of MFRP protein in wild-type and vector-treated *rd6* eyes. *Left* panel: Detection of endogenous MFRP by immunohistochemistry in wild-type retina. *Right* panel: Low-magnification view of a treated rd6 retina. *Bottom* panel: Vector-treated *rd6* retinal section depicting robust MFRP expression within the apical *RPE* membrane and its microvilli, as well as the inner segments of photoreceptor cells

was more effectively rescued by the AAV8 (Y733F) vector. The ratio values for the *rd6* group treated with the AAV8 (Y733F) vector were significantly different from 1.0 (*p* value of less than 0.05) at all light intensities examined. In contrast, those mice treated with the scAAV2 quadruple, displayed ratio values significantly greater than 1.0 only for light intensities that elicited a mixed rod-cone or cone-isolated responses. These results indicate that while the AAV2-quadruple vector prevents photoreceptor cell death, the AAV8 (Y733F) serotype provides more significant functional benefits for rods. In contrast, the ratios of cone-isolated photopic b-wave amplitudes at 25 cds/m$^2$ eliciting intensity were similar for both vector treatments, presumably because cones are less severely affected early in the disease process compared to rods, and thus can be rescued efficiently by both vectors.

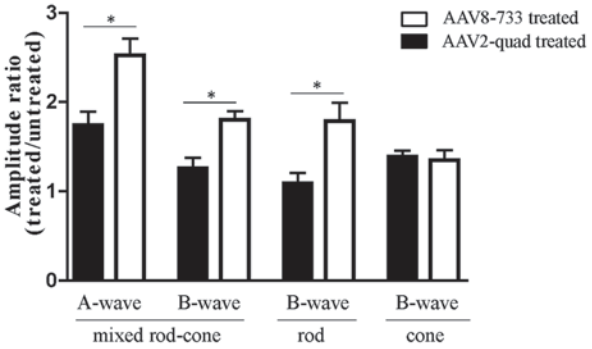


**Fig. 89.3** ERG analysis following subretinal treatment with either *AAV-2* quadruple or *AAV8-733* vectors in rd6 mice. Bar graph represents the ERG amplitude ratios (treated/untreated) of the maximum a-wave or b-wave amplitudes. Full-field scotopic (*dark-adapted*) measurements are in response to 0.025 cd.s/m$^2$ (rod-only) and 2.5 cd.s/m$^2$ (*mixed rod-cone*), while photopic (cone-mediated) flash recordings are in response to a 25 cd.s/m$^2$ eliciting intensity. Data are expressed as means ± SEM ($n = 5$ in each group). Unpaired Student's *t*-test was used for determination of the significance between *AAV2*-quadruple and *AAV8-733* treated rd6 groups for each light intensity ($^*p < 0.05$)

## 89.4 Discussion

Animal models of retinal degeneration combined with the AAV gene transfer technology represent valuable tools to evaluate potential therapeutic strategies for the treatment of ocular disorders, as well as for understanding the function and mechanism of proteins involved in retinal disease. The MFRP protein was shown in other studies to be expressed at the RPE apical membrane, where it appears to play a critical role in maintaining the integrity of RPE microvilli which nurture and support rod and cone photoreceptor cells [7]. Previously, we demonstrated the ability of a subretinally delivered AAV8 (Y733F) vector containing a smCBA promoter driving expression of a murine *Mfrp* gene to improve retinal function and prevent photoreceptor cell death in the early onset RPE-based model of MFRP-RP, the *rd6* mouse [8]. To gain further insight into the feasibility of treating *Mfrp*-RP with a gene based therapy, in the current study we used a scAAV2 quadruple (Y272, 444, 500, 730F) vector, which has been previously shown to penetrate retinal layers distal from the injection site, and thus has the ability to transduce RPE cells following an intravitreal delivery [9]. In order to evaluate its full therapeutic potential, this study characterized the effects of the high titer scAAV2 quadruple (Y272, 444, 500, 730F) subretinal vector delivery ($10^9$ total vector genomes) on the photoreceptor structure and function.

The natural history of the *rd6* mouse has been well documented previously, and it has been shown that by P25 the scotopic rod a-wave had decreased by approximately 50 % with both photoreceptor outer segments and RPE microvili displaying abnormal morphology [7]. Subretinal delivery of the scAAV2 quadruple (Y272,

444, 500, 730F) smCBA-MFRP vector at P14, as shown in this study, provides an effective structural benefit, with substantially improved photoreceptor morphology in treated eyes. Similar to our previous study [8], we also established that the AAV-mediated MFRP transgene expression is localized not only at the base of the RPE apical membrane, but also throughout the entire length of the RPE microvilli, which contain an internal core of actin filaments, as well as to the inner segments of photoreceptors. This supports the concept that MFRP may play a role in maintaining the normal morphology of RPE microvilli, perhaps by interacting with actin filaments and thus stabilizing their structure.

In contrast to the AAV8 (Y733F) vector used in our previous study [8], the AAV2 quadruple provided limited functional benefits for rod photoreceptors, which are affected early in the disease process. The superiority of the AAV8 (Y733F) vector could potentially arise from a rapid onset of transgene expression, combined with its ability to uniformly transduce the entire RPE apical surface following a single subretinal injection. The results also indicate that an AAV-based gene therapy approach for the RP caused by *Mfrp* mutations would benefit more if treatment is initiated early. Future studies focusing on the MFRP function and its role in maintaining a healthy RPE-photoreceptor interface may provide answers on developing new therapeutic strategies for later stages of this disorder.

**Acknowledgment** Foundation Fighting Blindness, Macula Vision Research foundation Research to Prevent Blindness, Inc.

## References

1. Katoh M (2001) Molecular cloning and characterization of MFRP, a novel gene encoding a membrane-type Frizzled-related protein. Biochem Biophys Res Commun 282:116–123
2. Mandal MN, Vasireddy V, Jablonski MM, Wang X, Heckenlively JR, Hughes BA et al (2006) Spatial and temporal expression of MFRP and its interaction with CTRP5. Invest Ophthalmol Vis Sci 47:5514–5521
3. Ayala-Ramirez R, Graue-Wiechers F, Robredo V, Amato-Almanza M, Horta-Diez I, Zenteno JC (2006) A new autosomal recessive syndrome consisting of posterior microphthalmos, retinitis pigmentosa, foveoschisis, and optic disc drusen is caused by a MFRP gene mutation. Mol Vis 12:1483–1489
4. Hawes NL, Chang B, Hageman GS, Nusinowitz S, Nishina PM, Schneider BS et al (2000) Retinal degeneration 6 (rd6): a new mouse model for human retinitis punctata albescens. Invest Ophthalmol Vis Sci 41:3149–3157
5. Kameya S, Hawes NL, Chang B, Heckenlively JR, Naggert JK, Nishina PM (2002) Mfrp, a gene encoding a frizzled related protein, is mutated in the mouse retinal degeneration 6. Hum Mol Genet 11:1879–1886
6. Shu X, Tulloch B, Lennon A, Vlachantoni D, Zhou X, Hayward C et al (2006) Disease mechanisms in late-onset retinal macular degeneration associated with mutation in C1QTNF5. Hum Mol Genet 15:1680–1689
7. Won J, Smith RS, Peachey NS, Wu J, Hicks WL, Naggert JK et al (2008) Membrane frizzled-related protein is necessary for the normal development and maintenance of photoreceptor outer segments. Vis Neurosci 25:563–574

8. Dinculescu A, Estreicher J, Zenteno JC, Aleman TS, Schwartz SB, Huang WC et al (2012) Gene therapy for retinitis pigmentosa caused by MFRP mutations: human phenotype and preliminary proof of concept. Hum Gene Ther 23:367–376
9. Petrs-Silva H, Dinculescu A, Li Q, Deng WT, Pang JJ, Min SH et al (2011) Novel properties of tyrosine-mutant AAV2 vectors in the mouse retina. Mol Ther 19:293–301
10. Pang JJ, Dai X, Boye SE, Barone I, Boye SL, Mao S et al (2011) Long-term retinal function and structure rescue using capsid mutant AAV8 vector in the rd10 mouse, a model of recessive retinitis pigmentosa. Mol Ther 19:234–242

# Chapter 90
# Gene Therapy for Stargardt Disease Associated with *ABCA4* Gene

**Zongchao Han, Shannon M. Conley and Muna I. Naash**

**Abstract** Mutations in the photoreceptor-specific flippase ABCA4 lead to accumulation of the toxic bisretinoid A2E, resulting in atrophy of the retinal pigment epithelium (RPE) and death of the photoreceptor cells. Many blinding diseases are associated with these mutations including Stargardt's disease (STGD1), cone-rod dystrophy, retinitis pigmentosa (RP), and increased susceptibility to age-related macular degeneration. There are no curative treatments for any of these dsystrophies. While the monogenic nature of many of these conditions makes them amenable to treatment with gene therapy, the *ABCA4* cDNA is 6.8 kb and is thus too large for the AAV vectors which have been most successful for other ocular genes. Here we review approaches to *ABCA4* gene therapy including treatment with novel AAV vectors, lentiviral vectors, and non-viral compacted DNA nanoparticles. Lentiviral and compacted DNA nanoparticles in particular have a large capacity and have been successful in improving disease phenotypes in the *Abca4*$^{-/-}$ murine model. Excitingly, two Phase I/IIa clinical trials are underway to treat patients with *ABCA4*-associated Startgardt's disease (STGD1). As a result of the development of these novel technologies, effective therapies for *ABCA4*-associated diseases may finally be within reach.

**Keywords** *ABCA4* · Gene therapy · Nanoparticles · Lentivirus · STGD1 · Viral · Non-viral

M. I. Naash (✉) · Z. Han · S. M. Conley
Department of Cell Biology, University of Oklahoma Health Sciences Center,
940 Stanton L. Young Blvd., BMSB 781, Oklahoma City, OK 73104, USA
e-mail: muna-naash@ouhsc.edu

Z. Han
Zongchao-han@ouhsc.edu

S. M. Conley
Shannon-conley@ouhsc.edu

J. D. Ash et al. (eds.), *Retinal Degenerative Diseases,* Advances in Experimental Medicine and Biology 801, DOI 10.1007/978-1-4614-3209-8_90,

## 90.1 Introduction

The *ABCA4* gene, encodes the ABCR protein, a photoreceptor-specific ATP-binding cassette transporter [1]. This protein is thought to act as a flippase for N-retinylidene phosphatidylethanolamine (PE), thereby facilitating the transport of all-*trans*-retinaldehyde from the disc lumen to the cytoplasm [2]. Mutations in *ABCA4* are associated with different forms of retinal disease. STGD1 patients exhibit delayed dark adaptation, severe macular vision loss and atrophy, as well as accumulation of lipofuscin granules in the RPE, increased levels of A2E (a major fluorophore of lipofuscin) in the RPE, and yellow fundus flecking [3]. The accumulation of A2E in the RPE is toxic, which eventually results in the degeneration of the RPE and the neural retina.

*Abca4*$^{-/-}$ mice were generated and show delayed dark adaptation, increased all-*trans*-retinaldehyde (all-*trans*-RAL) following light exposure, elevated PE in OSs, and increased accumulation of A2E in the RPE [2]. The fundus of aged *Abca4*$^{-/-}$ mice also exhibits yellow-white flecks and an atrophic appearance [4, 5]. Even though the mouse does not have a macula, this model has been widely used till date as many of the phenotypes are similar to those exhibited by STGD1 patients.

At present, there is no cure for ABCA4-associated disease. Studies have shown that *Abca4*$^{-/-}$ mice raised in darkness do not accumulate A2E, suggesting that avoiding excessive light might be beneficial for patients with ABCA4-associated retinal dystrophy [6]. Retinal dystrophy in *Abca4*$^{-/-}$ mice was also improved by treatment with isotretinoin (Accutane®), a drug commonly used for the treatment of severe acne [7]. However, long-term benefits of this approach are questionable, because prolonged exposure to isotretinoin is detrimental to the photoreceptors. Because of the monogenic nature of many ABCA4-associated diseases, effective *ABCA4* gene therapy has been a research target for some time now. A major limitation for successful gene delivery has been the large size of the *ABCA4* cDNA (6.8 kb [8]). However, several approaches have been tried, [5, 9–11] with varying degrees of success. Here, we review recent developments in gene and cell therapy for the treatment of ABCA4-associated diseases.

## 90.2 *ABCA4* Gene Therapy

### *90.2.1 AAV-Mediated* ABCA4 *Gene Transfer*

Gene replacement is a logical strategy for STGD1, particularly given the current success of AAV-mediated ocular gene delivery (e.g. [12–14]), but the large size of the *ABCA4* cDNA prevents its formulation as a traditional AAV (maximum capacity ~4.7 kb). In spite of this, some attempts to deliver *Abca4* via AAVs have been made using a modified AAV serotype 5 vector [11]. The authors provided evidence of phenotypic improvement in the *Abca4*$^{-/-}$ mouse model; however, the study was controversial and has not been replicated. Subsequent studies from three independent

groups have concluded that the original study delivered AAVs containing different, smaller parts of the *Abca4* expression cassette generated by random recombination, and that in no case was an intact *Abca4* expression cassette transferred [10, 15, 16].

### *90.2.2 Lentivirus-Mediated* ABCA4 *Gene Transfer*

Lentiviral-mediated gene delivery has been successfully used for treatment of ocular diseases [9, 17–19]. Lentiviruses, are members of the retrovirus family, but they are able to infect non-dividing cells. Compared to AAV, lentiviruses have one major advantage: a relatively larger carrying capacity (up to 8 kb) [20]. Kong et al. generated an equine infectious anemia virus-based lentiviral vector carrying the human *ABCA4* cDNA driven by the bovine rod opsin promoter and subretinally delivered it to *Abca4*$^{-/-}$ mice [9]. Animals were followed for 1 year and treated eyes exhibited reduced A2E accumulation compared to mock-treated or untreated eyes [9]. Though the study did not assess functional phenotypes, the reduced A2E levels suggest that RPE cell toxicity and subsequent retinal degeneration will also be reduced leading to functional benefits. One drawback of lentiviral-mediated gene delivery is random integration throughout the genome. To combat this, significant work has gone into developing non-integrating lentiviral vectors [21].

### *90.2.3 Non-Viral* ABCA4 *Gene Transfer*

Recently we have used novel self-compacted DNA nanoparticles made of polyethylene glycol-substituted polylysine (CK30PEG NPs) for ocular gene delivery [22–24]. These NPs can compact DNA up to 20 kb in size into particles ~8 nm in diameter [25]. In addition to the eye, they have been used successfully in the lung and brain as well as in a phase I/IIa clinical trial for cystic fibrosis [26–28]. We have shown that these NPs can mediate long-term rescue of the RP phenotype of *rds*$^{+/-}$ mice and the Leber's Congenital Amaurosis phenotype of *rpe65*$^{-/-}$ mice [29, 30]. Importantly, these particles are non-toxic in the eye, even after repeat injections, and can drive gene expression levels on a scale comparable to AAV [23, 31].

To take advantage of this technology for the treatment of ABCA4-associated disease, we constructed plasmid vectors carrying the human *ABCA4* cDNA and compacted into NPs. After subretinal delivery in *Abca4*$^{-/-}$ mice, persistent transgene expression was observed for up to 8 months post-injection (the longest time tested) [5]. Excitingly, we also observed significant correction of functional (dark adaptation by ERG) and structural (reduced fundus flecking) STGD1 phenotypes in treated animals [5]. This study suggested that NPs are a gene delivery method that may successfully target difficult-to-treat genetic diseases, particularly those associated with large genes. Future studies are needed to explore ways to increase distribution of expression after NP delivery and fully examine potential systemic immune responses to subretinally delivered NPs, but current evidence suggests that systemic toxicity will be minimal.

## 90.3 *ABCA4* Clinical Trials

Based on positive animal studies, clinical trials for STGD1 were initiated using StarGen™, a lentivirus-based drug carrying the *ABCA4* gene. Led by Dr. David Wilson, the first patient in the USA clinical trial (NCT01367444) was treated subretinally at Casey Eye Institute in Portland, OR, in mid-2011. Subsequently, a second clinical trial site led by Dr. Jose-Alain Sahel, in Paris, France, was opened. These phase I/IIa studies will enroll up to 28 patients and will evaluate three dose levels for safety, tolerability, and aspects of biological activity. Till date, there have been no study results published or posted on ClinicalTrials.gov, however a press release from Oxford Biomedica (August 2012, http://www.oxfordbiomedica.co.uk/page.asp?pageid=59&newsid=629), reports positive highlights from the Data Safety and Monitoring Board (DSMB) overseeing the study. They noted that 8 patients had been treated at the first dose level with no serious adverse events and that the DSMB supports proceeding to the next dose level.

In addition to the StarGen trial, another clinical trial for STGD1 was also initiated in 2011. This trial is led by Advanced Cell Technology, Inc. (Marlborough, MA, NCT01345006) and takes a cell therapy approach, utilizing human embryonic stem cell derived RPE cells. Twelve patients with advanced STGD1 were planned for this phase I/II study, but no results are currently available.

## 90.4 Conclusions

Successful development vectors for the delivery of large genes has significantly advanced the field of *ABCA4*-associated gene therapy. Many retinal disease genes are too large for AAV and even lentivirus, including some associated with Usher syndrome (USH2A, USH1B), Bardet-Biedl Syndrome (BBS1), and RP (CRB1, IMPG2) making development of large capacity delivery vehicles widely applicable to a broad range of blinding retinal degenerative conditions as well as myriad non-ocular diseases. In addition, the ability to transfer larger expression cassettes will allow for more sophisticated vector engineering approaches for optimal gene targeting.

In the past two decades, gene therapy for human ocular disorders has produced remarkable breakthroughs [12–14]. However, significant barriers remain for the development of truly curative therapies. Human ocular clinical trials have highlighted that subretinal delivery can be extremely damaging to the retina, specifically to macular cones, and that getting sufficient distribution of expression to effect improvements can be challenging. In addition, safety concerns regarding the development of an immune response to delivery agents persist, particularly in cases where repeat injection is needed or where the contralateral eye is treated some time after the first eye. Finally, often genetic treatments are not delivered until degeneration is advanced, and rescue at that stage in the disease process is very difficult. Such concerns have prompted development of cell based therapies, but significant work

remains to optimize this approach as well. Certainly outcomes from the gene and cell-based clinical trials for ABCA4-associated STGD1 are eagerly awaited and may inform future research directions.

**Acknowledgment** This work was supported by the NIH, the Foundation Fighting Blindness and the Oklahoma Center for the Advancement of Science and Technology.

## References

1. Illing M, Molday LL, Molday RS (1997) The 220-kDa rim protein of retinal rod outer segments is a member of the ABC transporter superfamily. J Biol Chem 272(15):10303–10310
2. Weng J, Mata NL, Azarian SM, Tzekov RT, Birch DG, Travis GH (1999) Insights into the function of Rim protein in photoreceptors and etiology of Stargardt's disease from the phenotype in abcr knockout mice. Cell 98(1):13–23
3. Molday RS (2007) ATP-binding cassette transporter ABCA4: molecular properties and role in vision and macular degeneration. J Bioenerg Biomembr 39(5-6):507–517
4. Conley SM, Cai X, Makkia R, Wu Y, Sparrow JR, Naash MI (2012) Increased cone sensitivity to ABCA4 deficiency provides insight into macular vision loss in Stargardt's dystrophy. Biochim Biophys Acta 1822(7):1169–1179
5. Han Z, Conley SM, Makkia RS, Cooper MJ, Naash MI (2012) DNA nanoparticle-mediated ABCA4 delivery rescues Stargardt dystrophy in mice. J Clin Invest 122(9):3221–3226
6. Mata NL, Weng J, Travis GH (2000) Biosynthesis of a major lipofuscin fluorophore in mice and humans with ABCR-mediated retinal and macular degeneration. Proc Natl Acad Sci USA 97(13):7154–7159
7. Radu RA, Mata NL, Nusinowitz S, Liu X, Sieving PA, Travis GH (2003) Treatment with isotretinoin inhibits lipofuscin accumulation in a mouse model of recessive Stargardt's macular degeneration. Proc Natl Acad Sci USA 100(8):4742–4747
8. Azarian SM, Megarity CF, Weng J, Horvath DH, Travis GH (1998) The human photoreceptor rim protein gene (ABCR): genomic structure and primer set information for mutation analysis. Hum Genet 102(6):699–705
9. Kong J, Kim SR, Binley K, Pata I, Doi K, Mannik J, Zernant-Rajang J, Kan O, Iqball S, Naylor S, Sparrow JR, Gouras P, Allikmets R (2008) Correction of the disease phenotype in the mouse model of Stargardt disease by lentiviral gene therapy. Gene Ther 15(19):1311–1320
10. Lai Y, Yue Y, Duan D (2010) Evidence for the failure of adeno-associated virus serotype 5 to package a viral genome > or = 8.2 kb. Mol Ther 18(1):75–79
11. Allocca M, Doria M, Petrillo M, Colella P, Garcia-Hoyos M, Gibbs D, Kim SR, Maguire A, Rex TS, Di Vicino U, Cutillo L, Sparrow JR, Williams DS, Bennett J, Auricchio A (2008) Serotype-dependent packaging of large genes in adeno-associated viral vectors results in effective gene delivery in mice. J Clin Invest 118(5):1955–1964
12. Bainbridge JW, Smith AJ, Barker SS, Robbie S, Henderson R, Balaggan K, Viswanathan A, Holder GE, Stockman A, Tyler N, Petersen-Jones S, Bhattacharya SS, Thrasher AJ, Fitzke FW, Carter BJ, Rubin GS, Moore AT, Ali RR (2008) Effect of gene therapy on visual function in Leber's congenital amaurosis. N Engl J Med 358(21):2231–2239
13. Cideciyan AV, Hauswirth WW, Aleman TS, Kaushal S, Schwartz SB, Boye SL, Windsor EA, Conlon TJ, Sumaroka A, Roman AJ, Byrne BJ, Jacobson SG (2009) Vision 1 year after gene therapy for Leber's congenital amaurosis. N Engl J Med 361(7):725–727
14. Maguire AM, Simonelli F, Pierce EA, Pugh EN Jr, Mingozzi F, Bennicelli J, Banfi S, Marshall KA, Testa F, Surace EM, Rossi S, Lyubarsky A, Arruda VR, Konkle B, Stone E, Sun J, Jacobs J, Dell'Osso L, Hertle R, Ma JX, Redmond TM, Zhu X, Hauck B, Zelenaia O, Shindler KS, Maguire MG, Wright JF, Volpe NJ, McDonnell JW, Auricchio A, High KA,

Bennett J (2008) Safety and efficacy of gene transfer for Leber's congenital amaurosis. N Engl J Med 358(21):2240–2248
15. Hirsch ML, Agbandje-McKenna M, Samulski RJ (2010) Little vector, big gene transduction: fragmented genome reassembly of adeno-associated virus. Mol Ther 18(1):6–8
16. Wu Z, Yang H, Colosi P (2010) Effect of genome size on AAV vector packaging. Mol Ther 18(1):80–86
17. Balaggan KS, Binley K, Esapa M, Iqball S, Askham Z, Kan O, Tschernutter M, Bainbridge JW, Naylor S, Ali RR (2006) Stable and efficient intraocular gene transfer using pseudotyped EIAV lentiviral vectors. J Gene Med 8(3):275–285
18. Miyoshi H, Takahashi M, Gage FH, Verma IM (1997) Stable and efficient gene transfer into the retina using an HIV-based lentiviral vector. Proc Natl Acad Sci USA 94(19):10319–10323
19. Greenberg KP, Geller SF, Schaffer DV, Flannery JG (2007) Targeted transgene expression in muller glia of normal and diseased retinas using lentiviral vectors. Invest Ophthalmol Vis Sci 48(4):1844–1852
20. Thomas CE, Ehrhardt A, Kay MA (2003) Progress and problems with the use of viral vectors for gene therapy. Nat Rev Genet 4(5):346–358
21. Sarkis C, Philippe S, Mallet J, Serguera C (2008) Non-integrating lentiviral vectors. Curr Gene Ther 8(6):430–437
22. Farjo R, Skaggs J, Quiambao AB, Cooper MJ, Naash MI (2006) Efficient non-viral ocular gene transfer with compacted DNA nanoparticles. PLoS One 1:e38
23. Han Z, Koirala A, Makkia R, Cooper MJ, Naash MI (2012) Direct gene transfer with compacted DNA nanoparticles in retinal pigment epithelial cells: expression, repeat delivery and lack of toxicity. Nanomedicine (Lond) 7(4):521–539
24. Koirala A, Makkia RS, Cooper MJ, Naash MI (2011) Nanoparticle-mediated gene transfer specific to retinal pigment epithelial cells. Biomaterials 32(35):9483–9493
25. Fink TL, Klepcyk PJ, Oette SM, Gedeon CR, Hyatt SL, Kowalczyk TH, Moen RC, Cooper MJ (2006) Plasmid size up to 20 kbp does not limit effective in vivo lung gene transfer using compacted DNA nanoparticles. Gene Ther 13(13):1048–1051
26. Konstan MW, Davis PB, Wagener JS, Hilliard KA, Stern RC, Milgram LJ, Kowalczyk TH, Hyatt SL, Fink TL, Gedeon CR, Oette SM, Payne JM, Muhammad O, Ziady AG, Moen RC, Cooper MJ (2004) Compacted DNA nanoparticles administered to the nasal mucosa of cystic fibrosis subjects are safe and demonstrate partial to complete cystic fibrosis transmembrane regulator reconstitution. Hum Gene Ther 15(12):1255–1269
27. Padegimas L, Kowalczyk TH, Adams S, Gedeon CR, Oette SM, Dines K, Hyatt SL, Sesenoglu-Laird O, Tyr O, Moen RC, Cooper MJ (2012) Optimization of hCFTR Lung Expression in Mice Using DNA Nanoparticles. Mol Ther 20(1):63–72
28. Yurek DM, Fletcher AM, Smith GM, Seroogy KB, Ziady AG, Molter J, Kowalczyk TH, Padegimas L, Cooper MJ (2009) Long-term transgene expression in the central nervous system using DNA nanoparticles. Mol Ther 17(4):641–650
29. Cai X, Conley SM, Nash Z, Fliesler SJ, Cooper MJ, Naash MI (2010) Gene delivery to mitotic and postmitotic photoreceptors via compacted DNA nanoparticles results in improved phenotype in a mouse model of retinitis pigmentosa. FASEB J 24(4):1178–1191
30. Koirala A, Makkia RS, Conley SM, Cooper MJ, Naash MI (2013) S/MAR-containing DNA nanoparticles promote persistent RPE gene expression and improvement in RPE65-associated LCA. Hum Mol Genet 22(8):1632–1642
31. Han Z, Conley SM, Makkia R, Guo J, Cooper MJ, Naash MI (2012) Comparative Analysis of DNA Nanoparticles and AAVs for Ocular Gene Delivery. PLoS One 7(12):e52189

# Chapter 91
# Assessment of Different Virus-Mediated Approaches for Retinal Gene Therapy of Usher 1B

**Vanda S. Lopes, Tanja Diemer and David S. Williams**

**Abstract** Usher syndrome type 1B, which is characterized by congenital deafness and progressive retinal degeneration, is caused by the loss of the function of *MYO7A*. Prevention of the retinal degeneration should be possible by delivering functional *MYO7A* to retinal cells. Although this approach has been used successfully in clinical trials for Leber congenital amaurosis (LCA2), it remains a challenge for Usher 1B because of the large size of the *MYO7A* cDNA. Different viral vectors have been tested for use in *MYO7A* gene therapy. Here, we review approaches with lentiviruses, which can accommodate larger genes, as well as attempts to use adeno-associated virus (AAV), which has a smaller packaging capacity. In conclusion, both types of viral vector appear to be effective. Despite concerns about the ability of lentiviruses to access the photoreceptor cells, a phenotype of the photoreceptors of *Myo7a*-mutant mice can be corrected. And although *MYO7A* cDNA is significantly larger than the nominal carrying capacity of AAV, AAV-*MYO7A* in single vectors also corrected *Myo7a*-mutant phenotypes in photoreceptor and RPE cells. Interestingly, however, a dual AAV vector approach was found to be much less effective.

**Keywords** Usher syndrome 1B · MYO7A · Gene therapy · Lentivirus · AAV

V. S. Lopes (✉)
Stein Eye Institute, UCLA David Geffen School of Medicine,
Los Angeles, CA 90095-7008, USA
e-mail: vslopes@ucla.edu

T. Diemer · D. S. Williams
Departments of Ophthalmology and Neurobiology, Stein Eye Institute,
UCLA School of Medicine, Los Angeles, CA 90095, USA
e-mail: tdiemer@gmail.com

D. S. Williams
e-mail: dswilliams@ucla.edu

J. D. Ash et al. (eds.), *Retinal Degenerative Diseases,* Advances in Experimental Medicine and Biology 801, DOI 10.1007/978-1-4614-3209-8_91,

## 91.1 Introduction

Many inherited retinal diseases are caused by loss of function of a single gene, expressed in the photoreceptor cells (PR) and/or the retinal pigment epithelium (RPE), and are characterized by progressive blindness. Introduction of a wildtype copy of the mutated gene prior to retinal degeneration should therefore be sufficient to prevent it. Clinical trials have demonstrated the efficacy of this type of gene therapy in treating Leber congenital amaurosis patients, lacking functional *RPE65*. In these trials, the cDNA of wild-type *RPE65* was delivered to the RPE via an adeno-associated virus (AAV) [1–4].

Usher syndrome is a genetic disorder, characterized by retinal degeneration and deafness. Usher syndrome type 1 is the most severe, with patients born profoundly deaf [5]. Due to their congenital deafness, Usher 1 patients can be readily identified prior to the onset of retinal degeneration. Usher 1B accounts for at least half the cases of Usher 1, and it is caused by mutations in the *MYO7A* gene [6]. MYO7A is an unconventional myosin, with a cDNA of ~7 kb. Mouse studies have shown that it performs several functions in the photoreceptor and RPE cells. Its deficiency results in the impairment of critical cellular processes in the retina, such as phagosome degradation [7]. Inheritance of Usher1B is recessive, with most of the known *MYO7A* mutations probably resulting in a lack of functional MYO7A protein [8]. This, combined with a very early identification of the mutation involved, makes Usher 1B patients suitable candidates for preventive gene replacement therapy, where a wildtype copy of *MYO7A* would be delivered to the photoreceptor and RPE cells.

AAV have been successfully used in pre-clinical and clinical retinal gene therapy trials, but their nominal carrying capacity of ~5.4 kb [9] potentially limits its general application to genetic retinal diseases involving large genes, such as *MYO7A*. Nevertheless, we have now explored the use of AAV vectors for delivering *MYO7A*, including the use of dual AAV vectors [10]. We review these results here, and compare them with published and some unpublished studies on lentiviral delivery.

## 91.2 Lentivirus-Mediated Gene Therapy

Lentiviral (LV) vectors are able to deliver large genes (up to 10 kb) to post-mitotic cells, and result in prolonged expression, due to efficient and permanent integration of the delivered gene into the host genome. Thus they are apparently good candidates for trials involving large genes, such as *MYO7A*. Two types of LVs are being used in retinal gene therapy trials: HIV-derived and equine infectious anaemia virus (EIAV).

### 91.2.1 HIV-Derived Vectors

The use of HIV-1 derived vectors for delivery of genes to the retina dates from 1997, with the delivery of GFP [11]. The ability to deliver LV-*MYO7A* to the RPE and photoreceptors was tested by Hashimoto et al. [12], by performing subretinal injections into *Myo7a*-null mice (see [13] for the discussion on the use of *Myo7a*-null mice as a murine Usher1B model). The *MYO7A* was driven by a chimeric promoter, composed of elements from CMV and a minimal region of the native *MYO7A* promoter [14]. MYO7A protein was detected in the RPE, although not in the photoreceptors. Correction of mutant phenotypes was nevertheless observed in both the photoreceptor and RPE cells, near the injection site. Expression was detected up to 3 weeks after injection ([12] and unpublished observations), and it is expected that it would be retained longer [15].

The integrating nature of lentiviruses resulted in variation in the levels of protein expressed among cells [12]. This characteristic may also result in insertional mutagenesis, through the disruption of a previously functional gene or in the activation of abnormal gene expression. Several studies have focused on determining the specific sites and preferences of LV integration, which seem to vary with the type of vector and tissue targeted. Transduction of post-mitotic tissues, such as the retina, with LV seems to result in near random integration. While targeting integration into a defined site is not yet possible, one can shift its preference towards inactive regions of DNA [16].

One way to circumvent the random integration of LVs is to use integration-deficient LVs, which result in the accumulation of viral genomes as circular double strands in the nucleus of transduced cells [17]. Mutations in the integrase coding sequence, such as the D64V mutation, can reduce integrations by 10,000-fold, while avoiding degradation and retaining long-term transgene expression (at least up to 9 months) [17, 18]. Subretinal injection into *Myo7a*-null mice of an integration-deficient D64V LV or a WT LV, encoding MYO7A, resulted in similar expression levels and comparable efficacy in the correction of mutant RPE and photoreceptor phenotypes (unpublished observations). These observations suggest that non-integrating LV may be efficacious for Usher 1B retinal therapy, while providing greater safety over integrating LV.

### 91.2.2 EIAV-Derived Vectors

In comparison with HIV-derived LV, equine infectious anaemia virus (EIAV) seems to result in a faster onset of expression (from 3 days to a peak at around day 14). Expression from the introduced gene has been demonstrated in both the RPE and photoreceptor cells for up to 16 months in mouse retinas [19]. Moreover, correction of a retinal phenotype in mutant mice indicated the successful delivery of the

large *ABCA4* cDNA, which is almost 7 kb [20]. Recently, we have made use of an EIAV vector to deliver *MYO7A* to *Myo7a*-deficient mice, under the control of the chimeric *CMV-MYO7A* promoter. Following injection, MYO7A was detected at wildtype levels in the photoreceptor connecting cilium, as well as in the RPE cells, and resulted in the rescue of mutant phenotypes. However, as reported with EIAV encoding eGFP, we noted areas with reduced photoreceptor nuclei, at 6 months post injection. EIAV has been considered a safer alternative to HIV-derived LVs, however a study has shown that in utero and neonatal delivery of FIX (Factor IX) resulted in 80% or all of the animals developing liver tumours [21]. As with HIV-derived LVs, this potential oncogenic activation may be diminished by using an integration-deficient version.

## 91.3 AAV Based Vectors

AAV has been the primary choice of viral vector so far, with the serotype 2 and 5 being the most used in the retinal field. They have been shown to result in long-term gene expression, transduce photoreceptors efficiently, have low toxicity, and result in mostly episomal DNA in the cells. One of its major drawbacks seems to be its limited ability to encapsulate efficiently genes that are smaller than 5.4 kb.

An initial study with *MYO7A* showed that AAV5 was able to mediate full-length expression of MYO7A in RPE primary cultures [22]. Detailed studies have then shown that the delivery of genes larger than 5.4 kb is most probably accomplished by fragmentation of the gene into sizes that can be packaged efficiently, followed by reassembly of the gene, via recombination, inside the cell [23–25]. Molecular strategies have been designed to circumvent this issue. One such strategy has been the use of mini-genes, containing only essential domains [26]. However, this approach results in the exclusion of protein domains, which may be more important than initially thought, as demonstrated in the case of dystrophin [27]. In the case of large molecular motors, like MYO7A, in which all domains appear to be important for its function, this strategy is also not applicable.

We have found that delivery of *MYO7A* by AAV2 or AAV5 single vectors results in MYO7A protein expression in RPE primary cultures, as shown previously with AAV5 [22]. Following subretinal injection into *Myo7a*-null mice of *MYO7A* in either serotype, MYO7A was immunodetected in the photoreceptor and RPE cells, similar to WT retinas. Mutant phenotypes were corrected in both cell types, indicating the expression of fully functional MYO7A [10].

In order to avoid fragmentation of *MYO7A* into unknown fragments, a dual AAV2 vector strategy was devised. *MYO7A* cDNA was divided into two overlapping fragments, and packaged into two separate AAV particles. A mixture of the two was then delivered simultaneously, with the aim of achieving full-length *MYO7A* by recombination. The results were, however, disappointing [10]. Subretinal injection of *Myo7a*-null mice resulted in only a very low proportion of the photoreceptor and RPE cells expressing functional protein, near the injection site. Rescue of mutant

phenotypes was sporadic. Following treatment of primary cultures of *Myo7a*-null RPE cells, again only a minority of cells expressed detectable MYO7A protein, and an additional concern was that some of these cells overexpressed MYO7A to levels that appeared to be toxic [10].

The above comparison of single and dual AAV vector systems indicates that the single vector approach is more effective, despite the likely involvement of random fragmentation of the *MYO7A* cDNA so that it can be packaged [10].

The efficacy of a dual system might be increased by engineering the two DNA fragments so that they trans-splice, or perhaps combining both trans-splicing and overlapping features. These approaches have been reported, with genes other than *MYO7A,* to be slightly more effective than the overlapping dual AAV, but they have always fallen short of single AAV strategies [28, 29].

## 91.4 Conclusions

Retinal gene therapy with large genes can be accomplished through the use of several viral strategies such as LV and AAV. Each has its own advantages and disadvantages. Retinal delivery of *MYO7A* has been attempted with both LV and AAV, and the results provide a relative assessment of each for the delivery of large genes to the retina. LV-*MYO7A* has proved effective for treating photoreceptor and RPE cells. The consequences of integration remain a concern, however, justifying further work on integration-deficient LV strategies. Single AAV-*MYO7A* vectors have been demonstrated to be efficacious, and the success of AAV vectors in clinical trials of retinal gene therapy supports their use for treating Usher 1B. However, the likely generation of unknown fragments of the gene, in order to package it, may be somewhat disconcerting, even though no deleterious consequences were observed in mice or cultured RPE cells. Unfortunately, a dual AAV-*MYO7A* vector approach was not successful.

**Acknowledgment** We are grateful to Katie Binley and William Hauswirth, and their respective laboratories for discussions and collaborative research. We are supported by grants from the NIH and NNRI. DSW is a Jules and Doris Stein RPB Professor.

## References

1. Bainbridge JW, Ali RR (2008) Success in sight: the eyes have it! Ocular gene therapy trials for LCA look promising. Gene Ther 15(17):1191–1192
2. Cideciyan AV, Aleman TS, Boye SL, Schwartz SB, Kaushal S, Roman AJ et al (2008) Human gene therapy for RPE65 isomerase deficiency activates the retinoid cycle of vision but with slow rod kinetics. Proc Natl Acad Sci U S A 105(39):15112–15117
3. Maguire AM, High KA, Auricchio A, Wright JF, Pierce EA, Testa F et al (2009) Age-dependent effects of RPE65 gene therapy for Leber's congenital amaurosis: a phase 1 dose-escalation trial. Lancet 374(9701):1597–1605

4. Maguire AM, Simonelli F, Pierce EA, Pugh EN Jr, Mingozzi F, Bennicelli J et al (2008) Safety and efficacy of gene transfer for Leber's congenital amaurosis. N Engl J Med 358(21):2240–2248
5. Williams DS (2008) Usher syndrome: animal models, retinal function of Usher proteins, and prospects for gene therapy. Vision Res 48(3):433–441
6. Weil D, Blanchard S, Kaplan J, Guilford P, Gibson F, Walsh J et al (1995) Defective myosin VIIA gene responsible for Usher syndrome type 1B. Nature 374(6517):60–61
7. Williams DS, Lopes VS (2011) The many different cellular functions of MYO7A in the retina. Biochem Soc Trans 39(5):1207–1210
8. Jacobson SG, Cideciyan AV, Gibbs D, Sumaroka A, Roman AJ, Aleman TS et al (2011) Retinal disease course in Usher syndrome 1B due to MYO7A mutations. Invest Ophthalmol Vis Sci 52(11):7924–7936
9. Wu Z, Yang H, Colosi P (2010) Effect of genome size on AAV vector packaging. Mol Ther 18(1):80–86
10. Lopes VS, Boye SE, Louie CM, Boye S, Dyka F, Chiodo VA et al (2013) Retinal gene therapy with a large MYO7A cDNA using adeno-associated virus. Gene Ther 20(8):824–833
11. Miyoshi H, Takahashi M, Gage FH, Verma IM (1997) Stable and efficient gene transfer into the retina using an HIV-based lentiviral vector. Proc Natl Acad Sci U S A 94(19):10319–10323
12. Hashimoto T, Gibbs D, Lillo C, Azarian SM, Legacki E, Zhang XM et al (2007) Lentiviral gene replacement therapy of retinas in a mouse model for Usher syndrome type 1B. Gene Ther 14(7):584–594
13. Williams DS, Lopes VS (2012) Gene therapy strategies for Usher syndrome type 1B. Adv Exp Med Biol 723:235–242
14. Orten DJ, Weston MD, Kelley PM, Cremers CW, Wagenaar M, Jacobson SG et al (1999) Analysis of DNA elements that modulate myosin VIIA expression in humans. Hum Mutat 14(4):354
15. Tolmachova T, Tolmachov OE, Wavre-Shapton ST, Tracey-White D, Futter CE, Seabra MC (2012) CHM/REP1 cDNA delivery by lentiviral vectors provides functional expression of the transgene in the retinal pigment epithelium of choroideremia mice. J Gene Med 14(3):158–168
16. Papayannakos C, Daniel R (2013) Understanding lentiviral vector chromatin targeting: working to reduce insertional mutagenic potential for gene therapy. Gene Ther 20(6):581–588
17. Wanisch K, Yanez-Munoz RJ (2009) Integration-deficient lentiviral vectors: a slow coming of age. Mol Ther 17(8):1316–1332
18. Yanez-Munoz RJ, Balaggan KS, MacNeil A, Howe SJ, Schmidt M, Smith AJ et al (2006) Effective gene therapy with nonintegrating lentiviral vectors. Nat Med 12(3):348–353
19. Balaggan KS, Binley K, Esapa M, Iqball S, Askham Z, Kan O et al (2006) Stable and efficient intraocular gene transfer using pseudotyped EIAV lentiviral vectors. J Gene Med 8(3):275–285
20. Kong J, Kim SR, Binley K, Pata I, Doi K, Mannik J et al (2008) Correction of the disease phenotype in the mouse model of Stargardt disease by lentiviral gene therapy. Gene Ther 15(19):1311–1320
21. Themis M, Waddington SN, Schmidt M, von Kalle C, Wang Y, Al-Allaf F et al (2005) Oncogenesis following delivery of a nonprimate lentiviral gene therapy vector to fetal and neonatal mice. Mol Ther 12(4):763–771
22. Allocca M, Doria M, Petrillo M, Colella P, Garcia-Hoyos M, Gibbs D et al (2008) Serotype-dependent packaging of large genes in adeno-associated viral vectors results in effective gene delivery in mice. J Clin Invest 118(5):1955–1964
23. Dong B, Nakai H, Xiao W (2010) Characterization of genome integrity for oversized recombinant AAV vector. Mol Ther 18(1):87–92
24. Lai Y, Yue Y, Duan D (2010) Evidence for the failure of adeno-associated virus serotype 5 to package a viral genome > or = 8.2 kb. Mol Ther 18(1):75–79

25. Bostick B, Shin JH, Yue Y, Duan D (2011) AAV-microdystrophin therapy improves cardiac performance in aged female mdx mice. Mol Ther 19(10):1826–1832
26. Zhang Y, Duan D (2012) Novel mini-dystrophin gene dual adeno-associated virus vectors restore neuronal nitric oxide synthase expression at the sarcolemma. Hum Gene Ther 23(1):98–103
27. Duan D, Yue Y, Engelhardt JF (2001) Expanding AAV packaging capacity with trans-splicing or overlapping vectors: a quantitative comparison. Mol Ther 4(4):383–391
28. Ghosh A, Yue Y, Lai Y, Duan D (2008) A hybrid vector system expands adeno-associated viral vector packaging capacity in a transgene-independent manner. Mol Ther 16(1):124–130.

# Chapter 92
# Gene Therapy Restores Vision and Delays Degeneration in the CNGB1$^{-/-}$ Mouse Model of Retinitis Pigmentosa

**Stylianos Michalakis, Susanne Koch, Vithiyanjali Sothilingam, Marina Garcia Garrido, Naoyuki Tanimoto, Elisabeth Schulze, Elvir Becirovic, Fred Koch, Christina Seide, Susanne C. Beck, Mathias W. Seeliger, Regine Mühlfriedel and Martin Biel**

**Abstract** Retinitis pigmentosa (RP) is a severe retinal disease characterized by a progressive degeneration of rod photoreceptors and a secondary loss of cone function. Here, we used CNGB1-deficient (CNGB1$^{-/-}$) mice, a mouse model for autosomal recessive RP, to evaluate the efficacy of adeno-associated virus (AAV) vector-mediated gene therapy for the treatment of RP. The treatment restored normal expression of rod CNG channels and rod-driven light responses in the CNGB1$^{-/-}$ retina. This led to a substantial delay of retinal degeneration and long-term preservation of retinal morphology. Finally, treated CNGB1$^{-/-}$ mice performed significantly better than untreated mice in a rod-dependent vision-guided behavior test. In summary, this study holds promise for the treatment of rod channelopathy-associated retinitis pigmentosa by AAV-mediated gene replacement.

S. Michalakis (✉) · S. Koch · E. Schulze · E. Becirovic · F. Koch · M. Biel
Center for Integrated Protein Science Munich (CIPSM), Department of Pharmacy—Center for Drug Research, Ludwig-Maximilians-Universität München, Butenandtstr. 5-13, 81377 Munich, Germany
e-mail: michalakis@lmu.de

S. Koch
e-mail: susanne.koch@cup.lmu.de

V. Sothilingam · M. G. Garrido · N.Tanimoto · C. Seide · S. C. Beck · M. W. Seeliger · R. Mühlfriedel
Division of Ocular Neurodegeneration, Institute for Ophthalmic Research, Centre for Ophthalmology, University of Tübingen, Schleichstr. 4/3, 72076 Tübingen, Germany
e-mail: Vithiyanjali.Sothilingam@med.uni-tuebingen.de

M. G. Garrido
e-mail: Marina.Garcia-Garrido@med.uni-tuebingen.de

N. Tanimoto
e-mail: Naoyuki.Tanimoto@med.uni-tuebingen.de

E. Schulze
e-mail: elisabeth.schulze@cup.lmu.de

J. D. Ash et al. (eds.), *Retinal Degenerative Diseases,* Advances in Experimental Medicine and Biology 801, DOI 10.1007/978-1-4614-3209-8_92,

**Keywords** Rod photoreceptor · Retinitis pigmentosa · Gene therapy · Adeno-associated virus vector · Cyclic nucleotide-gated channel · Gene replacement

## 92.1 Introduction

Retinitis pigmentosa (RP) is a family of hereditary eye disorders characterized by progressive retinal degeneration [1, 2]. RP primarily affects rod photoreceptors, but secondary to rods, cone photoreceptors also degenerate. Accordingly, RP patients suffer from night blindness at disease onset, and finally, central vision is also impaired, leading eventually to complete blindness. RP is genetically very heterogeneous and currently more than 50 RP genes are known. Mutations in the genes encoding the two rod cyclic nucleotide-gated (CNG) channel subunits cause autosomal recessive RP (arRP) [3]. The rod CNG channel is a heterotetramer composed of three CNGA1 subunits and one CNGB1 subunit. Mutations in CNGB1 are found in approximately 4% of arRP cases [1]. Knockout of CNGB1 in mice results in a phenotype that recapitulates the principal pathology of RP patients [4, 5]. In the present study we used CNGB1 knockout mice as a model for RP to evaluate AAV-mediated gene therapy as a potential treatment of RP caused by rod photoreceptor-specific gene mutations.

## 92.2 Materials and Methods

### *92.2.1 Cloning, Production, and Delivery of rAAV Vectors*

Cloning and mutagenesis were performed by standard techniques. All sequence manipulations were confirmed by sequencing. To construct pAAV2.1-Rho-CNG-

E. Becirovic
e-mail: elvir.becirovic@cup.lmu.de

F. Koch
e-mail: fred.koch@cup.lmu.de

C. Seide
e-mail: Christina.Seide@med.uni-tuebingen.de

S. C. Beck
e-mail: Susanne.Beck@med.uni-tuebingen.de

M. W. Seeliger
e-mail: see@uni-tuebingen.de

R. Mühlfriedel
e-mail: regine.muehlfriedel@med.uni-tuebingen.de

M. Biel
e-mail: mbiel@cup.lmu.de

B1a-SV40, we inserted a PCR-amplified 471 bp (−386 to + 86) mouse rhodopsin promoter fragment [6] and a PCR-amplified 221 bp long SV40 late Poly A fragment and PCR-amplified full-length mouse CNGB1a cDNA (3978 bp) into pAAV2.1-mcs [7]. pAAV2/8 Y733F encoding a Y733F-modified AAV8 capsid was obtained by site-directed mutagenesis using wild-type pAAV2/8 as a template. Single-strand AAV vectors were produced as described previously [7]. Physical titers (in genome copies/ml) were determined by quantitative PCR of CNGB1. All primer sequences are available on request. Subretinal delivery procedures were described elsewhere [8].

### *92.2.2 Electroretinograms*

ERG analysis was performed at 6 weeks to 4 months after injection according to procedures described elsewhere [9].

### *92.2.3 Immunohistochemistry*

Immunohistochemical staining was performed at 40 days to 12 months post injection according to procedures described previously [10]. We used the following primary antibodies: rabbit anti-CNGB1 (C-AbmCNGB1 [4], 1 : 30,000), mouse anti-CNGA1 (2G11 [11], 1 : 30), and rabbit anti-cone arrestin ([9], 1 : 300). Laser scanning confocal micrographs was performed using a LSM 510 meta microscope (Carl Zeiss, Germany) and images are presented as collapsed confocal z-stacks. Stainings were reproduced in ≥ 3 independent experiments.

### *92.2.4 Visual Water Maze Task*

Mice were housed separately in an inverse 12 h light–dark cycle. The experiment was performed in the dark cycle. Mice were trained for 3 days (eight trials a day) to locate a stable platform (10 cm in diameter) at dim light conditions of 0.32 cd/m$^2$ to ensure that vision is totally confined to the rod system. The platform was placed in a circular swimming pool (120 cm in diameter, 70 cm high, white plastic) filled with water. The starting position of the mouse was changed from trial to trial in a pseudorandom order whereas the platform was kept in a constant location. Distal cues in the testing room and the water maze, such as patterned cardboards, were provided as spatial references. Trials were terminated if the mouse climbed onto the platform or when it swam for 2 min. If the mouse did not find the platform, it was gently placed on the stable platform. After each trial the mouse was left on the platform for 10 s undisturbed. The experiment was performed and analyzed blindly to the animal genotype.

## 92.3 Results

### *92.3.1 Restoration of CNG Channel Expression in Rod Outer Segments of CNGB1$^{-/-}$ Mice*

AAVs expressing CNGB1a under control of a rhodopsin promoter were injected into the subretinal space of 2-week-old CNGB1$^{-/-}$ mice. Forty days after delivery we detected virally encoded CNGB1a protein in the treated, but not the untreated part of the retina. Figure 92.1 shows representative confocal scans from the treated (panels a, d) and untreated regions (panels b, e) of a CNGB1$^{-/-}$ retina as well as from wild-type control retina (panels c, f) immunolabeled for CNGB1. The treatment not only restored expression of CNGB1a (Fig. 92.1a) but also the levels of the previously missing endogenous CNGA1 protein (Fig. 92.1d). Comparison with wild-type mice showed that the treatment led to almost wild-type levels of expression of CNGB1 and CNGA1 in treated CNGB1$^{-/-}$ mice (Fig. 92.1a, c–d).

### *92.3.2 Restoration of Rod Photoreceptor Function in Treated CNGB1$^{-/-}$ Mice*

To probe how the treatment affected the rod system activity, we tested 8-week-old CNGB1$^{-/-}$ mice in dark-adapted (scotopic) electroretinography (ERG). In contrast to non-injected eyes (untreated eyes, UEs), eyes of CNGB1$^{-/-}$ mice that had received injections of CNGB1a AAV vector (treated eyes, TEs) were able to generate characteristic responses to dim light stimuli ($-2.0$ log cd*s/m$^2$), reflecting improved rod system activity (Fig. 92.1g, h).

### *92.3.3 AAV Treatment Restores Rod-Mediated Vision in CNGB1$^{-/-}$ Mice*

We next used a water maze test to assess visual responsivity (see Materials and Methods). The mice were tested on three consecutive days in a water maze for their ability to navigate to a visible escape platform. The experiment was performed at dim light conditions to ensure that vision is totally conferred to the rod system. On day 1, wild-type mice needed $47.9 \pm 10.6$ s to navigate to the escape platform, but gradually improved their performance to $7.3 \pm 1.1$ s on day 3 (Fig. 92.1i). Untreated CNGB1$^{-/-}$ mice needed significantly longer than wild-type mice ($p < 0.001$, two-way ANOVA) (Fig. 92.1i). However, treated CNGB1$^{-/-}$ mice were clearly able to improve during the three test days (day 1: $59.7 \pm 11.0$ s; day 3: $23.1 \pm 4.7$ s; $p = 0.0127$, one-way ANOVA) and performed significantly better than untreated CNGB1$^{-/-}$ mice ($p = 0.0123$, two-way ANOVA) (Fig. 92.1i). Treated mice did not

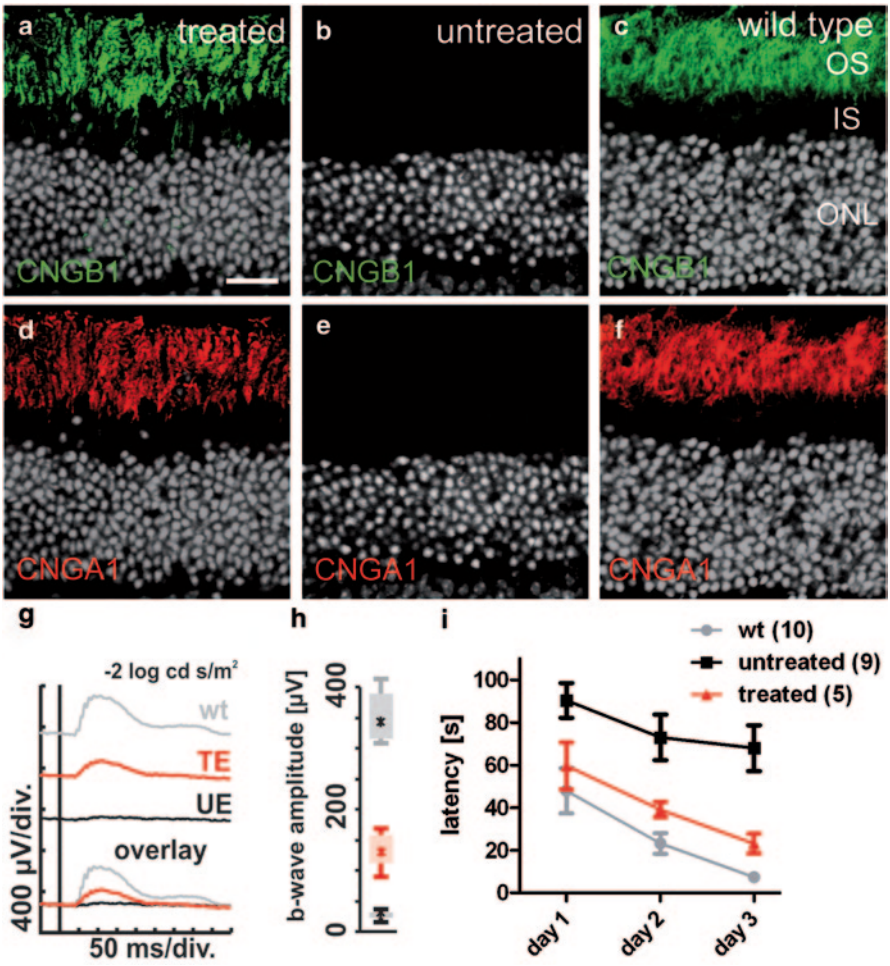


**Fig. 92.1** Gene replacement restores rod CNG channels and improves visual function in *CNGB1*$^{-/-}$ mice. **a**–**f** Confocal scans from retinal slices immunolabeled with antibodies specific for CNGB1a (*green*) and CNGA1 (*red*). The treatment results in expression of CNGB1a in rod outer segments of treated mice (**a**), which is absent in the untreated knockout retina (**b**). The CNGB1a expression levels in the treated knockout are comparable to wild type (**c**). The treatment also rescues the expression of *CNGA1* in rod outer segments (**d**), which is downregulated in the untreated knockout retina (**e**). Again, the levels of expression are comparable to wild type (**f**). Cell nuclei were stained with the nuclear dye Hoechst 33342 (*gray*). **g** Representative scotopic single flash ERG responses at −2 log cd*s/m$^2$ recorded from a wild-type (wt) eye, treated eye (TE), and untreated eye (UE). **h** The quantitative data of each group are shown as box-and-whisker plots. **i** Latency to locate a platform under dark conditions. In contrast to untreated *CNGB1*$^{-/-}$ mice (*black*), treated CNGB1$^{-/-}$ mice (*red*) significantly improved their performance during the three test days. Their performance did not significantly differ from wild-type control mice (*gray*). *IS*, photoreceptor inner segments; *ONL*, outer nuclear layer; *OS* photoreceptor outer segments. The scale bar marks 20 µm

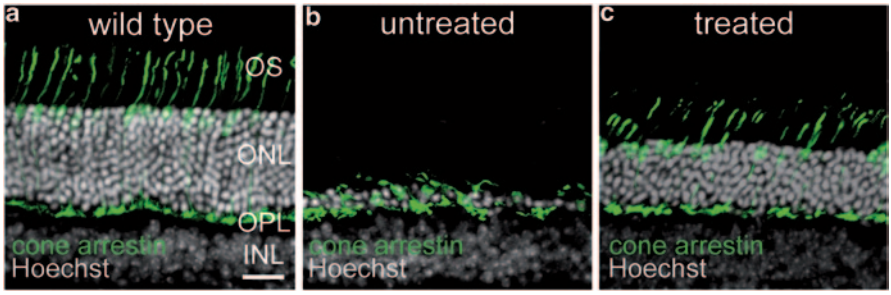


**Fig. 92.2** Long-term effect of gene therapy on photoreceptor degeneration in CNGB1$^{-/-}$ mice. **a–c** Confocal scans from retinal slices stained with the nuclear dye *Hoechst* 33342 (*gray*) and immunolabeled for the specific "cone marker" cone arrestin (*green*) demonstrate a beneficial effect of the treatment on photoreceptor cell loss and *ONL* thinning as well as cone morphology at 12 months. The scale bar marks 20 µm. *INL*, inner nuclear layer; *OPL*, outer plexiform layer; *ONL*, outer nuclear layer; *OS*, photoreceptor outer segments

significantly differ from wild type in their overall performance ($p=0.0834$, two-way ANOVA) (Fig. 92.1i).

### *92.3.4 Gene Therapy Delays Retinal Degeneration in CNGB1$^{-/-}$ Mice*

To test whether the treatment was able to delay the retinal degeneration in CNGB1$^{-/-}$ mice we isolated the retina at 12 months post injection and analyzed retinal histology. Figure 92.2 shows representative confocal scans from retinal slices of a treated knockout mouse 12 months after treatment labeled with the nuclear dye Hoechst 33342 and an antibody directed against the cone marker cone arrestin to reveal the thickness of retinal layers and the morphology of cone photoreceptors. The wild-type retina contains 11–12 rows of photoreceptors (Fig. 92.2a). The untreated region revealed the expected thinning of the outer nuclear layer (Fig. 92.2b). However, in the treated part 7–8 rows of photoreceptors remained indicating that the treatment significantly delayed photoreceptor cell loss (Fig. 92.2c). In addition, the treatment also resulted in significant preservation of cone photoreceptor morphology (Fig. 92.2a–c) confirming a beneficial effect on secondary cone degeneration.

## 92.4 Discussion

Until recently, RP has been considered to be incurable. With the advent of AAV-mediated gene replacement therapy, several groups succeeded in restoration of retinal function in RP animal models [12, 13]. In this study we present data on the successful restoration of vision in the CNGB1 knockout mouse model of RP us-

ing AAV-mediated gene therapy. The treatment resulted in efficient and long-term expression of high levels of full-length CNGB1a protein in rod outer segments. This led to significant preservation of outer segment morphology, a delay of retinal degeneration and long-term preservation of retinal morphology. Finally, the treatment significantly restored rod-driven light responses and improved rod-dependent vision-guided behavior.

Our data are very encouraging to launch AAV-based gene therapy studies in human patients suffering from CNG channelopathies.

**Acknowledgement** We thank James M. Wilson (University of Pennsylvania) and Alberto Auricchio (TIGEM) for the gift of AAV plasmids and Robert Molday (University of British Columbia) and Wolfgang Baehr (University of Utah) for the gift of antibodies. This work was supported by the Deutsche Forschungsgemeinschaft (DFG).

## References

1. Hartong DT, Berson EL, Dryja TP (2006) Retinitis pigmentosa. Lancet 368(9549):1795–1809
2. Sahel J, Bonnel S, Mrejen S, Paques M (2010) Retinitis pigmentosa and other dystrophies. Dev Ophthalmol 47:160–167
3. Biel M, Michalakis S (2007) Function and dysfunction of CNG channels: insights from channelopathies and mouse models. Mol Neurobiol 35(3):266–277
4. Hüttl S, Michalakis S, Seeliger M, Luo DG, Acar N, Geiger H et al (2005) Impaired channel targeting and retinal degeneration in mice lacking the cyclic nucleotide-gated channel subunit CNGB1. J Neurosci 25(1):130–138
5. Zhang Y, Molday LL, Molday RS, Sarfare SS, Woodruff ML, Fain GL et al (2009) Knockout of GARPs and the beta-subunit of the rod cGMP-gated channel disrupts disk morphogenesis and rod outer segment structural integrity. J Cell Sci 122(Pt 8):1192–1200
6. Flannery JG, Zolotukhin S, Vaquero MI, LaVail MM, Muzyczka N, Hauswirth WW (1997) Efficient photoreceptor-targeted gene expression in vivo by recombinant adeno-associated virus. Proc Natl Acad Sci U S A 94(13):6916–6921
7. Michalakis S, Mühlfriedel R, Tanimoto N, Krishnamoorthy V, Koch S, Fischer MD et al (2010) Restoration of cone vision in the CNGA3-/- mouse model of congenital complete lack of cone photoreceptor function. Mol Ther 18(12):2057–2063
8. Mühlfriedel R, Michalakis S, Garrido MG, Biel M, Seeliger MW (2013) Optimized technique for subretinal injections in mice. Methods Mol Biol 935:343–349
9. Tanimoto N, Muehlfriedel RL, Fischer MD, Fahl E, Humphries P, Biel M et al (2009) Vision tests in the mouse: functional phenotyping with electroretinography. Front Biosci 14:2730–2737
10. Michalakis S, Geiger H, Haverkamp S, Hofmann F, Gerstner A, Biel M (2005) Impaired opsin targeting and cone photoreceptor migration in the retina of mice lacking the cyclic nucleotide-gated channel CNGA3. Invest Ophthalmol Vis Sci 46(4):1516–1524
11. Molday RS, Molday LL, Dose A, Clark-Lewis I, Illing M, Cook NJ et al (1991) The cGMP-gated channel of the rod photoreceptor cell characterization and orientation of the amino terminus. J Biol Chem 266(32):21917–21922
12. den Hollander AI, Black A, Bennett J, Cremers FP (2010) Lighting a candle in the dark: advances in genetics and gene therapy of recessive retinal dystrophies. J Clin Invest 120(9):3042–3053
13. Smith AJ, Bainbridge JW, Ali RR (2012) Gene supplementation therapy for recessive forms of inherited retinal dystrophies. Gene Ther 19(2):154–161

# Chapter 93
# Therapy Strategies for Usher Syndrome Type 1C in the Retina

**Kerstin Nagel-Wolfrum, Timor Baasov and Uwe Wolfrum**

**Abstract** The Usher syndrome (USH) is the most common form of inherited deaf-blindness with a prevalence of ~1/6,000. Three clinical subtypes (USH1–USH3) are defined according to the severity of the hearing impairment, the presence or absence of vestibular dysfunction and the age of onset of retinitis pigmentosa (RP). USH1 is the most severe subtype with congenital severe to profound hearing loss and onset of RP before puberty. Currently only the amelioration of the hearing deficiency is implemented, but no treatment of the senso-neuronal degeneration in the eye exists.

In our studies we are focusing on the evaluation of gene-based therapies to cure the retinal degeneration of USH1C patients: (i) gene augmentation using recombinant adeno-associated virus, (ii) genome editing by homologous recombination mediated by zinc-finger nucleases and, (iii) read-through therapy using novel designer aminoglycosides and PTC124. Latter compounds target in-frame nonsense mutations which account for ~20 % of all USH cases.

All analyzed gene-based therapy strategies lead to the restoration of USH protein expression. These adjustments may be sufficient to reduce the progression of retinal degeneration, which would greatly improve the life quality of USH patients.

**Keywords** Retinal gene therapy gene addition · Gene editing · Translational read-through · Aminoglycosides · Deaf-blindness

K. Nagel-Wolfrum (✉) · U. Wolfrum
Department of Cell and Matrix Biology, Institute of Zoology,
Johannes Gutenberg University of Mainz, 55099 Mainz, Germany
e-mail: nagelwol@uni-mainz.de

U. Wolfrum
e-mail: wolfrum@uni-mainz.de

T. Baasov
Edith and Joseph Fischer Enzyme Inhibitors Laboratory, Schulich Faculty of Chemistry,
Technion-Israel Institute of Technology, Haifa, Israel
e-mail: chtimor@techunix.technion.ac.il

J. D. Ash et al. (eds.), *Retinal Degenerative Diseases,* Advances in Experimental Medicine and Biology 801, DOI 10.1007/978-1-4614-3209-8_93,

**Abbreviations**

| | |
|---|---|
| AAV | Adeno-associated viruses |
| HR | Homologous recombination |
| RP | Retinitis pigmentosa |
| TR | Translational read-through |
| TRIDs | Translational read-through inducing drugs |
| USH | User syndrome |
| ZFN | Zinc finger nucleases |

## 93.1 Introduction

The human Usher syndrome (USH) is the most frequent cause of combined deaf-blindness in man [1]. It is clinically and genetically heterogeneous and subdivided into three clinical USH types. USH1–USH3 differ in the severity of the symptoms namely hearing loss, balance problems, and retinal degeneration (*retinitis pigmentosa*), as well as the progression of the disease. Molecular analyses have demonstrated that functionally different USH proteins are organized in networks in the eye and the inner ear [1]. This knowledge explains why defects in proteins of different families are causative for similar symptoms.

Currently, the auditory deficit in USH can be compensated with hearing aids and cochlear implants [2]. In contrast, to date there is no therapy for the ophthalmic component of USH. Since all USH proteins are organized in protein networks, the lack of a specific protein may result in the disruption of the entire USH protein network, causing senso-neuronal degeneration in the inner ear and retina. Consequently, restoring the USH protein expression should reverse the clinical phenotype. The identification of USH genes in combination with patient screening has provided detailed knowledge about mutations in the genes causing USH, allowing the development of gene-specific therapies. Such personalized gene-based therapies include gene augmentation and genome editing induced by homologous recombination mediated by zinc finger nucleases. In addition, for nonsense mutations the application of novel translational read-through inducing drugs, like PTC124 or designer aminoglycosides are promising treatment options.

## 93.2 Gene Augmentation

Gene augmentation is based on the exogenous replacement of a mutated gene by a functional copy. It is certainly attractive for the treatment of hereditary retinal degenerations in general [2]. The subretinal injection of adeno-associated viruses (AAV) carrying the *RPR65* gene in patients with Leber congenital amaurosis already showed promising results in vision improvement [3]. However, both the

differentially expressed splice variants and the enormous size of several USH genes hamper gene augmentation for most genetic USH subtypes [2]. In particular, our transcriptome analysis in human retinas demonstrates that *USH1C* is transcribed in various harmonin isoforms [4]. The ambiguity concerning the activities of different harmonin isoforms makes *USH1C* a difficult target for gene augmentation. Therefore, alternative strategies are necessary for USH to enable at least some translation of functional protein from mutated genes which may delay the onset and/or progression of RP in USH patients. In this chapter we will provide recent findings for two alternatives therapy strategies focussing on a specific USH1C causing in-frame nonsense mutation namely the p.R31X mutation. The point mutation alters the wild-type cytosine at position 91 to a thymine, consequently the arginine (R) codon CGA is altered to the premature TGA (X) stop codon. The transcription/translation of this mutated *USH1C* gene results in a non-functional harmonin protein.

## 93.3 Genome Editing by Homologous Recombination Mediated by Zinc Finger Nucleases

The most elegant way of a therapy for USH is to repair the mutated gene on the genomic level. Genome editing, synonymic called gene repair can be achieved by homologous recombination (HR) which is a cell autonomous repair mechanism activated following a double strand break. However, under normal conditions HR occurs at a very low frequency and consequently cannot be applied for therapeutic approaches [5]. The efficiency can be increased by introducing double-strand breaks close to the mutation in the genome using zinc finger nucleases (ZFNs) [2, 5]. ZFNs are hybrid proteins composed of an engineered zinc finger DNA-binding domain, designed to bind to a specific target sequence and the non-specific cleavage domain of the FokI endonuclease (Fig. 93.1a). Proximate to the ZFN mediated DNA cleavage an exogenously introduced donor plasmid coding for the healthy gene replaces the mutated genomic DNA by HR.

In a recent study we demonstrated for the first time ZFN activated genome editing of the p.R31X mutation in the *USH1C* gene [6]. We specifically designed ZFN for the p.R31X mutation and proved ZFN mediated genome editing of the mutated *USH1C* in a cellular reporter system. We showed ZFNs induced DNA cleavage of their target sequence and demonstrated that simultaneous application of ZFN and donor DNA induce the repair of the disease causing nonsense mutation in the genomic context. Finally, we confirmed the recovery of the expression of the *USH1C* gene product harmonin (Fig. 93.1b).

Genome editing of the disease causing mutation in the endogenous context using ZFN or TAL effector nucleases, which are an alternative molecular scissor [7], are the most effective and elegant way to cure USH. Nevertheless, this strategy is far from being applied in patients and a lot of efforts have to be made to proceed in the direction of clinical trials.

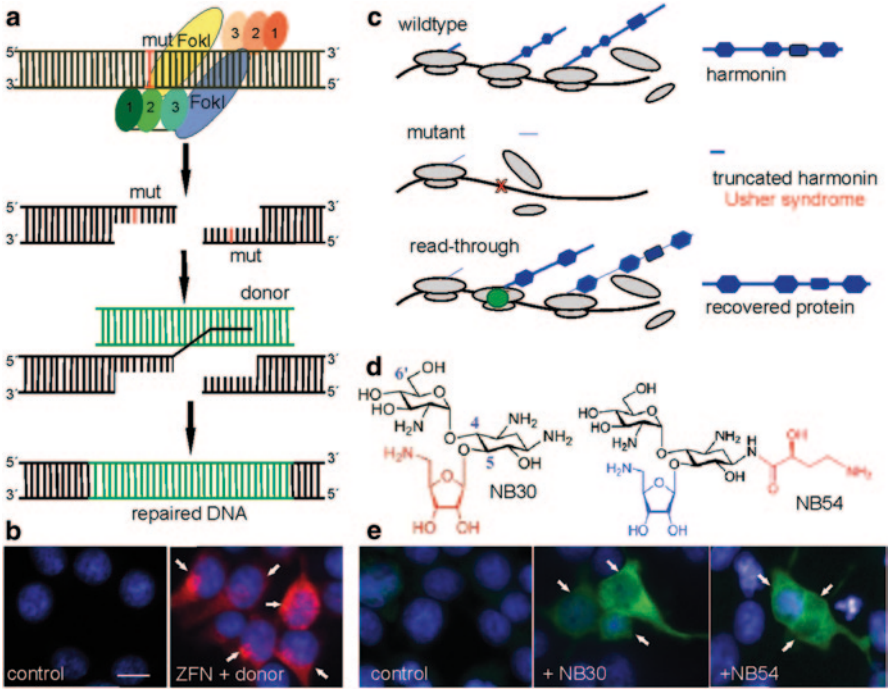


**Fig. 93.1** Mechanism of genome editing and translational read-through. **a** Genome editing. A pair of zinc finger nucleases (*ZFN*) binds to the DNA close to the mutation (*mut*), cause a double strand break and thereby activate homologous recombination. For DNA repair an introduced non-mutated donor DNA is used as template. **b** Restored harmonin expression in cells co-transfected with *ZFN* and *donor* (*arrows*). **c** Translational read-through (TR). Full-length protein is generated by the translation of mRNA. A nonsense mutation (*cross*) induces a premature stop of protein translation leading to a truncated and non-functional polypeptide. TRIDs (*circle*) allow the TR of the nonsense mutation resulting in full-length protein. **d** Chemical structures of the redesigned aminoglycosides. **e** Restored harmonin expression in cells treated with *NB30* or *NB54* (*arrows*)

## 93.4 Translational Read-Through of Nonsense Mutations

Translational read-through (TR) was identified as an innovative therapy for several non-ocular genetic diseases caused by in-frame nonsense mutations [8]. TR mediates the over read of nonsense mutations thereby inducing the expression of full-length functional proteins (Fig. 93.1c). So far, various chemicals, called TR inducing drugs (TRIDs), are known to promote TR. Known TRIDs include clinically used aminoglycoside antibiotics like gentamicin, designer aminoglycosides like NB30 or NB54, and the chemical compound PTC124 [8–15]. For PTC124 encouraging results already have paved the way to clinical trials on patients suffering from Duchenne muscular dystrophy and cystic fibrosis [16]. The use of clinically approved aminoglycosides for the read-through therapy is limited due to their unsatisfactory biocompatibility [17, 18]. As these side effects are unrelated to their

induced TR activity, we optimized the structure–activity–toxicity relationship of the paromamine scaffold resulting in the designer aminoglycosides of the first generation (NB30) and second generation (NB54) (Fig. 93.1d) [9, 13]. Previous studies demonstrated the sustained TR activity and reduced toxicity of the redesigned aminoglycosides compared to their parental substance [11, 15, 19]. In our most recent study we compared the relative efficacies of NB30, NB54, and the clinically approved PTC124 with regard to induce TR of the p.R31X mutation in *USH1C* and their retinal biocompatibility [13]. In cell culture experiments application of the designer aminoglycosides and the clinically approved PTC124 did not result in significant differences in the TR efficacy of the harmonin a1 and b3 isoforms (Fig. 93.1e). Furthermore, all three TRIDs restored the functionality of the different harmonin isoforms: the known interaction of harmonin a1 with the protein USH2a protein and the ability of harmonin b to bundle actin filaments.

In addition to TR efficacy biocompatibility of TRIDs in tissues and the organism is an important concern for read-through therapy. In previous independent studies systemic application of NB30, NB54, and PTC124 was analyzed [10, 19, 16]. To identify the TRID with the best safety profile for the treatment of retinal diseases we directly compared the retinal biocompatibility of the TRIDs in murine and human organotypic retina cultures [15]. No apparent difference in the retinal integrity was observed. However, the designer aminoglycoside of the first generation (NB30) increased the number of apoptotic nuclei (TUNEL assay) in retinal cultures. In contrast, the designer aminoglycoside of the second generation NB54 and PTC124 had an excellent retinal biocompatibility. Importantly, we observed no significant difference in retinal biocompatibility between NB54 and the clinical approved PTC124. These data underline the effectiveness and the importance of the continuous redesigning of aminoglycosides to TRIDs with even better TR activity and reduced toxicity.

The in vivo efficacy of NB54 and PTC124 was already demonstrated in several animal models of non-ocular diseases [16, 19, 20]. Our comparison of the in vivo administration of the redesigned NB54 and PTC124 in an USH1C mouse model revealed that both TRIDs increased TR of full-length harmonin a1 expression with the same efficacy.

Designer aminoglycosides of the second generation and PTC124 are currently considered as therapeutic agents to treat USH since in-frame nonsense mutations account for approximately 20 % of all USH cases [2]. Furthermore TRIDs serve as potential drugs for the treatment of genetic diseases caused by nonsense mutations.

## 93.5 Conclusion

Gene-based therapies are promising strategies for the retinal degeneration of USH patients. Recent success in gene augmentation approaches in other retinal dystrophies give hope for the cure of USH-related retinal degeneration. The combination of preclinical data related to USH as well as the outcome of clinical trials with

PTC124 in non-ocular diseases raise hope for near future treatment of the retinal degeneration of USH patients.

**Supports** DFG; EU/FP7 “SYSCILIA”, EU/FP7 “TREATRUSH”; FAUN-Stiftung, Nuremberg; Foundation Fighting Blindness; Forschung contra Blindheit; German Ministry of Education and Research, under the frame of E-Rare-2, the ERA-Net for Research on Rare Diseases.

## References

1. Wolfrum U (2011) Protein networks related to the Usher syndrome gain insights in the molecular basis of the disease. In: Satpal A (ed) Usher syndrome: pathogenesis, diagnosis and therapy. Nova Science Publishers, USA, pp 51–73
2. Overlack N, Goldmann T, Wolfrum U, Nagel-Wolfrum K (2011) Current therapeutic strategies for human Usher syndrome. In: Ahuja S (ed) Usher syndrome: pathogenesis, diagnosis and therapy. Nova Science Publishers, Inc. USA, pp 377–395
3. den Hollander AI, Black A, Bennett J, Cremers FP (2010) Lighting a candle in the dark: advances in genetics and gene therapy of recessive retinal dystrophies. J Clin Invest 120:3042–3053
4. Nagel-Wolfrum K, Becker M, Goldmann T, Muller C, Vetter J, Wolfrum U (2011) USH1C Transcripts and harmonin protein expression in human retina. Invest Ophthalmol Vis Sci 52:45
5. Händel EM, Cathomen T (2011) Zinc-finger nuclease based genome surgery: it’s all about specificity. Curr Gene Ther 11:28–37
6. Overlack N, Goldmann T, Wolfrum U, Nagel-Wolfrum K (2012) Gene repair of an Usher syndrome causing mutation by zinc-finger nuclease mediated homologous recombination. Invest Ophthalmol Vis Sci 53:4140–4146
7. Christian M, Cermak T, Doyle EL, Schmidt C, Zhang F, Hummel A, Bogdanove AJ, Voytas DF (2010) Targeting DNA double-strand breaks with TAL effector nucleases. Genetics 186:757–761
8. Keeling KM, Bedwell DM (2011) Suppression of nonsense mutations as a therapeutic approach to treat genetic diseases. Wiley Interdiscip Rev RNA 2:837–852
9. Nudelman I, Rebibo-Sabbah A, Shallom-Shezifi D, Hainrichson M, Stahl I, Ben Yosef T, Baasov T (2006) Redesign of aminoglycosides for treatment of human genetic diseases caused by premature stop mutations. Bioorg Med Chem Lett 16:6310–6315
10. Rebibo-Sabbah A, Nudelman I, Ahmed ZM, Baasov T, Ben Yosef T (2007) In vitro and ex vivo suppression by aminoglycosides of PCDH15 nonsense mutations underlying type 1 Usher syndrome. Hum Genet 122:373–381
11. Goldmann T, Rebibo-Sabbah A, Overlack N, Nudelman I, Belakhov V, Baasov T et al (2010) Beneficial read-through of a USH1C nonsense mutation by designed aminoglycoside NB30 in the retina. Invest Ophth Vis Sci 51:6671–6680
12. Hainrichson M, Nudelman I, Baasov T (2008) Designer aminoglycosides: the race to develop improved antibiotics and compounds for the treatment of human genetic diseases. Org Biomol Chem 6:227–239
13. Nudelman I, Rebibo-Sabbah A, Cherniavsky M, Belakhov V, Hainrichson M, Chen F et al (2009) Development of novel aminoglycoside (NB54) with reduced toxicity and enhanced suppression of disease-causing premature stop mutations. J Med Chem 52:2836–2845
14. Goldmann T, Overlack N, Wolfrum U, Nagel-Wolfrum K (2011) PTC124-Mediated translational readthrough of a nonsense mutation causing Usher syndrome type 1C. Hum Gene Ther 22:537–547
15. Goldmann T, Overlack N, Moller F, Belakhov V, van Wyk M, Baasov T et al (2012) A comparative evaluation of NB30, NB54 and PTC124 in translational read-through efficacy for treatment of an USH1C nonsense mutation. Embo Mol Med 4:1186–1199

16. Peltz SW, Morsy M, Welch EM, Jacobson A (2012) Ataluren as an agent for therapeutic nonsense suppression. Annu Rev Med 64:407–425
17. Lopez-Novoa JM, Quiros Y, Vicente L, Morales AI, Lopez-Hernandez FJ (2011) New insights into the mechanism of aminoglycoside nephrotoxicity: an integrative point of view. Kidney Int 79:33–45
18. Warchol ME (2010) Cellular mechanisms of aminoglycoside ototoxicity. Curr Opin Otolaryngol Head Neck Surg 18:454–458
19. Rowe SM, Sloane P, Tang LP, Backer K, Mazur M, Buckley-Lanier J, Nudelman I, Belakhov V, Bebok Z, Schwiebert E et al (2011) Suppression of CFTR premature termination codons and rescue of CFTR protein and function by the synthetic aminoglycoside NB54. J Mol Med 89:1140–1161
20. Wang D, Belakhov V, Kandasamy J, Baasov T, Li SC, Li YT, Bedwell DM, Keeling KM (2012) The designer aminoglycoside NB84 significantly reduces glycosaminoglycan accumulation associated with MPS I-H in the Idua-W392X mouse. Mol Genet Metab 105:116–125

# Part XI
# Therapy: Protection

# Chapter 94
# Nipradilol Promotes Axon Regeneration Through S-Nitrosylation of PTEN in Retinal Ganglion Cells

**Yoshiki Koriyama, Marie Kamiya, Kunizo Arai, Kayo Sugitani, Kazuhiro Ogai and Satoru Kato**

**Abstract** Nipradilol (Nip) is registered as an anti-glaucoma agent. More recently, a protective effect of Nip has been demonstrated in retinal ganglion cells (RGCs) mediated by S-nitrosylation of antioxidative-related Keap1 protein due to its nitric oxide (NO)-donating effect. It also has been reported that Nip promoted axon outgrowth in cat RGCs. However, the detailed mechanism remains unclear. NO physiologically regulates numerous cellular responses through S-nitrosylation of protein at cysteine residues. It has been reported that phosphatase and tensin homologue deleted on chromosome 10 (PTEN) deletion strongly showed axon regeneration after optic nerve injury. PTEN inactivation by S-nitrosylation results in the accumulation of phosphatidylinositol (3, 4, 5) triphosphate ($PIP_3$) and the activation of Akt/mammalian target of rapamycin (mTOR) signaling. The ribosomal S6 kinase 1 (S6K) which can monitor as phospho-S6 (pS6) is one of major target of mTOR. In this study, we investigated the possibility that Nip can promote axon outgrowth in RGCs by Akt/mTOR signaling thorough S-nitrosylation of PTEN.

Y. Koriyama (✉) · S. Kato
Department of Molecular Neurobiology, Graduate School of Medicine,
Kanazawa University, 13-1 Takaramachi,
Kanazawa 920-8640, Japan
e-mail: koriyama@med.kanazawa-u.ac.jp

S. Kato
e-mail: satoru@med.kanazawa-u.ac.jp

M. Kamiya · K. Arai
Department of Clinical Drug Informatics, Faculty of Pharmacy, Institute of Medical,
Pharmaceutical and Health Sciences, Kanazawa University, Kanazawa, Japan
e-mail: marie33@stu.kanazawa-u.ac.jp

K. Sugitani · K. Ogai
Division of Health Sciences, Graduate School of Medicine, Kanazawa University,
Kanazawa, Japan
e-mail: sugitani@staff.kanazawa-u.ac.jp

K. Ogai
e-mail: kazu0208@stu.kanazawa-u.ac.jp

J. D. Ash et al. (eds.), *Retinal Degenerative Diseases,* Advances in Experimental Medicine and Biology 801, DOI 10.1007/978-1-4614-3209-8_94,

**Keywords** Optic nerve regeneration · S-nitrosylation · Nipradilol · Retinal ganglion cells · PTEN · mTOR

## 94.1 Introduction

Nipradilol (Nip), which has α1- and β-adrenoceptor antagonist and nitric oxide (NO)-donating properties has clinically been used as an anti-glaucomatous agent [1–3]. NO mediates cellular signaling pathways that regulate physiological functions. The major signaling mechanisms mediated by NO are cGMP-dependent signaling and protein S-nitrosylation-dependent signalings. Nip has been described as having neuritogenic action in cat retinal ganglion cells (RGCs). However, the mechanism of Nip-induced optic nerve regeneration has not been fully elucidated. PTEN inactivation by S-nitrosylation results in the activation of Akt/mammalian target of rapamycin (mTOR) signaling [4]. Deletion of the *pten* gene in RGCs is enough to promote significant optic nerve regeneration, in part by increasing protein translation through mTOR pathway [5]. In this study, we investigated whether Nip can promote axon outgrowth in RGCs through Akt/mTOR signaling by S-nitrosylation of PTEN.

## 94.2 Materials and Methods

### *94.2.1 Cell Culture*

The cell line RGC-5, a transformed cell line with some ganglion cell characteristics, were cultured in low-glucose Dulbecco's modified Eagle's medium (DMEM) containing 10 % fetal bovine serum (FBS), penicillin, and streptomycin. Then, cells were cultured in medium containing 1 % FBS and 400 nM staurosporine to prevent over-proliferation and differentiation [6] before assessment of neurite outgrowth. To quantify neurite outgrowth, 20 random images were obtained per plate, and cells bearing processes 2-fold longer than the cell body were considered as positive [7].

### *94.2.2 S-Nitrosylation Analysis of PTEN*

S-nitrosylation of PTEN was assessed by a modified biotin switch assay [8] using the S-nitrosylated Protein Detection Assay Kit (Cayman Chemical, Ann Arbor, MI, USA). RGC-5 cells, exposed to 2-(4-carboxyphenyl)-4,4,5,5-tetramethylimidazoline-1-oxyl-3-oxide (c-PTIO, a NO scavenger) or dithiothreitol (DTT, an inhibitor of S-nitrosylation) for 1 h, were harvested and lysed with buffer at 4 °C. Biotinylated proteins were further purified by overnight incubation with Neutravidin-coupled

agarose beads (Pierce-Thermo Scientific). The quantity of S-nitrosylated PTEN protein in the samples was analyzed by western blot using anti-PTEN antibody (Cell Signaling Technology, USA).

### *94.2.3 Immunohistochemistry*

Tissue fixation and cryosectioning were performed as previously described [9]. Briefly, the eyes and optic nerves were isolated and fixed in 4% paraformaldehyde (PFA) containing 0.1 M phosphate buffer (pH 7.4) and 5% sucrose for 2 h at 4 °C. Sucrose concentration was gradually increased to 30%. The eyes were cryosectioned at 12 μm thickness. The frozen retinal sections were incubated with primary anti-pAkt, anti-pS6, and anti-NeuN antibodies. The sections were then incubated with Alexafluoro anti-IgG (Molecular probe, Eugene, OR, USA).

### *94.2.4 Observation of Optic Nerve Regeneration in Vivo*

Mice were sacrificed at 14 days after optic nerve injury and were perfused with 4% PFA. Regenerating optic axons were visualized by staining with mouse anti-GAP43 antibody (Santa Cruz Biotechnology, Santa Cruz, CA) followed by a fluorescently-labeled secondary antibody.

## 94.3 Results

### *94.3.1 Nip Promotes Axonal Outgrowth in RGC-5 Cells*

In previous paper, we tested that Nip (20 μM) could generate NO in RGC-5 cells [10]. At 20 μM, Nip significantly enhanced neurite outgrowth from RGC-5 cells within 24 h (Figs. 94.1b, d) compared to no treatment control (Figs. 94.1a, d). However, an mTOR inhibitor, rapamycin at 1 nM cancelled significant neurite outgrowth by Nip to the control levels (Figs. 94.1c, d). Either c-PTIO, a NO scavenger or S-nitrosylation inhibitor, DTT suppressed Nip-induced neurite outgrowth (Fig. 94.1d). Treatment of each reagent, rapamycin or DTT alone did not affect the neurite outgrowth of control (data not shown).

### *94.3.2 Nip S-Nitrosylates PTEN in RGC-5 Cells*

Nip increased S-nitrosylated PTEN 1.5-fold compared with no treatment (Fig. 94.2). The increase of S-nitrosylation of PTEN by Nip was significantly suppressed by pretreatment with either c-PTIO or DTT.

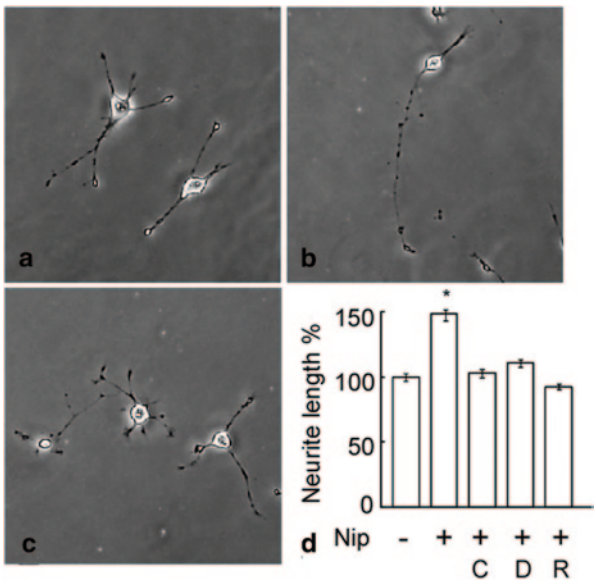


**Fig. 94.1** Nitric oxide/S-nitrosylation-dependent neurite outgrowth by *Nip*. **a-c** Photomicrographs of neurite outgrowth promotion in RGC-5 cells. **a** Control. Scale = 20 μm. **b** 20 μM Nip. **c** *Nip* plus rapamycin at 1 nM. **d** Quantification of neurite outgrowth by *Nip* (20 μM). c-PTIO (*C*: 100 μM), DTT (*D*: 1 mM), rapamycin (*R*: 1 nM) significantly inhibited neurite outgrowth by *Nip*. **p* < 0.01 vs control (*n* = 100)

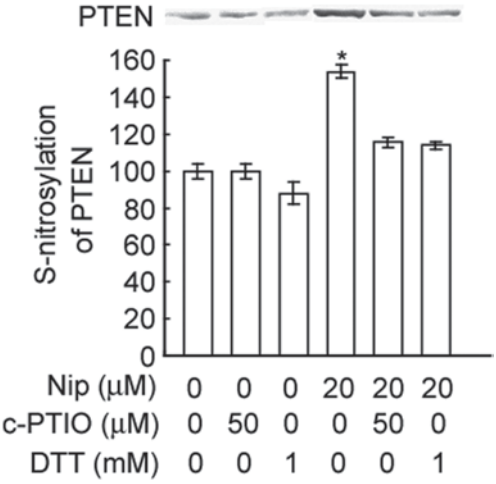


**Fig. 94.2** S-nitrosylation of *PTEN* by *Nip*. RGC-5 cells were exposed to *Nip* for 1 h and analyzed by biotin-switch assay. *Nip* at 20 μM significantly S-nitrosylated *PTEN*. Either *c-PTIO* or *DTT* completely inhibited the *PTEN* S-nitrosylation by *Nip*. **p* < 0.01 vs control (*n* = 3)

### *94.3.3 Nip Activates Akt and mTOR Signaling in Mouse RGCs*

The changes of phosphorylation of Akt or S6 in RGCs were examined for 5 days after treatment of Nip (Figs. 94.3a–c). The localizations of Akt or S6 activation were confirmed by anti-NeuN, a potent marker of RGCs. Intraocular injection of Nip increased Akt activation in RGCs at 1 day post-treatment (Figs. 94.3a, c) and the levels were gradually returned to normal levels by day 5 post-treatment (Fig. 94.3c). Phosphorylation of S6 levels also peaked in RGCs at 1 day and decreased by 5 days after Nip treatment (Figs. 94.3b and c).

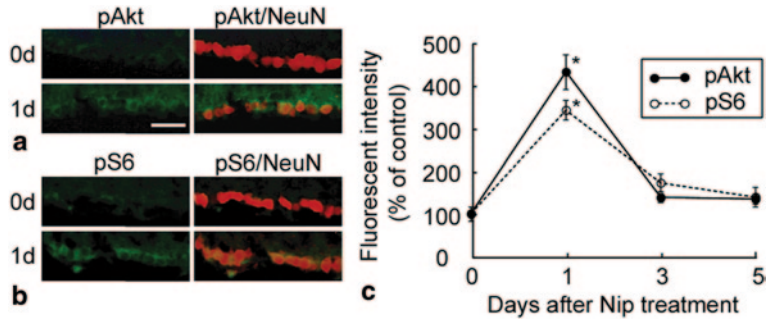


**Fig. 94.3** Cell signaling by intraocular injection of Nip in mouse RGCs. **a** Nip induced *Akt* phosphorylation at 1 days after injection in RGCs. Scale = 50 μm. **b** Nip induced *S6* phosphorylation at 1 days after injection in RGCs. **c** The levels of *pAkt* and *pS6* expression were quantified by analysis of fluorescence intensity and represented on the graph. *$p < 0.01$ vs 0 days ($n = 10$)

### *94.3.4 Nip-Induced Optic Nerve Regeneration*

We further confirmed optic nerve regeneration by Nip after injury. Longitudinal sections through the adult mouse optic nerve showing GAP-43 positive axons extending into the distal injury site (asterisks) at 2 weeks after optic nerve injury. Intraocular Nip induced optic nerve regeneration in vivo (Fig. 94.4b) compared to the injured optic nerve (Fig. 94.4a).

## 94.4 Discussion

Nip has vasodilator activity owing to NO released from its nitroxyl moiety [1]. Nip lowers intraocular pressure via selective α1-adrenoceptor [2] and non-selective β-adrenoceptor [3] antagonist properties. In the study of CNS regeneration, NO has been linked to numerous physiological and pathophysiological events on axonal outgrowth through cGMP dependent pathway [11]. However, whether NO/S-nitrosylation signaling is important for axonal regeneration is unclear. It has been reported that Nip promoted axon outgrowth in cat RGCs [12, 13]. As denitronipradilol could not induce axonal regeneration, the effect seems to be mediated by NO-dependent pathway. However, the detailed mechanism remains unclear. We focused on the molecule which is involved in axonal regeneration and its activities are controlled by S-nitrosylation of the cysteine residues. PTEN/mTOR is critical for controlling the regenerative capacity of mouse RGCs and corticospinal neurons [5, 14]. It has been reported that S-nitrosylation of PTEN activated PI3K and its downstream pathway [4, 15]. In this study, we could show the correlation between Akt/mTOR activities and optic nerve regeneration through S-nitrosylation of PTEN in RGCs. We already reported that the neuroprotective action of Nip is caused by induction of the antioxidant protein, heme oxygenase-1 in RGC-5 cells through

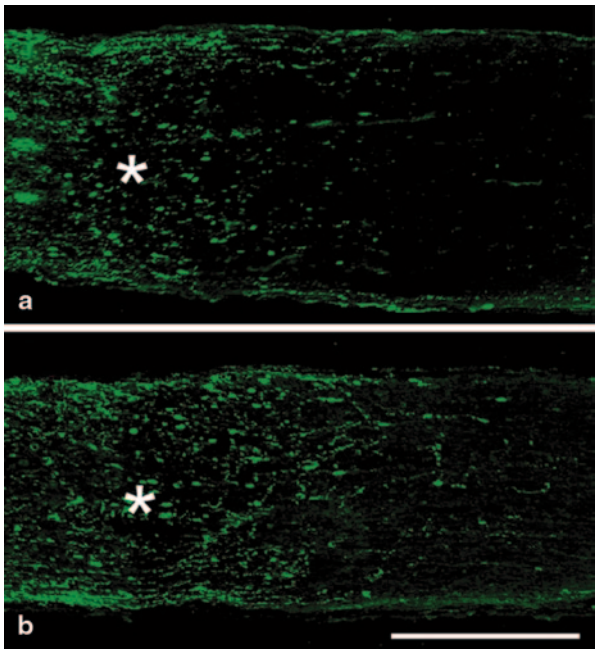


**Fig. 94.4** Nip-induced mouse optic nerve regeneration in vivo. Longitudinal sections of the mouse optic nerve showing GAP-43 positive axons extending proximally over the injury site (*asterisks*) at 2 weeks after optic nerve injury. Scale = 250 μm

activation of the Keap1/Nrf2 pathway by Keap1 S-nitrosylation [10]. The both neuroprotective and neuritogenic activities of Nip could be a new target for the regeneration of retinal ganglion cells after glaucomatous conditions.

## References

1. Adachi T, Hori S, Miyazaki K, Takahashi E, Nakagawa M, Udagawa A, Hayashi N, Aikawa N, Ogawa S (1995) Rapid increase in plasma nitrite concentration following intravenous administration of nipradilol. Eur J Pharmacol 286:201–204
2. Kou K, Ibengwe J, Suzuki H (1984) Effects of alpha-adrenoceptor antagonists on electrical and mechanical responses of the isolated dog mesenteric vein to perivascular nerve stimulation and exogenous noradrenaline. Naunyn Schmiedebergs Arch Pharmacol 326:7–13
3. Uchida Y, Nakamura M, Shimizu S, Shirasawa Y, Fujii M (1983) Vasoactive and beta-adrenoceptor blocking properties of 3,4-dihydro-8-(2-hydroxy-3-isopropylamino) propoxy-3-nitroxy-2H-1-benzopyran (K-351), a new antihypertensive agent. Arch Int Pharmacodyn Ther 262:132–149
4. Numajiri N, Takasawa K, Nishiya T, Tanaka H, Ohno K, Hayakawa W, Asada M, Matsuda H, Azumi K, Kamata H, Nakamura T, Hara H, Minami M, Lipton SA, Uehara T (2011) On-off system for PI3-kinase-Akt signaling through S-nitrosylation of phosphatase with sequence homology to tensin (PTEN). Proc Natl Acad Sci USA 108:10349–10354
5. Park KK, Liu K, Hu Y, Smith PD, Wang C, Cai B, Xu B, Connolly L, Kramvis I, Sahin M, He Z (2008) Promoting axon regeneration in the adult CNS by modulation of the PTEN/mTOR pathway. Science 322:963–966

6. Ganapathy PS, Dun Y, Ha Y, Duplantier J, Allen JB, Farooq A, Bozard BR, Smith SB (2010) Sensitivity of staurosporine-induced differentiated RGC-5 cells to homocysteine. Curr Eye Res 35:80–90
7. Koriyama Y, Takagi Y, Chiba K, Yamazaki M, Arai K, Matsukawa T, Suzuki H, Sugitani K, Kagechika H, Kato S (2011) Neuritogenic activity of a genipin derivative in retinal ganglion cells is mediated by retinoic acid receptor β expression through nitric oxide/S-nitrosylation signaling. J Neurochem 119:1232–1242
8. Jaffrey SR, Erdjument-Bromage H, Ferris CD, Tempst P, Snyder SH (2001) Protein S-nitrosylation: a physiological signal for neuronal nitric oxide. Nat Cell Biol 3:193–197
9. Koriyama Y, Ohno M, Kimura T, Kato S (2009) Neuroprotective effects of 5-S-GAD against oxidative stress-induced apoptosis in RGC-5 cells. Brain Res 1296:187–195
10. Koriyama Y, Kamiya M, Takadera T, Arai K, Sugitani K, Ogai K, Kato S (2012) Protective action of nipradilol mediated through S-nitrosylation of Keap1 and HO-1 induction in retinal ganglion cells. Neurochem Int 61:1242–1253
11. Nakazawa T, Tomita H, Yamaguchi K, Sato Y, Shimura M, Kuwahara S, Tamai M (2002) Neuroprotective effect of nipradilol on axotomized rat retinal ganglion cells. Curr Eye Res 24:114–122
12. Watanabe M, Tokita Y, Yata T (2006) Axonal regeneration of cat retinal ganglion cells is promoted by nipradilol, an anti-glaucoma drug. Neuroscience 140:517–528
13. Yata T, Nakamura M, Sagawa H, Tokita Y, Terasaki H, Watanabe M (2007) Survival and axonal regeneration of off-center retinal ganglion cells of adult cats are promoted with an anti-glaucoma drug, nipradilol, but not BDNF and CNTF. Neuroscience 148:53–64
14. Liu K, Lu Y, Lee JK, Samara R, Willenberg R, Sears-Kraxberger I, Tedeschi A, Park KK, Jin D, Cai B, Xu B, Connolly L, Steward O, Zheng B, He Z (2010) PTEN deletion enhances the regenerative ability of adult corticospinal neurons. Nat Neurosci 13:1075–1081
15. Pei DS, Sun YF, Song YJ (2009) S-nitrosylation of PTEN Invovled in ischemic brain injury in rat hippocampal CA1 region. Neurochem Res 34:1507–1512

# Chapter 95
# Reciprocal Changes in Factor XIII and Retinal Transglutaminase Expressions in the Fish Retina During Optic Nerve Regeneration

**Kayo Sugitani, Kazuhiro Ogai, Yoshiki Koriyama and Satoru Kato**

**Abstract** Unlike mammals, fish retinal ganglion cells have the capacity to repair their axons even after optic nerve transection. In the process of fish optic nerve regeneration, a large number of genes have been described as regeneration-associated molecules. Using molecular cloning techniques, we identified two types of cDNA clones belonging to the transglutaminase (TG) family which were upregulation genes; one is cellular factor XIII (cFXIII) and the other is a tissue type TG named retinal transglutaminase ($TG_R$). cFXIII mRNA started to increase in the retinal ganglion cells at 1–2 days, peaked at 5–7 days, and returned to the control level by 20 days post optic nerve injury. In contrast, $TG_R$ mRNA started to increase at day 5–10, peaked at day 20, and then gradually decreased by day 40 after nerve injury. To elucidate the molecular involvement of these TGs in optic nerve regeneration, we studied the effects of recombinant $TG_R$ protein or overexpression of cFXIII using a retinal explant culture system. cFXIII effectively induced neurite outgrowth only from naïve (intact) retinas. In contrast, the $TG_R$ protein significantly enhanced neurite outgrowth only from primed retinas, in which the optic nerve had been crushed 5–7 days previously. These reciprocal expressions of cFXIII and $TG_R$ suggest that these two types of TGs are important for the neurite sprouting and axonal elongation processes, respectively, during optic nerve regeneration processes.

K. Sugitani (✉) · K. Ogai
Division of Health Sciences, Graduate School of Medical Science, Kanazawa University,
5-11-80 Kodatsuno,
Kanazawa 920-0942, Japan
e-mail: sugitani@staff.kanazawa-u.ac.jp

K. Ogai
e-mail: kazu0208@stu.kanazawa-u.ac.jp

Y. Koriyama · S. Kato
Department of Molecular Neurobiology, Graduate School of Medicine, Kanazawa University,
Kanazawa, Japan
e-mail: koriyama@med.kanazawa-u.ac.jp

S. Kato
e-mail: satoru@med.kanazawa-u.ac.jp

J. D. Ash et al. (eds.), *Retinal Degenerative Diseases,* Advances in Experimental Medicine and Biology 801, DOI 10.1007/978-1-4614-3209-8_95,

**Keywords** Cellular Factor XIII · $TG_R$ · Optic nerve regeneration · Retinal ganglion cells · Wound healing · Transglutaminase · Neurite sprouting · Neurite elongation

**Abbreviations**

| | |
|---|---|
| FXIII-A | Factor XIII A subunit |
| cFXIII | Cellular factor XIII |
| CNS | Central nervous system |
| RGC | Retinal ganglion cell |
| TG | Transglutaminase |
| $TG_R$ | Retinal transglutaminase |

## 95.1 Introduction

Fish retinal ganglion cells (RGCs) have the capacity to repair their axons even after optic nerve transection. We screened for regeneration-associated genes using axotomized fish retinas to identify the molecules for the rescue and repair of mammalian CNS neurons. In our previous study [1–3], four periods of goldfish optic nerve regeneration were reported: (i) the first period, preparation for neurite sprouting (0–6 days after nerve injury); (ii) the second, axon elongation (1–6 weeks after nerve injury); (iii) the third, synaptic refinement in the tectum (2–5 months after nerve injury); and (iv) the last, restoration of visual function (6 months after nerve injury). To identify the genes whose expression was specifically upregulated in each optic nerve regeneration period, a cDNA library was prepared from goldfish optic nerves and retinas after nerve injury. Out of many candidate molecules, we cloned two types of transglutaminase (TG), protein cross-linking enzymes, were identified as upregulation molecules. Factor XIII-A was upregulated mainly in the first stage of regeneration [3, 4], and retinal transglutaminase ($TG_R$) increased and had axon elongation effects only in the second period of optic nerve regeneration after nerve injury [5].

## 95.2 Cellular Factor XIII (cFXIII)

Factor XIII (FXIII) was originally identified as a plasma TG heterotetramer ($A_2B_2$) consisting of two catalytic A subunits and two non-catalytic B subunits. It promotes clot stability by catalyzing the formation of covalent cross-linking reactions in polymerized fibrin as a blood coagulation factor [6]. Cellular FXIII (cFXIII) consists of a homodimer of A subunits ($A_2$); it exists as an intracellular form of FXIII in various tissues, platelet, monocytes, macrophages, and megakaryocytes [7, 8]. By the screening of a cDNA library prepared from goldfish retina at 1 day after optic nerve

**Table 95.1** Two types of TG expression in goldfish after optic nerve injury

| | Period of increase after optic nerve injury | Localization of protein | Function |
|---|---|---|---|
| Cellular Factor XIII (cFXIII) | 1–10 days | RGC | Neurite sprouting |
| | 2, 3 h ~ | Optic nerve | Wound healing? |
| | ~40 days | Optic nerve | Axonal elongation |
| Retinal TG ($TG_R$) | 5–40 days | RGC | Axonal elongation |

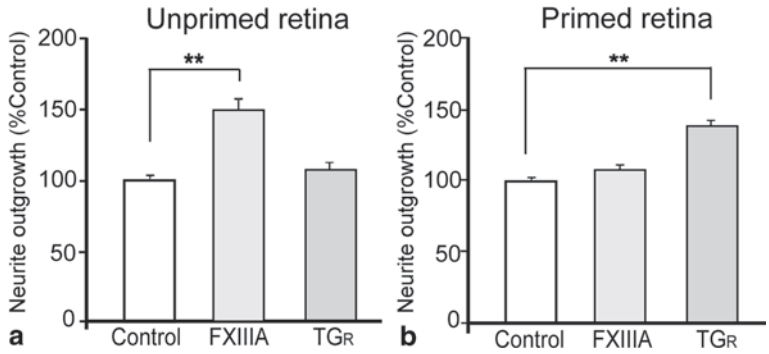


**Fig. 95.1** Neurite outgrowth effects of cFXIII or $TG_R$ protein in goldfish retinal explant cultures. Neurite outgrowth for 5 days of culture in the presence of FXIII-A or $TG_R$ protein in unprimed (naïve) goldfish retinal explants (**a**) and primed retinal explants (**b**) compared with controls (no addition). **a** Overexpression of FXIII-A protein increased the number of unprimed explants with neurite outgrowth compared with the controls and $TG_R$ (**$p<0.01$ increased relative to control). **b** Recombinant $TG_R$ protein (0.01 U/ml) increased the number of primed explants with neurite outgrowth compared with the controls (**$p<0.01$ increased relative to control)

injury, a positive clone with a 2,560 bps fragment was identified as the full-length cDNA clone of FXIII-A (DNA Data Bank of Japan; Accession No. AB622931) encoding a protein of 744 amino acid residues with a predicted molecular mass of 83.8 kDa [3]. FXIII-A mRNA signals in the retina started to increase at day 1 and peaked at 3–7 days, then had decreased by 20 days after optic nerve injury (Table 95.1). The distribution of FXIII-A was confined to the RGC layers [3, 4] during the period of neurite sprouting in the optic nerve regeneration process.

To investigate the functional role of upregulation of cFXIII in optic nerve regeneration, we induced overexpression of the FXIII-A gene using retinal explant cultures by lipofection. Neurite outgrowth was assessed as the ratio of the outgrowth in the control culture and the FXIII-A overexpression culture (Fig. 95.1). In this study, we compared the effect of neurite outgrowth using two types of retinas; one was an unprimed retina (naïve retina without optic nerve lesion), and the other was a primed one in which the optic nerve had been injured 5 days previously. As seen in Fig. 95.1, the FXIII-A overexpression experiments showed that cFXIII induced neurite outgrowth only from unprimed (naïve) retinas but not from primed retinas. Figure 95.1b shows that these inductive effects of neurite outgrowth were lost in

the primed retina. The levels of endogenous cFXIII in the primed retina had already increased in RGCs at this time.

On the other hand, a large number of FXIII-A positive cells accumulated in the area surrounding the optic nerve injury site within a few hours after nerve injury [3]. Nuclear staining of the crushed optic nerve sections with DAPI showed that DAPI-positive glial cells merged with FXIII-A expressing cells. These cFXIII positive cells in the injured optic nerves were identified as astrocytes/microglial cells by immunohistochemical study using the antiserum of some glial marker proteins. The increased level of FXIII-A mRNA was maintained for 1–40 days in the optic nerve after optic nerve injury [3].

## 95.3 Retinal Transglutaminase ($TG_R$)

Following the end of increasing cFXIII expression in the damaged retina, $TG_R$, a different type of TG, was identified as an upregulated gene (DNA Data Bank of Japan; Accession No. AB198723) encoding 678 amino acid residues, with a predicted molecular mass of 75.9 kDa [5]. The levels of $TG_R$ mRNA and protein increased only in the RGCs during the period 5–40 days, and peaked at 20 days after optic nerve injury (Table 95.1). This corresponds to the period of axonal elongation during the optic nerve regeneration process.

To investigate the functional role of upregulation of $TG_R$ in optic nerve regeneration, we prepared retinal explant cultures in the presence of recombinant $TG_R$ protein. The percentage of explants showing positive neurite outgrowth was compared under various culture conditions. As seen in Fig. 95.1, the $TG_R$ protein induced neurite outgrowth from the primed retina but not from the unprimed retina. The addition of recombinant $TG_R$ to the retinal culture also induced striking neurite outgrowth from adult rat RGCs [5]. These molecular and cellular data strongly suggest that $TG_R$ promotes axonal elongation at the surface of injured RGCs after optic nerve injury.

## 95.4 Conclusions

The TG family catalyzes post-translational, covalent protein cross-linking reactions in diverse processes in nervous systems [9]. During goldfish optic nerve regeneration, we observed expression of two types of TG gene, FXIII-A and $TG_R$, in the RGCs (Table 95.1). However, these different types of TG are upregulated at different stages in optic nerve regeneration (Fig. 95.2). $TG_R$ is upregulated in the second stage (1–6 weeks after injury), which corresponds to the period of axonal elongation to the target and the beginning of synaptic connection in the tectum [5]. On the other hand, FXIII-A is upregulated in the first stage, which corresponds to the period of preparation for axon regrowth [3]. In our culture study, we clearly demonstrated that

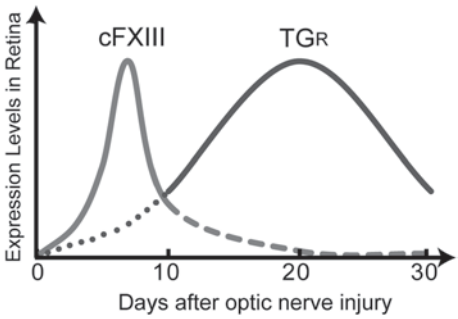


**Fig. 95.2** Pattern diagram of cFXIII and $TG_R$ expression in the goldfish retina during optic nerve regeneration

the endogenous FXIII-A protein (cFXIII) in RGCs induced neurite outgrowth from naïve retinas, but not from primed retinas. In contrast, recombinant $TG_R$ protein induced a drastic extension of long and thick neurites only from primed retinas in which the optic nerve had been injured 5–7 days previously. These results correspond to the peak period of upregulation for these two types of TGs. Additionally, it is strongly suggested that cFXIII produced by non-neuronal cells also induce the elongation of regenerating axons. These reciprocal changes in the expression of cFXIII and $TG_R$ in the RGCs in the early stage of regeneration suggest that the both types of TGs are important for neurite sprouting and axonal elongation, respectively, during optic nerve regeneration.

**Acknowledgement** This work was supported by Grants-in-Aid for Scientific Research to K.S. (No. 23618006) from the Ministry of Education, Culture, Sports, Science and Technology, Japan.

## References

1. Kato S, Koriyama Y, Matsukawa T, Sugitani K (2007) Optic nerve regeneration ingoldfish. In: Becker CG, Becker T (eds) Model organisms in spinal cord regeneration. Wiley-VCH, Germany, pp 355–372
2. Matsukawa T, Arai K, Koriyama Y, Liu Z, Kato S (2004) Axonal regeneration of fish optic nerve after injury. Biol Pharm Bull 27:445–451
3. Sugitani K, Ogai K, Hitomi K, Nakamura-Yonehara K, Shintani T, Noda M, Koriyama Y, Tanii H, Matsukawa T, Kato S (2012) A distinct effect of transient and sustained upregulation of cellular factor XIII in the goldfish retina and optic nerve on optic nerve regeneration. Neurochem Int 61:423–432
4. Sugitani K, Ogai K, Nakashima H, Kato S (2012) Factor XIIIA induction in the retina and optic nerve after optic nerve lesion in goldfish. Adv Exp Med Biol 723:443–448
5. Sugitani K, Matsukawa T, Koriyama Y, Shintani T, Nakamura T, Noda M, Kato S (2006) Upregulation of retinal transglutaminase during the axonal elongation stage of goldfish optic nerve regeneration. Neuroscience 142:1081–1092
6. Schwartz ML, Pizzo SV, Hill RL, McKee PA (1973) Human Factor XIII from plasma and platelets. Molecular weights, subunit structures, proteolytic activation, and cross-linking of fibrinogen and fibrin. J Biol Chem 248:1395–1407
7. Derrick EK, Barker JN, Khan A, Price ML, Macdonald DM (1993) The tissue distribution of factor XIIIa positive cells. Histopathology 22:157–162

8. Quatresooz P, Paquet P, Hermanns-Lê T, Piérard GE (2008) Molecular mapping of factor XIII-Ia-enriched dendrocytes in the skin. Int J Mol Med 22:403–409
9. Lesort M, Tucholski J, Miller ML, Johnson GV (2000) Tissue transglutaminase: a possible role in neurodegenerative diseases. Prog Neurobiol 61:439–463

# Chapter 96
# *N*-Acetylserotonin: Circadian Activation of the BDNF Receptor and Neuroprotection in the Retina and Brain

**P. Michael Iuvone, Jeffrey H. Boatright, Gianluca Tosini and Keqiang Ye**

**Abstract** TrkB is the cognate receptor for brain-derived neurotrophic factor (BDNF), a member of the neurotrophin family involved in neuronal survival, neurogenesis and synaptic plasticity. BDNF has been shown to protect photoreceptors from light-induced retinal degeneration (LIRD) and to improve ganglion cell survival following optic nerve damage. However, the utility of BDNF as a retinal neuroprotectant is limited by its short half-life, inability to cross the blood-brain and blood-retinal barriers, and activation of the proapoptotic p75 neurotrophin receptor. *N*-Acetylserotonin (NAS) is a naturally occurring chemical intermediate in the melatonin biosynthetic pathway in the pineal gland and retina. Its synthesis occurs in a circadian fashion with high levels at night and is suppressed by light exposure. Until recently, NAS was thought to function primarily as a melatonin precursor with little or no biological function of its own. We have now shown that TrkB activation in the retina and hippocampus is circadian in C3H/f$^{+/+}$ mice, which synthesize NAS, but not in C57BL/6 mice, which have a mutation in the gene encoding the enzyme that converts serotonin to NAS. In addition, treatment of mice exogenous

P. M. Iuvone (✉) · J. H. Boatright · G. Tosini
Department of Ophthalmology, Emory University School of Medicine,
30322 Atlanta, GA, USA
e-mail: miuvone@emory.edu

J. H. Boatright
e-mail: jeffboatright@emory.edu

G. Tosini
e-mail: gtosini@msm.edu

G. Tosini · K. Ye
Department of Pharmacology and Toxicology and Neuroscience Institute,
Morehouse School of Medicine, Atlanta, GA, USA
e-mail: gtosini@msm.edu

K. Ye
Department of Pathology and Laboratory Medicine,
Emory University School of Medicine, Atlanta, GA 30322 USA
e-mail: kye@emory.edu

J. D. Ash et al. (eds.), *Retinal Degenerative Diseases,* Advances in Experimental Medicine and Biology 801, DOI 10.1007/978-1-4614-3209-8_96,

NAS, but not with serotonin or melatonin, activates TrkB during the daytime in a BDNF-independent manner. NAS appears to have neuroprotective properties and its administration reduces caspase 3 activation in the brain in response to kainic acid, a neurotoxic glutamate analog. We have developed structural analogs of NAS that activate TrkB. One of these derivatives, *N*- [2-(-indol-3-yl)ethyl]-2-oxopiperideine-3-carboximide (HIOC), selectively activates TrkB with greater potency than NAS and has a significantly 5-hydroxy-1Hlonger biological half-life than NAS after systemic administration. HIOC administration results in long-lasting activation of TrkB and downstream signaling kinases. The compound can pass the blood-brain and blood-retinal barriers when administered systemically and reduces kainic acid-induced neuronal cell death in a TrkB-dependent manner. Systemic administration of HIOC mitigates LIRD, assessed electrophysiologically and morphometrically. Hence, NAS may function as an endogenous circadian neurotrophin-like compound and HIOC is a good lead compound for further drug development for treatment of retinal degenerative diseases.

**Keywords** Neuroprotection · TrkB receptor · BDNF · Light-induced retinal degeneration · Circadian rhythm · *N*-acetylserotonin

**Abbreviations**

| | |
|---|---|
| BDNF | Brain-derived neurotrophic factor |
| LIRD | Light-induced retinal degeneration |
| NAS | *N*-acetylserotonin |
| TrkB | Tropomyosin-related kinase B |
| AANAT | Arylalkylamine *N*-acetyltranferase |
| HIOC | *N*-[2-(5-hydroxy-1H-indol-3-yl)ethyl]-2-oxopiperidine-3-carboxamide |
| ERG | Electroretinogram |
| ONL | Outer nuclear layer |

## 96.1 Introduction

Melatonin is a neurohormone synthesized in the retina and pineal gland [1, 2]. It transmits circadian signals of darkness and nighttime. Melatonin is synthesized from serotonin and its robust circadian rhythm is attributable primarily to the circadian regulation of arylalkylamine *N*-acetyltransferase (AANAT) [3], which converts serotonin to *N*-acetylserotonin. Melatonin acts primarily through two subtypes of G protein-coupled receptors, MT1 and MT2 [4, 5], but the neurohormone may also have actions as a free radical scavenger and antioxidant [5]. Until recently, *N*-acetylserotonin was thought to be merely a metabolic intermediate in melatonin synthesis, although some data suggest that it may have cytoprotective effects due to its antioxidant properties [6].

Neurotrophins are a family of small proteins with neuroprotective effects that play important roles in development and maintenance of neurons, in neuroprogeni-

tor cell proliferation and neurogenesis, and in a variety of other important neuronal functions [7]. Brain-derived neurotrophic factor (BDNF) is a member of the neurotrophin family that acts primarily on high-affinity tropomyosin-related kinase B (TrkB) receptors, which are transmembrane proteins with an extracellular BDNF-binding domain and an intracellular tyrosine kinase domain [7, 8]. Binding of BDNF elicits homodimerization of TrkB and its autophosphorylation. Phospho-TrkB (pTrkB) couples to multiple signaling pathways, including ERK1/2 and AKT, through which it is thought to promote cell survival. BDNF also acts on the low affinity $p75^{NTR}$ receptor, which is also a tyrosine kinase receptor [7].

BDNF has been shown to protect against LIRD and to improve retinal ganglion survival following optic nerve injury through TrkB-dependent mechanisms [9–12]. However, the therapeutic potential of BDNF is limited because (1) it does not cross the blood-retinal barrier or blood-brain barrier and, therefore, must be administered centrally or intravitreally; (2) it has a relatively short half-life; (3) at higher concentrations, it acts on the $p75^{NTR}$ receptor, which has a pro-apoptotic effect. These limitations have led to the search for small molecule activators of TrkB. In a screen of small molecule libraries, Keqiang Ye et al. noted that compounds with an indole alkyl moiety, similar in structure to melatonin, *N*-acetylserotonin, and serotonin, had efficacy in promoting TrkB activation [13].

## 96.2 Circadian Activation of TrkB in the Retina and Brain

Melatonin synthesis and AANAT activity occur as circadian rhythms with peaks at night in darkness [1, 2]. The levels of pTrkB and total TrkB were examined during the day and night in two strains of mice [14]: C3H/$f^{+/+}$ mice, which have an intact melatonin synthetic pathway [15], and C57BL/6J mice, which have a mutation in AANAT that limits the production of melatonin [16]. Total TrkB protein did not evidently fluctuate as function of time of day in either strain of mouse. However, a circadian rhythm in the levels of pTrkB was observed in the retina and hippocampus of C3H/$f^{+/+}$ mice, with higher levels at night compared to day. In contrast, pTrkB levels were similar in the day and night, in retina and hippocampus of C57BL/6J mice.

## 96.3 *N*-Acetylserotonin Activates TrkB and Its Signaling Pathways

To determine if endogenous indole alkyl compounds can activate TrkB, the effects of serotonin, *N*-acetylserotonin and melatonin on pTrkB were examined in cultured cortical and hippocampal neurons [14]. Treatment of cultures with BDNF and *N*-acetylserotonin, but not with serotonin, 5-hydroxyindoleacetic acid, or melatonin, increased the level of pTrkB assessed by immunofluorescence and immunoblot

analyses [14]. The effect of *N*-acetylserotonin appeared to be specific for TrkB, as it had no effect on TrkA or TrkC. It was dose dependent and was observed in the low nM range. Systemic administration of *N*-acetylserotonin increased pTrkB in the retina and hippocampus, indicating that it crosses the blood-retinal and blood-brain barriers. This conclusion was verified by direct measurement of *N*-acetylserotonin in the retina and brain following systemic administration [17]. In vitro, *N*-acetylserotonin was shown to promote TrkB dimerization and activation of downstream signaling kinases, including ERK1/2 and AKT. The effects of *N*-acetylserotonin were BDNF-independent, as shown in neurons from forebrain-specific BDNF conditional knockout mice. They were blocked by 1NMPP1, a specific inhibitor of Trk tyrosine kinase in TrkB F616A knock-in mouse neurons [18], indicating that they are specifically mediated by TrkB activation.

## 96.4 Neuroprotective Effect of *N*-Acetylserotonin

Kainic acid administration promotes neuronal apotoptosis in brains of TrkB F616A mice. The effect of kainic acid was antagonized by systemic administration of *N*-acetylserotonin, but not of melatonin[14]. Moreover, the neuroprotective effect of *N*-acetylserotonin was blocked by 1NMPP1, indicating that it was mediated by activation of TrkB. Similarly, BDNF and *N*-acetylserotonin effectively blocked glutamate-induced apoptosis in cultured cortical neurons [14].

As mentioned, treatment with BDNF protects rats from LIRD [9]. In contrast, *N*-acetylserotonin had no protective effect against LIRD in mice, even at doses exceeding those required for maximal TrkB activation (K. Ghai and P.M. Iuvone, unpublished observations). The lack of neuroprotection could be due to species differences, protocol differences (constant light vs. short-term high-intensity light), or to the short half-life of *N*-acetylserotonin.

## 96.5 Neuroprotective Effect of HIOC, an *N*-Acetylserotonin Derivative

Several *N*-acetylserotonin derivatives were evaluated for efficacy in activating TrkB [17]. One of these, *N*-[2-(5-hydroxy-1H-indol-3-yl)ethyl]-2-oxopiperidine-3-carboxamide (HIOC) was potent and effective in activating TrkB and downstream signaling kinases. HIOC passed the blood-brain and blood-retina barriers following systemic administration, as assessed by pharmacokinetic measurements of the drug in blood, retina and brain [17]. It had a significantly longer biological half-life than *N*-acetylserotonin, and promoted persistent activation of TrkB following systemic administration [17]. HIOC protected cultured neurons from glutamate-induced neuronal cell death. It also protected against kainic acid-induced apoptosis in the brain following systemic administration; the neuroprotective effect of HIOC was TrkB

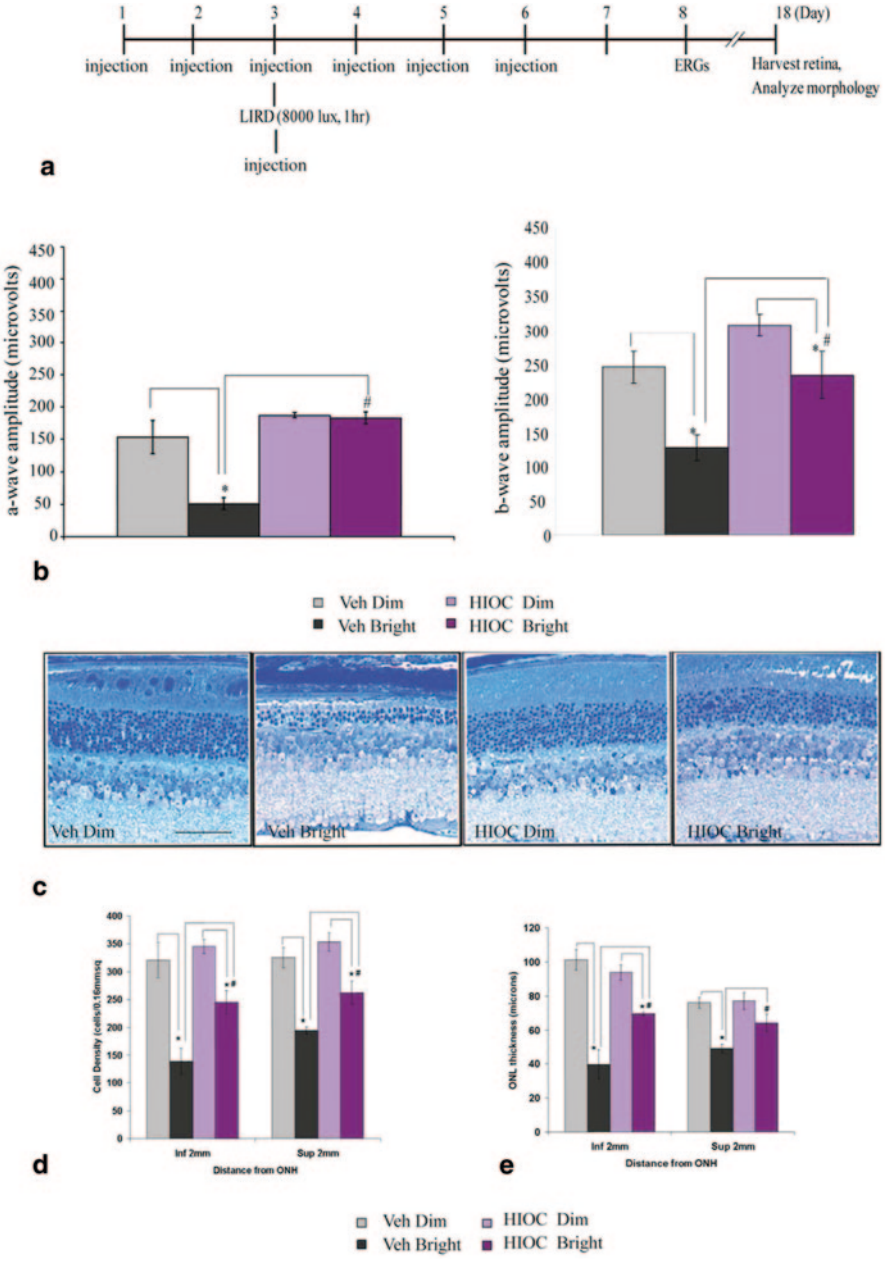


**Fig. 96.1** HIOC mitigates retinal damage caused by bright light exposure. **a** Experimental design. BALB/c mice ($n=4$–5/group) were injected with *HIOC* (40 mg/kg ip) or vehicle, subjected to bright light, ERG recordings, and histological analysis on the schedule depicted in the diagram. **b** ERG measured at a flash intensity of 6.28 cd-s/m$^2$. **c** Representative toluidine blue stained retinal sections from each treatment group. **d**, **e** Quantitative analysis of ONL cell density and thickness. $^{*,\#}p<0.05$. (Reproduced from [17] © The Authors)

dependent. In contrast to *N*-acetylserotonin, HIOC potently protected against LIRD, as assessed functionally and histologically [17]. Bright-light exposure (8000 lx for 1 h) markedly reduced a-wave and b-wave amplitudes of the dark-adapted electroretinogram (ERG), measured one week post exposure, and caused reduced thickness of the outer nuclear layer (ONL) and photoreceptor outer segment disruption, measured 16 days post exposure (Fig. 96.1). These deleterious effects of bright light were significantly attenuated with HIOC treatment (Fig. 96.1) [17]. The neuroprotective effect of HIOC was tightly associated with TrkB activation. When assessed 90 min after bright light exposure in vehicle-treated mice, a small increase in pTrkB immunoreactivity was observed just distal to the ONL in the vicinity of photoreceptor inner segments [17]. This may reflect TrkB activation in the microvilli of Müller cells, as photoreceptors are not thought to express TrkB [19]. There was also some increase in label in cells of the ganglion cell layer. In the retinas of mice exposed to bright light and treated with HIOC, there was a massive increase of pTrkB labeling in the retina. The labeling at the level of the inner segments was greatly enhanced, as was that in ganglion cell and inner nuclear layers [17]. TrkB activation in the Müller cell microvilli may be particularly relevant to the photoreceptor-survival effect of HIOC considering its location and a previous study showing that BDNF expression directed to Müller cells is protective in LIRD [10].

## 96.6 Conclusion

These recent studies suggest that *N*-acetylserotonin, previously thought to be just a precursor of melatonin, is an endogenous circadian neuroprotectant and activator of TrkB receptors. Exogenous *N*-acetylserotonin may have therapeutic benefit in short-term neurotoxic insults, but probably not for slowly developing neurodegenerative disease due to its short half-life. Synthetic, small molecule activators of TrkB based on the structure of *N*-acetylserotonin have potential for the treatment of retinal degenerative diseases and HIOC is a good lead compound for this purpose.

## References

1. Iuvone PM, Tosini G, Pozdeyev N, Haque R, Klein DC, Chaurasia SS (2005) Circadian clocks, clock networks, arylalkylamine N-acetyltransferase, and melatonin in the retina. Prog Retinal Eye Res 24:433–456
2. Klein DC, Coon SL, Roseboom PH, Weller JL, Bernard M, Gastel JA, Zatz M, Iuvone PM, Rodriguez IR, Begay V et al (1997) The melatonin rhythm-generating enzyme: Molecular regulation of serotonin *N*-acetyltransferase in the pineal gland. Recent Prog Hormone Res 52:307–358
3. Bernard M, Iuvone PM, Cassone VM, Roseboom PH, Coon SL, Klein DC (1997) Avian melatonin synthesis: photic and circadian regulation of serotonin *N*-acetyltransferase mRNA in the chicken pineal gland and retina. J Neurochem 68:213–224

4. Dubocovich ML, Markowska M (2005) Functional MT1 and MT2 melatonin receptors in mammals. Endocr 27:101–110
5. Hardeland R (2005) Antioxidative protection by melatonin: multiplicity of mechanisms from radical detoxification to radical avoidance. Endocr 27:119–130
6. Oxenkrug G (2005) Antioxidant effects of N-acetylserotonin: possible mechanisms and clinical implications. Ann NY Acad Sci 1053:334–347
7. Hennigan A, O'Callaghan RM, Kelly AM (2007) Neurotrophins and their receptors: roles in plasticity, neurodegeneration and neuroprotection. Biochem Soc Trans 35:424–427
8. Ohira K, Hayashi M (2009) A new aspect of the TrkB signaling pathway in neural plasticity. Curr Neuropharmacol 7:276–285
9. LaVail MM, Unoki K, Yasumura D, Matthes MT, Yancopoulos GD, Steinberg RH (1992) Multiple growth factors, cytokines, and neurotrophins rescue photoreceptors from the damaging effects of constant light. Proc Natl Acad Sci USA 89:11249–11253
10. Gauthier R, Joly S, Pernet V, Lachapelle P, Di Polo A (1 September 2005) Brain-Derived Neurotrophic Factor Gene Delivery to Muller Glia Preserves Structure and Function of Light-Damaged Photoreceptors. Invest Ophthalmol Vis Sci 46:3383–3392
11. Weber AJ, Harman CD, Viswanathan S (2008) Effects of optic nerve injury, glaucoma, and neuroprotection on the survival, structure, and function of ganglion cells in the mammalian retina. J Physiol 586:4393–4400
12. Mansour-Robaey S, Clarke DB, Wang YC, Bray GM, Aguayo AJ (1994) Effects of ocular injury and administration of brain-derived neurotrophic factor on survival and regrowth of axotomized retinal ganglion cells. Proc Natl Acad Sci USA 91:1632–1636
13. Jang SW, Liu X, Yepes M, Shepherd KR, Miller GW, Liu Y, Wilson WD, Xiao G, Blanchi B, Sun YE et al (2010) A selective TrkB agonist with potent neurotrophic activities by 7,8-dihydroxyflavone. Proc Natl Acad Sci USA 107:2687–2692
14. Jang SW, Liu X, Pradoldej S, Tosini G, Chang Q, Iuvone PM, Ye K (2010) N-acetylserotonin activates TrkB receptor in a circadian rhythm. Proc Natl Acad Sci U S A 107:3876–3881
15. Tosini G, Menaker M (1998) The clock in the mouse retina: melatonin synthesis and photoreceptor degeneration. Brain Res 789:221–228
16. Roseboom PH, Namboodiri MAA, Zimonjic DB, Popescu NC, Rodriguez IR, Gastel JA, Klein DC (1998) Natural melatonin 'knockdown' in C57BL/6J mice: rare mechanism truncates serotonin *N*-acetyltransferase. Mol Brain Res 63:189–197
17. Shen J, Ghai K, Sompol P, Liu X, Cao X, Iuvone PM, Ye K (2012) N-acetyl serotonin derivatives as potent neuroprotectants for retinas. Proc Natl Acad Sci USA 109:3540–3545
18. Chen X, Ye H, Kuruvilla R, Ramanan N, Scangos KW, Zhang C, Johnson NM, England PM, Shokat KM, Ginty DD (2005) A chemical-genetic approach to studying neurotrophin signaling. Neuron 46:13–21
19. Rohrer B, Korenbrot JI, LaVail MM, Reichardt LF, Xu B (1999) Role of neurotrophin receptor TrkB in the maturation of rod photoreceptors and establishment of synaptic transmission to the inner retina. J Neurosci 19:8919–8930

# Chapter 97
# A High Content Screening Approach to Identify Molecules Neuroprotective for Photoreceptor Cells

**John A. Fuller, Gillian C. Shaw, Delphine Bonnet-Wersinger, Baranda S. Hansen, Cynthia A. Berlinicke, James Inglese and Donald J. Zack**

**Abstract**
Purpose
Retinal degenerations are a heterogeneous group of diseases in which there is slow but progressive loss of photoreceptors (PR). There are currently no approved therapies for treating retinal degenerations. In an effort to identify novel small molecules that are (1) neuroprotective and (2) promote PR differentiation, we have developed microscale (1,536 well) cell culture assays using primary retinal neurons.

J. A. Fuller (✉) · G. C. Shaw · D. Bonnet-Wersinger · B. S. Hansen · C. A. Berlinicke · D. J. Zack
Wilmer Eye Institute, Johns Hopkins University School of Medicine,
400 N Broadway, Baltimore, MD 21231, USA
e-mail: jfulle19@jhmi.edu

G. C. Shaw
e-mail: gshaw6@jhmi.edu

D. Bonnet-Wersinger
e-mail: delphine.bonnet@inserm.fr

B. S. Hansen
e-mail: bhansen2@jhmi.edu

J. Inglese
National Center for Advancing Translational Sciences, NIH, Rockville, MD, USA
e-mail: jinglese@mail.nih.gov

National Human Genome Institute, NIH, Bethesda, MD, USA

D. J. Zack
Departments of Molecular Biology and Genetics, Neuroscience, and Institute of Genetic Medicine, The Johns Hopkins University School of Medicine,
Baltimore, MD, USA
e-mail: dzack@jhmi.edu

Institut de la Vision, Paris 75012, France

J. D. Ash et al. (eds.), *Retinal Degenerative Diseases,* Advances in Experimental Medicine and Biology 801, DOI 10.1007/978-1-4614-3209-8_97,

Methods
Primary murine retinal cells are isolated, seeded, treated with a 1,280 compound chemical library in a 7 point titration and then cultured under conditions developed to assay protection against an introduced stress or enhance PR differentiation. In the protection assays a chemical insult is introduced and viability assessed after 72 h using CellTiterGlo, a single-step chemiluminescent reagent. In the differentiation assay, cells are isolated from the rhodopsin-GFP knock-in mouse and PR differentiation is assessed by fixing cells after 21 days in culture and imaging with the Acumen plate-based laser cytometer (TTP Labtech) to determine number and intensity of GFP-expressing cells. Positive wells are re-imaged at higher resolution with an INCell2000 automated microscope (GE). Concentration-response curves are generated to pharmacologically profile each compound and hits identified by xx.

Results
We have developed PR differentiation and neuroprotection assays with a signal to background (S/B) ratios of 11 and 3, and a coefficient of variation (CV) of 20 and 9%, suitable for chemical screening. Staurosporine has been shown in our differentiation assay to simultaneously increase the number of rhodopsin positive objects while decreasing the mean rhodopsin intensity and punctate rhodopsin fluorescent objects.

Conclusions
Using primary murine retinal cells, we developed high throughput assays to identify small molecules that influence PR development and survival. By screening multiple compound concentrations, dose-response curves can be generated, and the false negative rate minimized. It is hoped that this work will identify both potential preclinical candidates as well as molecular probes that will be useful for analysis of the molecular mechanisms that promote PR differentiation and survival.

**Keywords** Neuroprotection · Photoreceptor · HTS · Screening · High content analysis

**List of Abbreviations**

| | |
|---|---|
| DMSO | Dimethyl sulfoxide |
| ER | Endoplasmic reticulum |
| GFP | Green fluorescent protein |
| HCA | High content analysis |
| qHTS | Quantitative high throughput screening |
| PBS | Phosphate buffered saline |
| PR | Photoreceptor |
| RP | Retinitis pigmentosa |

## 97.1 Introduction

The retinal degenerations, the prototype of which is retinitis pigmentosa (RP), are a group of genetically heterogeneous orphan diseases in which there is slow but progressive loss of Photoreceptor (PR) cells, resulting in concomitant loss of vi-

sion. The past several decades have witnessed tremendous strides to define many of the genes that when mutated can cause retinal degeneration. To date, more than 150 retinal degeneration related genes have been identified [1]. These findings have led to mechanistic insights and have opened up the possibility of new treatment strategies, such as gene therapy and related treatment approaches [2–6]. Although these avenues are exciting and have great potential, treatment strategies based on a particular gene or mutation have the limitation that even if they are effective, they generally are appropriate for only a small fraction of RP patients. An alternative and complementary approach is to develop so called "neuroprotective" treatments aimed at protecting PRs from degeneration, often independent of the nature of the initiating cellular insult. Neuroprotection may therefore be useful for a larger group of patients, since they may preserve vision in multiple different genetic forms of RP. Theoretically, such approaches could also be effective for the treatment of the "dry" (atrophic) form of age-related macular degeneration.

With the goal of identifying lead compounds for the development of such novel neuroprotective therapies, we have been carrying out phenotypic screens with primary retinal neurons to identify small molecules that promote the survival and/or differentiation of PR cells. Although not the traditional route to contemporary drug discovery, phenotypic screens actually have a well-established track record. Out of the 50 first-in-class small molecules given FDA approval between 1998 and 2008, 28 were discovered using phenotypic approaches and of these, 8 were approved without a known molecular mechanism of action [7].

For our phenotypic screens, we have developed cell-based assays that are compatible with quantitative high throughput screening (qHTS), which by assessing the compound library over multiple concentrations develops a full pharmacokinetic profile for each molecule tested [8]. We are using primary retinal neurons in a high content assay that measures the numbers of cells expressing endogenous levels of a knocked-in human rhodopsin-EGFP fusion protein [9]. For retinal cell survival following oxidative damage, we employ a single-step addition cell viability reagent that is amenable for ultra HTS (greater than 100,000 wells per day).

In addition to their potential as therapeutic lead compounds for further development, it is envisioned that small molecules discovered in this study may also be of use as molecular probes which will be useful for discovering and dissecting the mechanisms of PR development and survival.

## 97.2 Materials and Methods

### *97.2.1 Primary Cell Dissociation*

All animal procedures were performed according to the guidelines of the ARVO statement for the "Use of Animals in Ophthalmic and Vision Research" and were approved by the Institutional Animal Care and Use Committees at the Johns Hopkins University School of Medicine. Retinas from postnatal day 0 (GFP differentiation assay) or 4 (cell survival) are isolated from homozygous rhodopsin-GFP knock-in mice [9] or C57BL/6 mice, respectively. Animals are sacrificed by hypothermia followed by decapitation, eyes are enucleated, and retinas are dissected.

The retinas are dissociated into single cell suspensions by incubation with activated papain in Hibernate-E without $Ca^2$+ (BrainBits) for 15 min at 37 °C. The solution is neutralized by adding Hibernate-E with $Ca^2$+ plus B27 (Invitrogen), L-Glutamine, and Pen/Strep. The cells are then transported on ice to the screening facility.

### *97.2.2 1536 Well Cell Plating and Compound Library Treatment*

Prior to cell plating, 1,536 well plates are filled with 4 μL of neuronal culture medium consisting of Neurobasal-E, B-27, L-Glutamine, pen/strep (all Life Technologies) using a Multidrop Combi peristaltic bulk dispenser (ThermoFisher). Each plate is then "pinned" with 23 nL of a compound at a set stock concentration in DMSO that is delivered from a library plate using a robotic pintool transfer tool (Wako). Cells are resuspended at a concentration of $2.5 \times 10^5$ cells/mL, filtered through a 10 μm nylon filter (Amazon.com: Small Parts), dispensed at a final well culture volume of 8 μL (1,000 cells/well), and incubated for up to 21 days. Since we are using such low volumes for extended cultures, the plates are covered with a Breathe-Easy gas-permeable membrane (Diversified Biotech) and a Microclime vapor barrier lid (Labcyte).

### *97.2.3 Fixation and Imaging*

For the differentiation assay, cells are treated with 2 μL of 20% (4% final) fresh paraformaldehyde in PBS containing Hoechst 33342 (1:5000 final) for 15 min at room temperature. The plates are then aspirated and rinsed twice with PBS using an EL406 washer dispenser (BioTek Instruments) equipped with an aspirator and syringe dispenser for 1,536 well plates, and imaged with an Acumen Explorer (TTP Labtech) plate cytometer equipped with 405, 488, and 633 nm lasers [10]. PRs are defined as Hoecsht positive objects with size and GFP fluorescence intensity above defined threshold values. "On the fly" analysis allows for virtual 'cherry-picking' wells that display fraction of GFP positive cells or GFP intensity values greater or lesser than 3*SD relative to DMSO controls. These wells are then imaged with a microscope-based INCell2000 HCA platform (GE), with triple-channel images for nuclei, GFP, and brightfield acquired for each designated well.

### *97.2.4 CellTiterGlo Viability Assay*

For the neuroprotection assay, following treatment with 0.2 mM paraquat (Sigma), cell cultures are treated with compounds and incubated for 72 h. Plates are then equilibrated at room temperature for 10 min treated with 4 μL CellTiterGlo (Promega), treated for 10 min at room temperature, and then imaged using a Viewlux uHTS CCD-based imager (Perkin Elmer).

### *97.2.5 Analysis and Curve Fitting*

Plate data from GFP positive cell count data, GFP intensity, or viability (raw relative luminescence units) are exported from each respective instrument into .CSV files. Assay statistics are generated by analyzing activity of control compounds, as well as DMSO-treated control plates. The raw data is then normalized using the following formula: $Y=\left(\frac{x-N}{P-N}\right)*(100)$ where Y = percent activity, x = specific data value, N = median DMSO control value, and P = median positive control value [8]. Following normalization, the data is then fitted with either NIH CurveFit (http://tripod.nih.gov/curvefit), an open source curve fitting and classification software, or with Prism (Graphpad). The data is then ranked according to efficacy, potency, and curve class as defined by Inglese et al. [8].

## 97.3 Results

### *97.3.1 Rhodopsin-GFP Count*

In an effort to observe the effects of small molecules on PR development, we chose to use a fluorescent reporter to follow PR differentiation. The hRhoGFP knock-in mouse was generated by replacing the mouse rhodopsin (rho) open reading frame with a human Rho-GFP fusion construct, thus creating a rhodopsin reporter controlled by native regulatory mechanisms [9]. Since the peak of PR cell genesis in the mouse is near the time of birth of the animal, for the assay we chose to harvest and culture cells from postnatal day 0 retinas. After 21 days of culture, PRs in the culture develop bright GFP fluorescence with bright punctate ('peak rhodopsin') objects, believed to be proto-outer segments, that have a signal to background of 11-fold over pre-differentiated RhoGFP cells. As a demonstration of the capability of this screen identifying modulators of PR differentation, we have found that culture in the presence of staurosporine, a broad spectrum kinase inhibitor implicated in rhodopsin expression modulation [11, 12], increases the number of rhodopsin positive cells (Fig 97.1a, c, e). However, the number of cells with peak rhodopsin objects (Fig 97.1f, *arrows*) is significantly decreased.

### *97.3.2 Cell Titer Viability Screening*

Oxidative and ER stress have been implicated in the pathogenesis of PR degeneration [13–18]. In an effort to find novel PR protective small molecules, we have developed a primary cell-based screen for compounds protective against this type of cell damage. For this assay, the herbicide paraquat, an inducer of both oxidative and ER stress that has been used to model retinal degeneration in vivo, is used to

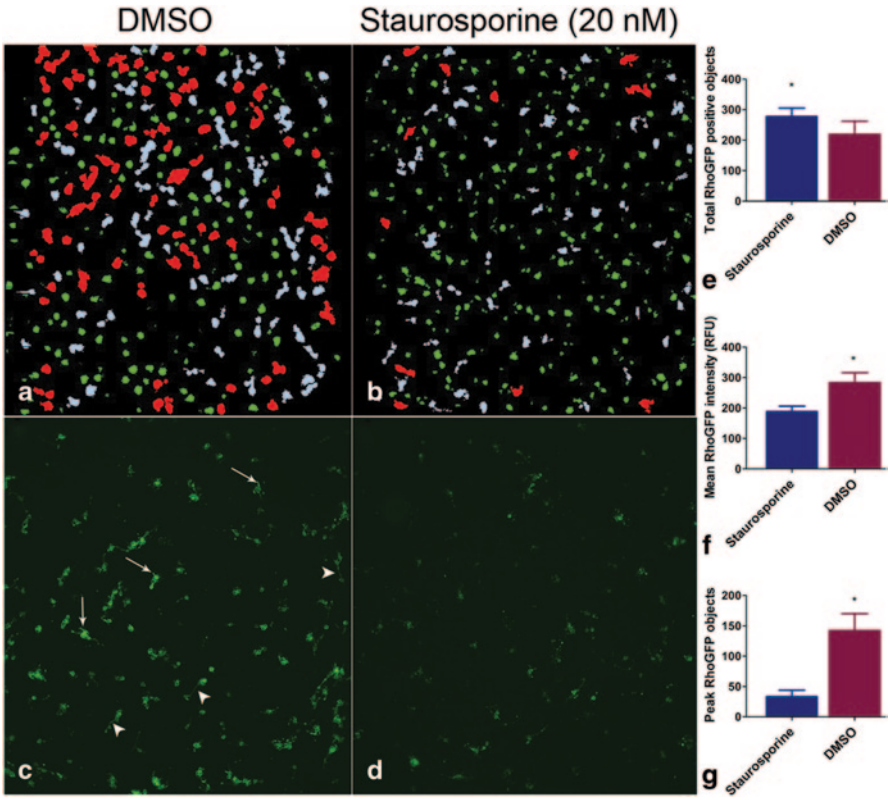


**Fig. 97.1** Extended culture of mature *RhoGFP* photoreceptors in 1536 qHTS format. Primary retinal neurons treated for 21 days with *staurosporine* (20 nM) show a small increase in total *RhoGFP*+cells (**b**: *green* objects, **d**, **e**). However total intensity and objects with a peak GFP area > 1200 RFU are decreased (**b**: *red*, **f**, **g**) **a**, **b**: Acumen GFP (*green*), 'peak GFP' objects (*red*), objects outside parameters (*gray*), **c**, **d**: corresponding INCell2000 images showing mature photoreceptors with 'peak' punctate GFP positive structures (*arrows*) and neurites (*arrowheads*). *$p < 0.0001$ (unpaired t-test)

induce acute oxidative damage to retinal cell cultures [13, 19–23]. The cells are treated with 0.2 mM paraquat, a concentration found to induce 75% cell death in 72 h. Cell survival is assayed at 72 h using CellTiterGlo (Promega), a single-step viability reagent. We have measured assay performance and have found a cell concentration correlation of 95% and CV below 10%. The difference between untreated and paraquat-treated cells as has a signal to background ratio of 3 and a Z' of 0.61. We have found that J147 (Cellagen), a known neuroprotective compound [24], has maximal protective activity at 27 μM, and used as a positive control for this assay (Fig. 97.2).

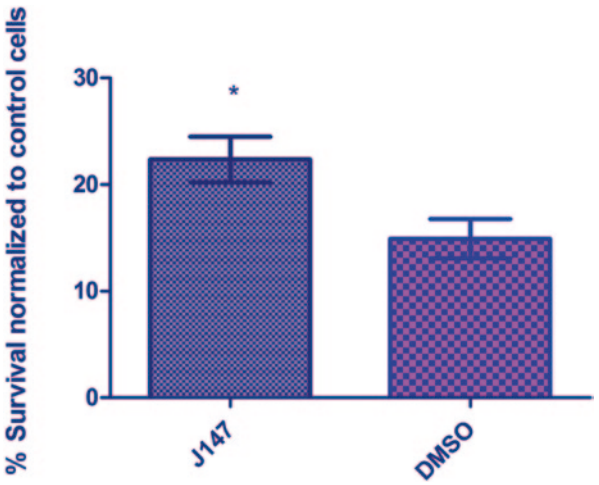


**Fig. 97.2** Neuroprotection of primary photoreceptors following paraquat-induced oxidative damage with *J147*, a reported neuroprotective molecule. *J147* is a single point positive with activity at 27 µM. *$p<0.0001$ (unpaired t-test)

## 97.4 Discussion

There is a clear need for drug therapies that target vision loss arising from retinal degeneration. Currently, the pharmaceutical and biotechnology sectors struggle with increasing R&D costs and dwindling development pipelines [25]. The so-called preclinical 'valley of death' particularly impacts rare disease therapeutic development due to increasing risks incurred in development with a reduced incentive (treatable patient populations). As such, there has been a trend towards increased involvement by academic and government laboratories in developing strategies for treating orphan diseases [26, 27]. One major benefit to this approach with respect to retinal degeneration will be the rapid establishment of new paradigms for discovery by pairing novel assay technologies (e.g. advanced high content imaging systems) with more appropriate models of retinal disease. In our work, rather than focusing on a single target in retinal degeneration, we are striving to find the most potent and efficacious molecules that are neuroprotective and modulate PR development.

High-throughput screening with retinal primary cells has many challenges to overcome. Issues such as day-to-day variability in cell preparation, variability in animal litters, and stochastic effects within each well can have tremendous effects on culture conditions. We have found that cells take at least 6 days to produce a measurable response with respect to RhoGFP numbers and rhodopsin intensity. In typical, 1,536 well assays in this time frame would be unacceptable due to variation arising from plate-edge and evaporation effects. However by taking precautions to mitigate edge and evaporation effects, we can consistently culture cells well over a period of three weeks under conditions in which the cells develop in a fashion that mirrors in vivo PR development.

Autofluorescence in the GFP emission spectrum is a major challenge for fluorescent protein-based reporter assay systems as many molecules in compound libraries

are also fluorescent in the FITC spectrum. To distinguish false positives, we have employed a far-red conjugated primary antibody to stain positive wells after primary GFP object identification. However, high throughput immunostaining in a large screening campaign can be expensive and labor intensive. An alternative approach would be to develop a consensus biocircuit that employs nonhomologous reporters separated by a 2A polycistronic peptide [28].

In this study, we have used primary retinal neurons in high-throughput format for studying small molecule effects on PR differentiation and survival. In addition to their potential as therapeutic leads, we believe that bioactive molecules identified though our ongoing screens will have applicability as molecular probes that are involved in retinal cell biology will serve as useful reagents for future studies.

**Acknowledgment** We thank John Wilson and Ted Wensel (Baylor College of Medicine) for generously providing Rho-GFP mice, and Patricia Dranchak, Sam Hasson, and Ryan MacArthur of the NIH NCATS DPI for their help and assistance. This work was funded by an FFB/Wynn-Gund Translational Research Acceleration Program Award.

## References

1. RetNet: Retinal Information Network. https://sph.uth.edu/retnet/
2. Cideciyan AV, Aleman TS, Boye SL, Schwartz SB, Kaushal S, Roman AJ, Pang JJ, Sumaroka A, Windsor EA, Wilson JM, Flotte TR, Fishman GA, Heon E, Stone EM, Byrne BJ, Jacobson SG, Hauswirth WW (2008) Human gene therapy for RPE65 isomerase deficiency activates the retinoid cycle of vision but with slow rod kinetics. Proc Nat Acad Sci USA 105(39):15112–15117
3. Barnett PJ (2009) Mathematical modeling of triamcinolone acetonide drug release from the I-vation intravitreal implant (a controlled release platform). Conference proceedings: annual international conference of the IEEE engineering in medicine and biology society IEEE engineering in medicine and biology society conference 2009:3087–3090
4. Jacobson SG, Cideciyan AV, Ratnakaram R, Heon E, Schwartz SB, Roman AJ, Peden MC, Aleman TS, Boye SL, Sumaroka A, Conlon TJ, Calcedo R, Pang JJ, Erger KE, Olivares MB, Mullins CL, Swider M, Kaushal S, Feuer WJ, Iannaccone A, Fishman GA, Stone EM, Byrne BJ, Hauswirth WW (2012) Gene therapy for leber congenital amaurosis caused by RPE65 mutations: safety and efficacy in 15 children and adults followed up to 3 years. Arch Ophthalmol 130(1):9–24
5. Maguire AM, Simonelli F, Pierce EA, Pugh EN Jr, Mingozzi F, Bennicelli J, Banfi S, Marshall KA, Testa F, Surace EM, Rossi S, Lyubarsky A, Arruda VR, Konkle B, Stone E, Sun J, Jacobs J, Dell'Osso L, Hertle R, Ma JX, Redmond TM, Zhu X, Hauck B, Zelenaia O, Shindler KS, Maguire MG, Wright JF, Volpe NJ, McDonnell JW, Auricchio A, High KA, Bennett J (2008) Safety and efficacy of gene transfer for Leber's congenital amaurosis. N England J Med 358(21):2240–2248
6. Sieving PA, Caruso RC, Tao W, Coleman HR, Thompson DJ, Fullmer KR, Bush RA (2006) Ciliary neurotrophic factor (CNTF) for human retinal degeneration: phase I trial of CNTF delivered by encapsulated cell intraocular implants. Proc Nat Acad Sci USA 103(10):3896–3901
7. Swinney DC, Anthony J (2011) How were new medicines discovered? Nat Rev Drug Discov 10(7):507–519
8. Inglese J, Auld DS, Jadhav A, Johnson RL, Simeonov A, Yasgar A, Zheng W, Austin CP (2006) Quantitative high-throughput screening: a titration-based approach that efficiently identifies biological activities in large chemical libraries. Proc Nat Acad Sci USA 103(31):11473–11478

9. Chan F, Bradley A, Wensel TG, Wilson JH (2004) Knock-in human rhodopsin-GFP fusions as mouse models for human disease and targets for gene therapy. Proc Nat Acad Sci USA 101(24):9109–9114
10. Bowen WP, Wylie PG (2006) Application of laser-scanning fluorescence microplate cytometry in high content screening. Assay Drug Dev Technol 4(2):209–221
11. Xie HQ, Adler R (2000) Green cone opsin and rhodopsin regulation by CNTF and staurosporine in cultured chick photoreceptors. Invest Ophthalmol Vis Sci 41(13):4317–4323
12. Bradford RL, Wang C, Zack DJ, Adler R (2005) Roles of cell-intrinsic and microenvironmental factors in photoreceptor cell differentiation. Dev Biol 286(1):31–45
13. Cingolani C, Rogers B, Lu L, Kachi S, Shen J, Campochiaro PA (2006) Retinal degeneration from oxidative damage. Free Radical Biol Med 40(4):660–669
14. Hackam AS, Strom R, Liu D, Qian J, Wang C, Otteson D, Gunatilaka T, Farkas RH, Chowers I, Kageyama M, Leveillard T, Sahel JA, Campochiaro PA, Parmigiani G, Zack DJ (2004) Identification of gene expression changes associated with the progression of retinal degeneration in the rd1 mouse. Invest Ophthalmol Vis Sci 45(9):2929–2942
15. Komeima K, Rogers BS, Campochiaro PA (2007) Antioxidants slow photoreceptor cell death in mouse models of retinitis pigmentosa. J Cell Physiol 213(3):809–815
16. Punzo C, Xiong W, Cepko CL (2012) Loss of daylight vision in retinal degeneration: are oxidative stress and metabolic dysregulation to blame? J Biol Chem 287(3):1642–1648
17. Usui S, Oveson BC, Lee SY, Jo YJ, Yoshida T, Miki A, Miki K, Iwase T, Lu L, Campochiaro PA (2009) NADPH oxidase plays a central role in cone cell death in retinitis pigmentosa. J Neurochem 110(3):1028–1037
18. Usui S, Oveson BC, Iwase T, Lu L, Lee SY, Jo YJ, Wu Z, Choi EY, Samulski RJ, Campochiaro PA (2011) Overexpression of SOD in retina: need for increase in H2O2-detoxifying enzyme in same cellular compartment. Free Radical Biol Med 51(7):1347–1354
19. Chinta SJ, Rane A, Poksay KS, Bredesen DE, Andersen JK, Rao RV (2008) Coupling endoplasmic reticulum stress to the cell death program in dopaminergic cells: effect of paraquat. Neuromolecular Med 10(4):333–342
20. Huang CL, Lee YC, Yang YC, Kuo TY, Huang NK (2012) Minocycline prevents paraquat-induced cell death through attenuating endoplasmic reticulum stress and mitochondrial dysfunction. Toxicol Lett 209(3):203–210
21. Kumar A, Singh BK, Ahmad I, Shukla S, Patel DK, Srivastava G, Kumar V, Pandey HP, Singh C (2012) Involvement of NADPH oxidase and glutathione in zinc-induced dopaminergic neurodegeneration in rats: similarity with paraquat neurotoxicity. Brain Res 1438:48–64
22. Somayajulu-Nitu M, Sandhu JK, Cohen J, Sikorska M, Sridhar TS, Matei A, Borowy-Borowski H, Pandey S (2009) Paraquat induces oxidative stress, neuronal loss in substantia nigra region and parkinsonism in adult rats: neuroprotection and amelioration of symptoms by water-soluble formulation of coenzyme Q10. BMC Neurosci 10:88
23. Yang W, Tiffany-Castiglioni E, Koh HC, Son IH (2009) Paraquat activates the IRE1/ASK1/JNK cascade associated with apoptosis in human neuroblastoma SH-SY5Y cells. Toxicology Lett 191(2–3):203–210
24. Chen Q, Prior M, Dargusch R, Roberts A, Riek R, Eichmann C, Chiruta C, Akaishi T, Abe K, Maher PA (2011) Novel neurotrophic drug for cognitive enhancement and Alzheimer's disease. PloS one 6(12):e27865
25. Silber BM (2010) Driving drug discovery: the fundamental role of academic labs. Sci Transl Med 2(30):30cm16
26. Reed JC, White EL, Aubé J, Lindsley C, Li M, Sklar L, Schreiber S (2012) The NIH's role in accelerating translational sciences. Nat Biotechnol 30(1):16–19
27. Frearson J, Wyatt P (2010) Drug discovery in academia: the third way? Expert Opin Drug Discov 5(10):909–919
28. Cheng KCC, Inglese J (2012) A coincidence reporter-gene system for high-throughput screening. Nat Methods 9(10):937

# Chapter 98
# Antioxidant Therapy for Retinal Disease

**Anna-Sophia Kiang, Marian M. Humphries, Matthew Campbell and Peter Humphries**

**Abstract** Disease mechanisms associated with retinal disease are of immense complexity, mutations within 45 genes having been implicated, for example, in retinitis pigmentosa, while interplay between genetic, environmental, and demographic factors can lead to diabetic retinopathy, age-related macular degeneration, and glaucoma. In light of such diversity, any therapeutic modality that can be targeted to an early molecular process instrumental in multiple forms of disease, such as oxidative stress, holds much attraction. Here, we provide a brief overview of a selection of compounds displaying antioxidant activity, which have been shown to slow down degeneration of retinal tissues and highlight suggested modes of action.

**Keywords** Antioxidant · Oxidative stress · ROS · Retinal disease · Lutein · CAPE · Curcumin · Alpha-lipoic acid · Cannabidiol · 8-OH DPAT · JHX-4

## 98.1 Introduction

Oxidative stress occurs when there is an imbalance between the production of reactive oxygen species (ROS) and activity of endogenous antioxidant defense systems and is often associated with nitrosative stress which results from a similar build-up of reactive nitrogen species. In the retina, photoreceptors are particularly vulnerable to these stresses due to the environment of high oxygen and lipid polyunsaturated

A.-S. Kiang (✉) · M. M. Humphries · M. Campbell · P. Humphries
Ocular Genetics Unit, School of Genetics and Microbiology,
Trinity College Dublin, Dublin 2, Ireland
e-mail: skiang@tcd.ie

M. M. Humphries
e-mail: mhumphri@tcd.ie

M. Campbell
e-mail: campbem2@tcd.ie

P. Humphries
e-mail: pete.humphries@tcd.ie

J. D. Ash et al. (eds.), *Retinal Degenerative Diseases,* Advances in Experimental Medicine and Biology 801, DOI 10.1007/978-1-4614-3209-8_98,

fat (PUFA) content coupled with phototransduction leading to increased ROS production, while phagocytosis of ROS-laden photoreceptor outer segments and the interaction of raised lipofuscin levels with light also places the RPE under considerable oxidative stress [1]. ROS generated by ischaemia/reperfusion [2], glutamate excitotoxicity [3], and raised glucose [4] in the inner retina mean that these cells are also under threat. Primary reactive species include superoxide anion, hydrogen peroxide ($H_2O_2$), hydroxyl radical, singlet oxygen, nitric oxide and peroxynitrate which can generate further products, for example, nitrotyrosine, formed by reaction between peroxynitrate and tyrosine residues of a protein. Additionally, oxidation of PUFA can generate 4-hydroxynonenal (4-HNE) and malondialdehyde (MDA) which can lead to chronic lipid-based immune responses which while initially protective can become pathological under prolonged oxidative stress [5]. Endogenous cellular defense mechanisms counteracting these reactive species include the tripeptide glutathione (GSH) which is oxidised to glutathione disulphide (GSSH) and reduced back to GSH. Thus, the GSH/GSSH ratio is an indication of the redox status of the cell: low ratios implying high oxidative stress which in turn can lead to activation of transcription factors, including, nuclear factor (erythroid-derived 2)-like 2 (Nrf2) which binds to antioxidant response elements up-regulating detoxification and antioxidant enzymes. Raised levels of protective enzymes such as superoxide dismutase (SOD) which catalyzes the dismutation of superoxide into oxygen and $H_2O_2$, glutathione peroxidase (GPx) which reduces lipid hydroperoxides to alcohols and catalase which along with GPx breaks down hydrogen peroxide to water and oxygen, are the cell's attempt to return to homeostasis. However, when the endogenous antioxidant systems of retinal cells fail to keep reactive species under a certain threshold level, disease processes culminating in cell death ensue [6]. Therapeutic intervention by exogenous application of antioxidant compounds is thus an attractive proposition for preventing retinal disease.

## 98.2 Lutein

Lutein is a blue light-absorbing xanthophyll carotenoid with clinically proven retinal protective effects [7]. Mechanistic studies carried out by Sasaki et al., in streptozotocin (STZ)-generated diabetic and light-induced retinal degeneration (LIRD) murine models fed with lutein showed amelioration of retinal thinning and electroretinographic (ERG) responses which was correlated with reduced levels of ROS [8, 9] and double-stranded DNA breaks [9] while similar improvements in retinal structure and function, also attributed to lutein, were observed in a second model of diabetic retinopthy in which GSH and GPx activity increased and levels of MDA decreased [10]. In addition, lutein also had a neuroprotective effect in ischaemia/reperfusion mouse models of acute glaucoma [11, 12] preventing ganglion and amacrine cell loss again via attenuation of oxidative stress as observed by increased GSH, and a reduction in nitrotyrosine, MDA, activated caspase-3 and nuclear localization of DNA damage-associated polyADP-ribose.

## 98.3 Caffeic Acid Phenethyl Ester (CAPE)

Derived from a lignin precursor, CAPE is found in all plants from where it is concentrated by bees in honeybee propolis. It has been shown to reduce pro-inflammatory signaling in cell culture while increasing activity of the protective Nrf2 [13]. Similarly, hemeoxygenase-1 (HO-1) expression was increased by CAPE administered to $H_2O_2$-stressed 661W cells and to albino rats reared in dim light leading to reduced cell death and improved animal ERG recordings [14]. Furthermore, histological and electrophysiological assessment of rats following ischaemia/reperfusion-injury where CAPE had been injected i.p both before and after reperfusion, indicated that retinal pathology had ameliorated. This was backed up by molecular evidence demonstrating reduction in MDA with concomitant increased levels of SOD, GPx, and catalase [15].

## 98.4 Curcumin

Curcumin, a constituent of turmeric, has been used in traditional Indian cuisine and medicine for over 2000 years. More recently, it has come to the fore as a pleiotropic therapeutic and is currently under clinical trial in over 60 studies. In the retina, Mandal et al. [16] observed improved ERG readings and ONL thicknesses in curcumin-fed rats subjected to LIRD compared to controls which correlated with reduced 4-HNE generation and significantly dampened light-induced expression of many genes involved in oxidative stress, inflammation, and apoptosis. In addition $H_2O_2$-treated cell lines were also protected by curcumin via up-regulation of the protective enzymes HO-1, thioredoxin-1 and Nrf-2 while Woo et al. [17], showed that reduction of ROS levels was mediated by HO-1. Antioxidant properties of curcumin were again exemplified by Gupta et al. [18], in diabetic rats where restoration of GSH, SOD, and catalase levels resulted in reduced endothelial cell organellar degeneration and capilliary basement membrane thickness. Curcumin has also been shown to alleviate ER-stress-induced retinal degeneration [19]. In these experiments Vasireddy et al. administered curcumin to the P23H rhodopsin rat model and observed enhanced expression levels of photoreceptor-expressed genes, corrected P23H rhodopsin trafficking and lowered ER stress response protein levels which correlated with protection of ONL thickness to about 60 % that of wild type controls and improved ERGs compared to untreated P23H controls.

## 98.5 Alpha-Lipoic Acid

A comparison between conventional glycemic control with insulin and daily administration of lipoic acid, a natural food supplement, in alloxan-induced diabetic mice, demonstrated a reduction in oxidative stress as observed by enhanced GSH

and GPx activity and normalisation of MDA levels, resulting in restoration of ERGs to control values by both treatments [20]. In addition, oral administration of lipoic acid to STZ-generated diabetic rats reduced superoxide formation and blocked hyperglycemia-induced increases in VEGF, angiopoetin 2 and erythropoetin [21].

## 98.6 Cannabidiol

Cannabidiol is a major, non-addictive constituent of cannabis which has antioxidant and anti-inflammatory properties. In microglial cells and rat retinas treated with lipopolysaccharide, cannabidiol attenuated high ROS and nitric oxide generation which resulted in down-regulation of p38 mitogen-activated protein kinase and associated tumor necrosis factor-α release and glial activation culminating in prevention of neuronal cell death [22]. In a later study carried out on STZ-diabetic rats by the same group, cannabidiol reduced rampant diabetes-induced oxidative and nitrosative stress in ganglion cells as well as Muller cell activation with the knock-on effect of reducing peroxynitrite and thus tyrosine nitration of glutamate synthase which would otherwise have resulted in neurotoxic accumulation of glutamate. In this way, neuronal cell death was prevented with the number of TUNEL and caspase-3 positive cells near to that of control, wild-type animals [23].

### *98.6.1 8-Hydroxy DPAT (8-OH DPAT)*

8-hydroxy DPAT (8-hydroxy-*N, N*-dipropyl-2-aminotetralin) and another serotonin 5-$HT_{1A}$ receptor agonist (AL-8309) shown by Collier et al., to protect the rat retina from blue light-induced photo-oxidative damage was associated with significant decreases in both microglial and alternative complement pathway activation [24, 25]. Definitive proof that 8-OH DPAT protects via reducing oxidative damage has been reported by the same group in both $H_2O_2$-treated ARPE-19 cells and murine eyes subretinally injected with AAV carrying a ribozyme targeting SOD2 [26]. Superoxide generation was reduced while SOD2 and GSH/GSSG ratio increased resulting in decreased lipid peroxidation, nitrotyrosine levels and mitochondrial damage in cell cultures treated with 8-OH DPAT while systemic administration of the same resulted in a reduction by 60% of lipofuscin accumulation and improved ERG and ONL thickness in the SOD2 knockdown model eyes. A phase III, multi-centred, randomized placebo-controlled clinical trial of AL-8309 for dry AMD (NCT ID: NCT00890097) has recently been completed.

## 98.7 Multifunctional Antioxidant JHX-4

Strong evidence that an initial trigger in light damage to photoreceptor is the generation of superoxide and release of iron from ferritin, and that these react chemically to form hydroxyl ions which then cause lipid peroxidation and membrane damage, has stimulated Jin et al., [27] to design multifunctional antioxidants containing both free radical scavenging and redox metal chelating groups. These researchers demonstrated that such compounds can protect $H_2O_2$-challenged ARPE-19 cells from hydroxyl radicals, reducing cell death. Further, in vivo proof of concept studies from this lab demonstrated that the compound, JHX-4 (4-(5-hydroxypyrimidin-2-yl)-N, N- dimethyl-3, 5-dioxopiperazine-1-sulfonamide) could combat LIRD in rat [28] since oxidative stress products 4-HNE and nitrotyrosine, increased in retinas by LIRD remained at levels similar to those of non-light damaged controls in LIRD rats pre-fed with JHX-4. ONL thicknesses of treated LIRD retinas were only about 15 % less than undamaged retinas and over 50 % greater than untreated LIRD controls while both scoptopic and photopic ERG responses were almost identical to those of undamaged controls indicating that JHX-4 protects both rods and cones.

## 98.8 Conclusion

ROS are essential for modulating signaling pathways involved in basic physiological responses including cell proliferation, gene expression, and apoptosis [29] and thus complete inhibition by antioxidant therapy would be undesirable. However, there is no doubt that if a certain threshold level is surpassed due to generation of excess oxidative products, pathological responses will predominate and ultimately lead to cell death. In this regard, small molecule compounds displaying antioxidant properties which can access the retina, together with enhanced delivery systems [31] which may help reduce effective doses, show great promise as therapeutics for retinal disease.

## References

1. Wright AF, Chakarova CF, Abd El-AzizMM, Bhattacharya SS (2010) Photoreceptor degeneration: genetic and mechanistic dissection of a complex trait. Nat Rev Genet 11:273–284
2. Osborne NN, Casson RJ, Wood JPM, Chidlow G, Graham M, Melena J (2004) Retinal ischemia: mechanisms of damage and potential therapeutic strategies. Prog Retin Eye Res 23:91–147
3. Nguyen D, Alavi MV, Kim KY, Kang T, Scott RT, Noh YH et al (2011) A new vicious cycle involving glutamate excitotoxicity, oxidative stress and mitochondrial dynamics. Cell Death Dis 2:e240. doi:10.1038/cddis.117
4. Kowluru RA, Chan PS (2007) Oxidative stress and diabetic retinopathy. Exp Diabetes Res. doi:10.1155/2007/43603:1-12

5. Handa JT (2012) How does the macula protect itself from oxidative stress? Mol Aspect Med 33:418–435
6. Jarrett SG, Boulton ME (2012) Consequences of oxidative stress in age-related macular degeneration. Mol Aspect Med 33:399–417
7. Kijlstra A, Tian Y, Kelly ER, Berendschot TTJM (2012) Lutein: More than just a filter for blue light. Prog Retin Eye Res 31:303–315
8. Sasaki M, Ozawa Y, Kurihara T, Yuki K, Kobayashi S, Ishida S et al (2010) Neurodegenerative influence of oxidative stress in the retina of a murine model of diabetes. Diabetologia 53:971–979
9. Sasaki M, Yuki K, Kurihara T, Miyake S, Noda K, Kobayashi S et al (2011) Biological role of lutein in light-induced retinal degeneration. J Nutr Biochem. doi 10.1016/j.jnutbio.2011.01.006
10. Muriach M, Bosch-Morell F, Alexander G, Blomhoff R, Barcia J, Arnal E et al (2006) Lutein effect on retina and hippocampus of diabetic mice. Free Radic Biol Med 41:979–984
11. Dilsiz N, Sahaboglu A, Yildiz MZ, Reichenbach A (2006) Protective effects of various antioxidants during ischaemia-reperfusion in the rat retina. Graefes Arch Clin Exp Ophthalmol 244:627–633
12. Li S-Y, Fu Z-J, Huan M, Jang W-C, So K-F, Wong D et al (2009) Effect of lutein on retinal neurons and oxidative stress in a model of acute retinal ischemia/reperfusion. Invest Ophthalmol Vis Sci 50:836–843
13. Lee Y, Shin DH, Kim JH, Hong S, Choi D, Kim YJ et al (2010) Caffeic acid phenethyl ester-mediated Nrf2 activation and IkappaB kinase inhibition are involved in NfkappaB inhibitory effect: sructural analysis for NfkappaB inhibition. Eur J Pharmacol 643:21–28
14. Chen H, Tran J-TA, Anderson RE, Mandal MNA (2012) Caffeic acid phenethyl ester protects 661W cells from $H_2O_2$-mediated cell death and enhances electroretinography response in dim-reared albino rats. Mol Vis 18:1325–1338
15. Shi Y, Xingwei W, Gong Y, Qiu Y, Zhang H, Huang Z et al (2010) Protective effects of caffeic acid phenethyl ester on retinal ischemia/reperfusion injury in rats. Curr Eye Res 35:930–937
16. Mandal MNA, Patlolla JMR, Zheng L, Agbaga M-P, Tran J-TA, Wicker L et al (2009) Curcumin protects retinal cells from light- and oxidant stress-induced cell death. Free Radic Biol Med 46:672–679
17. Woo JM, Shin D-Y, Lee SJ, Joe Y, Zheng M, Yim JH et al (2012) Curcumin protects retinal pigment epithelium cells against oxidative stress via induction of heme oxygenase-1 expression and reduction of reactive oxygen. Mol Vis 18:901–908
18. Gupta SC, Kumar B, Nag TC, Agrawal SS, Agrawal P, Saxena R et al (2011) Curcumin prevents experimental diabetic retinopathy in rats through its hypoglycemic, antioxidant, and anti-inflammatory mechanisms. J Ocul Pharmacol Ther 27:123–130
19. Vasireddy V, Chavali VRM, Joseph VT, Kadam R, Lin JH, Jamison JA et al (2011) Rescue of photoreceptor degeneration by curcumin in transgenic rats with P23H rhodopsin mutation. PLoS ONE 6(6):e21193. doi:10.1371/journal.pone.0021193.
20. Johnsen-Soriano S, Garcia-Pous M, Arnal E, Sancho-Tello M, Garcia-Delpech S, Miranda M et al (2008) Early lipoic acid intake protects retina of diabetic mice. Free Radical Res 42:613–617
21. Lee SG, Lee CG, Yun IH, Hur DY, Yang JW, Kim HW (2012) Effect of lipoic acid on expression of angiogenic factors in diabetic rat retina. Clin Experiment Ophthalmol 40:e47–e57. doi:10.1111/j.1442-9071.2011.02695.x.
22. El-Remessy AB, Khalifa Y, Ola S, Ibrahim AS, Liou GI (2010) Cannabidiol protects retinal neurons by preserving glutamine synthetase activity in diabetes. Mol Vis 16:1487–1495
23. El-Remessy AB, Tang Y, Zhu G, Matragoon S, Khalifa Y, Liu EK et al (2008) Neuroprotective effects of cannabidiol in endotoxin-induced uveitis: critical role of p38 MAPK activation. Mol Vis 14:2190–2203
24. Collier RJ, Patel Y, Martin EA, Deminska O, Hellberg M, Krueer DS et al (2011) Agonists at the serotonin receptor ($5\text{-}HT_{1A}$) protect the retina from severe photo-oxidative stress. Invest Ophthalmol Vis Sci 52:2118–2126

25. Collier RJ, Wang Y, Smith SS, Martin E, Ornberg R, Rhoades K et al (2011) Complement deposition and microglial activation in the outer retina in light-induced retinopathy: inhibition by a 5-HT1A agonist. Invest Ophthalmol Vis Sci 52:8108–8116
26. Thampi P, Rao HV, Mitter SK, Cai J, Mao H, Li H et al (2012) The $5HT_{1a}$ receptor agonist 8-Oh DPAT induces protection from lipofuscin accumulation and oxidative stress in the retinal pigment epithelium. PLoS ONE 7(4):e34468. doi:10.1371/journal.pone.0034468.
27. Jin H, Randazzo J, Zhang P, Kador PF (2010) Multifunctional antioxidants for the treatment of age-related diseases. J Med Chem 53:1117–1127
28. Randazzo J, Zhang Z, Hoff M, Kawada H, Sachs A, Yuan Y et al (2011) Orally active multifunctional antioxidants are neuroprotective in a rat model of light-induced retinal damage. PLoS ONE 6(7):e21926. doi:10.1371/journal.pone.0021926.
29. Groeger G, Doonan F, Cotter TG, Donovan M (2012) Reactive oxygen species regulate prosurvival ERK1/2 signaling and bFGF expression in gliosis within the retina. Invest Ophthalmol Vis Sci 53:6645–6654
30. Humphries P, Humphries MM, Tam LCS, Farrar JG, Kenna PF, Campbell M et al (2012) Hereditary retinopathies. SpringerBriefs in Genetics. doi:10.1007/978-1-4614-4499-2_1
31. Campbell M, Humphries MM, Humphries P (2013) Barrier modulation in drug delivery to the retina. Methods Mol Biol 935:371–380

# Chapter 99
# Pathophysilogical Mechanism and Treatment Strategies for Leber Congenital Amaurosis

**Yingbin Fu and Tao Zhang**

**Abstract** Mutations in retinoid isomerase, RPE65, or lecithin-retinol acyltransferase (LRAT) disrupt 11-*cis*-retinal recycling and cause Leber congenital amaurosis (LCA), the most severe retinal dystrophy in early childhood. We used $Lrat^{-/-}$, a murine model for LCA, to investigate the mechanism of rapid cone degeneration. We found that mislocalized M-opsin was degraded whereas mislocalized S-opsin accumulated in $Lrat^{-/-}$ cones before the onset of massive ventral/central cone degeneration. Since the ventral and central retina expresses higher levels of S-opsin than the dorsal retina in mice, our results may explain why ventral and central cones degenerate more rapidly than dorsal cones in $Rpe65^{-/-}$ and $Lrat^{-/-}$ LCA models. In addition, human blue opsin and mouse S-opsin, but not mouse M-opsin or human red/green opsins, aggregated to form cytoplasmic inclusions in transfected cells, which may explain why blue cone function is lost earlier than red/green-cone function in LCA patients. The aggregation of short-wavelength opsins likely caused rapid cone degenerations through an ER stress pathway as demonstrated in both the $Lrat^{-/-}$ retina and transfected cells. Based on this mechanism, we designed a new therapy of LCA by reducing ER stress. We found that systemic injection of an ER chemical chaperone, tauroursodeoxycholic acid (TUDCA), is effective in reducing ER stress, preventing apoptosis, and preserving cones in $Lrat^{-/-}$ mice.

**Keywords** aggregation · RPE65 · LRAT · Leber congenital amaurosis (LCA) · Short-wavelength sensitive opsins (SWS) · Medium/long-wavelength sensitive opsins (M/LWS) · Cone degeneration

Y. Fu (✉) · T. Zhang
Department of Ophthalmology & Visual Sciences, University of Utah,
65 Mario Capecchi Drive, Salt Lake City, UT 84132, USA
e-mail: Yingbin.fu@hsc.utah.edu

T. Zhang
e-mail: tao0905@gmail.com

J. D. Ash et al. (eds.), *Retinal Degenerative Diseases,* Advances in Experimental Medicine and Biology 801, DOI 10.1007/978-1-4614-3209-8_99,

## 99.1 Introduction

Both Retinoid isomerase (RPE65) and lecithin-retinol acyltransferase (LRAT) are required for 11-*cis*-retinal recycling in the RPE. Mutations in *RPE65* or *LRAT* cause Leber congenital amaurosis (LCA) [1]. Two mouse models, *Rpe65*$^{-/-}$ and *Lrat*$^{-/-}$, capture many salient pathologic features of human LCA [2–4]. Both rod and cone function are severely compromised due to the lack of 11-*cis*-retinal [2, 3]. The cone opsins (S-opsin and M-opsin) fail to traffic from the cone inner segment to the cone outer segment and the cone photoreceptors in the central/ventral regions degenerate rapidly (<4 weeks). Early loss of foveal cones also occur in RPE65-deficient patients [5]. The mechanisms responsible for early cone death in both mouse models and human patients are not well understood. Specifically, it is unclear why ventral and central cones in mouse models die much more rapidly than dorsal cones. Similarly, it is unclear why blue cone function is lost early in patients [5, 6]. Here, we used the *Lrat*$^{-/-}$ mouse, a model for LCA, to investigate the mechanism and treatment for cone photoreceptor degeneration.

## 99.2 Materials and Methods

### *99.2.1 Animals and TUDCA Injection*

*Lrat*$^{-/-}$ mice were generated and described previously [3]. WT (*C57BL/6J*) mice were purchased from Jackson Laboratory. All animal experiments were approved by the Institutional Animal Care and Use Committees (IACUC) at the University of Utah and were performed in accordance with the ARVO Statement for the Use of Animal in Ophthalmic and Vision Research. Mice were reared under cyclic light (12 h light/12 h dark). *Lrat*$^{-/-}$ and WT mice were treated with TUDCA (TCI America) or vehicle (0.15 M $NaHCO_3$, pH 7.0) following a published procedure [7].

### *99.2.2 Statistics*

Data were presented as mean ± SEM, and the differences were analyzed with unpaired two-sample Student's *t*-test. *P* values <0.05 were considered statistically significant.

## 99.3 Results

### *99.3.1 Different Protein Stability of M and S Opsins in the Lrat*$^{-/-}$ *Retina.*

By immunohistochemistry, we found that *Lrat*$^{-/-}$ cones accumulated more mislocalized S-opsin than M-opsin [8]. We proceeded to verify this finding by western

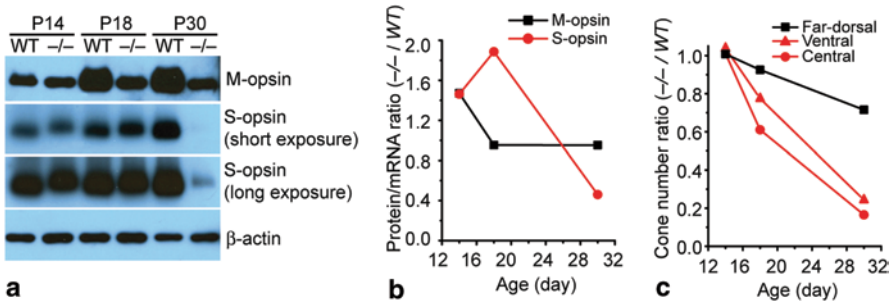


**Fig. 99.1** Expression of M and S opsins in *Lrat*$^{-/-}$ and WT retinas. **a** Western blot analysis of M and S opsins in the retinas of *Lrat*$^{-/-}$ and WT mice at P14, P18, and P30. Equal loading was indicated by β-actin. **b** The average protein/mRNA ratios of M and S opsins of *Lrat*$^{-/-}$ were normalized against those of WT. **c** The average cone numbers from *ventral*, *central*, and *far-dorsal* retina of *Lrat*$^{-/-}$ were normalized against those of *WT*. (Data were from Fig. 2 of [8]. Copyright National Academy of Sciences, USA)

blot at three stages of cone degeneration: (1) P14, pre-degeneration [9]; (2) P18, early-stage degeneration; (3) P30, late-stage degeneration. In P14 *Lrat*$^{-/-}$, the protein levels of both M-opsin and S-opsin were similar to those in WT (Fig. 99.1a) although their mRNA levels were slightly reduced [8]. However, in P18 *Lrat*$^{-/-}$ retina, the M-opsin protein was markedly reduced (~1.9 times) whereas the S-opsin level remained the same, as compared with WT (Fig. 99.1a). After we normalized the protein levels of cone opsins against their mRNA levels (i.e. protein/mRNA), this ratio almost doubled (~1.9 times) for S-opsin in P18 *Lrat*$^{-/-}$ compared to WT (Fig. 99.1b). In contrast, the protein/mRNA ratio of M-opsin in P18 *Lrat*$^{-/-}$ was similar to that in WT. Assuming the protein synthesis for cone opsins is minimally affected in the early stage of *Lrat*$^{-/-}$ cone degeneration, our results suggest that mislocalized S-opsin was more resistant to proteasome degradation than mislocalized M-opsin. Since the ventral and central retina express higher levels of S-opsin than the dorsal retina in mice [10], our results suggest that accumulation of mislocalized S-opsin may underlie the fast ventral/central cone degeneration in *Lrat*$^{-/-}$ mice. Cones at the far-dorsal region, which express more M-opsin than S-opsin, degenerated much more slowly, corresponding to less accumulation of mislocalized M-opsin. In P30 *Lrat*$^{-/-}$, both the protein (Fig. 99.1a) and mRNA [8] levels of S-opsin were drastically reduced, due to significant loss of ventral and central cones [4, 9] (Fig. 99.1c).

### *99.3.2 Mouse and Human SW Opsins Aggregate and Cause ER Stress in Transfected Cells*

By using a cell culture system (COS-7), we found that mouse S-opsin and human blue opsin showed prominent aggregations manifesting as green dots of varying sizes in the perinuclear region (Fig. 99.2a). This was not observed for mouse M-opsin and human red/green opsins. To examine the possibility that the aggregation of SW opsins may induce UPR and ER stress, COS-7 cells were co-transfected with

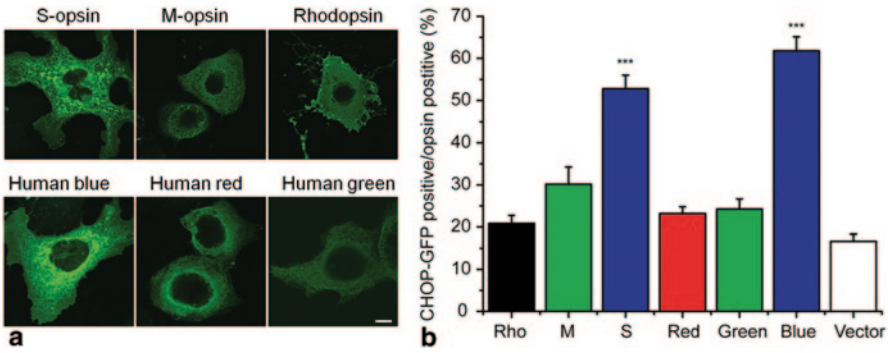


**Fig. 99.2** Mouse *S-opsin* and human blue opsin aggregated and induced *CHOP* activation in COS-7 cells. **a** COS-7 cells were transfected with plasmids encoding various opsins, and were labeled with opsin antibodies (*green*). Scale bar, 10 μm. **b** Quantification of *CHOP-GFP* positive cells as percentages of opsin expressing cells. COS-7 cells were co-transfected with plasmids encoding *CHOP-GFP* and various opsins (or control vector pRK5 and pmCherry-N1), and were labeled with opsin antibodies. The numbers of vector transfected cells were estimated from mCherry positive cells. $N=10$ for Rho; $N=11$ for M, *red*, *blue*; $N=12$ for S and *green* opsins; $N=6$ for *vector* control. Both mouse *S-opsin* (S) and human blue opsin induced significant more CHOP activation than mouse *M-opsin* (M), human red/green opsins, bovine rhodopsin, and vector control. ***, $p<0.001$. (Data were from Figs. 5 and 6 of [8]. Copyright National Academy of Sciences, USA)

various opsins and a CHOP-GFP reporter plasmid. CHOP (C/EBP homology protein) is a well characterized UPR (unfolded protein response) target gene and an ER stress marker associated with apoptosis. It has been shown that CHOP-GFP can track the expression of endogenous CHOP [11]. The expression of mouse S and human blue opsins induced significant CHOP activation compared with the expression of rhodopsin, mouse M-opsin or human red/green opsins (Fig. 99.2b, $p<0.001$). Consistent with the cell culture result, the CHOP signal was markedly increased in the ONL of the ventral retina of P18 *Lrat*$^{-/-}$, coinciding with the maximal S-opsin accumulation and the early stage of cone degeneration [8]. The CHOP signal was lower in the ventral retina of P14 *Lrat*$^{-/-}$ when S-opsin accumulation was much less. In the far-dorsal retina of *Lrat*$^{-/-}$ (P14 and P18) that mainly expresses M-opsin, no CHOP upregulation was observed [8].

### *99.3.3 TUDCA Significantly Slows Down Cone Degeneration in Lrat*$^{-/-}$ *Mice*

To determine whether TUDCA can prevent or slow down this rapid cone degeneration, *Lrat*$^{-/-}$ mice were injected subcutaneously once every 3 days starting at P9. Treated mice were euthanized at P28 and cone cell densities were determined at different retinal regions from fluorescence images of cone-arrestin stained retinal flatmounts. There was significant cone degeneration in the ventral and central regions of retina in vehicle injected *Lrat*$^{-/-}$ mice (Fig. 99.3). TUDCA treatment

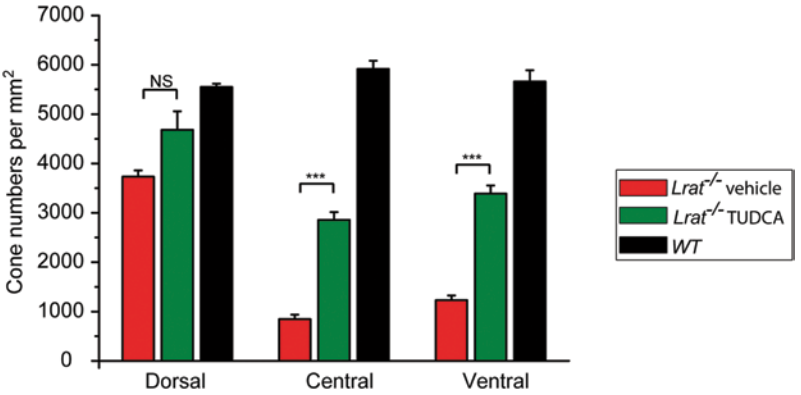


**Fig. 99.3** Quantification on the protective effect of TUDCA on *Lrat*$^{-/-}$ cones. Cone photoreceptors were counted in the *ventral*, *central*, and *dorsal* sections in TUDCA injected *Lrat*$^{-/-}$ ($n=8$), vehicle injected *Lrat*$^{-/-}$ ($n=6$), and untreated WT ($n=5$). Data were expressed as the average numbers of cones per mm$^2$ (mean ± SEM). Untreated *WT* mice were included as controls to evaluate the efficacy of TUDCA. ***$p<0.001$, NS, not significant. (From Fig. 1 of [12]. Copyright Association for Research in Vision and Ophthalmology)

resulted in a significant increase (~3-fold, $p<0.001$) in cone density in the ventral and central retina compared with the vehicle (Fig. 99.1). Cone cell morphology was greatly improved as evidenced by the presence of intact cone structures [12]. TUDCA treatment also increased cone numbers (25%) in the dorsal retina although the difference was not statistically significant ($p=0.057$). Although TUDCA provided significant protection of central and ventral cones of *Lrat*$^{-/-}$ mice, the cone densities are still lower than those of WT (54.5 and 62.7% lower for central cones and ventral cones, respectively). We observed a substantial reduction of CHOP in the ventral retina of TUDCA-treated *Lrat*$^{-/-}$ mice compared to that in vehicle-treated littermates at P18 [12]. Furthermore, TUDCA injection virtually eliminated apoptotic signals in the ONL of *Lrat*$^{-/-}$ mice judged by caspase-3 activation [12]. Our data suggest that TUDCA slows down cone degeneration by reducing ER stress and preventing apoptosis.

## 99.4 Discussion

Our studies showed that M and S opsins face very different fates in *Lrat*$^{-/-}$ mice: A significant amount of mislocalized M-opsin is degraded whereas S-opsin is resistant to proteasome degradation, resulting in far more toxic aggregation of S-opsin in the ventral and central cones than that of M-opsin in the dorsal cones. In addition, we found that aggregation of S-opsin activated the unfolded protein response (UPR) and caused ER stress. It is likely that the UPR in cones copes with mislocalized M-opsin more effectively than with mislocalized S-opsin. Thus, M-opsin is significantly degraded by the ER-associated degradation (ERAD) pathway, which relieves

ER stress. On the other hand, S-opsin is resistant to ERAD resulting in aggregation/accumulation, which induces apoptosis. As the ventral and central retina express higher levels of S-opsin than the dorsal retina in mice [10], our results explain the region-specific cone degeneration pattern in *Lrat*$^{-/-}$ and *Rpe65*$^{-/-}$ retinas. In addition, we demonstrated that systemic injection of TUDCA is effective in reducing ER stress, preventing apoptosis, and preserving cones in *Lrat*$^{-/-}$ mice. TUDCA has the potential to lead to the development of a new class of therapeutic drugs for treating LCA.

**Acknowledgment** We thank W. Baehr for providing the *Lrat*$^{-/-}$ mice. This study was supported by NIH grant EY022614, E. Matilda Ziegler Award, Career Initiation Research Grant Award from Knights Templar, Career Development Award from Research to Prevent Blindness, RPB), and an unrestricted grant to the Department of Ophthalmology at the University of Utah from RPB.

## References

1. den Hollander AI, Roepman R, Koenekoop RK, Cremers FP (2008) Leber congenital amaurosis: genes, proteins and disease mechanisms. Prog Retin Eye Res 27(4):391–419
2. Redmond TM, Yu S, Lee E, Bok D, Hamasaki D, Chen N et al (1998) Rpe65 is necessary for production of 11-cis-vitamin A in the retinal visual cycle. Nat Genet 20(4):344–351
3. Batten ML, Imanishi Y, Maeda T, Tu DC, Moise AR, Bronson D et al (2004) Lecithin-retinol acyltransferase is essential for accumulation of all-trans-retinyl esters in the eye and in the liver. J Biol Chem 279(11):10422–10432
4. Fan J, Rohrer B, Frederick JM, Baehr W, Crouch RK (2008) Rpe65-/- and Lrat-/- mice: comparable models of leber congenital amaurosis. Invest Ophthalmol Vis Sci 49(6):2384–2389
5. Jacobson SG, Aleman TS, Cideciyan AV, Heon E, Golczak M, Beltran WA et al (2007) Human cone photoreceptor dependence on RPE65 isomerase. Proc Natl Acad Sci U S A 104(38):15123–15128
6. Lorenz B, Poliakov E, Schambeck M, Friedburg C, Preising MN, Redmond TM (2008) A comprehensive clinical and biochemical functional study of a novel RPE65 hypomorphic mutation. Invest Ophthalmol Vis Sci 49(12):5235–5242
7. Phillips MJ, Walker TA, Choi HY, Faulkner AE, Kim MK, Sidney SS et al (2008) Tauroursodeoxycholic acid preservation of photoreceptor structure and function in the rd10 mouse through postnatal day 30. Invest Ophthalmol Vis Sci 49(5):2148–2155
8. Zhang T, Zhang N, Baehr W, Fu Y (2011) Cone opsin determines the time course of cone photoreceptor degeneration in Leber congenital amaurosis. Proc Natl Acad Sci U S A 108(21):8879–8884
9. Zhang H, Fan J, Li S, Karan S, Rohrer B, Palczewski K et al (2008) Trafficking of membrane-associated proteins to cone photoreceptor outer segments requires the chromophore 11-cis-retinal. J Neurosci 28(15):4008–4014
10. Applebury ML, Antoch MP, Baxter LC, Chun LL, Falk JD, Farhangfar F et al (2000) The murine cone photoreceptor: a single cone type expresses both S and M opsins with retinal spatial patterning. Neuron 27(3):513–523
11. Novoa I, Zeng H, Harding HP, Ron D (2001) Feedback inhibition of the unfolded protein response by GADD34-mediated dephosphorylation of eIF2alpha. J Cell Biol 153(5):1011–1022
12. Zhang T, Baehr W, Fu Y (2012) Chemical chaperone TUDCA preserves cone photoreceptors in a mouse model of Leber congenital amaurosis. Invest Ophthalmol Vis Sci 53(7):3349–3356

# Chapter 100
# Current and Emerging Therapies for Ocular Neovascularisation

**Alison L. Reynolds, David Kent and Breandán N. Kennedy**

**Abstract** Ocular neovascularisation (ONV) is a pathological feature of many human blinding diseases. Here, we review current pharmacological therapies for these disorders and highlight emerging therapies in clinical trial for ONV. Finally, we discuss desirable characteristics of future ONV therapies, including innovative strategies for novel delivery to the back of the eye.

**Keywords** Age-related macular degeneration · Clinical trials · Diabetic retinopathy · Ocular neovascularisation

## 100.1 Introduction

The growth of unwanted, abnormal blood vessels within the choroid and retina, is a pathological hallmark of blinding disorders, such as wet-age related macular degeneration (AMD), proliferative diabetic retinopathy (DR), retinopathy of prematurity (ROP) and retinal vein occlusions (RVO).

These diseases comprise the most common forms of visual impairment of old age (AMD), working age (DR) in the Western world [1, 2]. Fuelled by an ageing population and diabetes epidemic, the USA and European patients with wet AMD and PDR is predicted to rise to 3 and 16 million respectively by 2016 [3, 4].

A. L. Reynolds (✉) · B. N. Kennedy
School of Biomolecular and Biomedical Science, Conway Institute,
University College Dublin, Belfield, Dublin 4, Ireland
e-mail: alison.reynolds@ucd.ie

D. Kent
The Vision Clinic, Circular Road, Kilkenny, Ireland
e-mail: dkent@liverpool.ac.uk.

Pharmacology and Therapeutics, University of Florida, Gainesville, FL, USA

B. N. Kennedy
e-mail: brendan.kennedy@ucd.ie

J. D. Ash et al. (eds.), *Retinal Degenerative Diseases,* Advances in Experimental Medicine and Biology 801, DOI 10.1007/978-1-4614-3209-8_100,

While physiological angiogenesis is central to ocular development, the growth of abnormal blood vessels in ONV disease causes blindness by damaging the retina: leaking, haemorrhaging and forming scars, prompting photoreceptor death [1, 2]. Standard intervention is to block pro-angiogenic factors, particularly vascular endothelial growth factor (VEGF), preventing the formation of new blood vessels. Here, we review current and emerging therapies for treating ONV, highlighting novel mechanisms of action and innovative delivery methods.

## 100.2 Current Therapies for ONV

Anti-VEGF therapies (Lucentis, Avastin, Eylea) constitute the vast majority of the ONV market. Therapies used pre-2006 for ONV include photodynamic therapy with Verteporfin, intravitreal steroids, anti-VEGF aptamer (Macugen) and are now used infrequently.

Anti-VEGF therapies antagonise a key component of the angiogenesis pathway, preventing neovascularisation. The current gold standard since 2006 is the anti-VEGF monoclonal antibody ranibizumab (Lucentis®; Genentech/Roche). Approximately, 30 % of patients report a gain in visual acuity with at least an arrest of vision loss occurring in most cases [5]. Bevacizumab (Avastin®; Genentech/Roche), a less expensive anti-VEGF antibody, used in colorectal cancer, is used off-label for ONV. The Comparison of AMD Treatments Trials reported that Lucentis and Avastin are equivalent in terms of efficacy and safety [6]. In 2011, VEGF trap Aflibercept (Eylea®; Regeneron) was approved in the USA. This recombinant fusion protein binds to all VEGFA isoforms and has improved efficacy which may result in reduced dosing frequency [7].

The arrival of Lucentis revolutionised the treatment of ONV, not only halting blindness but also improving vision. The key limitation for anti-VEGF therapies is their delivery mode of monthly intravitreal injections which must be performed in a surgical setting by an ophthalmic surgeon. This exerts a large service-delivery burden on physicians, healthcare systems and patients, removing patient independence. Moreover, the long-term systemic and ocular effects of blocking VEGF are unknown.

## 100.3 Emerging Therapies

Here, we focus on emerging therapies that have progressed into clinical trials for ONV, DR or wet AMD. Table 100.1 gives a summary of each drug, known targets, promoters, delivery and clinical trial phase. This is an exciting time for ONV with many new therapies targeting different pathways and novel delivery methods coming on stream.

**Table 100.1** Summary of drugs in clinical trial for ONV, wet AMD and DR (MedTrack reports 12.12.2012). Shown is highest phase clinical trial undertaken for ONV, wet AMD or DR. $I^R$, $II^R$, $III^R$: recruiting for a phase I, II or III trial

| Drug | Company | Target | Size | Delivery | Phase |
|---|---|---|---|---|---|
| Arxxant | Eli Lilly/Takeda | Protein kinase C-beta | Small | Oral | Pending approval |
| Ad-PEDF | GenVec | PEDF | Large | Intravitreal | I |
| GS101/Aganirsen | Gene Signal International | Insulin receptor substrate 1 | Small | Topical | I[a] |
| ARC1905 | Ophthotech | Complement component 5 | Large | Intravitreal | I |
| AAV-sFLT01 | Genzyme/AGTC | VEGF | Large | Intravitreal | $I^R$ |
| JSM6427 | Shire Plc. | α5β1 integrin | Large | Intravitreal | I |
| Palomid 529 | Paloma Pharmaceuticals | PI3K/Akt/mTOR | Small | Topical | I |
| Retinostat | Oxford Biomedica | Endostatin, angiostatin | Large | Intravitreal | $I^R$ |
| TG-0054 | TaiGen Biotechnology | CXCR4 | Small | Topical | I |
| TG100801 | TargeGen/Sanofi | VEGFR2, SRC | Small | Topical | I |
| Vatalanib/PTK787 | Novartis | VEGFR1, 2, 3, PDGF | Small | Oral | I/II |
| Volociximab | Ophthotech | α5β1 integrin | Large | Intravitreal | I |
| AL 39324 | Alcon | VEGFR1 and 3, KDR, PDGFR-B | Small | Intravitreal | II |
| ATG3/mecamylamine | JDRF/CoMentis | Nicotinic acetylcholine receptor | Small | Topical | II |
| Evizon/squalamine lactate | Ohr Pharmaceutical | Growth factor signalling | Small | Topical | $II^R$ |
| Fovista/E10030 | Ophthotech | PDGF-B | Large | Intravitreal | IIb |
| Gly230 | Glycadia Pharm. | Glycation | Small | Oral | II |
| Hl-con1 | Iconic Therapeutics | Pathologic blood vessels | Large | Intravitreal | II |
| NT-503 | Neurotech | VEGF | Implant | Surgical | II[a] |
| Pazopanib/Votrient | Glaxo Smith Kline | VEGFR1,2,3, PDGFR-A,-B, c-KIT | Small | Topical | II |
| Sirolimus | MacuSight/Santen | mTOR | Small | Oral | II |
| Zybrestat | OXiGENE/Bristol Myers-Squibb | Vascular disrupting agent | Small | Intravenous/topical | II |
| Iluvien | pSividia/Alimera/Dainippon | Corticosteroid fluocinolone acetonide | Implant | Intravitreal | II |
| Posurdex/Ozurdex | Allergan | Corticosteroid dexamethasone | Implant | Intravitreal | II |
| KH902 | Chengdu/Kanghong Biotech | VEGF | Large | Intravitreal | $III^R$ |

[a] Unable to verify at www.clinicaltrials.gov

### *100.3.1 Anti-VEGF Therapies*

Due to the success of Lucentis, more anti-VEGF therapies are in the pipeline each attempting to improve efficacy and mode of delivery. KH902, a VEGF receptor decoy, blocks ONV by binding VEGF and placental growth factor (PlGF) [8]. AAV2-sFLT01 a gene therapy targets VEGF and gives persistent expression following a single intravitreal injection [9]. NT-503 an encapsulated cell technology implant (containing retinal pigment epithelial cells) secretes VEGF antagonists for 2 years [10].

### *100.3.2 Therapies Targeting Inflammatory System Components*

ONV is not only a disease of the vascular system but also an inflammatory disease as evidenced by aberrant activation of the complement system and an upregulation of inflammatory factors in AMD patients [11]. ARC1905 is a complement component 5 aptamer in development which inhibits the complement cascade [12].

### *100.3.3 Gene Therapies*

Gene therapy offers the potential of a one-off therapy: a single injection of a vector which can continuously express a chosen protein. Retinostat uses a lentiviral vector to deliver two anti-angiostatic proteins: endostatin and angiostatin [13]. AdPEDF, an adenovirus, delivers pigment epithelium-derived factor (PEDF), a potent anti-angiogenic protein [14]. GS-100, an anti-sense oligonucleotide acts by silencing the insulin receptor substrate 1 gene [15].

### *100.3.4 Integrin α5β1 Antagonists*

Integrins, adhesion molecules known as cellular "glue" mediate binding to the extracellular matrix and regulate endothelial cell survival, proliferation and migration. Antagonists of α5β1 integrin prevent it from binding to fibronectin, a key step in angiogenesis [16]. Two α5β1 antagonists are in development: JSM6427 and volociximab a monoclonal antibody [17, 18].

### *100.3.5 Tyrosine Kinase Inhibitors*

ONV can be prevented by targeting pathways downstream of VEGF using receptor tyrosine kinase inhibitors (RTKi) to block phosphorylation or bind receptors.

Four RTKis are in clinical trial for ONV: TG100801, a VEGFR2/SRC kinase inhibitor, PTK787, inhibiting all 3 VEGF receptors and platelet-derived growth factor (PDGF), AL-39324, inhibiting VEGFR1 & 3, KDR and PDGFR-B and pazopanib inhibiting all VEGF receptors, PDGF and c-kit [19–22]. These small molecules can be delivered orally or topically. Chapter 102 discusses inhibitors to PI3K/Akt/mTOR.

### *100.3.6 Corticosteroids*

Corticosteroids reduce inflammation and oedema. Two treatments for diabetic macular oedema are being developed as adjunct therapies for patients with ONV [23, 24]. Posurdex/Ozurdex and Iluvien have been formulated to be injected as slow release ocular implants to last 3 years and reduce the frequency of Lucentis injections.

### *100.3.7 Other Small Molecules*

Small molecules are in development as oral, topical or intravenous therapies for ONV. Arxxant, a protein kinase C inhibitor acts downstream of VEGF [25], TG-0054, a CXCR4 antagonist down regulates VEGF [26]. Evizon inhibits VEGF, PDGF and basic fibroblast growth factor (bFGF) [27]. ATG3, a non-specific nicotinic acetylcholine receptor antagonist suppresses ONV [28]. GLY-230, a selective glycation inhibitor, inhibits VEGF and PEDF [29]. Zybrestat, a vascular disrupting agent, depolymerises tubulin and disrupts cell junctions [30].

### *100.3.8 Other Large Molecules*

Fovista, a PDGF-B aptamer, disrupts neovascular pericytes causing CNV regression [31]. Used as a combination therapy, Fovista shows efficacy over Lucentis as a monotherapy [32]. hl-con1, a fusion protein targets pathologic blood vessels, which are selectively destroyed by the immune system [33].

## 100.4 Desirable Characteristics for ONV Therapies

It is possible to design a “wish list” of desirable characteristics for an ideal ONV therapy. The basics are a compound which is safe, efficacious, fast-acting, long-lasting, and reasonably priced. A compound which is anti-angiogenic, anti-inflammatory and which regresses ONV would be advantageous. The future is likely to involve combination therapies targeting a variety of elements within angiogenesis and inflammatory cascades, not limited to VEGF.

An improvement to drug delivery options is essential. Small molecules have the option to be formulated as a patient-administered tablet, eye drop or gel, reducing the service-delivery burden on physicians and potentially providing a prophylactic therapy. Gene therapies offer the promise of a once-off treatment. Drugs formulated in inserts and implants will reduce the number of injections and visits to the physician's office.

## 100.5 Conclusion

Current therapies for ONV, while efficacious, are limited in success by their delivery mode. Emerging therapies comprise a broad spectrum of drugs: from small molecule inhibitors of the targets of VEGF to vascular disrupting agents. Future treatment of ONV will involve safer, more efficacious combination therapies which target multiple anti-angiogenic and anti-inflammatory pathways. Patient administered tablets or eye drops as adjuncts will reduce clinic visits.

## References

1. Jager RD, Mieler WF, Miller JW (2008) Age-related macular degeneration. N Engl J Med 358:2606–2617
2. Cheung N, Mitchell P, Wong TY (2010) Diabetic retinopathy. Lancet 376:124–136
3. European ophthalmics pharmaceuticals market (2010) Frost & Sullivan report M4AC-52 Web. 08 Oct. 2013
4. U.S. retinal therapeutics market (2011) Frost & Sullivan report N85D-52. Web. 08 Oct 2013
5. Rosenfeld PJ, Brown DM, Heier JS, Boyer DS, Kaiser PK, Chung CY, Kim RY (2006) Ranibizumab for neovascular age-related macular degeneration. N Engl J Med 355:1419–1431
6. The CATT Research Group (2011) Ranibizumab and Bevacizumab for neovascular age-related macular degeneration. N Engl J Med 364:1897–1908
7. Heier JS, Brown DM, Chong V, Korobelnik J-F, Kaiser PK, Nguyen QD, Kirchhof B, Ho A, Ogura Y, Yancopoulos GD, Stahl N, Vitti R, Berliner AJ, Soo Y, Anderesi M, Groetzbach G, Sommerauer B, Sandbrink R, Simader C, Schmidt-Erfurth U (2012) Intravitreal Aflibercept (VEGF Trap-Eye) in wet age-related macular degeneration. Ophthalmology 119:2537–2548
8. Huang J, Li X, Li M, Li S, Xiao W, Chen X, Cai M, Wu Q, Luo D, Tang S, Luo Y (2012) Effects of intravitreal injection of KH902, a vascular endothelial growth factor receptor decoy, on the retinas of streptozotocin-induced diabetic rats. Diabetes Obes Metab 14:644–653
9. Lukason M, DuFresne E, Rubin H, Pechan P, Li Q, Kim I, Kiss S, Flaxel C, Collins M, Miller J, Hauswirth W, MacLachlan T, Wadsworth S, Scaria A (2011) Inhibition of choroidal neovascularization in a nonhuman primate model by intravitreal administration of an AAV2 vector expressing a novel anti-vegf molecule. Mol Ther 19:260–265
10. Neurotech (2012) NT-503 VEGF-Antagonist. http://www.neurotechusa.com/VEGF-Antagonist.html. Accessed 08 Oct 2013
11. Klein RJ, Zeiss C, Chew EY, Tsai J-Y, Sackler RS, Haynes C, Henning AK, SanGiovanni JP, Mane SM, Mayne ST, Bracken MB, Ferris FL, Ott J, Barnstable C, Hoh J (2005) Complement factor H polymorphism in age-related macular degeneration. Science 308:385–389
12. Ophthotech Corp (2013) ARC1905-Anti-C5 Aptamer. http://www.ophthotech.com/product-candidates/ arc1905/. Accessed 08 Oct 2013

13. Binley K, Widdowson P, Kelleher M, de Belin J, Loader J, Ferrige G, Carlucci M, Esapa M, Chipchase D, Angell-Manning D, Ellis S, Mitrophanous K, Miskin J, Bantseev V, Nork T, Miller P, Naylor S (2012) Safety and biodistribution of an equine infectious anemia virus-based gene therapy, RetinoStat(®), for age-related macular degeneration. Hum Gene Ther 23:980–989
14. Rasmussen H, Chu K, Campochiaro P, Gehlbach P, Haller J, Handa J, Nguyen Q, Sung J (2001) Clinical protocol. An open-label, phase I, single administration dose-escalation study of ADGVPEDF.11D (ADPEDF) in neovascular age-related macular degeneration (AMD). Hum Gene Ther 12:2029–2032
15. Cloutier F, Lawrence M, Goody R, Lamoureux S, Al-Mahmood S, Colin S, Ferry A, Conduzorgues J-P, Hadri A, Cursiefen C, Udaondo P, Viaud E, Thorin E, Chemtob S (2012) Antiangiogenic activity of aganirsen in nonhuman primate and rodent models of retinal neovascular disease after topical administration. Invest Ophthalmol Vis Sci 53:1195–1203
16. Kim S, Bell K, Mousa SA, Varner JA (2000) Regulation of angiogenesis in vivo by ligation of integrin α5β1 with the central cell-binding domain of fibronectin. Am J Pathol 156:1345–1362
17. Ramakrishnan V, Bhaskar V, Law D, Wong M, DuBridge R, Breinberg D, O'Hara C, Powers D, Liu G, Grove J, Hevezi P, Cass K, Watson S, Evangelista F, Powers R, Finck B, Wills M, Caras I, Fang Y, McDonald D, Johnson D, Murray R, Jeffry U (2006) Preclinical evaluation of an anti-alpha5beta1 integrin antibody as a novel anti-angiogenic agent. J Exp Ther Oncol 5:273–286
18. Zahn G, Vossmeyer D, Stragies R, Wills M, Wong C, Löffler K, Adamis A, Knolle J (2009) Preclinical evaluation of the novel small-molecule integrin Î± 5β1 inhibitor jsm6427 in monkey and rabbit models of choroidal neovascularization. Arch Ophthalmol 127:1329–1335
19. Caballero S, Sengupta N, Binghaman DP, Timmers A, Romano C, Grant MB (2007) Oral Administration of AL-39324 Can Both Suppress and Cause Regression of Vascular Lesion Volume in Experimental Choroidal Neovascularization. ARVO Meeting Abstracts 48:1470
20. Doukas J, Mahesh S, Umeda N, Kachi S, Akiyama H, Yokoi K, Cao J, Chen Z, Dellamary L, Tam B, Racanelli-Layton A, Hood J, Martin M, Noronha G, Soll R, Campochiaro PA (2008) Topical administration of a multi-targeted kinase inhibitor suppresses choroidal neovascularization and retinal edema. J Cell Physiol 216:29–37
21. Maier P, Unsoeld A, Junker B, Martin G, Drevs J, Hansen L, Agostini H (2005) Intravitreal injection of specific receptor tyrosine kinase inhibitor PTK787/ZK222 584 improves ischemia-induced retinopathy in mice. Graefes Arch Clin Exp Ophthalmol 243:593–600
22. Takahashi K, Saishin Y, Saishin Y, King AG, Levin R, Campochiaro PA (2009) Suppression and regression of choroidal neovascularization by the multitargeted kinase inhibitor pazopanib. Arch Ophthalmol 127:494–499
23. Kiernan DF, Mieler WF. Intraocular corticosteroids for posterior segment disease: 2012 update. Expert Opin Pharmacother. 2012; 13:1679–1694.
24 Comparison of Ranibizumab monotherapy and Ranibizumab combination therapies in recurrent or persistent choroidal neovascularization secondary to age-related macular degeneration. NCT01162746 http://www.ClinicalTrials.gov. Accessed 08 Oct 2013
25. Aiello L, Vignati L, Sheetz M, Zhi X, Girach A, Davis M, Wolka A, Shahri N, Milton R, PKC-DRS Group, PKC-DRS2 Group (2011) Oral protein kinase c β inhibition using ruboxistaurin: efficacy, safety, and causes of vision loss among 813 patients (1,392 eyes) with diabetic retinopathy in the protein kinase C β inhibitor-diabetic retinopathy study and the protein kinase C β inhibitor-diabetic retinopathy study 2. Retina 31:2084–2094
26. Liang Z, Brooks J, Willard M, Liang K, Yoon Y, Kang S, Shim H. CXCR4/CXCL12 axis promotes VEGF-mediated tumor angiogenesis through Akt signaling pathway. Biochem Biophys Res Commun. 2007; 359:716–722.
27. Connolly B, Desai A, Garcia C, Thomas E, Gast M (2006) Squalamine lactate for exudative age-related macular degeneration. Ophthalmol Clin North Am 19:381–391
28. Kiuchi K, Matsuoka M, Wu JC, Lima eSR, Kengatharan M, Verghese M, Ueno S, Yokoi K, Khu NH, Cooke JP, Campochiaro PA (2008) Mecamylamine suppresses basal and nicotine-stimulated choroidal neovascularization. Invest Ophthalmol Vis Sci 49:1705–1711

29. Cohen MP, Hud E, Wu V-Y, Shearman CW (2008) Amelioration of diabetes-associated abnormalities in the vitreous fluid by an inhibitor of albumin glycation. Invest Ophthalmol Vis Sci 49:5089–5093
30. Nambu H, Nambu R, Melia M, Campochiaro PA (2003) Combretastatin A-4 phosphate suppresses development and induces regression of choroidal neovascularization. Invest Ophthalmol Vis Sci 44:3650–3655
31. Jo N, Mailhos C, Ju M, Cheung E, Bradley J, Nishijima K, Robinson GS, Adamis AP, Shima DT (2006) Inhibition of Platelet-Derived Growth Factor B Signaling Enhances the Efficacy of Anti-Vascular Endothelial Growth Factor Therapy in Multiple Models of Ocular Neovascularization. Am J Pathol 168:2036–2053.
32. Ophthotech Corp (2012) Ophthotech's novel anti-PDGF combination agent fovista demonstrated superior efficacy over lucentis monotherapy in large controlled wet AMD trial. http://www.ophthotech.com/. Accessed 08 Oct 2013
33. Iconic Therapeutics (2010) hI-con1. http://www.iconictherapeutics.com/. Accessed 08 Oct 2013

# Chapter 101
# Targeting the PI3K/Akt/mTOR Pathway in Ocular Neovascularization

**Temitope Sasore, Alison L. Reynolds and Breandán N. Kennedy**

**Abstract** Ocular neovascularization, a common pathological feature of wet age-related macular degeneration (AMD), proliferative and diabetic retinopathy (PDR) leads to fluid and blood leakage, scar formation and ultimately blindness. Elucidation of vascular endothelial growth factor (VEGF) as a key mediator of angiogenesis led to clinically approved anti-VEGF agents. However, these drugs are associated with adverse side-effects, high costs and extensive clinical burden. The phosphatidylinositol-3-kinase (PI3K) pathway is an alternative therapeutic target in angiogenic diseases. The PI3K/Akt/mTOR pathway orchestrates an array of normal cellular processes, including growth, survival and angiogenesis. Here, we review the potential of targeting the PI3K pathway, to treat ocular neovascularization.

**Keywords** Phosphoinositol 3 kinase (PI3K) · Mammalian target of rapamycin (mTOR) · Protein kinase B/Akt · Neovascularization · Blindness · Vascular endothelial growth factor (VEGF)

**Abbreviations**

| | |
|---|---|
| AMD | Age-related macular degeneration |
| PDR | Proliferative and diabetic retinopathy |
| VEGF | Vascular endothelial growth factor |
| VEGFR | Vascular endothelial growth factor receptor |
| PI3K | Phosphatidylinositol-3-kinase |
| ONV | Ocular neovascularization |
| mTOR | Mammalian target of rapamycin complex |
| CNV | Choroidal neovascularization |

B. N. Kennedy (✉) · T. Sasore · A. L. Reynolds
School of Biomolecular and Biomedical Science, Conway Institute,
University College Dublin, Belfield, Dublin 4, Ireland
e-mail: brendan.kennedy@ucd.ie

T. Sasore
e-mail: temitope.sasore@ucdconnect.ie

A. L. Reynolds
e-mail: alison.reynolds@ucd.ie

J. D. Ash et al. (eds.), *Retinal Degenerative Diseases,* Advances in Experimental Medicine and Biology 801, DOI 10.1007/978-1-4614-3209-8_101,

## 101.1 Introduction

Proliferative and diabetic retinopathy (PDR) and wet Age-related macular degeneration (AMD) are responsible for ~4.89 and ~1.51 million, respectively, of severe cases of visual disability and irreversible blindness worldwide [1]. The direct medical costs of DR and AMD in the USA is ~$ 490 and $ 570 million, respectively [2]. These diseases while different in etiology, share common pathologies: vessel permeability, angiogenesis, inflammation and neurodegeneration. Although the molecular mechanisms of ocular neovascularization (ONV) are only partially elucidated, an imbalance between pro-angiogenic factors (e.g. VEGF) and anti-angiogenic signals (e.g. angiostatin) is responsible [3, 4]. The elucidation of these key regulators yielded therapeutic targets. Current treatments predominantly inhibit VEGF; the most prominent being Lucentis (Ranibizumab), and "off-label" Avastin (Bevacizumab) [5, 6]. These drugs delivered by intravitreal injection are effective in improving vision in 30–40 % of patients and stabilizes vision in ~90 % of treated patients [7, 8].

## 101.2 Current Anti-angiogenic Therapies: Promises and Problems

~6.4 million DR and AMD patients worldwide could benefit from anti-angiogenic therapy [1]. Currently, Lucentis, a monoclonal antibody, and Eylea, a soluble decoy receptor; all directed against VEGF, are the market leading prescriptions for wet AMD [5, 9]. In addition, Avastin is a popular off-label treatment [6, 10]. Another ~40 anti-angiogenic drugs are currently in clinical development, ~15 % of which also target VEGF and are a focus of this chapter. Despite the efficacy of approved agents, angiogenesis involves networks of factors, thus inhibition of one can cause compensatory up-regulation of another, leading to drug-resistance [11]. Current pharmacological options are associated with adverse side-effects, high drug costs, extensive clinical burden, invasive route of administration and limited population efficacy and inability to cause vascular regression [12]. Thus, sole inhibition of VEGF is an insufficient approach. In summary, these challenges highlight the need to develop improved pharmacological treatments for ocular neovascularization.

## 101.3 Phosphatidylinositol 3-Kinase (PI3K) Signalling Pathway

The PI3K/Akt/mTOR signalling pathway (Fig. 101.1) has emerged as an alternative target to inhibit angiogenesis [13, 14]. PI3K family members orchestrate a myriad of critical and essential cellular processes, including cell growth, metabolism, sur-

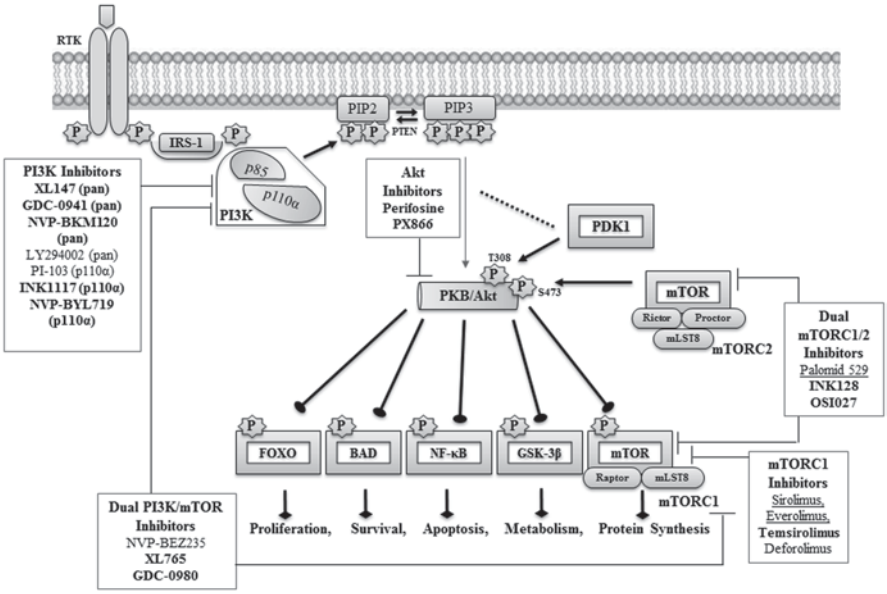


**Fig. 101.1** Figure shows a schematic diagram of the phosphatidylinositol 3-kinase (*PI3K*) signalling pathway, detailing known *PI3K* inhibitors (*square boxes*) and the target pathway nodes. Compounds *underlined* are in clinical trials for ocular indications and compounds in *bold* are in clinical trials for oncology. *RTK* receptor tyrosine kinase, *IRS*-1 insulin receptor substrate 1, *FKHR* forkhead, *NF-κB* nuclear factor-kappaB, and *GSK-3β* glycogen synthase kinase 3beta

vival and angiogenesis [15, 16]. The PI3K/AKT/mTOR pathway is the most frequently activated signalling pathway in human cancers [17]. Based on structural features and substrate specificity, PI3K family members are divided into class I, II and III [18], with class I being the most commonly investigated [19]. Class I PI3 yK enzymes form heterodimers composed of one of four closely related p110 catalytic subunits (α, β, δ or γ) along with an associated p85 regulatory subunit [18, 19]. Following receptor tyrosine kinase (RTK) activation (e.g. VEGF binding VEGFR) the RTK is phosphorylated, recruiting the regulatory subunit to the plasma membrane and activating the catalytic subunit. Then, PtdIns(4, 5)$P_2$ is phosphorylated to generate PtdIns(3, 4, 5)$P_3$, a second messenger that activates downstream signalling components, a prime example being the serine-threonine protein kinase AKT. Phosphoinositide-dependent protein kinase 1 (PDK1) can then phosphorylate AKT (protein kinase B) allowing it to activate downstream effectors, such as mammalian target of rapamycin complex 1 (mTORC1), which controls protein synthesis [20]. The other mTOR complex (mTORC2) phosphorylates Akt, thereby stimulating the activity of mTORC1 and modulating cellular processes.

## 101.4 Therapeutic Targeting of the PI3K Pathway

The PI3K/Akt/mTOR pathway is associated with human cancer [17, 21] and intense efforts are underway to discover and develop drugs targeting nodes of this pathway. These drugs are classified as inhibitors targeting specific isoforms (NVP-BYL719 'p110α'), specific nodes (NVP-BKM120 'pan-PI3K'), and multiple nodes (Palomid 529 'dual mTORC1/2') [22, 23].

LY294002, a broad spectrum PI3K inhibitor, is the archetypal PI3K inhibitor. LY294002 is a valuable tool in characterizing intracellular PI3K signalling in cells and VEGF pathways in angiogenesis [24]. Recent studies show LY294002 is efficacious as an inhibitor of ocular angiogenesis in animal models [14, 25]. Further clinical development stalled due to unfavourable pharmacological properties, poor solubility and toxicity [15]. Recently, the pro-drug SF1126 (Semafore Pharmaceuticals Inc), consisting of LY294002 conjugated to an RGD-targeting peptide [26] has enhanced localization to the vasculature higher aqueous solubility and is in clinical trial for solid tumours [27].

Anti-angiogenic therapies for oncology have moved on from the discovery of broad-spectrum PI3K inhibitors, to the development of isoform-selective PI3K inhibitors like NVP-BEZ235, a dual PI3K/mTOR inhibitor [21]. The same strategy should be possible for ocular indications or node specific inhibitors. To date, only the mTOR inhibitors Palomid 529 (Paloma Pharmaceuticals, Inc.) and Sirolimus (MacuSight, Inc.) are being clinically evaluated for ocular indications. Palomid 529 is a first-in-class, dual TORC1/TORC2 inhibitor in clinical trial for advanced AMD [28, 29]. Sirolimus (Rapamycin), originally designed as an immunosuppressant, is currently in clinical trial for diabetic macular oedema and choroidal neovascularization (CNV) [30]. A recent phase 2 trial of Everolimus/RAD001) (a derivative of Sirolimus) for neovascular AMD was terminated as the primary endpoint was not reached [31].

The p110α isoform (encoded by the *PIK3CA* gene) of the class I PI3K is selectively required for angiogenesis *in vivo* [32] and several inhibitors targeting this isoform are in clinical trials for cancer [33]. Targeting this angiogenesis-specific isoform may be particularly advantageous as it has the potential of maximising efficacy and improving the side-effect profile.

## 101.5 The Future for PI3K Inhibitors

Ocular drugs with low-molecular weight (e.g. PI3K inhibitors), as opposed to large monoclonal antibodies (e.g. Lucentis), offer treatment advantages in the management of ocular neovascularization. Small-molecule inhibitors can be delivered topically, orally, intravenously or by intraocular implant, delivery methods which can improve ocular drug bioavailability and decrease the frequency of intraocular injections. Based on the high degree of molecular interactions with other biologi-

cal pathways, targeting the PI3K/Akt/mTOR pathway in combination with other signalling pathways may improve therapeutic outcome and circumvent limitations imparted by the current anti-angiogenic inhibitors. To bridge this gap, recent studies shown that mTOR inhibitors significantly decrease VEGF mRNA stability [34], suggesting they may improve efficacy when combined with anti-VEGF agents [35].

## 101.6 Conclusion

Based on the current status of therapeutics for ocular neovascularization, it appears prudent that alternative molecular targets are warranted. Therapeutic targeting of the PI3K/Akt/mTOR pathway is an attractive option approach for the treatment of sight-threatening ocular neovascularization. PI3K/Akt/mTOR inhibitors alone or in combination with other anti-angiogenic agents hold promise for improving treatment of PDR and wet AMD.

## References

1. U.S. retinal therapeutics market (2011) Frost & Sullivan report N85D-01 Web. Accessed Oct. 08, 2013
2. Rein DB, Zhang P, Wirth KE, Lee PP, Hoerger TJ, McCall N, Klein R, Tielsch JM, Vijan S, Saaddine J (2006) The economic burden of major adult visual disorders in the United States. Arch Ophthalmol 124(12):1754–1760
3. Cao Y (2001) Endogenous angiogenesis inhibitors and their therapeutic implications. Int J Biochem Cell 33(4):357–369
4. Gao G, Ma J (2002) Tipping the balance for angiogenic disorders. Drug Discov Today 7(3):171–172
5. Rosenfeld PJ, Brown DM, Heier JS, Boyer DS, Kaiser PK, Chung CY, Kim RY (2006) Ranibizumab for neovascular age-related macular degeneration. New Eng J of Med 355(14):1419–1431
6. Rosenfield PJ, Moshfeghi AA, CA P (2005) Optical coherence tomography findings after an intravitreal injection of bevacizumab (avastin) for neovascular age-related macular degeneration. Opthalmic Surg Lasers Imaging 36(4):331–335
7. Campochiaro P (2007) Targeted pharmacotherapy of retinal diseases with ranibizumab. Drugs Today (Barc) 43:529–537
8. Narayanan R, Kuppermann BD, Jones C, Kirkpatrick P (2006) Ranibizumab. Nat Rev Drug Discov 5(10):815–816
9. Heier JS, Boyer D, Nguyen QD, Marcus D, Roth DB, Yancopoulos G, Stahl N, Ingerman A, Vitti R, Berliner AJ, Yang K, Brown DM (2011) The 1-year results of CLEAR-IT 2, a phase 2 study of vascular endothelial growth factor trap-eye dosed as-needed after 12-week fixed dosing. Ophthalmology 118(6):1098–1106
10. Rosenfeld PJ, Schwartz SD, Blumenkranz MS, Miller JW, Haller JA, Reimann JD, Greene WL, Shams N (2005) Maximum tolerated dose of a humanized anti-vascular endothelial growth factor antibody fragment for treating neovascular age-related macular degeneration. Ophthalmology 112(6):1048–1053.e4
11. Ribatti D (2010) The inefficacy of antiangiogeneic therapies. J Angiogenesis Res 2:27
12. Garber K (2010) Biotech in a blink. Nat Biotech 28(4):311–314

13. Cai J, Ahmad S, Jiang WG, Huang J, Kontos CD, Boulton M, Ahmed A (2003) Activation of vascular endothelial growth factor receptor-1 sustains angiogenesis and Bcl-2 expression via the phosphatidylinositol 3-kinase pathway in endothelial cells. Diabetes 52(12):2959–2968
14. Alvarez Y, Astudillo O, Jensen L, Reynolds AL, Waghorne N, Brazil DP, Cao Y, O'Connor JJ, Kennedy BN (2009) Selective inhibition of retinal angiogenesis by targeting PI3 kinase. PLoS One 4(11):e7867
15. Marone R, Cmiljanovic V, Giese B, Wymann MP (2008) Targeting phosphoinositide 3-kinase-Moving towards therapy. Biochim Biophys Acta 1784(1):159–185
16. Jiang BH, Zheng JZ, Aoki M, Vogt PK (2000) Phosphatidylinositol 3-kinase signaling mediates angiogenesis and expression of vascular endothelial growth factor in endothelial cells. Proc Natl Acad Sci U S A 97(4):1749–1753
17. Liu P, Cheng H, Roberts TM, Zhao JJ (2009) Targeting the phosphoinositide 3-kinase pathway in cancer. Nat Rev Drug Discov 8(8):627–644
18. Fruman DA, Meyers RE, Cantley LC (1998) Phosphoinositide kinases. Annu Rev Biochem 67:481–507
19. Cantley LC (2002) The phosphoinositide 3-kinase pathway. Science 296(5573):1655–1657
20. Engelman JA, Luo J, Cantley LC (2006) The evolution of phosphatidylinositol 3-kinases as regulators of growth and metabolism. Nat Rev Genet 7(8):606–619
21. Roper J, Richardson MP, Wang WV, Richard LG, Chen W, Coffee EM, Sinnamon MJ, Lee L, Chen P, Bronson RT, Martin ES, KE H (2011) The dual PI3K/mTOR inhibitor NVP-BEZ235 induces tumor regression in a genetically engineered mouse model of PIK3CA wild-type colorectal cancer. PLoS One 6:e25132
22. Fritsch CM, Schnell C, Chatenay-Rivauday C, Guthy DA, De Pover A, Wartmann M, Brachmann S, Maria S, Huang A, Quadt C, Hofmann F, Caravatti G (2012) NVP-BYL719, a novel PI3Kalpha selective inhibitor with all the characteristics required for clinical development as an anti-cancer agent [Abstract]. American Association for Cancer Research. Abstract nr 3748
23. Maira SM, Pecchi S, Huang A, Burger M, Knapp M, Sterker D, Schnell C, Guthy D, Nagel T, Wiesmann M, Brachmann S, Fritsch C, Dorsch M, Chène P, Shoemaker K, De Pover A, Menezes D, Martiny-Baron G, Fabbro D, Wilson CJ, Schlegel R, Hofmann F, García-Echeverría C, Sellers WR, Voliva CF (2012) Identification and characterization of NVP-BKM120, an orally available pan-class I PI3-kinase inhibitor. Mol Cancer Ther 11(2):317–328
24. Hu L, Hofmann J, Jaffe RB (2005) Phosphatidylinositol 3-kinase mediates angiogenesis and vascular permeability associated with ovarian carcinoma. Clin Cancer Res 11(22):8208–8212
25. Yu WZ, Zou H, Li XX, Yan Z, Dong JQ (2008) Effects of the phosphatidylinositol 3-kinase inhibitor in a mouse model of retinal neovascularization. Ophthalmic Res 40(1):19–25
26. Garlich JR, De P, Dey N, Su JD, Peng X, Miller A, Murali R, Lu Y, Mills GB, Kundra V, Shu HK, Peng Q, and DL D.A (2008) Vascular targeted pan phosphoinositide 3-kinase inhibitor prodrug, SF1126, with antitumor and antiangiogenic activity. Cancer Res 68(1):260–215
27. Schwertschlag US, Chiorean EG, Anthony SP, Sweeney CJ, Borad MJ, Von Hoff DD, Garlich JR, Shelton CF, RK R (2008) Phase 1 pharmacokinetic (PK) and pharmacodynamic(PD) evaluation of SF1126 a vascular targeted pan phosphoinositide 3- kinase (PI3K) inhibitor in patients with solid tumors. J Clin Oncol (May)20:(suppl) abstr 14532
28. Phase 1 study of Palomid 529 a dual TORC1/2 inhibitor of the PI3K/Akt/mTOR pathway for advanced neovascular age-related macular degeneration (P529010). http://clinicaltrials.gov/show/NCT01033721. Accessed 08 Oct 2013
29. Palomid 529 in patients with neovascular age-related macular degeneration. http://clinicaltrials. gov/show/NCT1271270. Accessed 08 Oct 2013
30. Sherris D (2007) Ocular drug development-future directions. Angiogenesis 10(2):71–76
31. The efficacy of oral everolimus in patients with neovascular age-related macular degeneration. http://clinicaltrials.gov/show/NCT00857259. Accessed 08 Oct 2013
32. Graupera M, Guillermet-Guibert J, Foukas LC, Phng L-K, Cain RJ, Salpekar A, Pearce W, Meek S, Millan J, Cutillas PR, Smith AJH, Ridley AJ, Ruhrberg C, Gerhardt H, Vanhaesebroeck B (2008) Angiogenesis selectively requires the p110[agr] isoform of PI3K to control endothelial cell migration. Nature 453(7195):662–666

33. Sanofi Study of XL147 (SAR245408) in advanced or recurrent endomentrial cancer. Accessed 08 Oct 2013
34. Basu A, Datta D, Zurakowski D, Pal S (2010) Altered VEGF mRNA stability following treatments with immunosuppressive agents: implications for cancer development. J Biol Chem 285(33):25196–25202
35. Dorrell MI, Aguilar E, Scheppke L, Barnett FH, Friedlander M (2007) Combination angiostatic therapy completely inhibits ocular and tumor angiogenesis. Proc Natl Acad Sci U S A 104(3):967–972

# Chapter 102
# Pigment Epithelium-Derived Factor Protects Cone Photoreceptor-Derived 661W Cells from Light Damage Through Akt Activation

**Matthew Rapp, Grace Woo, Muayyad R. Al-Ubaidi, S. Patricia Becerra and Preeti Subramanian**

**Abstract** Pigment epithelium-derived factor (PEDF) can delay and prevent the death of photoreceptors *in vivo*. We investigated the survival activity of PEDF on cone photoreceptor-derived 661W cells in culture, the presence of PEDF receptor (PEDF-R) in these cells and the activation of prosurvival Akt. Cell death was induced by light exposure in the presence of 9-*cis* retinal. Cell viability assays showed that PEDF increased the number of 661W cells exposed to these conditions. Western blots showed that PEDF-treated 661W cells had a higher ratio of phosphorylated Akt to total Akt than untreated cells. The PEDF receptor PEDF-R was immunodetected in the plasma membrane fractions of 661W cells. The results demonstrated that PEDF can protect 661W cells against light-induced cell death and suggest that the binding of PEDF to cell surface PEDF-R triggers a prosurvival signaling pathway.

**Keywords** PEDF · PEDF-R · Photoreceptor · 661W cells · Akt phosphorylation · Survival

P. Subramanian (✉) · M. Rapp · G. Woo · S. P. Becerra
National Eye Institute, National Institutes of Health, Bldg. 6, Rm. 131F, 6 Center Dr., MSC 0608, Bethesda, MD 20892-0608, USA
e-mail: subramanianp@nei.nih.gov

M. Rapp
e-mail: rappm1@umbc.edu

G. Woo
e-mail: gracebeewoo@gmail.com

S. P. Becerra
e-mail: becerrap@nei.nih.gov

M. R. Al-Ubaidi
Department of Cell Biology, University of Oklahoma Health Sciences Center, Oklahoma City, Oklahoma 73104, USA
e-mail: muayyad-al-ubaidi@ouhsc.edu

Oklahoma Center for Neurosciences, University of Oklahoma Health Sciences Center, Oklahoma City, Oklahoma 73104, USA

J. D. Ash et al. (eds.), *Retinal Degenerative Diseases,* Advances in Experimental Medicine and Biology 801, DOI 10.1007/978-1-4614-3209-8_102,

**Abbreviations**

| | |
|---|---|
| PEDF | Pigment epithelium-derived factor |
| PEDF-R | PEDF receptor |
| RPE | Retinal pigment epithelium |
| FBS | Fetal bovine serum |
| Akt | The serine/threonine kinase |
| PI3K | Phosphatidylinositol 3-kinase |
| DHA | Docosahexaenoic acid |

## 102.1 Introduction

Pigment epithelium-derived factor (PEDF) has potent retinal survival properties [1–3]. It is a natural glycoprotein (50-kDa) that is highly expressed in the retinal pigment epithelium (RPE) [4–5] and is secreted into the interphotoreceptor matrix [6]. PEDF is involved in the maintenance and promotion of photoreceptor and retinal neuron cell survival [1–2]. It also plays a role in the prevention of neovascular invasion [1, 3], [7–9]. Studies in animal models for inherited and light-induced retinal degeneration, retinal ischemia, and degeneration of spinal cord motor neurons have established a role for PEDF as a neurotrophic factor in the retina and CNS [10–15]. PEDF protects cultured cells of retinal origin from death induced by ischemia and cytotoxic agents [15–19]. In neurovascular ocular diseases such as age-related macular degeneration, diabetic retinopathy, and neuroretinal dystrophies, PEDF levels are reduced [20–22]. Although numerous studies have demonstrated the importance of PEDF as a neuroprotective factor, specific mechanisms of PEDF action are yet to be elucidated.

One of the proposed mechanisms is thought to be initiated via interaction with high-affinity receptors on cell surfaces. Pigment epithelium-derived factor (PEDF-R) is a phospholipase A (PLA) enzyme with high affinity for PEDF, whose activity is enhanced by PEDF binding [23, 24]. The PEDF-R sequence has four transmembrane domains and intracellular and extracellular regions. In the rat retina, active PEDF-R is detected in the plasma membranes of RPE cells and in the inner segments of the photoreceptors. Thus the location of PEDF and PEDF-R indicates that ligand and receptor are available to interact in the retina.

To investigate the molecular mechanism of action of PEDF in response to light-induced damage of photoreceptors, we used the 661W cell line, a mouse retinal tumor-derived cone-specific cell line expressing cone pigments, transducin, and arrestin [25]. These cells have been used as an in vitro model for studying light-induced cell death in cone photoreceptors [26].

## 102.2 Materials and Methods

### *102.2.1 Cell Culture*

661W cells were cultured in DMEM with 10% Fetal Bovine Serum (FBS) and 1% antimycotic-antibiotic cocktail. The media was also supplemented with 4.3 μg/ml hydrocortisone, 0.04 μg/ml progesterone, 32 μg/ml putrescine, and 4% β-mercaptoethanol. Cells were kept at 37° C with 5% $CO_2$.

### *102.2.2 Cell Viability Assays*

Three thousand cells were plated per well of a 96-well tissue culture plate and allowed to grow for 16 h in the dark. Then, the media was replaced with regular media, media containing 10 μM 9-*cis* retinal, or media with 9-*cis* retinal and PEDF. After 4 h, the plates were placed in a light box (~22,000 lx) at 30° C, either covered or not covered to obtain data from samples in the dark and in the light for the indicated time period. Cell viability measurements were made with a CellTiter-Glo viability assay kit (Promega) following the manufacturer's instructions, except that the extract mixture with the CellTiter-Glo reagent was pipetted up and down 2–3 times and transferred to a 96-well opaque-walled plate. The luminescence intensity was measured using an automated plate reader (Envision, Perkin Elmer, MA).

### *102.2.3 Western Blot and Protein Analysis*

Cells were harvested at various times with 1X SDS sample buffer and passed through a needle to shred DNA. The samples were boiled for 10 min, cooled on ice, and loaded on a 10–20% tricine polyacrylamide gel for SDS-PAGE [27]. After immunotransfer, the nitrocellulose membrane was incubated sequentially in blocking solution for 1 h at room temperature, rabbit anti-phospho-Akt diluted 1:1,000 (Cell Signaling Technology, Inc., cat #9271) for 16 h at 4° C, HRP-conjugated goat anti-rabbit IgG secondary antibody (1:5,000) for 1 h at room temperature, and finally SuperSignal West Dura Extended Duration Substrate (Pierce) as per the manufacturer's protocol. Washes were with TBS-T (50 mM Tris HCl pH 7.4, 150 mM NaCl plus 0.1% Tween-20, TBS-T) and stripping was with Restore™ Western Blot Stripping Buffer (Pierce). For total Akt detection, the stripped and blocked membrane was incubated with mouse anti-Akt diluted 1:1,000 (Cell Signaling Technology, Inc., cat #2967), followed with HRP-conjugated goat anti-mouse IgG (1:5,000). For PEDF-R detection, primary and secondary antibodies were 0.25 μg/ml anti-PEDF-R (R&D systems, cat# AF5365) and HRP-conjugated donkey anti-sheep IgG diluted 1:20,000 (SIGMA, cat# A3415) in 1% BSA/TBS-T, respectively. Blots were exposed to X-ray films to visualize chemiluminescent immunoreactive bands.

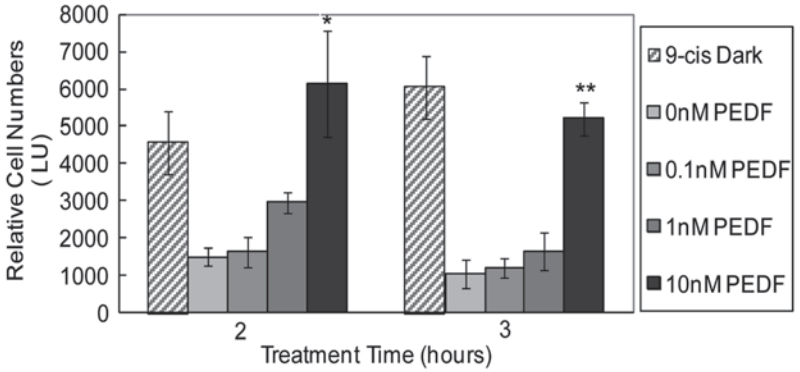


**Fig. 102.1** Effect of *PEDF* on 661W Cell Viability. The plot shows relative 661W cell numbers after treatments with indicated *PEDF* concentrations in the presence of 9-*cis* as a function of time (h) of light exposure. Control, 9-*cis dark*. Each point is the average of four replicate wells ± SD. (* $p < 0.002$ for 2 h, ** $p < 0.00001$ for 3 h)

### *102.2.4 Membrane Fractionation*

Confluent 661W cells (90%) were harvested and lysed with RIPA buffer (Pierce) to obtain total cell lysates or subjected to biochemical fractionation to separate cytosolic and membrane fractions [23]. Protein concentration was determined with BCA Protein Assay (Pierce).

## 102.3 Results

### *102.3.1 PEDF Promotes Survival Activity on 661W Cells*

Cells were treated with 9-*cis* retinal with or without PEDF before and during light exposure (22,000-lux). Figure 102.1 shows that when exposed to light, only 33% and 17% of the cells were viable after 2 and 3 h, respectively, as compared to cells kept in the dark (100%). However, in the presence of PEDF, the viable cell numbers increased and had a significant recovery (approximately 100%) with 10 nM PEDF. The results indicate that PEDF protected these cells from light-induced death.

### *102.3.2 PEDF Promotes Akt Activation*

To identify prosurvival pathways for PEDF protection of 661W cells, we investigated the activation of Akt, a known survival target. Cells were damaged by light and 9-*cis* in the presence and absence of PEDF, and phosphorylated Akt (pAkt)

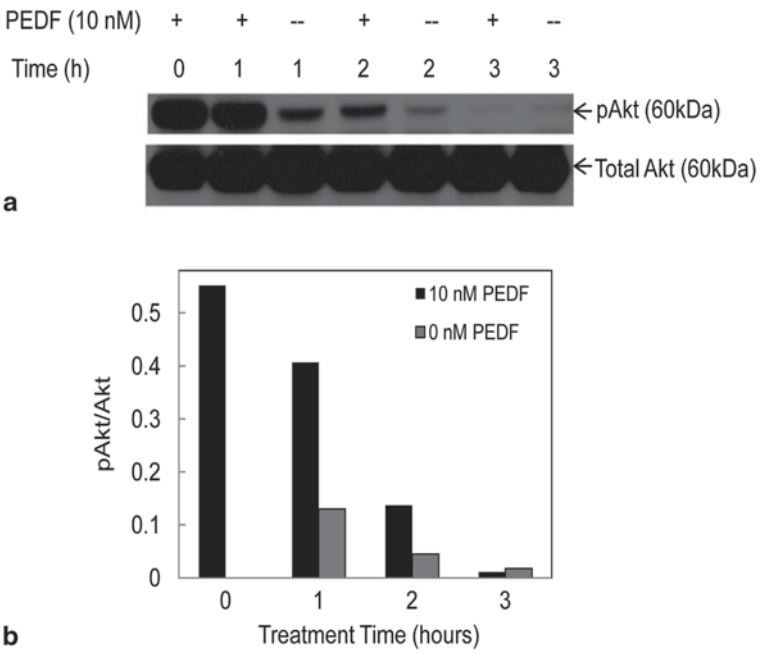


**Fig. 102.2** *PEDF* activates Akt in 661W cells. **a** 661W cells were treated with or without *PEDF* in the presence of 9-*cis* and exposed to light for the indicated times. Western blots of total lysates with antibodies to *pAkt* and total *Akt* are shown. **b** Plot showing the ratio of *pAkt* and *Akt* band intensities from (**a**) using UN-SCAN-IT software

levels were determined in cell lysates. The level of pAkt was normally high in the dark and dropped with light exposure (Fig. 102.2). Cells treated with 10 nM PEDF and exposed to light for 1 and 2 h had significant increases of pAkt relative to those without PEDF (Fig. 102.2). However, by the third hour, no pAkt was detected with or without PEDF. The results show that PEDF induced intracellular signaling events in the Akt pathway in 661W cells and further support our previous findings on photoreceptor protection by PEDF.

### *102.3.3 PEDF-R in 661W Cells*

Previous studies have shown that PEDF-R is a transmembrane protein present in plasma membranes [23]. Western blots of 661W total lysates and cell membrane fractions with antibody to PEDF-R show the presence of a single immunoreacting band that migrates as an 80-kDa protein (Fig. 102.3). The results demonstrate the presence of PEDF-R in 661W cells and imply its cell surface location and availability to interact with extracellular PEDF ligands.

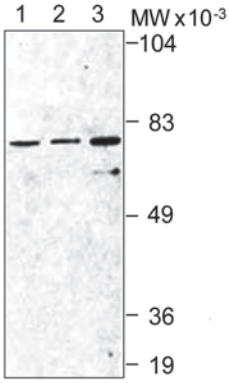


**Fig. 102.3** PEDF-R in 661W cells. Total RIPA lysate and membrane fractions from 661W cells were analyzed by western blotting for PEDF-R. Lane *1*, total lysate (20 μg protein); lanes *2* and *3*, membrane fractions isolated with NP-40 and CHAPS, respectively (5 μg protein). Molecular weight markers are shown to the right

## 102.4 Discussion

It was previously determined that 661W cells undergo apoptosis when exposed to light in the presence of 9-*cis* retinal [26]. In this study, we successfully demonstrate that PEDF prevents 661W cell death induced by light damage and that PEDF activates Akt, a known survival target.

While light exposure lowers the activated Akt levels with time, PEDF promotes Akt activation as early as 1 h post-addition and in agreement with the idea of pAkt being a precursor for survival. Interestingly, photoreceptor 661W cells contain PEDF-R on their surfaces indicating the availability of a PEDF receptor that could interact with a prosurvival signaling pathway in these cells.

A distinct signal transduction mechanism leading to the neurotrophic action of PEDF has not yet been established, but is implied by the following observations: (1) The phosphatidylinositol 3-kinase (PI3K)/Akt signaling is a critical downstream regulator for neuronal survival [28], (2) Several survival factors, including PEDF and docosahexaenoic acid (DHA), promote neuronal survival through the activation of Akt [28, 29], and (3) PEDF enhances the PLA activity of PEDF-R to liberate free-fatty acids, such as DHA, in the retina [23]. Our findings infer that PEDF interaction with PEDF-R to release DHA could serve to promote Akt as a prosurvival mediator, which would establish a signal transduction pathway in photoreceptor cell survival by PEDF.

## References

1. Barnstable CJ, Tombran-Tink J (2004) Neuroprotective and antiangiogenic actions of PEDF in the eye: molecular targets and therapeutic potential. Prog Retin Eye Res 23(5):561–577
2. Becerra SP (2006) Focus on Molecules: pigment epithelium-derived factor (PEDF). Exp Eye Res 82(5):739–740
3. Bouck N (2002) PEDF anti-angiogenic guardian of ocular function. Trends Mol Med 8(7):330–334

4. Becerra SP et al (2004) Pigment epithelium-derived factor in the monkey retinal pigment epithelium and interphotoreceptor matrix: apical secretion and distribution. Exp Eye Res 78(2):223–234
5. Perez-Mediavilla LA et al (1998) Sequence and expression analysis of bovine pigment epithelium-derived factor. Biochim Biophys Acta 1398(2):203–214
6. Tombran-Tink J et al (1995) Expression, secretion, and age-related downregulation of pigment epithelium-derived factor, a serpin with neurotrophic activity. J Neurosci 15(7 Pt 1):4992–5003
7. Crawford SE et al (2001) Pigment epithelium-derived factor (PEDF) in neuroblastoma: a multifunctional mediator of Schwann cell antitumor activity. J Cell Sci 114(Pt 24):4421–4428
8. Garcia M et al (2004) Inhibition of xenografted human melanoma growth and prevention of metastasis development by dual antiangiogenic/antitumor activities of pigment epithelium-derived factor. Cancer Res 64(16):5632–5642
9. Wang L et al (2003) Suppression of angiogenesis and tumor growth by adenoviral-mediated gene transfer of pigment epithelium-derived factor. Mol Ther 8(1):72–79
10. Bilak MM et al (1999) Pigment epithelium-derived factor (PEDF) protects motor neurons from chronic glutamate-mediated neurodegeneration. J Neuropathol Exp Neurol 58(7):719–728
11. Cao W et al (2001) In vivo protection of photoreceptors from light damage by pigment epithelium-derived factor. Invest Ophthalmol Vis Sci 42(7):1646–1652
12. Cayouette M et al (1999) Pigment epithelium-derived factor delays the death of photoreceptors in mouse models of inherited retinal degenerations. Neurobiol Dis 6(6):523–532
13. Dawson DW et al (1999) Pigment epithelium-derived factor: a potent inhibitor of angiogenesis. Science 285(5425):245–248
14. Duh EJ et al (2002) Pigment epithelium-derived factor suppresses ischemia-induced retinal neovascularization and VEGF-induced migration and growth. Invest Ophthalmol Vis Sci 43(3):821–829
15. Takita H et al (2003) Retinal neuroprotection against ischemic injury mediated by intraocular gene transfer of pigment epithelium-derived factor. Invest Ophthalmol Vis Sci 44(10):4497–4504
16. Pang IH et al (2007) Pigment epithelium-derived factor protects retinal ganglion cells. BMC Neurosci 8:11
17. Miyazaki M et al (2011) Pigment epithelium-derived factor gene therapy targeting retinal ganglion cell injuries: neuroprotection against loss of function in two animal models. Hum Gene Ther 22(5):559–565
18. Ogata N et al (2001) Pigment epithelium derived factor as a neuroprotective agent against ischemic retinal injury. Curr Eye Res 22(4):245–252
19. Unterlauft JD et al (2012) Pigment epithelium-derived factor released by Muller glial cells exerts neuroprotective effects on retinal ganglion cells. Neurochem Res. 37:1524–1533
20. Duh EJ et al (2004) Vitreous levels of pigment epithelium-derived factor and vascular endothelial growth factor: implications for ocular angiogenesis. Am J Ophthalmol 137(4):668–674
21. Holekamp NM, Bouck N, Volpert O (2002) Pigment epithelium-derived factor is deficient in the vitreous of patients with choroidal neovascularization due to age-related macular degeneration. Am J Ophthalmol 134(2):220–227
22. Ogata N et al (2004) Decreased levels of pigment epithelium-derived factor in eyes with neuroretinal dystrophic diseases. Am J Ophthalmol 137(6):1129–1130
23. Notari L et al (2006) Identification of a lipase-linked cell membrane receptor for pigment epithelium-derived factor. J Biol Chem 281(49):38022–38037
24. Subramanian P, Notario PM, Becerra SP (2010) Pigment epithelium-derived factor receptor (PEDF-R): a plasma membrane-linked phospholipase with PEDF binding affinity. Adv Exp Med Biol 664:29–37
25. Tan E et al (2004) Expression of cone-photoreceptor-specific antigens in a cell line derived from retinal tumors in transgenic mice. Invest Ophthalmol Vis Sci 45(3):764–768

26. Kanan Y et al (2007) Light induces programmed cell death by activating multiple independent proteases in a cone photoreceptor cell line. Invest Ophthalmol Vis Sci 48(1):40–51
27. Wu YQ et al (1995) Identification of pigment epithelium-derived factor in the interphotoreceptor matrix of bovine eyes. Protein Expr Purif 6(4):447–456
28. Akbar M et al (2005) Docosahexaenoic acid: a positive modulator of Akt signaling in neuronal survival. Proc Natl Acad Sci U S A 102(31):10858–10863
29. Sanchez A et al (2012) Pigment epithelium-derived factor (PEDF) protects cortical neurons in vitro from oxidant injury by activation of extracellular signal-regulated kinase (ERK) 1/2 and induction of Bcl-2. Neurosci Res 72(1):1–8

# Chapter 103
# Nanoceria as Bona Fide Catalytic Antioxidants in Medicine: What We Know and What We Want to Know…

**Lily L. Wong and James F. McGinnis**

**Abstract** Cerium oxide ($CeO_2$) nanoparticles, CeNPs or nanoceria are inorganic and possess catalytic antioxidant activity. They scavenge reactive oxygen species and act as an oxygen buffer. Their application in industry is well-established. However, their usage as bona fide antioxidants in biological systems has been recent and is quite revolutionary. Other reviews have documented nanoceria's protective effect in reducing oxidative stress in cell culture and in animal disease models that are associated with oxidative stress. We specifically have targeted CeNPs as ophthalmic therapeutics to slow the progression of retinal degeneration and as anti-angiogenic agents in rodent models. The radical scavenging activity of CeNPs is mainly due to the dramatic increase of surface area to volume ratio in these nanocrystalline structures. The parameters for CeNPs usage in industrial settings are decidedly not suitable for biological applications. In this short review, we report the pharmacokinetics, biodistribution, and toxicity evaluation of CeNPs when applied as ophthalmic therapeutic agents in an in vivo system. We highlight studies that examine how CeNPs behave in biological environments and how they interact with bio-macromolecules. We also discuss studies that examine the dynamic changes of the surface chemistry of CeNPs in physiological buffers. Finally, we raise a list of questions that we think ought to be answered for CeNPs to be considered the antioxidants of choice in medicine, specifically in the treatment of ocular diseases.

L. L. Wong (✉) · J. F. McGinnis
Department of Ophthalmology, College of Medicine,
University of Oklahoma Health Sciences Center (OUHSC) and Dean McGee Eye Institute,
608 Stanton L Young Blvd, DMEI PB L027, 73104 Oklahoma City, OK, USA
e-mail: lily-wong@ouhsc.edu

J. F. McGinnis
Cell Biology and Oklahoma Center for Neuroscience, OUHSC,
73104 Oklahoma City, OK, USA
e-mail: james-mcginnis@ouhsc.edu

J. D. Ash et al. (eds.), *Retinal Degenerative Diseases,* Advances in Experimental Medicine and Biology 801, DOI 10.1007/978-1-4614-3209-8_103,

**Keywords** Nanomedicine · Nanoparticles · Cerium oxide nanoparticles · Pharmacokinetics · Toxicity · Retention · Vitreous · ICP-MS · Oxidative stress · Radical scavenging · Antioxidant

**Abbreviations**

| | |
|---|---|
| CeNPs | Cerium oxide nanoparticles |
| ICP-MS | Inductively coupled plasma-mass spectrometry |
| ROS | Reactive oxygen species |

## 103.1 Introduction

The first in-depth inquiry into the radical scavenging and neuroprotective effect of cerium oxide nanoparticles (CeNPs or nanoceria) in biological systems was published in 2006 [1]. Schubert et al. compared nanomaterials including yttrium oxide, cerium oxide, aluminum oxide, silicon oxide that range from less than 10 nm to 1000 nm and compared these to their bulk counterparts with respect to cytotoxicity and neuroprotective effect using HT22 cells, an immortalized murine hippocampal cell line. They convincingly showed that nanoparticles of yttrium oxide and cerium oxide alone and not their bulk counterparts were the only ones that possessed radical scavenging property and neuroprotective effect when these cells were challenged with glutamate. Later that year, our laboratory published the first in vivo study of applying CeNPs in the vitreous of albino rats to inhibit rod cell death in the light-damage retinal degeneration model [2]. In that study, we also showed that CeNPs lowered reactive oxygen species (ROS) in primary rat retinal neurons when challenged with hydrogen peroxide. Since then, our laboratory has demonstrated that the radical scavenging CeNPs act as anti-angiogenic agents to reduce the pathologic expression of *vascular endothelial growth factor* (*vegf*), and retinal neovascularization in the retinas of the *very low density lipoprotein receptor* (*vldlr*) knockout mice [3]. We established the neuroprotective effect of CeNPs on photoreceptor cells in another retinal degeneration mouse model, the *tubby* mouse [4, 5]. We have evidenced that CeNPs delay photoreceptor degeneration in the P23H-1 rats, a model for autosomal dominant retinitis pigmentosa ([6] and unpublished results). We have demonstrated that CeNPs are effective therapeutic agents against intraocular malignancies in a rodent model [7]. An extensive list of studies on antioxidant properties of CeNPs in abiotic environment, in cell culture, and animal models are found in these reviews [8, 9].

## 103.2 Physical and Chemical Properties of Naked CeNPs

CeNPs belong to a unique class of nanomaterials that possess redox-active radical scavenging activities. Unlike other nanomaterials being developed for drug or nucleic acid delivery [10], CeNPs are investigated for use as bona fide catalytic antioxidants for treatment of diseases that are associated with oxidative stress

[8, 11]. The oxides of cerium, when synthesized in the nanometer range, have enhanced redox capacity. The cerium ions have both 3+ and 4+ valence states and therefore can act as electron donors or acceptors. Oxygen defects or vacancies on the surface or subsurface of the lattice crystals act as sites for radical scavenging [12, 13]. CeNPs in water are shown to have catalytic activities that mimic superoxide dismutase (SOD) and catalase [14–16], two major antioxidative enzymes that neutralize superoxide anions ($O_2^-$) and hydrogen peroxides ($H_2O_2$), respectively. The redox capacity of CeNPs is regenerative [14] although the mechanism is unclear. Celardo et al. [9] postulate two models for the redox cycle: the initial $H_2O_2$ oxidation step at a vacancy site is the same in the two models. The models differ at the conversion step of Ce3+ back to Ce4+; one is by reduction of two $O_2^-$ and the other by the reduction of $H_2O_2$ and uptake of 2H+. The combined auto-catalytic and regenerative properties of CeNPs make them desirable therapeutic agents.

In all of our experiments, we have used naked CeNPs synthesized by simple wet chemistry methods as described in [17] and [16]. Synthesized CeNPs were characterized by high resolution transmission electron microscopy for size and shape determination, by dynamic light scattering for zeta potential measurement, and by X-ray photoelectron spectroscopy for relative abundance of 3+ and 4+ oxidation state of cerium. The stable water-dispersed CeNPs are 3–5 nm in size and the particle size remains the same in a wide range of pH buffers and upon aging [18]. We dilute our concentrated stock from water to 1 mM or 172 μg/ml in saline for extended use. Before further dilution or intravitreal injection, we vortex the 1 mM suspension for 1 min to dissociate loose aggregates that may have formed in the saline solution. We have previously determined that 1 mM CeNPs formed two different families of aggregates in saline (76 and 295 nm; [3]) most likely due to the reduction in zeta potential in high salt environment (+40 mV of 5 mM in water vs +10 mV of 1 mM in saline). Despite the formation of agglomeration of CeNPs to these larger but still nanometer sizes, we did not observe any precipitation of particles.

## 103.3 Cytotoxic Assessment of Our Synthesized CeNPs

A large number of cell culture studies on the cytotoxic effects of CeNPs are published [8, 9]. However, the findings from these publications are challenging to interpret because the syntheses of these CeNPs are different, consequently, so are their properties. We confine the discussion to the naked CeNPs synthesized by simple wet chemistry as mentioned above. Any negative side effects of CeNPs appear to be cell type and concentration specific. While Hirst et al. [19] reported no toxic effect on a murine macrophage cell line (1 nM to 10 μM), Karakoti et al. [17] reported a slight reduction in viability at 5 μM on human epidermal keratinocytes. In our laboratory, we showed that CeNPs were not toxic to primary rat retinal neurons, instead they promoted the longevity of these cells in culture up to 29 days [11]. Additionally, we tested five cell types, including mouse cone photoreceptor precursor cells (661W), human retinal pigment epithelial cells (ARPE19), human corneal epithelial cells, primary human umbilical vein endothelial cells, and human microvascular

endothelial cells ([20] and unpublished results). CeNPs were not cytotoxic to any of the five cell types at low and medium dosages (1 nM to 5 μM) for up to 72 h of incubation. CeNPs exhibited cytotoxicity only to 661W cells but not the other four cell types at high dosages and only at 72 h of incubation (above 10 μM).

To validate the usage of CeNPs as ophthalmic agents, we also examined the effects of CeNPs in healthy retinas [21]. We assessed retinal function and performed quantitative morphometric analyses of the retinas at 9, 60, and 120 days after a single intravitreal injection of CeNPs to rat eyes. The highest dosage tested was 344 ng (or 2 μl of 1 mM CeNPs) per eye. We did not observe any deficits in rod and cone functions, or retinal morphology at all the time points tested when compared with saline injected animals. We therefore postulate that CeNPs administered at these equivalent dosages are not toxic to healthy human retinas. Our findings are also consistent with an in vivo systemic administration study by Hirst et al. [22]. They found no overt toxicity in mice after 5 weeks of weekly intravenous administration of CeNPs at 0.5 mg/kg.

## 103.4 Pharmacokinetics and Biodistribution of CeNPs After a Single Intravitreal Injection

Cell culture studies showed that CeNPs are taken up by cells via clathrin- and caveolae-dependent endocytic pathways and are found in multiple cellular compartments including the mitochondria, lysosomes, endoplasmic reticulum, the nucleus, and the cytoplasm [23]. Using inductively coupled plasma-mass spectrometry (ICP-MS), a highly sensitive method to detect trace elements in biological samples, we demonstrate that CeNPs are rapidly and preferentially taken up by retinal cells after intravitreal injection [21]. One hour after injection, the predominant amount of injected CeNPs is found in the retina (Fig. 103.1). The clearance of CeNPs from the retina is extremely slow (Fig. 103.2). The estimated elimination half-life of CeNPs in the retina is 414 days.

Our data suggest that CeNPs are eventually removed from the retina, however, the primary route of elimination is unclear. It can be by general circulation or locally in the eye, or both. The prolonged retention of CeNPs in the retina is especially desirable if the self-regenerative property of CeNPs is maintained. Currently, CeNPs are the only type of catalytic antioxidant that is non-toxic and does not require frequent dosing. We have shown that the longest duration observed for CeNPs neuroprotective effect in rodent models varies from 42 [5] to 120 days (unpublished results).

## 103.5 Nanoceria in Physiological Buffers and Interaction with Bio-Macromolecules

Due to the greatly increased surface area in nanomaterials, the surface charge and properties of nanomaterials can alter significantly under different physiological conditions such as pH, availability of free water molecules, and the interactions

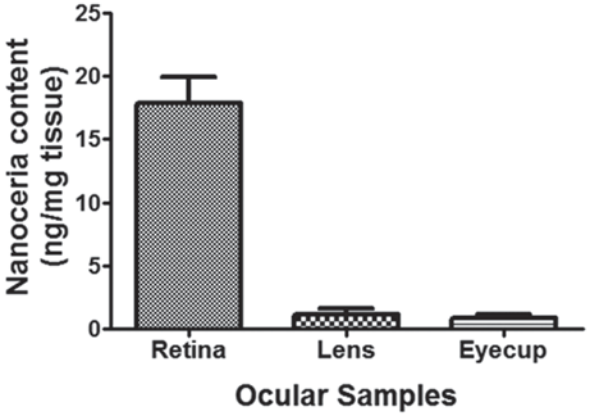


**Fig. 103.1** Bio-distribution of CeNPs in ocular tissues 1 h post intravitreal injection. Approximately 334 ng of CeNPs were injected into each eye. Whole eyes were dissected into component parts: *retina* (R), *lens* (L), and the rest of the *eyecup* which also included the cornea (EC) for ICP-MS analysis. Within 1 h of CeNPs application, retinal tissue accumulated the highest amount of CeNPs (17.89 ng/mg), followed by the lens tissue (1.13 ng/mg), and the lowest amount in the eyecup tissue (0.83 ng/mg). Uninjected eyes contained negligible amount of CeNPs. (Reprinted with permission from PLoS One)

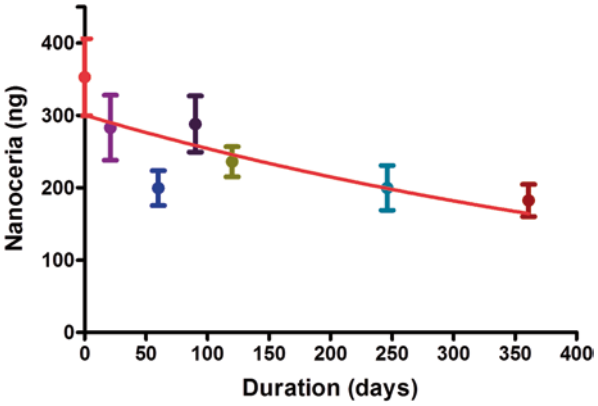


**Fig. 103.2** The rat retina retained CeNPs over prolonged periods following a single intravitreal injection. The injected CeNPs accumulated in the retina rapidly. We detected 94% of the injected CeNPs in the retina after 1 h of injection and about 70% of the injected CeNPs was retained for 120 days. The elimination half-life of CeNPs in the retina is 414 days. (Reprinted with permission from PLoS One)

with proteins and DNA. To address some of these unknowns, Singh et al. [24] examined changes in the surface chemistry, SOD, and catalase mimetic activities of CeNPs when exposed to biological media, buffers, and ions. They did not observe any changes of CeNPs in surface oxidation chemistry or SOD mimetic activity over a broad range of pH, when incubated with cell culture media with or without serum, and in buffers containing sulfate or carbonate anions. However, they did discover

the abolition of SOD mimetic activity when CeNPs were resuspended in phosphate buffers of 100 μM or higher. The loss of SOD mimetic activity was accompanied by a concomitant increase in catalase mimetic activity. The authors argued that phosphate anions might be stabilizing the 3+ state of Ce. In another study by Kuchma et al. [25], they discovered that CeNPs possessed mimetic phosphatase activity for cleavage of phosphate ester bonds in physiological conditions. However, they failed to find hydrolysis products when incubating high concentrations of CeNPs (5 mM to 37.5 mM) with DNA plasmids. They speculated that CeNPs could hydrolyze ATP and phosphorylated proteins, but not DNA in biological systems. In light of the findings that phosphate anions can modify the catalytic nature of CeNPs and the discovery of new catalytic activities of CeNPs for biomolecules, nanomedicine researchers must continue their effort to understand the molecular interaction of nanomaterials in various biological environments.

We use intravitreal injection of CeNPs as a paradigm for ophthalmic therapy. We confirm that CeNPs administered in the vitreous are able to penetrate through this complex structure and are taken up by one or more cell types in the retina [21]. The vitreous body contains collagen fibers embedded in a matrix of highly water-bound glycosaminoglycans [26]. Forty percent of the soluble proteins in the vitreous is albumin [26] which may adsorb to the injected positively-charged CeNPs by electrostatic interactions [27]. We convincingly show that this potential interaction did not impede the uptake of CeNPs by retinal cells, as 94% of injected CeNPs is found in the retina 1 h post injection. The vitreous is also abundant in iron-binding proteins. Thirty-five percent of the soluble proteins in the monkey vitreous are composed of transferrin and/or lactoferrin [28]. The high amount of transferrin or transferrin-like proteins in the vitreous may contribute to the rapid uptake of CeNPs by retinal cells. CeNPs complexed with transferrins are found to be taken up by cells more efficiently than naked CeNPs at a number of concentrations [29]. Transferrin receptors are ubiquitous in every cell type of the body including retinal cells. We hypothesize that the rapid uptake of CeNPs may be facilitated by binding to transferrin and/or lactoferrin in the vitreous. This hypothesis is consistent with our observation that CeNPs-mediated photoreceptor cell protection is not confined to the injection site but is found across the entire retina [2].

## 103.6 Conclusions

Our laboratory has demonstrated that CeNPs reduced ROS in retinas of the *vldlr* mutant and *tubby* mice [3, 4]. Concomitantly, pathological retinal vessels, both new and existing, are reduced in the *vldlr* mutants and rod and cone degenerations are delayed in the *tubby* mice. We and others hypothesize that CeNPs exert their primary function by lowering ROS in diseased tissues. However, besides modulating the redox environment, CeNPs possess additional catalytic activities and may directly and/or indirectly modulate activities of signaling proteins and transcription machinery to influence gene expressions. Lee et al. [30] examined the genomic effects of naked CeNPs in HT22 cells and found that specific genes were differentially expressed

according to nanoparticle species and particle size. In contrast, our preliminary microarray data of CeNPs in healthy rat retina suggested that CeNPs might not have specific but rather broad genomic effects in retinal cells. CeNPs maintained elevated gene expression of many genes that were elevated merely due to mechanical injury, such as injection of saline into the vitreous. Instead of only being elevated for 24 h, as in the case of saline injection, the elevated gene expressions were maintained for at least 72 h (unpublished results). In this regard, CeNPs administration may elicit a preconditioning or adaptive cellular stress response that is termed hormesis—"an adaptive response of cells and organisms to a moderate stress" [31]. This kind of response is very analogous to that described by Calabrese et al. [32], regarding how antioxidant administration modulates the expression of vitagenes.

To develop CeNPs as ophthalmic therapeutics, we need to understand how CeNPs are delivered from the vitreous to retinal cells, and to determine the retinal cell types that preferentially take up CeNPs. Results from these studies will illuminate the cellular mechanism(s) of how CeNPs slow the progression of blinding diseases.

As oxidative stress is involved in the progression of many blinding diseases such as age-related macular degeneration, diabetic retinopathy, and retinitis pigmentosa, targeting the reduction of ROS by CeNPs in these diseased eyes may be one way to prolong vision until cures become available.

## References

1. Schubert D, Dargusch R, Raitano J, Chan SW (2006) Cerium and yttrium oxide nanoparticles are neuroprotective. Biochem Biophys Res Commun 342(1):86–91
2. Chen J, Patil S, Seal S, McGinnis JF (2006) Rare earth nanoparticles prevent retinal degeneration induced by intracellular peroxides. Nat Nanotechnol 1(2):142–150
3. Zhou X, Wong LL, Karakoti AS, Seal S, McGinnis JF (2011) Nanoceria inhibit the development and promote the regression of pathologic retinal neovascularization in the *Vldlr* knockout mouse. PLoS ONE 6(2):e16733
4. Kong L, Cai X, Zhou X, Wong LL, Karakoti AS, Seal S, McGinnis JF (2011) Nanoceria extend photoreceptor cell lifespan in tubby mice by modulation of apoptosis/survival signaling pathways. Neurobiol Dis 42(3):514–523
5. Cai X, Sezate SA, Seal S, McGinnis JF (2012) Sustained protection against photoreceptor degeneration in tubby mice by intravitreal injection of nanoceria. Biomaterials 33(34):8771–8781
6. Wong LL, Pye QN, Chen L, Cai X, Seal S, McGinnis J.F (2012) Assessing the therapeutic effect of nanoceria in an autosomal dominant retinitis pigmentosa model Invest Ophthalmol Vis Sci E-Abstract:282
7. Klump KEKSV, Seal S, Dyer MA, McGinnis J.F (2012) Therapeutic inhibition of retinoblastoma by nanoceria. Invest Ophthalmol Vis Sci E-abstract:6549
8. Karakoti A, Singh S, Dowding JM, Seal S, Self WT (2010) Redox-active radical scavenging nanomaterials. Chem Soc Rev 39(11):4422–4432
9. Celardo I, Pedersen JZ, Traversa E, Ghibelli L (2011) Pharmacological potential of cerium oxide nanoparticles. Nanoscale 3(4):1411–1420
10. Thomas DG, Klaessig F, Harper SL, Fritts M, Hoover MD, Gaheen S, Stokes TH, Reznik-Zellen R, Freund ET, Klemm JD, Paik DS, Baker NA (2011) Informatics and standards for nanomedicine technology. Wiley Interdiscip Rev Nanomed Nanobiotechnol 3:511–532

11. McGinnis JF, Chen J, Wong L, Sezate S, Seal S, Patil S (2008) Inventors, Inhibition of reactive oxygen species and protection of mammalian cells. patent 7347987
12. Campbell CT, Peden CH (2005) Chemistry. Oxygen vacancies and catalysis on ceria surfaces. Science 309(5735):713–714
13. Inerbaev TM, Seal S, Masunov AE (2010) Density functional study of oxygen vacancy formation and spin density distribution in octahedral ceria nanoparticles. J Mol Model 16(10):1617–1623
14. Korsvik C, Patil S, Seal S, Self WT (2007) Superoxide dismutase mimetic properties exhibited by vacancy engineered ceria nanoparticles. Chem Commun (Camb) 2007(10):1056–1058
15. Pirmohamed T, Dowding JM, Singh S, Wasserman B, Heckert E, Karakoti AS, King JE, Seal S, Self WT (2010) Nanoceria exhibit redox state-dependent catalase mimetic activity. Chem Commun (Camb) 46(16):2736–2738
16. Self WT, Seal S (2009) Inventors, Nanoparticles of cerium oxide having superoxide dismutase activity patent 7504356
17. Karakoti AS, Monteiro-Riviere NA, Aggarwal R, Davis JP, Narayan RJ, Self WT, McGinnis J, Seal S (2008) Nanoceria as antioxidant: synthesis and biomedical applications (1989). JOM 60(3):33–37
18. Vincent A, Inerbaev TM, Babu S, Karakoti AS, Self WT, Masunov AE, Seal S (2010) Tuning hydrated nanoceria surfaces: experimental/theoretical investigations of ion exchange and implications in organic and inorganic interactions. Langmuir: ACS J Sur Coll 26(10):7188–7198
19. Hirst SM, Karakoti AS, Tyler RD, Sriranganathan N, Seal S, Reilly CM (2009) Anti-inflammatory properties of cerium oxide nanoparticles. Small 5(24):2848–2856
20. Wong LL, Yu X, Sezate SA, Seal S, McGinnis J.F (2010) Unique sensitivity of cone photoreceptor precursor tumor cells, 661W, to cerium oxide nanoparticles. Invest Ophthalmol Vis Sci E-abstract:1432
21. Wong LL, Hirst SM, Pye QN, Reilly CM, Seal S, McGinnis JF (2013) Catalytic nanoceria are preferentially retained in the rat retina and are not cytotoxic after intravitreal injection. PLoS ONE 8(3):e58431
22. Hirst SM, Karakoti A, Singh S, Self W, Tyler R, Seal S, Reilly CM (2011) Bio-distribution and in vivo antioxidant effects of cerium oxide nanoparticles in mice. Environ Toxicol 2011:107–118
23. Singh S, Kumar A, Karakoti A, Seal S, Self WT (2010) Unveiling the mechanism of uptake and sub-cellular distribution of cerium oxide nanoparticles. Mol Biosyst 6(10):1813–1820
24. Singh S, Dosani T, Karakoti AS, Kumar A, Seal S, Self WT (2011) A phosphate-dependent shift in redox state of cerium oxide nanoparticles and its effects on catalytic properties. Biomaterials 32(28):6745–6753
25. Kuchma MH, Komanski CB, Colon J, Teblum A, Masunov AE, Alvarado B, Babu S, Seal S, Summy J, Baker CH (2010) Phosphate ester hydrolysis of biologically relevant molecules by cerium oxide nanoparticles. Nanomed: Nanotechnol Biol Med 6(6):738–744
26. Kleinberg TT, Tzekov RT, Stein L, Ravi N, Kaushal S (2011) Vitreous substitutes: a comprehensive review. Surv Ophthalmol 56(4):300–323
27. Patil S, Sandberg A, Heckert E, Self W, Seal S (2007) Protein adsorption and cellular uptake of cerium oxide nanoparticles as a function of zeta potential. Biomaterials 28(31):4600–4607
28. Van Bockxmeer FM, Martin CE, Constable IJ (1983) Iron-binding proteins in vitreous humour. Biochim Biophys Acta 758(1):17–23
29. Vincent A, Babu S, Heckert E, Dowding J, Hirst SM, Inerbaev TM, Self WT, Reilly CM, Masunov AmE, Rahman TS (2009) Seal S. Protonated nanoparticle surface governing ligand tethering and cellular targeting. ACS Nano 3(5):1203–1211
30. Lee TL, Raitano JM, Rennert OM, Chan SW, Chan WY (2012) Accessing the genomic effects of naked nanoceria in murine neuronal cells. Nanomed: Nanotechnol Biol Med 8(5):599–608
31. Mattson MP (2008) Hormesis defined. Ageing Res Rev 7(1):1–7
32. Calabrese V, Cornelius C, Mancuso C, Pennisi G, Calafato S, Bellia F, Bates TE, Giuffrida Stella AM, Schapira T, Dinkova Kostova AT, Rizzarelli E (2008) Cellular stress response: a novel target for chemoprevention and nutritional neuroprotection in aging, neurodegenerative disorders and longevity. Neurochem Res 33(12):2444–2471

# Chapter 104
# Nanoceria and Thioredoxin Regulate a Common Antioxidative Gene Network in *tubby* Mice

**Xue Cai, Junji Yodoi, Sudipta Seal and James F. McGinnis**

**Abstract** Oxidative stress is a node common to the causes and effects of various ocular diseases. We have shown that thioredoxin has neuroprotective effects on *tubby* photoreceptors. We also demonstrated that nanoceria (cerium oxide nanoparticles), which are direct antioxidants, have long-term effects on prevention of retinal degeneration in *tubby* mice. Here, using commercially available PCR array plates, we surveyed the regulation in expression of 89 oxidative stress-associated genes in the eyes of P12 *tubby* mice which are either intravitreally injected with nanoceria or in which the *Trx* gene is overexpressed. Our data demonstrate that nanoceria and Trx regulate the same group of genes associated with antioxidative stress and antioxidant defense.

J. F. McGinnis (✉) · X. Cai
Department of Ophthalmology, Dean McGee Eye Institute, University of Oklahoma Health Sciences Center, 608 Stanton L. Young Blvd, 73104 Oklahoma City, OK, USA
e-mail: james-mcginnis@ouhsc.edu

X. Cai
e-mail: xue-cai@ouhsc.edu

J. Yodoi
Department of Biological Responses, Institute for Virus Research, Kyoto University, 606-8507 Kyoto, Japan
e-mail: yodoi@virus.kyoto-u.ac.jp

S. Seal
Materials Science and Engineering, Advanced Materials Processing Analysis Center and Nanoscience Technology Center, University of Central Florida, 32816 Orlando, FL, USA
e-mail: Sudipta.Seal@ucf.edu

J. F. McGinnis
Department of Cell Biology, University of Oklahoma Health Sciences Center, 73104 Oklahoma City, OK, USA

Neuroscience Center, University of Oklahoma Health Sciences Center, 73104 Oklahoma City, OK, USA

Department of Ophthalmology, Dean McGee Eye Institute, University of Oklahoma Health Sciences Center, 608 Stanton L. Young Blvd, 73104 Oklahoma City, OK, USA

J. D. Ash et al. (eds.), *Retinal Degenerative Diseases,* Advances in Experimental Medicine and Biology 801, DOI 10.1007/978-1-4614-3209-8_104,

**Keywords** *Tubby* mouse · Nanoceria · Thioredoxin · Oxidative stress and antioxidant defense · PCR array

**Abbreviations**

| | |
|---|---|
| Trx | Thioredoxin |
| ASK1 | Apoptosis signal kinase 1 |
| MAPKs | Mitogen-activated protein kinases |
| Nanoceria | Cerium oxide nanoparticles |
| P7 | Postnatal day 7 |
| Wt | Wild type |
| IACUC | Institutional Animal Care and Use Committee |
| Nrf2 | Nuclear factor erythroid 2-related factor |
| siRNA | Small interfering RNA |
| ROS | Reactive oxygen species |
| ICAM-1 | Intercellular adhesion molecule 1 |
| HMVEC | Human microvascular endothelial cells |
| Nxn | Nucleoredoxin |
| Cys | Cysteine residue |
| Wnt | Wingless/Intergration, Wg/Int |
| Dvl | Dishevelled |
| RPE | Retinal pigment epithelium |
| bZIP | Basic leucine zipper |
| ARACNE | Algorithm for the Reconstruction of Accurate Cellular Networks |
| CLR | Context Likelihood of Relatedness |

## 104.1 Introduction

Thioredoxin (Trx) is a well-known ubiquitous antioxidant protein involved in a variety of cellular activities in which it regulates redox activities to protect cells against various apoptotic stresses by binding and inactivating apoptosis signal kinase 1 (ASK1) which inhibits the activation of its downstream MAPKs (mitogen-activated protein kinases) [1, 2]. We demonstrated that overexpression of *Trx* reverses oxidative stress and prevents retinal degeneration in *tubby* mice [3]. Nanoceria (cerium oxide nanoparticles) are direct broad spectrum antioxidants having enzymatic activities of superoxide dismutase and catalase and neuroprotective functions. Our previous studies showed that they can protect photoreceptors from light-damage in rats [4] and prolong the lifespan of photoreceptors in *tubby* mice [5, 6].

To test if nanoceria and Trx regulate similar functions and target the same downstream genes, *tubby* pups were intravitreally injected at postnatal day 7 (P7) with 1 μl of 1 mM nanoceria (172 ng), whereas uninjected *tubby* served as a control.

Analysis of gene expression in transgenic *Tub/Trx* and nanoceria injected *tubby* mice was carried out at P12. The fold change of gene expression was compared to that of wild type (wt) and untreated *tubby* mice.

## 104.2 Materials and Methods

### *104.2.1 Animals and Genotyping*

Wild type (wt) C57BL/6J, *tubby* and transgenic *Tub*/*Trx* mice were used for this study. All procedures were approved by the Institutional Animal Care and Use Committees (IACUC) from the University of Oklahoma Health Sciences Center and the Dean McGee Eye Institute.

### *104.2.2 Intravitreal Injection*

Intravitreal injection of P7 t*ubby* pups with 1 µl of 1 mM nanoceria in saline was performed as previously reported [6]. After injection, the mice were returned to the original cages and maintained in the normal conditions until P12.

### *104.2.3 PCR Array and Semi-Quantitative RT-PCR*

Three to four pairs of retinas from each group (wt, *Tub*/*Trx*, uninjected and nanoceria injected *tubby*) were collected. PCR array using "mouse oxidative stress and antioxidant defense" plates (SABiosciences Corporation, Frederick, MD) were performed as previously reported [6]. The levels of gene expression were determined by the fold change of each gene compared to wt or *tubby* using the PCR Array Data Analysis Software. Semi-quantitative RT-PCR of Nrf2 (nuclear factor erythroid 2-related factor) and densitometric analysis of the bands normalized to GAPDH are the same as previously reported [6].

## 104.3 Results and Discussion

### *104.3.1 Nanoceria and Trx Regulate the Expression of Same Group of Genes*

Based on the gene function, the oxidative stress-associated genes we tested with the array plates can be categorized as two groups: antioxidants and oxidants. The antioxidants can be subdivided into the following groups: (1) Superoxide dis-

mutase (Sod 1-3 and Ccs); (2) Glutathione peroxidases (Gpx 1-6 and Gstk1) and other peroxidases (Cat, Ctsb, Prdx6-rs1, Ptgs1, Serpinb1b); (3) Peroxiredoxins (Prdx 1-6), Thioredoxins (Nxn, Txnip, Txnrd 1-3) and other antioxidants (Ercc2, Mpp4, Nqo1, Scd1, Zmynd17); (4) Oxygen transporter (Aqr, Cygb, Fancc, Mb, Slc38a1, Vim). The Oxidants (oxidase and ROS generators) include Cyba, Ncf2. Genes with changes in expression in untreated *tubby* mice (compared to age-matched wt, *tub*/wt), nanoceria injected *tubby* and *Tub*/*Trx* mice (compared to uninjected *tubby*, $CeO_2$/*tub* and *Tub*/*Trx*/*tub*) were summarized in Table 104.1 (Changes of 2-fold were determined as a threshold). Nanoceria and Trx similarly modulate the expression of some genes, e.g., they exhibit a similar effect on the down- or up-regulation of the expression of these genes. Those genes related to protection and antioxidant production, damaged DNA repair and apoptosis prevention, such as *Ccs*, *Gpx1*, *Nqo1*, *Prdx1-4*, *Psmb5*, *Sod1*, *Txnip*, *Txnrd3*, etc, were greatly down-regulated in *tubby* retinas but were up-regulated by nanoceria and Trx. However, another group of genes, having similar functions, such as *Cygb*, *Ercc2*, *Prdx6-rs1*, *Prnp*, and *Srxn1* were up-regulated in *tubby* retinas but were down-regulated by nanoceria and Trx. *Gpx4*, *Sod2*, and *Mpp4* were down-regulated in *tubby* retinas but were further down-regulated by nanoceria and Trx. Surprisingly, oxidants such as *Cyba* and *Ncf2* were up-regulated by nanoceria and Trx. Davies [7] reported that in a stress environment, temporal and spatial gene expression results in transcriptional and translational regulation which, at a given time point, up-regulates some genes and down-regulates others as adaptive responses for protection of proliferating cells against the stress. In addition, because multiple defense networks overlap and are fine-tune regulated by cross talk with each other, down-regulation of antioxidant genes or up-regulation of oxidant genes might involve in modulation of their downstream targeting genes thus indirectly reducing oxidative stress damage.

Overexpression of *SOD1* protects retinal cells against oxidative stress damage-induced retinal degeneration in transgenic *Sod1* mice, and *Sod1*$^{-/-}$ mice exhibit more extensive reduction in ERG amplitudes and apoptosis in the retina [8, 9]. SOD1 deficiency also caused an AMD-like phenotype [10]. Knockdown of *Gpx1* expression by siRNA (small interfering RNA) enhanced reactive oxygen species (ROS) production and *ICAM-1* (intercellular adhesion molecule 1) expression, but overexpression of Gpx1 resulted in inhibition of pro-inflammatory cytokines, ERK1/2, JNK and NF-κB pathways in human microvascular endothelial cells (HMVEC) [11].

Peroxiredoxins have highly conserved peroxidatic active sites (cysteines) and are distributed widely in cellular compartments. They are involved in many cytokine-induced signaling pathways via regulation of levels of hydrogen peroxide [12]. In this work, Prdx1, 2, 3 and 4 are down-regulated, but Prdx6 is up-regulated in *tubby* retina. Nanoceria and Trx reverse these effects. Prdx6 has a unique structural property (a single cysteine residue (1-Cys) different from the presence of 2-Cys of Prdx 1-4). It is located in cytosol and also in acidic lysosomes and lamellar bodies. It exhibits bifunctional enzymatic activities with glutathione peroxidase and phospholipase [13].

**Table 104.1** Mouse oxidative stress and antioxidant defense genes with changes in expression in *tubby* mice regulated by nanoceria and Trx (≥2-fold). $N = 3–4$, $*p < 0.05$, $**p < 0.01$

| Symbol | Gene name | *tub*/wt | | $CeO_2$/*tub* | | *Tub*/*Trx*/*tub* | |
|---|---|---|---|---|---|---|---|
| | | fold | *p* value | fold | *p* value | fold | *p* value |
| *Ccs* | Copper chaperone for superoxide dismutase | −2.14 | 0.1311 | 1.63 | 0.4737 | 1.46 | 0.5498 |
| *Ctsb* | Cathepsin B | −1.69 | 0.0554 | 1.70 | 0.0348* | 2.12 | 0.1597 |
| *Gpx1* | Glutathione peroxidase 1 | −2.48 | 0.0129* | 2.90 | 0.0353* | 3.03 | 0.0444* |
| *Mb* | Myoglobin | −1.31 | 0.6485 | 8.72 | 0.2710 | 6.95 | 0.3737 |
| *Nqo1* | NAD(P)H dehydrogenase, quinone 1 | −2.33 | 0.0681 | 1.82 | 0.2793 | 2.10 | 0.2538 |
| *Nxn* | Nucleoredoxin | −2.23 | 0.0407* | 3.37 | 0.0069** | 4.24 | 0.0176** |
| *Prdx1* | Peroxiredoxin 1 | −2.25 | 0.0370* | 1.69 | 0.0643 | 2.08 | 0.2188 |
| *Prdx2* | Peroxiredoxin 2 | −2.61 | 0.0071** | 1.66 | 0.0350* | 1.82 | 0.0349* |
| *Prdx3* | Peroxiredoxin 3 | −2.39 | 0.1103 | 1.38 | 0.3494 | 2.29 | 0.1870 |
| *Prdx4* | Peroxiredoxin 4 | −1.98 | 0.1799 | 2.73 | 0.0132* | 3.04 | 0.1669 |
| *Psmb5* | Proteasome (prosome, macropain) subunit, beta type 5 | −2.22 | 0.0069** | 1.85 | 0.0203* | 1.82 | 0.0082** |
| *Ptgs1* | Prostaglandin-endoperoxide synthase 1 | −1.12 | 0.8575 | 2.07 | 0.0195* | 2.67 | 0.1413 |
| *Sod1* | Superoxide dismutase 1, soluble | −2.65 | 0.0096** | 1.86 | 0.0629 | 2.92 | 0.1529 |
| *Txnip* | Thioredoxin interacting protein | −2.54 | 0.0162* | 2.24 | 0.0469* | 4.80 | 0.2087 |
| *Txnrd3* | Thioredoxin reductase 3 | −2.41 | 0.0283* | 1.70 | 0.0592 | 1.85 | 0.0760 |
| *Serpinb1b* | Serine (or cysteine) peptidase inhibitor, clade B, member 1b | −3.45 | 0.0057** | 1.37 | 0.3808 | 2.11 | 0.2611 |
| *Vim* | Vimentin | −2.49 | 0.0393* | 2.38 | 0.2638 | 5.79 | 0.0425* |
| *Xpa* | Xeroderma pigmentosum, complementation group A | −2.09 | 0.0026** | 1.54 | 0.0565 | 1.84 | 0.0045** |
| *Gstk1* | Glutathione S-transferase kappa 1 | −2.01 | 0.0207* | 1.02 | 0.9049 | 2.45 | 0.1845 |
| *Scd1* | Stearoyl-Coenzyme A desaturase 1 | −3.23 | 0.1138 | 1.16 | 0.5966 | 19.02 | 0.3671 |
| *Zmynd17* | Zinc finger, MYND domain containing 17 | −1.58 | 0.2002 | 1.02 | 0.8583 | 2.25 | 0.0286* |
| *Cat* | Catalase | −1.43 | 0.5013 | −1.32 | 0.9226 | 2.81 | 0.2921 |
| *Txnrd1* | Thioredoxin reductase 1 | −1.57 | 0.0460* | −2.28 | 0.0190* | 1.94 | 0.0163* |
| *Cygb* | Cytoglobin | 2.77 | 0.0009** | −1.95 | 0.0429* | −2.68 | 0.0012** |
| *Ercc2* | Excision repair cross-complementing rodent repair deficiency, complementation group 6 | 1.94 | 0.6509 | −1.90 | 0.3015 | −2.65 | 0.0466* |

**Table 104.1** (continued)

| Symbol | Gene name | *tub*/ wt | | $CeO_2$/ *tub* | | *Tub*/ *Trx*/*tub* | |
|---|---|---|---|---|---|---|---|
| | | fold | *p* value | fold | *p* value | fold | *p* value |
| *Prdx6* | Peroxiredoxin 6 | 1.02 | 0.7857 | −1.81 | 0.0499* | −2.34 | 0.0255* |
| *Prdx6-rs1* | Peroxiredoxin 6, related sequence 1 | 1.46 | 0.9708 | −6.63 | 0.0113* | −5.02 | 0.1785 |
| *Prnp* | Prion protein | 2.55 | 0.5953 | −2.50 | 0.3967 | −5.09 | 0.0149* |
| *Srxn1* | Sulfiredoxin 1 homolog (S. cerevisiae) | 1.26 | 0.8812 | −1.13 | 0.6807 | −2.20 | 0.0135* |
| *Aqr* | Aquarius | −1.05 | 0.9533 | −2.63 | 0.1071 | −2.72 | 0.0631 |
| *Fancc* | Fanconi anemia, complementation group C | −1.21 | 0.5909 | −1.77 | 0.1057 | −2.13 | 0.0674 |
| *Gpx4* | Glutathione peroxidase 4 | −1.26 | 0.5109 | −1.26 | 0.9961 | −2.71 | 0.0153* |
| *Slc38a1* | Solute carrier family 38, member 1 | −1.11 | 0.3782 | −2.20 | 0.0093** | −2.31 | 0.0828 |
| *Sod2* | Superoxide dismutase 2, mitochondrial | −1.41 | 0.2214 | −3.26 | 0.1673 | −1.66 | 0.1624 |
| *Mpp4* | Membrane protein, palmitoylated 4 (MAGUK p55 subfamily member 4) | −1.22 | 0.5733 | −3.14 | 0.0311* | −3.81 | 0.0229* |
| *Cyba* | Cytochrome b −245, alpha polypeptide | 1.29 | 0.3426 | 2.25 | 0.0638 | 2.46 | 0.0631 |
| *Ncf2* | Neutrophil cytosolic factor 2 | −1.43 | 0.3592 | 2.25 | 0.1370 | 3.27 | 0.1443 |

In the current study, we show that Nxn (Nucleoredoxin) is significantly reduced in *tubby* retinas whereas nanoceria and Trx significantly increased Nxn levels by 3- and 4-fold respectively. Nxn blocks the activation of the Wnt (Wingless/Intergration, Wg/Int) pathway by interacting with Dishevelled (Dvl), an essential adaptor protein for anti-apoptotic Wnt signaling. In the retina, when Nxn is oxidized and inactivated by ROS [14, 15], it no longer interacts with Dvl [15], which results in dysregulation of Wnt signaling and in retinal degeneration [16].

We have previously reported that rod and cone opsin mislocalize in *tubby* retinas [6]. The polarized secretion and translocation of these proteins and endocytosis are dependent on the interactions with cytoskeletal elements. Many proteins are required for cargo transportation and cellular motility. In this study, the genes associated with motility, such as *Dnm2* (*tub*/wt, −1.84-fold) (less than 2-fold are not shown in Table 104.1) and *Vim*, are down-regulated in the *tubby* mice (Table 104.1). Nanoceria and Trx up-regulate their levels (Dnm2: $CeO_2$/*tub*, 1.51-fold; *Tub/Trx/tub*, 1.27-fold) (less than 2-fold are not shown in Table 104.1), further supporting our previous report that nanoceria prevent mislocalization of rhodopsin and M-opsin in *tubby* mice [6].

### *104.3.2 Nanoceria and Trx Differentially Regulate the Expression of Another Group of Genes*

As shown in Table 104.1, nanoceria and Trx differentially regulated another group of genes having the same function in *tubby* mice. For example, *Gstk1*, *Scd1*, and *Zmynd17* are down-regulated in *tubby* mice with only slight changes induced by nanoceria treatment. However, Trx greatly up-regulated their expression more than 2-fold higher than in *tubby* mice. Similarly, nanoceria treatment resulted in further down-regulation of the expression of *Cat* and *Txnrd1*, but Trx significantly up-regulated their expression. It was reported that adenovirus-mediated delivery of catalase to the RPE (retinal pigment epithelium) cells of Balb/c mice protected photoreceptors against light damage [17]. It need to be indicated that nanoceria reduced the expression of *Cat* and *Sod2* because nanoceria themselves are antioxidants with the properties and activities of catalase and superoxide dismutase. Collectively, these data reveal that nanoceria and Trx similarly regulate expression of some genes. However nanoceria appear to have different mechanisms, which are distinct from those of Trx, for regulating expression of other genes possibly, by affecting other controllers or regulators which further modulate expression of these genes.

### *104.3.3 Oxidative Stress and Antioxidant Defense Genes are Targeted by Nrf2*

Nrf2 is a basic leucine zipper (bZIP) transcription factor which translocates into the nucleus under oxidative stress conditions. Taylor et al. [18], using computational ARACNE (Algorithm for the Reconstruction of Accurate Cellular Networks) and CLR (Context Likelihood of Relatedness) predicted and demonstrated that *Als2*, *Prnp*, *Sod2*, *Srxn1*, *Ppp1r15b*, *Nqo1*, *Idh1*, and *Ercc6* are Nrf2 target genes in the mouse lung. We have shown that Nrf2 expression was increased in *tubby* retina to a level equivalent to wt by Trx overexpression [3] or nanoceria treatment [5]. To test Nrf2 expression in this study, semi-quantitative RT-PCR was performed. Our data demonstrated that Nrf2 mRNA level was decreased 2-fold in *tubby* retina compared to wt, and nanoceria and Trx up-regulate Nrf2 expression by 1.5- and 2-fold higher than *tubby* mutant, respectively (data not shown).

In conclusion, nanoceria act as direct broad spectrum antioxidants, and regulate genes common to the Trx gene network. Therefore, nanoceria might have mechanisms similar to those by which Trx acts to decrease oxidative stress-induced cellular damage and thereby prevent retinal degeneration in *tubby* mice.

**Acknowledgment** This review was written with the partial support of NIH grant COBRE-P20 RR017703, R01EY018724, R01EY022111.

## References


1. Collet JF, Messens J (2010) Structure, function, and mechanism of thioredoxin proteins. Antioxid Redox Signal 13:1205–1216
2. Nakamura H, Hoshino Y, Okuyama H, Matsuo Y, Yodoi J (2009) Thioredoxin 1 delivery as new therapeutics. Adv Drug Deliv Rev 61:303–309
3. Kong L, Zhou X, Li F, Yodoi J, McGinnis J, Cao W (2010) Neuroprotective effect of overexpression of thioredoxin on photoreceptor degeneration in Tubby mice. Neurobiol Dis 38:446–455
4. Chen J, Patil S, Seal S, McGinnis JF (2006) Rare earth nanoparticles prevent retinal degeneration induced by intracellular peroxides. Nat Nanotechnol 1:142–150
5. Kong L, Cai X, Zhou X, Wong LL, Karakoti AS, Seal S et al (2011) Nanoceria extend photoreceptor cell lifespan in tubby mice by modulation of apoptosis/survival signaling pathways. Neurobiol Dis 42:514–523
6. Cai X, Sezate SA, Seal S, McGinnis JF (2012) Sustained protection against photoreceptor degeneration in tubby mice by intravitreal injection of nanoceria. Biomaterials 33:8771–8781
7. Davies KJ (1999) The broad spectrum of responses to oxidants in proliferating cells: a new paradigm for oxidative stress. IUBMB Life 48:41–47
8. Dong A, Shen J, Krause M, Akiyama H, Hackett SF, Lai H et al (2006) Superoxide dismutase 1 protects retinal cells from oxidative damage. J Cell Physiol 208:516–526
9. Hashizume K, Hirasawa M, Imamura Y, Noda S, Shimizu T, Shinoda K et al (2008) Retinal dysfunction and progressive retinal cell death in SOD1-deficient mice. Am J Pathol 172:1325–1331
10. Imamura Y, Noda S, Hashizume K, Shinoda K, Yamaguchi M, Uchiyama S et al (2006) Drusen, choroidal neovascularization, and retinal pigment epithelium dysfunction in SOD1-deficient mice: a model of age-related macular degeneration. Proc Natl Acad Sci USA 103:11282–11287
11. Lubos E, Kelly NJ, Oldebeken SR, Leopold JA, Zhang YY, Loscalzo J et al (2011) Glutathione peroxidase-1 deficiency augments proinflammatory cytokine-induced redox signaling and human endothelial cell activation. J Biol Chem 286:35407–35417
12. Wood ZA, Schroder E, Robin Harris J, Poole LB (2003) Structure, mechanism and regulation of peroxiredoxins. Trends Biochem Sci 28:32–40
13. Fisher AB (2011) Peroxiredoxin 6: a bifunctional enzyme with glutathione peroxidase and phospholipase A(2) activities. Antioxid Redox Signal 15:831–844
14. Funato Y, Miki H (2007) Nucleoredoxin, a novel thioredoxin family member involved in cell growth and differentiation. Antioxid Redox Signal 9:1035–1057
15. Funato Y, Miki H (2010) Redox regulation of Wnt signalling via nucleoredoxin. Free Radic Res 44:379–388
16. Hackam AS (2005) The Wnt signaling pathway in retinal degenerations. IUBMB Life 57:381–388
17. Rex TS, Tsui I, Hahn P, Maguire AM, Duan D, Bennett J et al (2004) Adenovirus-mediated delivery of catalase to retinal pigment epithelial cells protects neighboring photoreceptors from photo-oxidative stress. Hum Gene Ther 15:960–967
18. Taylor RC, Acquaah-Mensah G, Singhal M, Malhotra D, Biswal S (2008) Network inference algorithms elucidate Nrf2 regulation of mouse lung oxidative stress. PLoS Comput Biol 4:e1000166

# Chapter 105
# Intrascleral Transplantation of a Collagen Sheet with Cultured Brain-Derived Neurotrophic Factor Expressing Cells Partially Rescues the Retina from Damage due to Acute High Intraocular Pressure

**Toshiaki Abe, Yumi Tokita-Ishikawa, Hideyuki Onami, Yuki Katsukura, Hirokazu Kaji, Matsuhiko Nishizawa and Nobuhiro Nagai**

**Abstract** We constructed brain-derived neurotrophic factor (BDNF) expressing rat retinal pigment epithelial (RPE) cells by stable transfection of BDNF cDNA, and the RPE cells were cultured on a cross-linked collagen sheet (Coll-RPE-BDNF). BDNF expression of the Coll-RPE-BDNF was confirmed by western blot, and the Coll-RPE-BDNF was transplanted into the rabbit sclera. *In vivo* BDNF expression was confirmed by His expression that was linked to the expressing BDNF. The effect of the released BDNF was examined in a rabbit acute high intraocular pressure system by electroretinogram and histological examination. Statistically significant preservation of ERG b wave amplitude was observed in the rabbits treated by Coll-RPE-BDNF when compared to that of no treatment. Statistically significant preservation of the thickness of the inner nuclear layer at the transplanted area

T. Abe (✉) · Y. Tokita-Ishikawa · H. Onami · Y. Katsukura · N. Nagai
Division of Clinical Cell Therapy, Center for Advanced Medical Research and Development (ART), Graduate School of Medicine, Tohoku University, Sendai, Japan
e-mail: toshi@oph.med.tohoku.ac.jp

Y. Tokita-Ishikawa
e-mail: y.katsukura@med.tohoku.ac.jp

H. Onami
e-mail: honami@oph.med.tohoku.ac.jp

Y. Katsukura
e-mail: y.katsukura@med.tohoku.ac.jp

H. Kaji · M. Nishizawa
Department of Bioengineering and Robotics, Graduate School of Engineering, Tohoku University, Sendai, Japan
e-mail: kaji@biomems.mech.tohoku.ac.jp

M. Nishizawa
e-mail: nishizawa@biomems.mech.tohoku.ac.jp

N. Nagai
e-mail: nagai@med.tohoku.ac.jp

J. D. Ash et al. (eds.), *Retinal Degenerative Diseases,* Advances in Experimental Medicine and Biology 801, DOI 10.1007/978-1-4614-3209-8_105,

was observed in the rabbits treated by Coll-RPE-BDNF compared to that of no treatment. Intra-scleral Coll-RPE-BDNF transplantation may partially rescue retinal cells from acute high intraocular pressure.

**Keywords** Brain-derived neurotrophic factor · Collagen sheet · Transplantation · Sclera · Acute high ocular pressure

## 105.1 Introduction

Neurotrophic factors have been reported to be elevated in the ganglion cell and nerve fiber layer in an animal model of acute elevation of intraocular pressure (IOP) [1]. Elevated intraocular pressure has also been proposed as one of the risk factors for glaucoma [2], and neurotrophins are diffusible trophic molecules that exert a potent survival effect not only on adult CNS neurons, but also on retinal ganglion cells, in particular [3]. Neurotrophic factors have also been shown to protect photoreceptors from agents that induce apoptosis [4]. The transplantation of cells expressing neurotrophic factors can rescue photoreceptors from different types of toxic agents [5]. Neurotrophic factor therapies have been tried in some patients with retinitis pigmentosa [6]. In addition, intravitreal injection of anti-vascular endothelial growth factor (VEGF) has been reported to treat some retinal diseases [7]. These treatment required repeated intraocular injection, which may induce irreversible side effects, such as infection, vitreous hemorrhage, and retinal detachment [8].

Here, we examined whether transscleral neurotrophic factor delivery for retinal diseases can rescue retinal damage from acute intraocular pressure by transplanting a collagen sheet with cultured brain-derived neurotrophic factor (BDNF) expressing retinal pigment epithelial cells (RPE) into the rabbit sclera.

## 105.2 Materials and Methods

### *105.2.1 Animals and Surgical Procedure*

Twenty-eight male albino rabbits (3.0–3.5 kg; Kumagai-shigeyasu Co.Ltd, Sendai, Japan) were used in these experiments. Transplantations were performed in the right eye of each rabbit, and the left eye was used as an untreated control. For all procedures, the rabbits were anesthetized with an intramuscular injection of ketamine hydrochloride (35 mg/kg) and xylazine hydrochloride (5 mg/kg), and the pupils were dilated with topical 2.5 % phenylephrine and 1 % tropicamide. Oxybuprocaine hydrochloride (0.4 %) was also used for local anesthesia. The rabbits were immunosuppressed by intramuscular injection of cyclosporine A (20 mg in 1 ml; Novartis Pharmaceuticals, Cambridge, MA, USA). An approximately 4 mm half-thickness scleral incision was made at the equator of upper temporal region of the rabbits. Halfthickness scleral pockets between the optic disc and equator were made

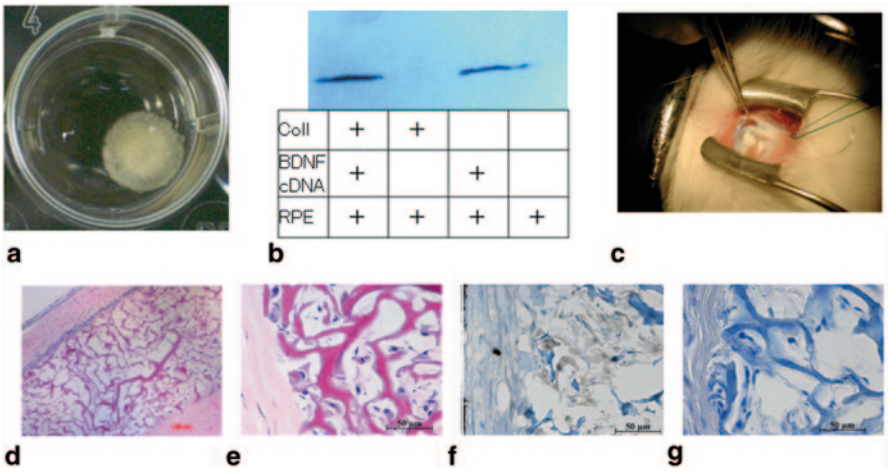


**Fig. 105.1** **a** *RPE-BDNF* cultured on a cross-linked collagen sheet (*Coll-RPE-BDNF*). **b** BDNF expression is confirmed by western blot. **c** *Coll-RPE-BDNF* was implanted intrasclerally. **d** and **e** Histological examination shows the intrascleral *Coll-RPE-BDNF* at 1 week after transplantation. **f** Immunohistochemistry shows HisG immunoreactivity in the cells cultured in *Coll-RPE-BDNF*. **g** Negative control. Bars are 50 or 100 μM

in order to insert the collagen sheets constructed as described in Fig. 105.1c. The wounds were closed by 8-0 Silk. Antibiotic ophthalmic solution was administered at the end of the surgery. A 25-gauge infusion cannula was inserted into the vitreous cavity through the pars plana to elevate the IOP. The pressure was set to 150 mmHg for 40 min by increasing the height of the bottle of balanced salt solution (BSS Plus; Alcon Laboratories, Fort Worth, TX USA) [9]. The procedures used in the animal experiments followed the guidelines of the Association for Research in Vision and Ophthalmology Statement for the Use of Animals in Ophthalmic and Vision Research, and were approved by the Animal Care Committee of Tohoku University Graduate School of Medicine.

### *105.2.2 Preparation of the RPE-BDNF Cross-Linked Collagen Sheets*

Rat RPE were prepared as reported previously [5]. Rat BDNF cDNA was inserted into the plasmid vector pcDNA/HisMax (Invitrogen, CA, USA), which has a polyhistidine (6xHis) region and a human cytomegarovirus promoter just upstream of the multiple cloning site according to the manufacture's instructions. We constructed BDNF expressing rat RPE cells by stable transfection of the BDNF cDNA vector (RPE-BDNF) as reported previously [5], and the RPEs were cultured on a cross-linked collagen sheet (Coll-RPE-BDNF). BDNF expression was confirmed by western blot.

### *105.2.3 Immunohistochemistry after Coll-RPE-BDNF Transplantation*

Anti-HisG immunohistochemistry was performed after intrascleral Coll-RPE-BDNF transplantation. Animals were euthanized by overdose of ketamine hydrochloride and xylazine hydrochloride. The eyes were enucleated, fixed, cryoprotected, and immersed in OCT compound (Tissue-Tec; Sakura Finetec USA, Inc., Torrance, CA, USA). The frozen segment was sectioned at the implanted area for 10 μm with a cryostat. The sections were incubated with anti-HisG, followed by anti-mouse IgG secondary antibody conjugated to an alkaline phosphatase (Dako, Glostrup, Denmark). Negative controls (four rabbits) incubated with just FITC-conjugated anti-rabbit IgG were also prepared.

### *105.2.4 Electroretinography and Measurement of Retinal Thickness*

One week after experiments, flash electroretinographies (ERGs) were recorded in the eyes of dark-adapted rabbits (Mayo, Aichi, Japan). A single flash of light (1000 cd/m$^2$, 3 ms) from a halogen source 30 cm from the eye was used as the light stimulus.

After ERG, the eyes were enucleated, immersion-fixed in 4% paraformaldehyde and embedded in paraffin wax. Tissue blocks were sectioned at 3 μm along the vertical plane through the optic nerve head and the transplanted and non-transplanted sites. The sections were stained with hematoxylin-eosin (H-E). The thickness of the total retina, inner retinal layer (nerve fiber layer to outer plexiform layer; INL) to outer nuclear layer (ONL), was determined on these images by an IPLab program (Scanalytics, Inc. Fairfax VA). We measured five points as described in Fig. 105.2b.

### *105.2.5 Statistical Analyses*

Analysis of variance (ANOVA) with Tukey's test was used to examine differences between animals. *P*-values less than 0.05 were considered significant.

## 105.3 Results

### *105.3.1 Collagen Sheet Preparation with RPE*

BDNF expression from Coll-RPE-BDNF (Fig. 105.1a) was confirmed by western blot (Fig. 105.1b). We also detected RPE in the Coll-RPE during successive culture at least 120 days after starting the culture (data not shown).

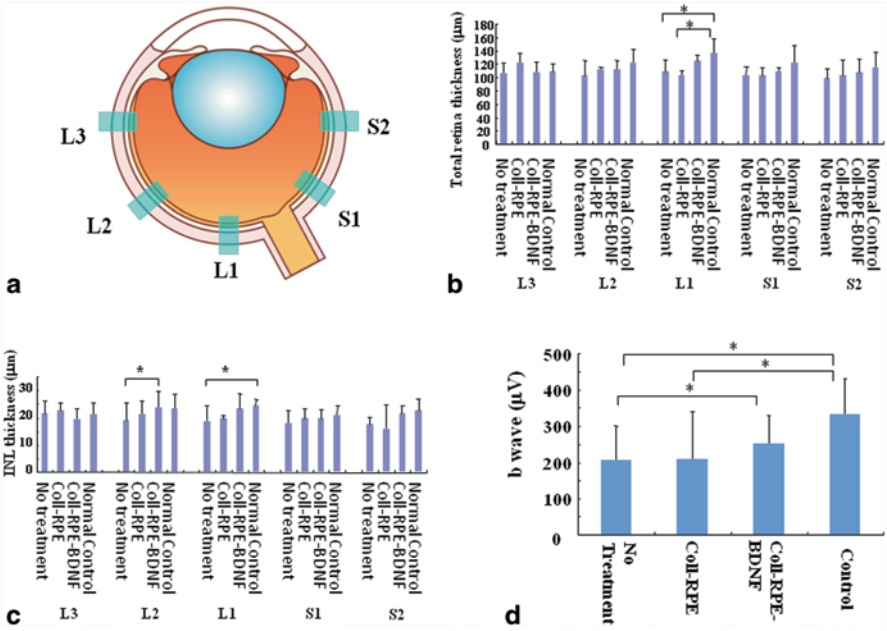


**Fig. 105.2** **a** Histological examination was performed at 5 points. **b** and **c** Statistically significant preservation of the thickness of the inner nuclear layers at the transplanted area was observed in the rabbit treated by *Coll-RPE-BDNF* when compared to those of *no treatment*. **d** Statistically significant lower amplitude of *b wave* was observed in the rabbits treated by only collagen sheet or *no treatment* when compared to those of *Coll-RPE-BDNF* and *control* ($n=5$)

### *105.3.2 Collagen Sheet Transplantation*

The Coll-RPE-BDNFs were transplanted intrasclerally (Fig. 105.1c). Histochemistry at 1 week after transplantation showed that the collagen sheet with RPE was detected in the intrascleral region (Fig. 105.1d, e). Immunohistochemistry demonstrated that HisG was detected at the cells in the collagen sheet (Fig. 105.1f, g). Bars are 50 and 100 μm.

### *105.3.3 Retinal Thickness*

We measured five different sites for retinal thickness (Fig. 105.2a). Statistically significant differences are shown as asterisks. Statistically significant preservation of INL was observed in the Coll-RPE-BDNF treatment group when compared to that of the no treatment group ($p=0.014$) (Fig. 105.2b). Statistically significant differences were not observed between the Coll-RPE-BDNF group and normal controls.

### *105.3.4 ERG*

Statistically significant preservation of ERG b wave was observed in the Coll-RPE-BDNF group when compared to that of the no treatment ($p=0.041$) (Fig. 105.2c). Statistically significant differences were not observed between the Coll-RPE-BDNF group and normal controls.

## 105.4 Discussion

During the retinal disease process, many types of cells produce multiple factors that affect retinal cell death [10]. Some of these factors lead the retinal cells to a common final death pathway or apoptosis, and many approaches to halt apoptosis, such as neurotrophic factor application, have been reported [11]. BDNF is a potent and frequently used neurotrophic factor for retinal neuroprotection [12]. However, topical application is limited by the significant barrier of the corneal epithelium [13], and systemic drug administration is not a viable alternative due to the blood-retinal barrier. Although intravitreal injections and intraocular implants deliver drugs effectively to the retina, this approach is invasive for the eyes [14]. A periocular or transscleral route is less invasive than intravitreal administration, and provides higher retinal and vitreal drug bioavailability compared to eye drops.[15] Some authors have reported that conjunctival blood and lymphatic vessel elimination limits transscleral drug delivery to the retina considerably [16]. Our results show that implantation of Coll-RPE-BDNF into the sclera rescued retinal cells from acute high-ocular pressure. Our methods safely deliver the BDNF from the outside of the retina and may also reduce the released BDNF removed by conjunctival blood and lymphatic vessels.

In conclusion, intrascleral Coll-RPE-BDNF transplantation may partially rescue retinal cells from acute high-intraocular pressure in rabbits.

**Acknowledgments** This study was supported by Health Labour Sciences Research Grant from the Ministry of Health Labour and Welfare (H23-kankaku-ippan-004, H24-nanchitoh-ippan-067).

## References

1. Wei Y, Wang HZ, Zhang FK, Zao JP, Jiang XH et al (2012) Enhanced expression of proneurotrophins in elevated introcular pressure-induced rat retinal ischemia. Chin Med J (Engl) 125:3875–3879
2. Leske MC, Heijl A, Hussein M, Bengtsson B, Hyman L et al (2003) Factors for glaucoma progression and the effect of treatment: the early manifest glaucoma trial. Arch Ophthalmol 121:48–56
3. Almasieh M, Wilson AM, Morquette B, Cueva Vargas JL, Di Polo A (2012) The molecular basis of retinal ganglion cell death in glaucoma. Prog Retin Eye Res 31:152–181

4. LaVail MM, Yasumura D, Matthes MT, Lau-Villacorta C, Unoki K et al (1998) Protection of mouse photoreceptors by survival factors in retinal degenerations. Invest Ophthalmol Vis Sci 39:592–602
5. Kano T, Abe T, Tomita H, Sakata T, Ishiguro S et al (2002) Protective effect against ischemia and light damage of iris pigment epithelial cells transfected with the BDNF gene. Invest Ophthalmol Vis Sci 43:3744–3753
6. Sieving PA, Caruso RC, Tao W, Coleman HR, Thompson DJ et al (2006) Ciliary neurotrophic factor (CNTF) for human retinal degeneration: phase I trial of CNTF delivered by encapsulated cell intraocular implants. Proc Natl Acad Sci U S A 103:3896–3901
7. Rosenfeld PJ, Brown DM, Heier JS, Boyer DS, Kaiser PK et al (2006) Ranibizumab for neovascular age-related macular degeneration. N Engl J Med 355:1419–1431
8. Pilli S, Kotsolis A, Spaide RF, Slakter J, Freund KB et al (2008) Endophthalmitis associated with intravitreal anti-vascular endothelial growth factor therapy injections in an office setting. Am J Ophthalmol 145:879–882
9. Marmor MF, Dalal R (1993) Irregular retinal and RPE damage after pressure-induced ischemia in the rabbit. Invest Ophthalmol Vis Sci 34:2570–2575
10. Kim MY, Kang SY, Lee SY, Yang MS, Kim MH et al (2012) Hypersensitivity reactions to oxaliplatin: clinical features and risk factors in Koreans. Asian Pac J Cancer Prev 13:1209–1215
11. Frasson M, Picaud S, Leveillard T, Simonutti M, Mohand-Said S et al (1999) Glial cell line-derived neurotrophic factor induces histologic and functional protection of rod photoreceptors in the rd/rd mouse. Invest Ophthalmol Vis Sci 40:2724–2734
12. Nagahara AH, Tuszynski MH (2011) Potential therapeutic uses of BDNF in neurological and psychiatric disorders. Nat Rev Drug Discov 10:209–219
13. Del Amo EM, Urtti A (2008) Current and future ophthalmic drug delivery systems. A shift to the posterior segment. Drug Discov Today 13:135–143
14. Geroski DH, Edelhauser HF (2001) Transscleral drug delivery for posterior segment disease. Adv Drug Deliv Rev 52:37–48
15. Ranta VP, Urtti A (2006) Transscleral drug delivery to the posterior eye: prospects of pharmacokinetic modeling. Adv Drug Deliv Rev 58:1164–1181
16. Lee SJ, He W, Robinson SB, Robinson MR, Csaky KG et al (2010) Evaluation of clearance mechanisms with transscleral drug delivery. Invest Ophthalmol Vis Sci 51:5205–5212

# Chapter 106
# Neuroprotective Effects of Low Level Electrical Stimulation Therapy on Retinal Degeneration

**Machelle T. Pardue, Vincent T. Ciavatta and John R. Hetling**

**Abstract** Low-level electrical stimulation applied to the eye has been shown to have neuroprotective effects on photoreceptors and retinal ganglion cells. In this review, we compare the effects of Subretinal Electrical Stimulation (SES), Transcorneal Electrical Stimulation (TES), and Whole Eye Stimulation (WES) on preserving retinal structure and function, and visual acuity, in retinal degeneration. Similarities and differences in stimulus parameters, targeted cells and growth factor expression will be discussed with emphasis on studies that have translated laboratory findings into clinical trials.

**Keywords** Retinal degeneration · Electrical stimulation · Subretinal · Transcorneal · Neuroprotection · Photoreceptors · Retinal ganglion cells

**Abbreviations**

BDNF Brain derived neurotrophic factor
CNTF Ciliary nerve trophic factor

M. T. Pardue (✉) · V. T. Ciavatta
Ophthalmology, School of Medicine, Emory University, Atlanta, GA, USA
e-mail: mpardue@emory.edu

V. T. Ciavatta
e-mail: vciavat@emory.edu

M. T. Pardue · V. T. Ciavatta
Rehab R&D Center of Excellence, US Department of Veterans Affairs, Decatur, GA, USA

M. T. Pardue
Research Service (151Oph), Atlanta VA Medical Center,
1670 Clairmont Rd., 30033 Decatur, GA, USA

J. R. Hetling
Bioengineering, University of Illinois at Chicago, Chicago, IL, USA
e-mail: JHetli1@uic.edu

J. D. Ash et al. (eds.), *Retinal Degenerative Diseases,* Advances in Experimental Medicine and Biology 801, DOI 10.1007/978-1-4614-3209-8_106,

| | |
|---|---|
| ERG | Electroretinogram |
| EST | Electrical stimulation therapy |
| FGF-2 | Fibroblast growth factor beta |
| IGF-1 | Insulin growth factor-1 |
| IL-1β | Interleukin-1 beta |
| RGC | Retinal ganglion cells |
| RP | Retinitis pigmentosa |
| SES | Subretinalelectrical stimulation |
| TES | Transcornealelectrical stimulation |
| TNF | Tumor necrosis factor |
| WES | Whole eye stimulation |

## 106.1 Introduction

Low-level electrical stimulation therapy (EST) is a common rehabilitative strategy to restore function in muscle and neurons. As early as 1873, the beneficial effects of EST on the eye were reported [1]. Recent interest in EST to treat retinal degenerative diseases has been driven, in part, by work on retinal prosthetics in which electrical stimulation designed to restore visual signaling also appeared to have neuroprotective effects [2]. This review will summarize the current literature on EST for retinal degenerative disease, both in animal models and initial clinical studies.

## 106.2 Types of EST Applied to the Retina

Three approaches to EST have been applied to the retina: Subretinalelectrical stimulation (SES), Transcornealelectrical stimulation (TES), and Whole eye stimulation (WES). SES uses an implanted microphotodiode array to stimulate the retina with low-level current proportional to incident light [3, 4]. The current density in response to white light is estimated to be less than 760 μA/cm$^2$ [5] and is driven by a localized electrical field that focuses stimulation at the level of the inner retina [6].

TES consists of placing a contact lens electrode on the cornea; the active and reference electrodes are concentric rings integral to the lens. Thus, the electrical field and resulting current are strongest in the anterior segment.

WES consists of placing an active electrode on the cornea and a reference electrode in the mouth or elsewhere on the head [7]. This configuration differs from TES and SES in that the applied electrical field, and thus the currents, are more uniformly distributed through the entire eye. It should be noted that this review will classify some studies identified as TES in the literature as WES due to reference

electrode placement away from the cornea [8, 9]. Neuroprotective current levels for TES and WES appear in the range of 1.5 to 1000 μA.

## 106.3 EST Preserves Photoreceptors

EST was applied to the RCS rat, a model of retinitis pigmentosa (RP), in early stages of the disease and showed neuroprotective results. SES preserved retinal function as measured by electroretinogram (ERG) b-wave [3, 4], maintained greater outer nuclear layer thickness [3], and increased activity in the superior colliculus [10]. Implanted RCS rats experienced protective effects proportional to the frequency with which SES microphotodiodes were stimulated with flashes from a Ganzfeld source [11, 12]. In addition to photoreceptor preservation, EST appears to delay inner retinal degeneration in RCS rats as evidenced by preservation of post-receptoral ERG parameters after SES [5] and decreased apoptosis in isolated RCS retinas after ex vivo stimulation [13]. TES preserved photoreceptors in the RCS rat after weekly 1 h stimulation, as indicated by significantly greater outer nuclear layer thickness and preserved ERG b-wave [14].

EST preserves photoreceptors in animal models with rhodopsin mutations that mimic many forms of RP. P347L rabbits received weekly TES for 1 h that resulted in preservation of ERG b-wave and photoreceptors in the visual streak [15]. Twice weekly WES treatments for 12 weeks preserved photoreceptor responsivity in P23H-1 rats, as measured by ERG a-wave sensitivity and preserved b-wave amplitudes [7]. In these experiments, photoreceptor morphology was not preserved, possibly due to the relatively small current levels applied. However, it is difficult to directly compare charge density at the retina between EST methods due to the marked differences in current paths between the different electrode geometries.

Another common model of photoreceptor degeneration is exposure to bright light. After WES stimulation every 3 days for 14 days with a contact lens electrode referenced to the opposite eye, albino rats exposed to bright light had significantly preserved a- and b-wave amplitudes [16]. EST for 2 h with a DTL fiber on the cornea (location of reference electrode not described) prior to a milder light exposure temporarily preserved b-wave amplitudes and some photoreceptors and rod outer segments after 3 weeks [8]. These effects were not as great as that reported by Ni et al. [16], possibly due to the different electrode configuration and the absence of repeated EST sessions.

## 106.4 EST Protects Retinal Ganglion Cells

In addition to photoreceptors, TES has been shown to be protective to retinal ganglion cells (RGC). Morimoto et al. demonstrated that a single 1 h exposure to TES can preserve RGCs [17]. Six hours of TES stimulation following optic nerve crush

in wild-type rats produced significantly larger visually evoked potentials [18]. Following ocular ischemia caused by elevated pressure in wild-type rats, TES every other day for 14 days preserved RGC density, retinal thickness, and ERG b-wave amplitudes [19]. A study on the optimal parameters of TES for RGC's found that 1–2 ms/phase and current of 100 and 200 μA at frequencies of 1, 5 and 20 Hz produced optimal results [20]. Furthermore, stimulation longer than 30 min and repeated exposures were more beneficial.

## 106.5 Mechanisms Underlying the Neuroprotective Effects of EST

Similar to the effects of electrical stimulation in other tissues, EST increases expression of neurotrophic factors in Muller cells. A number of studies have shown increased growth factor expression in vivo: fibroblast growth factor beta (FGF-2) mRNA expression was increased after SES [4], insulin growth factor-1 (IGF-1) mRNA and protein were upregulated in Muller cells after TES [18] and ciliary nerve trophic factor (CNTF) and brain derived neurotrophic factor (BDNF) levels increased in Muller cells after WES [16]. Similarly, cultured Muller cells exposed to biphasic pulses (10 μA, 1 ms pulse duration, 20 Hz) showed increased BDNF, FGF-2, and IGF-1 levels [21–23]. L-type calcium channels may control the release of these growth factors, as shown by using nifedipine, an L-type voltage dependent calcium channel blocker, to suppress the upregulation of IGF-1 and BDNF [21, 22]. In addition, EST downregulates proinflammatory cytokines such as interleukin-1 beta (IL-1β) and tumor necrosis factor (TNF)-alpha [24] and the pro-apoptotic gene Bax [16]. Finally, gene expression analysis of wild-type retina following 1 h of TES showed downregulation of Bax and differential expression of the TNF family [25]. It is interesting to note that different genes appear to be expressed depending on whether EST is applied to a diseased or healthy retina [25].

## 106.6 EST in Clinical Studies

The first reports of SES in patients was the retinal prosthetic trial by Chow et al. in which microphotodiode arrays were implanted in the subretinal space of RP patients. These patients showed improvement of retinal function that was not associated with direct activation of the retina overlying the device [2, 26]. More recent TES studies in RP patients chose current levels based on individual phosphene thresholds; [9] visual field area and ERG b-wave amplitude were significantly preserved.

Several studies have examined the potential of TES to benefit patients with RGC damage. Patients with non-arteritic ischemic optic neuropathy or traumatic optic neuropathy were found to have preserved visual acuity threshold and retinal function, as measured by critical flicker fusion, after a single 30 min treatment of TES [27]. TES was also reported to benefit patients with retinal artery occlusion by im-

**Table 106.1** Stimulation parameters and efficacy of approach for EST applied to the retina of animals or patients

| Disease model/*disease* | EST | Stimulation parameters[a] | Preservation[b] (fold change) | Ref |
|---|---|---|---|---|
| RCS rats | SES | 100 µA, n/a, chronic, chronic | b-wave amplitude: 4.3<br>ONL thickness: 3.4 | [3] |
| RCS rats | SES | 100 µA, n/a, chronic, chronic | LA b-wave amplitude: 1.6 | [4] |
| RCS rats | TES | 100 µA, 1 ms, weekly, 1 h | b-wave amplitude: 1.7<br>ONL thickness: 2.3 | [14] |
| P347L rabbits | TES | 700 µA, 10 ms, weekly, 1 h | LA a-wave amplitude: 1.4<br>ONL thickness: 1.75 | [15] |
| P23H-1 rats | WES | 1.5 µA, 5 Hz sinusoid, twice weekly, 0.5 h | a-wave amplitude: 2.2<br>b-wave amplitude: 1.6 | [7] |
| Bright light exposure in rats | WES | 200 or 300 µA, 3 ms, every 3 days, 1 h | a-wave amplitude: 13<br>b-wave amplitude: 11.5 | [16] |
| Bright light exposure in rats | WES | 200 µA, 2 ms, once, 1 h | ERG Vmax: 1.1<br>Photoreceptor length: 1.5 | [8] |
| Optic nerve transection in rats | TES | 100 µA, 0–3 ms, once, 1 h | RGC density: 1.4<br>IGF-1 RNA expression: 2 | [17] |
| Optic nerve crush in rats | TES | 500 µA, 50 ms, once, 6 h | VEP amplitude: 2.4 | [18] |
| Ischemia with elevated pressure in rats | TES | 300 µA, 3 ms, every 2 days, 1 h | b-wave amplitude: 2.2<br>RGC density: 1.2 | [19] |
| *Optic neuropathy* | TES | 600–800 µA, 10 ms, once, 0.5 h | Visual acuity threshold: 4<br>Flicker fusion frequency: 2.5 | [27] |
| *Retinal artery occlusion* | TES | ≤1000 µA, 10 ms, monthly, 0.5 h | LA b-wave amplitude: 1.6<br>mfERG N1-P1 amplitude: 3.75 | [28] |
| *Retinal artery occlusion* | TES | 500–900 µA, 10 ms, once, 0.5 h | mfERG N2 amplitude: 1.6 | [29] |
| *Retinitis pigmentosa* | WES | 150% of phosphene threshold, 5 ms, wkly, 0.5 h | b-wave amplitude: 1.3<br>Visual field area: 1.1 | [9] |

[a] Current, pulse duration, frequency of EST, duration of EST. All stimulation parameters included biphasic 20 Hz current, unless noted

[b] Preservation was calculated based on the reported maximal EST value compared to the sham control for each parameter in animal studies or the maximal difference reported between the first and last visit in patient studies

proving visual acuity and mfERG with monthly treatments [28], but also showed similar preservation with a single 30 min TES treatment [29]. Furthermore, TES significantly increased choroidal blood flow at 3 and 24 h after TES in healthy subjects, which might provide further beneficial nutrients to the diseased retina.

## 106.7 Conclusions

There is mounting experimental evidence that EST provides neuroprotective effects to photoreceptors and retinal ganglion cells. As summarized in Table 106.1, these effects are often modest. However, the non-invasive nature of TES and WES, as well as the demonstrated benefits after even a single treatment, makes EST attractive as one possible component in a management strategy aimed at maintaining vision in patients with retinal degenerations. With few treatment options for these blinding diseases, additional studies are needed to determine the optimal EST parameters that will preserve visual function.

## References

1. Dor H (1873) Beitrage zur Electrotherapie der Augenkrankheiten. Graefes Arch Clin Exp Ophthalmol 19:532
2. Chow AY, Chow VY, Packo KH, Pollack JS, Peyman GA, Schuchard R (2004) The artificial silicon retina microchip for the treatment of vision loss from retinitis pigmentosa. Arch Ophthalmol 122(4):460–469
3. Pardue MT, Phillips MJ, Yin H, Sippy BD, Webb-Wood S, Chow AY et al (2005) Neuroprotective effect of subretinal implants in the RCS rat. Invest Ophthalmol Vis Sci 46(2):674–682
4. Ciavatta V, Chrenek M, Wong P, Nickerson J, Pardue M (2006) Growth factor expression following implantation of microphotodiode arrays in RCS rats. Invest Ophthalmol Vis Sci ARVO E-abstract:3177
5. Ciavatta VT, Mocko JA, Kim MK, Pardue MT (2013) Subretinal electrical stimulation preserves inner retinal function in RCS retina. Molecular vision in-press
6. Mathieson K, Loudin J, Goetz G, Huie P, Wang L, Kamins TI et al (2012) Photovoltaic retinal prosthesis with high pixel density. Nat Photonics 6(6):391–397
7. Rahmani S, Bogdanowicz L, Thomas J, Hetling JR (2012) Chronic delivery of low-level exogenous current preserves retinal function in pigmented P23H rat. Vision Res 76:105–113
8. Schatz A, Arango-Gonzalez B, Fischer D, Enderle H, Bolz S, Rock T et al (2012) Transcorneal electrical stimulation shows neuroprotective effects in retinas of light-exposed rats. Invest Ophthalmol Vis Sci 53(9):5552–5561
9. Schatz A, Rock T, Naycheva L, Willmann G, Wilhelm B, Peters T et al (2011) Transcorneal electrical stimulation for patients with retinitis pigmentosa: a prospective, randomized, sham-controlled exploratory study. Invest Ophthalmol Vis Sci 52(7):4485–4496
10. DeMarco PJ Jr, Yarbrough GL, Yee CW, McLean GY, Sagdullaev BT, Ball SL et al (2007) Stimulation via a subretinally placed prosthetic elicits central activity and induces a trophic effect on visual responses. Invest Ophthalmol Vis Sci 48(2):916–926
11. Pardue MT, Phillips MJ, Yin H, Fernandes A, Cheng Y, Chow AY et al (2005) Possible sources of neuroprotection following subretinal silicon chip implantation in RCS rats. J Neural Eng 2(1):S39–S47
12. Pardue MT, Kim MK, Walker TA, Faulkner AE, Chow AY, Ciavatta VT (2012) Neuroprotective dose response in RCS rats implanted with microphotodiode arrays. Adv Exp Med Biol 723:115–120
13. Schmid H, Herrmann T, Kohler K, Stett A (2009) Neuroprotective effect of transretinal electrical stimulation on neurons in the inner nuclear layer of the degenerated retina. Brain Res Bull 79(1):15–25

14. Morimoto T, Fujikado T, Choi JS, Kanda H, Miyoshi T, Fukuda Y et al (2007) Transcorneal electrical stimulation promotes the survival of photoreceptors and preserves retinal function in royal college of surgeons rats. Invest Ophthalmol Vis Sci 48(10):4725–4732
15. Morimoto T, Kanda H, Kondo M, Terasaki H, Nishida K, Fujikado T (2012) Transcorneal electrical stimulation promotes survival of photoreceptors and improves retinal function in rhodopsin P347 L transgenic rabbits. Invest Ophthalmol Vis Sci 53(7):4254–4261
16. Ni YQ, Gan DK, Xu HD, Xu GZ, Da CD (2009) Neuroprotective effect of transcorneal electrical stimulation on light-induced photoreceptor degeneration. Exp Neurol 219(2):439–452
17. Morimoto T, Miyoshi T, Matsuda S, Tano Y, Fujikado T, Fukuda Y (2005) Transcorneal electrical stimulation rescues axotomized retinal ganglion cells by activating endogenous retinal IGF-1 system. Invest Ophthalmol Vis Sci 46(6):2147–2155
18. Miyake K, Yoshida M, Inoue Y, Hata Y (2007) Neuroprotective effect of transcorneal electrical stimulation on the acute phase of optic nerve injury. Invest Ophthalmol Vis Sci 48(5):2356–2361
19. Wang X, Mo X, Li D, Wang Y, Fang Y, Rong X et al (2011) Neuroprotective effect of transcorneal electrical stimulation on ischemic damage in the rat retina. Exp Eye Res 93(5):753–760
20. Morimoto T, Miyoshi T, Sawai H, Fujikado T (2009) Optimal parameters of transcorneal electrical stimulation (TES) to be neuroprotective of axotomized RGCs in adult rats. Exp Eye Res 90(2):285–291
21. Sato T, Fujikado T, Lee TS, Tano Y (2008) Direct effect of electrical stimulation on induction of brain-derived neurotrophic factor from cultured retinal Muller cells. Invest Ophthalmol Vis Sci 49(10):4641–4646
22. Sato T, Fujikado T, Morimoto T, Matsushita K, Harada T, Tano Y (2008) Effect of electrical stimulation on IGF-1 transcription by L-type calcium channels in cultured retinal Muller cells. Jpn J Ophthalmol 52(3):217–223
23. Sato T, Lee TS, Takamatsu F, Fujikado T (2008) Induction of fibroblast growth factor-2 by electrical stimulation in cultured retinal Mueller cells. Neuroreport 19(16):1617–1621
24. Zhou WT, Ni YQ, Jin ZB, Zhang M, Wu JH, Zhu Y et al (2012) Electrical stimulation ameliorates light-induced photoreceptor degeneration in vitro via suppressing the proinflammatory effect of microglia and enhancing the neurotrophic potential of Muller cells. Exp Neurol 238(2):192–208
25. Willmann G, Schaferhoff K, Fischer MD, Arango-Gonzalez B, Bolz S, Naycheva L et al (2011) Gene expression profiling of the retina after transcorneal electrical stimulation in wild-type Brown Norway rats. Invest Ophthalmol Vis Sci 52(10):7529–7537
26. Chow AY, Bittner AK, Pardue MT (2010) The artificial silicon retina in retinitis pigmentosa patients (an American Ophthalmological Association thesis). Trans Am Ophthalmol Soc 108:120–154
27. Fujikado T, Morimoto T, Matsushita K, Shimojo H, Okawa Y, Tano Y (2006) Effect of transcorneal electrical stimulation in patients with nonarteritic ischemic optic neuropathy or traumatic optic neuropathy. Jpn J Ophthalmol 50(3):266–273
28. Inomata K, Shinoda K, Ohde H, Tsunoda K, Hanazono G, Kimura I et al (2007) Transcorneal electrical stimulation of retina to treat longstanding retinal artery occlusion. Graefes Arch Clin Exp Ophthalmol 245(12):1773–1780
29. Oono S, Kurimoto T, Kashimoto R, Tagami Y, Okamoto N, Mimura O (2011) Transcorneal electrical stimulation improves visual function in eyes with branch retinal artery occlusion. Clin Ophthalmol 5:397–402

# Index



J. D. Ash et al. (eds.), *Retinal Degenerative Diseases,* Advances in Experimental Medicine and Biology 801, DOI 10.1007/978-1-4614-3209-8,